

---

# ANIMAL CELL TECHNOLOGY MEETS GENOMICS

---

Proceedings of the 18th ESACT Meeting  
Granada, Spain, May 11-14, 2003

Edited by  
Francesc Gòdia and  
Martin Fussenegger



European Society for Animal Cell Technology

 Springer

## ANIMAL CELL TECHNOLOGY MEETS GENOMICS

# Animal Cell Technology Meets Genomics

Proceedings of the 18th ESACT Meeting  
Granada, Spain, May 11–14, 2003

*Edited by*

Francesc Gòdia

and

Martin Fussenegger

 Springer

A C.I.P. Catalogue record for this book is available from the Library of Congress.

ISBN 1-4020-2791-5 (HB)  
ISBN 1-4020-3103-3 (e-book)

---

Published by Springer,  
P.O. Box 17, 3300 AA Dordrecht, The Netherlands.

Sold and distributed in North, Central and South America  
by Springer,  
101 Philip Drive, Norwell, MA 02061, U.S.A.

In all other countries, sold and distributed  
by Springer,  
P.O. Box 322, 3300 AH Dordrecht, The Netherlands.

*Printed on acid-free paper*

springeronline.com

All Rights Reserved  
© 2005 Springer

No part of this work may be reproduced, stored in a retrieval system, or transmitted in any form or by any means, electronic, mechanical, photocopying, microfilming, recording or otherwise, without written permission from the Publisher, with the exception of any material supplied specifically for the purpose of being entered and executed on a computer system, for exclusive use by the purchaser of the work.

Printed in the Netherlands.

## Contents

Meeting Committees	xxiii
ESACT Executive Committee	xxiv
Sponsors	xxv
Companies Participating in the Trade Exhibition	xxvi
Introduction: Animal Cell Technology Meets Genomics	xxvii
Acknowledgements	xxviii
List of Participants	xxix

### ***CHAPTER 1: CELLULAR MECHANISMS***

<b>Effect of osmotic pressure on GS-NSO expression system</b>	3–13
Wu M., Dimopolous G., Mantalaris A., Varley J.	
<b>Molecular approaches to influence epigenetic effectors of transient and stable transgene expression in mammalian cells</b>	15–22
Hacker D., Cotten M., Wurm F.	
<b>Genomic exploration on Chinese hamster ovary cells</b>	23–29
de Leon Gatti M., Wlaschin K., Rink A., Sanny, A., Tan, K.S., Nissom, P.M., Ong, P.F., Wong K., Philip, R.J., Cham, B., Wong, C.F., Lim, K.M., Yap, M., Hu W.-S.	
<b>Roles for glycosylation in receptor-ligand interactions in the immune system</b>	31–42
Rudd, P.M., Merry, A.H., Dwek, R.A.	
<b>Investigations on mannose-6-phosphate receptor mediated protein uptake</b>	43–49
Duerrschmid M., Jursik, C., Borth, N., Grabherr R., Doblhoff-Dier O.	
<b>Analysis of multiple apoptosis parameters using a microfluidic chip-based system</b>	51–57
Valer M., Preckel T., Luedke G., Buhlmann C.	
<b>Inhibiting apoptosis in cell culture using multiple inhibitors</b>	59–65
Figuroa, B., Ailor, E., Reff, M., Hardwick, J.M., Betenbaugh M.J.	
<b>Pausing of mammalian cells by cold exposure, limits and opportunities</b>	67–70
Hunt L., Hacker D., El Abridji H., Grosjean F., DeJesus M., Jordan M., Wurm F.	

<b>The functional competence of animal cells: analysis of the secretory pathway</b>	71–74
Racher A.J., Birch J.R., James D.C., Alete, D.E., Smales C.M.	
<b>Proteome analysis of recombinant CHO cells under hyperosmotic stress</b>	75–78
Lee M.S., Kim K.W., Kim Y.H., Lee G.M.	
<b>Expression profiling analysis of sodium butyrate-induced Chinese hamster ovary cells in defined medium</b>	79–82
Melville M.W., Sinacore, M., Hann L.E.	
<b>Intracellular nucleotide pools for optimizing product-oriented transient transfection of HEK293 cells in suspension</b>	83–86
Bassani Molinas M.M., Beer C., Hesse F., Wirth M., Durocher Y., Kamen A., Wagner R.	
<b>Impact of yeast pyruvate carboxylase on the productivity of animal host cell lines</b>	87–89
Bollati Fogolín M., Irani N., Beccaria A.J., Schulz C., Van den Heuvel J., Elias C.B., Carpentier E., Durocher Y., Bisson L., Etcheverrigaray M., Kratje R.B., Wirth M., Kamen A., Wagner R.	
<b>Environmental effects of lactate on High-Five™ insect cell metabolism</b>	91–99
Drugmand J.-C., Schneider Y.-J., Agathos S.N.	
<b>Correlation of intracellular nucleotide pools to amino acid concentrations in culture media by the application of multivariate methods</b>	95–98
Hesse F., Nelving A., Wagner R.	
<b>Engineering <i>Trichoplusia ni</i> (High Five™) insect cells to express a cytosolic pyruvate carboxylase enzyme improves the viability of the cells in batch, fed-batch and perfusion cultures.</b>	99–102
Locas M.-C., Elias C.B., Lanthier, S., Bisson, L., Perrier, M., Kamen A.	
<b>Insect cell culture medium selection and optimisation based on monitoring and economical considerations</b>	103–106
Lecina M., Soley A., Passamani P., Casablanca A., De Gracia, J., Vela C., Espuña E., Cairó J.J., Gòdia, F.	

- Antiapoptotic activity of synthetic and natural peptides** 107–110  
Franek F.
- Effect of antiapoptotic genes expression on cell growth and monoclonal antibody productivity in a hybridoma cell line** 111–113  
Juanola S., Vives J., Andersen, J., Prats E., Cornudella L., Cairó J., Gòdia F.
- Amplified dicistronic expression units mediate apoptosis protection in CHO-DG44 cells adapted for growth in serum-free media, impact on mitochondria copy number** 115–120  
Meents H., Enenkel B., Fussenegger M.
- Effect of reduced water on the apoptotic cell death triggered by oxidative stress in pancreatic  $\beta$  HIT-T15 cell** 121–124  
Shirahata S., Li Y., Teruya K., Katakura Y., Kabayama S., Otsubo K., Morisawa S., Ishii Y., Gadek Z.
- Characterization of apoptosis in a CHO cell line cultivated in batch and continuous culture: Effect of medium, specific perfusion rate and chemical inhibitors** 125–128  
Thrift J., Yamasaki G., Heidemann R., Abbas N., Konstantinov K.
- Hydrogen peroxide-induced cellular senescence is regulated via two different pathways** 129–131  
Yoshizaki K., Katakura Y., Fujiki T., Tsunematu T., Teruya K., Shirahata S.
- Identification of autocrine factors influencing proliferation in serum free cultures of *Trichoplusia ni* cells** 133–135  
Eriksson U., Häggström L.
- The effects of insulin and Long<sup>TM</sup>R<sup>3</sup>IGF-I on Chinese hamster ovary cells: cell survival, receptor activation and second messenger pathways** 137–141  
Yandell C.A., Butler I.P., Sheehan A.J., Wade B.J., Simula A.P., Goddard C.
- Conditioned medium factors in protein-free cultures of NS0 cells** 143–145  
Spens E., Häggström L.
- Production of human anti-peptide antibody for clinical use by in vitro immunization** 147–149  
Tamura, T., Katakura, Y., Yamashita, M., Aiba, Y., Matsumoto S., Teruya, K., Shirahata S.

<b>Optimization of in vitro immunization protocol to produce antigen specific human monoclonal antibody by demonstrating the role of IL-10</b>	151–153
Xu Q.H., Katakura Y., Yamashita M., Teruya K., Shirahata S.	
<b>Extracellular histone H4 from SF9 cells is antimicrobial</b>	155–157
Calles K., Lindskog E., Nossed Å., Svensson I., Häggström L.	
<b>Analyzing calcium phosphate transfection of adherent CHO cells using microscopic live imaging</b>	159–161
Grosjean F., Jordan M., Wurm F.M.	
<b>Effects of multiplicity of infection (MOI) and cell cycle on Baculovirus infection kinetics</b>	163–165
Haas R., Reid S., Nielsen L.K.	
<b>Non-freezing preservation and subsequent recovery of hepatocytes under pO<sub>2</sub>- and pH-controlled conditions for continuous supply of cells for bioartificial liver support</b>	167–170
Iding K., Büntemeyer H., Lehmann J.	
<b>Selection of MDCK subclones with various genotypic and phenotypic markers: sensitivity to influenza virus infection</b>	171–174
Kessler N., Roche G., Vernet A., Abismil C.	
<b>Extracellular metalloproteases and their inhibitors expressed by the IFN-<math>\gamma</math> producing CHO-320 cell line</b>	175–178
Mols J., Verhoeve F., Peeters-Joris C., Agathos S.N., Schneider Y.-J.	
<b>Novel small-molecule AKT1 inhibitors discovered by Redistribution<sup>TM</sup>-based high-throughput screening.</b>	179–181
Præstegaard M., Nielsen S.J., Lundholt B.K., Mikkelsen I., Loechel S., Heide M., Linde V.	
<b>Influence of mistletoe extracts and its components on in-vitro physiology of cancer cells</b>	183–185
Sidler F., Wermelinger, T., Rist, L., Hensel A., Viviani A.	
<b>Rapid in-process monitoring of antibody integrity, purity and titre-2100 Bioanalyser (Lab on a chip) study</b>	187–192
Nesredin A., Mussa N.A., Cheung K.Y., Alam I.M., Flatman S.	
<b>Toxicological evaluation of haine river waste-water samples to appropriately sensitised cultured Fathead Minnow cells compared with the microtox® method</b>	193–196
Dierickx P.J., Van der Wielen C.	



**CHAPTER 2: CELL BASED THERAPIES**

- 3D-cultivation and characterisation of osteogenic cells for the production of highly viable bone tissue implants** 199–205  
Barthold M., Majore I., Fargali S., Stahl F., Schulz R., Lose S., Mayer H., Jäger V.
- Carbon source has a considerable influence on extracellular matrix formation, demonstrated on specific collagen expression of primary human tenocytes** 207–212  
Möbest D., Jaeger M., Hoben G., Hamann D., Wollner S., Stark G.B.
- Design and characterization of cardiomyocyte-derived micro tissues** 213–214  
Kelm M.J., Ehler E., Perriard J.C., Fussenegger M.
- Process development for standardized generation of monocyte-derived dendritic cells: applicability in breast cancer immunotherapy** 221–227  
Bohnenkamp H.R., Noll T.
- Stemline™ hematopoietic stem cell expansion medium, a serum-free medium for expansion of CD34<sup>+</sup> hematopoietic stem cells and progenitors** 229–232  
Leugers S., Allison D., Pronold, B.J., Rennebeck, G., Van Zant, G., Tario J., Swartzwelder F., Donahue L.
- Mesenchymal stem cells: a very first step towards large scale cell culture strategies transplantation** 233–235  
Bensellam M., Bassens C., Toallati, M., Lowagie S., Wérenne J.
- Expansion of murine embryonic stem cells on microcarriers-functional characteristics and scale-up potential** 237–240  
Burg M., Quel G., Rüdiger M., Zweigerdt R.
- In vitro cultivation of rabbit mesenchymal stromal cells on 3D bioresorbable calcium phosphate scaffolds for the generation of bone tissue implants** 241–243  
Fargali S., Barthold M., Rohde, M., Majore I., Jäger V.
- Establishment and characterization of human medullary thyroid carcinoma cell lines for immunotherapy** 245–248  
Stradler G., Voglauer R., Wieser M., Katinger H., Pfragner R.

<b>Suppression of cell growth by platinum nanocolloids as scavengers against reactive oxygen species</b>	249–251
Hamasaki T., Kashiwagi T., Aramaki, S., Imada, T., Komatsu T., Li Y., Teruya K., Katakura Y., Kabayama S., Otsubo K., Morisawa S., Shirahata S.	
<b>Comparison of fluidized bed and fed batch reactor cultures for production of anti-HIV-antibody</b>	253–255
Hinterleitner P., Unterluggauer F., Landauer K., Müller D., Kunert R., Blüml G., Doblhoff-Dier O., Katinger H.	
<b>Suppression of oxidative stress-induced apoptosis of neuronal cells by electrolyzed-reduced water</b>	257–259
Kashiwagi T., Hamasaki, T., Kabayama, S., Takaki, M., Teruya, K., Katakura, Y., Otsubo, K., Morisawa, S., Shirahata, S.	
<b>Spheroid formation by encapsulation of cancer cells to mimic small size tumors</b>	261–263
Marc A., Markvicheva E., Jourdain C., Bezdetnaya L., Merlin J-L., Guillemin F., Zubov V., Goergen J-L.	
<b>Bioreactor for continuous biomechanical characterization of cellular systems and tissue-engineered biohybrid tissues</b>	265–267
Möbest D., Jaeger M., Guttman J., Schneider M., Stark G.B.	
<b>Membrane-separated cocultivation of cord blood hematopoietic stem cells with stromal cell lines</b>	269–271
Fischbach T., Noll T.	
<b>Anti-apoptotic genes protect an insulinoma cell line from cell death induced by hyperglycemia</b>	273–275
Ogawa A., Terada S., Miki M., Kumagai T., Kimura, T., Yamaguchi, A.	
<b>Preparation and characterization of an idiotype-dendritic cell vaccine for immunotherapy of multiple myeloma</b>	277–280
Opalka B., Schütt P., Brandhorst D., Buttkeleit U., Tewes M., Moritz T., Seeber S., Nowrousain M.R.	
<b>Pretreatment with polycations enhances Adenoviral infection levels in serum-free PER.C6™ cells as well as HEK 293 cells</b>	281–283
Padilla J., Burke V., Johnson J., Hartshorn J., McNorton S., Etchberger K.	
<b>Optimizing the production of cardiomyocytes from mouse embryonic stem cells in a 2L stirred tank reactor</b>	285–288
Schroeder M., Niebruegge, S., Werner A., Zweigerdt R., Burg	

- Establishment and characterization of CD4<sup>+</sup> Killer-T-Cells (KTCs)** 289–292  
Voglauer R., Jursik C., Prchal M., Jungfer, H., Grillari, J., Katinger H.

### **CHAPTER 3: GENE BASED THERAPEUTICS**

- Successful development of a robust adenovirus production process primarily relies on a better understanding of packaging cell line physiology and vector replication kinetics** 295–301  
Kamen A., Henry O., Jacob D., Bernier A.
- Retroviral vector stability: inactivation kinetics and membrane properties** 303–308  
Cruz P., Carmo M., Coroadinha, A.S., Bengala, A., Gonçalves, D., Texeira, M., Merten, O.-W., Geny-Fiamma, C., Carrondo, M.J.T.
- Comparison of host cell lines and production methods for a new generation of oncolytic adenoviral vectors** 309–316  
Forestell S., Celeri C., Dang C., Gong T., Olsen M., Sifi I., Yuk I., Geyer S.
- Process development for a veterinary vaccine against heartwater** 317–320  
Marcelino I., Sousa M., Verissimo C., Peixoto C., Carrondo M.J.T., Alves P.M.
- A new method for the quantitative determination of enveloped viral particles** 321–323  
Beer C., Wirth M.
- Development of a 293T cell line for the production of virus like particles in bioreactors** 325–328  
Costa M.J.L., Malhó, R., Gonçalves J., Ferreira G.N.M., Aires-Barros M.R.
- Effect of MOI and medium composition on adenovirus infection kinetics** 329–332  
Ferreira T., Alves P.M., Gonçalves, D., Carrondo M.J.T.
- ION-exchange chromatography based strategies for purification of viral vectors** 333–338  
Vasi J., Morenweiser, R., Eriksson, K., Lemmens R., Herzer S.

- Scaling up of endothelial cells culture for the production of a rickettsiae vaccine: evaluation of the importance of the interference effects** 339–344  
Hendrick V., Kagye N., Kamba Y., Simon, S., Thinsy A-L., Marigue, T., Wérenne J.

#### **CHAPTER 4: TARGET DISCOVERY**

- Inducible gene expression for antibiotic drug discovery and diagnostics** 345–350  
Weber W., Link N., Spielmann M., Weber, C.C., Keller B., Fussenegger M.

- Nucleic acid capture assay: a novel high-throughput method for direct mRNA quantitation** 351–357  
Van de Goor J., Tsai S.P., Wong A., Mehta S., Zheng L., Elliott L.O., Stephan J.P.

- High throughput transient transfections of HEK293EBNA cells: development of an integrated expression purification process at 100 ml scale** 359–364  
Heine H., Rey L., Arod C.Y., Gaudry J-P., Antonsson B., Feger G., Battle T.

- Transient gene expression in suspension HEK293 cells: application to large-scale protein production** 365–367  
Baldi L., Jacquet R., Picasso S., Tromba P., Derow E., Girard P., Hacker D., Wurm F.M.

- Monoclonal antibody production: determination of appropriate system and medium for production enhancement and decrease of overall production time** 369–371  
Fritchman K., Tilsaghani C., Sumnall T.

- The secrets of transfection in serum-free suspension culture** 373–376  
Geisse S., Di Maiuta N., Ten Buren B., Henke M.

- From genes to proteins: full open reading frame (ORF) clones and their application in functional research** 377–379  
Goedde A., Baars S., Czerny K., Schultz E., Gernold N., Scheuermann, T., Schatten R., Henze S., Schick M., Ebert L., Langlais C., Korn B.

<b>A versatile disposable culture system for high throughput screening of process parameters and production cell lines</b>	381–383
Jordan M., DeJesus M., Eigenmann C., Gleich T., Wurm F. M.	
<b>Long time storage of pre-inoculated multi-well plates for cell-based assay kits used for drug identification and characterisation</b>	385–387
Loa A., Gelli, C., Laffert B.	
<b>Comparative secretion levels of recombinant proteins between insect cell-baculovirus and mammalian HEK293EBNA cells</b>	389–391
Losberger C., Battle T.	
<b>Microfluidic technology applied to protein sizing and quantitation</b>	393–396
Valer M., Neumann T., Barthaier P., Kuschel M., Buhlman C.	
<b>CryoStock – a software for cell culture management</b>	397–400
Zerlin M., Greiffenberg L., Wurm Y., Winkler I., Kreusel D., Tomoe S., Ballabas L., Martin J.	
<b><u>CHAPTER 5: BIOPHARMACEUTICALS</u></b>	
<b>Targeting the human Immunoglobulin loci for high level heterologous gene expression</b>	403–409
Winkler K., Wermelinger T., Paul C., Koch S., Brecht, R., Zietze, S., Nuck, R., Thiel, G., Marx U., Sandig V.	
<b>MAR elements as tools to increase protein production by CHO cells</b>	411–415
Girod, P.-A., Zahn-Zabal, M.M. Mermod N.	
<b>Cell line engineering for production of therapeutic antibody glycoforms with increased biological activity</b>	417–422
Umana P., Bruenker P., Ferrara C., Moser S., Suter T., Gerdes C.A., Puentener U., Jean-Mairet, Buholzer P., Spaeni M.	
<b>Development of a metabolically optimized fermentation process based on glucose-limited CHO perfusion culture</b>	423–430

<b>Applications of quasi real-time metabolic flux analysis in mammalian cell culture process development</b>	431–438
Goudar C., Biener R., Michaels J., Zhang, C., Piret J., Konstantinov K.	
<b>Data-based modelling of cell cultures</b>	439–445
Cunha-Bakeev C., Glassey J., Montague G., Al-Rubeai M., Hardwicke, P.	
<b>Cell culture and downstream processing integration using ProteinChip® technology. Application to protein analysis and purification in biopharmaceutical manufacturing</b>	447–452
Bengio S., Santambien P., Cleverley S.	
<b>The prospects for insect cells for use as a cell substrate for the production of biotherapeutics</b>	453–458
Galbraith D.N.	
<b>High-performance cell culture platform technology for Mab production</b>	459–464
Chang D.Y.H., Garza P., Huang Y.M., Talabardon M., Rahmati S., Fallon E., Noe W.	
<b>Development and integration of a new animal-component-free process for the production of UK-279,276</b>	465–470
Pluschkell S., Blocker L., Geldart R., Hawrylik S., Mensah P., Okediadi C., Pias S., Subashi A., Zhu M.	
<b>Towards an affinity-based capture system for the isolation of high expression cells using a co-expressed surface protein</b>	471–473
Derouazi M., Pick H.M., Deluz C., Picasso S., Wurm F.M.	
<b>Effect of doxycycline-regulated calnexin and calreticulin expression on specific thrombopoietin productivity of recombinant CHO cells</b>	475–478
Chung J.Y., Lim S. W., Hong Y. J., Koh Y. W., Hwang S. O., Lee G.M.	
<b>Recombinant glycoprotein expression. Development of a homologous CHO expression system</b>	479–482
Noone C., Smith T., Cairns M.	

<b>Generation of recombinant antibody manufacturing cell lines using cell-cell fusion</b>	483–488
Zeng W., Puchacz E., Heineken K., Raymond I., Chang C., Ryll T., Chamow S.	
<b>Cloning and expression of biopharmaceuticals in CHO.K1 and BHK-21 cells</b>	489–492
Castilho L.R., Asensi G.F., Cavalcanti J.C., Sousa, P.M., Del Aguila, E.M., Silva J.T., Paschoalin V.M.F., Castilho, L.R.	
<b>Camel single-domain antibodies as modular building blocks to make bivalent constructs for use in immunotherapy of cancer</b>	493–495
Cortez-Retamozo V., Backmann N., Senter P.D., Wernery U., De Baetselier P., Muyldermans S., Revets H.	
<b>Establishment of efficient cloning method for variable region genes of antigen specific human monoclonal antibody</b>	497–499
Matsumoto S., Katakura Y., Yamashita M., Aiba Y., Noguchi E., Teruya K., Shirahata S.	
<b>From gene to monoclonal antibody: efficient screening by cell sorting</b>	501–504
Borth N., Böhm E., Grillari J., Löscher, M., Gross S., Voglauer R., Ferko B., Kunert R., Katinger H.	
<b>Development of an integrated strategy for recombinant cell line selection</b>	505–507
Castillo A.J., Victores, S., Faife, E., Rabasa, Y., De La Luz, K.R.	
<b>Gene transfer to animal cells in culture by microinjection: A novel tool to create recombinant cell lines?</b>	509–512
Derouazi M., Girard P., Jordan M., Denoya C., Wurm F.M.	
<b>Evaluation of the stability of NS0 cell lines expressing recombinant human IgG</b>	513–515
Forrest-Owen W., Daramola L., Hatton D., Field R.	
<b>High throughput screening and selection of single cells in suspension using fluorescence parameters</b>	517–520
Giese C., Demmler C., Gradl G., Marx U.	

<b>Control of key parameters in the development of mammalian production clones</b>	521–524
Kunert R., Wolbank, S., Chang, M., Preis S., Steinfeldner W., Borth N., Katinger H.	
<b>Establishment of screening systems for recombinant cell lines: early prediction of the suitability as a production clone</b>	525–527
Lattenmayer C., Kunert R., Katinger H.	
<b>Characterisation of CHO subclones showing profound changes in performance when propagated in different cultivation systems</b>	529–532
Trummer E., Müller D., Steinfeldner W., Kunert R., Steindl F., Hesse F., Katinger H.	
<b>High level production of recombinant IgG in the human cell line PER.C6™</b>	533–536
Yallop C., Raamsman M., Zuijderwijk M., van Noordenburg Y., Vooy A., Keehnen R., van Montfort B., Jansen M., Lagerwerf F., Dijkstra R., Birrento M., De Vocht M., Renger S., Bout A., Opstelten D.-J.	
<b>Creating a new medium to help meet the variable nutritional requirements of Chinese hamster ovary (CHO) cell clones</b>	537–540
Deeds Z.W., Albee A., Delong B., Gifford J., Ross J.S., Kao K., Caple M.V.	
<b>Development of an efficient medium optimization kit for factorial matrix design - a statistical approach to increase cell growth and productivity of recombinant CHO cells</b>	541–547
DeLong B., Albee A., Deeds Z., Gifford J., Ross J., Kao K., Caple M.	
<b>An efficient approach to cell culture medium optimization – a statistical method to medium mixing</b>	549–553
Gifford J., Albee A., Deeds Z.W., Delong B., Kao K., Ross J.S., Caple M.V.	
<b>Virus inactivation in foetal calf serum by a combined treatment of gamma-irradiation and UV-C irradiation</b>	555–559
Hermann H., Burian R., Waldmann R.	
<b>Advances in media optimization: two automated approaches that increase expression while reducing development time</b>	561–563



Holdread S., Hunt C., Haaland P., Chaney B., Porter, W.,  
Heidaran, M., Wannlund J.

**The importance of cholesterol for insect cell growth and  
baculovirus production** 565–568

Lua L.H.L., Reid S.

**Use of rapeseed proteins and peptides as supplements in  
insect cell cultures** 569–571

Marc A., Deparis V., Durrieu C., Marc I., Goergen J.L.,  
Chevalot I.

**Nutritional performance of wheat gluten -derived  
protein hydrolysates in hybridoma cell cultures** 573- 576

Martens D.E., Wegkamp H.B.A., Simpson N.H., Huttinga  
H.H., Kunst T., Siemensma A.D.

**SyntheChol<sup>TM</sup> synthetic cholesterol for cholesterol  
dependent cell culture. Development of non-animal  
derived chemically defined NS0 medium** 577- 580

Talley D., Cutak B., Rathbone E., Al-Kolla T., Allison D.,  
Blasberg J., Koa K. Caple M.

**NS0 derivatives: MAb production in large-scale SFM  
formats** 581-584

Manwaring J., Barnett B., Pence, B., Whitford W.

**Silk protein sericin accelerates proliferation of various  
mammalian cells** 585-587

Terada S., Yanagihara K., Kaito, K., Miki M., Sasaki M.,  
Tsujimoto K., Yamada H.

**Image analysis based realtime-control of glucose  
concentration** 589-592

Brueckerhoff T., Frerichs J., Joeris K., Konstantinov K.,  
Scheper T.

**On line analysis of microcarrier cultivations** 593-595

Burzlaff A., Kasper C., Scheper T.

**Error analysis during estimation of metabolic fluxes  
through metabolite balancing** 597-600

Goudar C., Biener R., Michaels J., Piret J., Konstantinov K.

**Generalized logistic equation modeling of mammalian  
cell batch cultures** 601-604

Goudar C., Heidemann R., Joeris K., Michaels J., Piret J.,  
Konstantinov K.

<b>In-situ microscopy based monitoring of mammalian cell culture processes</b>	605-608
Joeris K., Frerichs J-D., Scheper T., Konstantinov K.	
<b>A novel disposable microtube for rapid assessment of biomass in cell cultures</b>	609-612
Jordan M.	
<b>Intracellular monitoring of baculovirus infection of Sf9 insect cells and r-protein production using anti-alpha-1,3/4 fucosyltransferase antibodies and flow cytometry</b>	613-616
Marc A., Deparis V., Jestin A., Goergen J.L.	
<b>Effect of glucose and glutamine concentration on metabolism of animal cells in chemostat culture</b>	617-620
Matsuoka H., Takeda T.	
<b>Evaluation of a novel capacitance probe for on-line monitoring of viable cell densities in batch and fed-batch animal cell culture processes</b>	621-624
Schmid G., Zacher D.	
<b>Sodium butyrate enhancement of protein expression in HeLa cells: follow-up of a chimeric reporter gene behaviour for process development</b>	625-627
Bassens C., Rigaux P., Hendrick V., Cherlet, M., Sato, K. Kotarsky K., Wérenne J.	
<b>Scalable, serum-free, high efficiency transfection of CHO Cells using an economical DNA transfer vehicle</b>	629-632
Girard P., Derouazi M., Van Tilborgh, F. Wurm F. M.,	
<b>Process optimization for an NS0-derived hybridoma cell line in a chemically defined, protein-free medium</b>	633-636
Johnson J.M., Hartshorn J., McNorton S., Padilla-Zamudio J., Etchberger K.	
<b>Impact of change in fermentation process pH and dissolved carbon dioxide concentration on secreted antibody structure and cell physiology of a GS-NS0 cell line expressing a human antibody</b>	637-640
Ridley A., Dempsey J., Gee C., Turner R., Osborne M., Ruddock S., Ritchie C., Field R.	
<b>Experimental factorial design for the study of some variables in roller bottles cell culture</b>	641-643
Rodríguez E.N., Pérez M., Ordaz Y., Casanova P.R.,	

Martinez L., Herrera N.

**Evaluation of RollerCell system for high scale production of biopharmaceuticals** 645-647

Rodríguez E.N., Pérez M., Ordaz Y., Casanova P.R.,  
Martinez L., Herrera N.

**Strategies for the process development of monoclonal antibodies for therapeutic use** 649-653

De Mattei C., De Bernardi N., Gaspari F., Castiglioni S.,  
Orlandi A., Muru E., Cavenaghi C., Nolli M.

**Optimisation of Pei-mediated transient expression in Chinese hamster ovary cells** 655-657

Tait A., Hoare M., Birch J., Gailbraith, D. J., Hines, M.,  
Brown J.C., James D.C.

**Development of fed-batch process producing monoclonal antibodies using in-house media** 659-661

Huang Y.M., Huynh T., Ly L., Noe W., Chang D.Y.H.

**Production of an anti  $\beta 2$  integrin monoclonal antibody by a hybridoma cell line grown in a 2 liter bioreactor** 663-666

Kallel H., Bellila A., Fathallah D.M.

**Economic evaluation of disposables vs stainless steel within a modular pilot plant facility – a comparative analysis** 667-670

Monge M., Sinclair A.

**cGMP manufacturing of a fusion protein in mammalian cells using a large scale acoustic perfusion system** 671-674

Crowley J., Schlukebir C., Dijkstal M., Hoeksma S., Olthof E., Hußmann S., Esser S., Herrmann A., Coco  
Martin J.M., Hof R.

**Influence of culture parameters on viability in perfusion process** 675-677

Dalm M.C.F., Cuijten S.M.R., Van Grunsven W.M.J.,  
Oudshoorn A., Tramper J., Martens D.E.

**Use of hydrocyclone as an efficient tool for cell retention in perfusion cultures** 679-682

Elsayed E.A., Piehl G-W., Nothnagel J. Medronho R.A.,  
Deckwer W-D., Wagner R.

**Effect of different variables on the long-term spinfilter clogging during pilot-scale animal cell perfusion runs** 683-685

Figueredo A., Navarrete J., Vitón P., Martínez E., Castro A., Chico E.

**Integrating acoustic perfusion in mammalian cell culture: temperature control** 687- 691

Keijzer T., Trampler F., Oudshoorn A., Berg v/d H.

**Flexible fed-batch process control of animal cells** 693- 695

Frahm B., Pörtner R.

**Development of a fed-batch strategy for the production of NS0-derived humanised MAb in protein free medium** 697- 700

Ojito Magaz, E., Arias M.A., Chico Veliz E.

**Transfection to manufacturing: reducing timelines for high yielding GS-CHO processes** 701-704

Rendall M., Maxwell A., Tatham D., Khan P., Gay R.D., Kallmeier R.C., Wayte J.R.T., Racher A.J.

**Optimization of a fed-batch process producing humanized antibodies** 705-709

Sauer P.

**Optimized feeding strategy for NS0 cells** 711-714

Walowitz J., Tescione L., Paul, W., Jayme D., Gorfien S.

**Comparison of complementary interactions between synthetic ligands and t-PA by HPMDC** 715-717

Tappe A., Kretzmer G., Kasper C., Scheper T., Vlach E.G., Tennikova T.B., Platonova G.A.

**Effect of nutrient supplementation on the biological quality of t-PA produced by CHO cells on serum-free medium** 719- 722

Altamirano C., Illanes A., Canessa R., Becerra S., Berríos J.

**Modulation of the glycosylation repertoire of a recombinant human EPO expressing model cell line under different culture conditions** 723-725

Duvar S., Berlin J., Ziehr H., Conradt H.S.

**Physicochemical estimation of rhEPO potency produced in suspension culture** 727- 729

Etcheverrigaray M., Amadeo G.I., Didier C., Pereira Bacci D.A., Cavatorta F.A., Kratje R.B.

**Post-translational modification of recombinant human GM-CSF expressed by stable-transfected CHO cells**

<b>under different culture conditions</b>	731-734
Forno Á.G., Etcheverrigaray M., Nimtz M., Kratje R.B.	
<b>Softmix, a new scaleable mixing system for the cultivation of sensitive cells on microcarrier under protein-free conditions</b>	735-738
Naschberger S., Rütten K., Müller D., Katinger H.	
<b>Establishment of fermentation process for hrepo using stirred tank fermenters in perfusion mode using a commercial protein-free culture medium</b>	739-742
Bouzó L., Ojito E., Arias M.A., Suarez J., Chico E., Alvarez A., Chea M., Alvarez I., Diaz C., Valiente O.	
<b>Continuous GMP production in hollow fibre bioreactors-a viable alternative for the production of low volume biopharmaceuticals</b>	743-745
Brecht R., Bushnaq-Josting H., Zietze S., Nuck R., Kloth C., Schwadtke A., Obermayer N., Marx U., Koch S.	
<b>Optimizing cultivation strategies in different scales of hollow fiber bioreactors</b>	747-750
Rodríguez G., Arias M.A., Suárez J., Chea M., Bouzó L., Cuervo R., Álvarez, Chico E.	
<b>Increasing antibody production from hollow fiber systems</b>	751-753
Gramer M.J.	
<b>Production of poliovirus, rubella virus, measles virus and recombinant adenovirus in protein-free media</b>	755-759
Card C., Smith T., Hunsaker B., Barnett B.	
<b>Serum-free production of poliovirus: a comparative study using microcarriers, roller bottles and stationary cell culture</b>	761-765
Card C., Smith T., Hunsaker B., Barnett B.	
<b>Glutamine-free media for vaccine production processes</b>	767-770
Genzel Y., Alt R., Reichl U.	
<b>Serum free cultivation of primary chicken embryo fibroblasts in microcarrier systems for vaccine production</b>	771-774
Hundt B., Schänzler A., Reichl U.	
<b>Design of an animal protein free medium to sustain Vero cells growth in a stirred tank bioreactor</b>	775-778

Kallel H., Rourou S., Van Der ark A., Thalen M., Van Der Velden De Groot T.

**Use of on-line our measurements to monitor and improve insect cell cultures for recombinant protein production**

779-781

Lecina M., Casablanco A., Soley A., Vela, C., Espuña, E., de Gracia, J., Cairó J.J., Gòdia F.

**Production of live influenza vaccine in MDCK cell line**

783-785

Mazurkova N., Nechaeva E., Ryabicheva T., Varaksin N., Sen'kina T., Sviridenko T., Kolokoltsova S., Markushin S., Gendon Vu.

**Elaboration of the microencapsulated forms of the viral vaccines**

787-789

Nechaeva E., Varaksin N., Ryabicheva T., Getmanova T., Mazurkova N., Senkina T., Kolokoltsova T.

**HTS-based development of high-producing CHO cell lines**

791-792

Sautter K., Fieder J., Otto R., Enenkel B.

Author Index

793-800

Subject Index

801-813

## MEETING COMMITTEES

### Organising Committee

Francesc Gòdia (Chairman)	UAB, Barcelona, Spain
Oscar Cerezales	Grupo Pacífico, Barcelona, Spain
Elisabeth Fraune (Trade Exhibition and Sponsorship)	B. Braun Biotech, Melsungen, Germany
Fiona Godsmán (Trade Exhibition and Sponsorship)	Q-One Biotech, Glasgow, UK
Christophe Losberger (Web site)	Serono, Geneva, Switzerland
Carmen Vela	Ingenasa, Madrid, Spain

### Scientific Committee

Francesc Gòdia	U.A.B., Barcelona, Spain
Christel Fenge	AstraZeneca, Stockholm, Sweden
Martin Fussenegger	ETH, Zurich
Hansjörg Hauser	GBF, Braunschweig, Germany
Eleftherios T. Papoutsakis	Northwestern U., Evanston, USA
José Vicente Castell	Hospital La Fe, Valencia, Spain
Carmen Vela	INGENASA, Madrid, Spain
Bernd Schröder	MainGen, Frankfurt, Germany

### Poster Award Committee

Nathalie Chatzissavidou	Biovitrum, Stockholm, Sweden
Paula Marques Alves	IBET, Oeiras, Portugal

## **ESACT Executive Committee**

Otto-Wilhelm Merten, Chairman	AFM-Généthon, France
Alain Bernard, Secretary	Serono, Switzerland
Elisabeth Lindner-Olsson, Treasurer	Metcon Medicin, Sweden
Florian Wurm	EPFL, Switzerland
Manuel Carrondo	IBET, Portugal
Martin Fussenegger	ETH-Zürich, Switzerland
Stefanos Grammatikos	Boehringer-Ingelheim, Germany
Francesc Gòdia, Meeting Secretary	UAB, Spain
Rodney Smith	UK



## **SPONSORS**

ESACT and the Organising Committee wish to thank the following companies for their generous support:

### **MAIN SPONSORS**

Amersham Biosciences  
Boehringer Ingelheim GmbH  
Invitrogen  
JRH Europe  
Q-One Biotech  
Sigma-Aldrich GmbH

### **ADDITIONAL SPONSORS**

Abgenix  
AppliSens  
AstraZeneca  
Aventis Pasteur  
B. Braun Biotech International GmbH  
Beckman Coulter  
BioInvent  
BioProcess International  
BioReliance  
Biovitrum AB  
Chiron Behring GmbH  
Genentech  
GlaxoSmithKline Biologicals  
Guava Technologies, INC  
HyClone / Perbio  
Innovatis AG  
Intervet International bv  
Inveresk Research  
Kendro Laboratory Products  
NUNC  
Pall  
Roche Diagnostics GmbH / Hoffmann-La Roche  
Rütten Engineering  
Serologicals Corporation  
Serono International SA  
Wyeth Biopharma

## COMPANIES PARTICIPATING IN THE TRADE EXHIBITION

Aber Instruments Ltd	Innovatis AG
Amersham Biosciences	Inveresk Research
AMT	Invitrogen
Applikon. BV	JM Separations BV
AppliSens	JRH Europe
Areta International srl	Kendro Laboratory Products
B. Braun Biotech International GmbH	Kuhner AG
Beckman Coulter	Microsafe
Becton Dickinson	New Brunswick Scientific (UK) Ltd
Biogen Científica s.l. - Infors AG	NewLab BioQuality AG
BioInvent	NUNC
BioProcess International	PAA Laboratories GmbH
BioReliance	Pall
BioVest International	Papaspyrou biotechnologie GmbH
BioWest Laboratoire	Q-One Biotech
Boehringer Ingelheim GmbH	Quest International
Broadley Technologies Ltd	Rütten Engineering
Cambrex	Sensorix
Cayla / Invivogen	Serologicals Corporation
Cell Culture Technologies	Sigma-Aldrich GmbH
Cellon SA	Stedim S.A.
Cesco Bioengineering	Steris Ltd.
Charter Medical	Terracell International
ChemoMetec A/S	Texcell
Covance	The Automation Partnership Ltd
ECACC	Thermo Trace
Elnor Ibérica, S.A.	The Williamsburg BioProcessing F.
Genetic Engineering News	Wave Biotech AG
Greiner Bio-One GmbH	
Guava Technologies, INC	
HyClone / Perbio	

## **Introduction: Animal Cell Technology Meets Genomics**

Every two years, the Meeting of the European Society of Animal Cell Technology gathers the highest number of scientists and engineers from academia and industry in the field of Animal Cell Technology, and offers a unique opportunity for a comprehensive overview of its state-of-the-art.

The 18<sup>th</sup> ESACT meeting was celebrated in Granada (Spain) in May 2003, and was entitled “Animal Cell Technology Meets Genomics”, in order to reflect that the emerging technologies in the area of genomics, proteomics and other “-omics”-type disciplines will provide key technological assets to increase knowledge and open new horizons in animal cell technology. During the meeting a variety of top-class emerging technologies were presented together with the latest advances in more mature industrial areas. The meeting was opened by a first session devoted to the understanding of basic cellular mechanisms, and four sessions focused on applied aspects of animal cell technology: Cell-based therapies and gene-based therapies, target discovery and biopharmaceuticals. The Granada Meeting has also seen a special focus on forefront industrial case studies. The spirit and scientific excellence of the 18<sup>th</sup> ESACT meeting is now reflected in different chapters of the book.

Feedback confirmed that the participants highly enjoyed the scientific quality of the meeting as much as the parallel exhibition, the social programme and particularly the city of Granada, its nice atmosphere and the splendid and bright Spring days we all had. Once again, the Granada meeting was confirming the solid evolution of the ESACT meeting series, and the continued attention that it receives from the scientific and industrial communities involved in Animal Cell Technology.

This book presents, in the form of short papers, a high number of the contributions to the meeting, and has been prepared with the aim to provide a relevant reference of the current research efforts in Animal Cell Technology.

Francesc Gòdia and Martin Fussenegger  
Editors

## **Acknowledgements**

This book has been possible as a consequence on the realization of a very stimulating meeting in Granada, and the preparation of the different contributions by their authors. The Editors of the book would like to acknowledge all of them for their effort, first by preparing their poster or oral presentations to the meeting, second for the preparation of their contribution to this book.

We would like to acknowledge very sincerely all the people who contributed to the success of the Granada meeting: session chairpersons, delegates, exhibitors, sponsors, technicians from the Palacio de Congresos, support team from Grupo Pacífico, and especially all the members of the ESACT Executive Committee, and the Granada Meeting Committees: Scientific, Organizing and Poster Award. Thank you very much to all of them.

Finally, we would like to thank all the delegates in Granada meeting, 700, for their active participation, their interest in the meeting, and positive feed-back. It was the combination of all individuals that made the atmosphere of the meeting unique, together with the fabulous and rich background of the city of Granada.

Francesc Gòdia and Martin Fussenegger  
Editors

## List of Participants

BADARULHISAM ABDUL-RAHMAN, Inno Biologics Sdn Bhd,  
Prime Minister's Department, Level 2, Perdana Putra Building 62502  
Putrajaya, Malaysia, Phone: +60388881810, Fax: +60388883801, E-mail:  
badrul\_abdulrahman@hotmail.com

GITA ABRAHAM, Interpharm, Industrial Park, Kinyat Weizman,  
76110 Mess-Ziona, Israel, Phone: +97289382480, Fax: +97289301013,  
E-mail: gita.abraham@serono.com

SPIROS AGATHOS, Unit Of Bioengineering. Univ. Of Louvain,  
Place Croix du Sud 2/19, B-1348 Louvain-La-Neuve, Belgium, Phone:  
+3210473644, Fax: +3210473062, E-mail: agathos@gebi.ucl.ac.be

VIVIANA AGUS, Axxam S.R.L., Via Olgettina, 58, 10132 Milano,  
Italy, Phone: +39022105651, Fax: +390239786102, E-mail:  
viviana.agus.va@axxam.com

YONG-HO AHN, Lg Life Science / R&D Park, 104-1 Moonji-dong,  
Yusung-gu, 305-380 Daejeon, Korea, South, Phone: 82-42-866-2167,  
Fax: 82-42-862-0331, E-mail: yhahnd@lgls.co.kr

BERT AL, Sanquin (Clb), Plesmanlaan 125, 1066 CX Amsterdam,  
The Netherlands, Phone: +31205123658, Fax: +31205123658, E-mail:  
alconijn@hetnet.nl

TERI ALDRICH, Amgen, Inc., 51, University St., 98101 Seattle,  
USA, Phone: +2062654660, Fax: +2066217977, E-mail:  
ateri@amgen.com

DANIEL ALETE, The University Of Kent, Research School  
of Biosciences, Protein Science Group CT2 7NZ Canterbury, UK, Phone:  
+441227764000, E-mail: da7@ukc.ac.uk

CATHERINE ALLIOUX, Biosepra Sa, Division of CIPHERGEN,  
48 Avenue des Genottes 95800 Cergy Saint Christophe, France, Phone:  
+33134207824, Fax: +33134207878, E-mail: callioux@ciphergen.com

DAN ALLISON, Sigma-Aldrich, Eschenstr, 5, 82024 Taufkirchen,  
Germany, Phone: +49 896513 1901, Fax: +49 896513 1919, E-mail:  
HHellwig@europe.sial.com

CLAUDIA ALTAMIRANO, Universidad Catolica Valparaiso,  
Avenida Brasil 2147, Valparaiso, Chile, Phone: +5632273755, Fax:  
+5632273803, E-mail: claudia.altamirano@ucv.cl

PAULA MARQUES ALVES, Ibet, Apartado 12, 2781-901 Oeiras,  
Portugal, Phone: +351214469421, Fax: +351214421161, E-mail:  
marques@itqb.unl.pt

HANS JUUL ANDERSEN, Statens Serum Institut, Artillerivej 5,  
2300 Copenhagen, Denmark, Phone: +4532683645, E-mail: hju@ssi.dk

DANA ANDERSEN, Genentech, Inc, One DNA Way Ms-32, South  
San Francisco 94080 California, USA, Phone: +16502254443, E-mail:  
andersen@gene.com

DAN ANDERSSON, Bioinvent International Ab, Soelvegatan 41,  
22370 Lund, Sweden, Phone: +46 46 2868561, Fax: +46 46 2110806, E-  
mail: petra.klingberg.persson@bioinvent.com

CARLO ANDRETTA, Biospectra Ag, ZUERCHERSTRASSE 137,  
CH8952 ZURICH - SCHLIEREN, Switzerland, Phone: +4117556700,  
Fax: +4117556729, E-mail: andretta@biospectra.ch

WILLIAM ROBERT ARATHOON, Genentech, Inc., 1 DNA Way,  
MS 87, 94080 South San Francisco (CA), USA, E-mail: ra@gene.com

PAUL ARMSTRONG, Serologicals Corporation, The Magdalene  
Centre, Oxford Science Park OX4 4GA Oxford, UK, Phone:  
+441865784646, Fax: +441865784648, E-mail:  
jnicacio@serologicals.com

MURIEL AUDIT, Genethon, 1 bis rue de l'Internationale, 91002 Evry,  
France, Phone: +3369472945, Fax: +3360778698, E-mail:  
audit@genethon.fr

JOHN AUNINS, Merck, Po Box 4 WP17-201, 19486 West Point, PA,  
USA, Phone: +1 215 652 5577, Fax: +1 215 993 4880, E-mail:  
john\_aunins@merck.com

ANNA MAIJA AUTERE, National Agency For Medicines,  
Mannerheimintie 166, P.O.Box 55 FIN-00301 Helsinki, Finland, Phone:  
+358947334279, Fax: +358947334355, E-mail:  
anna-maija.autere@nam.fi

TORBEN L. BACHMANN, Novo Nordisk A/S, Novo Allé 3BM1.03,  
2880 Bagsvaerd, Denmark, Phone: +45 44426652, Fax: +4544421244,  
E-mail: tol@novonordisk.com

GIANNI BAER, Serono, Zone Industrielle B, 1809 Fenil-Sur-Corsier,  
Switzerland, Phone: +41219232000, Fax: +41219232013, E-mail:  
rachel.zohar@serono.com

KEVIN BAILEY, Regeneron Pharmaceuticals, Inc, 777 Old Saw Mill  
River Road, Tarrytown 07452 NY, USA, Phone: +19143457529, Fax:  
+19143457685, E-mail: kevin.bailey@regeneron.com

ANDREAS BALZER, Novartis - Pharma Ltd., WKL - 681.1.42,  
CH-4002 Basel, Switzerland, Phone: +41616966064, Fax: +41616963373,  
E-mail: andreas.balzer@pharma.novartis.com

YVES BARBIER, Texcell/Institut Pasteur, 25-28 RUE DU  
DOCTEUR ROUX, 75724 Paris cedex 15, France, Phone: +33 1 45 68 84  
35, Fax: +33 1 45 68 88 59, E-mail: ybarbier@pasteur.fr

SARAH BARLOW, Steris, Steris house, Jays Close, RG22 4AX  
Viables, Basingstoke, UK, Phone: +44 1256 840400, Fax: +44 1256  
866502, E-mail: sarah\_barlow@steris.com

LOUISE BARNES, Universtity Of Manchester, School of Biological  
Sciences, Stopford Bldg. Oxford Rd. M13 9PT Manchester, UK, Phone:  
+441612755101, Fax: +441612755082, E-mail:  
louise.m.barnes@man.ac.uk

DENIS BARRAL, Merial, 254 Avenue Marcel Merieux, 69007 Lyon,  
France, Phone: +33472723000, Fax: +33472725545, E-mail:  
agnes.simon@merial.com

YVES BARRANDON, Epfl - Chuv, Swiss Federal Inst. of Tech.  
Lausanne, Lausanne University Hospital 1015 Lausanne, Switzerland,  
E-mail: nadia.martel@hospv.ch

MARÍA DE LOS MILAGROS BASSANI MOLINAS, German  
Research Centre For Biotechnology, Mascheroder Weg 1, 38124  
Braunschweig, Germany, Phone: +495316181742, Fax: +495316181488,  
E-mail: mmb@gbf.de

CLEMENT BASSENS, Universite Libre De Bruxelles, 50, Av. F.D.  
Roosevelt, B-1050 Brussels, Belgium, Phone: +32 2 6503229,  
Fax: +3226503230, E-mail: biocelan@ulb.ac.be

THIERRY BATTLE, Serono Pharmaceutical Research Inst.,  
14 Chemin des Aulx, 1228 Plan-Les-Quates, Switzerland, Phone:  
+41227069644, E-mail: thierry.battle@serono.com

KATHRIN BAUMEISTER, Aventis Pharma Germany, Industriepark  
Hoechst, Building h777 65926 Frankfurt, Germany, Phone:  
+496930544966, E-mail: kathrin.baumeister@aventis.com

BECKMAN 1, Beckman Coulter, Europark Fichtenhain B13, 47807  
Krefeld, Germany, Phone: +49 2151 333 789, Fax: +49 2151 333 639,  
E-mail: jstucki@beckman.com

CHRISTIANE BEER, Gesellschaft Für Biotech. Forschung,  
Mascheroder Weg 1, D-38124 Braunschweig, Germany, Phone: +49 531  
6181432, Fax: +49 531 6181262, E-mail: chb@gbf.de

LAURENT BELLANGER, C.E.A. / D.S.V. / Sbtn, CEA / DSV /  
SBTN BP 17171, 30207 Bagnols- Sur- Ceze, France, Phone:  
+33466796763, Fax: +33466791905, E-mail: laurent.bellanger@cea.fr

ANDRE JOAO BENGALA, Ibet, Apartado 12, 2781-901 Oeiras,  
Portugal, Phone: +351214469424, Fax: +351214421161, E-mail:  
marques@itqb.unl.pt

SYLVIO BENGIO, Biosepra Sa, Division of CIPHERGEN, 48 Avenue  
des Genottes 95800 Cergy Saint Christophe, France, Phone:  
+33134207824, Fax: +33134207878, E-mail: sbengio@ciphergen.com

NISSIM BENVENISTY, The Hebrew Univ. Of Jerusalem, Herbert  
Cohn Chair in Cancer Research, Givat-Ram 91904 Jerusalem, Israel,  
Phone: +97226586774, Fax: +97226586975, E-mail:  
nissimb@mail.ls.huji.ac.il



MAGALI BERBEROF, Glaxosmithkline, Rue de l'Institut 89, 1330 Rixensart, Belgium, Phone: +3226567716, Fax: +3226569013, E-mail: magali.berberof@gsk.com

ALAIN BERNARD, Laboratoires Serono S.A., Route de Fenil ZIB, 1809 Fenil-sur-Corsier, Switzerland, Phone: +41 21 9232357, Fax: +41219232013, E-mail: Alain.Bernard@serono.com

SUZANNE BERRY, Trends In Biotechnology, Elsevier Science, 84 Theobald's Road, Holbrun WC1X 8RR London, UK, Phone: +442076114182, Fax: +442076114470, E-mail: suzanne.berry@elsevier.com

OLIVIER BERTEAU, Biogen Cientifica, Bejar, 36, 28028 Madrid, Spain, Phone: +34 (91) 361 10 27, Fax: +34 (91) 361 08 98, E-mail: rtrujillo@biogencientifica.com

MARTIN BERTSCHINGER, Epfl, FSB-ISP-LBTC, 1015 Lausanne, Switzerland, Phone: +41216936152, Fax: +41216936140, E-mail: martin.bertschinger@epfl.ch

MICHAEL BETENBAUGH, Johns Hopkins University, Dept. of Chemical and Biomolecular Eng., 21218 Baltimore (MD), USA, Phone: +14105165461, E-mail: beten@jhu.edu

ALLISON BIANCHI, Amgen, Inc., 51 University St, 98101 Seattle, USA, Phone: +2062654662, Fax: +2066247496, E-mail: bianchia@amgen.com

RICHARD BIENER, Bayer Technology Services, BTS-PT-PD-PA, Building E41 51368 Leverkusen, Germany, Phone: +492143071850, Fax: +492143062677, E-mail: richard.biener\_rb@bayertechnology.com

DAVID BIRCH, Covance, 7 Roxborough way, Maidenhead SL6 3UD Berkshire, UK, Phone: +44 1628 548000, Fax: +44 1628 826706, E-mail: lesley.smith@covance.com

RASMUS BJERRE-NIELSEN, Technical University Of Denmark, Brogaardsvej 137 1TV, 2820 Gentofte, Denmark, Phone: +4544432312, E-mail: rabn@biocentrum.dtu.dk

HENRI BLACHERE, 4 Rue Mareschal, 34000 Montpellier, France,  
Phone: +33 467 925614, Fax: +33 467 920599, E-mail:  
htblachere@aol.com

NICOLE BLECKWENN, National Institutes Of Health, 6 Center Dr.  
MSC 2715 Bldg 6, Rm B1-33 20892 Bethesda, MD, USA, Phone: +1 301  
4022981, Fax: +1 301 4515911, E-mail: nb115q@nih.gov

RACHEL BLOGG, Sensorix, Technoparkstrasse 1, 8005 Zurich,  
Switzerland, Phone: +32 9 220 3373, Fax: +32 9 220 3379, E-mail:  
susa.volker@sensorix.com

GERALD BLUEML, Amersham Biosciences, Bjorkgatan 30, 75182  
Uppsala, Sweden, Phone: +46 18 612 0505, Fax: +46 18 10 1403, E-mail:  
gerald.blueml@eu.amershambiosciences.com

ERNST BOEHM, Baxter Bioscience, Molecular Cell Biology,  
Industriestrasse 72 A-1221 Vienna, Austria, Phone: +43 1 201003687,  
Fax: +43 1 201005040, E-mail: ernst\_boehm@baxter.com

ELISABETH BOHLEN, Bioengineering Ag, Sagerainstrasse 9, 8636  
Wald, Switzerland, Phone: +41552568111, Fax: +41552568256, E-mail:  
n.watanabe@bioengineering.ch

HERMANN BOHNENKAMP, FORSCHUNGSZENTRUM JÜLICH  
GmbH, Leo-Brandt-Strasse 1, 52428 Jülich, Germany, Phone: +49 2461  
612254, Fax: +49 2461 613870, E-mail: h.bohenkamp@fz-juelich.de

STHEN BOISEN, Chemometec, Gydevang 43, 3450 Allerod,  
Denmark, Phone: +45 4813 1020, Fax: +45 481 31021, E-mail:  
sb@chemometec.dk

MARIELA BOLLATI FOGOLIN, Gbf - German Research C. For  
Biotech., Experimental Immunology, Mascheroder Weg 1 D-38124  
Braunschweig, Germany, Phone: +49 531 6181487, E-mail: mrb@gbf.de

GERT BOLT, Novo Nordisk, Novol Allé, 2880 Bagsvaerd, Denmark,  
Phone: +4544436654, E-mail: bolt@novonordisk.com

BRYAN BOLTON, Eccac, CAMR, Salisbury SP4 0JG Wiltshire, UK,  
Phone: +44 1980 612773, Fax: +44 1980 611315, E-mail:  
Lisa.Reynolds@camr.org.uk

*List of Participants*

xxxv

JENNIFER BOND, Chemical Engineering, Imperial College, South Kensington, SW7 2BY London, UK, Phone: +442075895111, E-mail: jennifer.bond@imperial.ac.uk

JOHN BONHAM CARTER, Adaptive Biosystems, 248 Toddington Road, LU4 9UR Luton, UK, Phone: +441582597676, Fax: +441582581495, E-mail: cheryl.pond@adaptive.co.uk

NICOLE BORTH, Institute For Applied Microbiology, Muthgasse 18, 1190 Vienna, Austria, Phone: +431360066232, Fax: +4313697615, E-mail: nicole.borth@boku.ac.at

HELLA BOSTEELS, Glaxosmithkline, South Eden Park Road, BR3 3BS Beckenham, UK, Phone: +4402086396277, Fax: +4402086396149, E-mail: hella.s.bosteels@gsk.com

JEAN-FRANÇOIS BOUQUET, Aventis Pasteur, 1541 Avenue Marcel Merieux - T1, 69280 Marcy l'Etoile, France, Phone: +33437373533, Fax: +33437379436

ETIENNE BOUTRY, Aventis Pasteur, 1541 Avenue Marcel Merieux, 69280 Marcy L'Etoile, France, Phone: +33437373498, Fax: +33437379436, E-mail: etienne.boutry@aventis.com

THIERRY BOVY, Cambrex, Parc Industriel de Petit Rechain, 4800 Verviers, Belgium, Phone: +32 87321 611, Fax: +32 87351 967, E-mail: roel.gordijn@cambrex.com

DAVID BRADY, Biogen, 5 Roxborough Way, Foundation Park, SL6 3UD Maidenhead, Berkshire, UK, Phone: +44 1628 501075, Fax: +441628 501010, E-mail: dave\_brady@biogen.com

STEFAN BRANTSCHEN, Berna Biotech, Ltd, Rehhagstrasse 79, 3018 Bern, Switzerland, Phone: +41319806378, Fax: +41319806785, E-mail: stefan.brantschen@bernabiotech.com

RENE BRECHT, Probiogen Ag, Goethestr 54, 13086 Berlin, Germany, Phone: +49309240060, Fax: +493092400619, E-mail: rene.brecht@probiogen.de

HENNER BRETTSCHEIDER, Biowest Laboratoire, Rue de la Caille, 49340 Nuaille, France, Phone: +33 241 464242, Fax: +33 241 463890, E-mail: h.Brettschneider@biowest.net

SYLVIE BRETTSCHEIDER, Biowest, France, E-mail: h.brettschneider@biowest.net

HERVÉ BROLY, Sorebio, Site Montesquieu, 1 avenue Jacques Monod 33650 Martillac, France, Phone: +330557960968, Fax: +330556647766, E-mail: herve.broly@serono.com

WILLIAM BRONDYK, Genzyme Corporation, One Mountain Road, 01701-9322 FRAMINGHAM, USA, Phone: +15082712847, Fax: +15088729080, E-mail: william.brondyk@genzyme.com

PETER BROWN, Biotechnology Solutions, 20 Woodcrest Dr., Orinda 94563 California, USA, Phone: +19252541601, Fax: +19252546584, E-mail: pwbrown@netwiz.net

MICHAEL BROWN, Kellogg Company Gb Ltd, Park Road, M328RA Manchester, UK, Phone: +01618693843, Fax: +01618693239, E-mail: michael.brown@kellogg.com

THOMAS BRÜCKERHOFF, Universität Hannover, Inst. für Technische Chemie, Callinstrasse 3 D-30167 Hannover, Germany, Phone: +49 511 7622381, Fax: +49 511 7623004, E-mail: brueckerhoff@iftc.uni-hannover.de

BARRY BUCKLAND, Merck & Co., Inc., PO Box 4 WP17-201, 19486 West Point, USA, Phone: +12156523612, Fax: +12159932238, E-mail: barry\_buckland@merck.com

HEINO BUENTEMEYER, University Of Bielefeld, Institute of Cell Culture Technology, 33594 Bielefeld, Germany, Phone: +495211066317, Fax: +495211066023, E-mail: hb@zellkult.techfak.uni-bielefeld.de

HERMANN BUJARD, Universitaet Heidelberg, Zentrum fuer Molekulare Biologie (ZMBH), Im Neuenheimer Feld 282 69120 Heidelberg, Germany, Phone: +496221548214, Fax: +496221545892, E-mail: h.bujard@zmbh.uni-heidelberg.de

SANDY BULLOCH, Gibco Invitrogen Corp., 3175 Staley Road,  
14072 Grand Island, USA, Phone: +17167743104, Fax: +17167746996,  
E-mail: jennifer.walowitz@invitrogen.com

MONIKA BURG, Cardion Ag, Max Planck Str 15a, 40699 Erkrath,  
Germany, Phone: +492112056516, Fax: +492112056598, E-mail:  
burg@cardion.de

CHRISTA BURGER, Merck Kgaa, Frankfurter Str. 250, 64271  
Darmstadt, Germany, Phone: +496151726032, Fax: +496151723447,  
E-mail: christa.burger@merck.de

ARNE BURZLAFF, Universität Hannover, Inst. für Technische  
Chemie, Callinstrasse 3 D-30167 Hannover, Germany, Phone: +49 511  
7622966, Fax: +49 511 7623004, E-mail: burzlaff@iftc.uni-hannover.de

HIKMAT BUSHNAQ-JOSTING, Probiogen Ag, Goethestr 54, 13086  
Berlin, Germany, Phone: +49309240060, Fax: +493092400660, E-mail:  
hikmat.bushnaq-josting@probiogen.de

MIKE BUTLER, University Of Manitoba, Department of  
Microbiology, 118 Buller Bldg R3T 2N2` Manitoba, Winnipeg, Canada,  
Phone: +12044746574, Fax: +12044747618, E-mail:  
butler@cc.umanitoba.ca

BRIAN CAINE, Bioprocess International, One Research Dr, Suite  
400 A 1581-0770 Westborough, MA, USA, Phone: +1508 614 1443, Fax:  
+1508 616 0476, E-mail: bcaine@bioprocessintl.com

MICHAEL CAIRNS, National Diagnostics Centre, National  
University of Ireland, Galway Galway, Ireland, Phone: +35391512405,  
E-mail: michael.cairns@nuigalway.ie

JORDI J. CAIRO, Universitat De Barcelona, BELLATERRA, 08193  
CERDANYOLA, Spain, Phone: +34 (93) 5812692, Fax: +34 (93)  
5812013, E-mail: jordijoan.cairo@uab.es

KARIN CALLES, Karo Bio Ab, Novum, Hasolvagen 7, 141 57  
Huddinge, Sweden, Phone: +4686086102, E-mail:  
karin.calles@karobio.se

PIERRE CALOZ, Abgenix, Inc., 6701 Kaiser Drive, Fremont 94555  
California, USA, Phone: +15102846869, Fax: +15107905106, E-mail:  
pierre.caloz@abgenix.com

SUSAN CAMERON, Invitrogen, 3 Fountain Drive Inchinnan  
Business Park, PA4 9RF Paisley, UK, Phone: +44 141 814 6108, Fax:  
+44 141 814 6287, E-mail: frainj@lifetech.com

JOSEPH CAMIRE, Hyclone Laboratoires, 1725 S. Hyclone Rd.,  
84321 Logan, USA, Phone: +14357920169, Fax: +14357920253, E-mail:  
joseph.camire@perbio.com

RAQUEL CAMPOS, Pall Lifesciences, Europa House, Havant Street  
PO13PD Portsmouth, UK, Phone: +442392303303, Fax:  
+442392302506, E-mail: ruth\_batson@europe.pall.com

MATTHEW CAPLE, Sigma-Aldrich, Eschenstr, 5, 82024  
Taufkirchen, Germany, Phone: +49 896513 1901, Fax: +49 896513 1919,  
E-mail: HHellwig@europe.sial.com

CORY CARD, Hyclone Uk Ltd, Unit 9 Atley Way, North Nelson  
Industrial Estate NE23 1WA Cramlington, Northumberland, UK, Phone:  
+44 141 583 2142, Fax: +44 141 583 2136, E-mail:  
Jarlath.Keating@perbio.com

NATALIE CARRICK, The Automation Partnership Ltd, York way,  
Royston, SG8 5WY Hertfordshire, UK, Phone: +44 1763 227336, Fax:  
+44 1763 227201, E-mail: slp@autoprt.co.uk

MANUEL CARRONDO, Ibet, Apartado 12, 2781-901 Oeiras,  
Portugal, Phone: +351 21 4427787, Fax: +351 21 4421161, E-mail:  
mjtc@itqb.unl.pt

KEITH CARSON, Williamsburg Bioprocessing Foundation, PO Box  
1229, 23451 Virginia Beach, USA, Phone: +17574238823, Fax:  
+17574232065, E-mail: kcarson@wilbio.com

ANA VERONICA CARVALHAL, Ibet, Apartado 12, 2781-901  
Oeiras, Portugal, Phone: +351214469424, Fax: +351214421161, E-mail:  
uva@itqb.unl.pt

JOHN CARVELL, Aber Instruments, Science Park, Aberystwyth  
SY23 3AH, UK, Phone: +44 1970 636300, Fax: +44 1970 615455,  
E-mail: jc@aber-instruments.co.uk

JOSÉ VICENTE CASTELL, Hospital Univ. La Fe, U. Hepatología  
Experimental, Invest., Avda. de Campanar, 21 46009 Valencia, Spain,  
Phone: +34 (961) 973048, Fax: +34 (961) 973018, E-mail:  
jose.castell@uv.es

LEDA CASTILHO, Federal University Of Rio De Janeiro,  
PEQ/COPPE/UFRJ, Centro de Tecnologia, Sala G-116, Ilha do Fundao  
21945-970 Rio de Janeiro, RJ, Brazil, Phone: +55 21 25628336, Fax: +55  
21 25628300, E-mail: leda@ufrj.br

JOSÉ CASTILLO, Glaxosmithkline Biologicals, Rue de L'Institut 89,  
1330 Rixensart, Belgium, Phone: +3226567595, Fax: +3226566159,  
E-mail: christine.wiame@gskbio.be

ADOLFO JOSE CASTILLO VITLLOCH, Center Of Molecular  
Immunology, Calle 216 y 15, Atabey, Playa, 11600 Havana City, Cuba,  
Phone: +5372716867, Fax: +537335049, E-mail: adolfo@ict.cim.sld.cu

LUIGI CAVENAGHI, Areta International, Via Roberto Lepetit, 34,  
21040 Gerenzano (VA), Italy, Phone: +39 0296489264, Fax: +39  
0295489260, E-mail: mlnolli@aretaint.com

AZIZ CAYLI, Boehringer Ingelheim, Birkenorferstrasse 65, D-88397  
Biberach, Germany, Phone: +49 73 51 54 48 01, Fax: +49 73 51 54 51  
31, E-mail: evelyn.schmucker@bc.boehringer-ingelheim.com

KARIN CEBALO, Institute Of Immunology, Rockefellerova 10,  
10000 Zagreb, Croatia, Phone: +38514684500, Fax: +38514684303,  
E-mail: kcebalo@imz.hr

STEVEN CHAMOW, Abgenix, Inc., 6701 Kaiser Drive, M/S 26,  
Fremont 94555 CA, USA, Phone: +15102846619, Fax: +15107905269,  
E-mail: melanie.schneider@abgenix.com

DAVID CHANG, Idec Pharmaceuticals, 11011 Torreyana Rd., 92121  
San Diego, USA, Phone: +18584318500, Fax: +18584318750, E-mail:  
dchang@idecpharm.com

KING-MING CHANG, Cesco Bioengineering, Rm 537, bldg 53, #195, Sec 4, Chung-Hsing Rd. Chutung, Hsin-Chu 310 R.O.C., Taiwan, Phone: +886 3 5910120, Fax: +886 3 5910123, E-mail: drsychang@cescobio.com.tw

CHRISTOPHER CHANG, Cesco Bioengineering, Rm 537, bldg 53, #195, Sec 4, Chung-Hsing Rd. Chutung, Hsin-Chu 310 R.O.C., Taiwan, Phone: +886 3 5910120, Fax: +886 3 5910123, E-mail: drsychang@cescobio.com.tw

CLAUDIO CIRO CHAPARRO, Lobo V Ycia, 1427 Capital Federal, Argentina, Phone: +541145237006, Fax: +541145237012, E-mail: cchaparro@lobov.com.ar

JEAN MARIE CHARPIN, Texcell/Institut Pasteur, 25-28 RUE DU DOCTEUR ROUX, 75724 Paris cedex 15, France, Phone: +33 1 45 68 84 35, Fax: +33 1 45 68 88 59, E-mail: ybarbier@pasteur.fr

NATHALIE CHATZISSAVIDOU, Biovitrum Ab, Lindhagensgatan 133, SE-11276 STOCKHOLM, Sweden, Phone: +4686973038, Fax: +4686972312, E-mail: nathalie.chatzissavidou@biovitrum.com

DOMINIQUE CHEVRIER, Cayla/Invivogen, 5, rue Jean Rodier, 31405 Toulouse, France, Phone: +33562716939, Fax: +33562716930, E-mail: cayla@cayla.com

GISELA CHIANG, Biogen, 14 Cambridge Center, 02142 Cambridge, MA, USA, Phone: +16176793856, Fax: +16176793200, E-mail: gisela\_chiang@biogen.com

ERNESTO CHICO, Center Of Molecular Immunology, Calle 15 y 216, Atabey Playa, P.O. Box 16040 11600 Havana, Cuba, Phone: +5372714335, Fax: +537335049, E-mail: chico@ict.cim.sld.cu

KLAUS CHRISTENSEN, Hoffmann La Roche Ag, Grenzacherstrasse, CH-4070 Basle, Switzerland, Phone: +41 61 6884356, Fax: +41 61 6882438, E-mail: klaus.christensen@roche.com

SOREN CHRISTIENSEN, Lundbeck A/S, Ottiliavej 9, DK2500 Valby, Denmark, Phone: +4536441425, Fax: +4536303747, E-mail: snc@lundbeck.com



JOO-YOUNG CHUNG, Daewoong Co. Ltd., San 84-1, Samgye Ri, Pokok-Myun 449-814 Yong-In, Korea, South, Phone: +82313343200, Fax: +82313227190, E-mail: [jychung@daewoong.co.kr](mailto:jychung@daewoong.co.kr)

JULIA CINO, New Brunswick Scientific, 163 Dixons Hill Road, North Mymms AL9 7JE Hatfield, UK, Phone: +44 1707 275733, Fax: +44 1707 267859, E-mail: [moritz@nbsuk.co.uk](mailto:moritz@nbsuk.co.uk)

THOMAS JAMES CLARK, La Tuilerie, 81630 Montaurausse, France, Phone: +33 5 63335519, Fax: +33 5 63335545, E-mail: [TClark5604@aol.com](mailto:TClark5604@aol.com)

MARTIN CLARKSON, Maxygen, Agern Alle 1, DK-2970 Horsholm, Denmark, Phone: +4570205550, Fax: +4570205530, E-mail: [mpc@maxygen.dk](mailto:mpc@maxygen.dk)

CATHERINE CLEUZIAT, Merial, 254 Avenue Marcel Merieux, 69007 Lyon, France, Phone: +33472723000, Fax: +33472725545, E-mail: [agnes.simon@merial.com](mailto:agnes.simon@merial.com)

WILLIAM CLOSS, Solohill Engineering, 43 Pinehurst Road, West Hartland 06091 CT, USA, Phone: +18606041781, Fax: +18604665908, E-mail: [salesflyer@aol.com](mailto:salesflyer@aol.com)

JOSE COCO MARTIN, Dsm, Zuiderweg 72/2, Groningen 9700, The Netherlands, Phone: +31505222308, Fax: +31505222333, E-mail: [jose.coco-martin@dsm.com](mailto:jose.coco-martin@dsm.com)

HARALD S. CONRADT, Gbf Braunschweig, Planscherider Weg 1, 38124 Braunschweig, Germany, Phone: +491703847564, E-mail: [hco@gbf.de](mailto:hco@gbf.de)

ANTONIO CONTRERAS-GOMEZ, Universidad De Almeria, Carrera de Sacramento, s/n, 04120 La Cañada, Spain, Phone: +34 (950) 015898, Fax: +34 (950) 015484, E-mail: [acontre@ual.es](mailto:acontre@ual.es)

ERIC CORNAVACA, Invitrogen Corporation, 3175 Staley Road, Grand Island NY, USA, Phone: +17167746660, Fax: +17147746998, E-mail: [eric.cornavaca@invitrogen.com](mailto:eric.cornavaca@invitrogen.com)

ANA SOFIA COROADINHA, Ibet, Apartado 12, 2781-901 Oeiras, Portugal, Phone: +351214469424, Fax: +351214421161, E-mail: [avalente@itqb.unl.pt](mailto:avalente@itqb.unl.pt)

VIRNA CORTEZ-RETAMOZO, Vrije Universiteit Brussel, Lab. of Molecular & Cellular Immunology, Gebouw E-8.7, Pleinlaan 2 1050 Brussel, Belgium, Phone: +3223590358, Fax: +3223590359, E-mail: [vcortez@vub.ac.be](mailto:vcortez@vub.ac.be)

MARIA JOAO LEITE COSTA, Instituto Superior Tecnico, Avenida Rovisco Pais, 1049-001 Lisboa, Portugal, Phone: +351218419065, Fax: +351218419062, E-mail: [mjsleite@hotmail.com](mailto:mjsleite@hotmail.com)

JOHN CROWLEY, Dsm Biologics, Zuiderweg 72/2, P.O.Box 454 9700AL Croningen, Netherlands Antilles, Phone: +31505222287, Fax: +31505281330, E-mail: [john.crowley@dsm.com](mailto:john.crowley@dsm.com)

PEDRO CRUZ, Ibet, Apartado 12, 2781-901 OEIRAS, Portugal, Phone: +351214469417, Fax: +351214421161, E-mail: [pcruz@itqb.unl.pt](mailto:pcruz@itqb.unl.pt)

HELDER CRUZ, Ecbio, Lab. 4.11 Edificio IBET/ITQB, Apartado 12 2781-901 OEIRAS, Portugal, Phone: +351214469467, Fax: +351214469364, E-mail: [cruz@itqb.unl.pt](mailto:cruz@itqb.unl.pt)

RENATA CUDNA, University Of Manchester, School of Biological Sciences, Stopford Bldg. Oxford Rd. M13 9PT Manchester, UK, Phone: +441612755101, Fax: +441612755082, E-mail: [renata.e.cudna@stud.man.ac.uk](mailto:renata.e.cudna@stud.man.ac.uk)

ARCHIE CS CULLEN, Jrh Biosciences, 13804 W 107th Street, Lenexa 66215 Kansas, USA, Phone: +1 913 469 5580 x-225, Fax: +1 913 469 5584, E-mail: [Susan.Bridges@jrhbio.com](mailto:Susan.Bridges@jrhbio.com)

ANTONIO CUNHA, Ibet, Apartado, 2781-901 Oeiras, Portugal, Phone: +351214469480, Fax: +351214469390, E-mail: [cunha@itqb.unl.pt](mailto:cunha@itqb.unl.pt)

CLAUDIA CUNHA-BAKEEV, Univ. Of Newcastle Upon Tyne, School of Chemical Eng. & Adv. Materials, Merz Court NE1 7RU Newcastle upon Tyne, UK, Phone: +441912225332, Fax: +441912225292, E-mail: [claudia.cunha-bakeev@ncl.ac.uk](mailto:claudia.cunha-bakeev@ncl.ac.uk)

MARK CUNNINGHAM, Centocor, 145 King of Prussia Road, PA 19087 Radnor, USA, Phone: +16106517567, Fax: +16102408150, E-mail: mcunnin2@centus.jnj.com

BRENDA CUTLER, Hyclone, 925 West 1800 South, 84321 Logan, UT, USA, Phone: +14357534584, Fax: +14357534589, E-mail: brenda.cutler@perbio.com

CISKA DALM, Diosynth Bv, Kloosterstraat 6, 5340 BA Oss, The Netherlands, Phone: +31412663474, Fax: +31412662556, E-mail: ciska.dalm@diosynth.com

THOMAS DANTES, Max-Planck-Inst. For Infection Biology, Campus Charite Mitte, Schumannstrasse 21/22 D-10117 Berlin, Germany, Phone: +493028460259, Fax: +493028460210, E-mail: dantes@mpiib-berlin.mpg.de

PAULA DAVIS, Biowest Laboratoire, Rue de la Caille, 49340 Nuaille, France, Phone: +33 241 464242, Fax: +33 241 463890, E-mail: h.Brettschneider@biowest.net

SABINE DE BEUF, Hyclone Uk Ltd, Unit 9 Atley Way, North Nelson Industrial Estate NE23 1WA Cramlington, Northumberland, UK, Phone: +44 141 583 2142, Fax: +44 141 583 2136, E-mail: Jarlath.Keating@perbio.com

FRANÇOISE DE FORESTA, Glaxo Smith Kline Biologics, 89 Rue de l'Institute, 1330 Rixensart, Belgium, Phone: +3226569947, Fax: +3226569013, E-mail: francoise.de-foresta@gskbio.com

JESUS DE LA FUENTE, Glaxosmithkline, C/ Santiago Grisolia 4, 28760 TRES CANTOS ( MADRID), Spain, Phone: +34918074029, Fax: +34918074062, E-mail: jesus.de.la.fuente@gsk.com

ANA MARIA DE MARTIN BARRY, Puleva Biotech, C/ Purchil 66, 18004 Granada, Spain, Phone: +34958240152, Fax: +34958240160, E-mail: ademartin@puleva.es

GUY DE MARTYNOFF, Bioprotein Technologies, 63-65 Boulevard Massena, 75013 Paris, France, Phone: +33144060616, Fax: +33144067525, E-mail: contact@bioprotein.com

VINCENT DEGOUYS, Amersham Biosciences, Bergrand 230,  
4707AT Roosendaal, The Netherlands, Phone: +31 165 580 622, Fax:  
+31 165 580 601, E-mail:  
vincent.degouys@eu.amserhambiosciences.com

MICHEL DELAFON, Becton Dickinson, Tullastr. 8-12, 69126  
Heidelberg, Germany, Phone: +49 6221 305416, Fax: +49 6221 305407,  
E-mail: Eva\_Miller@Europe.bd.com

MADIHA DEROUAZI, Epfl, FSB-ISP-LBTC, 1015 Lausanne,  
Switzerland, Phone: +41216936152, Fax: +41216936140, E-mail:  
madiha.derouazi@epfl.ch

FRITZ DIENER, Rütten Engineering, Industriestrasse 9, 8712 Stäfa,  
Switzerland, Phone: +41 1928 2930, Fax: +41 1926 2802, E-mail:  
info@rutten.com

PAUL DIERICKX, Institute Of Public Health, Wytzmanstraat, 14,  
B-1050 Brussels, Belgium, Phone: +32 2 642 5107, Fax: +32 2 642 5244,  
E-mail: p.dierickx@ipm.fgou.be

MATT DILLINGHAM, Serologicals Ltd., 4 Fleming Road, Kirkton  
Campus EH54 7BN Livingston, UK, Phone: +441506404000, Fax:  
+441506404001, E-mail: jwilson@serologicals.com

NANNI DIN, Novo Nordisk A/S, Novo Alle 1, Ba, 6B2.83 DK2880  
Bagsvaerd, Denmark, Phone: +4544426056, Fax: +4544444008, E-mail:  
din@novonordisk.com

OTTO DOBLHOFF-DIER, Igeneon, Brunnerstrasse 69/3, 1230  
Vienna, Austria, Phone: +43190250202, Fax: +43190250902, E-mail:  
otto.doblhoff@igeneon.com

ANNA DODDS, Angel Biotechnology Limited, 44 Colbourne  
Crescent, Nelson Park, Cramlington Northumberland, UK, Phone:  
+441670591920, Fax: +441670591921, E-mail:  
anna.dodds@angelbio.com

JANA DOLNIKOVA, Biogen, Inc, 14 Cambridge Center, Cambridge  
02142 Massachusetts, USA, Phone: +16176793319, Fax: +16176793200,  
E-mail: jana\_dolnikova@biogen.com

LAURIE DONAHUE, Sigma-Aldrich, Eschenstr, 5, 82024  
Taufkirchen, Germany, Phone: +49 896513 1901, Fax: +49 896513 1919,  
E-mail: HHellwig@europe.sial.com

HENRIK DORGE, Nunc, Kamstrupvej 90, 4000 Roskilde, Denmark,  
Phone: +45 4631 2181, Fax: +45 4631 2175, E-mail: cmn@nunc.dk

MAGNUS DOVERSKOG, Biovitrum, Strandbergsgatan 49, 11276  
Stockholm, Sweden, Phone: +4686973302, Fax: +4686972333, E-mail:  
magnus.doverskog@biovitrum.com

ROSMARY DRAKE, The Automation Partnership, York Way,  
Hertfordshire SG8 5WY, UK, Phone: +441763227200, Fax:  
+441763227201

JEAN-CHRISTPHE DRUGMAND, Unit Of Bioengineering, Univ.  
Of Louvain, Place Croix du Sud 2/19, B-1348 Louvain-La-Neuve,  
Belgium, Phone: +3210473039, Fax: +3210473062, E-mail:  
drugmand@gebi.ucl.ac.be

PAUL DUCOMMUN, Serono, Zone Industrielle B, 1809 Fenil-Sur-  
Corsier, Switzerland, Phone: +41219232000, Fax: +41219232013,  
E-mail: rachel.zohar@serono.com

MARKUS DUERRSCHMID, Institute Of Applied Microbiology,  
Muthgasse 18, 1190 Viena, Austria, Phone: +43 664 2200625, E-mail:  
h9040929@edv1.boku.ac.at

REINHARD DUNKER, Merck KgaA, Frankfurter Str. 250, 64271  
Darmstadt, Germany, Phone: +496151726574, Fax: +496151723447,  
E-mail: reinhard.dunker@merck.de

SEVIM DUVAR, Gesellschaft Für Biotechnologische F., Mascheroder  
Weg 1, 38124 Braunschweig, Germany, Phone: +495316181, Fax:  
+495312612334, E-mail: sdr@gbf.de

HORST EBERHARDT, Roche Diagnostics GmbH, Nonnenwald 2,  
82377 Penzberg, Germany, Phone: +498856602648, Fax:  
+498856602003, E-mail: horst.eberhardt@roche.com

ESBEN EGGERTSEN, Novo Nordisk, Novo Alle 3BM, 2880  
Bagsvaerd, Denmark, Phone: +4544428760, E-mail:  
egg@novonordisk.com

CHRISTINA EL-NAAMAM, Chemometec, Gydevang 43, 3450  
Allerod, Denmark, Phone: +45 4813 1020, Fax: +45 481 31021, E-mail:  
sb@chemometec.dk

ELSAYED AHMED ELSAYED, German Research Center (Gbf),  
Cell Culture Technology Dept., Mascheroder Weg 1 D-38124  
Braunschweig, Germany, Phone: +49 531 6181 116, Fax: +49 531 6181  
448, E-mail: esa@gbf.de

BARBARA ENENKEL, Boehringer Ingelheim, Birkenorferstrasse 65,  
D-88397 Biberach, Germany, Phone: +49 73 51 54 48 01, Fax: +49 73 51  
54 51 31, E-mail: evelyn.schmucker@bc.boehringer-ingelheim.com

DAVID EPSTEIN, Centocor, Inc., 200 Great Valley Pkwy, 19355  
Malvern, PA, USA, Phone: +16106517440, E-mail:  
depstei4@centus.jnj.com

ULRIKA ERIKSSON, Department Of Biotechnology, Royal Institute  
of Technology, 10691 Stockholm, Sweden, Phone: +46855378307, Fax:  
+46855378323, E-mail: ulrika@biotech.kth.se

DOMINIQUE ESBERT, Serologicals Corporation, The Magdalene  
Centre, Oxford Science Park OX4 4GA Oxford, UK, Phone:  
+441865784646, Fax: +441865784648, E-mail:  
jnicacio@serologicals.com

BARBARA ESCH, Boehringer Ingelheim, Birkenorferstrasse 65, D-  
88397 Biberach, Germany, Phone: +49 73 51 54 48 01, Fax: +49 73 51  
54 51 31, E-mail: evelyn.schmucker@bc.boehringer-ingelheim.com

SYBILLE ESSER, Cardion Ag, Max-Planck-Strasse 15A, 40699  
Erkrath, Germany, Phone: +492112056542, Fax: +492112056598, E-  
mail: esser@cardion.de

SCOTT ESTES, Genzyme Corporation, 1 Mountain Rd, Framingham  
Massachusetts, USA, Phone: +15082702096, Fax: +15088729080, E-  
mail: scott.estes@genzyme.com

KAREN ETCHBERGER, Jrh Biosciences, 13804 W 107th Street,  
Lenexa 66215 Kansas, USA, Phone: +1 913 469 5580 x-225, Fax:  
+1 913 469 5584, E-mail: Susan.Bridges@jrhbio.com

MARINA ETCHEVERRIGARAY, Univ. Nacional Del Litoral,  
Facultad de Bioquímica y Ciencias Biológicas, CC242 - Ciudad Universitaria  
S3000ZAA Santa Fe, Argentina, Phone: +543424575214, Fax:  
+543424575214, E-mail: marina@fcb.unl.edu.ar

EVELYN FAIFE, Centro De Inmunología Molecular, Calle 15 esq.  
216 Atabey Playa, 300.07694 Ciudad de La Habana, Cuba, Phone:  
+5372716867, Fax: +537335049, E-mail: faife@ict.cim.sld.cu

ALAIN FAIRBANK, Hyclone UK Ltd, Unit 9 Atley Way, North  
Nelson Industrial Estate NE23 1WA Cramlington, Northumberland, UK,  
Phone: +44 141 583 2142, Fax: +44 141 583 2136, E-mail:  
Jarlath.Keating@perbio.com

IMAN FAMILI, University Of California, 10185 Camino Ruiz #132,  
San Diego 92126 CA, USA, Phone: +18586938535, E-mail:  
ifamili@ucsd.edu

JOHN FANN, Abbott Bioresearch Center, 100 Research Drive,  
Worcester 01545 MA, USA, Phone: +15086883735, Fax: +15087934885,  
E-mail: john.fann@abbott.com

SAMIRA FARGALI, German Research Centre For Biotechnology,  
Mascheroder Weg 1, 38124 Braunschweig, Germany, Phone:  
+495316181181, Fax: +495316181488, E-mail: sfa@gbf.de

CHRISTEL FENGE, Astrazeneca, Biotech Laboratory, Building 841  
S-151 85 Sodertalje, Sweden, Phone: +46 8 552 54593, Fax:  
+46 8 552 53935, E-mail: christel.fenge@astrazeneca.com

CARMEN FERNANDEZ, Elnor Iberica, Centro Emp. Euronova,  
Rda. Poniente 6-2D 28760 TRES CANTOS ( MADRID), Spain, Phone:  
+34 (91) 806 04 09, Fax: +34 (91) 804 14 96, E-mail:  
elnoriberica@elnoriberica.com

CLAUDIA FERRARA, Glycart Biotechnology Ag, Wayistrasse 18,  
Schieren 8952 Zurich, Switzerland, Phone: +4117556161, Fax:  
+4117556160, E-mail: claudia.ferrara@glycart.com

TIAGO FERREIRA, Ibet, Apartado 12, 2781-901 Oeiras, Portugal,  
Phone: +351214469424, Fax: +351214421161, E-mail: [tbpsf@itqb.unl.pt](mailto:tbpsf@itqb.unl.pt)

CECILE FIAMMA-GENY, Genethon, 1, bis rue de l'Internationale,  
91000 Evry, France, Phone: +33169471022, E-mail:  
[fiamma@genethon.fr](mailto:fiamma@genethon.fr)

ALVIO FIGUEREDO, Center Of Molecular Immunology, Calle 216  
esq. 15, Atabey, Playa, 11600 Ciudad Habana, Cuba, Phone:  
+5372717933, Fax: +537335049, E-mail: [alvio@ict.cim.sld.cu](mailto:alvio@ict.cim.sld.cu)

DAVID FIORENTINI, Biological Industries Ltd., 25115 Kibbutz Beit  
Haemek, Israel, Phone: +97249960695, Fax: +97249565570, E-mail:  
[tech@bioind.com](mailto:tech@bioind.com)

THOMAS FLETCHER, Irvine Scientific, 2511 Daimler St., 92705  
Santa Ana (CA), USA, Phone: +19492617800, Fax: +19492616522,  
E-mail: [tfletcher@irvinesci.com](mailto:tfletcher@irvinesci.com)

JANYS FLETCHER, Lonza Biologics Plc., 228 Bath Rd., Slough,  
SL1 4DY Berkshire, UK, Phone: +441753716585, Fax: +441753716660,  
E-mail: [silvana.palumbo@lonza.com](mailto:silvana.palumbo@lonza.com)

INGO FOCKEN, Aventis Pharma, Industriepark Hoechst, Protein  
Production, Building G877 D-65926 Frankfurt, Germany, Phone:  
+4906930524594, E-mail: [ingo.focken@aventis.com](mailto:ingo.focken@aventis.com)

SEAN FORESTELL, Onyx Pharmaceuticals, 3031 Research Drive,  
94806 Richmond, CA, USA, Phone: +15102628736, E-mail:  
[sforestell@onyx-pharm.com](mailto:sforestell@onyx-pharm.com)

ANGELA GUILLERMINA FORNO, Univ. Nacional Del Litoral,  
Facultad de Bioquímica y Ciencias Biológicas, CC242 - Ciudad Universitaria  
S3000ZAA Santa Fe, Argentina, Phone: +54 342 4575214, Fax:  
+54 342 4575214, E-mail: [gforno@fbcb.unl.edu.ar](mailto:gforno@fbcb.unl.edu.ar)

WYN FORREST-OWEN, Cambridge Antibody Technology, Milstein  
Building, Garanta Park CB16GH Cambridge, UK, E-mail:  
[liz.browne@cambridgeantibody.com](mailto:liz.browne@cambridgeantibody.com)

BJOERN FRAHM, Technische Universität Hamburg-Harburg,  
Denickestr. 15, 21071 Hamburg, Germany, Phone: +49 4042878 4061,  
Fax: +49 4042878 2909, E-mail: [frahmb@yahoo.com](mailto:frahmb@yahoo.com)



FRANTISEK FRANEK, Institute Of Experimental Botany, Radiova,  
1, CZ-10227 Prague, Czech Republic, Phone: +420267008469, Fax:  
+420267008329, E-mail: franek@biomed.cas.cz

REINHARD FRANZE, ROCHE DIAGNOSTICS Gmbh,  
Nonnenwald, Penzberg, Germany, Phone: +498856602560, Fax:  
+498856606762, E-mail: reinhard.franze@roche.com

ELISABETH FRAUNE, B. Braun Biotech International,  
Schwarzenberger weg 73-79, 34212 Melsungen, Germany, Phone:  
+49 5661 713934, Fax: +49 5661 929943, E-mail:  
Elisabeth.Fraune@bioscipro.com

ELKE FREISSLER, Rentschler Biotechnologie, Erwin - Rentschler  
Str. 21, D-88471 Laupheim, Germany, Phone: +497392701734, Fax:  
+497392701725, E-mail: elke.freissler@rentschler.de

JAN-GERD FRERICHS, Institute For Technical Chemistry, Callinstr  
3, 30167 HANNOVER, Germany, Phone: +495117625679, Fax:  
+495117623004, E-mail: frerichs@iftc.uni-hannover.de

KATHIE FRITCHMAN, Bd Diagnostic Systems, 10971 Torreyana  
Rd, 92121 San Diego, CA, USA, Phone: +7607884577, Fax:  
+7607884535, E-mail: Kathie\_fritchman@bd.com

RICHARD FRX, Cellon Sa, 29 AM Bechler, Bereldange 7213  
Luxembourg, Luxembourg, Phone: +352 263 3731, Fax: +352 311 052,  
E-mail: cellon@gms.lu

ANTJE FUHRMANN, Greiner Bio-One Gmbh, Maybachstr. 2,  
D-72636 Frickenhausen, Germany, Phone: +4970229480, Fax:  
+497022948514, E-mail: g.jenisch@greinerbioone.com

MARTIN FUSSENEGGER, Eth / Institute Of Biotechnology, ETH  
Hougesberg, HPT, 8093 Zurich, Switzerland, Phone: +41 1633 3448,  
Fax: +41 1633 1051, E-mail: fussenegger@biotech.biol.ethz.ch

ZBIGNIEW GADEK, Center For Holistic Medicine And Naturopathy  
Co., Ltd., Talweg 14, 57392 Schmalleberg-Nordenau, Germany, Phone:  
+4929759622190, Fax: +4929759622200, E-mail: zgngmbh@t-online.de

ANA GAGO-MARTINEZ, Universidad De Vigo, Dpto. Química Analítica, Fac. de Ciencias, Campus Universitario de Vigo 36200 Vigo, Spain, Phone: +34986812284, Fax: +34986812556, E-mail: anagago@uvigo.es

DANIEL GALBRAITH, Q-One Biotech Ltd., West of Scotland Science Park, G20 0XA Glasgow, Scotland, UK, Phone: +44141946999, Fax: +441419460000, E-mail: dgalbraith@q-one.co.uk

GILAD GALLILI, Abic. Vet. Biolog. Lab. Teva, P.O.B. 489 W. Indust. Zone, 99100 Bet Shemesh, Israel, Phone: +97229906948, Fax: +97229906900, E-mail: gilad.gallili@teva.co.il

GALLMEIER, Biowest Laboratoire, Rue de la Caille, 49340 Nuaille, France, Phone: +33 241 464242, Fax: +33 241 463890, E-mail: h.Brettschneider@biowest.net

CATHERINE GARDNER, Moregate Tcs Ltd, Botolph Claydon, MK18 2LR Buckingham, UK, Phone: +441296713777, Fax: +441296714806, E-mail: alan@tcsgroup.co.uk

BOB GARRAHY, Broadley Technologies, Cain Hill Lodge, Wrest Park, Silsoe MK43 4HS Bedford, UK, Phone: +44 1525 862518, Fax: +44 1525 862811, E-mail: andrew\_hayward@btinternet.com

MONTSERRAT GARRELL, Biokit, Can Male s/n, 08186 Lliça D'Amunt, Spain, Phone: +34938609000, Fax: +34938609010, E-mail: mgarrell@biokit.com

MARTIN GAWLITZEK, Genentech, Inc., 1 DNA way, 94080 South San Francisco, USA, Phone: +1 650 225 8869, E-mail: martin@gene.com

SABINE GEISSE, Novartis Pharma Research Ct/Bmp, Building WSJ-506.3.04, CH-4002 Basel, Switzerland, Phone: +41613248274, Fax: +41613246303, E-mail: sabine.geisse@pharma.novartis.com

YVONNE GENZEL, Mpi Fur Dynamics Of Complex Tech. Syst., Sandtorstrasse 1, 39106 Magdeburg, Germany, Phone: +493916110257, Fax: +493916110203, E-mail: genzel@mpi-magdeburg.mpg.de

JACQUES GERARD, Glaxosmithkline Biologicals, Rue de L'Institut 89, 1330 Rixensart, Belgium, Phone: +3226569674, Fax: +3226569013, E-mail: jacques.gerard@gskbio.com

*List of Participants*

li

CHRISTOPH GIESE, Probiogen Ag, Goethestr. 54, 13086 BERLIN, Germany, Phone: +49309240060, Fax: +493092400660, E-mail: christoph.giese@probiogen.de

CELESTINO GIL, B. Braun Biotech International GmbH, Schwarzenberger Weg 73-79, D-34212 Melsungen, Germany, Phone: +495661713934, Fax: +495661753934, E-mail: elisabeth.fraune@bioscipro.com

CYRILLE GIMENEZ, Aventis Pasteur, 1541 Ava. Marcel Merieux - T1, 69280 Marcy l'Etoile, France, Phone: +33437373533, Fax: +33437379436

PHILIPPE GIRARD, Epfl, FSB-ISP-LBTC, 1015 Lausanne, Switzerland, Phone: +41216935562, Fax: +41216936140, E-mail: philippe.girard@epfl.ch

PETER GIRLING, Switzerland

BIRGITTE GISSEL, Novo Nordisk A/S, Novo Allé, 3BM1.08, 2880 Bagsvaerd, Denmark, Phone: +45 4443 3778, E-mail: bgis@novonordisk.com

CRISTINA GLAD, Bioinvent International Ab, Soelvegatan 41, 22370 Lund, Sweden, Phone: +46 46 2868561, Fax: +46 46 2110806, E-mail: petra.klingberg.persson@bioinvent.com

LOIC GLEZ, Serono, 14 Chemin des Aulx, 1228 Plan-Les-Ouates, Switzerland, Phone: +41 22 7069637, Fax: +41 22 7946965, E-mail: loic.glez@serono.com

CHRIS GODDARD, Gropep, 28 Dalglish St., 5031 Thebarton, Australia, Phone: +61883547705, Fax: +61883547788, E-mail: chris.goddard@gropep.com.au

FRANCESC GODIA, Universitat Autònoma De Barcelona, Dpt. d'Enginyeria Química, Escola Tècnica Superior d'Enginyeria 08193 Bellaterra, Barcelona, Spain, Phone: +34 (93) 581 28 10, Fax: +34 (93) 581 20 23, E-mail: francesc.godia@uab.es

FIONA GODSMAN, Q-One Biotech, Todd Campus,, West of  
Scotland Science Park G20 0XA Glasgow, UK, Phone: +44 141 946  
9999, Fax: +44 141 946 0000, E-mail: Fgodsman@q-one.co.uk

ASTRID GOEDDE, Rzpd, Im Neuenheimer Feld 580, 69120  
Heidelberg, Germany, Phone: +6221424713, Fax: +6221424704, E-mail:  
goedde@rzpd.de

MERLIN GOLDMAN, UK, E-mail: mhgoldman@blueyonder.co.uk

LUCIA GOLZIO, Rbm - Serono, Via Ribes, 1, 10010 Colletterto  
Giacosa (TO), Italy, Phone: +39 0125 222111, Fax: +39 0125 222599,  
E-mail: lucia.golzio@serono.com

RAFAEL GOMEZ TRUJILLO, Biogen Cientifica, Bejar, 36, 28028  
Madrid, Spain, Phone: +34 (91) 361 10 27, Fax: +34 (91) 361 08 98,  
E-mail: rtrujillo@biogencientifica.com

TOM GONG, Onyx Pharmaceuticals, 3031 Research Drive, 94806  
Richmond (CA), USA, Phone: +15102433618, E-mail: tgong@onyx-  
pharm.com

OSCAR GONZALEZ, Elnor Iberica, Centro Emp. Euronova, Rda.  
Poniente 6-2D 28760 TRES CANTOS ( MADRID), Spain, Phone:  
+34 (91) 806 04 09, Fax: +34 (91) 804 14 96, E-mail:  
elnoriberica@elnoriberica.com

KEITH GOODERHAM, Invitrogen Ltd, 3 Fountain Drive, Inchinnan  
Business Park PA49RF Inchinnan (Scotland), UK, Phone:  
+4401418146100, Fax: +44014148146117, E-mail:  
keith.gooderham@invitrogen.com

ROEL GORDIJN, Cambrex, Parc Industriel de Petit Rechain, 4800  
Verviers, Belgium, Phone: +32 87321 611, Fax: +32 87351 967, E-mail:  
roel.gordijn@cambrex.com

STEPHEN GORFIEN, Invitrogen Corporation, 3175 Staley Road,  
14072 Grand Island, NY, USA, Phone: +1 716 774 6633, Fax: +1 716  
774 6996, E-mail: steve.gorfien@invitrogen.com

*List of Participants*

liii

ALEXANDER GÖTZ, Greiner Bio-One GmbH, Maybachstr. 2,  
D-72636 Frickenhausen, Germany, Phone: +4970229480, Fax:  
+497022948514, E-mail: g.jenisch@greinerbioone.com

CHETAN GOUDAR, Bayer Corporation, 800 Dwight Way, B55N  
94701 Berkeley, CA, USA, Phone: +15107054035, E-mail:  
chetan.goudar.b@bayer.com

GERARD GOURDON, Applikon, 9 Rue Levassov, 78130 LES  
MUREAUX, France, Phone: +33134929999, E-mail:  
G.GOURDON@APPLIKON.FR

STEFANOS GRAMMATIKOS, Boehringer Ingelheim Pharma Kg,  
Birkendorfer Strasse 65, 88397 Biberach an der Riss, Germany, Phone:  
+497351544022, Fax: +4973515498681, E-mail:  
stefanos.grammatikos@bc.boehringer-ingelheim.com

MIKE GRAMMER, Biovest International, 8500 Evergreen  
Boulevard, MN55433 Minneapolis, USA, Phone: +441519245351, Fax:  
+441512222309, E-mail: BiovestEurope@aol.com

LOTHAR GRANNEMANN, Innovatis Ag., Technologiezentrum,  
Meisenstrasse 96 33607 Germany, Germany, Phone: +495212997300,  
Fax: +495212997285, E-mail: sabine.kappes@innovatis.com

ANDRE GREBE, B.BRAUN BIOTECH INTERNATIONAL GmbH,  
Schwarzenberger Weg 73-79, 34212 Melsungen, Germany, Phone:  
+495661713528, Fax: +495661929945, E-mail:  
andre.grebe@bioscipro.com

ANNE GREGOIRE, Cytheris, 21 Rue Astride Briand, 92170 Vanves,  
France, Phone: +33158883808, Fax: +33146444446, E-mail:  
agregoire@cytheris.com

NIKI GREGORIADES, Abgenix, Inc., 6701 Kaiser Drive, Mailstop  
26, Fremont 94555 CA, USA, Phone: +15102846451, Fax:  
+15107905269, E-mail: niki.gregoriades@abgenix.com

BRYAN GRIFFITHS, Esact Office, 5 Bourne Gardens Porton, SP4  
0NU SALISBURY, UK, Phone: +44 1980610405, Fax: +44 1980610405,  
E-mail: esact@giff.evesham.net

LEOPOLD GRILLBERGER, Baxter Vaccine Ag, uFERSTRABE 15,  
A2304 Orth/Donau, Austria, Phone: +431201004648, Fax:  
+431201004708, E-mail: leopold\_grillberger@baxter.com

PHILIPPE GRIMM, Q-One Biotech, West of Scotland Science Park,  
G20 0XA Glasgow, UK, Phone: +44 141 947 011, Fax: +44 141 9467  
011, E-mail: jrudd@q-one.co.uk

MAYA GROSH, Imclone Systems, Inc, 22 Chubb Way, Somerville  
08876 NJ, USA, Phone: +19085418094, Fax: +19082180344, E-mail:  
maya.grosh@imclone.com

MARIA JESUS GUARDIA ALBA, Puleva Biotech, C/ Purchil 66,  
18004 Granada, Spain, Phone: +34958240152, Fax: +34958240160,  
E-mail: mjguardia@puleva.es

FRANK GUDERMANN, Innovatis Ag., Technologiezentrum,  
Meisenstrasse 96 33607 Germany, Germany, Phone: +495212997300,  
Fax: +495212997285, E-mail: sabine.kappes@innovatis.com

EMMANUEL GUEDON, Cnrs - Lab. Des Sciences Du Genie  
Chimique, Ensaia - 2. Av. de la Foret de Haye, 54505 Vandoeuvre-les-  
Nancy, France, Phone: +33383595842, Fax: +33383595804, E-mail:  
emmanuel.guedon@ensaia.inpl-nancy.fr

ROS GUSTERSON, Glaxosmithkline, South Eden Park Road, BR3  
3BS Beckenham, UK, Phone: +4402086396584, Fax: +4402086396114,  
E-mail: roaslind.j.gusterson@gsk.com

IGGY GYEPI-GARBRAH, Pall Lifesciences, Europa House, Havant  
Street PO13PD Portsmouth, UK, Phone: +442392303303, Fax:  
+442392302506, E-mail: ruth\_batson@europe.pall.com

RICHARD HAAS, University Of Queensland, Dpt. of Chemical  
Engineering, QLD 4072 St Lucia, Australia, Phone: +61 733653568, Fax:  
+61 733654199, E-mail: richarh@cheque.uq.edu.au

DAVID HACKER, Epfl, FSB-ISP-LBTC, 1015 Lausanne,  
Switzerland, Phone: +41216936142, Fax: +41216936140, E-mail:  
david.hacker@epfl.ch

PAUL HAFFENDEN, Terracell International, Po Box 250 Nobleton,  
LOG 1NO Ontario, Canada, Phone: +1 905 859 4991, Fax: +1 905 859  
4992, E-mail: paulhaff@terracell.ca

DOMINIK HAFNER, Wave Biotech Ag, Ringstr. 24, 8317  
Tagelswangen/Schweiz, Switzerland, Phone: +41523542055, Fax:  
+41523542056, E-mail: pblanc@wavebiotech.ch

LENA HAGGSTROM, Department Of Biotechnology, Royal  
Institute of Technology, S-10691 Stockholm, Sweden, Phone:  
+46855378308, Fax: +46855378323, E-mail: lenah@biotech.kth.se

MEINHARD HAHN, Abt. Molekulare Genetik, Im Neuenheimer  
Feld 280, D-69120 Heidelberg, Germany, Phone: +496221424677, Fax:  
+496621491540, E-mail: m.hahn@dkfz.de

CHRISTIAN HAKEMEYER, University Of Bielefeld, Inst. for Cell  
Culture Technology, Universitätsstrasse 25 33615 Bielefeld, Germany,  
Phone: +49 521 1066230, E-mail: cha@zellkult.techfak.uni-bielefeld.de

TAKEKI HAMASAKI, Dep. Of Genetic Resources Tech. Fac. Of  
Agriculture. Kyushi Univ., 6-10-1 Hakozaki, Higashi-ku, 812-8581  
Fukuoka, Japan, Phone: +81926423045, Fax: +81926423052, E-mail:  
hamasan@mti.biglobe.ne.jp

TOBY HAMBLIN, Charter Medical, 3948A Westpoint Blvd,  
NC27103 Winston-Salem, USA, Phone: +13367144218, Fax:  
+13367144241, E-mail: mmilani@lydall.com

JULIAN HANAK, Cobra Biomanufacturing Plc, The Science Park,  
Keele, ST5 5SP Newcastle under Lyme, UK, Phone: +01782382205, Fax:  
+01782714168, E-mail: diane.davies@cobrat.com

YASMINE HANNABY, Paa Laboratoires, Unterm Bomarin 2,  
Germany, Phone: +49 6421 82013, Fax: +49 6421 85890, E-mail:  
adler@scm.de

JENS JACOB HANSEN, Novo Nordisk A/S, Krogshøjvej 6a1.104,  
2880 Bagsvaerd, Denmark, Phone: +4544420016, E-mail:  
jsjh@novonordisk.com

KURT HARBORDT, Bd Diagnostic Systems, 7 Loveton Circle,  
21152 Sparks, MD, USA, Phone: +14103164685, Fax: +14103164974,  
E-mail: kurt\_harbordt@bd.com

RETO R HARTMANN, Sensorix, Technoparkstrasse 1, 8005 Zurich,  
Switzerland, Phone: +32 9 220 3373, Fax: +32 9 220 3379, E-mail:  
susa.volker@sensorix.com

JEANETTE HARTSHORN, Jrh Biosciences, 13804 W 107th Street,  
Lenexa 66215 Kansas, USA, Phone: +1 913 469 5580 x-225, Fax:  
+1 913 469 5584, E-mail: Susan.Bridges@jrhbio.com

LORNA HARVEY, Inveresk Research, Elphinstone Research Centre,  
Tranent EH33 2NE Scotland, UK, Phone: +44 1875 618538, Fax: +44  
1875 614555, E-mail: jean.howieson@inveresk.com

HANSJÖRG HAUSER, Gbf, Mascheroder Weg 1, 38124  
Braunschweig, Germany, Phone: +49 531 6181250, Fax:  
+49 531 6181262, E-mail: hha@gbf.de

NICOLAS HAVELANGE, Henogen Sa., Rues des Prof. Jeneur et  
Brachet 12, B-6041 Gosselies, Belgium, Phone: +3271378901, Fax:  
+3271378973, E-mail: nicolas.havelange@henogen.com

ANDREW HAYWARD, Broadley Technologies, Cain Hill Lodge,  
Wrest Park, Silsoe MK43 4HS Bedford, UK, Phone: +44 1525 862518,  
Fax: +44 1525 862811, E-mail: andrew\_hayward@btinternet.com

CAROLE HEATH, Amgen, 51 University Street, 98101 SEATTLE,  
WASHINGTON, USA, Phone: +14258447117, Fax: +14254873791,  
E-mail: heathc@amgen.com

DANIEL HEID, Rütten Engineering, Industriestrasse 9, 8712 Stäfa,  
Switzerland, Phone: +41 1928 2930, Fax: +41 1926 2802, E-mail:  
info@rutten.com

RÜDIGER HEIDEMANN, Bayer Corporation, 800 Dwight Way,  
94710 Berkeley, CA, USA, Phone: +15107055617, Fax: +15107055451,  
E-mail: rudiger.heidemann.b@bayer.com



HOLGER HEINE, Serono Pharmaceutical Research Inst., 14, Chemin des Aulx, 1228 Plan-les-Quates, Switzerland, Phone: +41227069666, Fax: +41227946965, E-mail: holger.heine@serono.com

HORST HELLWIG, Sigma-Aldrich, Eschenstr. 5, 82024 Taufkirchen, Germany, Phone: +49 896513 1901, Fax: +49 896513 1919, E-mail: HHellwig@europe.sial.com

HERBERT HERMANN, Paa Laboratoires, Unterm Bomarin 2, Germany, Phone: +49 6421 82013, Fax: +49 6421 85890, E-mail: adler@scm.de

ANDREAS HERRMANN, Papaspyrou Biotechnologie, Karl-Heinz-Beckurts-Strasse 13, 52428 Jülich, Germany, Phone: +49 2461 890 578, Fax: +49 2461 690 860, E-mail: a.herrmann@papaspyrou.de

FRIEDEMANN HESSE, Acbt - Austrian Center Of Biopharmaceutical Technology, Muthgasse 18, A-1190 , Austria, Phone: +431360066806, Fax: +4313697615, E-mail: fhesse@edv2.boku.ac.at

PETER HINTERLEITNER, Institute Of Applied Microbiology, Muthgasse, 18, 1190 Vienna, Austria, Phone: +43 1 36006620, Fax: +43 1 3697615, E-mail: shakyma@gmx.at

KARMEN HODGES, Cmc Biopharmaceuticals, Fruebjergvej 3, 2100 Kobenhavn, Denmark, Phone: +4539179857, Fax: +4570209476, E-mail: ka@cmcbio.com

STACY HOLDREAD, Bd Diagnostic Systems, 7 Loveton Circle, 21152 Sparks, MD, USA, Phone: +4103163628, Fax: +4103163690, E-mail: stacy\_holdread@bd.com

CARSTEN HOLTORP, Chemometec, Gydevang 43, 3450 Allerød, Denmark, Phone: +45 4813 1020, Fax: +45 481 31021, E-mail: sb@chemometec.dk

DIETER HUBEST, Uniklinik Freiburg, Germany

BORIS HUNDT, Otto-Van Guericke University, Postfach 4120, 39016 magdeburg, Germany, Phone: +493916110213, Fax: +493916110203, E-mail: boris.hundt@vst.uni-magdeburg.de

HANS HUTTINGA, Quest International, Huizerstraatweg 28,  
LNL1411 GP Maarden, The Netherlands, Phone: +31 35 699 2458, Fax:  
+31 35 694 5684, E-mail: hans.huttinga@QuestIntl.com

CHRISTOPHER HWANG, Genzyme Corp., 45 New York Ave,  
P.O.BOX 9322 Framingham, USA, Phone: +15082713692, Fax:  
+15082713452, E-mail: chris.hwang@genzyme.com

THOMAS IRISH, Crucell N.V., Archimedsdweg 4, 2301 Leiden, The  
Netherlands, Phone: +31715248706, Fax: +31715248702, E-mail:  
t.irish@crucell.com

VOLKER JAEGER, Cell Culture Technology Dept., Mascheroder  
Weg 1, D-38124 Braunschweig, Germany, Phone: +495316181102, Fax:  
+495316181488, E-mail: vja@gbf.de

DAVID JAMES, University Of Queensland, St Lucia, 4068 Brisbane,  
Australia, Phone: +61733654638, Fax: +61733654199, E-mail:  
davidj@cheque.uq.edu.au

ERIC JANSSENS, B. Braun Biotech International GmbH,  
Schwarzenberger Weg 73-79, D-34212 Melsungen, Germany, Phone:  
+495661713934, Fax: +495661753934, E-mail:  
elisabeth.fraune@bioscipro.com

RACHEL JARMAN-SMITH, Jrh Biosciences, 13804 W 107th Street,  
Lenexa 66215 Kansas, USA, Phone: +1 913 469 5580 x-225, Fax: +1 913  
469 5584, E-mail: Susan.Bridges@jrhbio.com

DAVID JAYME, Gibco / Invitrogen Corporation, 3175 Staley Road,  
14072 Grand Island (NY), USA, Phone: +17167746771, Fax:  
+17177466996, E-mail: david.jayme@invitrogen.com

NANNI JELINEK, Biogenerix Ag, Jander Str. 3, 68199 Mannheim,  
Germany, Phone: +496218755651, Fax: +496218755633, E-mail:  
nanni.jelinek@biogenerix.com

DAVID JERVIS, The Automation Partnership Ltd, York way,  
Royston, SG8 5WY Hertfordshire, UK, Phone: +44 1763 227336, Fax:  
+44 1763 227201, E-mail: slp@autoprt.co.uk

YUN JIANG, Biovitrum, Visitors Lindhagensgatan 133, 11276  
Stockholm, Sweden, Phone: +4686972647, Fax: +4686972312, E-mail:  
yun.jiang@biovitrum.com

PETER JOHANSSON, Bioinvent, BioInvent International AB,  
Solvegatan41 SE-22370 LUND, Sweden, Phone: +46462868561, Fax:  
+46462110806, E-mail: petra.klingberg.persson@bioinvent.com

HELENA JOHANSSON, Bioinvent, BioInvent International AB,  
Solvegatan41 SE-22370 LUND, Sweden, Phone: +46462868561, Fax:  
+46462110806, E-mail: petra.klingberg.persson@bioinvent.com

LAUST BRUUN JOHNSEN, Novo Nordisk, Novo Alle, 6B3.99,  
2880 Bagsvaerd, Denmark, Phone: +4544422846, E-mail:  
lbjh@novonordisk.com

DAVID JONES., Crucell Holland Bv, Archimedesway 4, 2301  
Leiden, The Netherlands, Phone: +31715240777, Fax: +31715248702,  
E-mail: d.jones@crucell.com

MARTIN JORDAN, Epfl, FSB-ISP-LBTC, 1015 Lausanne,  
Switzerland, Phone: +41216936142, Fax: +41216936140, E-mail:  
martin.jordan@epfl.ch

ANNETTE JORGENSEN, Novo Nordisk A/S, Hagedornsvej 1, 2820  
Gentofte, Denmark, Phone: +4544430238, Fax: +4544439210, E-mail:  
annj@novonordisk.com

SANDRA JUANOLA JOURNÉ, Universitat Autònoma de  
Barcelona, Dept. Eng. Química, Edif. C., Campus UAB 08193 Bellaterra,  
Spain, Phone: +34 (93) 5811808, Fax: +34 (93) 5812013, E-mail:  
sandra.juanola@uab.es

MARTINA KAHL, Greiner Bio-One GmbH, Maybachstr. 2, D-72636  
Frickenhausen, Germany, Phone: +4970229480, Fax: +497022948514,  
E-mail: g.jenisch@greinerbioone.com

DANIEL KAISER, ALFA BIOVERFAHRENS TECHNIK GmbH,  
Heinrich - Hertz Str. 16, 14532 Kleinmachnov, Germany, Phone:  
+4933203804710, Fax: +4933203804720, E-mail: dkaiser@alphabvt.com

GREGORIO KAKLIS, Steris, Steris house, Jays Close, RG22 4AX  
Viables, Basingstoke, UK, Phone: +44 1256 840400, Fax: +44 1256  
866502, E-mail: sarah\_barlow@steris.com

HÉLA KALLEL, Institute Pasteur Of Tunis, 13 Place Pasteur. BP 74,  
1002 Tunis, Tunisia, Phone: +21671848903, Fax: +21671791833, E-mail:  
hela.kallel@pasteur.rns.tn

STEPHAN KALWY, Lonza Biologics, Plc., 228 Bath Road, SL1 4DY  
Slough, UK, Phone: +441753716855, Fax: +441753777001, E-mail:  
skalwy@lonza.co.uk

AMINE KAMEN, Nrc / Irb, 6100 Royalmount Ave., H4P 2R2  
Montreal, Canada, Phone: +15144962264, Fax: +15144467251, E-mail:  
sylvie.dupuis@cnrc-nrc.gc.ca

TAICHI KASHIWAGI, Dep. Of Genetic Resources Tech. Fac. Of  
Agriculture. Kyushu Univ., 6-10-1 Hakozaki. Higashi-ku, 812-8581  
Fukuoka, Japan, Phone: +81926423045, Fax: +81926423052, E-mail:  
ktaichi@grt.kyushu-u.ac.jp

CORNELIA KASPER, Institut Für Technische Chemie, Callinstr. 3,  
30167 Hannover, Germany, Phone: +49 511 7622967, Fax: +49 511  
7623004, E-mail: kasper@iftc.uni-hannover.de

RANDALL KAUFMAN, Howard Hughes Med. Institute, Univ. of  
Michigan Med. School, MSRB II, Room 4570, 1150 W. Medical Center  
Drive 48109-0650 Ann Arbor, MI, USA, Phone: +17347639037, Fax:  
+17347639323, E-mail: janmit@umich.edu

HITTO KAUFMANN, Walter & Eliza Hall Inst. Of Med. Research,  
1G Royal Parade, Parkville 3050 Victoria, Australia, Phone: +61 3  
93452548, Fax: +61 3 93470852, E-mail: kaufmann@wehi.edu.au

JARLATH KEATING, Hyclone Uk Ltd, Unit 9 Atley Way, North Nelson  
Industrial Estate NE23 1WA Cramlington, Northumberland, UK, Phone:  
+44 141 583 2142, Fax: +44 141 583 2136, E-mail:  
Jarlath.Keating@perbio.com

TIMO KEIJZER, Applisens, De Brauwweg, 13, 3125AE Schiedam,  
The Netherlands, Phone: +31 10 298 3555, Fax: +31 10 437 9648,  
E-mail: APPLISENS@APPLIKON.COM

KLAUS KELLINGS, Newlab Bioquality, Max-Planck str. 15A,  
40699 Erkrath, Germany, Phone: +49 211 9255 351, Fax: +49 211 9255  
333, E-mail: dippel@newlab.de

JENS KELM, Institute Of Biotechnology, ETH Hoenggerberg HPT  
E53, 8093 Zuerich, Switzerland, Phone: +41 1 63326, Fax: +41 1 63310,  
E-mail: kelm@biotech.biol.ethz.ch

RALPH KEMPHEN, Boehringer Ingelheim, Birkenorferstrasse 65,  
D-88397 Biberach, Germany, Phone: +49 73 51 54 48 01,  
Fax: +497351545131, E-mail: evelyn.schmucker@bc.boehringer-  
ingelheim.com

NICOLE KESSLER, Cambrex, Parc Industriel de Petit Rechain, 4800  
Verviers, Belgium, Phone: +32 87321 611, Fax: +32 87351 967, E-mail:  
roel.gordijn@cambrex.com

KEN KETLEY, Jrh Biosciences, 13804 W 107th Street, Lenexa  
66215 Kansas, USA, Phone: +1 913 469 5580 x-225, Fax: +1 913 469  
5584, E-mail: Susan.Bridges@jrhbio.com

FRANÇOIS KISLIG, Laboratoires Serono, Sa., Route de Fenil ZIB,  
1809 Fenil-Sur-Corsier, Switzerland, Phone: +41 21 9232000, E-mail:  
rachel.zohar@serono.com

ROBERT KISS, Genentech, Inc., 1 DNA Way, M94080 So. San  
Francisco, CA., USA, Fax: +6502255135, E-mail: kiss.robert@gene.com

IDA MOELGAARD KNUDSEN, Novo Nordisk A/S, Noveo Allé,  
DK 2880 Bagsvaerd, Denmark, Phone: +4544422917, Fax:  
+4544421244, E-mail: imq@novonordisk.com

SUSANN KOCH, Probiogen Ag, Goethestr. 54, 13086 Berlin,  
Germany, Phone: +49309240060, Fax: +493092400619, E-mail:  
susann.koch@probiogen.de

STEFAN KOCHANNEK, University Of Ulm, Dpt. of Gene Therapy,  
Helmholzstr. 8/1 89081 Ulm, Germany, Phone: +49731500336, Fax:  
+49731500336, E-mail: stefan.kochanek@medizin.uni-ulm.de

TAMARA KOLOKOLTSOVA, St. Research Ct. Of Virology And Biotechnology, Novosibirsk region, 630559 Koltsovo, Russian Federation, Phone: +73832366481, Fax: +73832366481, E-mail: kolokol@vector.nsc.ru

KONSTANTIN KONSTANTINOV, Bayer Corp., 800 Dwight Way, 94701 Berkeley, CA, USA, Phone: +5107057040, Fax: +5107055451, E-mail: konstantin.konstantinov.b@bayer.com

GEORG KOX, Dasgip Ag, Germany, Phone: +4924619800, Fax: +49246980100, E-mail: m.glier@dasgip.de

DANIELLA KRANJAC, Wave Biotech Ag, Ringstr. 24, 8317 Tagelswangen/Schweiz, Switzerland, Phone: +41523542055, Fax: +41523542056, E-mail: pblanc@wavebiotech.ch

RICARDO KRATJE, Universidad Nacional De Litoral, Lab. Cultivos Celulares / Bioquímica, C.C. 242 S3000ZAA Santa Fe - Pcia. Santa Fe, Argentina, Phone: +543424575214, Fax: +543424552928, E-mail: rkratje@fcb.unl.edu.ar

BARBARA KRAUS, Baxter Vaccine Ag, UFERSTRABE 15, A2304 Orth/Donau, Austria, Phone: +431201004648, Fax: +431201004708, E-mail: karin\_macho@baxter.com

CAROLINE KRAUSE, Jrh Biosciences, 13804 W 107th Street, Lenexa 66215 Kansas, USA, Phone: +1 913 469 5580 x-225, Fax: +1 913 469 5584, E-mail: Susan.Bridges@jrhbio.com

CLAUS KRISTENSEN, Novo Nordisk, Novo Alle 6B2.107, DK-2880 Bagsvaerd, Denmark, Phone: +4544423572, E-mail: clak@novonordisk.com

MERETE KRISTENSEN, Bioimage, Morkhojbygade 28, 2860 Soborg, Denmark, Phone: +4544433444, E-mail: merk@bioimage.com

BERND KRUEGER, Sigma-Aldrich, Eschenstr. 5, 82024 Taufkirchen, Germany, Phone: +49 896513 1901, Fax: +49 896513 1919, E-mail: HHellwig@europe.sial.com

LYNNE KRUMMENN, Genetech Inc., 1 Dna Way, 94080 San Francisco, CA, USA, Phone: +16502251997, Fax: +16502252006, E-mail: krummenn@gene.com

MARKUS KUEHNER, Adolf Kühner Ag, Dinkelbergstr. 1, 4127 Birsfelden, Switzerland, Phone: +41 61 319 93 93, Fax: +41 61 319 93 94, E-mail: mkuhner@kuhner.com

RENATE KUNERT, Institute For Applied Microbiology, Muthgasse 18, A-1190 Vienna, Austria, Phone: +431360066959, Fax: +4313697615, E-mail: r.kunert@iam.boku.ac.at

INCA KUSTERS, Aventis Pasteur, 1541 avenue Marcel Mérieux, 69280 Marcy L'Etoile, France, Phone: +33437373969, Fax: +33437373976, E-mail: inca.kusters@aventis.com

SHINOBU KUWAE, Mitsubishi Pharma Corporation, 2-25-1 Shodai-Ohtani, Hirakata 573-1153 Osaka, Japan, Phone: +81728569295, Fax: +81728642341, E-mail: kuwae.shinobu@mc.m-pharma.co.jp

RENATE LAMBERTI, Cell Culture Technologies, Buhnrain 14, 8052 Zurich, Switzerland, Phone: +41 1 301 2008, Fax: +41 1 301 2017, E-mail: info@cellculture.com

KARLHEINZ LANDAUER, Igeneon Ag, Brunner Strasse 69/3, 1230 Vienna, Austria, Phone: +4369918904242, Fax: +4319025091, E-mail: karlheinz.landauer@igeneon.com

UWE LANGER, Bayer Ag, Fiedrich Ebert Strasse 217, 42096 Wuppertal, Germany, Phone: +49202367531, Fax: +49202367524, E-mail: uwe.langer.ul2@bayer-ag.de

CHRISTINE LATTENMAYER, Acbt - Austrian Center Of Biopharmaceutical Technology, Muthgasse 18, A-1190 Vienna, Austria, Phone: +431360066805, Fax: +4313697615, E-mail: h9640202@edv2.boku.ac.at

LAUSSERMAIR, Q-One Biotech, West of Scotland Science Park, G20 0XA Glasgow, UK, Phone: +44 141 947 011, Fax: +44 141 9467 011, E-mail: jrudd@q-one.co.uk

TAMMY LAUVRAY, Charter Medical, 3948A Westpoint Blvd,  
NC27103 Winston-Salem, USA, Phone: +13367144218, Fax:  
+13367144241, E-mail: mmilani@lydall.com

SHAWN LAWRENCE, Regeneron Pharmaceuticals, 777 Old Saw  
Mill River Rd., 10522 Tarrytown, NY, USA, Phone: +19143457716, Fax:  
+19143457685, E-mail: shawn.lawrence@regeneron.com

ARYE LAZAR, Israel Institute For Biological Research, P. O. Box  
19, 74100 Ness - Ziona, Israel, Phone: +97289381485, Fax:  
+97289381464, E-mail: lazar@intersun.iibr.gov.il

ERIC LE GUERN, Cmc Biopharmaceuticals, Fruebjergvej, DK2100  
Copenhagen, Denmark, Phone: +4539179885, Fax: +4570209470,  
E-mail: eg@cmcbio.com

RICHARD LEACH, Sigma-Aldrich, eSCHENSTR. 5, 82024  
Taufkirchen, Germany, Phone: +49 896513 1901, Fax: +49 896513 1919,  
E-mail: HHellwig@europe.sial.com

MAX LECHNER, ROCHE DIAGNOSTICS GmbH, Nonnenwald 2,  
D-82372 Penzberg, Germany, Phone: +498856602889, Fax:  
+498856603760, E-mail: max.lechner@roche.com

MARTI LECINA VECIANA, Universitat Autònoma De Barcelona,  
Dept. Eng. Química. Edif. C., Campus UAB 08193 Bellaterra, Spain,  
Phone: +34 (93) 5811808, Fax: +34 (93) 5812013, E-mail:  
marti.lecina@uab.es

JEAN-PIERRE LEDIG, Laboratoires Fournier, 50 Rue de Dijon,  
21121 Daix, France, Phone: +33380447507, Fax: +33380447538, E-mail:  
f.cermelj@fournier.fr

GYUN MIN LEE, Kaist, 373-1 Kusong-dong Yusong-gu, 305-701  
TAEJON, Korea, South, Phone: +82428692618, Fax: +82428692610,  
E-mail: gmlee@mail.kaist.ac.kr

MOON SUE LEE, Kaist, Department of Biological Sciences, 373-1  
Kusong-Dong, Yusong-Gu 305-701 Taejon, Korea, South, Phone:  
+82428695618, Fax: +82428692610, E-mail: leems@mail.kaist.ac.kr



CHANYONG LEE, Merck Research, P.O.BOX 2000, R-804-105  
07065 Rahway, USA, Phone: +17325941193, Fax: +17325944400,  
E-mail: chanyong\_lee@merck.com

JUERGEN LEHMANN, Inst. Of Cell Culture Techn. Faculty Of  
Techn. Univ. Bielefeld, Universitaetsstr. 25, D-33615 Bielefeld,  
Germany, Phone: +495211066319, E-mail: jl@zellkult.techfak.uni-  
bielefeld.de

MICHAEL LEHNERER, OCTAGENE Gmbh, Am Klopferspitz 19,  
82152 Martinsried, Germany, Phone: +498970076960, Fax:  
+498970076961, E-mail: info@octagene.com

CHRISTIAN LEIST, Novartis Pharma Ltd., WKL-681.1.45, CH-4002  
Basel, Switzerland, Phone: +41616964651, Fax: +41616962643, E-mail:  
christian.leist@pharma.novartis.com

CHRISTINE LETTENBAUER, Wave Biotech Ag, Ringstr. 24, 8317  
Tagelswangen/Schweiz, Switzerland, Phone: +41523542055, Fax:  
+41523542056, E-mail: pblanc@wavebiotech.ch

PATRICIA LEUNG-TACK, Aventis Pasteur, 1541 Avenue Marcel  
Merieux, 69280 Marcy L'Etoile, France, Phone: +330437370918, Fax:  
+330437373148, E-mail: patricia.leung-tack@aventis.com

CINDEE LEVOW, Glaxo Smithkline Pharmaceuticals, 709  
Swedeland Road, UE 3836 King of Prussia PA, USA, Phone:  
6102707886, E-mail: cindie\_a\_levow@gsk.com

ANDREW LEWIN, Cobra Biomanufacturing Plc, Science Park,  
Keele, ST5 5SP Newcastle Under Lyme, UK, Phone: +441782382202,  
Fax: +441782714168, E-mail: diane.davies@cobrabio.com

LASSE LINDHARDT, Ssi - Statens Serum Institut, Artillerivej 5,  
2300 Copenhagen, Denmark, Phone: +4532683307, E-mail: llp@ssi.dk

ELISABETH LINDNER-OLSSON, Metcon Medicin Ab, Dalenum  
17, S18170 Lidings, Sweden, Phone: +4684115660, Fax: +4684115668,  
E-mail: elisabeth.lindner-olsson@metconmedicin.se

ALEXANDER LOA, Cell Culture Service, Falkenried 88, 20251  
Hamburg, Germany, Phone: +494047196560, Fax: +494047196566,  
E-mail: loa@cellcultureservice.com

JAVIER LOBO, B. Braun Biotech International GmbH,  
Schwarzenberger Weg 73-79, D-34212 Melsungen, Germany, Phone:  
+495661713934, Fax: +495661753934, E-mail:  
elisabeth.fraune@bioscipro.com

RENÉ LOHSER, Adolf Kühner Ag, Dinkelbergstr. 1, 4127  
Birsfelden, Switzerland, Phone: +41 61 319 93 93, Fax: +41 61 319 93  
94, E-mail: mkuhner@kuhner.com

CHRISTOPHE LOSBERGER, Serono, 14 Chemin des Aulx, 1228  
Plan-Les-Quates, Switzerland, Phone: +41 22 7069637, Fax: +41 22  
7946965, E-mail: christophe.losberger@serono.com

HANS-JÜRGEN LOTZ, Kendro Laboratory, Heraustrasse, 12-14,  
63450 Hanau, Germany, Phone: +49 1805 536376, Fax: +49 1805  
112110, E-mail: info@kendro.de

LINDA LUA, The University Of Queensland, Dpt. of Chemical  
Engineering, 4072 Brisbane, Queensland, Australia, Phone: +617  
33654920, Fax: +617 33654199, E-mail: lindal@cheque.uq.edu.au

HOLGER LUEBBEN, Chiron Behring, Emil V. Behring Str. 76,  
35041 Marburg, Germany, Phone: +496421385807, Fax:  
+496421392829, E-mail: holger.luebben@chiron-behring.com

REGINE LUEMEN, Innovatis Ag., Technologiezentrum,  
Meisenstrasse 96 33607 Germany, Germany, Phone: +495212997292,  
Fax: +495212997285, E-mail: regine.luemen@innovatis.com

ELKE LULLAU, Astrazeneca, Astrazeneca Biotech. Bldg. 841, S-  
15185 Sodertalje, Sweden, Phone: +46855251938, Fax: +46855253935,  
E-mail: elke.lullau@astrazeneca.com

BJÖRN LUNDGREN, Amersham Biosciences, Björkgatan 30, 75182  
Uppsala, Sweden, Phone: +46 18 612 0505, Fax: +46 18 10 1403, E-mail:  
bjorn.lundgren@eu.apbiotech.com

SHUN LUO, Jrh Biosciences, 13804 W 107th Street, Lenexa 66215  
Kansas, USA, Phone: +1 913 469 5580 x-225, Fax: +1 913 469 5584,  
E-mail: Susan.Bridges@jrhbio.com

DIRK LUTKEMEYER, University Of Bielefeld, Inst. of Cell Culture  
Technology, Faculty of Technology 33594 Bielefeld, Germany, Phone:  
+495211066324, Fax: +495211066328,  
E-mail: dlu@zellkult.techfak.uni-bielefeld.de

CHRISTOPHER LUX, Indiana University, School of Medicine, 821  
F Dr MLK Jr St 46202 Indianapolis, IN, USA, Phone: +13179724117,  
E-mail: ctlux@iupui.edu

IAN LYALL, Gibco Invitrogen Corp., 3175 Staley Road, 14072  
Grand Island, USA, Phone: +17167743104, Fax: +17167746996, E-mail:  
jennifer.walowitz@invitrogen.com

KURT A. MACK, Cell Culture Technologies, Buhnrain 14, 8052  
Zurich, Switzerland, Phone: +41 1 301 2008, Fax: +41 1 301 2017,  
E-mail: info@cellculture.com

MALCOM MACNAUGHTON, Inveresk Research, Elphinstone  
Research Centre, Tranent EH33 2NE Scotland, UK, Phone: +44 1875  
618538, Fax: +44 1875 614555, E-mail: jean.howieson@inveresk.com

DAVID MALINGE, The Automation Partnership Ltd, York way,  
Royston, SG8 5WY Hertfordshire, UK, Phone: +44 1763 227336, Fax:  
+44 1763 227201, E-mail: slp@autoprt.co.uk

MARCOS MALUMBRES, Centro Nac. De Investigacions  
Oncologicas, Melchor Fernández Almagro, 3, 28029 Madrid, Spain,  
Phone: +34 (91) 2246938, Fax: +34 (91) 7328010, E-mail:  
barbacid@cnio.es

ROLF MANSER, Bioengineering Ag, Sagerainstrasse 9, 8636 Wald,  
Switzerland, Phone: +41552568111, Fax: +41552568256, E-mail:  
n.watanabe@bioengineering.ch

ANNIE MARC, Cnrs - Lab. Des Sciences Du Genie Chimique,  
Ensaia, 2 Av. de la Foret de Haye, 54505 Vandoeuvre-les-Nancy, France,  
Phone: +33383595785, Fax: +33383595804, E-mail:  
annie.marc@ensic.inpl-nancy.fr

ISABEL MARCELINO, Ibet, Apartado 12, 2781-901 Oeiras,  
Portugal, Phone: +351214469424, Fax: +351214421161, E-mail:  
isabelm@itqb.unl.pt

DINO MARCUS, Israel Institute For Biological Research, P.O Box  
19, 74100 Ness Ziona, Israel, Phone: +97289381518, Fax:  
+97289401094, E-mail: biot1@iibr.gov.il

MARTINE MARIGLIANO, Transgene, 11 Rue de Molsheim, 67082  
Strasbourg, France, Phone: +33388279113, Fax: +33388225807, E-mail:  
marigliano@transgene.fr

JAVIER MARQUEZ, Sigma-Aldrich, Eschenstr, 5, 82024  
Taufkirchen, Germany, Phone: +49 896513 1901, Fax: +49 896513 1919,  
E-mail: HHellwig@europe.sial.com

DIRK E. MARTENS, Wageningen University, Bomenweg 2, 6703  
HD Wageningen, Netherlands Antilles, Phone: +31317482683, Fax:  
+31317482237, E-mail: dirk.martens@wur.nl

CARL MARTIN, Covance, 7 Roxborough way, Maidenhead SL6  
3UD Berkshire, UK, Phone: +44 1628 548000, Fax: +44 1628 826706,  
E-mail: lesley.smith@covance.com

MONIQUE MARTIN, Bio-Rad, 3 Bld. Raymond Poincare, 32430  
Marnes la Coquette, France, Phone: +33147356128, Fax: +33147953133,  
E-mail: monique.martin@bio-rad.com

UWE MARX, Probiogen Ag, Goethestr. 54, 13086 BERLIN,  
Germany, Phone: +49309240060, Fax: +493092400619, E-mail:  
christoph.giese@probiogen.de

STEFANIA MASSA, Molmed Spa, Via Olgettina 58, 20132 Milano,  
Italy, Phone: +3902212771, Fax: +390221277220, E-mail:  
stefania.massa@molmed.com

ALISON MASTRANGELO, Abbott Bioresearch Center, 100  
Research Drive, Worcester 01605 , USA, Phone: +15088492755, Fax:  
+15087547481, E-mail: dorothy.jacques@abbott.com

SHIN-EI MATSUMOTO, Dept. Of Genetic Resources Techn. Fac. Of Agriculture. Kyushu Univ., 6-10-1 Hakozaki, Higashi-ku, 812-851 Fukuoka, Japan, Phone: +8192642304, Fax: +8192642305, E-mail: shinei@grt.kyushu-u.ac.jp

HIROSHI MATSUOKA, Teikyo Univ. Of Science And Technology, 2525 Uenohara-machi, 409-0193 Yamanashi, Japan, Phone: +81554634411, Fax: +81554634431, E-mail: matsuoka@ntu.ac.jp

NATALIA MAZURKOVA, St. Research Ct. Of Virology And Biotechnology, Novosibirsk region, 630559 Koltsovo, Russian Federation, Phone: +73832366481, Fax: +73832366481, E-mail: nechaeva@vector.nsc.ru

JOHN Mc MANUS, Inveresk Research, Elphinstone Research Centre, Tranent EH33 2NE Scotland, UK, Phone: +44 1875 618538, Fax: +44 1875 614555, E-mail: jean.howieson@inveresk.com

PETER MCGRADY, Biovest International, 8500 Evergreen Boulevard, MN55433 Minneapolis, USA, Phone: +441519245351, Fax: +441512222309, E-mail: BiovestEurope@aol.com

JACKIE MCINTOSH, Invitrogen Ltd, 3 Fountain Drive, Inchinnan Business Park PA49RF Inchinnan (Scotland), UK, Phone: +4401418146100, Fax: +4401418146117, E-mail: keith.gooderham@invitrogen.com

RICARDO MEDRONHO, Universidade Federal Do Rio De Janeiro, Escola de Quimica, Bloco E, Ilha do Fundao 21949-900 Rio de Janeiro, Brazil, Phone: +552125627635, Fax: +552125627567, E-mail: medronho@eq.ufrj.br

HEIKO MEENTS, Novartis Pharma Ltd., WKL-681.1.43, CH-4002 Basel, Switzerland, Phone: +41616961035, Fax: +41616963373, E-mail: heiko.meents@pharma.novartis.com

BERNARD MEIGNIER, Aventis Pasteur, Campus Merieux, 1541 Avenue Marcel Merieux 69280 Marcy L'Etoile, France, Phone: +33437373481, Fax: +33437373976, E-mail: bernard.meignier@aventis.com

PETRA MEISSNER, Micromet Ag, Staffelseestr, 2, 81477 Munich, Germany, Phone: +4989895277410, Fax: +4989895277405, E-mail: michaela.schaefer@Micromet.de

MICHAEL MELLOR-CLARK, Q-One Biotech, West of Scotland Science Park, G20 0XA Glasgow, UK, Phone: +44 141 947 011, Fax: +44 141 9467 011, E-mail: jrudd@q-one.co.uk

MARK MELVILLE, Wyeth Biopharma, 1 Burtt Rd, 01810 Andover, USA, Phone: +19782471725, Fax: +19782472603, E-mail: mmelville@wyeth.com

LEE MERMELSTEIN, Scios Inc., 820 West Maude Ave, 94085 Sunnyvale (California), USA, Phone: +1 408 616 8330, Fax: +1 408 616 8502, E-mail: mermelstein@sciosinc.com

NIC MERMOD, University Of Lausanne, Center for Biotechnology UNIL-EPFL, Lab. Molecular Biotechnology 1015 Lausanne, Switzerland, Phone: +41216936151, E-mail: desiree.atkinson@iba.unil.ch

OTTO-WILHEM MERTEN, Genethon Ii, Gene therapy programme, 1 rue internationale bp60 91002 Evry cedex 2, France, Phone: +33 1 6947 2590, Fax: +33 1 6947 2838, E-mail: omerten@genethon.fr

FERRUCCIO MESSI, Cell Culture Technologies, Buhnrain 14, 8052 Zurich, Switzerland, Phone: +41 1 301 2008, Fax: +41 1 301 2017, E-mail: info@cellculture.com

FATHIA METHNANI, Microsafe, Niels Bohrweg 11-13, 2333 CA Leiden, The Netherlands, Phone: +31 71 523 1886, Fax: +31 71 523 5980, E-mail: Fathia@microsafe.nl

FREDERIC MEUWLY, Serono, Zone Industrielle B, 1809 Fenil-Sur-Corsier, Switzerland, Phone: +41219232226, Fax: +41219232013, E-mail: rachel.zohar@serono.com

JAMES MICHAELS, Bayer Biotechnology, Bayer Corporation, 800 Dwight Way, Bldg. 56A, 94701-1986 Berkeley, USA, Phone: +15107055468, Fax: +15107055451, E-mail: jim.michaels.b@bayer.com

DOUGLAS MILLER, Amgen Inc., 51 University Street, Seattle  
98101 Washington, USA, Phone: +14258447377, Fax: +14254873791,  
E-mail: millerda@amgen.com

ALAIN MILLER, C.I.L. S.A, Rue de la Marlette 14, B-7180 Seneffe,  
Belgium, Phone: +3264520561, Fax: +3264558617, E-mail:  
alain.miller@wanadoo.be

JEAN-MAURICE MIMRAN, Jrh Biosciences, 13804 W 107th Street,  
Lenexa 66215 Kansas, USA, Phone: +1 913 469 5580 x-225, Fax: +1 913  
469 5584, E-mail: Susan.Bridges@jrhbio.com

EMILIO MOLINA GRIMA, Universidad De Almeria, Carrera de  
Sacramento, s/n, 04120 La Cañada, Spain, Phone: +34 (950) 015032, Fax:  
+34 (950) 015484, E-mail: emolina@ual.es

JOHANN MOLS, Université Catholique De Louvain, Cellular  
Bioengineering Group, Place Louis Pasteur 1 1348 Louvain La Neuve,  
Belgium, Phone: +3210473039, Fax: +3210474895, E-mail:  
mols@bioc.ucl.ac.be

MIRIAM MONGE, Stedim, Z.I. Des Paluds, Avenue de Jouques  
BP1051 13781 Aubagne cedex, France, Phone: +33 4 42 84 56 31, Fax:  
+33 4 42 84 56 17, E-mail: m-monge@stedim.fr

MONICA MONTOUTE, Glaxo Smith Kline Pharmaceuticals, 709  
Sweedland Road, King of Prussia 19406 Pennsylvania, USA, Phone:  
+16102705145, Fax: +16102705860, E-mail:  
monica.n.montoute@gsk.com

MURRAY MOO-YOUNG, University Of Waterloo, Department of  
Chemical Engineering, Waterloo N2L3G1 Ontario, Canada, Phone:  
+15198884006, Fax: +15197464979, E-mail: mooyoung@uwaterloo.ca

JAVIER MORENO, Sigma-Aldrich, Eschenstr, 5, 82024 Taufkirchen,  
Germany, Phone: +49 896513 1901, Fax: +49 896513 1919, E-mail:  
HHellwig@europe.sial.com

DIANA MORGAN, Bioreliance, Innovation Park Hillfoots Road, FK9  
4NF Stirling, UK, Phone: +44 1786 451318, Fax: +44 1786 464764,  
E-mail: atullu@bioreliance.com

ANA MARIA MORO, Instituto Butanan, Av. Vital Brasil 1500,  
05503-900 Sao Paulo, Brazil, Phone: +551137223608, Fax:  
+551137261505, E-mail: anamoro@butantan.gov.br

JOHN MOWLES, Pharmsouce Information Services Inc, 17  
Northbrook, Market Lavington SN104AN Devizes, UK, Phone:  
+441380812374, Fax: +441380812374, E-mail:  
jon.mowles@easynet.co.uk

ELIANE MUELLER, Cellntec Advanced Cell Systems,  
Laeggasstrasse 122, CH 3012 Bern, Switzerland, Phone: +41316312508,  
E-mail: eliane@cellntec.com

DETHARDT MULLER, Institute For Applied Microbiology,  
Muthgasse 18, A-1190 Vienna, Austria, Phone: +431360066230, Fax:  
+4313697615, E-mail: dmueller@edv2.boku.ac.at

ANTONY MUNN, Lonza, 224 Bath Road, SL1 4DY Slough, UK,  
Phone: +441753777000, E-mail: amunn@lonza.co.uk

TOM MURPHY, Jm Separations Bv, Boschdijk 780, 5624 CL  
Eindhoven, The Netherlands, Phone: +31402197480, Fax:  
+31402197499, E-mail: info@jmseparations.com

NESREDIN MUSSA, Lonza Biologics Plc, 228 Bath Road, SL1 4DY  
Slough, UK, Phone: +441753777000, Fax: +441753716595, E-mail:  
nesredin.mussa@lonza.com

CHO MYUNG-SAM, Bayer Biotechnology, 800 Dwight Way, 94701  
Berkeley, USA, Phone: +15107055424, Fax: +15107054860, E-mail:  
myung-sam.cho.b@bayer.com

ISABELLE NADEAU, Biomarin Pharmaceutical, 371 Bel Marin  
Keys, Suite 210 94949 Novato, CA, USA, Phone: +14158846700,  
E-mail: inadeau@bmrn.com

FRANK-JAN NAGEL, Centocor, Einsteinweg 92, 2333 CB Leiden,  
The Netherlands, Phone: +31715242089, Fax: +31715216511, E-mail:  
FNagel@cntnl.jnj.com



STEFAN NASCHBERGER, Institute For Applied Microbiology,  
Muthgasse 18, A-1190 Vienna, Austria, Phone: +43 1360066805, Fax:  
+43 13697615, E-mail: s.naschberger@iam.boku.ac.at

ELENA NECHAEVA, St. Research Cent. Of Virology And  
Biotechnology, Novosibirsk region, 630559 Koltsovo, Russian  
Federation, Phone: +73832366481, Fax: +73832366481, E-mail:  
nechaeva@vector.nsc.ru

JANOS FALHOF NIELSEN, Statens Serum Institut, Artillerivej 5,  
2300 Copenhagen, Denmark, Phone: +4540592249, E-mail: jfn@ssi.dk

VILLY NIELSEN, Nunc, Kamstrupvej 90, 4000 Roskilde, Denmark,  
Phone: +45 4631 2181, Fax: +45 4631 2175, E-mail: cmn@nunc.dk

OLE NIELSEN, Biowest Laboratoire, Rue de la Caille, 49340  
Nuaille, France, Phone: +33 241 464242, Fax: +33 241 463890, E-mail:  
h.Brettschneider@biowest.net

LARS S. NIELSEN, Symphogen A/S, Elektrovej 375, DK-2800  
Lyngby, Denmark, Phone: +45 45265066, Fax: +45 45265060, E-mail:  
lsn@symphogen.com

LENA NIELSEN, Bioinvent, BioInvent International AB,  
Solvegatan41 SE-22370 LUND, Sweden, Phone: +46462868561, Fax:  
+46462110806, E-mail: petra.klingberg.persson@bioinvent.com

KJELL NILSSON, Percell Biolytica Ab, Ji-Te gatan 9, SE-265 38  
Ästorp, Sweden, Phone: +464250282, Fax: +464250191, E-mail:  
kjell.nilsson@percell.se

INGE NILSSON, Bioinvent International Ab, Soelvegatan 41, 22370  
Lund, Sweden, Phone: +46 46 2868561, Fax: +46 46 2110806, E-mail:  
petra.klingberg.persson@bioinvent.com

WOLF NOE, Idec Pharmaceuticals, 11011 Torreyana Road, 92121  
San Diego (CA), USA, Phone: +18584318326, Fax: +18584318750,  
E-mail: wnoe@idecpharm.com

THOMAS NOLL, Research Center Jülich, Leo-Brand-Strasse, 52425 Jülich, Germany, Phone: +492461613870, Fax: +492461613870, E-mail: th.noll@fz-juelich.de

M& LUISA NOLLI, Areta International, Via Roberto Lepetit, 34, 21040 Gerenzano (VA), Italy, Phone: +39 0296489264, Fax: +39 0295489260, E-mail: mlnolli@aretaint.com

CATHY NOONE, National University Of Ireland, University Road, Galway, Galway, Ireland, Phone: +353 91 586559, Fax: +353 91 586570, E-mail: cathy.b.noone@nuigalway.ie

HENRIK NORGAARD, Nunc, Kamstrupvej 90, 4000 Roskilde, Denmark, Phone: +45 4631 2181, Fax: +45 4631 2175, E-mail: cmn@nunc.dk

MARTA NORTON DE MATOS, Itqb, Avenida da Republica, Apt. 127, 2781-901 Oeiras, Portugal, Phone: +351214469758, Fax: +35214411277, E-mail: mmatos@itqb.unl.pt

PHIL OFFIN, The Automation Partnership Ltd, York way, Royston, SG8 5WY Hertfordshire, UK, Phone: +44 1763 227336, Fax: +44 1763 227201, E-mail: slp@autoprt.co.uk

AKIKO OGAWA, Fukui University, 3-9-1 Bunkyo, 910 8507 Fukui, Japan, Phone: +81776278645, Fax: +81776278747, E-mail: akky@acbio2.acbio.fukui-u.ac.jp

YVONNE OHGREN, Bioinvent, BioInvent International AB, Solvegatan41 SE-22370 LUND, Sweden, Phone: +46462868561, Fax: +46462110806, E-mail: petra.klingberg.persson@bioinvent.com

EDUARDO OJITO, Center Of Molecular Immunology, Calle 216 esq. 15, Atabey, Playa, 11600 Ciudad Habana, Cuba, Phone: +5372717211, Fax: +537335049, E-mail: ojito@ict.cim.sld.cu

YEMI ONAKUNLE, Lonza Biologics, Plc., 228 Bath Road, Slough, SL1 4DY Berkshire, UK, Phone: +441753716643, Fax: +441753716660, E-mail: silvana.palumbo@lonza.com

BERTRAM OPALKA, Universitaetsklinikum, Essen, Innere Klinik (Tumorf.), Hufelandstrasse 55, D-45122 Essen, Germany, Phone: +492017232020, Fax: +492017232020, E-mail: bertram.opalka@uni-essen.de

DIRK-JAN OPSTELTEN, Crucell, Archimedesweg 4, 2333 Leiden, The Netherlands, Phone: +31715248776, Fax: +31715248702, E-mail: dj.opstelten@crucell.com

JASON JOHN OSMAN, Lonza Biologics, 224 Bath Road, SL1 4DY Slough, UK, Phone: +441753716523, Fax: +441753777001, E-mail: josman@lonza.co.uk

ANDREW O'TOOLE, Elnor Iberica, Centro Emp. Euronova, Rda. Poniente 6-2D 28760 TRES CANTOS ( MADRID), Spain, Phone: +34 (91) 806 04 09, Fax: +34 (91) 804 14 96, E-mail: elnoriberica@elnoriberica.com

LAURIE OVERTON, Glaxo Smithkline, 5 MOORE DRIVE, 27709 Research Triangle Park. Nort Carolina, USA, Phone: +19194836209, Fax: +19194836470, E-mail: lko8763@gsk.com

SADETTIN OZTURK, Glaxosmithkline, 709 Swedeland Road, Ve 4021 PA19406 King of Prissia, USA, Phone: +16102393912, Fax: +16102393917, E-mail: s\_ozturk@earthlink.net

JORGE ARTURO PADILLA - ZAMUDIO, Jrh Biosciences Inc., 13804 W 107th Street, Lenexa 66215 KS, USA, Phone: +19134695580, Fax: +19134695584, E-mail: jorge.padilla@jrhibio.com

UTE PAEGELOW, Gbf, Mascheroderweg 1, 38124 Braunschweig, Germany, Phone: +495316181762, E-mail: utp@gbf.de

BRIAN PAGE, Biowest Laboratoire, Rue de la Caille, 49340 Nuaille, France, Phone: +33 241 464242, Fax: +33 241 463890, E-mail: h.Brettschneider@biowest.net

LAURA PALOMARES, Instituto De Biotecnologia, Avenida Universidad 2001, Col. Chamilpa 62210 Cuernavaca, Mor, Mexico, Phone: +525556227646, Fax: +527773138811, E-mail: laura@ibt.unam.mx

BERNHARD PALSSON, University Of California, Dept. of Bioengineering, 9500 Gilman Drive - San Diego 92093-0412 La Jolla, CA, USA, Phone: +18585344272, Fax: +18585345722, E-mail: bpalsson@ucsd.edu

STEFAN PAPADILERIS, Paa Laboratoires, Unterm Bomarin 2, Germany, Phone: +49 6421 82013, Fax: +49 6421 85890, E-mail: adler@scm.de

ELEFTHERIOS T. PAPOUTSAKIS, Northwestern U., Dpt. Chemical Engineering, 2145 Sheridan Road 60208-3120 Evanston, IL, USA, Phone: +1 847 4917455, Fax: +1 847 4913728, E-mail: e-paps@northwestern.edu

CHANDRA PATEL, New Brunswick Scientific, 163 Dixons Hill Road, North Mymms AL9 7JE Hatfield, UK, Phone: +44 1707 275733, Fax: +44 1707 267859, E-mail: moritz@nbsuk.co.uk

NELS PEDERSON, Biogen, 14 Cambridge Center B6-6, 02142 Cambridge, MA, USA, Phone: +16179144858, E-mail: nels\_pederson@biogen.com

SUE PEFFER, The Automation Partnership Ltd, York way, Royston, SG8 5WY Hertfordshire, UK, Phone: +44 1763 227336, Fax: +44 1763 227201, E-mail: slp@autoprt.co.uk

BRANDON PENCE, Hyclone Uk Ltd, Unit 9 Atley Way, North Nelson Industrial Estate NE23 1WA Cramlington, Northumberland, UK, Phone: +44 141 583 2142, Fax: +44 141 583 2136, E-mail: Jarlath.Keating@perbio.com

CARINA PERSSON, Biovitrum, Strandbergsgatan 47, 11276 Stockholm, Sweden, Phone: +4686972731, Fax: +4686972533, E-mail: carina.persson@biovitrum.com

BO PERSSON, Zymo Genetics, Inc, 1201 Eastlake Ave E., Seattle 98102 WA, USA, Phone: +12064426824, Fax: +12064426608, E-mail: bop@zgi.com

BERND PESCHKE, Becton Dickinson, Tullastr. 8-12, 69126 Heidelberg, Germany, Phone: +49 6221 305416, Fax: +49 6221 305407, E-mail: Eva\_Miller@Europe.bd.com

JORN MEIDAHN PETERSEN, NOVO NORDISK A/S Dept. Of Assay & Cell Technology, No Alle, DK 2880 Bagsvaerd, Denmark, Phone: +4544422634, E-mail: jmp@novonordisk.com

DAVID PHELAN, Thermo Trace, 189-199 Browns Road, Noble Park, 3174 Victoria, Australia, Phone: +61 3 9790 4100, Fax: +61 3 9790 4155, E-mail: scott\_sinclair@thermotrace.com.au

LAURENT PIERARD, Glaxosmithkline Biologicals, Rue de L'Institut 89, 1330 Rixensart, Belgium, Phone: +3226569674, Fax: +3226569013, E-mail: laurent.pierard@gskbio.com

HERVE PINTON, Aventis Pasteur, 1541 Avenue Marcel Merieux, 69280 Marcy L'Etoile, France, Phone: +330437379377, Fax: +330437373197, E-mail: herve.pinton@aventis.com

JORDI PLANAS, Laboratorios Hipra, Sa., Avda. La Selva 135, 17170 Amer, Spain, Phone: +34 (972) 330660, Fax: +34 (972) 430661, E-mail: jpcu@hipra.com

STEFANIE PLUSCHKELL, Pfizer Inc., Eastern Point Road, CT 06340 Groton, USA, Phone: +18607153325, Fax: +18607159675, E-mail: stefanie\_b\_pluschkell@groton.pfizer.com

LOURDES PORQUET, Laboratorios Hipra, Sa., Avda. de La Selva, 135, 17170 Amer, Spain, Phone: +34 (972) 430660, Fax: +34 (972) 430661, E-mail: lpg@hipra.com

ALISON PORTER, Lonza Biologics, Plc., 228 Bath Road, Slough, SL1 4DY Berkshire, UK, Phone: +441753716525, Fax: +441753716660, E-mail: silvana.palumbo@lonza.com

JEROME POUZET, Texcell/Institut Pasteur, 25-28 RUE DU dOCTEUR rOUX, 75724 Paris cedex 15, France, Phone: +33 1 45 68 84 35, Fax: +33 1 45 68 88 59, E-mail: ybarbier@pasteur.fr

MORTEN PRAESTEGAARD, Bioimage A/S, Moerkhoej Bygade 28,  
2860 SOEBORG, Denmark, Phone: +4544437524, E-mail:  
morten.praestegaard@bioimage.com

ALAIN PRALONG, Werthenstein Chemie Ag, Industriestrasse, 6105  
Schachen, Switzerland, Phone: +41414999680, Fax: +41414999600,  
E-mail: alain.pralong@spcorp.com

DAVID PRUDHOE, Cellon Sa, 29 AM Bechler, Bereldange 7213  
Luxembourg, Luxembourg, Phone: +352 263 3731, Fax: +352 311 052,  
E-mail: cellon@gms.lu

SEBASTIEN QUESMEY, Biomerieux, Chemin de L'Orme, 69280  
Marcy L'Etoile, France, Phone: +33478877567, Fax: +33478875319

GIANLUCA QUINTINI, Altana Pharma Ag, Byk - Gulden - Str. 2,  
78467 Konstanz, Germany, Phone: +497531843508, Fax:  
+4975318493350, E-mail: gianluca.quintini@altanapharma.de

SOREN RASMUSSEN, Symphogen A/S, Elektrovej, Building 375,  
2800 Lyngby, Denmark, Phone: +45 45 265084, Fax: +45 45 265060,  
E-mail: skr@symphogen.com

SRIDHAR REDDY, Vaxgen, 347 Oyster Point Blvd., 94080 South  
San Francisco, USA, Phone: +16506242376, Fax: +16506242436,  
E-mail: sreddy@vaxgen.com

ALISON REES, Xenova, 310 Cambridge SCZ. Park, Milton Road  
CB4 0WG Cambridge, UK, Phone: +441223436566, Fax:  
+441223423458, E-mail: alison\_rees@xenova.co.uk

UDO REICHL, Max Planck-Inst. Fur Dynamik Komplexer Tech.  
Syst., Sandtorstrasse 1, 39106 Magdeburg, Germany, Phone:  
+493916110200, Fax: +493916110203, E-mail: ureichl@mpi-  
magdeburg.mpg.de

JON REID, Hyclone Uk Ltd, Unit 9 Atley Way, North Nelson  
Industrial Estate NE23 1WA Cramlington, Northumberland, UK, Phone:  
+44 141 583 2142, Fax: +44 141 583 2136, E-mail:  
Jarlath.Keating@perbio.com

JUERGEN REINHARDT, Novartis Institute Of Biomedical Research,  
Lichtstr 35, CH 4002 Basel, Switzerland, Phone: +41613242273, Fax:  
+41613242870, E-mail: juergen.reinhardt@pharma.novartis.com

MARK RENDALL, Lonza Biologics, 228 Bath Road, SL1 4DY  
Slough, UK, Phone: +441753716552, Fax: +441753777001, E-mail:  
mrendall@lonza.co.uk

SHAUL REUVENY, Israel Institute For Biological Research, P.O  
Box 19, 74100 Ness Ziona, Israel, Phone: +97289381518, Fax:  
+97289401094, E-mail: reuveny@iibr.gov.il

PER REXEN, Novo Nordisk A/S, Brennum Park 25K1.1.13, 3400  
Hillerod, Denmark, Phone: +4544435412, E-mail:  
prex@novonordisk.com

ANTHONY RICHARDS, Hyclone Uk Ltd, Unit 9 Atley Way, North  
Nelson Industrial Estate NE23 1WA Cramlington, Northumberland, UK,  
Phone: +44 141 583 2142, Fax: +44 141 583 2136, E-mail:  
Jarlath.Keating@perbio.com

ANDREAS RICHTER, Newlab Bioquality, Max-Planck str. 15A,  
40699 Erkrath, Germany, Phone: +49 211 9255 351, Fax: +49 211 9255  
333, E-mail: dippel@newlab.de

ALISON RIDLEY, Cambridge Antibody Technology, Milstein  
Building, Granta Park CB1 6GH Cambridge, UK, Phone: +441223898,  
Fax: +441223471487, E-mail: liz.browne@cambridgeantibody.com

MARCO RIEDEL, Probiogen Ag, Goethestr 54, 13086 Berlin,  
Germany, Phone: +49309240060, Fax: +493092400619, E-mail:  
marco.riedel@probiogen.de

JARNO ROBIN, Maxygen, Agern Allé 1, 2970 Horsholm, Denmark,  
Phone: +4545178498, Fax: +4570205530, E-mail: jro@maxygen.dk

CAROLINA RODENAS, Glaxosmithkline, C/ Santiago Grisolia 4,  
28760 TRES CANTOS ( MADRID), Spain, Phone: +34918074029, Fax:  
+34918074062, E-mail: carolina.2.rodenas@gsk.com

ROMAN RODRIGUEZ, Hyclone Uk Ltd, Unit 9 Atley Way, North Nelson Industrial Estate NE23 1WA Cramlington, Northumberland, UK, Phone: +44 141 583 2142, Fax: +44 141 583 2136, E-mail: Jarlath.Keating@perbio.com

MARCEL ROELL, Wave Biotech Ag, Ringstr. 24, 8317 Tagelswangen/Schweiz, Switzerland, Phone: +41523542055, Fax: +41523542056, E-mail: pblanc@wavebiotech.ch

MARIETTE ROESINK, Amt, PO Box 22506, 1100 DA Amsterdam, The Netherlands, Phone: +31205667585, Fax: +31205669272, E-mail: m.roesink@amtbv.com

DOMINIQUE ROLLAND, Biomerieux, Chemin de L'Orme, 692 80 Mercy L'etoile, France, Phone: +33478872099, Fax: +33478872 101, E-mail: dominique.rolland@eu.biomerieux.com

GUNTER ROMER, Boehringer Ingelheim, Birkenorferstrasse 65, D-88397 Biberach, Germany, Phone: +49 73 51 54 48 01, Fax: +49 73 51 54 51 31, E-mail: evelyn.schmucker@bc.boehringer-ingelheim.com

FILIPA ISABEL ROSA, Ibet, Apartado 12, 2781-901 Oeiras, Portugal, Phone: +351214469424, Fax: +351214421161, E-mail: frosa@itqb.unl.pt

MARTY ROSENBERG, Promega Corporation, USA, E-mail: ccorral@promega.com

SCOTT ROSS, Sigma-Aldrich, Eschenstr, 5, 82024 Taufkirchen, Germany, Phone: +49 896513 1901, Fax: +49 896513 1919, E-mail: HHellwig@europe.sial.com

MONIKA ROTHWEILER, Rütten Engineering, Industriestrasse 9, 8712 Stäfa, Switzerland, Phone: +41 1928 2930, Fax: +41 1926 2802, E-mail: info@rutten.com

EDWARD ROUTLEDGE, Angel Biotechnology Limited, 44 Colbourne Crescent, Nelson Park, Cramlington Northumberland, UK, Phone: +441670591920, Fax: +441670591921, E-mail: edward.routledge@angelbio.com



VIBEKE ROWELL, Nunc, Kamstrupvej 90, 4000 Roskilde, Denmark,  
Phone: +45 4631 2181, Fax: +45 4631 2175, E-mail: cmn@nunc.dk

PAULINE RUDD, Oxford University, Dpt. of Biochemistry, South  
Park Road OX1 3QU Oxford, UK, Phone: +441865275340, Fax:  
+441865275796, E-mail: pauline.rudd@bioch.ox.ac.uk

NICOLINE RUIJS, Hyclone Uk Ltd, Unit 9 Atley Way, North Nelson  
Industrial Estate NE23 1WA Cramlington, Northumberland, UK, Phone:  
+44 141 583 2142, Fax: +44 141 583 2136, E-mail:  
Jarlath.Keating@perbio.com

KURT RUSS, Rentschler Biotechnologie, Erwin Rentschler Str. 21,  
D-88471 Laupheim, Germany, Phone: +497392701510, Fax:  
+497392701525, E-mail: kurt.russ@rentschler.de

KURT RÜTTEN, Rütten Engineering, Industriestrasse 9, 8712 Stäfa,  
Switzerland, Phone: +41 1928 2930, Fax: +41 1926 2802, E-mail:  
info@rutten.com

THOMAS RYLL, Abgenix, 6701 Kaiser Drive, CA 94555 Fremont,  
USA, Phone: +1 510 284 6495, Fax: +1 510 790 5280, E-mail:  
thomas.ryll@abgenix.com

SONIA SA SANTOS, Ibet, Apartado 12, 2781-901 OEIRAS,  
Portugal, Phone: +351214469424, Fax: +351214421161, E-mail:  
sasantos@itqb.unl.pt

PATRICK SALOU, Novartis Pharma S.A.S, Centre de  
Biotechnologie, 26 Rue de la Chapelle BP 349 68333 HUNINGUE,  
France, Phone: +33389895224, Fax: +33389895252, E-mail:  
patrick.salou@pharma.novartis.com

VOLKER SANDIG, Probiogen Ag, Goethestr 54, 13086 Berlin,  
Germany, Phone: +49309240060, Fax: +493092400619, E-mail:  
volker.sandig@probiogen.de

PATRICK SANTAMBIEN, Biosepra Sa, Division of CIPHERGEN, 48  
Avenue des Genottes 95800 Cergy Saint Christophe, France, Phone:  
+33134207824, Fax: +33134207878, E-mail:  
psantambien@ciphergen.com

PAUL SAUER, Protein Design Labs, 34801 Campus Drive, 94555 Fremont, CA., USA, Phone: +15105741549, Fax: +15105741500, E-mail: psauer@pdl.com

KERSTIN SAUTER, Boehringer Ingelheim, Birkenorferstrasse 65, D-88397 Biberach, Germany, Phone: +49 73 51 54 48 01, Fax: +49 73 51 54 51 31, E-mail: evelyn.schmucker@bc.boehringer-ingelheim.com

SARAH SCARTH, Avecia, P.O.Box 2, Belasis Avenue TS23 1YN Billingham, Cleveland, UK, Phone: +441642304117, Fax: +441642364463, E-mail: sarah.scarth@avecia.com

STEFAN SCHAEFER, Biogen Cientifica, Bejar, 36, 28028 Madrid, Spain, Phone: +34 (91) 361 10 27, Fax: +34 (91) 361 08 98, E-mail: rtrujillo@biogencientifica.com

KLAUS SCHARFENBERG, Fachhochschule Oldenburg - Ostfriesland - Wilhemshaven, Constantiaplatz 4, D-26723 Emden, Germany, Phone: +1604545594, Fax: +49218071593, E-mail: scharfenberg@fho-emden.de / scharfenberg@gmx.de

HUUB SCHELLEKENS, The Netherlands, E-mail: h.schellekens@gdl.uu.nl

PETER SCHLENKE, Rentschler Biotenchnlogie, Erwin Rentschler Srt. 21, D-88471 Laupheim, Germany, Phone: +497392701537, Fax: +497392701521, E-mail: peter.schlenke@rentschler.de

GEORG SCHMID, F. Hoffmann - La Roche, Non-Clinical Development, Biotechnology, Bldg. 66/112A 4070 Basel, Switzerland, Phone: +41616882986, Fax: +41616882420, E-mail: georg.schmid@roche.com

JÜRGEN SCHMITZ, Papaspyrou Biotechnologie, Karl-Heinz-Beckurts-Strasse 13, 52428 Jülich, Germany, Phone: +49 2461 890 578, Fax: +49 2461 690 860, E-mail: m.papaspyrou@papaspyrou.de

EVELYN SCHMUCKER, Boehringer Ingelheim, Birkenorferstrasse 65, D-88397 Biberach, Germany, Phone: +49 73 51 54 48 01, Fax: +49 73 51 54 51 31, E-mail: evelyn.schmucker@bc.boehringer-ingelheim.com

MARKUS SCHNEIDER, Laboratoires Serono, S.A, Zone Industrielle B, CH-1809 Fenil-Corsier, Switzerland, Phone: +41219232369, Fax: +41219232070, E-mail: markus.schneider@serono.com

YVES-JACQUES SCHNEIDER, Universite Catholique De Louvain, Pl. L. Pasteur, 1, B 1348 Louvain-La-Neuve, Belgium, Phone: +3210472791, Fax: +3210474895, E-mail: yjs@bioc.ucl.ac.be

WOLFGANG SCHNEIDER, Hyclone Uk Ltd, Unit 9 Atley Way, North Nelson Industrial Estate NE23 1WA Cramlington, Northumberland, UK, Phone: +44 141 583 2142, Fax: +44 141 583 2136, E-mail: Jarlath.Keating@perbio.com

IRIS SCHONIGER, Boehringer Ingelheim, Birkenorferstrasse 65, D-88397 Biberach, Germany, Phone: +49 73 51 54 48 01, Fax: +49 73 51 54 51 31, E-mail: evelyn.schmucker@bc.boehringer-ingelheim.com

BERND SCHRÖDER, Maingen, Lab. Zellsystems, Weismullerstr 45 60314 Frankfurt am Main, Germany, Phone: +49 69 426023264, Fax: +49 69 426023274, E-mail: bernd.schroeder@maingen.de

MAGNUS SCHROEDER, University Of Bielefeld, Inst. of Cell Culture Technology, Postfach 10 01 31 33501 Bielefeld, Germany, Phone: +49 521 1066318, Fax: +49 521 1066023, E-mail: msc@zellkult.techfak.uni-bielefeld.de

DIANA SCHUHBAUER, La Roche Ag, Switzerland, Phone: +41616885871, Fax: +41616882420, E-mail: diana.schuhbauer@roche.com

DIETER SCHULLER, Boehringer Ingelheim, Birkenorferstrasse 65, D-88397 Biberach, Germany, Phone: +49 73 51 54 48 01, Fax: +49 73 51 54 51 31, E-mail: evelyn.schmucker@bc.boehringer-ingelheim.com

JOANNE SCHULTZ, Zymo Genetics, Inc, 1201 Eastlake Ave E., Seattle 98102 WA, USA, Phone: +12064426824, Fax: +12064426608, E-mail: josz@zgi.com

EDWIN SCHWANDER, Nunc, Kamstrupvej 90, 4000 Roskilde, Denmark, Phone: +45 4631 2181, Fax: +45 4631 2175, E-mail: cmn@nunc.dk

SCHWEIZER, Paul Ehrlich Institut, Paul Ehrlich Strasse 51-59,  
63225 Langen, Germany, Phone: +49 6103 771008, Fax: +49 6103  
771240, E-mail: treal@pei.de

JORG SCHWINDE, Dasgip Ag, Rudolf-Schulten-Str. 5, 52428 Julich,  
Germany, Phone: +4924619800, Fax: +492461980100, E-mail:  
m.glier@dasgip.de

CHERYL SCOTT, Bioprocess International, executive Parkway  
#255, Eugene 97401 OREGON, USA, Phone: +15413452761, Fax:  
+15413455055, E-mail: cscott@bioprocessintl.com

CECILIA SENDRESEN, Molmed Spa, Via Olgettina 58, 20132  
Milano, Italy, Phone: +3902212771, Fax: +390221277220, E-mail:  
cecilia.sendresen@molmed.com

WONGI SEOL, Toolgen, Inc., Daedeok Biocommunity, 461-6,  
Jeonmin-dong, Yuseong-gu 305-390 Daejeon, Korea, South, Phone:  
+82428638166, Fax: +82428633840, E-mail: wseol@toolgen.com

STEPHANIE SHAFFER, Bioprocess International, One Research Dr,  
Suite 400 A 1581-0770 Westborough, MA, USA, Phone: +1508 614  
1443, Fax: +1508 616 0476, E-mail: bcaine@bioprocessintl.com

JOSEPH SHILOACH, Nih, Niddk, Biotechnology Unit, Bldg. 6 Rm  
B1-33 6 central Drive, 20892-2715 Bethesda, Maryland, USA, Phone:  
+13014969719, Fax: +13014515911, E-mail: yossi@nih.gov

YUVAL SHIMONI, Genentech, Inc, 1 DNA Way, MS32, 94080  
South San Francisco, CA, USA, Phone: +16502254711, Fax:  
+16502257203, E-mail: yshimoni@gene.com

SANETAKA SHIRAHATA, Dept. Of Genetic Resources Tech. Fac.  
Of Agriculture, Kyushu Univ., 6-10-1 Hakozaki, Higashi-ku, 812-8581  
Fukuoka, Japan, Phone: +81926423045, Fax: +81926423052, E-mail:  
sirahata@grt.kyushu-u.ac.jp

WILHELM SIEBERTZ, Greiner Bio-One GmbH, Maybachstr. 2,  
D-72636 Frickenhausen, Germany, Phone: +4970229480, Fax:  
+497022948514, E-mail: w.siebertz@greinerbioone.com

ANDRE SIEMENSMA, Quest International, Huizerstraatweg 28,  
LNL1411 GP Maarden, The Netherlands, Phone: +31 35 699 2458, Fax:  
+31 35 694 5684, E-mail: hans.huttinga@QuestIntl.com

ANDRÉ SILVESTRO, Bioreliance, Innovation Park Hillfoots Road,  
FK9 4NF Stirling, UK, Phone: +44 1786 451318, Fax: +44 1786 464764,  
E-mail: atullu@bioreliance.com

PATRICK SIMPSON, Innovatis Ag., Technologiezentrum,  
Meisenstrasse 96 33607 Germany, Germany, Phone: +495212997300,  
Fax: +495212997285, E-mail: sabine.kappes@innovatis.com

TONY SIMULA, Gropep Limited, PO BOX 10065 BC, 5000  
Adelaide, Australia, Phone: +61883547759, Fax: +61883547788, E-mail:  
tony.simula@gropep.com.au

SCOTT SINCLAIR, Thermo Trace, 189-199 Browns Road, Noble  
Park, 3174 Victoria, Australia, Phone: +61 3 9790 4100, Fax: +61 3 9790  
4155, E-mail: scott\_sinclair@thermotrace.com.au

WILLIAM SISK, Biogen, 14 Cambridge Center B6-6, 02142  
Cambridge, MA, USA, Phone: +16176792799, Fax: +16176793200,  
E-mail: william\_sisk@biogen.com

JAE SLY, Biovest International, 8500 Evergreen Boulevard,  
MN55433 Minneapolis, USA, Phone: +441519245351, Fax:  
+441512222309, E-mail: BiovestEurope@aol.com

MARK SMITH, Probiogen Ag, Goethestr. 54, 13086 BERLIN,  
Germany, Phone: +49309240060, Fax: +493092400660, E-mail:  
mark.smith@probiogen.de

RODNEY SMITH, Essex House 19 Hgh Street Earith, Huntingdon,  
Cambs PE28 3PP Cambridge, UK, Phone: +441487842869, E-mail:  
dr.rodders@tesco.net

ANN SMITH, Lorantis Ltd., 307 Cambridge Science Park, CB4 0WG  
Cambridge, UK, Phone: +4401223702500, Fax: +4401223702599,  
E-mail: ann.smith@lorantis.com

ALBERT SOLEY ASTALS, Universitat Autònoma De Barcelona,  
Dept. Eng. Química. Edif. C., Campus UAB 08193 Bellaterra, Spain,  
Phone: +34 (93) 5811808, Fax: +34 (93) 5812013, E-mail:  
albert.soley@uab.es

CORINNA SONDEREGGER, BIOCHEMIE GmbH, Biochemiestrasse  
10, 6250 Kundl, Austria, Phone: +4353382003852, Fax: +435338200461,  
E-mail: corinna.sonderegger@gx.novartis.com

VERENA SONNENMOSER, Boehringer Ingelheim, 88397 Biberach,  
Germany, Phone: +497351547861, Fax: +497351837861, E-mail:  
verena.sonnenmoser@bc.boehringer-ingelheim.com

MARCOS SOUSA, Ibet, Apartado 12, 2781-901 Oeiras, Portugal,  
Phone: +351214469424, Fax: +351214421161, E-mail:  
msousa@itqb.unl.pt

ERIKA SPENS, Department Of Biotechnology, Royal Institute of  
Technology, 10691 Stockholm, Sweden, Phone: +46855378305, Fax:  
+46855378323, E-mail: erika@biotech.kth.se

KAREN SPLINTER, Rütten Engineering, Industriestrasse 9, 8712  
Stäfa, Switzerland, Phone: +41 1928 2930, Fax: +41 1926 2802, E-mail:  
info@rutten.com

GUIDO STADLER, Iam (Inst. For Applied Microbiology),  
Muthgasse, 18, A-1190 Vienna, Austria, Phone: +43 1 360066248, Fax:  
+43 1 3697615, E-mail: h9240486@edv1.boku.ac.at

WILLIAM STAFFOPOULOS, Guava Technologies, Ciplastraat 2,  
2440 Geel, Belgium, Phone: +32475448313, Fax: +3214570560, E-mail:  
bstaffopoulos@guavatechnologies.com

OLAF STAMM, Newlab Bioquality, Max-Planck str. 15A, 40699  
Erkrath, Germany, Phone: +49 211 9255 351, Fax: +49 211 9255 333,  
E-mail: dippel@newlab.de

THOMAS STEENSTRUP, Novo Nordisk A/S, Novo Alle, 2880  
Bagsvaerd, Denmark, Phone: +4544424167, E-mail:  
stee@novonordisk.com

JAN STELLS, Cellon Sa, 29 AM Bechler, Bereldange 7213  
Luxembourg, Luxembourg, Phone: +352 263 3731, Fax: +352 311 052,  
E-mail: cellon@gms.lu

JOHN STERLING, Genetic Engineering News, 2 Madison Avenue,  
10538-1961 Larchmont, USA, Phone: +1 914 834 3100, Fax: +1 914 834  
3689, E-mail: nriviera@liebertpub.com

MARC STIJBOS, Hyclone Uk Ltd, Unit 9 Atley Way, North Nelson  
Industrial Estate NE23 1WA Cramlington, Northumberland, UK, Phone:  
+44 141 583 2142, Fax: +44 141 583 2136, E-mail:  
Jarlath.Keating@perbio.com

ANKE STOCK, Newlab Bioquality Ag, Max-Planck Srt. 15 A, 40699  
Erkrath, Germany, Phone: +492119255351, Fax: +492119255333,  
E-mail: dippel@newlab.de

THIBAUD STOLL, Novartis Pharma S.A.S, Centre de  
Biotechnologie, 26 Rue de la Chapelle BP 349 68333 HUNINGUE,  
France, Phone: +33389895224, Fax: +33389895252, E-mail:  
thibaud.stoll@pharma.novartis.com

PATRICK STRAGIER, Cambrex, Parc Industriel de Petit Rechain,  
4800 Verviers, Belgium, Phone: +32 87321 611, Fax: +32 87351 967,  
E-mail: roel.gordijn@cambrex.com

JOCHEN STRASSNER, Altana Pharma Ag, Byk-Gulden-Strasse 2,  
78467 Konstanz, Germany, Phone: +497531843538, Fax:  
+4975318493538, E-mail: jochen.strassner@altanapharma.com

CLAUDIO STREBEL, University Of Applied Science Wandenswil,  
Gruntal, 8820 Wandenswil, Switzerland, Phone: +4117899738, Fax:  
+41434778422, E-mail: c.strebel@hswzfh.ch

JÖRG STUCKI, Beckman Coulter, Europark Fichtenhain B13, 47807  
Krefeld, Germany, Phone: +49 2151 333 789, Fax: +49 2151 333 639,  
E-mail: jstucki@beckman.com

MARC STURZ, Innovatis Ag., Technologiezentrum, Meisenstrasse  
96 33607 Germany, Germany, Phone: +495212997300, Fax:  
+495212997285, E-mail: sabine.kappes@innovatis.com

RICK SULLIVAN, Hy Clone, 925 West 1800 South, 84321 Logan, UT, USA, Phone: +14357534584, Fax: +14357534589, E-mail: rick.sullivan@perbio.com

TISH SUMMAL, Becton Dickinson, Tullastr. 8-12, 69126 Heidelberg, Germany, Phone: +49 6221 305416, Fax: +49 6221 305407, E-mail: Eva\_Miller@Europe.bd.com

TAKAMOTO SUZUKI, Kirin Brewery Co. Ltd, Pharmaceutical Co., 6-26-1 Jingumae Shibuya-ku, 150-8011 Tokyo, Japan, Phone: +81354856207, Fax: +81334996152, E-mail: tak-szk@jcom.home.ne.jp

JUDITH SYMES, Lonza Biologics, Plc., 228 Bath Road, Slough, SL1 4DY Berkshire, UK, Phone: +441753716588, Fax: +441753716660, E-mail: silvana.palumbo@lonza.com

MICHAEL SZARDENINGS, Osleweg 20, D38302 Wolfenbittel, Germany, Phone: +4953311977794, Fax: +491707625431, E-mail: msz@winet.de

ANDREW TAIT, University College London, Torrington Place, WC1 7JE London, UK, Phone: +61 422947164, E-mail: a.tait@ucl.ac.uk

TAMURA TAKASHI, Dept. Of Genetic Resources Tech. Kyushu Univ., 6-10-1 Hakozaki, 812-8581 Fukuoka, Japan, Phone: +81926423045, Fax: +81926423050, E-mail: tatamura@grt.kyushu-u.ac.jp

MYLENE TALABARDON, Idec Pharmaceuticals, 110011 Torreyana Rd., 92121 San Diego (CA), USA, Phone: +18584318500, Fax: +18584318750, E-mail: mtalabardon@idecpharm.com

CHRISTINE TANS, Glaxosmithkline Biologicals, Rue de L'Institut 89, 1330 Rixensart, Belgium, Phone: +3226569674, Fax: +3226569013, E-mail: christine.tans@gskbio.com

LINA TAO, Serologicals Corporation, The Magdalene Centre, Oxford Science Park OX4 4GA Oxford, UK, Phone: +441865784646, Fax: +441865784648, E-mail: jnicacio@serologicals.com



ALEXANDER TAPPE, Institut Für Technische Chemie, Callinstr. 3,  
30167 Hannover, Germany, Phone: +49 511 7622966, Fax: +49 511  
7623004, E-mail: tappe@iftc.uni-hannover.de

JEAN-MARC TEISSIER, Stedim, Z.I. Des Paluds, Avenue de  
Jouques BP1051 13781 Aubagne cedex, France, Phone: +33 4 42 84 56  
31, Fax: +33 4 42 84 56 17, E-mail: m-monge@stedim.fr

SATOSHI TERADA, Fukui University, 3-9-1 Bunkyo, 910-8507  
Fukui, Japan, Phone: +81776278645, Fax: +81776278747, E-mail:  
terada@acbio.fukui-u.ac.jp

LINDA THOMPSON, Hyclone Uk Ltd, Unit 9 Atley Way, North  
Nelson Industrial Estate NE23 1WA Cramlington, Northumberland, UK,  
Phone: +44 141 583 2142, Fax: +44 141 583 2136, E-mail:  
linda.thompson@perbio.com

JOHN THRIFT, Bayer Corporation, 800 Dwight Way, 94701-1986  
Berkeley, California, USA, Phone: +5107055426, Fax: +5107055451,  
E-mail: john.thrift.b@bayer.com

ANNIE TIRABY, Cayla/Invivogen, 5, rue Jean Rodier, 31405  
Toulouse, France, Phone: +33562716939, Fax: +33562716930, E-mail:  
cayla@cayla.com

STEFAN TOEMOE, Tecan, Schmalweg 50, 55252 Mainz-Kastel,  
Germany, Phone: +496134181424, E-mail: stefan.toemoe@tecan.com

GUNTER TRAUB, Greiner Bio-One GmbH, Maybachstr. 2, D-7263 6  
Frickenhausen, Germany, Phone: +4970229480, Fax: +497022948514,  
E-mail: g.jenisch@greinerbioone.com

HELMUT TRAUTMANN, Biospectra Ag, ZUERCHERSTRASSE  
137, CH8952 ZURICH - SCHLIEREN, Switzerland, Phone:  
+4117556700, Fax: +4117556729, E-mail: trautmann@biospectra.ch

WILTRUD TREFFENFELDT, DOW DEUTSCHLAND GmbH &  
Co OHG, Am Kronberger Hang 4, 65824 Schwalbach/Taunus, Germany,  
Phone: +496196566232, Fax: +496196566440, E-mail:  
wtreffenfeldt@dow.com

MANISHA TRIVEDI, Williamsburg Bioprocessing Foundation,  
P.O.Box 1229, Virginia Beach 23451 , USA, Phone: +17574238823, Fax:  
+17574232065, E-mail: mtrivedi@wilbio.com

EVELYN TRUMMER, Acbt - Austrian Center Of Biopharmaceutical  
Technology, Muthgasse 18, A-1190 Vienna, Austria, Phone:  
+431360066230, Fax: +4313697615, E-mail: h9740207@edv1.boku.ac.at

TATJANA TRUMMER, Roche Diagnostics GmbH, Nonnenwald 2,  
82377 Penzberg, Germany, Phone: +498856602165, Fax:  
+498856603529, E-mail: ulrich.behrendt@roche.com

FRITZ TSCHOPP, Sensorix, Technoparkstrasse 1, 8005 Zurich,  
Switzerland, Phone: +41 1 4451246, Fax: +41 1 4451247, E-mail:  
info@sensorix.com

HILARY TURNBULL, Genetic Engineering News, 2 Madison  
Avenue, 10538-1961 Larchmont, USA, Phone: +1 914 834 3100, Fax: +1  
914 834 3689, E-mail: nrivera@liebertpub.com

AXEL ULLRICH, Max-Planck-Institut Für Biochemie, Am  
Klopferspitz 18A, 82152 Martinsried, Germany, Phone: +4989857825,  
Fax: +4989857786, E-mail: ullrich@biochem.mpg.de

PABLO UMAÑA, Glycart Biotechnology Ag, Wayistrasse 18,  
Schieren 8952 Zurich, Switzerland, Phone: +4117556161, Fax:  
+4117556160, E-mail: pablo.umana@glycart.com

MARC VALER, Agilent Technologies, Hewlett Packard Stra. 8,  
76337 Waldbronn, Germany, Phone: +497243602470, Fax:  
+497243602149, E-mail: marc\_valer@agilent.com

JANA VAN DE GOOR, Genentech, Inc., 1 DNA way, 94080 South  
San Francisco (CA), USA, Phone: +16502252018, E-mail:  
goor@gene.com

HANS VAN DEN BERG, Applisens, De Brauwweg, 13, 3125AE  
Schiedam, The Netherlands, Phone: +31 10 298 3555, Fax: +31 10 437  
9648, E-mail: APPLISENS@APPLIKON.COM

ARNO VAN DER ARK, Nvi, Antonie van Leeuwenhoeklaan 11.,  
3720 AL Bilthoven, The Netherlands, Phone: +31 302743218, Fax: +31  
302744426, E-mail: arno.van.der.ark@nvi-vaccin.nl

TINY VAN DER VELDEN, Netherlands Vaccin Institute (Nvi), PO  
Box 457, 3720 AL Bilthoven, The Netherlands, Phone: +31 30 2742360,  
Fax: +31 302744426, E-mail: tiny.van.der.velden@nvi-vaccin.nl

K. VAN DONGEN, Jm Separations Bv, Boschdijk 780, 5624 CL  
Eindhoven, The Netherlands, Phone: +31402197480, Fax:  
+31402107499, E-mail: info@jmseparations.com

KIRK VAN NESS, Amgen, 51 University St., Seattle, USA, Phone:  
+14258447115, E-mail: vannessk@amgen.com

NADINE VAN OPSTAELE, Hyclone Uk Ltd, Unit 9 Atley Way,  
North Nelson Industrial Estate NE23 1WA Cramlington,  
Northumberland, UK, Phone: +44 141 583 2142, Fax: +44 141 583 2136,  
E-mail: Jarlath.Keating@perbio.com

EDWIN VAN WEERT, New Brunswick Scientific, 163 Dixons Hill  
Road, North Mymms AL9 7JE Hatfield, UK, Phone: +44 1707 275733,  
Fax: +44 1707 267859, E-mail: moritz@nbsuk.co.uk

MARC VANDER KELEN, Henogen, Sa., Rue des Prof. Jeener et  
Brachet 12, B-6041 Gosselies, Belgium, Phone: +3271378901, Fax:  
+3271378973, E-mail: marc.vanderkelen@henogen.com

JOZSEF VASI, Amersham Biosciences Ab, Bjorkgatan 30, 751 84  
Uppsala, Sweden, Phone: +46186120736, Fax: +46186121844, E-mail:  
jozsef.vasi@eu.amershambiosciences.com

CARMEN VELA, Ingenasa, Inmunología y genética aplicada, C/  
Hermanos García Noblejas, 41 28037 Madrid, Spain, Phone: +34 (91)  
388 05 01, Fax: +34 (91) 408 75 98, E-mail: cvela@ingenasa.es

DANIEL VELEZ, Im Clone Systems, 22 Chubb Way, Somerville  
08876 New Jersey, USA, Phone: +19085418016, Fax: +19082180344,  
E-mail: danv@imclone.com

DAVID VENABLES, Q-One Biotech, West of Scotland Science Park, G20 0XA Glasgow, UK, Phone: +44 141 947 011, Fax: +44 141 9467 011, E-mail: jrudd@q-one.co.uk

FARLAN VERAITCH, The University Of Birmingham, Chemical Engineering, Edgbaston B15 2TT Birmingham, UK, Phone: +447815310342, Fax: +441214145324, E-mail: farlanveraitch@hotmail.com

UTE VESPERMANN, CORNING GmbH, Melchersstr. 73, 48149 , Germany, Phone: +491709350017, Fax: +31206597673, E-mail: vespermau@corning.com

JOAQUIM VIVES, UNIVERSITY OF EDINBURGH-The Institute For Stem Cell Research, West Mains Road, The Roger Land Building, Kings Building EH9 3JQ Edinburgh, Scotland, UK, E-mail: quimv@hotmail.com

ANGELIKA VIVIANI, Hochschule Wädenswil, Einsiedlerstr. 29b, 8820 Wädenswil, Switzerland, Phone: +4117899717, Fax: +4117899950, E-mail: a.viviani@hswzfh.ch

REGINA VOGLAUER, Institute For Applied Microbiology, Muthgasse 18, A-1190 Vienna, Austria, Phone: +431360066231, Fax: +4313697615, E-mail: r.voglauer@iam.boku.ac.at

DAMIEN VOISARD, Serono, Zone Industrielle B, 1809 Fenil-Sur-Corsier, Switzerland, Phone: +41219232000, Fax: +41219232013, E-mail: rachel.zohar@serono.com

MICHAEL VON PEIN, Cambrex, Parc Industriel de Petit Rechain, 4800 Verviers, Belgium, Phone: +32 87321 611, Fax: +32 87351 967, E-mail: roel.gordijn@cambrex.com

BENEDICTE VONACH, Novartis Pharma Ltd., WKL-681.1.05, 4002 Basel, Switzerland, Phone: +41616961270, Fax: +41616963373, E-mail: benedicte.vonach@pharma.novartis.com

JURGEN VORLOP, Chiron Behring GmbH @ Co., Emil-Von-Behring Str. 76, 35041 Marburg, Germany, Phone: +496421394919, Fax: +496421392829, E-mail: juergen\_vorlop@chiron-behring.com

ROLAND WAGNER, Cell Culture Technology (Zkt) / Gbf,  
Mascheroder Weg 1, D-38124 Braunschweig, Germany, Phone:  
+495316181104, Fax: +495316181488, E-mail: wagner.roland@gbf.de

ERNST WAGNER, Ludwig-Maximilians-Universität, Biotechnology,  
Butenandtstr 5-13, Building D D-81377 Munich, Germany, Phone: +49  
89 21807841, Fax: +49 89 21807798, E-mail: ernst.wagner@cup.uni-  
muenchen.de

JENNIFER WALOWITZ, Gibco Invitrogen Corp., 3175 Staley Road,  
14072 Grand Island, USA, Phone: +17167743104, Fax: +17167746996,  
E-mail: jennifer.walowitz@invitrogen.com

FRANZ WALZ, Boehringer Ingelheim, Birkenorferstrasse 65, D-  
88397 Biberach, Germany, Phone: +49 73 51 54 48 01, Fax: +49 73 51  
54 51 31, E-mail: evelyn.schmucker@bc.boehringer-ingelheim.com

SALLY WARBURTON, Eccac, CAMR, Salisbury SP4 0JG  
Wiltshire, UK, Phone: +44 1980 612773, Fax: +44 1980 611315, E-mail:  
Lisa.Reynolds@camr.org.uk

BRENDA WEBB, Global Meeting Planning, World Trade Center,  
Cardiff Intl. Arena, Mary Ann Street, Cardiff CF10 2EQ Wales, UK,  
Phone: +442920232322, Fax: +442920232325, E-mail:  
brenda@global-meeting.co.uk

WILFRIED WEBER, Swiss Federal Institute Of Technology, Inst. of  
Biotechnology, ETH Hönggerberg CH-8093 Zürich, Switzerland, Phone:  
+41 1 6332107, Fax: +41 1 6331051, E-mail: weber@biotech.biol.ethz.ch

HU WEI-SHOU, University Of Minesota, 421 Washington Ave SE,  
55455 Mineapolis, USA, Phone: +1 612 625 0546, E-mail:  
bioeng@cems.umn.edu

ZENG WENLIN, Abgenix Inc., 6701 Kaiser Dr., CA94555  
FREMONT, USA, Phone: +15102846466, E-mail:  
wenlin.zeng@abgenix.com

JOHN WERENNE, Universite Libre De Bruxelles, 50 Av. F. D.  
Roosvelt, 1050 Brussels, Belgium, Phone: +3226503229, Fax:  
+3226503230, E-mail: biocelan@ulb.ac.be

ANDREAS WERNER, BOEHRINGER INGELHEIM Gmbh, Binger Strasse 173, 55216 Ingelheim, Germany, Phone: +49 77 97488, Fax: +49 77 98287, E-mail: andreas.werner@ing.boehringer-ingelheim.com

BILL WHITFORD, Hyclone UK Ltd, Unit 9 Atley Way, North Nelson Industrial Estate NE23 1WA Cramlington, Northumberland, UK, Phone: +44 141 583 2142, Fax: +44 141 583 2136, E-mail: Jarlath.Keating@perbio.com

MATTHIAS WIESER, Institute For Applied Microbiology, Muthgasse, 18, A-1190 Vienna, Austria, Phone: +431360066802, E-mail: mwieser@edv2.boku.ac.at

BERND-ULRICH WILHELM, B Braun Biotech International, Spain, Phone: +495661713636, Fax: +495661929945, E-mail: yadigar.aydin-talay@bioscipro.com

GILES WILSON, Novo Nordisk, Hageornsvej 1 Gentofte, G2820 Copenhagen, Denmark, Phone: +45 4443 8299, Fax: +45 4443 9210, E-mail: gcw@novonordisk.com

JAMES WILSON, Serologicals Ltd., 4 Fleming Road, Kirkton Campus EH54 7BN Livingston, UK, Phone: +441506404000, Fax: +441506404001, E-mail: jwilson@serologicals.com

KARSTEN WINKLER, Probiogen Ag, Goethestr 54, 13086 Berlin, Germany, Phone: +49309240060, Fax: +493092400619, E-mail: claudia.schulz@probiogen.de

MARC WINTGENS, Hyclone UK Ltd, Unit 9 Atley Way, North Nelson Industrial Estate NE23 1WA Cramlington, Northumberland, UK, Phone: +44 141 583 2142, Fax: +44 141 583 2136, E-mail: Jarlath.Keating@perbio.com

LIN WIRTH, Adolf Kühner Ag, Dinkelbergstr. 1, 4127 Birsfelden, Switzerland, Phone: +41 61 319 93 93, Fax: +41 61 319 93 94, E-mail: mkuhner@kuhner.com

MANFRED WIRTH, Gbf, Mascheroder Weg 1, 38124 Braunschweig, Germany, Phone: +495316181473, Fax: +495316181262, E-mail: mwi@gbf.de

*List of Participants*

xcv

JENS CHRISTIAN WORTMANN, Genmab A/S, Toldbodgade 59B,  
1253 Denmark, Denmark, Phone: +4533779601, Fax: +4525403021,  
E-mail: jcw@genmab.com

GARY WRIGHT, Biovest International, 8500 Evergreen Boulevard,  
MN55433 Minneapolis, USA, Phone: +441519245351, Fax:  
+441512222309, E-mail: BiovestEurope@aol.com

MON-HAN WU, Imperial College London, Department of Chemical  
Engineering, SW7 2BY London, UK, Phone: +442075895111, Fax:  
+442075945629, E-mail: mon-han.wu@ic.ac.uk

KARSTEN WUNSCHHEL, Quest International, Huizerstraatweg 28,  
LNL1411 GP Maarden, The Netherlands, Phone: +31 35 699 2458, Fax:  
+31 35 694 5684, E-mail: ann.goebel@QuestIntl.com

FLORIAN WURM, Epfl, Dpt. de chimie. Centre de Biotechnologie,  
FSB-ISP-LBTC 1015 Lausanne, Switzerland, Phone: +41 21 693 6141,  
Fax: +41 21 693 6140, E-mail: florian.wurm@epfl.ch

QUIANGHUA XU, Dept. Of Genetic Resources Tech. Fac. Of  
Agriculture. Kyushu Univ., 6-10-1 Hakozaki - Higashiku, 812-8581  
Fukuoka, Japan, Phone: +81926423045, Fax: +81926423052, E-mail:  
qianghua369@yahoo.com

CHRIS YALLOP, Crucell, Archimedesweg 4, 2333 Leiden, The  
Netherlands, Phone: +31715248959, Fax: +31715248702, E-mail:  
c.yallop@crucell.com

KANA YANAGIHARA, Eukui University, 3-9-1 Bunkyo, 910-8507  
Fukui, Japan, Phone: +81776278645, Fax: +81776278747, E-mail:  
terada@acbio.fukui-u.ac.jp

MEIJIA YANG, Serono Reproductive Biology Institute, 1 Technology  
Place, MA02370 Rockland, USA, Phone: +17816812375, Fax:  
+17816812910, E-mail: meijia.yang@serono.com

JEFF YANT, Amgen Inc., One Amgen Center Drive., MS 185-1-A  
91320-1799 Thousand Oaks (CA), USA, Phone: +18054472690, Fax:  
+18054996819, E-mail: jyant@amgen.com

KAICHI YOSHIZAKI, Faculty Of Agriculture, Kyushu University,  
Dep. Of Genetic, 6-10-1 Hakozaki, Higashi-ku, Fukuoka 812-8581 ,  
Japan, Phone: +81926423045, Fax: +81926423052, E-mail:  
y-kaichi@grt.kyushu-u.ac.jp

STEFANIE ZAHN, Papaspyrou Biotechnologie, Karl-Heinz-  
Beckurts-Strasse 13, 52428 Jülich, Germany, Phone: +49 2461 890 578,  
Fax: +49 2461 690 860, E-mail: i.landen@papaspyrou.de

MICHAEL ZANG-GANDOR, Eugenex Biotechnologies,  
Konstanzerstr. 19, CH-8274 Taegerwilen, Switzerland, Phone:  
+41716664361, Fax: +49753397624, E-mail:  
m.o.zang-gandor@eugenex.com

ED ZAPPEIJ, Applikon Bv, De Brauwweg, 13, 3125AE Schiedam,  
The Netherlands, Phone: +31 10 298 3555, Fax: +31 10 437 9648,  
E-mail: APPLISENS@APPLIKON.COM

TRACEY ZECCHINI, Astex Technology, 436 Cambridge Science  
Park, Milton Road CB4 0QA Cambridge, UK, Phone: +441223434992,  
Fax: +441223226201, E-mail: t.zecchini@astex-technology.com

CHUN ZHANG, Bayer Corporation, 800 Dwight Way, 94710  
Berkeley, CA, USA, Phone: +15107054416, E-mail:  
chun.zhang.b@bayer.com

THIERRY ZIEGLER, Sorebio, Site Montesquieu, 1 avenue Jacques  
Monod 33650 Martillac, France, Phone: +330557960968, Fax:  
+330556647766, E-mail: thierry.ziegler@serono.com



## CHAPTER 1

### CELLULAR MECHANISMS

MON-HAN WU<sup>1</sup>, GEORGE DIMOPOULOS<sup>2</sup>, ATHANASIOS  
MANTALARIS<sup>1</sup> AND JULIE VARLEY<sup>1</sup>

## EFFECT OF OSMOTIC PRESSURE ON GS-NS0 EXPRESSION SYSTEM

*1Department of Chemical Engineering, Imperial College, London, London  
SW7 2AZ, U.K. 2Centre for Molecular Microbiology & Infection, Imperial  
College, London, London SW7 2AZ, U.K.*

Abstract. It has been widely reported that metabolism, cell growth, cell density, product secretion and specific antibody productivity in mammalian cells is strongly affected by osmotic conditions. However, because hyper- and hypo-osmotic pressure suppresses cell growth, the enhanced final product concentration of the culture is not observed. Therefore by understanding the basic cellular processes of a GS-NS0 mammalian cell culture system would not only assist in the design of a more efficient mammalian cell culture systems but it will also aid the optimization of the production. Various properties of mammalian culture systems, such as, productivity, cell viability, metabolism, ion balance and the genes regulated during the culture of the GS-NS0 system under osmotic pressure of 210, 290, 370 and 450 mOsm/kg have been identified, and it is shown that there is a decrease in the growth rate of hyper- and hypo-osmotic cultures. Further differences have been identified in calcium accumulation, metabolism of glucose, glutamate and lactate. Additionally it is shown that there are over 600 genes involved in ion transport, accumulation of osmolytes, cell cycle distribution, proliferation, cytoskeletal organization and cell metabolism that are regulated by the changes in osmotic pressure.

### 1. INTRODUCTION

In numerous studies it has been reported that osmotic pressure affects cellular behaviour during antibody production processes [1]; an improved understanding of these effects might lead to the development of methodologies which might provide economically attractive means of increasing the specific antibody productivity in both hybridoma and transfectoma [2]. However, as hyper- and hypo-osmotic pressure is known to suppress cell growth, the enhanced antibody productivity of the produced cells in a hyperosmotic batch culture does not necessarily result in a substantial increase in final antibody concentration [3]. Some efforts have been made towards understanding aspects of cell function relevant to osmolarity effects. Various cellular functions have been found to relate to osmotic pressure, including cell growth rate [4], accumulation of osmoprotectants [5], cell cycle distribution [6], cell volume change and cellular metabolic rate [7], antibody production rate [3], total RNA and IgG mRNA transcription rate [2], translation rate [8] and antibody stability. However, without a more detailed understanding of the biological effects of osmolarity on the antibody production process in cells, a systematic method of improving the antibody production under hyperosmotic cultures will remain elusive.

To understand these effects at a genetic level, DNA microarrays hold great promise [9]. This gene expression-profiling technique permits the analysis of the expression levels of thousand of genes simultaneously. Here, a systematic method for investigating the role of osmolarity on the production processes from the level of growth, metabolism and gene expression is proposed. The expression profiles of the GS-NS0 system under different osmotic cultures are studied by identifying the regulation and the expression levels of around 7000 genes of the cells. During the cell culture process, expression of mRNA is analysed using oligo-DNA microarrays and metabolism and ion balance are analysed using a BioProfile Analyser (Nova Biomedical).

## 2. MATERIALS AND METHODS

### 2.1. Cell Line, Medium and Culture Maintenance

The GS-NS0 mouse myeloma cell line 6A1(100)-3 supplied by Lonza Biologics (UK) was used in all experiments. The cell line has been transfected with the glutamine synthetase selectable marker with expression of a chimeric B72.3 IgG4 antibody. Cells were cultured using Dulbecco's Modified Eagles's Medium with 2%(v/v) FBS. Different osmotic culture medium was prepared by varying the amount of NaCl in the standard medium to create 210, 290, 370 and 450 mOsm/kg medium. Cells growing in exponential phase were inoculated at  $2.0 \times 10^5$  cells/ml into a 1-L shake flask with 200 ml working volume, and 5% CO<sub>2</sub> was gased in the head space and agitated at 125 rpm in an orbital shaking incubator at a temperature of 36.5°C.

### 2.2. Viability, Metabolism and Medium Ion Concentration

Samples were taken daily at specific intervals during the culture duration. Cell concentration was estimated using a hemacytometer, and the trypan blue dye-exclusion method was used to distinguish between viable and dead cells. Na<sup>+</sup>, K<sup>+</sup>, Ca<sup>2+</sup>, NH<sup>4+</sup>, glucose, glutamate, glutamine and lactate concentrations were measured using a BioProfile 200 Analyser (Nova Biomedical).

### 2.3. Gene Expression Analysis

$2 \times 10^7$  cells were taken and palleted from the culture during mid-log phase of growth. Total cytoplasmic RNA was isolated using RNeasy total RNA extraction kit (Qiagen) and mRNA isolated using Oligotex mRNA extraction kit (Qiagen). Cy-3 and Cy-5 dye (Amersham Pharmacia) was incorporated into cDNA through a reverse transcription from the isolated mRNA according to methods described by Celis *et al* [9] and hybridized to Mouse Known Gene Oligo-DNA Microarray Chips provided by Human Genome Mapping Project Research Centre (Hinxton, U.K.). After the hybridization process of 20 hour, the microarray chips were washed and

scanned with a confocal laser scanner GenePix 4000B (Axon Instruments) and the scanned images were analysed using GenePix Pro software.

### 3. RESULTS AND DISCUSSION

#### 3.1. Effect of Osmotic Pressure on Cell Growth and Cell Viability

The viable cell count and cell viability for all four different osmotic pressures are shown in Figure 1 as a function of culture duration. In the present study, a slower growth rate was observed under both the hyper- and hypo-osmotic pressure environments as compared to growth at the normal osmotic condition. As shown in Fig. 1, the normal osmotic culture (290mOsm/kg) reached its peak around 100 hours while the cultures grown at osmotic pressure of 370 mOsm/kg and 450 mOsm/kg reached their peak around 120 hours and 145 hours, respectively. The maximum cell density for the normal osmotic culture was also higher than those of the hyper- and hypo-osmotic culture; calculated values show  $1.2 \times 10^6$  cells/ml,  $1 \times 10^6$  cells/ml and  $9.1 \times 10^5$  cells/ml for the 290 mOsm/kg, 370 mOsm/kg and 450 mOsm/kg cultures respectively. GS-NS0 cells did not survive under the hypo-osmotic culture condition of 210 mOsm/kg.

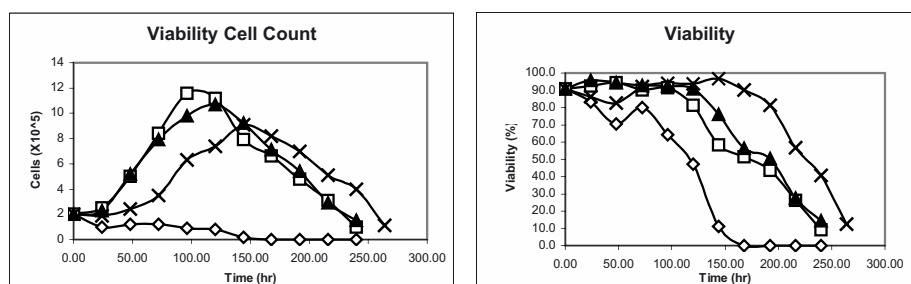


Fig. 1. Viable cell count and cell viability data for 210 mOsm/kg ( $\diamond$ -), 290 mOsm/kg ( $\square$ -), 370 mOsm/kg ( $\blacktriangle$ -) and 450 mOsm/kg ( $\times$ -)

It had been widely reported that cell growth is suppressed and cell viability drops for mammalian cells under hyper- and hypo-osmotic cultures [10]. For KR12H-2 transfectoma, when the osmotic pressure was increased from 285 mOsm/kg to 425 mOsm/kg, the specific growth rate and maximum viable cell concentration decreased by 20% and 48%, respectively [2]. In OKT3 hybridoma cells, it has been shown that cells were unable to proliferate above osmolarities of 500 mOsm/kg, and the maximal viable cell density dropped by 50%, with the specific cell growth rate also decreasing by 43%, when osmolarity increased from 335 to 425 mOsm/kg [6].

Even though earlier studies suggest that cell viability declines in hyperosmotic culture [6], in the present study using a GS-NS0 cell line, the results show that the

cell viability remained around 90% for all three normal- and hyper- cultures during the growth phase, and subsequently in all cases began to decay after the stationary phase of the culture (see Fig. 1).

### 3.2. Effect of Osmotic Pressure on Ion Balance and Metabolism

The effect of osmotic pressure on the concentration of  $\text{NH}_4^+$ , glucose, glutamate and lactate during the cultures are shown in Figure 2. Due to differences in the growth and viability profiles, the metabolic profile of the 210 mOsm/kg culture was very different to that for other osmotic culture conditions. However, even with a similar growth profile for the 290 and 370 mOsm/kg culture, the metabolic profile of the cultures were significantly different, with higher production of lactate and  $\text{NH}_4^+$  in the 290 mOsm/kg culture. Ion concentration measurements are shown in Fig. 3; these results indicate that the sodium concentration did not change dramatically over the culture period, and also that the trend in calcium concentration was similar in all cultures. However, even though it was observed that potassium did accumulate at the beginning of 290, 370 and 450 mOsm/kg cultures (within the cell environment), a greater accumulation was observed in the 370 and 450 mOsm/kg culture, as compared to the 290 mOsm/kg culture.

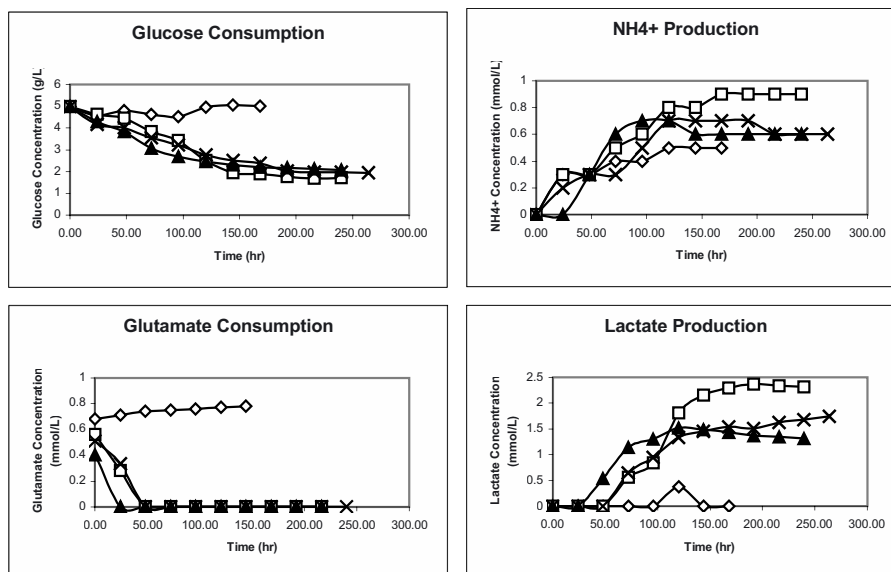


Fig. 2. Metabolism data for 210 mOsm/kg (-◇-), 290 mOsm/kg (-□-), 370 mOsm/kg (-▲-) and 450 mOsm/kg (-×-)

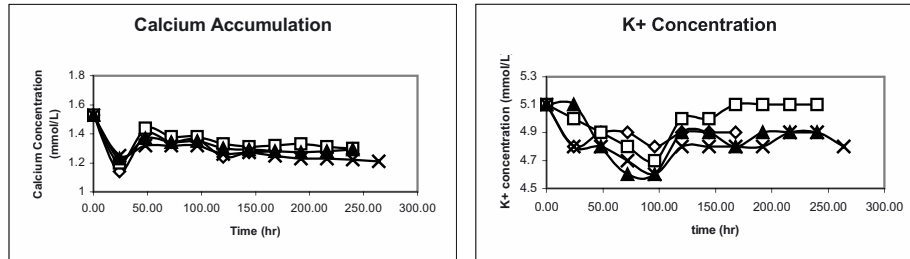


Fig. 3. Ion concentration data for 210 mOsm/kg (-◇-), 290 mOsm/kg (-□-), 370 mOsm/kg (-▲-) and 450 mOsm/kg (-×-)

In many studies of other mammalian culture systems, cellular metabolic rates have shown an increase during hyper-osmotic culture conditions. In NS0, after a shift of osmotic pressure from 275 mOsm/kg to 400 mOsm/kg, the glucose and glutamate uptake rate have been shown to increase by 2 and 6-fold, respectively, and lactate production to increase 4-fold [7]. In transfectoma, both glucose uptake rate and lactate production rate were significantly elevated at higher osmolarity, but the ratio of lactate production to glucose consumption did not change significantly, regardless of osmolarity increasing from 285 mOsm/kg to 425 mOsm/kg [2].

### 3.3. Effect of Osmotic Pressure on Gene Expression

DNA microarray techniques have been developed to examine thousands of genes *in situ*. They can be applied to expression monitoring, which involves measuring transcription levels under various physiological conditions; thus one is then able to identify regulatory expression patterns [11]. In the experiments conducted here, it was observed that out of 7,445 genes, transcription of 377 genes were changed by at least 2 fold under 210 mOsm/kg osmotic culture conditions, 720 genes under 370 mOsm/kg osmotic culture conditions and 680 genes under 450 mOsm/kg osmotic culture conditions. In Table 1 the categorized gene expression data is shown.

Table 1. Number of genes with greater than two fold up or down regulation in 210, 370 and 450 mOsm/kg cultures

Cultures Classifications	210 mOsm/kg		370 mOsm/kg		450 mOsm/kg	
	Up Regulated	Down Regulated	Up Regulated	Down Regulated	Up Regulated	Down Regulated
Cell Cycle and Proliferation	30	50	46	29	38	38
Cell Physiology	5	13	45	11	52	15
Cell Metabolism	44	15	71	63	57	75
Signaling and Transport	43	52	126	78	183	86
Others	62	63	169	82	82	54

Various genes related to cell cycle distribution, growth, transcription and translation regulation and cell proliferation were found to be affected by changes in osmotic pressure. Osmotic shock inhibits cell proliferation and also affects cell cycle control [12]. It was observed that in both hyper- and hypo-osmotic cultures, genes related to cell cycle and cell cycle control were up regulated; genes related to cell growth and maintenance were mostly down regulated; and genes related to transcriptional regulation were also mostly down regulated. In terms of apoptosis related genes, it was observed that most were down regulated in hypo-osmotic culture (210 mOsm/kg), whilst these genes were up regulated in hyper-osmotic cultures (370 and 450 mOsm/kg). The same trend was observed in DNA replication related genes.

In previous studies, hyperosmotic pressure has been shown to induce G1 phase arrest. A study using a CHO cell line showed that, under 335 mOsm/kg culture conditions, the percentage of cells in G1 and S phase was 33% 54%, respectively; under 425 mOsm/kg conditions, the distribution of cells in the cell cycle was 51% G1 phase and 38% S phase [13]. It has been observed that specific growth rates of antibody production cells in bioreactors are depressed at higher osmolarities. Lee *et al.* [2], showed that when osmotic pressure was increased from 285 to 425 mOsm/kg, the specific growth rate and maximum viable cell concentration decreased by 20% and 48%, respectively, also the transcription rate of Ig mRNA increased by more than 476% when the conditions were changed from 285 mOsm/kg to 425 mOsm/kg, and the stability of Ig mRNAs decreased at the higher osmolarity. Previous studies have shown that osmotic stress triggers the MAPK pathway, leading to an activation of JNK via the MAPK kinase, which has been shown to be involved in the onset of apoptosis [14].

Although the detailed mechanism of alterations in the cell cycle distribution and proliferation due to osmotic pressure is not yet clearly understood, numerous

hypotheses have been postulated. Lee *et al.* [2], have suggested that the change in transcriptional activity is due to the alteration in the chromatin structure or possibly the pressure may stimulate the expression of chaperone-like proteins in the endoplasmic reticulum which induces G1-phase arrest. Furthermore, it has also been suggested that since G1-phase arrested cells do not need to devote cellular resources to increase biomass, higher productivity may be a general feature of G1-phase arrested production [5].

Membranes of animal cells are highly permeable to water [15]. Thus water movement parallels any imbalance in intracellular and extracellular osmolarities across the cell membrane with subsequent alterations of cell volume; this can induce a variety of cell physiological changes in, for example, cell adhesion [16], cell size [17], cell shape and cytoskeletal organization [18]. In the 210 mOsm/kg culture, it was observed that genes related to cell adhesion, cell shape and cell size control and defence response were mostly down regulated, while in 370 and 450 mOsm/kg cultures these genes were mostly up regulated. The expression levels of these genes were also observed to be higher in 450 mOsm/kg as compared to 370 mOsm/kg culture.

A study by Servuss *et al.* [16], has shown that osmotic change is able to modulate cell-substrate and cell-cell adhesion, and in addition this also been shown to affect the set point for cell size, the function of membrane protein and organisation of cytoskeleton, which determines the shape of the cells [10]. In terms of genes related to defence and immune response, results from various studies imply that antibody production rate increases at higher osmolarities [2]. Hyperosmotic pressure was found to enhance transcription levels of immunoglobulin mRNAs preferentially, compared with non-IgG mRNA. However, further studies are needed to understand the specific regulation of immune response related genes by hyperosmotic pressure.

In many studies, cellular metabolic rates have shown an increase during hyperosmotic culture conditions. In NS0 as a result of a shift of osmotic pressure from 275 to 400 mOsm/kg, the glucose and glutamate uptake rate has been shown to increase by 2-fold and 6-fold, respectively, and a lactate production increase of 4-fold [7]. Various genes related to carbohydrate, protein, amino acid metabolism and other metabolic reactions have shown a difference of more than two fold in expression levels. It was observed that in both hypo- and hyper-osmotic cultures conditions, genes related to protein biosynthesis were mostly up regulated while genes related to proteolysis and peptidolysis were mostly down regulated, and those related to steroid metabolism were mostly up regulated. Carbohydrate metabolism related genes were observed to be greatly affected by osmotic change but with no consistent up or down regulation. Glycolysis related genes were mostly up regulated in 210 and 370 mOsm/kg cultures, but mostly down regulated in 450 mOsm/kg cultures. It was also observed that nitrogen metabolism and energy pathways were mostly up regulated and membrane lipid metabolism mostly down regulated in 450 mOsm/kg culture.

Cell swelling and shrinkage also exert profound effects on intracellular signalling mechanisms, which in turn modify a multitude of cellular functions including the volume regulation mechanism [18]. Ion transport across the cell



membrane is the most efficient and rapid means of altering cellular osmolarities [19]. During cell shrinkage, cells accumulate ions to achieve regulatory cell volume increase [20]. Various genes related to signal transduction, signalling pathways, ion transport, protein and amino acid transport have shown a difference of more than two fold in expression levels. It was observed in hypo-osmotic cultures that genes related to cation transport, potassium transport, signal transduction and JNK cascade were mostly down regulated. In hyper-osmotic cultures, genes related to potassium transport, protein trafficking, water transport and JNK cascade were mostly up regulated. In 450 mOsm/kg culture, it was also observed that genes related to anion transport, amino acid transport and calcium transport were mostly up regulated while genes related to electron transport and intracellular signalling cascade were mostly down regulated.

#### 4. CONCLUSION

The results of this study have shown that culture osmolarity has a profound effect on growth, metabolism, ion balance and gene expression of GS-NS0 cells. Cells did not survive under hypo-osmotic cultures (210 mOsm/kg) conditions, and a slower growth rate was observed for cells under hyper-osmotic conditions, as compared to growth under normal osmotic condition. Even with a similar growth profile for the 290 and 370 mOsm/kg cultures, the metabolic profiles for these cultures were significantly different with a higher lactate and  $\text{NH}_4^+$  production in 290 mOsm/kg culture. In the gene expression experiments conducted using oligo-DNA microarray, it has been shown that around 700 genes related to various cellular functions, such as cell cycle and proliferation, cell metabolism, signalling and transport and cell physiology, were significantly up or down regulated. Currently the pathways related to metabolism and genes identified to date are being obtained, subsequently, strategies for improvement in metabolic engineering, process control and plasmid design could be achieved.

#### 5. REFERENCES

1. V.M. deZengotita, R.K., W.M. Miller, Effect of CO<sub>2</sub> and osmolality on hybridoma cells: growth, metabolism and monoclonal antibody production. *Cytotechnology*, 1998. **28**: p. 213-227.
2. M.S. Lee, G.M.L., Hyperosmotic pressure enhances immunoglobulin transcription rates and secretion rates of KR12H-2 transfectoma. *Biotechnology and Bioengineering*, 2000(68): p. 260-268.
3. J. Lin, M.T., Y. Qu, P. Gao, T. Yoshida, Enhanced monoclonal antibody production by gradual increase of osmotic pressure. *Cytotechnology*, 1999. **29**: p. 27-33.
4. W. Zhou, C.C.C., B. Buckland, J. Aunins, Fed-batch culture of recombinant NS0 myeloma cells with high monoclonal antibody production. *Biotechnology and Bioengineering*, 1997. **55**(5): p. 783-792.
5. J.S. Ryu, T.K.K., J.Y. Chung, G.M. Lee, Osmoprotective effect of glycine betaine on foreign protein production in hyperosmotic recombinant Chinese hamster ovary cell culture differs among cell line. *Biotechnology and Bioengineering*, 2000(70): p. 167-175.
6. M. Cherlet, A.M., Stimulation of monoclonal antibody production of hybridoma cells by butyrate: evaluation of a feeding strategy and characterization of cell behaviour. *Cytotechnology*, 2000. **32**: p. 17-29.

7. P.J. Duncan, H.A.J., G. Hobbs, The effect of hyperosmotic conditions on growth and recombinant protein expression by NS0 myeloma cells in culture. *The Genetic Engineer and Biotechnologist*, 1997. **17**: p. 75-78.
8. L.M. Bell, M.L.L.L., B. Kim, E. Wang, J. Park, B.A. Hemmings, G.L. Firestone, Hyperosmotic stress stimulates promoter activity and regulates cellular utilization of the serum and glucocorticoid-inducible protein kinas (Sgk) by a p38 MAPK-dependent pathway. *The Journal of Biological Chemistry*, 2000. **275**(33): p. 25262-25272.
9. J.E. Celis, M.K., I. Gromova, C. Freferikson, M. Ostergaard, T. Thykjaer, P. Gromov, J. Yu, H. Palsdottir, N. Magnusson, T.F. Orntoft, Gene expression profiling: monitoring transcription and translation products using DNA microarray and proteomics. *FEBS Letters*, 2000(480): p. 2-16.
10. F. Lang, G.L.B., M. Ritter, H. Volkl, S. Waldegger, E. Gulbins, D. Haussinger, Functional significance of cell volume regulatory mechanisms. *Physiological Review*, 1998. **78**(1): p. 247-306.
11. H.C. Causton, B.R., S.S. Koh, C.T. Harbison, E. Kanin, E.G. Jennings, T.I. Lee, H.L. True, E.S. Lander, R.A. Young, Remodeling of yeast genome expression in response to environmental change. *Molecular Biology of the Cell*, 2001. **12**: p. 323-337.
12. J.S. Ryu, M.S.L., G.M. Lee, Effect of cloned gene dosage on the response of recombinant CHO cells to hyperosmotic pressure in regard to cell growth and antibody production. *Biotechnology Progress*, 2001. **17**: p. 993-999.
13. M. Cherlet, A.M., Hybridoma cell behavior in continuous culture under hyperosmotic stress. *Cytotechnology*, 1999(29): p. 71-84.
14. S. Matsuda, H.K., T. Moriguchi, Y. Gotoh, E. Nishida, Activation of protein kinas cascades by osmotic shock. *Journal of Biological Chemistry*, 1995. **270**: p. 12781-12786.
15. F. Guharay, F.S., Stretch-activated single ion channel currents in tissue cultured embryonic chick skeletal muscle. *Journal of Physiology*, 1984(352): p. 685-701.
16. R.M. Servesss, W.H., Mutual adhesion of lecithin membranes at ultralow tension. *Journal of Physiology*, 1989(50): p. 809-827.
17. G.R. Erickson, L.G.A., F. Guilak, Hyper-osmotic stress induces volume change and calcium transients in chondrocytes by transmembrane, phospholipid, and G-protein pathways. *Journal of Biomechanics*, 2001. **34**: p. 1527-1535.
18. Haussinger, D., The role of cellular hydration in the regulation of cell function. *Journal of Biochemistry*, 1996(313): p. 697-710.
19. Yancey, P.H., Compatible and coneracting solutes, in *Cellular and Molecular Physiology of Cell Volume Regulation*, K. Strange, Editor. 1994, CRC. p. 81-109.
20. Berg, M.B., Molecular basis for osmoregulation of organic osmolytes in renal medullary cells. *Journal of Experimental Zoology*, 1994(268): p. 171-175.

## QUESTIONS AND ANSWERS

**Bernard Palsson, University of California, San Diego, US:**

Your talk exemplified the challenge of what I was talking earlier, this needs to integrate multiple different data types. So, how are you planning to integrate these data ?

**Mon-Han Wu, Imperial College London, UK:**

At the moment we are in collaboration with the bioinformatics team at Imperial College. There are a few things we are planning to do. First, there is the plasmid design part, where, from the genomic data we analyse the promoter sequence and find the similarity between the promoters. Hopefully we can design a better plasmid from that promoter region, from the metabolic and genomic data, and hopefully the proteomic data. We hope to isolate the key metabolic pathways which are altered through osmolarity and hope to change that pathway through metabolic engineering, to increase productivity, as a final goal.

**Charny, Merck Inc. Company:**

Could you tell us about how you maintain your osmotic pressure and if it stayed the same throughout your cultivation, or if the choice of additives makes any kind of difference to your measurements ?

**Mon-Han Wu, Imperial College London, UK:**

The experience is actually quite simple: we just used a shake flask, so it is actually not fully controlled, but the osmolarity value stays quite constant throughout the cultivation.

**Iman Famili, University of California, San Diego, US:**

I was wondering when you showed your slide, and you showed that the secretion of a number of metabolites goes up and down, in an opposite trend for hyperosmotic conditions with respect to the normal case. Do you think that it has anything to do with the fact that for instance the transporters for these different metabolites are coupled with protons, and the cell is trying to compensate for the osmotic pressure through the exchange of these metabolites and if not, how would you rank the influence of regulation, the change of for instance protein folding because of the osmotic pressure or other factors when you change the osmolarity of the solution ?

**Mon-Han Wu, Imperial College London, UK:**

First of all, the metabolisms do change and do compensate for the osmolarity. In respect to the second part of the question, we are still not analyzing these aspects yet, but hopefully we will analyze all the genes, and the proteins and metabolisms, so we can paint a better picture and we can prioritize our concern and what we can do to the process.

**Barry Buckland, Merck Inc. Company, US:** Your data were very interesting, I am just curious whether you run enough replicates to know their reproducibility.

**Mon-Han Wu, Imperial College London, UK:**

The data shown are just from one experiment. We have done three replicates, but we are still analyzing them, and these data were not shown yet.

**Martin Jordan, EPFL, Switzerland:**

Did you see an effect on cell size when you cultured the cells at different osmolarities ?

**Mon-Han Wu, Imperial College London, UK:**

Yes, we did measure cell size and the osmolarity tends to effect cell size during mid-logarithmic phase, but according to papers it would not have any significant effect within the first eight hours of exposure to hyper- or hypo-osmotic pressure, but cells go more or less back to the normal size.

**Sadettin Ozturk, Centocor, US:**

Did you maintain the sodium to potassium ratio the same ?

**Mon-Han Wu, Imperial College London, UK:**

I did not, sodium was added, but in other papers it has been said that no matter what kind of salt you add the productivity still increases by the same amount. But, what we also did was cultures with salt variants, although they were not shown yet. Actually it does have a significant effect on cell growth either we add potassium, sodium or sorbitol. It will effect the growth, production and metabolism of the cell.

**David Jayme, Gibco/Invitrogen, US:**

My question is related to the last two. Clearly, by increasing the sodium chloride levels you will impact not only the osmolarity but the cell volume, at very least transiently, is going to effect membrane potential, is going to effect sodium-coupled nutrient co-transport, and that may effect your metabolic rates and a variety of other things as well. I wonder if you have really been able to tease out, to divorce the osmotic effect versus some effects that might be secondary.

**Mon-Han Wu, Imperial College London, UK:**

Yes, that is why we did specific experiments to isolate the osmolarity effect and the ionic balance effects.

D. L. HACKER, M. COTTEN\*, AND F. M. WURM

## MOLECULAR APPROACHES TO INFLUENCE EPIGENETIC EFFECTORS OF TRANSIENT AND STABLE TRANSGENE EXPRESSION IN MAMMALIAN CELLS

*Laboratory of Cellular Biotechnology (LBTC), Swiss Federal Institute of Technology (EPFL),  
CH-1015 Lausanne, Switzerland; \*Axxima Pharmaceuticals AG, D-82152 Martinsried,  
Germany*

**Abstract.** Transient and stable transgene expression in mammalian cells is influenced by epigenetic factors such as histone modifications and DNA methylation. Here we demonstrate the feasibility of using molecular approaches to overcome the potentially negative effects of these factors. Chinese hamster ovary cells (CHO) were co-transfected with the CELO adenovirus Gam1 gene and either the enhanced green fluorescent protein (EGFP) gene or the IgG heavy and light chain genes. In both cases the expression of the reporter protein was increased in the presence of Gam1. Transient expression of Gam1 in YIGG2 cells, a stable CHO cell line that carries a silenced enhanced yellow fluorescent protein (EYFP) gene, resulted in higher expression of this reporter protein. Lastly, targeting of the adenovirus E1A mRNA in HEK293 cells for degradation by RNAi resulted in a two-fold increase in the transient expression of a co-transfected reporter gene. These results demonstrate that epigenetic factors do play a role in stable and transient transgene expression and that molecular approaches can be developed to relieve the negative effects of these factors on recombinant protein expression in mammalian cells.

### 1. INTRODUCTION

Epigenetic effectors such as histone modifications and DNA methylation have profound effects on gene expression in mammalian cells (Jenuwein and Allis, 2001; Bird, 2002). For example, histone acetylation and deacetylation are associated with transcriptionally active and inactive chromatin, respectively, and histone methylation has negative or positive effects on transcription depending upon the site of modification (Jenuwein and Allis, 2001). Transcription is also inhibited by methylation of promoter sequences (Bird, 2002). Epigenetic modifications also affect the expression of stable and transient transgenes in mammalian cells. The histone deacetylase inhibitors sodium butyrate and trichostatin A enhance both transient and stable transgene expression, and the DNA methylation inhibitor 5-azacytidine reactivates stable transgenes silenced by DNA methylation (Jones and Taylor, 1980; Gorman et al., 1983; Yoshida et al., 1990; Hunt et al., 2002). However, the cost and cytotoxicity of these compounds are drawbacks to their use for large-scale recombinant protein production.

Molecular approaches may be attractive alternatives for enhancing transgene expression via modifications of epigenetic pathways. Some mammalian viruses have already provided examples of this strategy. The bovine herpesvirus 1 protein

bICP0 and the CELO adenovirus Gam1 protein activate viral transcription by inhibiting cellular histone deacetylases (Zhang and Jones, 2001; Chiocca et al., 2002). Gam1 has also been shown to enhance transient transgene expression from a number of different promoters in COS cells (Chiocca et al., 2002). In addition, the E1A proteins of human adenovirus function as transcriptional repressors by binding and inactivating the histone acetylases PCAF and p300/CRB (Chakravarti et al., 1999). Since the E1A proteins are expressed in HEK293 cells, they may have a negative effect on transient transgene expression in this cell line. In this study we demonstrate that the Gam1 protein enhances stable and transient transgene expression in CHO cells and that targeting of the E1A mRNAs for degradation using RNA interference (RNAi) results in higher transient expression of recombinant proteins in HEK293 cells.

## 2. MATERIALS AND METHODS

The construction of pGAM1 (Chiocca et al., 2002) and pEAK8-EGFP (Meissner et al., 2001) have been described. The expression vectors for the anti-human RhD IgG1 heavy chain gene, pMZ36 and pLH1, and for the anti-human RhD light chain gene, pMZ57 and pLH2, have been described (Zahn-Zabel et al., 2001; Meissner et al., 2001). pEGFP-N1 was purchased from Clontech (Palo Alto). The vector pHS containing the U6 promoter was a gift of Richard Iggo (ISREC, Switzerland). pHS-E1A was constructed by cloning the two annealed oligonucleotides CGAAAAGATCCCAACGAGGAGGCGGTTCAAGAGACCGCCTCCTCGTTGG GATCTTTTG (adenovirus E1A mRNA nucleotides 723-743 are underlined) and GATCCAAAAGATCCCAACGAGGAGGCGGTCTCTTGAACCGCCTCCTCGT TGGGATCTTTT into pHS digested with *Bam*HI and *Bst*BI.

## 3. RESULTS

### 3.1. *Gam1* enhances reporter gene expression in transiently transfected CHO cells

CHO-DG44 cells were co-transfected with pEGFP-N1 (10% of the total DNA) and varying amounts of pGAM1 (0-90% of the total DNA) using polyethylenimine as a transfection vehicle. At three days post-transfection GFP expression was 2-3 fold higher in the presence of Gam1 than in its absence (Fig. 1, left panel). By comparison, Gam1 did not increase the expression of EGFP in HEK293-EBNA cells following co-transfection with either pEGFP-N1 or pEAK-EGFP (data not shown). To determine the effects of Gam1 on the expression of a secreted protein, CHO-DG44 cells were co-transfected with varying amounts of pGAM1 (0-40% of the total DNA) and a 1:1 (w:w) mix of pMZ57 and pMZ36 (60% of the total DNA). These two vectors express the IgG light and heavy chain genes, respectively, under the control of the HCMV promoter. At three days post-transfection the level of

secreted IgG was three times higher in the presence of Gam1 than in its absence (Fig. 1, right panel). The results demonstrated that Gam1 enhances the expression of both cytoplasmic and secreted recombinant proteins in transiently transfected CHO cells.

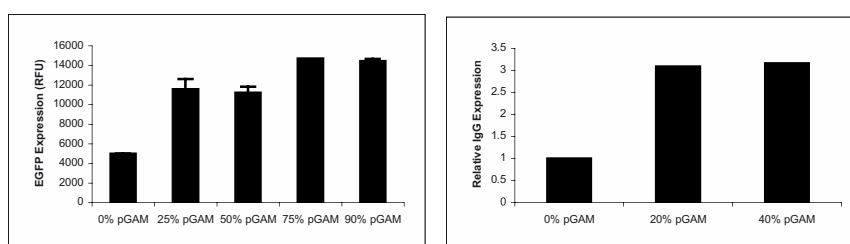


Figure 1. Transient transfection of CHO cells. (Left). Transfection with varying amounts of pGAM1 and 10% pEGFP-N1. Relative fluorescence units (RFU). (Right). Transfection with varying amounts of pGAM1 and a 1:1 mix of pMZ57 and pMZ36 (60% of the total DNA).

### 3.2. Gam1 activates a silenced transgene in a stable CHO cell line

The YIGG2 cell line carries the IgG heavy and light chain genes under the control of the SV40 promoter and the EYFP gene under the control of the HCMV promoter (Hunt et al., 2002). Immediately after the subcloning of YIGG2, 10-20% of the cells expressed EYFP, but after one month of cultivation only 0.1% of the cells still expressed EYFP (data not shown). To determine if gene silencing may have been the reason for the reduction in EYFP expression and to determine if the presence of Gam1 enhances EYFP expression, YIGG2 cells were transfected with varying amounts of pGAM1. By three days post-transfection the level of EYFP was increased 15-20 fold in the presence of pGAM1 (Fig. 2). Analysis of the transfected cell population by flow cytometry indicated that 8-10% of the cells expressed EYFP after transfection. This is equivalent to the transfection efficiency under the conditions used in this experiment. In contrast, the expression of IgG was enhanced at most 20-30% in the presence of Gam1 (data not shown). The results demonstrated that Gam1 increases the expression of a silenced transgene in a stable CHO cell line.

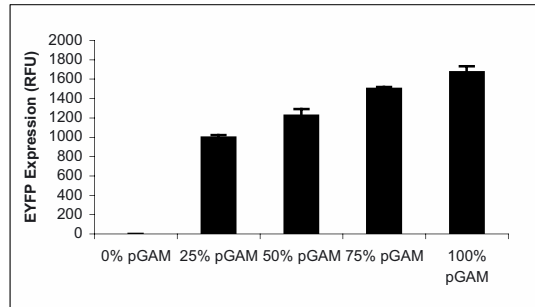


Figure 2. Transfection of YIGG2 cells with pGAM1.

### 3.3. Reporter gene expression is enhanced following RNAi-targeting of the adenovirus E1A mRNA in transiently transfected HEK293-EBNA cells

The adenovirus E1A proteins may be responsible for reduced transient transgene expression in HEK293 cells. Decreasing the E1A level in this cell line might therefore increase transcription from some promoters used for transient transgene expression. To investigate this possibility a vector to target E1A mRNA for cleavage by RNAi was constructed. pHS-E1A expresses a 53 nucleotide RNA polymerase III transcript that includes nucleotides 723-743 of the 12S and 13S E1A mRNAs plus the complement of this sequence. This RNA is expected to be cleaved to form a 21 base short interfering RNA (siRNA) targeting both the 12S and 13S E1A mRNAs for degradation. Cells were co-transfected with pEAK-EGFP (10% of the total DNA) and varying amounts of pHS-E1A (0-90% of the total DNA). The level of EGFP expression was three fold higher in cells transfected with the highest level of pHS-E1A (Fig. 3, left panel). Similar results were found when pHS-E1A was co-transfected with pEGFP-N1 (data not shown). To confirm these results with a second reporter protein, HEK293-EBNA cells were co-transfected with varying amounts of pHS-E1A (0-40% of the total DNA) and a 1:1 (w:w) mix of pLH1 and pLH2 (60% of the total DNA), vectors that express the IgG light and heavy chain genes, respectively, under the control of the EF-1 $\alpha$  promoter. At six days post-transfection IgG expression was two fold higher in cells co-transfected with pHS-E1A than in cells co-transfected with the empty pHS vector (Fig. 3, right panel). These results support the notion that E1A may be responsible for reduced transient transgene expression in HEK293 cells.



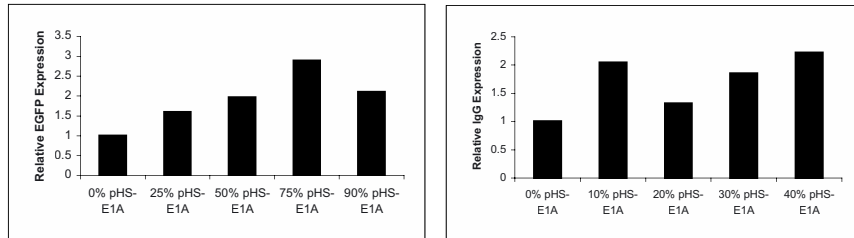


Figure 3. Transient transfection of HEK293-EBNA cells. (Left). Transfection with 10% pEAK-EGFP and varying amounts of pHS-E1A. (Right). Transfection with varying amounts of pHS-E1A and a 1:1 mix of pLH1 and pLH2 (60% of the total DNA).

#### 4. DISCUSSION

We have presented evidence demonstrating the feasibility of two genetic strategies for enhancing recombinant protein expression in stable cell lines and in transiently transfected cells. It was shown in CHO cells that Gam1 increased the transient expression of reporter genes under the control of the HCMV promoter. Transfection of YIGG2 cells with pGAM1 also resulted in an increase in the expression of the silenced EYFP gene in this stable CHO cell line. In contrast to these results, no enhancement of reporter gene expression by Gam1 was observed following transient transfection of HEK293-EBNA cells. Further studies on the molecular basis of Gam1 action on stable and transient transgenes in CHO and HEK293 cells are needed to resolve this difference.

The second strategy concerns the use of RNAi to enhance recombinant protein expression in mammalian cells. It was demonstrated in transient transfections of HEK293-EBNA cells that targeting the adenovirus E1A mRNA for degradation by RNAi results in increased expression from a co-transfected reporter plasmid. It may be concluded from these observations that the E1A proteins can have a negative effect on transient transgene expression in this cell line. In more general terms, these experiments demonstrate the potential utility of RNAi for targeting cellular mRNAs whose protein products have a negative effect on recombinant protein synthesis. It should be possible to insert one or more RNAi cassettes into expression vectors that are used for transient transfection of HEK293 cells.

#### 5. REFERENCES

- Bird, A. (2002). DNA methylation patterns and epigenetic memory. *Genes Dev.* 16:6-21.  
 Chakravarti, D., Ogryzko, V., Kao, H.-Y., Nash, A., Chen, H., Nakatani, Y., and Evans, R.M. (1999). A viral mechanism for inhibition of p300 and PCAF acetyltransferase activity. *Cell* 96:393-403.

- Chiocca, S., Kurtev, V., Colombo, R., Boggio, R., Sciarpi, M.T., Brosch, G., Seiser, C., Draetta, G.F., and Cotten, M. (2002). Histone deacetylase 1 inactivation by an adenovirus early gene product. *Curr. Biol.* 12:594-598.
- Gorman, C.M., Howard, B.H., and Reeves, R. (1983). Expression of recombinant plasmids in mammalian cells is enhanced by sodium butyrate. *Nucl. Acids Res.* 11:7631-7648.
- Hannon, G.J. (2002). RNA interference. *Nature* 418:244-251.
- Hunt, L., Batard, P., Jordan, M., and Wurm, F.M. (2002). Fluorescent proteins in animal cells for process development: optimization of sodium butyrate treatment as an example. *Biotechnol. Bioeng.* 77:529-537.
- Jenuwein, T., and Allis, C.D. (2001). Translating the histone code. *Science* 293:1074-1080.
- Jones, P.A., and Taylor, S.M. (1980). Cellular differentiation, cytidine analogs and DNA methylation. *Cell* 20:85-93.
- Meissner, P., Pick, H., Kulangara, A., Chatellard, P., Friedrich, K., and Wurm, F.M. (2001). Transient gene expression: recombinant protein production with suspension-adapted HEK293-EBNA cells. *Biotechnol. Bioeng.* 75:197-203.
- Yoshida, M., Kijima, M., Akita, M., and Beppu, T. (1990). Potent and specific inhibition of mammalian histone deacetylase both in vivo and in vitro by trichostatin A. *J. Biol. Chem.* 265:17174-17179.
- Zahn-Zabal, M., Kobr, M., Girod, P.-A., Imhof, M., Chatellard, P., deJesus, M., Wurm, F.M., and Mermod, N. (2001). Development of stable cell lines for production or regulated expression using matrix attachment regions. *J. Biotechnol.* 87:29-42.
- Zhang, Y., and Jones, C. (2001). The bovine herpesvirus 1 immediate-early protein (bICP0) associates with histone deacetylase 1 to activate transcription. *J. Virol.* 75:9571-9578.

## QUESTIONS AND ANSWERS

**Alain Bernard, Serono, Switzerland:**

Is pGAM1 acting differently on different promoters ? You showed in your stable work that you had the IgG under the SV40 promoter and then you are coming with fluorescent protein under the human CMV promoter.

**David Hacker, EPFL, Switzerland:**

Yes, that was an experiment done with the human CMV promoter. I did another experiment that I thought I had not enough time to include here, looking at promoter specificity of the *gam1* gene. With the human CMV promoter you see this two-fold increase in *gam1*, when you have a hybrid promoter with the human CMV promoter and the EF-1alpha promoter, then you see about a 30% increase in GFP expression, and with EF-1alpha promoter itself you see actually a decrease in expression. So, similar to the cell specificity you see also promoter specificity of the *gam1* activity.

**Gianluca Quintini, Altana Pharma, Germany:**

You showed that histone deacetylase inhibitors can negatively effect cell survival. *gam1*, if I got it right from the slide, promotes cell survival. Could you comment on that contradiction ? Second question: you expressed *gam1* transiently, what happens if you express it stably?

**David Hacker, EPFL, Switzerland:**

Regarding the second question, as far as I know, nobody is trying to produce a stable cell line with *gam1*. It is not clear what are the effects of sodium butyrate on cell survival, so you can not associate. Histone deacetylation is not necessarily involved in apoptosis or cell survival, these are clearly different pathways. Gam1 is acting on apoptosis and also acting on another pathway that is involved in histone deacetylation through separate activities. So, I do not see the contradiction you mentioned.

**Jana van de Goor, Genetech, US:**

In the initial few graphs that you showed us, I was wondering, since *gam1* has possibly a positive effect on cell growth and proliferation. Can some of the initial graphs that you showed be explained by higher viable cell numbers in the experiments, or were they normalized to viable cell counts, so that the effect can be attributed directly to each cell instead of higher viable numbers overall?

**David Hacker, EPFL, Switzerland:**

In the PEI transfections we counted the cells but there was no difference in the presence or absence of *gam1*. However, this is different for the calcium phosphate transfection. In that case you see cell viability increasing with increasing amounts of *gam1*. I do not know the differences between these two transfection methods.

**Allan Miller, CIL, Belgium:**

Deacetylation occurs during mitosis, so, if you expose your cells for a long period to *gam1* you should block mitosis and stop chromosome condensation. So, it is difficult for me to reconcile cell viability, chromosome condensation, normal cell-cycle progression with *gam1*, which stops deacetylation.

**David Hacker, EPFL, Switzerland:**

I do not know how to answer that either. In the PEI transfected cultures we do see cell division. As I have just said, there is no difference in cell number in the presence or absence of *gam1*, so cells continue to divide. The problem is that we do not know what has been affected when we transfect *gam1* into these cells, what cellular genes are being affected. We are only looking at one parameter, which is our reporter gene expression, and no other parameters such as the acetylation or deacetylation of histones or nucleosomes associated with that plasmid DNA are followed. That is one thing that will be important to know in order to determine the mechanism of action of *gam1* and the transgenes.

M. DE LEON GATTI<sup>1</sup>, K. WLASCHIN<sup>1</sup>, A. RINK<sup>2</sup>, A. SANNY<sup>3</sup>,  
K.S. TAN<sup>3</sup>, P.M. NISSOM<sup>3</sup>, P.F. ONG<sup>3</sup>, K. WONG<sup>3</sup>, R.J. PHILIP<sup>3</sup>,  
B. CHAM<sup>3</sup>, C.F. WONG<sup>3</sup>, K.M. LIM<sup>3</sup>, M. YAP<sup>3</sup>, AND W.-S. HU<sup>1</sup>,

## GENOMIC EXPLORATION ON CHINESE HAMSTER OVARY CELLS

<sup>1</sup>*University of Minnesota, U.S.A.*, <sup>2</sup>*University of Nevada at Reno, U.S.A.*, and  
<sup>3</sup>*Bioprocessing Technology Center, Singapore*

**Abstract.** Industrially important recombinant CHO cell clones carry many desirable phenotypic traits that differentiate them from the parental clone. The molecular basis for these traits at the genomic level is not well understood. A better understanding of key genetic alterations related to these traits will greatly facilitate the development of new cell lines and new processes. To advance this goal, we are constructing a CHO cDNA microarray. A phage library was constructed using mRNA pooled from different CHO clones under different cultivation conditions. Over four thousand sequences have been randomly isolated and sequenced. A cDNA microarray based on these sequences was constructed and used in gene expression studies. The differentially expressed genes identified by the CHO cDNA microarray were compared to those observed in cross-species hybridization to mouse cDNA microarrays. Sequence comparison with known mouse genes indicates only a moderate degree of homology. The results represent a significant step toward large-scale gene expression profiling for industrial mammalian cell culture processes.

### INTRODUCTION

The key to establishing an efficient cell culture process is the selection of stable, high-producing cell clones with desired growth and physiological characteristics. The current scheme for cell selection, adaptation and other process improvements is largely empirical and based on macroscopic phenotypic characteristics. Little is known about the molecular regulation associated with phenotypic changes. Large scale gene expression profiling can potentially reveal the molecular changes incurred in the selection and adaptation processes, providing further insight for genetic intervention to create a better host cell lines, and for more rational process development strategies.

Chinese hamster ovary (CHO) cells are the most common host cells used for the production of heterologous proteins; however, little genomic sequence information is available for this species. We are embarking on an effort to develop genomic tools for CHO cells. We have constructed a CHO cDNA library, sequenced and isolated over 4000 sequences, and constructed a cDNA microarray. Sequencing and annotation of the CHO cDNA library, along with the construction of a CHO cDNA microarray, will provide the much-needed tools for studying this economically important cell line. The objective of this project is to use these genomic tools to

establish a systematic way to uncover the genes and pathways that may affect the growth and production characteristics desired in bioprocessing.

## MATERIALS AND METHODS

### *Construction of a CHO cDNA library*

To ensure that the library represents gene expression under the most relevant and representative conditions, a 50/50 mixture of mRNA isolated from CHO DXB-11 cells and from an IgG producing cell line derived from CHO DXB-11 was used. DXB-11 is a dihydrofolate reductase deficient (DHFR-) cell line with a single point mutant allele. The other dhfr allele has been deleted [1]. The DXB-11 cell line is widely used for the production of recombinant proteins [2]. The IgG producing clone was grown in suspension using a semi-defined medium with intra-lipid® as the only undefined additive. DXB-11 was grown under adherent conditions in the presence of 5% fetal bovine serum, as is typically done in the early stages of clone selection after the transfection of the heterologous gene. Cells were harvested at the mid-exponential growth phase for RNA extraction. Total RNA was isolated using the standard guanidine isothiocyanate treatment, followed by phenol-chloroform extraction [3]. A cDNA library was constructed using the ZAP Express®  $\lambda$ -Phage cDNA Library Kit (Stratagene), along with the Gigapack III Gold Packaging Extract (Stratagene). cDNA was directionally cloned into the pBK-CMV vector, which allows both prokaryotic and eukaryotic expression of large sequences, and in vivo excision of cloned fragments into a phagemid vector. A second library was constructed using mRNA isolated from a recombinant CHO line producing  $\gamma$ -interferon. RNA was extracted from cells isolated in exponential growth phase, stationary phase, and death phase. cDNA from this pool was directionally cloned into the pDNR-LIB vector using the SMART cDNA Library kit (Clontech).

### *Construction of a CHO cDNA microarray*

CHO sequence inserts were amplified from the libraries using primers specific to the cloning vector (M13 forward and reverse primers or T3/T7 primers) and purified. Aliquots of each purified probe were analyzed on agarose gels and quantified using a Tecan Genios spectrophotometer. The remaining PCR product was desiccated in a Speedvac and re-suspended in phosphate printing buffer for a final DNA concentration of at least 150 ng/ $\mu$ l. Probes were spotted on polylysine coated slides using a Biorad Chipwriter equipped with quill-type steel pins at a nominal center-to-center spacing of 200  $\mu$ m. Arrays were re-hydrated over a 42°C water bath and subsequently exposed to 65mJ/cm<sup>2</sup> UV in a Stratalinker. Arrays were then blocked with succinic anhydride and 1,2 dichloroethane as previously described [4]. Prior to hybridization, slides were transferred to boiling water for 2 minutes, then dipped in 95% ethanol and dried by centrifugation at 500 rpm for 2 minutes.

### *Hybridization and Scanning*

Total RNA was isolated from suspension cell cultures using Trizol (Invitrogen) as per manufacturer’s instructions. Total RNA (30µg) was labeled by incorporation of amino-allyl dUTP (Sigma-Aldrich) by reverse transcription followed by conjugation to Cy3- or Cy5- dyes (Amersham Biosciences). Labeled targets were combined with equal volume of hybridization buffer (50% formamide, 10X SSC, 0.2% SDS) to a final volume of 50µl. Hybridization chambers containing the arrays were placed into a 42°C waterbath. After approximately 16 hours the arrays were washed at room temperature with decreasing concentrations of SSC and SDS and then dried by quick spinning in a centrifuge. The microarray images were obtained with ScanArray® Express (Packard BioScience Company, Billerica, MA). Image and data analysis were performed with GenePix Pro 4.1 (Axon Instruments) and GeneSpring 5.1 (Silicon Genetics), respectively.

RESULTS AND DISCUSSION

*Preliminary results of sequencing*

After transformation with the vector from the cDNA library, colonies of transformed XL0LR *E. coli* cells were picked using Genetix Q-Bot, and sequenced with the ABI 3700 96-well capillary machine. The median insert size for the library was 1100-1200 bp. Longer sequences were up to 2000bp. Over 4,000 sequences have been obtained. A modified version of phredPhrap was used to process the sequence data into strings, which were compared to the GenBank nucleotide database using the BLASTN algorithm. A major hurdle in annotating our sequences is that little genetic data for the Chinese Hamster is publicly available. Less than 500 unique sequences are available in GenBank. The results from initial annotation are summarized in Figure 1. A score greater than 300 indicates a fairly confident annotation. Sequences with scores less than 300 will be re-blasted and re-annotated periodically. The functional distribution of those sequences is shown in Figure 2.

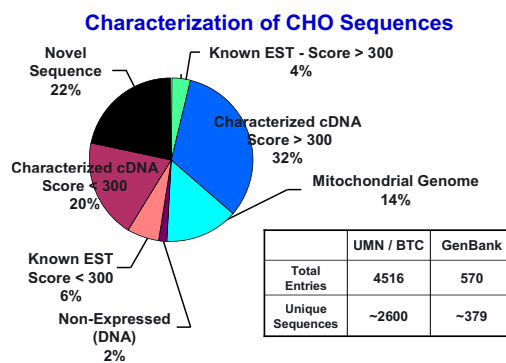


Figure 1. Characterization of isolated CHO sequences

An unusual abundance of mitochondrial transcripts were found in the mRNA isolates, as compared to typical tissue cDNA libraries. We obtained the entire mitochondrial genome sequence, except for the portions encoding for the D-Loop, by filling in the gaps in the mitochondrial sequences derived from random sequencing. The CHO mitochondrial sequence data was aligned with the complete mouse mitochondrial genome. Like other mammalian mitochondrial DNA, it encodes for 13 proteins, 2 ribosomal subunits, and 22 tRNAs.

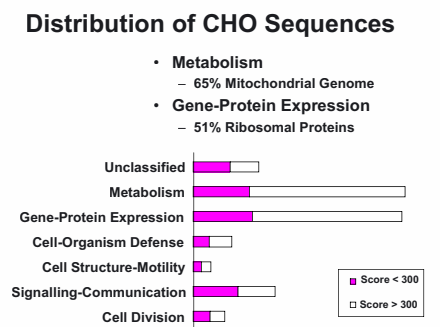


Figure 2. Distribution of functional class of isolated sequences

Phylogenetic analysis of the CHO mitochondrial genome is currently underway. In general, the CHO mitochondrial genes are more similar to the mouse and rat than to human. The cytochrome oxidase subunits appear more highly conserved, as compared to the NADH dehydrogenases, with the exception of NADH dehydrogenase subunit 1.

Attempts were also made to isolate particular sequences from the library using primers designed from the conserved sequences of corresponding genes in mouse, rat, and human. Nine sequences involved in apoptosis were obtained. However, unsuccessful isolations based on this strategy accounted for over 70% of all attempts.

#### *Effect of butyric acids on transcriptional profiles of cho and mouse hybridoma cells*

Butyric acid is often used to boost rDNA protein production in cell culture [5-7]. Gene expression profiles of recombinant CHO cells producing IgG were examined under treatment with butyric acid. As a control, a mouse hybridoma MAK cell line was used under identical conditions. The optimal concentration of butyric acid used for both cell lines was determined to be 1mM. The concentration was chosen by comparing the effect of butyric acid on IgG production and cell growth at four different concentrations ranging from 0 to 2mM. Sodium butyrate was added at



mid-exponential growth phase. Gene expression profiling was performed on mRNA cell samples withdrawn from the culture at 8 hours after sodium butyrate addition. The reference sample for all arrays was the zero time point, corresponding to the moment previous to sodium butyrate addition. Both cell line samples were hybridized to mouse BMAP arrays constructed at the University Minnesota. The mRNA sample from the CHO cells was additionally hybridized to the CHO array.

The same hybridization conditions were used for both CHO and mouse cells. The microarrays were run in quadruplicate, and 2:2 dye swaps were performed to minimize dye-labeling effects.

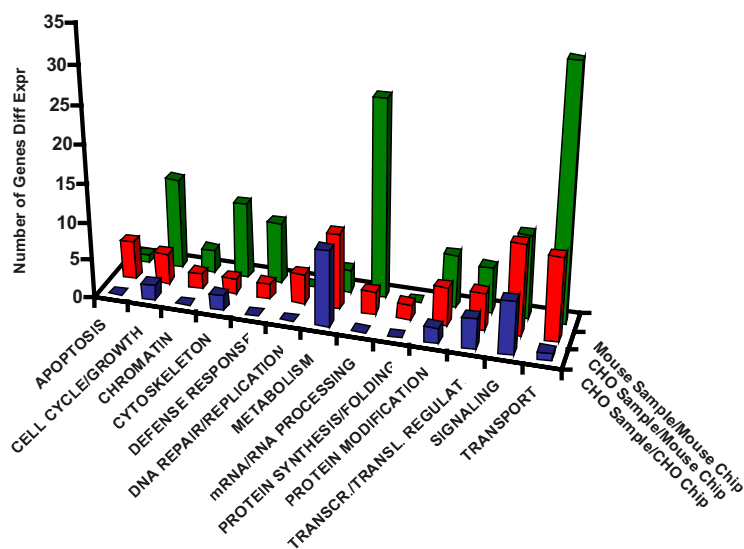


Figure 3. Distribution of Functional Class of Differentially Expressed Genes

### CONCLUDING REMARKS

Preliminary sequence and hybridization data has shown that hamster is not highly homologous to other well-sequenced rodent species. Using tools and data specific to these industrially important cell lines is necessary to conduct meaningful genomic studies. The construction of a cDNA microarray along with the availability of CHO sequence information will greatly facilitate the understanding of the molecular mechanisms involved in conferring key phenotypes and will provide a means to the reliable design of more optimal production cell lines.

## ACKNOWLEDGEMENTS

We thank the support of Minnesota Supercomputing Institute for bioinformatics support. The technical assistance of Dr. Zheng Jin Tu and Dr. Wen Dong in developing the sequence management data is gratefully acknowledged. We would like to thank Ms. Lo Siaw Ling and Ms. Chew Yen Cheng for technical assistance in implementing the phrad/phred/consed program in BTC.

## REFERENCES

1. Urlaub, G. and L.A. Chasin, *Isolation of Chinese Hamster Cell Mutants Lacking Dihydrofolate Reductase Activity*. Proc Natl Acad Sci U S A, 1980. **77**: p. 4216-4220.
2. Kaufman, R.J., *Selection and coamplification of heterologous genes in mammalian cells*. Meth Enzymol, 1990. **185**: p. 537-566.
3. Bairoch, A. and R. Apweiler, *The SWISS-PROT protein sequence data bank and its supplement TrEMBL in 1999*. Nucleic Acids Res, 1999. **27**(1): p. 49-54.
4. Diehl, F., et al., *Manufacturing DNA microarrays of high spot homogeneity and reduced background signal*. Nucleic Acids Res, 2001. **29**(7): p. E38.
5. Santell, L., et al., *Aberrant metabolic sialylation of recombinant proteins expressed in Chinese hamster ovary cells in high productivity cultures*. Biochemical & Biophysical Research Communications, 1999. **258**(1): p. 132-7.
6. Oh, S.K.W., et al., *Substantial overproduction of antibodies by applying osmotic pressure and sodium butyrate*. Biotechnology & Bioengineering, 1993. **42**(5): p. 601-610.
7. Oyaas, K., et al., *Transport Of Osmoprotective Compounds In Hybridoma Cells Hyperosmotic Stress*. Cytotechnology, 1995. **17**(3): p. 143-151.

M. de Leon Gatti – University of Minnesota, U.S.A.  
K. Wlaschin – University of Minnesota, U.S.A.  
A. Rink – University of Nevada at Reno, U.S.A.  
A. Sanny – Bioprocessing Technology Center, Singapore  
K.S. Tan – Bioprocessing Technology Center, Singapore  
P.M. Nissom – Bioprocessing Technology Center, Singapore  
P.F. Ong – Bioprocessing Technology Center, Singapore  
K. Wong – Bioprocessing Technology Center, Singapore  
R.J. Philip – Bioprocessing Technology Center, Singapore  
B. Cham – Bioprocessing Technology Center, Singapore  
C.F. Wong – Bioprocessing Technology Center, Singapore  
K.M. Lim – Bioprocessing Technology Center, Singapore  
M. Yap – Bioprocessing Technology Center, Singapore  
W.-S. Hu – University of Minnesota, U.S.A.

## QUESTIONS AND ANSWERS

**Thierry Battle, Serono Research, Switzerland:**

More a comment than a question. When you see only a few genes being modified or stimulated you should be happy, because anyway with the variants you will have various balances of protein to protein interactions. My comment is that by mixing suspension CHO cells and adherent CHO cells is adding extra complexity to your study.

**Wei-Sho Hu, University of Minnesota, US:**

But also with that you assure that all the genes are in the library, which is very important, otherwise you will be missing genes. What I should emphasize is that it is very important in this analysis is to apply very stringent statistics.

PAULINE M. RUDD, ANTHONY H. MERRY AND  
RAYMOND A. DWEK

## ROLES FOR GLYCOSYLATION IN RECEPTOR- LIGAND INTERACTIONS IN THE IMMUNE SYSTEM

*The Glycobiology Institute, Department of Biochemistry, University of  
Oxford, South Parks Road, Oxford OX1 3QU, U.K. email:  
pmr@glycob.ox.ac.uk*

**Abstract:** The fundamental importance of correct protein glycosylation is abundantly clear in a group of diseases known as congenital disorders of glycosylation (CDG). In these diseases, where sugars may be entirely absent or incorrectly processed, many proteins are affected [1] such that their biological functions are compromised. This disorder gives rise to a wide range of severe clinical conditions, including some that involve the immune system. Most of the key molecules involved in the innate and adaptive immune response are glycoproteins and the glycans play important roles in recognition events that are critical for triggering the biological functions of the proteins. Such roles include quality control to ensure correct protein folding, the loading of major histocompatibility class I (MHC I) peptide antigens, the geometry of the T-cell synapse and the interaction of MHC I with CD8. In the humoral immune response, multiply presented IgA glycans bind pathogenic bacteria and specific glycoforms of IgG can, when clustered, activate the complement pathway through engaging the mannose binding lectin. The recognition of an unusual cluster of mannose residues on the HIV gp120 envelope glycoprotein by a novel domain swapped antibody, isolated from a patient's serum, represents a new paradigm for antigen recognition. The broadly neutralising 2G12 IgG antibody has four closely spaced potential combining sites and may suggest a novel means to target clustered glycan arrays on pathogens.

### N- AND O-LINKED GLYCOSYLATION

In the primary sequence of a protein, the sequon AsnXaaSer (where Xaa is any amino acid other than Pro) is a necessary, but not sufficient, signal for N-glycosylation of the Asn residue with the oligosaccharide precursor, Glc<sub>3</sub>Man<sub>9</sub>GlcNAc<sub>2</sub>, an event that occurs in the endoplasmic reticulum (ER). After glucose and mannose trimming, the nascent glycoproteins are transferred to the Golgi apparatus where the N-linked oligomannose glycans can be processed to hybrid or complex glycans. In the Golgi, O-glycosylation is also normally initiated by the transfer of a GalNAc residue to the hydroxyl side chain of some Ser or Thr residues [2]. The chains are extended by the addition of single monosaccharide residues by processing enzymes.

Glycoproteins generally exist as populations of glycosylated variants (glycoforms) of a single polypeptide (See Review: [3]). Although the same glycosylation machinery is available to all proteins which enter the secretory pathway in a given cell, the 3D structure of the protein plays a major role in determining the glycan processing, and most glycoproteins emerge with a characteristic glycosylation pattern and heterogeneous populations of glycans at each glycosylation site [4]

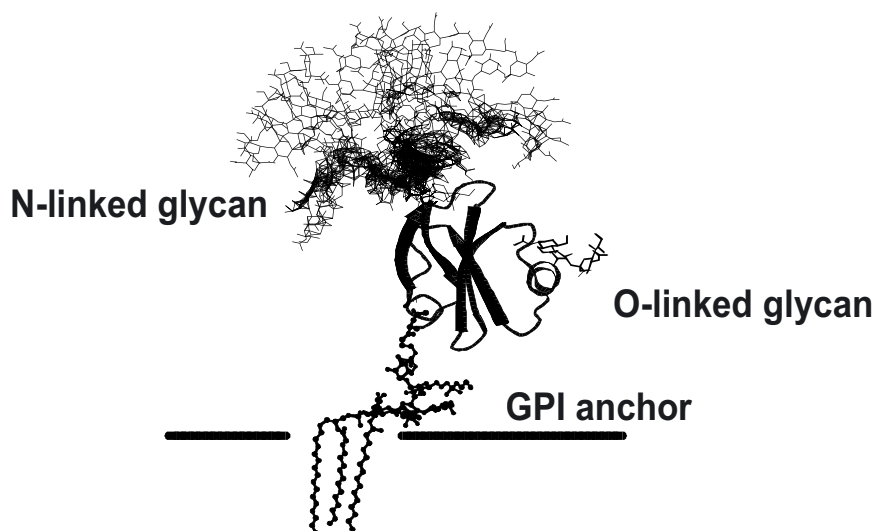


*Figure 1 Glycosylation of human erythrocyte CD59 [4] showing the conformational space available to the N-glycan chain resulting mainly from the flexible N-glycosidic linkage to asparagine in the peptide.*

#### FUNCTIONAL RECOGNITION OF GLYCAN EPITOPES

Almost all of the key molecules involved in the innate and adaptive immune response are glycoproteins. In the humoral immune system, all of the immunoglobulins and most of the complement components are glycosylated. A major function for sugars is to contribute to the stability of the proteins to which they are attached, and in addition specific glycoforms are involved in important recognition events. The affinity of a single monosaccharide for a protein receptor is in the micromolar range. This low affinity is, in general, insufficient for functional recognition. Biological responses depend on high affinity or avidity to ensure that functions are not triggered inadvertently. In the case of sugars, the requirement for high affinity binding or avidity can be provided either by multiple interactions of several monosaccharide residues in an oligosaccharide with a single protein binding site, or by interactions of multiple carbohydrate recognition domains on a protein with multiply presented glycans. This paper discusses ways in which such binding is achieved, as well as other roles for sugars in some important events in the immune system.

#### FOLDING OF MHC I AND THE LOADING OF ANTIGENIC PEPTIDE.

Inside the cell a major function for sugars is in the quality control of protein folding [5]. In the ER, the lectin-like chaperones calnexin (C1x) and calreticulin

(Clr) bind nascent glycoproteins through  $\text{Glc}_1\text{Man}_9\text{GlcNAc}_2$ . Unfolded glycoproteins are retained in the folding pathways until either they are fully folded and the terminal Glc residue is finally removed, releasing them from the chaperones, or the misfolded glycoproteins are targeted for degradation. The proposed ligand for both Clx and Clr is the terminal tetrasaccharide on the D1 arm of  $\text{Glc}_1\text{Man}_9\text{GlcNAc}_2$  (Figure 2) and high affinity binding is provided by multiple interactions of the mannose residues with the protein [6]

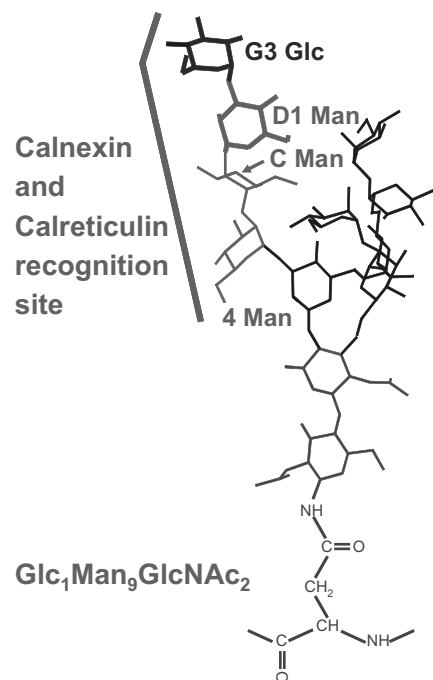
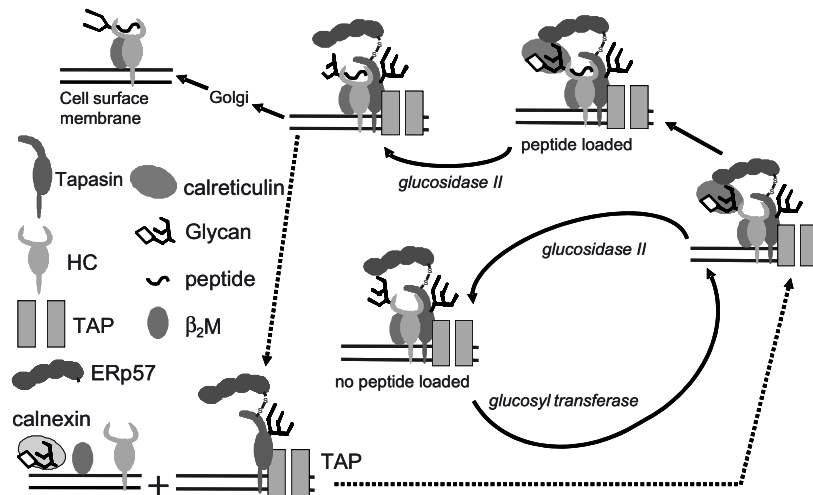


Figure 2 NMR solution structures of  $\text{GlcNAc}_2\text{Man}_9\text{Glc}_3$  showing the proposed recognition sites of Clx, Clr.

The Mature Major Histocompatibility Complex class I (MHC I) consists of two subunits: the heavy chain (HC), which is a transmembrane glycoprotein, and a small soluble non-glycosylated protein,  $\beta$ 2-microglobulin ( $\beta$ 2m). A peptide must be inserted into the peptide binding groove before MHC I can be transported to the cell membrane (Figure 3). Class I assembly requires multiple co-ordinated intra- and inter-molecular events to ensure the continuous reporting of cellular contents to cytotoxic T-lymphocytes.



*Figure 3 Proposed mechanism for the MHC class I peptide loading pathway Nascent glycoproteins are translated across the lumen of the ER and become immediately associated with the membrane bound calnexin (Clx). Interaction of with the binding complex with Clr continues until the peptide is in the groove.*

In the ER, unassembled HCs interact first with membrane bound Clx through  $\text{Man}_9\text{-}_7\text{GlcNAc}_2\text{Glc}_1$  sugars which are attached (in human HLA) to Asn86 in the early stages of glycan processing. When  $\beta_2\text{m}$  associates with HC, the sugar is released from Clx and MHC I binds to the soluble lectin-like chaperone, Clr. One or both of these chaperones recruits the thiol oxidoreductase (ERp57) into the complex, facilitating the formation of the intrachain disulfide bonds of the class I HC. The assembled class I- $\beta_2\text{m}$  dimer, together with associated Clr and ERp57, are associated with a larger complex that also contains the TAP transporter of antigenic peptides and the transmembrane glycoprotein tapasin. The complex is retained in the ER in the Clr quality control pathway until the peptide is in the groove. The terminal glucose residue is then finally removed and the complex dissociates allowing peptide loaded MHC I to exit the ER for the Golgi. Thus the efficient loading of MHC class I requires the presence of the  $\text{Glc}_1\text{Man}_9\text{GlcNAc}_2$  N-linked glycan and exploits the Clx/Clr quality control mechanism [7].

#### GLYCOSYLATION AND T-CELL RECOGNITION OF ANTIGEN PRESENTING CELLS

Multiple events and stages are involved in the T-cell recognition of antigen presenting cells (APC's). These include the formation of a junction between the two cells known as the immunological synapse [8] [9]), recognition of antigenic peptide-loaded MHC molecules by the T cell receptors (TCR's) and signal transduction. Sugars are likely to be important in many of these processes. Oligosaccharides

located on the membrane proximal domains of molecules in the immunological synapse tend to be conserved across species and may restrict the binding faces and orientations of the cell adhesion molecules CD2 and CD48 [10] contributing to the alignment of the opposing cell surfaces.

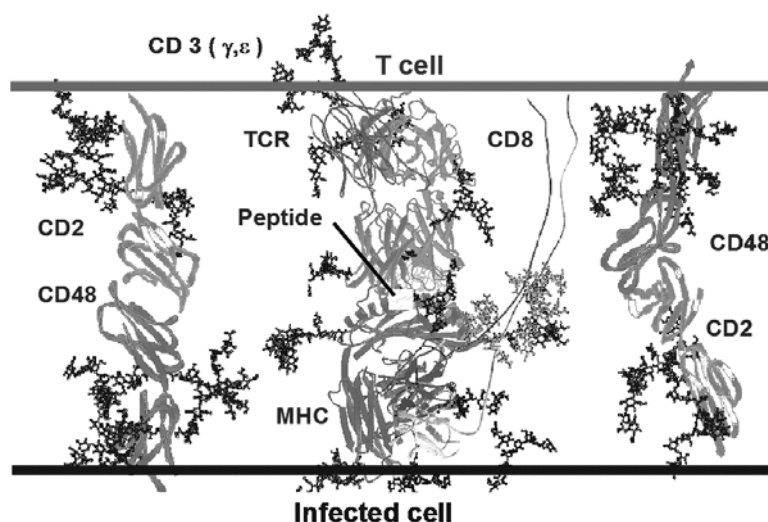
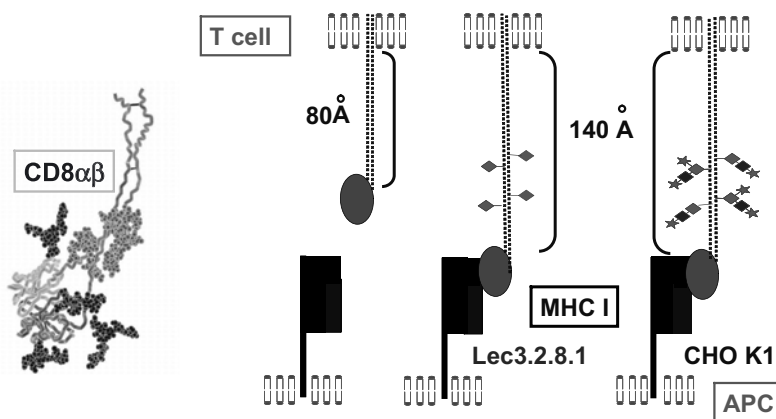


Figure 4 Some of the glycoproteins involved in the Immunological Synapse

The glycans may also be important in preventing non-specific protein-protein interactions, for example between TCRs, thus contributing to the spatial organisation of the junction. Certainly they cover large areas of the surface of the proteins, presenting a significant barrier to protease degradation of molecules at the synapse. MHC I interacts with TCRs on CD8+ T cells. CD8 hetero- ( $\alpha\beta$ ) and homo- ( $\alpha\alpha$ ) dimers, enhance T-cell activation by forming ternary complexes with the T cell receptor and peptide-MHCI molecules and recruiting the kinase p56lck to the complex. In CD8, the globular head containing the MHC binding site is tethered to the T-cell membrane by a polypeptide stalk that contains four O-linked sugars. The stalk region of CD8 plays a critical role in co-receptor interactions, spanning the nascent immunological synapse and orienting the CD8 binding face to the MHC. The conformational properties of the stalk are maintained by the O-linked glycans (Figure 5).





*Figure 5 O-glycans in the stalk region of CD8 affect the overall shape. The attachment of a single O-linked GalNAc residue (Lec 3.2.8.1 cell line) extends the stalk from 80Å to 140 Å [11]. Further elongation of the O-glycans (CHO-K1 cell line) does not result in further extension of the stalk.*

Analytical ultracentrifugation analyses of sCD8 $\alpha\alpha$ , expressed with normal O-glycosylation in CHO cells and truncated O-glycans in the Lec 3.2.8.1 cell line, indicate that O-glycans in the stalk region affect the overall shape of the molecule causing considerable extension of the stalk region from 80Å to 140 Å [11]. The GalNAc residue linked to the protein provides the majority of the chain extension and even the relatively few O-linked glycans on this cell surface molecule can significantly affect the presentation of the ligand binding domains.

In addition the O-glycans are expected to confer some rigidity to this extended peptide chain, protect it from digestion by proteases, and inhibit non-specific interactions of the stalk with the adjacent TCR.

#### ANTIBODY-ANTIGEN RECOGNITION BY IMMUNOGLOBULINS

In the extracellular space, two forms of non-self recognition are currently recognised. The first is the recognition of repetitive arrays of sugars, for example on bacteria or yeast by the mannose binding lectin. The second is the classical recognition of antigen by immunoglobulins.

In human IgG Fc (Figure 6), the two CH2 domains interact through an interstitial region that is formed by oligosaccharides, attached at Asn 297 on each heavy chain. Protein-oligosaccharide and oligosaccharide-oligosaccharide interactions play a role in maintaining the relative geometry of the CH2 domains. The location of the sugars in the interstitial region restricts the processing of the glycans and in normal control serum a significant proportion of the glycans are not fully galactosylated.

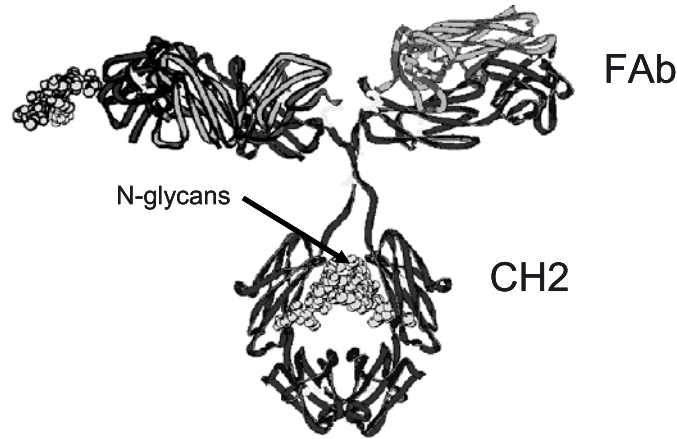


*Figure 6 Glycoform of human serum IgG showing conserved glycosylation in CH2 domain and non-conserved glycosylation in Fab region. The interstitial region between the CH $\gamma$ 2 domains accommodates the oligosaccharides which are attached at Asn 297.*

In rheumatoid arthritis (RA), an autoimmune disease, significant increases in the population of agalactosyl IgG0 glycoforms containing terminal GlcNAc residues have been described [12]. Aggregated IgG0 that can deposit in joints can be specifically recognised by the mannose binding lectin. This process may lead to inappropriate activation of the innate immune system providing an additional route to inflammation over and above classical antibody-antigen recognition. Functional recognition of IgG0 by the multiply presented carbohydrate recognition domains (CRDs) of MBL depends on multiple presentation of IgG0 glycans [13]. The mechanism by which specific IgG sugars initiate complement activation in rheumatoid arthritis is particularly important in the synovial cavity where IgG0 and MBL levels are elevated and IgG is clustered.

#### SECRETORY IGA1 BINDS BACTERIA THROUGH GLYCAN EPITOPES

In contrast to IgG, IgA1 (Figure 7) does not contain an interstitial space large enough to accommodate the Fc sugars and the Asn258 side chains are fully exposed and point out into solution[14,15].

Processing of the IgA1 N-glycans in the ER and Golgi is unhindered, and most serum IgA1 N-linked sugars, which include tri- and biantennary structures, are fully galactosylated and sialylated. The hinge region of IgA1, which contains 5 O-glycosylation sites, is resistant to many common proteases. The sugars, which on serum IgA1 mainly consist of sialylated Gal $\beta$ 1,3GalNAc, shield large areas of the hinge region (Figure 7) and produce an extended rigid structure.

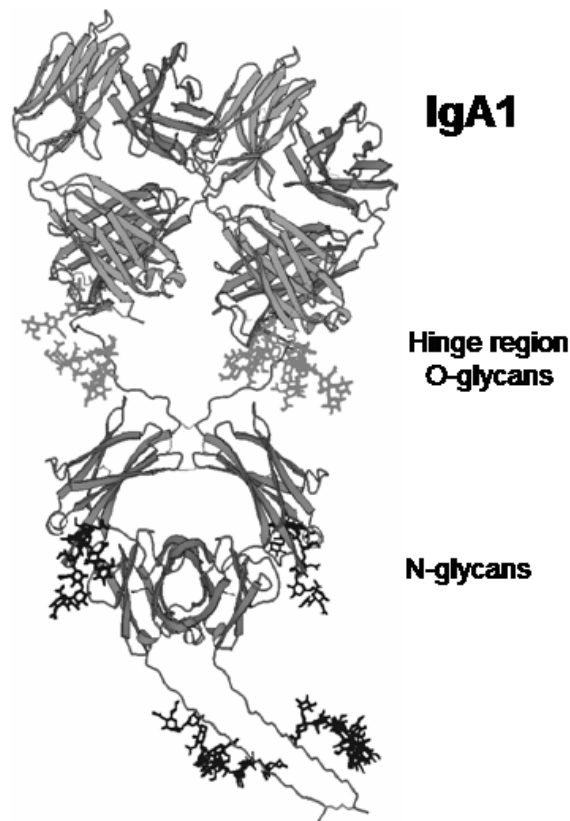


*Figure 7 Human Serum IgA1 showing O-glycosylation of hinge region. N-glycans attached to the CHa2 region of IgA1 are exposed on the outside of the molecule and more than 95% of them are significantly larger than the sugars on IgG. In IgA1, the O-linked glycans are located in the hinge region and the N-glycans are attached at Asn258 and Asn459 in the CHa2 domain and the tailpiece respectively.*

Secretory IgA1 (sIgA1) is a multi-polypeptide complex (Figure 8) consisting of a secretory component (SC) covalently attached to dimeric IgA containing one joining (J) chain. Secretory IgA1, J-chain and SC all have different N-glycosylation profiles. The N-glycans on the H chains are shorter than on serum IgA1, and present terminal GlcNAc and mannose residues which are normally masked by SC. The terminal residues can be unmasked and recognized by mannose binding lectin, by disrupting the SC-H chain non covalent interactions. The O-glycan regions on the heavy (H) chains of sIgA1 and the SC N-glycans have adhesin-binding glycan epitopes including galactose linked  $\beta$ 1-4 and  $\beta$ 1-3 to GlcNAc, fucose linked  $\alpha$ 1-3 and  $\alpha$ 1-4 to GlcNAc and  $\alpha$ 1-2 to galactose, and  $\alpha$ 2-3 and  $\alpha$ 2-6 linked sialic acids. These multiply

presented glycan epitopes provide SIgA1 with multiple glycan sites to which bacteria can bind, in addition to the four Fab binding sites, thus enabling SIgA to participate in both innate and adaptive immunity [16].

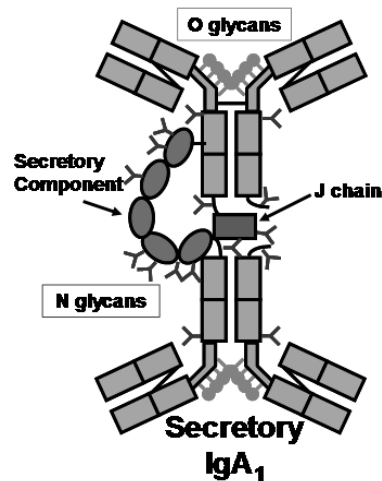


Figure 8 Multipeptide complex in Human Secretory IgA showing location of N- and O-glycans

#### AN UNUSUAL CLUSTER OF $\alpha 1 \rightarrow 2$ MANNOSE RESIDUES ON THE OUTER FACE OF GP120 ARE RECOGNIZED BY DOMAIN SWAPPED ANTI-HIV-1 ANTIBODY, 2G12.

Glycans attached to envelope glycoproteins protect viruses from the host immune system by virtue of the size of the sugars which cover potential immunogenic epitopes. Moreover, since the glycans are attached and processed by the host glycosylation machinery, it is unlikely that antibodies will be raised against them. Human IgG 2G12, first isolated and characterised as a mannose binding antibody by Stiegler et al [17], is therefore remarkable for its ability to neutralise a broad range of human immunodeficiency virus type 1 (HIV-1) isolates by binding a cluster of N-linked oligosaccharides on the "silent" face of gp120 with nanomolar affinity. Sugars at three N-glycosylation sites were strongly implicated in high affinity binding of gp120 to 2G12 by alanine scanning. Examination of the crystal structure of gp120 indicated that glycans at these sites are separated by only 35Å, too close for the Fab combining sites of a conventional antibody to engage simultaneously. This tight clustering of glycosylation sites is uncharacteristic of mammalian glycoproteins, is consistent with the finding that they contain only partially processed oligomannose glycans and may explain how the sugars can provide an

antigenic epitope. Inhibition assays and exoglycosidase digestions of the sugars on gp120 indicated that terminal mannose residues on the D1 arms of Man<sub>9</sub>-7GlcNAc<sub>2</sub> sugars were essential for binding [18]. Further insights into the recognition of gp120 by 2G12 were obtained from the crystal structures of the Fab fragment of 2G12 and its complexes with the disaccharide Man $\alpha$ 1-2Man and with the oligosaccharide Man<sub>9</sub>GlcNAc<sub>2</sub>. The data revealed that two Fabs assemble into an interlocked VH domain-swapped dimer (Figure 8). The configuration of this remarkable 'I' shaped antibody, isolated from a patient, showed two novel VH/VL combining sites for sugars that are only 35Å apart, as well as two additional novel sites within the VH/VH interface that are generated by the domain exchange [19]. Together these sites provide an extended surface for multivalent interaction with the conserved cluster of three oligomannose type sugars on the surface of gp120, the spatial orientation of which matches precisely to the antibody surface.

Glycans at Asn392 and Asn332 locate to the VH/VL combining sites, while the groove at the VH/VH interface can accommodate the glycan at Asn339. The unique arrangement of the Fab domains suggests a mechanism for high-affinity recognition of carbohydrate or other repeating, closely spaced epitopes on viral, microbial or cell surfaces.

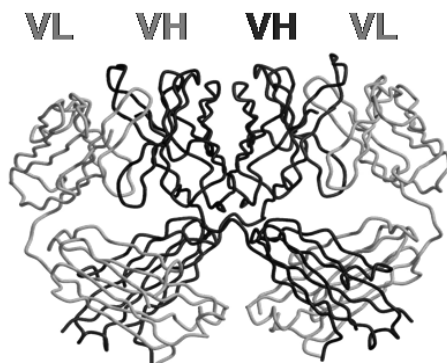


Figure 9 VH domain swapped dimer of 2G12 antibody [19]

## CONCLUSION

Glycans play many and varied roles in the functions of the proteins to which they are attached. In general, their relatively large size provides proteins with protection from proteases, for example in IgA1, and non-specific interactions, as in the T-cell synapse. Specific recognition epitopes are critical for efficient folding of some proteins via the Clx/Clr pathway. For example MHCI, and loading of antigenic peptide to MHCI uses an adaptation of the Clx/Clr folding pathway. Specific glycoforms of IgG may contribute to the pathogenesis of RA through binding MBL when aggregated, while sIgA presents multiple epitopes that bacteria can recognise.

Finally, a cluster of  $\alpha$ 1 $\rightarrow$ 2 mannose residues on the outer face of gp120 are recognized by the domain swapped ('I' shaped, rather than 'Y' or 'T' shaped) anti-HIV-1 antibody 2G12 demonstrating both a remarkable glycan epitope and a new paradigm in antibody recognition that may prove a useful therapeutic lead for targeting pathogens presenting closely spaced glycans on their surfaces.

## NOTES

### Abbreviations

APC: antigen presenting cell  
CDG: congenital disorders of glycosylation  
Clr: calreticulin  
Clx: calnexin  
ER: endoplasmic reticulum  
Glc: glucose  
GlcNAc: N-acetylglucosamine  
HC: heavy chain  
IgG0: agalactosyl glycoforms of immunoglobulin G  
Man: mannose  
MHC I: major histocompatibility class I  
RA: rheumatoid arthritis  
TCR: T cell receptor

## REFERENCES

1. Butler M, Quelhas D, Critchley AJ, Carchon H, Hebestreit HF, Hibbert RG, Vilarinho L, Teles E, Matthijs G, Schollen E, et al.: **Detailed glycan analysis of serum glycoproteins of patients with congenital disorders of glycosylation indicates the specific defective glycan processing step and provides an insight into pathogenesis.** *Glycobiology* 2003.
2. Wandall HH, Hassan H, Mirgorodskaya E, Kristensen AK, Roepstorff P, Bennett EP, Nielsen PA, Hollingsworth MA, Burchell J, Taylor-Papadimitriou J, et al.: **Substrate specificities of three members of the human UDP-N-acetyl-alpha-D-galactosamine:Polypeptide N-acetylgalactosaminyltransferase family, GalNAc-T1, -T2, and -T3.** *J Biol Chem* 1997, **272**:23503-23514.
3. Rudd PM, Dwek RA: **Glycosylation: heterogeneity and the 3D structure of proteins.** *Crit Rev Biochem Mol Biol* 1997, **32**:1-100.
4. Rudd PM, Morgan BP, Wormald MR, Harvey DJ, van den Berg CW, Davis SJ, Ferguson MA, Dwek RA: **The glycosylation of the complement regulatory protein, human erythrocyte CD59.** *J Biol Chem* 1997, **272**:7229-7244.
5. Chevet E, Cameron PH, Pelletier MF, Thomas DY, Bergeron JJ: **The endoplasmic reticulum: integration of protein folding, quality control, signaling and degradation.** *Curr Opin Struct Biol* 2001, **11**:120-124.
6. Ellgaard L, Helenius A: **ER quality control: towards an understanding at the molecular level.** *Curr Opin Cell Biol* 2001, **13**:431-437.
7. Radcliffe CM, Diedrich G, Harvey DJ, Dwek RA, Cresswell P, Rudd PM: **Identification of specific glycoforms of major histocompatibility complex class I heavy chains suggests that class I peptide loading is an adaptation of the quality control pathway involving calreticulin and ERp57.** *J Biol Chem* 2002, **277**:46415-46423.
8. Anton van der Merwe P, Davis SJ, Shaw AS, Dustin ML: **Cytoskeletal polarization and redistribution of cell-surface molecules during T cell antigen recognition.** *Semin Immunol* 2000, **12**:5-21.
9. Grakoui A, Bromley SK, Sumen C, Davis MM, Shaw AS, Allen PM, Dustin ML: **The immunological synapse: a molecular machine controlling T cell activation.** *Science* 1999, **285**:221-227.

10. Dustin ML, Ferguson LM, Chan PY, Springer TA, Golan DE: **Visualization of CD2 interaction with LFA-3 and determination of the two-dimensional dissociation constant for adhesion receptors in a contact area.** *J Cell Biol* 1996, **132**:465-474.
11. Merry AH, Gilbert RJ, Shore DA, Royle L, Miroshnychenko O, Vuong M, Wormald MR, Harvey DJ, Dwek RA, Classon BJ, et al.: **O-glycan sialylation and the structure of the stalk-like region of the T cell co-receptor CD8.** *J Biol Chem* 2003, **278**:27119-27128.
12. Parekh RB, Dwek RA, Sutton BJ, Fernandes DL, Leung A, Stanworth D, Rademacher TW, Mizuuchi T, Taniguchi T, Matsuta K, et al.: **Association of rheumatoid arthritis and primary osteoarthritis with changes in the glycosylation pattern of total serum IgG.** *Nature* 1985, **316**:452-457.
13. Malhotra R, Wormald MR, Rudd PM, Fischer PB, Dwek RA, Sim RB: **Glycosylation changes of IgG associated with rheumatoid arthritis can activate complement via the mannose-binding protein.** *Nat Med* 1995, **1**:237-243.
14. Mattu TS, Pleass RJ, Willis AC, Kilian M, Wormald MR, Lellouch AC, Rudd PM, Woof JM, Dwek RA: **The glycosylation and structure of human serum IgA1, Fab, and Fc regions and the role of N-glycosylation on Fc alpha receptor interactions.** *J Biol Chem* 1998, **273**:2260-2272.
15. Baenziger J, Kornfeld S: **Structure of the carbohydrate units of IgA1 immunoglobulin. I. Composition, glycopeptide isolation, and structure of the asparagine-linked oligosaccharide units.** *J Biol Chem* 1974, **249**:7260-7269.
16. Royle L, Roos A, Harvey DJ, Wormald MR, van Gijlswijk-Janssen D, Redwan el RM, Wilson IA, Doha MR, Dwek RA, Rudd PM: **Secretory IgA N- and O-glycans provide a link between the innate and adaptive immune systems.** *J Biol Chem* 2003, **278**:20140-20153.
17. Stiegler G, Kunert R, Purtscher M, Wolbank S, Voglauer R, Steindl F, Katinger H: **A potent cross-clade neutralizing human monoclonal antibody against a novel epitope on gp41 of human immunodeficiency virus type 1.** *AIDS Res Hum Retroviruses* 2001, **17**:1757-1765.
18. Scanlan CN, Pantophlet R, Wormald MR, Ollmann Saphire E, Stanfield R, Wilson IA, Katinger H, Dwek RA, Rudd PM, Burton DR: **The broadly neutralizing anti-human immunodeficiency virus type 1 antibody 2G12 recognizes a cluster of alpha1-->2 mannose residues on the outer face of gp120.** *J Virol* 2002, **76**:7306-7321.
19. Calarese DA, Scanlan CN, Zwick MB, Deechongkit S, Mimura Y, Kunert R, Zhu P, Wormald MR, Stanfield RL, Roux KH, et al.: **Antibody domain exchange is an immunological solution to carbohydrate cluster recognition.** *Science* 2003, **300**:2065-2071.

M. DÜRRSCHMID, C. JURSIK, N. BORTH, R. GRABHERR, O.  
DOBLHOFF-DIER\*

## INVESTIGATIONS ON MANNOSE-6-PHOSPHATE RECEPTOR MEDIATED PROTEIN UPTAKE

*Institute of Applied Microbiology (IAM), University of Natural Resources  
and Applied Life Sciences, Heiligenstädter Lände 11, A-1190 Vienna,  
Austria\* Igeneon AG, Brunner Strasse 69, A-1230 Vienna, Austria*

**Abstract.** Efficient and targeted uptake of functional proteins is a key to successful application of recombinant proteins in enzyme replacement therapy as for example for mucopolysaccharidosis VI (MPS VI). As a model protein arylsulfatase B (ASB), which is the enzyme deficient in the inherited storage disease MPS VI, was used in this study. The protein exhibits a mannose-rich glycosylation site which binds to the cell-surface presented cation independent mannose-6-phosphate receptor and is subsequently uptaken. In the current study we have designed various vectors all containing green fluorescent protein (GFP), as a marker-protein, fused to the C-terminal portion of ASB. In addition the original ASB signal sequence was included in order to provide correct folding and targeting. The effect of the leader sequence of plasmids and glycosylation was investigated in terms of product location and quality. Transfections were performed in COS cells.

**Keywords:** mannose-6-phosphate receptor, arylsulfatase B, mammalian cells, shuttle, gfp, MPS VI

### 1. INTRODUCTION

Therapeutic application of proteins is very much dependent on intra- and intercellular transport mechanisms. Pino-, phago-, and endocytosis are examples for the cellular uptake of such substances. Receptor mediated endocytosis, a very specific uptake mechanism, is also responsible for the transport of arylsulfatase B, the enzyme deficient in the inherited lysosomal storage disease mucopolysaccharidosis VI, into the cells and further to the lysosomes. Therefore the enzyme binds to the mannose-6-phosphate receptor (Lobel et al., 1988; Oshima et al., 1988), which is represented on the cell surface (Dahms et al., 1989; von Figura, 1991; Amara et al., 1992; Hille-Rehfeld, 1995; Denzer et al., 1997; York et al., 1999). In the current study we have designed constructs that allow binding at the specific M6PR and thus induce a transport of the connected protein into the cell.

### 2. MATERIAL AND METHODS

#### 2.1. Cell Line and Medium



For the transient expression of recombinant proteins a CHO-K1 and a COS cell line was used. Flow cytometry analysis was done with a serum free cultivated dehydrofolate reductase (dhfr) -negative CHO cell line.

Cells were grown in a 1:1 mixture of DMEM and HAM's F12 containing Phenol Red (Biochrom Corp., Berlin, Germany) supplemented with 6 mM L-glutamine (Sigma Aldrich Corp., St. Louis MO, USA) and 5 % FCS (Pan Biotech GmbH, Aidenbach, Germany).

### 2.2. Cloning

RNA was isolated from CHO342/MCB I cells (J.J.Hopwood, Lysosomal Diseases Research Unit, Department of Chemical Pathology, Women's and Children's Hospital; Adelaide, Australia) and the yield determined at 260 nm and 280 nm with the Eppendorf Biophotometer 6131 (Eppendorf, Germany). Single-stranded cDNA was synthesised with Superscript II Reverse Transcriptase (Invitrogen, Carlsbad CA, USA) and amplified by PCR. DNA was first purified with Qiaquick-Kit (Qiagen, Hilden, Germany) and again purified after separation on a preparative agarose gel (Qiaquick DNA gel purification kit, Qiagen). The inserts were ligated into the vector pQBI-f25 (Promega, Mannheim, Germany). Electroporation of electrocompetent bacteria (dh5 $\alpha$ -strain) (Hanahan et al., 1985) was done in electroporation cuvettes at 2.500 V, 25  $\mu$ F and 1000  $\Omega$ . The constructs were subsequently purified by Midi- or Maxiprep (Midi Kit, Maxi Kit, Qiagen) and used to transfect CHO or COS cells according to a standard protocol (Jordan et al., 1996; Batard et al., 2001).

### 2.3. Transfection

One day before transfection 1 to 4 x 10<sup>5</sup> cells mL<sup>-1</sup> were seeded in 12 well plates (Nalge Nunc, Wiesbaden, Germany) and put into the incubator overnight. One hour prior to addition of the precipitate, partially depleted medium was exchanged to fresh medium (pH 7.4). For the transfection itself 100  $\mu$ L 2.5 M CaCl<sub>2</sub> solution was mixed with 25  $\mu$ g DNA and filled up to 1 mL with 1/10 TE-buffer. After 1 mL HEPES-solution was added immediately, the mixture was mixed once and applied to the cells. Per mL medium 100  $\mu$ L precipitate were used. Finally the plates were incubated at 37 °C (pH 7.3 – 7.6) for 2 to 6 hours prior to applying a glycerine shock by addition of 20 % glycerol in PBS. Glycerol was removed after 1 minute and fresh medium was added. The cultures were aspirated and fresh medium added again. The evaluation of the plates was done 1-5 days after the transfection by fluorescence microscopy .

For PAGE- and Western-analysis samples were taken after 24 to 72 hours. Samples of the culture's supernatant were taken, centrifuged to get rid of any suspended cells, and stored until analysis at -20 °C. Attached cells were washed with PBS and treated with lysis buffer. The liquid was collected and stored again at -20 °C.

#### 2.4. PAGE and Western Analysis

Samples were diluted with sample buffer according to the assumed protein concentration (usually 1:1) and incubated at room temperature for 30 minutes. A polyacrylamide gradient-gel (Pre-cast Tris-Glycin Gel, 4-20 % Polyacrylamid, Novex, San Diego CA, USA) was loaded with the denatured samples and a prestained PAGE standard protein marker (BIORAD Control 90677, Broad Range, BIORAD, Munich, Germany). The electrophoresis run was performed in a NOVEX electrophoresis system (Novex, San Diego CA, USA) at 125 V and up to 50 mA for 2 hours.

After the SDS-PAGE, Western blotting was done on a PVDF membrane (Inc. Schleicher & Schuell, Dassel, Germany) in the NOVEX Blotting Device (Novex, San Diego CA, USA). The protein transfer from gel to membrane was executed at 125 mA and 6 V for 1.5 hours. After this procedure the membrane was blocked 30 minutes with blocking buffer. The membrane was subsequently incubated for 1. hour with the biotinylated polyclonal goat  $\alpha$ -gfp antibody (Abcam, Cambridge, UK) solution followed by 3 washing steps. The membrane was then again incubated for 1 hour with the HRP-avidin conjugate (Amersham Biosciences, Uppsala, Sweden), again washed 3 times for 15 minutes and finally incubated for 5 minutes, wrapped in a plastic foil, with 5 mL Lumi-substrate (ECL Plus™, Amersham Biosciences, Uppsala, Sweden). Analysis was performed with the Lumi-Imager and the Lumi-Analyst software package (Boehringer-Mannheim, Mannheim, Germany).

#### 2.5. FACS-Analysis

A FACS Vantage (Becton Dickinson) flow cytometer equipped with sort enhancement module and automatic cell deposition unit was used for cell sorting. Uptake of constructs containing ASBEST was checked by cell sorting. Therefore the CHO dhfr<sup>-</sup> cells were incubated with culture supernatant of transfected COS-cells containing the fusion-protein. The cells were then stained either in the viable or in the ethanol-fixed form. Staining was done with mouse  $\alpha$  GFP antibody (Sigma Aldrich Corp.; #G6539, St. Louis MO, USA) and phycoerythrin-labelled anti mouse antibody (Sigma Aldrich Corp., St. Louis MO, USA) for detection with FACS.

### 3. RESULTS

#### 3.1. Role of Leader-Sequence

PAGE, followed by Western-Blot with ECL+ detection technique, revealed that the leader sequence which was previously suspected to be responsible for the transport of the enzyme out of the cells, indeed fulfilled the proposed function. Figure 1 shows Western Blot results for samples of cell suspension and lysed cells. Gfp in culture supernatant of COS cells transfected with construct leagfpASBEST is displayed in lane 4, gfp in a sample of lysed cells transfected with leagfpASBEST

construct in lane 3, gfp in culture supernatant of a gfpASBEST transfected culture in lane 2, and finally gfp in a sample of lysed cells previously transfected with gfpASBEST in lane 1. Samples of lysed cells are 10-fold concentrated as compared to the samples of culture supernatants. The figure confirms strongly the thesis that the leader sequence is absolutely necessary to ensure the efficient transport of ASB protein out of the cells. Samples of cultures with cells containing the construct with the leader, the ASBEST and the gfp sequences (here referred as leaASBESTgfp) are able to transport most of the product into the supernatant. This is stressed by the finding that most of the product can be found in the supernatant (lane 4 in Figure 1) and that only a small part of the product can be detected in the samples of lysed cells. In samples of cultures with cells containing the construct without the leader sequence (here referred as ASBESTgfp), most product could be proved to appear in the sample of the lysed cells (lane 1 in Figure 1) and only a small amount of product could be detected in the supernatant of the cultures, which again stresses the assumption that protein without the leader can not exit the cells efficiently.



*Figure 1- Western Blot of culture supernatant and lysed COS cells with ASBESTgfp and leaASBESTgfp. Detection with biotinylated anti-gfp-antibody followed by anECL<sup>+</sup> staining. Lane 1: gfp of lysed cells with ASBEST; lane 2: gfp in lysed cells with leaASBEST; lane 3: gfp in ASBEST culture supernatant; lane 4: gfp in leaASBEST culture supernatant.*

### 3.2. Role of ASBEST (Glycosylation)

In the case of enzyme replacement therapy ASB has to be able to reenter any cell, to be able to evolve its pharmacological function. Several studies so far show that the ASB contains a mannose-rich glycosylation site. This glycosylation site, which is responsible for the enzyme's binding to the cation-independent mannose-6-phosphate receptor is located on the C-terminus (here referred to as the ASBEST part of the gene). ASBEST samples were applied to a M6PR-coated plate and then detected with an antibody-ELISA. FACS analysis revealed that ASBEST-labelled fusion protein enters the cells quite rapidly, as receptor-bound protein could only be detected after 1 hour, albeit only in small quantities, but none could be detected after 4 hours. Furthermore the fusion protein could be found intracellularly after 1 hour but not after 4 hours (see Figure 2).

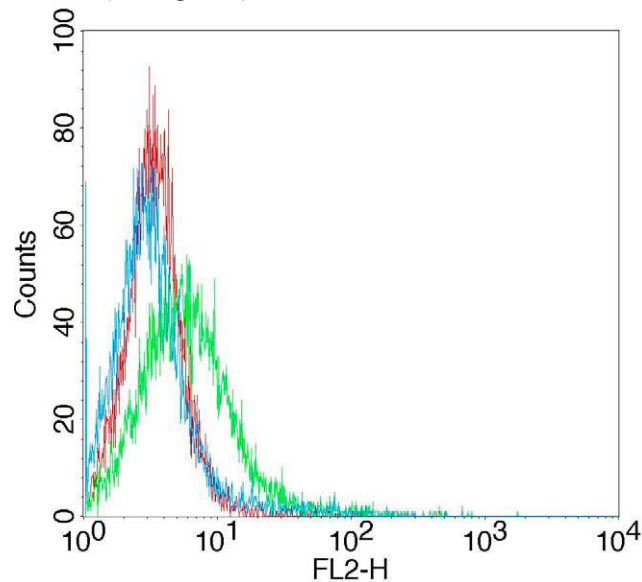


Figure 2 – FACS-diagram showing the shift caused by cells which had previously uptaken the fusion-protein.

#### 4. DISCUSSION

Receptor mediated endocytosis is the mechanism that underlies enzyme replacement therapy (Kakkis et al., 2002), which itself is a relatively simple method of continuously substituting the lacking enzyme in a distinct metabolic disease (Anson et al., 1992). In the case of human arylsulfatase B, the enzyme deficient in MPS VI, the region which is responsible for receptor binding is glycosylated and contains mannose-6-phosphate residues. These residues enable binding to the cation independent mannose-6-phosphate receptor and subsequently uptake of the protein into the cell.

The current study provides evidence that a distinct C-terminal gene-region is responsible for receptor binding, as a recombinant protein consisting of the receptor binding part of ASB and GFP can be internalised into the cell efficiently. Furthermore we could demonstrate that the leader sequence is necessary for product release into culture medium.

## 5. REFERENCES

- Amara J.; Cheng S.H.; Smith A.; Intracellular protein trafficking defects in human disease; Trends Cell Biol. 1992, 2:145-149
- Batard P.; Jordan M.; Wurm F.; Transfer of high copy number plasmid into mammalian cells by calcium phosphate transfection; Gene 2001, 270(1-2): 61-68
- Byers S.; Crawley A.C.; Brumfield L.K.; Nuttall J.D.; Hopwood J.J.; Enzyme replacement therapy in a feline model of MPS VI: modification of enzyme structure and dose frequency; Pediatr. Res. 2000, 47(6):743-749
- Dahms N.M.; Lobel P.; Kornfeld S.; Mannose-6-phosphate receptors and lysosomal enzyme targeting; J. Biol. Chem. 1989, 264:12115-12118
- Denzer K.; Weber B.; Hille-Rehfeld A.; von Figura K.; Pohlmann R.; Identification of three internalization sequences in the cytoplasmic tail of the 46 kDa mannose 6-phosphate receptor; Biochem. J. 1997, 326:497-505
- Hille-Rehfeld A.; Mannose 6-phosphate receptors in sorting and transport of lysosomal enzymes; Biochim Biophys Acta 1995, 1241:177-194
- Jordan M., Schallhorn A., Wurm F.M.; Transfecting mammalian cells: optimization of critical parameters affecting calcium-phosphate precipitate formation; Nucleic Acids Res 1996, 24(4):596-601
- Kakkis E.; Enzyme replacement therapy for the mucopolysaccharide storage disorders; Expert Opin. Investig. Drugs 2002, 11(5):675-685
- Lobel P.; Dahms N.P.; Kornfeld S.; Cloning and sequence analysis of the cation-independent mannose 6-phosphate receptor; J. Biol. Chem. 1988, 263:2563-2570
- Oshima A.; Nolan C.M.; Kyle J.W.; Grubb J.H.; Sly W.S.; The human cation-independent mannose 6-phosphate receptor – cloning and sequence of the full-length cDNA and expression of functional receptor in COS cells; J. Biol. Chem. 1988, 263(5):2553-2562
- von Figura K.; Molecular recognition and targeting of lysosomal proteins; Curr. Opin. Cell Biol. 1991, 3:642-646
- York S.J.; Arneson L.S.; Gregory W.T.; Dahms N.M.; Kornfeld S.; The rate of internalization of the mannose-6-phosphate/insulin-like growth factor II receptor is enhanced by multivalent ligand binding; J Biol Chem 1999, 274(2):1164-1171
- Hanahan D.; Jessee J.; Bloom F.R.; Techniques for transformation of E. coli, In: DNA cloning: a practical approach, ed. Glover D.M. and Hames B.D., 2nd edition, volume 1, 1-36; Oxford University Press, New York (1985)

## 6. ACKNOWLEDGEMENT

Work supported in part by the European Commission's TMR Programme, Contract No. ERBFMRXCT97-0156, EuroUltraSonoSep and by the Austrian Federal Ministry of Education, Science and Culture's research grant GZ 70.0161/1 - Pr/4/97: "Process development MPS VI"

## QUESTIONS AND ANSWERS

**José Vicente Castell, Hospital La Fe, Spain:**

Do you have a working hypothesis for the low levels of intracellular protein within the cells, for example degradation ?

**Markus Duerrschmid, Institute of Applied Microbiology, Austria:**

We know there is an intracellular degradation, so you have to apply the enzyme permanently.

M. VALER, T. PRECKEL, G. LUEDKE, C. BUHLMANN

## ANALYSIS OF MULTIPLE APOPTOSIS PARAMETERS USING A MICROFLUIDIC CHIP-BASED SYSTEM

*Assay Support Biochemist, Agilent Technologies GmbH, Hewlett-Packard  
Strasse, 8. 76337 Waldbronn, Germany*

**Abstract.** We have developed miniaturized assays for detection of phosphatidylserine exposure, caspase activity and DNA laddering using lab-on-a-chip technology. A readout system capable of two-color fluorescence detection was used to run disposable glass chips with various analytical functionalities. The chips contain an interconnected network of microchannels that permits either electrophoretic separations of biomolecules or simple flow cytometric analysis of cells.

Translocation of phosphatidylserine to the outer leaflet of the membrane bi-layer was monitored in treated cells by binding of annexin V-biotin and streptavidin-Cy5. Counterstaining the sample with the live cell dye calcein allowed for the discrimination of live apoptotic and dead cells. Activation of caspase-3 was measured in fixed, permeabilized cells by intracellular staining with an anti-active caspase-3 MAb and a Cy5-labeled secondary antibody. Importantly, the small microfluidic chip-based system used here requires only 20,000 cells per sample for the flow cytometric analysis and allows for on-chip optimization of the staining.

Results obtained with the microfluidic chips showed good correlation with data obtained using a conventional flow cytometer, while consuming fewer cells and automating data acquisition of 6 cell samples. In addition, as a third apoptosis parameter fragmentation of genomic DNA was measured using the same microfluidic system, where the microchannels of the chips were filled with a sieving polymer and DNA was electrophoretically size fractionated using an intercalating dye for detection.

### 1. INTRODUCTION

Apoptosis, or programmed cell death, is a highly regulated metabolic cascade leading to cell self-destruction. It is used in multicellular organisms to tightly control cell numbers and tissue size during development<sup>1</sup> and to protect itself from altered cells that threaten homeostasis. Defects of apoptosis control lead to unexpected cell behavior, related to such diseases as cancer, Alzheimer's<sup>2</sup>, and Parkinson's. Apoptosis is characterized by a distinct set of morphological events involving plasma membrane blebbing and asymmetry loss, reduction in cell volume, loss of mitochondrial membrane potential, nuclear condensation, fragmentation of chromatin at nucleosomal intervals, and other cytoplasmic changes. Cells may respond with distinct pathways to different death triggers. Mitochondrial and death-receptor pathways may operate independently<sup>3,4</sup>. The number of pathways combined with differences in cell line behavior and cell dynamics during the process demand that alternative assays be used under certain circumstances. Apoptosis assay development must include a battery of tests to confirm assay usability and permit understanding of the ongoing metabolic processes.

### 1. 1. Analytical assays

The measurement of phosphatidylserine (PS) in the outer layer of the cell membrane with fluorescently labelled annexin V is widely used because of its relative ease of measurement and quantitative properties.

On the other hand, direct measurement with fluorescently labeled antibodies against executors or antagonists is also preferred, like active-caspases or Bcl-2 markers. The flow cytometry assays evaluate single cells for apoptosis and a percentage of the live cell population is then reported to be apoptotic. The microfluidic platform makes these flow cytometric assays<sup>5-7</sup> compatible with the more traditional DNA laddering. DNA laddering, as visualized by the DNA electrophoresis of cell extracts, is a result of the activity of the caspase-activated DNase (CAD). CAD cuts the genomic DNA between nucleosomes to generate DNA fragments with lengths corresponding to multiples of 180 base pairs<sup>8</sup>. DNA laddering is then an indication of the average health of a complete population, and is not dependent on the viability status of the cells. The appearance of DNA laddering is unambiguously connected to apoptosis. The combined measurement of exposed PS and the extracted DNA of apoptotic cells with one platform are compared here. A rapid protocol for DNA preparation that is compatible with the chip platform is discussed.

## 2. EXPERIMENTAL

### 2.1. Cell culture and apoptosis induction

Jurkat cells (ATCC, Manassas, VA) were cultured in RPMI 1640 medium supplemented with 10% FBS, 10 U/mL Pen-Strep, 20  $\mu$ M l-glutamine, 1 mM sodium pyruvate, and 0.05  $\mu$ M b-mercaptoethanol. Apoptosis was induced in Jurkat cells by resuspension in a solution of 5  $\mu$ M camptothecin (# C9911, Sigma Chemical Co., St. Louis, MO). Cells were harvested and counted at the times indicated.

### 2.2. DNA preparation

DNA extraction and purification of Jurkat cells was performed as described in the rapid protocol below (based on the original protocol from Kratzmeier et al.<sup>9</sup>). Eluted samples were loaded directly into the chip wells and prepared according to the manufacturer's instructions.

- Pellet  $1-2 \times 10^6$  cells by centrifugation (2 min  $\times 400$  g); remove medium
- Resuspend cells in 100  $\mu$ L 4 °C lysis solution (0.2% Triton X-100, 10 mM Tris-10 mM EDTA).



- Incubate for 5 min at 4 °C
- Centrifuge for 5 min at 13,000 g
- Transfer supernatant to a new vial and discard the pellet
- Purify DNA using a low-volume elution method; for this process, a polymerase chain reaction (PCR) purification kit was used (MinElute PCR purification kit, cat. no. 28004, QIAGEN, Hilden, Germany). As an alternative, a salt-cold ethanol precipitation is possible.
- Run in an Agilent 2100 bioanalyzer with the DNA 12000 LabChip® kit (both from Agilent Technologies GmbH, Waldbronn, Germany) selecting the DNA 12000 laddering assay.

If an alternative DNA purification method is used, special attention must be given to the injection of large amounts of genomic non-fragmented DNA, since whole cell lysates may lead to clogging of the chip. The recommended extraction protocol eliminates such interference of genomic DNA. In addition, extracted DNA is concentrated to a small volume, and only 1 µL of the DNA is used in the chip, thus permitting the apoptosis measurement of low cell numbers.

#### 2.4. Annexin V apoptosis measurements

The chip-based flow cytometric assay for annexin staining was used as described<sup>10</sup>. Briefly; treated cells were harvested to a cell density of  $1 \times 10^6$  cells/mL. 100µl of the cell suspension was mixed with 2 µL of 200 µg/mL annexin V-biotin in a microcentrifuge tube and incubated for 10 min at RT. After washing, the cells were resuspended in 100 µL of binding buffer containing 1 µg/mL Fluorolink-Cy5 streptavidin (Amersham Biosciences, Buckinghamshire, U.K.) and 1 µM Calcein-AM (Molecular Probes, Eugene, OR) for live cell staining. Following incubation for 10 min at RT, centrifugation, and medium aspiration, the cells were resuspended in 50 µL of Cell Buffer (Agilent Technologies) by gentle pipetting. Ten microliters of cell suspension (20,000 cells) was added directly to the cell chip and analyzed on the Agilent 2100 bioanalyzer.

### 3. RESULTS AND DISCUSSION

Jurkat cells treated for 6 hours with 5µM camptothecin were analyzed with the cytometric assay Annexin V (Fig. 1B). Calcein-AM was used to select life cells, by detecting emission fluorescence at 525nm while Annexin was simultaneously measured in the second channel at 680nm. After switching the instrument to electrophoresis mode (<1min), the extracted DNA from cells treated for 48H was analyzed using the DNA 12000 LabChip® kit. The characteristic DNA laddering further confirmed apoptosis in the sample (Figure 1B).

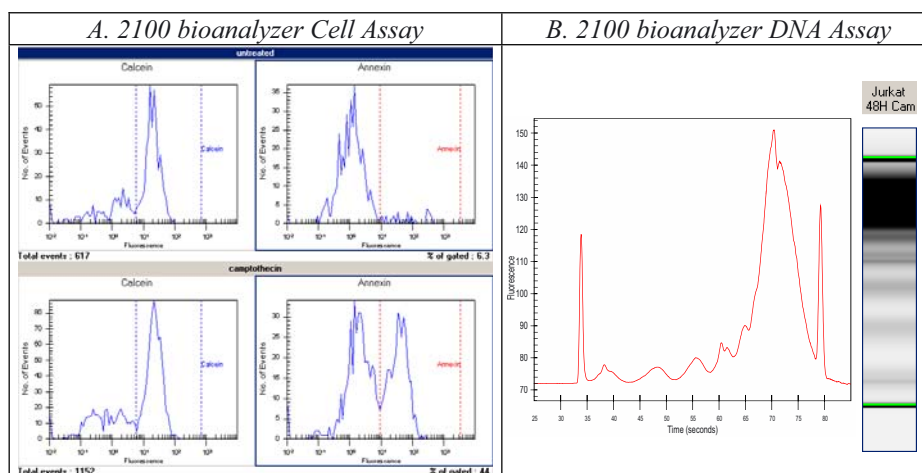


Figure 1 A. Histogram view of the two-color flow cytometric analysis showing annexin V-Cy5® staining of phosphatidyl serine in untreated (upper panel) and apoptosis induced (lower panel). Left panels show life reference staining with calcein, as annexin also stains cells with a damaged membrane (e.g.: necrotic and dead cells). B Apoptosis confirmation by DNA laddering assay, electropherogram and gel like image are shown.

Sizing information, provided by the instrument software, shows nucleosomal fragmentation of chromatin by evenly distributed peaks in the electropherogram (figure 2). Apoptosis is confirmed in samples by fragmentation in 180-200bp intervals.

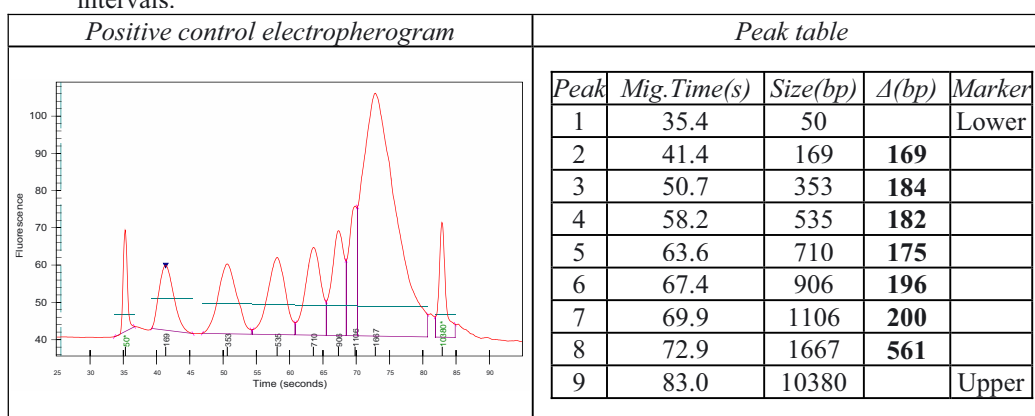


Figure 2. Electropherogram of U937 cells lyophilized positive control. Automated size calibration allows a quick verification of DNA fragmentation sizes. DNA peaks at 180-200bp intervals were well according the expected values for nucleosomal fragmentation.

Typical DNA extraction with the described fast protocol leads to 10 $\mu$ l of 2-30ng DNA/ $\mu$ l depending on cell type and number of apoptotic cells. Concentration of each band was calculated to be approximately 1ng/ $\mu$ l (1 $\mu$ l loaded on the chip). Even at this low concentration, apoptotic samples are clearly distinguishable from the negative control and necrotic samples (Figure 3, lanes 1 to 7). The positive sample in lane 4 (sample 2, incubated for 6 hours) turned out to be 35% apoptotic as confirmed by the Annexin V assay. Intracellular antibody detection against active Caspase 3 proved similar results (results not shown). A clear discrimination of samples that contain a lower number of apoptotic cells is achieved by overlaying negative controls and samples in the electropherogram view (figure 4). This software option enormously expands the concentration range usability of the assay, as the gel view image cannot be scaled to intense and small bands at the same time.

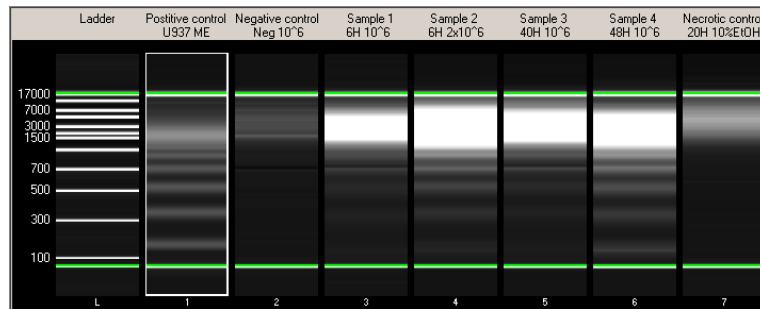


Figure 3 Gel like image showing positive (lane 1) and negative controls (lanes 2 and 7) together with 4 apoptotic samples (lanes 3 to 6) showing different degrees of apoptosis. Negative and necrotic samples display an overall smaller DNA signal and no trace of laddering.

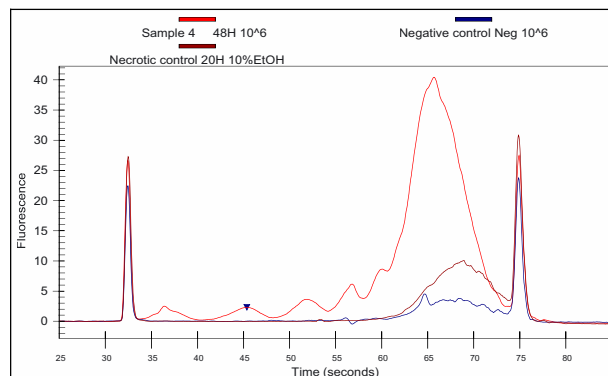


Figure 4 Electropherogram overlay of apoptotic sample, necrotic and negative controls (lanes 6, 7 and 2 in figure 5). Electropherogram view shows laddering as a succession of broad peaks between 150 and 1000bp. (Peaks at 33 and 75 s belong to assay markers).

#### 4. CONCLUSION

A combination of complementary assays is usually wanted to confirm apoptosis in cell samples. The chip-based approach offers the flexibility to quantitatively measure flow cytometric parameters including cell viability and apoptotic markers and subsequently perform a DNA fragmentation electrophoresis assay. It makes use of minimum volumes of samples and reagents and the turn around time is greatly improved by automation of the analysis.

#### 5. REFERENCES

1. Jacobson MD, Weil M, Raff MC. Programmed cell death in animal development. *Cell* 1997; 88:347–54.
2. Su JH, Kesslak JP, Head E, Cotman CW. Caspase-cleaved amyloid precursor protein and activated caspase-3 are co-localized in the granules of granulovacuolar degeneration in Alzheimer's disease and Down's syndrome brain. *Acta Neuropathol (Berlin)* 2002; 104(1):1–6.
3. Gross A, Yin XM, Wang K, et al. Caspase cleaved BID targets mitochondria and is required for cytochrome c release while BCL-XL prevents this release but not tumor necrosis factor-R1/Fas death. *J Biol Chem* 1999; 274:1156–63.
4. Krohn AJ, Wahlbrink T, Prehn JH. Mitochondrial depolarization is not required for neuronal apoptosis. *J Neurosci* 1999; 19(17):7394–7404.
5. Ferrance J, Snow K, Landers JP. Evaluation of microchip electrophoresis as a molecular diagnostic method for Duchenne muscular dystrophy. *Clin Chem* 2002; 48:380–3.
6. Preckel T, Luedke G, Chan S, Wang B, Dubrow R, Buhlmann C. Detection of cellular parameters using a microfluidic chip-based system. *J Assoc Lab Autom* 2002; 7(4):85–9.
7. Preckel T, Luedke G. Apoptosis detection by Annexin V and active Caspase 3 with the Agilent 2100 bioanalyzer. Agilent Technologies appl note 5988-4319EN, 2001.
8. Wyllie AH. Glucocorticoid-induced thymocyte apoptosis is associated with endogenous endonuclease activation. *Nature* 1980; 284:555–6.
9. Kratzmeier M, Albig W, Meergans T, Doenecke D. Changes in the protein pattern of H1 histones associated with apoptotic DNA fragmentation. *Biochem J* 1999; 337:319–27.
10. Preckel T, Chan S, Luedke G. A fast protocol for apoptosis detection by Annexin V with the Agilent 2100 bioanalyzer. Agilent Technologies appl note 5988-7297EN, 2002.

## QUESTIONS AND ANSWERS

**Florian Wurm, EPFL, Switzerland:**

I am sure very few in this room have used your technology so far, could you explain more details about what kind of equipment one has to buy, and the cost of the chips, and if it is possible to reuse them ?

**Marc Valer, Agilent Technologies, Belgium:**

There are two posters giving more information about this technology. Basically, it is a fluorescence-based equipment, with the size of a printer, it uses disposable chips, that are different for cells and for nucleic acids, and as for the cost for analysis we are aiming at one USD per sample for DNA, and for cells we are still a bit further, about 2.5 USD per sample.

**José Vicente Castell, Hospital La Fe, Spain:**

Can the chips be reutilized ?

**Marc Valer, Agilent Technologies, Belgium:**

The nucleic acid chips cannot be reutilized, for various technical reasons, mainly due to the polymers used and the small size of the channels. The cell systems uses bigger channels, and it should be possible to clean them up, but it will also take a lot of time to make sure you do not have cross-contamination between samples.

BRUNO FIGUEROA<sup>1</sup>, ERIC AILOR<sup>2</sup>, MITCHELL REFF<sup>2</sup>,  
J. MARIE HARDWICK<sup>3</sup>, AND MICHAEL BETENBAUGH<sup>1</sup>

## INHIBITING APOPTOSIS IN CELL CULTURE USING MULTIPLE INHIBITORS

<sup>1</sup>*Department of Chemical and Biomolecular Engineering, Johns Hopkins University, Baltimore, Maryland USA,* <sup>2</sup>*IDEC Pharmaceuticals, San Diego, California, USA,* <sup>3</sup>*Department of Molecular Microbiology and Immunology, Bloomberg School of Public Health, Johns Hopkins University, Baltimore, Maryland USA*

**Abstract.** Mammalian cell culture is widely used for the production of therapeutic proteins and for the generation of cells for cell and gene therapies. During cell culture, these cells can be exposed to a number of external and internal insults including nutrient depletion, toxin accumulation, viral infections, and external shear stress among others. These events can trigger the biochemical cascade called apoptosis in which the cells actively participate in their own demise. This program cell death (PCD) cascade decreases the viable cells in a bioreactor and lowers productivity since valuable bioreactor resources are needed to replace dead or dying cells rather than being applied to generate target proteins and cells. As a result, methodologies that limit the apoptosis pathway are desirable and represent a major application of cell engineering for mammalian culture. A number of natural anti-apoptosis genes have been identified in both eucaryotes and viruses that inhibit apoptosis at both upstream and downstream points in the apoptosis cascade. Anti-apoptosis proteins may be used to prevent the loss of mitochondrial membrane integrity or block cellular caspases from degrading the cell. Apoptosis pathways include feedback and feedforward loops that lead to amplification of the apoptotic response. Therefore, strategies that block cell death at multiple points along the cascade may limit the amplification of these apoptosis signals. As a result, combinatorial strategies that include anti-apoptosis proteins blocking apoptosis at different steps in the cascade are being implemented. In particular, the inhibitors of mitochondrial activity are being combined with proteins that block caspase activation. In this way, it may be possible to extend mammalian cell lifetimes and function for multiple biotechnology and bioengineering applications.

### 1. INTRODUCTION

Apoptosis is an essential process that selectively eliminates compromised cells in multicellular organisms. Apoptosis is important in organ development and tissue homeostasis and during certain conditions that result in degenerative diseases. Also, apoptosis plays an important role in regulating the multiplication of a number of viruses and their pathogenicity. Much of the apoptosis pathway is also retained for cells in culture. As a result, mammalian cells grown in culture will undergo apoptosis in response to varying stimuli including nutrient deprivation, toxin accumulation, and virus infection. Developing methodologies to inhibit apoptosis

can be used to limit the level of cell death in mammalian cell culture systems. One approach that can be used to limit cell death is to engineer the cells with genes that are inhibitors of the programmed cell death cascade (Figure 1). Viral inhibitors of apoptosis such as E1B-19K from the adenovirus offer one potential option for inhibiting cell death in mammalian cultures. The recently discovered protein, Aven, is another natural cell death inhibitor that can block apoptosis at a different step in the cascade. In the following section, we will describe these genes and their effects on the apoptosis pathway.

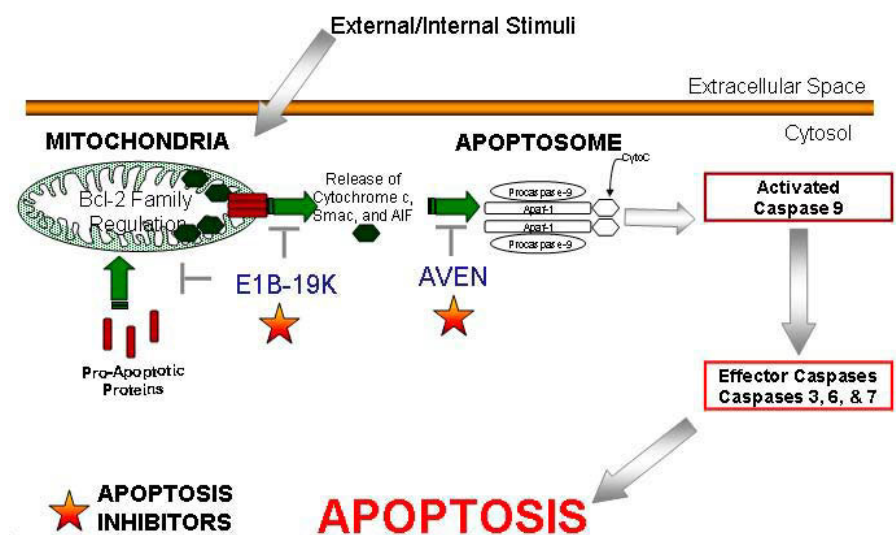


Figure 1. Apoptosis pathway and E1B-19K and Aven inhibitors of apoptosis.

## 2. BACKGROUND

### 2.1. Adenoviral Anti-apoptosis Protein E1B-19K

Apoptosis plays an important role in regulating the multiplication of a number of viruses and their pathogenicity. A cell's defence against viral infection is to initiate the apoptosis process. However, certain viruses have developed methods to combat the initiation of apoptosis and encode proteins that suppress cell death in order to facilitate efficient viral replication and pathogenesis. One such virus is the human adenovirus, composed of a linear duplex DNA molecule of 36,000 base pairs.

Following infection, the viral genes are expressed in the cell nucleus in two broad phases: "early," which is the stage prior to viral DNA replication, and "late," following DNA replication. Early phase genes encode proteins that function to

suppress the infected cell's apoptosis process and to counteract immunosurveillance. Late phase genes encode primarily viral structural proteins. The oncogenic transformation of primary cells and gene expression in infected cells is regulated by the E1 region of the adenovirus genome. The E1 region is composed of two transcription units, E1A and E1B. Nuclear phosphoproteins which are necessary to transactivate transcription of viral early promoters, stimulate cellular DNA synthesis, and immortalize primary cells are encoded by the E1A unit. The E1B unit is essential for proper regulation of viral gene expression and for full manifestation of the transformed phenotype. The E1B unit encodes two distinct tumor antigens of adenovirus, 19 kDa and 55 kDa proteins. While E1A expression will induce apoptosis during transformation, the viral protein E1B-19K functions to inactivate the apoptosis program stimulated by E1A (White et al., 1991). In addition, E1B-19K can suppress the effects of certain external cell death-inducing stimuli, such as TNF-alpha and other agents that induce apoptosis (Gooding et al., 1991, Hashimoto et al. 1991).

Indeed, E1B-19K is a functional homolog of the cellular anti-apoptosis protein Bcl-2 (Cuconati and White, 2002). In addition, both proteins also share limited but significant amino acid sequence homology, especially in the BH1 and BH3 structural domains (Tarodi et al., 1993, Chiou et al., 1994). However, the E1B-19K protein lacks the BH2 and the C-terminal membrane targeting domains present in many Bcl-2 family members. Both Bcl-2 and E1B-19K proteins bind and inhibit Bcl-2 family members including Bax, Bak and Nbk/Bik via their BH3 domains (Cuconati and White, 2002). Since Bax and Bak can activate the apoptosis cascade by initiating the release of cytochrome c and other pro-apoptotic factors from the mitochondria, E1B-19K binding to these proteins may be one mechanism by which this protein inhibits the programmed cell death cascade.

## 2.2. Cellular Anti-apoptosis protein Aven

A novel 38 kDa protein designated Aven was identified using a mutant of Bcl-x<sub>L</sub>, another member of the Bcl-2 family (Chau et al., 2000). The Aven protein was subsequently found to bind to a number of other Bcl-2 family proteins including human Bcl-2 and homologs from herpesviruses. The protein did not interact with pro-apoptotic Bcl-2 family members including Bax and Bak.

Aven's activity in the cell death pathway was elucidated by exposing mammalian FL5.12 cells stably expressing Aven to apoptosis induced by IL-3 withdrawal. The Aven-expressing cells had 20% higher viability compared to control-transfected cells. In contrast, expression of Aven did not protect BHK cells against apoptosis induced by caspase-1, but the concurrent expression of both Bcl-x<sub>L</sub> and Aven increased the anti-apoptosis activity of Bcl-x<sub>L</sub> by 20-30% above the levels obtained using Bcl-x<sub>L</sub> alone. Subsequent experiments indicated that Aven interacted independently with the pro-apoptosis protein Apaf-1. Apaf-1 associates with cytochrome c released from the mitochondria during the formation of an oligomeric multi-protein complex that leads to the subsequent activation of caspase-9 (see



Figure 1). In addition, Apaf-1 was found to inhibit the activation of cell death caused by the co-transfection of caspase-9 and Apaf-1.

The mechanism by which Aven acts to prevent apoptosis is not yet defined. Aven clearly acts to inhibit apoptosome assembly and caspase activation. However, Aven is also observed to enhance Bcl-x<sub>L</sub> function in cells exposed to caspase-1-induced apoptosis. The alternative anti-apoptosis activities of Aven may be related or represent separate mechanisms to slow the cell death cascade.

In order to investigate further the role of E1B-19K and Aven in preventing cell death in cultures, CHO-K1 cell lines were genetically modified in order to express these two anti-apoptosis proteins. CHO cell lines were created containing one or more of the heterologous genes of interest. Experiments were then performed in which the cells were exposed to a model cell culture insult in order to elucidate the protective capacity of Aven, E1B-19K, or Aven and E1B-19K in combination.

### 3. RESULTS AND DISCUSSION

CHO cells were transfected with the Invitrogen pIND vector, which has been modified to include sites for the insertion of three foreign genes. This cell line has been manipulated to include the ecdysone expression system so that foreign genes encoded on the vector are induced in the presence of an inducer such as ponasterone A. Four different cell lines were generated for the current study as shown in Table 1. A control CHO cell line was generated containing the GFP gene only. Three additional cell lines were created in which the gene for GFP was integrated into the cells in combination with either Aven, E1B-19K, or both anti-apoptosis genes together. In the absence of the ponasterone A, expression of these heterologous genes was repressed. The addition of ponasterone A to the cultures facilitated the high level expression of GFP, GFP and Aven, GFP and E1B-19K, or GFP, Aven and E1B-19K in the four engineered cell lines of interest. Western blot analysis using anti-Aven and anti-E1B-19K antibodies confirmed the expression of these genes in the genetically engineered cells following the addition of ponasterone A.

In order to evaluate the effects of expressing these heterologous genes on cell survival, the engineered CHO cell lines were exposed to a model insult which can induce apoptosis. The exhaustion of critical nutrients is one common insult that occurs in animal cells cultured in bioreactors for extended periods. In order to simulate nutrient depletion, the different CHO cell lines were grown in normal medium and then resuspended in culture medium without glucose. Preliminary experiments indicated that the removal of glucose from the culture medium indeed induced the programmed cell death cascade in CHO cells. Next, viabilities of the different cell lines were monitored in order to evaluate the effect of expressing either Aven, E1B-19K, or Aven and E1B-19K in combination. Experiments were performed both in the presence (+) and absence (-) of ponasterone A as indicated in Table 1. The number of viable cells were observed to increase following the expression of either Aven or E1B-19K alone as well as Aven and E1B-19K in combination. Viable cells numbers were significantly lower in cell lines expressing GFP alone and in the engineered cells cultured in the absence of ponasterone A.

Therefore, the over-expression of Aven and E1B-19K independently and in combination represents a possible cell engineering strategy that can limit apoptosis and enhance survival of mammalian cells cultured for extended periods in bioreactors.

*Table 1. Engineered CHO cell lines exposed to apoptosis insult. Experiments were performed in the absence(-) or presence (+) of ponasterone A inducer.*

<i>Cell Line</i>	<i>No Inducer</i>	<i>With Ponasterone A</i>
CHO-GFP	CHO-GFP (-)	CHO-GFP (+)
CHO-GFP-Aven	CHO-GFP-Aven (-)	CHO-GFP-Aven (+)
CHO-GFP- E1B-19K	CHO-GFP-E1B-19K (-)	CHO-GFP-E1B-19K (+)
CHO-GFP-Aven - E1B-19K	CHO-GFP-Aven - E1B-19K (-)	CHO-GFP-Aven-E1B-19K (+)

#### 4. REFERENCES

- White, E., Cipriani, R., Sabbatini, P., and Denton, A. The adenovirus E1B 19-kilodalton protein overcomes the cytotoxicity of E1A proteins. *J. Virol.* 65: 2968-2978 (1991).
- Gooding, L. R., Aquino, L., Duerksen-Hughes, P. J., Day, D., Horton, T. M., Yei, S., and Wold, W. S. M. The E1B-19K protein of group C adenoviruses prevents cytolysis by tumor necrosis factor of human cells but not mouse cells. *J. Virol.* 65: 3083-3094 (1991).
- Hashimoto, S., Ishii, A., and Yonehara, S. The E1B oncogene of adenovirus confers cellular resistance to cytotoxicity of tumor necrosis factor and monoclonal anti-Fas antibody. *Intl. Immunol.* 3: 343-351 (1991).
- Cuconati, A., and White, E. Viral homologs of Bcl-2: role of apoptosis in the regulation of virus infection. *Genes Dev.* 16: 2465-2478 (2002)
- Tarodi, B., Subramanian, T., and Chinnadurai, G. Functional similarity between adenovirus E1B 19K gene and Bcl-2 oncogene: Mutant complementation and suppression of cell death. *Intl. J. Oncol.* 3: 467-472 (1993).
- Chiou, S.-K., Tseng, C. C., Rao, L., and White, E. Functional complementation of the adenovirus E1B 19K protein with Bcl-2 in the inhibition of apoptosis in infected cells. *J. Virol.* 68: 6553-6566 (1994).
- Chau, B. N., Cheng, E. H.-Y., Kerr, D. A., and Hardwick, J. M. Aven, a novel inhibitor of caspase activation, binds Bcl-x<sub>L</sub> and Apaf-1. *Mol. Cell* 6: 31-40 (2000).

## QUESTIONS AND ANSWERS

**Herman Katinger, Institute of Applied Microbiology, Vienna, Austria:**

What concentration do you consider critical with respect to glucose? Do you use defined medium or not ?

**Michael Betenbaugh, John Hopkins University, Baltimore, US:**

I do not know exactly what is the critical concentration of glucose, since we did glucose deprivation experiments. The medium we used is a defined, serum-free proprietary medium from IDEC, although it was not totally optimized.

**Stephanos Grammatikos, BI Pharma, Germany:**

You were only measuring viability although they are several other assays for measuring apoptosis. Were you able to show at any time that what you were doing genetically actually does?

**Michael Betenbaugh, John Hopkins University, Baltimore, US:**

Although we are not able to afford sophisticated techniques to make massive measurements, we do follow the loss of viability with other apoptosis assays, such as microscopic observation, flow cytometry and DNA laddering, and there is always a correlation. The cell death in these experiments is mainly apoptotic, although I cannot provide the exact data.

**Alain Bernard, Serono, Switzerland:**

Is there a reason why you chose inducible expression rather than constitutive, and, what is the ratio of expression of E1B-19K and Aven in terms of copy number and so on ?

**Michael Betenbaugh, John Hopkins University, Baltimore, US:**

It would also have been OK to use constitutive expression of the antiapoptotic genes, but in previous studies with other genes such as *bcl-x<sub>L</sub>* and *bcl-2* we have observed an effect on cell growth rates. This effect can be avoided using inducible systems. On the other part of the question, I do not have the specific activity numbers, but the effect is primarily due to the fact that E1B-19K is a potent apoptosis inhibitor when compared to Aven. It is not so much an expression effect but an activity effect. E1B-19K is a powerful inhibitor of apoptosis, and it is also non proprietary, another important aspect to take into account.

**Ralph Kemphen, Boehringer Ingelheim, BI Pharma, Germany:**

Do you think that the cells really want to commit suicide or do you think they are trying to attain a resting cell situation but they finally collapse ?

**Michael Betenbaugh, John Hopkins University, Baltimore, US:**

There are certainly different options between arrest and apoptosis. When you deplete the cells of glucose, the signal is so strong for the apoptotic mechanisms, that there are no possibilities for the cell to evolve to a resting cell situation.

**Satoshi Terada, Fukua University, Japan:**

Transfection with the genes improved cell viability but the maximum cell density is decreased, is that right?

**Michael Betenbaugh, John Hopkins University, Baltimore, US:**

No, the cell viability and the total cell density were increased, on a total basis.

**Satoshi Terada, Fukua University, Japan:**

But on the other hand the amount of the antibody is not so much higher.

**Michael Betenbaugh, John Hopkins University, Baltimore, US:**

I said that this is a non-optimized experiment. There are many different ways to inhibit apoptosis, and there are many different ways to induce higher production levels of antibodies. What we are showing in this case is for a non-optimized system. For other things being equal you can certainly increase total productivity on a per volume basis by inducing anti-apoptosis genes.

**Meijia Yang, Serono Reproductive Biology Institute, US:**

You have prolonged the production phase, and in the last phase, under more stress for the cells, have you measured the antibody production of this phase in comparison to the normal situation, and if any changes occurred in the glycosylation patterns ?

**Michael Betenbaugh, John Hopkins University, Baltimore, US:**

I do not know that by increasing the production phase the quality of the antibody in terms of glycosylation may have changed.

L. HUNŦ, D. HACKER, H. EL ABRIDI, F. GROSJEAN,  
M. DEJESUS, M. JORDAN, F. M. WURM

## PAUSING OF MAMMALIAN CELLS BY COLD EXPOSURE, LIMITS AND OPPORTUNITIES

*Swiss Federal Institute of Technology Lausanne, Faculty of Basic Sciences,  
Institute of Biological and Chemical Process Sciences*

### 1. INTRODUCTION

The use of mammalian cells for research and for numerous applications could be facilitated significantly if pausing, i.e. reduction and reactivation of cellular activity, could be executed at will without negative effects. Preferably, pausing should be possible at any phase of a cell culture and at any scale of operations. In this communication we report our first observations to pause cell cultures by temperature reduction. Little information is available in the literature on cold exposure of mammalian cells (1). For this study, we took advantage of the availability of stable GFP-transfected CHO cells whose biomass in culture could be fast and non-invasively monitored by a standard fluorescence reader (2).

### 2. RESULTS

*Optimal pausing temperature is not near 0° C.*

All living systems are constrained by a well-defined range of temperature. The optimal temperature for mammals and cell in culture derived from them is probably among the most narrowly defined in nature. Starting from GFP-expressing CHO cell cultures, we explored the possibility to reduce the environmental temperature within the range of 0° C to 37° C. For practical reasons, six different temperature settings were studied initially: 0° C (ice-water bath), 4° C (cold room), 7° C (+/- 2°, refrigerator), 16° C (+/-1° C, tube incubator for ligations), 23° C (+/- 2° C, ambient temperature in the laboratory) and 37° C (cell culture incubator). Cells for the data shown below were obtained from an adherent T-flask culture. The cells were trypsinized, resuspended in fresh culture medium and transferred as aliquots in 1.5 ml Eppendorf tubes that were subsequently closed and incubated at the indicated temperature. After pausing cells were transferred into 12-well plates with fresh medium. For growth assessment the 12 well plates were incubated in a standard

CO<sub>2</sub> incubator and total fluorescence was measured using a standard fluorescence plate reader.

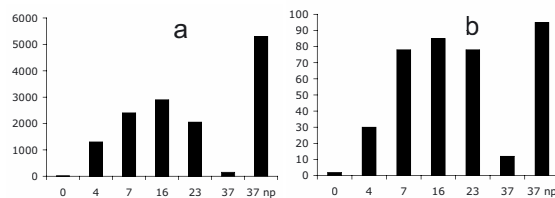


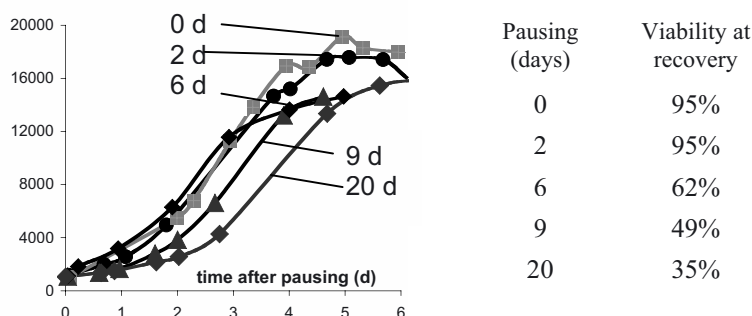
Fig.1 Pausing for 4 days at different temperatures (np= not paused).

a: Cell mass (rfu) assessed after 2 days of growth  
b: Viability after pausing (%)

Surprisingly, after 4 days of pausing, the optimal temperature allowing rigorous growth and good viability was not found near 0° C, but in the 10-20° C range. As expected, non-paused cells showed the highest obtained cell mass after two days of culture. In comparison to these, the better performing cells (7-23° C) showed about half the cell mass obtained by the control culture, indicating a delay in reinitiated growth. Pausing in an eppendorf tube at 0° C and at 37° C for 4 days resulted in an unrecoverable culture. Cultures paused at 7-23° C reached eventually a final maximal cell density similar to control cells (data not shown).

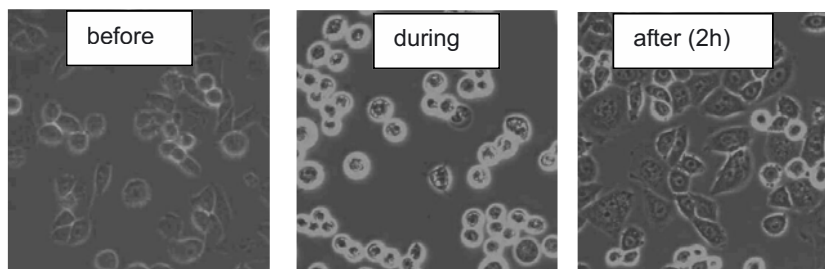
*Cells can be paused 3 weeks at 4-8° C.*

In a subsequent study, the pausing time period was investigated and, for practical reasons, the incubation of samples was done in a refrigerated incubator, maintaining temperature between 4° and 8° C. We paused cells for 0, 2, 6, 9 and 20 days. The cells were distributed, at a cell density of about  $1 \times 10^6$  c/ml as 1 ml aliquots into closed eppendorf tubes and replated after pausing into prewarmed medium (0.5 ml) in 24 well plates. Each well received 50µl of the paused cell suspension. Subsequent growth was assessed by fluorescence quantification, 2-3 times per day.



The table shows that extending periods of time under pausing condition decreases the viability of the culture, but even after 3 weeks, more than 30% of the cells are viable. Subsequent seeding of paused cultures results in full recovery of the cells, albeit with a delay for exponential growth, most pronounced in cultures that have been stored for longer periods.

We have also executed a number of pausing experiments with cells that were left in cell culture flasks or multiwell plates and then left at 4°C for a week-end or longer, i.e. they were not trypsinized prior to pausing. In all cases, care was taken prevent gas exchange during pausing. Pausing of adherent CHO cells under these conditions results in detachment and rounding up. Subsequent to returning the cell culture flasks to 37°C the cells reattach to the surface of the culture flask and continue to grow. The images below show the morphology of cells prior to, during and after pausing for 3 days.



### 3. FURTHER STUDIES AND DISCUSSION

We performed a number of studies concerning the medium composition for cells under pausing and have found that pH and the availability of glucose and glutamine are important for long-term pausing (data not shown). Pausing for 1-2 days can be performed with PBS solutions. Also, we have extended these studies to subpopulations of cells derived from those used here. These subpopulations were adapted to grow under serum free conditions in free suspension mode (spinner and shaker). Our observations reported above could be verified in principle, but we need to accumulate more data for providing sufficient support for a general statement. In addition, we have used HEK-293 cells and found them to be amenable to pausing as well, with a broad optimal temperature range similar to the one observed with our CHO cells (data not shown). Also, cells can be prepared for transfections, paused for at least one week and re-incubated at 37° C for a few hours. It appears that such cells are as transfectable as “fresh” cells.

Obviously, the preliminary data presented here do not provide sufficient evidence for a generally applicable pausing regimen for all mammalian cells in culture. We would not be surprised if individual cell types and different cell culture modes affect both the temperature range and the time frames during which cells can be paused. However, literature data from the 1970ies support our surprising observation that very cold pausing (near 0° C) is detrimental for survival of cells.

#### 4. REFERENCES

- L. A. Sonna, J. Fujita, S. L. Gaffin, C.M. Lilly 2002: Invited review: Effects of heat and cold stress on mammalian gene expression. *J. Appl Physiol.* 92, 1725-1742
- Hunt, L., M. Jordan, M. Dejesus, F.M. Wurm 1999: GFP expressing mammalian cells for fast, sensitive, noninvasive cell growth assessment in a kinetic mode. *Biotechn. Bioeng* 65; 201-205

The first author of this paper, Dr. Lisa Hunt passed away following a mountain hiking accident, late in 2002. Dr. Hunt was an enthusiastic scientist who has touched and inspired the scientific and personal life of many who knew her.



DANIEL E. ALETE<sup>1</sup>, ANDREW J. RACHER<sup>2</sup>, JOHN R. BIRCH<sup>2</sup>,  
DAVID C. JAMES<sup>3</sup> AND C. MARK SMALES<sup>1</sup>.

## THE FUNCTIONAL COMPETENCE OF ANIMAL CELLS: ANALYSIS OF THE SECRETORY PATHWAY.

<sup>1</sup>Research School of Biosciences, University of Kent, Canterbury, CT2 7NJ, UK. <sup>2</sup>Lonza Biologics plc, 228 Bath Road, Slough, SL1 4DY, UK. <sup>3</sup>Dept of Chemical Engineering, University of Queensland, St. Lucia, Brisbane, Qld 4072, Australia.

### 1. INTRODUCTION

The development of highly efficient expression systems (such as the Glutamine synthetase (GS) and Dihydrofolate reductase (DHFR) systems) has resulted in the generation of cell lines with high levels of recombinant gene transcription (i.e. the production of relatively high levels of recombinant protein mRNA) (Bebbington, 1992; Grillari, 2001). However, the correlation between the amount of mRNA produced and the yield of fully functional secreted recombinant protein in these cell lines is variable (Merten *et al.*, 1994). Several reports have now suggested that one of the possible reasons for this anomaly is that there are 'bottlenecks' within the cell that are major rate-limiting steps in achieving high level recombinant protein production from mammalian cells in culture (Fann *et al.*, 1999). It has been suggested that the most likely bottlenecks in mammalian cells include the efficient folding, transport, modification and degradation of recombinant proteins (Fann *et al.*, 1999). We have utilised a proteomic approach for the comparative analysis of a series of NS0 cell lines differing in cell specific productivity in order to further our current understanding of the cellular processes that result in high level monoclonal antibody (Mab) secretion. Specifically, we have investigated the processes catalysed by a variety of proteins that constitute the secretory pathway. Our model system for this investigation is the GS-NS0 cell line expressing B72.3 antibody.

### 2. MATERIALS AND METHODS

Parental NS0 cells were transfected with a glutamine synthetase (GS) expression vector containing the B72.3 H and L chain genes by electroporation in protein free medium. Primary transfectants were identified by transferring the cells into medium containing 10% dFCS and 2 mM glutamine before limiting dilution in 96-well microtiter plates. After 24 hours the B72.3 and GS genes were co-amplified by

inclusion of 10 mM methionine sulphoximine (MSX) and the exclusion of glutamine. The plates were then left for 2-3 weeks before being screened for colonies. From this point onwards the medium did not contain glutamine or MSX. Selected colonies were then moved into 24 well plates. Subsequently, transfected GS-NS0 cells were routinely cultured in DMEM/F-12 medium containing 10% dFCS without either glutamine or MSX.

Five cell lines (4O, 4R, 2X, 2P, 2N2) differing in Mab specific productivity, a mock transfectant blank (transfected with GS vector lacking Mab genes) and the parental NS0 cell population were selected for further comparative analyses. All experiments reported here are based on 100 mL batch cultures in 0.5 L shake flasks. Cultures were initially seeded at a density of  $2 \times 10^5$  cells mL<sup>-1</sup>. Cell specific productivities were determined by ELISA assay. Microsome fractions were prepared from GS-NS0 cells were harvested at mid-exponential phase of growth as described by Han *et al.* (Han *et al.*, 2001). The microsome fraction was solubilised for 1 h at RT with agitation in lysis buffer (9.5 M Urea, 4% CHAPS, 0.8% Pharmalytes (pH 3-10) and 1% DTT). Solubilised proteins were separated by isoelectric focussing on pH 3-10, 24 cm IPG strips on an IPGphor machine (Amersham Biosciences) for a total of 70,000 Vh. IPG strips were run in the second dimension on large format (24cm) 12.5% tris-glycine polyacrylamide gels using an Ettan Dalt II system (Amersham Biosciences). Proteins spots were visualised by silver staining as described by Smales *et al.*, 2003. Image analysis was performed using Image Master™ 2D Elite software (Amersham Biosciences). Protein spots were identified by in-gel tryptic digest followed by MALDI-TOF mass spectrometry peptide mass fingerprinting.

### 3. RESULTS AND DISCUSSION

A summary of growth and production kinetics is shown in Figure 1. A range of specific productivities was observed in the cell lines investigated. Transfection appeared to adversely affect the specific growth rate of NS0 cells. Productivity did not (inversely) correlate with growth rate (Figure 1). The fractionation procedure resulted in the enrichment of secretory pathway proteins GRP78 and PDI while minimal contamination of mitochondrial (HSP60) and cytosolic (tubulin) proteins was observed as determined by western analysis (data not shown). After 2D-electrophoresis between 600 and 850 discrete protein spots were observed in the enriched microsome fractions across all gels and cell lines. This compares with analysis of the whole cell proteome using the same IEF and SDS-PAGE procedures whereby approximately 2500 discrete protein spots are observed in each gel (Smales *et al.*, 2003).

Comparative analysis of the proteomic maps generated in this study shows, as expected, that there is no change in the abundance of many proteins between the different cell lines (Figure 2). However, there were many cell line specific changes in protein abundance that did not correlate with cell specific productivity. Very few examples of changes in protein abundance that correlate with higher Mab productivity were observed (see Figure 2 for example).

The data present here therefore clearly demonstrates that the majority of changes in protein expression observed in the NS0 microsome proteome are cell line specific, and that there are very few changes that correlate with increased monoclonal antibody productivity. Those proteins whose expression does correlate with increased productivity (7 in total) are present in low abundance. These results imply that a productive cell has a ‘bias’ (cell specific bias) to its range of proteins involved in integrated cellular functions such as productivity and cellular metabolism.

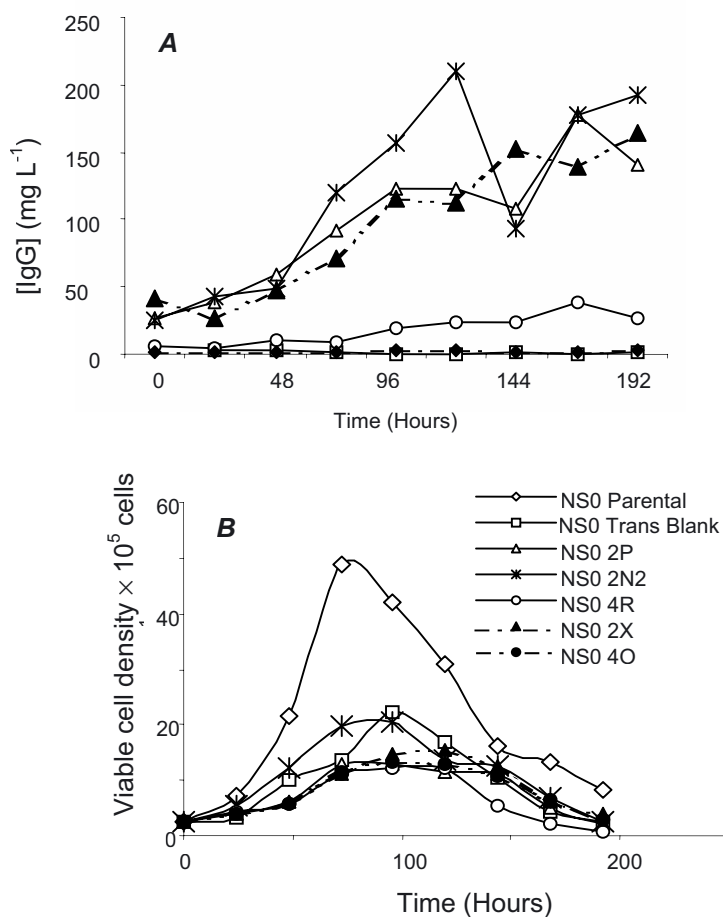


**Figure 1.** Characteristics of the GS-NS0 cell lines utilised in this study. (A) Mab productivity over batch culture assayed by ELISA (B) Cell growth based on 100 mL batch cultures.

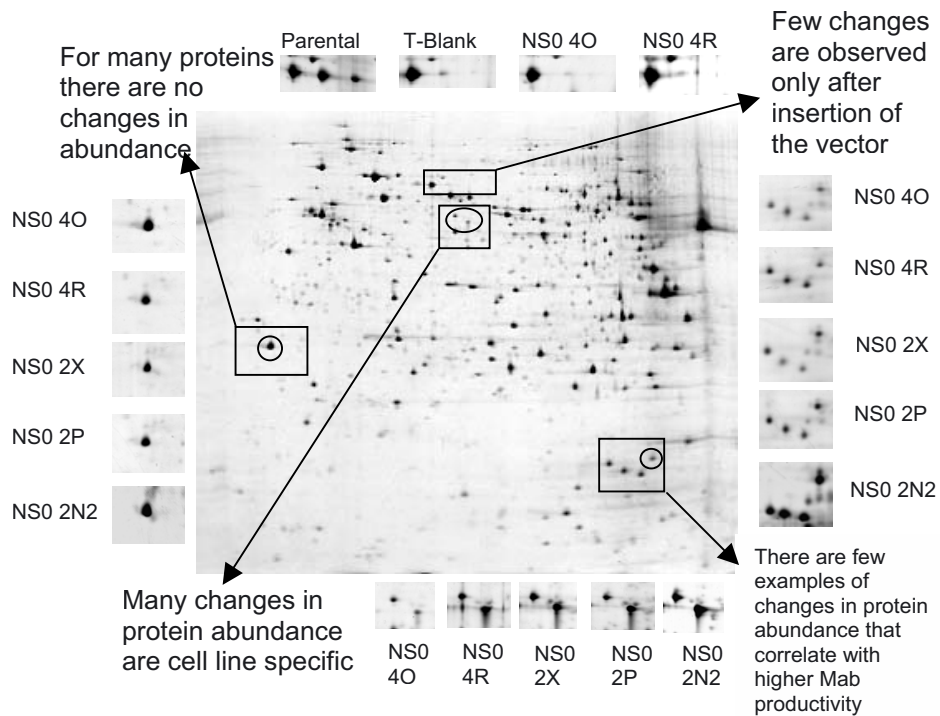


Figure 2. Comparative analysis of microsomal fractions of GS-NS0 cell line differing in specific productivity by 2D-PAGE. Protein spots were visualized using silver staining and image analysis performed using Image Master™ 2D Elite software (Amersham Biosciences).

## REFERENCES

- Bebbington C.R., Renner G., Thompson S., King D., Abrams D., and Yarranton, G.T. (1992). *Biotechnology*, **10**:169-175.
- Grillari J., Fortschegger K., Grabherr R.M., Hohenwarter O., Kunert R., and Katinger H. (2001) *J. Biotech.*, **87**:59-65.
- Merten O.W., Moeurs D., Keller H., Leno M., Palfi G.E., Cabanie L., and Couve E. (1994) *Biotech. Bioeng.*, **44**:753-764.
- Fann C.H., Guarna M.M., Kilburn D.G., and Piret J.M. (1999) *Biotech. Bioeng.*, **63**:464-472.
- Han D.K., Eng J., Zhou H., and Aebersold. 2001. *Nature Biotech.*, **19**:946-951.
- Smales C.M., Birch J.R., Racher A.J., Marshall C.T., and James D.C.(2003) *Biochem. Biophys. Res. Com.*, **306**:1050-1055.

MOON SUE LEE<sup>A</sup>, KYOUNG WOOK KIM<sup>B</sup>, YOUNG HWAN  
KIM<sup>B</sup>, GYUN MIN LEE<sup>A,\*</sup>

## PROTEOME ANALYSIS OF RECOMBINANT CHO CELLS UNDER HYPEROSMOTIC STRESS

<sup>a</sup> *Department of Biological Sciences, Korea Advanced Institute of Science  
and Technology, 373-1 Kusong-Dong, Yusong-Gu, Daejeon 305-701, Korea*

<sup>b</sup> *Proteome Analysis Team, Korea Basic Science Institute, P.O. Box 41,  
Daejeon 305-333, Korea*

### ABSTRACT

To better understand intracellular responses rCHO cells expressing an antibody to hyperosmotic pressure, we have taken a proteomics approach. Using two-dimensional electrophoresis and mass spectrometry, a proteome profile of rCHO cells comprising 23 identified proteins was established. Based on this proteome profile, we found 3 proteins of which expression levels were significantly changed at 450 mOsm/kg. Compared to the results at 300 mOsm/kg, two glycolytic enzymes, glyceraldehyde-3-phosphate dehydrogenase and pyruvate kinase, were found to be up-regulated, probably leading to an increased metabolic energy for antibody synthesis. The elevation of specific glucose consumption rate at 450 mOsm/kg agreed with the up-regulation of these glycolytic enzymes. On the other hand, tubulin expression was down-regulated, reflecting a depressed cell growth rate at 450 mOsm/kg. Taken together, this study shows the potential of the proteomics approach in understanding intracellular and physiological changes in cells and seeking a better insight into possible environmental or genetic manipulation approaches for increasing foreign protein production in rCHO cells.

### 1. INTRODUCTION

Hyperosmotic pressure, which can be induced by adding cheap salts or sugars to culture media, has been suggested as an economical solution to increase the specific foreign protein productivity ( $q$ ) in rCHO cell culture [1, 2]. However, studies on intracellular responses of rCHO cells to hyperosmotic pressure have not been fully substantiated as yet, though they could eventually lead to a better insight into possible environmental or genetic manipulation approaches for increasing foreign protein production [3]. Two-dimensional polyacrylamide gel electrophoresis (2-D PAGE) followed by mass spectrometric analysis is a commonly used method for the identification of proteins in a complex mixture. When these technologies are used in concert to the study on cell culture, their impact on the foreign protein production can be maximized.

## 2. MATERIALS AND METHODS

### 2.1. 2-D PAGE.

Exponentially growing cells were harvested at 72 h. Whole cell extracts were prepared using rehydration buffer (8 M urea, 2% CHAPS, 50 mM DTT, 0.2% (w/v) Bio-Lyte 3/10 ampholyte, and 0.002% bromophenol blue). Two milligrams of proteins were loaded onto 17 cm ReadyStrip IPG strips, and IEF was performed to 50,000 Vh using PROTEAN<sup>®</sup> IEF Cell System (Bio-Rad) at 20°C.

### 2.2. MALDI-TOF-MS and MALDI-TOF/TOF tandem MS.

Spots of interest were excised manually, and digested with sequencing grade trypsin. The resulting tryptic peptides were dissolved in 0.5% trifluoroacetic acid (TFA) solution, and then desalted using ZipTipC18 (Millipore, Bedford, MA). Peptides were eluted directly onto MALDI target by CHCA matrix solution. All mass spectra were acquired at a reflection mode by a 4700 Proteomics Analyzer (Applied Biosystems, Framingham, MA). When the protein spots were not identified by peptide mass fingerprinting (PMF), fragmentation patterns of tryptic peptide molecular ions ( $[M+H]^+$ ) were analyzed by MS/MS methods for obtaining their partial sequences using MALDI-TOF/TOF technique.

## 3. RESULTS AND DISCUSSION

### 3.1. Cell growth and antibody production

To determine the effect of hyperosmotic pressure on rCHO cells (CS13\*-1.00) in regard to growth and antibody production, batch cultures with various osmolalities in the range of 300 to 450 mOsm/kg were performed. The osmolality did not change significantly during the culture (data not shown).

As shown in Figure 1A, hyperosmotic pressure depressed cell growth. On the other hand, the maximum antibody concentration at the osmolality ranging from 300 to 450 mOsm/kg was similar despite the depressed cell growth at elevated osmolalities (Figure 1B). This result implies that hyperosmotic pressure significantly enhanced  $q_{Ab}$ . The  $q_{Ab}$  at 450 mOsm/kg was increased by 139%, compared with that at 300 mOsm/kg.

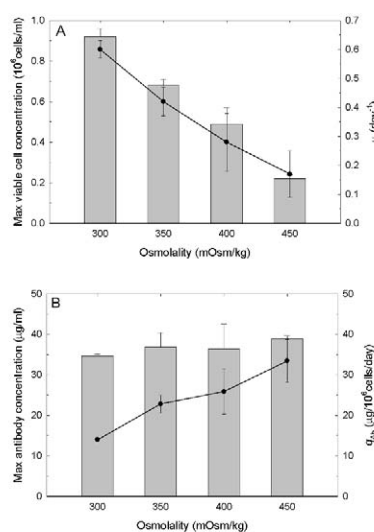


Figure1. Cell growth and antibody production.

3.2. Proteome profile of rCHO cells

Proteome expression profiles of rCHO cells grown at 300 mOsm/kg were shown in Figure 2. To achieve more protein spots, overlapping pH range analysis was carried out; (A) pH range 3-6, linear, and (B) pH range 5-8, linear. Over 800 spots were detected on the map with PDQuest™ image analysis software. From the silver-stained

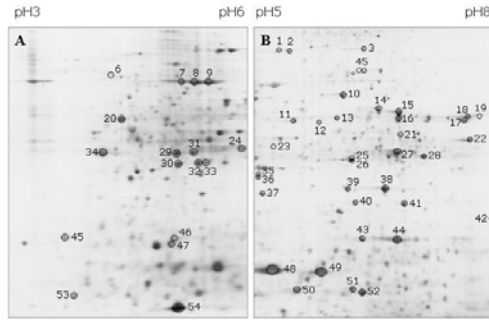


Figure 2. Proteome expression profiles of rCHO cells. 2-D gels,

abundant 54 spots were excised and analyzed by MALDI-TOF-MS. Since the complete database of CHO cells has not been established, all mass spectra were searched in the database of rodent species or all entries. Among 54 spots, 29 protein spots were identified by MALDI-TOF-MS database search. After MS/MS analysis, additional 12 protein spots were identified by database search.

Figure 3 shows the representative MALDI tandem mass spectrum of a peptide molecular ion with a molecular mass of 2183.542 Da found in Spot No.44. The spot was identified as a homologous protein similar to superoxide dismutase by MASCOT MS/MS ion searching of fragmentation patterns. As a result, the protein expression profile of rCHO cells was constructed using 41 identified protein spots.

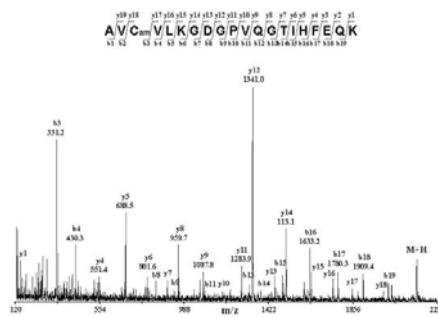


Figure 3. Representative MALDI tandem mass spectrum of peptide molecular ion with a molecular mass of 2183.54 Da.

### 3.3. Identification of proteins regulated by hyperosmotic pressure

To identify the proteins that are regulated in response to the hyperosmotic pressure, 2-D PAGE of proteins (2 mg each) extracted from cells grown at 300 and 450 mOsm/kg was performed. Compared to the results at 300 mOsm/kg, we have found at least 8 spots with significantly different expression levels at 450 mOsm/kg. These spots were identified as glyceraldehyde-3-phosphate dehydrogenase (GAPDH), pyruvate kinase (PK), and tubulin by MS. The metabolic enzymes, GAPDH and PK, were found to be up-regulated, suggesting that hyperosmotic pressure alters the metabolic state. The up-regulated expressions of these two glycolysis enzymes could activate the generation of metabolic energy. On the other hand, tubulin was found to be down-regulated.

In conclusion, in an effort to better understand intracellular responses of rCHO cells to hyperosmotic pressure, we have established a CHO cellular protein map comprising 23 identified proteins. From this map, we found out that hyperosmotic pressure up-regulates GAPDH and PK and down-regulates tubulin. Furthermore, 2-D database obtained in this study contributes to the construction of an improved CHO reference map, which is a useful tool in seeking a better insight into possible environmental or genetic manipulation approaches for increasing foreign protein production.

## 4. REFERENCES

- [1] Ryu JS, Lee MS, Lee GM, Effects of cloned gene dosage on the response of recombinant CHO cells to hyperosmotic pressure in regard to cell growth and antibody production, *Biotechnol. Prog.* 17 (2001) 993-999.
- [2] Lee MS, Lee GM, Hyperosmotic Pressure Enhances Immunoglobulin Transcription Rates and Secretion Rates of KR12H-2 Transfectoma, *Biotechnol. Bioeng.* 68 (2000) 260-268.
- [3] Gauss C, Kalkum M, Löwe M, Lehrach H, Klose J, Analysis of the mouse proteome. (I) Brain proteins: Separation by two-dimensional electrophoresis and identification by mass spectrometry and genetic variation, *Electrophoresis* 20 (1999) 575-600.



MARK W. MELVILLE, MARTIN SINACORE, AND  
LOUANE E. HANN

## EXPRESSION PROFILING ANALYSIS OF SODIUM BUTYRATE-INDUCED CHINESE HAMSTER OVARY CELLS IN DEFINED MEDIUM

*Wyeth BioPharma, Drug Substance Development, 1 Burt Road, Andover,  
MA 01810*

**Abstract.** The production of recombinant protein for biopharmaceutical application typically requires vast numbers of cells, and agents that induce expression of the desired product to even higher levels. A typical strategy employed by the biotech industry is to express the protein of interest in Chinese Hamster Ovary (CHO) cells stably transfected with the gene. Where even higher levels of expression are desired, inducing agents such as sodium butyrate or valeric acid are added to the media. Current research suggests that these chemicals increase expression by blocking deacetylation of histone proteins bound to DNA. This has the effect of relaxing DNA structure, and allowing greater access to the transcription machinery. Thus, higher levels of mRNA are achieved. However, these agents have the ultimate effect of blocking cell proliferation, and eventually inducing apoptosis in treated cells. We have undertaken an expression profiling approach to identify the genes up and down-regulated in induction conditions.

### 1. INTRODUCTION

DNA microarray technology has allowed researchers to survey the expression of thousands of genes and identify key genes involved in various cellular processes including those associated with disease states, cellular signaling pathways, and development. We designed a DNA oligo microarray based on the Affymetrix platform specific for CHO cells to identify genes that are differentially expressed during various cell culture processes. The microarray contains genes identified from a CHO-cell library constructed by our group as well as additional sequences derived from public databases. Using the microarray technology we hope to identify CHO genes that negatively influence cellular productivity or alter host cell behavior in order to design better production processes and increase our understanding of CHO cell biology. In this study, we present expression profiling results identifying genes associated with butyrate induction using a product cell line.

## 2. MATERIALS AND METHODS

### 2.1. CHO CHIP DESIGN

Two normalized cDNA expression libraries were created from log and stationary phase CHO DUKX cultures. The library was screened for sequence redundancy and overlaps and ultimately yielded 2835 unique sequences. An additional 732 CHO sequences, collected from public data bases, were included on the chip as well as 22 product-specific genes and 122 controls sequences that were used for normalizing data and determining RNA quality. Each sequence on the chip was represented by 55 separate 25-mer oligo probes; the specificity of each probe set was confirmed by BLAST analysis against the other sequences on the microarray.

### 2.2. EXPRESSION PROFILING

The product cell line used in these experiments was derived from a CHO DG44 host cell line. Cultures were seeded at  $2 \times 10^6$  cells/ml on day 0 in 125 mL polycarbonate shake flasks. Twenty-four hours later, the medium was replaced with fresh medium containing 0.5 mM sodium butyrate ( $n = 3$ ). The medium from all cultures was removed by centrifugation on day 4, and replaced with the fresh medium containing butyrate. Cultures were terminated on day 6. Cell density and viability were monitored daily using a hemacytometer and trypan blue dye exclusion. Total RNA was purified from  $3 \times 10^6$  cells on each culture day using the RNeasy Mini Kit (Qiagen) and quantified by  $A_{260}$ . RNA integrity was assessed using an Agilent Bioanalyzer 2100. cRNA was prepared as recommended by Affymetrix and was hybridized onto the microarray. Hybridized chips were placed in an Agilent GeneArray Scanner. All subsequent analyses were conducted using the GeneLogic GeneExpress 2000 software suite. Taqman quantitative RT PCR was performed on an ABI PRISM 7000 Sequence Detection System.

## 3. RESULTS AND DISCUSSION

Over the course of butyrate induction, 604 transcripts were identified that exhibited a 2-fold change or more in replicate cultures ( $p\text{Value} < 0.05$ ). These genes fall into several categories based on their expression pattern (Figure 1). The number of differentially expressed genes was reduced to 25 when the data set was limited to transcripts having at least a 3-fold change at 24 hours post-butyrate addition. Sequence analysis of the 25 differentially expressed genes identified 22 unique genes that fell into a several categories including those involved with cell cycle control, DNA synthesis and repair, and the ER-stress response. The differential regulation of genes involved in cell cycle control and DNA synthesis and repair is consistent with the reported role of butyrate in cell cycle arrest<sup>1</sup>, apoptosis<sup>2</sup> and histone deacetylation<sup>3</sup>. The induction of ER-stress response genes is likely due to the high expression level observed for the product-specific transcript that encodes a secreted protein (Figure 2).

For the product-specific transcript, comparison of the microarray data with Taqman-generated data showed a similar expression pattern. However, the absolute fold change values determined by the two methods varied. For example, on day 4 a 119-fold increase in product transcript was observed by Taqman compared to a 42-fold

increase as determined by microarray analysis. This result is consistent to that observed for other transcripts where the absolute fold change values may vary between the two methods (data not shown). Nonetheless, Taqman analysis provides a reliable method for confirming differentially regulated genes identified by microarray analysis.

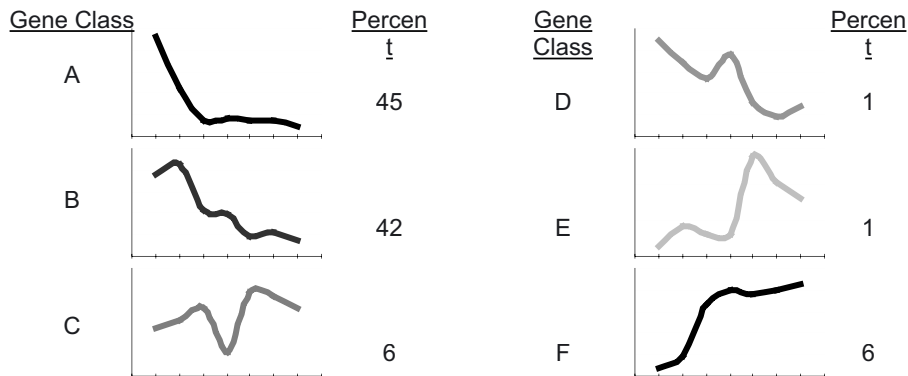


Figure 1. Expression profiles of 604 sequences differentially expressed in butyrate-induced culture over 6 days. The genes were grouped by expression pattern. The distribution is shown as a percentage.

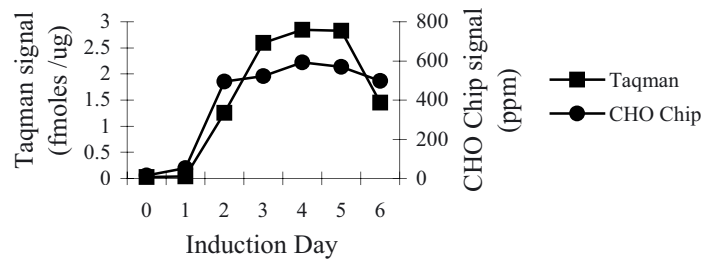


Figure 2. Expression profile of product mRNA

In this study, we have shown that our CHO microarray is a useful tool to monitor gene expression changes associated with butyrate induction. Identification of novel genes associated with other industrially relevant culture processes such as fed-batch, perfusion or high cell density cultures should provide an invaluable tool to understand and improve CHO cell production systems.

## REFERENCES

1. Cuisset L. et al. *Biochem Biophys Res Comm* (1998) **246**, 760-764.
2. Kim N.S. and G.M. Lee. *Biotech and Bioengin* (2000) **71**, 184-193.
3. Lee D.Y. et al. *Cell* (1993) **72**, 73-84.

**Acknowledgements.** We would like to thank Peter Lapan and Bo Gou for their work in sequencing and analyzing the cDNA libraries used for the chip. We would also like to thank Bill Mounts and Maryann Whitley for their help in chip design and data analysis.

M.M. BASSANI MOLINAS<sup>1</sup>, C. BEER<sup>1</sup>, F. HESSE<sup>3</sup>, M. WIRTH<sup>1</sup>,  
DUROCHER<sup>2</sup>, A. KAMEN<sup>2</sup>, R. WAGNER<sup>1</sup>

## INTRACELLULAR NUCLEOTIDE POOLS FOR OPTIMIZING PRODUCT-ORIENTED TRANSIENT TRANSFECTION OF HEK293 CELLS IN SUSPENSION

<sup>1</sup>*German Research Centre for Biotechnology, Braunschweig, Germany*

<sup>2</sup>*Biotechnology Research Institute, Montréal, Quebec, Canada*

<sup>3</sup>*pres. add: Austrian Center of Biopharmaceutical Technology, Vienna,  
Austria*

**Abstract.** Cells and productivity of HEK293s taken from a low and a high passage number and transfected by polycation-mediated gene delivery in serum-containing and a special chemically defined protein-free medium were compared using nucleotide ratio monitoring. Using a DNA:PEI ratio of 0.5:1.5 ( $\mu\text{g } \mu\text{g}^{-1}$ ) a high transfection efficiency of about 80 % was achieved. The NTP/U ratio has been shown to detect the age of the cell line and to monitor the transfection process. It revealed a high energy level and an exponential growth as best prerequisite for obtaining a high productivity in transiently transfected HEK293 cells in suspension culture.

### 1. INTRODUCTION

The transfection efficiency of mammalian cells depends on a multitude of different factors. In particular, the cation-mediated gene delivery has been used together with different cell lines cultured in suspension and even scale-up to larger volumes has been reported (Girard et al., 2002). However, there remains a high demand for simplification or reduction of handling steps, and reduction in the amount of DNA especially for large-scale transfection and the complete elimination of serum and undefined components from the production process. In our study, we used intracellular nucleotide ratios for characterizing the cellular age and for optimizing the transfection process using HEK293 cells cultured in suspension based on the cation-mediated gene delivery using polyethyleneimine.

### 2. MATERIALS AND METHODS

#### *2.1. Cell Line and Culture Conditions*

HEK293s cells taken from early and late passage numbers were cultured at 37 °C in 200 mL spinner flasks (Techne, Cambridge, UK) in suspension using calcium-free DMEM supplemented with MEM vitamin solution, 0.1 % Pluronic F68 and 5 %

FCS and a new chemically defined protein-free medium formulation. Cell concentration, viability, substrates and metabolites as well as intracellular nucleotides were quantified as described elsewhere (Ryll et al., 1990, Ryll and Wagner, 1992).

## 2.2. Transient Transfection and Expression Rate

Cells from the exponential growth ( $5\text{--}10 \times 10^5 \text{ mL}^{-1}$ ) were directly transfected with a bicistronic plasmid harbouring the genes for human erythropoietin (EPO) and green fluorescence protein (EGFP) under control of the cytomegalovirus (CMV) promoter using an optimised DNA and linear polyethylenimine (PEI, 25 kDa) mixture at a ratio of  $0.5 \mu\text{g} : 1.5 \mu\text{g}$ . Transfection efficiency was quantified by a FACScan (Becton-Dickinson Immunocytometry Systems, San Jose, CA, USA).

## 3. RESULTS AND DISCUSSION

Figure 1A shows, that the maximum of the characteristic increase of the combined nucleotide ratio (NTP/U) during the phase of reduced exponential growth appeared one day later in cells of a late passage number ( $> 100$ ) compared to an early passage number (40-77) under serum-containing conditions indicating a change in the cell character during aging of these cells. When cells from an early passage number were transfected with DNA:PEI, the maximum value of the NTP/U ratio reached only 50% compared to untransfected cells (Fig. 1B, Fig. 2A). Although the NTP/U ratio in transfected cells of a late passage number also increased one day later compared to transfected cells of an early passage number, they did not show the reduced increase of the NTP/U ratio compared to untransfected cells (Fig. 1B). This suggested nucleotide ratios for monitoring the process of DNA uptake in transient transfection systems.

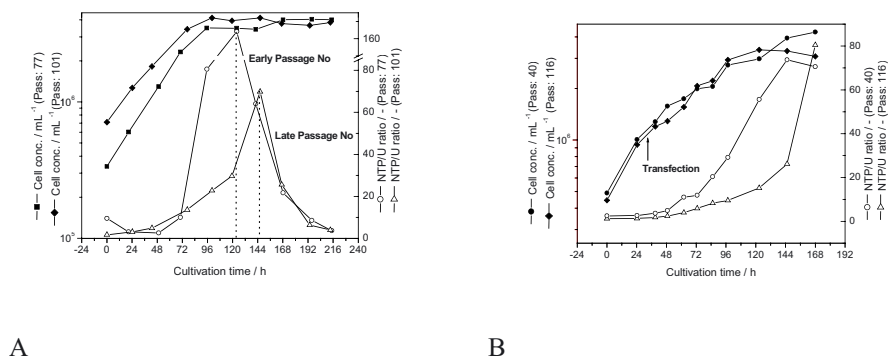
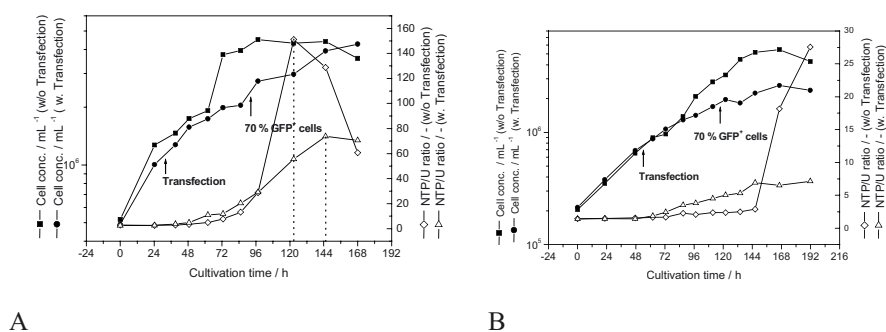


Figure 1. Cultivation of HEK293s cells taken from early (77, A; 40 B) and late (101, A; 116, B) passage numbers and cultivated in serum-containing medium. Nucleotides were analysed from untransfected (A) and transfected (B) cells. Expression expressed as EGFP positive cells was 70 % for the early and 80 % for the late passage number (B).

In addition, transfected HEK293 cells also showed the maximum of the NTP/U ratio one day later compared to their untransfected counterparts of the same passage number under serum-containing medium conditions (Fig. 2A). In contrast, transfected and untransfected cells of the same passage number cultured under protein-free medium conditions (Fig. 2B) both showed the characteristic increase in the NTP/U ratio more than one day later compared to the serum-containing culture.



A

B

Figure 2. Cultivation and transient transfection of HEK293s cells taken from passage number 40 and cultivated under serum-containing medium (A) and from passage number 76 and cultivated under protein-free medium conditions (B)

#### 4. CONCLUSION

Previously, we reported that specific nucleotide ratios (NTP and U ratio) can monitor the exact phases of the growth cycle of cultured continuous mammalian cell lines (Ryll and Wagner, 1992). Here, we demonstrate that the NTP/U ratio can also be used to distinguish between HEK293 cells from an early and a late passage number. Moreover, the nucleotide ratios of transfected HEK293 cells clearly differ from those obtained in untransfected cells and also differ in cell cultured under serum-containing and protein-free medium conditions. These results suggest intracellular nucleotide ratios as a reliable tool for the optimisation of the transient transfection process under defined culture conditions. In addition, we could demonstrate that the transfectability and productivity of transiently transfected HEK2943 cells was independent on the passage number.

#### 5. REFERENCES

Girard P, Derouazi M, Baumgartner G, Bourgeois M, Jordan M, Jacko B, Wurm FM. 2002. 100-liter transient transfection. *Cytotechnology* 38, 15–21, 2002

- Ryll T, Lucki-Lange M, Jäger V, Wagner R. 1990. Production of recombinant human Interleukin-2 with BHK cells in a hollow fibre and a stirred tank reactor with protein-free medium. *J Biotechnol* 14, 377-392
- Ryll T, Wagner R. 1992. Intracellular ribonucleotide pools as a tool for monitoring the physiological state of in vitro cultivated mammalian cells during production processes. *Biotechnol Bioeng* 40, 934-946



M. BOLLATI FOGOLIN<sup>1,4</sup>, N. IRANI<sup>1</sup>, A.J. BECCARIA<sup>4</sup>,  
C. SCHULZ<sup>1</sup>, J. VAN DEN HEUVEL<sup>3</sup>, C.B. ELIAS<sup>5</sup>,  
E. CARPENTIER<sup>5</sup>, Y. DUROCHER<sup>5</sup>, L. BISSON<sup>5</sup>,  
M. ETCHEVERRIGARAY<sup>4</sup>, R. KRATJE<sup>4</sup>, M. WIRTH<sup>2</sup>,  
A. KAMEN<sup>5</sup>, R. WAGNER<sup>1</sup>

## IMPACT OF YEAST PYRUVATE CARBOXYLASE ON THE PRODUCTIVITY OF ANIMAL HOST CELL LINES

<sup>(1)</sup> Cell Culture Technology, <sup>(2)</sup> Regulation and Differentiation, <sup>(3)</sup> Structural Biology - German Research Center for Biotechnology, Braunschweig, Germany. <sup>(4)</sup> Facultad de Bioquímica y Ciencias Biológicas, Universidad Nacional del Litoral, Santa Fe, Argentina. <sup>(5)</sup> Biotechnology Research Institute, Montréal, Québec, Canada

**Abstract.** Continuous cell lines are not capable of complete oxidising glucose via the TCA cycle. Recently, we presented a strategy of inverse metabolic engineering to increase the glycolytic flux into the TCA. This work summarises the effect of yeast pyruvate carboxylase 2 (PYC2) expressed in the cytoplasm of different host systems: BHK-21, CHO-K1, CHO-DG44, HEK293 and BTI-Tn-5B1-4 (High Five<sup>TM</sup>) cells.

### 1. INTRODUCTION

Mammalian cell lines are the prominent producers for complex recombinant proteins. Unfortunately, they have the disadvantage of being unable to completely oxidise glucose. Improvement of the energy metabolism by metabolic engineering has been considered as an efficient strategy. Increasing the flux of glucose into the TCA can perform a more efficient exploitation of glucose to form ATP (Irani et al., 1999). Therefore, in the present work, we summarise the effect of PYC2 by comparing the productivity of five different host systems, commonly used for recombinant protein expression: BHK-21, CHO-K1, CHO-DG44, HEK293 and High Five<sup>TM</sup> cells.

### 2. MATERIALS AND METHODS

#### 2.1. Cell Lines and Culture Conditions

BHK-21A cells expressing PYC2 and hEPO (Irani et al., 1999 and 2002), CHO-K1 cells expressing PYC2 and hGM-CSF (Bollati Fogolin et al., 2001), and CHO-DG44

cells expressing PYC2 and the hGH were cultivated as described in the respective references. HEK293 cells expressing the PYC2 and SEAP as well as producing adenovirus Ad5CMV5GFPq particles (Elias et al., 2003) were cultivated in 1% BCS-containing LC-SFM medium. High Five<sup>TM</sup> cells expressing the PYC2 were cultivated in Excell-405 medium and infected with baculovirus expressing  $\beta$ -galactosidase (Elias et al., 2003).

## 2.2. Analytical Methods

Cell numbers and viability were estimated by nuclei staining using crystal violet and the trypan blue exclusion method. Glucose and lactate were routinely determined using a Glucose/Lactate analyzer (Yellow Springs Instruments, Yellow Springs, OH, USA). Amino acid concentrations and intracellular nucleotide pools were quantified by RP-HPLC as described previously (Ryll et al., 1990; Ryll and Wagner, 1991). Pyruvate carboxylase expression and the enzyme activity were determined as reported elsewhere (Irani et al., 1999).

## 2.3. Quantification of Recombinant Proteins

EPO and hGH concentrations were quantified by ELISA Kits (Roche Diagnostics GmbH). GM-CSF was determined using a competitive ELISA (Bollati Fogolín et al., 2002). Secreted SEAP and  $\beta$ -galactosidase activities were monitored according to the methods described by Elias et al., 2003.

## 3. RESULTS AND DISCUSSION

Table 1 summarises the results of the impact of PYC2 on different host cell lines.

*Table 1. Impact of PYC2 expression on the cell growth, metabolism and productivity. Data are shown as improvement factor between the PYC2-expressing cells and their controls*

Parameters	Animal host cell lines				
	BHK-21	CHO-K1	CHO-DG44	HEK293	High Five <sup>TM</sup>
PC activity	1.7	1.8	3.0	N.D.	N.D.
Final cell density	1.0	0.6	1.5	1.0	2.0
Prolonged viability	Yes	Yes	No	Yes	No
q <sub>glucose</sub>	4.0	1.5	1.0	1.2	1.0
q <sub>glutamine</sub>	1.8	1.0	1.0	1.2	1.2
q <sub>lactate</sub>	2.6	1.5	1.0	1.6	1.7
Intracellular ATP	1.4	1.3	1.0	N.D.	N.D.
Productivity	1.8	2.0	1.0	1.0	1.0

N.D.: not determined

PYC2-expressing BHK-21 cells showed 30% prolonged viability, a decreased cell specific glucose and glutamine consumption rate, and a reduced lactate formation rate of less than 50%. Additionally, a 40% higher intracellular ATP

content and up to 2 fold higher yields of EPO were achieved. In contrast, PYC2-expressing CHO-K1 cells revealed a reduced growth rate but also a prolonged cell viability. Furthermore, a 50% reduction in the lactate production rate, a 30% higher cellular ATP content and a 2 fold increase in the yield of GM-CSF were achieved in CHO-K1 cell clones expressing PYC2. Although a 3 fold higher pyruvate carboxylase activity in CHO-DG44 was reached, the metabolism could not be improved and showed no effect on the production of hGH suggesting a maximum possible reduction of lactate synthesis by long-term cell selection *in vitro*. PYC2-expressing HEK293 cells revealed a 60% reduced lactate production rate and 170% prolonged cell viability. However, no significant effect on the cellular productivity of SEAP and adenovirus particles were observed but the prolonged cellular lifetime resulted in higher product yields. Finally, higher cell concentrations and reduced lactate as well as ammonium secretion rates were achieved with PYC2-expressing High Five<sup>TM</sup> cells, whereas the productivity was not significantly affected. These results suggested that the cytosolic expression of PYC2 dominantly reduces the lactate formation by a more efficient nutrient exploitation resulting in a prolonged cellular lifetime which maintains the production phase at a higher level. All standard cell lines characterised by a high lactate rate were susceptible to PYC2 expression except clones that have been optimised for minimum lactate production, such like the CHO-DG44.

#### 4. REFERENCES

- Bollati Fogolin, M., Schulz, Ch., Wagner, R., Etcheverrigaray, M. and Kratje, R.B. (2001). Expression of yeast pyruvate carboxylase in hGM-CSF-producing CHO cells. In: Lindner-Olsson, E., Chatzissavidou, N. and Lüllau, E. (Eds.), *Animal Cell Technology: From Target to Market*, Kluwer Academic Publishers, Dordrecht, The Netherlands, pp. 241-243.
- Bollati Fogolin, M., Oggero Eberhardt, M., Kratje, R.B. and Etcheverrigaray, M. (2002). Choice of the adequate quantification method for recombinant human GM-CSF produced in different host systems. *Electronic J. of Biotech.* 5, 243-250.
- Elias, C.B., Carpentier, E., Durocher, Y., Bisson, L., Wagner, R. and Kamen, A. (2003) Improving glucose and glutamine metabolism of human HEK 293 and *Trichoplusia ni* insect cells engineered to express a cytosolic pyruvate carboxylase enzyme. *Biotechnol. Prog.* 19, 90-97.
- Irani, N., Wirth, M., van den Heuvel, J., Wagner, R. (1999) Improvement of the primary metabolism of cell cultures by introducing a new cytoplasmic pyruvate carboxylase reaction. *Biotechnol. Bioeng.* 66, 238-246.
- Irani, N., Beccaria, A.J. and Wagner, R. (2002) Expression of recombinant cytoplasmic yeast pyruvate carboxylase for the improvement of the production of human erythropoietin by recombinant BHK-21 cells. *J. Biotechnol.* 93, 269-282.
- Ryll, T., Lucki-Lange, M., Jäger, V. and Wagner, R. (1990) Production of recombinant interleukin 2 with BHK cells in a hollow fibre and a stirred tank reactor with protein-free medium. *J. Biotechnol.* 14, 377-392.
- Ryll, T. and Wagner, R. (1991) An improved ion-pair HPLC method for the quantification of a wide variety of nucleoside and sugar-nucleoside in animal cells. *J. Chromatogr.* 570, 77-88.

J.-C. DRUGMAND, Y.-J. SCHNEIDER AND S.N. AGATHOS

## ENVIRONMENTAL EFFECTS OF LACTATE ON HIGH-FIVE™ INSECT CELL METABOLISM

*Cellular Bioengineering Group, Université Catholique de Louvain,  
Louvain-la-Neuve, Belgium*

**Abstract.** In batch suspension culture of High-Five™ insect cells without oxygen limitation, we observed that during the growth phase the presence of exogenous lactate in the medium seems to increase its accumulation by the cells and inhibits cell growth. At the end of culture, after glucose exhaustion from the medium, High-Five™ cells are able to use the produced lactate as a carbon source.

### 1. INTRODUCTION

The use of insect cells for the production of recombinant (glyco)-proteins by the Insect Cell Baculovirus Expression Vector System (ICB-BEVS) is a well-established technology. Among the industrially important cell lines, High-Five™ insect cells cultivated in serum-free medium have shown great potential for the production and can reach high cell densities.

Contrary to mammalian cell culture, insect cells are known to accumulate little lactate during the growth phase. But under stress conditions, these cells tend to produce more by-products (lactate, ammonium, alanine) (Rhiel et al.1997). These insect cells are generally grown in rich medium. However, in such medium cells waste glucose and have a higher rate of lactate production as a by-product. We report here experimental results of lactate effects on insect cell growth and recombinant protein production.

### 2. MATERIALS AND METHODS

High-Five™ cells were a gift from the Laboratory of Virology, University of Wageningen, The Netherlands. *Autographa californica* recombinant for  $\beta$ -galactosidase ( $\beta$ -gal) was supplied by Invitrogen (Carlsbad, CA, U.S.A.). The serum-free medium used was YPR formulated and optimised by us previously (Ikonomou et al., 2001). Metabolites were determined using a automatic Bioprofile 100 Analyser (Nova Biomedical, Waltham, MA, U.S.A.).  $\beta$ -gal activities were determined according to Miller et al. (1972). The growth and production phases of the cells were studied in 250 ml shake flasks with 50 ml medium at 28°C and 130 rpm. L-lactate sodium salt, D-lactate sodium salt and alls chemicals were supplied from Sigma (Saint-Louis, MO, U.S.A.)

## 3. RESULTS AND DISCUSSION

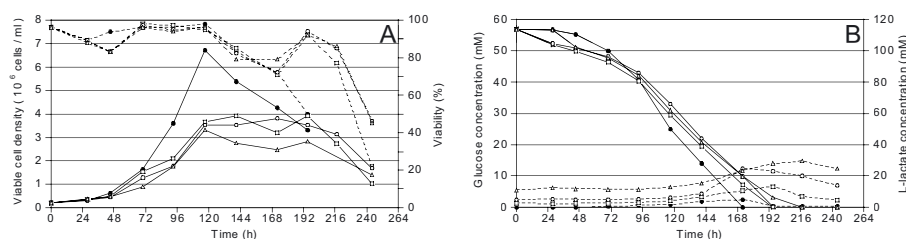


Figure 1: Representative time course profiles of High-Five™ cell density (full lines, panel A), viability (dashed lines, panel A), glucose (full lines, panel B) and lactate concentration (dashed lines, panel B) inoculated in presence of different initial exogenous L-lactate concentration (● control, □ 2.5 mM, ○ 5 mM, Δ 10 mM) in the medium.

We have previously observed that in a fixed-bed culture, immobilized High-Five cells have a different metabolism compared to suspension culture (results not shown). In agitated bioreactor conditions a slight lactate accumulation occurs in the exponential cell growth phase, but in a fixed bed culture, High-Five™ cells tend to produce high lactate concentration apparently due to oxygen limitation. This accumulation of lactate (in lactic acid form) leads to a decrease in the medium pH, thus adversely affecting cell viability. To control lactate accumulation, a strategy of base addition is usually adopted, which increases the pH and buffers the medium but increases its osmolarity.

Nevertheless, in batch suspension culture without apparent oxygen limitation, we observed that the presence of exogenous L-lactate in the medium seemed to increase the lactate production rate and to inhibit cell growth (Figure 1). This inhibition was probably due to the pH decrease (uncontrolled) associated with lactate production. At the end of the culture, after glucose exhaustion from the medium, High-Five cells were able to use the lactate produced as carbon source thus extending the stationary phase. With glucose-limited medium, similar results were observed but with a lower rate of lactate production and lower final cell densities (results not shown). This accumulation and consumption of lactate did not occur with exogenous D-lactate (results not shown).

Table 1: Effects of exogenous L-lactate added in the medium on  $\beta$ -gal production by High-Five<sup>TM</sup> cells (MOI of 2 at  $3.6 \times 10^6$  cells/ml) after total change-over of medium before infection.

L-lactate concentration (mM)	Volumetric productivity (Units / ml)	Specific productivity (Units / $10^6$ cells)
0 (control)	1744	484
5	1401	389
10	980	272
20	543	150

In regard to production, lactate seemed to have different effects than in the growth phase. Without exogenous lactate addition, infected cells produced in the first 2 days post-infection little lactate (3 mM) that decreased pH slightly and then consumed the lactate upon glucose depletion by the end of the infection phase. With exogenous addition, cells directly consumed lactate and no lactate accumulation was observed. With lactate supplementation during infection, cell density and viability decreased more rapidly than the unsupplemented control (Figure 2). This presence of lactate seemed to be slightly toxic for the cells and to decrease the recombinant protein production by the BEVS (Table 1).

In this case, the monitoring of lactate concentration and of the pH profile in insect cell culture using BEVS becomes a critical strategy to obtain high production mainly in a process not involving a total change-over of medium before infection.

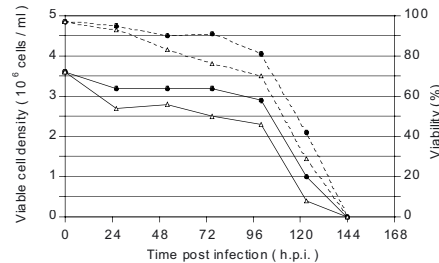


Figure 2: Representative time course of cell density (full lines) and viability (dashed lines) during infection of High-Five<sup>TM</sup> (MOI of 2 at  $3.6 \times 10^6$  cells/ml) after total change-over of medium before infection ( $\bullet$  control,  $\Delta$  10 mM exogenous L-lactate).

#### 4. CONCLUSIONS

We can conclude that the presence of lactate in the medium seems to increase the lactate accumulation by growing High-Five<sup>TM</sup> cells when glucose is in excess. The accumulation may not be due solely to the lack of oxygen, but also reflect a wider repertoire of metabolic responses as a function of pH, lactate and glucose concentration. When glucose depletion occurs, High-Five<sup>TM</sup> cells are able to use lactate as a carbon source.

The presence of lactate impacts significantly the protein production. Thus, to obtain high productivity, preventing lactate accumulation during the growth phase and before infection is a key point particularly in fed-batch, perfusion and fixed-bed culture.

## 5. REFERENCES

- Rhiel, M.; C.M. Mitchell-Logean, and D.W. Murhammer. "Comparison of *Trichoplusia ni* BTI-Tn-5B1-4 (High Five™) and *Spodoptera frugiperda* Sf-9 Insect Cell Line Metabolism in Suspension Cultures." *Biotechnol. Bioeng.* 55 (1997): 909-920.
- Ikonomou, L.; G. Bastin, Y.-J. Schneider, and S.N. Agathos. "Design of an Efficient Medium for Insect Cell Culture and Recombinant Protein Production." *In Vitro Cell. Dev. Biol.-Animal* 37 (2001): 549-559.
- Miller, J.H. "Assay of  $\beta$ -Galactosidase." In *Experiments in Molecular Genetics*, 352-55. New York: Cold Spring Harbor Laboratory Press, 1972.

F. HESSE<sup>1</sup>, A. NELVING<sup>2</sup>, R. WAGNER<sup>3</sup>

## CORRELATION OF INTRACELLULAR NUCLEOTIDE POOLS TO AMINO ACID CONCENTRATIONS IN CULTURE MEDIA BY THE APPLICATION OF MULTIVARIATE METHODS

<sup>1</sup>*present address: Austrian Center of Biopharmaceutical Technology, Vienna, Austria*

<sup>2</sup>*present address: AstraZeneca Biotech Laboratory, Södertälje, Sweden*  
<sup>3</sup>*Cell Culture Technology, German Research Centre for Biotechnology, Braunschweig, Germany*

### 1. INTRODUCTION

Special ratios of intracellular nucleotide pools were shown to provide valuable information on the state of cultures of recombinant cell lines (Ryll and Wagner, 1992). In theory, these ratios could be used as control parameters in cultivation processes. However, as the determination of intracellular parameters is labor, time and cost intensive, this method can not be applied for routine process control. A strategy to overcome this restriction is to find more easily accessible parameters that can be reliably correlated to the intracellular nucleotide pools and ratios. Here we demonstrate in principle that this can be achieved by the application of multivariate methods such as principal component analysis (PCA) and partial least squares regression (PLS).

### 2. EXPERIMENTS AND RESULTS

#### *2.1. Analysis of Nucleotide Data with PCA*

In order to investigate whether PCA can be applied to obtain information on the state of a culture from nucleotide data, interpolated curves derived from the raw data of five cultivation experiments performed with two different cell culture media (Dulbecco's Modified Eagle Medium (DMEM) and Serum Free 293 II Medium (SFM), respectively) were analysed. Figure 2 reveals that the methods provide information on the dynamics and changes of cellular metabolism. The observed turns, for example, could be correlated to the time when glucose was depleted from



the culture medium. The loading plot provides valuable information on the influence of the investigated parameters on the dynamic behavior.

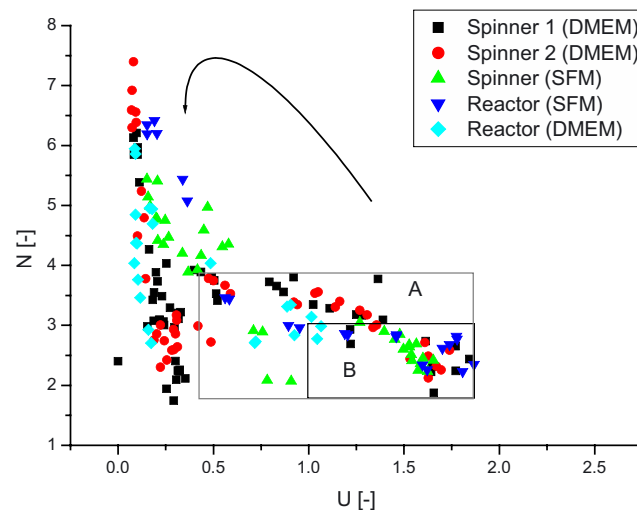


Figure 1. NTP over  $U$  plot for the five experiments performed illustrating the “log-box” theory proposed by Ryll and Wagner (1992). It is possible to define areas corresponding to the exponential growth phase. (A) shows the area defined for experiments performed with DMEM medium, (B) shows the area for experiments where SFM 293 II medium was used.

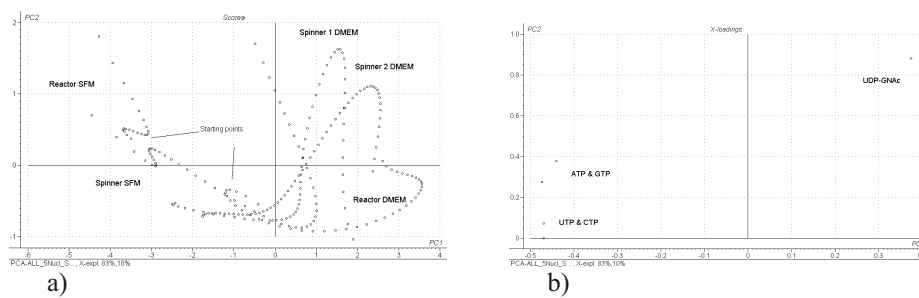


Figure 2. Score (a) and loading (b) plot obtained by applying PCA to the nucleotide data from all five experiments. The first principal component (PC) describes 83 % of the total variation, the second PC 10 %.

### 2.2. Correlation of Nucleotide Pools to Free Amino Acid Concentrations

PLS was used to correlate intracellular nucleotide pools to the concentrations of free amino acids in the culture supernatant and to the respective amino acid uptake rates. For a number of intracellular nucleotide pools and even ratios correlation models could be built indicating a true relationship between these intracellular and extracellular parameters (Tab. 1). Surprisingly, models built on free amino acid concentrations were more reliable than those built on the respective uptake rates. Significant correlation could be easily found by analysing the respective loading plots (Tab.2).

Table 1. Overview of all correlation models built. For parameters indicated by bold letters, the majority of the models was classed as successful.

<i>Models build from amino acid concentrations</i>					
	Spinner 1 DMEM	Spinner 2 DMEM	Spinner SFM	Reactor SFM	Reactor DMEM
ADP	-	-	-	n.m.	+
ATP	-	-	-	-	+/-
CTP	+/-	+/-	+/-	-	+
GTP	-	-	-	-	+/-
NAD	-	-	-	-	-
<b>UDP-GNAc</b>	+/-	+/-	-	+/-	+
<b>UTP</b>	+	+	+/-	-	+
<b>NTP ratio</b>	+/-	+	+	+	+
<b>U-ratio</b>	+	+	+	-	+/-
NTP/U ratio	-	-	-	-	-
<i>Models build from amino acid uptake rates</i>					
ADP	-	+	-	n.m.	
ATP	-	-	-	n.m.	
CTP	-	-	-	n.m.	
GTP	-	-	-	n.m.	
NAD	-	-	-	n.m.	
UDP-GNAc	+/-	+	-	n.m.	
UTP	-	+/-	+	n.m.	
NTP ratio	-	-	+	n.m.	
<b>U ratio</b>	+	+	+	n.m.	
NTP/U	-	-	-	n.m.	
(+)= good model possible to build, (+/-)= satisfying model possible to build, (-)= no model possible to build, n.m = not modeled					

### 3. CONCLUSIONS

PCA is an excellent tool to analyze dynamic changes in intracellular nucleotide pools during the course of cultivation experiments.

The results obtained with PCA were consistent to the information obtained from NTP/U-plots.

Applying PLS correlation of intracellular nucleotide pools to free amino acid concentrations in the culture medium could be shown in principle.

This correlation could be used to determine or at least estimate intracellular nucleotide pools and their relevant ratios by means of measuring amino acid concentrations in the culture medium. As these extracellular parameters are more easily accessible than the intracellular nucleotide pools, this method could be used for process control.

*Table 2. Correlation between nucleotides and amino acids, obtained from the loading plots of the PLS regression models.*

<b>Free amino acids models</b>	
<b>Nucleotide</b>	<b>Amino acid relationships</b>
<b>CTP</b>	Ala and Glu negatively correlated. Remaining amino acids positively correlated.
<b>UDP-GNAc</b>	Glu, Ala and Asn positively correlated. Remaining amino acids negatively
<b>UTP</b>	Ala negatively correlated. Glu and Gly in some cases negatively correlated. Remaining amino acids positively correlated.
<b>NTP-ratio</b>	Ala, Glu and Gly positively correlated. Remaining amino acids negatively.
<b>U-ratio</b>	Ala, Glu and Gly slightly or strongly negatively correlated. Remaining amino acids positively
<b>Uptake rate models</b>	
<b>Nucleotide</b>	<b>Amino acid relationships</b>
<b>U-ratio</b>	Opposite relations compared to U-ratio model obtained in the free amino acid case.

#### 4. REFERENCE

- Ryll T., Wagner R. (1992). Intracellular Ribonucleotide Pools as a Tool for Monitoring the Physiological State of In Vitro Cultivated Mammalian Cells during Production Processes, *Biotechnol. Bioeng.* **40**, 934-946.

M.-C. LOCAS, C. B. ELIAS, S. LANTHIER, L. BISSON,  
M.PERRIER AND A.A. KAMEN

ENGINEERING *Trichoplusia ni* (HIGH-FIVE™) INSECT  
CELLS TO EXPRESS A CYTOSOLIC PYRUVATE  
CARBOXYLASE ENZYME IMPROVES THE  
VIABILITY OF THE CELLS IN BATCH, FED-BATCH  
AND PERFUSION CULTURES

*Animal Cell Technology, Biotechnology Research Institute (NRC),  
Montréal, Qc, Canada*

**Abstract.** Cultures of *Trichoplusia ni* High-Five™ cells show accumulation of large amounts of lactate and ammonia, which may be deleterious to the cell growth and final product quality. In this work we have investigated the metabolism of these cells with respect to the utilization of glucose and glutamine and we have used a metabolic engineering approach to overcome this problem demonstrating the successful culture of these cells at high cell densities. The cells have been modified to express a cytosolic pyruvate carboxylase (PYC2), an enzyme which had been earlier identified as a key enzyme in the flux of glucose to the TCA cycle. The modified cells showed a more efficient utilization of glucose and glutamine and a marked decrease, in the amount of lactate (up to 70%) and ammonia (up to 60%) produced when compared to the non-modified host cells. This resulted in maintaining cells at a higher viability for a prolonged time, a major advantage in high cell density cultures especially when combined with stable insect cell lines. These changes in the metabolism were further evaluated in 3L-bioreactor studies, under controlled conditions. The implications of these changes to the operation conditions have been evaluated under batch, fed-batch and perfusion culture modes.

## 1. INTRODUCTION

Recent advances in the insect cell technology field such as, high cell density cultures, the ability to generate stable expression systems using insect cells, the demonstration of baculovirus mediated gene expression in mammalian cells, and the use of insect cells for the production of recombinant viral vectors for gene transfer applications have led to a renewal of interest in this technology. There is however, a relative lack of information in the literature on the metabolism of cultured insect cells, which is one of the limitations in designing media and for large scale operations at high cell densities. In this work, we describe the metabolism of the *Trichoplusia ni* (High-Five™) insect cells with respect to the utilization of glucose and glutamine.

## 2. RESULTS AND DISCUSSION

### 2.1. Batch culture

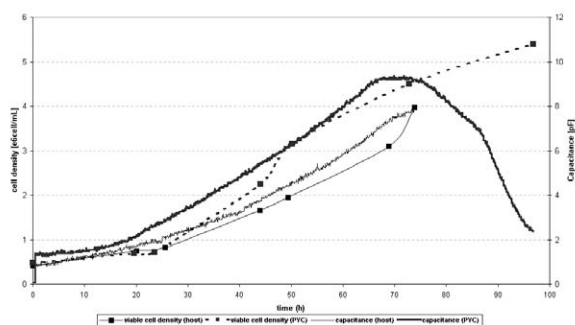


Figure 1. Batch culture of High-Five™ insect cells

The final cell density obtained was higher in the case of the transformed cells. The specific growth rates for the two cell lines as well the corresponding specific consumption rates of glucose and glutamine and production rates in mmol/hr/(E6 cells/mL) of lactate and ammonia are shown in Table 1.

Table 1. Kinetic rates for growth, consumption and production of metabolites in a batch culture

High-Five™	Growth rate ( $h^{-1}$ )	Glucose	Glutamine	Lactate	Ammonia
Host	0.0318	0.098	0.048	0.018	0.110
PYC	0.0297	0.058	0.032	0	0.103

From the results it is evident that there is a decrease in the consumption of both glucose and glutamine accompanied by a decrease in production of waste metabolites. The lower glucose consumption did not result in a lower growth rate and did not affect the final cell densities achieved.

## 2.2. Fed-Batch culture

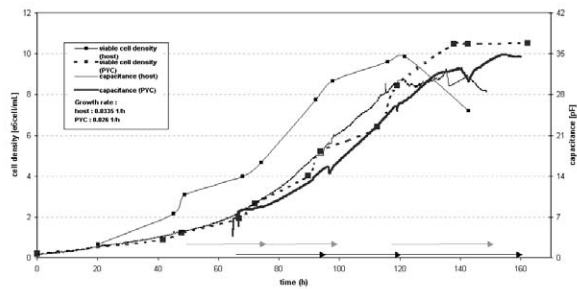


Figure 2. Fed batch culture of High-Five™ insect cells

The time and duration of the feed addition are indicated by horizontal arrows. The viable cell density obtained with the PYC expressing cells was higher than in the case of the untransformed host cells and could be maintained at a higher viability for a longer time.

## 2.3. Perfusion culture

Perfusion culture experiments were carried out using IPL-41 medium and compared with the performance of the host cells under similar conditions of cultivation. The perfusion rate used in these experiments was 1VVD. The profiles for the cell density and the capacitance measurement shown in Figure 3 indicate that the PYC transformed cells could be maintained for a longer period at the plateau conditions in a perfusion mode.

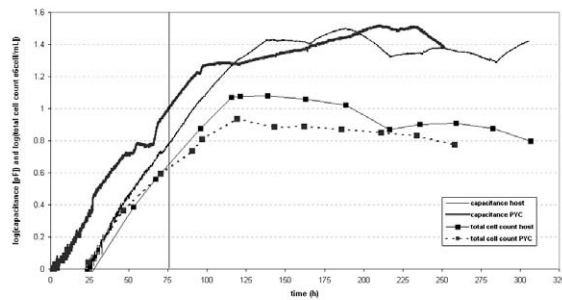


Figure 3 : Perfusion culture of High-Five™ insect cells

### 3. CONCLUSION

The results obtained in this study confirm that the glucose and glutamine metabolism of cells can be changed by the introduction of the cytosolic PYC enzyme. There was no marked change in the growth rates of the transformed cells in batch culture. The PYC transformed cells achieved the same or higher final cell densities as the host cells. The transformed cells have a lower glucose consumption rate and glutamine consumption rate. The PYC transformed cells can be maintained at higher viabilities for longer time in fed batch cultures. These cells can be maintained at a stable high cell density for a prolonged time in perfusion culture.

### 4. REFERENCES

- Bédard C et al. **1997**. *Biotechnol. Lett.* **19**: 629-632  
Elias, C et al. **2000** *Biotechnol. Bioeng.* **68** (4), 381-388.  
Elias C et al. **2003**. *Biotechnol. Prog.* **19**, 90-97  
Kamen A.A. et al. **1996**. *Biotechnol. Bioeng.*, **50**: 36-48  
Irani, N. et al. **1999**. *Biotechnol. Bioeng.*, **66**, 238-246.  
Irani, N et al. **2002**. *Biotechnol.*, **93**, 269–281.  
Neermann and Wagner. **1996**, *J Cell Physiol.*, 166, 152-169.

M. LECINA<sup>1</sup>, A. SOLEY<sup>1</sup>, P. PASSAMANI<sup>1</sup>, A. CASABLANCAS<sup>1</sup>,  
J. DE GRÀCIA<sup>1</sup>, C. VELA<sup>2</sup>, E. ESPUÑA<sup>3</sup>, J.J. CAIRÓ<sup>1</sup>, F. GÒDIA<sup>1</sup>

## INSECT CELL CULTURE MEDIUM SELECTION AND OPTIMISATION BASED ON MONITORING AND ECONOMICAL CONSIDERATIONS

*Departament d'Enginyeria Química, ETSE, Campus Universitat Autònoma  
de Barcelona (UAB), 08193 Bellaterra, Barcelona, Spain.*

*[Albert.Soley@uab.es](mailto:Albert.Soley@uab.es)*

*INGENASA, Departamento de Investigación. C/Hnos. García Noblejas 41,  
2º, 28037 Madrid, Spain.*

*LABORATORIOS HIPRA S.A., Departamento de Investigación y Desarrollo.  
Avda. La Selva 135, 17170 Amer, Spain.*

**Abstract.** The culture of insect cells is currently done using different media specifically developed for these cells (among them, IPL-41, Grace's, and TC-100). The growth of a Sf9 cell line was studied in each of these media, and IPL-41 showed the best results. Nevertheless, this medium contains various carbohydrates as carbon and energy sources, and this fact supposes a complication for the monitoring of the culture. In order to make possible the control of the sugar exhaustion, its formulation was simplified to a unique saccharide source, as it was seen that one of this nutrients was sufficient to enable an efficient growth of the cells.

### INTRODUCTION

The two major application areas of insect cells are related to the production of baculoviruses, where the aim is whether to produce the virus itself, or to produce recombinant proteins using the baculovirus expression system. The importance gained by these fields in biotechnology has fostered the interest in the development of suitable and economical insect cell media.

The first synthetic medium for the culture of insect cells (Wyatt, 1961) contained high concentrations of amino acids, organic acids, inorganic salts and various carbohydrates supplemented with heat-treated hemolymph. Subsequently, the utilisation of several media has been explored. In 1962 Grace proposed various modifications to Wyatt's medium (Grace, 1962), that included the addition of diverse vitamins and changed certain characteristics of the medium. Afterwards numerous variations have been proposed on Grace's original medium, among them that leading to TC-100 (Gardiner and Stockdale, 1975), a medium that omits the addition of organic acids, uses only one sugar source (glucose), and is supplemented with tryptose extract and foetal bovine serum. Another medium developed specifically for insect cell culture is IPL-41 (Weiss et al., 1981), which is a more



complex medium, with increased amounts amino acids, vitamins and other components, that targets the needs of large-scale cultures.

## MATERIALS AND METHODS

*Cell line, medium and culture conditions.* The insect cell line used was a strain of Sf9 provided by LABORATORIOS HIPRA S.A.. The basal media used were Grace's (Sigma G9771), IPL-41 (Sigma I0638, Biol. Industries 06-1824-01-1A), and TC-100 (Gibco 43000-017). 3.33 g/l of yeast extract (Sigma Y-1000) and lactalbumin hydrolysate (Sigma L90) were supplemented. 5% (V/V) of FBS (HyClone SH30071.03) was added. Cultures were performed in 250 ml spinner flasks with 60 ml of working volume, using  $3\text{-}3.5 \times 10^5$  cells/ml as seeding density, stirred at 40 rpm, grown at 27°C, 95% humidity, in an incubator (Forma Scientific HEPA filtered IR incubator 3862). *Analytical methods.* Cell density and viability were assessed by the trypan blue exclusion method using a hemocytometer (Neubauer improved, Brand). Glucose was measured using an automatic analyser (YSI, 2700 Select). Sucrose and maltose were detected by HPLC (Waters, LC module I plus).

## RESULTS AND DISCUSSION

In the present work the growth of Sf9 cells in various media was studied (TC-100, Grace's, and IPL-41). In the figure 1, it is seen that the medium which supported a greater growth of the cells was IPL-41. In addition, at the operating scale the cost of IPL-41 is lower than the cost of Grace's medium and as low as TC-100's cost (Grace's, 64 €/l; IPL-41, 17€/l; TC-100, 17 €/l). For both reasons, IPL-41 was the medium chosen for a further development of the interest production process.

Although IPL-41 shows better results concerning growth, it presents a complication for the monitoring of the exhaustion of the culture medium, due to the presence of various saccharide sources (glucose, maltose and sucrose). In order to overcome this drawback, various experiments were performed using IPL-41 containing only one of the sugars. In figure 2 it is shown that media containing only glucose or maltose allow a similar culture growth to that supported by the control medium (having sucrose, glucose and maltose). Consequently, the need of sucrose in the medium was discarded.

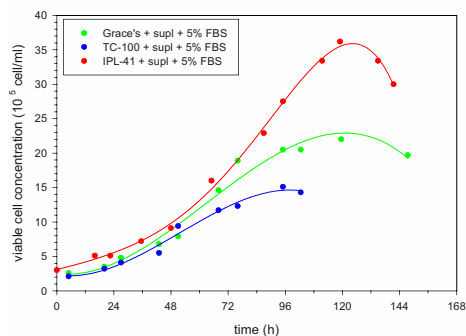


Figure 1. Batch growth curves of *Sf9* cultures using IPL-41, TC-100 and Grace's insect cell medium.

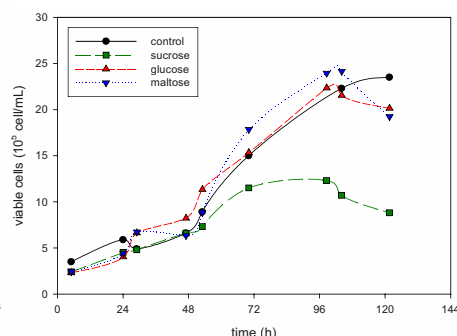


Figure 2. Batch growth curves of *Sf9* cultures using IPL-41 containing only one of the saccharide sources (sucrose, glucose, or maltose).

Additional experiments with analysis of the carbohydrate consumption were conducted in order to select whether glucose or maltose should be used as unique saccharide source. Before further considerations, it has to be stated that since the cultures were supplemented with yeast extract and lactalbumin hydrolysate, all of them had certain basal amounts of glucose, sucrose and maltose. Besides, supplements of the sugar-to-test were added to reach the same total amount of monosaccharide in each experiment. Figure 3 shows the profiles of glucose, as well as sucrose and maltose. In the control culture (glucose, maltose, sucrose), glucose is consumed preferably to maltose, as it is seen similarly in the culture with glucose as main carbohydrate. In the culture with maltose as main saccharide, it is degraded to glucose, which is subsequently consumed by the cells. The main conclusion of this experiment was the selection of glucose as unique sugar source, since it is the sugar consumed preferably by the cells and allows an easiest monitoring of the sugar exhaustion.

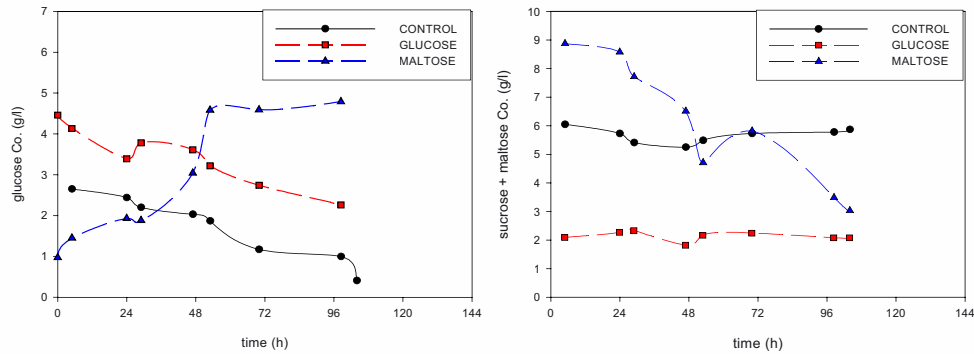


Figure 3. Saccharide concentration in Sf9 cultures using glucose and maltose as main carbohydrates. The concentration of maltose is referred as sucrose+maltose since the used HPLC does not permit distinguishing among these sugars.

## CONCLUSION

The analysis of three potential media for Sf9 cell culture allowed the selection of IPL-41, and its further simplification by reducing the three carbon sources in its formulation to one.

## REFERENCES

- Gardiner G.R., and Stockdale H. (1975). Two tissue culture media for production of Lepidopteran cells and nuclear polyhydrosis viruses. *J. Invertebr. Path.* **25**: 363-370.
- Grace T.D.C. (1962). Establishment of four strains of cells from insect tissue grown in vitro. *Nature* **195**: 788-789.
- Weiss S.A., Smith G.C., Kalter S.S., and Vaughn J.N. (1981). Improved method for the production of insect cell cultures in large volume. *In Vitro* **17**: 495-502.
- Wyatt G.R. (1961). The biochemistry of insect hemolymph. *Ann. Rev. Entomol.* **6**: 75.

FRANTIŠEK FRANĚK

## ANTIAPOPTOTIC ACTIVITY OF SYNTHETIC AND NATURAL PEPTIDES

*Laboratory of Growth Regulators, Institute of Experimental Botany,  
Radiová 1, CZ-10227 Prague 10, Czech Republic. E-mail:  
franek@biomed.cas.cz.*

### 1. INTRODUCTION

Hybridoma cultures producing diagnostic and therapeutic monoclonal antibodies suffer from premature termination by apoptosis triggered spontaneously in parallel with gradual exhaustion of nutrients. Thus, high attention is being paid to media additives, such as protein digests [1], capable of suppressing cell suicide. Our previous work has indicated that protein hydrolysates do not only contribute to optimization of nutrition, but that they may provide peptides mimicking growth factors or survival factors [2]. Our further studies carried out with pure synthetic peptides have corroborated this notion, and have pointed to anti-apoptotic activity of a variety of peptides [3-4].

### 2. MATERIALS AND METHODS

Synthetic peptides used in this work were products of Bachem (Bubendorf, Switzerland) and of PolyPeptide Laboratories (Prague, Czech Republic). Chromatography fractions of wheat gluten enzymic hydrolysate were prepared as reported earlier [2].

Mouse hybridoma ME-750 was cultured in DMEM/F12/RPMI 1640 (3:1:1) medium supplemented with amino acids, and with the iron-rich protein-free growth promoting mixture [5]. The cultures (volume 6.0 ml) kept in 25 cm<sup>2</sup> T-flasks were inoculated at a density of  $(250 \pm 50) \times 10^3$  cells/ml and the culture parameters were evaluated on day 6, i.e., at the decline phase of the cultures.

The antibody concentration was determined by immunoturbidimetry [6]. The apoptotic index, i.e. the percentage of apoptotic cells relative to total cells, was determined by microscopic counting of the morphologically distinct shrunken cells with ruffled membrane.

## 3. RESULTS AND DISCUSSION

Our previous work has shown increased cell viability in cultures supplemented with oligoglycines, oligoalanines, and with several lysine-containing peptides [3,4]. In the present experiments, anti-apoptotic activity was found also with some peptides containing glutamic acid, serine, threonine or D-alanine residues (Tab.1).

*Table 1. Apoptotic index in hybridoma cultures supplemented with various peptides*

Supplement	Apoptotic index, %	Supplement	Apoptotic index, %
None (Control)	46		
Gly-Gly-Glu-Ala 0.1%	20	Ser-Ser-Ser 0.1%	28
dtto 0.2%	18	dtto 0.2%	24
Gly-Glu-Gly 0.1%	22	Ala-Ala-Ala 0.1%	26
dtto 0.2%	24	dtto 0.2%	22
Thr-Thr-Thr 0.1%	26	D-Ala-Ala-Ala 0.1%	27
dtto 0.2%	22	dtto 0.2%	20

The anti-apoptotic component of the complex effect of wheat gluten hydrolysate fractions on hybridoma cultures [2] was investigated in comparison with the effect of synthetic peptides representing one of the repeat motifs of the high molecular weight glutenin subunit [7] (Tab.2). The glutamine-containing synthetic peptides and the combination of a natural peptide fraction with tetraglycine showed the highest suppression of apoptotic death rate.

Table 2. Hybridoma cultures supplemented with synthetic and natural gluten-derived peptides

Supplement		Viable cells x 10 <sup>-3</sup> cells/ml	Apoptotic index, %	Monoclonal antibody, mg/l
None(Control)		1180	48	33
<i>A) Synthetic peptides</i>				
Pro-Gly-Gln-Gly-Gln-Gln	0.1%	1630	31	66
dtto		1110	42	57
0.05%				
Pro-Gly-Gln-Gly-Gln	0.1%	1580	33	60
dtto		1400	33	65
0.05%				
<i>B) Chromatography fractions of wheat gluten enzymic hydrolysate [1]</i>				
Fraction a1	0.2%	1390	40	56
Fraction a21	0.2%	1950	36	67
Fraction a22	0.2%	1400	43	58
<i>C) Combination of a chromatography fraction with a synthetic peptide</i>				
Fraction a1 +	0.2%			
+ Tetraglycine	0.2%	2050	26	98

Under condition of modelled starvation, i.e., in media deliberately diluted with saline, the anti-apoptotic effect of synthetic peptides, as well as of hydrolysate fractions was very pronounced (Tab.3). The present data confirm that the cell-proliferation modulating activity of some peptides [3-5], is accompanied with pronounced anti-apoptotic activity. Significant effects can be achieved at peptides concentrations in the millimolar range.

Table 3. Hybridoma cultures starving in media diluted to 40% by saline. Effect of supplementation with synthetic peptides and with gluten hydrolysate fractions

Supplement		Viable cells x 10 <sup>-3</sup> cells/ml	Apoptotic index %	Monoclonal antibody, mg/l
None(Control)		250	55	12
<i>A) Synthetic peptides</i>				
Tetraglycine	0.2%	260	44	14
Tetraalanine	0.2%	380	34	16
Gly-Phe-Gly	0.2%	520	24	14
<i>B) Chromatography fractions of wheat gluten enzymic hydrolysate [1]</i>				
Fraction a1	0.2%	330	48	14
Fraction a21	0.2%	600	32	16
Fraction a22	0.2%	720	47	17

The anti-apoptotic activity is not confined to any specific amino acid residue(s). The peptides are effective both in rich protein-free media suited to biotechnological production, and under conditions of starvation in media diluted with saline. The findings indicate that the mechanism of peptides action is complex, and cannot be interpreted solely as a beneficial contribution to cell nutrition.

#### ACKNOWLEDGEMENTS

This work was supported by the Grant OC 844.10 of the Ministry for Education, and by the Grant No. 521/02/0479 of the Grant Agency of the Czech Republic.

#### REFERENCES

1. Schlaeger, E.-J. (1996) The Protein Hydrolysate, Primaton RL, Is a Cost-Effective Multiple Growth-Promoter of Mammalian Cell Culture in Serum-Containing and Serum-Free Media and Displays Anti-Apoptotic Properties. *J. Immunol. Methods* 194, 191-199.
2. Franěk, F., Hohenwarter, O., and Katinger, H. (2000) Plant Protein Hydrolysates: Preparation of Defined Peptide Fractions Promoting Growth and Production in Animal Cell Cultures. *Biotechnol. Prog.* 16, 688-692.
3. Franěk, F., and Katinger, H. (2002) Specific Effects of Synthetic Oligopeptides on Cultured Animal Cells. *Biotechnol. Prog.* 18, 155-158.
4. Franěk, F., and Katinger H. (2001) Specific Effects of Synthetic Oligopeptides in Animal Cell Culture. In: "Animal Cell Technology: From Target to Market" (E. Lindner-Olsson et al., eds.) Kluwer Academic Publishers, Dordrecht 2001, pp.164-167.
5. Franěk, F., Eckschlager, T., and Katinger, H. (2003) Enhancement of Monoclonal Antibody Production by Lysine-Containing Peptides. *Biotechnol. Prog.* 19, 169-174.
6. Franěk, F., and Šrámková, K. (1996) Cell Suicide in Starving Hybridoma Culture: Survival-Signal Effect of Some Amino Acids. *Cytotechnology* 21, 81-89.
7. Feeney, K.A., Tatham, A.S., Gilbert, S.M., Fido, R.J., Halford N.G., and Shewry, P.R. (2001) Synthesis, expression and characterisation of peptides comprised of perfect repeat motifs based on a wheat seed storage protein. *Biochim. Biophys. Acta* 1546, 346-355.

S. JUANOLA<sup>1</sup>, J. VIVES<sup>1</sup>, J. ANDERSEN<sup>1</sup>, E. PRATS<sup>2</sup>,  
L. CORNUDELLA<sup>2</sup>, J.J. CAIRÓ<sup>1</sup>, F. GÒDIA<sup>1</sup>

## EFFECT OF ANTIAPOPTOTIC GENES EXPRESSION ON CELL GROWTH AND MONOCLONAL ANTIBODY PRODUCTIVITY IN A HYBRIDOMA CELL LINE

<sup>1</sup> Dept. d'Eng. Química, UAB/U. d'Eng. Bioquímica, CeRBa. Edifici C,  
08193 Bellaterra, Barcelona, Spain. <sup>2</sup> Dept. de Biologia Molecular i  
Cel·lular, IBMB-CSIC/U. de Biotecnologia de Cèl·lules Animals, CeRBa. C/  
Jordi Girona 18-26, 08034 Barcelona, Spain.

**Abstract.** Different proteins that interfere with the apoptosis biochemical pathways, such as Bcl-2 and various viral homologues, has been investigated in a hybridoma cell line (KB 26.5). Our results indicate that the over-expression of cellular *bcl-2* and viral *bhrf-1* (from Epstein Barr virus positive cell lines) and *ks-bcl-2* (from Kaposi sarcoma tissues) genes under apoptosis triggering conditions (i. e., glutamine depletion) not only delays cell death process but also allows the recovery of the cultures when re-exposed to non-inducing apoptosis conditions. Thus, the over-expression of these genes delays PCD, therefore expanding the life span of the cultures and enhancing cell productivity. Nevertheless, despite the significant effect of these genes on apoptosis, total antibody productivity in cultures of *ks-Bcl-2* and *bhrf-1* expressing cells is lesser than *bcl-2* expressing cells and control cultures. However, specific antibody productivities in Bcl-2 and control cultures are similar. These results lead to the conclusion that the use of viral proteins, in particular BHRF-1, increases cell survival but reduces antibody production. Due to the need of operating bioreactors for long periods of time, it is important to achieve a stable expression system to express the desired genes over a large number of generations. To improve the efficiency of stable cell line production, bicistronic vectors has been evaluated. The bicistronic vectors contain an Internal Ribosome Entry Site (IRES) that permits the simultaneous expression of the interest gene and antibiotic resistant marker and, consequently, it ensures the expression of desired genes for long periods of time.

### 1. INTRODUCTION

Productivity of monoclonal antibodies by hybridoma cells is limited by the onset of a programmed cell death process known as apoptosis. We previously reported two different approaches to delay cell death in presence of apoptotic stimuli: one based on the addition of Caspase inhibitors to the culture (Tintó et al., 2002); and another based on the over-expression of endogenous and viral homologues of Bcl-2 (Vives et al., 2003). The effect of the over-expression of antiapoptotic genes, with potentiality to block apoptosis pathways at the mitochondrial level, on the antibody productivity in batch cultures has been investigated. Moreover, due to the need of culturing these cells for long periods of time, it is important to develop more robust cell lines harbouring these genes. In this sense, stable cell lines engineered with bicistronic vectors have been evaluated. The first attempt of using bicistronic vectors



is reported, employing the GFP (Green Fluorescent Protein) as reporter gene and 293N cells, due to their high transfection efficiency.

## 2. MATERIALS AND METHODS

*Cell line, medium and culture conditions.* KB26.5 murine hybridoma was cultured as described (Sanfeliu et al., 1997). 293 N human embryonic kidney cell line was grown in DMEM + 10% FCS (Biological industries). Transfected hybridoma and 293 N cells were maintained under selective pressure with G-418 sulphate at a final concentration of 3 mg/mL and 1.5 mg/mL respectively.

*Plasmid constructs and DNA transfections.* Sequences encoding cDNA from Bcl-2, BHRF-1 and Ks-Bcl-2 were isolated as previously described (Vives et al., 2003). These cDNAs were cloned into a pcDNA3 vector (Invitrogen). The plasmid p-EGFP-IRES-neo was constructed from pIRESneo (Clontech) and pIRES2-EGFP (Clontech). Hybridomas and 293 N cells were transfected using DMRIE-C (Life Technologies) and Superfect (Qiagen), respectively.

*ELISAs.* A standard sandwich-type ELISA (Butler et al., 1978) was used to quantify monoclonal antibodies (Mabs) concentration.

*Apoptosis detection.* Cell viability was measured as described (Tintó et al., 2002).

## 3. RESULTS AND DISCUSSION

The over-expression of cellular gene *bcl-2* and viral genes *ks-bcl-2* and *bhrf-1* in glutamine free medium delayed the process of hybridoma cell destruction (Vives et al., 2003). Furthermore, in a batch culture, *bcl-2* expressing cells reached higher cell densities than the control culture (Figure 1a) as also described (Bierau et al. 1998) and the results of the ELISA test evidenced a higher antibody production of *bcl-2* expressing cells than the others cultures. However, the specific antibody productivities of *bcl-2* transfected cells and the control culture are similar, but greater than cells transfected with viral genes (Figure 1b).

These results show that the expression of viral genes not only increases cell survival but also affects in a negative way the antibody productivity in this particular cell line. In this sense, the use of antiapoptotic genes generates a compromise between productivity and protection.

The pcDNA3 vector employed does not ensure a stable expression of the desired genes over a large number of generations. Therefore, a stable expression system based on bicistronic vectors is needed. In order to check the expression of the bicistronic vectors, the p\_EGFP\_IRES\_neo plasmid was constructed (Figure 2a). 293 N cells transfected with this vector expressed the GFP throughout a relevant number of subcultures (>10). The GFP fluorescence after this period is shown in Figure 2b. In this way, a stable hybridoma cell line protected against apoptosis could be developed.

## 4. FIGURES

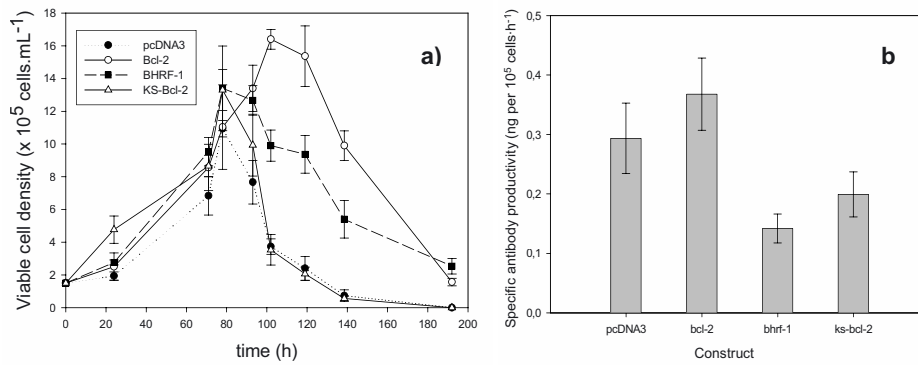


Figure 1. Effect of the expression of *bcl-2*, *ksbc1-2* and *bhrf-1* on KB26.5 hybridoma cell viability in batch culture (a) and specific antibody productivity of these cultures at maximum cell density (b). *pcDNA3* transfected cells was used as control culture.

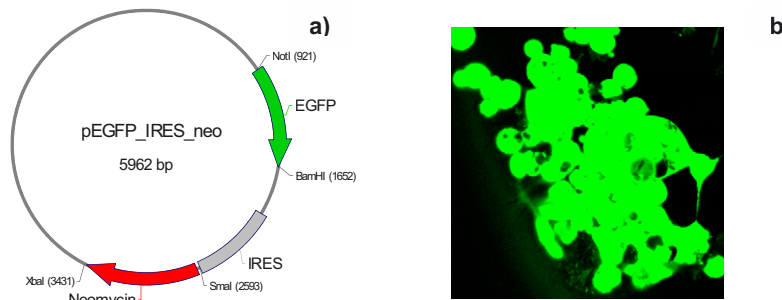


Figure 2. Diagram of *pEGFP\_IRES\_neo* vector (a) and photograph of the EGFP-transfected 293 N cells obtained with a confocal microscope (b).

## 4. REFERENCES

- Bierau H., Perani A., Al-Rubeai M., Emery A.N. "A comparison of intensive cell culture bioreactors operating with hybridomas modified for inhibited apoptotic response." *J. Biotechnol.* **16** (1998), 195-207. Butler J.E., Feldbush T.L., McGivern P.L., Stewart N. "The enzyme-linked immunosorbent assay (ELISA): a measure of antibody concentration or affinity". *Immunochem.* **15** (1978), 131-136.
- Sanfeliu A., Paredes C., Cairó J.J., Gòdia F. "Identification of key patterns in the metabolism of hybridoma cells in culture". *Enz. Micr. Tech.* **21** (1997), 421-428. Tintó A., Gabernet C., Vives J., Prats E., Cairó J.J., Cornudella L., Gòdia F. "The protection of hybridoma cells from apoptosis by caspase inhibition allows culture recovery when exposed to non-inducing conditions". *J. Biotechnol.* **95** (2002), 205-214.
- Vives J., Juanola S., Cairó J.J., Prats E., Cornudella L., Gòdia F. "Protective effect of viral homologues of *bcl-2* on hybridoma cells under apoptosis-inducing conditions". *Biotechnol. Prog.* **19** (2003), 84-89.

H. MEENTS<sup>1,3</sup>, B. ENENKEL<sup>2</sup>, AND M. FUSSENEGGER<sup>1\*</sup>

AMPLIFIED DICISTRONIC EXPRESSION UNITS  
MEDIATE APOPTOSIS PROTECTION IN CHO-DG44  
CELLS ADAPTED FOR GROWTH IN SERUM-FREE  
MEDIA, IMPACT ON MITOCHONDRIA COPY  
NUMBER

<sup>1</sup>*Institute of Biotechnology, Swiss Federal Institute of Technology, ETH  
Zurich, CH-8093 Zurich, e-mail: fussenegger@biotech.biol.ethz.ch;*

*\*corresponding author*

<sup>2</sup>*Boehringer Ingelheim Pharma KG, D-88397 Biberach, Germany;*

<sup>3</sup>*Present address: Biotechnology Development, Novartis Pharma AG,  
CH-4057 Basel, Switzerland*

**Abstract.** We have constructed dicistronic expression vectors for one-step antiapoptosis engineering and product expression. Expression units encoding the soluble intercellular adhesion molecule 1 (sICAM), a potential therapeutic for treatment of the common cold, and *bcl-2/bcl-x<sub>L</sub>* were integrated and amplified in Chinese hamster ovary- (CHO) DG44 cells adapted for anchorage-independent growth in serum-free media. sICAM expression was translated in a cap-dependent and survival gene expression in a cap-independent manner based on the encephalomyocarditis virus (EMCV) internal ribosome entry site (IRES). Batch cultivations of engineered CHO-DG44 cells containing amplified transgene expression units exhibited improved viability and delayed onset of apoptosis compared to cell lines harboring monocistronic control constructs. *bcl-x<sub>L</sub>*-mediated apoptosis protection was significantly higher compared to *bcl-2*-based survival engineering. High-level expression of *bcl-2* and *bcl-x<sub>L</sub>* seem to be required to compensate for increased mitochondria numbers found to be associated with production cell lines grown in serum-free medium.

## 1. INTRODUCTION

Chinese hamster ovary (CHO) cell derivatives have emerged as the number one production cell line in the past decades due to their straightforward adaptation for growth in serum-/protein-free media, and their compatibility with *dhfr*-based amplification protocols to increase the copy number of product gene-encoding chromosomal loci. One of the major problems associated with standard bioreactor operation is cell death by apoptosis. Serum components have been identified as major apoptosis-protective agents and their absence in modern biopharmaceutical manufacturing results in increased sensitivity of production cell lines to programmed cell death (Zanghi et al., 1999). Bcl-2, the prototype apoptosis suppressor and key member of the Bcl-2 family of highly conserved pro- (for example bid and bax) and anti-apoptotic (for example *bcl-2*, *bcl-x<sub>L</sub>*) response regulators, has been the prime choice of antiapoptosis engineering in the biotech community. Bcl-2 family

members have been shown to modulate the caspase-9-dependent apoptosis pathway in response to a molecular rheostat localized at the outer mitochondrial membrane consisting of homo- and heterodimerized pro- and antiapoptotic Bcl-2-type proteins. This assembly of crucial players in the apoptosis-controlling machinery within the outer mitochondrial membrane bring these cellular power stations into the focus for antiapoptosis engineering (Follstad et al., 2000). However, bioengineers have not yet discovered mitochondria as a potential target for improving desired characteristics of production cell lines.

## 2. MATERIAL AND METHODS

### *Cell culture, plasmid constructs and flow cytometry*

CHO-DG44/dhfr<sup>-/-</sup> adapted for growth in suspension was used as parental cell line throughout this report and cultivated like its transgenic counterparts in serum-free CHO-S-SFM-II-derived medium (Invitrogen). The basic vector pBID, which was used throughout this study, mediates constitutive expression of desired transgenes (Meents et al., 2002). In addition, pBID encodes the *dhfr* mini gene as selection and amplification marker. pBID-sICAM, pBID-sICAM-bcl-2, and pBID-sICAM-bcl-xL have been described elsewhere (Meents et al., 2002). Fragmented DNA levels were quantified using a fluorescence-based TUNEL-assay (PharMingen). Cells were analyzed according to the manufacturer's protocol using a FACSCalibur (Becton-Dickinson).

### *Fluorescence microscopy of labeled mitochondria*

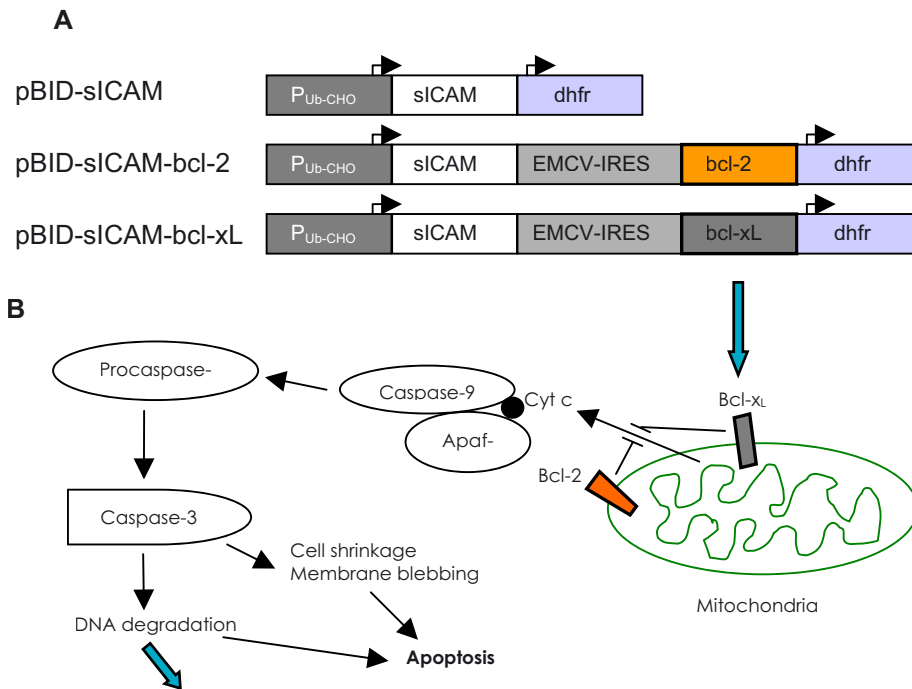
0.5 x 10<sup>6</sup> cells per sample were harvested and treated with 1% paraformaldehyde in PBS before cells were ready for the fluorescence-based staining of their mitochondria. A PBS solution containing 500 pM of the mitochondrion-selective MitoTracker Green FM dye (Molecular Probes) was prepared. Cells were incubated in 200 µl staining solution for 15 min at 37 °C. Subsequently, the cells were resuspended in 400 µl PBS and subjected to flow cytometric analysis. 100 µl of the remaining cell solutions were centrifuged on poly-L-lysine-coated slides at 800 x g for 5 min and examined under a fluorescence microscope (laser scanning microscope, Leica TCS).

## 3. RESULTS AND DISCUSSION

We constructed dicistronic expression units which contained sICAM in the first cistron, and either *bcl-2* or *bcl-x<sub>L</sub>* in the second cistron. Translation of the second cistron was driven by an internal ribosome entry site (IRES) derived from the encephalomyocarditis virus (Fig. 1A). Although the mechanisms by which these survival genes suppress apoptosis is not fully understood, a significant pathway is associated with the subcellular localization of Bcl-2 and Bcl-x<sub>L</sub> to the mitochondrial

membrane (Fig. 1B). Both proteins prevent apoptosis-induced release of cytochrome c from the mitochondrial inter-membrane space into the cytoplasm.

To assess the viability extending activity of *bcl-2* and *bcl-x<sub>L</sub>* when expressed from the second cistron stable mixed populations have been generated. Batch cultivations with these transgenic cells revealed no positive impact on viability in comparison to the monocistronic, sICAM only, control mixed populations (data not shown). This is consistent with previous reports demonstrating only marginal or no cell death protection of *bcl-2*- and *bcl-x<sub>L</sub>*-based antiapoptosis engineering strategies. However, we established clonal stable cell lines by a single round of methotrexate induced amplification and selected the highest sICAM producers. HMNI-3/HMNI-4 encode the control vector pBID-sICAM, HMIBC-1/HMIBC-2 contains pBID-sICAM-*bcl-2* and HMIBX-1/HMIBX-2 harbor pBID-sICAM-*bcl-x<sub>L</sub>*. Percent viability assessments of the amplified *bcl-2* and *bcl-x<sub>L</sub>* expressing cell clones revealed significant increases in cell viability during the decline phase of batch cultivations (data not shown). *bcl-x<sub>L</sub>* was superior to *bcl-2* with respect to cell death protection.



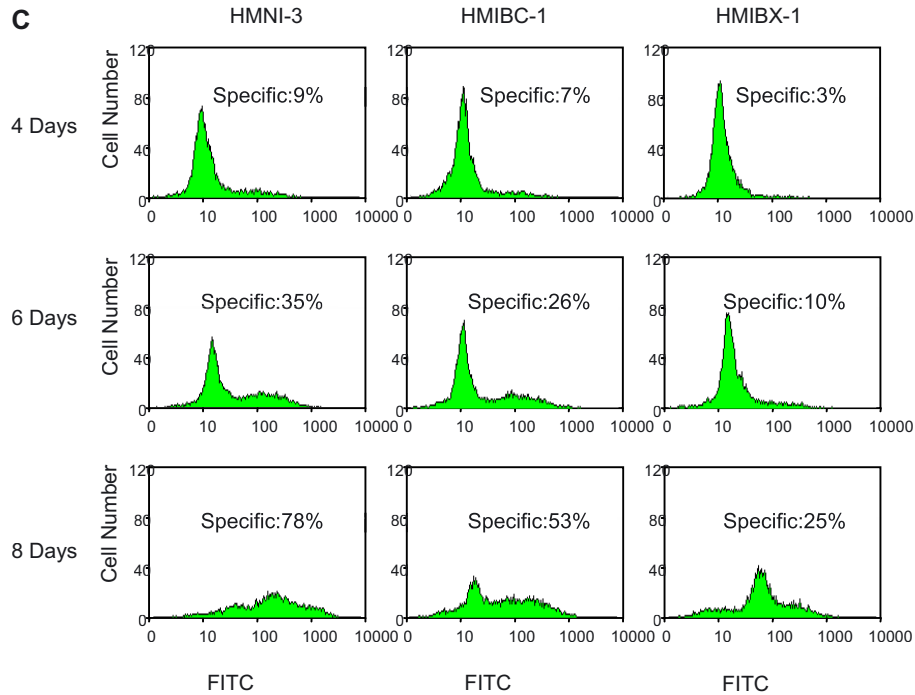


Figure 1. (A) Schematic presentation of expression vectors used. (B) Molecular pathways of *bcl-2*- and *bcl-x<sub>L</sub>*-mediated survival induction. (C) Apoptosis characteristics of engineered CHO cells.

A later event during apoptosis is the activation of endonucleases, which cleave DNA resulting in a characteristic “ladder” of DNA fragments. Apoptosis can be efficiently quantified by using FITC-labeling of the DNA breaks, referred to as TUNEL-assay, followed by flow cytometric analysis. The FITC profile of HMNI-3, HMIBC-1, and HMIBX-1 at day 4, 6, and 8 in batch cultures is shown in Fig. 1C. Percent values in the graphs represent the proportion of specific apoptotic cells. Correlating with an increase in viability amplified cell clones also exemplified a dramatically reduced percentage of apoptotic cells. The apoptosis-suppressing potential of *bcl-x<sub>L</sub>* was 2-fold higher compared to *bcl-2*.

High-level expression of survival genes seem to be necessary to significantly protect CHO-DG44 grown under serum-free conditions. We speculated whether an elevated mitochondria content in serum-depleted CHO-DG44 could be the cause for the required high *bcl-2* or *bcl-x<sub>L</sub>* dosages. Therefore, we cultivated CHO-DG44 in serum-free and serum-containing media. The specific mitochondria content of both cultures was quantified after two weeks using MitoTracker Green FM, a

mitochondrion-specific fluorescent dye. As MitoTracker Green FM accumulates in mitochondria in a membrane potential-independent manner it is an excellent tool for the quantification of these organelle. Mitochondria-specific staining was significantly increased in cells cultivated in the absence of serum as assessed by fluorescence microscopy (Fig. 2). FACS-mediated analysis of mitochondria counts exemplified an up to 3-fold boost in specific mitochondria content (data not shown).

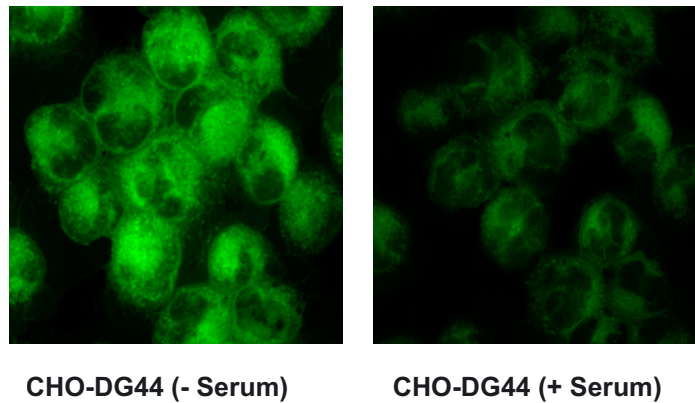


Figure 2. Fluorescence micrographs (original magnification 630x) of MitoTracker-stained CHO-DG44 cells grown in the absence (-Serum) and presence (+ Serum) of serum.

#### 4. CONCLUSIONS

- *bcl-2* and *bcl-x<sub>L</sub>*, showed apoptosis-suppressing only at high expression levels. It was therefore not surprising that apoptosis-suppressing and viability-enhancing characteristics were only detectable following *dhfr*-based amplification of *bcl-2* and *bcl-x<sub>L</sub>*.
- *bcl-x<sub>L</sub>* outperformed *bcl-2* with respect to cell death protection. If ectopic expression of this survival genes was chosen to improve cell culture performance, the use of *bcl-x<sub>L</sub>*, rather than *bcl-2* is highly recommended.
- The mitochondria content of production cell lines grown in serum-free media was about three-fold higher compared to cultures maintained in serum-containing medium, suggesting that increased *bcl-2* and *bcl-x<sub>L</sub>* expression levels were required to compensate for the higher intracellular concentration of apoptosis machineries associated with these organelles.

## 5. REFERENCES

- Follstad, B.D., Wang, D.I., and Stephanopoulos, G. 2000. Mitochondrial membrane potential differentiates cells resistant to apoptosis in hybridoma cultures. *Eur J Biochem* 267:6534-6540.
- Meents, H., Enenkel, B., Eppenberger, H.M., Werner, R.G., and Fussenegger, M. 2002. Impact of coexpression and coamplification of sICAM and antiapoptosis determinants bcl-2/bcl-x<sub>L</sub> on productivity, cell survival and mitochondria content in CHO-DG44 grown in suspension and serum-free media. *Biotechnol Bioeng* 80:706-716.
- Zanghi, J. A., Fussenegger, M., and Bailey, J. E. 1999. Serum protects protein-free competent Chinese hamster ovary cells against apoptosis induced by nutrient deprivation in batch culture. *Biotechnol Bioeng* 64:108-119.



Y. P. LI, K. TERUYA, Y. KATAKURA, S. KABAYAMA<sup>1</sup>,  
K. OTSUBO<sup>1</sup>, S. MORISAWA<sup>1</sup>, Y. ISHII<sup>2</sup>, Z. GADEK<sup>3</sup> AND  
S. SHIRAHATA

## EFFECT OF REDUCED WATER ON THE APOPTOTIC CELL DEATH TRIGGERED BY OXIDATIVE STRESS IN PANCREATIC $\beta$ HIT-T15 CELL

*Department of Genetic Resources Technology, Faculty of Agriculture,  
Kyushu University, Fukuoka 812-8581, Japan; <sup>1</sup>Nihon Trim Co. Ltd., 1-8-  
34 Oyodonaka, Kita-ku, Osaka 531-0076, Japan; <sup>2</sup>Hita Tenryosui Co. Ltd.,  
Nakanoshima-machi, Hita 877-0074, Japan; <sup>3</sup>Centre for Holistic Medicine  
and Naturopathy, 57392 Nordenau, Germany*

**Abstract.** Recent studies have demonstrated that reactive oxygen species (ROS) and the resulting oxidative stress play an important role in apoptosis. Apoptosis is implicated in pathophysiology of diabetes mellitus. Antioxidants can block or delay apoptosis. We have demonstrated that reduced water (RW) such as hydrogen-rich electrolysed-reduced water (ERW) and natural reduced waters (NRW) like Hita Tenryosui water in Japan and Nordenau water in Germany could scavenge ROS and stimulate glucose intake into muscle and adipocytes. This study investigated the effect of reduced water (RW) on oxygen radicals and apoptosis of pancreatic  $\beta$ -cells by alloxan. Incubation of HIT-T15 cells with alloxan, a diabetogenic compound, resulted in the increased intracellular ROS level, a decrease in viability of cells, the formation of DNA fragmentation and Sub-G1 phase. The generation of ROS, the formation of DNA fragmentation and Sub-G1 phase, the lowering of cell viability by alloxan toxicity can be suppressed by treatment with RW. In contrast, HIT-T15 cells treated with Mineral water were not observed. These results suggest that RW protected pancreatic  $\beta$ -cell from the alloxan-induced apoptosis by preventing the alloxan-derived oxygen radical generation.

### 1. INTRODUCTION

Reactive oxygen species (ROS) play an important role in apoptosis. Alloxan, a potent diabetogenic agent, has been widely used for the induction of experimental diabetes by the production of ROS. HIT-T15 cells, a hamster  $\beta$ -cell line, treated with alloxan caused  $\beta$ -cell apoptosis with increase of intracellular ROS level, elevation of cytosolic-free  $\text{Ca}^{2+}$ , decrease of intracellular ATP level, inhibition of glucose-stimulated insulin release (1,2). In the previous study, we showed that electrolysed-reduced water (ERW) and natural reduced water (NRW) could inhibit the decrease of  $\beta$ -cell viability by scavenging ROS, suggesting that RW might be effective for preventing type 1 diabetes (3, 4). A statistical analysis of the clinical data on 219 diabetes patients also demonstrated that Nordenau water could significantly improve the symptoms of diabetes mellitus. However, the effect of RW on apoptosis or necrosis of pancreatic  $\beta$ -cell in relation to type 1 diabetes has not been understood.

Here we report that protective effect of RW to alloxan-diabetes may be due to prevented alloxan-induced apoptosis by scavenging intracellular ROS.

## 2. MATERIALS AND METHODS

### *2.1. Preparation of reduced water*

Electrolyzed-reduced water (ERW) was prepared by the electrolysis of Milli-Q water containing 0.002N NaOH using an electrolyzing device, TI-200S (Nihon Trim, Osaka), equipped with a platinum-coated titanium electrodes at direct current of 100 V for 60 min. Nordenau Water was supplied by Mr. Theo Tommes in Nordenau in Germany. Hita Tenryosui water was obtained from Hita Tenryosui Co. in Japan. Natural mineral water was purchased from the market in Japan. The medium was prepared using RW instead of Milli-Q water.

### *2.2. Cell culture*

Hamster pancreatic  $\beta$ -cell line, HIT-T15, was cultured in RPMI 1640 medium containing 10% fetal bovine serum (FBS), 2 mM L-glutamine, 25 mM HEPES, 100 IU/ml penicillin-G and 100  $\mu$ g/ml streptomycin. The medium was exchanged every 2 days.

### *2.3. Measurement of sub-G1 phase and DNA fragmentation*

After pre-incubation with RW for 24 h, HIT-T15 cells were incubated with 1 mM alloxan for 4 h, the cell numbers of Sub-G1 phase in cellular suspension were determined using flow cytometric analysis, and DNA fragmentation was determined by DNA fragmentation assay kit and 2% agarose gel electrophoresis, according to the manufacturer's instructions..

## 3. RESULT AND DISCUSSION

Alloxan-derived ROS disturb intracellular  $\text{Ca}^{2+}$  homeostasis and decrease the ATP level, resulting in death of pancreatic  $\beta$ -cells. Cell death can occur by either of two mechanism, necrosis or apoptosis. The biochemical hallmark of apoptosis is the fragmentation of the genomic DNA. Free radicals play important roles in alloxan-diabetes. Alloxan can cause accumulation of enough ROS to induce the fragmentation of DNA in  $\beta$ -cells. The DNA fragmentation by alloxan is a critical step in the induction of alloxan-diabetes. In order to evaluate the effect of RW on alloxan-induced apoptosis, HIT-T15 cells were treated with various waters and then exposed to 1mM alloxan for 4 h. Alloxan increased DNA fragmentation and caused

Table 1. Effects of various waters treated on alloxan-induced DNA fragmentation of HIT-T15 cells.

	Control	ERW	Hita W	Rordenau W	Mineral W
alloxan -	100.00±9.56	-	-	-	-
lloxan +	824.32±9.25	129.07±27.48	185.85±10.71	199.22±8.1	830.04±163.92

DNA ladder, however, the DNA fragmentation induced by alloxan was remarkably inhibited by RW. Whereas, the commercial natural mineral water examined did not exhibit the protective effect (Table 1). Each value denotes the mean  $\pm$  S.D. of three separate experiments.

Under the conditions of mild oxidative stress, cell cycle-related genes are repressed to increase the lengthening of G1-phase. Alloxan increased number of cells with fragmented nuclei, the DNA content of these cells was lower than that at G1 phase (in sub-G1 phase). These sub-diploidy cells with fragmented nuclei thus were undergoing apoptosis. RW could remarkably inhibited alloxan-induced increase of number of cells at sub-G1 phase. However, the commercial natural mineral water did not (Figure 1). Each value denotes the mean  $\pm$  S.D. of three separate experiments.

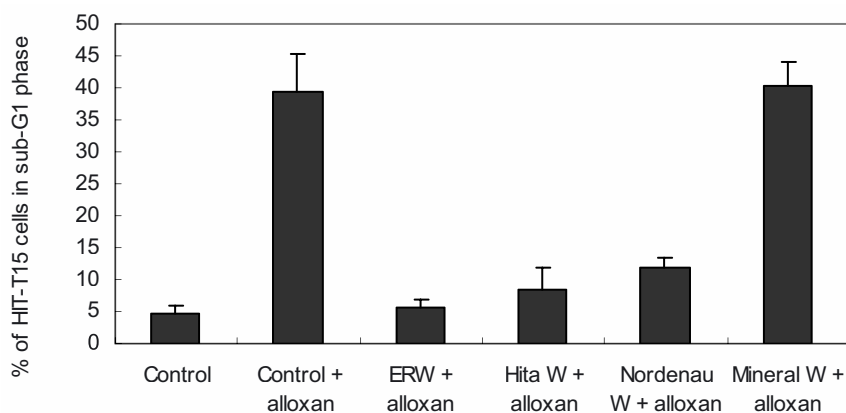


Figure 1. Effects of various waters on alloxan-induced apoptosis to HIT-T15 cells in sub-G1 phase

In conclusion, RW could scavenge intracellular ROS induced by alloxan in pancreatic  $\beta$ -cells, HIT-T15, and protected pancreatic  $\beta$ -cell from the alloxan-induced apoptosis by preventing the alloxan-derived oxygen radical generation. These results suggested that RW is effective to prevent alloxan-induced diabetes.

## 4. REFERENCES

1. Rho H, Lee J, Kim H, Park B & Park J (2000) Protective mechanism of glucose against alloxan-induced  $\beta$ -cell damage: pivotal role of ATP. *Exp Mol Med*, **32**: 12-17.
2. Sakurai K, Katoh M, Someno K & Fujimoto Y (2001) Apoptosis and mitochondrial damage in INS-1 cells treated with alloxan. *Biol Pharm Bull*, **24**: 876-882.
3. Shirahata S, Kabayama S, Nakano M, Miura T, Kusumoto K, Gotoh M *et al.* (1997) Electrolyzed-reduced water scavenges active oxygen species and protects DNA from oxidative damage. *Biochem Biophys Res Commun*, **234**:269-274.
4. Li Y, Nishimura T, Teruya K, Maki T, Komatsu T *et al.* (2003) Protective mechanism of reduced water against alloxan-induced pancreatic  $\beta$ -cell damage. *Cytotechnology*, **40**, in press.

JOHN THRIFT, GLEN YAMASAKI, RUDIGER HEIDEMANN,  
NADA ABBAS AND KONSTANTIN KONSTANTINOV

## CHARACTERIZATION OF APOPTOSIS IN A CHO CELL LINE CULTIVATED IN BATCH AND CONTINUOUS CULTURE: EFFECT OF MEDIUM, SPECIFIC PERFUSION RATE AND CHEMICAL INHIBITORS

*Bayer HealthCare, 800 Dwight Way, Berkeley, CA 94710 USA*

**Abstract.** In this study apoptosis is characterized in a CHO cell line cultivated in both batch and continuous perfusion culture. Data is presented which shows that apoptosis can be induced in this cell line with camptothecin and detected using DNA gel electrophoresis and annexin-V & caspase-3 flow cytometric analysis. Time profiles of caspase-3 and DNA laddering gels indicate that apoptosis is the predominant form of cell death experienced by this cell line in batch culture. Several reported apoptosis inhibitors are evaluated for their ability to improve batch performance (NAC, suramin, cyclosporin A, Ac-DEVD-CHO, z-VAD-fmk), of which only one, z-VAD-fmk, is shown to significantly improve batch survivability. However z-VAD-fmk's effectiveness at improving continuous culture is less profound, possibly due to this cell lines ability to die by an alternative apoptotic pathway. Finally, reduced productivity at ultra-low feed rates in perfusion culture is shown to be correlated to the induction of apoptosis.

### 1. INTRODUCTION

The ability to block apoptosis presents the possibility of extending the productive lifetime of cultured cells and so improve the productivity of biopharmaceutical manufacturing process. For this work the degree of apoptosis in an industrially important CHO cell line secreting recombinant protein was characterized. Understanding the role of apoptosis in this cell line could provide insights into more productive operation and could have profound economic benefits. For the study, characterization was performed in both batch and continuous culture systems.

### 2. METHODS

Several distinguishing characteristics of apoptosis were used to quantitate the degree of apoptosis in the CHO cell culture. Three assay methods were investigated and optimized for this purpose: **DNA gel electrophoresis.** Cells undergoing apoptosis cleave their dna into non-random fragments that can be used to characterize the degree of apoptosis in a culture. **Annexin V binding.** Cells undergoing apoptosis translocate phosphatidylserine (ps) from its usual residence in the inner leaflet of the cell membrane to the outside of the cell membrane. **Caspase activation.** Caspases

are commonly thought to be the most important effector molecules inducing apoptosis.

3. RESULTS

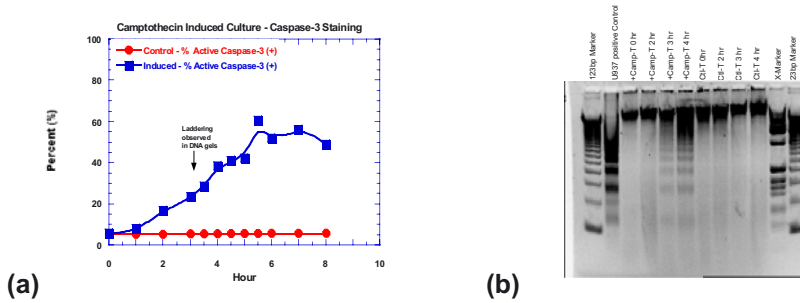


Figure 1. Apoptosis can be induced and detected in the Bayer CHO cell line with 20 $\mu$ M camptothecin. (a) time profile of caspase-3 activation (b) agarose DNA fragmentation gel.

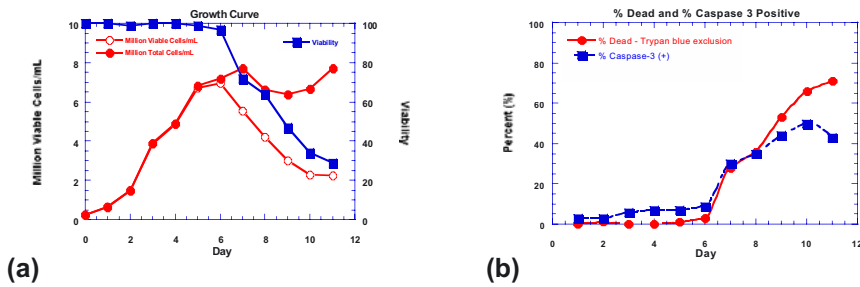


Figure 2. The Bayer CHO cell line dies predominantly by apoptosis in batch culture. (a) time profile of cell density and viability in batch culture, trypan blue exclusion (b) Time profile of caspase-3 activation.

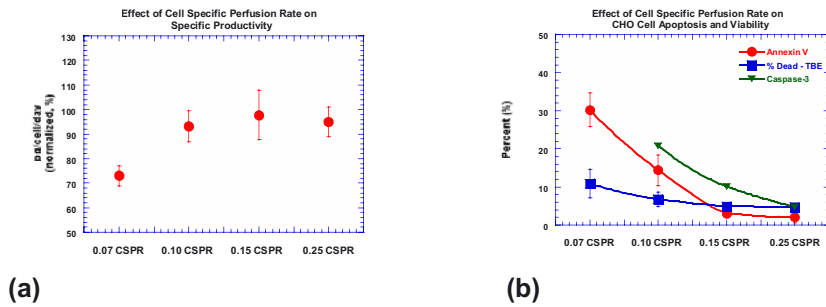


Figure 3. Reduced cell specific productivity in at low specific perfusion rates can be correlated to the induction of apoptosis. (a) effect of specific perfusion rate on cell specific productivity (b) effect of specific perfusion rate on annexin V and caspase-3 apoptosis indicators.

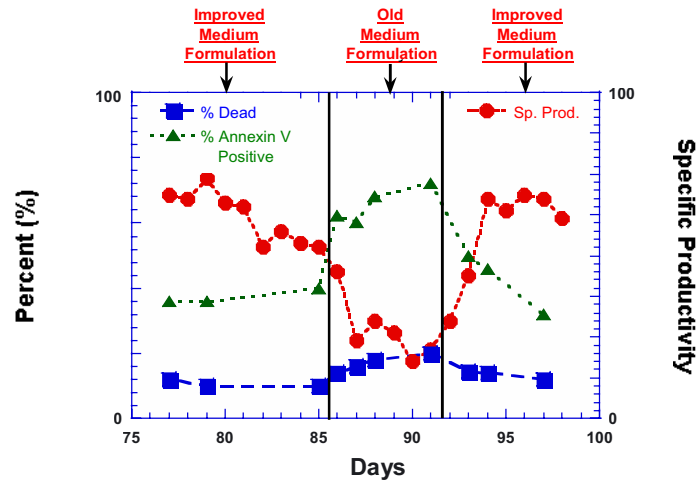


Figure 4. Improvements in media formulation can reduce apoptosis and increase productivity at low perfusion rate in perfusion bioreactors.

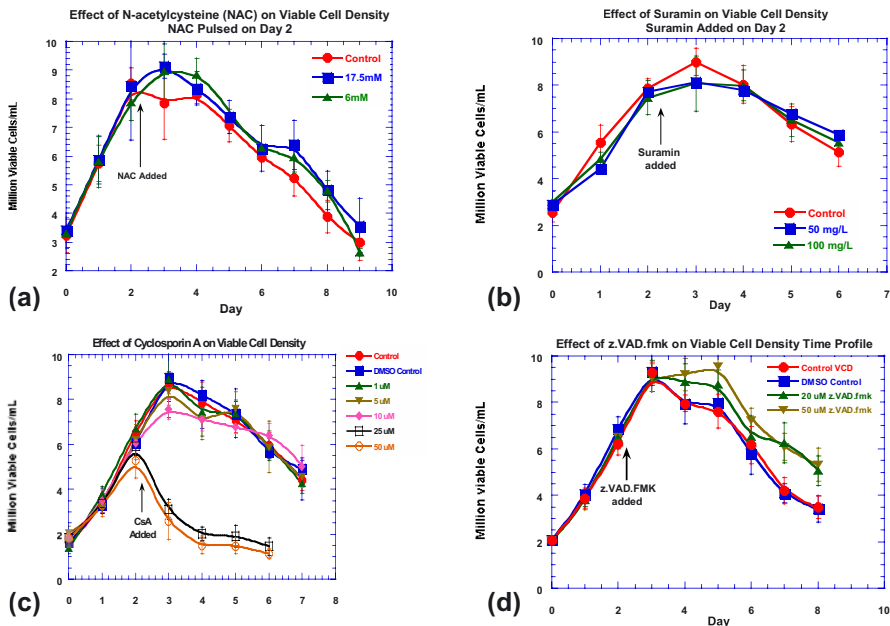


Figure 5. Effect of apoptosis inhibitors on cell survivability in batch culture. (a) N-acetylcysteine (b) suramin (c) cyclosporin A (d) z.VAD.fmk. Only z.VAD.fmk improved survivability.

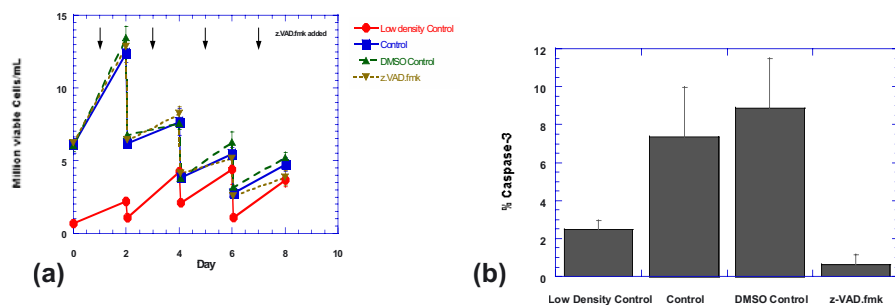


Figure 6. No improvement in a high cell density serial passage experiment was observed with *z.VAD.fmk*, even in the absence of caspase-3 activity. (a) time profile of cell density during serial passage (b) average caspase-3 at passage.

#### 4. CONCLUSIONS

We have shown in this study that batch cultures of a Bayer CHO cell line die by a predominately apoptotic mechanism. It is also shown that a reduction in specific productivity observed at low specific perfusion rates in a continuous perfusion bioreactor can be correlated to an increase in apoptosis, and that this phenomenon can be mitigated by an improved medium formulation. In addition it is shown that the pan caspase inhibitor *z.VAD.fmk* can increase cell density and prolong cell viability in batch culture, however this improved culture survivability does not result in higher product concentrations. *zVAD.fmk* did not improve survivability in a longer term passage culture in higher product concentrations.

#### 5. REFERENCES

- Singh RP, Finka G, Emery AN, Al-Rubeai M: Apoptosis and its control in cell culture systems. *Cytotechnology* 1997, 23:87-93.
- Mutsumi Z, Takagi M, Yoshida T. Effect of antioxidants on the apoptosis of CHO cells and production of tissue plasminogen activator in suspension culture. *J Biosci Bioengineer* 2001, 91 581-585.
- Pritchard D, Singh J, Carlisle D, Patierno S. Cyclosporin inhibits chromium(VI)-induced apoptosis and mitochondrial cytochrome c release and restores clonogenic survival in CHO cells. *Carcinogenesis* 2000, 21: 2027-2033.
- Zhang G, et al. Caspase inhibition prevents staurosporine-induced apoptosis in CHO-K1 cells. *Apoptosis* 1998, 3:27-33.
- Harding CL, Lloyd DR, McFarlane CM, Al-Rubeai M: Using the Microcyte flow cytometer to monitor cell number, viability and apoptosis in mammalian cell culture. *Biotechnol Prog* 2000, 16:800-802.
- Zanghi J, Renner W, Bailey J, Fussenegger M. The growth factor suramin reduces apoptosis and cell aggregation in protein-free CHO cell batch culture. *Biotechnol Prog* 2000, 16:319-325.
- Kidd V, Lahti J, Teitz T. Proteolytic regulation of apoptosis. *Cell & Develop Bio* 2000, 11:191-201.



YOSHIKAZI K., KATAKURA Y. I. FUJIKI T., TSUNEMATU T.,  
TERUYA K., SHIRAHATA S.

## HYDROGEN PEROXIDE-INDUCED CELLULAR SENESCENCE IS REGULATED VIA TWO DIFFERENT PATHWAYS

*Laboratory of Cellular Regulation Technology, Department of Genetic  
Resources Technology, Graduated School of Bioresource and  
Bioenvironmental Sciences, Kyushu University, Japan 6-10-1 Hakozaki,  
Higashi-ku, Fukuoka city, Japan*

**ABSTRACT.** Cellular senescence is thought to be an anti-tumor mechanism similar to apoptosis, which suggests that signal mediators participating in the cellular senescence programs might be a novel target for cancer therapy. Until now, several different cellular senescence pathways were reported. One is the telomere shortening dependent pathway called “replicative senescence”[1]. Another is the telomere shortening independent pathway, which is activated by oncogenic *ras*, called “premature senescence”[2]. Furthermore, we and other researchers have demonstrated that lethal concentration of hydrogen peroxide induces apoptosis, while sublethal concentration of hydrogen peroxide triggers premature senescence in normal cells[3] and A549, human lung adenocarcinoma. In this research, we attempted whether oxidative stress-inducible cellular senescence in A549 cancer cells can function as tumor suppression.

### 1. INTRODUCTION

Normal somatic cells undergo a limited number of division when cultured *in vitro* before entering an irreversible state of cell cycle arrest known as replicative senescence [1]. This process has been demonstrated to occur also *in vivo* and is believed to play a major role in safeguarding against tumor formation by suppressing the emergence of immortal cells besides to apoptosis. While it has been believed that cell lines lacking cell cycle checkpoint molecules become tumor cells. In fact it has been known that cancer cells are deficient in the pathway at least either p19<sup>ARF</sup>-p53 or p16<sup>INK4b</sup>-RB, which are known as cell cycle checkpoint regulators. It has been also reported that A549, human lung adenocarcinoma, is p15<sup>INK4a</sup>, p16<sup>INK4b</sup> null cell line. We has been reported that sublethal oxidative stress triggered cellular senescence in A549 cancer cells, suggesting that oxidative stress-inducible cellular senescence might not require the function of p15<sup>INK4a</sup> and p16<sup>INK4b</sup>. Recently it has been thought that there exist cellular senescence checkpoint mechanisms which is different from cell cycle checkpoint. In the present study, we tried to demonstrate whether A549 cells (p15<sup>-/-</sup>, p16<sup>-/-</sup>) undergo cellular senescence in response to

sublethal concentration of hydrogen peroxide, and whether senesced A549 cells impairs tumorigenicity.

## 2. RESULTS AND DISCUSSION

Previously we reported that sublethal (100  $\mu\text{M}$ ) hydrogen peroxide-treatment for 2h triggers cellular senescence evidenced phenotypic and morphological changes. In this research we attempted whether sublethal oxidative stress can function as a tumor suppression. So we evaluated the ability of colony formation in soft agar 10 days after the treatment with hydrogen peroxide for 2h in A549 cells. As a positive control we used A549 cells treated with lethal hydrogen peroxide-treatment for 2h. The result showed that sublethal hydrogen peroxide-treatment dramatically diminished the ability of colony formation in soft agar compared with non-treatment A549 cells (Table 1). Furthermore it was observed morphological enlargement compared with lethal hydrogen peroxide-treatment A549 cell. To demonstrate that

**Table.1 Colony formation after treatment with lethal/ sublethal hydrogen peroxide in A549 cells.**

	Ratio of colony formation (%)
non-treatment	79.1
lethal hydrogen peroxide (500 $\mu\text{M}$ )	13.1
sublethal hydrogen peroxide (100 $\mu\text{M}$ )	18.2

this impaired ability of colony formation is not caused by cell death, we evaluated cell death with PI (Propidium Iodide) staining methods, one of the necrosis marker. Lethal/ sublethal hydrogen peroxide-treatment A549 cells were staining with 10  $\mu\text{g/ml}$  of PI for 30 minutes and analyzed with flow cytometry. PI was incorporated by only dead cell and detected as PI-positive cell. The result showed that PI positive cells did not increase in A549 cells treated with sublethal concentration of hydrogen peroxide as compared to non-treated A549 cells. While PI positive cells dramatically increase in A549 cells treated with lethal concentration of hydrogen peroxide (Table 2). In conclusion, sublethal oxidative stress triggered cellular senescence in A549 cells as well. Furthermore this cellular senescence induction might apply to a novel method to suppress tumorigenicity. Molecules involved in this process might be a novel target for a cancer therapy.

**Table.2 Cell death after treatment with lethal/ sublethal hydrogen peroxide in A549 cells.**

	Ratio of dead cells (%)
non-treatment	1.42
lethal hydrogen peroxide (300 $\mu\text{M}$ )	15.5
sublethal hydrogen peroxide (100 $\mu\text{M}$ )	1.52

## REFERENCES

- Hayflick, L., and Moorhead, P. S. (1961) *Exp. Cell. Res.* **25**, 585-621  
Manuel S., and Scott W. L. (1997) *Cell* **88**, 593-602  
Chen Q.M. (2000) *Ann N Y Acad Sci.* **908**, 111-25

U. ERIKSSON AND L. HÄGGSTRÖM

## IDENTIFICATION OF AUTOCRINE FACTORS INFLUENCING PROLIFERATION IN SERUM-FREE CULTURES OF *TRICHOPLUSIA NI* CELLS

*Department of Biotechnology, Royal Institute of Technology,  
SE-106 91 Stockholm, Sweden*

**Abstract.** The aim of this study is to understand how proliferation of *Trichoplusia ni* cells is regulated in serum-free cultures. The hypothesis is that *T. ni* (Hi5) cells produce extracellular factors, which influence growth and productivity. To study this, the effect of conditioned medium (CM) on cell growth was investigated. Addition of 10 – 20 % CM shortened the lag phase and increased the maximum cell density. CM was further concentrated and fractionated on a gel filtration column. Fractions which either inhibit or stimulate proliferation have been identified. These results suggest that extracellular protein factors are involved in regulation of proliferation.

### 1. INTRODUCTION

The problem with insect cell cultures is the dramatic decrease in productivity which occurs when cells are infected with baculovirus occurs above a critical cell density. This puts a definite limit to the obtainable product yield. The aim of this study is to understand the mechanisms behind *Trichoplusia ni* cell proliferation and investigate how these mechanisms affect productivity. The hypothesis is that *T. ni* (Hi5) cells produce extracellular factors, which influence growth and productivity in serum-free cultures. Therefore, extracellular protein factors will be identified and their roles in proliferation and productivity evaluated.

### 2. RESULTS

#### *2.1. Effects of conditioned medium on *T. ni* proliferation*

To investigate whether extracellular factors produced by the cells themselves might be involved in regulation of proliferation, the effect of conditioned medium (CM) on cell growth was first studied. Different concentrations (10, 20, and 30%) of CM were mixed with fresh medium and tested on new cultures inoculated at different cell densities ( $1.5 \times 10^5$  and  $3 \times 10^5$  cells mL<sup>-1</sup>, Figure 1). The data show that 10 and 20% CM resulted in a shorter lag phase and a higher maximum cell density compared to fresh medium, whereas 30% CM shortened the lag phase but did not affect the maximum cell density. The effect becomes more pronounced with

decreasing inoculum cell densities. These results suggest that factors present in CM stimulate proliferation.

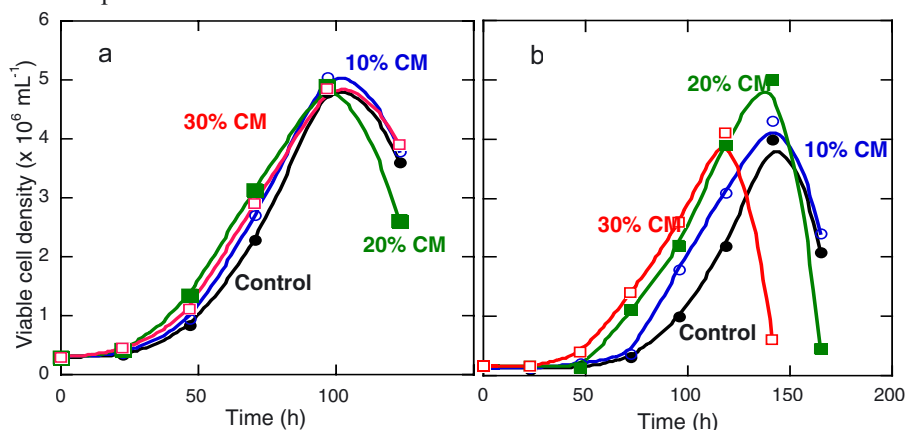


Figure 1. Effect of CM on *T. ni* proliferation.. Inoculum density, a)  $3 \times 10^5$  cells  $\text{mL}^{-1}$  b)  $1.5 \times 10^5$  cells  $\text{mL}^{-1}$ . Symbols: Control in 100% fresh medium (closed circles), 10% CM (open circles), 20% CM (closed squares), and 30% CM (open squares).

## 2.2. Identification of extracellular protein factors

To further investigate the possible presence of extracellular factors, cells were incubated in yeast extract-free ExpressFive medium (Invitrogen) for three days. CM from such cultures was concentrated on a 3 kDa cut-off filter, and then fractionated on a gel filtration column. Fractions were selected on basis of the gel column elution profile and the proteins in each fraction were further studied by SDS-PAGE analysis (not shown). Selected fractions were added to *T. ni* cultures (50% fraction, 50% fresh medium) to test their effect on proliferation. The results indicated that both inhibitory and stimulatory components were present in CM. So far, three different fractions have been shown to influence cell proliferation. Two of these fractions, one eluting at  $\approx 10$  kDa (Fig. 2a) and the other eluting at  $>400$  kDa, inhibit cell proliferation, while a fraction at  $\approx 45$  kDa stimulated proliferation (Fig. 2b).

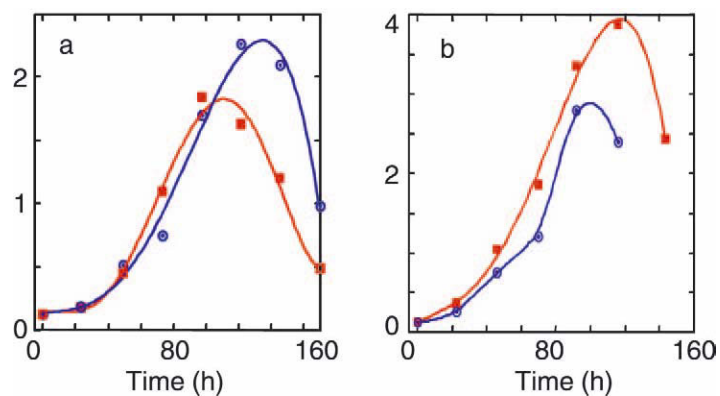


Figure 2. Effect of CM fractions on cell proliferation. A) 10 kDa fraction, b) 45 kDa fraction. Symbols: Control culture in 100% fresh medium (filled circles), culture with 50% CM fraction and 50% fresh medium (filled squares).

### 3. DISCUSSION

Our data clearly show that CM contains factors, produced by the cells themselves, which affect cell proliferation. Obviously, both stimulatory and inhibitory components are present in CM. We speculate that these factors take part in a complex pattern of autocrine regulation. We are currently working on identifying and characterising these proteins.

### 4. ACKNOWLEDGEMENTS

This work was supported by a grant from the Swedish Centre for Bioprocess Technology, and by AstraZeneca Biotech Laboratory, Gärtuna, Södertälje.

C.A. YANDELL, I.P. BUTLER, A.J. SHEEHAN, B.J. WADE,  
A.P. SIMULA AND C. GODDARD.

## THE EFFECTS OF INSULIN AND LONG<sup>TM</sup>R<sup>3</sup>IGF-I ON CHINESE HAMSTER OVARY CELLS: CELL SURVIVAL, RECEPTOR ACTIVATION AND SECOND MESSENGER PATHWAYS

*GroPep Ltd. PO Box 10065 BC, Adelaide, SA 5000, Australia.*

**Abstract.** Serum-free media for CHO cell culture has traditionally been supplemented by the addition of insulin or more recently by an insulin-like growth factor-I (IGF-I) analogue Long<sup>TM</sup>R<sup>3</sup>IGF-I. We, and others, have demonstrated that Long<sup>TM</sup>R<sup>3</sup>IGF-I is capable of supporting the growth of CHO cells and the production of recombinant proteins in serum-free cultures, at concentrations 200-fold lower than required for insulin. As CHO cells have fewer insulin receptors (IR) than Type I IGF receptors (IGF-IR) and as insulin is used at supra-physiological concentrations, it is believed to be also acting via the IGF-IR. However, the differences in the cellular responses to the two growth factors in CHO cells are not well understood.

In this study we have examined the activation of IR, IGF-IR and second messenger molecules upon stimulation of CHO cells with insulin and Long<sup>TM</sup>R<sup>3</sup>IGF-I. We have demonstrated that insulin at supra-physiological levels stimulates both the IR and the IGF-IR. However, Long<sup>TM</sup>R<sup>3</sup>IGF-I activates these receptors to a greater degree than does insulin, at 200-fold lower concentrations. Insulin also does not appear to activate some of the anti-apoptotic signalling molecules to the same degree as Long<sup>TM</sup>R<sup>3</sup>IGF-I. Indeed, insulin stimulation of CHO cells in serum-free culture results in less phosphorylation of Akt, a protein kinase that plays a key role in controlling the balance of cell survival and apoptosis, than stimulation by Long<sup>TM</sup>R<sup>3</sup>IGF-I. The levels of MAPK phosphorylation however, were comparable regardless of whether the serum-free media adapted cells were stimulated by insulin or Long<sup>TM</sup>R<sup>3</sup>IGF-I. This appears to be due to the high basal levels of MAPK phosphorylation in cells adapted to serum-free media.

### 1. INTRODUCTION

The production of therapeutic proteins relies heavily on the large-scale culture of eukaryotic cells that secrete the protein of interest into the media. There is a strong drive within the biopharmaceutical industry towards the development of serum-free manufacturing processes primarily because of the potential for introducing pathogenic contaminants, such as viruses, bacteria or prions. Chinese hamster ovary (CHO) cells can be maintained in serum-free media by the addition of insulin or an insulin-like growth factor-I (IGF-I) analogue, Long<sup>TM</sup>R<sup>3</sup>IGF-I. It has been demonstrated that Long<sup>TM</sup>R<sup>3</sup>IGF-I is capable of supporting growth of CHO cells and the production of recombinant proteins in serum-free culture at concentrations 100-1000-fold lower than required for insulin (1,2,3). CHO cells have 10-fold fewer insulin receptors (IR) than Type I IGF receptors (IGF-IR) (2) and insulin maintains

cell viability only at supra-physiological concentrations. Therefore, it has been hypothesised that insulin's actions are also mediated via the IGF-IR.

In this study we have examined the role of IR and IGF-IR activation and activation of two key anti-apoptotic signalling molecules in CHO cells in response to stimulation by insulin and Long<sup>TM</sup>R<sup>3</sup>IGF-I at concentrations relative to those used to maintain cell viability.

## 2. MATERIALS AND METHODS

CHO K1 cell lines (ATCC) were maintained in a 1:1 mix of DMEM and Ham's F12 medium (D/F12). Recombinant Long<sup>TM</sup>R<sup>3</sup>IGF-I was manufactured at GroPep Ltd, and bovine insulin was obtained from Sigma (St Louis, MO, USA). Anti-phosphotyrosine, anti-phospho-Akt and anti-phospho-MAPK antibodies (Cell Signaling Technology, Beverly, MA, USA), anti-IR $\beta$  antibody (GroPep), anti-IGF-IR $\beta$  antibody (Santa Cruz Biotechnology Inc, Santa Cruz, CA, USA), or anti- $\beta$ -actin antibody (Sigma) were prepared at the appropriate dilutions in 5% skim milk in tris buffered saline containing 1% Tween-20.

CHO K1 cells adapted to grow in serum-free media (SFA cells) were stimulated for 10 minutes with various concentrations of insulin or Long<sup>TM</sup>R<sup>3</sup>IGF-I. Cells were also grown in D/F12 with 10% FBS to confluence, starved for 48 hours, before being stimulated with insulin or Long<sup>TM</sup>R<sup>3</sup>IGF-I. Stimulated cells were lysed with a buffer containing phosphatase inhibitors. The cell lysates were incubated with the appropriate anti-receptor antibody followed by protein-G-sepharose. The immunoprecipitated receptors and lysates were prepared in SDS sample buffer, separated by SDS-PAGE and transferred to nitrocellulose membranes. Membranes were immunoblotted with the appropriate dilutions of primary antibody, the appropriate HRP-conjugated secondary antibody and detection was by enhanced chemiluminescence (Pierce, Rockford, IL, USA). The ratio of phosphorylated protein to total protein was calculated as the relative intensities for the protein band of interest.

## 3. RESULTS AND DISCUSSION

We have examined the activation of both the IR and the IGF-IR in CHO K1 cells after stimulation with insulin or Long<sup>TM</sup>R<sup>3</sup>IGF-I at various concentrations. The concentrations used in these stimulation experiments are 10 times that required for maintenance of cell cultures because of the insensitive nature of the immunoblots and the short time period of stimulation. We have shown that Long<sup>TM</sup>R<sup>3</sup>IGF-I and insulin both stimulate the IR and IGF-IR (Fig. 1). However, Long<sup>TM</sup>R<sup>3</sup>IGF-I stimulates both receptors to a greater degree than does insulin, at 200-fold lower concentrations.



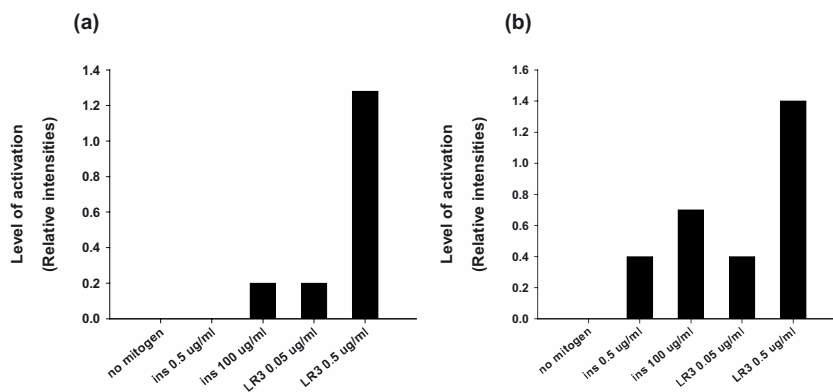


Figure 1: The levels of activation of the IR (a) and the IGF-IR (b) after stimulation of SFA CHO K1 cells with insulin (ins) or Long<sup>TM</sup>R<sup>3</sup>IGF-I (LR3). This is represented as the relative intensities of phosphorylated receptor as a ratio of the total amount of receptor immunoprecipitated as detected by immunoblot.

We hypothesise that there are IGF-IR/IR hybrid receptors that have a higher affinity for IGF-I than insulin as the greater activation of the IR at these concentrations of Long<sup>TM</sup>R<sup>3</sup>IGF-I would be unexpected with homodimeric IR alone. The role of hybrid receptors is currently being investigated by the transfection of kinase-defective, dominant-negative IGF-IR and IR into CHO cells.

The phosphorylation of Akt and the MAP kinases (MAPK) was also examined after stimulation with various concentrations of Long<sup>TM</sup>R<sup>3</sup>IGF-I and insulin. Akt is a key signalling molecule that regulates the balance of cell survival and apoptosis. Phosphorylation of Akt leads to inhibition of Bad, caspase-9 and other apoptotic signalling molecules. The MAPKs are involved in many signalling pathways and the phosphorylation of these proteins leads to cell proliferation, survival and differentiation. Both the IR and the IGF-IR have been demonstrated to mediate their effects through these two signalling intermediates. In SFA CHO K1 cells Akt phosphorylation is greater with Long<sup>TM</sup>R<sup>3</sup>IGF-I than with insulin, at 200-fold lower concentrations (Fig. 2). MAPK phosphorylation was similar with both Long<sup>TM</sup>R<sup>3</sup>IGF-I and insulin treatment (results not shown). However, the basal levels of MAPK phosphorylation in these cells was high. When the same experiments were performed in cells grown in FBS and starved for 48 hours, basal levels of MAPK and Akt phosphorylation were negligible and Long<sup>TM</sup>R<sup>3</sup>IGF-I stimulated both to a greater degree than did insulin (Fig.3). This suggests that high basal levels of MAPK phosphorylation may be a consequence of the adaptation of CHO K1 cells to serum-free D/F12 media.

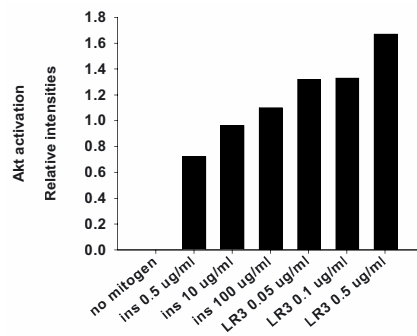


Figure 2: The level of activation of Akt after stimulation of SFA CHO K1 cells with insulin (ins) or Long<sup>TM</sup>R<sup>3</sup>IGF-I (LR3). This is represented as the relative intensities of phosphorylated Akt as a ratio of the total amount of protein loaded as detected by immunoblot.

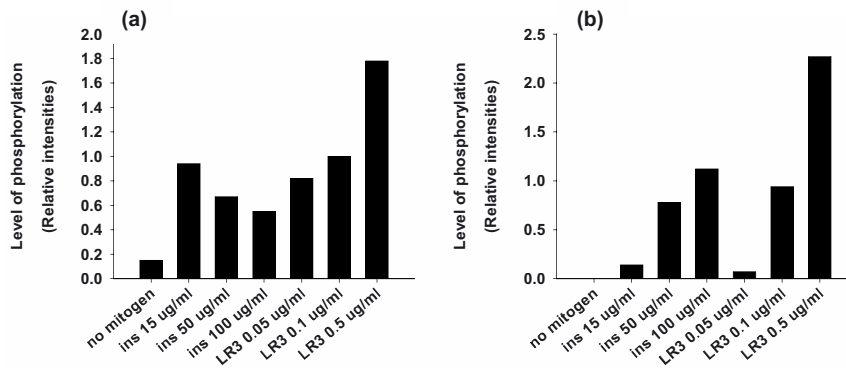


Figure 3: The level of activation of Akt (a) and p42/MAPK (b) after stimulation with insulin (ins) or Long<sup>TM</sup>R<sup>3</sup>IGF-I (LR3) in CHO K1 cells, grown in 10% FBS and starved for 48 hours.

These results demonstrate why LongTMR3IGF-I is better able to stimulate cell proliferation and maintain cell viability than insulin even though LongTMR3IGF-I is used at 200-fold lower concentrations. It also indicates that LongTMR3IGF-I may be useful for adapting CHO K1 to serum-free conditions as it reduces cell death on removal of serum. Indeed, it has previously been demonstrated that LongTMR3IGF-I potentiated the rapid adaptation of a recombinant CHO cell line to manufacturing media (3), decreasing the time taken to obtain stable clones and to scale-up to production levels.

#### 4. REFERENCES

1. Morris, A.E. and Schmid J. 2000. *Biotechnol. Prog.* **16**, 693-697.

2. Yandell, C.A., Wade, B.W., Sheehan, A.J., Simula, A.P. and Goddard, C. 2002. In *Cell Engineering VIII*, Snowmass, CO: United Engineering Foundation, Inc.
3. Chun, C., Heineken, K., Szeto, D., Ryall, T., Chamow, S and Chung, J.D. 2003. *Biotechnol. Prog.* **19**, 52-57.

E. SPENS AND L. HÄGGSTRÖM

## CONDITIONED MEDIUM FACTORS IN PROTEIN-FREE CULTURES OF NS0 CELLS

*Department of Biotechnology, Royal Institute of Technology, SE-106 91  
Stockholm, Sweden*

**Abstract.** An NS0 myeloma cell line has successfully been adapted to a protein-free medium without animal-derived components. The antibody yield in this medium is almost three-fold that in a traditional serum-medium. Kinetic studies of specific growth rate and specific product formation show that the antibody production in the serum-medium is strongly coupled to cell division while in the protein-free medium it is not. We propose that the large difference in growth and productivity profiles is due to the difference in supply and origin of growth factors. In the serum-medium proliferation is dependent on and related to factors present in the serum while in the protein-free medium the cells have adapted to an environment without serum-derived factors. Instead, the cells have started to produce their own factors through which they control their proliferation. We are currently trying to identify and characterise such conditioned medium factors and so far we have discovered at least one factor at about 20 kDa with a clear positive effect on cell growth.

### 1. INTRODUCTION

Animal cells have traditionally been cultured in serum supplemented media. Clinical applications of produced recombinant proteins however demands fully defined protein-free media without animal derived components. Designing such a medium for NS0 cells is more difficult than for other mammalian cell lines due to their need for cholesterol and lipid supplementation (Keen and Hale, 1996). The frequent proprietary of commercial media further complicates research on medium composition. In this study we show that it is possible to culture NS0 cells in a fully defined protein-free media without animal derived components.

### 2. RESULTS

#### *2.1. Growth and production in traditional serum-medium and protein-free medium*

A batch shake-flask culture of NS0 myeloma cells in serum-medium is characterised by fast growth and rapid onset of apoptosis at day three (Figure 1a). The final antibody concentration is 70 mg/L. Successful adaptation of the NS0 cell-line to a protein-free medium without animal-derived components resulted in a five-day culture with a final antibody concentration of 195 mg/L (Figure 1b).

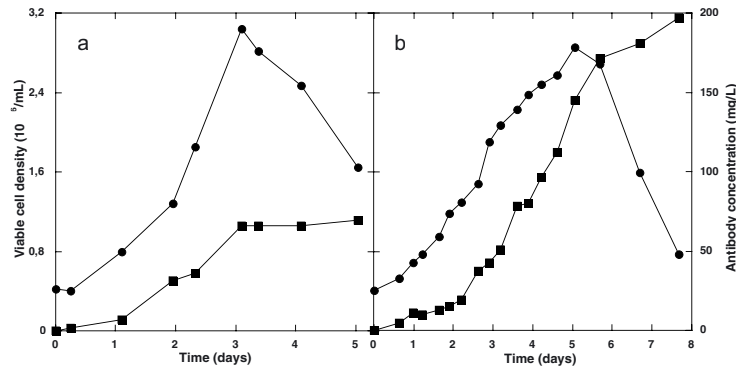


Figure 1. Growth and production of NS0 myeloma in DMEM with 10% FBS (a) and modified Serum-free and Protein-free Hybridoma Medium (Sigma-Aldrich, Sweden) (b). Viable cells ( $\square$ ) and antibody concentration ( $\circ$ ).

### 2.2. Specific growth rate and specific product formation rate

Calculation of specific growth rate and specific product formation rate shows that the kinetics in the two media is very different. In the serum-medium product formation is strongly coupled to cell division (Figure 2a) while in the protein-free medium it is not (Figure 2b).

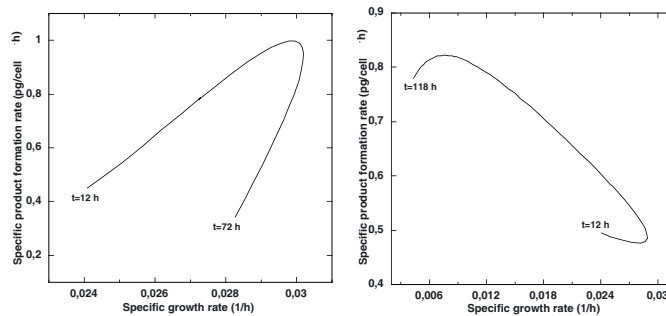


Figure 2. Specific product formation rate plotted as a function of specific growth rate for NS0 myeloma cultured in serum-medium (a) and protein-free medium (b).

### 2.3. Conditioned medium factors

Conditioned medium was concentrated using a 3 kDa cut-off filter and then fractionated on a gel-filtration column with a separation span of 3-70 kDa. The effect of different fractions on cell growth was investigated using fractionated fresh

medium and running buffer as controls. So far, at least one fraction with a clear positive effect has been discovered (Figure 3). The protein content in this fraction is shown in Figure 4. Proteins with suspected activity are now being identified with N-terminal sequencing.

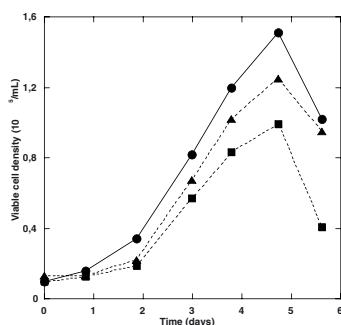


Figure 3. Effect of chromatography fraction from concentrated conditioned medium. Conditioned medium (●), fresh medium (◻) and running buffer (◻).

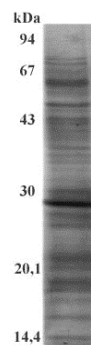


Figure 4. Protein content in chromatography fraction from concentrated conditioned medium.

### 3. DISCUSSION

The successful adaptation of NS0 myeloma cells to a protein-free medium and the profound difference in growth and productivity profiles in this medium compared to the serum-medium indicates that the cells themselves possess a proliferative control system. During the adaptation process the removal of serum-derived growth factors forces the cells to activate this system. By producing different factors the cells start to, in an autocrine manner, control their growth and maybe also the termination of proliferation. Understanding the role of these conditioned medium factors is of vital importance for developing novel strategies to improve growth and productivity in NS0 cell cultures.

### 4. ACKNOWLEDGEMENTS

This work was supported by a grant from The Swedish Centre for BioProcess Technology and by BioInvent International AB (Lund, Sweden). We also want to thank ESACT for the bursary awarded to E. Spens.

### 5. REFERENCE

- M. J. Keen and C. Hale (1996) The use of serum-free medium for the production of functionally active humanised monoclonal antibody from NS0 mouse myeloma cells engineered using glutamate synthetase as selectable marker. *Cytotechnology* 18: 207-217.

T. TAMURA<sup>1,2</sup>, Y. KATAKURA<sup>1</sup>, M. YAMASHITA<sup>1</sup>, Y. AIBA<sup>1</sup>,  
S. MATSUMOTO<sup>1</sup>, K. TERUYA<sup>1</sup> and S. SHIRAHATA<sup>1</sup>

## PRODUCTION OF HUMAN ANTI-PEPTIDE ANTIBODY FOR CLINICAL USE BY *IN VITRO* IMMUNIZATION

<sup>1</sup>*Department of Genetic Resources Technology, Kyushu University,  
Fukuoka 812-8581, Japan;* <sup>2</sup>*R&D Division, SEIWA Pharmaceutical Co.,  
Ltd., Kitaibaraki 319-1535, Japan*

### 1. INTRODUCTION

Human monoclonal antibodies have a large potential to be used for diagnosis and therapy of various diseases, such as cancer, allergy, and so on. However, there exist some problems on sensitizing antigens to the human in order to obtain the antigen-specific human antibodies because of ethical and moral reasons. *In vitro* immunization method (IVI), in which primary B cells are activated to produce antigen-specific B lymphocytes, was established to solve this problem. In our previous study, we have established an IVI of human peripheral blood lymphocytes (PBL) against soluble proteins such as Cholera toxin B subunit (CTB), KLH or Rice allergic protein (RA) (Ichikawa et al., 1999). Furthermore, using a fragment peptide of CTB or RA, we have demonstrated that peptide antigen can be useful as sensitising antigen on IVI. However, some of proteins were difficult to produce antibodies because of serious effect on PBL on IVI, such as cytotoxicity, autoimmune response, change in the cytokine balance, and so on. TNF- $\alpha$  is a pleiotropic cytokine primarily produced by activated macrophages to response to a variety of inflammatory agents, so it is difficult to use as sensitizing antigen on IVI. Furthermore, Anti-TNF- $\alpha$  chimeric monoclonal antibody Infliximab have been reported to improve symptoms of rheumatoid arthritis and Crohn's disease, and approved for treatment of these disease (Targan et al., 1997, Maini et al., 1999). In this study, we tried to establish an *in vitro* immunization protocol against peptide fragments derived from tumor necrosis factor- $\alpha$  (TNF- $\alpha$ ) for production of antibody for clinical use.

### 2. MATERIALS AND METHODS

### 2.1. Antigenes

Recombinant human IL-2 were purchased from Genzyme corporation (Cambridge, MA, USA). Recombinant human IL-4 and recombinant human TNF- $\alpha$  were purchased from Pepro Tech EC LTD. (London, England). Two synthetic peptides, TNF- $\alpha$ pep(1) (<sup>1</sup>VRSSSRTPSDKPVA<sup>14</sup>: rich-hydrophilic region) and TNF- $\alpha$ pep(2) (<sup>83</sup>AVSYQTKVNLLS<sup>94</sup>: TNF receptor binding region), and their peptides coupled with KLH (TNF- $\alpha$ pep(1)-KLH, TNF- $\alpha$ pep(2)-KLH) were obtained from Sigma Genosys Japan Co. Ltd. (Hokkaido, Japan).

### 2.2. Isolation of human lymphocytes

Human peripheral blood lymphocytes (PBL) were separated by density-gradient centrifugation from several healthy donors. After separation, the lymphocyte layer was harvested and them washed three times with ERDF medium. Lymphocytes from peripheral blood were treated with 0.25 mM Leu-Leu-OMe (LLME) to remove the cytotoxic T cells, CD8+ suppressor T cells, and natural killer cells before use.

### 2.3. In Vitro Immunization

*In vitro* immunization of PBL was performed in 24 well culture plates. LLME-treated PBL were cultured for 8 days in ERDF medium containing 10 % fetal bovine serum, 2-mercaptoethanol, Muramyl dipeptide (MDP), IL-2, IL-4 and TNF- $\alpha$  antigens.

### 2.4. Measurement of antibody production

Antibody production levels in culture supernatants were measured by a sandwich enzym-linked immunosorbent assay (ELISA). Antigen specificity of produced antibody was tested by a direct ELISA and enzyme-linked immunospot (ELISPOT) assay.

## 3. RESULT AND DISCUSSION

First, in order to examine the effect of TNF- $\alpha$  antigen, we performed IVI of PBL derived from healthy donors against various dose of TNF- $\alpha$ , TNF- $\alpha$ pep(1), and TNF- $\alpha$ pep(1)-KLH with IL-2 (10 units/ml), IL-4 (1 ng/ml) and MDP (10  $\mu$ g/ml). Eight days after sensitization, we harvested culture supernatants of each treatment and measured antibody production levels by ELISA. As a result, IgM or IgG antibody production of PBL was not enhanced by adding each antigen in comparison with control. Using TNF- $\alpha$  protein form as sensitizing antigens, we couldn't detect antigen-specific antibody production response from PBL on IVI. But we found that TNF- $\alpha$ -specific antibodies were generated in IVI by using TNF- $\alpha$ pep(1) or TNF- $\alpha$ pep(1)-KLH, especially 0.1  $\mu$ g/ml TNF- $\alpha$ pep(1) (Table.). In addition, by an ELISPOT assay analysis, TNF- $\alpha$ -specific IgM-generated B cells were demonstrated to increase by immunization with 0.1  $\mu$ g/ml TNF- $\alpha$ pep(1).



Furthermore, we examined IVI of PBL derived from different donors against TNF- $\alpha$  antigens with same conditions of previous study. As a result, we observed increase

Table. Effect of antigen form and antigen dose on antigen production of immunized PBL.

Antigen	Dose ( $\mu\text{g/ml}$ )	Concentration of immunoglobulins ( $\mu\text{g/ml}$ )		Anti-TNF- $\alpha$ antibody production	
		IgM	IgG	IgM	IgG
Control	0	1.805	9.076	-	-
TNF- $\alpha$	10	0.690	11.622	-	-
	1	1.954	11.096	+	+
	0.1	2.432	10.810	+	-
TNF- $\alpha$ pep(1)	10	2.760	10.847	+	+
	1	6.362	11.084	++	-
	0.1	4.516	11.462	+++	-
TNF- $\alpha$ pep(1)- KLH	10	2.624	10.318	++	-
	1	3.205	10.535	++	-
	0.1	2.401	10.306	-	+

of TNF- $\alpha$  specific IgM antibodies production of every donor's PBL which were stimulated against TNF- $\alpha$ pep(1) *in vitro*. Next, we studied IVI of PBL against TNF- $\alpha$ pep(2), which was composed hydrophobic amino acid residue and was a TNF receptor binding region. As a result, we couldn't detect antibody production response of PBL with the same condition of using TNF- $\alpha$ pep(1). However, restudied and changed concentrations of IL-4 from 1 ng/ml to 10 ng/ml or MDP from 10  $\mu\text{g/ml}$  to 1  $\mu\text{g/ml}$ , we could detect the increase of TNF- $\alpha$  specific antibody production from PBL stimulated with TNF- $\alpha$ pep(2). These results indicate that anti-TNF- $\alpha$  antibody can be produced by the IVI method using TNF- $\alpha$  fragment peptide as sensitizing antigens. Moreover, a fragment peptide can be useful as a sensitizing antigen on IVI instead of protein form which is difficult to use as an antigen.

Taken together with our previous report, we have succeeded in the production of antigen specific human antibodies by IVI of PBL against three distinct proteins and their peptides as shown above, we conduct here that IVI of human PBL is a useful method of generating antigen-specific human antibody *in vitro*.

#### 4. REFERENCES

- Ichikawa A., Katakura Y., et al. (1999) *In Vitro* Immunization of Human Peripheral Blood Lymphocytes: Establishment of B Cell Lines Secreting IgM Specific for Cholera Toxin B Subunit from Lymphocytes Stimulated with IL-2 and IL-4, *Cytotechnology* **31**, 131-139
- Targan SR., Hanauer SB., et al. (1999) A Short-Term Study of Chimeric Mnoclonal Antibody cA2 to Tumor Necrosis Factor  $\alpha$  For Crohn's Disease, *N. Engl. J. Med.* **337**, 1029-1035
- Mainai R., St Clair EW., et al. (1999) Infliximab (chimeric anti-tumour necrosis factor a monoclonal antibody) versus placebo in rheumatoid arthritis patients receiving concomitant methotrexate: a randomised phase III trial, *Lancet.* **354**, 1932-1939

Q.H. XU<sup>1,2</sup>, Y. KATAKURA<sup>1</sup>, M. YAMASHITA<sup>1</sup>, K. TERUYA<sup>1</sup>,  
S.G.FANG<sup>2</sup> AND S. SHIRAHATA<sup>1</sup>

## OPTIMIZATION OF IN VITRO IMMUNIZATION PROTOCOL TO PRODUCE ANTIGEN SPECIFIC HUMAN MONOCLONAL ANTIBODY BY DEMONSTRATING THE ROLE OF IL-10

<sup>1</sup>*Department of Genetic Resources Technology, Kyushu University, Fukuoka  
812-8581, Japan* <sup>2</sup>*College of Life Sciences, Zhejiang University, Hangzhou  
310029, China*

**Abstract** We have previously reported that *in vitro* immunization (IVI) protocol enables antigen specific antibody production from Leu-Leu-Ome (LLME)-treated human peripheral blood lymphocytes (PBL) by stimulating with antigen in the presence of IL-2, IL-4 and muramyl dipeptide (MDP). In the course of our studies to optimize the antibody production, we evaluated the cytokine production profiles in the IVI protocol. IL-10 was produced in non-treated PBL, which was thought to be one of reasons for inability of non-treated PBL to produce antibody, and also produced in LLME-treated PBL 1 wk after the antigen sensitization, where antibody production was strongly enhanced. Furthermore, IL-10 added to the LLME-treated PBL before the antigen sensitization, antibody production decreased. However, IL-10 added to the LLME-treated PBL at the antigen sensitization augmented antibody production level. These results strongly suggest that IL-10 might play an important role in the activation and/or inactivation of T cells, B cells and antigen presenting cells at the antigen sensitization, where IL-10 might alter the cellular milieu, resulting in the suppression or activation of antibody production. In the present study, we tried to further evaluate the function of IL-10 in antibody production in the IVI protocol. Results showed that IL-10 added before the antigen sensitization targets CD8 T cells, which might lead to elicit the suppressive function of T cells, while IL-10 added at the antigen sensitization elicits Th2 type responses via suppressing IFN-gamma and augmenting IL-4 production.

### 1. INTRODUCTION

Human monoclonal antibodies are thought to be best suited for clinical use, but techniques to produce human mAb haven't yet been well established. One method to produce human mAb is the *in vitro* immunization technique, in which antigen-specific B lymphocytes taken from peripheral blood are activated by specific antigen, and are induced to produce antigen specific mAb [1]. We have previously improved this technique and demonstrated that muramyl dipeptide (MDP), interleukin-2 (IL-2) and IL-4 were effective as additive for inducing the production of antigen-specific antibody from human PBLs *in vitro* [2]. We previously found that antibody production can be seen in the LLME-treated PBL, but not in non-treated PBL [3]. During our study, we evaluated the cytokine production profiles in the IVI protocol. IL-10 was produced in non-treated PBL, which was thought to be one of reasons for inability of non-treated PBL to produce antibody; while IL-10

existing in later period of LLME-treated PBL would enhance antibody production. In the course of our studies to optimize the antigen specific antibody production, we evaluated the function of IL-10 in the IVI protocol.

## 2. MATERIALS AND METHODS

### 2.1. *In vitro* immunization

Human peripheral blood lymphocytes (PBL) were separated from healthy donors by using lymphocyte separation medium. PBLs were treated with Leu-Leu-OMe to remove the cytotoxic T cells, CD8<sup>+</sup> suppressor T cells and natural killer T cells. LLME-treated PBLs were cultured in ERDF medium containing 10% heat inactivated FBS, MDP (10 µg/ml), IL-2 (10 units/ml), IL-4 (10 ng/ml), 2-mercaptoethanol (20 µM), and mite extract (10 µg/ml). IL-10 (50 or 100 ng/ml) was simultaneously added with antigen.

### 2.2. Enzyme-linked immunosorbent assay (ELISA)

Supernatants were collected on IVI 2 days, 4 days, and 7 days and applied to ELISA. Absorbance at 405nm was measured using ELISA reader. Total antibody production and specific antibody production were detected by ELISA.

### 2.3. Cytokine expression profiles

PBLs were collected on IVI 2 days, 4 days and 7 days. CD4<sup>+</sup>, CD8<sup>+</sup> T-cell subsets and CD19<sup>+</sup> B cells were separated by using MS Separation column and MiniMACS according to manufacturer's recommendations. Two hundred ng of total RNA of each sample was used in reverse transcription. The same amount of each cDNA sample was amplified under the following condition: 94°C 30 s, 60°C or 62°C 30s and 72°C 1 min by using specific primers for GAPDH and several cytokines.

## 3. RESULTS AND DISCUSSION

PBLs isolated from healthy donors were immunized *in vitro*. IL-10 added with mite extract (10 µg/ml). The concentration of IL-10 is 0 ng/ml, 50 ng/ml or 100ng/ml respectively. Supernatants were collected on IVI 2 days, 4 days, and 7 days and applied to ELISA. As showed in Figure 1, total IgG production was enhanced by IL-10 addition. With regard to other types of immunoglobulins and antigen-specific antibodies, we obtained almost the same results. In order to further evaluate the function of IL-10 on antibody production in the IVI protocol, we separated CD4<sup>+</sup>, CD8<sup>+</sup> T cell subsets and CD19<sup>+</sup> B cells on IVI 2 days, 4 days and 7 days. We then evaluated the effects of IL-10 added simultaneously with antigen on cytokine gene expressions of those cells. As showed in Figure 2, gene expression levels for IL-2 and IFN-gamma were greatly repressed by IL-10 addition, demonstrating that IL-10 added with antigen suppressed Th1 type cytokine production both in CD4<sup>+</sup> and CD8<sup>+</sup> T cells. Furthermore, IL-10 added with antigen enhanced the gene expression

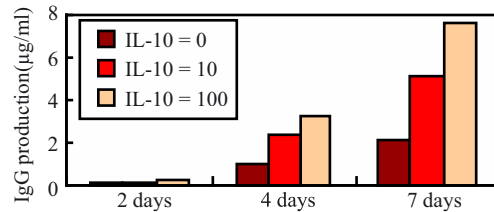


Fig. 1 The effect of IL-10 added with antigen on antibody production

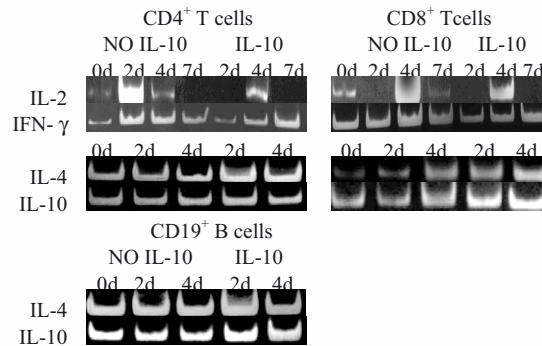


Fig. 2 The Effect of IL-10 Added With Antigen on Gene Expression of Cytokines

levels of IL-4 and IL-10 in CD4<sup>+</sup>, CD8<sup>+</sup> T-cell subsets and CD19<sup>+</sup> B cells, indicating that IL-10 addition in the IVI protocol would stimulate Th2 type responses, which led to enhancement of antibody production. Previous studies showed that IL-10 added to the LLME-treated PBL before antigen sensitization, antibody production decreased. These results suggest that IL-10 might play an important role in the activation and/or inactivation of T cells, B cells and antigen presenting cells at the antigen sensitization.

In conclusion, our study has showed that IL-10 added before the antigen sensitization targets CD8 T cells, which might lead to elicit the suppressive function of T cells. Moreover, IL-10 added at the antigen sensitization elicited Th2 type responses via suppressing IFN-gamma and augmenting IL-4 production.

#### 4. REFERENCES

1. James K & Bell GT (1987) Human monoclonal antibody production. Current status and future prospect. *J Immunol Method* 100: 5-40.
2. Ichikawa A, Katakura Y, Hashizume S & Shirahata S (1999) *In vitro* immunization of human peripheral blood lymphocytes: establishment of B cell lines secreting IgM specific for cholera toxin B subunit from lymphocytes stimulated with IL-2 and IL-4. *Cytotechnology* 31: 131-139.
3. Yamashita M, Katakura Y, Ichikawa A, Teruya K, Shirahata S (2002) *Animal Cell Technology: Basic & Applied Aspects*, Volume 12, 231-234.

K. CALLES<sup>1</sup>, E. LINDSKOG<sup>2</sup>, Å. NOSSED<sup>2</sup>, I. SVENSSON<sup>2</sup>,  
L. HÄGGSTRÖM<sup>2</sup>

## EXTRACELLULAR HISTONE H4 FROM SF9 CELLS IS ANTIMICROBIAL

<sup>1</sup>*KaroBio AB, SE-141 57 Huddinge, Sweden,* <sup>2</sup>*Department of Biotechnology,  
Royal Institute of Technology, SE-106 91 Stockholm, Sweden*

**Abstract.** *Spodoptera frugiperda* Sf9 cells produces an extracellular, truncated form of histone H4 (H4-N12). H4-N12 was suspected to have antimicrobial effects. To investigate this, conditioned medium from Sf9 cell cultures was concentrated and fractionated on a gel filtration column. The fractions containing H4-N12, were collected, pooled and the buffer exchanged (to citrate buffer). *Bacillus megaterium* was incubated in the histone H4 fraction and a drastic loss in viability could be observed already after a couple of minutes compared to a control culture in the same buffer. Incubation of *Escherichia coli* showed similar results, however with a slower decrease in viability. Further, the bacteria displayed a substantial leakage of intracellular proteins after exposure to the histone H4 fraction. Cell lysis was confirmed by microscopic investigation.

### 1. INTRODUCTION

We have identified an extracellular protein in Sf9 cell culture supernatants as a truncated form of histone H4 (H4-N12), by N-terminal sequencing.

Extracellular histones or histone-fragments are known to have antimicrobial activity (1). For example, histone 2A has been shown to be a precursor of buforin I, which is an antimicrobial peptide in the stomach of the toad *Bufo bufo gargarizans* (2).

The effects of the extracellular histone H4 on different bacteria were therefore investigated.

### 2. MATERIAL AND METHODS

Medium from a seven day Sf9 cell culture was used for histone preparation. After concentration and gel chromatography of the medium a purified fraction of Histone H4 was collected (Figure 3, lane 2). Compared to the original medium the proteins in this fraction were concentrated 27-fold.

To investigate the antimicrobial activity, 0.1 mL of either *Escherichia coli* or *Bacillus megaterium*, was mixed with 0.9 mL of the histone fraction in 10mM citrate buffer (pH 5.6) to a final OD of 0.5. As a control 0.1 mL bacterial culture was mixed with 0.9 mL of the citrate buffer. The mixtures were incubated at 37°C for *E. coli* and 30°C for *B. megaterium*. Samples for viable count, OD measurements and SDS-PAGE gel analysis were taken at different time points.

## 3. RESULTS

The addition of histone fraction to *Bacillus megaterium* cultures decreased the cell viability and optical density drastically (Figure 1 and 2). Addition of histone fraction to *E. coli* cultures showed similar results, however with a less drastic drop in viability (not shown).

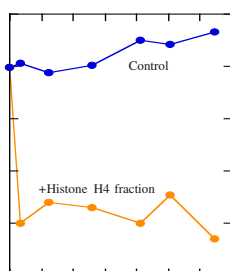


Figure 1. Survival of *B. megaterium* in buffer with or without histone fraction

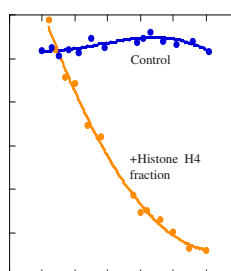


Figure 2.  $OD_{600}$  profiles of *B. megaterium* in buffer with or without histone fraction

Analysis of culture supernatant on SDS-PAGE showed that the amount of extracellular proteins had increased in the culture with histone fraction, indicating that cell lysis had occurred (Figure 3). Further, micrographs of *B. megaterium* after exposure to the histone fraction confirmed this (Figure 4). These results indicate that H4-N12 interferes with membrane permeability.

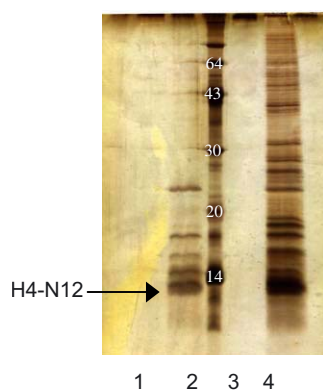


Figure 3. SDS-PAGE. Samples taken at 0 and 60 minutes from the culture supernatant of the control and of the *B. megaterium* and Histone H4 mixture. Lane 1: Control at 0 min, lane 2: Histone fraction at 0 min, lane 3: Molecular weight marker, lane 4: Control after 60 min, lane 5: *B. megaterium* and histone fraction mixture after 60 min.

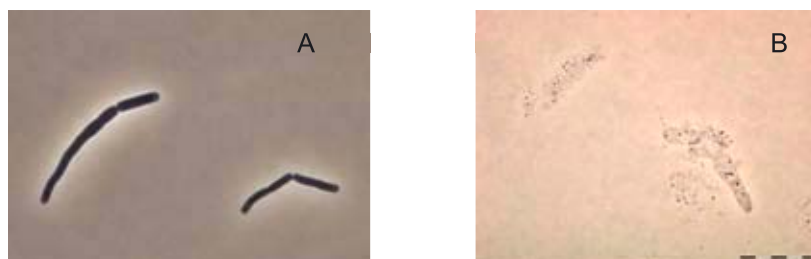


Figure 4. *Bacillus megaterium* after 25 minutes of incubation in buffer (A) and in histone fraction (B)

#### 4. DISCUSSION

The results from this study show that a histone fraction, obtained from conditioned medium of Sf9 cell cultures, displayed an antimicrobial effect. An interesting question is whether an Sf9 culture would have the ability to defeat a microbial contamination. Since the environment would be different in the culture compared to the conditions in these experiments, the bacterial response is difficult to foresee. The histone fraction used for these experiment was concentrated 27-fold compared to the original conditioned medium. Experiments with a histone fraction at the same concentration as in the culture is being carried out at present.

#### 5. ACKNOWLEDGEMENTS

This work was supported by a grant from the Swedish Centre for Bioprocess Technology, CBioPT, and by KaroBio AB.

#### 6. REFERENCES

- Hirsch, J.G., Bactericidal action of Histone, *J.Exp. Med.* 108:925-944 (1958)  
Kim, H.S., Park, C.B., Kim, M.S., Kim, S.C., cDNA cloning and characterization of Buforin I, An antimicrobial peptide: A cleavage Product of Histone H2A, *Biochem Biophys Res Commun* 229, 381-387 (1996)

F. GROSJEAN, M. JORDAN AND F. M. WURM

## ANALYZING CALCIUM PHOSPHATE TRANSFECTION OF ADHERENT CHO CELLS USING MICROSCOPIC LIVE IMAGING

*Laboratory of Cellular Biotechnology (LBTC), Institute of Chemical and Biological Process Science (ISP), Faculty of Basic Sciences, Swiss Federal Institute of Technology (EPFL), 1015 Lausanne, Switzerland. Email: Frederic.Grosjean@epfl.ch*

**Abstract.** Using a motorized Zeiss-Axiovert 200M microscope equipped with a gas- and temperature-controlled incubation chamber, we performed studies on calcium phosphate (CaPi) transient transfection of CHO-DG44 cells. Over a 24-hour period, images were captured every 10 minutes with both fluorescent and normal light. Enhanced green fluorescent protein (EGFP) was used as a reporter. The following observations were made:

1. CaPi gene transfer and subsequent recombinant protein expression is fast; within 2.5 hours after transfection the first EGFP positive cells became visible.
2. Cells with detectable EGFP expression exhibited an extended cell cycle that was 6 – 10 hours longer than that of EGFP-negative cells.
3. The first cells to express EGFP were cells that underwent mitosis 1 – 2 hours after CaPi addition. EGFP expression in both daughter cells post-mitosis occurred only for cells that underwent mitosis after the glycerol shock.
4. Cells with exceptionally high EGFP expression level remained round for unusually long periods of time.

**Keywords:** calcium phosphate, Chinese Hamster Ovary cells (CHO), Green Fluorescence Protein (GFP), live imaging, transient transfection, mitosis.

### INTRODUCTION

Live imaging microscopy is an excellent tool to study transient transfection using fluorescent proteins as markers. Cells can be monitored visually before, during and after transfection. Counting fluorescent and non-fluorescent cells gives the transfection efficiency as well as information on cell proliferation when correlated with time. Live imaging has the advantage over flow cytometry to allow morphological and time-dependent cell-by-cell analysis of the observed adherent populations. It also allows us to obtain information on the global time frames that encompass the activities between transgene transport to the nucleus and subsequent intracellular product accumulation.



## RESULTS AND DISCUSSION

In the transfected cell population the first EGFP expression became visible approximately 2.5 hours post-glycerol shock. About 90% of the EGFP positive cells either underwent mitosis or appeared to prepare for mitosis (rounding up) but did not divide. The ratio of executed and non-executed mitosis in the early EGFP-expressing cells was around 3 to 5.

The first visible EGFP-positive cells eventually developed a strong fluorescence, indicative of accumulation of a large intracellular quantity of EGFP. None of these cells underwent a second mitosis. They all became round after 7 to 15 hours post first observation of EGFP and some of them lost fluorescence after a few hours. Only cells that proceeded through mitosis post glycerol shock resulted in two EGFP-positive daughter cells (Fig. 1). None of the cells undergoing mitosis between the time of DNA addition and glycerol shock (first visible EGFP-positive cells) produced two EGFP-positive daughter cells – only one of them was positive. We assume that a non-homogeneous plasmid distribution within the cell was responsible for the asymmetry in expression.

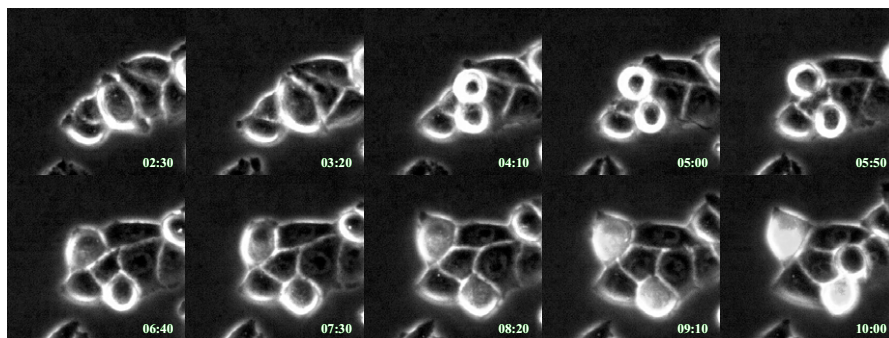


*Fig 1. EGFP-positive daughter cells appear post mitosis. ~90% of the positive cells express EGFP post-mitosis or post-aborted mitosis. The time passed since glycerol shock is indicated in hours and minutes in the lower part of each image. GFP-positive cells appear brighter than the others.*

It appears that mitosis facilitates DNA entry into the nucleus. The same may be said for the glycerol shock since it results in a 50% reduction of cell volume (own observation) and thus an increase in the intracellular plasmid concentration.

Batard et al. (2001) have recently shown that cells with a high copy number of plasmid following transfection exhibit reduced cell proliferation and decreased survival. Our studies support these results since EGFP-positive cells have an extended cell cycle compared to negative cells (Table 1). Cells with very high levels of EGFP often rounded up and detached after a few hours. The occasional loss of fluorescence in these cells may have been indicative of membrane leakage and eventual cell death as blebbing was frequently observed.

Table 1. EGFP-positive cells have a longer cell cycle compared to negative cells.

	Doubling time [hours]
EGFP-negative cells	12 - 14
EGFP-positive cells	18 - 22

EGFP-positive cells reached a maximum of about 20% of the population by 14 hours after glycerol shock (Fig. 2). Results in Figure 2a represent the number of cells counted by microscopy within a surface area of 0.34 mm<sup>2</sup>. Both EGFP-positive and negative cells increased in number over a 24-hour time frame, with the growth of EGFP-negative cells outpacing EGFP-positive cells. For this reason, the EGFP-positive subpopulation of cells fell to about 15% at 24 hours post-glycerol shock.

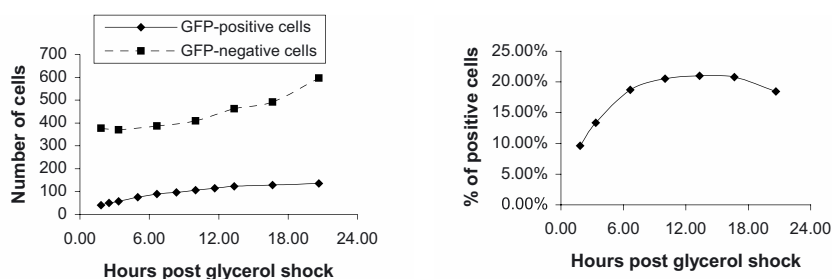


Fig 2. a: Number of EGFP-positive and negative CHO cells post-transfection. b: Percentage of EGFP-positive cells post-transfection.

We observed first visible EGFP expression in cells just 2.5 hours post-glycerol shock. For these transfections we used a shortened protocol, requiring just one hour of interaction between cells and DNA. Since maturation of GFP to its fully fluorescent state takes about one hour in mammalian cells (Tsien et al., 1998), processes for transfer to the nucleus, transcription and translation took approximately 1.5 hours.

#### ACKNOWLEDGEMENTS

Part of this work was financially supported by ZLB Bioplasma AG (Bern, Switzerland)

#### REFERENCES

- Batard P., Jordan M. and Wurm F.M., Transfer of high copy number plasmid into mammalian cells by calcium phosphate transfection. *Gene* (2001) **270**: 61-68.  
 Tisen R. Y., The green fluorescent protein. *Annu. Rev. Biochem.* (1998) **67**:509-544.

R.HAAS, S.REID, AND L.K.NIELSEN

## EFFECTS OF MULTIPLICITY OF INFECTION (MOI) AND CELL CYCLE ON BACULOVIRUS INFECTION KINETICS

*Division of Chemical Engineering, The University of Queensland, Brisbane,  
Qld 4072, Australia ; e-mail: RicharH@cheque.uq.edu.au*

**Abstract.** Synchronously infected cells show a large spread in the timing of cell death. This asynchrony is caused neither by the number of viruses a cell receives nor by the cell cycle status of the cell at the time of infection. However, the cell cycle status at the time of infection influences the productivity and budding rate.

### 1. INTRODUCTION

Baculoviruses are increasingly used as an expression vector system and as a bio-pesticide. A thorough understanding of the *in-vitro* kinetics of virus infection helps to design and scale up processes that involve recombinant or wild-type baculovirus infections.

Up to an optimal peak cell density (OPCD) – usually 30 to 40% of maximal peak cell density – the yield increases with cell density; thereafter the volumetric yield drops sharply (Wong *et al.* 1996). Due to this reason, cell densities are kept around or below the OPCD in most processes.

All available infection kinetics models are based on the assumption that the infection is entirely controlled by the virus and thus determined right at the start of the infection. Infected cells proceed through a certain sequence of events such as virus genome reproduction, viral protein expression, and finally cell lysis.

The simpler models are based on the assumption that all infected cells proceed with the same pace and intensity through these different stages (Nielsen 2000). However, this assumption is inconsistent with the observed behaviour as cell lysis occurs anywhere between 40 and 80 hours post infection (hpi) (Figure 1c).

More complex models are based on the assumption that the timing and intensity of these events depend on the number of viruses each individual cell receives (Licari and Bailey 1992; Hu and Bentley 2000), which provides a possible explanation for the spread in the timing of cell death.

Other explanations could be the cell cycle state of the infected cell at the time of infection or various unspecified events that occur within a cell.

This study investigates whether the number of infectious viruses and/or the cell cycle state at the time of infection causes the observed asynchrony of baculovirus infection kinetics.

## 2. RESULTS AND DISCUSSION

## 2.2. Multiplicity of Infection (MOI)

If a cell culture is infected with more than 3 active viruses (or plaque forming units – PFU) per cell, all cells become infected within a short time-frame; this constitutes a synchronous infection. If a culture is infected with an MOI of 15 PFU/cell, it can be assumed that <1% of all cells will receive less than 6 PFU/cell and <1% of all cells will receive more than 25 PFU/cell.

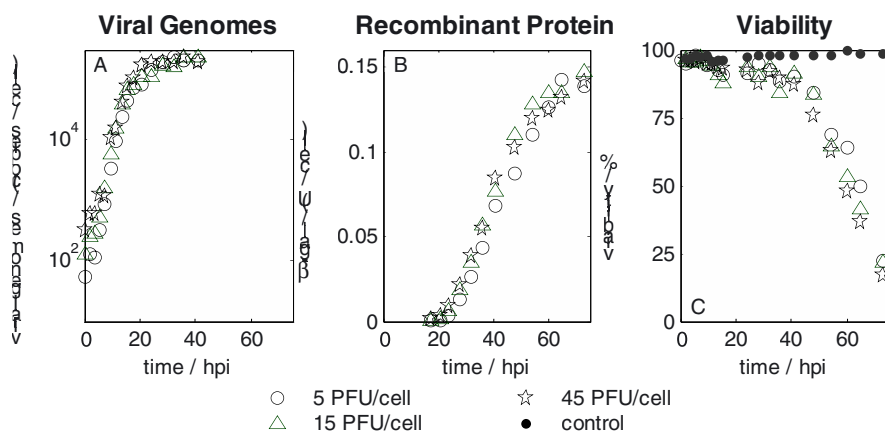


Figure 1. Infection using different MOIs.

Three Sf9 insect cell cultures at a cell density of  $1.4 \times 10^6$  cells/ml (30% of the OPCD) were infected at an MOI of 5, 15, and 45 PFU/cell. The infection kinetics of these cultures were identical in viral genome replication (determined by real time PCR), recombinant protein ( $\beta$ -galactosidase) production, and viability (Figure 1). Further they were also identical in cell volume increase and viral budding rate (data not shown).

Therefore, the assumption that the timing and intensity of these events depend on the number of viruses each individual cell receives can be dismissed for synchronous baculovirus infection at a cell density below or at the OPCD.

## 2.2. Cell Cycle

Immediate early genes of the baculovirus influence the cell cycle of the host cell (Prihod'ko and Miller 1998). Hence, it seems likely that the cell cycle phase at the time of infection has an influence on the infection kinetics.

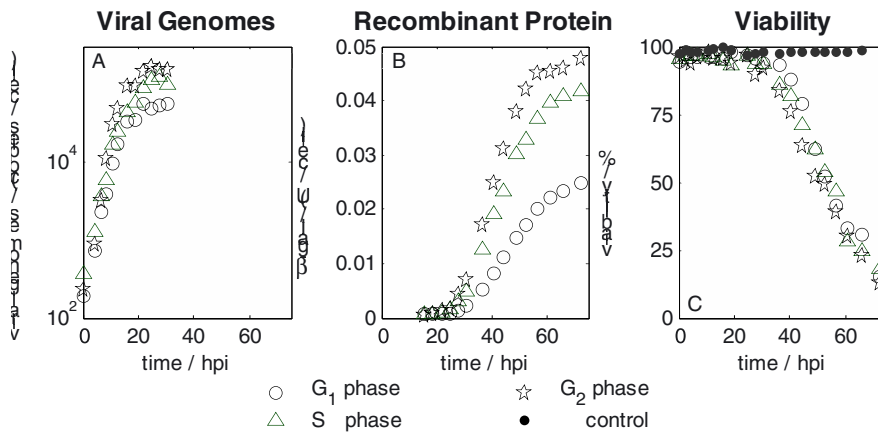


Figure 2. Infection of cells at different cell cycle phases.

Cells at a cell density of  $1.8 \cdot 10^6$  cells/ml (35% of the OPCD) were separated according to their sizes (or cell cycle phase) by means of centrifugal elutriation. Subsequently, the cells were infected at an MOI of  $\sim 30$  PFU/cell to ensure synchronous infection.

No difference in the timing of cell death was observed between cells infected at different cell cycle phases (Figure 2c). Hence, the cell cycle phase does not cause the observed asynchrony in the timing of cell death.

An increased viral genome replication, recombinant protein production (Figure 2A & B), and viral budding rate (data not shown) were observed with a later positioning in the cell cycle at the time of infection. This is the first time that this cell cycle dependent asynchrony in synchronously infected culture has been observed. We speculate that this effect is caused by an increased protein production system of cells at a later stage of the cell cycle phase rather than the genetic cell cycle status itself.

### 3. REFERENCES

- Hu, Y. C. and W. E. Bentley (2000), *Chemical Engineering Science* **55** (19): 3991-4008.  
 Licari, P. and J. Bailey (1992), *Biotechnology and Bioengineering* **39** (4): 432-441.  
 Nielsen, L. K. (2000), *The Encyclopedia of Cell Technology*. R. E. Spier, John Wiley & Sons NY: 1217-1230.  
 Prikhod'ko, E. A. and L. K. Miller (1998), *Journal of Virology* **72** (1): 684-92.  
 Wong, K. T. K., C. Peter, et al. (1996), *Biotechnology and Bioengineering* **49** (6): 659-666.

KAI IDING, HEINO BÜNTEMEYER AND JÜRGEN LEHMANN

NON-FREEZING PRESERVATION AND SUBSEQUENT  
RECOVERY OF HEPATOCYTES UNDER PO<sub>2</sub>- AND  
PH-CONTROLLED CONDITIONS FOR CONTINUOUS  
SUPPLY OF CELLS FOR BIOARTIFICIAL LIVER  
SUPPORT

*Institute of Cell Culture Technology, University of Bielefeld, 33594  
Bielefeld, Germany, kid@zellkult.techfak.uni-bielefeld.de*

1. INTRODUCTION

Bioartificial liver support using immobilized hepatocytes in a hollow fiber bioreactor is the most encouraging approach to overcome the increasing problem of donor organ shortage in liver transplantation surgery. One of the main challenges is the continuous supply of hepatocytes at any time a medical application is needed. The coordination of hepatocyte propagation and their medical application without any intermediate step is a complicated venture and hardly practicable since any application of the bioartificial liver system is unpredictable. Therefore, after cultivation the cells have to be maintained under conditions which enables storage over a certain period of time and subsequently facilitates a rapid recovery of the hepatocytes. Cryopreservation is a well established method in cell culture technology. Investigations with primary hepatocytes of several species including man provided maintenance at 90% viability (1). However, cell recovery is decreased – values as low as 22% of the initial cell amount have been reported (2). Furthermore, cryopreservation requires the addition of potentially toxic compounds like dimethyl sulfoxide. These compounds have to be removed from the hepatocyte culture prior to medical application. This is unreliable, costly and time-consuming. Methods which avoid harmful cryoprotective additives are preferable. Such a method can be the storage at temperatures slightly above the freezing point. Hence, we investigated the preservation potential of an enriched standard cultivation medium at 4°C and physiological pH with a special focus on the impact of controlled oxygen concentrations during the chilling procedure and the subsequent hypothermic storage on cell survival and recovery in a pO<sub>2</sub>- and pH-controlled 1-L bioreactor.

## 2. MATERIALS AND METHODS

Two immortalized murine hepatocyte cell lines (HepT and K105) and the human hepatoma cell line C3A were used. The murine lines were propagated by microcarrier cultivation (CultiSpher® G, Percell, Astorp, Sweden); C3A was expanded by spheroid cultivation. The hepatocytes were cultivated and subsequently preserved in a pO<sub>2</sub>- and pH-controlled 1-L-bioreactor. The main feature of the bioreactor itself is a membrane stirrer with 2 m of a polypropylene hollow fiber membrane tubing for bubble free aeration. Temperature was adjusted by a cooling and heating circulator bath. Hypothermic preservation was performed according to table 1.

Table 1. Oxygen concentration (O<sub>2</sub>) of the different preservation modes during chilling and subsequent preservation of the hepatocyte cell lines in the pO<sub>2</sub>- and pH-controlled bioreactor system. The pH was each perpetuated at its physiological value (pH 7.2). AHP = anoxic hypothermic preservation, NHP = normoxic hypothermic preservation, HHP = hyperoxic hypothermic preservation, MAHP = modified anoxic hypothermic preservation

Mode	Chilling (37°C → 4°C)	→	reser ation (at 4°C)
AHP	O <sub>2</sub> = 0.00 mg L <sup>-1</sup>	→	O <sub>2</sub> = 0.00 mg L <sup>-1</sup>
NHP	O <sub>2</sub> = 2.75 mg L <sup>-1</sup>	→	O <sub>2</sub> = 2.75 mg L <sup>-1</sup>
HHP	O <sub>2</sub> = 8.76 mg L <sup>-1</sup>	→	O <sub>2</sub> = 8.76 mg L <sup>-1</sup>
MAHP	O <sub>2</sub> = 8.76 mg L <sup>-1</sup>	→	O <sub>2</sub> = 0.00 mg L <sup>-1</sup>

Cell densities were estimated automatically by the CEDEX system (Innovatis, Bielefeld, Germany) based on the trypan blue exclusion method. Glucose and lactate were determined with an automatic analyzer system based on enzymatic and electrochemical reactions (YSI 2700, Yellow Springs Instruments, Yellow Springs, OH, USA). The free amino acids in the culture supernatants were analysed with an automated reversed phase high performance liquid chromatography system (RP-HPLC) with precolumn derivatization using the *o*-phthaldialdehyde method. Ammonia detection was performed by using a spectrofluorimetric method based upon *o*-phthaldialdehyde (OPA) derivatisation.

## 3. RESULTS

The maintenance of cell viability was depending both on the type of preservation procedure and the hepatocyte cell line. Independent from conditions during chilling and hypothermic preservation, the human hepatoma cell line C3A died rapidly within approximately 24 hours (fig. 1). Comparable results were achieved with K105, except under modified anoxic conditions (MAHP). In this case the decrease of the viable cell number could be reduced to a rate of 25.8 ± 4.8% per day (fig. 1).

Figure 1. Cell loss of HepT, C3A and K105 during hypothermic preservation in the 1-L bioreactor in relation to the preservation mode. AHP: anoxic hypothermic preservation; NHP: normoxic hypothermic preservation; HHP: hyperoxic hypothermic preservation; a) cell loss within the first 48 hours of preservation, b) cell loss during preservation beyond 48 hours; MAHP: modified anoxic hypothermic preservation.

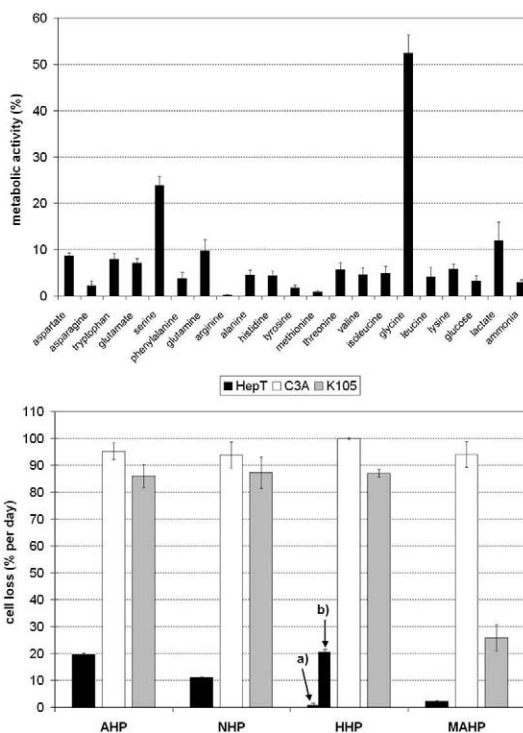
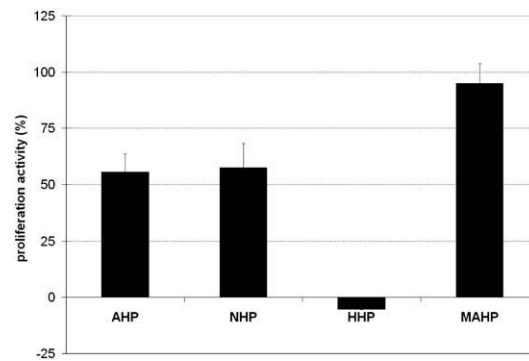


Figure 2. Residual metabolic activity (percentage) of Hep T during modified anoxic hypothermic preservation (MAHP) in the 1-L bioreactor in relation to the metabolic activity of HepT during cultivation under physiological conditions.

The most robust hepatocyte cell line under hypothermic conditions was HepT. Remarkably, cell viability of HepT was stable within the first 48 hours of hypothermic storage under hyperoxic conditions (HHP) but decreased subsequently with a rate of  $20.1 \pm 0.5\%$  per day. Modified anoxic conditions (MAHP) emerged as the best way to preserve HepT hypothermically over several days. In this case the decrease of the number of viable cells could be limited to a rate of  $2.3 \pm 0.3\%$  per day (fig. 1). The metabolic activity of HepT under modified anoxic hypothermic conditions (MAHP) was reduced to a minimum in relation to the normal metabolic activity under physiological conditions (fig.2). Cell recovery correlated inversely with cell impairment during hypothermic preservation (fig 3). Preservation of HepT under modified anoxic hypothermic conditions (MAHP) for up to 9.5 days, resulting in a comparative moderate loss of viable cells, facilitated a rapid subsequent recovery. Hypothermic, non-freezing storage under defined  $pO_2$  and pH conditions is an alternative to cryopreservation for a comparatively short period of time. Rapid recovery of the hepatocytes can be obtained. Nevertheless, the ideal conditions for a successful preservation have to be estimated discretely for each hepatocyte cell line.



Figure 3. Proliferation activity (percentage) of HepT during normothermic recovery proportional to proliferation activity under physiological conditions in relation to the preceded hypothermic preservation mode in the 1-L bioreactor.



#### REFERENCES

- (1) Guillouzo A., Riolland L., Fautrel A., Guyomard C. Survival and function of isolated hepatocytes after cryopreservation. *Chemico-Biological Interactions* 121, 7-16 (1999).
- (2) Utesch D., Diener B., Molitor E., Oesch F., Platt K.L. Characterization of cryopreserved rat liver parenchymal cells by metabolism of diagnostic substrates and activities of related enzymes. *Biochemical Pharmacology* 44, 309-315 (1992).

NICOLE KESSLER, GHISLAINE ROCHE, AUDREY VERNET,  
ALEXANDRA ERNY AND CHRISTOPHE ABISMIL

SELECTION OF MDCK SUBCLONES WITH VARIOUS  
GENOTYPIC AND PHENOTYPIC MARKERS:  
SENSITIVITY TO INFLUENZA VIRUS INFECTION

*Laboratoire de Virologie, Université Claude Bernard Lyon1, 8 avenue  
Rockefeller, 69373 Lyon cedex 08, France*

**Abstract.** The epithelial MDCK cell line which is considered as an alternative system for influenza virus vaccine production is known to consist of different cell subtypes. We showed previously that phenotypic and genotypic characteristics of cells were profoundly modified with cell culture conditions, i.e., culture medium and passage number (KESSLER et al.; 2001). Questions arose as to 1) whether changes occur as a consequence of cell subtype selection or result from cell de-differentiation and 2) whether these changes are capable to influence MDCK cell responsiveness to influenza virus infection. In order to bring some piece of information to these questions, we cloned MDCK cells cultivated in serum-supplemented medium or adapted to serum-free Ultra-MDCK medium (BioWHITTAKER). Several sub-clones were selected under each culture conditions on the basis of morphological characteristics and were then studied in terms of karyotype and phenotypic markers (PNA binding, TEER). In addition susceptibility to influenza virus infection was analyzed by using a pannel of fourteen A/H3N2 strains ranging from A/Hong Kong/1/68 virus to A/Sydney/5/97 virus

**Key words:** MDCK, Trans-epithelial electrical resistance (TEER), peanut lectin (PNA), carbonic anhydrase (CA), influenza virus.

## 1. MATERIALS AND METHODS

For cloning, MDCK cells grown in either FCS-supplemented EMEM or serum-free Ultra-MDCK medium (BioWhittaker/Cambrex) were seeded in 96 well plates, at limiting dilution (1 cell / well) in the same medium and medium changes were performed twice a week. After subsequent trypsinization, cells were controlled for PNA binding and CA activity. Clones of interest were selected and cells were frozen 6-8 passages post cloning. PNA (Peanut lectin) binding was controlled using a biotinylated PNA (Vector and an HRP-avidin (Zymed) Trans-epithelial electrical resistance (TEER) was measured across cell monolayers grown on permeable supports (T-Clear inserts, Costar) using the Millicell ERS system (Millipore). Karyotype analysis was performed using a modification of the GTG banding procedure described by Seabright (1971).

Fourteen A/H3N2 influenza strains isolated from 1968 to 1999 were selected and used after three passages in MDCK cells adapted to Ultra-MDCK medium. All infections of MDCK clone cells were performed at a  $10^{-5}$  m.o.i. Susceptibility of clones to influenza infection was tested in terms of infectious particle productivity on wild-type MDCK cells, hemagglutination activity using using hen red blood

cells, neuraminidase activity on fetuin substrate (Aymard-Henry et al, 1973) and immunofluorescence with anti nucleoprotein monoclonal antibody and polyspecific polyclonal anti-serum.

## 2. RESULTS AND DISCUSSION

### 2.1. Analysis of MDCK clones

Six clones derived from Ultra-MDCK medium-adapted cells at p62 FBS-EMEM, p9 Ultra-MDCK (**2E2**, **2B11**, **2G10**, **1H8**) or p72FBS-EMEM, p155 Ultra-MDCK (**B11** **A8**) and six clones derived from FBS- EMEM grown cells at p89 (AD8, BF12, AG1, BD7, BF5, BH2) were selected for subsequent analysis. Table1 summarized the results obtained when analyzing the karyotype, PNA binding and TEER of SFM grown and FBS grown clones which were used twelve passages and ten passages post cloning respectively.

Table1. Phenotypic and genotypic characteristics of clones

	PNA			No	TEER		
	+++	++/+	±/-		Low <500Ω.cm <sup>2</sup>	Medium <4000Ω.cm <sup>2</sup>	High 5000Ω.cm <sup>2</sup>
78-81 chr	<u>AD8</u> <u>BF12</u>	<b>2G10</b> <b>B11</b> <b>2E2</b>	<b>A8</b> <u>AG1</u> <u>BD7</u> <u>BF5</u> <u>BH2</u>	<u>BF5</u> <u>BH2</u>	<u>AD8</u>	<b>A8-</b> <b>2G10</b> <b>B11</b>	<u>AG1</u> <u>BD7</u> <b>2E2</b> <u>BF12</u>
>84 chr.	<b>2B11</b>		<b>1H8</b>				<b>2B11</b> <b>1H8</b>
No TEER			<u>BF5</u> <u>BH2</u>	<b>A</b>	<b>B</b>	<b>C</b>	
Low TEER	<u>AD8</u>						
		<b>2G10</b> <b>B11</b>	<b>A8</b>				
High TEER	<u>BF12</u> <b>2B11</b>	<b>2E2</b>	<u>AG1</u> <u>BD7</u> <b>1H8</b>				

Figure1. PNA binding  
A- +++, B-++/+, C-±/-

Ultra-MDCK grown clones (in bold in Tables) were shown to belong to two different genotypes as a function of their low (78-81 chromosomes) or high (>84 chromosomes) modal number while all six FBS-grown clones (underlined in Tables)

exhibited a unique low modal number. Seven different phenotypes resulted from the different combinations between PNA binding (Figure1) and TEER activity of clones; five of them were associated with the low modal number genotype exclusively while the two others were found associated with both low and high modal number genotype (Table2). Two clones, 1H8 and AD8, exhibited both genotypic and phenotypic profiles similar to those of C7 and C11 clones which were previously described by Gekle et al (1994) and Wunsch et al (1995) as representative of Principal cells and Intercalated cells respectively. The isolation of seven additional phenotype/genotype clone profiles demonstrated without ambiguity the extraordinary plasticity of MDCK cells which were shown capable to completely modify their phenotype and/or genotype with culture conditions.

Table2. MDCK cell phenotypic/genotypic profiles

	No/Low PNA			Medium PNA		High PNA	
	TEER=0	Medium TEER	High TEER	Medium TEER	High TEER	Low TEER	High TEER
Low chr.	<u>BF5</u> <u>BH2</u>	<b>A8</b>	<u>AG1</u> <u>BD7</u>	<b>2G10</b> <b>B11</b>	<b>2E2</b>	AD8	<u>BF12</u>
High chr.			<b>1H8</b>				<b>2B11</b>

## 2.2. Susceptibility of MDCK clones to influenza virus infection

Cells from 1H8, 2B11, 2G10 and 2E2 clones were tested for their comparative susceptibility to infection with A/H3N2 influenza strains. Results showed: 1- a difference in susceptibility of clones to A/H3N2 infection, with a frequently highest sensitivity of 2E2 cells. The difference observed with each virus, between the highest and lowest values of infectious titre as a function of clones allowed ranging viruses in three groups (Table3). 2- For each virus/MDCK clone pair, a differential sensitivity was observed when considering the different antigens : hemagglutinin, neuraminidase and infectious particles. 3- Using immunofluorescence test, differences were shown as a function of clones in the kinetic of synthesis of viral antigens.

Table 3. Grouping of A/H3N2 viruses with clone differences in sensitivity

Difference between highest/lowest log TCID50 values with clones	A/H3N2 strains
<0.5 log	A/Vic/3/75- A/Shang/16/89- A/Beij/32/92
0.5 <log<1	A/Bgk/1/79- A/Sich/2/87- A/Guiz/54/89
>1 log	A/HK/1/68- A/Miss/1/85- A/Beij/353/89 A/Shangd/9/93- A/Johan/33/94- A/Nanch/933/95- A/Syd/5/97- A/Pan/2007/97

## 3- REFERENCES

- Gekle M, Wunsch S, Oberleithner H, Silbernagl S. Characterization of two MDCK-cell subtypes as a model system to study Principal and Intercalated cell properties. *Eur. J. Physiol* (1994) 428, 157-162
- Wunsch S, Gekle M, Kersting U, Schuricht B, Oberleithner H. Phenotypically and karyotypically distinct Madin-Darby canine kidney cell clones respond differently to alkaline stress. *J Cell Physiol* (1995) 164, 164-171.
- Kessler N, Roche G. The influence of culture conditions on the development of trans-epithelial electrical resistance and the junctional complex of MDCK cells. In E Lindner-Olsson et al (eds). *Animal Cell Technology: from Target to Market*, Kluwer Academic. Publishers, (2001) 244-246

J. MOLLS, F. VERHOEYE, C. PEETERS-JORIS, S.N. AGATHOS  
AND Y.-J. SCHNEIDER.

## EXTRACELLULAR METALLOPROTEASES AND THEIR INHIBITORS EXPRESSED BY THE IFN- $\gamma$ PRODUCING CHO-320 CELL LINE.

*Cellular Bioengineering group. Institut des Sciences de la Vie & Université  
Catholique de Louvain, 1348 Louvain la Neuve, Belgium.*

### 1. INTRODUCTION

Chinese Hamster Ovary (CHO) cells are among the most widespread expression system for production of proteins requiring post-translational modifications for their biological activity. Serum- and animal protein-free cultivation increases biosafety and facilitates purification procedures, but it raises the problem of recombinant product proteolysis due to loss of several inhibitors present in serum. Here we report nutritive medium dependent and independent expression of matrix metalloproteases (MMP) and natural inhibitors by the IFN- $\gamma$  producing CHO-320 cell line.

### 2. MATERIALS AND METHODS

CHO-320 cell line, a gift from Dr. A. Marc (Nancy, France), was cultivated in suspension in BDM [1] supplemented with ITS (1%, v/v), pluronic F-68 (0.1%, w/v) and rice protein hydrolysates from either Quest (Maarsen, The Netherlands) (Q-CBDM) or CWBI (Liège, Belgium) (C-CBDM). Zymographies were performed under non-reducing conditions in a SDS-PAGE gel enclosing gelatin (0.5%, w/v) as substrate. Proteases were visualized as clear bands on a dark background. Reverse zymographies were performed similarly but with 10 times concentrated conditioned media and exogenous active MMP added during incubation to allow the visualization of inhibitors as dark bands. Western-blotting were performed with polyclonal antibodies raised to human IFN- $\gamma$  (Endogen, Woburn, USA), mouse MMP-14 or mouse TIMP-2 (Santa Cruz Biotechnology, Santa Cruz, USA).

### 3. RESULTS AND DISCUSSION

We have previously identified a secreted MMP, as proMMP-9, in the culture medium of CHO-320 cells. This MMP is continuously expressed with limited

activation occurring along the death phase [2]. We now describe MMP-14, another member of the MMP family, but detected at the outer side of the plasma membrane. Fig. 1 shows that MMP-14 is expressed under three different molecular forms: proMMP-14, active MMP-14 and an inactive degradation product. The type of rice peptones added to the nutritive medium did not affect the expression at the transcriptional level, since MMP-14 mRNA levels are not different when CHO-320 cells were cultivated in either Q-CBDM (panel b, lane 1) or C-CBDM (panel b, lane 2). At a post-translational level, the proteic activity decreased during cultivation in C-CBDM (panel b, lane 2).

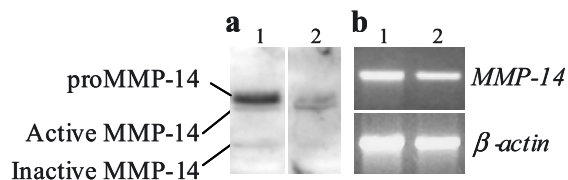


**Figure 1: MMP-14 expression.** CHO-320 cells cultivated for 4 days in Q- (1) or C-CBDM (2). 50  $\mu$ g of whole cell lysates were analysed by western-blotting detecting MMP-14 (panel a). mRNA from the same cells were isolated, reverse transcribed and amplified by PCR using primers of  $\beta$ -actin and MMP-14 cDNA (panel b).

We also found that natural inhibitors of the tissue inhibitors of metalloproteases (TIMPs) are secreted by the CHO-320 cells to counteract proteases expression.

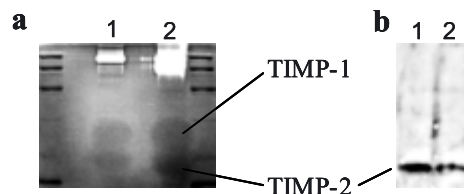


**Figure 2: TIMPs expression.** CHO-320 cells were cultivated for 4 days in either Q-(1) or C-CBDM (2). Media were then concentrated 10x and analysed by gelatin reverse zymography (panel a) or western-blotting with polyclonal antibodies raised against TIMP-2 (panel b).

Gelatin reverse zymography and western-blotting (fig. 2) revealed that two members of the TIMPs family are expressed in the conditioned media. In fact, TIMP-1 is the only member of the family displaying glycosylation and has an apparent MW of 28 kDa. TIMP-2 that is not glycosylated, has been identified by western-blotting at 22 kDa. The expression of these proteins was unaffected by the cultivation in either Q- (1) or C-CBDM (2). Interestingly, TIMP-1 is the natural inhibitor of MMP-9 and TIMP-2 is implicated in MMP-14 inhibition. This strongly suggests a coordinated expression of proMMP-9/TIMP-1 and (pro)MMP-14/TIMP-2 in CHO-320 cells.

When CHO-320 cells were cultivated in C-CBDM (fig. 3, upper panel), a 70 kDa MMP appeared in the conditioned medium which is immunologically distinct from (pro)MMP-9 and still under characterisation by mass spectrometry. In the same culture conditions, western-blotting analysis of recombinant IFN- $\gamma$  (fig. 3, lower panel) revealed proteolysis as bands of lower molecular weight than the non-glycosylated (0N) protein appeared after 4 days of cultivation.

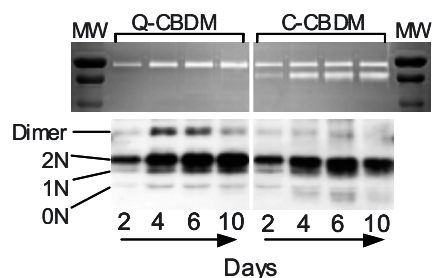


*Figure 3: Medium dependant expression and proteolysis. Conditioned media of CHO-320 cells cultivated in Q-CBDM (left part) or C-CBDM (right part) were subjected to gelatin zymography (upper panel) or western-blotting (lower panel) with polyclonal antibodies raised against human IFN- $\gamma$ . 0N, 1N and 2N are respectively the non-, mono- and bi-glycosylated forms of the recombinant IFN- $\gamma$  monomer.*

Experiments are in progress to further characterise proteases and their inhibitors in CHO-320 cells as well as the different effects of plant peptones on these pathways.

#### 4. CONCLUSIONS

Expression of proteases and IFN- $\gamma$  proteolysis are tightly depending on the culture conditions. MMP-14 expression is lower in C-CBDM than in Q-CBDM while the 70 kDa metalloprotease only appeared in C-CBDM conditioned media. We showed also that IFN- $\gamma$  undergoes proteolysis when the 70 kDa metalloprotease was expressed.

#### 5. REFERENCES

- 1 Schneider, Y.-J. (1989) *J. Immunol. Methods* **116**, 65-77.
- 2 Mols, J., Burteau, C., Verhoeve, F., Peeters-Joris, C., Bastin, G., Agathos, S. N. and Schneider, Y.-J. (2001) in *Animal cell technology : from target to market* (Lindner-Olsson, E., Chatzissavidou, N. and Lüllau, E., eds.), pp. 227-229, Kluwer Academic publishers, Dordrecht

#### 6. ACKNOWLEDGMENTS

J.Mols received a grant from the belgian FRIA and this work was supported by the Walloon Region.



MORTEN PRÆSTEGAARD, SØREN JENSBY NIELSEN, BETINA  
KERSTIN LUNDHOLT, IVAN MIKKELSEN, STEVEN LOECHEL,  
MORTEN HEIDE, VIGGO LINDE

## NOVEL SMALL-MOLECULE AKT1 INHIBITORS DISCOVERED BY REDISTRIBUTION™-BASED HIGH- THROUGHPUT SCREENING

*BioImage A/S, Copenhagen, Denmark, www.bioimage.com*

### 1. INTRODUCTION

#### *1.1 Redistribution™*

Redistribution™ is a novel approach for discovering drugs that specifically modulate the function of intracellular signalling proteins by modulating their translocation behaviour without affecting their inherent catalytic activity. Intracellular translocation of selected targets labelled with a proprietary Green Fluorescent Protein (GFP) is quantified in living cells in high throughput. Redistribution™ allows identification of drug candidates aimed at targets which previously have proven difficult to modulate with high selectivity.

#### *1.2 Akt1 as a target for translocation modulating drugs*

The PI3-Kinase pathway regulates multiple cellular responses such as cell proliferation, growth and survival. One of the main effectors of PI3-K is the kinase Akt/PKB. Akt activity is frequently elevated in primary carcinomas most frequently due to PTEN gene loss. Akt activation provides growth factor-mediated cell survival by phosphorylating and inactivating Bad, Caspase 9, and Forkhead transcription factors, all of which can induce apoptosis. A drug that inhibits translocation of Akt to the plasma membrane is predicted to specifically decrease Akt activity

### 2. RESULTS

#### *2.1 Akt1 Redistribution™ assay*

Activation of growth factor receptors induces PI3-K dependent formation of PIP3 at the plasma membrane. The PH domain of Akt has high affinity for PIP3, and mediates transient translocation of Akt from the cytoplasm to the plasma membrane

following growth factor stimulation. We have developed a cell-based assay to screen for drug candidates that selectively inhibit Akt1 translocation using insulin signalling as our model system.

A CHO cell line stably expressing the human insulin receptor and GFP-tagged Akt1 is utilized in an antagonist-type assay. Akt1 translocation to the plasma membrane is initially stimulated by insulin. Subsequently, cells are treated with compounds that potentially reverse the insulin-induced translocation using the PI3-Kinase inhibitor wortmannin as a reference compound. The redistribution of Akt1-GFP is measured as a change in fluorescence intensity over time using a FLIPR (figure 1a).

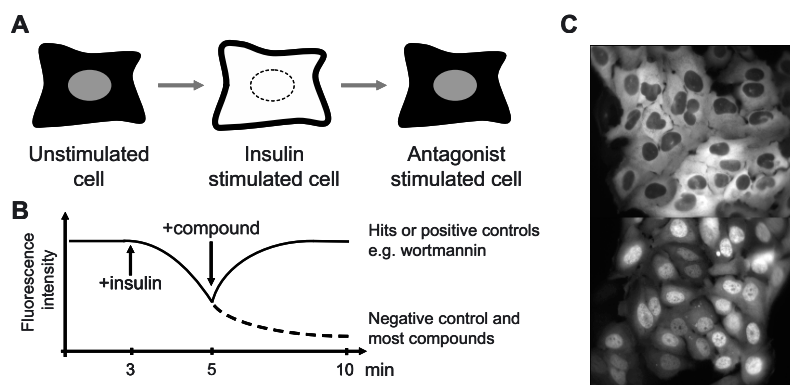


Figure 1. A) Schematic presentation of Akt1-GFP translocation in our Redistribution<sup>TM</sup> assay. B) Schematic diagram showing the FLIPR trace throughout the experiment. C) Representative images of FKHR-GFP-expressing U2OS cells with (top) and without (bottom) stimulation with 10  $\mu$ M LY294002

## 2.2 High Throughput Screening and Secondary Characterisation of Hits

We have screened a library of 65000 compounds in our Akt1 Redistribution<sup>TM</sup> assay. The potency to inhibit translocation expressed as percent activity was determined for all compounds by normalising to wortmannin treated cells. The average Z'-factor of the screen was 0.59. The screen yielded 130 hits that were confirmed in retest.

To further characterise our hit compounds, we developed a set of secondary assays. One such assay, measures the induction of nuclear translocation of FKHR-GFP. FKHR (forkhead) is a direct Akt target and is retained in the cytoplasm during periods of high Akt activity. Therefore, Akt pathway inhibitors are expected to lead to accumulation of FKHR in the nucleus. Nuclear accumulation of FKHR is thus a good downstream readout of Akt pathway inhibition (figure 1c, table 2).

Our second characterisation assay measures translocation of Btk-GFP from the cytoplasm to the plasma membrane. Like Akt, Btk contains a PH domain and translocates to the plasma membrane in response to the same stimuli as Akt. This

assay therefore allows us to discriminate between compounds that affect Akt directly *and* specifically, and those that act either upstream of Akt or antagonise PH domains non-specifically (table 2).

Furthermore, we have tested hit compounds for their inhibitory activity in a set of kinase assays, including Akt1 itself, PI3-Kinase, and the Insulin receptor tyrosine kinase (InsR-TK). Finally, selected hit compounds have been assayed for specific growth inhibitory effects in a panel of human tumour cell lines that are either dependent or independent of PI3-Kinase/Akt pathway activity (table 2).

To illustrate the type of hit compounds that result from a pathway-type screen such as ours, partial data for two different compounds is shown below. Table 2 outlines the activity profiles of the two compounds in the Akt1 screening assay and secondary assays.

Compound A is conceivably a PI3-kinase inhibitor like the reference compound wortmannin. Compound B has no inhibitory effect on upstream selectivity assays. Therefore compound B most likely works at the level of Akt although this remains to be formally proven in binding assays. Both compounds show selectivity in the tumour cell line proliferation assays, indicating that inhibitors at multiple levels in the PI3-kinase pathway are candidates for anti-cancer drugs (table 1).

Table 1. Mean IC<sub>70</sub> of compounds A and B in 4 day cell proliferation assays

Cell line	Origin	PI3-K pathway dependency	Cmpd A IC70 ( $\mu$ M)	Cmpd B IC70 ( $\mu$ M).
OVCAR-3	ovarian	dependent	9.7	1.3
SKOV-3	ovarian	independent	55.0	6.4
MDA-MB-468	breast	dependent	6.3	0.4
MDA-MB-231	breast	independent	35.6	5.0

Table 2. Assay summary for two compound examples

Assay	Assay Level	Cmpd A	Cmpd B
Akt1 translocation	screening	inhibition	inhibition
FKHR translocation	functional, downstream	translocation	translocation
Btk-PH translocation	selectivity, upstream	inhibition	none
Akt1 kinase assay	characterisation	none	none
InsR-TK kinase assay	selectivity, upstream	none	none
PI3-K kinase assay	selectivity, upstream	inhibition	inhibition
Cell Proliferation	functional, downstream	selectivity	selectivity
Likely activity		PI3K inh.	Akt1 inh.

### 3. CONCLUSION

We conclude that the Redistribution<sup>TM</sup> approach is a valid strategy for discovering novel drug candidates that specifically and efficiently targets the dynamics of important signalling pathways, here exemplified by an Akt1 translocation inhibitor.

F. SIDLER<sup>A</sup>, T. WERMELINGER<sup>A</sup>, L. RIST<sup>B</sup>, A. HENSEL<sup>A</sup>,  
A. VIVIANI<sup>A</sup>

## INFLUENCE OF MISTLETOE EXTRACTS AND ITS COMPONENTS ON IN VITRO PHYSIOLOGY OF CANCER CELLS

*a: HSW, Hochschule Wädenswil, Grüntal, CH-8820 Wädenswil, Switzerland*

*b: Paracelsus-Spital, Bergstrasse 16, CH-8805 Richterswil, Switzerland*

**Abstract.** The effect of various mistletoe preparations on cancer cells are well known [1]. We compared the induced cytotoxicity of ash and apple mistletoe extracts with common cytostatics such as Cisplatin, Paclitaxel and Doxorubicin. The effectiveness of these cancer therapeutics were depending on the concentration of the active agent, the cancer cell line and the presence of fetal calf serum (FCS) or mistletoe polysaccharides in the culture medium.

### 1. INTRODUCTION

The actual cancer therapy with mistletoe preparations is based on the tumor progression and the physical and mental health of the patient in general. The mistletoe therapy was established in 1922 by Rudolf Steiner and Ita Wegmann and is the most common in Germany today [3]. Mistletoe extracts contain a multitude of substances that have immunostimulatory and cytotoxic or anti-tumorigenic and antimetastatic effects, including viscotoxins and lectins (ML-I, ML-II, ML-III, VisalbcBA).

The mistletoes for the preparations derive from different trees. The final mistletoe extract is available as freshly pressed or fermented juice depending on the specific production process of the manufacturer. These different treatments result in a wide range of products.

The variety of the mistletoe preparations and the individual responsiveness of the patient to the mistletoe extract demand an effort to prognosticate the optimal therapy with the best individual medicament. In this sense we showed that the cytotoxicity of a distinct mistletoe extract is different regarding different cancer cell lines.

### 2. RESULTS

#### *2.1. Effect of mistletoe extracts and cytostatics on the proliferation of the breast cancer cells MFM-223 and KPL-1*

The extract of fresh apple mistletoe (Abnoba®Mali-2) and ash mistletoe (Abnoba®Fraxini-2) as well the chemotherapeutics Cisplatin, Paclitaxel and Doxorubicin were

added to the breast tumor cells MFM-223 and KPL-1 in decreasing concentrations from  $10^{-1}$  to  $10^{-4}$   $\text{mg}\cdot\text{ml}^{-1}$ . The toxic influence on the cells was controlled observing the cell proliferation (BrdU incorporation), the mitochondrial activity (MTT) and the cell viability (LDH). It was shown that mistletoe preparations have comparable, dose-de-pendent cytotoxic effect on cancer cells to common cytostatica. The viability of KPL-1 cells was diminished in the range of 60-80% when the concentration of chemothera-peutics was  $10^{-1}$   $\text{mg}\cdot\text{ml}^{-1}$ . Lower doses from  $10^{-2}$  to  $10^{-4}$   $\text{mg}\cdot\text{ml}^{-1}$  of Abnoba®Mali-2, Abnoba® Fraxini-2, Cisplatin and Doxorubicin had no influence on the cell prolifera-tion. Paclitaxel showed no effect on KPL-1. In contrast, the MFM-223 cell line reacted very sensitive to Paclitaxel in all concentrations tested, even at  $10^{-4}$   $\text{mg}\cdot\text{ml}^{-1}$  80% of the cells were killed.  $10^{-1}$  and  $10^{-2}$   $\text{mg}\cdot\text{ml}^{-1}$  Doxorubicin and the two mistletoe extracts lo-wered the viability of MFM-223 to 10-20%, whereas Cisplatin had a cytotoxic effect only at a concentration of  $0.1 \text{ mg}\cdot\text{ml}^{-1}$ .

### *2.2. The influence of mistletoe lectins, viscotoxin and mistletoe polysaccharides on the growth of MOLT-4*

The most powerful, cytotoxic agent of mistletoe extract was described to be the mistletoe lectin I (ML I) and viscotoxin [2]. We tested how isolated ML I and viscotoxin influenced the proliferation of MOLT-4 in the presence and absence of FCS. Finally, we supplemented the culture medium with mistletoe polysaccharides in com-bination with ML I or viscotoxin. We found, that viscotoxin only destroyed cells in high concentrations of  $9 \mu\text{g}\cdot\text{ml}^{-1}$ , whereas ML I stopped cell proliferation in the range of  $2.5 \text{ ng}\cdot\text{ml}^{-1}$  in the presence of FCS. In the culture medium without FCS, the ML I were diluted to  $0.0025 \text{ ng}\cdot\text{ml}^{-1}$  without any loss of toxicity compared to the highest dose of  $250 \text{ ng}\cdot\text{ml}^{-1}$ . The addition of mistletoe polysaccharides (MS) reduced the toxic effect of ML I. However, viscotoxin seemed to stimulate the cell proliferation when mistletoe polysaccharides were present.

### *2.3. Mistletoe applications on primary breast cancer cells*

Isolated breast cancer cells of three patients were cultured in the presence of three different mistletoe preparations: Abnoba Fraxini-2 (ash) corresponds to a fresh pressed extract, Isacador M (apple) and Q (oak) were fermented mistletoe juices. All prepara-tions showed cytotoxic effects in the highest concentrations of  $01 \text{ mg}\cdot\text{ml}^{-1}$ : only 20% of the cells from patient 2 survived, the viability of the cells from patient 1 and 3 was re-duced in the range of 40 to 50 %. Cells of patient 1 reacted the most sensitive to Fraxi-ni-2, whereas cells of patient 3 were sensitive to Iscador M.

## 3. CONCLUSION

We conclude, that mistletoe extracts show comparable results to common cytosta-tics regarding the mitochondrial activity of tumor cells in vitro.

The active agents of mistletoe, the mistletoe lectins and viscotoxin, can be influenced by FCS or mistletoe polysaccharides regarding cell proliferation.

Different mistletoe preparations have different cytotoxic effects on primary breast cancer cells from different patients.

#### 4. REFERENCES

- Schlodder D (1996) Die Misteltherapie im Spannungsfeld zwischen Empirie und Wissenschaft, In  
Hornung J.: Forschungsmethoden in der Komplementärmedizin. Schattauer, Stuttgart  
Büssing A (2001) *Viscum album* L. – Mechanismen der Zytotoxizität. KVC Verlag, Essen.  
Grossarth-Maticek R, Kiene H, Baumgartner SM, Ziegler R (2001). Use of iscador, an extract of  
european mistletoe (*viscum album*), in cancer treatment: prospective nonrandomized and randomized  
matched-pair studies nested within a cohort study. *Alternative Therapies*: 7(3), 57-78.

The project was supported by the “Kommission für Technologie und Innovation” (KTI grant 5732.2 FHS).

NESREDIN A. MUSSA PHD, KEE Y. CHEUNG, IMTIAZ M.  
ALAM & STEVE FLATMAN

## RAPID IN-PROCESS MONITORING OF ANTIBODY INTEGRITY, PURITY AND TITRE- 2100 BIOANALYSER (LAB ON A CHIP) STUDY

*Lonza Biologics plc, Research and Development, 228 Bath Road, Slough,  
Berkshire SL1 4DY, U.K.*

### 1. INTRODUCTION

The number of therapeutic antibodies and recombinant proteins developed has risen dramatically over the past decade. This explosion in therapeutic antibody research was followed with immediate success as Rituxan® and Herceptin®, the first therapeutic antibodies accepted by the FDA for non-Hodgkin's lymphoma and breast cancer respectively and lately immunotherapeutics showed indications in the inhibition of prion replication and slowing down the disease (White *et al*, 2003). Over 90% of the potential therapeutic antibodies are at the clinical trial stages. This trend is likely to increase with the timing of proteomic research. The type of diseases targeted include arthritis (Kevorkov & Futlik, 2000), Asthma (Nelson, 2003), HIV (Tsamis, 2003) and stroke (Wiessner, 2003). Clinical trials and in market therapeutic antibodies are produced in vast quantities depending on the market requirements and trial demands.

Analysis of these products is vital throughout the product life cycle from development to final release. The widely employed techniques for such purposes are SDS-PAGE electrophoresis, Protein A HPLC and ELISA assays which require multiple operators and can result in protruded time line. The use of these techniques is necessitated to have an understanding of the product quality issues and titre assessment. The current advances in proteomic research and increased therapeutic antibody development requires more efficient technologies and platforms with multi analytical/parameter capabilities to deliver the data with minimum resource and at a rapid speed to facilitate the anticipated throughput, this is were the 2100 Bioanalyser (Figure 1) proves its usefulness. This technique has been evaluated at Lonza Biologics for the analysis of monoclonal antibody (IgG4). This is referred to as Lab Chip technology and is based on microfluidics where sample preparation, fluid handling and biochemical analysis are carried out within the confines of a microchip. The chips comprise of microchannels fabricated in glass that create an

interconnected network of gel matrix reservoirs and pathways. This technology has fully automated analytical and data processing capability.

At Lonza Biologics we have employed the 2100 Bioanalyser at selected stages of product manufacturing development and compared it with the conventional techniques. Some promising data were obtained. Lonza Biologics, part of Swiss-based Lonza Group, is a contract manufacturer of biotherapeutics derived from mammalian cell culture.

## 2. METHOD AND SAMPLE PREPARATION

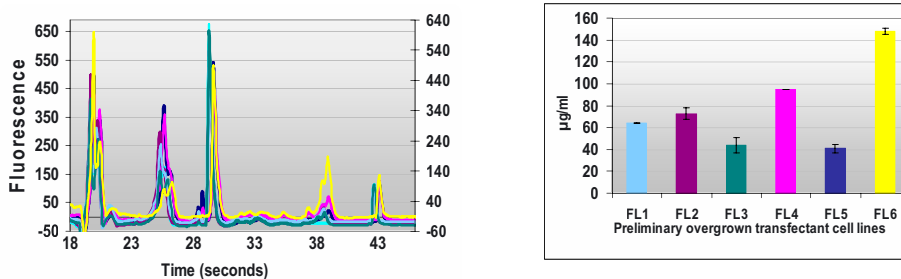
4  $\mu$ l of sample was added to 2  $\mu$ l of sample buffer ( $\pm$   $\beta$ -MCE). Sample was heated in boiling water for 1 minute. After cooling the sample was spun at 13K RPM for 15 seconds. This was followed by the addition of 84  $\mu$ l of distilled water. 6.0  $\mu$ l of sample and ladder was applied into the protein chip wells where proteins are separated by the acrylamide sieving process. The protein chip was loaded onto the 2100 Bioanalyser and each protein is then induced by fluorescent excitation at 633 nm. All the reagents are provided in the 2100 Bioanalyser protein 200 plus kit (<http://www.chem.agilent.com/Scripts/PCol.asp?lPage=50>).

## 3. RESULTS AND DISCUSSION

Antibody analysis using 2100 Bioanalyser at early stages of the manufacturing development process (Figure 1a & 1b) showed that titre and antibody integrity information are essential in the selection process of cell line clones. Rapid trending of the product titre and overall profile of the fermentation medium containing the product in real time *at line* was only realised using the 2100 Bioanalyser and specific Lonza Biologics sample preparation method. The titre, total % and quality of the product and other product related fragments were trended *at line* (Figure 2 & 3). Product purification processes require on-going monitoring of the status of the antibody after each purification steps for titre, % purity and quality of the product. 2100 Bioanalyser provided these data *at line*. The data have direct impact on the purification process development strategy (Figure 4). The 2100 Bioanalyser was used for the medium selection process. Various medium specifications, including protein free media were used to grow CHO cells and the intact antibody, light chain (LC), and heavy chain (HC) products were analysed (data not shown).



3.1 Antibody Assembly Development Process



Figures 1a and 1b  
 Electropherograms for the profile of culture supernatant containing intact monoclonal antibody and other fragment obtained from preliminary overgrown transfectant cell lines.  
 Figure 2b Intact monoclonal antibody titre

3.2 Fermentation Development Process

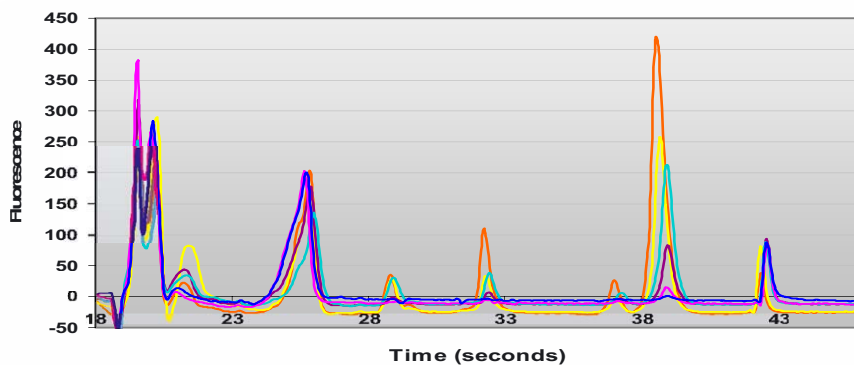


Figure 2 Electropherograms of intact monoclonal antibody and other fragments in culture supernatant analysed using 2100 Bioanalyser at line. Samples were collected at different intervals across two weeks pilot scale fermentation process

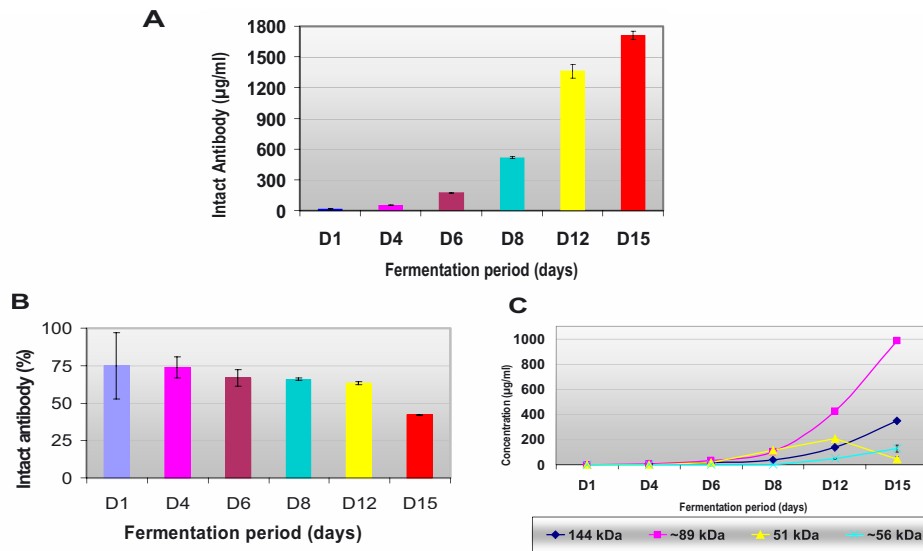


Figure 3

A The titre of the intact antibody in culture supernatant analysed at-line.

B The % total of the intact monoclonal antibody.

C-The rise in antibody fragments across fermentation process.

3.3 Purification Development Process

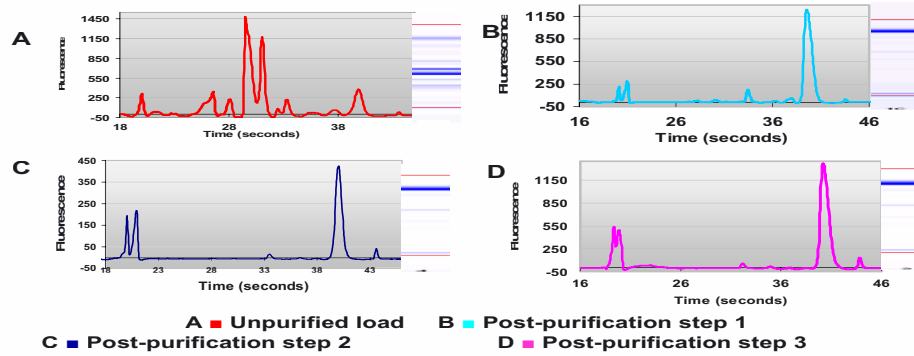


Figure 4 Monoclonal antibodies undergo several stages of purification. At each stage of purification process development, the 2100 Bioanalyser was used to assess product quality and purity.

Table 1 Purification and separation process of the intact antibody, antibody fragments and other contaminants. P1 to P3 are the different purification processes, P3 being the final purification step.

Protein Size (kDa)	Load (Unpurified)	P1	P2	P3	Final purified product
13.7	√	√			
14.6	√	√			
32.5	√				
37.6	√	√			
42.8	√		√		
51.4	√	√			
56			√		
63.8	√	√			
141.1	√		√		
113.8	√				
117.6	√				
123			√	√	
91	√		√	√	√ (<1%)
163	√	√	√	√	√ (>99%)

### 3.4 Concluding remarks

The data presented here shows for the first time the applicability of 2100 Bioanalyser for the simultaneous determination of the titre, integrity, and % purity of monoclonal antibodies throughout the manufacturing and purification development process.

2100 Bioanalyser can be used for the analysis of both monoclonal antibodies and other recombinant proteins produced in mammalian cell culture.

The 2100 Bioanalyser allows *at line* analysis at a rapid pace relative to the conventional techniques. This introduces improved efficiency in the process of therapeutic antibody manufacturing development. This ultimately reduces the time line required to manufacture products for clinical trials and market supply.

### REFERENCES

- <http://www.chem.agilent.com/Scripts/PCol.asp?lPage=50>
- Keverkov NN and Futlik DM; 2000, Peculiarities of the rheumatoid arthritis pathogenesis and some current approaches to its treatment; Russ J immunol, 5 (1 ), 5-18.
- Nelson HS; 2003, Advances in upper airway diseases and allergen immunotherapy; J Allergy Clin Immunol; 111(3 Suppl), S793-8.
- Tsamis F, Gavrilov S, Kajumo F, Seibert C, Kuhmann S, Ketas T, Trkola A, Palani A, Clader JW, Tagat JR, McCombie S, Baroudy B, Moore JP, Sakmar TP, Dragic T; 2003, Ananalysis of the mechanism by which the small molecule CCR5 Anatagonists SCH-351125 and SCH-350581 inhibition of HIV-1 entry; J Virol, 1, 77 ( 9 ), 5201-5208.
- White AR, E Perry, Tayebi M, Mushens R, Linehan J, Brandner S, Anstee D, Collinge J, Hawke S; 2003, Monoclonal antibodies inhibit prion replication and relay the development of prion disease; Nature, 422, 80-83
- Wiessner C, Bareyre FM, Allegrini PR, Mir AK, Frentzel S, Zurini M, Schnell L, Oertle T, Schwab ME; 2003, Anti-Nogo-A antibody infusion 24 hours after experimental stroke improved behavioral outcome and corticospinal plasticity in normotensive and spontaneously hypertensive rats; J Cereb Blood Flow Metab, 23( 2 ), 154-65

P.J. DIERICKX<sup>A</sup> AND C. VAN DER WIELEN<sup>B</sup>

## TOXICOLOGICAL EVALUATION OF HAINE RIVER WASTE-WATER SAMPLES TO APPROPRIATELY SENSITIZED CULTURED FATHEAD MINNOW CELLS COMPARED WITH THE MICROTOX<sup>®</sup> METHOD

*IPH, Afdeling Toxikologie, Wytsmanstraat 14, B-1050 Brussel, Belgium<sup>a</sup> and  
ISSeP, Section Environnement, rue du Chéra 200, B-4000 Liège, Belgium<sup>b</sup>*

Abstract. Our previously described neutral red uptake (NRU) inhibition assay on cultured fathead minnow (FHM) fish cells revealed a good correlation as well with fish as with *Daphnia magna* toxicity data. The major drawback was the lower sensitivity of the cytotoxicity assay. This was, therefore, adapted in several ways, and was used to evaluate the cytotoxicity of waste-water samples. A good correlation with the Microtox results was observed [1]. In order to validate these results we repeated these experiments on water samples obtained from another river.

### INTRODUCTION

The waste-water samples were taken on the Haine river (Belgium) in 2001. It concerned waste-water from a water collector (samples s), metal industry (samples x), sewage treatment plants (samples t and u), and petrochemical industry (samples v, w, y and z). The samples were sterilized by filtration on a Millex-GS filtre (0.22 µm). The NRU was measured on cells seeded at a density of  $90 \cdot 10^3$  per microtiter plate well after 24h, with or without 400 µM buthionine-sulfoximine (BSO) [1]. FHM cells were considered to be intoxicated when the NRU was reduced by at least 15% compared with that of control cultures. The results are compared with toxicity data obtained by the Microtox assay, which is based on the inhibition of luminescence of the bacterium *Vibrio fischeri* [2], and was performed as described [3]. These results were quantified by the TU20 and TU50, corresponding to respectively 100/EC20 and 100/EC50, EC20 and EC50 being the exposure concentrations causing 20 and 50% inhibition of luminescence.

The results are summarized in Table 1. The sampling points covered different kinds of industrial activity. In the course of the year the largest NRU differences were observed for sampling places w, y and z. Only 11 samples were toxic to FHM cells in the absence of BSO, but 20 samples were toxic in the presence of BSO. This shows that a reduced glutathione content in the cells increased the sensitivity of the assay. Dose-response toxicity was obtained for most toxic samples. In the Microtox assay 17 samples were toxic based on the TU20 and 11 based on the TU50. The toxicity in both assays is compared in Table 2. These results correlate

well with those obtained before on a series of waste-water samples collected in another river basin [1].

Our results confirm that the FHM assay in the presence of BSO allows to detect the toxicity of environmental water samples with a sensitivity which is comparable to

*Table 1. Toxicity results for the whole series of waste water samples. The cytotoxicity in FHM cells is expressed as the neutral red uptake in % of the control cells.*

Sample		Microtox <sup>®</sup>			
N <sup>o</sup>	Date	50% water (- BSO)	50% water (+ BSO)	TU20 <sup>a</sup>	TU50 <sup>a</sup>
s1	12/02	110 ± 2	70 ± 9 <sup>b</sup>	9.4	-
s2	19/03	106 ± 7	76 ± 10 <sup>b</sup>	29.0	7.5
s3	28/05	46 ± 19 <sup>b</sup>	55 ± 10 <sup>b</sup>	8.6	-
s4	01/10	94 ± 9	90 ± 10	-	-
s5	19/11	114 ± 4	85 ± 13 <sup>b</sup>	-	-
t1	05/02	111 ± 19	99 ± 15	-	-
t2	26/02	110 ± 12	122 ± 13	-	-
t3	07/05	103 ± 14	109 ± 8	-	-
t4	03/09	121 ± 17	121 ± 12	-	-
t5	05/11	98 ± 12	87 ± 9	-	-
u1	05/02	104 ± 14	112 ± 26	-	-
u2	26/02	108 ± 17	120 ± 17	-	-
u3	07/05	108 ± 18	106 ± 5	-	-
u4	03/09	101 ± 13	109 ± 2	3.6	-
u5	05/11	120 ± 9	109 ± 3	-	-
v1	12/02	139 ± 7	104 ± 10	12.0	2.8
v2	19/03	134 ± 7	123 ± 9	7.2	-
v3	28/05	105 ± 15	114 ± 8	8.8	2.2
v4	01/10	113 ± 8	134 ± 27	-	-
v5	19/11	114 ± 9	158 ± 11	-	-
w1	19/02	41 ± 9 <sup>b</sup>	14 ± 1 <sup>b</sup>	200.0	89.0
w2	26/03	65 ± 7 <sup>b</sup>	12 ± 1 <sup>b</sup>	88.0	24.0
w3	11/06	8 ± 2 <sup>b</sup>	20 ± 4 <sup>b</sup>	150.0	68.0
w4	17/09	46 ± 18 <sup>b</sup>	11 ± 1 <sup>b</sup>	35.0	17.0
w5	26/11	83 ± 6 <sup>b</sup>	71 ± 6 <sup>b</sup>	14.0	5.1
x1	19/02	92 ± 19	78 ± 7 <sup>b</sup>	9.0	-
x2	26/03	115 ± 19	73 ± 26 <sup>b</sup>	-	-
x3	11/06	90 ± 17	95 ± 8	-	-
x4	17/09	110 ± 12	76 ± 13 <sup>b</sup>	-	-
x5	26/11	115 ± 8	102 ± 14	-	-

Table 1. (continued)

y1	12/03	110 ± 5	90 ± 10	-	-
y2	02/04	110 ± 1	79 ± 3 <sup>b</sup>	-	-
y3	18/06	14 ± 4 <sup>b</sup>	18 ± 1 <sup>b</sup>	-	-
y4	10/09	116 ± 19	81 ± 9 <sup>b</sup>	-	-
y5	03/12	114 ± 4	110 ± 12	-	-
z1	12/03	85 ± 7	82 ± 4 b	5.2	-
z2	02/04	111 ± 6	78 ± 9 <sup>b</sup>	-	-
z3	18/06	18 ± 5 <sup>b</sup>	18 ± 1 <sup>b</sup>	16.0	7.7
z4	10/09	15 ± 3 <sup>b</sup>	18 ± 2 <sup>b</sup>	290.0	150.0
z5	03/12	13 ± 2 <sup>b</sup>	16 ± 1 <sup>b</sup>	24.0	13.0

<sup>a</sup>The TU20 and TU50 represent the number of times the water sample has to be diluted to obtain the EC20 and EC50, respectively; - = lower than the quantitation limit of 2.2. <sup>b</sup>Toxic.

Table 2. Comparison of the toxicity of the 40 waste water samples in the FHM assay (in the presence of BSO) and in the Microtox assay. The numbers of water samples are given.

	Toxic in FHM assay & Microtox	Only toxic in Microtox	Only toxic in FHM assay	Not toxic in FHM assay or Microtox
Based on TU20	13	4	7	16
Based on TU50	9	2	11	18

that of the Microtox method. Since the results of this study are highly comparable with those of the previous study [1], we can conclude that toxicity data obtained with cultured fish cells can be used for ecotoxicological research. Any in vitro cytotoxicity laboratory can perform this kind of assays. No concentration or fractionation of the water samples is necessary.

The General Direction for Natural Resources and Environment is acknowledged for providing the waste-water samples. We thank Patricia Naport (ISSeP) and Els Jonckers (IPH) for their excellent technical assistance.

## REFERENCES

1. Scheers, E.M., Van der Wielen, C. and Dierickx, P.J. (2002). Toxicological evaluation of waste-water samples to appropriately sensitized cultured fathead minnow cells compared with the Microtox assay. *Bull. Environ. Contam. Toxicol.* 68:352-260.
2. Van der Wielen, C. and Halleux, I. (2000). Toxicity of the Scheldt and Meuse Rivers in Wallonia (Belgium) by conventional and micro-biotests. In : Persoone, G., Janssen, C. and De Coen, W. (eds.) *New Microbiotests for Routine Toxicity Testing and Biomonitoring*, Kluwer, Dordrecht, Netherlands and Plenum, New York, USA, p. 295-303.
3. Dierickx, P.J., Van der Wielen, C. and Lemaire, S. (2000). Toxicological evaluation of surface-water samples in sensitised cultured fish cells compared with the Microtox method. *ATLA* 28/509-515.



## CHAPTER 2

### CELL BASED THERAPIES

M. BARTHOLD, I. MAJORE, S. FARGALI, F. STAHL,  
R. SCHULZ, S. LOSE, H. MAYER, V. JÄGER

## 3D-CULTIVATION AND CHARACTERISATION OF OSTEOGENIC CELLS FOR THE PRODUCTION OF HIGHLY VIABLE BONE TISSUE IMPLANTS

*German Research Centre for Biotechnology (GBF), Braunschweig*

### 1. INTRODUCTION

Bone tissue engineering represents a novel strategy to restore the function of bone in various indications in orthopaedic reconstructive surgery such as high impact trauma, anterior/posterior spinal fusions, non-union fractures, tibial plateau fractures, hip fractures or total hip revisions, bone void fillings after tumor removal or cranio-maxillofacial applications. It is based on the *in vitro* 3D-cultivation of osteoprogenitor cells on biocompatible and bioresorbable, osteoconductive scaffold materials. The engineered tissue is then used for implantation instead of scaffolds without cells, which lack satisfactory mechanical long-term stability or autologous material from the iliac crest which requires subsequent filling of the void volume after transplantation.

For comprehensive monitoring of the proliferation, directed differentiation and mineralisation of osteogenic cells an assortment of invasive and non-invasive analytical methods is necessary.

A novel bone-specific DNA microarray for simultaneous determination of tissue-associated genes has been developed and used for the identification of relevant non-invasive analytical methods which are essential for an adequate in-process control during the manufacturing of scaffold materials settled with cells which are intended for implantation. This analytical tools have been used to monitor cultivation processes performed with a novel miniaturised fixed-bed perfusion bioreactor system.

### 2. MATERIALS AND METHODS

Experiments were performed with primary cells isolated from femura and tibiae of 6 weeks old female New Zealand White rabbits with a weight of approx. 800 g (Charles River Laboratories) or femura of 5 weeks old female Wistar WKY rats. Human primary cells were isolated from specimens of a heterotopic ossification and from spongiosa arising after hip bone surgery. Cell proliferation was monitored by WST-1 assay (Roche), DNA-quantification with Hoechst 33258, counting of viable

cells in a hemocytometer with trypan blue as well as the determination of D-glucose, L-lactate and LDH in the culture medium. Cell differentiation was analysed by determination of membrane-bound and soluble alkaline phosphatase (AP), ELISAs for Collagen I C-terminal propeptide (Quidel) and Osteocalcin (BTI), as well as calcium deposition (calcein fluorescence). Further analysis was performed on the transcriptional level by reverse transcriptase-polymerase-chain-reaction (RT-PCR) and a cDNA chip containing 57 bone-specific gene markers.

3-dimensional culture was carried out on camceram calcium phosphate scaffolds (Camimplants) with a porosity of approximately 90% and a volume of 1 cm<sup>3</sup>. Seeded carriers were cultured in small-scale fixed-bed bioreactors (working volume = 30 ml, meredos) with a batchwise or continuous media exchange (10 ml per day) and an internal perfusion of the carriers of 200 µl min<sup>-1</sup>.

### 3. RESULTS AND DISCUSSION

#### 3.1 Development of Serum-reduced Media

After establishment of suitable isolation and cultivation protocols for osteogenic cells from rat, rabbit and human serum-reduced media with improved performance were developed. Because of the higher risk of an immune response due to the use of xenogenic (FBS) or allogenic serum in high concentrations of usually 10 to 15%, a substantial reduction of serum is of great importance for maximising the rate of success in implantation experiments. The cells isolated from different species turned out to have different requirements for optimum cell proliferation and differentiation. Results of the media optimisation for rat osteogenic cells are shown in Fig. 1. Best performance was obtained using a medium based on our in-house formulation ZKT-I and supplemented with 1% FBS, insulin, transferrin, albumin plus bFGF and PDGF-BB as cytokines (11). The addition of osteogenic supplements (13) resulted

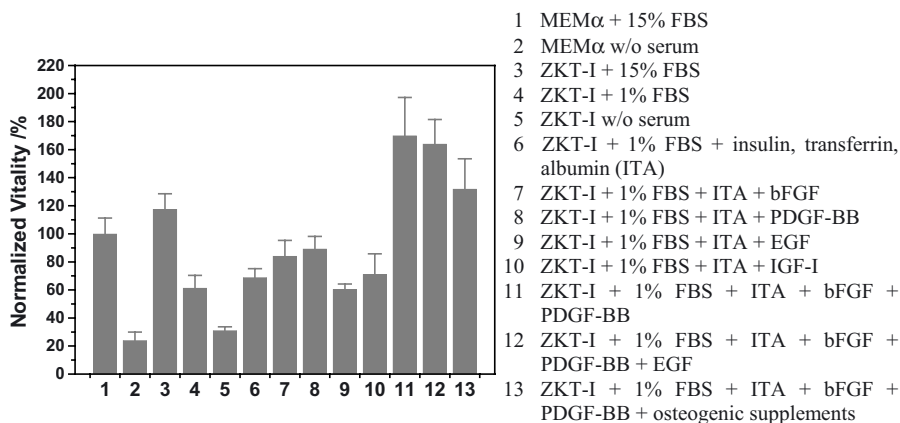


Figure 1. Comparison of different serum-reduced media formulations for an improved cultivation of osteogenic rat cells. Vitality was measured using the WST-1 assay and normalised setting MEMα supplemented with 15% FBS (1) to 100%.

in a reduced cell proliferation but accelerated differentiation into the osteoblast lineage. In contrast to the optimised medium for rabbit cells EGF showed no beneficial effects in cultures of rat cells. Principally, rabbit cells in culture medium supplemented with allogenic rabbit serum grew faster than those in medium supplemented with FBS. However, rabbit serum was found to significantly support rabbit cell differentiation into the adipocyte lineage even after removal of the majority of lipids by ultracentrifugation. For both species cell growth and differentiation was markedly improved using the optimised culture media when compared to culture media supplemented with 15% serum. In addition, the directed alteration of the composition of cytokines and specific osteogenic factors allowed a better control of the maturation of cells.

### 3.2 DNA Microarray and In-process Analytics

During the cultivation of osteogenic cells it is very important to get detailed information about the differentiation status of the osteogenic cells. In 3-dimensional culture cells are not directly accessible without damaging the structure of the newly developed tissue. Thus, scaffolds with cells intended for use as an implant require

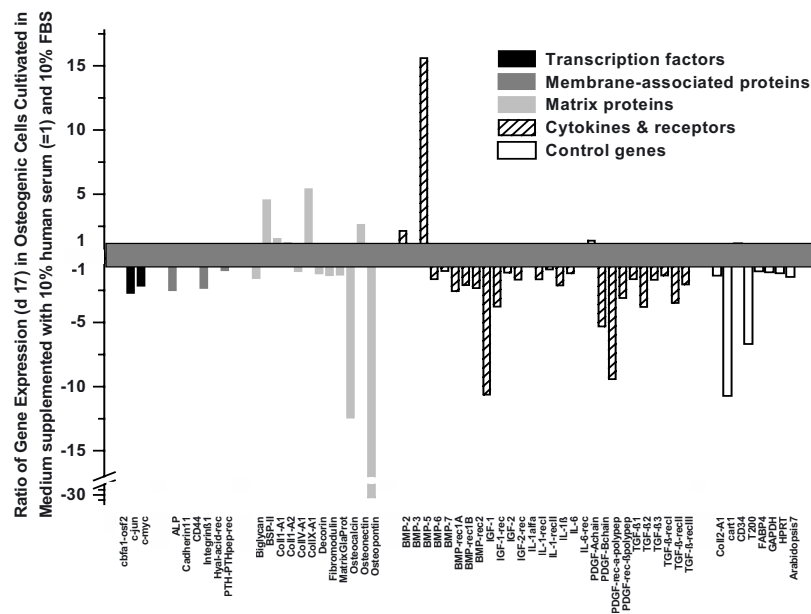


Figure 2. Comparison of gene expression levels of human osteoblasts obtained from a heterotopic ossification, which are cultivated in medium supplemented with either 10% human serum (expression level set to 1) or 10% FBS as measured with a DNA microarray.

the use of non-invasive analytical methods. These are based on the analysis of soluble factors which can be quantified in the cell culture supernatant. We have identified the formation of l-lactate as a good parameter for the measurement of the overall metabolic activity, the release of lactate dehydrogenase as an indicator for cell death, collagen I C-terminal propeptide as a marker for early stage differentiation, soluble alkaline phosphatase as a marker for the intermediate stage of differentiation and osteocalcin as a marker for matrix mineralisation. To get a more comprehensive overview about the expression of bone-specific genes a DNA microarray has been developed for human osteogenic cells. Requiring the isolation of a large amount of RNA from cells this technology can only be used for the analysis of samples which are not intended for subsequent implantation. The microarray allows a direct comparison of different cultures of human cells as it is shown in Fig. 2.

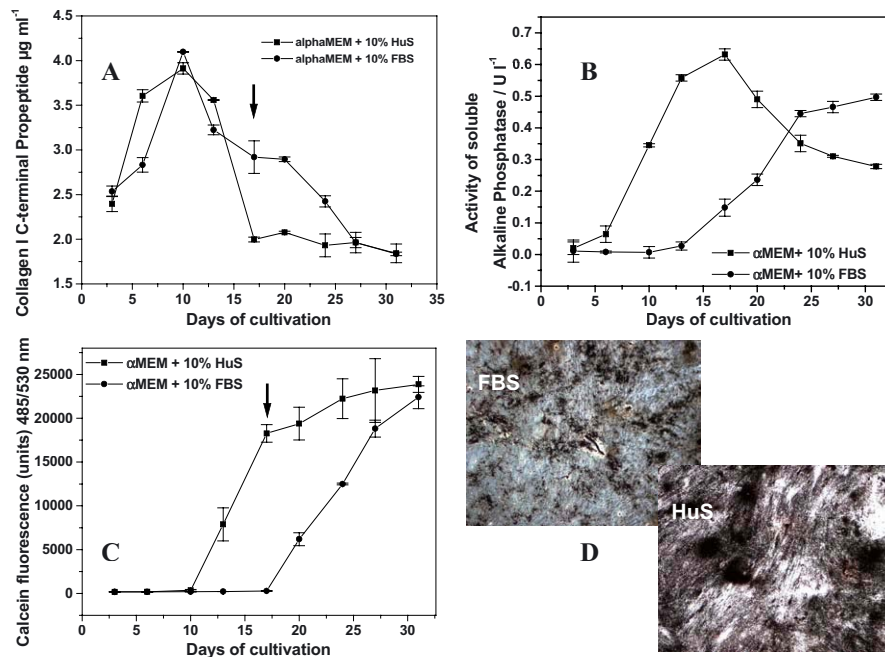


Figure 3. Comparison of the cultivation of human osteogenic cells grown in different culture media. Analysis of selected marker genes on the proteinous level after 17 days of cultivation. A - Expression of an early differentiation marker (collagen I as measured by the cleaved, soluble C-terminal propeptide). B - Expression of an intermediate differentiation marker (soluble alkaline phosphatase). C - Late differentiation marker as measured by calcium deposition in the extracellular matrix. D - von-Kossa-stain of mineralised matrix (after 31 days).

Cells cultivated in a medium supplemented with 10% human serum were compared with cells grown in the same medium supplemented with 10% FBS. Gene expression on the transcriptional level was verified for selected proteins and calcium

deposition as shown in Fig. 3. Since the cell differentiation in the presence of human serum is accelerated, collagen I, a differentiation marker characteristic for the early phase is already down-regulated at day 17 when compared to the culture with 10% FBS. In contrast, markers characteristic for later phases of cell differentiation (alkaline phosphatase, calcium deposition) can be found at considerably higher concentrations. In summary, cell differentiation, the formation of extracellular matrix and its mineralisation are significantly accelerated in the presence of human serum. The quantitative determination of collagen I and alkaline phosphatase together with an osteocalcin ELISA (not suitable at high FBS concentrations) represent valuable tools for a non-invasive in-process control.

### 3.3 Three-Dimensional Culture

Tissue engineered implantable bone is based on suitable bioresorbable and osteoconductive scaffold materials which are settled with osteogenic cells *in vitro*. Preferably this cultivation should be performed under well-defined and reproducible conditions. However, most of the cultivations were carried out using relatively simple, non-controlled equipment such as spinner flasks and roller bottles (Sikavitsas et al., 2002), rotating centrifuge tubes kept at an angle (Baksh and Davies, 2000) or perfusion chambers (Goldstein et al., 2001). We have developed a novel continuously perfused cultivation system based on a miniaturised bioreactor which can be operated as a fixed-bed system (Fig. 4).

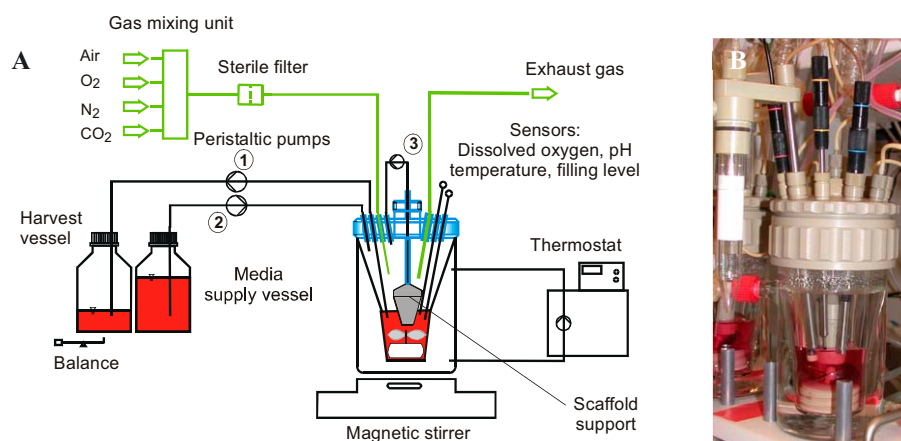


Figure 4. A - Schematic diagram of the bioreactor set-up. Medium circulation is performed by pump no. 3. Continuous medium exchange is accomplished by pumps 1 and 2, and controlled by a level sensor. B - Reactor vessel.

The development and optimisation of 3D bone cultures in this bioreactor system was first established in the rat model as shown in Fig. 5. A circulation of  $200 \mu\text{l min}^{-1}$  and an oxygen concentration of 20% air saturation were found to be optimal for the

cultivation. Based on the optimised process parameters a process with continuous medium exchange was set-up and compared to a conventional static culture as described (Fargali et al., 2003). This process proved to be superior with regard to cell growth and directed differentiation as well as extracellular matrix formation and mineralisation.

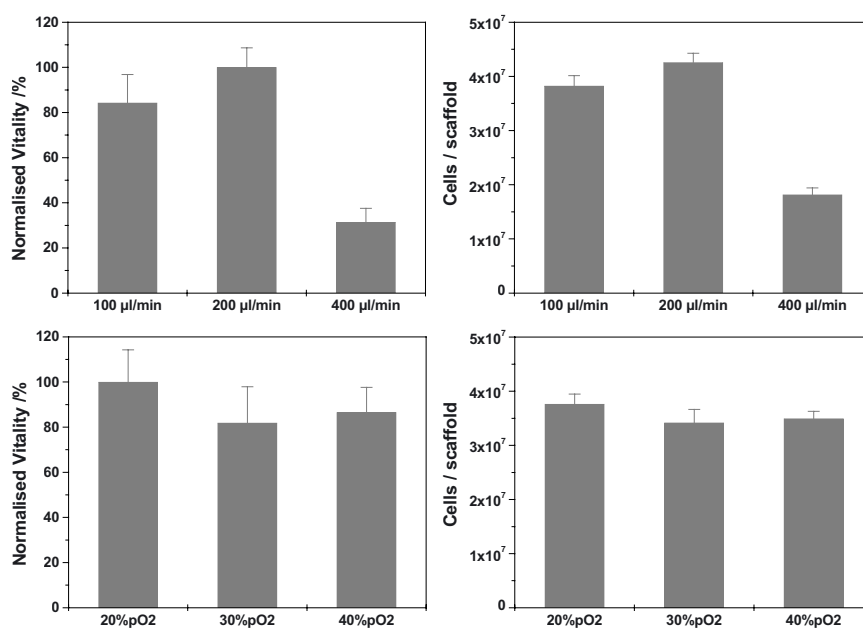


Figure 5. Optimisation of different process parameters for the 3D cultivation of rat osteogenic cells of the 4<sup>th</sup> passage. Cells were grown in a serum-reduced medium (no. 13) as described above.

The developed cultivation process based on suitable, serum-reduced culture media, an adequate in-process control and well-defined culture conditions showed promising results for the generation of implantable bone tissue.

#### 4. REFERENCES

- Baksh D, Davies JE (2000) Design strategies for 3-dimensional in vitro bone growth in tissue-engineering Scaffolds. In: JE Davies (ed.), Bone engineering, em squared, Toronto, pp. 488-495.
- Fargali S, Barthold M, Rohde M, Majore I, Jäger V (2003) In vitro cultivation of rabbit mesenchymal stromal cells on 3D bioresorbable calcium phosphate scaffolds for the generation of bone tissue implants. *This volume*.
- Goldstein AS, Juarez TM, Helmke CD, Gustin MC, Mikos AG (2001) Effect of convection on osteoblastic cell growth and function in biodegradable polymer foam scaffolds. *Biomaterials* **22**: 1279-1288.
- Sikavitsas VI, Bancroft GN, Mikos AG (2002) Formation of three-dimensional cell/polymer constructs for bone tissue engineering in a spinner flask and a rotating wall vessel. *J. Biomed. Mat. Res.* **62**: 136-148.

QUESTIONS AND ANSWERS

**Elephterios Papoutsakis, Northwestern University, US:**

How much material you need to make the microarray analysis ? how many cells do you need to harvest ?

**Volker Jäger, GBF, Germany:**

It is about 1 or 2 million cells. You have to sacrifice the whole scaffold for such an experiment.



D. MÖBEST<sup>1</sup>, M. JAEGER<sup>2</sup>, G. HOBEN<sup>1</sup>, D. HAMANN<sup>1</sup>,  
S. WOLLNER<sup>1</sup>, G.B. STARK<sup>1</sup>

## CARBON SOURCE HAS A CONSIDERABLE INFLUENCE ON EXTRACELLULAR MATRIX FORMATION, DEMONSTRATED ON SPECIFIC COLLAGEN EXPRESSION OF PRIMARY HUMAN TENOCYTES

1 Dept. Plastic- & Hand Surgery, University Medical Center, University of  
Freiburg, Hugstetterstr. 55, D-79106 Freiburg, Germany  
2 Dept. Traumatology, University Medical Center, University of Freiburg,  
Hugstetterstr. 55, D-79106 Freiburg, Germany

Key words: metabolism, extracellular matrix formation, Tissue Engineering

### INTRODUCTION

Tissue-Engineering was defined by R. Langer and J. P. Vacanti in 1993: „Tissue

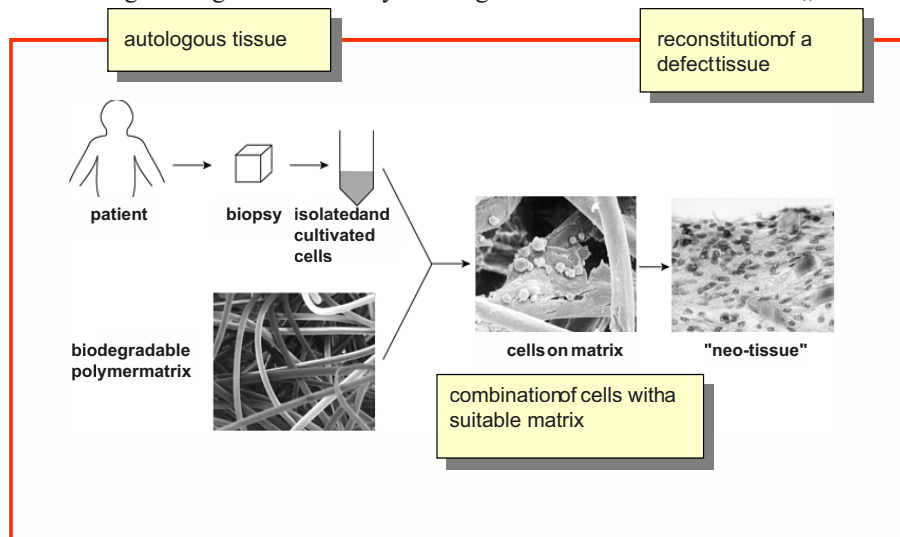


Figure 1. Principle of „Tissue Engineering“

engineering is an interdisciplinary field that applies the principles of engineering and the life sciences toward the development of biological substitutes that restore, maintain, or improve tissue function“[1].

Ideally autologous cells are isolated and combined *in vitro* with a biologically degradable matrix to form a temporary tissue substitute, which should develop into new, functional tissue at the implantation site degrading the synthetic components (figure 1). For generation of neo- or pre-tissue constructs in Tissue Engineering not only cell amplification and proliferation is of relevance, but also the formation of appropriate extracellular matrix components to generate functional tissues. In fascia substitute construction there are high demands on tissue mechanics and proper development of a functional connective tissue is crucial. The formation of an appropriate extracellular matrix has not been a current focus in research, though it is known that the activation of the pentose phosphate pathway is of benefit for the formation of secondary metabolites. Also the use of fructose instead of glucose as a carbon source increased the specific vector production of TeFly cells significantly [2]. In our study we compared fructose as an alternative carbon source for the cultivation of human primary tenocytes and measured specific collagen I and collagen III formation, the major extracellular matrix components of tendon tissue. In addition we took the major components in collagen synthesis (glycine, L-proline, L-aspartic acid, L-methionine) into consideration and elevated the concentration by factor 10 compared to the base Medium (DMEM), or added missing amino acids at the same molarity.

#### MICROTITER ASSAY TO DETERMINE SPECIFIC COLLAGEN EXPRESSION

Collagen I and III is specifically stained by the sirius red dye. This was used by Tullberg-Reinert et al. [3] to develop a spectrophotometric microtiter assay. In addition the sirius red staining method allows a morphological observation of cells as well as a localization of collagen deposition. With regard to that this method is superior to radioactive tracing methods or hydroxyproline measurements. In figure 2 an example of a sirius red stained cell culture is shown.

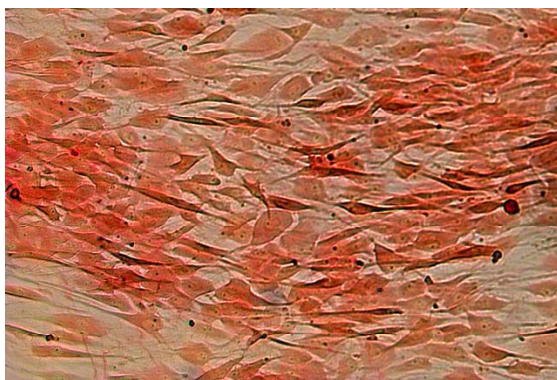


Figure 2. Cell culture stained with sirius red

We combined this method with the Alamar Blue<sup>®</sup> [4] cell count without causing interference. This allows specific collagen expression rates of *in vitro* cultured cells to be determined. These combined assays are an ideal tool for screening experiments with focus on matrix formation as a basis for Tissue Engineering.

#### INFLUENCE OF CARBON SOURCE ON ALAMAR BLUE<sup>®</sup> METABOLISM

Initially we believed one could neglect the altered metabolic state of cells on Alamar Blue<sup>®</sup> metabolism fed by alternative carbon sources. However, while preparing calibration curves, it was clearly seen that a switch of carbon source from glucose to fructose had a considerable effect on the slope of the calibration curves with cultured primary human tenocytes (figure 3) reflecting the activation of different metabolic pathways.

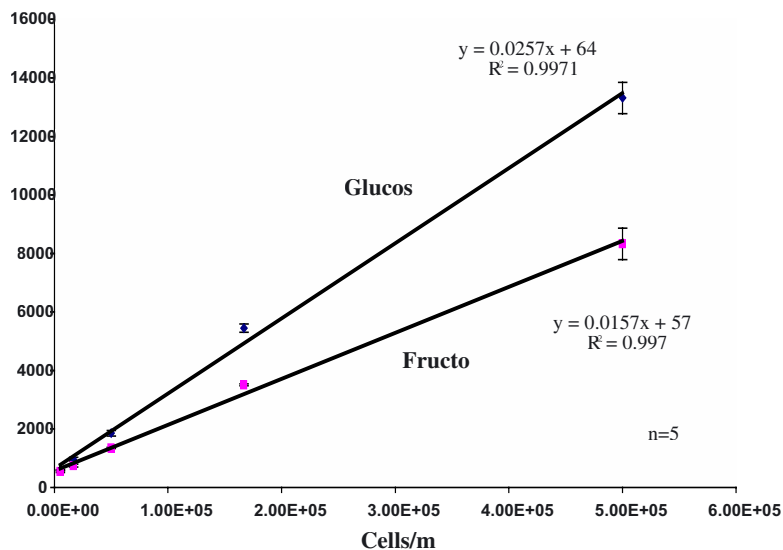


Figure 3. Calibration curves of Alamar Blue<sup>®</sup> with human primary tenocytes cultivated under different carbon sources for 3 weeks

Thus, it was important to cultivate corresponding cultures under the same conditions as the experimental cultures to generate reliable calibration curves for analysis.

### INFLUENCE OF MEDIUM COMPONENTS: GLUCOSE VS. FRUCTOSE AND AMINO ACID SUPPLEMENTATION

The change from glucose to fructose as a carbon source resulted in an increase in the specific collagen I, III expression in cultivated primary human tenocytes after 3 weeks of cultivation (figure 4). At that time all cultures reached confluency and showed about equal levels of cell concentration (figure 5).

Surprisingly the addition of amino acids, being the major components in collagen

#### Specific Collagen Expression

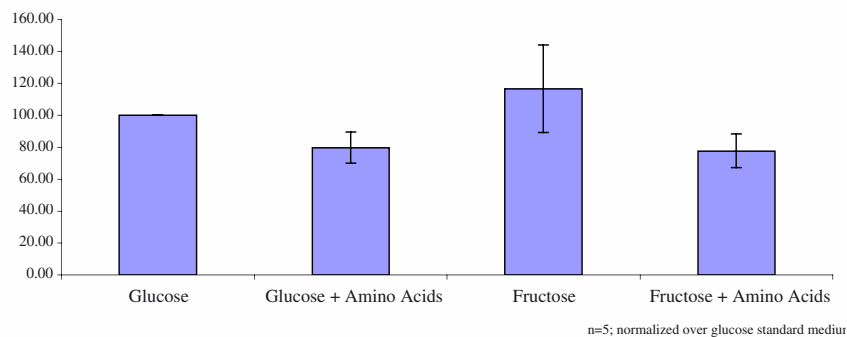


Figure 4. Specific collagen expression of primary human tenocytes after 3 weeks of cultivation with different media compositions

#### Cell Count

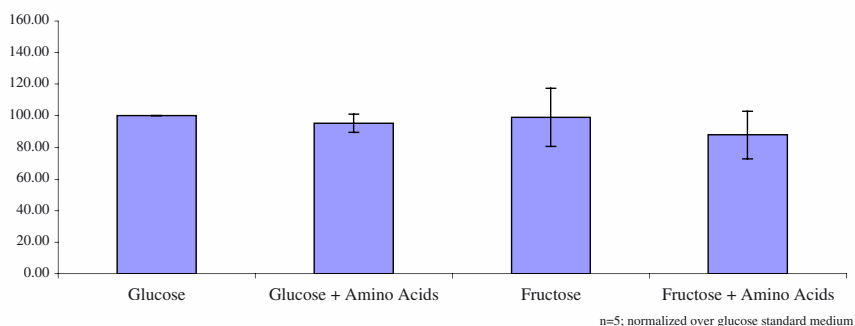


Figure 5. Cell count of primary human tenocytes after 3 weeks of cultivation with different media compositions

synthesis, at those high levels had an unexpected adverse effect and resulted in a decrease in specific collagen expression (figure 4) without having a considerable effect on cell growth itself (figure 5).

#### SUMMARY

A microtiter assay for specific collagen expression was established as shown in the example of cultivation of primary human tenocytes, which could be a nice tool in Tissue Engineering. Working with cells under different metabolic states clearly showed an alteration in metabolism of Alamar Blue<sup>®</sup> indicating that cells conditions have to be considered when using this method for cell counting, but they also could suggest that this method could be used as a potential indicator for metabolic alterations in cells. Fructose replacing glucose as carbon source favours specific collagen I,III expression in primary human tenocytes, without having a visible effect on total cell numbers after 3 weeks of cultivation. In contrast to expectations, addition of amino acids relevant for collagen synthesis lowers specific collagen expression at the high concentrations used in this study.

#### REFERENCES

- Langer, R. Vacanti, J.P.: Science 260, 920-6. (1993)  
Merten, O.-W. Rochette, C. Fiamma-Geny, C. Leger, W. Danos, O.: ESACT-Abstracts, O7.04 (2001)  
Tullberg-Reinert, H. Jundt, G.: Histochem Cell Biol, 112(4), 271-6 (1999)  
Ahmed, S.A. Gogal Jr., R.M. Walsh, J.E.: J Immunol Meth 170, 211-24 (1994)

## QUESTIONS AND ANSWERS

**Allan Miller, CIL, Belgium:**

You rightly emphasized the role of the extracellular matrix as well as the chemistry of the microenvironment in the differentiation of stem cells. People normally use feeder layers which are made of gamma-irradiated or mytomycin-treated mouse embryonic and then they put the cells they want to differentiate onto these feeder layers. Do you have the same results if you grow these mouse embryonic fibroblast, detach the cells to leave the extracellular matrix and then using the mouse embryonic fibroblasts' conditioned medium plus this conditioned surface. Do you obtain the same results as when you just grow your cells onto gamma-irradiated or mytomycin-treated fibroblasts ?

**Dieter Möbest, Chirurgische Universitätsklinik Freiburg, Germany:**

Our first aim is to have a practical approach and find media as defined as possible, and try to get a platform such as conditioned medium, but it would be interesting to find out specific factors and we have related projects ongoing to check the influence of extracellular matrix components on the differentiation status of the cells. But for this project we are trying to keep it as simple as possible.

**David Jayme, Gibco, Invitrogen, US:**

You noted that there is an improved specific production rate of ECM with the fructose substitution, but you also noticed that there was a decreased proliferative rate, and I wonder if you have been able to dissociate these two reasons for the increased specific production: fructose substitution or slower proliferation. Secondly, your amino acids substitution information was kind of surprising. I wonder if you have some dose-response data, or individual additions, or whether you add all of them together at one single concentration.

**Dieter Möbest, Chirurgische Universitätsklinik Freiburg, Germany:**

About the kinetics, after three weeks you had a confluent layer of cells, and also the same cell amount. We also tried some other strategies, such as one week on glucose to increase cell numbers, and then switch to the fructose medium and we got similar results. Regarding the amino acids, this was a preliminary experiment. It would certainly be a good idea to check them one by one, and do dose-response tests.

JENS M. KELM<sup>1</sup>, ELISABETH EHLER<sup>2</sup>, JEAN-CLAUDE  
PERRIARD<sup>2</sup> AND MARTIN FUSSENEGGER<sup>1\*</sup>

## DESIGN AND CHARACTERIZATION OF CARDIOMYOCYTE-DERIVED MICROTISSUES

<sup>1</sup>*Institute of Biotechnology, Swiss Federal Institute of Technology, ETH Hoenggerberg, CH-8093 Zurich, Switzerland, Phone: +41 1 633 3448, Fax: +41 1 633 1234, e-mail [fussenegger@biotech.biol.ethz.ch](mailto:fussenegger@biotech.biol.ethz.ch); \*corresponding author*

<sup>2</sup>*Institute of Cell Biology, Swiss Federal Institute of Technology, ETH Hoenggerberg, CH-8093 Zurich, Switzerland*

**Abstract.** Classical mammalian cell culture focuses on growing established cell lines as two-dimensional monolayers or suspension cultures. However, in such cultivation conditions mammalian primary cells may lose key morphological characteristics and specialized functions. By contrast, three-dimensional (3D) cell culture may preserve specific function and cell phenotypes since the 3D arrangement of cells favors (i) *in vivo*-like cell shape, (ii) intercellular crosstalk as well as (iii) development of a complex extracellular matrix. Thus, 3D cultivation may create unique microenvironments required for key processes including differentiation, proliferation, apoptosis and angiogenesis. We have refined the hanging drop technology to produce fully functional and beating myocardial microtissues that maintain the differentiated morphology typical for cardiomyocytes. Myocardial microtissues derived from primary mouse and rat cardiomyocytes as well as mixed populations, reflecting the cell type composition of rodent hearts, were characterized for muscle-specific cell morphologies, extracellular matrix components as well as VEGF (vascular endothelial growth factor) production. Novel findings included (i) a linear correlation between cell number and microtissue size, (ii) intensive cell-cell contacts, (iii) maintenance/development of cardiomyocyte-specific cell structures, (iv) development of an extracellular matrix, and (v) size-dependent VEGF production of microtissues which is expected to increase vascularization and tissue integration following implantation. We also established human HIV-1-based transduction of cardiomyocytes that revealed increased specific productivity of microtissues compared to isogenic populations cultivated as monolayers.

### INTRODUCTION

Heart disease is the major cause of morbidity and associated mortality in industrialized countries affecting over sixty million patients per year in the USA alone [1]. Therefore, cardiac tissue engineering remains a high priority as transplantations and artificial hearts only cover about 10% of current clinical needs and/or fail to offer any long-term therapeutic perspectives. For the treatment of smaller heart lesions, engineered heart cell suspensions and undersized cell aggregates may be sufficient [2].

So far, 3D cultivation for production myocardial tissues was often dependent on artificial scaffolds consisting for example of alginate polymers [3] or cell/collagen mixtures [4]. Although scaffolds enable artificial tissues to grow in a desired shape they may cause post-transplantation side effects resulting from toxic degradation products, induction of inflammatory reactions and poor resorption [5]. Alternative strategies to produce scaffold-free artificial tissues are taking advantage of the

aggregation of mammalian cells following cultivation in shake flasks, on non-adhesive surfaces [6] or gravity-enforced assembly in hanging drops [7]. Attempts to shape artificial cardiac-like cell aggregates have mainly been based on physical assembly of isolated primary cardiomyocytes since the emergence of cardiomyocytes in spheroid cultures of human embryonic stem cells was stochastic and strategies for rational differentiation of this pluripotent cell type into cardiac cells are still in its infancy [8].

We have refined the hanging drop cultivation technology to design functional heart microtissues from purified primary neonatal rat (NRC) and mouse (NMC) cardiomyocytes as well as cardiomyocyte-containing cell mixtures reflecting the natural cell composition of neonatal rodent hearts. Owing to the 3D cultivation method the size of the microtissue could be adjusted and contraction maintained for over 3 weeks.

One of the major challenges associated with implantation of bioartificial tissues is their connection to the host vascular system. We could induce the endogenous production of the vascular endothelial growth factor (VEGF), a potent inducer of vascularization, by modulating the size of the myocardial microtissue.

In order to enable rational molecular interventions in myocardial microtissues to refine cell phenotypes or to engineer production of desired protein therapeutics, we have evaluated lentiviral transduction systems for straightforward transgene delivery into cardiomyocytes cultivated in two or three dimensions.

## RESULTS AND DISCUSSION

### *Production of myocardial microtissues*

The hanging drop cultivation technology was successfully adapted and refined to produce myocardial microtissues of neonatal rat (NRC) and mouse (NMC) cardiomyocytes. Under optimized culture conditions 1'200 rat cardiomyocytes form in a single hanging drop a myocardial spheroid of  $130 \pm 11 \mu\text{m}$  in diameter with near 100% efficiency within four days (Figure 1A; B). Microtissues derived from mouse populations of 1'200 cardiomyocytes reached  $170 \pm 12 \mu\text{m}$  in diameter at the same time point. As myocardium-derived cells are terminally differentiated and proliferation-inert corresponding myocardial microtissues show an invariant size/time profile when cultivated for a period of several days. Pure NRC cultures as well as mixed NRC populations reflecting the cell type composition of rodent heart produce myocardial microtissues of comparable size ( $130 \pm 11 \mu\text{m}$ ). Since the overall size of myocardial microtissues is a direct function of the proliferation-incompetent cardiomyocyte cell number it can be varied over a wide range (NRC:  $130 \pm 11 \mu\text{m} - 230 \pm 11 \mu\text{m}$ ; NMC  $170 \pm 12 \mu\text{m} - 320 \pm 19 \mu\text{m}$ ) by adjusting the concentration of the cell suspension between 1'200 to 10'000 cells/hanging drop (Figure 2).

NRC-derived microtissues started rhythmic contraction 48 h after addition of phenylephrin, which could be maintained for over three weeks. A video motion of



contracting mouse and rat myocardial microtissue can be accessed at <http://www.biotech.biol.ethz.ch/martinf/staff/jens.html>. Myocardial spheroids rapidly synchronized their beating frequencies upon inter-microtissue contacts, which exemplifies the capacity of myocardial microtissues to form functional tissue interactions. In contrast to NRC-derived microtissues, NMC-based myocardial spheroids initiate sustained contraction in the absence of any chemical stimuli following aggregation.

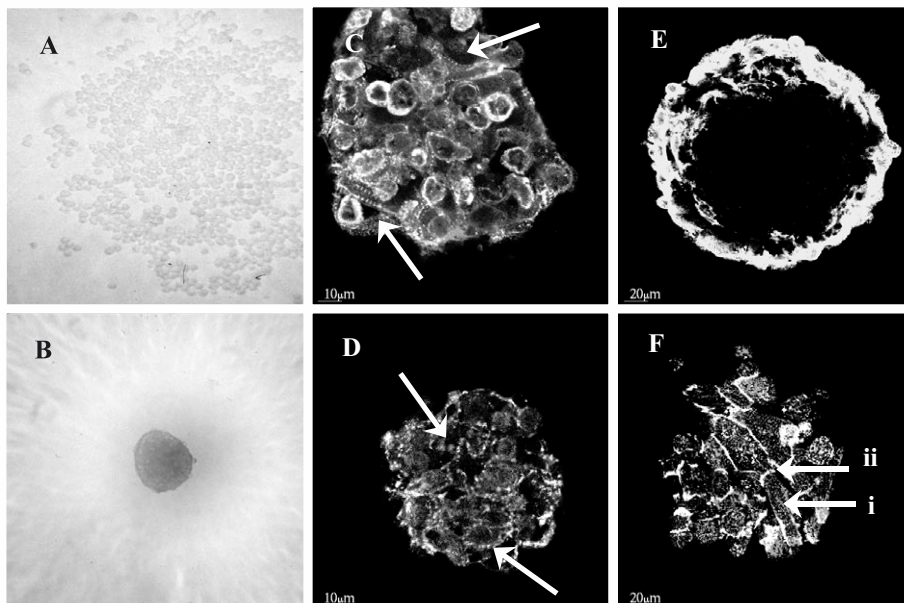


*Figure 1. Generation of a myocardial microtissue in hanging drops after 1 day (A) and 4 days (B). Immunohistological characterization of seven-days-old neonatal rat (NRC; D), mouse (NMC; C) myocardial microtissues as well as NRC-coated fibroblast feeder spheroids (E, F). (A-C). Striation of cardiomyocytes was visualized by staining sarcomeric alpha-actinin indicated by the arrows (C; D; E; Fi). Cell-cell contacts were visualized by  $\square$ -catenin staining (Fii).*

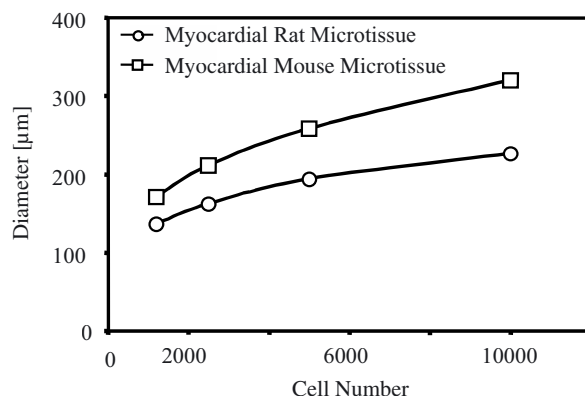


Figure 2. Cell number-size correlations of NRC and NMC-derived myocardial microtissues cultivated for four days in hanging drops. Since NRC's as well as NMC's are proliferation-incompetent, the microtissue size is a function of the initial cell concentration inoculated in the hanging drop.

#### Characterization of Myocardial Microtissues

*In vitro* generation of three-dimensional heart structures from isolated cardiomyocytes requires maintenance of shape and myofibrils while keeping the mechanical flexibility. Also, electrical continuity between the cells has to be maintained by intercalated disks, specialized cell-cell junctions, which are abundant in heart structures. We have used a combination of immunofluorescence labeling and confocal microscopy to characterize whether cardiomyocytes retained *in vivo*-like morphology when grown as myocardial microtissues. In NRC- and NMC-derived myocardial microtissues striation of myofibrils could be observed (Figure 1C; D). Also,  $\beta$ -catenin-specific expression throughout the entire myocardial microtissues indicates tissue-like cell-cell interactions within these myocardial spheroids while individual cells retain their typical cell morphologies associated with mature cardiomyocytes.

Similarly, cardiomyocytes coated directly onto a feeder spheroid assembled from myocardial fibroblasts, the cardiomyocytes were evenly distributed on the surface, showed intact cell-cell contacts as evidenced by  $\beta$ -catenin staining and demonstrated characteristic orientated rod-shaped morphology as well as intercalated discs (Figure 1E; F).

As the extracellular matrix is an important modulator of differentiation we analyzed the composition of the ECM in myocardial microtissue compared to monolayer cardiomyocytes. Differences could be observed in Collagen I and IV expression, which could be detected solely in microtissues whereas fibronectin and laminin were observed in both cultivation types (data not shown).

Rational generation of artificial tissues beyond a certain size as well as their connection to the host capillary system following implantation requires vascularization [10]. Therefore, we have analyzed vascular endothelial growth factor (VEGF) expression, a potent inducer of angiogenesis, which is induced under hypoxic conditions [11], in cardiomyocyte monolayers and myocardial microtissues. Whereas NRC's cultivated in monolayers and myocardial microtissues up to  $130 \pm 11 \mu\text{m}$  in diameter show no VEGF expression, oversized ( $230 \pm 11 \mu\text{m}$  in diameter) myocardial microtissues assembled from produce this growth factor at high levels suggesting hypoxic conditions inside the spheroid. Similar results were obtained with NMC's cultivated as monolayers and microtissues (Figure 3).

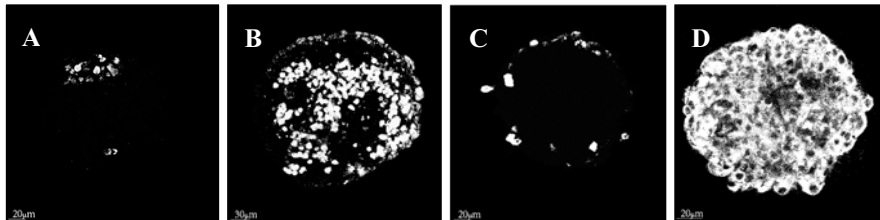


Figure 3. VEGF (vascular endothelial growth factor) -specific immunostaining of neonatal rat (C; D) and mouse (A, B) myocardial microtissues. Myocardial microtissue produced from 1'200 NRCs (A,  $130 \mu\text{m}$  in diameter) and NMC's (B,  $170 \mu\text{m}$  in diameter) show only low level VEGF expression. By contrast, VEGF-specific immunostaining of oversized myocardial microtissue produced from 10'000 NRC's and NMC's (NRC:  $230 \mu\text{m}$  in diameter; NMC:  $320 \mu\text{m}$ ) display increased VEGF expression.

#### Lentiviral Transduction

Therapeutic interventions in mammalian tissues and artificial organs require an efficient DNA transfer technology. We have assessed the potential of third-generation self-inactivating lentiviral particles encoding either the enhanced yellow fluorescent protein (EYFP; pMF351,  $5'LTR-\psi^+-P_{hCMV}-EYFP-3'LTR_{\Delta U3}$ ; [12]) or the secreted  $\alpha$ -amylase (SAMY; pMF364,  $5'LTR-\psi^+-P_{EF1\alpha}-SAMY-3'LTR_{\Delta U3}$ ; [13]) under control of the human  $P_{hCMV}$  or  $P_{EF1\alpha}$  promoters to transduce cardiomyocyte monolayers as well as NRC-derived myocardial microtissues.

In order to assess the specific heterologous protein production capacity of mammalian cells grown in monolayers and microtissues, freshly isolated NRCs and ERCs (embryonic rat cardiomyocytes) were transduced with SAMY-encoding lentiviral particles. Whereas the monolayer culture produced respectable  $5 \mu\text{U}/\text{cell}$   $\alpha$ -amylase NRCs assembled in myocardial microtissues secreted over 6-fold more SAMY per cell. Owing to their high ectopic protein production capacity microtissues may eventually become as valuable for *in vivo* delivery of protein therapeutics in gene therapy scenarios as for tissue engineering/replacement therapies.

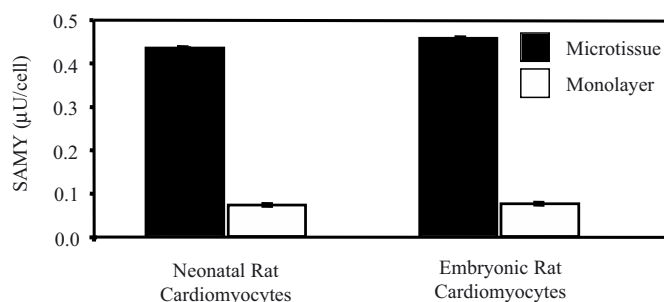


Figure 4. Quantification of SAMY production of 1'200 NRCs and ERC's (embryonic rat cardiomyocytes) transduced with pMF364 (5'LTR- $\psi^+$ -P<sub>EF1 $\alpha$</sub> -SAMY-3'LTR <sub>$\Delta$ U3</sub>)-derived SAMY (secreted  $\alpha$ -amylase)-encoding lentiviral particles followed by four-day maintenance in monolayer cultures or hanging drop cultures to form myocardial microtissues.

#### REFERENCES

1. Claycomb, W., Proliferative potential of the mammalian ventricular cardiac muscle cells, in The development and regenerative potential of cardiac muscle, J.A. Oberpiller, M.A., Editor. 1991, Harwood Academic: New York. p. 351-362.
2. Akins, R.E., Can tissue engineering mend broken hearts? *Circ Res*, 2002. 90(2): p. 120-2.
3. Dar, A., et al., Optimization of cardiac cell seeding and distribution in 3D porous alginate scaffolds. *Biotechnol Bioeng*, 2002. 80(3): p. 305-12.
4. Eschenhagen, T., et al., Three-dimensional reconstitution of embryonic cardiomyocytes in a collagen matrix: a new heart muscle model system. *Faseb J*, 1997. 11(8): p. 683-94.
5. Yang, S., et al., The design of scaffolds for use in tissue engineering. Part I. Traditional factors. *Tissue Eng*, 2001. 7(6): p. 679-89.
6. Sperlakis, N., Cultured heart cell reaggregate model for studying cardiac toxicology. *Environ Health Perspect*, 1978. 26: p. 243-67.
7. Kelm, J.M., Timmins, N., Brown, C.J., Fussenegger, M., Nielsen, L.K., An efficient cultivation method to generate homogeneous multicellular tumor spheroids that can be applied to a wide variety of cell types. *Biotechnol Bioeng*, 2003, in press.
8. Boheler, K.R., et al., Differentiation of pluripotent embryonic stem cells into cardiomyocytes. *Circ Res*, 2002. 91(3): p. 189-201.
9. Auerbach, D., et al., Different domains of the M-band protein myomesin are involved in myosin binding and M-band targeting. *Mol Biol Cell*, 1999. 10(5): p. 1297-308.
10. Griffith, L.G. and G. Naughton, Tissue engineering--current challenges and expanding opportunities. *Science*, 2002. 295(5557): p. 1009-14.
11. Maulik, N. and D.K. Das, Potentiation of angiogenic response by ischemic and hypoxic preconditioning of the heart. *J Cell Mol Med*, 2002. 6(1): p. 13-24.
12. Mitta, B., Rimann, M., Ehrbar, M., Djonov, V., Ehrenguber, M.U., Kelm, J., Fussenegger, M., Advanced modular self-inactivating lentiviral expression vectors for multigene interventions in mammalian cells and in vivo transduction. *Nucleic acids research*, 2002.
13. Schlatter, S., et al., SAMY, a novel mammalian reporter gene derived from *Bacillus stearothermophilus* alpha-amylase. *Gene*, 2002. 282(1-2): p. 19-31.

## QUESTIONS AND ANSWERS

**Hitto Kaufmann, Walter and Eliza Hall Institute of Medicine, Australia:**

A general question regarding viability of the cells. Is there anything known about the cell death mechanisms of the cells in these droplets, is apoptosis or necrosis occurring ? Does this depend on the size of the droplets ?

**Jens Kelm, Institute of Biotechnology, ETH-Zurich, Switzerland:**

We have not evaluated if the cells were becoming apoptotic after a while, but as we see that the VEGF secretion is induced only in large-sized tissues (up to a size of 200-250  $\mu\text{m}$  in diameter) and we can maintain the myocardial microtissues for over three weeks in culture while still contracting, I do not think the cells undergo apoptosis.

**Nesredin Mussa, Lonza Biologics, UK:**

It is very interesting to see how you increase the size of the cells. My question refers to alpha-actinin. Did you compare the structure of alpha-actinin in your culture to the structure of *in vivo*-extracted alpha-actinin ?

**Jens Kelm, Institute of Biotechnology, ETH-Zurich, Switzerland:**

We use alpha-actinin mainly to visualize the spheroid and the location of the cardiomyocytes, we have not done any comparison of the alpha-actinin cytoskeleton of our *in vitro*-generated tissues compared to the *in vivo* situation.

**Juergen Lehmann, University of Bielefeld, Germany:**

If you use the hanging drop technology over a long time you may need to renew the medium, how is the technology for this ?

**Jens Kelm, Institute of Biotechnology, ETH-Zurich, Switzerland:**

If you use very large-sized microtissues of 10'000 cells the medium will last for about 10 to 15 days. This time span is long enough to generate those microtissues. After you have generated those microtissues you can harvest them and you continue to cultivate them in non-adhesive culture dishes, so that there will be no nutrient limitations.

H. R. BOHNENKAMP AND T. NOLL

## PROCESS DEVELOPMENT FOR STANDARDIZED GENERATION OF MONOCYTE-DERIVED DENDRITIC CELLS: APPLICABILITY IN BREAST CANCER IMMUNOTHERAPY

*Institute of Biotechnology 2, Forschungszentrum Jülich GmbH, 52425  
Jülich, Germany; h.bohnenkamp@fz-juelich.de*

**Abstract.** There is increasing interest in the generation of dendritic cells (DC) for cancer immunotherapy. In order to utilize DC in clinical trials the necessity of standardized, reproducible and easy to use protocols are the matter of interest. We describe here the process development for the generation of DC as the result of investigation of culture conditions as well as consumption rates of medium and cytokines. Furthermore we compared cells from healthy donors and breast cancer patients. Our studies demonstrate that highly viable DC (94±2%) can be produced from CD14<sup>+</sup> monocytes enriched via immunomagnetic beads in a high yield (28±6%) with X-VIVO 15, 400 U/mL GM-CSF and 2000 U/mL IL-4 without serum and feeding. For maturation different cocktails (TNF- $\alpha$ , IL-1 $\beta$ , IL-6, PGE<sub>2</sub> and TNF- $\alpha$ , PGE<sub>2</sub>) were compared. The cells expressed typical surface molecules of mature DC and induced high proliferative response in mixed lymphocyte reactions which led to IFN- $\gamma$  producing T-lymphocytes. DCs from breast cancer patients were found similar to those from healthy donors. These data suggest that the using of this optimized protocol result in highly mature DC suitable for clinical application.

### 1. INTRODUCTION

The use of dendritic cells as potent stimulators for immunotherapeutic vaccination of cancer is a very promising approach to overcome the tumour escape in immune surveillance (Costello et al., 1999). To date, several clinical trials have been performed utilizing DC preparations, which demonstrated anti-tumour responses (Nestle et al., 1998; Thurner et al., 1999; Kikuchi et al., 2001; Kobayashi et al., 2001). Mainly monocyte derived DC were used because they are easy to obtain after enrichment of monocytes by magnetic separation or adherence, followed by differentiation using GM-CSF and IL-4 (Romani et al., 1994; Sallusto and Lanzavecchia, 1994). For studies where DCs are to be cultured ex vivo and then reintroduced to the patient, it is advisable to avoid fetal calf serum or any kind of foreign antigen due to possible infections and immunogenicity. However, the use of autologous serum or plasma may cause non-standardized cultivation conditions and so is best to avoid.

Here we describe the development of a standardized protocol, which circumvents the disadvantages of non-uniform culture conditions caused by supplemented serum, non-defined cell densities and adherence steps. Furthermore, the protocol eliminates the need for feeding the cells, which increases the risk of contamination. In this

study we have examined the influence of several important cultivation parameters to optimize and setup the serum-free generation of DC in X-VIVO 15. Cell density, GM-CSF and IL-4 concentration, medium components like glucose, lactate and amino acids were assessed. Moreover the influence of different maturation cocktails (TNF- $\alpha$ , IL-1 $\beta$ , IL-6, PGE<sub>2</sub> and TNF- $\alpha$ , PGE<sub>2</sub>) on the maturation status of DC was investigated. This protocol was transferred to clinical application by using cells from breast cancer patients of different clinical stages. The generated moDCs were found similar to those from healthy donors indicating the suitability of the developed protocol.

## 2. MATERIALS AND METHODS

Cells:	mononuclear cells from peripheral blood of healthy donors and breast cancer patients
Isolation of cells:	Ficoll density gradient followed by Miltenyi MACS CD14 <sup>+</sup> enrichment
Culture Medium:	X-VIVO 15 (Bio Whittaker)
Cytokines:	rhuGM-CSF (Leucomax <sup>TM</sup> , Novartis), rhuIL-4, rhuTNF- $\alpha$ , rhuIL-1 $\beta$ , rhuIL-6 (all from R&D), PGE <sub>2</sub> (Sigma) and rhuIL-2 (from BHK 21 cells, kindly provided by Dr. Wagner, GBF)
Cytokine analysis:	enzyme linked immunosorbent assay (ELISA, Becton Dickinson), ELISpot (IFN- $\gamma$ , R&D), cytometric bead array (Beckton Dickinson)
Cell analysis:	Flow cytometer (FACSCalibur, Becton Dickinson) Mixed lymphocyte reaction, phagocytosis, wash-out test

## 3. RESULTS

### 3.1. Bioprocess development

#### 3.1.1. Cell density

To investigate different cell densities  $3.3 \cdot 10^5$ ,  $6.6 \cdot 10^5$ ,  $1.3 \cdot 10^6$  and  $2.6 \cdot 10^6$  monocytes mL<sup>-1</sup> were inoculated and cultivated in X-VIVO 15 supplemented with 800 U mL<sup>-1</sup> GM-CSF and 500 U mL<sup>-1</sup> IL-4 for 6 days. For 2 additional days a maturation cocktail (TNF- $\alpha$ : 1000 U mL<sup>-1</sup>, IL-1 $\beta$ : 1000 U mL<sup>-1</sup>, IL-6: 1000 U mL<sup>-1</sup>, PGE<sub>2</sub>: 1  $\mu$ g mL<sup>-1</sup> (0.003  $\mu$ M)) was added. No significant differences in yield and phenotype have been observed between a cell density of  $3.3 \cdot 10^5$  and  $1.3 \cdot 10^6$  mL<sup>-1</sup>, while  $2.6 \cdot 10^6$  mL<sup>-1</sup> resulted in a 25% lower cell number and a reduced HLA-DR, CD80, CD86 and CD83 expression. Metabolic analysis showed an increase in lactate concentration at the highest cell density at  $\geq 25$  mmol L<sup>-1</sup> which caused a decreased culture pH and might be responsible for the lower yield. Accumulation of

metabolic products like lactate produces an acidic environment and therefore inhibits proliferation (Carswell and Papoutsakis, 2000; Bohnenkamp and Noll, 2002). Due to a cost-effective utilization of the cultivation system in terms of highest yield of matured moDC per volume, all further experiments were performed at a cell density of  $1.3 \cdot 10^6 \text{ mL}^{-1}$  inoculated monocytes.

### 3.1.2. GM-CSF and IL-4 concentration

Before determination of the necessary cytokine concentration a stability test was done. Vials containing medium and cytokines were incubated at  $37^\circ\text{C}$  and 5%  $\text{CO}_2$  for 8 days. Both cytokines remained stable during the investigated period of time. The GM-CSF concentration was tested using 200, 400 and  $800 \text{ U mL}^{-1}$  while the IL-4 concentration remained at  $500 \text{ U mL}^{-1}$ . For 400 and  $800 \text{ U mL}^{-1}$  yield and phenotype was comparable to the previous experiment.  $200 \text{ U mL}^{-1}$  GM-CSF resulted in the same number of DCs but in a lower expression of CD80, CD83 and CD86. A GM-CSF ELISA showed that the  $200 \text{ U mL}^{-1}$  were exhausted completely while in the other two experiments about  $300 \text{ U mL}^{-1}$  were consumed ( $296 \text{ U mL}^{-1}$  and  $320 \text{ U mL}^{-1}$  respectively).

In an experimental setup, similar to that described above, IL-4 concentrations of 500, 1000 and  $2000 \text{ U mL}^{-1}$  have been compared. The GM-CSF concentration remained at  $800 \text{ U mL}^{-1}$ . The IL-4 ELISA indicated that only at an initial concentration of  $2000 \text{ U mL}^{-1}$  the IL-4 was not limiting, as we could still measure  $25 \text{ U mL}^{-1}$  after 8 days of cultivation and phenotypic analysis showed a homogenous population of matured moDC only for the highest IL-4 concentration. However, yield and viability of DCs was found similar with all concentrations.

### 3.1.3. Maturation cocktails

To simplify the used maturation cocktail containing the four cytokines: TNF- $\alpha$ :  $1000 \text{ U mL}^{-1}$ , IL-1 $\beta$ :  $1000 \text{ U mL}^{-1}$ , IL-6:  $1000 \text{ U mL}^{-1}$  and PGE<sub>2</sub>:  $1 \mu\text{g mL}^{-1}$  ( $0.003 \mu\text{M}$ ), we analyzed a cocktail consisting of just two: TNF- $\alpha$ :  $1000 \text{ U mL}^{-1}$  and PGE<sub>2</sub>:  $18 \mu\text{g mL}^{-1}$  ( $0.054 \mu\text{M}$ ). We found in 12 experiments similar results in yield, viability and phenotype for both cocktails.

## 3.2. Immunobiological analysis

### 3.2.1. Phenotype

Using the optimized cultivation parameters ( $1.3 \cdot 10^6$  monocytes  $\text{mL}^{-1}$ ,  $400 \text{ U mL}^{-1}$  GM-CSF,  $2000 \text{ U mL}^{-1}$  IL-4, no feeding), determined in the prior experiments, generation of moDC in  $75 \text{ cm}^2$  T-flasks has been performed. No difference was observed regardless of the cultivation system. The mean yield as calculated from inoculated CD14<sup>+</sup> monocytes was  $28 \pm 6\%$  with a mean viability of  $94 \pm 2\%$  ( $n = 6$ ). Figure 1 indicates the mean percentage of positive dendritic cells for important



surface antigens like HLA-DR, HLA-A,B,C, costimulatory molecules like CD40, CD80 and CD86, the intracellular adhesion molecule (ICAM-1) CD54 and the standard maturation marker CD83.

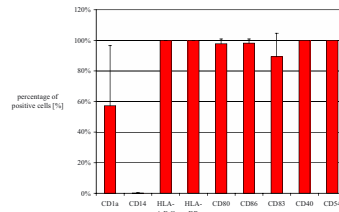


Figure 1. Phenotype of moDC generated with the optimized protocol. Illustrated are results as mean ( $\pm$ SD) from six independent experiments.

### 3.2.2. Phagocytosis

The phagocytosis capacity of immature and matured moDCs were analysed using fluorescence-labeled latex beads (2  $\mu$ m). Dendritic cells were incubated for 2h and 20h at 37°C and 5% CO<sub>2</sub>. Immature dendritic cells showed a very much higher uptake of beads than matured (figure 2).

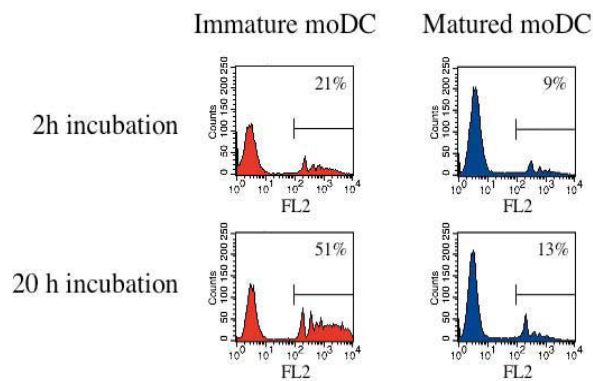


Figure 2. Uptake of fluorescence-labeled latex beads of immature and matured moDC.

### 3.2.3. Mixed lymphocyte reaction

Dendritic cells matured with TNF- $\alpha$ : 1000 U mL<sup>-1</sup>, IL-1 $\beta$ : 1000 U mL<sup>-1</sup>, IL-6: 1000 U mL<sup>-1</sup> and PGE<sub>2</sub>: 1  $\mu$ g mL<sup>-1</sup> (0.003  $\mu$ M) or TNF- $\alpha$ : 1000 U mL<sup>-1</sup> and PGE<sub>2</sub>: 18  $\mu$ g mL<sup>-1</sup> (0.054  $\mu$ M) were either cultivated with T-cells at a ratios of 1:10 in the

presence of 100 U mL<sup>-1</sup> IL-2 after 92h and 163h or incubated with T-cells at ratio of 1:5, 1:10 and 1:20 without IL-2. Determination of proliferation by counting (IL-2 cultivation) or BrdU incorporation (without IL-2 - colorimetric) showed a strong allostimulatory response.

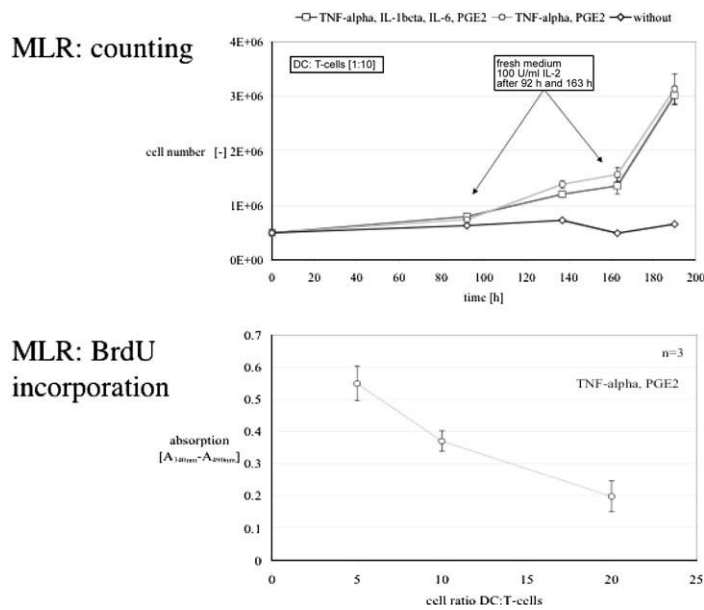


Figure 3. Mixed lymphocyte reaction: determination of T-cell proliferation by counting and by BrdU incorporation.

### 3.2.4. Cytokine profile

Supernatant after DC generation was tested for following cytokines: IL-2, IL-4, IL-5, IL-10, IL-12p70, GM-CSF, TNF- $\alpha$  and IFN- $\gamma$ . Supernatant of matured dendritic cells were positive for IL-4, GM-CSF and TNF- $\alpha$ , indicating no limitation of these cytokines. IL-10 could be found in low amounts ( $\leq 35$  pg mL<sup>-1</sup>) while IL-12p70 could not be determined (detection limit  $\leq 5$  pg mL<sup>-1</sup>) after 8 days of cultivation.

Using an IFN- $\gamma$  secretion assay and CD25 staining after mixed lymphocyte reaction 66% to 72% of T-cells could be analyzed positive for the cytokine and the high affinity IL-2 receptor.

### 3.2.5. Wash-out test

After 8 days dendritic cells were inoculated in fresh medium without cytokines and incubated for one more day. Over 95% of all cells remained non-adherent, showed the same morphology and phenotype.

### 3.3. Transfer to clinical application

For the transfer to clinical application blood samples from 8 different breast cancer patients were used. Following the setup of the optimized protocol dendritic cells were generated resulting in same yield, viability and phenotype than in prior experiments with healthy donors.

## 4. ACKNOWLEDGEMENTS

The authors gratefully acknowledge J. Taylor-Papadimitriou and J. Burchell (Cancer Research UK, Breast Cancer Biology Group, Guy's Hospital) for their support and help. We also like to thank B. Schwartzkopff for performing medium analysis and cytokine ELISA and C. Herfurth for amino acids analysis.

## 5. REFERENCES

- Bohnenkamp, H.R. and Noll, T. (2002) Bioprocess development for the cultivation of human T-lymphocytes in a clinical scale. *Cytotechnology* 38, 135.
- Carswell, K.S. and Papoutsakis, E.T. (2000) Extracellular pH affects the proliferation of cultured human T cells and their expression of the interleukin-2 receptor. *J Immunother* 23, 669-74.
- Costello, R.T., Gastaut, J.A. and Olive, D. (1999) Tumor escape from immune surveillance. *Arch Immunol Ther Exp* 47, 83-8.
- Kikuchi, T., Akasaki, Y., Irie, M., Homma, S., Abe, T. and Ohno, T. (2001) Results of a phase I clinical trial of vaccination of glioma patients with fusions of dendritic and glioma cells. *Cancer Immunol Immunother* 50, 337-44.
- Kobayashi, T., Shinohara, H., Toyoda, M., Iwamoto, S. and Tanigawa, N. (2001) Regression of lymph node metastases by immunotherapy using autologous breast tumor-lysate pulsed dendritic cells: report of a case. *Surg Today* 31, 513-6.
- Nestle, F.O., Aljagic, S., Gilliet, M., Sun, Y., Grabbe, S., Dummer, R., Burg, G. and Schadendorf, D. (1998) Vaccination of melanoma patients with peptide- or tumor lysate-pulsed dendritic cells. *Nat Med* 4, 328-32.
- Romani, N., Gruner, S., Brang, D., Kampgen, E., Lenz, A., Trockenbacher, B., Konwalinka, G., Fritsch, P.O., Steinman, R.M. and Schuler, G. (1994) Proliferating dendritic cell progenitors in human blood. *J Exp Med* 180, 83-93.
- Sallusto, F. and Lanzavecchia, A. (1994) Efficient presentation of soluble antigen by cultured human dendritic cells is maintained by granulocyte/macrophage colony-stimulating factor plus interleukin 4 and downregulated by tumor necrosis factor alpha. *J Exp Med* 179, 1109-18.
- Thurner, B., Haendle, I., Roder, C., Dieckmann, D., Keikavoussi, P., Jonuleit, H., Bender, A., Maczek, C., Schreiner, D., von den Driesch, P., Brocker, E.B., Steinman, R.M., Enk, A., Kampgen, E. and Schuler, G. (1999) Vaccination with mage-3A1 peptide-pulsed mature, monocyte-derived dendritic cells expands specific cytotoxic T cells and induces regression of some metastases in advanced stage IV melanoma. *J Exp Med* 190, 1669-78.

## QUESTIONS AND ANSWERS

**Martin Fussenegger, ETH-Zürich, Switzerland:**

In one of your slides you mentioned magnetic beads separation of monocytes. Is there a particular reason for that ?

**Hermann Bohnenkamp, Forschungszentrum Jülich, Germany:**

There are a couple of reasons, especially that you can easily analyse six different cytokines at once, in one specimen of about 50 µl, and this is also easier to analyse in the computer after the FACS analysis. Otherwise you have to do a lot of ELISA tests to get the same results. So we use this technology simply because it is easier.

**Diana Schuhbauer, Hoffmann La Roche, Basel, Switzerland:**

I have a question regarding the cytokine profile from the dendritic cells, that you showed in your last slide. If you said that they are only producing IL-10, if you want to use them in breast cancer, then you would prefer to have dendritic cells actually stimulating the TH1 or CTL pathway ?

**Hermann Bohnenkamp, Forschungszentrum Jülich, Germany:**

IL-10 is also present at a very low amount, that means 35 picograms/mL if we use this very high cell density, and I would wonder if such low amounts would do anything.

**Alain Miller, Celltech:**

In your FACS analysis you showed high expression of dendritic markers, I wonder what is your negative control there ?

**Hermann Bohnenkamp, Forschungszentrum Jülich, Germany:**

As a negative control we compared with immature dendritic cells and of course with monocytes, you can analyse them and see the difference in expression between immature and mature dendritic cells, and the second is the mean fluorescence intensity increase with the HLA-A,B,C and HLA-DR, but as well you have of course to make lymphocyte reactions for the control to check the stimulation of T-cells.

S.L. LEUGERS, D.W. ALLISON, B.J. PRONOLD,  
G. RENNEBECK, G. VAN ZANT, J.D. TARIO, JR.,  
F.J. SWARTZWELDER , AND L.M. DONAHUE

STEMLINE™ HEMATOPOIETIC STEM CELL  
EXPANSION MEDIUM, A SERUM-FREE MEDIUM  
FOR THE EXPANSION OF CD34<sup>+</sup> HEMATOPOIETIC  
STEM CELLS AND PROGENITORS

<sup>1</sup>Cell Culture, Sigma-Aldrich, St. Louis, MO, United States, <sup>2</sup>University of  
Kentucky, College of Medicine, Markey Cancer Center, Lexington, KY,  
United States. <sup>3</sup>Stemgenix, Amherst, NY, United States.

## 1. INTRODUCTION

Hematopoietic stem cells (HSC) have the ability to repopulate the hematopoietic system by differentiating into all of the necessary erythroid, lymphoid, and myeloid lineages. Due to this rare ability, HSC are used as therapeutic agents in the treatment of malignant and benign diseases of the blood forming and immune systems. There have been many advances in the area of clinical HSC research, but the availability of suitable cells for transplantation still remains a major limiting factor.

HSC can be isolated from three different sources: umbilical cord blood (CB), bone marrow, and mobilized peripheral blood. CB is currently the preferred source because it has been shown to have a lower risk of graft versus host disease (GVHD), presumably due to its immunological naiveté. However, because the volume of CB is limited, each umbilical cord has only enough cells to successfully transplant a small child. In order to transplant an adult, the HSC from CB must be expanded *ex vivo*. The expansion must be performed in a manner to ensure that the HSC not only differentiate along appropriate hematopoietic lineages, but also self-renew, leaving undifferentiated stem cells in the expanded culture. In order to expand these very specific cell types, an optimized serum-free medium and cytokine cocktail are needed.

To this end, Stemline™ Hematopoietic Stem Cell Expansion Media were developed for the expansion of HSC. They are serum-free media that allow for expansion of both differentiated and undifferentiated HSC. Stemline™ and Stemline™ II are both able to expand HSC from CB, bone marrow, and mobilized peripheral blood. In bench-scale and clinical-scale expansions, both media have

shown promising results in expanding a mixed population of cells that remain fully functional.

## 2. MATERIALS AND METHODS

Cell Preparation. For all experiments, cryopreserved, human CD34<sup>+</sup> cells were obtained from independent suppliers (Stemgenix; AllCells, LLC) and were handled in a manner consistent with the supplier's instructions with regard to storage and reconstitution.

Serum-Free Expansion Medium Preparation. Stemline™ Hematopoietic Stem Cell Expansion Media (Sigma-Aldrich; also marketed as HSC GEM™ (Stemgenix)), X-VIVO-15 (BioWhittaker), HPGM (BioWhittaker), QBSF-60 (Quality Biological), StemPro-34 (Life Technologies), and StemSpan H3000 (Stem Cell Technologies) were purchased fresh and stored according to the manufacturer's recommendations. One ml of each medium was pipetted in triplicate in 24-well culture plates to which SCF, TPO and G-CSF were added to a final concentration of 100 ng/ml each. CD34<sup>+</sup> cells were added to each well at  $1.0 \times 10^4$  cells/ml and allowed to proliferate in a humidified incubator at 37°C and 5% CO<sub>2</sub> for 10-14 days.

Flow Cytometry. Cells were stained with CD34-FITC and CD38-PE (Becton Dickinson). Single color controls were used to set the color compensation and PI was included to determine cell viability. 50,000 events were collected for each sample on a BD FACScan.

Clinical-Scale Expansion. A 2-step, clinical-scale assay (McNiece, et al., *Experimental Hematology* 2000. 28: 1181-1186) was set up for a comparison study between Stemline™ and Stemline™ II.

## 3. DISCUSSION

Stemline™ media were developed for the ex vivo expansion of hematopoietic stem cells from cord blood, mobilized peripheral blood, and bone marrow. Stemline™ media expand CD34<sup>+</sup> cells from all three sources better than other commercially available, serum-free HSC media. Figure 1 is a representative graph of a bench-scale expansion of CD34<sup>+</sup> cells from cord blood. As demonstrated in Figure 1, Stemline™ expands CD34<sup>+</sup> cells from CB better than or equal to the other HSC media. Stemline™ II is a newer version of the medium that demonstrates an increased expansion potential for CD34<sup>+</sup> cells. Similar results have been seen for several CB, mobilized peripheral blood, and bone marrow donors (data not shown).

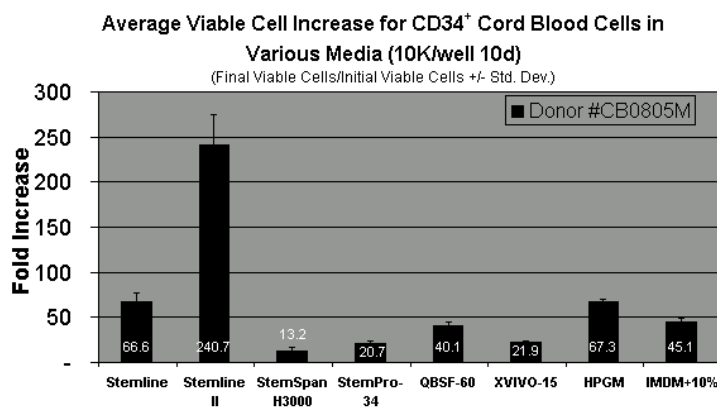


Figure 1: Expansion of CD34<sup>+</sup> cells from cord blood in Stemline<sup>TM</sup> and Stemline<sup>TM</sup> II compared to other commercially available, serum-free, HSC media.

To further determine the media's potential for expanding CD34<sup>+</sup> cells, a two-step clinical-scale expansion was performed using both Stemline<sup>TM</sup> and Stemline<sup>TM</sup> II. Figure 2 (left) illustrates the fold increase of total nucleated cells after 14 days in culture. Both media are able to expand CD34<sup>+</sup> cells, but Stemline<sup>TM</sup> II has an increased expansion potential (approximately 2X) as demonstrated in figure 2. This increased expansion is necessary in the early stages of a transplant to ensure its success.

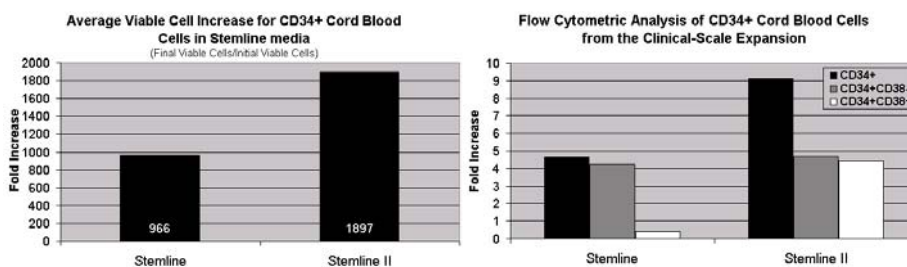


Figure 2: (Left) Comparison of Stemline<sup>TM</sup> to Stemline<sup>TM</sup> II in a clinical-scale expansion of CD34<sup>+</sup> cells from cord blood. (Right) Flow cytometric analysis on CD34<sup>+</sup> cord blood cells from clinical-scale expansion.

After expansion, the cells were characterized using flow cytometry (Figure 2, right) and colony-forming unit assays (data not shown). Testing the functionality of the expanded cells is important in order to determine if the cell population is a mix of early and late progenitors that will ensure a successful transplantation. The cells were analyzed for expression of CD34 and CD38. Flow cytometric analyses of the

clinical-scale expansions reveal that Stemline™ and Stemline™ II expand comparable numbers of early progenitor cells (CD34<sup>+</sup>/CD38<sup>-</sup>). Stemline™ II also has the additional benefit of a higher capacity for the expansion of the CD34<sup>+</sup>/CD38<sup>+</sup> late progenitors required for short-term engraftment. NOD/SCID mouse studies are also underway in order to determine the long-term engraftment potential of the expanded cells.

The excellent performance of the Stemline™ media for the expansion and maintenance of functionality of CD34<sup>+</sup> cells makes both media superior to all other commercially available, serum-free, HSC media. Additionally, Stemline™ media have Device Master Files (DMF) and are formulated in a state-of-the-art cGMP facility making them well suited for clinical applications.



M. BENSELLAM, C. BASSENS, M. TOALLATI, S. LOWAGIE,  
AND J. WERENNE

## MESENCHYMAL STEM CELLS: A VERY FIRST STEP TOWARDS LARGE SCALE CELL CULTURE STRATEGIES.

*Laboratory of Animal Cell Biotechnology, Department of Bioengineering,  
Faculty of Sciences, Université Libre de Bruxelles, Brussels, Belgium.*

**Abstract :** The aim of the project for which the present work is a very first step is to define cell culture conditions and devices that increase the ability of mesenchymal stem cells (MSC) to proliferate *in vitro*. Adhesion, mobility and growth of the cells on different microcarriers were tested in different conditions in order to select the most appropriate strategy to scale-up production for future cell therapy

### 1. INTRODUCTION

Recent studies (1,2) demonstrated that mesenchymal stem cells (MSC) derived from mesoderm could differentiate into cells of the the germ layers (ecto- and endoderm), showing therefore a previously unexpected "plasticity". In particular, MSC can differentiate into neurons.

As MSC proliferate extensively *in vitro* without obvious senescence or loss of differentiation potential, they may be an ideal source for therapy of inherited or degenerative neurological diseases including spinal cord injury.

One of the numerous challenges of cell-based tissue engineering strategies is to expedite the delivery of large number of progenitor cells (of the order of 500 million cells) to the repair and/or regeneration site. The aim of the project for which the present work is a very first step is to define cell culture conditions and devices that increase the ability of MSC to proliferate *in vitro* so that they can be used as a sufficient source of tissue for transplantation. The final goal of this approach will be the development of a process to produce adult MSC cells at large scale in conditions where differentiation potentialities can be maintained .

### 2. MATERIAL AND METHODS

Early passages of the cells used ( kindly supplied by Dr B. Rogister and S. Wislet), were tested for their adhesion and mobility properties on a number of relevant substratum, including different kinds of commercial microcarriers.

They were grown as it will be published elsewhere (3), essentially using DMEM with 10% of foetal calf Serum. Cells were tested as reported before briefly (4) in one series of experiments between passage 16 and 19, and further studied at

passages higher than 22 (from cells frozen at passage 17 by our suppliers). The data reported here concerned mainly studies made using Cytodex 3 at 5 mg/ml.

### 3. RESULTS

#### 3.2. MSC culture in monolayer

Using 75 cm<sup>2</sup> Tissue Culture flasks (Nunc) for MSC culture, cells of different morphological aspects and size can still be observed after passage 16-19. In some culture plates, cells are standing for long periods of time as foci of about 1000 cells without obvious multiplication after slight trypsinisation procedure. In some other culture plates cells spread on all the available surface after seeding. This indicates that some signals, that should be better studied and controlled in the future, affect the behaviour of the cells.

#### 3.3. Migration of MS cells from the monolayer

In confluent monolayers of MSC (between passage 16 and 19), added Cytodex 3 microcarriers were fully colonised in 24 to 48 hours in static conditions.

The free space left on the plate after harvesting part of the microcarriers after colonisation was slowly reoccupied in function of time by newly dividing cells. An immediate readdition of more Cytodex 3 does not lead to an immediate colonisation of the fresh beads. This indicates that either we selected some kind of cells on the first round of the migration test, or that some factors of unknown nature which were consumed in the first wave of cell migration, are necessary for the subsequent step.

#### 3.4. Transfer of colonised microcarriers to TC treated or untreated plates

After transfer to fresh 24 wells plates, depending on the case (either "TC treated" or "untreated"), one of the following observations are made:

- On "TC treated" dishes: most of the cells (at passage 16-19) were maintained on the microcarriers in the static conditions and some cells detached from the microcarriers, and spread and divide after 48 hours on the plate surface. However, up to now a long term propagation of the few cells attached to the plate after leaving microcarriers in these conditions was not obtained; cells are dying after one or two rounds of division.
- On "untreated" dishes: cells were detached readily from the microcarriers and aggregated in suspension to each other before rapidly dying. At the present time we have not investigated further what is the critical factor causing those different behaviours.

It should be mentioned that these mobility properties as observed with early passage cells are not reproduced with cells at later passages (higher than 22).

#### 4. CONCLUSIONS AND PROSPECTS

The present very first step taken towards large scale production of MSC indicate that at early passages (lower than 16-19):

- MSC attach, spread and divide on Cytodex 3.
- MSC migrate from monolayer to fresh Cytodex 3, indicating that they present very active mobility properties.
- MSC colonising microcarriers when transferred to a "TC treated dish" may leave the beads to form a new monolayer on the plate.
- The TC treated plate left free from cells after migration of an early passage monolayer to microcarriers were invaded by new dividing cells. Only one round of this propagation was observed with the cells at passage higher than 19 used for this experiment.

The observed properties provided useful information to control expansion of stem cells in the required amounts needed for cell therapy.

A careful study should however now extend our observations in order to characterize and control the differentiation state of the dividing MSC in the different steps we have taken. We should also investigate the effect of the factors affecting the different MSC behaviours observed in the different conditions studied, leading either to non dividing foci or continuously dividing monolayers.

**Acknowledgments :** We wish to thank Dr B. Rogister and S. Wislet from the University of Liège for kindly supplying to us the initial cells we used in our approach and for providing the appropriate information to establish MSC culture from rats.

#### 5. REFERENCES

- D. Woodbury, E.J. Schwarz, D. Prockop and I.B. Black, Adult rat and human bone marrow stromal cells differentiate into neurons, *J. neuroscience res.* **61**, 364-370, 2000.
- Y. Jiang, B.N. Jahagirdar, R.L. Reinhardt, R.P.E. Schwartz, C.D. Keene, X.R. Ortiz-Gonzalez, M.Reys, T. Lenvik, T Lund, M. Blackstad, J. Du, S. Aldrich, A. Lisberg, W.C. Low, D.A. Largaespada and C. Verfaillie, Pluripotency of Mesenchymal Stem Cells derived from adult marrow, *Nature*, 418, 41-49, 2002.
- S.Wislet, B. Rogister, P. Leprince and G. Moonen, *J. Cell Science*, to be published
- M. Bensellam, M. Toallati, S. Lowagie, S. Wislet, B. Rogister and J. Wérenne, BELACT Meeting, Brussels, March 2003.

BURG M., QUEL G., RUEDIGER M., ZWEIGERDT R.

## EXPANSION OF MURINE EMBRYONIC STEM CELLS ON MICROCARRIERS-FUNCTIONAL CHARACTERISTICS AND SCALE-UP POTENTIAL

*Cardion AG, Erkrath, Germany*

### 1. INTRODUCTION

Embryonic stem cells (ESC) are derived from the inner cells mass of blastocysts. They are capable of unlimited, undifferentiated proliferation in vitro (self-renewal) [1], [2] and can form various somatic cell types [3] including beta-like cells, cardiomyocytes and neural cells upon differentiation via embryoid bodies (EBs). Stem cells are of increasing importance as a potential source for cell based therapies [4]. Therefore, scalable technologies are required to provide cell sources that may be used for tissue replacement. Aim of this study was to develop a scalable bioprocess to propagate embryonic stem cells in suspension, while maintaining their pluripotentiality.

### 2. MATERIALS AND METHODS

We investigated culture and functional characteristics of J1 murine embryonic stem cells (mESC) grown in conventional monolayer culture or on microcarriers in suspension (figure 1). Cells were seeded on gelatine-coated 100mm dishes at  $2 \times 10^6$  cells in 10 ml culture volume and cultivated for 7 passages (48 h per passage) in the presence of 10% FCS and leukemia inhibitory factor (LIF) [5] (figure 2, A). Prior to cultivation on beads in stirred suspension culture a variety of microcarriers was pretested in stationary culture with regard to supporting mESC attachment and growth. Based on this analysis fibronectin-coated Cytodex 1 beads were chosen for spinner flask cultures. Spinner flasks were inoculated with 50 ml culture volume at  $2 \times 10^5$  cells/ml with or without 3 mg fibronectin-coated Cytodex 1 beads/ml. Cells were cultivated in spinner flasks (100 ml Bellco spinner vessels, 30 rpm) for 3 passages (72 h per passage). At the end of every passage cells were harvested by trypsinization and reseeded on freshly prepared microcarriers. Cell numbers were determined by trypan blue and crystal violet staining. Expression of embryonic stem cell specific markers SSEA-1 [6] and E-cadherin [7] was determined via flow cytometry. To investigate differentiation capacity of mESC, expanded on

fibronectin-coated Cytodex 1 beads, ability to form cardiomyocytes (4 days EB-formation without LIF, 5 days differentiation in gelatine-coated dishes) was tested.

### 3. RESULTS

In stirred suspension cultures without microcarriers mESC formed large aggregates resulting in poor proliferation. FACS analysis of these cultures after 3 passages revealed an extensive decrease of SSEA-1 and E-cadherin expression indicating loss of stem cell characteristics (data not shown). Formation of large aggregates was also observed in the presence of various micro-carriers tested (plastic beads, Cytodex 3, Cytodex 1 without fibronectin coating; figure 1, B). In contrast, addition of fibronectin-coated Cytodex 1 microcarriers resulted in improved adhesion of mESC to the beads and overall aggregate formation was reduced (figure 1, C). Cell densities of up to  $10^6$  cells/ml were observed in spinner cultures with fibronectin-coated Cytodex 1, resulting in a 5fold cell expansion within 72 h (figure 3, B). Such growth rates corresponded to values observed in conventional monolayer cultures (figure 3, C). Stem cell morphology and expression of SSEA-1 and E-cadherin remained unchanged over 3 passages (table 1) in suspension. Also, cells expanded on fibronectin-coated Cytodex 1 beads efficiently differentiated towards cardiomyocytes indicated by beating clusters and cardiomyocyte specific immunohistochemistry upon differentiation (data not shown).

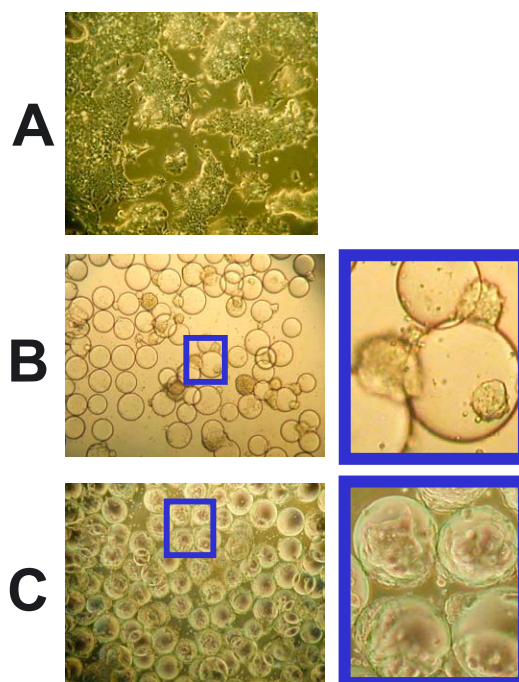


Figure 1. Microscopic analysis of mESC grown in dishes (A), on Cytodex 1 (B), and on fibronectin-coated Cytodex 1 microcarriers (C).

## 4. DISCUSSION

In summary, we have successfully established a bioprocess to propagate murine embryonic stem cells in suspension, on fibronectin-coated Cytodex 1 microcarriers. Stem cell characteristics including growth rates, expression of stem cell markers and differentiation capacity were unaltered. Scale-up of the established spinner flask process to larger bioreactor volumes deemed feasible compared to conventional monolayer cultures

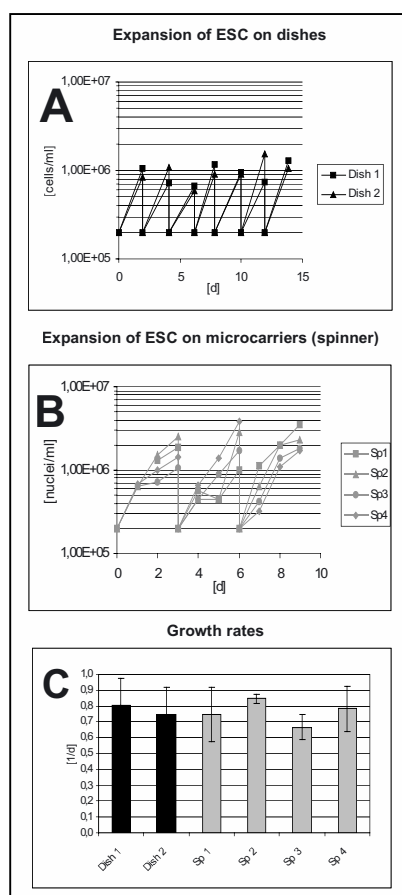


Figure 2. Growth curves (A, B) and mean growth rates (C) of J1 mESC cultures.

Table 1. Expression of embryonic stem cell specific markers SSEA-1 and E-cadherin was measured via flow cytometry

<i>Cells</i>	<i>SSEA-1</i>	<i>E-cadherin</i>
mESC (expanded in monolayer culture)	97.22%	94.42%
mESC, (expanded on microcarriers)		
Spinner 1	97.72%	89.49%
Spinner 2	98.05%	89.75%
Spinner 3	94.93%	81.58%
Spinner 4	96.35%	91.46%
mESC (5 days differentiation)	7.46%	27.73%

## 5. REFERENCES

- Evans MJ, Kaufman MH., Establishment in culture of pluripotential cells from mouse embryos. *Nature* 1981 Jul 9;292(5819):154-6
- Burdon T, Smith A, Savatier P. Signalling, cell cycle and pluripotency in embryonic stem cells. *Trends Cell Biol* 2002 Sep;12(9):432-8
- Mueller M, Fleischmann BK, Selbert S, Ji GJ, Endl E, Middeler G, Mueller OJ, Schlenke P, Frese S, Wobus AM, Hescheler J, Katus HA, Franz WM., Selection of ventricular-like cardiomyocytes from ES cells in vitro. *FASEB J* 2000 Dec;14(15):2540-8
- Thomson JA, Itskovitz-Eldor J, Shapiro SS, Waknitz MA, Swiergiel JJ, Marshall VS, Jones JM., Embryonic stem cell lines derived from human blastocysts. *Science*. 1998 Nov 6;282(5391):1145-7.
- Murray P, Edgar D., The regulation of embryonic stem cell differentiation by leukaemia inhibitory factor (LIF). *Differentiation* 2001 Oct;68(4-5):227-34
- Knowles BB, Aden DP, Solter D., Monoclonal antibody detecting a stage-specific embryonic antigen (SSEA-1) on preimplantation mouse embryos and teratocarcinoma cells. *Curr Top Microbiol Immunol* 1978;81:51-3
- Burdsal CA, Damsky CH, Pedersen RA., The role of E-cadherin and integrins in mesoderm differentiation and migration at the mammalian primitive streak. *Development* 1993 Jul;118(3):829-44

S. FARGALI, M. BARTHOLD, M. ROHDE, I. MAJORE, V. JÄGER

## IN VITRO CULTIVATION OF RABBIT MESENCHYMAL STROMAL CELLS ON 3D BIORESORBABLE CALCIUM PHOSPHATE SCAFFOLDS FOR THE GENERATION OF BONE TISSUE IMPLANTS

*German Research Centre for Biotechnology (GBF), Braunschweig*

### 1. INTRODUCTION

Bone substitution products have been identified as the major products in demand for state-of-the-art orthopaedic reconstructive surgery including spinal fusions, trauma, fracture non-unions and cranio-maxillofacial applications. One promising strategy is to use highly porous scaffold structures of bioresorbable and osteoconductive materials such as calcium phosphate ceramics for *in vitro* propagation and directed differentiation of preferably autologous osteogenic cells. These viable scaffolds are intended for subsequent implantation. As a necessary prerequisite a suitable animal critical-sized defect model has to be established. New Zealand White rabbits were chosen for that purpose and standardised protocols for the isolation and characterisation of mesenchymal stromal cells (MSCs) had to be developed including the ability of these cells to differentiate into bone tissue *in vitro*.

### 2. MATERIALS AND METHODS

All experiments were performed with cells isolated either from bone marrow of femura and tibiae of 6 weeks old female New Zealand White rabbits or from bone marrow of the femura of 4-6 week old female Wistar WKY rats. Cell proliferation was screened by WST-1 assay (Roche). DNA was quantified by Hoechst 33258 and viable cells were counted with a hemocytometer using the trypan blue exclusion method. Cell differentiation was monitored by the analysis of characteristic markers (e.g. osteocalcin ELISA or histological staining). 3D-culture was carried out on camceram calcium phosphate scaffolds with a porosity of approximately 90% and a total volume of 1 cm<sup>3</sup> in a miniaturised fixed-bed bioreactor system or static cultures. Cell attachment, proliferation and matrix formation were also followed by electron microscopy (DSM 982, Zeiss, Jena).



### 3. RESULTS AND DISCUSSION

#### 3.1 Cell Characterisation in 2D Culture

To characterise rabbit MSCs of the first four passages after isolation with regard to their potential for proliferation, differentiation and mineralisation, cells were cultured in ZKT-I basal medium containing 10% FBS and the osteogenic supplements L-ascorbic acid,  $\beta$ -glycerophosphate and dexamethasone for 30 days. All subcultures showed the typical sequence of differentiation stages with proliferation as well as development, maturation and mineralisation of extracellular matrix. Distinct nodules are formed which can be identified by staining for membrane-bound alkaline phosphatase (Fig. 1A) and by von-Kossa-staining for calcium deposition (black nodules; Fig. 1B).

#### 3.2 Effect of Different Growth Factors on *in vitro* Expanded Rabbit MSCs

To minimise the risk of virus contamination and immune response after implantation, the use of serum-free or serum-reduced media for rabbit MSCs is preferable. Rabbit MSCs were grown in different culture media supplemented with recombinant growth factors, hormones, vitamins and two different sera (FBS and rabbit serum) in the presence of osteogenic supplements as mentioned above. After 5 days of culture the proliferation of cells was measured. The best performance was achieved in ZKT-I supplemented with PDGF-bb, b-FGF, EGF, insulin, transferrin, and albumin. Epidermal growth factor (EGF) was showing the strongest synergistic effect as a mitogenic factor in combination with other cytokines. Cells with a typical elongated, spindle-shaped morphology of mesenchymal progenitor cells were found (Fig. 1C). FBS was shown to be superior to rabbit serum, since the presence of higher concentrations of rabbit serum supported also differentiation into adipocytes.

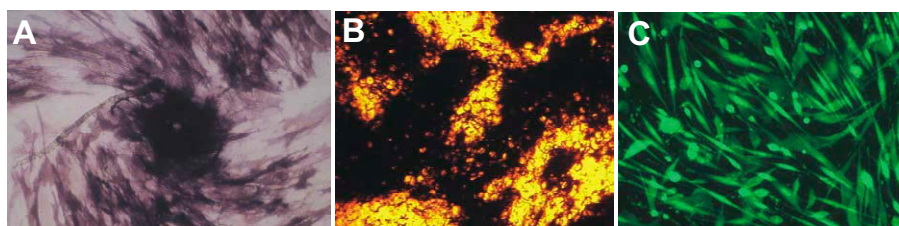


Figure 1. Fixed cells on 48-well plates 18 days post confluence stained either for membrane-bound alkaline phosphatase (A) or calcium (von-Kossa-staining) (B). Viable osteogenic progenitor cells were fluorescence-stained with the LIVE/DEAD kit (Molecular Probes) (C).

### 3.3 Three-Dimensional Culture

For the manufacturing of implantable bone tissue based on scaffold materials under well-defined and reproducible conditions a novel continuously perfused bioreactor system was developed. The development and optimisation of 3D bone cultures was first established in the rat model. Rat osteogenic cells of the 4<sup>th</sup> passage were cultivated in a serum-reduced medium containing PFGF-bb, b-FGF, insulin, transferrin, albumin and osteogenic factors. 7 days post inoculation the cytokines were removed to enhance the differentiation. Compared to a static 3-D culture proliferation and mineralisation of the cells was substantially improved in the bioreactor (Fig. 2). Rabbit cells were also tested in 3D culture with regard to attachment, growth and production of collagen I (Fig. 3).

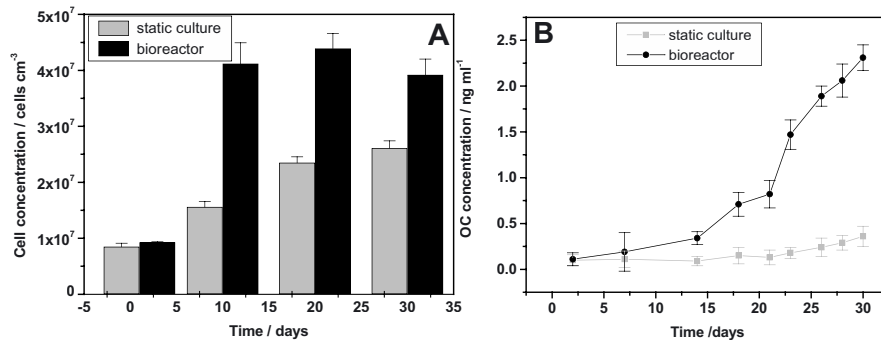


Figure 2. Proliferation (A) and mineralisation (B) of rat osteoblasts on calcium phosphate scaffolds in static culture and in the bioreactor system.

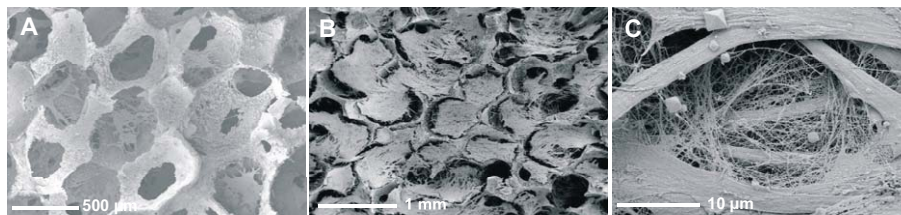


Figure 3. SEM study of osteoblast-like rabbit cells cultivated in the novel serum-reduced culture medium on calcium phosphate scaffolds in static culture : A – Scaffold 24 h after inoculation. B- Scaffold 10 days after inoculation. C- Cells 10 days after inoculation forming collagen fibrils.

A novel culture medium with reduced serum content was shown to have a superior performance with regard to proliferation and directed differentiation of osteogenic rabbit cells. Protocols for a standardised cell isolation and 2-D culture were established and optimised. In 3-D culture the use of the novel bioreactor system resulted in a significantly improved cell growth, formation of extracellular matrix and mineralisation when compared to static culture conditions.

G. STADLER<sup>1</sup>, R. VOGLAUER<sup>1</sup>, M. WIESER<sup>1</sup>, H. KATINGER<sup>1</sup>,  
R. PFRAGNER<sup>2</sup>

## ESTABLISHMENT AND CHARACTERIZATION OF HUMAN MEDULLARY THYROID CARCINOMA CELL LINES FOR IMMUNOTHERAPY

<sup>1</sup> *Institute of Applied Microbiology, University of Natural Resources and Applied Life Sciences, Vienna, Austria,* <sup>2</sup> *Department of Pathophysiology, Karl-Franzens University, Graz, Austria*  
*h9240486@edv1.boku.ac.at*

### 1. INTRODUCTION

The prognosis for patients with medullary thyroid carcinoma (MTC), a rare tumor of the parafollicular C cells of the thyroid gland, is very poor as the tumor metastasizes very early and presently the only curative therapeutic option is radical surgery. Thus, the search for new therapeutic strategies is of fundamental importance.

A highly promising approach in antitumor therapy is the activation of the patient's immune system against the malignant cells. One of these strategies aims at the stimulation of resting T-cells by dendritic cells (DCs)<sup>1</sup>. The ability of MTC tumor lysate pulsed DCs to stimulate anti tumor response against MTC has been published<sup>2</sup>. In the case of MTC the small tumor size and hence small amounts of tumor lysates impede repeated treatment of the patients, a drawback we want to overcome by establishing autologous tumor cell lines. These cells are difficult to cultivate and the spontaneous outgrowth of continuously growing cell lines is rare. Although we have succeeded in establishing several MTC cell lines<sup>3,4</sup>, clinical application is hampered by low success rates and the long time necessary for generation of sufficient cell material to pulse DCs. Therefore, a fast and efficient protocol for generation of cell lines is required. Since telomerase is considered to play a crucial role in maintenance of cell growth<sup>5</sup>, our project is focused on the introduction of hTERT into MTC cells after explantation. In order to elucidate the role of telomerase biology in our already established MTC cell lines, we characterized these cells for telomerase activity and telomere length as well as for maintenance of cell specific markers. Additionally, we started to establish a transfection protocol for MTC cells.

## 2. METHODS AND RESULTS

### 2.1. Establishment of MTC cell lines

Primary MTC cultures were established from patients with progressive MTC using optimized protocols<sup>3,4</sup>. The majority of cell lines have been derived from metastatic tumor tissue (e.g. MTC-SK, RARE, SINJ), however, recently we have been successful in establishing two cell lines from primary tumors (e.g. SHER I).

MTC-SK has been continuously cultured for over 4 years (more than 200 passages), RARE and SHER have been propagated for about 30 passages, so far. In contrast, SINJ ceased growth after 47 population doublings.

### 2.2. Characterization of MTC cell lines

#### *Immunocytochemical characterization*

Cell line characterization was performed as described before<sup>3,4</sup>. Cells were analyzed for neuroendocrine markers such as calcitonin (CT), calcitonin gene-related peptide (CGRP), bombesin (GRP), neuron specific enolase (NSE) and somatostatin (SRIF). Positive reactivity was assessed semi-quantitatively and data were demonstrated by multiplying the staining intensity and the number of positive cells (+: weak, ++: moderate, +++: strong). The cell lines show characteristics of the original tumor tissue such as the positive reaction with antibodies directed against CT, CGRP and GRP (table 1).

Table 1. Immunocytochemical characterization of MTC cell lines (n.d....not determined).

<i>Cell line</i>	<i>CT</i>	<i>CGRP</i>	<i>GRP</i>	<i>NSE</i>	<i>SRIF</i>
MTC-SK	++	+++	+++	+++	-
RARE	n.d.	++	+	+++	n.d.
SINJ	+ / ++	+ / ++	++	++	-

#### *Determination of telomerase activity*

Telomerase-activity was determined by a modified protocol of the conventional TRAP-assay optimized for real-time PCR<sup>6</sup> (Figure 1 left). A serial dilution of Hek293, a human adenovirus immortalized kidney epithelial cell line, served as standard and positive control. Cell lysates treated with RNase were used as negative control. Telomerase-activity of samples was expressed in relative values corresponding to the activity of a calculated number of Hek293.

#### *Determination of telomere length*

Telomere length was determined by Flow-FISH analysis (Figure 1 right)<sup>7</sup>. Whole cells were labeled in situ with a telomere specific fluorescein conjugated PNA-

probe. For negative control the PNA-probe was substituted by  $H_2O_{dd}$ . Cells were counterstained with propidium iodide and analyzed using flow cytometry. G1 population was gated and telomere specific fluorescence was determined. Quantum™ 24 FITC-labeled standard beads were used to convert the mean fluorescence values into Molecules of Equivalent Soluble Fluorochromes (MESF).

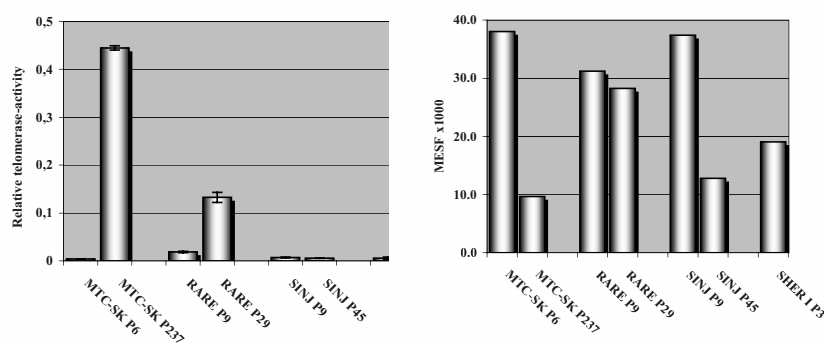


Figure 1. Relative telomerase-activity (left) and telomere length expressed as MESF (right) of the MTC cell lines MTC-SK, RARE, SINJ and SHER I, at different passage levels.

### 2.3. Optimization of transfection efficiency of MTC cells

Gene transfer into MTC cells was performed using the Nucleofector™ Technology (AMAXA). For optimization of gene introduction we used the Cell Line Optimization Nucleofector™ Kit and the *gfp* reporter gene. Flow cytometric analysis of transfected SHER I showed a transfection efficiency of up to 40%. Figure 2 shows *gfp* expressing SHER I cells.

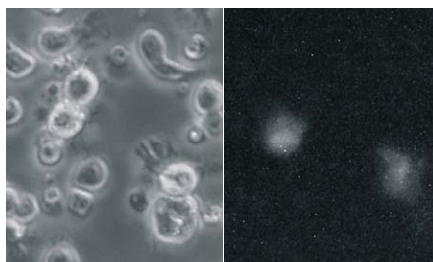


Figure 2. MTC cell line SHER I was transfected with a plasmid encoding the fluorescent protein *gfp* for optimization of gene introduction. Cells were analyzed by light (left) and fluorescence microscopy (right).

### 3. DISCUSSION

Since telomerase is considered to play an essential role in maintaining cell growth in vitro<sup>5</sup> we analyzed the impact of telomere biology on the growth capacity of MTC cells. All analyzed metastatic MTC tumor cell lines show low telomerase activity after in vitro explantation and long telomeres. Additionally, we detected a loss of DNA from the ends of the telomeres over the cultivation period. Nevertheless, reactivation of telomerase at higher passage level allows the metastatic cell line MTC-SK to enter a phase of continuous cell growth. In contrast, when telomerase is not reactivated cells stop dividing such as SINJ cell line, having about 47 generations before entering senescence. Cells from primary tumor tissue show shorter telomeres and low telomerase activity compared to metastatic tumor cells. Although more data are required to confirm our preliminary results, we suggest that telomerase activity as well as the maintenance of telomere structure are intrinsic and crucial components for fast and efficient expansion of MTC cell lines in vitro. This hypothesis is currently tested by ectopic expression of the catalytic subunit of human telomerase (hTERT) in primary MTC tumor cells, the protocol for which has been established during this study. Using hTERT we will be able to establish new MTC cell lines within a minimum time frame. Therefore we are convinced that this technology will allow the generation of sufficient and appropriate tumor cell material for pulsing autologous DCs.

### ACKNOWLEDGEMENTS

G.S. was supported by the doctoral scholarship program of the Austrian Academy of Sciences.

### 4. REFERENCES

- Zitvogel, L., Angevin, E. & Tursz, T. (2000). *Ann Oncol*, 11, 199-205.
- Bachleitner-Hofmann, T., Stift, A., Friedl, J., Pfragner, R., Radelbauer, K., Dubsky, P., Schuller, G., Benko, T., Niederle, B., Brostjan, C., Jakesz, R., Gnant, M. (2002). *J Clin Endocrinol Metab*, 87(3), 1098-104.
- Pfragner, R., Höfler, H., Behmel, A., Ingolic, E., Walser, V. (1990). *Cancer Res*, 50, 4160-4166.
- Pfragner, R., Wirnsberger, G., Behmel, A., Wolf, G., Passath, A., Ingolic, E., Adamiker, D., Schauenstein, K. (1993). *Int J Oncol*, 2, 831-836.
- Meyerson, M., Counter, C.M., Eaton, E.N., Ellisen, L.W., Steiner, P., Caddle, S.D., Ziaugra, L., Beijersbergen, R.L., Davidoff, M.J., Liu, Q. et al. (1997) *Cell*, 90, 785-795.
- Wege, H., Chui, M.S., Le, H.T., Tran, J.M., Zern, M.A. (2003). *Nucleic Acids Res*, 31(2):E3-3.
- Bacchetti S, Haber DA, Weinberg RA, Baerlocher, G.M., Mak, J., Tien, T. & Lansdorf, P.M. (2002). *Cytometry*, 47, 89-99.

T. HAMASAKI, T. KASHIWAGI, S. ARAMAKI, T. IMADA  
T. KOMATSU, Y. LI, K. TERUYA, Y. KATAKURA,  
S. KABAYAMA\*, K. OTSUBO\*, S. MORISAWA\* AND  
S. SHIRAHATA

## SUPPRESSION OF CELL GROWTH BY PLATINUM NANOCOLLOIDS AS SCAVENGERS AGAINST REACTIVE OXYGEN SPECIES

*Department of Genetic Resources Technology, Faculty of Agriculture,  
Kyushu University, Fukuoka 812-8581, Japan; \*Nihon Trim Co. Ltd., Osaka  
531-0076, Japan*

**Abstract.** Electrolysed-reduced water (ERW) contained Platinum nanocolloids (PtNCs) of 1-10 nm, suggesting that PtNCs in ERW functioned as active hydrogen donors and scavenge intracellular reactive oxygen species (ROS). Electron paramagnetic resonance (EPR) analysis revealed that synthesized PtNCs of about 2 nm scavenged superoxide anion radicals and DPPH radicals. Synthesized PtNCs scavenged intracellular ROS and suppressed the growth of human leukemia K562 cells.

### 1. INTRODUCTION

Electrolyzed reduced water is molecular hydrogen-rich alkaline water, which is produced near cathode during electrolysis of water. ERW can scavenge reactive oxygen species (ROS) *in vitro* and in cultured cells. The ROS-scavenging activity of ERW was correlated with the content of platinum eluted from platinum electrodes, suggesting that Platinum nanocolloids (PtNCs) of nm sizes in ERW functioned as active hydrogen donors. Here, we synthesized PtNCs and examined their ROS-scavenging activity and the growth suppressing effect on K562 cells.

### 2. MATERIAL AND METHODS

#### *2.1. Preparation of chemically synthesized PtNCs*

The PtNCs were synthesized by ethanol reduction from  $\text{H}_2\text{PtCl}_6$ . The solution containing with 0.04 %  $\text{H}_2\text{PtCl}_6$ , 0.5 % Tween 80, 40 mM Phosphate buffer (pH 7.0) and 10 % ethanol was incubated for 10 hours at 60 °C. The solution was then filtrated for desalt and concentrated by ultrafiltration using the 10,000 molecular weight cut membrane.

#### *2.2. Determination of superoxide anion radical- and DPPH radical-scavenging activity of PtNCs*

The reaction mixture for measuring DMPO-OOH spin adducts specific to superoxide radical contained 0.2 mM hypoxanthine, 125  $\mu$ M diethylenetriamine-pentaacetic acid, 40 mM sodium phosphate buffer (pH 7.8), 10 mU of xanthine oxidase, 0.19 M 5,5-dimethylpyrroline 1-oxide (DMPO) and 150  $\mu$ l of sample. The samples for measuring 1,1-diphenylpicryl-2-hydrazyl (DPPH) radical were mixed with 100  $\mu$ l of 200  $\mu$ M DPPH, 40 mM phosphate buffer (pH 6.0) solution in a tube. Electron paramagnetic resonance (EPR) spectra were recorded 90 sec after mixing the solution on a JEOL JESREIX spectrometer using an aqueous quartz flat cell.

### 2.3. Cell culture and measurement of cell proliferation.

Human leukemia K562 cells were cultured in RPMI 1640 medium supplemented with 10% inactivated FBS under an atmosphere of 5% CO<sub>2</sub>/95% air at 37°C. Cells were seeded in a 35 mm dish at the density of 1 $\times$ 10<sup>5</sup> cells/ml and measured the cell number three days after treatment with PtNCs in hydrogen gas-saturated water.

### 2.4. Measurement of intracellular ROS scavenging activities by flowcytometer

The amount of intracellular ROS, especially the intracellular H<sub>2</sub>O<sub>2</sub>, was determined by using a fluorescent dye, 2',7'-dichlorofluorescein-diacetate (DCFH-DA). Cells were pre-cultured for 10 min in Ca<sup>2+</sup>, Mg<sup>2+</sup>-free HBSS buffer with hydrogen gas ventilated ultrapure water containing each amount of PtNCs. After the removal of the supernatant, 5  $\mu$ M DCFH-DA was added and incubated for 10 min. After resuspended in PBS, intracellular redox state of cells was analysed immediately using a flowcytometer.

## 3. RESULT AND DISCUSSION

### 3.1. Scavenging activity of PtNCs on superoxide radical and DPPH-radical

Transmittance electron microscopic analysis and dynamic light scattering analysis revealed that ERW contained PtNCs of 1-10 nm, suggesting that PtNCs functioned as active hydrogen donors and scavengers against ROS (data not shown). Antioxidative activity of PtNCs was examined using biological *in vitro* system. DMPO-OOH signal which is from superoxide anion radical was inhibited by 10 ppm of PtNCs compared with 0 ppm of PtNCs (Figure 1 a), suggesting that PtNCs scavenged ROS. Effects of PtNCs on EPR signal of DPPH radical were investigated with saturated hydrogen water. As shown in Figure 1 b, 1 ppm of PtNCs completely scavenged the DPPH radical, suggesting that PtNCs has the ability of generating active hydrogen from hydrogen molecule.





Figure 1. a. 0 ppm of PtNCs (an upper signal), 10 ppm of PtNCs (a lower signal). b. 0 ppm of PtNCs with hydrogen (an upper signal), 1 ppm of PtNCs with hydrogen (a lower signal)

### 3.2. Intracellular ROS-scavenging effect and growth-suppressive effects on K562 cells of PtNCs

We examined the intracellular ROS-scavenging activity of PtNCs. As shown in Figure 2, PtNCs in the hydrogen gas-saturated solution scavenged intracellular ROS of K562 cells. However, PtNCs only did not scavenge intracellular ROS, suggesting that active hydrogen generated by the catalytic action of PtNCs scavenged intracellular ROS. In order to examine a physiological function of PtNCs, the effect of PtNCs on the proliferation of K562 cells were examined by measuring the cell number three days after PtNCs treatment. The suppression of the proliferation of K562 cells was not observed by the treatment with PtNCs only. However, in the presence of hydrogen gas, PtNCs suppressed the proliferation in a dose-dependent manner (Figure 2). PtNCs in the nitrogen gas-saturated solution did not suppress the proliferation. These results suggested that active hydrogen generated from hydrogen gas by the catalyst of PtNCs suppressed the proliferation of K562 cells.

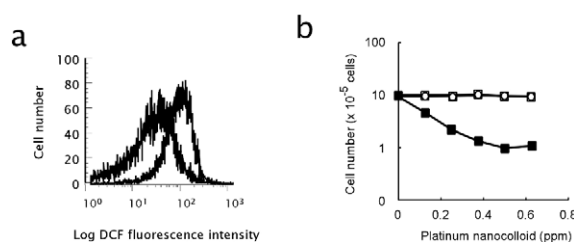


Figure 2. a. Left peak; PtNCs with  $H_2$ , right peak; PtNCs with  $N_2$ . b. Open square; none saturated water (control), closed circle; nitrogen saturated water, closed square; hydrogen saturated water.

## 4. REFERENCES

- 1, Shirahata S., Kabayama S., Nakano M., Miura T., Kusumoto K., Gotoh M., H. Hayashi, Otsubo K., Morisawa S., and Katakura Y. 1997. *Electrolyzed-reduced water scavenges active oxygen species and protects DNA from oxidative damage. Biochem. Biophys. Res. Commun.*, 234, 269-74.
- 2, Helmut B and Ryan M. R. 2001. Nanoscopic metal particles – synthetic methods and potential applications. *Eur. J. Inorg. Chem.* 10, 2455-2480

P. HINTERLEITNER<sup>1</sup>, F. UNTERLUGGAUER<sup>2</sup>, K. LANDAUER<sup>1</sup>,  
D. MÜLLER<sup>2</sup>, R. KUNERT<sup>1</sup>, G. BLÜML<sup>3</sup>, O. DOBLHOFF-DIER<sup>1</sup>,  
H. KATINGER<sup>1</sup>

## COMPARISON OF FLUIDIZED BED AND FED BATCH REACTOR CULTURES FOR PRODUCTION OF ANTI- HIV-ANTIBODY

<sup>1</sup> *Institute of Applied Microbiology, University of Natural Resources and Applied Life Sciences, Muthgasse 18, A-1190 Vienna, Austria* <sup>2</sup> *Polymun Scientific, Nussdorfer Lände 11, A-1190 Vienna, Austria* <sup>3</sup> *Amersham Biosciences c/o Institute of Applied Microbiology, Muthgasse 18, A-1190 Vienna, Austria E-mail: Blueml@edv1.boku.ac.at*

**Abstract.** High product yield, product quality and stable reactor culture conditions are a key to economically viable pharmaceutical bioprocesses. Two types of culture methods for production of recombinant anti-HIV-antibody were applied within this study. The tested cell line was a DHFR<sup>r</sup> recombinant CHO cell line expressing anti-HIV antibodies (CHO-4E10; Polymun Scientific, Vienna, Austria). Cells were cultured in a perfused lab-scale fluidized bed Cytopilot Mini™ reactor (Amersham Biosciences, Uppsala, Sweden) attached to macroporous Cytoline 1™ (Amersham Biosciences, Uppsala, Sweden) microcarriers and as suspension cells in a pilot scale stirred tank bioreactor fed-batch process. Both processes were performed using protein-free media. The systems were compared in terms of cell growth, product yield and product quality.

Both systems were equally well suited for production of the recombinant protein in terms of product yield and product quality, however demonstrating an economic advantage of the fluidized bed process.

### FLUIDISED BED LAB-SCALE CULTURE

#### *Specification of fluidised bed bioreactor set-up*

This alternative commercial system is based on a bioreactor with a net volume of 2 L. The starting carrier-bed volume was 300 ml (Cytoline 1), the seeding density was  $2 \times 10^6$  cells mL<sup>-1</sup> microcarrier. Media used were a 1:1 mixture of Dulbecco's Modified Eagle medium and Ham's F-12 medium (Biochrom, Berlin, Germany). Additional 100 mM ferric citrate, 6mM L-Glutamine and 0,38mM methotrexate (Sigma, St.Louis, USA), 0,25 % soy-peptone and protein free additive (Polymun Scientific, Vienna, Austria) were supplemented. Dissolved oxygen set-point of 50 % was controlled via a PID loop of the process control unit (PCS AG, Switzerland) and maintained by supplying spare oxygen to the reactor by either a simple sparger or at higher cell densities via a microsparger (Fujiplate Tube element, Fuji Filter

Manufacturing Co., Tokyo, Japan). The pH was controlled automatically by the process-control unit (PID loop) using CO<sub>2</sub> and 1 M NaOH to balance deviations with a pH set-point of 7.1.

#### *Regime of fluidised bed culture*

Aim of this labour scale reactor culture was to achieve a stable production process and a product concentration comparable to the pilot plant fed-batch culture.

Only about 7 % of the cells could be found in the supernatant 24 h after inoculation. 25 days after inoculation, microcarriers were fully colonised with an achieved average growth rate of 0.3 d<sup>-1</sup>.

On day 35, after ten days after stable culture conditions and full colonisation of microcarriers, perfusion rate of previous 13 times the settled microcarrier bed volume was decreased to 4 times. This was achieved by diminishing the residual glucose concentration and increasing the initial glucose concentration of the media from 4 to 6 and 8 g L<sup>-1</sup>, respectively. As a result product concentrations increased up to 102.5 µg mL<sup>-1</sup>, although specific productivity decreased from 6.3 to 3.7 µg per day and 10<sup>6</sup> cells. Continuous accumulation of lactate (2.5 to 4.3 g L<sup>-1</sup>) during the increase of glucose concentration in the media could be noticed.

### PILOT SCALE AIRLIFT FED-BATCH CULTURE

#### *Specification*

The pilot scale fed-batch culture was performed in an airlift bioreactor (Chemap, Volketswil, Switzerland) with a working volume of 500 L by Polymun scientific, Austria in a row of repeated fed-batch cultures. Two stirred tank bioreactor processes (MBR, Wetzikon, Switzerland) served to scale up the inoculum, whereupon the second process was operated in repeated batch mode, in order to achieve sufficient amounts of inoculum. Starting cell number was 6.6 x 10<sup>5</sup> mL<sup>-1</sup>. Media used for this process was in principle the same as for the FBR-culture, except in the content of ferric citrate, which was 250 mM for pilot scale cultures. Shot solution (Polymun scientific, Vienna, Austria) was continuously added over a period of 4 days to an extent of maximum 5% of working volume.

### METHODS FOR PRODUCT QUALITY CONTROL

- SDS PAGE of samples, either pre-treated with a reducing agent or untreated, on a continuous gel (PhastGel Gradient Media, Gradient 8 – 25 %) with Phast-System™ (Amersham Biosciences, Uppsala, Sweden). Gels were either silver stained to detect pattern of bands or western blots were performed followed by immunodetection (g- heavy chain and k -light chain specific).

- Isoelectric focusing (IEF) of native samples: This was performed with the LKB 2117-001 Multiphor II Electrophoresis System (Amersham Biosciences, Uppsala, Sweden) on a polyacrylamide gel, kindly provided by Polymun Scientific, Vienna, Austria for a pI range of 5.2 – 11. For detection silver staining was carried out after focussing.

### CONCLUSIONS

- 102.5  $\mu\text{g mL}^{-1}$ , the highest titer achieved in fluidised bed culture was comparable to titers achieved by pilot scale fed-batch cultures, thus fulfilling the aim of the lab-scale experiment.
- Before decreasing perfusion rate fluidised bed culture could be kept in a stable state.
- Due to the decrease of the perfusion rate of more than 3 times, lactate accumulated in the culture media to a moderate extent (less than double). Furthermore, this
- decrease had a negative effect on specific productivity and depletion of certain amino acids at the end of the culture had to be compensated.
- All tested samples showed equal pattern of bands (1), even samples collected at critical stages like at the end of fluidised bed and fed-batch culture. Thus it was verified that the reduction of perfusion rate had no negative effect on product quality in fluidised bed culture. Potential economical advantages of FBR culture for antibody production with this cell line could be calculated. For a desired yield of 72 kg antibody a fluidised bed bioreactor culture with a settled bed volume of 1000L would need 180 days (7000 L bioreactor, perfusion rate of 8 bed volumes per day, achieved product concentration of 85  $\mu\text{g mL}^{-1}$ , two carrier to carrier transfers and a calculated specific productivity of 5.6  $\mu\text{g}$  per day and 1 million cells). Calculating with an average yield of 100  $\mu\text{g mL}^{-1}$  and an operating time of 10 days for a fed batch 60 repeated fed-batches in a 12000 L bioreactor would be necessary to produce the same amount of antibody, resulting in 600 days of fermentation. In this calculation of time further labour days for cleaning and restarting are not included. For further calculations see (2).

### REFERENCES

- (1) Garfin, D. E. Electrophoretic Methods, ed. by J.A. Glaser and M. P. Deutscher, Academic Press, 2000, 69-71.
- (2) Landauer, K. (2002); Influence of Media Additives on the Adhesion of Animal Cells on Microcarriers. PhD thesis, Institute of Applied Microbiology, pp 78, University of Natural Resources and Applied Life Sciences, Vienna, Austria.

T. KASHIWAGI, T. HAMASAKI, S. KABAYAMA\*, M. TAKAKI,  
K. TERUYA, Y. KATAKURA, K. OTUBO\*, S. MORISAWA\*,  
AND S. SHIRAHATA

## SUPPRESSION OF OXIDATIVE STRESS-INDUCED APOPTOSIS OF NEURONAL CELLS BY ELECTROLYZED-REDUCED WATER

*Department of Genetic Resources Technology, Faculty of Agriculture,  
Kyushu University, Fukuoka 812-8581, Japan  
\*Nihon Trim Co. LTD., Osaka 531-0076 Japan*

**Abstract.** We have proposed an active hydrogen reduced water theory that active hydrogen produced by electrolysis of water is stabilized in the form of hydrogenated metal nanocolloids in electrolyzed reduced water (ERW) and scavenges intracellular reactive oxygen species (ROS). Because various brain diseases are caused by oxygen stress, we examined the effect of ERW on oxidative stress-induced apoptosis of neuronal cells. ERW suppressed the H<sub>2</sub>O<sub>2</sub>-induced cell death of mouse neuroblastoma N1E115 cells, rat pheochromocytoma PC12 cells and mouse neuronal stem SFME cells. ERW lowered the intracellular ROS level of N1E115 cells, suppressing the H<sub>2</sub>O<sub>2</sub>-induced decrease of mitochondrial membrane potential and intracellular ATP level, which are markers of apoptosis. These results suggested the effectiveness of ERW for prevention of various brain diseases caused by oxidative stress.

### 1. INTRODUCTION

Neuronal cell death associates with aging and neurodegenerative diseases including Alzheimer's disease [1], Parkinson's disease [2], Huntington's disease [3], and pathological conditions such as ischemia, stroke, and excitotoxicity [4][5]. In these diseases, it has been considered that oxidative stress is one of the causes of the neuronal cell death. Oxidative stress is caused by reactive oxygen species (ROS) such as hydroxyl radical (OH), hydrogen peroxide (H<sub>2</sub>O<sub>2</sub>), and superoxide anion radical (O<sub>2</sub><sup>-</sup>) generated in the process of respiration, associated with mitochondrial electron transport. It has been a challenge to find out new anti-oxidants which can protect brain from oxidative damage. We proposed an active hydrogen reduced water theory that ERW contained active hydrogen as hydrogenated metal nanocolloids, which can scavenge intracellular ROS. We found that ERW scavenged ROS and protected DNA from oxidative damage [6] and stimulated glucose uptake into myotubes and adipocytes [7]. Anti-oxidative reduced water will be beneficial for prevention of oxidative stress in brain, because water can freely pass through the blood-brain barrier. Here, we investigated whether ERW could suppress the apoptosis of neuronal cells caused by oxidative stress.

### 2. MATERIALS AND METHODS

257

*F. Gòdia and M. Fussenegger (Eds.), Animal Cell Technology meets Genomics, 257-259.  
© 2005 Springer. Printed in the Netherlands.*

*Preparation of ERW.* ERW was prepared by electrolysis of ultrapure water containing 0.01% NaCl using an electrolyzing device TI-8000 or TI-200S (Nihon Trim, Osaka, Japan) equipped with platinum-coated titanium electrodes. ERW was easily neutralized by a HEPES buffer in medium.

*Cell culture.* Mouse neuroblastoma N1E115 cells were cultured in DMEM/F12 medium supplemented with 10 % fetal bovine serum (FBS). To differentiate N1E115 cells to neuron like cells, cells were cultured in the medium with 1% DMSO and 1% FBS for 4 days on poly-D-lysine coated dishes. PC12 cells were cultured in DMEM supplemented with 5% FBS and 5% horse serum (HS). To differentiate PC12 cells to neuron-like cells, cells were cultured in the medium with 0.5 % FBS, 0.5 % HS and nerve growth factor (NGF) for 4 days. SFME cells were cultured in D-MEM/F12 supplemented with insulin, transferrin, chemically defined lipid concentrate, sodium selenite and epidermal growth factor (EGF).

*Viability assay.* Cells were plated on a 24-well plate and differentiated. Differentiated cells were treated with H<sub>2</sub>O<sub>2</sub> for 24 hr. Cell viability was assayed by using WST-8 [7].

*Measurement of intracellular ROS.* Intracellular ROS were measured by using 2',7'-dichlorofluorescein diacetate (DCFH-DA) which is converted to fluorescent DCF when reacting with intracellular ROS [8]. DCF fluorescence was measured by confocal laser scanning microscopy.

### 3. RESULTS AND DISCUSSION

#### 3.1. Suppressive effect of ERW on neuronal cell death induced by H<sub>2</sub>O<sub>2</sub>

N1E115 cells were treated with various concentration of H<sub>2</sub>O<sub>2</sub>. As shown in Figure 1, the viability decreased in a dose-dependent manner. ERW significantly prevented the H<sub>2</sub>O<sub>2</sub>-induced cell death. ERW did not affect the cell viability in the absence of H<sub>2</sub>O<sub>2</sub>. Similar results were obtained in the case of PC12 cells and SFME cells (data not shown). Furthermore, ERW suppressed the decrease of intracellular ATP and mitochondrial membrane potential that is the markers of apoptosis, indicating that ERW could suppress apoptosis of neuronal cells induced by H<sub>2</sub>O<sub>2</sub> (data not shown).

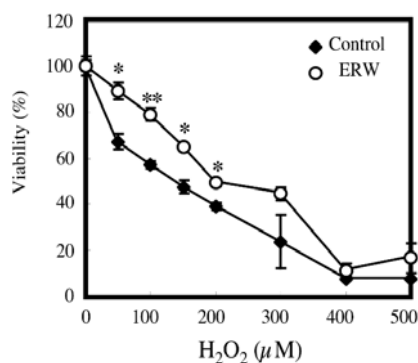


Figure. 1 Suppressive effect of ERW prepared by TI-8000 on neuronal cell death of N1E115 cells induced by H<sub>2</sub>O<sub>2</sub>. All values represent the mean  $\pm$  S.D. \*,  $p < 0.05$ , \*\*,  $p < 0.01$

### 3.2. Scavenging effect of ERW on intracellular ROS and suppression of apoptosis

Intracellular ROS was significantly scavenged in N1E115 cells by the treatment with ERW for 10 minutes in comparison with non-treated cells (control) (Figure 2). N1E115 cells were exposed to 200  $\mu\text{M}$   $\text{H}_2\text{O}_2$  for 3 hr, and the mitochondrial membrane potential (MMP) was measured using rhodamin 123. Fluorescence was measured by flow cytometry. ERW suppressed the  $\text{H}_2\text{O}_2$ -induced decrease of MMP. After the exposure to 200  $\mu\text{M}$   $\text{H}_2\text{O}_2$  for 24 hr, intracellular ATP in N1E115 cells were measured by ATP Bioluminescence Assay kit CLS II (Roche). ERW suppressed the  $\text{H}_2\text{O}_2$ -induced decrease of intracellular ATP. These results suggested that ERW could suppress the  $\text{H}_2\text{O}_2$ -induced apoptosis of N1E115 cells.

Further investigation will be necessary to demonstrate that ERW is effective to prevent neurodegenerative diseases *in vivo*.

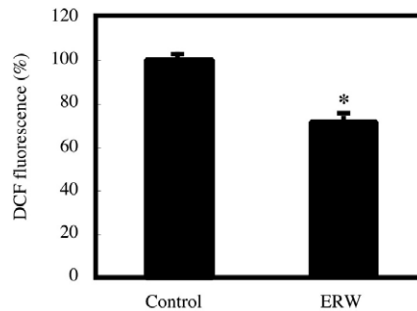


Figure. 2 Effect of ERW prepared by TI-8000 on intracellular ROS of N1E115 cells All values represent the mean  $\pm$  S.D. \*,  $p < 0.05$

## 4. REFERENCES

1. Miranda S. et al. (2000) *Prog Neurobiol*, **62**, 633-684.
2. Koutsilieri E. et al. (2002) *J Neurol*, **249**, Suppl 2: 111-115
3. Browne SE. et al. (1999) *Brain Pathol*, **9**, 147-163.
4. Love S. (1999) *Brain Pathol*, **9**, 119-31.
5. Coyle JT. et al. (1993) *Science*, **262**, 689-695.
- Shirahata S. et al. (1997) *Biochem Biophys Res Commun*, **234**, 269-274.
- Oda M. et al. (1999) In: *Animal Cell Technology: Products from Cells, Cells as Products*, (ed. by A. Bernard et al.), Kluwer Academic Publishers, the Netherlands, pp. 425-427.
8. Kanemura Y. et al. (2002) *J Neurosci Res*, **69** (6), 869-79.
9. Bass DA. et al. (1983) *J Immunol*, **130** (4), 1910-7

A. MARC<sup>1</sup>, E. MARKVICHEVA<sup>2</sup>, C. JOURDAIN<sup>3</sup>,  
L. BEZDETAY<sup>3</sup>, J.L. MERLIN<sup>3</sup>, F.GUILLEMIN<sup>3</sup>, V. ZUBOV<sup>2</sup>,  
J.L. GOERGEN<sup>1</sup>

## SPHEROID FORMATION BY ENCAPSULATION OF CANCER CELLS TO MIMIC SMALL SIZE TUMORS

*1-Laboratoire des Sciences du Génie Chimique, CNRS-ENSAIA, BP 172, F-54505 Vandoeuvre-lès-Nancy; 2- Shemyakin Inst. Bioorganic Chemistry, Russian Academy of Science, Moscow; 3- Laboratoire de Recherche en Oncologie, CAV, Nancy*

### 1. INTRODUCTION

Multicellular spheroids are three-dimensional structures that are used to mimic small tumors. Cellular organization of spheroids allows the formation of *in vivo* tumors much better than two-dimensional *in vitro* models. Spontaneous spheroid generation is presently performed in T-flask, on agarose layer to prevent cell attachment at the bottom of the flasks and spheroids can then be expanded in agitated systems such as spinner flasks. The aim of the current research is to develop a novel spheroid model based on tumour cells cultivated in polymer microcapsules, which could mimic *in vivo* tumors. We mainly focused on the effect of the operating conditions on the capsule size and stability, with the objective to reach small size spheroids with a narrow distribution.

### 2. PREPARATION OF MICROCAPSULES

To get microcapsules with polyelectrolyte semi-permeable membrane, two natural biocompatible polymers, namely oppositively charged polysaccharides, alginate and chitosan, have been used. The cell encapsulation was based on a first step of cell entrapment in calcium alginate beads coated with alginate-chitosan membrane and on a second step by dissolving the alginate core using EDTA. We used either a classical spray device or a lab-made electrostatic bead generator for the smaller capsules.

The encapsulated cells (e.g. MCF-7 cells) were then cultivated in RPMI medium supplemented with 10% FCS in Roux bottles or Erlenmeyer flasks to get the desired cellular spheroids.



### 3. INFLUENCE OF THE OPERATING CONDITIONS

#### 3.1. Effect of incubation time and pH of chitosan solution on membrane thickness

The thickness of the polyelectrolyte membrane could be varied within the range of 30-60  $\mu\text{m}$  as a function of several parameters. For example, it was found higher with a chitosan solution of pH 6.0 (table 1). Besides, though cell death occurred after 20 min of incubation, the thickness increases with the incubation time of Ca-alginate beads in chitosan solution (table 2).

Table 1. Membrane thickness as a function of the pH of the chitosan solution

pH	5.0	5.5	6.0	6.5	7.0
Membrane thickness, $\mu\text{m}$	36 $\pm$ 6	40 $\pm$ 8	63 $\pm$ 7	25 $\pm$ 2	5 $\pm$ 2

Table 2. Membrane thickness as a function of incubation time in chitosan solution

Incubation time, min	2	4	6	8	10	15	20
Membrane thickness, $\mu\text{m}$	36 $\pm$ 6	45 $\pm$ 8	54 $\pm$ 8	60 $\pm$ 6	63 $\pm$ 7	72 $\pm$ 9	85 $\pm$ 8

#### 3.2. Effect of chitosan type on the membrane stability

Three chitosan samples have been tested with molecular weights of 3.5, 30 and 50 kDa. The 3.5 and 30 kDa were obtained as described earlier (Bartkowiak and Hunkeler, 2000) and were kindly provided by Prof. Bartkowiak (Poland) and Vikhoreva (Russia). The last one was purchased from Kitozyme (Belgium). The capsules obtained with 3.5 and 30 kDa chitosans had a nice spherical shape and were stable at storage for more than 20 days both in physiological solution and in FCS containing culture medium. In contrast, the microcapsules based on 50 kDa chitosan were completely destroyed after 3 days of incubation in culture medium.

#### 3.3. Effect of polymer concentration and needle diameter on microcapsule size

The mean size of microcapsules could be decreased up to a value between 300 and 400  $\mu\text{m}$  by lowering the concentration of alginate solution (table 3) and by using a smaller needle diameter as part of the electrostatic bead generator (figure 1). Elsewhere a 1.2 % chitosan solution increased the bead stability by comparison with 0.2 %, but appeared to be toxic for the cells.

Table 3. Microcapsules size as a function of the alginate concentration

Alginate concentration, %	1.5	2.0
Mean bead size, $\mu\text{m}$	370	425

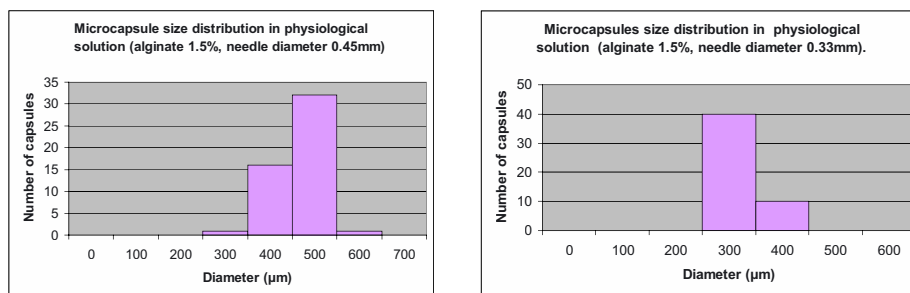


Figure 1. : Microcapsules size as a function of needle diameter

#### 4. LONG TERM CULTIVATION OF TUMOR CELLS

MCF-7 cells have been encapsulated from an initial concentration of  $3 \times 10^6$  cells/ml of alginate solution. The proliferation of the cells has been monitored using a light microscope. The cells grew in aggregates increasing with time in large cell clusters, which filled all the capsule volume. Multicellular spheroids of MCF-7 tumour cells have been generated after one month culture without cytotoxicity of the membrane.

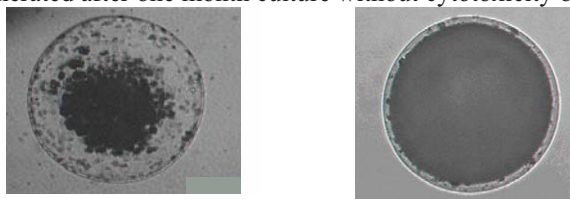


Figure 2: MCF-7 cells in microcapsules after 20 days (left) and 35 days (right)

#### 5. CONCLUSIONS AND PERSPECTIVES

Some microcapsules of alginate-chitosan polymers have been studied. The thickness of the membrane depends on several operating parameters. A small size of microcapsules between 300 and 400 µm can be reached with a narrow distribution. Some tumor cells can grow in the microcapsules and multicellular spheroids have been generated. Further studies will assess photodynamic therapy on spheroids obtained by encapsulation of tumour cells and co-cultures of tumor and endothelial cells inside microcapsule to mimic the cell interactions occurring in *in vivo* tumors.

#### 6. REFERENCES

Bartkowiak, A. and Hunkeler, D., Chemistry of Materials, 12, 206-212 (2000)

D. MÖBEST<sup>1</sup>, M. JAEGER<sup>3</sup>, J. GUTTMANN<sup>2</sup>, M. SCHNEIDER<sup>2</sup>,  
G.B. STARK<sup>1</sup>

## BIOREACTOR FOR CONTINUOUS BIOMECHANICAL CHARACTERIZATION OF CELLULAR SYSTEMS AND TISSUE-ENGINEERED BIOHYBRID TISSUES

<sup>1</sup>*Dept. Plastic- & Hand Surgery, University Medical Center, University of  
Freiburg, Hugstetterstr. 55, D-79106 Freiburg, Germany*

<sup>2</sup>*Dept. Anaesthesiology & Intensive Care, University Medical Center,  
University of Freiburg, Hugstetterstr. 55, D-79106 Freiburg, Germany*

<sup>3</sup>*Dept. Traumatology, University Medical Center, University of Freiburg,  
Hugstetterstr. 55, D-79106 Freiburg, Germany*

Key words: Tissue-Engineering, analysis of biomechanical properties

### INTRODUCTION

In Tissue Engineering it is essential for the generation of „neo-tissues“ to maintain functionality (e.g. mechanical stability) during development. Closest to biology would be a *in vivo* model, but this only allows endpoint observations and gives very limited possibilities to follow up the development of the „neo-tissues“. To circumvent these limitations we try to use suitable *in vitro* systems. Currently we are developing an integrated reactor-/ analysis system. For analysis of cellular systems in response to mechanical stimuli we introduce a bioreactor system allowing online analysis of biomechanical properties of cellular and biosynthetic systems. The effect of mechanostimulation will be investigated on pulmonary cells and in engineering of fascia substitutes, where neo-formation of cellular tissue should parallel the degradation kinetics of biodegradable scaffolds to guarantee a minimum mechanical stability.

### APPROACH

#### *Bioreactor design*

This system should allow defined culture conditions, application of mechanical stimuli, microscopic observation, and destructive free online monitoring of mechanical parameters. To achieve these requirements we designed a reactor consisting of 2 compartments separated by an elastic membrane carrying the

„tissue“. Mechanical stimulus is generated by changing pressure and volume in the 2 compartments which is measured for biomechanical online-characterization (figure 1). Elongation will be measured by using autofocus systems of microscopes or by deformation of optical grids projected on the construct thus allowing to determine local differences in the construct. This system also allows continuous microscopic observation.

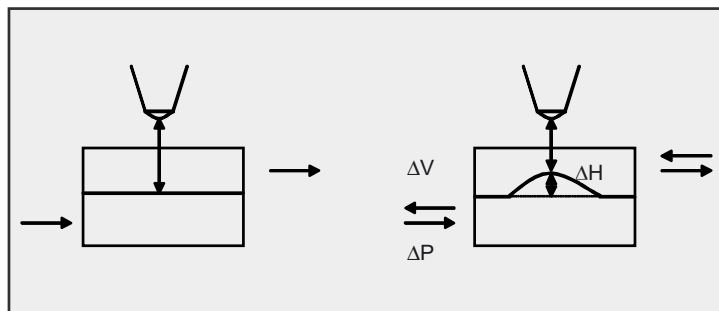


Figure 1. The bioreactor consists of 2 compartments divided by the biosynthetic hybrid tissue. Through volume changes ( $\Delta V$ ) a mechanical stimulus can be induced; pressure

#### Mechanical parameters derived from pressure volume data

The mechanical strain  $\sigma$  is not homogeneously distributed, but depends on the radius  $r$  on the circular membrane. We are interested in analysing the geometric distribution  $\sigma(r)$ .

$$\sigma = E \cdot \varepsilon \quad [1]$$

$E$ : modulus of elasticity,  $\varepsilon$ : relative elongation

$E$  is determined by the pressure-volume curve of one bioreactor-compartment by taking the elastance:

$$El = \Delta p / \Delta V \quad [2]$$

$$El = (F/A) / (A \cdot h) \quad [3]$$

$F$ : force acting on membrane,  $A$ : area of membrane,  $h$ : (mean) elongation of the membrane

With  $E = F/A$  follows:

$$E = El \cdot (A \cdot h) = El \cdot V(p) \quad [4]$$

By determining elongation  $\varepsilon$  related to radius  $r$  the distribution of mechanical strain  $\sigma$  can be described as function of  $r$ : with [1] and [4] follows:

$$\sigma(r) = EI \cdot V(p) \cdot \varepsilon(r) \quad [5]$$

Linear and/or non-linear changes in elasticity can be determined using multiple linear regression analysis within consecutive volume portions: SLICE-analysis<sup>1,2,3</sup> as established in respiratory mechanics analysis.

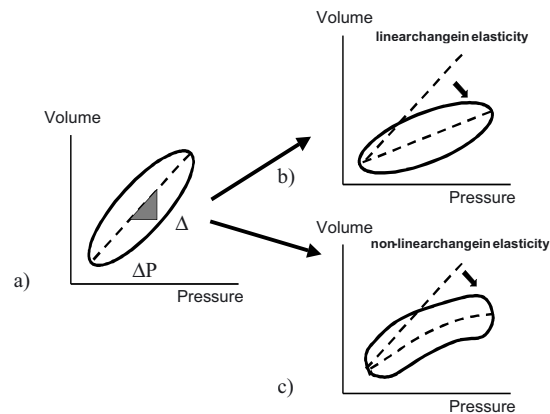


Figure 2 a) Volume/pressure diagram reflecting initial mechanical status, b) linear change in elasticity. c) non-linear change in elasticity

## SUMMARY

A bioreactor was designed and characterized allowing a controlled mechanical stimulation of biosynthetic hybrid tissues, which in addition is continuously microscopable. Continuous biomechanical destructive free characterization of tissue engineered constructs is possible. A control system is under development to determine P/V-diagrams for online determination of mechanical properties of the construct e.g. elasticity.

## REFERENCES

1. Guttman J. et al. "The analysis of linear and/or non-linear changes in elasticity can be performed by using the SLICE-analysis, which allows determination of elasticity within consecutive volume portions" *Technol Health Care* 2: 175-191, 1994
2. Kessler V. et al. "Analysis of nonlinear volume-dependent respiratory system mechanics in pediatric patients" *Pediatr Crit Care Med* 1: 111-118, 2000.
3. Mols G. et al. "Volume-dependent compliance and ventilation-perfusion mismatch in surfactant depleted isolated rabbit lungs" *Crit Care Med* 29: 144-151, 2001.

T. FISCHBACH AND T. NOLL

## MEMBRANE-SEPARATED COCULTIVATION OF CORD BLOOD HEMATOPOIETIC STEM CELLS WITH STROMAL CELL LINES

*Institute of Biotechnology 2, Research Center Jülich, 52425 Jülich,  
Germany, [TH.NOLL@FZ-JUELICH.DE](mailto:TH.NOLL@FZ-JUELICH.DE)*

**Abstract.** Cord blood hematopoietic stem and progenitor cells (HSPC) represent an important cell source for transplantation of cancer patients after high dose chemotherapy if autologous cells are not suitable (e.g. patients with hematopoietic malignancies) and no adult allogeneic donor is available. The main disadvantage of cord blood is the low number of cells obtained due to the small volume of blood collectable from umbilical cords. Without an expansion of the HSPC a transplantation is mostly limited to juvenile patients. We developed a novel small scale membrane bioreactor for parallelized membrane-separated cocultivation of HSPC with stromal cells. This system imitates the natural hematopoietic environment with stromal growth factors, ECM components and direct cell-cell contact between HSPC and stromal cells while maintaining a physical separation of the cells. The mini membrane bioreactor consists of a turnable insert for conventional 12-well plates, wherein a thin, porous polyethylene membrane is fixed. Murine stromal cells adhere to the underside on the membrane and HSPC are co-cultured on top of it. Soluble factors and stromal extensions travers the membrane, whereas cell bodies are retained. Thus, stroma directly supports HSPC expansion without contaminating the future transplant. Purified CD34<sup>+</sup> cells are cultured for 7 days in X-Vivo10 supplemented with four cytokines (Tpo, SCF, IL-3 and FL). Many important parameters have been investigated using this system (membrane material, pore size, type of stromal cells, cell density, agitation, feeding, etc.). With the novel membrane reactor we are able to expand HSPC to high cell densities. On average, after 12 days total cells and progenitor cells (CFC) expand 242 and 29fold. Early progenitors (CAFC) could even be expanded 39fold.

### 1. INTRODUCTION

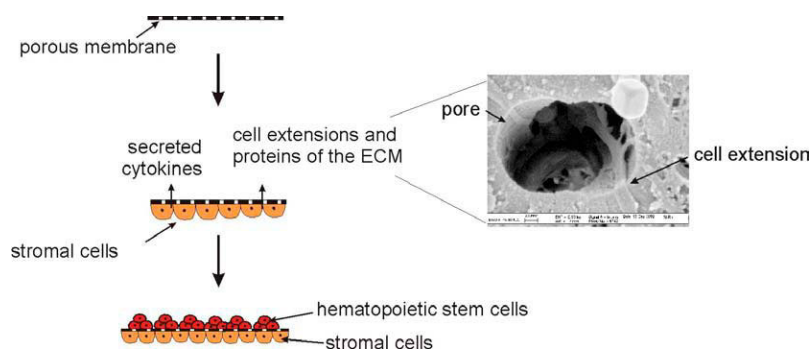


*Figure 1. Schematic picture showing the principle of the membrane-separated co-culture.*

Human umbilical cord blood (CB) is an attractive alternative to bone marrow or growth factor mobilized peripheral blood as source of hematopoietic stem cells because CB contains a high proportion of primitive progenitor cells. However, there are limitations to the widespread use of CB as the cell number available is sufficient to reconstitute children, but the ability to engraft an adult from CB may require ex vivo expansion at least in most cases. Therefore several strategies have been developed for ex vivo expansion. Out of these, coculture of CB derived stem cells with stromal cell lines, mostly of murine origin, has been shown to be superior to the cultivation of isolated stem cells. Major drawback of this strategy is that the stem cells have to be isolated prior to transplantation, making cocultivation possible while maintaining a physical separation of the different cells.

## 2. MATERIALS AND METHODS

Cells:	cord blood CD34+, 5*10 <sup>3</sup> /mL Stromal cell lines SI/SI, M2-10B4 mod and MS-5
Volume:	1 mL for suspension control (well plate) 3,6 mL for mini-membrane bioreactor
Culture medium:	X-Vivo 10, serum-free
Cytokines:	TPO (20ng/mL), SCF (50 ng/mL), IL-3 (10 ng/mL), FL (50 ng/mL)
Culture time:	7-12 days
Readout:	cell count, CFC and CAFC assays
Animal experiment:	irradiated NOD/SCID mice were transplanted with cells and after 6 weeks the percentage of human cells in the blood and bone marrow was determined

## 3. RESULTS

### 3.1 Design and use of the system for membrane-separated cocultivation

The culture system consists of a turnable insert made from stainless steel fitting into conventional 12-well plates. Within the insert a polyethylene membrane (thickness 11  $\mu\text{m}$ ) with  $2 \cdot 10^7$  pores /  $\text{cm}^2$  is fixed between silicon and teflon rings. In the first step irradiated stromal cells ( $5 \cdot 10^4$ ) were immobilized on one side of the membrane, subsequently the insert was turned around and the CD34+ cord blood cells placed on the other side of the membrane.

### 3.2 Comparison of different pore sizes

Three different pore sizes (0.45 / 1 / 3  $\mu\text{m}$ ) were compared. While a pore size of 0.45  $\mu\text{m}$  is too small to allow stromal cell extensions or extracellular proteins to pass the membrane and a pore size of 3  $\mu\text{m}$  bears the risk of stromal cells passing the membrane especially if pore overlapping occurs, a pore size of 1  $\mu\text{m}$  enables direct

cell-cell contact through the membrane while the stromal cells are retained effectively (Fig. 2).

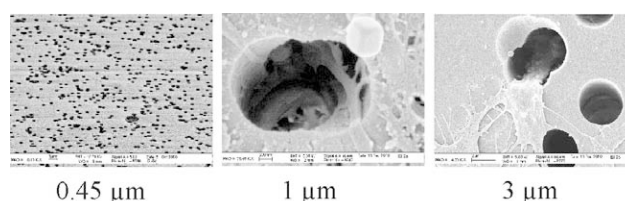


Figure 2. SEM pictures showing the cell-free top side of the membrane with stromal cells immobilized on the opposite side

### 3.3 Comparison of different stromal cell lines

Three different stromal cell lines (SI/SI, M2-10B4 mod and MS-5) were compared for their supportive effect on hematopoietic stem cell expansion in the membrane-separated co-culture. Expansion factors are given relative to a standard suspension culture. While the expansion of the total cell number and of the CFC is mainly unaffected, the expansion of the CAFC is strongly increased for the MS-5 cell line, which was used for all subsequent experiments.

### 3.4 Expansion of cord blood CD34<sup>+</sup> cells under optimised conditions

Optimised parameters were used for the ex vivo expansion of cord blood CD34<sup>+</sup> cells for 12 days. Membrane-separated cocultivation allows prolonged cultivation compared to suspension culture, resulting in strongly increased expansion factors.

Table 1. Expansion factors under optimised conditions

cell population	suspension culture day 7	membrane coculture day 7	suspension culture day 12	membrane coculture day 12
MNC	25	33	81	242
CFC	8	11	16	29
CAFC	3	6	7	39

### 3.5 Transplantation of NOD/SCID mice

CD34<sup>+</sup> cells were cultivated for 7 days either in standard suspension culture or in the membrane-separated coculture system using the MS-5 stroma cell line. Afterwards cells were transplanted to irradiated NOD/SCID mice. 30% of the BM cells and 6% of the PB cells of the mice transplanted with cells from the co-culture were of human origin. Cells from co-culture showed a more than 2fold higher engraftment potential than cells from suspension culture.



AKIKO OGAWA<sup>1</sup>, SATOSHI TERADA<sup>1</sup>, MASAO MIKI<sup>1</sup>  
TOSHIHISA KIMURA<sup>2</sup>, AKIO YAMAGUCHI<sup>2</sup>

## ANTI-APOPTOTIC GENES PROTECT AN INSULINOMA CELL LINE FROM CELL DEATH INDUCED BY HYPERGLYCEMIA

<sup>1</sup>*Department of Applied Chemistry and Biotechnology, Faculty of  
Engineering, Fukui University, 3-9-1 Bunkyo, Fukui 910-8507, Japan*

<sup>2</sup>*Department of Surgery, Fukui Medical University, 23-3 Shimoaizuki,  
Matsuoka-Cho, Yoshida-Gun, Fukui 910-1193, Japan*

### 1. INTRODUCTION

Type I diabetes results from the destruction of beta cells in the islets of Langerhans, where insulin is produced. There are more than 700,000 in Japan with severe type I diabetes who need to precisely control the level of glucose in blood. These patients must increase the insulin concentration in their blood in order to avoid blindness and other possible complications caused by hyperglycemia, abnormally high glucose level in the blood. Although insulin injection is effective, it involves problems. The patients must measure their glucose level daily and inject the proper amount of insulin. If glucose level is excessively suppressed, the patient will go into a hypoglycemic coma and sometimes die. Therefore, a novel treatment that is less dangerous is urgently required and islet beta cell or islet transplantation is one of the most promising treatment. The transplanted islets or cells would then secrete the appropriate amount of insulin and thereby maintain normal glucose homeostasis in diabetic patients.

However, many challenges remain to be overcome. Transplanted recipients would need to take immunosuppressive drugs for the rest of their lives in order to keep from rejecting the tissue [1], and the supply of islets is quite thin [2]. In addition, islet cells are damaged during organ procurement, preservation, isolation, and transplantation [3, 4]. An especially serious problem is post-transplant damage to the cells. Transplanted cells are exposed to several stresses, such as toxic effects from hyperglycemia. These stresses decrease functional islet cell numbers, which often prevents maintenance of normal glycemic levels.

In this study, we aimed to effectively prevent the death of transplanted islets. For this purpose, we examined anti-apoptotic genes. Bcl-2 is an anti-apoptotic membrane protein that strongly inhibits apoptosis induced by multiple stimuli [5]. We previously reported that introduction of Bcl-2 prevented a hybridoma cell line

from death and increased its monoclonal antibody productivity [6] and improved hepatoma culture [7].

Several researchers have already reported that introduction of *bcl-2* protects islet beta cells from cytokine- and hypoxia-induced destruction [3]. But there are multiple apoptosis pathways and Bcl-2 protein cannot inhibit all of these pathways. Therefore it is important to investigate other anti-apoptotic genes to find the most effective at preventing hypoxia-induced islet cell death. We attempted to introduce *crmA* into an islet cell line. CrmA is derived from cowpox virus and strongly inhibits caspases, the initiating factor for apoptosis [8].

## 2. MATERIALS AND METHODS

The rat insulinoma cell line RIN-5F, ATCC CRL-2058 (American Type Culture Collection, Manassas, Virginia, USA) was used throughout this work. The basal medium used was RPMI 1640 medium (Nissui, Tokyo, Japan) supplemented with 10% (vol/vol) FBS. BCMG-*bcl-2*-neo vector and BCMG-*crmA*-neo vector were successfully transfected to Rin-5F cells. Viable and non-viable cell densities were determined by the trypan blue exclusion method using a Neubauer improved hemocytometer (Erma, Tokyo, Japan). Insulin concentration in the culture supernatant was determined with ELISA kit (Shibayagi, Japan).

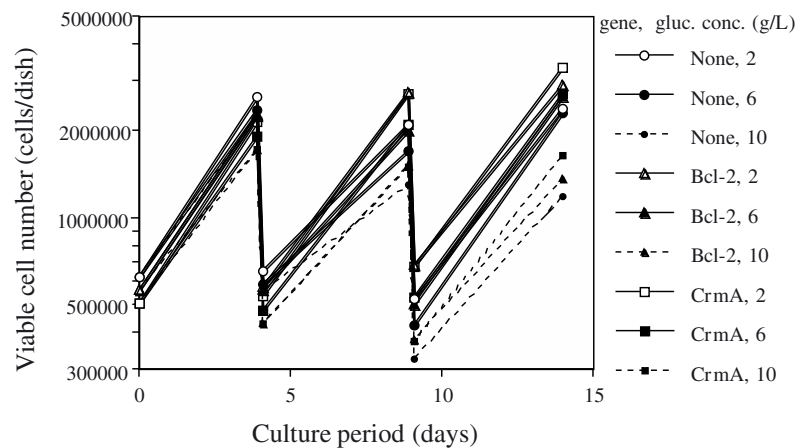


**Fig.1** Growth curve of Rin-5F cells transfected with gene in the presence of glucose. Cells were treated with trypsin and harvested to fresh media at 1: 4 dilution rate at every 4-5 days.

## 3. RESULTS AND DISCUSSIONS

Rin-5F cells transfected with anti-apoptotic genes including *Bcl-2* and *crmA* were cultured in the presence of glucose at different concentration. 2 g/L is normal

glucose level in RPMI medium, and 6 g/L is glucose level in blood of rat diabetes. 10g/L is extremely high concentration. As shown in Fig.1 and Fig.2, the proliferations of cells under hyperglycemia were inhibited and the viabilities were decreased. But over-expression of anti-apoptotic genes, including Bcl-2 and CrmA, significantly improved the proliferation and viability of the cell line.

Then we determined insulin synthesis of the cells under hyperglycemia condition. Although insulin concentrations in the culture supernatant of cells under hyperglycemia were lower, over-expression of anti-apoptotic genes partly neutralized this decrease. For example, while wild type in the presence of 6 g/L of glucose synthesized one fifth as much as cells in normal condition did, Bcl-2 transfectants in the presence of 6 g/L of glucose synthesized half as much as cells in normal condition did.

These results suggest that anti-apoptotic technique would be useful for cell therapy to improve efficiency of curing diabetes.

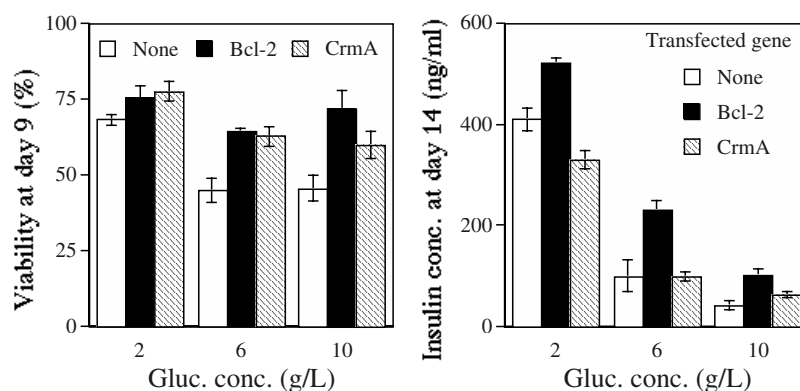


Fig. 2. Viability of Rin-5F transfected with gene. Fig.3. Insulin production of Rin-5F

#### 4. REFERENCES

- [1] T. Zwillich, Islet transplants not yet ready for prime time, *Science*, 289 (2000), 531
- [2] P. W. Burridge *et al.* Future trends in clinical islet transplantation, *Transplant. Proc.*, 34 (2002), 3347
- [3] J. L. Contreras *et al.* Cytoprotection of pancreatic islets before and soon after transplantation by gene transfer of the anti-apoptotic bcl-2 gene, *Transplantation*, 71 (2001), 1015
- [4] G. Nakagawa *et al.* Preservation of pancreatic islets in rodent models, *Pancreas*, 16 (1998), 392
- [5] Y. Tsujimoto, Stress-resistance conferred by high level of bcl-2 alpha protein in human B lymphoblastoid cell, *Oncogene*, 4 (1989), 1331
- [6] S. Terada, *et al.* Improvement of mammalian cell survival by apoptosis-inhibiting genes and caspase inhibitors for effective use of mammalian cells, *Seibutsukougakukaishi*, 77 (1999) 2-11.
- [7] S. Terada, *et al.*, Generation of a novel apoptosis-resistant hepatoma cell line, *J. Biosci. Bioeng.*, 95 (2003), 146
- [8] M. Miura *et al.* Induction of apoptosis in fibroblasts by IL-1 beta-converting enzyme, a mammalian homolog of the *C. elegans* cell death gene *ced-3*, *Cell* 75 (1993), 653

B. OPALKA, P. SCHÜTT, D. BRANDHORST, U. BUTTKEREIT,  
M. TEWES, T. MORITZ, S. SEEBER, M.R. NOWROUSIAN

## PREPARATION AND CHARACTERIZATION OF AN IDIOTYPE-DENDRITIC CELL VACCINE FOR IMMUNOTHERAPY OF MULTIPLE MYELOMA

*Establishing a Protocol for Generation of Mature Dendritic Cells  
Pulsed with Idiotype Protein in Preparation of a Clinical Phase-I  
Vaccination Study in Multiple Myeloma Patients after Conventional or  
High Dose Chemotherapy*  
*Universitätsklinikum Essen, Innere Klinik (Tumorforschung), Hufelandstr.  
55, D-45122 Essen, Germany*

### INTRODUCTION

Multiple myeloma (MM) is a malignant disease characterized by the accumulation of clonal plasma B cells in the bone marrow, osteolytic lesions, progressive bone marrow failure and renal insufficiency. In the majority of cases the malignant plasma cells produce a monoclonal immunoglobulin of the IgG-, IgA or Bence Jones-type. Despite recent progress in pharmacological therapy, MM is still considered incurable and novel therapeutic approaches are demanded [1]. As the clone-specific idiotypic determinant (Id) on the immunoglobulin can be regarded as a specific tumor antigen, vaccination therapy with the Id as antigen have been suggested and performed [2, 3]. In particular dendritic cells (DCs) loaded with the Id antigen appear as an attractive approach in this context [4, 5]. Therefore, in preparation of a clinical vaccination trial of MM patients with Id-loaded DCs we have investigated protocols to prepare autologous DCs as well as Id protein from MM patients and evaluated their capacity to stimulate T cell activation in vitro.

### MATERIALS AND METHODS

**Preparation of Id protein:** The Id was isolated from patients serum prior to the beginning of chemotherapy. Purification was performed by protein G-Sepharose affinity chromatography followed by neutralization and sterilization.

**DC-preparation:** Peripheral blood mononuclear cells were isolated from 100 ml of blood by density gradient centrifugation, resuspended in serum-free medium

(XVIVO15) and cultured in tissue culture dishes for 2 h. The adherent cells were incubated in XVIVO medium supplemented with IL-4 ( $10^3$  U/ml) and GM-CSF ( $0.8-1 \times 10^3$  U/ml) for 7 days. The Id or control antigens were added at days 1 and 4. Optimal doses of Id protein in our hands were 35-40  $\mu$ g/ml. After 7 days the medium was exchanged and maturation was induced with IL-4, GM-CSF (concentrations see above), TNF- $\alpha$  (10 ng/ml), and IL-1 $\beta$  (10 ng/ml) in the continuous presence of Id or control antigen. Phenotypes of immature and mature DCs were analysed by flow cytometry at day 7 and at day 14, respectively.

Immunophenotyping of the DCs was performed by flow cytometry on days 7 and 14 using the following antigens: CD 14, CD 40, CD 83, CD 86, CD1a, and HLA-DR

Functional activity of DCs: Function of the DCs was assessed by co-culturing immature day 7 DCs with autologous lymphocytes, which were derived from the non-adherent fraction of peripheral blood cells and pre-cultured for 7 days in XVIVO medium supplemented with 5 U/ml IL-2. Co-culture of antigen-pulsed DCs and lymphocytes was performed for another 7 days. On day 14 stimulation of CD4 and CD8 T cells was analyzed by FACS after staining with anti-CD25 and anti-CD71 mABs while T cell proliferation was assessed by flow cytometric cell cycle analysis of CD 4 and CD 8 lymphocytes using propidium iodide staining. In addition, cluster formation of lymphocytes in the presence of antigen pulsed DCs was scored by light microscopy and documented by photography. Size and number of clusters were evaluated. In one patient, INF- $\gamma$  secretion of activated lymphocytes was verified by flow cytometry and ELISPOT after enrichment of INF- $\gamma$  secreting cells using anti-CD45/anti-INF- $\gamma$  bi-specific antibodies and MACS selection.

## RESULTS AND DISCUSSION

Using a protocol suitable for the preparation of monoclonal immunoglobulin idiotype (Id) pulsed DCs for immunotherapeutic purposes the generation of mature day14 DCs from peripheral blood was analysed in 27 multiple myeloma (MM) patients. As depicted in table 1 the efficiency of DC generation from MM patients was similar for patients at different stages of disease and therapy. In the majority of patients (19/27) more than  $2 \times 10^6$  DCs (sufficient for at least one round of vaccination) were obtained from 100 ml of peripheral blood. This compared similar to DC yield obtained from five normal donors on d7 ( median 6.0, range 1.3 –  $12.0 \times 10^6$ ).

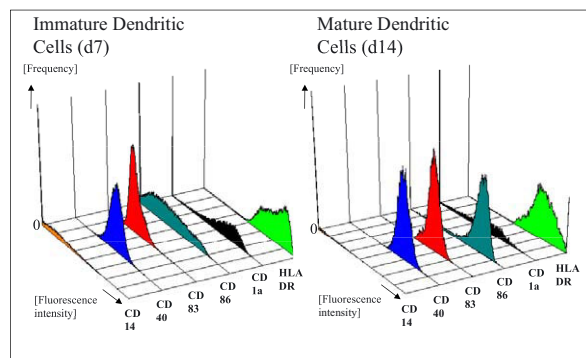
Table 1. Dendritic cell yield from peripheral blood

Donors /patients	Samples (n)	Median (x 10 <sup>6</sup> )	Range	Total yield <2x10 <sup>6</sup> cells
27 MM patients including	27	5.6	(0-34.7)	8/27
- TH	15	5	(0.05-15.6)	5/15
+ TH	12	8	(0-34.7)	3/12
- HD	17	5	(0.05-9.25)	5/17
+ HD (< 6 months)	5	5.2	(0-34.7)	2/ 5
+ HD (>12 months)	5	8.3	(1.7-15.6)	1/ 5
- CTX(untreated)	8	4.15	(0.8-7.5)	3/ 8
- CTX (>6 weeks)	11	6.3	(1.5-15.6)	2/11
+ CTX (<6 weeks)	7	5	(0-34.7)	3/ 7

- TH; +TH = patients without (-) or with (+) thalidomide treatment, - HD, + HD (< 6months), + HD (> 12 months) = patients without (-) or within 6 months of (< 6 month) or 12 months after (>12 month) high dose chemotherapy. - CTX; + CTX = patients with last conventional chemotherapy longer than 6 weeks ago (- CTX) or within 6 weeks of conventional chemotherapy (+ CTX) and no treatment with HD-CTX.

Mature DCs generated by our protocol showed high expression of CD40, CD83, CD86, HLA-DR, and downregulation of CD14 (figure 1). Addition of IL-6 to the cultures had only marginal influence on maturation. Again, no differences in surface phenotype were found when DCs from MM patients and healthy donors were compared.

Figure 1. Surface phenotype of DCs



Results of flow cytometric analyses of monocyte (CD14) and DC (CD40, CD83, CD86, and HLA-DR) surface markers at day 7 and day 14 of DC maturation are depicted (representative experiment). In selected

patients, also functional properties of DCs generated by our protocol were assessed. This was done by exposing autologous T cells to Id-pulsed DCs and subsequent measurement of T cell activation. In comparison to non-pulsed DC controls, DCs pulsed with an allogeneic Bence Jones Protein (BJP) or the autologous Id protein exhibited a markedly increased capability to activate CD8 lymphocytes during the 7 day co-culture. Following co-culture with BJP- or Id-pulsed DCs CD8 cells expressed significantly more CD25- as well as CD71-activation marker on their surface. Proliferation of CD8 cells, as measured by the percentage of cells in the G2/M-phase of the cell cycle, also was significantly increased. In addition, when cluster formation of lymphocytes during co-culture with DCs was analysed semiquantitatively as another parameter of lymphocyte activation, more and bigger lymphocyte-clusters were detected in the presence of BJP- or Id-pulsed DCs. In one patient, INF- $\gamma$  secretion of lymphocytes after co-culture with Id-pulsed DCs was assessed by enrichment of INF- $\gamma$  secreting cells with anti-CD45/anti-INF- $\gamma$  bi-specific antibodies and MACS selection and subsequent confirmation of INF- $\gamma$  secretion by ELISPOT or FACS-analysis of intracellular INF- $\gamma$  production. No INF- $\gamma$  secreting lymphocytes were detected following co-culture with non-pulsed DCs.

#### SUMMARY

Using a clinically applicable protocol the preparation of mature DCs from the peripheral blood of MM patients at various stages of disease and therapy was demonstrated. While there were substantial interindividual variations, on average no major differences in yield and maturity of the DCs were detected between MM patients and healthy controls. In addition, the functionality of Id-pulsed DCs was demonstrated in selected patients by antigen-dependant activation of both CD4+ and CD8+ T cells. In view of these results a phase I study using autologous Id-pulsed DCs for vaccination of MM patients has been designed at our institution.

#### REFERENCES

1. Barlogie, B., et al., *Advances in the treatment of multiple myeloma*. Adv Intern Med, 1998. **43**: p. 279-320.
2. Lynch, R.G., et al., *Myeloma proteins as tumor-specific transplantation antigens*. Proc Natl Acad Sci U S A, 1972. **69**(6): p. 1540-4.
3. Wen, Y.J., B. Barlogie, and Q. Yi, *Idiotype-specific cytotoxic T lymphocytes in multiple myeloma: evidence for their capacity to lyse autologous primary tumor cells*. Blood, 2001. **97**(6): p. 1750-5.
4. Titzer, S., et al., *Vaccination of multiple myeloma patients with idiotype-pulsed dendritic cells: immunological and clinical aspects*. Br J Haematol, 2000. **108**(4): p. 805-16.
5. Lim, S.H. and R. Bailey-Wood, *Idiotypic protein-pulsed dendritic cell vaccination in multiple myeloma*. Int J Cancer, 1999. **83**(2): p. 215-22.

PADILLA, J.<sup>1</sup>, BURKE, V.<sup>2</sup>, JOHNSON, J.<sup>1</sup>, HARTSHORN, J.<sup>1</sup>,  
MCNORTON, S.<sup>1</sup> AND ETCHBERGER, K.<sup>1</sup>

## PRETREATMENT WITH POLYCATIONS ENHANCES ADENOVIRAL INFECTION LEVELS IN SERUM-FREE PER.C6™ CELLS AS WELL AS HEK 293 CELLS

<sup>1</sup>*JRH Biosciences, Inc., 13804 W. 107<sup>th</sup> Street, Lenexa, Kansas 66215 USA.  
Corresponding author phone (913) 469 5580 e-mail. [jorge.padilla@jrhbio.com](mailto:jorge.padilla@jrhbio.com)*

<sup>2</sup>*Univ. of the Virgin Islands.*

### 1. INTRODUCTION

Adenoviral vectors are ideal for the high-level, short-term gene expression required in gene therapy protocols. Human adenovirus 5 (Ad5) offers great promise in cancer gene therapy. Ad5 is very well characterized and can be grown in culture to a high titer. This virus is stable and capable of replicating in many human cancer cell types. More recently developed cell lines such as PER.C6™ eliminate overlapping sequences resulting in significantly lower rates of RCA. The transduction efficiency of adenovirus has been reported to increase in the presence of pharmacological agents, used in conjunction with adenovirus administration in vivo and in vitro. This report describes the effects of pharmacological agents on adenovirus infection using two different cell systems: PER.C6™ and HEK 293 cells.

### 2. MATERIALS AND METHODS

#### 2.1. Cells and virus

Two cell lines were used in this study: Transformed primary human embryonic kidney cells 293 (HEK 293), and PER.C6™, Crucell NV. HEK 293 cells were cultivated in DMEM/Modified with high glucose, supplemented with 6 mM L-glutamine, and 10% FBS, and washed with Phosphate Buffered Saline (PBS),

PER.C6™ cells were cultivated in EX-CELL™ VPRO Medium, supplemented with 6 mM L-glutamine.

The adenovirus used for infection was adenovirus 5 containing GFP under the control of a modified Cytomegalovirus-IE promoter enhancer (Adv5CMV5-GFP). The viral stock titer was  $4.5 \times 10^{11}$  TCID50/mL.



### 2.1.1. Polycations

Protamine; poly-L-lysine, DEAE-dextran, spermine, spermidine and polybrene, were from Sigma-Aldrich Co.

#### 2.1.1.1. Culture and infection in spinner flasks

PER.C6<sup>TM</sup> cells were inoculated at approximately  $4 \times 10^5$  cells/mL. Cells in log phase growth were pretreated with the polycations or polyamines two hours before infection. After pretreatment with the chemical compounds, resuspended cells were infected with Adv5CMV5-GFP at a MOI of 10. In the case of HEK 293 cells, 96-well plates were seeded at the appropriate cell density followed by pretreatment with the polycations for two hours. Cells infected with Adv5CMV5-GFP at a MOI of 10. Cells were monitored by fluorescence microscopy and the intensity of fluorescence was quantified.

##### 2.1.1.1.1. Quantification of adenoviral vector by fluorometry

The level of GFP was quantitated by fluorescent microscopy using a Spectra MAX Gemini XS plate reader ( $\lambda_{ex}=473$  nm,  $\lambda_{em}=509$  nm).

## 3. RESULTS

Since polycations have been shown to enhance adenovirus infection of epithelial cells, applying this could increase the number of cells infected with adenoviral vectors which could improve the success of gene therapy applications.

In this study, we wanted to determine which polycations such as DEAE-dextran, protamine, polybrene and poly-L-lysine were able to facilitate uptake of adenoviral particles. Polybrene at 4  $\mu$ g/mL resulted in the greatest increase of infection on HEK 293 cells at day 13. Since there is little information about PER.C6<sup>TM</sup> cell line, we evaluated the possible effect of polycations on adenoviral infection using this cell line. Based upon the data obtained with the HEK 293 cell line, we selected those polycation concentrations that had the greatest increase in virus yield. As shown in Figure 1, the addition of 100  $\mu$ g/mL or 500  $\mu$ g/mL protamine, 5  $\mu$ g/mL poly-L-lysine, 0.5  $\mu$ g/mL DEAE-dextran and 1 mM spermine before infection did not increase the efficiency of adenovirus infection in PER.C6<sup>TM</sup> cells. However, adding 4  $\mu$ g/mL polybrene before adenovirus infection increased the levels of infection compared to those of the non-treated infected control (Figure 2).

## 4. CONCLUSIONS

The infection with adenovirus in either HEK 293 or PER.C6<sup>TM</sup> cells was markedly increased by the addition of polycations. These data demonstrate that the presence of polymers such as polybrene before viral adsorption in both cell systems increases the efficiency of viral infection.

## 5. FIGURES

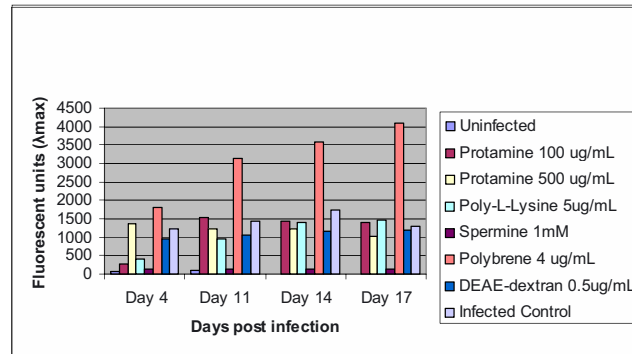


Figure 1. Effect of polycations on the ADV infection on PER.C6<sup>TM</sup> cells. PER.C6<sup>TM</sup> cells were incubated with polycations for two hours before infection, and the fluorescence intensity levels were determined on days 4, 11, 14 and 17. Polybrene at 4 $\mu$ g/mL before adsorption with adenovirus supported an increase on the level of fluorescence intensity.

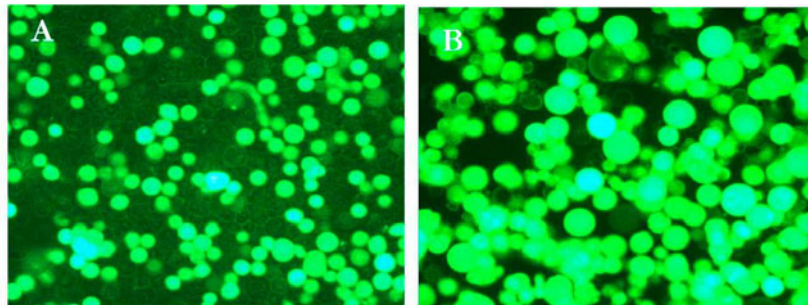


Figure 2. Fluorescence microscopy of PER.C6<sup>TM</sup> cells infected with adenovirus. Panel A illustrates cells infected with Adv5CMV5-GFP without pre-treatment with polycations. Panel B illustrates infected cells pretreated with 4 $\mu$ g/mL polybrene. The amount of fluorescence was increased by the addition of polycations.

M. SCHROEDER<sup>1,3</sup>, S. NIEBRUEGGE, A. WERNER<sup>1</sup>,  
R. ZWEIGERDT<sup>2</sup>, M. BURG<sup>2</sup>, J. LEHMANN<sup>1</sup>

## OPTIMIZING THE PRODUCTION OF CARDIOMYOCYTES FROM MOUSE EMBRYONIC STEM CELLS IN A 2L STIRRED TANK REACTOR

<sup>1</sup>*Institute of cell culture technology, University of Bielefeld, Bielefeld, Germany* <sup>2</sup>*Cardion AG, Erkrath, Germany,* <sup>3</sup>*Institute of Biotechnology 2, Research Center Juelich GmbH, Germany*

### 1. INTRODUCTION

Embryonic stem (ES) cells are a promising potential source for the derivation of specific cell types for therapeutical applications. Currently, conventional technologies such as cell culture plates and spinner flasks are used for the expansion and differentiation of ES cells. Both systems are difficult to scale up and pose serious limitations on the control of culture parameters like pH, pO<sub>2</sub> and shear force. For the clinical-scale production of specific cell types reproducible bioprocesses at a relevant scale have to be established. Cell transplantation is emerging as a potential treatment for heart failure. The left ventricle of the human heart contains ~5.8x10<sup>9</sup> cardiomyocytes (CMs, Kajstura et al., 1998). Consequently, cell transplantation therapies aimed at replacing tissues lost to myocardial infarction could require the successful seeding of as many as 5-10x10<sup>8</sup> donor CMs per patient. The robust generation of such large CM numbers is only feasible in controlled bioreactors with active aeration. In addition a reliable method for the exclusion of non-CM and of potentially remaining stem cells is mandatory to provide highly purified cells for transplantation purposes. In this work the scale up and purity issues are addressed and findings on the expansion and differentiation of ES cells and the production of pure CMs in a 2L standard stirred tank reactor are presented.

### 2. RESULTS

#### *2.1. Expansion and differentiation of J1 ES cells: Stirrer-speed optimization*

J1 ES cells were expanded on tissue culture plates to inoculate a standard 2L stirred tank reactor (B.Braun). The following culture parameters were kept constant over the course of the bioprocess: 37°C, pH 7.2 and 40% pO<sub>2</sub>. The process was

inoculated with a single-cell suspension of  $2 \times 10^5$  cells/mL in a culture volume of 1L. EB formation was performed via stirring directly in the bioreactor. At day 2 culture volume was adjusted to 2L. After 9 days in suspension EBs were harvested and replated on gelatine-coated cell culture dishes. Seeded cells were analyzed for the presence of contracting colonies (indicating CM-formation). Immunohistochemistry using the Myosin-heavy-chain specific MF20 antibody was performed. Specific processes were performed at stirrer speeds of 35, 50, 65, 80 and 125 rpm aiming to determine the optimum stirrer speed regarding proper EB formation, cell yield and differentiation towards CMs.

Fig. 1 is a comparison of cell densities depending on specific stirrer speeds tested. The optimum stirrer speed was determined to be 65 rpm in our system resulting in  $1,3 \times 10^7$  viable cells/mL at day 9. In contrast, the 35 rpm process resulted in the formation of large cell aggregates and only limited cell expansion and differentiation. In addition, aggregates attached to the bioreactor wall and electrodes at this specific speed. A stirrer speed of 125 rpm was the upper limit for expansion and differentiation in our system and EBs were seriously damaged at this speed resulting in low cell growth and high LDH-activity levels.

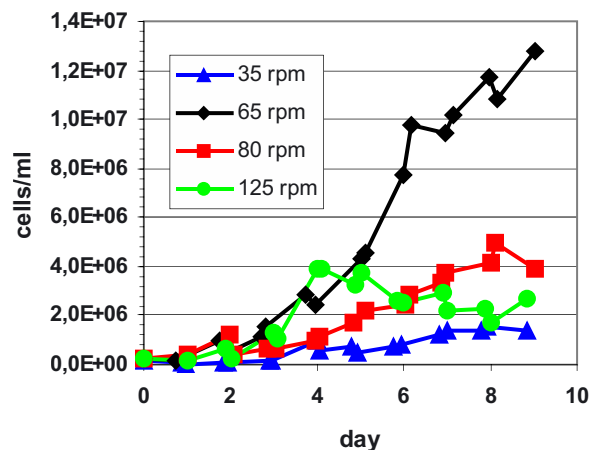


Figure 1. Cell densities at different stirrer speeds.

## 2.2. Genetic selection of pure CMs from ES cells in clinical scale

Based on the optimized EB formation process described above we next aimed to select CMs in our bioreactor setting. To facilitate the large-scale production of ESC-derived CMs, this bioengineering approach was performed in conjunction with a CM-specific genetic selection technique. The genetic selection utilized the alpha-cardiac-MHC promoter to target expression of neomycin resistance exclusively in

CMs; addition of G418 and retinoic acid (RA) to the cultures results in a substantive enrichment of stem-cell derived CMs (Klug et al., 1996, Zandstra et al., 2003).

After nine days of EB formation and differentiation at 65 rpm a selection phase of another nine days was initiated via G418 (400 µg/mL) and RA (10 nM). At the end of the process cells were harvested, enzymatically dispersed and replated on cell culture plates to assess cardiomyocyte purity. Fig. 2 presents cell densities observed during the production process. Fig. 3 exhibits MF20 staining of the enzymatically digested cardiac bodies at day 18 (cells were stained two days after plating). Persistence of embryonic stem cells has been analyzed via FACS analysis. It is important to underscore that the number of SSEA-1 and E-cadherin positive cells was below detectable limits (data not shown) in our system. In summary, we have generated more than 1e9 essentially pure CMs in a 2L stirred tank reactor, demonstrating feasibility of such clinical scale bioprocess for the derivation of specific cell types from embryonic stem cells.

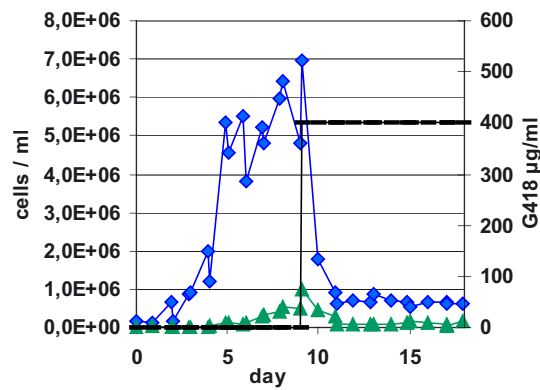


Figure 2. Cell densities of production process. Square: viable cell density. Triangle: dead cell density.

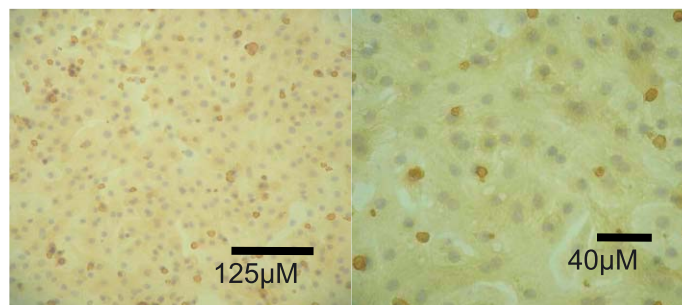


Figure 3. MF20 (DAB) and hemalaun stain of attached and dispersed cells. Seeding density 7e4 CMs per cm<sup>2</sup>. Purity >99%.

### 3. REFERENCES

- Bader, D. *et al.* (1982). Immunochemical analysis of myosin heavy chain during avian myogenesis in vivo and in vitro. *J Cell Biol* 95: 763–770.
- Kajstruta, J. *et al.* (1998). Myocyte proliferation in end-stage cardiac failure in humans. *Proc Natl Acad Sci USA* 95: 8801-8805.
- Klug, M.G. *et al.* (1996). Genetically selected cardiomyocytes from differentiating embryonic stem cells form stable intracardiac grafts. *J Clin Invest* 98: 216-224.
- Zandstra et al., Scalable production of embryonic stem cell derived cardiomyocytes. *Tissue Eng* 2003 Aug.;9(4)

R. VOGLAUER<sup>1</sup>, C. JURSIK<sup>1</sup>, M. PRCHAL<sup>1</sup>, H. JUNGFER<sup>2</sup>,  
J. GRILLARI<sup>1</sup>, H. KATINGER<sup>1</sup>

## ESTABLISHMENT AND CHARACTERIZATION OF CD4+ KILLER-T-CELLS (KTCS) A PROMISING NEW TOOL FOR ADOPTIVE IMMUNOTHERAPY

<sup>1</sup> *Institute of Applied Microbiology, University of Natural Resources and Applied Life  
Sciences, Vienna, Austria,* <sup>2</sup> *Roche Diagnostics, Penzberg, Germany,*  
*R.Voglauer@iam.boku.ac.at*

### 1. INTRODUCTION

Normally the immune system recognizes arising tumor cells and thus plays an important role in the prevention of cancer. However, many tumor cells possess mechanisms that allow them to escape initial immune response and destruction. Over the last years different tumor therapy strategies have been developed, one of which deals with the “reinvolvedment” of the patients immune system. In the case of adoptive immunotherapy, immune competent cells are activated and expanded ex-vivo, followed by reinfusion into the patient<sup>1</sup>. Successful adoptive T-cell therapy has been demonstrated in viral diseases and several types of cancer. Nevertheless, preclinical and clinical studies have elucidated several issues that have to be addressed to improve the success rates of these therapy forms. These issues include the selection of appropriate target antigens, the optimization of the methods for generating functional immune cell populations in vitro and the assurance of effector cell survival and function by administration of cytokines and proinflammatory signals. Here we describe the generation of a novel subset of highly reactive anti-tumor lymphocytes. These cells represent an oligoclonal population of cytotoxic CD4<sup>+</sup>T-cells, that attack a large variety of different tumor cell lines, while sparing normal cells. Simple and fast isolation and expansion of these Killer T-cells make them a highly promising new tool for adoptive immunotherapy.

### 2. METHODS AND RESULTS

#### 2.1. Generation of Killer-T-Cells

Peripheral blood mononuclear cells (PBMCs) were isolated using Ficoll-Hypaque gradient centrifugation. After depletion of monocytes, natural killer (NK) cells, suppressor-T-cells and dendritic cells by incubation with L-leucyl-L-leucine-methylester hydrochloride the remaining cells were activated by a three days

incubation with a glutaraldehyde fixed antibody-producing cell line. Further cell propagation was carried out in serum-free medium supplemented with interleukin 2 and cyclosporin A.

## 2.2. Allogeneic cytotoxicity assay

KTCs from healthy donors were generated from PBMCs and cocultivated with human tumor cells as target cells. For quantification of cytotoxicity we established a recently published flow cytometric assay<sup>2</sup>. Therefore, the tumor targets were stained with the lipophilic membrane dye PKH-26. Thereafter, effector and target cells were incubated for 20-24 h at various target : effector ratios (1:10, 1:20). The percentages of vital, early apoptotic and necrotic cells within the target cell population were determined after costaining with Annexin-V-FITC (Ann-FITC) and propidium iodide (PI) (figure 1). For quantification of KTC cytotoxicity, the percentage of non-specific annexin-positive cells (including apoptotic and necrotic cells), which was determined in control samples without effector cells was subtracted from the percentage positive events at the indicated effector : target ratios (figure 2).

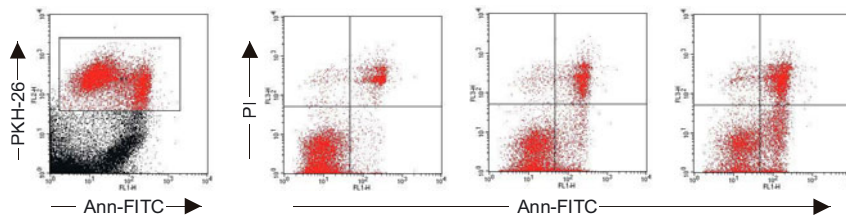
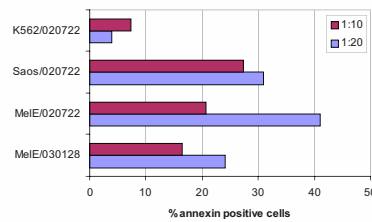


Figure 1. KTC cytotoxicity on human melanoma cells after 20 h. Target cells were selected by gating on the PKH26 positive cell population (left picture). 10000 of these gated cells were further analyzed for Ann-FITC/PI stained subpopulation: target cells without KTCs, target :



effector ratio 1:10, target : effector ratio 1:20 (from left to right).

Figure 2. Percentage of annexin-positive human melanoma, fibrosarcoma and K562 cells after 20 h cocultivation with KTCs at target : effector ratios of 1:10 and 1:20.



### 2.3. Autologous cytotoxicity assay

KTCs from three different colorectal carcinoma (CRC) patients were generated and cocultured with autologous tumor as well as normal cells. While stromal cells were not attacked, CRC cells were killed (table 1). Same results were obtained when allogeneic pairs of and CRC cells / stromal cells KTCs isolated from tumor patients were cocultured (data not shown). Killing properties were followed by trypan-blue dye exclusion assays.

Table 1. Effect of KTCs on autologous tumor and stromal cells

Patient	Coculture of	Surviving target cells (% of control)
1	CRC + KTCs	< 1
	stromal cells+KTCs	105
2	CRC + KTCs	2
	stromal cells+KTCs	97
3	CRC + KTCs	< 1
	stromal cells+KTCs	106

### 2.4. Characterization of the Killer-T-Cell population upon their CD profiling

Killer-T-Cells were stained with antibodies directed against various surface markers and a second, fluorescent labeled antibody. Percentage of viable, positively stained cells is shown in figure 3. Cells were negative for NK- and B-cell markers (data not shown).

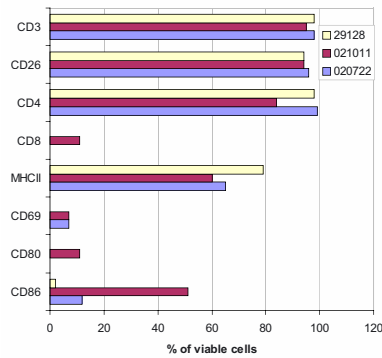


Figure 3. The expression of various surface markers was determined on KTC populations of 3 different donors. Only a small assortment of surface markers tested is shown.

### 3. DISCUSSION

Here we describe a novel approach to generate/expand a subpopulation of immunoreactive T-cells from PBMCs. In vitro these cells recognize and kill all different tumor cell lines tested so far, but leave normal cells as well as the typical NK target cell line K562 intact. Autologous cytotoxicity assays have shown that the distinction between tumor and normal cells was exactly the same as it was for allogeneic ones, suggesting that the killing mechanism is not MHC restricted. However, characterization of the cytotoxic properties of these cells by conventional methods was limited due to the slow killing mechanism. In order to circumvent this problem, we established a novel cytotoxicity assay. Thereby, we confirmed that the cells need more time than other known cytotoxic cells to initiate cell death in vitro. Additionally, we demonstrated that apoptosis is induced in target cells and that the killing efficiency is dependent on the effector to target cell ratio.

The profile of surface markers demonstrates that we have generated a novel subset of cytotoxic CD4<sup>+</sup> T-cells, expressing various activation markers. These results suggest that we have expanded a to date unknown T-cell population that represents a highly promising tool for adoptive immunotherapy against cancer.

### ACKNOWLEDGEMENT

The authors like to thank POLYMUN SCIENTIFIC Immunbiologische Forschung GmbH for financially supporting this work.

### 4. REFERENCES

1. Knutson, K.L., Almand, B., Mankoff, D.A., Schiffman, K. and Disis, M.L. (2002). *Expert Opin Biol Ther*, 2, 55-66.
2. Fischer, K., Andreesen, R., Mackensen, A. (2002). *J Immunol Methods*, 259(1-2):159-69.

## CHAPTER 3

### GENE BASED THERAPEUTICS

A. KAMEN, O. HENRY, D. JACOB AND A. BERNIER

## SUCCESSFUL DEVELOPMENT OF A ROBUST ADENOVIRUS PRODUCTION PROCESS PRIMARILY RELIES ON A BETTER UNDERSTANDING OF PACKAGING CELL LINE PHYSIOLOGY AND VECTOR REPLICATION KINETICS

*Animal Cell Technology, Biotechnology Research Institute (NRC), Montréal,  
Qc, Canada, Email: amine.kamen@cnrc-nrc.gc.ca*

**Abstract.** *This report will focus on demonstrating how the fundamental understanding of complementing cell line physiology and metabolism, viral infection kinetics, culture conditions and viral particle stability is a prerequisite to defining optimal operating conditions for improving final adenoviral yield and activity. Steps involved in developing and optimising a robust integrated process for adenovirus production using HEK-293 cells cultured in suspension and serum free medium will be reviewed using data generated in batch, fed-batch and perfusion culture modes from 3, 20L and 60L bioreactor runs. Development of new monitoring tools (in-situ GFP probe, permittivity) and quantification techniques (HPLC-determination of total particles) greatly contributed to acceleration of process development. On-line monitoring of physiological parameters such as respiration and biovolume during the course of infection/production allowed a real-time supervision and control of critical phases of the process.*

### 1. INTRODUCTION

Adenoviral vectors (AdV) have a number of advantages including their ability to infect post-mitotic tissue including muscles. They are produced at high titres and have been used in 28% of clinical protocols targeting mainly cancer diseases. Although there is a preponderance of literature describing vector design and pre-clinical and clinical AdV mediated therapies (Vorberg and Hunt, 2002), documentation on AdV processing and production at large scale is scarce (Nadeau and Kamen, 2003). The availability of large quantities of clinical grade AdV is recognized as an important limitation to in-vitro experimentations, as well as pre-clinical and clinical studies. In this report challenges and strategies involved in AdV production technologies are discussed based on data generated in authors' laboratory during the last 5 years.

### 2. MATERIAL AND METHODS

#### *2.1. Adenoviral vectors and cell lines*

First generation E1-E3 deleted AdV expressing marker genes such as  $\beta$ -galactosidase, luciferase, GFP (S65T mutant as well as enhanced GFP-Q) and

therapeutic genes such as dystrophin (6.3 kB) and utrophin under control of early promoters CMV or RSV-LTR were used. HEK-293 cells (Graham, 1977) adapted to suspension culture (293S) and further adapted to serum free medium as described elsewhere (Coté *et al.* 1998) were used for AdV production. Serum-free clones were cultured in Low Calcium Serum Free Medium (LC-SFM) or a low protein proprietary formulation NSFM13 (Nadeau *et al.*, 2000). MOI for infection was 10. Viable and total cells were counted using a haemocytometer (Hausser Scientific, Horshaw, PA). Viability was assessed by dye exclusion method using erythrosine B. Infectious virus titer was measured as described by Cote *et al.*, 1997. and total viral particle concentration following the method developed by Shabram *et al.*, 1977, and further optimised in our laboratory (Transfiguracion *et al.*, 2001). The GFP positive cells were scored using a flow cytometer (FCM, EPICS XL-MCL, Coulter, Miami, USA).

### 2.2 Bioreactor and perfusion set-up

Cultures were performed in Chemap CF2000 (Mannedorf, Switzerland) 3 L and 20 L bioreactors and a 60 L Applikon bioreactor (Applikon Inc., Clinton, N.J.). The primary operating conditions have been described in previous reports (Nadeau *et al.*, 2002). The biomass was evaluated using a capacitance probe (Aber Instruments Ltd., Aberystwyth, U.K.) that allows for viable cell biovolume estimation (Zeiser *et al.*, 1999). The fluorescence probe is described elsewhere (Gilbert *et al.*, 2000). Perfusion cultures were performed in a Chemap 3 L bioreactor equipped with an Applikon BioSep™ acoustic filtration system (model ADI 1015, Sonosep Biotech Inc., Richmond, BC, Canada) as the cell retention device.

## 3. RESULTS AND DISCUSSION

For large-scale productions, suspension culture is the method of choice over processes using adherent cells. Suspension culture is characterized by a homogeneous concentration of cells, nutrients, metabolites and products, there by facilitating scale-up and enabling accurate monitoring and control of the culture. Therefore, HEK-293 cells have been adapted to suspension and serum free medium Proprietary serum-free medium (NSFM13) supporting high cell density, high viability during the infection phase and high adenoviral specific yield was developed.

### 3.1 HEK-293 metabolic changes following adenovirus infection

Upon infection, the cell size as well as the cell dry weight, protein content and DNA content increase. In the case of HEK-293 cells cultured in serum free medium, the mean cell diameter increased from 15  $\mu\text{m}$  to approximately 17  $\mu\text{m}$  (Nadeau *et al.*, 2000) This increase is associated with viral DNA replication 9 hours after the infection. Due to this delay, up to 50% cell growth after infection might be observed. We reported that the rates of consumption of glucose and production of

ammonia and lactate is increased by 30% to 100% (Garnier *et al.*, 1994). This trend has also been observed for O<sub>2</sub> consumption and for the theoretical ATP production. This may be not only due to the increase in cell weight but also to the infection process that requires more energy. Results of <sup>14</sup>C-glc and <sup>14</sup>C-gln labelling experiments (table 1) show that 14% of glutamine is metabolized through TCA, 3%-metabolized glucose goes through PPC and that glucose is minimally oxidized through TCA. However, glucose is more efficiently metabolised through the TCA cycle during infection, while less glutamine was driven into this pathway during the infection (Nadeau *et al.*, 2000; 2002). Similar to most transformed mammalian cells, lactate and ammonia are the main by-products accumulated in HEK-293 adenovirus infected or non-infected cultures.

	293SF in LC-SFM			
	Growth		Infection	
	%	nmole/10 <sup>6</sup> cells/min	%	nmole/10 <sup>6</sup> cells/min
PPC-flux (max)	3.38	0.086	3.05	0.076
PPC-flux (min)	3.12	0.079	2.09	0.052
Glc-TCA	0.26	0.007	0.95	0.024
Gln-TCA	14.3	0.06	3.35	0.014

Table 1: <sup>14</sup>C-glc and <sup>14</sup>C-gln labelling experiments and determination of ratio for the pentose phosphate cycle (PPC) and tricarboxylic acid (TCA) pathways

### 3.2 The "Cell density effect"

Maximal viable cell densities as high as 5x10<sup>6</sup> cells/mL can be achieved in suspension bioreactor cultures at scales ranging from 3 to 20L. However, productions of adenovirus vectors that maintain a high specific yield in batch operation were limited at cell densities in the range of 5x10<sup>5</sup> cells/mL, which is an order of magnitude lower than the maximal cell densities achievable

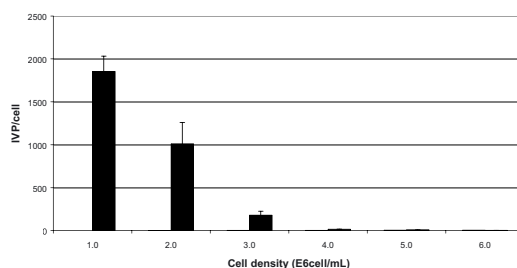


Figure 1: Infectious viral particles (IVP) per cell produced at different cell densities in NSF13 medium.

Results in figure 1 clearly demonstrate a decrease in the cell specific production of the infectious viral particles expressing a GFP-Q marker gene at cell densities higher than 5x10<sup>5</sup> cells/mL. Beyond 2x10<sup>6</sup> cells/mL, no infectious particles are detectable.

These results strongly suggest a limitation either due to key nutrient depletion or inhibitor by-product accumulation. Medium development remains a critical approach to improve the process. Alternatively to elevate the “cell density” limitation, different feeding strategies were evaluated. Sequential-batch, fed-batch and perfusion modes are of incremental difficulty in implementation and operation.

### 3.3 Batch production

The infection phase requires that the media be exchanged in order to have a successful production at cell densities higher than  $0.3 \times 10^6$  cells/mL. Figure 2 shows production of total GFP-expressing adenovirus particles as well as infectious particles obtained in a 60 L Applikon bioreactor infected at  $1 \times 10^6$  cells/mL. The culture medium was exchanged at ~90% using fresh NSFM13 medium prior to infection using a large-scale Sorvall Centrifuge Cell (Kendro Laboratory Products, Newton, CT). Maximum specific productions of ~22,000 particles and ~6,000 infectious particles per cell were reached and a ratio of infectious to total particles of 33% was obtained at 72 hpi. These yields are significantly higher than yields routinely obtained in shake flasks and indicate a successful scale-up.

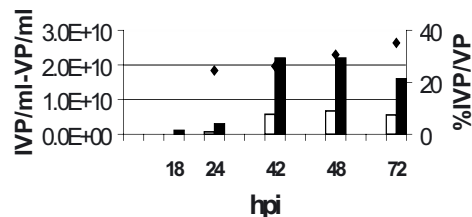


Figure 2: Time course of infectious particles (IVP), total particles (VP) and ratio of the two obtained in a 60L. The culture was infected at  $1 \times 10^6$  cells/mL in NSFM13.

Solid bar=VP/ml; empty bar= IVP/ml and  $\blacklozenge$  = viability

### 3.4 Fed-batch production

Fed-batch addition of glucose, glutamine and amino acids allowed infections at cell densities up to  $2 \times 10^6$  cells/mL; however, the productivities attained at high cell densities were lower than those obtained with infection at cell density of  $1 \times 10^6$  cells/mL. These results have been presented in detail by Nadeau *et al.* (2000, 2002). Despite modest improvements, efforts are still dedicated to developing an efficient fed-batch feeding strategy because this process is easy to operate and readily scalable

### 3.5 Perfusion production

An acoustic filter was used for cell retention in the perfusion experiments, in view of the increased shear sensitivity of the cell during the infection phase. The perfusion system permitted the *in situ* medium exchange and a better control of the culture

environment. Additionally, toxic by-products were removed. A perfusion rate of 2 vol/d allowed to reach virus titers of  $4.7 \times 10^{10}$  VP/mL, a significant increase compared to typical batch productions. Moreover, the specific productivity was maintained for cell densities up to  $3 \times 10^6$  cells/mL at infection.

### 3.6 On-line monitoring of the infection process

Various tools exist to monitor and assess the success of an infection during a culture, as illustrated in Figure 3. Prior to infection, both the capacitance and oxygen uptake rate (OUR) signals correlated well with the cell growth profile. Following infection, the cells continued to grow and there was a concomitant increase in the oxygen uptake rate and the cell capacitance signals (Figure 3). It was followed by a sharp decrease in cell viability and oxygen consumption as a result of the lytic process. The mean cell diameter increases after the onset of viral DNA replication. This change in the biovolume was reflected in the capacitance signal that reached a maximum 18 hours after the cell concentration and OUR peaks and only started to decline when the viability dropped below 70 %. The maximum virus titre was attained at 65 hpi and occurred just before the peak in fluorescence (74 hpi). Although not correlated to adenovirus production, the fluorescence measurement allows the monitoring of the viral protein expression kinetics.

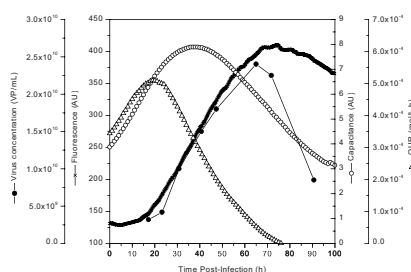


Figure 3: Total viral particle concentration, fluorescence, capacitance and oxygen uptake rate profiles post-infection during a perfusion culture. The virus titres were assayed by HPLC.

### 3.3 Adenoviral vector production kinetics and vector stability

The adenovirus production kinetics was evaluated beyond 48 hours post infection under different modes of culture, batch, fed-batch and perfusion. Decrease of specific total particle counts over time is systematically observed independently of the mode of culture while infectious titres were generally maintained constant till 96 hpi. In all experiments, including production of a wild type 5 adenovirus, the rate of decrease over time of total particle count was correlated with the rate of decrease in



cell viability. A net result of the selective decrease in total particles is an apparent increase of the ratio of infectious particle to total particle counts. Observation of adenoviral particles aggregation has been well documented in recent literature (Obenauer-Kutner *et al.*, 2002). Decrease of total particle counts occurs during the adenovirus production cycle. During this period, most of the adenoviral particles are within the cells. Aggregation alone cannot explain our results. Vellekamp *et al.* (2001) reported that empty and immature adenoviral particles were more susceptible to degradation at 37°C over time. Moreover, presence of empty particles was correlated with the presence of a 31kD precursor of adenovirus protein VIII (pVIII). An assay based on the measure of the 31kD pVIII was proposed to monitor ratio of empty to complete adenoviral particles. The assumption that immature adenovirus particles and empty capsids are degraded more rapidly than mature adenovirus particle is consistent with the observed increase of infectious to total particle ratio over adenovirus production time course. These results suggest that by selective degradation of immature particles the ratio of infectious to total particle may be increased at time periods of greater than 48 hours post infection.

#### 4. REFERENCES

- Côté J. *et al.* *Biotechnol Prog* 1997; **13**:709-714.  
Côté J, *et al.* *Biotechnol Bioeng* 1998; **59**:567-575.  
Garnier A. *et al.*. *Cytotechnology* 1994; **15**:145-155  
Gilbert PA. *et al.* *Biotech Letters* 2000; **22**:561-567.  
Graham FL. *J Gen Virol* 1977; **36**: 59-74.  
Nadeau I. and Kamen A, *Advanc Biotechnol.*, 2003, **22** : 475-489  
Nadeau I, *et al.* *Biotechnol Bioeng* 1996; **51**:613-623.  
Nadeau I. *et al.* *Biotechnol Prog* 2000; **16**:872-884.  
Nadeau I *et al.* *Biotechnol Bioeng* 2002 ; **77**:91-104.  
Transfiguracion *et al.* *J Chromatogr B* 2001; **761**:187-194.  
Obenauer-Kutner L.J. *et al.*, *Hum Gene ther* 2002; **13**:1687-1696  
Shabram PW *et al.* *Hum Gene ther* 1997; **8**:453-465  
Vellekamp G. *et al.* *Hum Gene ther* 2001; **12**:1923-1936  
Vorberg SA and Hunt KK, *Oncologist* 2002; **7**:46-59  
Zeiser A, *et al.* *Biotechnol Bioeng* 1999; **60**: 122-127

## QUESTIONS AND ANSWERS

**John Aunins, Merck, US:**

In your perfusion cultures, are you losing viral cells through your perfusion screen ?

**Amine Kamen, NRC/IRB, Canada:**

The perfusion rates are reasonable, about one volume per day up to three volumes per day. At some point we infect the cells at a MOI of 10, and we keep the perfusion. The experiments were designed to look at the kinetics, and you have noticed that we get beyond 48 hours. We do not lose cells at the early stage of perfusion, but later we do observe loss of viral cells in the perfusion system.

**Ernst Wagner, Ludwig-Maximilians Universität, Germany:**

You mentioned about 15-20% of infectious particles per total particle, which is quite nice, but obviously one would like to further increase the ratio. You mentioned also the aggregation problem. What would be your advice. How high can you get in percentage of infectious particles and will this also include purification methods?

**Amine Kamen, NRC/IRB, Canada:**

It is a complex question, because there is also an influence as well of the assay that is used to determine the infectious particles. There is certainly an underestimation of the real infectious particles. When the adenovirus is produced people harvest it at the maximum, normally this is after 48 hours in a batch mode. Very probably what is happening is that if you delay the harvesting at 37°C, part of the particles may fall apart, apparently, because they are incomplete, and this is something that may occur as well during the purification process. The ratio I mentioned is already in the high range, some people have reported 30 % and even 40 % as the highest, but often they are in the range of 10 %.

P.E. CRUZ<sup>1,2,3</sup>, M. CARMO<sup>1</sup>, A.S. COROADINHA<sup>1</sup>,  
A. BENGALA<sup>1</sup>, D. GONÇALVES<sup>1</sup>, M. TEIXEIRA<sup>1</sup>, O.-W.  
MERTEN<sup>4</sup>, C. GENY-FIAMMA<sup>4</sup>, M.J.T. CARRONDO<sup>1,5</sup>

## RETROVIRAL VECTOR STABILITY: INACTIVATION KINETICS AND MEMBRANE PROPERTIES

<sup>1</sup> - IBET/ITQB, Apartado 12, P-2780-901 Oeiras, Portugal;

<sup>2</sup> - ECBio, Lab 4.11, Ed. ITQB, Apartado 98, P-2781-901 Oeiras, Portugal;

<sup>3</sup> - Universidade Atlântica, Antiga Fábrica da Pólvora, P-2745-615  
Barcarena, Portugal

<sup>4</sup> - Généthon 3, Ibis, Rue de l'Internationale, 91000 Evry, France

<sup>5</sup> - Laboratório de Engenharia Bioquímica, FCT/UNL, P-2825 Monte da  
Caparica, Portugal

**Abstract.** Previous papers concerning the inactivation of retroviral vectors have focused either the kinetic aspects of the inactivation process or the factors affecting vector stability. The present work aims at bridging this previous knowledge by simultaneously studying inactivation kinetics and structural aspects of retroviral vectors. For this purpose, two human derived cell lines (TE Fly cells) producing retroviral vectors with amphotropic and GALV envelopes were used. Vectors with amphotropic envelope exhibit a higher stability than those with GALV envelope. Using an Arrhenius-like plot it was possible to observe two inactivation kinetic phases for amphotropic enveloped vectors but only one for GALV enveloped vectors. Electron Paramagnetic Resonance (EPR) results show that the production temperature exerts an important effect upon vector membrane rigidity, with a consistency between kinetic phase and membrane transition temperatures being observed. Since cell and vector membrane physico-chemical properties are affected as a response to changes in culture temperature and medium composition, such changes can be used more prospectively to improve the stability of retroviral vectors.

### 1. INTRODUCTION

Recombinant retroviruses are one of the most commonly used vectors for gene therapy (Mountain, 2000). However, the low stability of retroviral vectors, namely that of mouse leukaemia virus (MLV) derived vectors containing amphotropic or Gibbon Ape Leukaemia Virus – GALV envelopes, is still hampering a large-scale production, purification, and application of these vectors (Pizzato et al., 2001; LeDoux et al., 1999). The negative impact of a low stability is reflected not only in the dramatic reduction of the concentration of infectious particles but also in the efficacy of their use in clinical applications. Recently, it was shown that cell cultivation temperature and the cell type has a considerable impact upon the

temperature stability of amphotropic enveloped vectors (Beer et al., 2003). Finally, an earlier study by Aloia et al. (1988) showed that manipulation of membrane rigidity of retroviruses could affect virus stability and infectivity of HIV. These observations constitute an evidence of the complexity of the factors influencing the loss of infectivity of retroviral vectors.

The present work aims at studying in an integrated approach both the inactivation kinetics of retroviral vectors with amphotropic and GALV envelopes produced in TE Fly cells and their corresponding physico-chemical properties. The inactivation rates measured for each set of conditions enabled the analysis of the kinetics of vector loss of infectivity. Furthermore, vector physico-chemical properties, namely their rigidity as assessed by EPR (Electron Paramagnetic Resonance) (Slosberg and Montelaro, 1982) was studied in order to provide some explanations for the variation of the inactivation kinetics with storage temperature and to devise strategies for improving vector stability.

## 2. MATERIALS AND METHODS

### 2.1. Cell Culture

TE Fly A7 and TE Fly GA18, two TE 671 (human) derived cell lines producing retroviruses with amphotropic and Gibbon Ape Leukeamia Virus (GALV) envelopes, respectively, were used in this work. Both retroviral vectors code for the reporter gene lacZ. The cells were cultured in T-flasks in DMEM (4.5 g/l glucose, Glutamax I) (Life Technologies, Paisley, UK) supplemented with penicillin/streptomycin (100 U/ml; 100 µg/ml) and 5% FBS (Life Technologies) and incubated in a humidified incubator with 7% CO<sub>2</sub> in the gas phase, at 37°C.

### 2.2. Virus Production and Purification

For viral vector production cells were grown nearly to confluence in DMEM with 5% FBS supplement (Life Technologies). Fresh medium was added to cells 24 hours before the virus supernatant was harvested and filtered with 0.45 µm filters (Whatman, Maidstone, UK). The filtered viral supernatant was concentrated by ultra-centrifugation using a Beckman L8-55M centrifuge: 100 000g for 1.5 hours at 4°C in a Beckman 45Ti rotor. The pelleted virus was resuspended in PBS pH 7.2 and purified by centrifugation on a 20% (w/v) sucrose solution (Merck, Darmstadt, Germany) at 200 000g for 2 hours at 4°C in a Beckman 90Ti rotor. The titer of the purified vectors was assessed as mentioned below.

### 2.3. Virus stability assay

The inactivation rates were determined by titration of the infective virus on the purified samples. For that purpose, target cells were infected with different dilutions of the cited samples and tested for expression of the lacZ gene (Cruz et al., 2000). The temperature inactivation profiles of the vectors were determined by measuring

vector titer versus time (0, 1, 2, 4, 8, 16, 24, 48, 72 and 96h) at several temperatures: 4, 12, 17, 22, 27, 32 and 37°C. All determinations were performed in triplicate.

### 2.3. EPR spectroscopy

After the purification, the pelleted virus was suspended in 137mM NaCl/15mM Na<sub>2</sub>HPO<sub>4</sub>/2.7mM KCl/0.5mM MgCl<sub>2</sub>, pH 7.5. Spin label working solution (1mg/ml 5-doxyl-stearic acid (Sigma, St. Louis, MO) plus 50mg/ml crystallized BSA (Sigma) as carrier) was added to the purified virus (200ml per mg of viral protein) and PBS was added up to 1ml. The mixture was incubated for 2 hours at room temperature, after which unbound spin label was removed from the mixture by centrifugation on a 20% (w / v) sucrose solution, for 2 hours at 200 000g and 4°C, in a Beckman 90Ti rotor. The pelleted virus was resuspended in PBS pH 7.2 and transferred to a quartz EPR flat cell for aqueous samples. EPR spectra were measured in a Bruker ESR300 spectrometer, equipped with an Oxford Instruments variable temperature flow system. Spectra were obtained with a microwave power of 24 mW, from 5 to 37°C, after stabilization (typically 5 min) at each temperature. The hyperfine splitting constant 2T<sub>II</sub> was measured using the spectrometer software.

## 3. RESULTS AND DISCUSSION

The inactivation rates (*k*) were determined as described under Materials and methods. Table 1 shows the first order inactivation rates determined at 4 and 37°C for these vectors. Table 1 shows that the vectors with amphotropic envelope are generally more stable than GALV enveloped vectors produced under the same conditions. This corroborates the impact of envelope proteins upon vector stability that has been reported in the literature (DePolo et al., 1999). However, this difference in the stability may be due to the different protein structure or to the different amount of protein being incorporated in the viral envelope. The production temperature also affects the inactivation rates, with the vectors produced at 37°C being more stable than those produced at 32°C at low temperatures (Table 1).

Table 1. Vector first order inactivation rates measured at different temperatures for purified retroviral vectors produced at 37°C and 32°C. The standard error is shown.

<i>k</i> (h <sup>-1</sup> )	TE Fly A7 37°C	TE Fly A7 32°C	TE Fly GA18 37°C	TE Fly GA18 32°C
37°C	0.239±0.005	0.25±0.02	0.35±0.05	0.37±0.05
4°C	0.014±0.005	0.09±0.02	0.16±0.05	0.25±0.02

Vector inactivation kinetics were studied by plotting the inactivation rate and corresponding incubation temperature data according to the linearized form of the Eyring equation, an Arrhenius-like equation, given by:

$$\ln\left(\frac{k}{T}\right) = -\frac{\Delta H^\ddagger}{R} \cdot \frac{1}{T} + \ln\left(\frac{k_B}{h}\right) + \frac{\Delta S^\ddagger}{R}$$

where  $k$  is the rate constant – the first order inactivation rate -  $T$  is the temperature in Kelvin,  $k_B$  is the Boltzmann constant ( $1.38 \times 10^{-23}$  J/K),  $h$  is Planck's constant ( $6.626 \times 10^{-34}$  J s) and  $R$  is the ideal gas constant ( $8.314$  J/mol-K).  $\Delta H^\ddagger$  and  $\Delta S^\ddagger$  are, respectively, the enthalpy and entropy of activation for the reaction.

Figure 1 shows that amphotropic enveloped vectors exhibit two different kinetic phases while GALV enveloped vectors show only one. This shows that the two types of vectors differ not only in their stability but also in the way such stability is affected by the temperature.

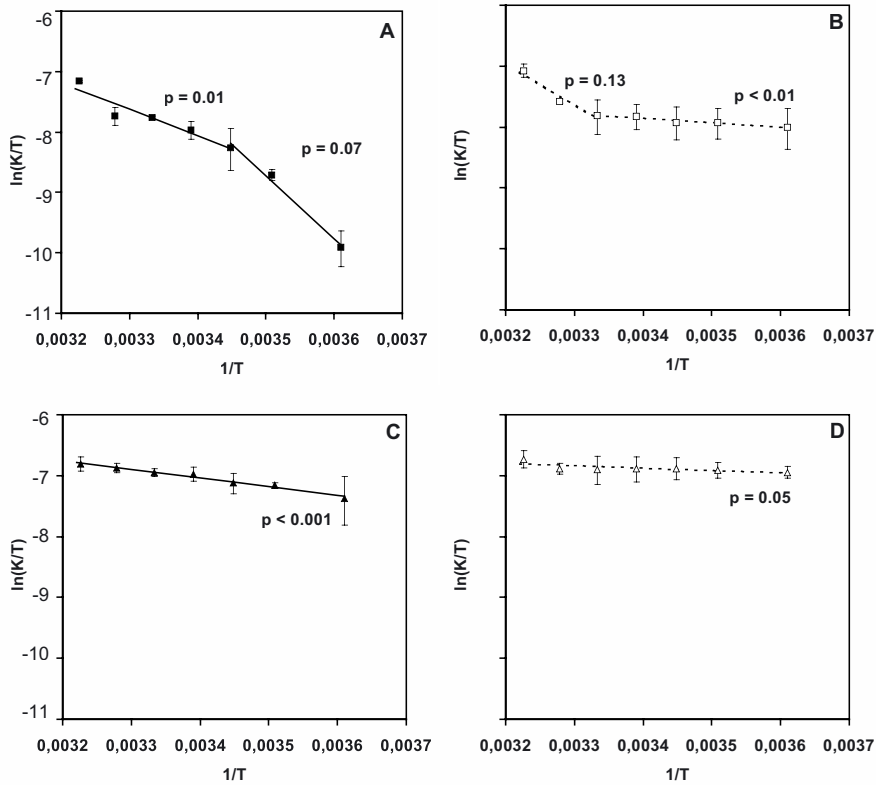


Figure 1. Temperature dependence of the first order inactivation rate of amphotropic (A,B) and GALV (C,D) enveloped purified retroviral vectors produced at 37°C (A,C) and 32°C (B,D). The  $p$  value is provided for each fitting.

The existence of different profiles and kinetic phases shown in Figure 1 suggests that production and incubation temperature must affect the vectors themselves. Thus, vector envelope rigidity was measured to test if the inactivation mechanism

was somewhat related to the envelope properties. Under these conditions, some correlation should be observed between the profiles shown in Figure 1 and the rigidity. To test this hypothesis, Electron Paramagnetic Resonance (EPR) (Slosberg and Montelaro, 1982) was used. Figure 2 depicts the hyperfine splitting constant  $2T_{II}$  measured using this technique. The increase in temperature caused a general decrease in the value of the spectral parameter  $2T_{II}$ . Since  $2T_{II}$  correlates with the lipid bilayer rigidity this decrease corresponds also to a decrease in the envelope rigidity. The plots of  $2T_{II}$  values versus temperature also allows the definition of the thermal transition temperatures, determined from the slope changes.

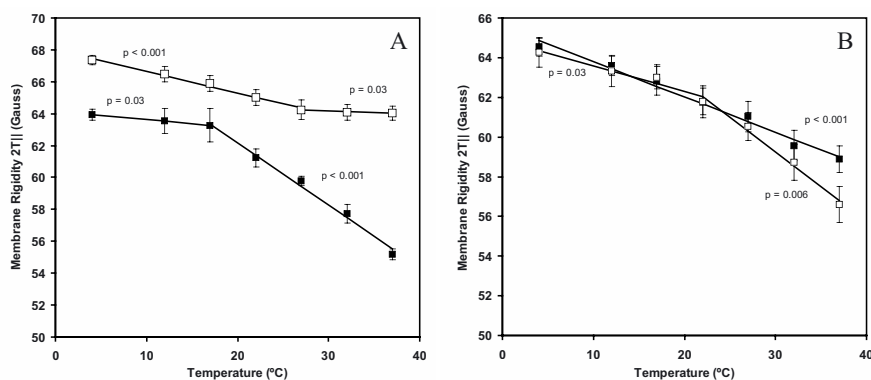


Figure 2. Plot of the hyperfine splitting constant  $2T_{II}$  versus temperature for purified retroviral vectors with amphotropic (A) and GALV (B) envelopes produced at  $32^{\circ}\text{C}$  ( $\square$ ) and  $37^{\circ}\text{C}$  ( $\blacksquare$ ). The  $p$  value is provided for each fitting.

The first conclusion that can be taken from Figure 2 is that the production temperature has a marked effect upon the rigidity of the envelope of the retroviral vector, this effect depending on the type of vector. Retroviral vectors with the amphotropic envelope protein produced at  $32^{\circ}\text{C}$  by TE Fly cells are more rigid (higher  $2T_{II}$ ) than those produced at  $37^{\circ}\text{C}$  (Figure 2A), the opposite being observed for vectors with the GALV envelope protein (Figure 2B).

Viral envelopes containing the amphotropic envelope protein have one thermal break point (Figure 2A). Nevertheless, the existence of break points of the vectors containing GALV envelope protein depends on the production temperature, with no breaks being observed for the vectors produced at  $37^{\circ}\text{C}$  (Figure 2B). However, the most interesting observation was that the results presented in Figure 2 regarding the thermal break points were consistent with the kinetic phase transition temperatures shown in Figure 1 reinforcing the relevance of the vector envelope properties upon vector inactivation kinetics. The only exception concerns the GALV pseudotyped vectors produced at  $32^{\circ}\text{C}$  where one membrane rigidity break existed (Figure 2B) but no kinetic phase transition was observed (Figure 1D). The explanation for this is the fact that the activation energy for the inactivation of these vectors (calculated from the slope of Figure 1D) is very close to zero; this means that the inactivation

reaction is practically spontaneous. Therefore, eventual changes in the envelope properties, such as membrane rigidity, should only have an impact on inactivation kinetics if they increase the activation energy of the vector inactivation reaction; from the results presented here it can be concluded that this was not the case for the GALV pseudotyped vectors produced at 32°C.

It has been shown that the cell membrane composition can be manipulated in several ways from cholesterol sequestration or depletion to the inhibition of cholesterol biosynthesis (Simons and Toomre, 2000, Beer et al., 2003); thus, production temperature may also affect membrane composition and physico-chemical properties. Since cholesterol is known for its stiffening and regulating effects upon membrane lipid phase behavior (Brown and London, 2000) it is likely that extreme variations in cholesterol content may lead to significant variations upon vector stability.

#### 4. CONCLUSIONS

The results obtained corroborate previous observations that the type of envelope and culture temperature significantly affect vector stability and inactivation kinetics. Furthermore, the inactivation kinetics are strongly affected by the culture temperature and the vector envelope proteins, with the different envelope proteins determining the existence of one (GALV pseudotyped vectors) or two (amphotropic vectors) kinetic phases.

Vector envelope properties, namely membrane rigidity, seem to affect the inactivation profiles. Membrane transitions are consistent with changes in the inactivation kinetics and vector sensitivity to temperature. This also suggests that the effect of the culture temperature upon vector stability is exerted through changes in the physico-chemical properties of the vector. Thus, since the concentration or ratios of individual lipid components affect the stability of retroviral vectors, more attention has to be paid as to how quantitative changes in individual lipids and cholesterol caused by cultivation conditions (e.g. temperature) or by the host cell type affects vector temperature stability.

#### 5. REFERENCES

- Aloia, R.C., Jensen, F.C., Curtain, C.C., Mobley, P.W., and Gordon, L.M. (1988). *Proc Natl Acad Sci U S A*. **85**, 900-904.
- Beer, C., Meyer, A., Müller, K., and Wirth, M. (2003). *Virology* **308**, 137-146.
- Brown, D.A., and London, E. (2000). *J. Biol. Chemistry* **275**, 17221-17224
- Cruz, P.E., Almeida, J.S., Murphy, P.N., Moreira, J.L., and Carrondo, M.J.T. (2000). *Biotechnol. Prog.* **16**, 213-221.
- DePolo, N.J., Harkleroad, C.E., Bodner, M., Watt, A.T., Anderson, C.G., Greengard, J.S., Murphy, K.K., Dubensky, T.W., and Jr, Jolly, D.J. (1999). *J Virol.* **73**, 6708-6714.
- Le Doux, J.M., Davis, H.E., Morgan, J.R., and Yarmush, M.L. (1999). *Biotechnol. Bioeng.* **63**, 654-662.
- Mountain, A. (2000). *Trends in Biotechnol.*, **18**, 119-128.
- Pizzato, M., Merten, O.-W., Blair, E.D., and Takeuchi, Y. (2001). *Gene Therapy* **8**, 737-745.
- Simons, K., and Toomre, D. (2000). *Nature Reviews / Mol. Cell Biology* **1**, 31-39.
- Slosberg, B.N., and Montelaro, R.C. (1982). *Biochim Biophys Acta.* **689**, 393-402.



SEAN FORESTELL, CHRIS CELERI, CHRIS DANG, TOM GONG,  
MATTHEW OLSEN, INESSE SIFI, INN YUK AND  
SCOTT GEYER

## COMPARISON OF HOST CELL LINES AND PRODUCTION METHODS FOR A NEW GENERATION OF ONCOLYTIC ADENOVIRAL VECTORS

*Onyx Pharmaceuticals Inc., 3031 Research Drive, Richmond, CA 94806.*

### INTRODUCTION

The ONYX-4XX family of vectors is designed to replicate in cells with defects in the retinoblastoma tumor suppressor protein (pRB) pathway (Johnson *et al.* 2002). Disruption of the RB tumor suppression pathway is common in a variety of tumor types including lung, colon, pancreatic, breast, glioma, bladder and prostate. Selective replication of ONYX-4XX vectors in pRB-defective cells has been accomplished by placing the control of adenoviral E1A proteins under the control of the human E2F promoter. To support the production of ONYX-4XX vectors, a producer cell line which provides E1 functions, such as HEK293, or a cell line with defects in the RB signaling pathway is required. The problem with HEK293 cells is the theoretical risk of homologous recombination between vector and adenoviral sequences in the cell which could lead to a recombinant vector that is unrestricted in its ability to replicate in normal cells. To overcome this risk, a decision was made to screen tumor cell lines for their ability to support the ONYX-4XX vectors. The selection criteria used were set a priori and are listed in Table 1. Cell lines which met these criteria were tested in different production platforms including Nunc Cell Factories™, batch-fed suspension culture, and perfusion using the Refine Technology ATF™ hollow fiber apparatus.

*Table 1: Selection Criteria for Cell Lines Supporting ONYX-4XX Production*

Parameter	Test System(s)	Criteria
<i>Vector Production</i>	Cell Specific Productivity in serum-free suspension culture	>20,000 vp/cell measured by HPLC
Cell Growth	Serum-free adapted cultures Maximum cell density in batch culture	MGT <36 hours >1.5E6 cells/ml
Generation of Recombinants	Probe for wt AdV by PCR	None detected
Regulatory Acceptability	No regulatory hurdles from FDA. Contamination with known human pathogens unacceptable.	Input required from consultant
Licensing Issues	Freedom to operate without large licensing fees.	Preferred status is unrestricted use.

## RESULTS

### *Adaptation of HeLaS3 and H1299 to Suspension Culture*

Based upon internal data and external publications, twelve human cell lines were selected for their ability to support wild-type adenovirus replication. Experiments with were performed to determine the ability of the cells to grow and support the production of ONYX-411 and ONYX-443 in adherent serum-containing culture. The results from these experiments are summarized in Table 2 and show mean cell generation time (MGT) and cell specific vector production based upon Anion-Exchange HPLC analysis of cell lysates.

Table 2. Results of preliminary screening of various tumor cell lines in adherent culture.

Cell Line	Cell Type	Growth Rate MGT (h)	ONYX- 443 (vp/cell)	ONYX- 411 (vp/cell)
HEK293	AdV transformed embryonic kidney	26.2	ND**	14,715
H1299	Lung large cell carcinoma	29.8	52,600	97,027
C-33A	Cervical carcinoma	22.3	BLQ*	11,053
HeLa-S3	Cervical carcinoma	31.1	49,880	75,263
Y79	Suspension retinoblast	30.9	20,064	ND
COLO-320DM	Colorectal Adenocarcinoma	24.7	20,758	BLQ
WiDR	Colorectal Adenocarcinoma	29.2	BLQ	ND
WERI-RB-1	Suspension Retinoblast	> 70	ND	ND
HT-3	Cervical carcinoma	> 100	ND	ND
HepG2	Hepatocellular Carcinoma	38.1	BLQ	ND
DU-145	Prostate Carcinoma	29.9	22,279	ND
A549	Lung Carcinoma	37.3	19,750	ND
NCI-H69	Small Cell Lung Carcinoma	24.2	BLQ	ND

\* BLQ: Below Limit of Quantitation (8,400 vp/cell)

\*\*ND: Not Done

*Adaptation of HeLaS3 and H1299 to Suspension Culture*

Applying the criteria established in Table 1, only the H1299 and HeLaS3 cell lines produced enough vector and had suitable growth characteristics to go to the next phase, adaptation to serum-free suspension culture. Several commercially available media were screened for suitability, and the media in which the cells grew best were selected. The H1299 were grown in the Gibco HEK293 SFMII medium supplemented with a trace element cocktail and an HEK supplement comprised of plant hydrolysates. The HeLaS3 cells were successfully adapted to growth in the JRH Ex-Cell 293 medium. Post adaptation, both cell lines grew extremely well with mean generation times of approximately 24 hours, with the HeLaS3 reaching a maximum cell density in batch culture of  $1.0 \times 10^7$  cells/ml, and the H1299 reaching a maximum cell density in batch culture of  $2.5 \times 10^6$  cells/ml. In shaker flask experiments, the HeLaS3 cell line was capable of supporting the production of ONYX-411 and ONYX-443 at 34,000 and 12,000 vp/cell respectively, while the H1299 cell line was only capable of supporting production of ONYX-411 at 28,000 vp/cell, while ONYX-443 was below the level of detection. Based on these results, it was decided that both the HeLaS3 and H1299 cell lines passed the criteria initially set for selection for ONYX-411 and were placed into further testing.

*Comparison of HeLaS3 and H1299 in Different Production Platforms**Nunc Cell Factories*

Several experiments were performed with the adherent HeLaS3 and H1299 cell lines with the ONYX 411 and 443 vectors to determine the productivity using 10-stack Nunc Cell Factories (CF10s). Some of the variables examined were culture medium, need for serum post-infection, need for medium exchange post-infection, cell density at infection, and viral concentration at infection. The factors with the biggest impact on productivity were: medium exchange post-infection; cell density at infection; and the presence of serum post-infection. In general, there was little difference in overall productivity between the HeLaS3 and H1299 cell lines, or the 411 and 443 vectors. On average, approximately 4-6E13 viral particles were produced per 10-stack Cell Factory with FBS at harvest as summarized in Table 3.

*Table 3: Summary of Vector Production in Cell Factories (total vector produced per CF10)*

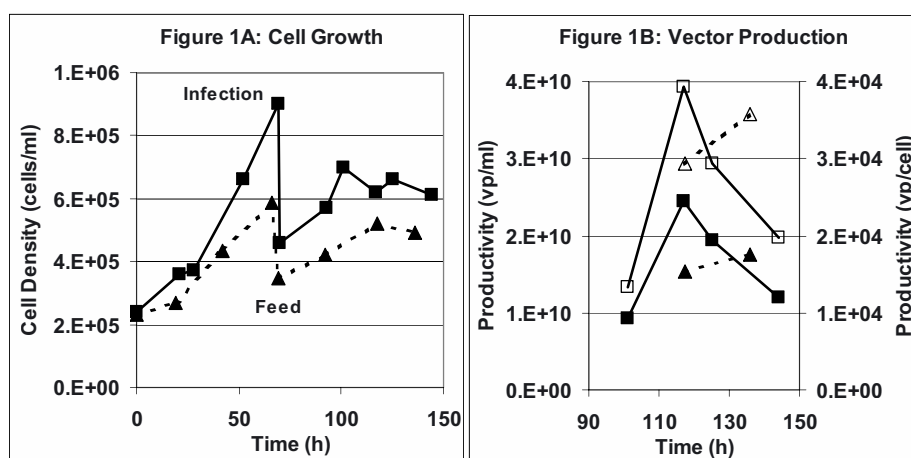
Exp. Conditions	# Experiments	Mean	Standard Deviation
<b>HeLa-S3</b>			
ONYX-411 + FBS	20	6.12E13	± 2.21E13
ONYX-411 w/o FBS	3	1.65E13	± 0.16E13
ONYX-443 + FBS	4	4.06E13	± 1.47E13
ONYX-443 w/o FBS	3	2.92E13	± 0.59E13
<b>H1299</b>			
ONYX-411 + FBS	9	4.32E13	± 1.80E13
ONYX-411 w/o FBS	4	2.91E13	± 3.00E13
ONYX-443 + FBS	2	4.16E13	ND
ONYX-443 w/o FBS	0	ND	ND

*10L Batch-Fed Bioreactor*

Experiments were performed in 10L Applikon bioreactors to determine the ability to produce ONYX-411 in batch culture according to the following protocol. Cells were seeded into the vessels at half volume and allowed to grow for three days. At this point, cells were infected and fresh medium added up to the full volume. Results from a typical experiment are summarized in Figures 1A and 1B comparing cell growth and vector production respectively. The H1299 cells have a significantly higher glucose uptake rate than the HeLaS3 cells, consuming approximately 1.7 g of glucose per 1E9 cells per day compared with 0.6 g of glucose per 1E9 cells per day for HeLaS3. While the volumetric productivity was higher for

the HeLaS3 cells due to the higher cell density achieved, the cell specific productivity was comparable at 30,000-40,000 vp/cell (Figure 1B). This cell specific productivity is in good agreement with data generated in the Nunc Cell Factories.

Figure 1. Comparison of ONYX-411 production in H1299 and HeLaS3 cells cultured in a 10L bioreactor. Cells were infected with vector at  $5E8$  vp/ml 72 hours post-seeding as seen by the dilution of the cells in Figure 1A. Figure 1B shows volumetric productivity (closed symbols) and cell specific productivity (open symbols) as measured by AEX HPLC.

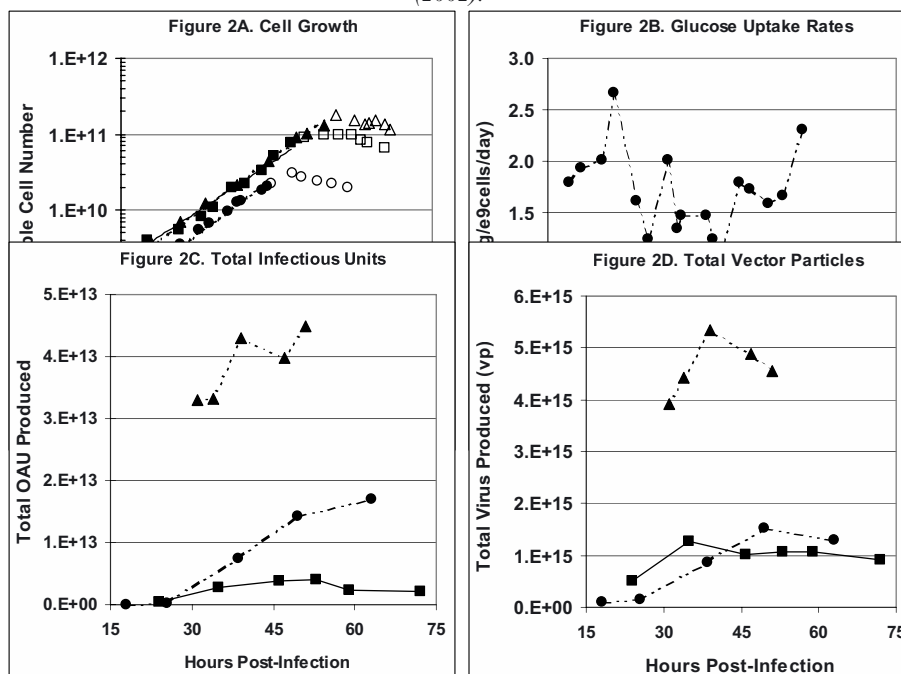


#### 10L Perfusion Bioreactor

Experiments were performed in a 10L Applikon reactor equipped with a Refine Technology hollow fiber perfusion apparatus operating with the alternating tangential flow (ATF) technology. In one experiment with H1299 cells, perfusion was initiated when the glucose level dropped below 3 g/L, and the viable cell density exceeded  $6E5$  cells/ml. Due to the high glucose uptake rate of these cells ( $1.69$  g/ $1E9$ cells/day, Figure 2B), the perfusion rate was kept at a high level (maximum  $2.5$  V day<sup>-1</sup>). When the density exceeded  $2E6$  cells/ml, cells were infected with ONYX-411 at a final concentration of  $1E9$  vp/ml. Cells continued to grow post-infection to a maximum viable cell density of  $3E6$  cells/ml. Looking at vector production, total vector produced peaked at 50 hours post-infection (hpi), but the maximum oncolytic activity unit (OAU) concentration was reached upon harvest 63 hpi. To reach peak productivity (50 hpi), the H1299 cells consumed a total of 81L medium. In another experiment, HeLaS3 cells grew rapidly to  $>2E6$  cells/ml before perfusion was necessary, and grew to a peak cell density of  $1E7$  cells/ml post-infection with ONYX-443. To reach the peak productivity, a total of 64L of medium was consumed. In a third experiment, the goal was to reach a higher cell density with HeLaS3 while minimizing medium consumption. In this experiment,

the cell density reached  $2E7$  viable cells/ml but consumed only a total of 63L of medium to reach peak productivity (39 hpi with ONYX-411). The key difference between the two cell lines is in the glucose uptake rate, which is approximately 3-fold higher for H1299 compared with the HeLaS3 (Figure 2B). With the HeLaS3 culture, there is an obvious peak in OAU concentration at 57 hpi, which is close to the peak time with the H1299 culture (63 hpi).

Figure 2. Data from Perfusion bioreactors. Circles: H1299 with Onyx-443. Squares: HeLaS3 with Onyx-443. Triangles: HeLaS3 with Onyx-411. Total infectious "Oncolytic Activity Units" or OAU were measured using an assay developed at Onyx as described by Sluzky et al (2002).



#### Scale-up to 70L Pilot Scale

The batch-fed and perfusion processes were next evaluated using a pilot scale 70L Applikon Bioclave vessel. Given the ability of the JRH Ex-cell 293 medium to support high densities, the batch-fed process was run allowing the cell density to achieve  $>2E6$  cells/ml before infection and addition of the feed medium. The higher volumetric productivity in the 70L vessel (Table 4) is due to the higher final cell density as the cell specific productivity remained roughly 38,000 vp/cell. Results obtained for both the HeLaS3 and H1299 cell lines with both the ONYX-411 and ONYX-443 vectors are summarized in Table 4. Note, the volumetric productivities reported reflect tank volume and not total volume of medium consumed.

Table 4. Comparison of production of ONYX-411 and ONYX-443 in the HeLaS3 and H1299 cell lines in different production platforms at the bench and pilot scale.

Production Platform And Scale	HeLa S3		H1299	
	ONYX-411	ONYX-443	ONYX-411	ONYX-443
Nunc 10-Stack Cell Factory	8.1E13 vp/L	4.5E13 vp/L	6.9E13 vp/L	4.9E13 vp/L
10L Batch Suspension	2.5E13 vp/L	ND	1.8E13 vp/L	BLD
70L Batch Suspension	7.8E13 vp/L	ND	ND	ND
10L ATF Perfusion	5.0E14 vp/L	1.1E14 vp/L	1.4E14 vp/L	ND
70L ATF Perfusion	3.5E14 vp/L	ND	ND	ND

## DISCUSSION

The final selection of a cell line for the production of the ONYX-4XX series of vectors comes back to the original criteria set in Table 1. Of the cell lines screened, only the HeLaS3 and H1299 cell lines met the technical criteria established. Both cell lines were adapted to growth in serum-free suspension culture with mean generation times of approximately 24 hours. Both the H1299 and HeLaS3 cells were capable of producing approximately 4E13 vp of vector in Cell Factories. The key difference between the cell lines became apparent upon adaptation to serum-free suspension culture. Under this mode of operation, the maximum cell density achieved with the H1299 in batch culture was 2E6 cells/ml, while the HeLaS3 cells were able to reproducibly grow to 1E7 cells/ml in batch culture. The reason for the difference was the significant difference in glucose uptake rate which was approximately 3 fold higher for the H1299. As a result of the lower nutrient uptake rate, HeLaS3 cells achieved higher cell densities and consequently, higher volumetric productivity than the H1299 in both batch and perfusion experiments. Another difference between the two cell lines was the inability of the H1299 cell line to produce the ONYX-443 vector in batch suspension culture, despite repeated attempts. Of the non-technical criteria for cell line selection, there were no regulatory concerns apparent which would favor one cell line over another. Feedback obtained from industry experts and the FDA indicated that the use of a tumor cell line is reasonable, and that no cell line would be excluded a priori. The theoretical risk of using a tumor cell line would be weighed against the potential benefit a therapy would have. The biggest concern with these cell lines is the presence of residual host cell DNA in the drug product. For these reasons, ONYX has decided to proceed with the HeLaS3 cells for production of the ONYX-4XX vectors. The main advantage being the higher volumetric productivity, greater ease of scale-up, and the ability to produce both the ONYX-411 and ONYX-443 vectors in all platforms tested.

## REFERENCES

- Johnson, L. *et al.* Selectively replicating adenoviruses targeting deregulated E2F activity are potent, systemic antitumor agents. *Cancer Cell* (2002) 1:325-337.
- Sluzky, V. *et al.* Analytical challenges for characterization and safety testing of a selectively replicating adenovirus in late stages of clinical development. Presented at The Williamsburg Bioprocessing Foundation Viral Vectors and Vaccines, 9<sup>th</sup> Annual Meeting, New Orleans, Louisiana, 2002.

## QUESTIONS AND ANSWERS

**Ernst Wagner, Ludwig-Maximilians Universität, Germany:**

You have noticed that the vector carrying the cytidine deaminase should lower growth properties. Is there a reason for this ?

**Sean Forestell, Onyx Pharmaceuticals, US:**

Cytidine deaminase is not the only one vector we have been working on. It just seems to be a vector-specific phenomenon. Some vectors are good producers and give very favourable particle to pfu ratios. In case of CD-1 we do not get very favourable ones. I think it is just vector specific.



I. MARCELINO<sup>1</sup>, M. SOUSA<sup>1</sup>, C. VERÍSSIMO<sup>2</sup>, C. PEIXOTO,  
M.J.T.CARRONDO<sup>1,2</sup>, P.M. ALVES<sup>1</sup>

## PROCESS DEVELOPMENT FOR A VETERINARY VACCINE AGAINST HEARTWATER

<sup>1</sup>ITQB/IBET, Apt. 12, 2781 Oeiras, Portugal; <sup>2</sup>FCT/UNL,  
2825 Monte da Caparica, Portugal

**Abstract:** This work describes the optimization of a cost-effective bioreaction strategy for the production of an inactivated bacterial vaccine against Heartwater and, the first attempt to produce the causative agent of this disease, the rickettsia *Ehrlichia ruminantium* (ER), in stirred tanks. *In vitro*, it is possible to produce ER using finite cultures of ruminant endothelial cells [1]. Herein, mass production of these cells was optimized for stirring conditions. The effect of inoculum size and microcarrier type upon maximum cell concentration was evaluated. Afterwards, using the optimized parameters for cell growth, their ability to support ER production was assessed. For that purpose, two ER strains (Gardel and Welgevonden) were studied. Critical bioprocess parameters related with the infection strategy such as serum concentration at infection time and refeeding strategy were analyzed. The results obtained clearly indicate that it is possible to produce ER in stirred tank bioreactors and that the production yields can be increased by a factor of 6.5 when serum-free medium is used during and after the infection process. The suitability of this process was validated upon to a 2L scale. Since process economics are critical for veterinary vaccines, these results are of major importance, as they will be used to define a scalable manufacturing culture process for the production of a Heartwater vaccine.

### INTRODUCTION

The rickettsia *Ehrlichia ruminantium* (ER) is an obligate intracellular bacterium that infects brain endothelial cells. It is the etiologic agent of Heartwater, an infectious disease of domestic and wild ruminants with high mortality rates in sub-Saharan countries and West Indies. Currently, a vaccine based on the chemically inactivated ER elementary bodies produced in finite culture of ruminant endothelial cells is the best candidate for protection against Heartwater [1]. To overcome the socio-economical impact of Heartwater, it is imperious to establish an industrial cost-effective production process that will permit the widespread application of the vaccine.

### MATERIALS AND METHODS

Cell Culture: Caprine Jugular (CJE) and Bovine Aortic Endothelial cells (BAE), supplied by Dr. D. Martinez (CIRAD/EMVT, France), were cultivated in static conditions as described previously [1]. Experiments in stirred tanks (spinner vessels – Wheaton and/or 2 L bioreactors - Braun) were performed using a non-porous (Cytodex 3<sup>TM</sup> from Amersham Pharmacia) and a porous microcarrier (Cultispher-

S<sup>TM</sup> from Percell Biolytica AB, Sweden). The microcarriers were prepared according to the manufacturers.

*Ehrlichia ruminantium* culture: ER Gardel (ERG) was supplied by Dr. D. Martinez and ER Welgevonden (ERW) by Dr. E. Zweygarth (Onderstepoort Institute, South Africa). ER was cultivated in static conditions as described elsewhere [1,2]. For stirred tank ER production, two culture media were tested: a Glasgow based medium supplemented with 10% FBS (Invitrogen, UK) and a special serum free formulation based on the commercial DMEM/HAM'S F12 (referred as SFMC-23) [2]. ER was quantified by SYBR Green I based real time PCR developed by our group [3].

## RESULTS AND DISCUSSION

### *Mass Production of Ruminant Endothelial Cells*

Microcarrier cell culture has been previously used by our group to produce large quantities of ruminant endothelial cells [4]. Herein, we show that cell growth yields are highly dependent on the cell origin (Table 1). Maximum cell density ( $1.4 \times 10^6$  cells/ml) was achieved for BAE cells when an inoculum of  $0.25 \times 10^6$  cells/ml was seeded on a non-porous microcarrier (Cytodex 3). Although similar results were obtained for CultiSpher S (porous microcarrier), there was a 24 h delay to attain maximum cell concentration. Therefore, 6 g/l of Cytodex 3 were used to obtain high amounts of host cells for ER infection experiments under stirring conditions.

Table 1. Optimized bioreaction parameters for CJE and BAE cells under stirring conditions.

	CJE cells		BAE cells	
	Cytodex 3 <sup>TM</sup>	Cytodex 3 <sup>TM</sup>	CultiSpher S <sup>TM</sup>	CultiSpher S <sup>TM</sup>
Microcarrier designation	Cytodex 3 <sup>TM</sup>	Cytodex 3 <sup>TM</sup>	CultiSpher S <sup>TM</sup>	CultiSpher S <sup>TM</sup>
Microcarrier weight	6 g/l	6 g/l	3 g/l	3 g/l
Inoculum size ( $\times 10^6$ cells/ml)	0.10	0.10	0.25	0.25
Maximum Cell Concentration ( $\times 10^6$ cells/ml)	0.68	0.96	1.38	1.30
Days for max. cell .conc.	8*	5	4	5

(\* Two complete media refeed were required to stimulate cell growth)

### *Ehrlichia ruminantium Life Cycle in Stirred Tank Culture Conditions*

Under static culture conditions, ER has been described to have a *Chlamydophila*-like developmental cycle consisting of an extracellular infectious form designated by elementary body (EB) and a non infectious, metabolically active, intracellular form

designated by reticular body (RB) [5]. To ensure that ER was able to colonize and proliferate inside the host cells, its growth was monitored using phase contrast microscopy (Figure 1). In Figure 1b, it is shown that the host cells exhibit a substantial swelling when compared to non-infected cells (Fig 1.A); this is an indicator of successful infection and ER development inside host cells. EBs maturation into RBs, forming inclusion bodies called *morula*, can be visualized in Fig. 1 C. After successive rounds of binary fission, non-infectious RBs reorganize to EBs that are released from the host cell after complete cell lysis (Fig. 1 D). This is the first evidence of successful ER growth under stirring conditions, supporting the development of a large-scale process for ER production.

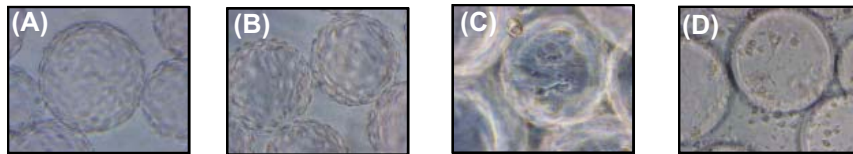


Figure 1 – *E. ruminantium* Gardel life cycle in microcarrier cells culture. **A** - non infected BAE cells; **B** - infected cells; **C** - reticulate bodies (*morula*); **D** - elementary bodies release.

#### Mass Production of *Ehrlichia ruminantium*

Two chemically distinct culture media were tested in their ability to support two ER isolates (ERW and ERG): a serum-containing medium based on Glasgow MEM and a serum free medium [4].

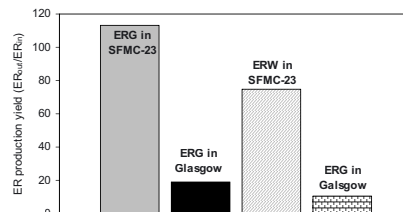


Figure 2 – ER production yield in stirred tank conditions: effect of serum

A 6.5-fold increase in ER production yield was obtained when serum free medium was used during and after infection. The elimination of serum oligosaccharides or glycoproteins, that normally inhibit host cell-bacterium interaction, could have contributed for an increase in the susceptibility of endothelial cells to ER infection therefore augmenting the final amount of produced bacteria. Considering the industrial demands for a biotechnological process, the use of this medium will reduce the production costs and minimize the interference of serum proteins on vaccine dosage (still based on total protein content). Preliminary results indicate that a better productivity is obtained when only one complete medium replacement is

done at infection time. These optimized parameters were validated up to a 2L scale and approximately 300 vaccine doses per litre were produced. The first doses produced at this mid-scale are currently undergoing field trial in cattle and sheep in Kenya and Burkina Faso; the preliminary results obtained are quite satisfactory and demonstrate the effectiveness of the vaccine in inducing protection against homologous challenge (data not shown).

#### REFERENCES

- [1] Totté P. *et al.* 1999. *Parasitol Today* 15: 286-90.
- [2] Zweygarth, E. & A.I. Josemans. 2001. *Onderstepoort J vet Res* 68: 37-40
- [3] Alves P.M. *et al.* 2003. *Journal of Microbiological Methods* (Submitted )
- [4] Moreira, J.L. *et al.* 2002. *ACS Symposium* (In press).
- [5] Jongejan, F. *et al.* 1991. *Onderstepoort J vet Res* 58: 227-237.

C. BEER AND M. WIRTH

## A NEW METHOD FOR THE QUANTITATIVE DETERMINATION OF ENVELOPED VIRAL PARTICLES

*German Research Centre for Biotechnology, Division of Molecular  
Biotechnology, Braunschweig*

**Abstract.** A method has been developed for the qualitative and quantitative detection of viral particles containing a lipid shell. The method is based on the specific binding of a fluorescent dye to cholesterol of the viral lipid shell. The fixed virus samples were examined using a fluorescence microscope at 1000x magnification. The method is fast, easy and reliable. It can be used to evaluate the infectious quality of virus vector batches (infectious/ total viral particle number). Further applications are the screening of cell lines for viral contaminations, determining the viral load in cell supernatants and the virus removal in downstream purification processes.

### 1. INTRODUCTION

Viruses represent unwanted companions of mammalian cell cultures, e.g. retroviruses of mouse hybridomas and myelomas. Thus, it is obvious that cell lines have to be screened for virus contamination particularly if cell lines are used for protein production for pharmaceutical applications. Furthermore, in cases of virus contamination the effectiveness of virus removal strategies of downstream processes has to be documented. Several methods are applicable for the general or specific detection and quantification of viral loads (e.g. electron microscopy, nucleic acid quantitation, immunostaining, MAP assays). Due to the limitations of current methods we have developed a new and simple assay, which uses the binding of a fluorescent dye to the cholesterol of the viral membrane.

### 2. METHODS

Cells were propagated in DME (10% FCS) in T25 flasks at 37°C, 5%CO<sub>2</sub>. After 24 hours production the supernatants were harvested, filtrated (0.45 µm) and analysed. The total viral particles were quantified via the cholesterol staining method. The endpoint titers were determined by a β-gal assay (TE671) or a G418 titer assay [5]. For the staining of viral particles the cell supernatants were filtrated to remove cells and cellular debris (0.45 µm pore size), fixed to chamber slides and stained with cholesterol binding fluorescent dye. Cholesterol stained particles were visualized using a bfp filter set (Ex 387/ Em 450) and 1000x magnification [6]. Immunohistochemical staining of amphotropic mouse leukemia virus was done as described by Pizzato et al. [1].

## 2. RESULTS

### 2.1. Development of a new staining method for enveloped viruses

The membrane of many enveloped viruses is acquired from the plasma membrane of the host cell. As cholesterol is a common component of the plasma membrane of most cells types cholesterol also represents a constituent of the viral membrane. We wondered whether a cholesterol binding fluorescent dye could be used to detect enveloped viral particles e.g. the amphotropic mouse leukemia virus (MLV-A), a retrovirus. Interestingly, the halos of the MLV-A particles (100nm diameter) could be detected using a fluorescence microscope (1000x magnification) (Fig. 1c).

Besides MLV-A we could detect the enveloped vesicular stomatitis virus (VSV) and the retroviral contamination of Sp2/0 cells [3]. As expected, type 5 adenoviruses (AdV5) could not be detected since they do not contain a lipid shell [4] (not shown).

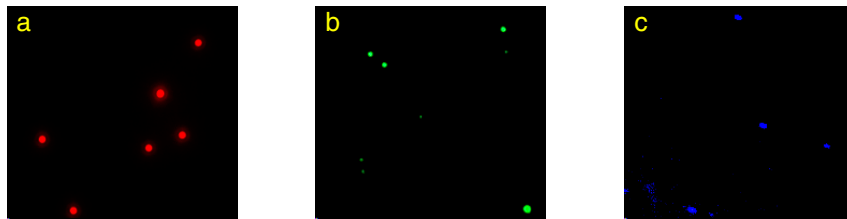


Figure 1. Cholesterol staining of MLV-A particles. a) 110 nm Texas Red labelled beads, b) Immunohistochemical detection of MLV-A using an antibody specific for the envelope protein, c) Fluorescent cholesterol staining of MLV-A derived from infected mouse NIH3T3 cells

To determine the reliability of the cholesterol staining method we compared the assay with the specific detection of the MLV-A using immunohistochemical staining of envelope proteins as described by Pizzato et al. [1] (figure 1). The quantification was performed after particle counting using commercially available beads (100 nm in diameter, Texas Red labelled) of known concentration as quantitation standard. The immunohistochemical and cholesterol staining resulted in similar viral counts (data not shown). The average variance of the new method of 13.5% was calculated from multiple determinations in 15 independent experiments (data not shown).

### 2.2. The infectious quality of a retroviral production depends on the host cell line

Retroviral vectors, defective in replication, are often used for gene transfer experiments. As the cholesterol staining method for enveloped viruses allows the easy quantification of total viral particles, we applied this method together with standard methods for measurement of retroviral titers to determine the infectious

quality (ratio infectious particle/ total particle numbers) of retrovirus productions of different cell lines. For that purpose, the potential of NIH3T3 (mouse), TE671 (human), BHK-A and BHK21B (both hamster) was compared. Due to the lack of retroviral producer cell lines based on BHK-A and BHK21B a helper virus approach was used (cotransfection of replication competent and retroviral vector). In addition, the TE671 based human packaging cell line TE FlyA7 [2] was used for the investigations. Interestingly, the productivity for retroviruses differed only marginally between the cell lines (total particles) while the population of infectious viruses varied drastically between cell lines of different origin (species and tissue) (mouse, human versus hamster).

### 3. DISCUSSION

We present a new method for qualitative and quantitative detection of enveloped viruses using cholesterol binding fluorescent dye and fluorescence microscopy. The method allowed us to detect MLV-A retrovirus derived from different cell lines, VSV and retroviral contaminations of cell cultures. A specific knowledge about the viruses (viral antigens, genome, proteins) is not necessary as all cholesterol containing enveloped viral particles should be detectable. Presently we are collecting data on the specificity using viruses of other families and maturation characteristics. The cholesterol staining method allows a rapid, sensitive, reliable and direct determination of the total viral load of cell culture samples and exhibits advantages compared to established methods of virus quantification with respect to cost, reliability and time-consumption. Especially, the method can be used to assess the infectious quality of retrovirus vectors derived from different cell lines and culture conditions. We could show that the quality of retrovirus production depends strongly on the used host cell line. While all cell lines investigated released reasonable total viral particles numbers, the level of infectious particles differed considerably. This results in infectious quality indices differing in three order of magnitudes (ranking: TE 671 (human) > NIH3T3 (mouse) > BHK-A (hamster) > BHK-B (hamster)). The molecular basis of this phenomenon is focus of current investigations. Our results suggest that a careful choice of the packaging cell line for retrovirus production is necessary.

### 4. REFERENCES

- [1] Pizzato, M. et al. (1999). *J. Virol.* 73, 8599-8611.
- [2] Cosset, F.L. et al. (1995). *J. Virol.* 69, 7430-7436.
- [3] Lovat, A. et al. (1999). *J. Virol. Methods* 82, 185-200.
- [4] Shenk, T. in *Fields Virology*, 3rd edition, pages 2111-2148.
- [5] Wirth, M. et al. (1994). *J. Virol.* 68, 566-569.
- [6] patent pending (Wirth M. and Beer C., Procedure for quantitative determination of viral or bacterial particles having a cholesterol-containing envelope; international PCT/EP02/11640; USA US 10/033,041; Germany DE 101 50 959.6 and 10151 898.612)

MARIA JOÃO L. COSTA<sup>(1,4)</sup>, RUI MALHÓ<sup>(2)</sup>, JOÃO  
GONÇALVES<sup>(1)</sup>, GUILHERME N.M. FERREIA<sup>(3,4)</sup> & MARIA  
RAQUEL AIRES-BARROS<sup>(4)</sup>

## DEVELOPMENT OF A 293T CELL LINE FOR THE PRODUCTION OF VIRUS LIKE PARTICLES IN BIOREACTORS

*(1) URJA-Faculdade Farmácia, Lisboa-Portugal; (2) Faculdade Ciências,  
Lisboa-Portugal; (3) FERN, Universidade Algarve-Portugal (4) CEBQ-IST,  
Lisboa-Portugal*

### 1. INTRODUCTION

Molecular therapy has become increasingly important for the treatment of some diseases. Although several protocols are currently in evaluation using viral and non viral delivery vectors, safety concerns and low delivery efficiency are important disadvantages on using these vectors, respectively. Virus like particles (VLPs) are delivery vectors aiming at combining the advantages of both viral and non viral vectors. Over the past ten years it has been demonstrated that structural proteins of many virus have the ability to self assembly into VLPs when expressed in eukaryotic or prokaryotic expression systems (Cho et al. 2001).

The Human Immunodeficiency Virus type 1 (HIV-1) and Simian Immunodeficiency Virus (SIV) Gag precursor, like those in other retrovirus, which is capable of assembling into virus-like particles without the requirement of any other viral factors, is composed of four major domains matrix (MA), capsid (CA), nucleocapsid (NC) and p6 (Demirov et al. 2002). The MA (p17) protein form the outer shell of the core of the virion (González et al. 1996). It has already been demonstrated that the expression of SIV MA protein alone by means of a vaccinia virus expressed system assembles into lentivirus-like particles which are released into the medium of infected cells (Gonzalez et al. 1993, Angela et al. 1998).

The goal of this work was to construct smaller VLPs able to delivery therapeutic and effective proteins to the target cell. The VLP was constructed using the p17 domain of SIV fused through a long peptide linker to the small domain p6 from HIV-1. The linker was used in order to avoid conformational problems. An expression cell line derived from 293T cells was developed for the production of these particles and is being adapted to suspension growth in serum-free medium. For delivery, the trans-activator protein (Tat) from HIV was used. To evaluate the role



of matrix-only for VLP formation and the dependence of p6 for Tat incorporation, the expression of SIV MA protein alone was also studied. Expression of chimeric proteins and presence in the culture medium was evaluated by immunoassay and electronic microscopy. Current studies evaluate the biochemical delivery of the Tat protein to cells.

## 2. RESULTS

### 2.1. Development of an expression cell line derived from 293T cells

To express the chimeric protein (p17-p6) in mammalian cells, 293T cells were transfected with pcDNA 3.1 – p17/p6 and placed under zeocin selection to obtain stable colonies. Several clones were analysed for protein expression. This detection was observed by immunofluorescence (figure 1a) and western-blot (figure 1b), either in cell lysates and in culture medium.

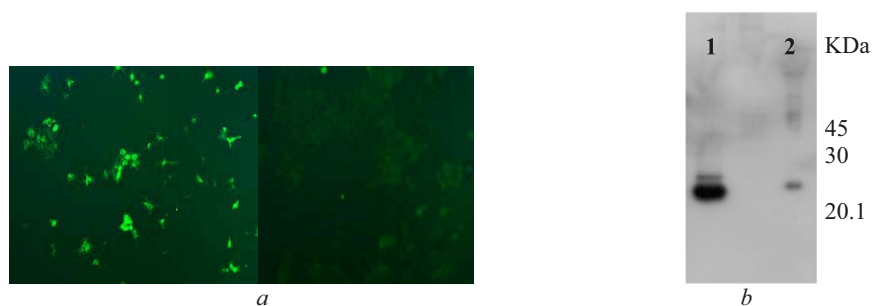


Figure 1. a) Immunofluorescence analysis (left – expression cell line; right – negative control- cells not transfected). Cells were incubated with anti-HA fluorescein (1:40) (Roche); b) Western-blot analysis (1 – Cell extract; 2 – Culture medium ultracentrifugated through a 20% sucrose cushion). Proteins were probed with anti-HA HRP (1:7500) (Roche)

To confirm that the chimeric protein (p17-p6) detected in the pelleted material was an indication of VLP formation and release, the stably transfected 293T cells culture medium was examined by electron microscopy (EM). The EM analysis (figure 2) demonstrated that we are in the presence of small particles surrounded by a lipidic membrane corresponding to the VLPs.

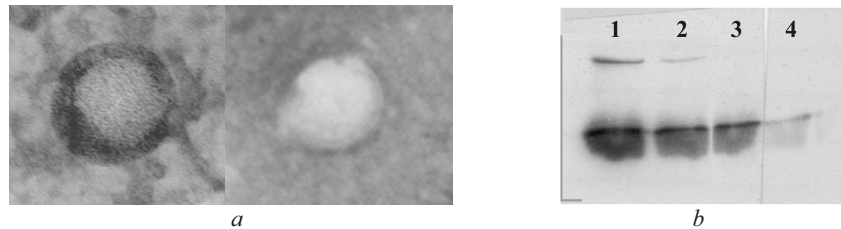


Figure 2. a) Electron microscopy; b) Protease protection assay (1 – Untreated; 2 – 1 % Triton X-100; 3 – Proteinase K 1  $\mu$ g/mL; 4 – 1 % Triton X-100 and proteinase K 1  $\mu$ g/mL)

To further investigate that the p17-p6 assembled as membrane-bound particles a protease protection assay was performed (figure 2b). Culture supernatant from stably transfected 293T cells was ultracentrifuged at 120 000 g, through 20% (w/v) sucrose cushion and the pellet was resuspended in PBS and divided into 4 aliquots. Proteinase K degraded p17-p6 VLP only in the presence of Triton X-100 (Figure 2b line 4), which indicates that protease digestion required disruption of the lipidic membrane surrounding the protein.

### 2.2. Increase of VLP production

To confirm the increase of VLP released, the 293T cells were transfected either by pcDNA 3.1-p17/p6 and pcDNA 3.1-p17, to compared the VLP production. The western-blot analysis of the culture medium (figure 3) showed a decreased of the particle released by the 293T cells expressing the matrix alone.

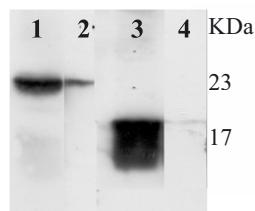


Figure 3. Western-blot analysis (1-cell extract, 2 – culture medium both from 293T cells transfected with p17/p6; 3 – cell extract, 4 – culture medium both from 293T cells transfected with p17)

## 3. DISCUSSION

Here we demonstrated that the fusion between the matrix protein of SIV with the p6 domain from HIV-1, when expressed in 293T cells, in the absence of other viral proteins assembles into chimeric VLPs. Electron microscopy analysis and protease

protection assay confirmed that the produced VLPs were surrounded by a lipidic membrane, that confer resistance to proteinase K degradation.

We also showed that this fusion increased the VLP release by 293T cells, when compared to the expression of MA protein alone. This suggested that the p6 will have a positive influence in the particle release. Studies are being made to evaluate the role of p6 in chimeric VLP released.

#### 4. REFERENCES

- Angela M, Giddings GD, Ritter Jr & Mulligan MJ (1998) The matrix protein of HIV-1 is not sufficient for assembly and released of virus-like particles. *Virology* 248: 108-116
- Cho C-W, Cho Y-S, Kang B-T, Hwang P & Yoon D-Y (2001) Improvement of gene transfer to cervical cancer cell lines using non-viral agents. *Cancer letters* 162: 75-85
- Demirov D, Orenstein J, Freed R (2002) The late domain of Human Immunodeficiency Virus release in a cell type-dependent manner. *Journal of Virology* 76: 105-117
- González SA, Affranchino JL, Gelderblom HR & Burny A (1993) Assembly of the matrix protein of Simian Immunodeficiency Virus-like particles. *Virology* 194: 548-556
- González SA, Burny A & Affranchino JL, (1996) Identification of domains in the Simian Immunodeficiency Virus matrix protein essential for assembly and envelope glycoprotein incorporation. *Journal of Virology* 70: 6384-6389

TIAGO B. FERREIRA<sup>1</sup>, PAULA M. ALVES<sup>1</sup>,  
DÉLIA GONÇALVES<sup>1</sup> & M.J.T. CARRONDO<sup>1,2</sup>

## EFFECT OF MOI AND MEDIUM COMPOSITION ON ADENOVIRUS INFECTION KINETICS

<sup>1</sup>*IBET/ITQB, Ap.12, 2781-901 Oeiras, Portugal;* <sup>2</sup>*FCT /UNL,  
2825-114 Monte da Caparica, Portugal.*

### INTRODUCTION

Recombinant adenoviral (AV) vectors are highly efficient for gene transfer in a broad spectrum of cell types and had become one of the vectors of choice for delivery and expression of foreign proteins for gene therapy and vaccination purposes. The market requirements for AV are constantly increasing causing a high demand of methodologies for the production in large scale of concentrated vectors.

The importance of infection kinetics on viral and protein production and the significance of variables such as MOI (Multiplicity Of Infection) and HPI (Hours Post Infection) in process optimisation have been demonstrated in previous studies with other viral/eukaryotic expression systems e.g. baculovirus-insect cells<sup>1</sup>, reinforcing that an optimized strategy of MOI and HPI is mandatory to increase production yields. Other important parameter affecting the viral infection process is serum concentration in the culture media<sup>2,3</sup>.

In this work, AV production kinetics was investigated. Factors such as medium composition, serum content, MOI, and harvest time were studied. A first generation recombinant adenovirus type 5 was used. Medium supplementation with a chemically defined lipid mixture, as a possible serum substitute, was also assessed.

### MATERIAL AND METHODS

Cell Growth: 293 cells (ATCC-CRL-1573), were grown in MEM supplemented with 2 mM glutamine and 5% (v/v) FBS (all from Gibco, UK), at a humidified atmosphere of 5% CO<sub>2</sub> in air at 37°C or in CD293 (a serum and protein-free medium Invitrogen, UK) supplemented with 2 mM glutamine at a humidified atmosphere of 8% CO<sub>2</sub> in air at 37°C; AV Quantification: AV titration was performed by the end-point dilution method (TCID<sub>50</sub>) using 96 well plates and 293 cells. The titer was calculated according to the method of Reed and Muench<sup>4</sup>. Virus titer were normalized to the maximum one in the experiment.

## RESULTS AND DISCUSSION

*Effect of MOI on AV production*

To evaluate the effect of MOI on AV production, 293 cells were infected with a MOI of 1, 5, 10 and 20. The AV production profiles are shown in Figure 1. The maximum vector titer increased by a factor of  $10^4$  when the MOI was increased from 1 to 5. Further increase in MOI did not affect vector titer but caused a shift of the optimal harvest time; taking into account the AV net output ( $AV_{Out}/AV_{In}$ ) it is clear that the best yields are obtained when a MOI of 5 is used. The profiles of AV release into the supernatant (due to cell lysis) were similar for MOI of 1, 5 and 10. The results show that for 48 HPI the amount of AV released into the supernatant is not significant as compared with the intracellular content, simplifying the downstream processing that can be designed taking into account only a cell concentration step, mechanical cell lysis and AV purification by ion exchange chromatography (data not shown).

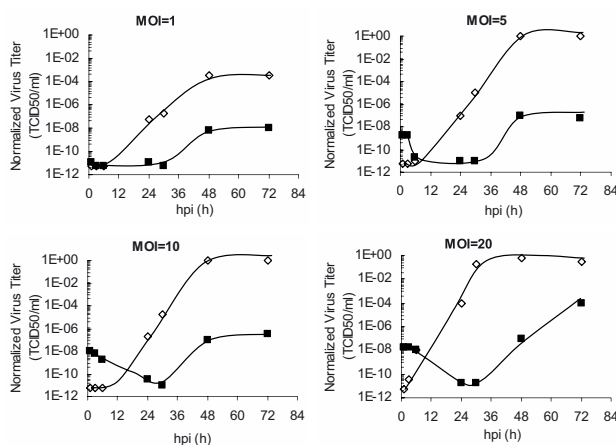


Figure 1. Effect of MOI on normalized virus titer ( $\diamond$  intracellular,  $\blacksquare$  extracellular).

*Effect of culture media composition on AV production*

In order to understand the effect of serum concentration on AV production, cells were grown in MEM supplemented with 10% FBS and at the time of infection (MOI 5) the total volume of the culture medium was replaced by MEM supplemented with 10, 5, 1 and 0% of FBS. AV were harvested at 48 HPI. The highest AV yields were obtained in MEM supplemented with 5% FBS (Figure 2). AV production decreased by a factor of  $10^3$  when 0 and 1% FBS concentrations were used indicating the importance of serum in viral infection as extensively reported in the literature<sup>2,3</sup>.

Interestingly a decrease on AV production was observed for 10% FBS containing medium, suggesting that when in excess some serum components (e.g. proteins) can compete with AV for cell receptors by blocking viral receptors and consequently decreasing the probability of viral entrance into the cell. A concomitant decrease in cell viability was observed with the decrease in serum content (Figure 2). An alternative approach to serum containing medium formulations is the use of commercially available defined media supplemented with known concentrations of lipids and amino acids solutions. We tested two chemically defined media (CD293 and MEM supplemented with a chemically defined lipid solution from Invitrogen) in their performance to produce AV. The results are presented in Figure 3. Cells were unable to grow in MEM supplemented with lipids, thus a complete replacement was done only at infection time. The highest AV yields were obtained in CD293 medium. When MEM supplemented with lipids was used a decrease in the maximum vector titer by a factor of  $10^2$  when compared with the CD293 medium and by a factor of 10 when compared with the MEM supplemented with 5% FBS was observed. Thus, the CD293 was chosen for further process development.

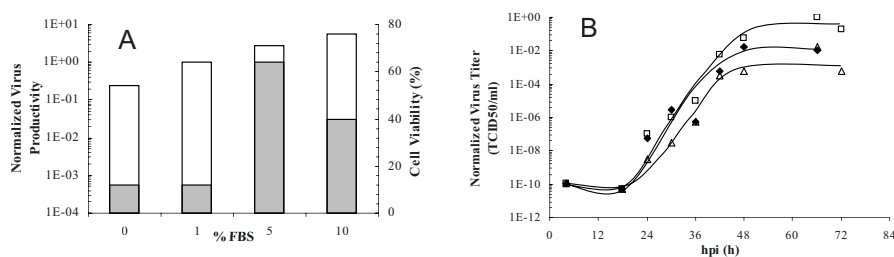


Figure 2. Normalized virus productivity (■) and cell viability (□) at different serum concentration for a MOI of 5 at 48 HPI.

Figure 3. Normalized virus titer at MOI 5 (□ CD293, △ MEM+lipids, ◆ MEM+5% FBS).

## CONCLUSIONS

The best AV production yields were obtained for a MOI of 5 at 48 HPI. Serum concentration affected AV production yields and also cell viability. The best FBS concentration was 5%. Surprisingly, AV infection seems to be hindered by the presence of a higher serum concentration (10%). CD293, a serum and protein free medium, prove its potentiality as the best alternative for AV production, not only because it supports higher AV yields but also because it is possible to simplify the downstream process, since virus and prions contamination are avoid in the bioprocess.

## REFERENCES

- 1 Cruz, PE, Martins, PC, Alves, PM, Peixoto, CC, Santos, H, Moreira, JL, and Carrondo, MJ (1999), *Biotechnol Bioeng* **65**(2) 133-43.
- 2 Maranga L, Coroadinha AS, Carrondo MJ (2002) *Biotechnol Prog* **18**(4) 855-61.
- 3 Petricevich VL, Palomares LA, Gonzalez M, Ramirez OT (2001) *Enzyme Microb Technol* **29**(1) 52-61.
- 4 Summers MD, Smith GE (1987) Texas A and M University Experimental Station Bulletin N° 1555.

J. VASI<sup>1</sup>, R. MORENWEISER<sup>2</sup>, K. ERIKSSON<sup>1</sup>, R. LEMMENS<sup>1</sup>  
AND S. HERZER<sup>3</sup>

## ION-EXCHANGE CHROMATOGRAPHY BASED STRATEGIES FOR PURIFICATION OF VIRAL VECTORS

<sup>1</sup>*Amersham Biosciences AB, R&D protein separations, Björkgatan 30,  
751 84 Uppsala, Sweden*

<sup>2</sup>*Amersham Biosciences Corp., P.O. Box 1327, Piscataway, NJ 08855, USA*

<sup>3</sup>*Amersham Biosciences Europe GmbH, Munzingerstrasse 9,  
D-79111Freiburg, Germany*

### 1. INTRODUCTION

The increasing numbers of pre-clinical and clinical trials where recombinant viral vectors are used for gene delivery require a cost-effective large scale production of biologically active, highly purified viral particles (Kay *et al.*, 2001). Traditional methods like CsCl density gradient centrifugation are time consuming, can process only limited volumes and involve the use of toxic reagents. Column chromatography can be an attractive alternative technique because of its well-known scalability, flexibility and capability to meet cGMP requirements. Chromatographic purification of virus particles mainly exploits size, surface charge or specific receptor-binding properties of the virions. Here we describe two ion-exchange chromatography based strategies, developed for the purification of adenovirus and adeno-associated virus. We demonstrate that this is a rapid, versatile and scalable technique suitable for large-scale production of high quality viral vectors.

### 2. MATERIALS AND METHODS

All chromatographic resins (SP Sepharose™ High Performance (Amersham Biosciences), Q Sepharose XL, SOURCE™ 15Q (Amersham Biosciences)) used in the study were products of Amersham Biosciences, Uppsala, Sweden.

Adeno-associated virus (AAV) serotypes 2 and 5 were produced in HEK 293 cells using a triple plasmid system (Brument *et al.*, 2002). The same cell line was used also for production of the Adenoviral vector (Ad5).

Electrophoretic titration curves of viral particles and whole lysates were generated on 2% agarose and on poly-acrylamide IEF gels, respectively. Viruses were labelled with CyDye™ fluor (Amersham Biosciences), while IEF gels were SYPRO™ Ruby



(Molecular Probes Inc.) or Coomassie™ (ICI plc.) stained. SDS-PAGE and western blot techniques were used for analysis of chromatographic samples.

Cells were lysed by three freeze/thaw cycles to release the viral particles. Cell debris were removed from the lysate by centrifugation. In case of Ad5 the lysate was benzonase treated prior to clarification. In case of AAV the clarified lysate was subjected to heat treatment (30 min at 56°C) and to filtration (5 and 0.45 µm) to remove the precipitate. In both AAV and Ad5 cases one half of the clarified lysate was subjected to chromatography and the other half to CsCl gradient purification.

Chromatography of AAV-5: SP Sepharose High Performance resin: Application buffer: 2 mM MgCl<sub>2</sub>, 100 mM NaCl, 25 mM NaHPO<sub>4</sub> pH 6.5. Elution buffer: Application buffer containing 500 mM NaCl.

SOURCE 15Q resin: Application buffer: 2mM MgCl<sub>2</sub>, 1 mM CaCl<sub>2</sub>, 20 mM NaCl, 20 mM Tris-HCl pH 8.2. Elution buffer: Application buffer containing 500 mM NaCl.

Chromatography of Ad5: Q Sepharose XL resin: Application buffer: 50 mM Tris-HCl pH 8.0 in 5% glycerol. Elution buffer: Application buffer containing 1 M NaCl.

### 3. RESULTS AND DISCUSSION

#### 3.1. Two step purification strategy for AAV

The result from electrophoretic titration curve indicated that the viral particles had a net positive charge under pH 7 (Figure 1A), while most of the impurities were negatively charged at this pH (Figure 1B). This suggests that cation-exchange chromatography is a favourable step for capturing the virus particles from the lysate.

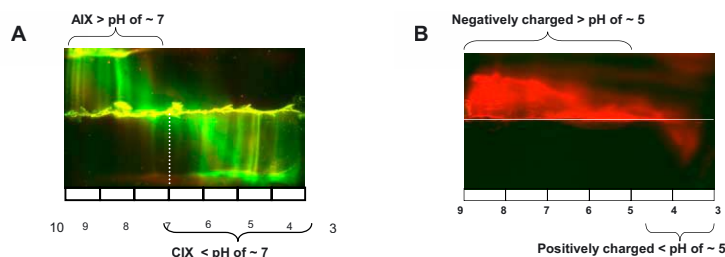


Figure 1. Electrophoretic titration curves. A: Cy3 Direct™ (Amersham Biosciences) labelled AAV. B: SYPRO Ruby stained whole cell lysate.

SP Sepharose High Performance was used to capture the rAAV5. The bound rAAV5 was eluted at 238mM NaCl (Figure 2A).

The anion-exchanger SOURCE 15Q was used for removal of the remaining impurities from the rAAV5 fractions. The binding of viral particles to the column was achieved by increasing the sample pH to 8.2 and lowering the salinity to 20mM (negative charge of the virus particles). When applying a linear salt gradient to the

column, rAVV5 was eluted in the first peak at a NaCl concentration of 93 mM (Figure 2B).

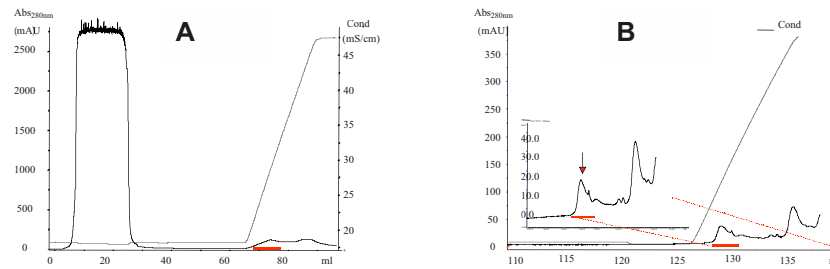


Figure 2. Capturing AAV on SP Sepharose High Performance (A) and final polishing on SOURCE 15Q (B) (A): virus-containing peak underlined. Insert in (B): the elution part of the chromatogram was enlarged. The arrow indicates the virus peak.

SDS-PAGE and western blot analysis of the virus-containing fractions confirmed the very effective removal of impurities (Figure 3). These results together with data of transducing activity and the empty particle/PFU ratio of the viral stock (data not shown) revealed a superior purity and biological activity of virus particles purified by chromatography in comparison to those isolated with the CsCl method.

Applying the same purification strategy on AAV serotype 2, a viral stock with a quality equal to AAV5 described above, was obtained (data not shown).

Scale-up experiments performed on columns containing 2, 8 or 20 ml of resins generated highly reproducible results with both AAV serotypes (data not shown).

These data indicates a general applicability of the IEX approach for purification of different AAV serotypes (Brument *et al.*, 2002).

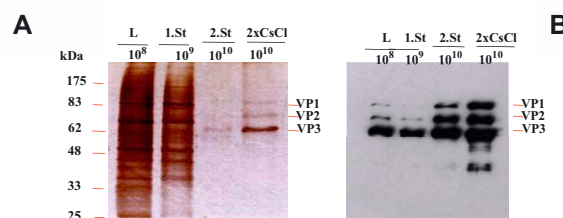


Figure 3. Silver staining (A) and western blot (B) analysis of rAVV5 samples. L: initial cell lysate, 1St: virus peak from SP Sepharose High Performance, 2St: virus peak from SOURCE 15Q, 2xCsCl: viruses purified by double CsCl gradient centrifugation,  $10^8$ : Number of rec. AAV particles present in the sample. VP1-3: indicates virus proteins

### 3.2. Single step purification strategy for Ad5 (Herzer *et al.*, 2000)

Empirical determination of the charge characteristic of Ad5 particles and clarified cell lysate showed moderate negative charge from pH 6-7 and strong negative charge of the virions above pH 7.5 (Figure 4A). ETC of contaminants indicated a slower migration towards the anode in the pH range of 7.5-8.5 (Figure 4B).

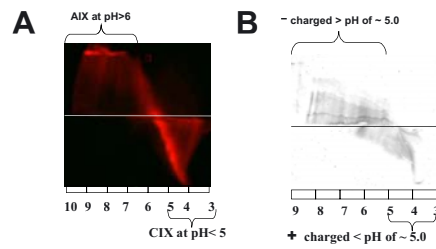


Figure 4. Electrophoretic titration curves. A: adenovirus. B: whole cell lysate.

Taking into consideration virus stability and the charge characteristics, Q Sepharose XL chromatography at pH 8.0 was chosen for the purification (Blanche *et al.*, 2003). By applying a linear salt gradient we were able to separate the majority of impurities from the peak containing most of the viral particles (Figure 5).

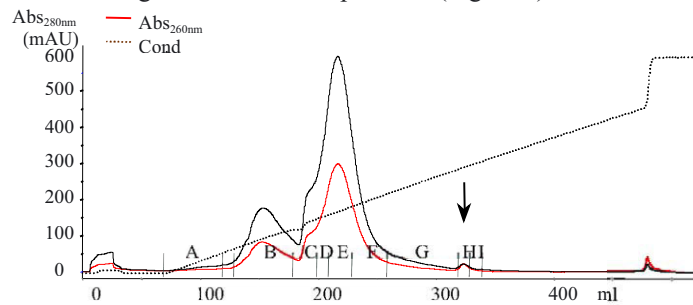


Figure 5. Q Sepharose XL purification of Ad5. A-I: indicates the analysed fractions. The arrow indicates the virus peak

The purity was confirmed by SDS-PAGE – western blot analysis (Figure 6) and PCR amplifications performed on the collected fractions.

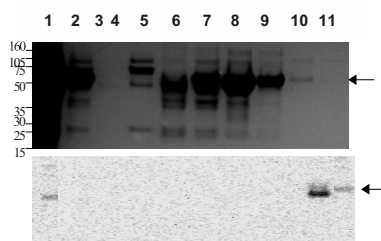


Figure 6. SDS-PAGE and western blot analysis of fractions. 1: loaded sample, 2: FT, 3: fraction A, 4: fraction B, 5: fraction C, 6: fraction D, 7: fraction E, 8: fraction F, 9: fraction G, 10: fraction H, 11: fraction I. Arrows indicate hexon band

Similar purities could also be obtained at salt concentrations up to 300 mM NaCl where contaminants will no longer bind to the column and an easy one step procedure allows elution of the virus from the column after sample application at 300 mM NaCl and elution at 600mM NaCl (data not shown). However, binding capacity at higher salt concentration is about half due to competition with chloride anions (data not shown).

Although the overall quality of Ad5 stocks obtained with a single step AIX chromatography is comparable to those isolated by double CsCl gradient, further improvement can be achieved by an additional size-exclusion chromatography on Sepharose 4 Fast Flow (Amersham Biosciences) (data not shown) or HIC/IMAC chromatographic step (Huyghe *et al.*, 1995).

#### 4. CONCLUSION

We presented two ion-exchange chromatography based strategies for purification of recombinant adeno-associated and adenovirus. This technique can handle crude, clarified cell lysate and generate viral stocks in high purity and with biological activity similar to particles obtained by traditional methods. As a chromatographic technique it has the vast advantages of easy, linear scalability, capability to meet cGMP requirements and short process time over the CsCl gradient density centrifugation. Moreover, the presented strategies demonstrated that ion-exchange chromatography can be a general method for large scale production of a variety of viral vectors.

#### ACKNOWLEDGEMENT

We thank to all our collaborators, Nicole Brument and Anna Salvetti (INSERM ERM; Nantes, France) for their contribution to this work. We also thank Thomas A. Gardner (Dept. of Urology, Indiana University Medical Centre, Indianapolis, IN, USA) and Alan R. Davis (Centre for Cell and Gene Therapy, Baylor College of Medicine, Houston, TX, USA) for providing us with adenovirus samples.

## REFERENCES

- Brument, N., Morenweiser, R., Blouin, V., Toubance, E., Raimbaud, I., Cherel, Y., Folliot, S., Gaden, F., Boulanger, P., Kroner-Lux, G., Moullier, P., Rolling, F., and Salvetti, A. (2002). A versatile and scalable two-step ion-exchange chromatography process for the purification of recombinant adeno-associated virus serotypes-2 and-5. *Molecular Therapy*. 6, 678-686.
- Blanche, F., Barbat, A., and Cameron, B. (2003). Method of separating viral particles (USP 6.537.793).
- Herzer, S., Olmsted, E. A., Palladino J., Eriksson K., Moore, P and Davis I.A.R. Rapid Adenovirus Purification Using Q Sepharose XL. Poster. Presented on 8th Meeting of the European Society of Gene Therapy (ESGT) Stockholm, Sweden, October 7-10, 2000.
- Huyghe, B. G., Liu, X., Sutjipto, S., Sugarman, B.J., Horn, M.T., Shepard, H.M., Scandella, C.J., and Shabram, P. (1995). Purification of a type 5 recombinant adenovirus encoding human p53 by column chromatography. *Hum Gene Ther*. 6, 1403-16.
- Kay, M. A., Glorioso, J. C. and Naldi, L. (2001). Viral vectors for gene therapy: the art of turning infectious agents into vehicles of therapeutics. *Nature Medicine* 7, 33-40.

V. HENDRICK, N. KAGYE, Y. KAMBA, S. SIMON,  
A-L.THINSY, T. MARIQUE AND J. WERENNE

## SCALING UP OF ENDOTHELIAL CELLS CULTURE FOR THE PRODUCTION OF A RICKETTSIAE VACCINE: VALUATION OF THE IMPORTANCE OF THE INTERFERENCE EFFECTS

*Laboratory of Animal Cell Biotechnology, Department of Bioengineering,  
Faculty of Sciences, Université Libre de Bruxelles, Brussels, Belgium.*

**Abstract:** We showed here that the scale-up of the production of the rickettsiae could benefit of the control of the migration properties of the host cells. Indeed, bead to bead transfer of endothelial cells, either normal or SV40 transformed and immortalized, was shown to be efficient in cell subculturing using Cytodex 3 microcarriers either if grown in roller-bottles or stirred tank. It should be mentioned however that a phenomenon of interference due, at least in part to in-situ interferon induction by the infection with the rickettsiae, occurs.

### INTRODUCTION

The infection by the rickettsiae *Cowdria ruminantium* transmitted from animal to animal by ticks of the *Amblyoma* species is one of the three main causes of economical losses for cattle breeders in Africa, South of Sahara. Attenuated or killed rickettsiae vaccine was however shown to be efficient. ( Martinez et al. 1996, Totté et al. 1999, Mahan et al. 2001) It should be produced in endothelial cells, which are the only efficient permissive cell type for the rickettsiae.

We have previously shown that mobility of endothelial cells is related to the expression of a 92 kD Metalloproteinase. (Blankaert et al, 1994, Marique and Wérenne, 2001) This property was taken into account in the present work.

We have shown before that interferon is playing an important role in *in vitro* infection (Totté et al. 1996) and in the resistance against the disease ( Totté et al. 1993 -Totté et al. 1994) .

We therefore evaluated here the possible role of the interferon system in the productivity of the vaccine.

### MATERIAL AND METHODS

*Cells used:* MDBK cells were used to titrate interferons and to titrate the VSV used for the CPE tests. (obtained from Dr K. Huygen , Pasteur Institute, Brussels). Endothelial cells : either the Bovine Umbilical Endothelial Cells -BUEC

(provided originally to us by Prof. F. Jongejan, Utrecht University), or murine Endothelial Cells immortalized by SV40 T antigen -HEC, were used.

*Rickettsiae stocks used* : the stock of *Cowdria ruminantium* "Senegal" was supplied originally to us by Prof. F. Jongejan. The rickettsiae were routinely stained in infected cells using the Diff-Quick coloration procedure (Bayer KIT).

*Culture media and procedure used*: Different culture media were tested (essentially DMEM, BHK21 and Optimem, from Gibco or Bio-Whtakker) with or without FCS (5-20 %), and with pen-sm (50 U and 50 µg/ml respectively). For "Spinner-flasks" growth, Cytodex 1, 2 and 3 were tested.

Growth was operated in <CO<sub>2</sub> incubators in "TC flasks" (80 cm<sup>2</sup>), "Roller-Bottles" (700 cm<sup>2</sup>) or Techne "Spinner-flasks" (100 or 250 ml) on Techne agitation plates. Pr

*Interferon* : for control we used HuIFN alfa, supplied to us by Boehringer-Ingelheim. The VSV reduction Cytopathogenic Effect (CPE) test is used for Interferon titration, as descriobed previously (Totté et al. 1994)

## RESULTS

### *Medium , Microcarriers and Cells selection:*

By comparing the different media and microcarriers used, the final selection of Optimem for cells growth and DMEM without Serum for the rickettsia production, Cytodex 3 (5mg/ml) , and immortalized HEC cells. BHK21 medium, either with Serum or not was not efficient for our purpose.

*Maintenance of cells*: cells already attached to their substratum remained alive for more than 20 days ( with Optimem , more than 80 % of the cells remained attached) and for DMEM without Serum, 50 % were maintained.

*Cell culture Procedures used*: for "Roller bottles" using a high HEC cells seeding concentration ( 7.10<sup>5</sup> cells in 100 ml medium), with a regular feeding procedure (every 3 days) , cells can reached a high density and may be maintained healthy for the long periods required for the rickettsiae production (more than 15 days).

Infected at day 12, a follow up of the rickettsia production was made and the process is efficient. In "Spinner-flasks" we showed that addition of fresh microcarriers and fresh medium at day 4 when reaching the first confluence, permitted a more than a doubling of the quantity of cells obtained after 10 days ( over 9.10<sup>7</sup> cells are obtained , using a 30 minutes static condition when adding fresh microcarriers followed by a stepwise increase in agitation (10, 20 and 50 rpm). *Infection with Cowdria ruminantium* : was giving rise to efficient production either in "Roller-Bottles" ( starting from day 5 to 9 essentially) and in "Spinner-Flasks", in which the process can be maintained longer.

*Interference effects* : rickettsiae titration (using a quantification of cell lysis essay) showed that supernatant from infected cells contained an interfering factor affecting the cell lysis process. Part of this effect is due to interferon.

## CONCLUSIONS

We developed a procedure to produce the rickettsiae *Cowdria ruminantium* using immortalized endothelial cells growing on microcarriers in "Spinner-Flasks" as an alternative to grow them in "Roller-bottles". The process involved scale-up conditions permitting the control of the adhesion of the endothelial cells on microcarriers for the prolonged time necessary for the development of infectious rickettsiae and the mobility of the endothelial cells from confluent microcarriers to empty beads. It should be mentioned that a phenomenon of interference due, largely to in-situ interferon induction by the infection with the rickettsiae, occurs. This should be taken into account in optimizing the process of *Cowdria ruminantium* production and in the downstream processing of the vaccine product.

## REFERENCES

- Blankaert, D., Simonart, Th., Van Vooren, J.P., Parent, D., Liesnard, C., Farber, C.M., Marique, T. and Wérenne, J. (1998), *JAIDS Hum. Retrovirology*, 18, 203-209.
- Mahan, S.M., Smith, G.E., Kumbula, D., Burridge, M.J. and Barbet, A.F. (2001), Reduction in mortality from heartwater in cattle, sheep and goats exposed to field challenge using an inactivated vaccine, *Vet. Parasit.* 97, 295-308.
- Marique, T., Blankaert, D., Hendrick, V., Raschella, A., Declercq, B., Alloin, C., Teixeira-Guerra, I., Sandron, D., Cherlet, M., Parent, D., Kirkpatrick, C., Van Vooren, J.P., and Wérenne, J. (1997), Biological response of endothelial cells and its modulation by cytokines: prospects for therapy and bioprocesses, *Cytotechnology*, 25, 183-189.
- Marique, T. and Wérenne, J. (2001), Control of 92kDa Collagenase secretion in mammalian cells by modulation of AP-1 activity: an experimentally based theoretical study, *J. Theoret. Biol.* 209, 3-8.
- Martinez, D., Perez, J.M., Sheikboudou, C., Debus, A., and Bensaid, A. (1996), Comparative efficacy of Freund's and Montanide ISA50 adjuvants for the immunisation of goats against heartwater with inactivated *Cowdria ruminantium*, *Vet. Parasit.* 67, 175-184.
- Totté, P., Bensaid, A., Mahan, S.M., Martinez, D. and McKeever, D.J. (1999), Immune responses to *Cowdria ruminantium* infections, *Parasit. Today* 15, 286-290.
- Totté, P., Jongejans, F., de Gee, A.L.W. and Wérenne, J. (1994), Production of alpha interferon in *Cowdria ruminantium*-infected cattle and its effect on infected endothelial cell cultures, *Infect. Immun.* 62, 2600-2604.
- Totté, P., Vachieri, N., Heremans, H., Biliau, A. and Wérenne, J. (1993), Protection against *Cowdria ruminantium* infection in mice with gamma interferon produced in animal cells, in Kobayashi, T., Kitagawa, Y. and Okumura, K. Eds, "Animal Cell Technology: Basic and Applied Aspects", 6, 595-599.
- Totté, P., Vachieri, N., Martinez, D., Trap, I., Ballingall, K.T., MacHugh, N.D., Bensaid, A., and Wérenne, J. (1996), Recombinant bovine interferon gamma inhibits the growth of *Cowdria ruminantium* but fails to induce major histocompatibility complex class II following infection of endothelial cells, *Vet. Immunol. Immunopath* 53, 61-71.



## CHAPTER 4

### TARGET DISCOVERY

WILFRIED WEBER, NILS LINK, MANUELA SPIELMANN,  
BETTINA KELLER, CORNELIA C. WEBER AND  
MARTIN FUSSENEGGER

## INDUCIBLE GENE EXPRESSION FOR ANTIBIOTIC DRUG DISCOVERY AND DIAGNOSTICS

*Institute of Biotechnology, Swiss Federal Institute of Technology,  
ETH Hoenggerberg, CH-8093 Zurich, Switzerland. Tel.: +41 1 633 3448;  
Fax: +41 1 633 1234; fussenegger@biotech.biol.ethz.ch*

**Abstract.** The rapid spreading of multi-drug-resistant human-pathogenic bacteria in industrialized countries and the thereto related increased morbidity and mortality urgently require decisive countermeasures to contain this imminent threat: (i) Discovery of novel anti-infectives has to outperform the emergence of novel resistance mechanisms, and the use of clinically licensed antibiotics in stock farming will have to be restricted or banned. Both of these key actions require highly sensitive and rapid technology to discover and validate novel antibiotic lead structures as well as detect trace amounts of illegal antibiotics in food samples including milk or meat. To increase the discovery rate for novel anti-infective lead structures, we have designed the Mammalian Antibiotic Sensor Technology (MAST), a mammalian cell-based screening platform with integrated cytotoxicity and bioavailability assessment of novel antibiotic structures. The basis of MAST are antibiotic biosensors derived from prokaryotic transcriptional regulators, which are highly responsive to potent antibiotic core structures of a desired class. In order to enforce the ban of certain antibiotics in food samples we developed an in vitro Biosensor ImmunoAssay (BIA) for which we have engineered prokaryote-derived biosensors into a cell-free test system for rapid and sensitive detection of antibiotics in biological samples like milk or serum.

### 1. INTRODUCTION

In the past decades spreading of multi-drug-resistant human-pathogenic bacteria has been favoured by excessive antibiotic prescriptions in human therapy as well as undue use of antibiotics as a growth promotant in stock farming. Today, more than 60% of all nosocomial infections are caused by multi-drug-resistant bacteria resulting in over 14.000 deaths per year in the USA alone. The World Health Organization as well as the European Commission have reacted to this new threat by banning antibiotics from use in stock farming. Current scientific reports suggest reduced prevalence of multi-drug-resistant bacteria to correlate with restricted use of clinically licensed anti-infectives in large-scale animal husbandry<sup>1</sup>. In this study we describe the potential and characteristics of antibiotic biosensors for discovery of novel antibiotics as well as for detection of anti-infectives in food samples.

## 2. RESULTS AND DISCUSSION

## 2.1. Mammalian Antibiotic Sensor Technology (MAST) for antibiotics discovery

For rapid identification of novel antibiotics against resistant bacteria, we designed the mammalian antibiotic sensor technology (MAST) which can be used for class-specific discovery of potent anti-infective core structures. The basis of MAST are biosensor proteins, which adjust their binding affinity to specific operators in response to different antibiotic classes<sup>2-5</sup>. Capitalizing on this reversible antibiotic-responsive protein-DNA interaction, we designed a mammalian cell-based screening system in which biosensor binding to a cognate operator module flanked by the viral P<sub>SV40</sub> promoter and the reporter gene SEAP (human secreted alkaline phosphatase) modulates reporter gene expression in response to biosensor-specific antibiotic structures<sup>3-5</sup>. In the absence of antibiotics, the biosensor-operator interaction blocks P<sub>SV40</sub>-driven SEAP expression, whereas class-specific antibiotic core structures bind the biosensor and change its allostery which results in disruption of the biosensor-operator interaction and derepression of the reporter gene. Thus, SEAP production quantified by a highly sensitive chemiluminescence assay<sup>6</sup> indicates the presence of an antibiotic structure (Figure 1). Engineering of the aforementioned biosensor-operator configuration into a mammalian cell context provides further information on the detected compounds<sup>7</sup>: (i) Undesired cytotoxic compounds kill the transgenic reporter cell line and escape detection and (ii) MAST only detects antibiotics which diffuse through the cellular membranes to reach the biosensor and produce a positive readout. Such bioavailability is essential to target intracellular pathogens like *Mycobacterium tuberculosis* or *Yersinia pestis* and to cross key body barriers following oral administration of the anti-infective. Overall, MAST enables a straightforward integrated 3-in-1 screening which assesses in a single step three main characteristics of novel anti-infective candidates (class-specific antibiotic core structure, non-cytotoxicity of the selected compound and bioavailability of the anti-infective) and therefore substantially speeds up the discovery process. MAST can be used to screen either biological or chemical libraries for new antibiotic lead structures (Figure 1).

Today, several biosensor proteins are available for the discovery of potent antibiotic core structures active against multi-drug-resistant bacteria (Table 1). Additional biosensors have recently been engineered for MAST-based screening of butyrolactones which have recently been associated with immunomodulatory activities<sup>3</sup>.

Table 1. Biosensors available for MAST-based screening.

Biosensor	Operator Site	Responsive to	Reference
TetR	<i>tetO</i>	Tetracycline antibiotics	(2)
PIP	PIR	Streptogramin antibiotics	(5)
E	ETR	Macrolide antibiotics	(4)
ScbR	O <sub>ScbR</sub>	Butyrolactones	(3)

Owing to the composite nature of streptogramin antibiotics it is difficult for pathogens to acquire or evolve resistance against this class of antibiotics<sup>7</sup>. Therefore, MAST-based discovery of novel streptogramins is a current priority.

Initial pilot discovery studies using streptogramin-specific MAST for screening a *Streptomyces* collection has resulted in several hits showing high activity against multi-drug-resistant human-pathogenic bacteria. Isolation, structure determination and characterization of the active compounds are currently underway<sup>7</sup>.

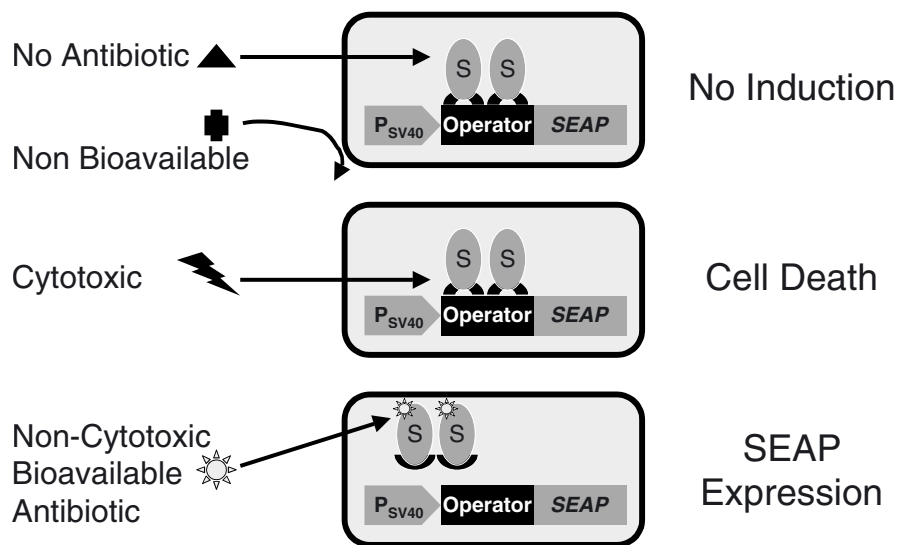


Figure 1. MAST (Mammalian Antibiotic Sensor Technology) in action. Mammalian cells (e.g. Caco-2, shaded rectangular box) engineered for MAST detection express the biosensor (S) and harbor the reporter construct consisting of a biosensor-specific operator flanked by the P<sub>SV40</sub> promoter and SEAP (secreted alkaline phosphatase). Only class-specific, non-cytotoxic, bioavailable antibiotics bind to S, induce an allosteric change and release it from its operator, which results in derepression of the SEAP. However, cytotoxic, non-bioavailable as well as non-antibiotic compounds do not produce a positive SEAP readout.

## 2.2. Biosensor ImmunoAssay (BIA) for antibiotic detection in food samples

In the previous chapter antibiotic biosensors have successfully been engineered in mammalian cells to enable 3-in-1 discovery of non-cytotoxic, bioavailable anti-infective core structures of a specific class. Biosensors can also be adapted for *in vitro* detection of trace antibiotic amounts in biological samples such as serum, milk and meat. We have designed a rapid, multiwell and high-throughput-compatible cell-free diagnostic system based on quantifying the antibiotic-responsive biosensor-operator interaction (Figure 2).

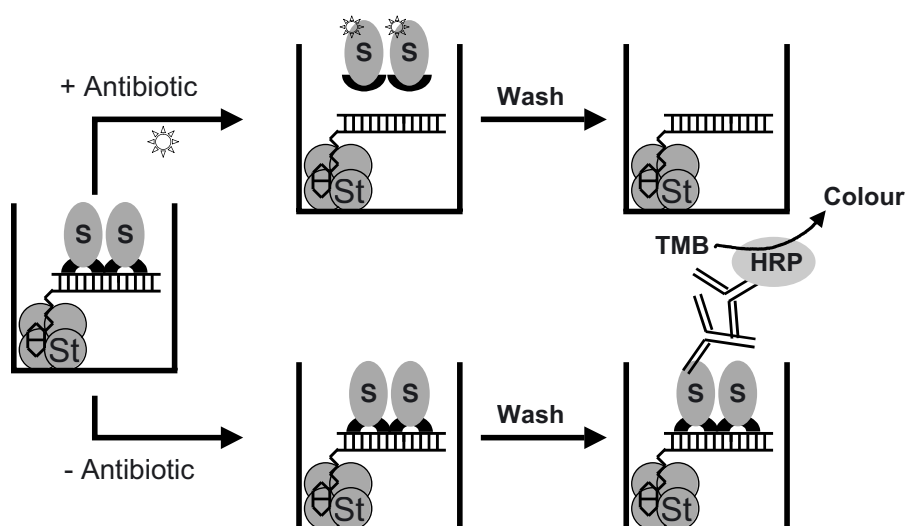


Figure 2. Diagram of the Biosensor ImmunoAssay (BIA). The biosensor (S) is bound to its operator sequence which is immobilized via a streptavidin (St)-biotin linkage in a 96-well microtiter plate. Only when the S-operator interaction is intact (- Antibiotic) it can be quantified by a primary and a secondary antibody coupled to horseradish peroxidase (HRP) which produces a colour readout in the presence of chromogenic TMB. However, in the presence of antibiotics (+ Antibiotic), no colour signal occurs.

BIA consists of a biosensor-specific operator-containing DNA fragment immobilized via a biotin-streptavidin linkage in the well of a microtiter plate which also contains lysate of a biosensor-producing *E.coli* in appropriate buffers (see Weber *et al.*<sup>8</sup> for a detailed protocol). Ready-to-use microtiter plates containing operator DNA and biosensor can pre-manufactured and stored vacuum-dried at 4°C for several month. Following activation by re-hydration with appropriate buffers, the test sample is added and its antibiotic content quantified by the capacity to disrupt the biosensor-operator interaction. The amount of biosensor protein which remains bound to the operator is detected by a primary antibody specific for a C-terminally fused hexahistidine tag and converted into a color readout using a secondary horseradish peroxidase-coupled antibody and the chromogenic substrate 3,3',5,5'-tetramethylbenzidine (TMB). Thus, decreasing antibiotics concentrations in the test samples correlate with increased color readout<sup>9</sup>.

We adapted this generic BIA set-up for the three antibiotic-responsive biosensors, TetR, PIP and E, which are responsive to antibiotics of the tetracycline, streptogramin and macrolide classes, respectively. These class-specific BIAs have been validated for detection of cow serum samples spiked with different concentrations of tetracycline, the streptogramin antibiotic pristinamycin and the macrolide antibiotic erythromycin (Table 2).

Table 2. Dose-response characteristics of the biosensor immunoassay used for the detection of tetracycline, streptogramin and macrolide antibiotics in cow serum. Cow serum was spiked with indicated antibiotic concentrations and subjected to antibiotic-specific BIAs.

Antibiotic (ng/ml)	Tetracycline	Pristinamycin	Erythromycin
500	10.5 ± 0.8	5.3 ± 0.7	8.2 ± 2.2
100	6.4 ± 0.4	4.6 ± 0.2	8.6 ± 1.1
50	18.2 ± 0.5	7.0 ± 1.2	9.5 ± 0.4
10	17.3 ± 0.8	6.4 ± 0.3	16.4 ± 1.3
5	47.3 ± 5.1	11.5 ± 1.7	19.4 ± 2.2
0	100.0 ± 8.3	100.0 ± 9.1	100.0 ± 10.3

The detection limits of the three BIAs specific for different antibiotics determined with a 95% confidence interval were in the ng per ml range, which is at least two orders of magnitude below EC maximum threshold values tolerated in food (Figure 3). Based on these promising results we are currently validating additional biosensors for detection of other substance classes in biological samples. Rapid test devices like lateral flow designs are under development.

In conclusion, antibiotic-responsive biosensors engineered into a MAST or BIA configuration are powerful systems which detect novel class-specific, non-cytotoxic and bioavailable antibiotic lead structures with unmatched precision (MAST) and trace minute amounts of illegal antibiotics in food samples with supreme ease and sensitivity (BIA). MAST and BIA systems are expected to become forefront technologies for the detection and/or preservation of efficient anti-infectives used in last-line-of-defence treatment of multi-drug-resistant human-pathogenic bacteria.

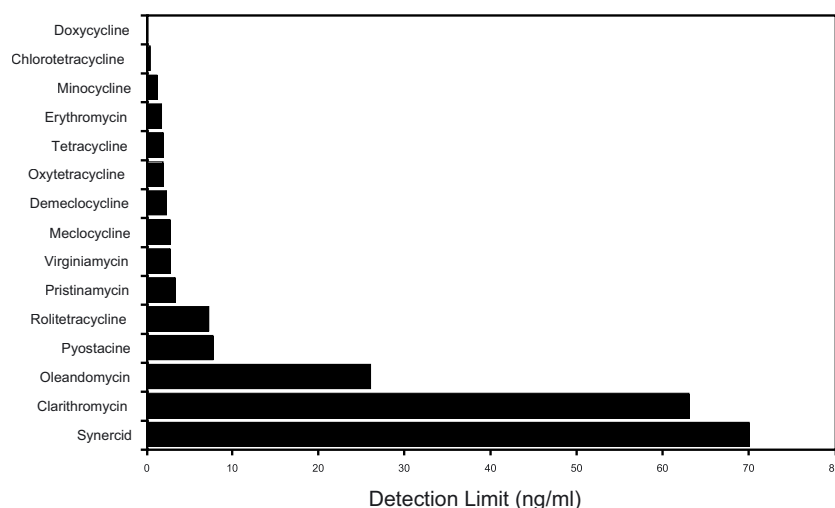


Figure 3: Detection limits for different antibiotics using the BIA assay. The detection limits are with an 95% confidence interval for each antibiotic. The maximum residual limits in food are 40 ng/ml and 100 ng/ml for erythromycin and tetracycline, respectively (European Agency for the Evaluation of Medicinal Products, EMEA).

## 3. REFERENCES

1. Aarestrup, F. M., Seyfarth, A. M., Emborg, H. D., Pedersen, K., Hendriksen, R. S. & Bager, F. Effect of abolishment of the use of antimicrobial agents for growth promotion on occurrence of antimicrobial resistance in fecal enterococci from food animals in Denmark. *Antimicrob Agents Chemother* **45**, 2054-9 (2001).
2. Gossen, M. & Bujard, H. Tight control of gene expression in mammalian cells by tetracycline-responsive promoters. *Proc Natl Acad Sci U S A* **89**, 5547-51 (1992).
3. Weber, W., Schoenmakers, R., Spielmann, M., Daoud-el Baba, M., Folcher, M., Keller, B., Weber, C. C., Link, N., van de Wetering, P., Heinzen, C., Jolivet, B., Séquin, U., Aubel, D., Thompson, C. J. & Fussenegger, M. Streptomyces-derived quorum sensing systems engineered for adjustable transgene expression in mammalian cells and mice. *Nucleic Acids Res* **in press** (2003).
4. Weber, W., Fux, C., Daoud-el Baba, M., Keller, B., Weber, C. C., Kramer, B. P., Heinzen, C., Aubel, D., Bailey, J. E. & Fussenegger, M. Macrolide-based transgene control in mammalian cells and mice. *Nat Biotechnol* **20**, 901-7 (2002).
5. Fussenegger, M., Morris, R. P., Fux, C., Rimann, M., von Stockar, B., Thompson, C. J. & Bailey, J. E. Streptogramin-based gene regulation systems for mammalian cells. *Nat Biotechnol* **18**, 1203-8 (2000).
6. Schlatter, S., Rimann, M., Kelm, J. & Fussenegger, M. SAMY, a novel mammalian reporter gene derived from *Bacillus stearothermophilus* alpha-amylase. *Gene* **282**, 19-31 (2002).
7. Aubel, D., Morris, R., Lennon, B., Rimann, M., Kaufmann, H., Folcher, M., Bailey, J. E., Thompson, C. J. & Fussenegger, M. Design of a novel mammalian screening system for the detection of bioavailable, non-cytotoxic streptogramin antibiotics. *J Antibiot* **54**, 44-55 (2001).
8. Weber, W., Marty, R. R., Link, N., Ehrbar, M., Keller, B., Weber, C. C., Zisch, A. H., Heinzen, C., Djonov, V. & Fussenegger, M. Conditional VEGF-mediated vascularization in chicken embryos using a novel temperature-inducible regulation system (TIGR). *Nucleic Acids Res* **in press** (2003).
9. Weber, C.C., Link, N., Fux, C., Zisch, A. H., Weber, W. & Fussenegger, M. Broad-spectrum protein biosensors for class-specific detection of antibiotics. Submitted (2003).

## QUESTIONS AND ANSWERS

**Alain Bernard, Serono, Switzerland:**

How reliable is the system that you used based on Caco-2 cells ?

**Wilfried Weber, ETH-Zurich, Switzerland:**

Caco-2 cells are widely used to determine the potential of compounds to diffuse through cell membranes.

**Alain Bernard, Serono, Switzerland:**

But Caco-2 will eliminate some compounds that later on could be found interesting. How do you address this point ?

**Wilfried Weber, ETH-Zurich, Switzerland:**

We tested the system in different cell types, and we also implemented it in *in vivo* cells, where you have also the effects of potential metabolites.

**David Hacker, EPFL, Lausanne:** What was the strain collection you were using ?

**Wilfried Weber, ETH Zürich, Switzerland:**

We have a very large collection of *Streptomyces* and *Actinomyces* strains.

VAN DE GOOR J., TSAI S.P., WONG A., MEHTA S., ZHENG L.,  
ELLIOTT L.O., STEPHAN J.P.

## NUCLEIC ACID CAPTURE ASSAY: A NOVEL HIGH- THROUGHPUT METHOD FOR DIRECT MRNA QUANTITATION

*Genentech, Inc., 1 DNA way, South San Francisco, CA94080, USA.*

**Abstract.** Generating industrial production cell lines with high productivity is a labor-intensive process with a limited throughput. As part of this process, hundreds of clones are screened using immunoassay and cell count data in multiple plates and dilutions, significantly decreasing the throughput of this traditional method. To overcome these limitations we developed a new solution phase hybridization technique, called Nucleic Acid Capture Assay (NACA) that allows the quantification of specific mRNA species directly from lysed cells. Target mRNAs are captured on a solid support and signaled through multiple sequence-specific synthetic oligos. Detection of the capture event is achieved using probes labeled with digoxigenin combined with alkaline phosphatase conjugated anti-digoxigenin antibody. In the current study, we show that mRNA correlates in most cell lines well with specific productivity and that the NACA assay can support high-throughput clone screening during drug development.

### 1. INTRODUCTION

During the process of drug development substantial resources and time are required to generate stable cell lines with high productivity. Chinese hamster ovary (CHO) cells are the predominantly used host in the biotechnology industry to produce therapeutic drugs. Mammalian expression vectors that use dihydrofolate reductase (DHFR) as a selectable and amplifiable marker (1-3) are often used to ensure high specific productivity. Indeed, an amplification process that leads to an increase in gene copy number of the transgene is often necessary to generate high producing stable cell lines.

Typically, expression plasmid carrying a transgene driven from a strong promoter is transfected into cells using one of many available transfection methods (4-6). Transfected cells are grown in a medium under an appropriate selection pressure until clones are formed. Hundreds of clones are picked and subjected to screens for specific productivity based traditionally on detection of the protein product of the transgene. ELISA is often the method of choice in many laboratories. The need to sample each clone multiple times in order to obtain an accurate measure of productivity combined with the necessity to prepare several different sample dilutions to fit into the linear range of the immunoassay dramatically decreases the throughput of this approach.



To overcome these limitations we have developed a new technology called Nucleic Acid Capture Assay (NACA), which allows high throughput direct quantitation of mRNA of the transgene directly from lysed cells (7). NACA involves several capture and signaling sequences (Figure 1). Target nucleic acid is hybridized to a set of capture polymers, that are specific for the target nucleic acid and also for the DNA extender oligonucleotides covalently bound to the capture wells. A second set of probes, named analyte-binding oligonucleotides, is used to signal the target molecule captured on the solid support. The different capture polymers and analyte-binding oligos hybridize to different regions on the target molecule. To reduce non-specific binding and stabilize the target nucleic acid, blockers are also designed. The NACA technology takes advantage of a simple and versatile signaling method. The immobilized target sequence is signaled through a stem oligonucleotide that hybridizes with the analyte-binding oligo present on the target molecule and allows hybridization of digoxigenin, fluorescein isothiocyanate or biotin labeled oligonucleotides. Alkaline phosphatase conjugated anti-digoxigenin, anti-fluorescein isothiocyanate antibodies or streptavidin/alkaline phosphatase conjugates, respectively, are subsequently used to signal the capture event. These signaling strategies allow a strong amplification of the signal without affecting the background of the assay and represent one of the particularities of the NACA compare to existing technologies.

We show that the concentration of transgene mRNA correlates well with specific productivity and that mRNA is indeed a good surrogate for cell productivity in cell lines. Unlike quantitative PCR, NACA does not require purification of total mRNA from each sample, thus, reducing the number of operational steps.

## 2. MATERIALS AND METHODS

### 2.1 Nucleic acid capture assay (NACA)

DNA oligomers (Figure 1) were synthesized with an amino-group at the 3' end for covalent coupling to 96-well DNA Immobilizer™ plates (Exiqon, Vedbaek, Denmark). Human Fc mRNA specific capture extenders and analyte-binding oligonucleotides were added to the transfected CHO cell lysates before mixing with capture hybridization buffer (6X SSC buffer (Sodium chloride/Sodium Citrate); 0.1% SDS; 50 mg/ml salmon sperm DNA) and loading onto the coated DNA Immobilizer™ plates. Hybridization occurred overnight at 53°C in the dark. The next day, the plates were cooled to room temperature and washed with wash buffer (0.1X SSC buffer; 0.1% SDS). The diluted stem oligonucleotide in label buffer (6X SSC; 10% BM block (Boehringer Mannheim)) was then added before incubating at 53°C for 30 minutes. After cooling to room temperature again, the plates were washed with wash buffer before the addition of the digoxigenin labeled oligonucleotide. After another 30 minutes of incubation at 53°C, the plates were cooled back down to room temperature. Then plates were washed with wash buffer and incubated at room temperature for 30 minutes in the presence of anti-

digoxigenin antibody conjugated to alkaline phosphatase. Finally, the plates were treated with alkaline phosphatase substrate (CDP-Star, InnoGenex) and incubated at 37°C for 15-30 minutes. The chemiluminescence was read using an MLX Microplate luminometer (Dynex). NACA data were expressed as relative luminescence units divided by the relative fluorescence (rFU) from the viable cells determined by the calcein AM assay (see below).

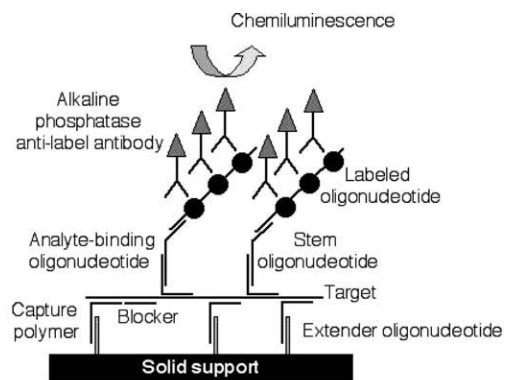


*Figure 1: In NACA target RNA hybridizes in solution to a set of specifically designed capture polymers and analyte-binding oligonucleotides. Blockers were also designed to reduce non-specific binding and stabilizes the target. Capture of target RNA on a solid support subsequently results from the binding of capture polymers to extender oligonucleotides covalently bound to the solid support.*

*The signaling of the captured RNA is accomplished through hybridization of stem and labeled oligonucleotides. Finally, alkaline phosphatase conjugated anti-label antibodies are introduced into the assay. Addition of chemiluminescent substrate results in luminescent signaling.*

## 2.2 Specific productivity assay

Confluent clones in a 96-well plate have reached confluency were trypsinized and split 1:2 into a new 96-well plate with 50  $\mu$ l of serum free medium. The second day after trypsinization, 100  $\mu$ l of a calcein AM/propidium iodide solution (see below) was added to each well. Plates were incubated for 20 minutes at 37°C. The fluorescence was read on a fluorescence plate reader (Millipore model 2350). After the fluorescence was determined, the supernatant in each well was collected by centrifugation and the titer of recombinant antibody was determined by an ELISA immunoassay (9, 10). Specific productivity was expressed as an antibody concentration (ng/ml) divided by the relative fluorescence (rFU) from viable cells obtained by the calcein AM assay.

Calcein AM/propidium iodide solution: 1 mg of calcein AM (Molecular Probes #C1430) was dissolved in 104  $\mu$ l of DMSO. Thirty three  $\mu$ l of the calcein AM

solution and 60  $\mu$ l of 1 mg/ml propidium iodide in ethanol were added to 10 ml of phosphate buffered saline.

### 3. RESULTS AND DISCUSSION

The dynamic range of the NACA assay (Figure 2) was evaluated using known concentrations of specific mRNA (recombinant human hemoglobin mRNA) ranging from pg/ml to ng/ml concentrations. Figure 2 shows that the relation between mRNA concentration and the relative luminescence obtained by NACA is linear over at least 3 orders of magnitude.

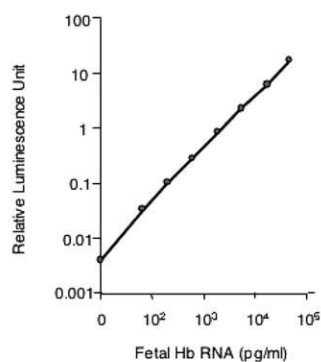


*Figure 2: Dynamic range of the NACA assay. The NACA was initially developed to measure the fetal hemoglobin mRNA (Fetal Hb). The Hb NACA generated a linear luminescent signal over at least 3 LOG dynamic range using recombinant human fetal Hb RNA.*

In order to validate the human Fc NACA technology, NACA data generated for fourteen different clones were compared to the data generated for the same clones using human IgG ELISA (Figure 3). A strong correlation ( $R= 0.95$ ) was observed between the Fc NACA and the IgG ELISA demonstrating that mRNA is a good surrogate for specific productivity and that NACA is an attractive tool that offers high-throughput for screening clones during drug development.

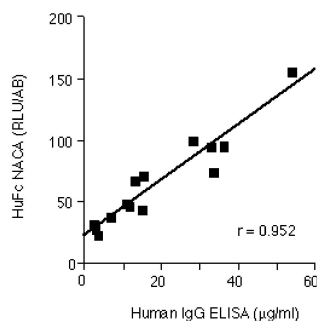


Figure 3: Fourteen different CHO clones producing a recombinant human monoclonal antibody were seeded in 96 well plates at a density between  $1 \times 10^3$  and  $80 \times 10^3$  cells/well. Conditioned media was collected to measure human IgG concentration using an intact IgG immunoassay and cells were subsequently lysed using the NACA lysis buffer. The NACA was performed as described in Material and Methods. Human Fc NACA data correlated well with the intact human IgG immunoassay data confirming the correlation between specific productivities and mRNA levels. This result also validates the NACA as a reliable strategy to screen CHO clones.

#### 4. REFERENCES

1. Urlaub G. and Chasin L.A. (1980) Isolation of Chinese hamster cell mutant deficient in dihydrofolate reductase Proc. Natl. Acad. Sci USA 77, 4216.
2. Levinson et al. (1990) Section V. Expression in mammalian cells. Methods in Enzymology (D.V.Goedell ed.) Academic Press 485.
3. Wood C.R., Dorner A.J., Morris G.E., Alderman E.M., Wilson D., O'Hara R.M. and Kaufman, R.J. (1990) High level synthesis of immunoglobulins in Chinese hamster ovary cells. J. Immunol. 143, 3011.
4. Graham F.L. and van der Eb A.J. (1973) A new technique for the assay of infectivity of human adenovirus 5 DNA. Virology 246, 148.
5. Xie T.D. and Tsong T.Y. (1993) Study of mechanisms of electric field-induced DNA transfection v. effects of DNA topology on surface binding, cell uptake, expression and integration into host chromosomes and DNA in the mammalian cell. Biophysical J. 65, 1684.
6. Felgner P.L. and Rinegold G.M. (1989) Cationic liposome mediated transfection. Nature 337, 387.
7. Tsai S. P., Wong A., Mai E., Chan P., Mausisa G., Vasser M., Jhurani P., Jakobsen M.H., Wong W. L. T., Stephan J. P. (2003) Nucleic acid capture assay, a new method for direct quantitation of nucleic acids. *Nucleic Acids Research* 31, e25.
8. Gilson U. E. M., Heid C. A., Williams P. M. (1996) A novel method for real time quantitative RT-PCR. *Genome research* 6, 995.
9. Kung W., Tran D., Hanson J., Yen R., Wong W.L., Bennett G.L. (2000) Automated robotic systems for ELISAs and protein radioiodinations. 32<sup>nd</sup> Annual Oak Ridge Conference, poster 8487392.
10. Tsai S. P., Wong A., Zheng L., Elliott L. O., van De Goor J., Stephan J. P. (2002) Development of direct quantitation methods for nucleic acid: Application to cellular clone selection. 42<sup>nd</sup> American Society for Cell Biology, poster 2302.

## QUESTIONS AND ANSWERS

**Chan Young Lee; Merck, US:**

Your linear correlation, within one single transgene, is indicating that the difference between a high producer and a low producer is based on the transcriptional level. But is there any other case indicating correlation with secretion or folding? A second question: this is a rapid screening method, but is there any other way to also induce the diversity during the transfection and bias the probability of identifying a high producer. Just because you mentioned that in the beginning there is not any control during the transfection. Have you identified the localization of your gene, and along your screening method, have you tried different transfection protocols to enhance your chance of identifying high producers ?

**Jana van de Goor, Genentech, US:**

Actually we have looked at some other transgenes that are not monoclonal antibodies, and the correlation of specific productivity across different transgenes was not there. It is definitely so that these methods are looking amongst one transgene where the transcription is directly related. There are of course other parameters that are desirable in cell culture to find high-producing clones, and this assay will not capture them all. But so far, we had really good experience using this assay for cell line screening, and the correlation is holding up for this particular transgene. This is using the traditional approach, without having a control on the integration events, and although every biologist would like to have more control on the system, we also know how much complex are the systems we are working with. Every bit of accuracy and control is really wanted, and we are also looking at various ways of how to use homologous recombination for targeting purposes, as many other labs are also investigating.

**Nicolas Mermod, University of Lausanne, Switzerland:**

Do you know how much of the total cell mRNA actually corresponds to the IgG transgenes ?

**Jana van de Goor, Genentech, US:**

We have never made that calculation, but I am sure some others have done, maybe somebody would like to comment on his cell line.

**Nicolas Mermod, University of Lausanne, Switzerland:**

Well, I know in our case this figure is about 16%, I was wondering about your case in order to make some comparison.

**Jana van de Goor, Genentech, US:**

What is the productivity of your cell line ?

**Nicolas Mermod, University of Lausanne, Switzerland:**

It is about 20 pg/cell-day.

**Nesredin Mussa, Lonza Biologics UK:**

A very interesting technology. Is the dynamic range of mRNA, in nanogram levels, very low for hyper-producing cell lines ? Have you done any correlation studies between reverse transcription PCR with this technology ?

**Jana van de Goor, Genentech, US:**

No, we have not done anything, we have done some comparisons to TAQ-Man assay, and the correlation is very good. Regarding the dynamic range, we do runs with three dilution ratios, and this is coming from a confluent 96 well plate, that is then passaged in a 1 to 10 ratio into the plates where you do your assay. So, there is a range of cell numbers that we normally harvest, but I do not know the exact numbers, because for a HTS you do not want to be counting cells in all your wells. We know from experience that taking the mentioned conditions will bring us to the dynamic range of the assay.

HOLGER HEINE, LAURENCE REY, CHRISTIAN Y. AROD,  
JEAN-PHILIPPE GAUDRY, BRUNO ANTONSSON,  
GEORG FEGER AND THIERRY BATTLE

## HIGH THROUGHPUT TRANSIENT TRANSFECTIONS OF HEK293EBNA CELLS - DEVELOPMENT OF AN INTEGRATED EXPRESSION PURIFICATION PROCESS AT 100 ML SCALE

*Serono Pharmaceutical Research Institute, Geneva, Switzerland*

**Abstract.** This work describes the set-up and optimisation of a simple, robust and cost effective process for the high throughput production of recombinant proteins using HEK293EBNA cells at 100 ml scale. Several transfection reagents were tested and evaluated for simplicity of transfection procedure, cost, reproducibility and expression yield. A purification process was set-up, which allows the fast purification of tagged proteins via a robotized system. The reproducibility and robustness of the whole process was monitored by inclusion of a well-expressed protein into the daily production batches. The statistical analysis of the purification yields of this control protein revealed that the process is operator independent and uncritical to cell density and nutrient conditions within the seed cultures. Over a period of more than a year more than 1,200 transfections were carried out yielding more than 630 different proteins in microgram quantities for screening purposes.

### 1. INTRODUCTION

The capability to express large numbers of unknown cDNAs in significant amounts becomes more and more important in the post-genome era.

To accommodate the flow of new genes discovered by genome mining and other techniques, a process had to be developed to achieve the following three main goals: Highest possible yield based on a maximum scale of 100 ml culture volume, low costs and simple experimental design, so that the process is robust and reproducible on a day to day basis.

Three different expression systems could be suitable for this approach, *E.coli*, insect or mammalian cells. Each of these systems has its specific advantages, which have to be considered as well as their disadvantages. Small-scale *E.coli* parallel expression systems are fast and commercially available, but the recombinant proteins lack glycosylation and are often not functional. Baculo-virus insect cell cultures produce glycosylated proteins but the lytic character of the system could be a disadvantage for a further scale-up. Mammalian cells produce functional proteins with correct glycosylation but the systems is slower and the expression yield could be lower than in the other systems.

Since the process should yield proteins to be used in cellular assays the recombinant proteins needed to be purified from the culture supernatant. To achieve

this goal the proteins were engineered to have a tag at the C-terminus, which allows for easy purification. The purification process was designed in a way that the proteins would be purified within 24 hours post-harvest to minimize the possibility of protein degradation.

## 2. MATERIALS AND METHODS

### 2.1 *Seed train*

Suspension-adapted HEK293EBNA cells (Invitrogen, USA) were grown in EXCELL V-PRO (JHR, UK) culture medium supplemented with 4mM L-Glutamine (Invitrogen, USA) and 1 ppm Phenol-red-solution (0.5% (w/v) solution in PBS) in spinner flasks (Techne, UK or DASGIP, Germany) in a humidified atmosphere containing 5% CO<sub>2</sub> at 37°C. The cells were counted on a daily basis and viability assessed using the Trypan blue exclusion method. A cell split was carried out if the glucose concentration in the culture medium is below 3g/l or the L-Lactate concentration was higher than 1.35g/l.

### 2.2 *Transfection*

Two T225-flasks per protein to be transfected were inoculated 16-20 hours prior to transfection at 2x10<sup>5</sup> cells/ml in FEME medium (DMEM/Ham's F-12 (1:1) (Invitrogen, USA) supplemented with 4mM L-Glutamine, 2 % FCS (JRH, UK) and 4ml/L ITS-X supplement (Invitrogen, USA). For the transfection 115µg plasmid cDNA, constituted of 113µg of the relevant plasmid and 2µg of reporter gene plasmid, was diluted in 4.7ml 150mM NaCl solution in tube 1. In another tube 230µl jetPEI transfection reagent (PolyPlus transfection, France) were diluted in 4.7ml 150 mM NaCl solution. Both tubes were well vortexed and then tube 2 added to tube 1. The mixture was vortexed and incubated for 30 minutes at room temperature. After the incubation the transfection mix was added to the two corresponding T225 flasks. The transfected cells were grown for 6 days in a humidified atmosphere in a CO<sub>2</sub> incubator.

### 2.3 *Harvest*

Immediately before harvest the cells were photographed using a fluorescence-microscope (Axioinvert, Zeiss, Germany). Positively transfected cells could be identified by their fluorescence due to the expression of the reporter gene. The supernatant of the two T225 transfected with the same cDNA were pooled and centrifuged at 1,900xg for 10 minutes at 4°C to remove debris.



#### 2.4 Purification

The centrifuged culture supernatant was diluted 1:1 with equilibration buffer and filtered through a 0.2µm filter. After this pre-treatment the supernatant was loaded onto a fully automated FPLC system (Vision Workstation, Applied Biosystems, USA). The recombinant protein was bound via the tag, eluted and desalted using a 10ml Sephadex G-25 column (Pharmacia, Sweden). The final elution volume was 2.2ml, which corresponds to a 48-fold concentration of the recombinant protein. The quality and purity of the proteins was assessed by SDS page (Coomassie stain) and Western-blot. If a band was seen on the Coomassie stained gel the protein concentration was determined using the BCA protein assay from Pierce.

### 3. RESULTS AND DISCUSSION

At the beginning of the definition of the process was the decision of the expression system. *E.coli* were not selected as expression host due to the lack of glycosylation of the recombinant protein and the fact that most proteins would be produced in inclusion bodies. This would imply challenging renaturation steps during protein purification, which is not possible for the automated standardized system we wanted to set-up.

HEK293EBNA cells were chosen as expression host due to their known high expression levels for secreted proteins and their ability to produce proteins with human glycosylation.

Starting with the target of 20 parallel transfections per day, which allowed the purification within 24 hours post-harvest, three production strategies were evaluated (table 1). For all strategies a production phase of 144 hours (6 days) was chosen to maximize the protein production. Due to the large quantity amount of cell splitting the flask-only variant was considered as not being feasible and the spinner only variant was rejected due to high investment costs for the equipment.

Production strategy			
	All flasks	All spinners	Mixed
Transfection	40 flasks per day (2 flasks per protein)	20 spinners	40 flasks per day (2 flasks per protein)
Seed train	40 flasks per day	2 spinner continuous	2 spinner continuous
Total per week	160+40 flasks	20+2 spinner	160 flasks 2 spinner

*Table 1 Possible production strategies for high throughput transfection*

To optimize the transfection several different reagents were tested. Each of them was optimized separately and the best conditions were compared head to head. For the final decision multiple aspects were taken into consideration. The ease of the protocol, the price, the amount of plasmid DNA needed, the reproducibility of the

transfection and the expression yield (table 2). The two best methods (Ca-Pi co-precipitation<sup>1</sup> and jetPEI) were tested head to head during the first period of the routine transfections with total 85 of proteins. Thereafter jetPEI was chosen due to the more convenient transfection protocol.

Reagent	DNA per 100ml	Price	Easiness	Robustness	Yield
Ca-Pi <sup>1</sup>	250µg	Very low	Fair	Good	Good
JetPEI	115µg	High	Good	Good	Good
Superfect <sup>2</sup>	200µg	Very high	Poor	Poor	Poor
Lipofectamine <sup>3</sup>	160µg	Very high	Good	Good	Poor
Effectene	80µg	High	Poor	Poor	Poor

Table 2 Comparison of transfection reagents

To be able to assess the success of the transfection a reporter gene was co-transfected with the genes of interest. This fluorescent protein allowed for monitoring of the evolution of the positively-transfected culture. Control pictures were taken 24 hours post transfection and directly before harvest (figure 1). Since the expression of the reporter gene was influenced by the expression of the gene of interest, a well-expressed control gene was transfected with every day's batch of unknown genes. This second internal control allowed additionally monitoring of the purification process.

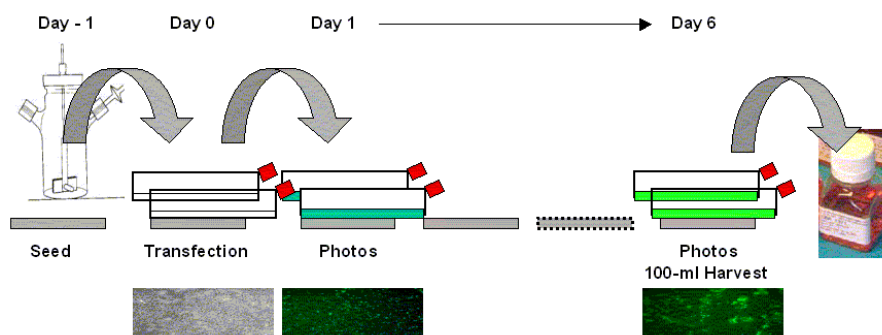


Figure 1: Final high throughput process

Even though all care was taken during the process, the recovery yield after purification of this protein varied in the range of  $185 \pm 66$  µg/100 ml culture volume ( $n=66$ ) (figure 2). To further investigate into this variation the operator independence of the process was assessed (figure 3). Other parameters as cell age of the seed train or cell-density before inoculation were analysed and found to have no significant influence on the process itself (figure 4). Even the residual nutrient and accumulated metabolite concentrations in the medium of the seed spinner were analysed and no significant influence on the transfection could be found (data not shown).

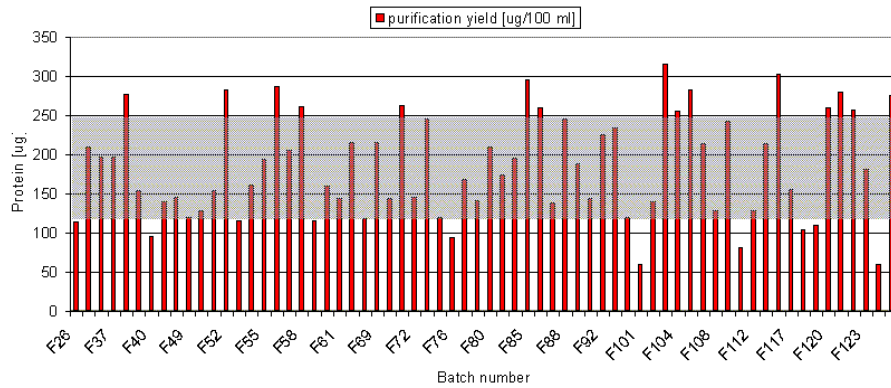


Figure 2: Purification yield of internal control protein. (Shaded is the mean value plus-minus standard deviation)

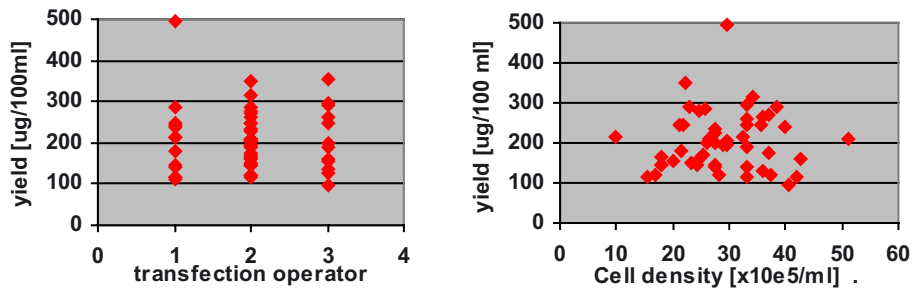


Figure 3 and 4: Operator independence and independence of seed spinner cell density of the final process

#### 4. CONCLUSION

We have set-up a robust and user-friendly universal expression process, which allows for the daily parallel transfection of 20 proteins using HEK293EBNA cells at 100 ml scale. The purification method was adapted to be able to process all samples within 24 hours post harvest. The inclusion of a well-expressed control protein in the daily batches allowed assessing its robustness. Using this process we performed more than 1200 transfections yielding more than 630 different proteins within 18 months.

## 5. ACKNOWLEDGEMENTS

The authors would like to thank the cloning group of SPRI for its support and plasmid supply and the BioProcessing group for plasmid storage, help with the transfections and pre-purification QC.

## 6. REFERENCES

- 1 Jordan M., Schallhorn A. and Wurm, F. M. (1996) Transfecting mammalian cells: optimization of critical parameters affecting calcium-phosphate precipitate formation *Nucl. Acids Res.* **24**, 4, 596
- 2 Shi C.-S. and Kehl J.H.(1997) Activation of stress-activated protein kinase /c-Jun N-terminal kinase, but not NF- $\kappa$ B, by the tumor necrosis factor (TNF) receptor1 through a TNF receptor associated factor 2- and germinal center kinase related-dependent pathway, *J. Biol. Chem.* **272**, 32, 102
- 3 Tolmachova T., Simpson K. and Huxley C. (1999) Analysis of a YAC with human telomeres and oriP from epstein-barr virus in yeast and 293 cells, *Nucl, Acids Res* **27**, 18, 3736

## QUESTIONS AND ANSWERS

**Chan Young Lee, Merck, US:**

Could you tell us whether your production medium contains serum ?

**Holger Heine, Serono, Switzerland:**

Yes, it contains 1% serum.

**Chan Young Lee, Merck, US:**

What is then the typical purification recovery yield ? Is that depending on the productivity as well ?

**Holger Heine, Serono, Switzerland:**

Yes, it depends on the productivity, and the average purification recovery was higher than 80 %.

L. BALDI, R. JACQUET, S. PICASSO, P. TROMBA, E. DEROW,  
P. GIRARD, D. HACKER, F. M. WURM

## TRANSIENT GENE EXPRESSION IN SUSPENSION HEK293 CELLS: APPLICATION TO LARGE-SCALE PROTEIN PRODUCTION

*Laboratory of Cellular Biotechnology (LBTC), Institute of Chemical and Biological Process  
Science (ISP), Faculty of Basic Sciences, Swiss Federal Institute of Technology (EPFL), CH-  
1015 Lausanne, Switzerland*

### 1. INTRODUCTION

Mammalian cell technology has allowed the market-scale production of recombinant proteins (r-proteins) of the highest complexity (i.e. antibodies) using stable cell lines (1). For the production of small to moderate quantities (1–500 mg) of research-grade r-proteins, transient gene expression (TGE) in animal cells is the method of choice. HEK293 cells have been used extensively for transient transgene expression due to their transfectability and their ability to grow to a high cell density (1, 2, 3). We have optimized a calcium phosphate (CaPi) based transient transfection method for HEK293 cells that has been scaled up to 100 L (4, 5). In this report we present the successful application of this method to the expression of various secreted r-proteins representing different degrees of complexity.

### 2. MATERIALS AND METHODS

HEK293-EBNA cells were adapted to serum-free suspension growth in Excell™-293 medium (JRH Biosciences) and transiently transfected in a DMEM/F12-based medium at a density of  $1 \times 10^6$  cells/ml in spinner flasks or bioreactors (Applicon) (6). Included in the DNA mix was pEGFP (Clontech) in order to allow direct visual estimation of the transfection efficiency. At 16 to 20 hrs post-transfection, one volume of Pro293 medium (Biowhittaker) was added. After 3-7 days the culture was centrifuged, and protein was purified from the supernatant or the cell pellet, as necessary. Human IgG1 antibodies and Fc-tagged proteins were purified on Streamline™ Protein A (Amersham Pharmacia Biotech) after overnight batch incubation with cell-free supernatants at 4°C.

### 3. RESULTS AND DISCUSSION

Some examples of r-protein expression by transient transfection with CaPi are presented in Table 1. Titers ranging between 1 and 20 mg/L were obtained, with the

highest titers for some antibodies reaching more than 25 mg/ml. However, some antibodies were expressed in the range of 1-3 mg/L in spite of high amino acid sequence conservation with antibodies that expressed at high levels. The reason for such significant differences in expression levels is under investigation, but may lay at the level of post-transcriptional modification. The highest transient expression of human IgG1 antibodies was achieved by co-transfecting vectors coding for heavy and light chain genes in an equimolar ratio (not shown). The inclusion of 1% EGFP-expressing plasmid in the DNA cocktail allowed us to easily judge transfection efficiency by microscopic observation of the cell culture as early as 16 hrs after transfection (Fig.1). The intensity of GFP expression directly correlated with the efficiency of the transfection procedure without interfering with product expression (7).

Table 1. Examples of secreted r-proteins yields per batch and total purified protein

<i>r-Protein</i>	<i>Expression time (d)</i>	<i>Max Expression level (mg/L)</i>	<i>Max batch volume (L)</i>	<i>Total purified (mg)</i>
<i>α-RhD</i> <sup>(a)</sup>	7	19.8	110	n/a
<i>agm-1</i> <sup>(b)</sup>	6	7	4.5	50
<i>α-HP</i> <sup>(a)</sup>	6	27.8	2	41
<i>Ltm-α15</i> <sup>(a)</sup>	6	23.9	2	30
<i>Ab62</i> <sup>(a)</sup>	7	22	1.5	25
<i>Ab69</i> <sup>(a)</sup>	7	19.4	1.5	8
<i>mIBPd</i> <sup>(c)</sup>	5	2.5	4	20
<i>mIBPFc</i> <sup>(b)</sup>	5	14.1	4	n/a
<i>MamFc</i> <sup>(b)</sup>	6	4.3	3	15
<i>Cals-1</i> <sup>(c)</sup>	5	20	1.5	46
<i>s407/408</i> <sup>(b)</sup>	7	7	4	20
<i>HRS-T</i> <sup>(b)</sup>	6	2.5	1	2.5

<sup>(a)</sup> Human IgG1 antibody; <sup>(b)</sup>Fc fusion; <sup>(c)</sup>His-tagged; n/a = not available

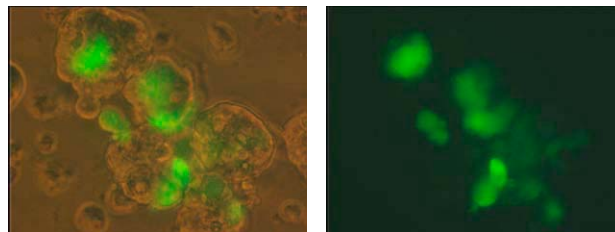


Figure 1. HEK293-EBNA cells at 16 hrs after transfection with 1% pEGFP-N1 DNA. Left: Visible and fluorescent light; Right: Fluorescent light only.

#### 4. OUTLOOK

The scalability of bioprocesses for the production of r-proteins is dependent on a balance between method efficiency and cost, with the ideal process being applicable to any protein and scalable to industrial facilities. The method applied in this work meets some of these criteria, and we have attempted to demonstrate its versatility by presenting some examples of different proteins that we have been able to express. We have successfully expressed not only secreted proteins but also intracellular and membrane proteins (data not shown). Transient expression of some intracellular (hormones) and membrane proteins (G protein-coupled receptors) revealed, in some cases, a certain degree of cytotoxicity, but we were still able to detect r-protein expression (unpublished data). Current research is aimed at the identification of the critical parameters for increasing r-protein yield. The general cost-effectiveness and versatility of our method make it a valuable tool for providing research material for several applications including functional genomic/proteomic studies, protein structure analysis, and high-throughput screening of complex r-proteins. However, further work is needed to make the system more reproducible and productive.

#### 5. ACKNOWLEDGMENTS

We thank S. Miescher, K. Leuthauser, L. Goffin, C. Renner, and L. Anders for providing some of the vectors used in this work and for discussions; M. Jordan for comments and discussion; H. Phan Thanh and H. ElAbridri for technical help; and S. Fabris for secretarial assistance.

#### 6. REFERENCES

1. Wurm, F., and Bernard, A. (1999). *Curr. Opin. Biotechnol.* 10:156-159.
2. Geisse, S., and Kocher, H. P. (1999). *Methods Enzymol.* 306:19-42.
3. Durocher, Y., Perret, S., and Kamen, A. (2002). *Nucleic Acids Res.* 30: 9.
4. Jordan, M., Schallhorn, A., and Wurm, F. M. (1996). *Nucleic Acids Res.* 24:596-601.
5. Girard, P., Jordan, M., Tsao, M., and Wurm, F. M. (2001). *Eng. J.* 7:117-119.
6. Meissner, P., Pick, H., Kulangara, A., Chatellard, P., Friedrich, K., and Wurm, F. M. (2001). *Biotechnol. Bioeng.* 75:197-203.
7. Pick, H. M., Meissner, P., Preuss, A. K., Tromba, P., Vogel, H., and Wurm, F. M. (2002). *Biotechnol. Bioeng.* 79:595-601.

K. FRITCHMAN<sup>1</sup>, C. TILSAGHANI<sup>2</sup> T. SUMNALL<sup>1</sup>

## MONOCLONAL ANTIBODY PRODUCTION: DETERMINATION OF APPROPRIATE SYSTEM AND MEDIUM FOR PRODUCTION ENHANCEMENT AND DECREASE OF OVERALL PRODUCTION TIME

<sup>1</sup>*BD Diagnostic System*, <sup>2</sup>*BD Biosciences, PharmingenT*

### 1. INTRODUCTION

In the production of an antibody or similar protein there is a vast selection of methods and materials to choose from for first the development of the target product and then scale up and manufacture of the product. While the final goal is more yield for less cost many factors need to be considered and weighed in the choice of the culture system and appropriate medium. In selecting the production system it is necessary to take into account current facilities and staff versus the cost of bringing in new systems and staff to support them. In selecting a medium, it is important to be aware of requirements farther down in the process.

### 2. MATERIALS

IMDM Medium, BD Cell<sup>TM</sup> MAb Medium Quantum Yield, Serum Free, (SF) and Animal Component Free, (AF), Hyclone low IgG Fetal Bovine Serum (FBS), Falcon<sup>TM</sup> Roller Bottles, SiCulture<sup>TM</sup> Gas Permeable Bags, Accusyst R Bioreactors and cartridges, BD CELLLine<sup>TM</sup> Flask.

### 3. METHODS

A comparison was performed in roller bottles, CELLLine flasks, and hollow fiber bioreactors to ascertain which system would result in the highest yield while at the same time increase capacity and decrease overall costs. In table 1 a rat cell line, XMG1, was used to demonstrate differences between the use of a traditional medium, IMDM, and a specialty hybridoma medium, BD CELL<sup>TM</sup> MAb, Quantum Yield. The table shows the differing amounts of medium, labor requirements, and time commitments required in the production of 1 gram of antibody. While at first appearance the roller bottle appears to be the most economical, other factors such as capacity, ROI of capital expenditures, etc. may carry a heavier weight in cost over



time. Figure number one shows the overall yield (ug/ml) achieved in the culture systems.

A comparison was done with multiple cell lines in gas permeable bags, roller bottles, and CELLline flasks to determine whether comparable yield could be obtained using a serum free formulation or an animal free hydrolysate supplemented formulation as compared to BD Cell Quantum Yield with 10% fetal bovine serum. An SDS Gel, figure 2, demonstrates the overall starting purity for the three media. As the AF media does not contain any complete proteins no bands are present in the lane on the SDS gel.

Figure number 4 shows the cell density obtained over time with the 3 systems. Figure number 5 demonstrates that comparable or even better yields can be obtained with the serum free media and animal free media. An SDS page gel was run on the unpurified supernatant, figure 6.

A cost analysis chart, table 2, was designed to demonstrate overall cost of various systems in traditional media versus specialty media from initial growth of the cell culture thru clarification and concentration of the antibody containing supernatant. This is a dynamic table designed so that fields in the bottom of the table can be modified for changes in cost, labor, culture system, etc. Thus, this table can provide a continuing cost monitor for changes in production methods. Production goal was 1 gram of antibody.

Table 1. RAT 1 Cost Analysis IMDM vs BD Cell Lot Size = 1 Gram

Medium	System	Yield	Media/FBS	Labor	Run Time	Cost/Mg*
IMDM	Roller Bottle	20 ug/ml	\$3,500	\$324	6 weeks	\$3.82
BD Cell	Roller Bottle	239 ug/ml	\$377	\$126	4 weeks	\$0.52
IMDM	Bioreactor	409 ug/ml	\$4,490	\$405	5 weeks	\$4.89
BD Cell	Bioreactor	452 ug/ml	\$1,890	\$180	5 weeks	\$2.09
BD Cell	CELLline Flask	2860 ug/ml	\$410	\$144	6 weeks	\$0.55
<b>Cost Calculations</b>						
BD Cell Medium		\$32 Per Liter		Hyclone low IgG FBS		\$580 Per Liter
IMDM Medium		\$12.00 Per Liter		Labor Costs		\$18.00 Per Hour

Table 2. Cost Comparison:Roller Bottle vs Gas Permeable Bag vs CELLline FLASK

Description	Unit	Roller Bottle		Gas Permeable Bag		CELLline Flask	
		IMDM	BD Cell	IMDM	BD Cell	IMDM	BD Cell
MAb Production	mgs	1000	1000	1000	1020	1094	1000
Harvest Volume	mls	25000	2500	10000	1200	1920	200
MAb Concentration	ug/ml	40	400	100	850	570	5000
Media Consumption	ltrs	25.00	2.50	10.00	1.20	96.00	4.00
Serum Consumption	ltrs	2.50	0.25	1.00	0.12	0.29	0.03
CELLline Flasks Used	ea					4	2
Roller Bottles Used	ea	20	5				
Production Run Time	wks	6	4	4	4	10	7
Gas Permeable Bags Used	ea			10	2		
Labor/Cell Culture	\$	\$162.00	\$18.00	\$36.00	\$18.00	\$432.00	\$90.00
Labor/C/C	\$	\$72.00	\$18.00	\$36.00	\$18.00	\$72.00	\$22.50
Media Cost	\$	\$300.00	\$86.63	\$120.00	\$41.58	\$1,152.00	\$138.60
Serum Cost	\$	\$1,450.00	\$145.00	\$580.00	\$69.60	\$167.04	\$17.40
Culture Vessel Cost	\$	\$160.00	\$40.00	\$600.00	\$120.00	\$580.00	\$290.00
Total Cost	\$	\$2,144.00	\$307.63	\$1,372.00	\$267.18	\$2,403.04	\$558.50
Cost/mg MAb	mg	\$2.14	\$0.31	\$1.37	\$0.26	\$2.20	\$0.56

4. CONCLUSIONS

Multiple systems, methods, and media are available for the successful production of a secreted product such as a monoclonal antibody or recombinant protein. The selection of the method, system, and medium will need to be done carefully after determining the parameters of the current needs while keeping in mind the future needs of the product. To avoid differences in the protein itself, similar systems should be selected for both the initial pilot work and scaled up production. Does not include costs for overhead, systems, downstream processing, etc

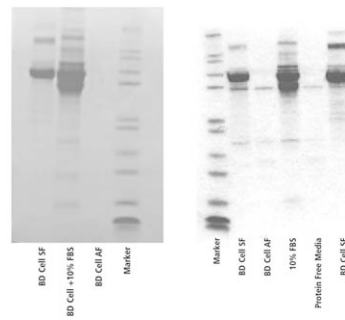
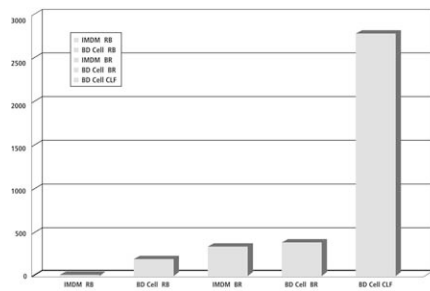


Figure 1. XMG1 Antibody Yield (ug/ml)

Figure 2. SDS Gel Media

Figure 6. SDS Page

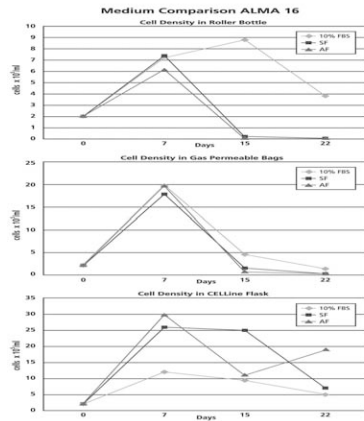


Figure 4.

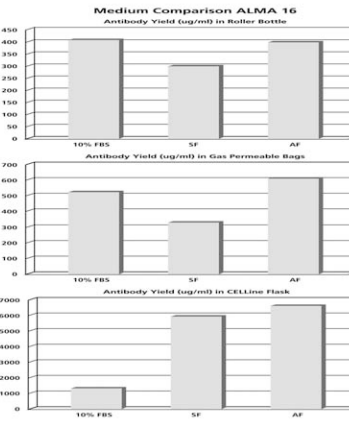


Figure 5.

S. GEISSE, N. DI MAIUTA\*, B. TEN BUREN AND M. HENKE

## THE SECRETS OF TRANSFECTION IN SERUM-FREE SUSPENSION CULTURE

*Novartis Pharma Research, CTA/Biomolecules Production,  
CH-4002 Basel/Switzerland*

*\* present address: HSW Wädenswil, CH-8820 Wädenswil*

### INTRODUCTION

Expression of recombinant proteins using mammalian expression systems is still considered to be costly, tedious and labour-intensive, and thus disadvantageous to high throughput applications. However, a breakthrough in the rapid generation of recombinant proteins in mammalian cells was recently achieved by applying large-scale transient transfection protocols. In particular the HEK.EBNA expression system has significantly contributed to this success. To date, two approaches to transient transfection of HEK.EBNA cells on large scale have been described in detail: CaPO<sub>4</sub>-mediated transfection [1] and Polyethylenimine (PEI) mediated transfection [2]. The data presented here evaluate both transfection methods in conjunction with cultivation of cells in serum-free suspension culture using commercially available as well as in-house developed cell culture media.

### MATERIALS AND METHODS

HEK.EBNA cells (Invitrogen) were grown in adherent mode in DMEM (Gibco/Life Technologies) with 10% fetal calf serum at 37°C/5% CO<sub>2</sub>. For suspension cultivation in roller bottles the cells were adapted to the following media: 293 SFM II, CD 293, FreeStyle 293 (all Invitrogen), Pro 293s CDM (BioWhittaker), Hektor S (Cell Culture Technologies), EX-CELL VPRO (JRH Biosciences) as well as to our in-house developed media formulations M11, M11V3, 2055 and its calcium-free counterpart 2055cf.

The expression plasmid used for transfection carries the cDNA coding for the cytokine IL-13 followed by an IRES element and the eGFP gene. Recombinant IL-13 production determined by affinity HPLC and green fluorescence of the cultured cells, indicative of transfection efficiency, served as read-out parameters.

CaPO<sub>4</sub>-mediated transfection was performed according to the protocol published by Meissner et al. [1]. Transfection using PEI as reagent was pursued as described by Durocher et al. [2]. All experiments were carried out on small-scale in multi-well-plates as well as in small and normal sized roller bottles; for PEI-mediated

transfection the scale-up to 10 l Wave Bioreactor™ (Wave Biotech AG, Tagelswangen, CH) volume was also assessed.

## RESULTS AND DISCUSSION

Upon step-wise adaptation of the HEK.EBNA cell line to the panel of different culture media listed above, the growth performance of the cells cultivated in roller bottles was analyzed as shown in Figure 1.

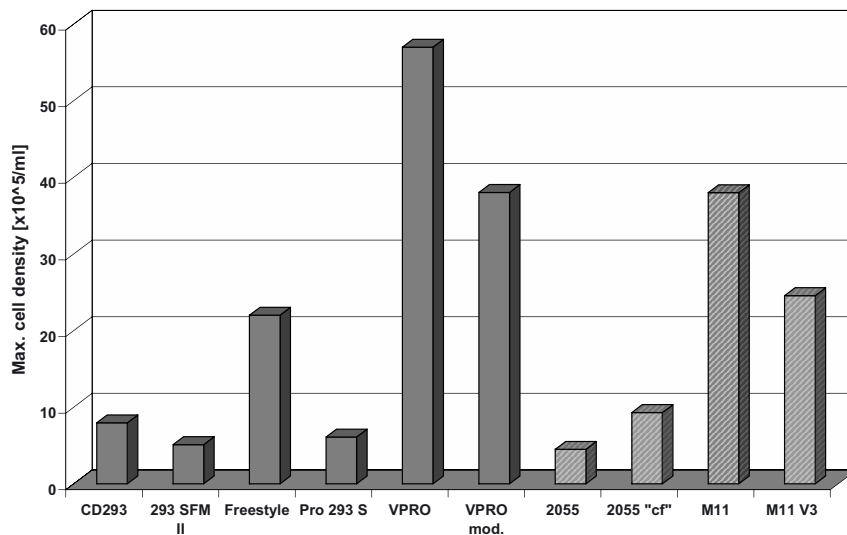


Figure 1: Maximal cell densities achieved for HEK.EBNA cells cultivated in different serum-free media. Following media adaptation the cells were seeded in roller bottles at a density of  $3 \times 10^5$  cells/ml. Cell densities and viabilities were monitored in 24 hour intervals using a Cedex cell counting device (Innovatis, Bielefeld/FRG). Medium VPRO mod. was prepared on special request and does not contain dextran sulfate. Solid bars: commercially available media; hatched bars: media developed in Novartis.

Only in five of the media tested the cells showed good growth performance: FreeStyle™, EX-CELL VPRO™ and EX-CELL VPRO mod. as well as M11/M11V3 media supported growth of the cells to densities higher than  $2 \times 10^6$  cells/ml. All other media gave unsatisfactory results. As we were unsuccessful in adapting HEK.EBNA cells to logarithmic growth in HEKTOR™ medium, no data are reported.

$\text{CaPO}_4$ - mediated transfection of HEK.EBNA cells, as described by Meissner et al. was successful only, if the cells were transferred into DMEM/F12 medium prior to transfection. Several serum-free media were suitable for pre-cultivation of the cells, but presumably because of their low calcium content the change of medium was absolutely mandatory for transfection. Additionally we observed a rapid decline in viability of the cultures during the production phase post transfection. Despite

being fully reproducible, these two observations strongly limit the usefulness of the CaPO<sub>4</sub>- mediated gene transfer approach.

In contrast, PEI-mediated transfection according to the protocol of Durocher et al. was simple to perform and worked in some of the commercially available media (CD 293, FreeStyle) as well as in-house developed formulations (2055, M11, M11V3). Cells cultivated in media Pro 293 S, 293 SFM II, EX-CELL VPRO or HEKTOR S could not successfully be transfected. The in-house developed medium M11V3 outperformed the original M11 medium with respect to transfection efficiency and recombinant protein expression.

A summary of all media tested with respect to growth performance, transfectability and cost-effectiveness is given in Table 1.

Medium	Price [CHF/L]	Growth characteristics HEK.EBNA cells	Transfectability HEK.EBNA cells	
			Calciumphosphate	PEI
CD 293	140	✓	✓	✓
PRO 293 S	85	✓	✓	✗
293 SFM II	140	✓	✓	✗
FreeStyle	134	✓✓	n.d.	✓
Hektor S	23	✗	✗	✗
EX-CELL VPRO	30	✓✓✓	n.d.	✗
2055	44	✓	✗	✓
M11	24	✓✓✓	✓	✓
M11V3	50	✓✓	n.d.	✓✓✓
DMEM/F12	45	✓	✓✓✓	n.d.

Table 1: Comparison of growth performance and transfectability of HEK.EBNA cells cultivated in commercially available as well as in-house developed serum-free culture media.

Symbols: ✓ = possible, ✓✓ = results acceptable, ✓✓✓ = very good results; ✗ = not possible; n.d. = not done.

## SUMMARY

In conclusion, we report on a thorough evaluation of commercially available cell culture media developed for HEK 293 cell lines in comparison to our in-house developed media formulations with respect to growth performance and utility in transfection. Apparently these two parameters are not linked: media supporting good growth of cultures do not automatically render the cells transfectable and vice-versa. Which media components are responsible for promoting or inhibiting cell growth and transfection remains speculative for the commercially available media; such investigations for our own media formulations are currently ongoing.

## REFERENCES:

1. Meissner, P, Pick, H, Kulangara A, Chatellard P, Friedrich K, Wurm FM. (2001) *Biotechnol. Bioeng.* 75:197-203.
2. Durocher Y, Perret S, Kamen A. (2002) *Nucleic Acids Res.* 30:2e9

A. GOEDDE, S. BAARS, K. CZERNY, E. SCHULTZ,  
N. GERNOLD, T. SCHEUERMANN,  
R. SCHATTEN, S. HENZE, M. SCHICK, L. EBERT,  
C. LANGLAIS, B. KORN

## FROM GENES TO PROTEINS: FULL OPEN READING FRAME (ORF) CLONES AND THEIR APPLICATION IN FUNCTIONAL RESEARCH

*RZPD – Ressourcenzentrum für Genomforschung, INF 580,  
69120 Heidelberg, Germany*

### 1. INTRODUCTION

As the human genome has been fully sequenced, our attention turns to proteomics, the large-scale identification and characterization of proteins. The better understanding of the functional roles of all proteins will be one of the most challenging steps. There are two possible sources to study the protein products of the genome and their interactions and functions:

1. Cells that natively express the protein of interest and
2. recombinant proteins that can be produced in homologous and heterologous expression systems.

### 2. FULL ORF CDNA CLONING

The sequencing of the human genome resulted in the identification of a large number of novel proteins whose function and interaction with other proteins are not yet well characterized. RZPD has started to establish a collection of full open reading frame (ORF) cDNA clones. With use of bioinformatic tools in total 5.200 human genes that lack annotated function, or poorly predicted function are identified.

To allow rapid and reliable subcloning of such a large number of ORFs we use a cloning system that supports subcloning without restriction and ligation (GATEWAY<sup>TM</sup>, Invitrogen<sup>TM</sup>). It is base-specific and relies on homologous recombination. It allows protein expression in a wide range of hosts as well as *in vitro* and *in vivo* functional studies at different scales. Up to now 3.120 full length ORFs have been cloned in this recombination vector system. 2.112 of these full length ORF clones have been completely sequence verified and annotated to characterize differences to the already published sequence data in respect to bp and

aa exchanges and alternative splice forms. Only clones showing stop codon mutations and frame shifts were discarded. Overall more than 90% of the ORF sequences passed our rigorous quality control.

#### *From Genes to Proteins*

As the initial cloning was done in a recombination shuttle vector system, in a second step ORFs are moved into destination vectors to produce expression clones (Baculovirus Expression Vector System (BEVS), *E.coli*, Yeast Two-Hybrid system). This ORF transfer reaction can easily be performed in high-throughput (96 well scale) using two or more vectors in one reaction. Using this technology there is good access to the respective proteins via Baculovirus Expression Vector and *E.coli* systems in consideration of speed, cost and their ability of post translational modifications.

### 3. EXPRESSION STUDIES

In addition, full length ORFs are used in an automated yeast two-hybrid screening (in cooperation at the Max Delbrück Center; Berlin; H. Göhler and E. Wanker, data not shown). Resulting protein-protein interactions from this system will be verified and characterized via *in vitro* methods. For this purpose different protein expression systems are established at the RZPD:

- Baculovirus Expression Vector system (BEVS)
- *in vivo* and *in vitro* *E.coli* expression system (*in vitro* system data not shown).

For analytical analysis specific antibodies for a large number of protein products of the full length ORFs are not yet available. Therefore different expression vectors are established that allow the fusion of the ORF of interest to an additional affinity fusion tag. Routinely GST and 6xHis tags are used in our expression systems. For special purpose other affinity tags are available. The fusion tags are very helpful in the protein purification step as well as in protein identification and the setting up of *in vitro* or *in vivo* protein-protein interaction assays.

In this study the results of the comparative expression of a set of nuclear receptors are presented. In the BEVS we used *Spodoptera frugiperda* (Sf9) cells, *Autographa californica* nuclear polyhedrosis virus (AcMNPV) and the destination vector pAcGHLT (BD, Pharmingen) in which the multiple cloning site (MCS) was exchanged by the corresponding GATEWAY™ MCS. For the *E.coli* system we used One Shot® BL21 Star™(DE3) and One Shot® BL21(DE3)pLysS (Invitrogen™) cell lines. As destination vectors for GST fusion proteins we used the Gateway compatible pGEX vector and for 6xHis fusion constructs the pDEST17 vector (Invitrogen™). To use both vectors in the shuttling step in one reaction the resistance gene in pDEST17 was changed to the tetracyclin resistance gene.

The comparison of protein expression and protein solubility of this set of proteins in BEVS and *E.coli* show significant differences in the access to certain proteins (Fig. 1). The examined proteins in most cases show good to low expression



levels in the *E.coli* expression system but mostly the produced proteins show accumulation of improper processed protein and aggregates (7 ORFs of 12).

In contrast most of the BEVS expressed nuclear receptors were properly processed and could easily be purified in milligram scale via one step affinity chromatography (13 ORFs of 15).

ORFNo	BEVS	<i>E.coli</i>	
		Expression	Solubility
574	+	+*	++*
645	+	++*	(-)*
646	++	(+)*	-*
653	+	++*	++*
655	-	(+)*	-*
667	++	-*	-*
669	++	+*	+*
2722	++	+	+
2725	++	+	-
2727	++	+	-
2728	++	+	-
2729	+	-	-
2731	+	+	+
2738	+	-	-
2739	-	+	-

\* Tag = 6His

Table. 1.

Comparison of expression and solubility of selected proteins in BEVS and *E.coli*. Verification of BEVS expressed proteins were quantified after one step affinity purification (GST tag) via coomassie stained SDS-PAGE gels. *E.coli* expression (GST and 6xHis tag) was performed by SDS-PAGE followed by coomassie staining. Western Blot analysis was performed without any purification step.

#### 4. OUTLOOK

The bacterial systems provide important advantages, like the ease of use, low cost and high expression level. In contrast they impose a number of limitations for synthesis of eucaryotic proteins like in our case improper processing and protein aggregation. In high-throughput studies for a large number of proteins this expression system will still be the method of choice. Insect cell based expression seems less advantageous in comparison to the bacterial system in handling and costs. For efficient expression of recombinant complex mammalian proteins in biologically active form the Baculovirus Expression Vector system remains to be the suitable technology.

Therefore a combination of both protein expression systems allow us to gain access to the respective proteins in question for *in vitro* interaction experiments. In cooperation with other groups, the produced proteins will also be used for the production of specific antibodies.

All data of our ORF cloning and the functional studies will be stored in the Primary Database at RZPD ([www.rzpd.de](http://www.rzpd.de)).

M. JORDAN, M. J. DE JESUS, C. EIGENMANN, T. GLEICH AND  
F. M. WURM

## A VERSATILE DISPOSABLE CULTURE SYSTEM FOR HIGH THROUGHPUT SCREENING OF PROCESS PARAMETERS AND PRODUCTION CELL LINES

*Swiss Federal Institute of Technology Lausanne, Faculty of Basic Sciences,  
Institute of Biological and Chemical Process Sciences, Switzerland*

### 1. INTRODUCTION

There is no doubt that fully equipped and controlled bioreactors are the only valid system for industrial production of large amounts of proteins with classical cell culture technology. However, valuable information for bioprocesses can be obtained much faster and easier using alternative cultivation systems. For attached cells, different disposable culture plates or flasks satisfy most of these needs. Since fewer choices are available for suspension cultures, we wanted to develop a reliable and versatile system that fits routine applications in our laboratory. To support high cell densities, the system needs to provide good mixing of the medium and efficient exchange rates for oxygen and carbon dioxide.

We used 50 ml centrifugation tubes with ventilation caps (Techno Plastic Products, Trasadingen, Switzerland) having five holes with different diameters above a gas permeable sterile filter (Fig. 1, right panels). The holes can be closed easily by covering them with adhesive tape to regulate gas exchange rates between the inside and the outside of the tube. Here we present the first results demonstrating the flexibility of these tubes for growing suspension cells to high densities.

### 2. RESULTS

The 50 ml centrifugation tube with a ventilation cap is an open system with tuneable permeability for gases such as O<sub>2</sub> and CO<sub>2</sub>. The permeability or mass transfer coefficient of the filter caps is not only relevant for O<sub>2</sub> and CO<sub>2</sub> exchange but also defines the evaporation rate, an important parameter for small culture volumes since the humidity within the tube is approximately 100%, while outside the tube it is typically 30% - 85%. Measuring the evaporation rate is straightforward and yields valid information about the mass transfer coefficient of the caps. Tubes containing 10 ml of DMEM/F12 medium were shaken at 37°C for 5 days (200 rpm with a shaking diameter of 5 cm, humidity about 35%). One or more holes of each cap was left open during the course of the experiment. For each tube the loss of medium due to evaporation is plotted in Fig. 1.

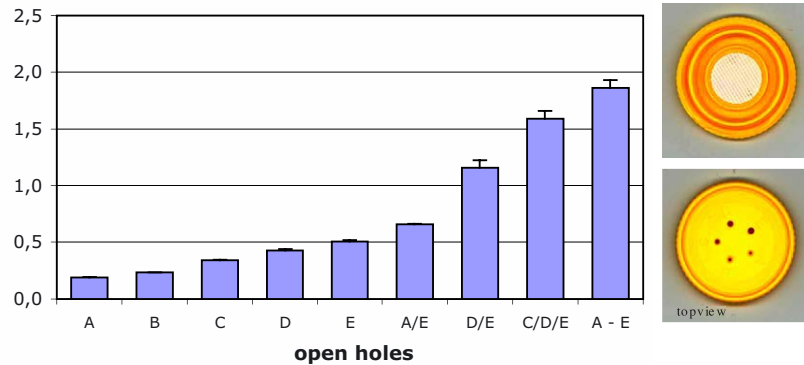


**Figure 1:** Permeability of the filter caps. Left: evaporation during 5 days at 200 rpm in a 37° room without control of humidity. The five holes were opened individually or in various combinations ( $n=2$ , except for B where  $n=8$ ). Right: Interior of cap with gas permeable sterile filter (top) and exterior of cap with five holes of different diameter (bottom).

Evaporation from the tubes correlated with the diameter of the open hole and was additive if several holes were left open. When all the holes were closed there was no evaporation (data not shown). The results demonstrated that the evaporation can be precisely modulated over a wide range. The maximum loss of water (2 ml per 5 days) exceeds the actual needs for animal cell cultures. This is twice the amount we have seen for a 1L Bellco spinner with a 300 ml culture volume and one cap opened.

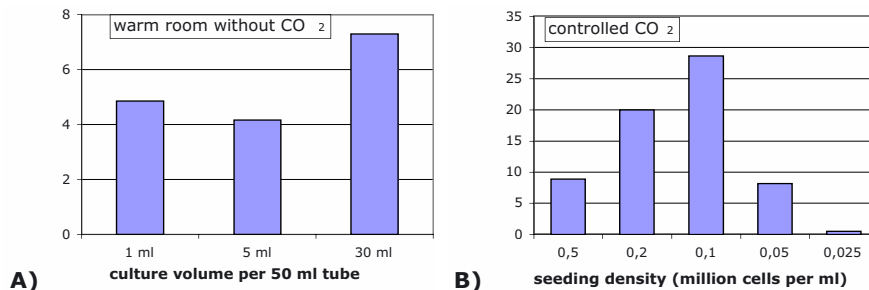


**Figure 2:** Growth of CHO DG 44 shaken at 180 rpm in serum free medium. **A)** Tested culture volumes: 1 ml (tubes were preincubated for 1 hour at 5%  $CO_2$  and then closed), 5 ml (hole A open) and 30 ml (hole E open). **B)** 5 ml cell suspension of 25'000 to 500'000 cells per ml were incubated for 5 days in a  $CO_2$  incubator (hole E open).

Based on these results and previous studies addressing the impact of carbon dioxide exchange on the medium pH, a variety of growth conditions in the ventilated centrifuge tubes were tested using CHO DG44 cells. In one experiment the culture volume ranged from 1 ml to 30 ml and the initial cell density was 500,000 cells/ml. The cultures were incubated for 2.5 without feeding, pH adjustments, or changes in filter permeability. Cells grew in volumes of 1 – 30 ml under normal atmosphere (Fig. 2A). In a second experiment the culture volume was maintained at 5 ml and the

initial seeding density was varied from 25,000 to 500,000 cells/ml. The cultures were maintained for 5 days in a shaker with CO<sub>2</sub> control. In all cases hole E of the cap was left open. Only at an initial density of 25'000 cells/ml did the cells fail to grow, while for the other cases an increase in biomass up to 30-fold was obtained (Fig. 2B). Cell viabilities were over 90% even for the highest seeding density (data not shown). For this culture the maximum cell density was expected much earlier than day 5. Surprisingly, no aggregate formation or cell settling was observed in this culture.

The effect of CO<sub>2</sub> control on cell growth in 50 ml tubes was investigated with HEK293 cells starting at 350,000 cells/ml in a volume of 5 ml. Under a controlled CO<sub>2</sub> atmosphere (5%), different permeabilities of the caps worked well (Fig. 3). If CO<sub>2</sub> was not present in the atmosphere, the permeability of the caps was crucial for cell growth; increasing the permeability had negative effects (Fig. 3). The tubes that were opened at day 0 did not support cell growth due to the basic pH of the bicarbonate buffered medium. Surprisingly, there were no pH differences at day 4 for all the other cases.

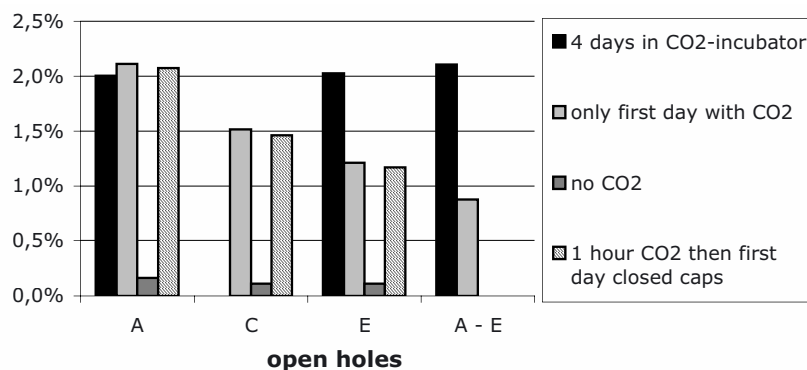


**Figure 3:** The effect of the permeability of the filter caps on the growth of HEK 293 cells under serum free conditions (a packed cell volume of 2% corresponds to a density of 4.5 million cells/ml).

### 3. CONCLUSION

The first results from cell growth experiments in the ventilated centrifuge tubes are promising. The geometrically defined caps avoid physical differences between individual tubes. The need for only a few ml of culture to launch experiments that can run for up to two weeks under a CO<sub>2</sub> and humidity controlled atmosphere make these tubes a unique system for growth of suspension cells. Due to their ease of handling, these tubes represent a valuable tool for high throughput experiments for screening and for process optimization. The system is also suitable for the routine passaging of cells. With tuneable filter caps the system can be adapted to a large variety of culture conditions ranging from 1 ml to 30 ml and from 0.1 – 6 million cells per ml.

ALEXANDER LOA; CLAUDIA GELLI, BERND LAFFERT

## LONG TIME STORAGE OF PRE-INOCULATED MULTI-WELL PLATES FOR CELL-BASED ASSAY KITS USED FOR DRUG IDENTIFICATION AND CHARACTERISATION

*CCS Cell Culture Service GmbH, Falkenried 88, 20251 Hamburg, Germany*

### INTRODUCTION

Cell-based assays are widely used to analyse diverse cell biological mechanisms. However, cells in general are sensible systems and, therefore, it is not surprising that different culture conditions will influence their performance in any assay. Even cells of same origin can behave differently if treated not identically. Hence, the multiplicity of laboratories and culturing techniques has created many cell lines with the same name but different biological properties. In a given laboratory alterations in cells can occur even under constant culture conditions (e.g. MRC-5).

To obtain reproducible results it is important to use the cells of same origin with comparable culture histories and nearly identical doubling numbers. This can be achieved by preparation of sufficiently large stocks of cryopreserved cells providing the user with cells of the same quality over a long period of time. However, prior to their use in an assay cells have to be scaled up, and this procedure is time-consuming. On the other hand, freezing of cells in the assay plates often causes problems due to the toxicity of cryoprotectants.

To achieve our aim, namely the production of ready-to-use assay plates, we had to establish a cryopreservation procedure that circumvents these problems and allows the storage of cells in 96-well plates for several months. Commonly cryoprotectants with toxic side effects such as DMSO are used to protect cells from damage induced by the freezing procedure. Only a few publications describe cryopreservation procedures without DMSO, and in most cases mixtures of sugars like sucrose, raffinose or trehalose are used to replace DMSO [1, 2, 3, 4]. However, while these sugars exhibit their cryoprotective effects best when located intracellularly, they do not penetrate the cell membrane except for sucrose. Thus, their use requires elaborate efforts including poration of the cell [4] to achieve results comparable to DMSO containing cryo-media.

The examination of thermodynamic and mechanical effects during the freezing process of the cells [5, 7] reveals a variety of starting points to solve the problem.

Investigations of the osmotic behaviour [6] clearly demonstrate the importance of this parameter in cryoprotective solutions.

In transplantation medicine solutions for organ protection were used which are adapted to hypothermia. To avoid intracellular increase in sodium-ions at lower temperature these media have an altered sodium/potassium ration. Hypo-Thermosol (HTS) [8] and University of Wisconsin Solution (UW) [9] were tested as basis for cryoprotective media.

### EXPERIMENTAL

Based on all theoretical and practical experiences in cryobiology a new cryoprotective medium without any toxic compounds was designed. Therefore, all compounds of an ordinary medium were carefully balanced and adapted to the needs of the cells in hypothermia. The osmotic pressure of the medium was optimised for the requirements during the freezing procedure. Scavengers have no effect on the freezing-procedure but were beneficial during long-term storage of the cells. A satisfactory buffer system e.g. HEPES, which is independent from carbon dioxide and less temperature sensitive, was chosen for the cryo-medium. Additional compounds like adenosine have positive effects on revitalisation. For Vero cells growing under serum-free conditions we were able to replace serum by methylcellulose and conditioned medium without any loss in cell revitalisation.

Using this new medium for cryopreservation of cells in 96-well plates, very good revitalisation rates were achieved. Rapid freezing is essential for the success of this method. A freezing rate at about 13K/min. was the best with L-929 cells. After freezing L-929 in plates and storage for several weeks at  $-80^{\circ}$  the plates were revitalised. Microscopical examinations revealed morphological differences between frozen and non-frozen cells. Plates were stained with Resazurin (metabolic activity of living cells) and measured in a fluorescence reader (Genios, TECAN) at ex/em 560/590 nm. Compared to non-frozen cells a loss in activity of about 5% was detected. In figure 1 the well-to-well conformity is shown. The signal variability of less than 10% is sufficient for a proper usage of the plates in assays.

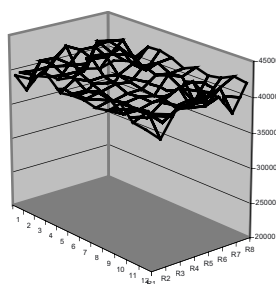


*Fig. 1 Well to well variation of cryopreserved assay plates*

One application for the plates is the determination of  $IC_{50}$ -values of toxic compounds. The comparison of results determined with non-frozen and thawed plates are nearly identical (fig. 2).

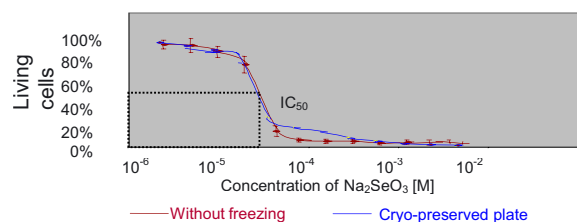


Fig. 2 Comparison of non-frozen and thawed plates for the  $IC_{50}$  determination of  $Na_2SeO_3$ .

First experiments with a stable cell line for a reporter gene assay are promising. The cells were frozen in plates at  $-80^{\circ}C$  and revitalised after a few days. Activation of  $NF\kappa B$  activity with a pro-inflammatory cytokine was still possible. This cell line in combination with the new cryopreservation procedure will be the basic platform for a 96-well plate based assay, screening for inflammatory compounds or anti-inflammatory agents.

## REFERENCES

- [1] J.M. Szein et al., Comparison of permeating and nonpermeating cryoprotectants for mouse sperm cryopreservation, *Cryobiology* 41 (2001) 28-39
- [2] R. Fabbri et al., Human oocyte cryopreservation: new perspectives regarding oocyte survival, *Human Reproduction* 16 (3) (2001) 411-416
- [3] P.H. Glenister, C.E. Thronton, Cryconservation – archiving for the future, *Mammalian Genome* 11 (2000) 565-571
- [4] A. Eroglu et al., Intracellular trehalose improves the survival of cryopreserved mammalian cells, *Nature Biotechnology* 18 Feb. (2000) 163-167
- [5] J. Wolf, G. Byrant, Cellular cryobiology: thermodynamic and mechanical effects, *International Journal of Refrigeration* 24 (2001) 438- 450
- [6] S. Kaidi et al., Osmotic behaviour of in vitro produced bovine blastocysts in cryoprotectant solutions as a potential predictive test of survival, *Cryobiology* 41 (2000) 106-115
- [7] R.T. Pfaff et al., Cryobiology of rat embryos I, *Biology of Reproduction* 63 (2000) 1294-1302
- [8] J.M. Baust et al., Modulation of the cryopreservation cap : elevated survival with reduced DMSO concentration, *Cryobiology* 45 (2002) 97-108
- [9] E.R. Gizewski et al., Rapid decrease in cellular sodium and chloride content during cold incubation of cultured liver endothelial cells and hepatocytes, *Biochem. J.* (1997) 322, 693-699

CHRISTOPHE LOSBERGER AND THIERRY BATTLE

COMPARATIVE SECRETION LEVELS OF  
RECOMBINANT PROTEINS BETWEEN INSECT CELL-  
BACULOVIRUS AND MAMMALIAN HEK293EBNA  
CELLS

*Serono Pharmaceutical Research Institute, Plan-les-Ouates, Geneva,  
Switzerland*

*Email: Christophe.Losberger@Serono.com*

1. INTRODUCTION

For our cell based screening activities we have set up a high throughput mammalian (Hek293EBNA) secreted protein expression flow (50-200µg purified target, 320 proteins a month). For proteins required in large amounts for *in vivo* testing we are currently relying on the scale-up capacity and easiness of the baculovirus expression system (from 1.7-L up to 64-L).

In order to streamline the scale-up flow, we compared the expression/secretion properties in insect cells of proteins initially produced via the mammalian throughput mode.

2. MATERIALS AND METHODS

Twenty-two C-terminal tagged proteins expressed at various levels in Hek293EBNA were selected. They were originally cloned into a pEAK vector and transfected with either a calcium-phosphate, lipofectamin or polyethylenimine reagent.

These genes were subcloned into pDEST8 vectors (Invitrogen Gateway System) and the virus stocks generated were titrated. Sf9 cultures in SF900II media (Gibco) were infected at MOI 5 and the expression was carried on for 72 hours. Samples were taken at 48 and 72 hours after infection.

3. RESULTS AND DISCUSSION

The level of expression in Sf9's cell lysates and supernatants ( $n \geq 2$ ) was determined by western blotting.



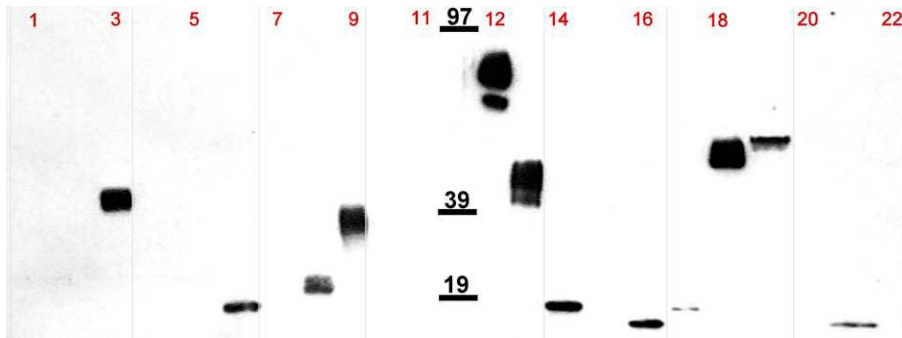


Figure 1. Western Blot of Hek293EBNA culture supernatant.

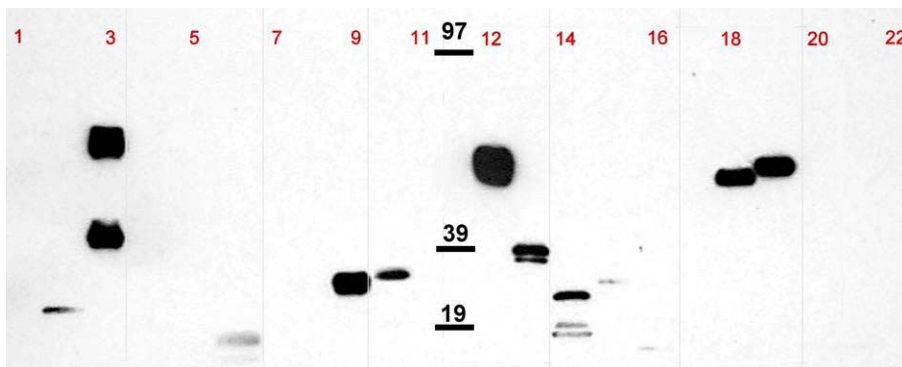


Figure 2. Western Blot of Sf9 culture supernatant.

The levels of secretion were compared side by side to those from the mammalian expression (n=2 to 93) and the bands were scored to discriminate between non-detected (0), low (1), medium (2) and high secretors (3) by the relative intensity of the bands.

In the mammalian system, 19/22 proteins were secreted. In the baculovirus system, 17/22 proteins were secreted with a very good correlation of low (n=7), medium (n=5) and high (n=5) secretors with those found via mammalian expression.

	Secretion		Expression Insect
	Hek293	Insect	
SP01	0.8	0.7	3.0
SP02	0.5	2.0	2.0
SP03	<b>2.8</b>	<b>3.0</b>	3.0
SP04	0.1	1.0	3.0
SP05	0.0	0.0	1.0
SP06	1.8	1.7	2.0
SP07	0.2	0.3	0.5
SP08	1.0	0.7	1.0
SP09	<b>3.0</b>	<b>2.7</b>	2.5
SP10	0.6	1.7	1.5
SP11	0.0	0.0	1.5
SP12	<b>2.5</b>	<b>3.0</b>	2.5
SP13	<b>2.3</b>	2.0	1.0
SP14	2.0	<b>3.0</b>	3.0
SP15	1.2	1.0	2.0
SP16	1.6	1.0	1.0
SP17	0.7	0.0	2.0
SP18	<b>2.5</b>	<b>2.2</b>	2.5
SP19	1.5	2.0	2.0
SP20	0.1	0.0	1.5
SP21	0.4	0.0	1.5
SP22	0.0	0.5	2.7
	<b>19/22</b>	<b>17/22</b>	<b>22/22</b>
	0.1-1.0	1.1-2.0	<b>2.1-3.0</b>

Table 1. Scores of secretion of Hek293EBNA vs insect and expression in insect cells

#### 4. CONCLUSION

In conclusion, within the panel of proteins tested so far, we found a high degree of correlation between proteins secreted in baculovirus and those generated via the Hek293EBNA mammalian system. Bearing the differences of glycosylation in mind, insect-cell baculovirus expression is a powerful scale-up expression system for proteins expressed via a high throughput mammalian expression system.

#### ACKNOWLEDGEMENTS

The SPRI Protein Expression Group for Hek293EBNA high throughput expression.  
The SPRI Gene Discovery Group for the DNA constructs.

M. VALER<sup>1</sup>, T. NEUMANN<sup>1</sup>, P. BARTHMAIER<sup>2</sup>, M. KUSCHEL<sup>1</sup>,  
C. BUHLMAN<sup>1</sup>

## MICROFLUIDIC TECHNOLOGY APPLIED TO PROTEIN SIZING AND QUANTITATION

<sup>1</sup> *AGILENT TECHNOLOGIES, WALDBRONN, GERMANY*

<sup>2</sup> *AGILENT TECHNOLOGIES, PALO ALTO, CA, USA*

### 1. INTRODUCTION

A universal task involved in protein characterization is purification, quantitation and identification. For example, protein quantitation is required to calculate and monitor the protein yield after various enrichment or purification processes as well as to optimize and standardize downstream experiments such as protein-protein-interaction studies or protein-drug interaction studies. Protein sizing is commonly used to identify proteins oligomers and monomers. In addition the recombinant protein expression technology facilitates to achieve high throughput protein expression and purification and keep up with the increasing pace of pharmaceutical research [1]. Recombinant protein technology is also increasingly used for manufacturing of proteins to be used as research or diagnostic tools, or as protein therapeutics [2].

With these advances there is a need for standardized, more automated and faster analysis of proteins. Recent development of microfluidic technology offers an interesting alternative to traditional protein analysis methods, such as denaturing polyacrylamide gel electrophoresis (SDS-PAGE) or capillary gel electrophoresis (CGE).

### AGILENT 2100 BIOANALYZER

Microfluidics technology allows integrating multiple experimental procedures, such as sample handling, separation staining/destaining, detection and analysis in a single process. The Agilent 2100 bioanalyzer, which was developed in collaboration with Caliper Technologies Corp. (Mountain View, CA, USA), is the first fully commercialized implementation of microfluidics technology to date [3, 4]. The system can be used for the rapid and automated analysis of proteins, DNA, RNA and cells. Together with the Protein LabChip<sup>®</sup> kits it allows for sizing, purity analysis, relative quantitation or absolute quantitation determination for proteins ranging in size from 5 to 200 kDa. The principle of the protein analysis is an electrophoretic process, where denatured proteins negatively charged through the interaction of SDS molecules are moved across micro-fabricated chips with distinct microfluidic channels. The channels are filled with a sieving polymer in order to separate the

proteins according to their size, and an intercalating fluorescent dye, which stains the proteins. Before the laser induced fluorescence detection of the different proteins a destaining step is integrated on the chip. Thus 10 protein samples can be analyzed unattended within less than 30 minutes. The software automatically evaluates the data and displays a detailed result table.

### 2.1. Sizing and resolution

To achieve accurate sizing of unknown protein samples, a sizing ladder is run on each chip, however sizing accuracy is dependent on the individual protein characteristics. The sizing precision ranges from 0.5 % to 5%. Proteins between 5 and 200 kDa can be analyzed with a resolution of 5% to 10% within a broad linear dynamic range (e.g. 20-2000 ng/ $\mu$ l BSA in PBS).

The analysis of a bispecific antibody consisting of two different heavy and light chains stemming from diverse organisms is shown in figure 1 as an example. The gel-like image of the analysis under reduced conditions (fig. 1A) shows a clear separation between the sets of two different light and heavy chains. This level of resolution was not achieved using a 4-12 % gradient SDS-PAGE gel (fig. 1A). Although the light chains were separated on the SDS-PAGE gel, the two heavy chains were not; they merged into one band. The overlay of the electropherograms of the analysis under reduced and non-reduced conditions is shown in figure 1B. Both conditions can be analyzed on the same chip. The automated data analysis assigned a size of 159 kDa to the intact antibody. The reduced antibody analysis revealed two light chain peaks at 23 kDa and 30 kDa and two heavy chain peaks at 57 kDa and 62 kDa.

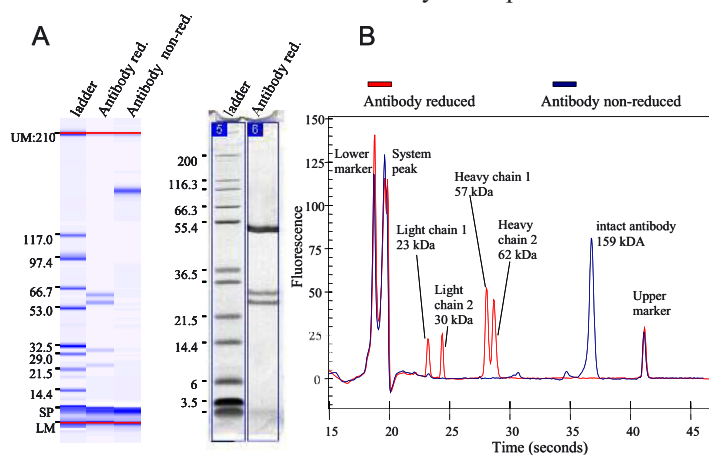


Figure 1. Analysis of a bispecific antibody on the Agilent 2100 bioanalyzer (A) Comparison of the gel-like image (left) and a scanned, Coomassie stained 4-12 % SDS-PAGE gel (right) The numbers indicate the molecular weight in kDa. (B). Overlay of the 2100 bioanalyzer electropherograms of reduced and non-reduced antibody sample is shown.

## 2.2. Quantitation

The Agilent 2100 Bioanalyzer software provides two functionalities for quantitation. The first possibility is to determine the relative concentration of the individual proteins. This value is determined automatically by the software based on a one-point calibration with the upper marker, which is used as an internal quantitation standard in every sample (fig. 1B). However, due to staining variability between the upper marker and the protein of interest, this value is not as accurate as absolute quantitation, using a pure sample of the target protein as reference. The Agilent 2100 Bioanalyzer software supports absolute quantitation, which can be obtained by a user generated protein quantitation calibration curve.

Table 1 shows that quantitation accuracy was greatly improved with the absolute quantitation feature compared to the relative concentration. The quantitation error for carbonic anhydrase (CA) was reduced from an average error of 42 % to 6 %, from 28 % to 11 % for ovalbumin (OV) and for bovine serum albumin (BSA) from 19 % to 15 %. The quantitation reproducibility was approximately 10 % and comparable between both quantitation methods.

	Target Conc. (µg/ml)	Agilent 2100 Bioanalyzer					
		Rel. conc. (µg/ml)	CV (%)	Error (%)	Calib. conc. (µg/ml)	CV (%)	Error (%)
BSA	1250	1523.5	9.8	21.9	1430.8	8.1	14.5
	750	911.6	8.9	21.5	856.1	6.9	14.1
	200	245.2	9.5	22.6	230.2	6.7	15.1
	40	36.4	9.5	9.1	34.2	6.1	14.6
OV	1250	985.7	3.4	21.1	1438.2	4.0	15.1
	750	597.6	3.7	20.3	872.7	6.2	16.4
	200	138.5	6.0	30.8	202.4	9.3	1.2
	40	24.3	12.9	39.3	35.6	15.1	11.1
CA	1250	1663.2	11.0	33.1	1142.0	12.0	8.6
	750	1083.8	10.0	44.5	742.7	8.6	1.0
	200	315.3	13.2	57.6	215.4	8.9	7.7
	40	53.7	28.8	34.3	36.8	27.7	8.1

Table 1 Comparison of relative and absolute quantitation for bovine serum albumin (BSA), ovalbumin (OV) and carbonic anhydrase (CA), (n=6) – accuracy and precision.

## 3. CONCLUSION

Although microfluidics technology is a relatively new technology, the microfluidic product, the Agilent 2100 bioanalyzer, for protein analysis has rapidly established itself as a viable alternative tool to conventional methods for protein sizing and quantitation. Since we are now entering the postgenomic era the number of biological products will increase and the technology will find further applications.

## 4. REFERENCES

- 1) Doyle SA, Murphy MB, Massi JM, Richardson PM; High-Throughput Proteomics: A Flexible and Efficient Pipeline for Protein Production; *J. Proteome Research*; 1(6) (2002) 531-536

- 2) Ohashi R, Manuel JM, Chwistek A, Hamel JF; Determination of monoclonal antibody production in cell culture using novel microfluidic and traditional assays; *Electrophoresis* 23(20) (2002) 3623-3629
- 3) Bousse L., Mouradian S., Minalla A., Yee H., Williams K., Dubrow R. (2001). Protein sizing on a microchip. *Anal. Chem.* 73(6), 1207-1212.
- 4) Kuschel M, Neumann T, Barthaier P and Kratzmaier M; Use of Lab-on-a-Chip Technology for Protein Sizing and Quantitation; *J. Biomolecular Techniques*; 13(3) (2002) 172-178

Dr. Tanja Neumann, Biochemist, Agilent Technologies Deutschland GmbH, Waldbronn, Germany, contact: <a href="mailto:tanja_neumann@agilent.com">tanja_neumann@agilent.com</a>
--

MARION ZERLIN\*, LARS GREIFFENBERG\*, YANNICK  
WURM\*, IRVIN WINKLER\*, DIETER KREUSEL\* AND STEFAN  
TOEMOE#, LASZLO BALLABAS#, JENS MARTIN#

## CRYOSTOCK A SOFTWARE FOR CELL CULTURE MANAGEMENT

*\*Aventis Pharma Deutschland GmbH; Industriepark Hoechst; D-65926  
Frankfurt am Main  
#T-SCC, Schmalweg 50; D-55252 Mainz-Kastel*

Abstract. Abstract. During the last years the requirements on modern cell culture have rapidly increased, comprising quality control, global administration and global availability of cell lines. To meet these demands we developed CryoStock as a new software tool for cell culture management. This application combines a database for the storage of stocks and a LIMS for tracking all tasks during handling and transfer of cell lines. The data collected during the cell culture process can be used to follow parent/child relationships and to generate user friendly queries and reports. CryoStock will put another layer of quality on our cell culture handling to increase reproducibility and outcome of cell-based assays and to accelerate the knowledge transfer among Aventis' scientists.

### 1. GLOBAL INFORMATION MANAGEMENT

In CryoStock each cell line is registered with a uniform and unique identifier as a numeric coding system. Each cell line with its corresponding batches gets a cell data sheet with an ID card to get a complete overview and a fast access to all relevant information, e.g. functional expression of target(s), stability of a clonal cell line, microscopical pictures, or the number of frozen vials (Figure 1). CryoStock allows to add documents like cultivation instructions, GMO- recordings or SOPs for cell-based assays to improve the quality and reproducibility of experiments.

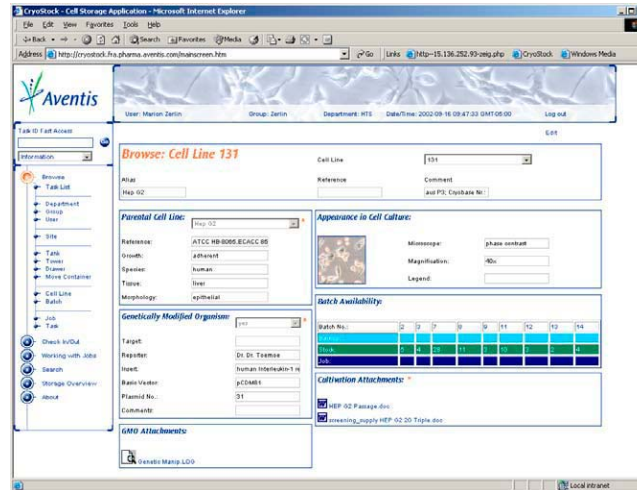


Figure 1. Cell data sheet in CryoStock (“ID-Card”)

## 2. STORAGE SYSTEM

CryoStock manages three kinds of storage environments: a stock platform (master bank), a backup facility and a Job module (working bank), in a company wide and consistent standard. These storage facilities can be configured flexible, even within one tower. The Stock module as the core of the storage platforms in CryoStock implements a controlled cryovial administration, combined with a backup storage system. Easy to use predefined administration queries help to control the extent of tank utilization. In addition, “out of age” and “out of stock” warnings increase the safety of the warehouse system.

## 3. WORKING WITH TASKS

Tasks are the most important feature in CryoStock. Tasks create a link between originally received vials, checked out vials and modified checked in vials. “Check In” and “Check out” activities are presented in an interactive overview chart, which guides the user through all working processes (see Figure 2 – Check In/Out) in the different storage modules. The generated task lists track the daily business of a working group to get a fast overview of the workflows in their cell culture lab (see Figure 3 – User Task List). Basing on the tasks, batch pedigrees of a cell line can be generated and all transfer processes can be tracked and documented.



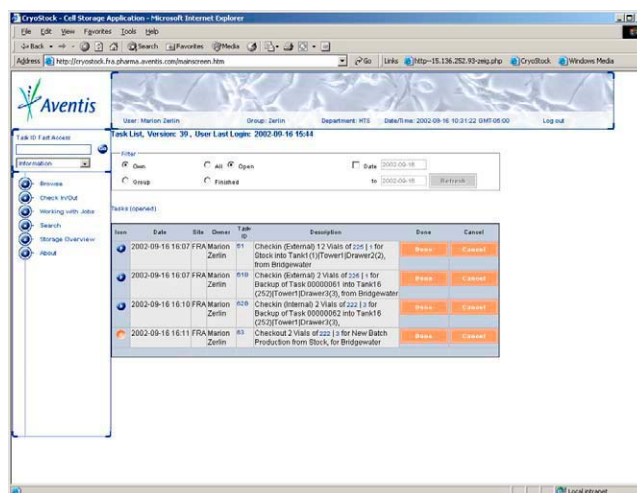


Figure 3. User Task List

#### 4. WORKING WITH JOBS

The Job module is a flexible storage system, which can be practically used as a temporary storage platform (working bank) to store frozen stocks e.g. during cell line generation processes or screening supplies. This module fits to heterogeneous workflows in cell culture labs. The user can reserve a job drawer and assign it to procedures within each distinct project. Each job drawer is visualized by a user defined Excel sheet, being linked to the origin cell line used for the job application. All jobs are listed in an job overview, where the user can choose to see either the own jobs or all jobs within his working group. This individual storage platform is not automatically controlled by the application and is only viewable for the members of the working group of a user.

#### 5. NO INSTALLATION / HIGH PERFORMANCE

CryoStock can be used without any client software installation. Once the server is installed and available in the (intra)net clients can connect and work with CryoStock simply using the already installed Internet Explorer on the system. All software updates are centrally managed on the server. The user interface is designed in pure HTML, thus preventing time consuming and expensive Java applet download. This method provides fast access to relevant data wherever the company intranet is accessible.

## 6. SECURITY

The CryoStock security is controlled by the ORACLE database. All user restrictions and password options can be used. The CryoStock application concept provides three user roles to allow highest possible access control with lowest possible admin effort:

- Admin: Administrator per site, manage documents, register users
- User: Person that works with vials and storage, manage documents for owned cell lines
- Observer: View only user, for queries. All scientists in the intranet can start queries for the allowed information without need to be set up by the administrator.

## 7. CUSTOMIZED APPLICATION

The unique CryoStock application concept with encapsulated application layers for Database operation, User interface and Business Logic facilitates the reuse of an existing implementation. Also easy redesign of a new interface to reflect individual needs of a site is supported by this concept. Advanced modularity allows for versatile and easy modification and enhancement of already existing CryoStock installations and provides a highly adaptive basis for further projects.

## 8. SYSTEM REQUIREMENTS

Server: Windows 2000, Sun Solaris, HP UX 11 Server, ORACLE 8i / 9i database with Apache JSP Web Server or Tomcat 4.1.24, Client: Internet Explorer 5.5 or higher, Intranet access

## CHAPTER 5

### BIOPHARMACEUTICALS

K. WINKLER <sup>1</sup>, T. WERMELINGER <sup>2</sup>, C. PAUL <sup>1</sup>, S KOCH <sup>1</sup>,  
R. BRECHT <sup>1</sup>, S. ZIETZE <sup>1</sup>, R. NUCK <sup>3</sup>, G. THIEL <sup>4</sup>, U. MARX <sup>1</sup>,  
V. SANDIG <sup>1\*</sup>

## TARGETING THE HUMAN IMMUNOGLOBULIN LOCI FOR HIGH LEVEL HETEROLOGOUS GENE EXPRESSION

<sup>1</sup>ProBioGen AG Goethestrasse 54, 13086 Berlin, Germany, <sup>2</sup>Hochschule  
Wädenswil, <sup>3</sup>Free University Berlin, <sup>4</sup>Institute of Medical Molecular  
Diagnostic,

\* corresponding author. Phone +493092400670 Email:

[Volker.Sandig@probiogen.de](mailto:Volker.Sandig@probiogen.de)

Abstract. A human / mouse heterohybridoma obtained by fusion of a B-lymphocyte from a patient with chronic thrombozytopenia with the mouse myeloma cell line P3X63Ag8, was selected as a potential protein producer cell line for its stability, preferable growth characteristics, and endogenous production capacity. The cell line secretes an IgM antibody at titers between 30 and 100µg/ml.

We have characterized the genomic organization of the IgH and Ig loci and have constructed targeting vectors. The IgH targeting construct contains 2kb of VH upstream sequences, the entire Igµ intron and a Leptin Fc fusion gene driven by either hybrid CMV EF1alpha or the endogenous VH promoter. The vectors were introduced by electroporation and clones losing IgM and gaining Leptin Fc expression were detected by an in situ staining technique. Whereas expression of several clones originating from non-homologous integration decreased over time, Leptin Fc expression of clones with gene targeting aimed at the IgH locus remained stable. Using recombinase mediated expression cassette exchange, we have replaced the Leptin Fc gene for several target genes. Homogenous expression levels were obtained in all clones selected for gene exchange.

The Leptin Fc product was purified and subjected to extensive glycosylation analysis showing complex oligosaccharide structures and signs of a partially human glycosylation pattern. The resulting cell line will be used for the manufacture of recombinant antibodies.

### 1. INTRODUCTION

Although, several hybridoma cells have been widely used to produce the respective antibodies, other recombinant glycoproteins have been predominantly generated in two cell lines: CHO and NS0. These cell lines have been selected for their growth properties, ease of transfection and the functionality of amplifiable selectable markers. Vectors containing strong viral or cellular promoters, appropriate polyadenylation signals, and sometimes in combination with specific signals to enhance RNA stability or translation are transfected into these cell lines. This is followed by drug selection. When these highly optimised vectors integrate into the host genome at a random position, the expression level of the individual cell clone is determined to a large extent by the position, rather than the vector itself.

This phenomenon is mediated by transcription promoting sequences in the genome such as S/MAR elements, which are thought to prevent methylation and heterochromatinisation of the chromosomal locus and make the promoter highly accessible to transcription factors and the basic transcription machinery. Extensive screening is required to identify extremely rare, high producer clones which represent highly active chromosomal positions. Therefore, it is desirable to re-use advantageous, fortuitously found loci, for a whole set of proteins to be produced. Homologous recombination as a potential strategy which has been shown to be rather ineffective for somatic cells and may be well masked by illegitimate recombination. As an alternative, targeting techniques using site specific recombinases (cre, flp) have been explored. Locus selection and replacement are becoming increasingly difficult when two genes eg. heavy and light chains of an antibody have to be produced at high levels.

We have explored a human mouse heterohybridoma, which expresses a human IgM antibody in a stable configuration over two years as a potential protein producer cell line. Using homologous recombination and an in situ screening strategy, we have replaced the *Ig $\mu$*  gene for a fusion protein Leptin Fc. In the resulting cell line, the modified locus is labeled with sites recognised by flp recombinase, which allow a simple exchange for a secondary gene. A similar, independent exchange system has been designed for the light gene ( $\lambda$ ) locus.

## 2. RESULTS AND DISCUSSION

### 2.1. Characteristics of the original heterohybridoma

The heterohybridoma CB03 was created by fusing human B lymphocytes, from a patient with chronic thrombocytopenia, obtained by therapeutic splenectomy, with the mouse myeloma line P3X63Ag8. CB03 secretes human autoantibodies of the IgM type which react with human platelets and double stranded and single stranded DNA [1]. The hybridoma secretes the antibody in a stable manner at a rate of 45pg/cell\*day over a period of two years. This is in striking contrast to the majority of heterohybridomas, which tend to quickly lose human chromosomes resulting in unstable immunoglobulin expression. Moreover, expression was preserved when the cell line was cultivated in high density fermentation systems of the CellPharm family (Unisyn Technologies Inc.) and remained stable in 5 independent fermenter runs which had a mean duration of 66 days. Expression did not decrease below 30 pg/cell\*day when the medium was exchanged for a protein free medium (Iscov's MEM/HamsF12 1:1, 330mg/l Sodium Pyruvate, w/o HEPES).

This suggests that the Ig loci of CB03 seem to be highly accessible and stable and are, therefore, well suited to drive a heterologous transgene. To assess the possibility to target these loci, thereby not only introducing a transgene cassette, but also abolishing IgM expression, the cell line was submitted to spectral Karyotype analysis to find out whether the respective loci are present as single copies. The typical cell contains 69 to 94 chromosomes with a dominance of mouse

chromosomes. Via hybridisation with specifically labelled human chromosome libraries, 8 complete human chromosomes (4, 5, 7, 10, 14, 17, 18, 22) and fragments of others (4, 8, 9, 10, 11, 14, 16), each linked to a mouse chromosome, were identified. Since a complete and a partial copy of chromosome 14 (the chromosome harbouring the IgH genes) were found, in situ hybridisation with an IgH probe was performed and a single copy of the human IgH region was identified. With a single chromosome 22 present, a single copy of the Ig lambda locus was expected as well.

### *2.2. Homologous targeting of the immunoglobuline loci*

Using the known cDNA sequence and the IMGT database, we have identified V1-2, D1, J6 and  $\mu$  as the elements participating in constitution of the heavy chain gene. A sequence map of the rearranged IgH locus of CB03 was built including sequences located upstream of the VH promoter region of V1-2. Using PCR primers located 2000bp upstream of the transcription start point for V1-2 and within JH6, the predicted structure was confirmed. A typical targeting vector for the IgH locus was constructed using a proofreading PCR system (Roche, Expand High Fidelity). This vector consists of a short flank (1930bp), which represents sequences upstream of the VH promoter, the promoter itself, the transcription initiation point and the RNA leader sequence without the start codon and a long flank (7400bp) ranging from JH6 to CH1 spanning the entire C $\mu$  intron.

The targeting vector was equipped with an SV40 driven blasticidin gene for selection. As a reporter, we have introduced the Leptin gene linked to an IgG4 Fc domain (hobFc) representing the large group of Fc fusion proteins with therapeutic potential. The gene was cloned either immediately behind the VH promoter or downstream of a human CMV promoter linked to the first intron of EF1 alpha gene. The composition of the lambda gene locus was investigated and a targeting construct was designed using a similar approach. V $\lambda$  3-19 gene (upstream) and JC2 (downstream) are the components forming the active lambda gene of CB03. The flanks were limited to 4000bp (V $\lambda$ ) and 4500bp (JC2) in order to exclude highly repetitive sequences located further upstream and downstream. Hygromycin and alpha-1 antitrypsin were used as selection marker and reporter respectively.

The targeting constructs, were introduced into the cell line by electroporation. In order to screen clone numbers large enough to detect homologous recombinants, we developed direct cell staining techniques for secreted IgM and IgG (Fc) using texas red and AMCA labelled antibodies. By optimising the concentration and incubation time, we were able to form antibody precipitates in situ in the absence of methyl cellulose or agarose which are usually employed to limit product diffusion. This procedure allowed not only the identification of high producers, but also the quick isolation of these clones with cloning cylinders. From approximately 800 clones, 32 with intense IgG staining were identified. Of these clones, 14 showed no staining for IgM, which was confirmed by Western blot for a total of 11 clones. PCR tests using primer pairs located outside the targeting vector and in the transgene region, confirmed a homologous targeting event in the clones analysed. Interestingly, expression remained stable over 3 months in clones originating from homologous

recombination, whereas several clones resulting from random integration lost expression. We observed the highest expression levels of 25pg/cell\*day for clones containing the CMV-EF1alpha hybrid promoter. The resulting cell line was named G-line.

### 2.3. Studies of the glycosylation pattern of Leptin Fc

Leptin Fc from the G line was generated in roller bottle culture and purified by a generic process including affinity chromatography, gel filtration and membrane filtration. The protein was digested with trypsin and the resulting peptides were deglycosylated by PNGase F digestion. The glycans were labeled with 2-amino-benzamide and separated by HPLC on a Phenomenex Hypersil APS-2-column (Fig.1). We used MALDI-TOF-MS (BRUKER BIFLEX™) with the desialylated, labelled samples to further characterize the respective fractions shown in Table1.

The single N-glycosylation site on Fc carries complex oligosaccharide structures which are sialylated at 37% , a rate close to average sialylation on antibodies in human blood. Sialic acids were further characterized by sialidase treatment, DMB labelling and separation on a Bischoff Hypersil-ODS-column and compared with the Sialic Acid Reference Panel (Oxford GlycoSciences). Typically, N-acetylneuraminic acid was found. Only 2% were represented by N-glycolylneuraminic acid, the dominating form in mouse myeloma cells, which was shown to be immunogenic [2]. Alpha 1,3 Gal structures, which are not made in human cells and are known to increase clearance via preexisting antibodies, were only found in 1.3% of the glycans.

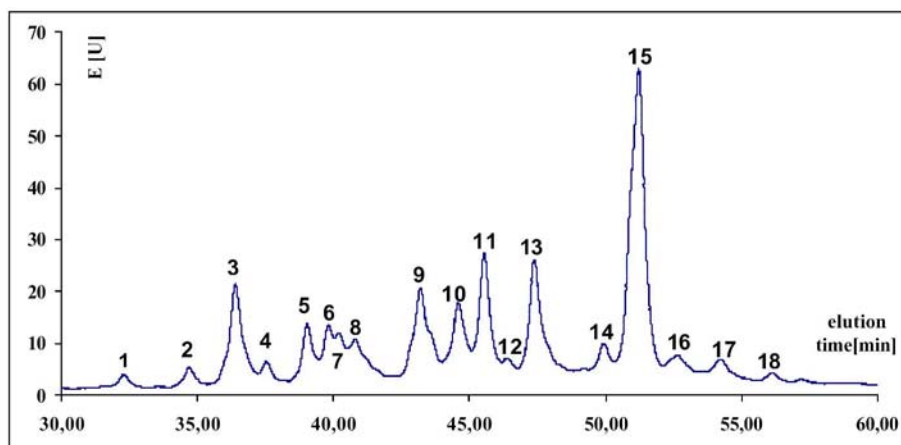


Figure1. Aminophase-HPLC of PBG04, peak numbers represent the fractions which were used for the MALDI-TOF-MS analysis

Table 1.  
Interpretation of the MALDI-TOF-MS-spectra of PBG04, \*denotes Gal $\alpha$ 1,3Gal epitopes

Peak	Area (%)	Monoisotopic mass (m/z)	Proposed structure
1	1,2	1256,9	Man3HexNAc1
2	1,4	1402,9	Man3HexNAc1Fuc
3	8,0	1378,4 Main	High Man5
4	1,6	1377,9 1419,0	High Man5 Man3HexNAc1Hex1
5	4,3	1606,5	Man3HexNAc2Fuc
6	3,1	1565,5	Man3HexNAc1Hex1Fuc
7	2,7	1540,7 Trace 1581,7 Main	HighMan6 Man5HexNAc
8	4,7	1540,5 1581,5 Main 1622,7	HighMan6 Man5HexNAc Man3HexNAc2Hex1
9	9,3	1768,8	Man3HexNAc2Hex1Fuc
10	6,6	1743,8 Main 1784,9 Trace	Man5HexNAc1Hex1 Man3HexNAc2Hex2
11	8,7	1784,7	Man3HexNAc2Hex2
12	1,6	1784,5 1889,7 1930,7 Trace	Man3HexNAc2Hex2 Man5HexNAc1Hex1Fuc Man3HexNAc2Hex2Fuc
13	10,9	1930,8	Man3HexNAc2Hex2Fuc
14	3,0	1664,5 1946,9 Trace 2093,0	Bi – 2AB Man3HexNAc2Hex3 (Bi + Gal*) Man3HexNAc2Hex3Fuc (Bi+Fuc+Gal*)
15	25,7	2150,0	Man3HexNAc3Hex3
16	3,2	N.D.	
17	2,8	N.D.	
18	0,9	2031,2 2514,2	Tri – 2AB Man3HexNAc4Hex4

#### 2.4. Flp mediated exchange of the transgene

To reduce the effort required to create producer lines for multiple transgenes, we intended to build in a mechanism for quick exchange of the transgene using recombinase mediated cassette exchange [3]. Therefore, the targeting vector was equipped with mutated incompatible flp sites (F3, wt and F5 [4]) flanking the hybrid promoter and following the transgene cassette respectively. In addition, a promoter-less neo gene lacking the ATG was introduced next to F5 (Fig1). Whereas recombinations with single recombinase sites promote the excision reaction far more than integration, this system should provide efficient replacement.

Transfection of a promoterless gfp and a minimal promoter linked to an ATG flanked by wt and F5 sites, together with a flp recombinase plasmid [5] resulted in a neomycin resistant cell pool with homogenous gfp expression.



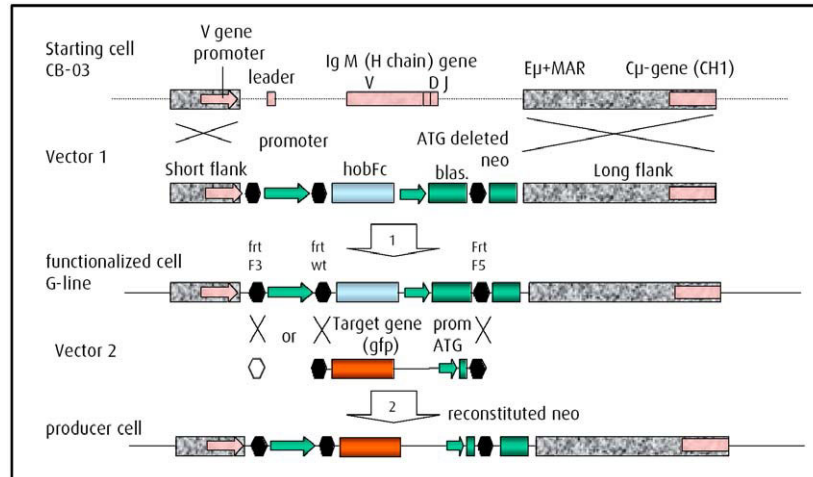


Figure 2. homologous recombination and flp mediated gene exchange to create producer cell lines

Recombination with an alpha 1 antitrypsin (aat) gene flanked by F3 and F5 sites resulted in neomycin resistant cell clones with homogenous aat expression of 9pg/cell\*day. An independent recombination system using F5 and wt frt sites and an ATG deficient histidinol resistance gene has been designed for the light chain locus. This system should allow the placement of genes for recombinant antibodies in a natural, favourable environment.

## REFERENCES

1. Jahn, S., et al., Expansion of a B-lymphocyte clone producing IgM auto-antibodies encoded by a somatically mutated VHI gene in the spleen of an autoimmune patient. *Rheumatol Int*, 1994. **13**(5): p. 187-96.
2. Noguchi, A., et al., Immunogenicity of N-glycolylneuraminic acid-containing carbohydrate chains of recombinant human erythropoietin expressed in Chinese hamster ovary cells. *J Biochem (Tokyo)*, 1995. **117**(1): p. 59-62.
3. Seibler, J. and J. Bode, Double-reciprocal crossover mediated by FLP-recombinase: a concept and an assay. *Biochemistry*, 1997. **36**(7): p. 1740-7.
4. Schlake, T. and J. Bode, Use of mutated FLP recognition target (FRT) sites for the exchange of expression cassettes at defined chromosomal loci. *Biochemistry*, 1994. **33**(43): p. 12746-51.
5. Buchholz, F., et al., Different thermostabilities of FLP and Cre recombinases: implications for applied site-specific recombination. *Nucleic Acids Res*, 1996. **24**(21): p. 4256-62.

## QUESTIONS AND ANSWERS

**Nicolas Mermod, University of Lausanne, Switzerland:**

Did you have to permeabilise the cells in order to stain them with the texas red-labelled IgG ?

**Volker Sanding, ProBioGen, Germany:**

We did not have to do anything, the protein was secreted into the medium, and when the clone produced sufficient amounts of protein, the antibody precipitates did form. In order to achieve that, you had to titrate the antibody concentration in a well-adjusted timing, otherwise you get a precipitate anywhere, and not for specific clones. We did try the same approach for a number of proteins and for the same protein in CHO, but because the expression level was much lower there, we did not observe precipitation. It is a method that is pretty nice, and works well, but only for a number of proteins.

**Reinhard Franze, Roche Diagnostics, Germany:**

Can you comment on the biological safety pattern of the cell line, specially on the retroviral particle load ?

**Volker Sanding, ProBioGen, Germany:**

We have not done any studies on that yet. It is clear that it has to be done, we just could conclude from what we know about the cell line, we have access to the data of the donor, and the donor is still traceable. On the other side, we have the typical cell line that has been used to make most of the hybridomas as a starting point. So, there are still open questions to solve.

**Florian Wurm, EPFL, Switzerland:**

You said something about low success rate or low expression level when you used CHO cells ?

**Volker Sanding, ProBioGen, Germany:**

We also have tried it in CHO cells, and we encountered problems as the selection was very difficult to achieve.

P.-A. GIROD, M. M. ZAHN-ZABAL, N. MERMOD

## MAR ELEMENTS AS TOOLS TO INCREASE PROTEIN PRODUCTION BY CHO CELLS

*Laboratory of Molecular Biotechnology, University of Lausanne CBUE, FSB-ISP, EPFL, 1015 Lausanne Switzerland*

**Abstract.** One of the major hurdles of isolating stable, inducible or constitutive high-level producer cell lines is the time-consuming selection, analysis and characterization of the numerous clones required to identify one with the desired characteristics. Various boundary elements, matrix attachment regions, and locus control regions were screened for their ability to augment the expression of heterologous genes in CHO and other cells. The 5'-matrix-attachment region (MAR) of the chicken lysozyme gene was found to significantly increase stable gene expression, in culture dishes and in bioreactors. These MAR elements can be easily combined with various existing expression systems, as they can be added in trans (i.e. on a separate plasmid) in co-transfections with previously constructed expression vectors. Using cell population analysis, we found that the use of the MAR increases the proportion of high-producing CHO cell clones, thus reducing the number of cell lines that need to be screened while increasing maximal productivity. Random cDNA cloning and sequencing indicated that over 12% of the ESTs correspond to the transgene. Thus, productivity is no longer limited by transcriptional events in such MAR-containing cell lines. The identification of small and more convenient active MAR portions will also be summarized. Finally, we will show examples of how MAR elements can be combined with short term expression to increase the simultaneous synthesis of many proteins in parallel by CHO cells. Overall, we conclude that the MAR sequence is a versatile tool to increase protein expression in short and long term production processes.

### 1. INTRODUCTION

The generation of highly productive CHO stable cell lines is a lengthy and costly process. One of the bottlenecks to the establishment of efficiently producing cell lines is the drastic and uncontrollable variation in the specific productivity of different clones. This variation is thought to result from the effect of the local chromatin structure at the site of integration of the transgenic DNA within the chromosome.

One approach to abolish this effect is to use chromatin elements capable of shielding the transgene locus from the repressive effects of flanking chromatin, such as S/MARs. These genetic elements, originally described as MARs (Matrix Attachment Regions) or SARs (Scaffold Attachment Regions), are 300 to 3000 bp long DNA elements that were proposed to attach chromatin to proteins of the nuclear matrix and thereby partition eukaryotic genomes in independent chromatin loops. Because of their co-localization with transcription regulatory elements, S/MARs have also been implicated in the regulation of gene expression, for instance by facilitating interactions of genes with chromatin activating complexes and thereby protecting transgenes from silencing effects. These properties have therefore

attracted considerable interest for use in industrial production processes and in gene therapies (1).

## 2. RESULTS AND DISCUSSION

One of the S/MAR elements, the chicken lysozyme MAR, improves significantly the generation of stable cell lines, including CHO cells. For instance, this 2.9 kb MAR can be added either in *cis*, as an element of the expression vector, or in *trans*, that is co-transfected onto a separate plasmid (2). We have found that one of the optimal settings consists of combining both approaches, and introduce the MAR elements both in *cis* and in *trans* (Fig. 1a). With this setting, the total polyclonal population of primary transformants produces 3 to 4 mg/L/day in culture dishes, using standard laboratory vectors and without further optimisation or process development (Fig. 1b). Use of MARs in *cis* and *trans* together allowed an eight to ten-fold improvement of the average cellular productivity.

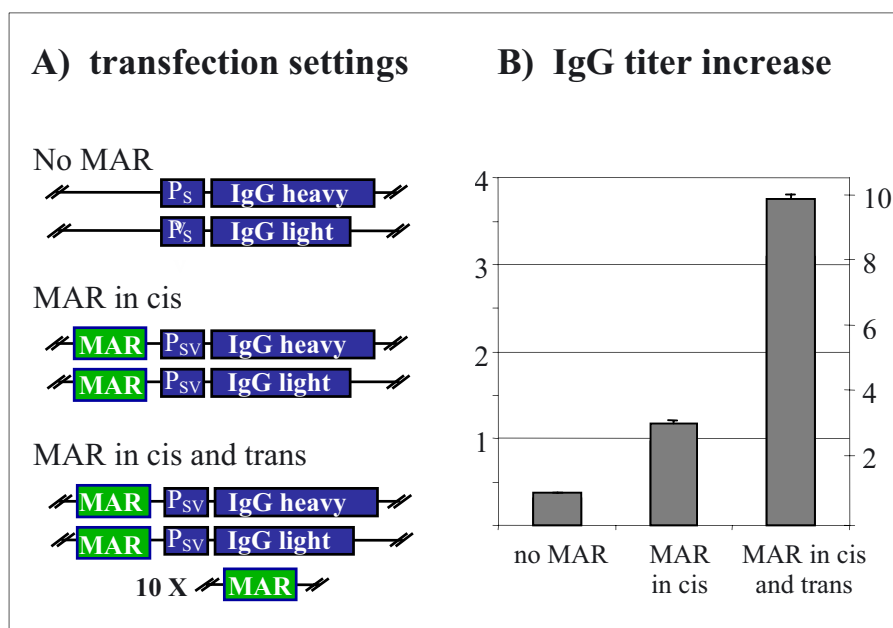


Figure 1. A) Transfection settings. CHO DG44 cells were transfected with the indicated IgG heavy and light chain expression vectors in the absence of MAR, with one MAR element inserted upstream of the SV40 early promoter (MAR in cis), or with the further addition of a 10-fold molar excess of MAR containing DNA fragment (cis and trans). B) Transfected cells were selected with neomycin during 14 days and IgG secreted by the polyclonal pool of primary transfectants was expressed as mg per liter per day (left-hand side scale), or as fold increase in IgG titre as compared to cells transfected without MAR elements (right-hand side scale).

Analysis of the population by FACS and by cellular cloning indicated that clonal productivity is also significantly increased, and that it generally shifts up protein production over the entire range of productivity (Fig. 2 and reference 3). Stable productivity was obtained in seed trains over periods of several weeks in the absence of selection.

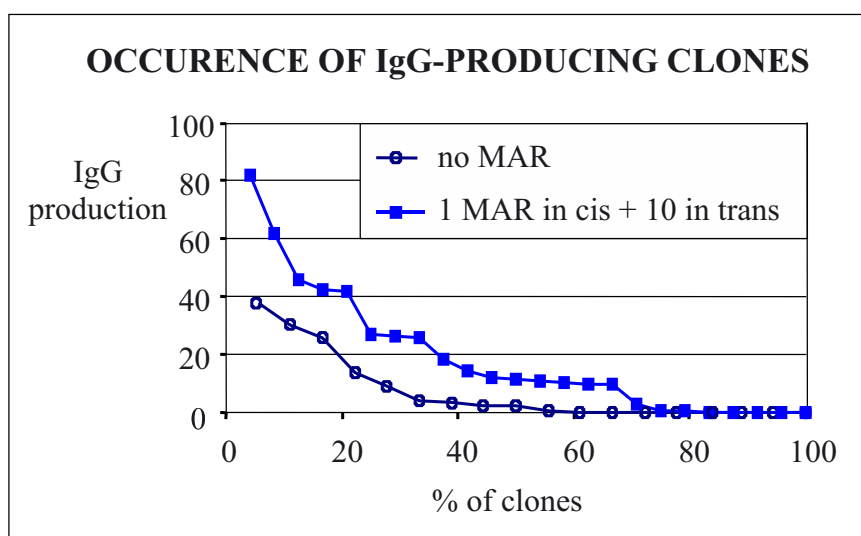


Figure 2. CHO DG44 cells were transfected either without MAR, or with one MAR element in cis and a ten-fold molar excess of MAR elements in trans, as in Figure 1. Stable transfectant cells were selected with neomycin, cell clones were picked randomly and analysed for IgG production. The titer of IgG secreted by individual cell clones, ranked in decreasing order, is expressed in arbitrary units

The total mRNA population of MAR containing CHO cell clones were analysed by poly-A primed reverse transcription and cDNA cloning and sequencing. This indicated that over 12% of the ESTs correspond to properly synthesized transgene mRNA. Analysis of high producer clones suggested that protein synthesis is no longer significantly limited by transgene transcription, but that it may be limited by the cell translation or protein secretion activities.

Use of MARs in transient transfection assays was also evaluated. Interestingly, we found that it can also be used to increase recombinant protein synthesis transiently. Furthermore, it can be combined with other productivity-increasing treatments, such as the addition sodium butyrate, an inhibitor of histone deacetylases thought to mediate a general chromatin decondensation. Overall, this allows the rapid synthesis of many proteins in parallel, for screening purposes. For instance, CHO cells transiently transfected in micro-titer plates can produce 5-10  $\mu\text{g}$  of proteins in a few days.

### 3. CONCLUSIONS

We conclude that the incorporation of MAR elements helps generate high producing mammalian cell clones at a high frequency. Use of these elements can be combined with other strategies aiming at increasing production (i.e. gene amplification, butyrate treatment, etc.), and productivity remains stable. These elements are compatible with various expression settings and vectors, and they can be easily combined with existing vectors. For instance, in the most simple setting, MAR elements can simply be added in trans, by cotransfecting the MAR-containing plasmid with existing vectors. MAR elements may therefore be used to quickly generate high-producing cell clones for further process development. Alternatively, they may be useful for the small-scale expression of multiple proteins in parallel, for research or screening purposes, by transient transfection of mammalian cells.

### 4. REFERENCES

- Zahn-Zabal, M., Kobr, M., Imhof, M. O., Chatellard, P., de Jesus, M., Wurm, F. and Mermod, N. (2001). Development of stable cell lines for production or regulated expression using matrix attachment regions. *J. Biotechnol.* , **87**, 29-42.
- Girod P.-A., and Mermod N. Use of Scaffold/Matrix-Attachment Regions for protein production. (2003). In: *New Comprehensive Biochemistry, Gene transfer and expression in mammalian cells*. Makrides S., ed. Elsevier Science. In press.
- Girod P.-A., and Mermod N. Generation of high producer CHO cell lines using S/MAR elements in trans. Manuscript in preparation.

## QUESTIONS AND ANSWERS

**Meijia Yang, Serono Reproductive Biology Institute, US:**

My question is regarding the mechanism of the MAR element. I assume you selected with methotrexate, and in the same plasmid you also have the DHFR resistance and your transgene. Since you have a mixed population, I wonder if there is an interaction effect of your mouse element.

**Nicolas Mermod, University of Lausanne, Switzerland:**

Your first question was about the mechanism of MAR functioning. We believe MAR is a regulation element, just like promoters and enhancers, and it is my fantasy that in the future people will not only work with enhancers and promoters, but will also incorporate the MAR as one of the final elements of the gene. Its function is for instance to allow the recruitment of histone acetyltransferases and other enzymes which will regulate the chromatin structure. Regarding the second question, in fact we first selected with neomycin, not with DHFR, and then in some cases we applied the methotrexate selection at a high concentration. Regarding the orientation, it is not believed to be orientation dependent. What we have found important is that the distance between the MAR and the gene of interest is relevant, so we are putting the MAR very close to the promoter and enhancer, and we find it to be the optimal setting.

**Nesredin Mussa, Lonza Biologics, UK:**

It is very interesting to see how you could improve the productivity of the cell lines using MAR. You mentioned that productivity can also be increased for existing stable cell lines. Have you tried this in your laboratory ?

**Nicolas Mermod, University of Lausanne, Switzerland:**

Yes, we did try that in our laboratory. For instance, we had a cell line which did not produce satisfactory IgG levels, so we diagnosed the problem as an imbalance between mRNA levels (analysed by quantitative PCR) between the light and the heavy chains. So, in that case we introduced the missing expression vector to restore the balance, and we could increase productivity.

**Lynne Krummen, Genentech, US:**

What constrains CHO to be a cell type with a particular MAR element ? Secondly, have you looked at other promoter combinations ?

**Nicolas Mermod, University of Lausanne, Switzerland:**

The MAR element was the most potent element we found in CHO cells. The other ones showed either marginal or no activity. We also looked at LCRs, however, they are typically cell type specific, while MAR is clearly not cell type specific. We used this MAR with several promoters, here we wanted to use non-optimized vectors, with very standard promoters, such as SV40, CMV or EF1-alpha, and it works as well, so it is not promoter dependent, at least for those promoters we have tested.

PABLO UMANA, PETER BRUENKER, CLAUDIA FERRARA,  
SAMUEL MOSER, TOBIAS SUTER, CHRISTIAN GERDES,  
URSULA PUENTENER, JOEL JEAN-MAIRET, PATRICK  
BUHOLZER, MANUEL SPAENI

## CELL LINE ENGINEERING FOR PRODUCTION OF THERAPEUTIC ANTIBODY GLYCOFORMS WITH INCREASED BIOLOGICAL ACTIVITY

*GLYCART Biotechnology, Wagistrasse 18, Zurich 8952, Switzerland.*

### CYTOTOXIC UNCONJUGATED MABS AS DRUGS

The clinical successes of the antibodies rituximab and alemtuzumab, for hematological malignancies, and trastuzumab, for solid breast tumors, have demonstrated that unconjugated antibodies can be useful drugs for the treatment of cancer. All of these antibodies have been approved and are currently in the market. Yet, a large need remains for improving this kind of drugs. For instance, rituximab induces a response in approximately 60% of the patients with relapsed/refractory low-grade non-Hodgkin's lymphoma. Of these, only 6% are complete responses and response durations are typically around 1 year (1).

The preferred type of unconjugated antibody for target-cell killing applications is an IgG1-type mAb, where at least the constant (or the Fc) region is of human origin (*i.e.*, chimeric, humanized, or fully-human IgG1s). Unconjugated IgG1 mAbs can exert their therapeutic effects via three classes of mechanisms. The variable region of the antibody molecule mediates the first class, while the other two involve the constant Fc region. Direct binding of the antibody via its variable region to the target molecule on the surface of cancer cells can lead to cell death or inhibition of tumor growth, for example by triggering apoptosis upon cross-linking of target molecules by the antibody. The Fc region operates in the other two-types of mechanisms: complement-mediated cytotoxicity, and Fc $\gamma$  receptor (Fc $\gamma$ R)-dependent effector functions. While complement is an Fc-receptor-independent mechanism, the other Fc effector functions of IgG1s are mediated by the interactions of the Fc region of target-cell bound antibody molecules and Fc $\gamma$  receptors on the surface of immune cells. For example, in antibody-dependent cellular cytotoxicity (ADCC), target-cell bound antibodies crosslink Fc $\gamma$ Rs on the surface of natural killer (NK) cells and this in turn triggers a lytic attack on the antibody-targeted cell by the immune effector cells.



Studies in mouse models have highlighted the importance of FcR-mediated mechanisms. Recently, the activity of rituximab and trastuzumab in mice engrafted with human tumor cells was studied (2). It was found that most of the *in vivo* activity of both antibodies was lost when FcR-mechanisms were abrogated. A similar effect has also been observed for a different antibody in a mouse model with intracranial tumors, where all of the *in vivo* anti-tumor activity of the antibody was lost when Fc $\gamma$ R knockout mice were used (3).

In addition to the data from mouse models, a correlation has been found between the efficacy of an anti-tumor unconjugated mAb in human patients and the binding affinity of a particular Fc $\gamma$ R to the antibody Fc region (4). There is a naturally occurring polymorphism in the gene encoding Fc $\gamma$ RIIIA that gives rise to two variants of the receptor differing in their binding affinity for the IgG Fc region. Approximately 10-20% of the population carries two copies of gene for the higher affinity variant. Recently the efficacy of rituximab within this patient population was investigated, finding a dramatically increased efficacy compared to the average efficacy in the total population. The study found an enhanced objective response rate (90% vs. 51% of patients after 1 year) and a large increase in molecular responses (5 out of 6 patients vs. 1 out of 6) for patients with the homozygous high affinity genotype relative to patients carrying at least one copy of the lower affinity variant of this receptor, respectively.

#### GLYCOENGINEERING OF ANTIBODY PRODUCTION CELL LINES

We have developed a technology that boosts the biological activity of antibodies by enhancing an important class of mechanisms employed by unconjugated, cell-killing antibodies. The technology, called GlycoMAb, enhances Fc-receptor-mediated effector functions via glycosylation engineering of the antibody Fc region. The IgG Fc carries two oligosaccharide molecules attached at conserved glycosylation sites and the presence of these carbohydrates is important for Fc $\gamma$ R binding and effector functions such as ADCC (5-7). GlycoMAb is based on genetically modifying antibody production cell lines for stable, constitutive overexpression of a particular glycosyltransferase gene encoding an enzyme with N-acetylglucosaminyltransferase III (GnTIII) activity (6). The antibodies produced by those cells have an engineered glycosylation pattern and increased ADCC and binding to the activating Fc $\gamma$ RIIIA receptor on immune effector cells. The new molecular variants of the antibody carry special types of oligosaccharides that are not synthesized by the standard cell lines used for antibody production in the biotechnology and pharmaceutical industries, but that can be found at relatively low levels in natural antibodies in humans and at higher levels in other human glycoproteins. The glycoengineered antibodies are highly enriched (at levels much higher than those found in nature) in glycosylation variants carrying bisected oligosaccharides, including both bisected, core-fucosylated and bisected, non-fucosylated, the second ones resulting from competition between recombinant GnTIII and the endogenous fucosyltransferase (6). Such glycoengineered antibodies have increased binding affinity to the activating Fc $\gamma$ RIII receptor on immune effector cells and increased ADCC.

By introducing a stable genetic modification to the antibody-producing cell line, large increases in potency of whole antibodies can be obtained while maintaining a simple production process that lacks chemical-conjugation and extra purification steps. Although a regulated expression system was used initially for proof-of-concept, the technology normally employs standard constitutive promoters. Industrial antibody production cell lines have been engineered by this approach. GlycoMAB conserves the bivalent target-binding nature and long serum half-life of antibodies and do not use toxic, immunogenic or radioactive moieties that can lead to higher side effects, elevated production costs or complex logistics from production to administration to patients.

Standard antibody production cell lines (CHO and mouse myeloma cells) were engineered for GnTIII overexpression and therapeutic antibody production. The antibodies included an antihuman neuroblastoma antibody (Fig. 1), an anti-renal carcinoma antibody (Fig. 2), and the anti-CD20 antibody with identical sequence to rituximab (Fig. 3). In all three cases, large increases in ADCC activity (measured ex-vivo with human tumor cell lines and immune effector cells freshly isolated from blood donors) were obtained.

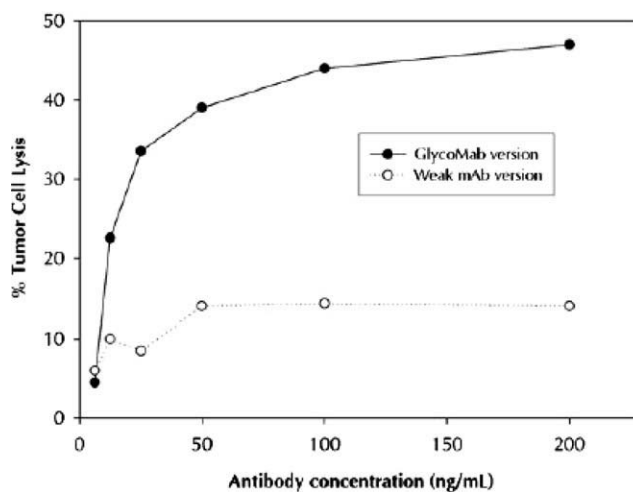


Figure 1. Increased ADCC of glycoengineered anti-neuroblastoma antibody. A chimeric IgG1 that binds to an isoform of L1-CAM expressed in human neuroblastoma cells was produced in CHO cells engineered for GnT-III overexpression. The unmodified and GlycoMAB-modified versions of the antibody were compared in an ex-vivo assay for ADCC using a human neuroblastoma cell line as a target (T) and peripheral blood mononuclear cells (PBMC) as effectors (E). An E:T ratio of 19:1 was used.

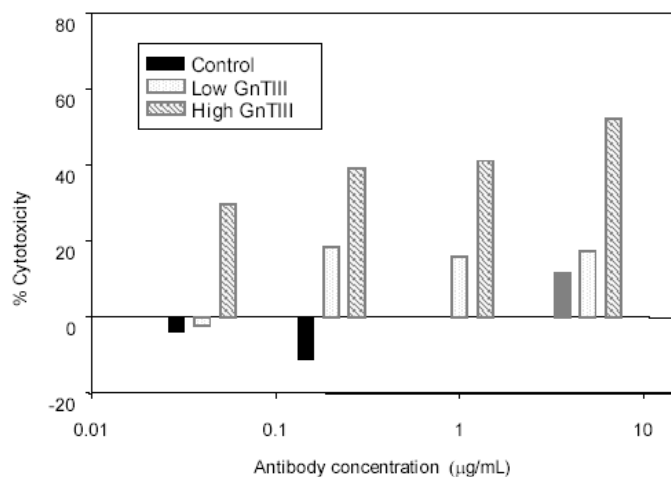


Figure 2. Increased ADCC of anti-renal carcinoma antibody. An industrial SP2/0-mouse myeloma cell line producing a chimeric anti-tumor IgG1 was engineered for GnTIII overexpression. Engineered cells with low and high levels of GnTIII overexpression were isolated and antibodies produced by these cells were compared in ADCC activity with the original unmodified antibody. A large increase in ADCC activity was observed at the higher levels of GnTIII overexpression. Assay conditions were: E:T of 25:1, 4 h incubation, PBMCs as effectors.

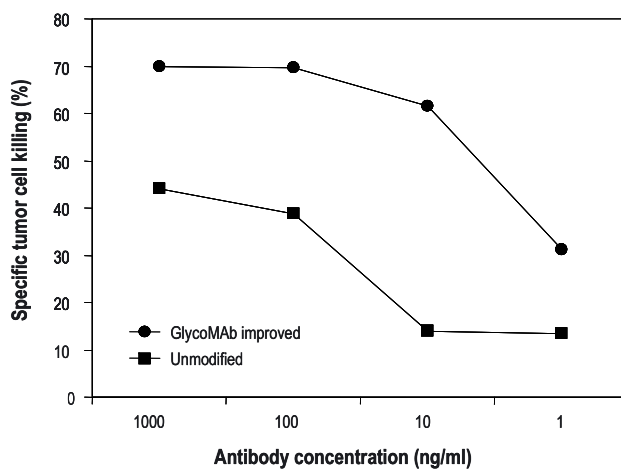


Figure 3. ADCC activity of anti-CD20 IgG1 improved via GlycoMAb technology. A chimeric IgG1 with identical protein sequence to rituximab was produced in cells engineered for GnT-III overexpression leading to high levels of bisected, non-fucosylated oligosaccharides in the antibody Fc-region. PBMCs were used as effectors, human lymphoma SKW6.4 cells were used as targets at a E:T ratio of 30:1 in a 4 h assay.

The correlation found in lymphoma patients receiving rituximab between efficacy and the homozygous higher-affinity Fc $\gamma$ RIIIA receptor genotype (4, see above) gives an indication of the impact that enhanced Fc-FcR interactions could potentially have on the outcome of anti-tumor antibody therapy. This was the single parameter found to correlate with the vastly enhanced objective response rate and the molecular responses. Modification of therapeutic IgG1s with GlycoMAb leads to increased binding for the Fc- Fc $\gamma$ RIIIA interaction (Fig. 4). The next step in the validation of this glycoengineering technology is to find out in non-human primates, and eventually in humans, how the obtained increase in receptor binding and ADCC translate into increased efficacy.

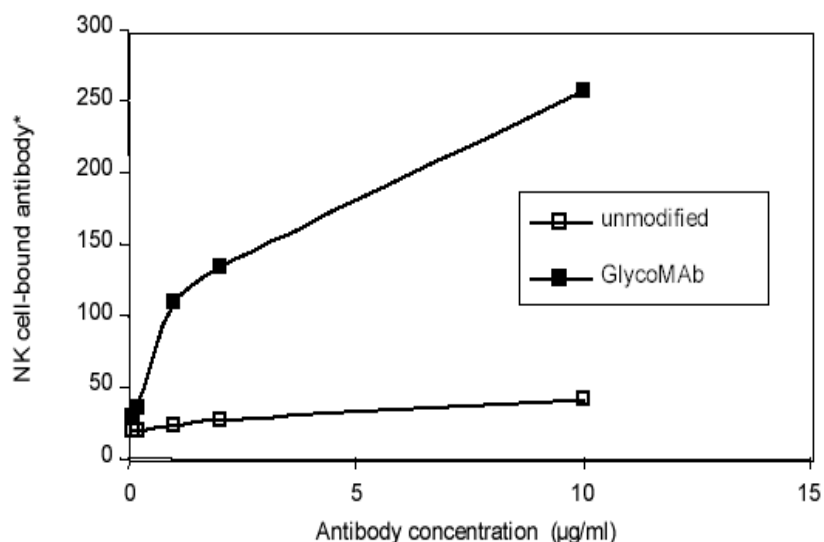


Figure 4. Binding of anti-CD20 antibodies to activating Fc $\gamma$ RIIIA receptor on human natural killer cells. Anti-CD20 antibodies (un-modified and glycoengineered versions) were incubated with freshly-isolated human NK cells. (\* Proportional to mean fluorescence by FACS analysis using an FITC-labeled anti-human IgG Fab).

## REFERENCES

1. J. Lab. Clin. Med. (1999) 134: 445.
2. Nat. Med. (2000) 6: 443.
3. P.N.A.S. USA (2000) 97: 7503.
4. Blood (2002) 99: 754.
5. Glycobiology (1995) 5: 813.
6. Nat. Biotechnol. (1999) 17: 176.
7. J. Biol. Chem. (2002) 277: 26733.

## QUESTIONS AND ANSWERS

**Meijia Yang, Serono Reproductive Biology Institute, US:**

Since you are adding another branch of sugar in your molecule, in terms of regulation, is it considered a complete new molecule, since you are introducing significant change to its activity, and therefore you need to go through new clinical trials and so on ?

**Pablo Umana, GlycArt Biotechnology AG, Switzerland:**

Yes, we believe that if you are significantly increasing the potency of the molecule, we imagine you would have to re-do the trials. So, this is best applied to molecules that are just at the pre-clinical stage.

**Steven Charmow, Abgenix, US:**

Nice talk. I want to focus on what you said about the correlation between an increase in GnTIII activity with a decrease in fucosyltransferase activity, so that the presence of bisecting GlcNAc necessitates a lower level of core fucose. I think there is evidence in the literature, particularly from a group in Japan that a decrease in core fucose without an increase in bisecting GlcNAc generates the same effect. Are you familiar with these results ?

**Pablo Umana, GlycArt Biotechnology AG, Switzerland:**

Thanks for bringing that up, I did not have enough time to go into a lot of detail. Basically what we have seen is that in the context of bisected oligosaccharides, removing the fucose also has a very big impact on the increase of the Fc receptor binding and in biological activity, so, basically the same thing that has been described by the group in Japan. For the non-bisected oligosaccharides, the same thing can be extrapolated. When you overexpress GnTIII, you always produce a little bit of bisected non-fucosylated oligosaccharides. What we can say solidly is that if you overexpress GnTIII to a level where you have high amounts of bisected non-fucosylated oligosaccharides, then you have a much bigger increase in the ADCC activity. So, we think the family of bisected oligosaccharides, removing the fucose has a much bigger effect than just having the bisecting GlcNAc.

LINK T<sup>1</sup>, ESSERS R<sup>1</sup>, ZÖRNER K<sup>1</sup>, GÄTGENS J<sup>1</sup>, DE GRAAF A,<sup>2</sup>  
BACKSTROM M<sup>3</sup>, HANSSON G<sup>3</sup> AND NOLL T<sup>1</sup>

## DEVELOPMENT OF A METABOLICALLY OPTIMIZED FERMENTATION PROCESS BASED ON GLUCOSE- LIMITED CHO PERFUSION CULTURE

<sup>1</sup> *Research Center Jülich, IBT-2, Germany* <sup>2</sup> *METabolic Explorer S.A.,  
Biopôle Clermont-Limagne, Saint-Beauzire, France* <sup>3</sup> *Department of Medical  
Biochemistry, University of Gothenburg, Gothenburg, Sweden*

**Abstract.** Many researchers are interested in glucose-limited perfusion culture in order to improve cellular metabolism towards more efficient substrate consumption and reduced production of cytotoxic metabolites (e.g. lactate).

We developed a highly reproducible glucose-limited perfusion process using a recombinant CHO cell line producing human MUC-1 glycoprotein (currently under evaluation for immunotherapy of breast cancer) in a standard stirred vessel bioreactor with cell retention by spin filter using serum-free culture medium. The strategy is easy to perform and does not need any online glucose or other invasive measurement making the process highly stable against disturbances. Using this strategy, glucose consumption rate decreases, glucose concentration in the bioreactor drops and remains below detectable levels and the cells do not longer produce any lactate, while cell specific productivity and space time yield increase 5fold and 4fold respectively (250 mg/L/day). Cell density remains very high at  $1-2 \cdot 10^7$  cells/mL. Process time can easily be extended to more than 1000 hours. The glycosylation of the product is unaffected as shown by glycoanalysis.

Preliminary results from metabolite quantification by LC-MS and from <sup>13</sup>C-lactate feeding experiments prove a switch in metabolism towards an increased TCA-cycle activity and indicate that gluconeogenesis takes place. Confirmation experiments are underway.

This strategy has already been transferred successfully to a second recombinant CHO cell line secreting another human Mucin. Other CHO cell lines producing an enzyme and a humanized antibody and a murine hybridoma cell line are under investigation.

### 1. INTRODUCTION

Mammalian cells are of increasing interest for the production of therapeutic proteins and vaccines especially if correct posttranslational modifications (e.g. glycosylation) is required for functionality.

In the last decades intensive research has been done to improve the low efficiency of mammalian cell culture which is mainly caused by slow growth, low cell densities and low cell specific productivity compared to microorganisms. One interesting approach is the manipulation of the cellular metabolism by controlled feeding aiming at a reduced production of toxic and inhibiting metabolites.

Especially lactate is cited as one of the factors that inhibit cell growth and limit the maximum cell density and product concentration in the culture. As the metabolism of glucose is greatly affected by its concentration (at high glucose levels about 70-95% of of the glucose consumed is converted to lactate) a number of feeding strategies in fedbatch and continuous fermentations have been developed to maintain the residual glucose concentration at low levels. In most cases this results in an increase in maximum cell density and therefore in maximum product concentration as the cell specific productivity remains constant. To our knowledge there is only one example of chemostatic hybridoma fermentation where a strong increase in cell specific productivity has been observed.

Most of the techniques applied for maintaining glucose concentrations on very low levels include online glucose analysis or other invasive analysis which are susceptible to troubles limiting the industrial applicability of these techniques. That makes the development of a strategy for glucose-limited perfusion culture which is easy to perform and stable against disturbances highly desirable. It has also to be ensured that the glycosylation pattern of the product is unaffected by the glucose-limitation.

## 2. MATERIALS AND METHODS

- Cells and product: CHO-K1 cells producing a fusion protein of human MUC-1 fused to the Fc part of an IgG antibody. The product which is expressed under the control of a CMV promotor has a molecular weight of 170 kDa and contains 80 potential O-glycosylation sites.
- Culture medium: ProCHO-IV (Biowhittaker) with additional buffering using 20 mmol/L NaHCO<sub>3</sub>.
- Fermentation system: 2L stirred vessel bioreactor (Applicon Biotek) with a working volume of 1L equipped with a propeller stirrer (200 rpm), bubblefree aeration and cell retention by using a spin filter (75 µm). The pH and the dissolved oxygen concentration were controlled at 7.2 and 40% of air saturation, respectively.
- Analysis: Samples were taken every 24 hours and cell concentration and viability were estimated using hemacytometer and trypan blue exclusion. Glucose and lactate concentration were determined using automatic enzymatic analysors (EBIO compact, Eppendorf and YSI 1500L, Yellow Springs). Product quantity was estimated by ELISA and product integrity analysed by SDS-Page. The glycosylation of the product was determined by LS-ESI mass spectrometry.

3. RESULTS

3.1 High glucose perfusion culture

After adapting the CHO cells which originally grew adherently in IMDM culture medium containing 10% FCS to suspension culture in protein-free medium and optimizing the most relevant fermentation parameters a cell density of  $3 \cdot 10^7$  mL<sup>-1</sup> and a space-time-yield of nearly 100 mg/L/d were obtained. The SDS-Page showed that only a few number of proteins is present in the supernatant with the product being the main one, easing the downstream processing (fig.1).

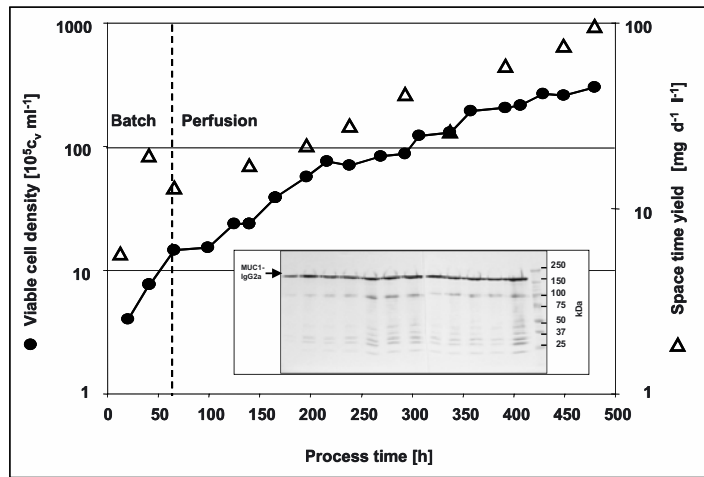


Figure 1. cell concentration, space time yield and SDS-Page during continuous high glucose fermentation

The perfusion rate was increased during the fermentation to avoid limiting levels in glucose and glutamine concentration (fig.2). Despite the high perfusion rate of 0.155 h<sup>-1</sup>, lactate accumulated to relatively high concentrations indicating that most of the glucose consumed is converted to lactate (fig.3).



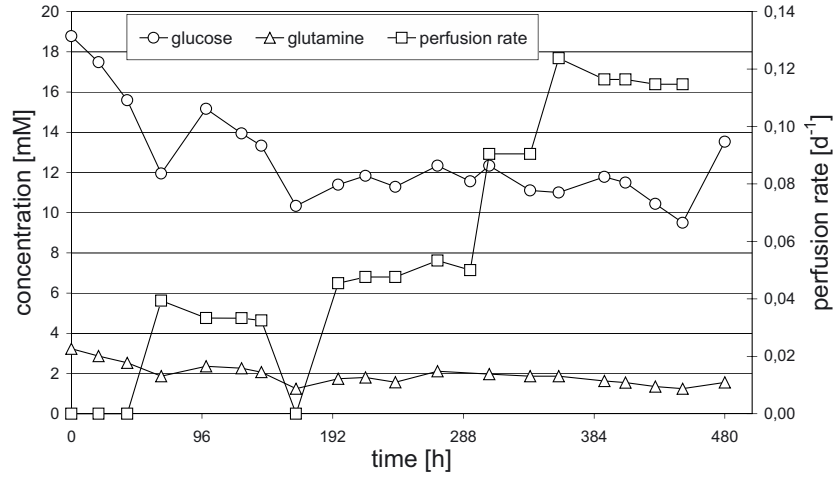


Figure 2. Perfusion rate, glucose and glutamine concentration during continuous high glucose fermentation

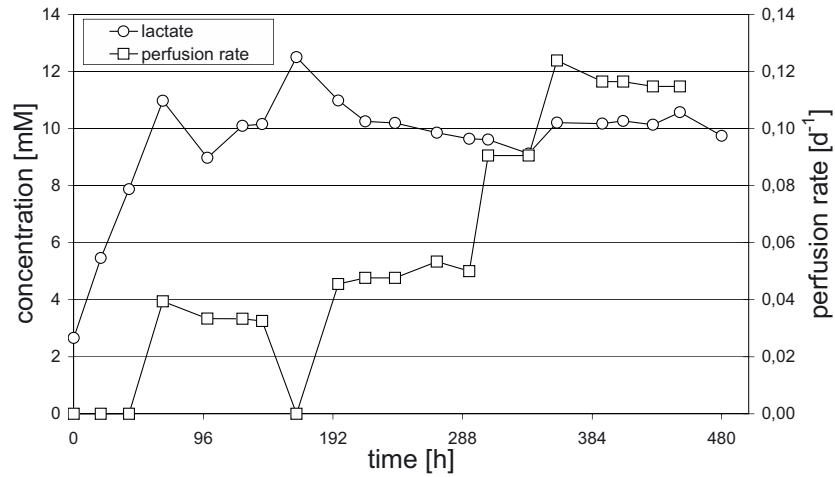


Figure 3. Perfusion rate and lactate concentration during continuous high glucose fermentation

### 3.2 Low glucose perfusion culture

To maintain very low glucose levels without using online glucose analysis or other invasive techniques, a constant perfusion rate was adjusted at 25% of the maximum perfusion rate in the high glucose fermentation (fig.4).

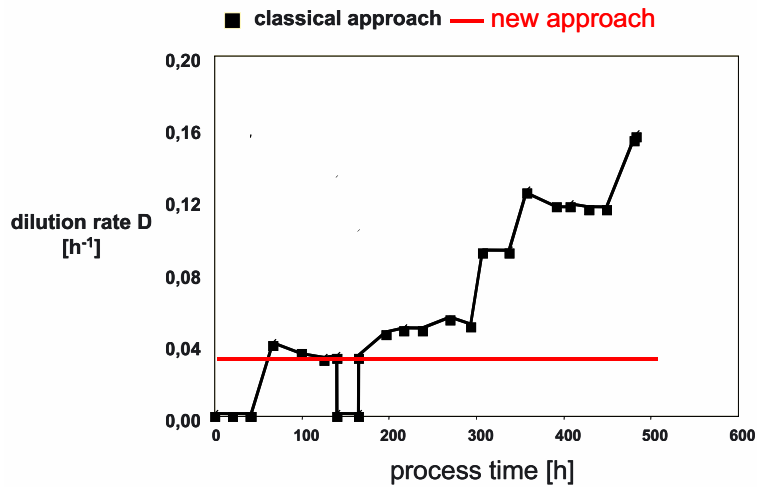


Figure 4. Comparison of perfusion rates during continuous high and low glucose fermentations

Using this strategy the glucose consumption rate decreases, the residual glucose concentration fell below detection levels and the cells did not produce any lactate (fig.5). Simultaneously, the cell specific productivity increases by >200% and as the cell density decreases only slightly ( $1-2 \cdot 10^7/\text{mL}$ ), the space time yield was increased by >100% (up to 250 mg/L/d) (fig.6). A process time of more than 30 days could be realised without any problems.

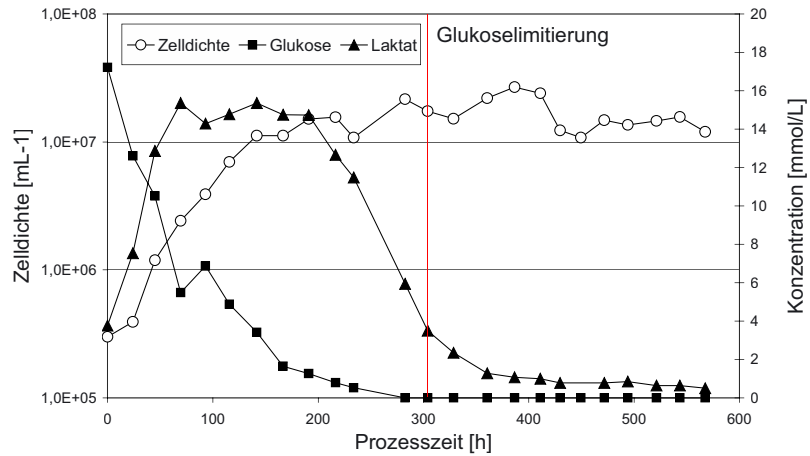


Figure 5. Cell concentration, glucose and lactate concentration during continuous low glucose fermentation

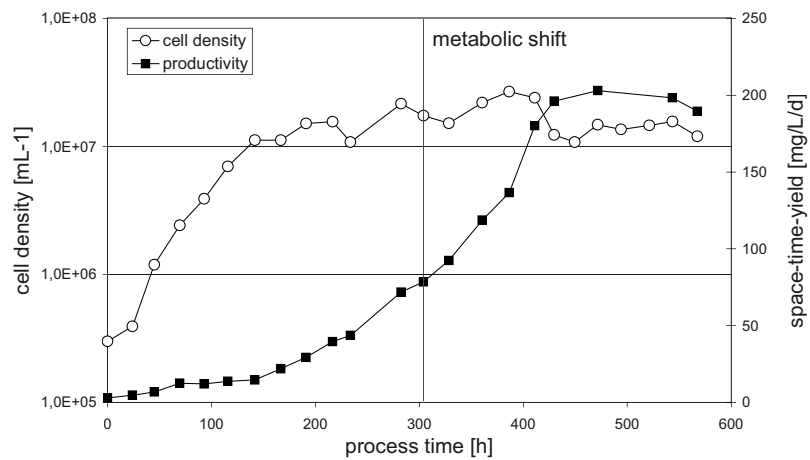


Figure 5. Cell concentration, glucose and lactate concentration during continuous low glucose fermentation

The increase in cell specific productivity started when the degree of glucose limitation (ratio between the current specific glucose uptake rate and the maximum specific glucose uptake rate) decreases below 0.4 (fig.6).

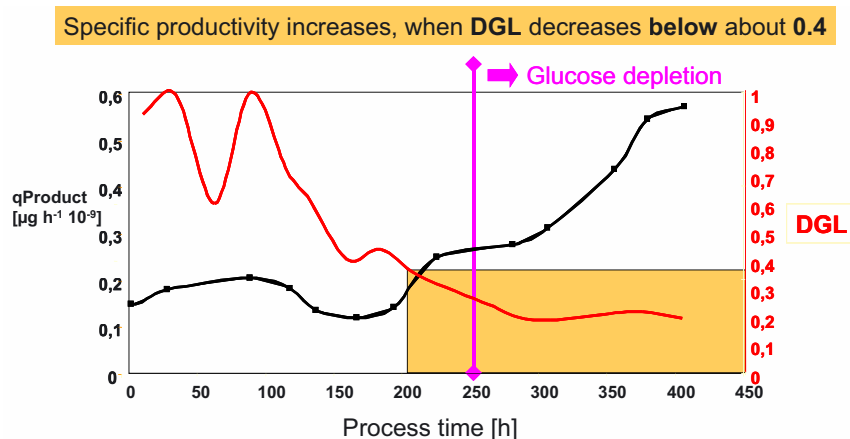


Figure 6. Degree of glucose limitation (DGL) and cell specific productivity during low glucose fermentation

Most important, the glycosylation of the product remains unaffected (glycostructures and site occupancy). First metabolite balancing and results from a  $^{13}\text{C}$ -Lactate feeding experiment show an increased TCA cycle activity and indicate that gluconeogenesis takes place.

This strategy could already be transferred successfully to another recombinant CHO cell line producing a second human mucin. Other CHO cell lines producing an enzyme and an antibody, respectively are currently under investigation.

#### 4. SUMMARY

- Development of a CHO perfusion process for the production of a highly glycosylated protein at very low glucose levels
- increase in cell specific productivity >200% and space time yield >100%
- product integrity and glycosylation remain unaffected

#### 5. AFFILIATIONS

T.Link, R. Essers, K.Zörner, J. Gägens and Thomas Noll, Institute of Biotechnology 2, Research Center Jülich, 52425 Jülich, Germany, [TH.NOLL@FZ-JUELICH.DE](mailto:TH.NOLL@FZ-JUELICH.DE)  
 A.de Graaf, METabolic EXplorer S.A., Biopôle Clemont-Limage, F-63360 Saint-Beauzire  
 M.Bäckström and G.Hansson, Department of Medical Biochemistry, University of Gothenburg, S-41390 Gothenburg

## QUESTIONS AND ANSWERS

**Otto Merten, Genethon, France:**

Thank you for your interesting presentation. Did you consider the use of other sugars that are metabolized differently than glucose ?

**Thomas Noll, Research Center Julich, Germany:**

No, not yet, that is a very important point. I think the first to be checked will be fructose. It is a very interesting thing.

**Dirk Lutkemeyer, University of Bielefeld, Germany:**

I have a question regarding the cell retention. You mentioned a spin filter with a 75  $\mu\text{m}$  mesh size. Can you comment on the retention rate and on the media composition ? Do you have proteins in the media ?

**Thomas Noll, Research Center Julich, Germany:**

The retention efficiency was between 85-90 %, that is quite OK. We first used a spin filter with 20  $\mu\text{m}$ , but that tends to block after about 200 hours, so we switched to the 75  $\mu\text{m}$  version. Regarding the medium, it is completely free of animal components, there is one recombinant protein in it, but I should not disclose the details since it is a proprietary medium.

CHETAN GOUDAR<sup>1,2</sup>, RICHARD BIENER<sup>3</sup>, JAMES MICHAELS<sup>1</sup>,  
CHUN ZHANG<sup>1</sup>, JAMES PIRET<sup>2</sup> AND KONSTANTIN  
KONSTANTINOV<sup>1</sup>

## APPLICATIONS OF QUASI REAL-TIME METABOLIC FLUX ANALYSIS IN MAMMALIAN CELL CULTURE PROCESS DEVELOPMENT

<sup>1</sup>*Bayer HealthCare, Biological Products Division, 800 Dwight Way,  
Berkeley, CA 94710*

<sup>2</sup>*Department of Chemical and Biological Engineering, University of British  
Columbia, Vancouver, BC Canada V6T 1Z3*

<sup>3</sup>*Bayer AG Technology Services, Process Analysis, 51368, Leverkusen,  
Germany*

**Abstract.** Metabolic flux analysis offers a means of quantifying changes in cellular physiology and metabolism and thus has the potential to play an important role in accelerating bioprocess development towards optimizing protein productivity. Most implementations of MFA to date have been of an off-line nature while to be most useful for on-line process diagnosis and control, effectively real-time estimation of metabolic fluxes is necessary. We have developed a framework that allows for quasi real-time estimation of metabolic fluxes for mammalian cells in high-density perfusion cultures by using a combination of on-line and rapid off-line measurements of experimental variables. The above approach was used on experimental data obtained from long-term perfusion experiments with CHO cells at  $\sim 20 \times 10^6$  cells/mL. Metabolic fluxes were estimated for various steady states over the course of the experiment resulting in useful information on the changes in cellular physiology and metabolism in response to changes in bioreactor conditions. The approach we present allows for robust estimation of metabolic fluxes in a quasi real-time fashion and has the potential to accelerate bioprocess development by reaching desired protein yields with fewer experiments.

### 1. INTRODUCTION

Mammalian cells are widely used for the production of therapeutic proteins that require their ability to effectively fold and glycosylate proteins. However, productivities from typical mammalian cell processes are low and a variety of approaches have been taken to overcome this limitation. These include bioprocess engineering of perfusion culture reactors to  $20 \times 10^6$  cells/mL cell densities (Konstantinov et al., 1994; Trampl et al., 1994), and developing improved feeding strategies to optimize cellular metabolism (Glacken et al., 1989; Zhou et al., 1997). Another tool for productivity engineering is metabolic flux analysis (MFA) which determines carbon fluxes in the central carbon metabolism and related pathways

(Bonarius et al., 1995; Nyberg et al., 1999; Stephanopoulos and Vallino, 1991; Zupke et al., 1995). MFA provides insights into cellular metabolism, especially under varied environmental bioreactor conditions, rapidly clarifying cellular responses to culture conditions that can influence productivities.

Most applications of metabolic flux analysis to date have been of an off-line nature which limits the impact that such an analysis can have on bioprocess development. To fully realize the potential of MFA for bioprocess diagnostics and decision-making, real-time metabolic flux information should be coupled with automated process control strategies to more rapidly optimize bioreactor operation.

In the present study, we present a framework for a quasi real-time metabolic flux analysis (QRT-MFA) system and illustrate its application for studying the metabolism of Chinese hamster ovary (CHO) cells in high cell-density perfusion culture. Specifically, the effect of changing basic process control variables such as pH, DO and temperature on cellular metabolism was studied and this was used to examine the operating ranges for these variables. Upon transfer of the developed process to the manufacture of a licensed product, this information can be readily used during validation efforts and for defining operating ranges for the bioprocess.

## 2. MATERIALS AND METHODS

### 2.1. Cell Line, Culture Medium and Bioreactor Operation

CHO cells were grown in perfusion culture in 15-L bioreactors (MBR Bioreactor AG, Switzerland) with 12 L working volume and a heated water jacket. The bioreactor was maintained at 37°C, with agitation constant at 40 rpm. Dissolved oxygen (DO) was maintained at 50% air saturation by sparging mixed oxygen and nitrogen. Bioreactor pH was maintained at 6.8 by the addition of 0.3 M NaOH. The bioreactor was inoculated at  $1.0 \times 10^6$  cells/mL and cell concentrations during the experiment were maintained at  $20 \times 10^6$  cells/mL by automatically bleeding cells from the bioreactor based on optical density measurements. The bioreactors were operated in a perfusion mode by continuously withdrawing reactor fluid and passing it through a cell separation device. The cells were recycled back to the bioreactor while the clarified liquid was harvested for subsequent purification steps to isolate the protein of interest.

### 2.2. Analytical Methods

Samples from the bioreactor and the harvest stream were taken daily for cell density and viability analysis using a hemacytometer and the trypan blue dye-exclusion method. These samples were then centrifuged in a Beckman CS-6 centrifuge (Beckman Coulter, CA) and the supernatant analyzed for nutrient and metabolite concentrations. Glucose, lactate, glutamine and glutamate concentrations were determined using a YSI Model 2700 analyzer (Yellow Springs Instruments,

OH) while ammonia was measured using an Ektachem DT60 analyzer (Eastman Kodak, NY). DO and pH were measured online using retractable Ingold electrodes (Ingold Electrodes, MA). The accuracy of these measurements was verified off-line using a Stat Profile 9 blood gas analyzer (Nova Biomedical, MA). The same instrument also measured the dissolved CO<sub>2</sub> concentration. On-line measurements of cell density were made with a retractable optical density probe (Aquasant Messtechnik, Switzerland) calibrated with cell density estimated by the hemacytometer. Amino acids were analyzed on a HP 1090 HPLC (Hewlett Packard, CA) using the AminoQuant protocol (Series II Operator's Handbook) with pre-column derivitization by ortho-phthalaldehyde and 9-fluorenylmethyl chloroformate for detection of primary and secondary amino acids, respectively.

### 2.3. Metabolic Flux Estimation

To obtain metabolic flux estimates in a quasi-real time fashion for on-line physiological state identification, the computation of metabolic fluxes was integrated with on-line data acquisition and process monitoring. Specifically, LabVIEW (National Instruments, TX) was used for on-line data acquisition and process control while all flux calculations were performed using FluxAnalyzer (Klamt et al., 2001) in MATLAB (Mathworks, Natick, MA). Seamless communication between these two environments allowed transfer of specific rate data from LabView to MATLAB followed by subsequent transfer of the computed metabolic fluxes in the reverse direction.

The bioreaction network used in the study was similar to the one proposed by Nyberg et al., 1999 for CHO cells with modifications to include reactions for all amino acids. A series of mass balance equations were written for each of the metabolites in the bioreaction network resulting in

$$\mathbf{Ax} = \mathbf{r} \quad (1)$$

where  $\mathbf{A}$  is the stoichiometric coefficient matrix,  $\mathbf{x}$ , the vector of unknown metabolic fluxes, and  $\mathbf{r}$ , the vector of uptake and production rates. Nutrient consumption and metabolite production rates were incorporated in  $\mathbf{r}$  and intermediate metabolite production rates were assumed to be zero based on the pseudo-steady-state hypothesis (Zupke and Stephanopoulos, 1995). As the stoichiometric matrix,  $\mathbf{A}$ , was not square, and estimation of the metabolic flux vector,  $\mathbf{x}$ , was done using the weighted least squares approach as the matrix  $\mathbf{A}$  was of full rank

$$\mathbf{x} = (\mathbf{A}^T \boldsymbol{\Psi}^{-1} \mathbf{A})^{-1} \mathbf{A}^T \boldsymbol{\Psi}^{-1} \mathbf{r} \quad (2)$$



where  $\Psi$  is the variance-covariance matrix associated with the rate vector  $\mathbf{r}$ .

### 3. RESULTS AND DISCUSSION

#### 3.1. Perfusion Experiment with CHO Cells

The perfusion experiment with CHO cells was conducted over a period of 120 days with 12 different steady states that each lasted for 10 days. The time profiles of viable cell density along with the corresponding steady state information are shown in Figure 1. Viability was greater than 90% for all the steady states presented in Figure 1. Steady states corresponding to  $T=30.5$  °C and  $pH=6.6$  were characterized by lower cell densities as significant reduction in growth rates was seen under these experimental conditions.

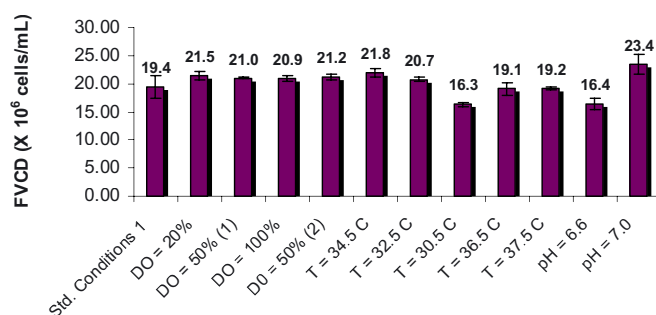


Figure 1. Viable cell densities for the 12 steady states examined in this study. The duration of the entire experiment was 120 days while that of the individual steady states was 10 days.

#### 3.2. Effect of DO on Cellular Metabolism

The DO set point for the process was 50 % air saturation and a lower limit of 20 % and an upper limit of 100 % were examined in this study. These correspond to steady-states 2 and 5 in Figure 1. For both these steady states, no significant changes in glycolytic and TCA cycle fluxes were seen. The magnitudes of most of the amino acid fluxes were also very similar and were comparable to those for the 50 % air saturation condition. Thus no significant changes in cellular metabolism were seen for the three DO concentrations examined in this study.

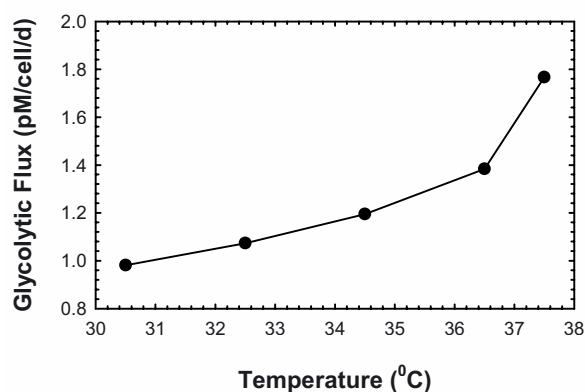


Figure 2. Glycolytic flux as a function of temperature for CHO cells in perfusion culture

### 3.3. Effect of Temperature on Cellular Metabolism

A temperature range of 30.5 – 37.5 °C was examined in this study. As expected, cellular growth and metabolic rates increased with higher temperatures and this manifested as increased glycolytic and TCA cycle fluxes (Figure 2). Specific productivity however, was inversely related to temperature as the lowest temperatures resulted in the highest protein production.

### 3.4. Effect of pH on Cellular Metabolism

The pH set point for the process was 6.8 and a lower limit of 6.6 and an upper limit of 7 were examined in this study (steady states 11 and 12 in Figure 1). A 39 % increase in glycolytic flux was seen at pH = 6.8 when compared to that at pH = 6.6 while a 146 % increase was seen when the pH value was 7.0. It is hypothesized that this is due to the enzyme phosphofructokinase which is strongly influenced by pH. The effect of pH on the fluxes at the pyruvate branch-point was also examined and the results are presented in Figure 3. The fluxes shown in Figure 3 include the pyruvate flux into the TCA cycle, the pyruvate flux to lactate and the pyruvate flux to  $\alpha$ -ketoglutarate expressed as a percentage of the flux entering pyruvate. No significant changes in the percentage values of these fluxes is seen suggesting that despite an increased glycolytic flux at elevated pH, the flux distribution at the pyruvate branch-point is unaffected.

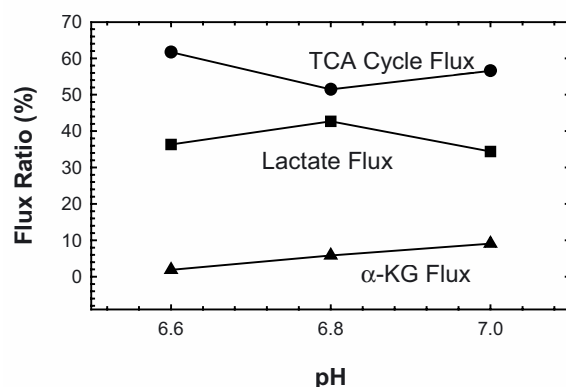


Figure 3. Flux distribution at the pyruvate branch-point for varying pH values

#### 4. CONCLUSIONS

We have illustrated application of QRT-MFA for studying the effect of changes in DO, temperature and pH on cellular metabolism for CHO cells cultivated in perfusion culture. Rapid estimation of metabolic fluxes was possible through seamless integration of the process control and metabolic flux computation environments. Changes to DO in the 20 – 100 % air saturation range had no effect on cellular metabolism as seen from the unchanged magnitudes of most fluxes in the bioreaction network. Higher temperatures were accompanied by increased cellular growth and metabolic rates whereas specific protein productivity decreased with increasing temperature. Increases in pH significantly increased the flux through glycolysis while the flux distribution at the pyruvate branch-point remained largely unchanged despite changes in the glycolytic flux. The approach presented in this study allows for rapid quantification of cellular metabolism and the insights gained from this study will be valuable during transfer of the fully developed bioprocess for manufacturing the licensed product.

#### 5. REFERENCES

1. Bonarius, H.P.; de Gooijer, C.D.; Tramper, J.; Schmid, G. Determination of the respiration quotient in mammalian cell culture in bicarbonate buffered media. *Biotechnol. Bioeng.* **1995**, *45*, 524-535.
2. Glacken, M.W.; Huang, C.; Sinskey, A.J. Mathematical description of hybridoma culture kinetics. III. Simulation of fed-batch reactors. *J. Biotechnol.* **1989**, *10*, 39-66.
3. Klamt, S.; Kremling, A.; Gilles, E.D. "FluxAnalyzer: A graphical interface for stoichiometric and quantitative analysis of metabolic networks."; 8th International Conference on Computer Applications in Biotechnology, 2001, Quebec City, Canada.

4. Konstantinov, K.; Chuppa, S.; Sajan, E.; Tsai, Y.; Yoon, S.; Golini, F. Real-time biomass-concentration monitoring in animal-cell cultures. *Trends Biotechnol* **1994**, *12*, 324-33.
5. Nyberg, G.B.; Balcarcel, R.R.; Follstad, B.D.; Stephanopoulos, G.; Wang, D.I. Metabolism of peptide amino acids by Chinese hamster ovary cells grown in a complex medium. *Biotechnol Bioeng* **1999**, *62*, 324-35.
6. Stephanopoulos, G.; Vallino, J.J. Network rigidity and metabolic engineering in metabolite overproduction. *Science* **1991**, *252*, 1675-1681.
7. Trampl, F.; Sonderhoff, S.A.; Pui, P.W.; Kilburn, D.G.; Piret, J.M. Acoustic cell filter for high density perfusion culture of hybridoma cells. *Bio/Technology* **1994**, *12*, 281-284.
8. Zhou, W.C.; Rehm, J.; Europa, A.F.; Hu, W.S. Alteration of mammalian cell metabolism by dynamic nutrient feeding. *Cytotechnology* **1997**, *24*, 99-108.
9. Zupke, C.; Sinskey, A.J.; Stephanopoulos, G. Intracellular flux analysis applied to the effect of dissolved oxygen on hybridomas. *Appl. Microbiol. Biotechnol.* **1995**, *44*, 27-36.
10. Zupke, C.; Stephanopoulos, G. Intracellular flux analysis in hybridomas using mass balances and In Vitro <sup>13</sup>C NMR. *Biotechnol. Bioeng.* **1995**, *45*, 292-303.

#### QUESTIONS AND ANSWERS

**Sadettin Ozturk, Centocor, US:**

At low pH I guess, there are lots of lactate coming from glutamine, could you differentiate how much lactate is coming from glutamine and how much from glucose ?

**Chetan Goudar, Bayer, US:**

Most of the lactate in this system is coming from glucose, almost 80 to 90 % of lactate is coming from glucose.

**Sadettin Ozturk, Centocor, US:**

Even at a low pH ?

**Chetan Goudar, Bayer, US:**

Yes, we did not see a significant shift.

**Sadettin Ozturk, Centocor, US:**

How can you tell whether that lactate is coming from glucose or from glutamine ?

**Chetan Goudar, Bayer, US:**

I am not showing all the fluxes in this talk, just the major ones, but there are about 95 reactions in the network, and we can look at the other fluxes which link glutamine to lactate.

**Steven Charmow, Abgenix, US:**

This is an steady-state system, where you are going from 3 to 7 months. What does determine how long a run goes ?

**Chetan Goudar, Bayer, US:**

Ideally we would like to run this forever, but what typically happens is that when you are running the system for 2 to 3 months you observe a decline in productivity.

**Steven Charmow, Abgenix, US:**

Why?

**Chetan Goudar, Bayer, US:**

Because your protein expression is not stable. In the cell lines we have, after 2 to 3 months, you can observe 30 to 40 % drops in productivity.

**David Jayme, Invitrogen, US:**

Is your system able to provide any advance warning when the cells might be becoming unstable in terms of their production, even though most of these major metabolic fluxes are still constant ?

**Chetan Goudar, Bayer, US:**

This is what I was planning to show in the animation that did not really work, but what you can do is to have a map of the flux distribution at a given physiological state, and if you observe shifts in the distribution, and if they are not desirable, you can make appropriate process changes. This is where the real value is. Regarding the loss of productivity, normally you have to look at the titers of the product, but if there is some way that you can correlate productivity to your metabolic fluxes, then you could use the changes in the fluxes to know if you are going in a given direction.

C. CUNHA-BAKEEV<sup>1</sup>, J. GLASSEY<sup>1</sup>, G. MONTAGUE<sup>1</sup>,  
M. AL-RUBEAI<sup>2</sup>, P. HARDWICKE<sup>3</sup>

## DATA-BASED MODELLING OF CELL CULTURES

<sup>1</sup> *School of Chemical Engineering and Advanced Materials, University of  
Newcastle, Newcastle upon Tyne, NE1 7RU, UK*

<sup>2</sup> *School of Chemical Engineering, The University of Birmingham,  
Birmingham, UK*

<sup>3</sup> *GSK, STEVENAGE, UK*

**Abstract.** The ever expanding use of animal cell cultures for production of valuable therapeutic products has highlighted the importance of effective control and optimisation. Whilst data-based modelling techniques proved to be a valuable tool in microbial processes for such a purpose, they have yet to be investigated in detail for animal cell cultures. This contribution investigates how successfully well-established data-based techniques can describe the process behaviour given the limited amount of data available. Numerical techniques are developed and tested in an attempt to overcome problems of limited data. It is shown that cross-validation and bootstrapping in particular improve the estimation of most of the process parameters. Cell cycle information included in the model development improved the estimation of the specific growth and production rates. This raises the possibility of using these estimates in a mechanistic model used to infer cell count and product concentration.

### 1. INTRODUCTION

The expanding use of animal cell cultures in pharmaceutical industry demands better monitoring and control schemes in order to obtain high productivity, while minimising the production costs. Past experience with microbial processes demonstrated that an accurate process model is an important component of an improved process control scheme. Successful attempts to model different cell lines have been presented in the literature using fundamental process knowledge<sup>1-2</sup> but this is not always available, particularly when dealing with industrial data.

Linear and non-linear data based modelling techniques have been widely applied for the monitoring, control and optimisation of microbial processes. In particular, artificial neural networks have been shown to provide satisfactory estimates of process parameters that are difficult to obtain on-line<sup>3</sup>. They can subsequently be used for improved supervision<sup>4</sup>, optimisation<sup>5</sup> and control<sup>6</sup>. However, the application of these techniques for modelling animal cell cultures remains limited.

The present work aims to investigate the application of data-based modelling methods to estimate important state variables of different cell lines. Such an estimate would allow important process decisions to be taken. In the first case study the model will provide estimation of parameters to improve the substrate feed regime. In the second case study, the estimated values will provide important information about the state of the cultivation and allow the optimisation of the infection procedure.

Also this will allow the scientists to operate the cultivation in such a way that the productivity can be optimised. Clearly, these objectives are critical from an industrial point of view and reflect the importance of a study of this type.

A Radial Basis Function (RBF) neural network was used for model development in both case studies. It is rapid to train, offers locally based non-linear responses and provides the ability to calculate confidence limits on the predictions if required<sup>7-8</sup>. A problem encountered during model development was the limited number of batches. Data augmentation techniques, noise addition and bootstrapping were used to generate 'new batches'. In addition, cross validation was used to determine the best training data set and model without increasing the size of the data set.

The data use in this work consisted of a set of batches of CHO cell cultivations producing INF- $\gamma$  obtained from Birmingham University and batches of insect cell cultivations obtained from GSK. These two data sets were modelled separately, taking into account the differences in the processes and available measurements.

## 2. METHODOLOGY

### 2.1. RBF artificial neural networks

The term "Artificial Neural Networks" originated from attempts to model and understand how the human brain works<sup>9</sup>. A Radial Basis Function (RBF) neural network consists of three layers of nodes interconnected in a feedforward manner. The first layer distributes the input data into the hidden layer containing the RBF units, which are non-linear transfer functions that calculate the outputs. Finally, the output layer gives the process parameter values predicted by the network<sup>10</sup>.

Neural networks "learn" from the information that is presented, and thus a suitable training data set is required. This selection is usually accomplished by using process knowledge<sup>8</sup>, but also depends on data availability. The data matrix is separated into a *training* set (for model development), a *test* set (to determine the most appropriate network structure) and *validation* set (to assess the model efficiency on independent data). The identification of the best network structure and the efficiency of the RBF model can be assessed by calculating the error between the actual and predicted values expressed as the Root Mean Squared Error (RMSE).

### 2.2. Data augmentation / Cross validation

Data augmentation techniques are used to increase a limited data set in order to improve the quality and robustness of data-based models. In the present work, two different methods of data augmentation were used, namely noise addition and bootstrapping. In the noise addition method<sup>11</sup>, a random number matrix is generated from a normal distribution, taking into account the variance of each variable. This matrix is then added to the original data to provide a new data set. The bootstrapping technique consists of taking random samples of the original data set<sup>12</sup>. These samples are then replaced in the data matrix to obtain a new data set.

In contrast, cross validation does not increase the data set. Instead, the data set is divided into subsets removing one for testing. This process is repeated until all

subsets have been left out for testing once. In this way, it is possible to determine the most suitable training data resulting in the best performing model as assessed by the RMSE achieved on the testing set.

### 3. DATA AVAILABILITY

#### 3.1. CHO cell culture

Five batches of the culture of a recombinant CHO 320 cell line were available for the present study. Each of these batches was initialised with a different concentration of foetal calf serum (FCS), namely, 1%, 2.5%, 5%, 7.5% and 10%. The detailed description of this process was presented elsewhere<sup>13</sup>. Off-line measurements were available for viable cell density and glucose, ammonia, lactate and product concentrations. In addition, the percentage of the cells in different cell cycle phases (G1, S, G2) were also available. The viable cell density and the product concentration were used as outputs. The specific growth rate ( $\mu$ ) and the specific production rate ( $q_P$ ) were calculated and used as additional outputs.

#### 3.2. Insect cell/baculovirus expression system

Twenty-one batches were available from the production of a recombinant protein by a baculovirus expression vector system in insect cells. The insect cells are cultivated until a certain cell count is achieved. The culture is then infected by a baculovirus containing the gene coding for the desired recombinant protein. Additional information about this process has been published previously<sup>14</sup>.

A number of measurements were available: respiration activity, pH, glucose, lactate, cell count and cell viability. The culture stages prior and post infection were modelled separately, using cell count and cell viability as their respective outputs. The cell count was considered the most important parameter to estimate prior to infection since its estimate will allow the optimisation of the infection procedure. In the post infection stage the cell viability is critical to achieve high productivity.

## 4. RESULTS

#### 4.1. CHO culture

From the five batches available, one was assigned to be the independent validation data set leaving four for model development/selection of structure. The data augmentation techniques were applied to the data set used for model development, but the resulting model compared on the same set. This was also the case for cross validation. Fig. 1 shows the summary of the lowest prediction errors for the validation data set obtained for the four process parameters estimated. Results for alternative training data generation approaches are indicated.

In general, the cross-validation technique resulted in the lowest RMSE errors. Figs. 2a and 2b demonstrate the quality of cell count and product concentration



estimation for the testing set. Clearly both the process parameters are accurately estimated, but on the independent validation set (Figs. 2c-d) the estimation is less accurate. However, the estimation of  $\mu$  and  $q_p$  (Figs. 2e-f) is satisfactory.

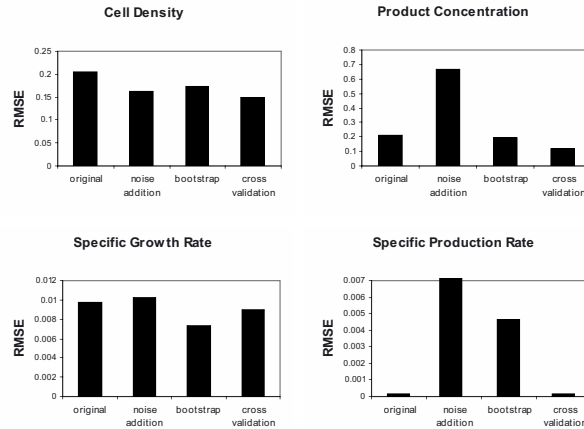


Figure 1. Summary of the RMSE obtained for the 'best' RBF models on the CHO cell process

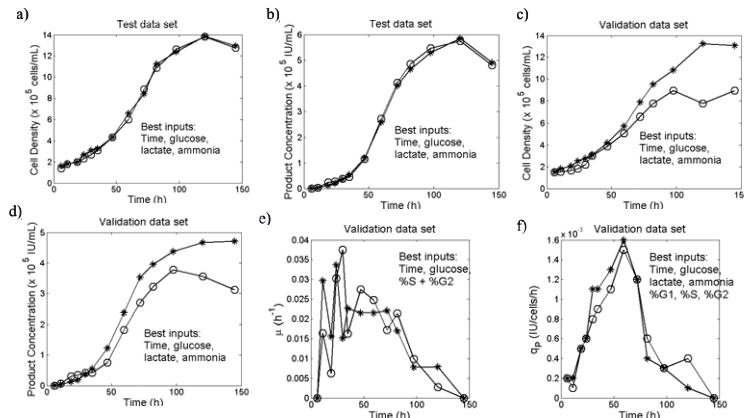


Figure 2. Comparison of the RBF network predictions with the actual measurements of the outputs of the CHO culture data. \*- Actual values, o- Predicted values.

This may be due to the fact that different input combinations were used to obtain the estimates. For  $\mu$  and  $q_p$  information on cell cycle (flow cytometric data reflecting the proportion of cells in G1, S, G2 phases) was included. This is in agreement with the expectations based on fundamental process understanding. Given the accuracy of the specific growth and production rate estimation, it is possible that estimates provided by the data-based model could be used in a mechanistic model predicting biomass and product concentration.

#### 4.2. Insect cell culture

Six out of the original 21 batches were selected for model validation. Following initial poor results, noise addition and bootstrapping were used to attempt to improve model accuracy. Fig. 3 shows the lowest prediction errors obtained with the validation data set for the pre- and post-infection data, when the model was trained with the original and the augmented data sets. Clearly the difference in the model performance for the cell count (pre-infection) can be considered insignificant. In the case of viability estimation (post-infection), bootstrapping leads to more accurate estimation.

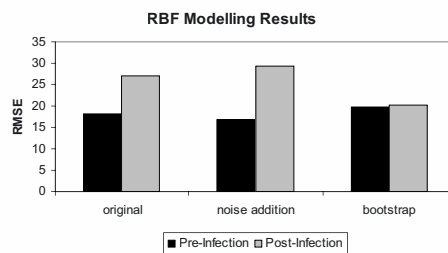


Figure 3. Summary of the RMSE for the 'best' RBF models of the insect cell/baculovirus expression system.

Fig. 4 shows the comparison of the predictions of the 'best' model obtained for each output with the respective actual measurements through parity plots. The values of cell count and cell viability were scaled between 0 and 1 in order to protect industrial confidentiality. The experimental error bounds are indicated by solid lines either side of the parity line.

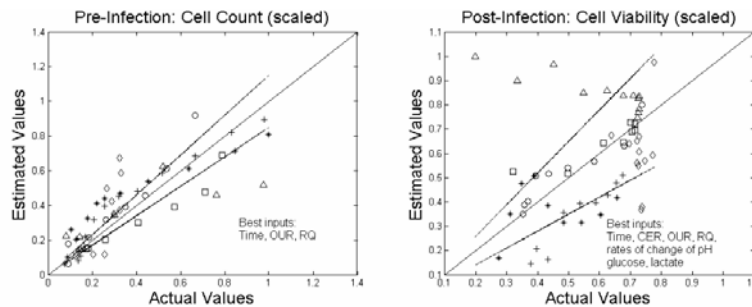


Figure 4. Parity plots of the predictions with the actual measurements of the outputs of the insect cell data (validation). \* batch 1, o batch 2, + batch 3, □ batch 4, Δ batch 5, ◇ batch 6.

The results indicate that the cell count estimation captured certain process characteristics although deviations consistent with un-modelled dynamics can be seen in some batches. The quality of cell viability estimation is less than ideal. Whilst this is expected given the experimental errors associated with the viability measurements and also the significant limitation in data availability, it is necessary to include further process information (either in the form of cell death kinetics or

infection kinetics) and/or alternative modelling approach to improve the accuracy of estimation.

## 5. CONCLUSIONS

RBF neural networks have been used to estimate the process parameters in the CHO cell culture cultivations producing INF- $\gamma$ . Three different techniques were used in an attempt to address the issue of the limited quantity of process data. For the first case study cross validation proved the most effective. It was found that the estimation of cell count and product concentration was less accurate than that of the specific growth and production rates. For the estimation of the latter parameters, cell cycle information in the form of flow cytometry data reflecting the proportion of cells in G1, S and G2 phases respectively was included. In order to improve the accuracy of cell count and product concentration estimation, the estimates of specific growth and production rates provided by the data-based models could be used within a hybrid model scheme combining data-based and mechanistic models.

Whilst the above cell culture cultivations were performed in a University environment and benefited from the availability of measurements reflecting the physiological state of the culture more explicitly, it is important to assess the ability of data-based models to estimate process parameters for industrial cell culture cultivations. Thus data from an insect cell/baculovirus system were also analysed using the same techniques. The model for cell count estimation provided reasonable estimates and these did not improve significantly by applying noise addition or bootstrapping. However, the estimates of cell viability have improved by the application of bootstrapping, although the results for the validation sets are still not ideal and alternative approaches for this parameter are being currently investigated.

**Acknowledgements:** Financial support from BBSRC is acknowledged (grant number E15014).

## REFERENCES

1. Jang JD, Sanderson CS, Chan LCL, Barford JP, Reid S (2000). *Cytotechnology* **34**: 71-82.
2. Faraday DBF, Hayter P, Kirkby NF (2001). *Biochem Eng J* **7**: 49-68.
3. Jeyamkondan S, Jayas DS, Holley RA (2001). *Int J Food Microbiol* **64**: 343-354.
4. Glassey J, Montague GA, Ward AC, Kara BV (1994). *Process Biochemistry* **29**: 387-398.
5. Dong D, McAvoy TJ, Zafiriou E (1996). 13<sup>th</sup> Triennial World Congress IFAC, San Francisco, 253-258.
6. Gehlen S, Tolle H, Kreuzig J, Friedl P (1992). IFAC Modeling and Control of Biotechnical Processes, Colorado, USA, 379-382.
7. Moody J, Darken CJ (1989). *Neural Computation* **1**: 281-294.
8. Warnes MR, Glassey J, Montague GA, Kara B (1998). *Neurocomputing* **20**: 67-82.
9. Quantrille TE, Liu YA (1991) *Artificial Intelligence in Chemical Engineering*. San Diego: Academic Press.
10. Cunha CCF, Glassey J, Montague GA, Albert S, Mohan P (2002). Submitted to *Trans Inst Measur Control*.
11. Conlin AK (1996) *Complex Sensor Data Analysis Through Data Augmentation*. PhD Thesis, University of Newcastle upon Tyne.
12. Efron B, Tibshirani RJ (1993) *An Introduction to the Bootstrap*. New York: Chapman & Hall.

13. Leelavatcharamas V, Emery AN, Al-Rubeai M (1996). In: *Flow Cytometry Applications in Cell Culture*, M. Al-Rubeai and A.N. Emery (eds), Marcel Dekker, 1-15.
14. Burr K, Glassey J, Montague GA, Hardwicke PI, Smith JJ (2001). *CAB8 Proceedings*, 251-256.

## QUESTIONS AND ANSWERS

### **Bjoern Frahm, Technische Universität Hamburg-Harburg, Germany:**

I do not quite see the intention of generating artificial data by adding noise to existing data. In one case you already have 21 batches, would it not have been better to experiment under different conditions, for example substrate limitations, and then try to model these circumstances instead of just creating artificial data ?

### **Claudia Cunha-Bakeev, University of Newcastle upon Tyne, UK:**

This is what we are trying to get, these were data from the University of Birmingham. They do changes in the fermentation, so that we can actually study it using this data technique. So, we are working at the moment with what we have. Also, these techniques have also been used for microbial systems previously, and it is possible to use them correctly without compromising the model.

### **Nicolas Mermod, University of Lausanne, Switzerland:**

Is over training a problem for you, and if so, how it is solved ? Do you think that approach will be generalizable to other bioreactors ? It was not clear to me if you always used data from the same bioreactor, or whether they were different processes.

### **Claudia Cunha-Bakeev, University of Newcastle upon Tyne, UK:**

They are different processes, yes. We have the laboratory conditions at University of Birmingham, then pilot plant at GSK, and we are also working with Lonza Biologics, although we could not show their results yet. So, the technique can be used for any kind of process.

### **Sadettin Ozturk, Centocor, US:**

I was just curious, I think may be things change, but long time ago neural networks were limited to the ranges of your study. You could make intrapolation, but not extrapolation, so you could not get out of the ranges of your study. Is there any recent development making this possible ?

### **Claudia Cunha-Bakeev, University of Newcastle upon Tyne, UK:**

No, you are right, we can not extrapolate in neural networks. That is, when we were selecting the training data, we tried to get the largest variation.

S. BENGIO, P. SANTAMBIEN AND S. CLEVERLEY

CELL CULTURE AND DOWNSTREAM PROCESSING  
INTEGRATION USING PROTEINCHIP®  
TECHNOLOGY APPLICATION TO PROTEIN  
ANALYSIS AND PURIFICATION IN  
BIOPHARMACEUTICAL MANUFACTURING

*Ciphergen, Biosepra Process Division, Cergy (France)*

**Abstract.** Ciphergen Biosystems has recently developed a novel technology called the ProteinChip® System that enables analysis of complex biological mixtures. The ProteinChip System employs a unique family of protein biochip arrays carrying functional groups (e.g. ion exchange, reverse phase, IMAC). These ProteinChip Arrays have been designed to bind proteins and peptides from complex biological mixtures such as fermentation or cell culture supernatants.

The technology is referred to as SELDI (Surface Enhanced Laser Desorption Ionization – Mass Spectrometry) which highlights the key elements of the technique: selective sample binding/desorption on functionalized surfaces followed by mass spectral analysis of retained components.. This molecular weight-based analysis also reveals important information about protein integrity (e.g. proteolytic degradation, glycosylation) that can be exploited for the purpose of process optimization, lot acceptance criteria or product specifications.

Applications of Surface enhanced laser desorption ionization for protein expression analysis and fast purification optimization from cell culture and fermentation media are discussed in this paper.

## 1. INTRODUCTION

Process Proteomics is a novel approach to protein expression monitoring and protein purification optimization, at both small and large-scale.

The approach is based on Retentate Chromatography SELDI mass spectrometry (RC-SELDI-MS), introduced by Ciphergen BioSystems. It employs two components : ProteinChip® Arrays and the ProteinChip reader.

ProteinChip Arrays consist in a family of functional surfaces that carry chemical groups equivalent to those used for chromatography sorbents (e.g., anion and cation exchange, IMAC, reverse phase and hydrophobic surfaces, refer to *Figure 1.*). These arrays bind proteins and peptides from complex biological mixtures, such as cell culture supernatants or fermentation feedstreams.

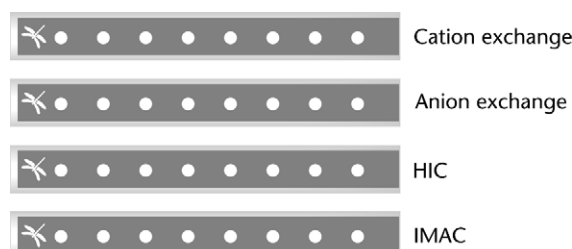


*Figure 1 : ProteinChip® Arrays carry functional groups similar to chromatography sorbents.*

*All spots on an array have the same functional group. A few microliters of sample (cell culture supernatant or clarified fermentation) can be loaded on each spot, and analyzed using a specially designed Time of flight mass spectrometer. Accurate molecular weight of the sample components is obtained in minutes.*

After applying a cell culture or fermentation sample on the array, the spots are rinsed with buffer. Bound proteins can be selectively « eluted » from the chip surface using appropriate buffer, as would be done using a chromatography sorbent. In practice, a few microliters of sample is sufficient to run an analysis . The array is analyzed using the ProteinChip® reader, a specially designed time-of-flight mass spectrometer (TOF-MS). Proteins in the 1-500 kDa range can be detected, with a sensitivity down to the femtomole level.

This approach can be used to monitor in « quasi real-time » the expression level of a target protein from a crude sample, and gives access to relative quantification data..

## 2. PROTEIN EXPRESSION MONITORING

Significant advances in the production of therapeutic and diagnostic proteins using cell-based systems have been achieved in recent years. Improved mammalian cell cultivation systems can produce proteins now routinely at the >1 g protein per liter scale.. These improvements in productivity, however, are often accompanied by increases in cell death and the release of damaging proteases and glycosylases. The presence of these hydrolases can result in a substantial decrease in final antibody yield, purity, and homogeneity. In addition, numerous host cell proteins (HCP) and media-derived proteins are typically present along with the target protein that can be co-purified and may contaminate the final product. A critical element in industrial manufacturing processes is the establishment of specific, sensitive and robust analytical methods to detect and track both product-related and process-related impurities throughout the process and in the final product.

Current methods of protein expression analysis rely mostly on gels and western blots ; these methods are time consuming,, less sensitive in the low molecular weight mass range, and provide insufficient real-time information about protein integrity. The RC-SELDI-MS approach is simple (see *Figure 2*), and can be applied to both tagged and untagged proteins. Analysis time is much shorter than with using conventional gel-based methods, total analysis per sample is as little as 10 minutes.

Moreover, the RC-SELDI-MS technology provides accurate information about protein molecular mass, and gives greater insight into sample composition. For high-throughput analysis, the approach can also be automated, using an autoloader or commercially available robots .

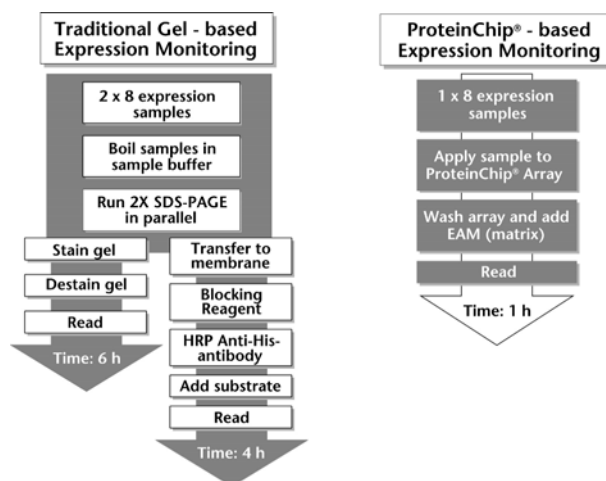


Figure 2 : RC-SELDI-MS analysis and comparison with traditional gel-based methods

In the example shown (Figure 3.), crude expression samples from an *in vitro* expression system were analyzed using the RC-SELDI-MS technology. 6xHis tagged recombinant proteins were selectively bound by IMAC (Nickel) surfaces in a 96-well bioprocessor. The impact of nutrients (amino acids) on the expression level of a model protein (GFP, 28 kDa) was assessed.

Fast results like presence or absence of protein after induction, time courses or relative expression levels can be obtained in a few hours, allowing to take decisions on the cell culture conditions. This approach can help to bridge the gap sometimes existing between cell culture or fermentation monitoring and downstream purification, with a single integrated platform.

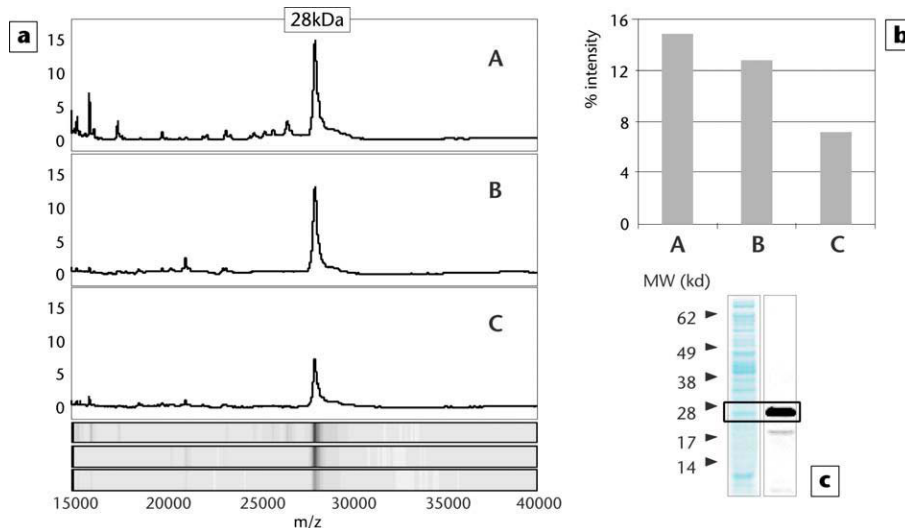


Figure 3. Expression monitoring : 6xHis tagged GFP (28 kDa, produced in an *in vitro* translation system . Expressed protein is captured on IMAC (Ni<sup>2+</sup>) Arrays. A,B,C represent 3 different amino acid mixtures, which have an impact on the model protein expression. Fig 3c represents SDS-PAGE and Western blot of a single GFP sample.

### 3. PROTEIN PURIFICATION OPTIMIZATION

ProteinChip Arrays and matching chromatography sorbents have been developed. This approach has been recently applied to the purification of a recombinant endostatin expressed in *Pichia pastoris*.

In a first step, a crude clarified fermentation sample was applied on four different types of arrays : CM, Q, RP and IMAC.

On chip screening principle is shown in *Figure 4* . Results from endostatin binding experiments on various surfaces (CM, Q, RP and IMAC arrays) showed that the cation exchange surface (equivalent to a CM chromatography sorbent) was the best candidate to retain endostatin at a given pH, while impurities could be retained on other surfaces.

After selecting and fine tuning a binding pH (pH 5.0), endostatin elution conditions were determined from the CM surface, and found to start at about 200mM. Conditions determined «on-chip» were then transferred on a regular chromatography sorbent (CM HyperZ, BioSeptra). This sorbent is an ion exchange resin, with a particle size of 70µm and a density of 3,2 g/L, specially designed for expanded bed adsorption. Analysis of collected fractions showed that endostatin was fully adsorbed and eluted in the pH and ionic strength conditions « predicted » on-chip (*Figure 5*).



Other examples with various recombinant proteins have demonstrated the value of this «on-chip predictive chromatography» to accelerate the process of chromatography step selection. Using a combination of chips and beads with matching chemistry, process purification development time for an unknown recombinant protein can be substantially reduced from weeks or months to days.

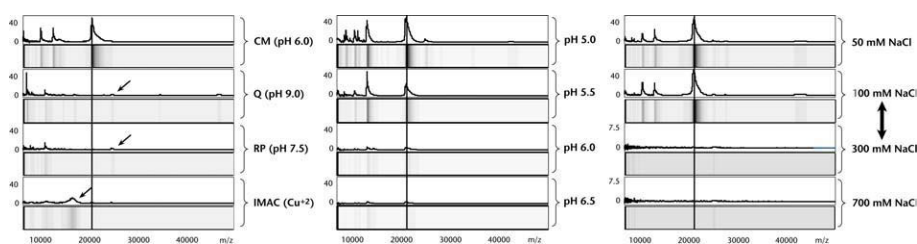


Figure 4. : Principle of «on-chip» purification optimization.

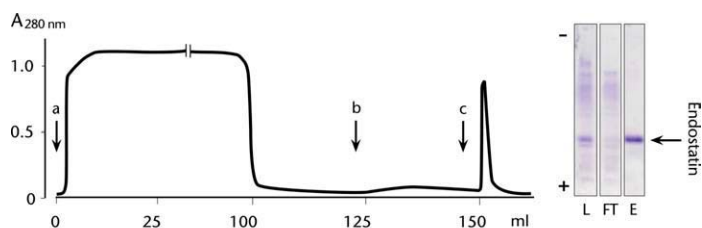


Figure 5. : On-chip recombinant endostatin purification optimization using the ProteinChip® technology .b and c represent elution of the protein using NaCl based on-chip prediction.

#### 4. CONCLUSION : A VERSATILE INTEGRATION TECHNOLOGY FOR « UPSTREAM » AND « DOWNSTREAM »

One of the key strengths of the RC-SELDI-MS approach is its simplicity of use and its power as an analytical tool to monitor in real-time a process flow. Having access to accurate molecular weight information can be exploited for « pre-QC » steps, like lot acceptance criteria. As an example, global evolution of glycosylation patterns can be monitored, and linked to cell culture conditions and biological activity. Post-translational modifications and protein integrity can also be followed. Process Proteomics represents therefore an integration tool, that can be exploited both by protein expression groups and downstream purification : upstream, the approach allows to follow in quasi real-time protein expression monitoring much faster than conventional gel-based methods ; downstream, predictive

chromatography performed « on-chip » and transferred to regular chromatography sorbents allows to save process development time.

Finally, at a « pre-QC » step, this approach gives valuable information about target protein integrity, as well as product or process-related impurities.

In certain cases, this approach can be applied for monitoring Host Cell Proteins and process-related impurities in commercial-scale production of therapeutic proteins, in complement to conventional techniques such as ELISA or Western-Blots.

Recent developments allow to couple the ProteinChip® technology with sophisticated tandem MS-MS analysis, giving access to protein identification by peptide mapping and Collision induced decay for sequence analysis. Peptide mapping using the tandem MS interface provides high accuracy M/z information from all available surfaces for database searching with high protein coverage, and then provides amino acid composition information.

For more information consult [www.ciphergen.com](http://www.ciphergen.com) or contact : Dr. Sylvio Bengio [sbengio@ciphergen.com](mailto:sbengio@ciphergen.com).

#### QUESTIONS AND ANSWERS

**Otto Merten, Genethon, France:**

I think this is a very interesting system, but we are working with viruses, and viral vectors, and the chromatographic matrix can affect the purification. Do you think that this can also be used for evaluating different column properties for the purification of viruses or not ?

**Sylvio Bengio, BioSeptra, France:**

So far, we have no experience with viruses. You are absolutely right, I think. A chromatography mechanism is by definition a three dimensional mechanism, where not only the properties of the matrix will play a role, but also what is happening in the internal porosities of the matrix, and this is particularly true for viruses. For viruses we have never tried such an approach, however, with different types of proteins we have seen, using different manufacturers' resins that, especially for ion exchangers the correspondences were surprisingly good, including we were the first sceptical as chromatographers.

D.N. GALBRAITH

## THE PROSPECTS FOR INSECT CELLS FOR USE AS A CELL SUBSTRATE FOR THE PRODUCTION OF BIOTHERAPEUTICS

*Q-One Biotech Ltd., Todd Campus, West of Scotland Science Park, Glasgow  
G20 0XA, United Kingdom.*

### 1. INTRODUCTION

Since the development of viral vaccines in the early years of last century, animal cell technology has been used for the production of biologicals for prophylaxis and therapy of humans and animals. It was not until the late 1980s, however, before industry adopted the large-scale culture of prokaryotic or eukaryotic cells for the production of (recombinant) therapeutic proteins. At present, more than 50 drugs containing active ingredients produced in cell culture systems have been approved for marketing in the USA and Europe. All of the cell culture systems currently in use have their advantages and disadvantages. Prokaryotic systems such as those based on *Escherichia coli* provide high yields, but the proteins produced can be without the post-translational modifications such as glycosylation and protein folding/secretion present in the equivalent proteins produced in mammalian cells. The differences seen with the recombinant proteins may affect their therapeutic activity. Eukaryotic systems on the other hand have the advantage that they are capable of some post-translational modifications. The production of recombinant proteins in insect cell systems is seen as robust, efficient and is low cost when compared to other cell based systems. These systems have been used to manufacture recombinant proteins for research and *in vitro* investigations for a number of years. The production of biotherapeutics in insect cells may also present an advantage in producing safer products over the equivalent production in mammalian cells. Proteins can be produced in insect cells without animal supplements such as foetal calf serum. In the current climate of concerns over Bovine Spongiform Encephalopathies and bovine viral risks this represents a significant safety, as well as a cost advantage over other production methods. Theoretically, the use of such systems could be advantageous from a therapeutic, as well as a commercial point of view.

Given the benefits for the production of recombinant proteins using *Baculovirus* in insect cells, the question arises as to why there are currently no licensed human clinical products in the marketplace developed using this technology? One reason

for this could be the uncertainty of how these products would be accepted by the regulatory authorities worldwide. As the investment costs of developing novel clinical products continue to escalate, pharmaceutical companies may be wary of investing significant amounts in this technology while the regulatory and safety aspects remain unknown.

In principal, producing recombinant proteins from insect cells should be no different to Chinese hamster ovary or other cells. On deciding to move to pre-clinical and clinical investigation, a rigorous study of the safety of the materials and processes will take place to comply with the safety milestones and regulatory requirements. In Europe the recently published Clinical Trials Directive make a clear indication that all materials used in clinical trials are required to be produced under cGMP (current Good Manufacturing Practice). It is likely that this requirement will be worldwide in the very near future. In the case of production in insect cells this will normally require banks of the cells and seed stocks of the *Baculovirus*, and a safety testing and validation plan for the downstream production of the protein.

Specific regulatory guidance for the characterisation and testing requirements of insect cells and products derived from them is not available. Therefore manufacturers are encouraged to use the generic guidelines already in place. The principal guidance notes are the International Conference on Harmonisation Q5A: Quality of biotechnological products: Viral safety evaluation of biotechnology products derived from cell lines of human and animal origin and Q5D Derivation and characterisation of cell substrates used for production of biotechnological / biological products. The stated objectives of these guidelines are to provide guidance and appropriate standards for cell lines and other materials used to prepare biological products and to provide a general framework for the viral testing and clearance studies required for products with intended clinical use. The guidelines are designed for a cell/reagent bank system, as this is the most practical, safe and cost effective method of generating clinical product.

When assessing the suitability of cell lines, the history of the cells must be documented. As insect cells and *Baculovirus* are very infrequently used for clinical production, these materials will require a clear documented culture history. Frequently cell lines have been passed between a number of laboratories before they are used for the production of a clinical product. For example the Sf9 cells were cloned in 1983 from parental line (IPLB-SF 21 AE) originally derived from the ovarian tissue of *Spodoptera frugiperla* described by Vaughn *et al* (1977). Finally in the late 1980's the cells were transferred to the American Type Culture collection where they were expanded and laid down as a bank; these are now available for release to any laboratory. It can be assumed that between 1977 and today there has been considerable culturing and sub-culturing of the cells by different operators using a number of different media types. Therefore there is the potential for the cells to be exposed to any number of materials that could affect the safety profile. Documenting the cultivation history of the use of physical, chemical or biological procedures can present difficulties, as this may be unavailable or incomplete. The guidelines note that on some occasions it is impossible to document all of the

manipulations carried out before the final point of use and this will be taken into consideration. However, the significant manipulations that affect the production characterisation of the cells should be recorded. Note should also be made of the potential exposure to infectious agents, here the regulators require to know if bovine serum, enzymes or other cell growth promoters of animal origin were used during the culture/manipulation of the cells. The accumulation of such data allows a thorough risk analysis of the potential entry of adventitious agents to the cell line and directs the testing strategy to establish product safety. Companies such as Protein Life Sciences or Invitrogen now offer characterised cell banks available for use in the production of products. These are based on clones from Sf9 or Hi5 cells. Care should be taken to determine that the characterisation carried out by the companies selling these cells will satisfy the current guidelines and that these are applicable.

*Baculovirus* expression vectors undergo a greater level of manipulation than the production cell lines. The *Baculovirus* genome is modified to include the foreign transgene capable of producing the desired recombinant protein. The methodology of the procedures used to insert these genes and to produce the vectors vary, but are reviewed by Kitts, 1996. In a similar way to the history of the cell line, the history of the vector requires to be documented, including all of the significant manipulations. *Baculovirus* vectors can be obtained from commercial sources that are suitable for production with modification for use to produce a clinical product. Again care should be exercised on relying on the suppliers safety data that may not be sufficient to satisfy current guidelines.

## 2. CURRENT AND POTENTIAL USE OF INSECT CELL SYSTEMS

The insect cell system is currently very well suited for the production of glycosylated or non-glycosylated products for research purposes. For example, the system can be used for the rapid production of large amounts of protein for structural studies. The system has also been particularly useful for the production of "difficult" proteins that are hard to express in other systems. *Baculoviruses* are frequently used to express genes that have been impossible to express in bacterial or other eukaryotic systems. Another use is the expression of putative gene products from genome projects, thereby serving as a high throughput system for the analysis of targets for drug screening.

With respect to the commercial production of biopharmaceuticals, a first target of choice has been the production of immunogenic proteins, for example vaccines. Already, the production of virus-like particles (VLPs) to be used as viral vaccines seems promising because of the already proven high efficacy of the VLPs in inducing immune response in animals. Due to the advantages associated with the insect cell system, work is in progress to overcome the disadvantages mentioned earlier and to optimise insect cell systems. As a consequence, the time rapidly approaches that the production of proteins of interest using the *Baculovirus*/insect cell system will no longer be confined to proteins for the research market. An increasing number of pharmaceutical companies are showing an interest in using the

*Baculovirus*/insect cell systems for the commercial production of bioactive proteins. Insect cell technology is appearing in an increasing number of patents filed. Furthermore, in the USA, a number of therapeutic proteins are currently in Phase III clinical trials, with an increase in the number of candidates that are in Phase II trials. Vaccine applications are emerging strongly. In Europe, two sub-unit vaccines based on envelope glycoprotein E2 of *Classical Swine Fever virus* produced in the BEV system have been licensed as a veterinary vaccine already. Porcilis Pesti is a vaccine used to prevent infection of piglets with *Classical Swine Fever virus (CSF)* marketed by Intervet [EMA/V/C/046/01/0/0]. This vaccine is given by intramuscular injection of the emulsion at age 5 weeks. The active ingredient of the vaccine is the CSF E2 antigen produced in an insect cell / *Baculovirus* expression system. The reason the insect cell / *Baculovirus* production system was chosen was for the high level of antigen productivity able to be achieved by the insect system, this reduces costs and makes the process commercially viable. The glycosylation of the protein mimics that of the native circumstances of E2 processing during replication of the virus, this processing aids in the immunogenicity of the protein facilitating the usefulness of this as a vaccine. And finally, the production system is bovine serum free, which again reduces costs and also reduces the concerns linked to the transmission of bovine viruses in the product (as this is a veterinary product used in pigs this is potentially even more significant than in humans due to the increased risk of cross species transmission). Overall the efficacy of the product and the commercial concerns made this product viable. When the European veterinary regulators reviewed the dossier on the product there were limited concerns raised with the insect cell / *Baculovirus* production system specifically. Other than the need to show that any *Baculovirus* was inactivated during the processing of the vaccine, no specific insect testing was requested. The position of the veterinary regulators was encouraging for manufacturers, however the concerns in the veterinary market are considerably different from those of human clinical products. The potential concerns of insect viruses being present, contaminating the product or insect proteins or nucleic acid present in the product have already raised concerns and may require further investigations before licensed products would be approved.

### 3. THE FUTURE

Clearly there is an interest and move for human biotherapeutics synthesised on insect cells to be manufactured and used. The efficacy, safety and cost issues all appear to indicate that for some products this production system will be useful. Therefore the likelihood is that we shall see such products being approved for use in humans in the future. A significant drawback to the use of insect cells for some biotherapeutics has been the worry that the glycosylation pattern in insect cells is so different from the mammalian version that these may not be able to be efficacious in humans. Recent advances in the use of modified cell lines to express a "human-like" glycosylation pattern have given rise to the potential for insect derived proteins to be useful in these products. Insect cells have been modified to eliminate "insect-like" glycosylation patterns and replace these with genes coding for enzymes that will

mimic the mammalian forms. A new promise of insect derived proteins has recently been published by Masahiro Tomita and co-workers. They describe the generation of transgenic silkworms that produce cocoons containing recombinant human collagen. The genes encoding human type III procollagen mini-chain, a fibroin light chain (from the insect silk), and an enhanced green fluorescent protein gene were synthesised in a vector construct. The genes used a fibrin promoter. Silkworm eggs were injected with the vectors, producing worms displaying EGFP fluorescence in their silk glands. On examination the cocoons emitted EGFP fluorescence, indicating that the promoter and fibroin L-chain cDNAs directed the synthesized products to be secreted into cocoons. From this work it is clear that other proteins may be expressed in this way further reducing the costs associated with such production systems and potentially allowing novel therapeutics to be marketed. Such methodologies may be particularly useful in the less developed world where the cost of large manufacturing sites may be prohibitive.

#### 4. REFERENCES

- Vaughn JL, Goodwin RH, Tompkins GJ and McCrawley P. The establishment of two cell lines from the insect *Spodoptera frugiperda* (Lepidoptera; Noctuidae). In Vitro. 1977 Apr;13(4):213-7.
- Kitts PA. Construction of *Baculovirus* recombinants. Current applications of cell culture engineering Vol 2. Insect cell cultures. 1996, p111-123, Eds Vlak JM, de Gooijer CD, Tramper J and Mittenburger HG.

## QUESTIONS AND ANSWERS

**John Aunins, Merck, US:**

I was a bit surprised too to hear about the lack of adventitious agents testing required for that. We know about contamination of rodent cell lines by adventitious viruses coming in from different sources including media components. Do you know of any examples about insect cell lines being contaminated by viruses ?

**Daniel Galbraith, Q-One Biotech, UK:**

Yes, there is a number of examples, unfortunately I did not have enough time to discuss them. People have been using baculovirus and insect cells for a long time, and we know that there are at least six known different viruses that can infect them.

**Herman Katinger, Institute of Applied Microbiology, Vienna, Austria:**

There are systems available completely protein-free for CHO cells, for a cost of less than a dollar per liter. Do you think that you can reduce further the cost with a protein-free medium, for the Baculo system, for example to half a dollar per liter ?

**Daniel Galbraith, Q-One Biotech, UK:**

I think we should mainly focuss on the amount of protein we are getting per cell and per liter, rather than cost per liter of medium. I think with the Baculovirus system, using the appropriate insect cells, and I know there has been a lot of work done on engineering insect cells to produce a higher amount of protein. So, I have never seen any calculations where the insect cell production has been at a higher cost than the equivalent CHO system, so I think that with the appropriate modifications we can go very low in costs.



DAVID Y. H. CHANG, PAUL GARZA, YAO-MING HUANG,  
MYLENE TALABARDON, SOHEIL RAHMATI, ERIC FALLON,  
WOLFGANG NOE

## HIGH PERFORMANCE CELL CULTURE PLATFORM TECHNOLOGY FOR MAB PRODUCTION

*IDEC pharmaceuticals Co, Cell Culture Process Sciences, 11011 Torreyana  
Road, San Diego, CA 92121, USA*

**Abstract.** Various optimization approaches using 5L bioreactors and spinner flasks, including manipulation of culture physical parameters (pH, temperature, osmolarity, pCO<sub>2</sub>) and design of cell culture basal and feed media, and feed scheme that prevent nutrient depletion or by-product accumulation, have been pursued in the interest of increasing productivity and delaying cell death. Using this strategy, final scale-up processes for 6 MABs led to harvest titers of 0.3 to 3 g/L, pending on the specific cellular productivity. This platform cell culture process is proven simple, robust, productive and scalable for IDEC clinical and commercial manufacturing.

### 1. INTRODUCTION

IDEC Pharmaceuticals has devoted efforts for maximizing monoclonal antibody (MAB) production to fulfil increasing clinical and market demand. Process Sciences Department endeavours to increase process productivity and decrease process variability. To achieve this goal, IDEC has focused on the development of an effective, reproducible, scalable and robust fed-batch cell culture process. A typical IDEC cell culture process flow diagram (PFD) is shown in Figure-1. With dedicated resources and efforts based on this PFD, we have successfully developed a platform supporting all IDEC clinical and future commercial MAB production. The strategy, methods and results for this development will be discussed in the following sessions.

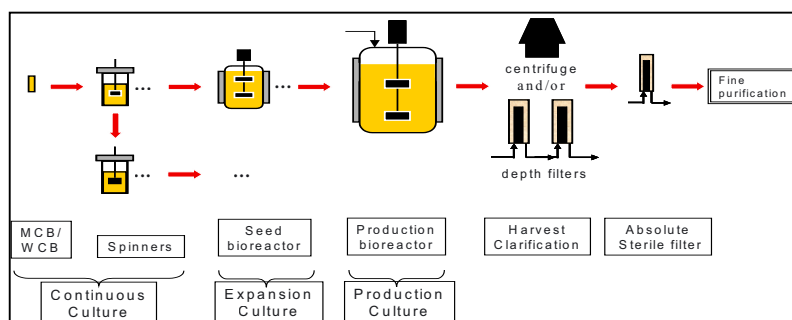


Figure 1. typical IDEC cell culture process flow diagram.

## 2. STRATEGY AND METHODS

### 2.1. Cell line and Expression system:

The cell culture platform starts with the development of production cell line, which is derived from CHO DG44 parental cells transfected with IDEC proprietary vector, NEOSPLA. The parental cells have been pre-adapted to serum-free and suspension culture prior to banking. This enables the prompt establishment of the MCB and MWCB. The production cell lines typically exhibit long-term (> 200 days) stability in MAb productivity, as shown in Figure 2.

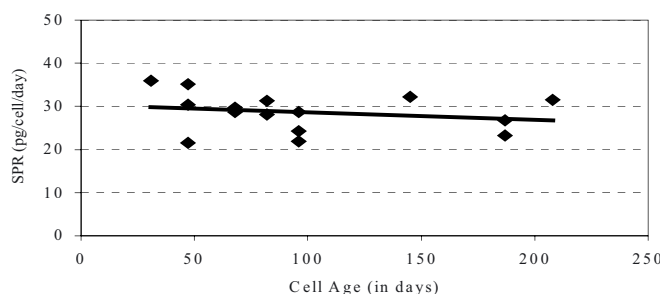


Figure 2. Typical cell line production stability over 200 days

### 2.2 IDEC cell culture manufacturing platform

IDEC cell culture Platform development focused on (1) the basal and feed media, (2) the fed-batch operation, and (3) the optimal bioreactor operation environment. IDEC developed this platform based on MAb1, and then immediately applied to 5 other MABs with minimal fine-tuning to achieve acceptable and satisfactory performance. Most importantly, all raw materials and unit operations are identical for all 6 different MABs processes.

The platform process originally used customized vendor proprietary media because of time and resource constraints. Concurrently, IDEC devoted significant resources to develop IDEC-own media (IM) and refined the platform process to accommodate it. In consequence, IDEC has the benefit of full sourcing control of qualified vendors to manufacture media at reasonable price and controlled quality, and the ownership of complete formulation know-how, which significantly benefits process development and trouble-shooting if needed. The development of IDEC in-house media started with commonly used commercial media as building blocks. The appropriate “balanced” concentrations of amino acids, vitamin and trace elements were defined through systematic approach using factorial experimental design. Major efforts were also devoted to identify critical supplement and their optimal dosage to maximize the performance in productivity and culture longevity. The

final medium formulation was proven feasible for powder form, and stable for extended period of time for both liquid and powder format.

Once the basal medium was defined, the feed medium was then developed based on the basal medium without inorganic salts. The feeding scheme was designed according to the overall metabolic profiles in order to replenish depleted nutrients as well as minimize the accumulation of inhibitory metabolites. The feeding was accomplished through discrete bolus additions instead of daily or continuous additions, and one bulk feed concentrate stock was prepared and stored in a feed tank with sufficient quantity to supply feeds throughout the course of run without additional preparation.

The bioreactor environmental conditions were systematically evaluated in appropriate scale-down models (spinner flasks and 5L bioreactors) to identify the optimal combination of pH, temperature, osmolarity, dissolved O<sub>2</sub> and CO<sub>2</sub>. Appropriate sparging strategy concerning sparger type, gas mixture composition (O<sub>2</sub>/air ratio), impeller design and agitation rate was identified critical to control dissolved O<sub>2</sub>, CO<sub>2</sub> and foaming.

### 3. RESULTS AND DISCUSSION

The platform culture performance for MAb1 (the model system for the development of platform) is shown in Figure 3. It clearly shows that the platform process is not only productivity and but also scalable from 5L, 100L/250L to 3000L bioreactors.

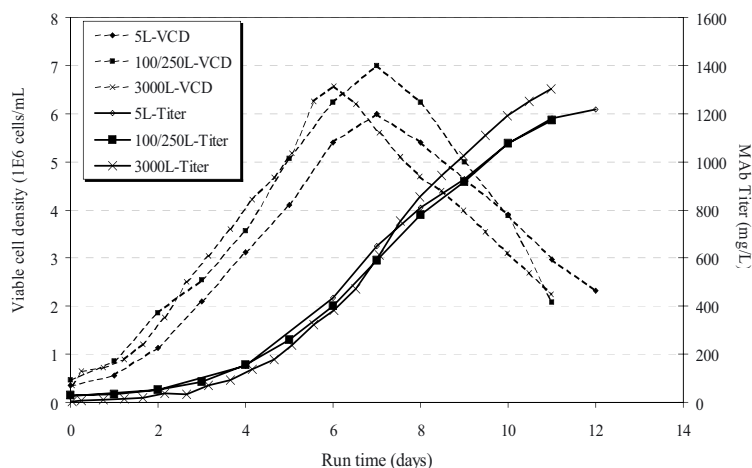


Figure 3. Performance and scalability of platform process for MAb1

This platform process was applied to five other MAbs in different phases of clinical development with minor fine adjustment in order to accommodate the different growth characteristics. The growth profiles are shown in Figure 4. All these processes fit into the two-week production cycle, which greatly simplifies the production logistics planning. Two of the 6 cell lines were able to grow to peak

viable cell densities of  $13 \times 10^6$  cells/ml, and the others to  $7 \times 10^6$  cells/ml. The corresponding MAb production profiles are shown in Figure 5. For the non-amplified cell lines used in Phase I/II production (MAb 5 and 6), the final harvest MAb titers range from 250-500 mg/L in 11-14 days. For the other fully amplified cell lines used in late clinical development, the final harvest titers range from 1200 to 3000 mg/L in a 2-week production cycle. This translates to volumetric productivity of 100 to 220 mg/L/day.

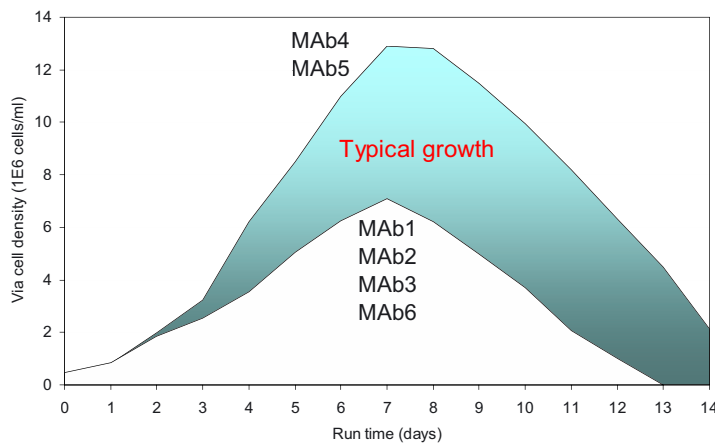


Figure 4. Growth profiles of platform process for 6 MAbs

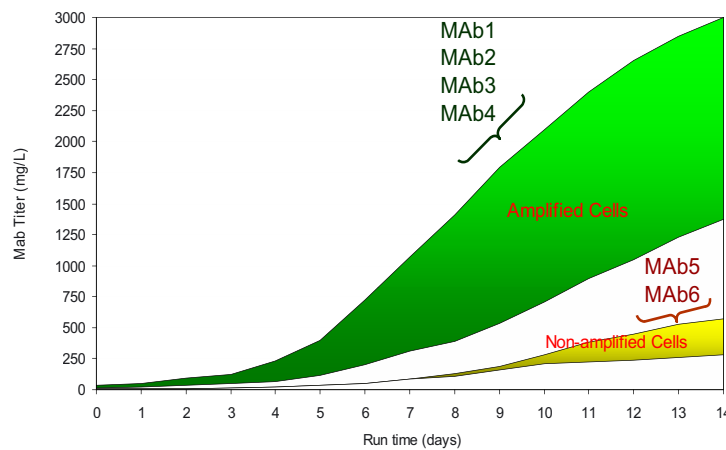


Figure 5. Productivity profiles of platform process for 6 MAbs

The IDEC in-house media (IM) was developed based on MAb4, and its performance is shown in Figure 6. It clearly shows that IM performance is comparable to vendor proprietary media. The impact of using IM on MAb4 glycosylation (galactose content on the biantenary glycan) is shown in Figure 7. It shows that the

replacement of vendor proprietary media with IM has no effect on MAb4 glycosylation.

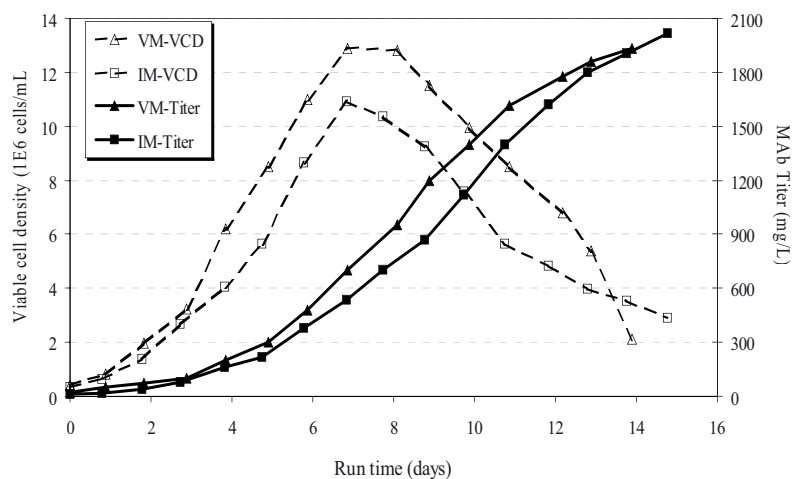


Figure 6. Performance of IDEC-medium versus vendor medium for MAb4

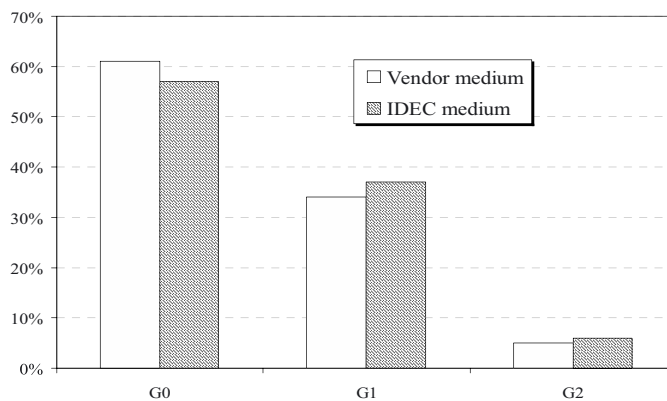


Figure 7. Glycosylation pattern for MAb4 using IDEC-medium and vendor medium

#### 4. CONCLUSIONS

The IDEC platform cell culture process has been proven simple, robust, productive and scalable. The platform process can readily deliver the MAb volumetric productivity of greater than 100 mg/L/day using the fully amplified cell lines. We have also applied the state-of-art analytical techniques early to identify process impacts on MAb quality. If the MAb quality such as glycosylation is shown to vary, this platform process needs to be implemented the latest before the Phase III manufacturing. Finally and most importantly, the “team-oriented” approach is

essential for the success of development and implementation of this platform process. It is not possible for this accomplishment without the joint efforts of R&D, pre-clinical and clinical development, marketing, process sciences, manufacturing, quality, compliance and regulatory at the first place.

## 5. ACKNOWLEDGEMENT

We thank various IDEC departments for their contributions and involvement in this work, including the remaining members of Cell Culture Process Sciences, Dr Mitchell Reff and his Molecular Biology department, Dr. Jorg Thommes and his Protein Purification Process Sciences department, Dr David Broad and his Biological Bulk Manufacturing department, Mr. Michael Molony and his Drug Testing Service group, Dr Michael LaBarre and his Analytical Sciences department, and finally Dr Wolfgang Berthold and his BioPharmaceuticals Sciences department.

## QUESTIONS AND ANSWERS

**Aziz Cayli, Boehringer Ingelheim, Germany:**

You have an amplified cell line. What was the amplification step ? How much MTX did you add to the culture medium ? The feed solution that you used: did you have just one single feed or two or three different feeds ?

**David Chang, IDEC Pharmaceuticals, US:**

Regarding the feed solution, you have to minimise it, normally it is between one and three.

**Herman Katinger, Institute of Applied Microbiology, Vienna, Austria:**

We cloned a lot of antibodies in recombinant CHO cells and we found out that each antibody is somehow an individual protein. It is not possible to predict in advance higher yields. We have some with very high yield and productivity and some that are not willing to become high producers. Did you have a similar experience ?

**David Chang, IDEC Pharmaceuticals, US:**

The data I showed are on the six antibodies we have in development phases, they were all treated through our platform technology, and I did not intentionally hide any low productivity cases.

S. PLUSCHKELL, L. BLOCKER, R. GELDART, S. HAWRYLIK,  
P. MENSAH, C. OKEDIADI, S. PIAS, A. SUBASHI, M. ZHU

## DEVELOPMENT AND INTEGRATION OF A NEW ANIMAL-COMPONENT-FREE PROCESS FOR THE PRODUCTION OF UK-279,276

*Pfizer Inc, Connecticut, USA*

**Abstract.** UK-279,276 is a 257 amino acid glycosylated and highly sialylated protein with a relative molecular weight of 36 to 61 kDa. This compound, a neutrophil inhibitory factor, was investigated for the potential prevention of neutrophil-dependent ischaemia-reperfusion injury in stroke patients. Early clinical lots were produced using a Chinese Hamster Ovary cell line in culture medium containing bovine serum albumin. It was then decided to develop a new process using a protein- and animal-component-free culture medium produced by fluidized-bed granulation. Many challenges were faced in this development, but ultimately productivity was increased approximately five-fold, while retaining robust and reproducible product glycosylation and sialylation. Pharmacokinetic analysis in rats resulted in essentially the same clearance properties for both products.

### 1. INTRODUCTION

UK-279,276 is a recombinant glycoprotein produced by transfected Chinese Hamster Ovary cells (CHO). The compound was originally isolated from the canine hookworm *ancylostoma caninum* in which it functions as a neutrophil inhibitory factor (NIF) in host defence (1). The recombinant protein was investigated as a potential drug for preventing ischaemic reperfusion injury in stroke patients or other indications (2). UK-279,276 has a molecular mass of approximately 36 kDa to 61 kDa, with usually 30% to 50% being contributed by glycosylation. The protein is 257 amino acids long, a monomer with five disulfide bonds and seven potential N-linked glycosylation sites. The glycan structures can have up to four branches and occur zero-, mono-, di-, tri-, or tetra-sialylated (2, 4). Manufacture of drug substance for Phase I and II clinical studies was carried out using a CHO cell line dependent upon bovine serum albumin, transferrin and insulin. Because of the increased concern about the risk of transmitting animal spongiform encephalopathy, a new process was planned to be introduced for Phase III and beyond. All raw materials were of non-animal origin and no proteins were added except for peptides stemming from the addition of hydrolysates.

## 2. NIF PRODUCING CELL LINES

Recombinant cell lines producing UK-279,276 (NIF) were derived from transfections of a CHO-K1 (ATCC CCL-61) host cell with the NIF gene as shown in Figure 1. The 7B4 Master Cell Bank or Working Cell Bank was used for the production of Phase I and II clinical material. For the animal-component-free (ACF) process, several options were initially pursued, either derived from new transfections or from the suspension culture 7B4, the parent of PF7. The culture PF211 was progressed based on its high productivity of UK-279,276, but was later discontinued because of cell line stability concerns and the preference for a cell line derived from the same transfection as PF7. Finally, it was decided to switch to the ACF-adapted cell line PFG01, which met all targets with respect to stability, productivity, and product quality (glycosylation, sialylation) (2).

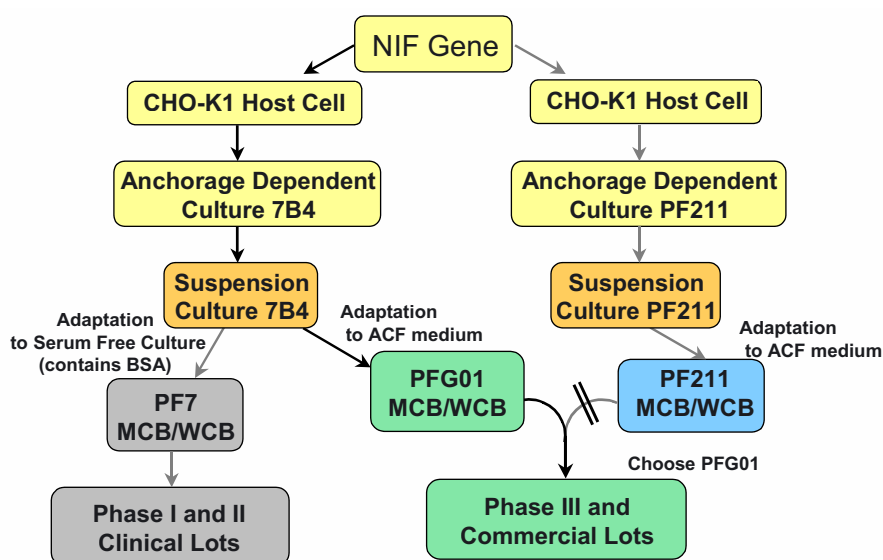


Figure 1. NIF producing cell lines.

## 3. THE ACF-V1 PROCESS

In the development of an ACF process for NIF production, the goal was to both improve productivity and maintain a robust and acceptable pattern of product glycosylation and sialylation during scale-up. As an initial test of product comparability during the process development phase, pharmacokinetic studies were conducted in rats to compare the PFG01-produced material with drug substance from the non-ACF process.



The strategy for the new process, named “ACF-v1” in its final configuration, relied on a customized, but commercially available protein-free cell culture medium which resulted in superior product quality at small scale. This medium was further improved by amino acid and yeast extract supplementation (2). Only the production stage, but not the inoculum culture, contained added yeast extract. The fed-batch stirred tank process also relied on a concentrated nutrient feed, containing the majority of the components of the basal medium plus added yeast extract at five-fold concentration (2). Osmolality of this feed was controlled by eliminating sodium chloride and sodium bicarbonate, and the concentrations of amino acids such as cystine and tyrosine were adjusted to remain within solubility limits. The fed-batch process also used a 400 g/l glucose feed, which could be fed either continuously or as once-per-day shot additions to maintain a glucose concentration near 2.0 g/l in the reactor. Significant productivity improvements were made by switching from the non-ACF process to the new ACF process. Time in the production bioreactor was reduced by at least seven days, with the ACF-v1 process time set to  $11 \pm 1$  days. Combined with a 2.5 to three-fold increase in harvest product titer, the productivity was increased approximately five-fold – exceeding the commercial target by 20% to 50% depending on the day of harvest.

Figure 2 shows example time profiles of the in-process product concentration and product quality typical of the ACF-v1 process. The product concentration is shown normalized relative to the commercial target estimated from capacity and cost of goods considerations. Good reproducibility and robustness was achieved at four reactor scales ranging from one liter to 100 liters. Day 11 product titers of 30% to 40% larger than the commercial target were reproducibly reached in different laboratories and at different scales up to 2000-L (data not shown). To support process development efforts, a rapid multi-sample in-process purification protocol was developed, consisting of an anion exchange chromatography step followed by a hydrophobic interaction chromatography step (2). Samples purified by this two-column method were subjected to enzymatic release of the glycan structures, which were then analysed by anion exchange HPLC to determine the oligosaccharide charge profile (2, 4). Data in Figure 2 indicate that sialylation of the glycans decreased over time. Highly sialylated structures such as tri- and tetra-sialylated glycans decreased from approximately 50% on day 7 to approximately 39% on day 13. At the same time, the fraction of zero-sialylated glycans increased from approximately 7% on day 7 to approximately 13% on day 13. At this stage in development, it was expected that two-column purified material needed to have at least 40% tri- and tetra-sialylated glycan structures, and no more than 10% zero-sialylated glycans to deliver acceptable pharmacokinetic results in the rat model (4). For complete purification of UK-279,276, a third anion exchange chromatographic step was necessary, which did impact final product yield and quality (2). Figure 3 shows typical results for final product quality at the one liter through 100 liter scale in comparison to the non-ACF process. While the sialylation pattern achieved in the new process was different from the non-ACF material, it was in itself comparable at all scales. Many (>20) batches produced under the default ACF-v1 conditions provided confidence in the reproducibility of final product quality. In addition, pharmacokinetic studies in rats resulted in a clearance rate of  $0.08 \pm 0.01$  ml/(min·kg)

and a half life of  $10.6 \pm 1.5$  hours for ACF-v1 material, which was equivalent to the non-ACF product (0.08 ml/(min·kg) and 11.5 hours respectively). Further pharmacokinetic and toxicology studies in animals were planned prior to initiating clinical comparability investigations and possible transition to the new manufacturing process.

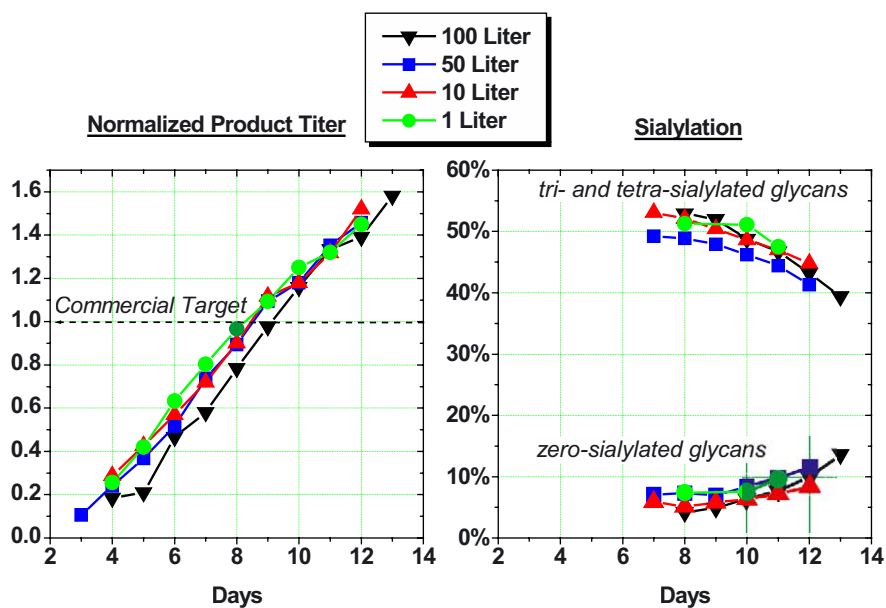


Figure 2. Time profiles of product formation

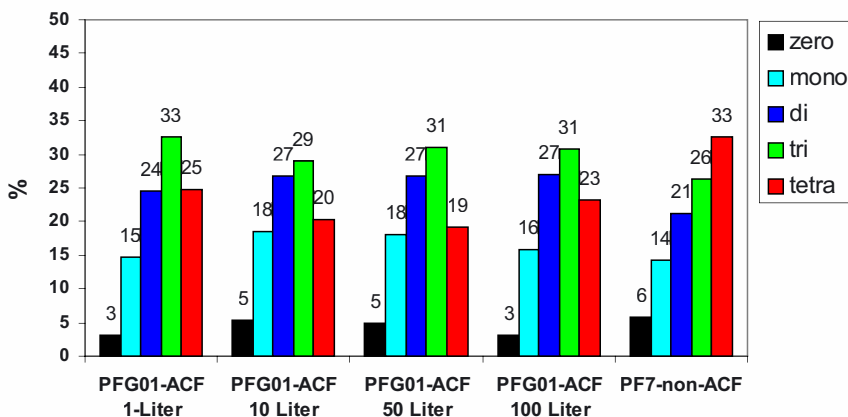


Figure 3. Sialylation profiles of fully purified drug substance and quality in the ACF-v1 process.

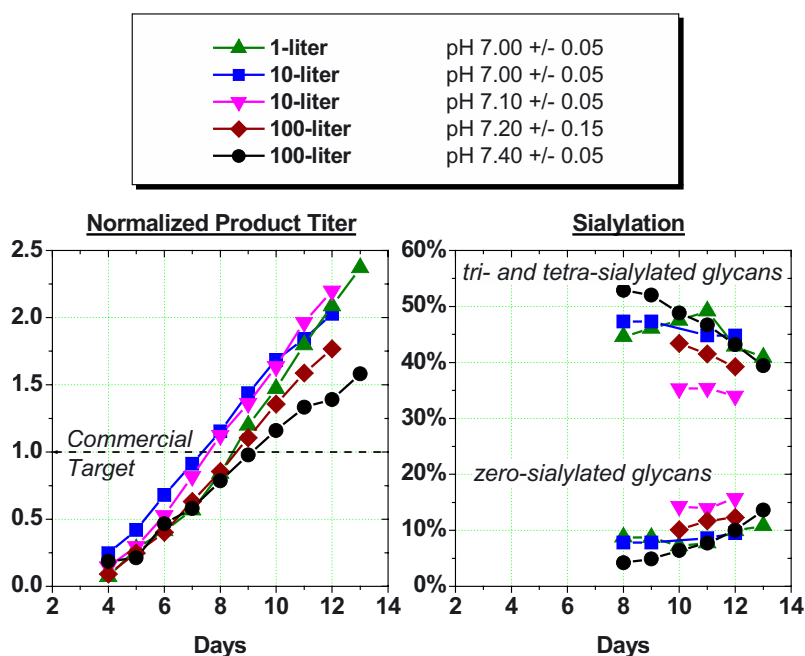


Figure 4. Effect of the pH on product titer and quality.

During development of the ACF-v1 process, the process pH set point was investigated carefully. In the default process, the pH was controlled at pH 7.4 ( $\pm 0.05$  to  $\pm 0.15$  pH units for the dead band). Range-finding studies, however, had shown that a significant increase in NIF production could be achieved by reducing the pH set point. Figure 4 illustrates that a pH set point of pH 7.2 to pH 7.0 resulted in a product concentration on day 11 approximately a factor 1.6 to 2.0 higher than the commercial target, whereas this factor was only approximately 1.4 at pH 7.4. Unfortunately, this opportunity could not be realized in the final process protocol due to a lack of robustness in product sialylation. The product quality data in Figure 4 show that some – but not all – batches controlled at a lower pH had significantly less tri- and tetra-sialylated glycan structures compared to the pH 7.4 reference. At the same time, these batches also had increased fractions of zero-sialylated glycans. In contrast, pH set points of 7.30 to 7.55 were found to generate reproducible product quality equivalent to the pH 7.4 default process. Small scale experimental design studies suggested that increased lactate accumulation, as seen at pH 7.3 or higher, was associated with better product sialylation.

During further scale-up and transfer to a manufacturing environment, the cell culture medium was switched from a liquid formulation to a solid raw material. This granulated material was produced by fluidized-bed granulation (AGT™, Invitrogen Corporation) (3). With respect to harvest titer and final product quality, no changes were observed. However, the granulated material resulted in an approximately 18% larger integral of the viable cell concentration over process time and approximately 14% lower cell-specific productivity.

#### 4. CONCLUSIONS

A new animal-component-free process, ACF-v1, was developed to produce the highly glycosylated and sialylated protein UK-279,276 (NIF) in a fed-batch stirred tank process using the recombinant CHO cell line PFG01. Process modifications lead to an approximately five-fold increase in productivity, exceeding the commercial target for harvest product titer by 20% to 50%. With a process time of 11±1 days and a pH control set point of pH 7.4, the glycosylation and sialylation profile of the final product was robust and reproducible. Pharmacokinetic studies in a rat model verified that NIF produced in the ACF-v1 process had clearance and half-life properties comparable to the material used for early clinical studies.

The authors would like to acknowledge and thank Robert Webster, Pfizer Inc, UK, for conducting the pharmacokinetic experiments.

#### 5. REFERENCES

- Moyle M., Foster D.L., McGrath D.E., Brown S.M., Laroche Y., De Meutter J., Stanssens P., Bogowitz C.A., Fried V.A., Ely J.A. A hookworm glycoprotein that inhibits neutrophil function is a ligand of the integrin CD11b/CD18. *Journal of Biological Chemistry* 1994; 269: 10008-15.
- Pluschkell S.B., Geldart R.W., Ho L., Koehler, M.A., Okediadi, C.A., Pias, S.J., Zhu, M.M., Hawrylik, S.J., Moyle, M. Process for preparation of recombinant *Ancylostoma caninum* neutrophil inhibitory factor, including its molecular cloning in mammalian cells and growth of transformed mammalian cells in animal protein and serum free medium. (Pfizer Products Inc., USA; Corvas International, Inc.). PCT Int. Appl. (2002), WO 02/16584 A2.
- Radominski, R., Hassett, R., Dadey, B., Fike, R., Cady, D., Jayme, D. Production-scale qualification of a novel cell culture medium format. *BioPharm* 2001; 14: 34-36,38-39.
- Webster R., Taberner J., Edgington A., Guhan S., Varghese J., Feeney H., Blocker L., Jezequel S.G. Role of sialylation in determining the pharmacokinetics of neutrophil inhibitory factor (NIF) in the Fisher 344 rat. *Xenobiotica* 1999; 29:1141-1155.

M. DEROUAZI<sup>\*1</sup>, H.M. PICK<sup>\*2</sup>, C. DELUZ<sup>2</sup>, S. PICASSO<sup>1</sup>,  
R. JACQUET<sup>1</sup> AND F.M. WURM<sup>1</sup>

## TOWARDS AN AFFINITY-BASED CAPTURE SYSTEM FOR THE ISOLATION OF HIGH EXPRESSION CELLS USING A CO-EXPRESSED SURFACE PROTEIN

<sup>1</sup>*LBTC, Center of Biotechnology, EPFL, 1015 Lausanne Switzerland.*

<sup>2</sup>*LCPPM, Institut of Biomolecular Science, EPFL,  
1015 Lausanne Switzerland*

*\*these authors contributed equally to this work*

### 1. INTRODUCTION

Identification, selection and expansion of the highest producing mammalian cell lines is tedious and often dependent on chance. We are attempting to establish a novel cell identification and selection system, based on the expression of a tagged plasma membrane protein that serves as a capturing device for rare cells overproducing a co-expressed recombinant protein. Here we studied the feasibility of this approach with transiently transfected CHO cells in suspension culture. Cells expressing an epitope-tagged plasma membrane protein were selected with antibody-coated protein A beads. We found that with increased expression of the tagged protein the level of the co-expressed recombinant protein was reduced. However, the data do support the notion that immobilized antibodies can be employed to select cells displaying an epitope-tagged protein.

### 2. RESULTS

#### *2.1. Stable transfections of CHO cells can be done in suspension culture*

We have developed an efficient method for the bulk transfection of suspension-adapted CHO cells promising to yield at least 10 to 100 times more stable cell lines from a single transfection than is possible with the transfection of adherent cells. In this study, we executed single-procedure transfections of suspension cultures at the 100 ml scale (i.e. with  $2 \times 10^8$  cells), equivalent to the transfection of sixty-six 10 cm cell culture plates. We have also shown that this procedure can be scaled-up to 1-10L, allowing one-step transfection of  $10^9$ - $10^{10}$  cells (see Girard et al. in this volume).

### 2.2. Co-expression of proteins having shared processing pathways may reduce the level of the recombinant protein of interest

For the cell selection procedure we chose to investigate an epitope-tagged mouse serotonin 5-HT<sub>3</sub> receptor as a potential cell surface marker. This protein can be expressed at very high levels (up to  $1 \times 10^7$  receptors per cell) in heterologous systems (Pick et al, 2003). Suspension-adapted CHO cells were transiently transfected with human IgG and receptor DNA at different ratios. When the level of the receptor plasmid was more than 5% of the total transfected DNA decreased expression of the recombinant antibody was observed (Fig. 1). One explanation for this negative interference is that both of the exogenously expressed proteins utilize overlapping pathways for protein processing (endoplasmic reticulum, Golgi apparatus).

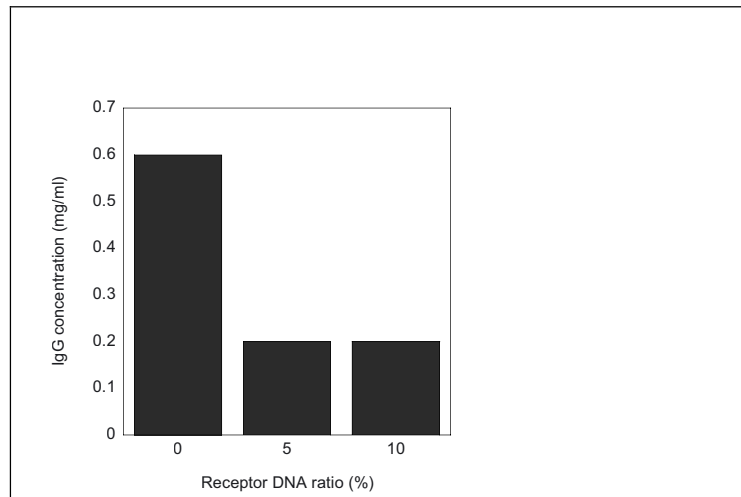


Figure 1. Suspension-adapted CHO DG44 cells were transiently transfected with IgG DNA ( $x\%$  of the total DNA) and varying amounts of receptor DNA. The antibody titer in the culture medium was determined by ELISA at 24 hours post-transfection.

### 2.3. Antibody-coated beads may be useful in capturing high expressor cells that exhibit tagged receptor protein on the surface

The specificity of the interaction between the Flag-tagged serotonin receptor and the antibody was investigated using laser-scanning confocal microscopy. Beads were pre-coated with a fluorescently labeled anti-Flag antibody (Cy3; Ex. 543 nm/ Em. 560 nm), and CHO cells transiently expressing the Flag-tagged 5HT<sub>3</sub> receptor were incubated overnight with the antibody-coated beads. Cells bound to the beads were stained with GR-fluorescein, a 5-HT<sub>3</sub> specific fluorescent antagonist (Valloton et al., 2001). Only cells expressing the cell surface target were found attached to the beads (Fig. 2).

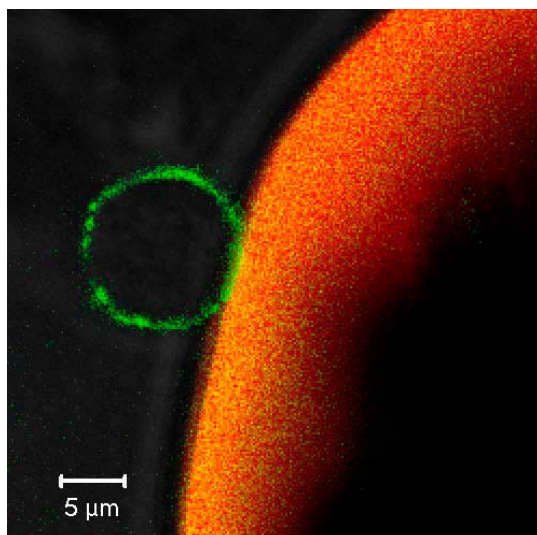


Figure 2. Fluorescence laser-scanning confocal micrograph visualizing the specific interaction of GR-fluorescein-labeled 5-HT<sub>3</sub> receptors (Ex 488 nm /Em 510 nm) on the cell surface of a transfected CHO cell with the Cy3-labeled antibodies (Ex 543 nm/Em 560 nm) fixed to the bead.

The specific labeling of the 5-HT<sub>3</sub> receptors on the cell surface allowed the determination of transient transfection efficiencies using laser-scanning confocal microscopy. We generally achieved transfection efficiencies between 20-30 % of the total cell number (data not shown). The cell viability was assessed using trypan blue staining. After overnight incubation with the beads 90 % of the cells were still viable and continued dividing after a shift to normal growth conditions (data not shown).

### 3. CONCLUSION

As a proof of principle the epitope-tagged 5-HT<sub>3</sub> receptor may be able to serve as cell surface target to allow the trapping of transiently transfected cells from polyclonal cell suspensions using antibody-coated protein A beads. Affinity trapping of transfected cells with subsequent antibiotic selection for highly expressing cells is expected to be an attractive procedure for the rapid production of stable clones from suspension cultures.

### 4. REFERENCES

- Pick H, Preuss AK, Mayer M, Wohland T, Hovius R, Vogel H. (2003) Monitoring expression and clustering of the ionotropic 5HT<sub>3</sub> receptor in plasma membranes of live biological cells. *Biochemistry* 42:877-884
- Vallotton P, Hovius R, Pick H, Vogel H. (2001) In vitro and in vivo ligand binding to the 5HT(3) serotonin receptor characterised by time-resolved fluorescence spectroscopy. *Chembiochem* 2:205-211

JOO YOUNG CHUNG<sup>B</sup>, SEUNG WOOK LIM<sup>B</sup>,  
YEON JOO HONG<sup>B</sup>, YEO WOOK KOH<sup>B</sup>, SUN OK HWANG<sup>A</sup>,  
GYUN MIN LEE<sup>A,\*</sup>

## EFFECT OF DOXYCYCLINE-REGULATED CALNEXIN AND CALRETICULIN EXPRESSION ON SPECIFIC THROMBOPOIETIN PRODUCTIVITY OF RECOMBINANT CHO CELLS

<sup>a</sup> *Department of Biological Sciences, Korea Advanced Institute of Science  
and Technology,*

*373-1 Kusong-Dong, Yusong-Gu, Daejeon 305-701, Korea*

<sup>b</sup> *R & D center, Daewoong Co. Ltd., San 84-1 Samgye-Ri, Pogok-Myun,  
Yongin, Kyunggi-do, 449-814, Korea*

**ABSTRACT** In an attempt to increase the specific TPO productivity ( $q_{\text{TPO}}$ ) of rCHO cells (CHO-TPO), the effect of expression level of calnexin (CNX) and calreticulin (CRT) on  $q_{\text{TPO}}$  was investigated. To regulate the CNX and CRT expression level simultaneously, the Tet-Off system was first introduced in CHO-TPO cells and stable Tet-Off cells (TPO-Tet-Off) were screened by the luciferase assay. The rCHO cells with a doxycycline-regulated CNX and CRT expression system (TPO-CNX/CRT) were established by cotransfection of CNX and CRT expression vector and pTK-Hyg vector into TPO-Tet-Off cells and subsequent screening by Western blot analysis of CNX and CRT. The expression levels of CNX and CRT in TPO-CNX/CRT cells could be tightly regulated by adding different concentrations of doxycycline to a culture medium. Compared with the basal level (2  $\mu\text{g}/\text{mL}$  doxycycline), a 2.9-fold increase in CNX expression and a 2.8-fold increase in CRT expression were obtained in the absence of doxycycline. This increased expression level of CNX and CRT resulted in a 1.9-fold increase in  $q_{\text{TPO}}$  without growth inhibition. Furthermore, *in vivo* biological activity of TPO was not changed by increasing the CNX and CRT expression level. Taken together, the results obtained here demonstrate that a simultaneous overexpression of CNX and CRT can increase the  $q_{\text{TPO}}$  of rCHO cells.

### 1. INTRODUCTION

For the production of therapeutic glycoproteins, CHO cells have been the most popular probably because CHO cells are able to perform complex post-translational modification, including glycosylation, in an authentic manner. To assess the effect of CNX and CRT expression level on  $q$  of foreign protein in rCHO cells, we selected TPO as a model protein. Human TPO, which is a hematopoietic growth factor inducing thrombopoiesis [1], is a very complex glycoprotein with 6 sites of N-linked glycosylation and 18 putative sites of O-linked glycosylation. The heavy glycosylation of TPO suggests that the post-translational process is most likely to be a limiting step in TPO secretion and overexpression of CNX and CRT in rCHO cells may increase specific TPO productivity ( $q_{\text{TPO}}$ ). We established a TPO-producing,



Tet-Off rCHO cell line with regulated expression of the CNX and CRT. The Tet-Off cell line is based on regulatory elements of the tetracycline-controlled transactivator (tTA) and a tTA-dependent promoter that is virtually silent in the absence of tetracycline [2]. Here, we report the effect of CNX and CRT expression level on the  $q$  and *in vivo* biological activity of TPO in rCHO cells.

## 2. MATERIALS AND METHODS

### 2.1. Vector for Simultaneous CNX and CRT Expression.

Figure 1 shows the schematic representation of procedure for the establishment of a vector for simultaneous expression of CNX and CRT, pBICC. The plasmids encoding the genes of CNX and CRT were constructed using the cDNA pool of CHO cells prepared in our laboratory. The cDNA templates were prepared from mRNAs of CHO cells (DUKX-B11, ATCC CRL-9096) using Marathon<sup>TM</sup> cDNA amplification kit.

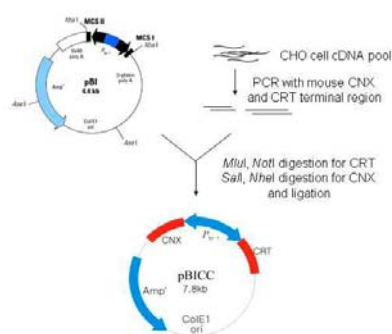


Figure1. Schematic representation of procedure for the establishment of a vector for simultaneous expression of CNX and CRT, pBICC.

### 2.2. Development of Double-Stable Cell Line.

The rCHO cell line expressing a human TPO (CHO-TPO) was established in our laboratory. To regulate the CNX and CRT expression level simultaneously, the Tet-Off system was first introduced in CHO-TPO cells and stable Tet-Off, CHO-TPO cells (TPO-Tet-Off) were screened by the luciferase assay, as described previously.

### 2.3. Slot and Western Blot Analyses.

To determine the expression level of CNX and CRT, slot and Western blot analyses were performed. Cells were lysed for 30 min at a concentration of  $1 \times 10^7$  cells/mL in cell lysis buffer (Cell Signaling Technology, Beverly, MA) at 4°C. Cell lysate was centrifuged at 12,000 g for 5 min at 4°C and supernatants were collected for slot and Western blot analysis. Western blot analysis of TPO in culture supernatants was performed in the same manner as used in that of CNX and CRT, except that a TPO polyclonal antibody (R&D systems, Minneapolis, MN) as a primary antibody for TPO expression and an alkaline phosphatase-conjugated anti-goat IgG (Sigma) as a secondary antibody.

#### 2.4. Biological Activity of TPO.

The *in vivo* biological activities of TPO were tested in mice. Female Balb/c mice (20-22g) were administered with the concentration of 30  $\mu\text{g}/\text{kg}$  as a single subcutaneous injection. Each test group consisted of five mice. On each sampling day, the mice were anesthetized with diethylether. About 200  $\mu\text{L}$  of peripheral blood was obtained from the abdominal artery for measuring the hematological parameters into EDTA tubes. The blood cell counts were determined using a Cell-Dyn 3500 analyzer (Abbott Laboratories, Abbott Park, IL). Statistical significance of difference in platelet levels between the vehicle and treated groups was assessed by Student's *t*-test.

### 3. RESULTS AND DISCUSSION

Figure 2 shows Western blot analysis of CNX and CRT in TPO-CNX/CRT cells. The expression levels of CNX as well as CRT in TPO-CNX/CRT cells could be regulated tightly by the doxycycline concentrations. When the doxycycline concentration decreased from 100 ng/mL to 0.1 ng/mL, the expression levels of CNX and CRT were increased in a dose-dependent manner. The expression levels of CNX and CRT in the absence of doxycycline were 2.9-fold and 2.8-fold higher than those at 2  $\mu\text{g}/\text{mL}$  of doxycycline (data not shown). Thus, CNX and CRT were coordinately expressed in TPO-CNX/CRT cells.

Figure 3 shows Western blots of secreted TPO in culture supernatants under the reducing condition. Regardless of doxycycline concentrations, the MW of TPO was approximately 90 kDa, which falls into the range of MW (80-100 kDa)

of TPO in human plasma. The MW of TPO calculated from its amino acid sequence is approximately 35 kD. Accordingly, TPO produced from CHO cells was heavily glycosylated and the MW was not influenced significantly by CNX and CRT overexpression. Figure 4 shows the changes in platelet levels of mice after a single injection of TPO samples at a concentration of 30  $\mu\text{g}/\text{kg}$ . The biological activity of TPO produced at various doxycycline concentrations was similar, suggesting that overexpression of CNX and CRT enhances  $q_{\text{TPO}}$  of rCHO cells without deteriorating the quality of TPO. The biological activity of TPO produced in the absence of doxycycline was significantly higher than that of negative control, as shown by statistical analysis using *t*-test ( $P < 0.001$ ,  $n = 5$ ).

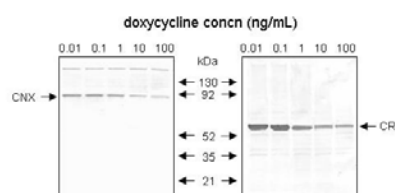


Figure 2. Western blot analysis of CNX and CRT expression levels in TPO-CNX/CRT cells at various concentrations of doxycycline.

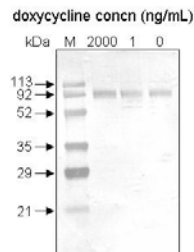


Figure3. Western blot analysis of secreted TPO in culture supernatants produced by TPO-CNX/CRT cells with regulated CNX and CRT expression at the corresponding doxycycline concentration.

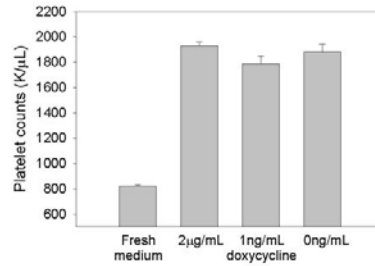


Figure4. Thrombopoietic activity of TPO produced at the corresponding doxycycline concentrations in normal female mice.

In conclusion, overexpression of CNX and CRT protein in CHO cells producing TPO significantly increased  $q_{TPO}$  without growth inhibition, resulting in the increased TPO production. Furthermore, in vivo biological activity of TPO was not changed by overexpression of CNX and CRT, demonstrating its potential as a means to increase  $q$  of rCHO cells producing therapeutic proteins.

#### 4. REFERENCES

- [1] De Sauvage FJ, Hass PE, Spencer SD, Malloy BE, Gurney AL, Spencer SA, Darbonne WC, Henzel WJ, Wong SC, Kaung WJ, Oles KJ, Hultgren B, Solber LA, Goeddel DV, Eaton DL, Stimulation of megakaryocytopoiesis and thrombopoiesis by the c-Mpl ligand, *Nature* 369 (1994) 533-538.
- [2] Gossen M, Bujard H, Tight control of gene expression in mammalian cells by tetracycline-responsive promoters, *Proc. Natl. Acad. Sci. USA* 89 (1992) 5547-5551.

NOONE C.B.<sup>1</sup>, SMITH T.J.<sup>2</sup> & CAIRNS M.T.<sup>3</sup>

## RECOMBINANT GLYCOPROTEIN EXPRESSION DEVELOPMENT OF A HOMOLOGOUS CHO EXPRESSION SYSTEM

<sup>1</sup> *National University of Ireland, Galway* <sup>2</sup> *National Centre for Biomedical Engineering and Science, NUI, Galway.* <sup>3</sup> *National Diagnostics Centre, NUI, Galway.*

### 1. INTRODUCTION

Glycosylation is a major post-translational modification of proteins that involves attachment of glycan/oligosaccharide chains to the protein (1). In producing recombinant glycoproteins it is essential to exactly replicate the native glycosylation pattern in order to ensure proper functional activity of the glycoprotein. For this reason the mammalian Chinese Hamster Ovary (CHO) cell line has generally been the host of choice. In order to evaluate the adopted dual vector expression system, we have chosen to express the glycoprotein bovine FSH. This glycoprotein is difficult to purify in substantial quantities from bovine pituitaries. A commercial form is available, however, it is frequently contaminated by other hormones such as lutenizing hormone, which it is believed, leads to some of the variability that is encountered with the superovulation procedure for cows. The aim of this project is to develop a system for expression of recombinant FSH by improving upon current CHO expression systems. The gene promoter is an obvious feature where expression levels can be controlled and/or maximised (2). An important aspect of this project was ultimately to replace the existing viral promoters with strong constitutive promoters native to CHO cells (i.e. homologous).

### 2. EXPERIMENTAL

#### *2.1. Northern and Virtual Northern Analysis*

Total RNA from CHO cells was analysed on 1.5% formaldehyde gel, transferred to nylon membrane by the northern blot procedure and probed with a variety of CHO genes that were expected to be highly expressed (fig 1). Labelling of probes was balanced in order that signal strength was representative of expression level and therefore of promoter strength. Candidate genes were also tested for the stability of

the message. There are two main reasons for this. One is that ultimately other features of these genes may be incorporated into the expression system to improve mRNA stability and therefore the steady-state level of translatable message. A second reason is that a stable gene will generally be a housekeeping gene and as such would also expect to be expressed constitutively. Virtual Northern analysis of cDNA generated from RNA of cells treated for different periods of time with actinomycin D (to inhibit *de novo* RNA transcription) confirmed stability of mRNA.

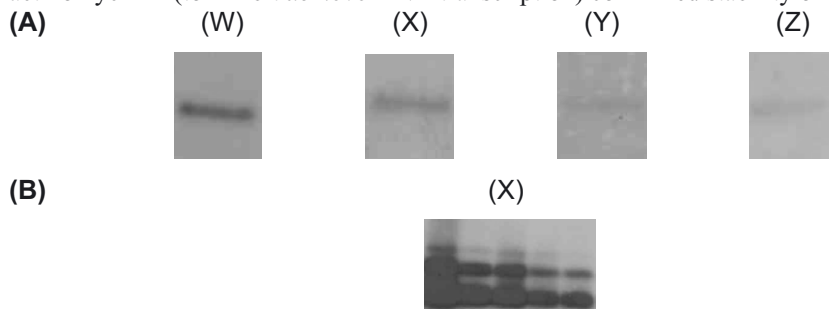


Figure 1. Comparative expression levels of several candidate CHO genes. Four candidate CHO genes (W, X, Y, Z) were analysed by northern blot. Exposures were restricted to ensure linearity of response. Gene X was further analysed on virtual northern (B). Lanes represent CHO RNA decayed for 0h, 9h, 12h, 15h and 18h. Each band (1.5kb, 900bp, 400bp) is representative of gene X.

## 2.2. Characterization of Promoter

A CHO genomic library was screened with a number of different probes derived from cDNA's of genes X and Y. Relevant lambda clones were isolated and purified. A genomic fragment of 18kb of gene X was digested further and subcloned into pGL3-Basic. Sequence analysis of a 7kb EcoRI fragment confirmed the presence of the entire gene X promoter. Expression levels were comparable to those of HCMV and SV40 viral promoters (fig.2).

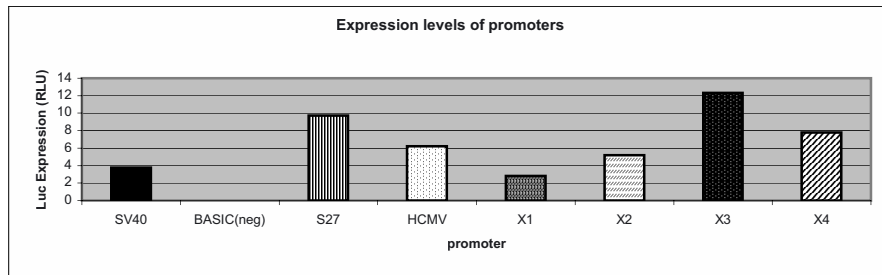


Figure 2. Relative expression levels of CHO promoter X to SV40, HCMV and s27 promoter levels. All promoters were compared within the pGL3-reporter vector backbone. The gene X promoter was dissected into segments of length 471bp, 739bp, 1021bp and 1350bp (X1 -X4 respectively). Luciferase levels were measured in relative luminescence units (RLU).

#### 2.4. Immunocytochemistry

In parallel to the promoter studies transient transfections were carried out using a dual vector expression system to express the separate  $\alpha$  and  $\beta$  FSH subunits under the control of the HCMV promoter. Transfected cells were analysed for FSH expression using immunocytochemistry and confocal microscopy. Primary antibodies to both  $\alpha$  and  $\beta$  FSH (kindly provided by Alan McNeilly, Edinburgh) were used along with a FITC labelled secondary antibody. Primary antibody to luciferase and a Texas Red labelled secondary were used as positive control (fig 3).

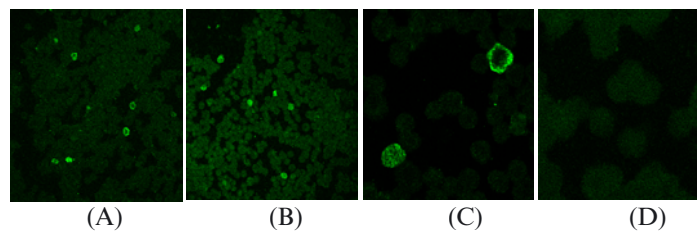


Figure 3. Immunocytochemistry of FSH-expressing cells. A and B are views of cells probed with the  $\alpha$  and  $\beta$  FSH antibodies respectively. C is a magnified view of cells at two different stages: cell full of vesicles containing FSH and a cell with vesicles being secreted into media. A and B are at 10 x magnification, C and D are at 40 x magnification. Non-transfected cells were also stained for beta FSH as a negative control (D).

### 3. DISCUSSION AND CONCLUSION

The promoter of a stable and highly expressed CHO gene was isolated. Reporter analysis confirmed it to be a strong promoter generating luciferase levels higher than that of both the viral SV40 and HCMV promoters. FSH expression was confirmed by staining with specific antibodies. The novel homologous CHO gene X promoter is now ready for introduction into expression cassette in place of HCMV.

### 4. REFERENCES

1. Savage A.V: Mammalian Cell Biotechnology in Protein Production. Walter de Gruyer, Berlin pp 233-276, 1997.
2. Latchman D.S: Eukaryotic Transcription Factors, 3<sup>rd</sup> edition (academic Press), pp 1-34, 1998.

WENLIN ZENG, ELA PUCHACZ, KATY HEINEKEN,  
ISAAC RAYMOND, CONWAY CHANG, THOMAS RYLL,  
AND STEVE CHAMOW

## GENERATION OF RECOMBINANT ANTIBODY MANUFACTURING CELL LINES USING CELL-CELL FUSION

*Abgenix, Inc, California, USA*

### INTRODUCTION

Human IgG is a heterotetrameric glycoprotein comprised of two heavy (H) and two light (L) chains. Traditionally, production of recombinant antibodies has been achieved by co-transfecting genes encoding both H and L chains into mammalian cells, such as CHO or NS0.

Abgenix and Japan Tobacco developed a novel method, cell-cell fusion (CCF), as an alternative to co-transfection to generate recombinant antibody manufacturing cell lines. In CCF, as shown in Figure 1, instead of co-introducing both HC and LC into the same cells, vectors encoding the HC and LC of an antibody are transfected separately into the host cells. Stable transfectants expressing either HC or LC are selected using different selection markers. The HC and LC producing cells are then fused to form hybrid cells that produce fully assembled and functional antibodies containing both HC and LC. We find that both H and L genes can be amplified using DHFR as the amplification marker.

We have evaluated and compared the productivity and stability profiles of production cell lines derived from CCF and co-transfection methods. The biological activity and the quality of antibody products from CCF cell lines were also examined and compared to antibody produced from co-transfected cell lines. This poster focuses on our progress in establishing our proprietary Cell-Cell Fusion technology for the generation of recombinant antibody manufacturing cell lines.

### MATERIALS AND METHODS

CHO cells were transfected with a HC vector or LC vector. Stable HC or LC clones were selected using Hygromycin or Neomycin as selective markers. High expressing HC or LC chain transfectants were selected by ELISA. Gene amplification was done using MTX. Fusion of CHO cells was preformed by standard PEG fusion. Figure 1 shows the cell-cell fusion procedure.



4-day titer analysis was performed on supernatants from 4 day cultures seeded with  $2 \times 10^5$  cells in 1mL in 24 well. The glycosylation pattern of antibody products was evaluated by enzymatically cleaving the oligosaccharides from the antibody with PNGase F and analyzing the oligosaccharides by P/ACE MDQ Capillary Electrophoresis (Beckman). Antigen binding activity was determined by an antigen specific ELISA.

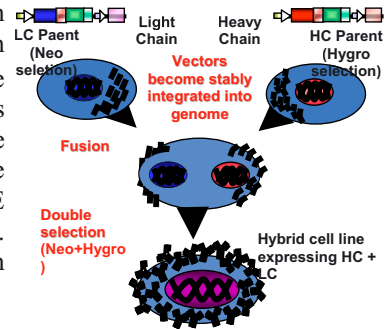


Figure 1. Cell-cell fusion procedure

EXPERIMENTS AND RESULTS

*Cell-Cell Fusion Cell Line Development Protocols*

A potential concern with developing antibodyproduction cell lines with cell-cell fusion is amplification. With co-transfection, both HC and LC vectors tend to be co-integrated into the genome. The HC and LC genes are more likely to be co-amplified during MTX amplification process. In cell-cell fusion cell line development process there are two places that we can perform MTX amplification. One is pre-fusion amplification by amplifying the HC and LC genes separately in the parental HC and LC cell lines. The other is post-fusion amplification by amplifying both HC and LC at the same time in the fused cell lines.

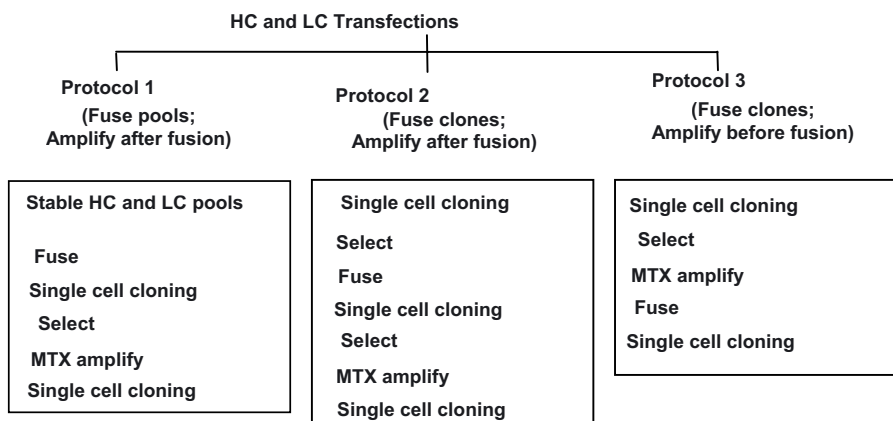


Figure 2. Cell-cell Fusion Protocols

There are potential concerns with either approach. With post-fusion amplification, it is not clear whether both HC and LC will be amplified at the same time since the HC and LC are located on two different chromosomes in the fused cells and amplification of the DHFR gene associated with either the HC or the LC vector can allow the cells survive MTX treatment. With pre-fusion amplification, it is not clear if HC alone can be well amplified since it has been reported that heavy chain protein alone is not secreted well and high levels of intracellular heavy chain protein is toxic to the cells. To identify the best amplification strategy, we tested three different cell-cell fusion cell line development protocols, CCF1, CCF2, and CCF3 as shown in Figure 2. In CCF1 and 2, HC and LC expressing cells are fused first and then amplified. In CCF3, HC and LC cells are amplified separately first and the MTX amplified HC and LC cells are then fused. We compared productivity of cells derived from the three CCF protocols and co-transfection protocol, and antibody products derived from cell lines developed from both CCF and co-transfection protocols.

*Productivity Comparison of Cell lines Generated by Cell-cell Fusion and Co-transfection Protocols.*

Table 1 shows the 4-day culture titers of the five best single cell clones generated by the CCF1, CCF2, and co-transfection protocols. The five clones were then amplified with various concentrations of MTX. For CCF3 1, HC and LC parental clones were amplified with MTX. The best amplified HC and LC cells were then fused. The productivity of the amplified cells from the four protocols were compared and the results are shown in Table 2.

Method	Clone ID	4-day Titer
Co-trans	22E6	3 ug/ml
CCF1	22C6	1.7 ug/ml
CCF1	7A6	1.2 ug/ml
CCF2	3-6B8	8.9 ug/ml
CCF2	4-5F12	21 ug/ml

Table 1. Productivity of best un-amplified clones

Protocol	MTX Pool ID	4-day Titer
Co-trans	22E6-250nM	50 ug/ml
CCF1	22C6-150nM	38.8 ug/ml
CCF1	7A6-300nM	37.2 ug/ml
CCF2	4-5F12-500nM	98.4 ug/ml
CCF2	3-6B8-500nM	58.9 ug/ml
CCF3	250nM	37.2 uf/ml

Table 2. Productivity of best amplified pools. CCF2 cells were lost due to equipment failure

*Stability of MTX amplified CCF Cell Lines*

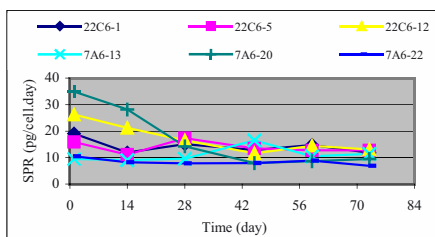


Figure 3. spr of CCF clones over time

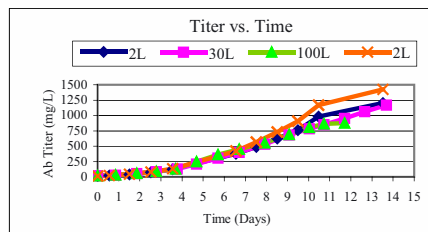


Figure 4. Titer of CCF clone 4C7 in fed-batch bioreactors at 2L, 30L, and 100L scales.

Figure 3 shows the specific productivity of six CCF cell lines over time. Some of the CCF clones are relatively stable for over two months and others are not as stable. This is similar to MTX amplified co-transfected clones in which the stability varies from clone to clone.

*Productivity of CCF Clones in Fed-batch Bioreactor*

Clone ID	CHO-S SFMII	CD-CHO	ABX-CHO2
CCF1-3G10	1.09 g/L	0.66 g/L	0.92 g/L
CCF1-4C7	1 g/L	0.8 g/L	1.07 g/L
CCF3-4C8	0.45 g/L	0.58 g/L	1.00 g/L
CCF3-9E10	0.32 g/L	0.70 g/L	0.71 g/L

Table 3. Titers of CCF clones in 2L fed-batch bioreactors.

Table 3 shows the productivity of four CCF clones in 2L fed batch bioreactors lines in 3 different media supplemented with PP3. Figure 4 shows the productivity of CCF1 clone 4C7 at scales of 2L, 30L, and 100L fed-batch bioreactors in our proprietary animal component free medium.

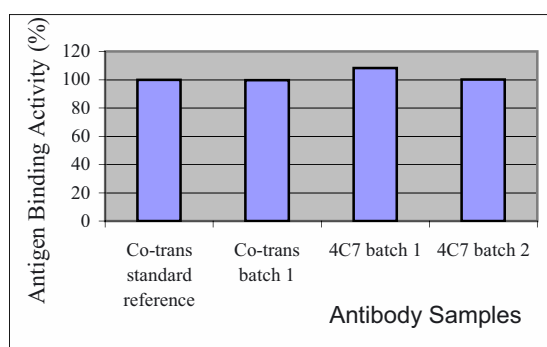
*Comparison of Antibody Products from CCF and Co-transfection Derived Cell Lines*

Antibody produced from CCF clones were purified with protein A column. The glycosylation pattern and the antigen binding activity of the purified antibody materials were analyzed and compared to that produced from a co-transfection derived cell line. Table 4 summarizes the percentage of G0, G1, and G2 glycoforms of antibody protein produced by each clone. The range of different glycoforms from the 4 CCF antibody products is comparable with that observed for the two control batches of antibody. Figure 5 shows that the antigen binding activity of CCF clone 4C7 is very similar to antibody from the co-transfection derived cell line.

Protocol-Clone ID	% G0	% G1	% G2
CCF1-3G10	70.9	25.3	3.8
CCF1-4C7	71.9	24.5	3.6
CCF3-4C8	75.8	21.5	2.7
CCF3-9E10	76.8	20.5	2.3
Co-trans batch1	69.5	26.7	3.8
Co-trans batch2	78.9	19.3	1.8

*Table 4. Comparison of the glycosylation pattern of antibody products. G0, G1 or G2 refer to forms containing 0, 1 or 2 terminal galactose residues, respectively, in biantennary structure.*

*Figure 5. Comparison of antigen binding activity of antibody products from CCF and co-transfected cell lines*



### CONCLUSIONS

In conclusion, we have shown that (1) cell-cell fusion (CCF) is a viable method for generating recombinant manufacturing cell lines. (2) Both LC and HC genes can be amplified using DHFR as the amplification marker to optimize cell line productivity. (3) The stability profile of CCF-derived clones is similar to that of co-transfection-derived clones (4) We have achieved greater than 1g/L titer at 2 L and 30 L scales using a CCF clone and a proprietary animal component-free medium in a fed-batch process(5) The antibody product derived from CCF clones is comparable in both glycosylation pattern and antigen binding activity to that derived from co-transfection clones.

G.F. ASENSI<sup>3</sup>, J.M. CAVALCANTI<sup>3</sup>, P.M. SOUSA<sup>4</sup>, E.M. DEL AGUILA<sup>2</sup>, J.T. SILVA<sup>2</sup>, V.M.F. PASCHOALIN<sup>2</sup>, L.R. CASTILHO<sup>1</sup>

## CLONING AND EXPRESSION OF BIOPHARMACEUTICALS IN CHO.K1 AND BHK-21 CELLS

<sup>1</sup> *Chemical Engineering Program/COPPE, Federal University of Rio de Janeiro,* <sup>2</sup> *Dept. of Biochemistry/IQ, Federal University of Rio de Janeiro,* <sup>3</sup> *Institute of Microbiology, Federal University of Rio de Janeiro,* <sup>4</sup> *Faculty of Pharmacy, Federal University of Rio de Janeiro*

### 1. INTRODUCTION

Since mammalian cells are able to correctly carry out protein folding and glycosylation, they are the host of choice for the expression of human glycoproteins of therapeutic use. Currently approved biopharmaceuticals derived from mammalian cell culture include monoclonal antibodies, blood coagulation factors, colony stimulating factors and other recombinant proteins (Castilho and Medronho, 2002).

Factor IX (FIX) is a coagulation glycoprotein that is either absent or deficient in hemophilia B patients. Administration of recombinant Factor IX to patients does not present the risk of virus contamination associated with hemodialysis or with Factor IX derived from human plasma. Human granulocyte colony stimulating factor (G-CSF) is a cytokine that stimulates the proliferation and terminal differentiation of neutrophilic granulocytes from progenitor cells. Therefore, G-CSF is employed in the treatment of illnesses such as neutropenia and leucopenia.

The aim of the present work was to construct recombinant vectors to be employed in the transfection of CHO.K1 and BHK-21 cells, in order to obtain recombinant cell lines stably expressing human Factor IX and G-CSF.

### 2. MATERIALS AND METHODS

#### 2.1. Human Factor IX

The cDNA coding for human FIX was obtained from *E. coli* cells (ATCC 79870) carrying the plasmid pCMV5FIX. Plasmid DNA was extracted through SDS

alkaline lysis. The plasmid was digested using *EcoR* I and the 2.4-kb fragment containing the FIX cDNA was purified from a non-stained agarose gel using the “GFX PCR DNA Gel Band Purification” kit (Amersham Biosciences).

The mammalian expression vector pCI-neo (Promega) was digested using *EcoR* I. The purified 2.4-kb fragment was linked to the digested plasmid using the “Ready to go - T4 DNA ligase” kit (Amersham Biosciences).

Competent *E. coli* DH5 $\alpha$  cells were prepared by the Ca<sup>2+</sup> methods (Sambrook and Russell, 2001). Competent cells were transformed with the pCI-neo plasmid with and without the insert and with *EcoR* I-digested pCI-neo plasmid. Non-transformed competent cells and the three types of transformed cells were incubated in solid LB medium with and without ampicillin (50  $\mu$ g/mL).

Colonies of transformed *E. coli* DH5 $\alpha$  cells were transferred to tubes containing liquid LB medium with ampicillin (50  $\mu$ g/mL). The pCI-neo plasmid was extracted by alkaline lysis with SDS and digested with *EcoR* I.

### 2.2. Human granulocyte colony stimulating factor (*G-CSF*)

Genomic DNA was extracted from cheek and blood cells. DNA and protein contents were quantified by measuring absorbance at 260 and 280 nm. DNA was purified using the “GFX Genomic Blood DNA Purification” kit (Amersham Biosciences).

The ORF of the *G-CSF* gene was amplified by PCR using a GeneAmp PCR System 2400 thermocycler (Perkin Elmer). Two different reaction conditions were tested (Table 1). In both cases, 0.25  $\mu$ g DNA, 20 pmoles of each primer, 0.5  $\mu$ moles of each nucleotide and 0.1  $\mu$ mol MgSO<sub>4</sub> were used, at a final volume of 50  $\mu$ L. The enzyme “Platinum Taq DNA Polymerase High Fidelity” (Invitrogen) was employed.

Table 1 – PCR conditions tested for *G-CSF* amplification.

<b>PCR-1:</b> 2 min/94°C 35 cycles: 1 min/94°C; 15 s/68°C; 1 min/72°C  7 min/72°C – 1 h/4°C	<b>PCR-2:</b> 2 min/94°C 15 cycles: 1 min/94°C; 15 s/62°C; 3 min/68°C 20 cycles: 1 min/94°C; 15 s/64°C; 3 min/68°C 7 min/72°C – 1 h/4°C
--	--

### 2.3. Electrophoresis

In all steps of the present work electrophoresis gels were carried out to analyse the DNA fragments obtained. Agarose gels (1.4%) were run in TAE buffer and stained either with 0.1-mg/mL ethidium bromide or SYBR Green I Nucleic Acid Gel Stain (Molecular Probes).  $\lambda$  DNA digested with *Hind* III, containing 23130, 9416, 6557, 4361, 2322, 2027 and 564 b fragments, was used as standard. Electrophoresis was run at 220V and 85mA, for 100 min.

## 3. RESULTS AND DISCUSSION

### 3.1. Human Factor IX

The gene coding for human FIX is found at chromosome X and consists of 8 exons and 7 introns, with approximately 34 kb (Walsh, 1998). Due to the large size of this

gene, a strain carrying the cDNA for human FIX (1.4 kb) was purchased from the ATCC Library of human cDNA clones.

After extracting the plasmid pCMV5FIX from the ATCC 79870 *E. coli* strain, it was digested with *EcoR* I and the fragments so obtained were analysed through electrophoresis (Fig. 1a). The fragment, which was 2.4 kb in length, contained the FIX cDNA. From a non-stained part of the gel the 2.4-kb fragment was recovered and purified.

The mammalian expression vector pCI-neo was also digested with *EcoR* I. Using a commercial DNA ligase kit, the 2.4-kb fragment was linked to the open pCI-neo plasmid. The recombinant plasmid so obtained was used to transform competent *E. coli* DH5 $\alpha$  cells, which were incubated in LB agar medium containing 50  $\mu$ g/mL ampicillin. As controls, non-transformed competent cells and cells transformed with the pCI-neo plasmid (without the insert) and with an open pCI-neo (digested with *EcoR* I) were also tested for growth in this medium. The recombinant vector so obtained will be sequenced and then employed to transfect CHO.K1 and BHK-21 cells previously adapted to serum-free suspension growth.

### 3.2. Human granulocyte colony stimulating factor (G-CSF)

The ORF of the human G-CSF gene is relatively short (1.5 kb). Therefore, we decided to amplify this ORF directly from genomic DNA extracted either from cheek or blood cells. Since both the DNA concentration and the  $A_{260}/A_{280}$  ratio were larger for the blood cell DNA, this was used in the PCR.

From the two different PCR conditions, only under the PCR-1 conditions it was possible to amplify the G-CSF ORF, as shown in Figs. 1b and 1c. The amplified fragment will be inserted in the pCI-neo vector and used to transfect CHO.K1 and BHK-21 cells previously adapted to serum-free suspension growth.

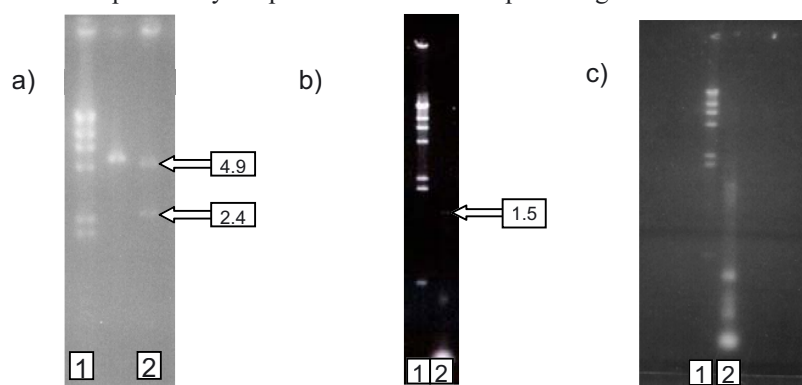


Figure 1 – (a) pCMV5FIX digested with *EcoR* I; (b) PCR-1 and (c) PCR-2 products (fragment standard – lane 1; sample – lane 2).



## 4. REFERENCES

- Castilho LR, Medronho RA (2002), *Advances in Biochemical Engineering/Biotechnology*, 74, 127-167.  
Sambrook J, Russell DW (2001), *Molecular Cloning - A Laboratory Manual*, CSHL Press, New York.  
Walsh G (1998), *Biopharmaceuticals: Biochemistry and Biotechnology*, John Wiley & Sons, New York.

VIRNA CORTEZ-RETAMOZO\*, N. BACKMANN\*, P. SENTER†, U. WERNERY‡, P. DE BAETSELIER\*, S. MUYLDERMANS\* AND H. REVETS\*

## CAMEL SINGLE-DOMAIN ANTIBODIES AS MODULAR BUILDING BLOCKS TO MAKE BIVALENT CONSTRUCTS FOR USE IN IMMUNOTHERAPY OF CANCER

\**Vlaams Interuniversitair Instituut voor Biotechnologie, Vrije Universiteit Brussel, E 8, Pleinlaan 2, B-1050 Brussels, Belgium*; †*Seattle Genetics, 21823 30th Dr. SE, Bothell, WA 98021, USA* and ‡*Central Veterinary Research Laboratories, PO-Box 591, Dubai, UAE*

*ABSTRACT* Over the last years there has been a growing interest in the use of antibodies and antibody fragments as therapeutic entities to treat cancer. Identification of the smallest antibody fragment still capable of binding to antigen has progressed from full antibody molecules to Fab and recombinant single chain Fv fragments. A further reduction to single-domain binding proteins based upon immuno-globulin VH and VH-like domains is being pursued since they offer exciting prospects in the development of novel immunotherapeutics. Unfortunately, the poor solubility and reduced antigen affinity requires additional engineering. By serendipity, it was discovered that this engineering is already performed in nature. Part of the humoral immune response of camels and llamas is based largely on heavy-chain antibodies where the light chain is totally absent. These unique antibody isotypes interact with the antigen by virtue of only one single variable domain, referred to as VHH. Here we describe the properties of camel VHH that offer added value over conventional antibody fragments as treatment modality for tumour patients.

### CAMELID HEAVY-CHAIN AND SINGLE-DOMAIN ANTIBODIES

Immunoglobulins found throughout the vertebrate phylum are composed of two identical heavy and two identical light chain polypeptides, except in *Camelidae* (camels, dromedaries and llamas) where an important fraction of the functional serum antibodies are homodimers of heavy chains only (HCAbs)<sup>1</sup>. In these bivalent HCAb molecules, the antigen is bound by one single domain, the N-terminal variable domain, referred to as VHH. The VHH's possess a number of amino acid substitutions that distinguish VHH's from the conventional variable domain of the heavy chain of conventional antibodies (VH). A VHH has a MW of only 15 kDa, which is at least half the size of the intact antigen-binding site of a conventional antibody, the Fv or scFv (*i.e.* the variable fragment consisting of paired VH and VL domains, or a scFv a construct where the VH is tethered by a flexible linker to a VL in one polypeptide chain, to enhance the stability of the recombinant protein). The presence in serum of camelids, of heavy-chain antibodies devoid of light chains and

the CH1 domain, in conjunction with the possibility to immunise these animals, allows for a straightforward cloning and selection procedure, and for the production of an antigen-binding unit consisting of a single-domain only, the VHH<sup>2</sup>. Thus, a technology was designed aimed at obtaining *in vivo* matured antigen binders in a single-domain format. To this end a dromedary (or a llama) is first immunised with the purified antigen (or a mixture of purified antigens). The lymphocytes from the peripheral blood are isolated and used to extract mRNA that is used in an RT-PCR with VHH-specific primers to amplify the VHH genes. The VHH gene fragments are then ligated in a phage display vector and an 'immune' library is created from which potent antigen binders can be selected<sup>2</sup>. These VHH's or cAbs are well expressed in the periplasm of bacteria, are very stable, and interact with the antigen with nM affinity, an affinity that is similar to what is obtained for the best scFv's. Surprisingly, many VHH's directed against enzymes act as competitive inhibitors<sup>3</sup>. Moreover, VHHs can access antigenic epitopes not generally recognized by conventional antibodies (unpublished results) and were recently shown to transmigrate across human blood-brain barrier endothelium<sup>4</sup>. Lastly, the comparative low complexity, high affinity and specificity of the antigen-binding site of these single-domain antibodies consisting of only three loops offer particular advantages over classical antibodies in the design of inhibitors or cell receptor blockers.

#### SINGLE-DOMAIN ANTIBODIES TARGETING CANCER CELLS

Two camel single-domain fragments, cAb-Lys2 and cAb-Lys3, recognizing an overlapping epitope of lysozyme, and a bivalent cAb-Lys3 were investigated for their ability to target transgenic tumours expressing lysozyme on their membrane. Biodistribution experiments with these cAbs in mice confirmed their extremely fast blood clearance in absence of accessible antigen. In contrast, the animals bearing tumours exposing the antigen retained the cAbs specifically at the tumour site<sup>5</sup>.

Having established the tumour targeting potential of VHHs, we went on using cAbs as modular building block in the generation of more complex constructs that have a favourable therapeutic effect. Indeed, the strict single domain nature of the cAbs promotes them as ideal molecular recognition unit into more complex entities, e.g. bivalent or bispecific constructs obtained by cloning two VHH's spaced by a flexible linker such as the natural hinge of antibodies, immuno-toxins and other immuno-conjugates generated by fusing the genes of a VHH to that of a toxic protein or of an enzyme. A series of five camelid single-domain antibody fragments (VHH/cAb) with specificity to carcinoembryonic antigen (CEA) were isolated from the phage displayed VHH repertoire of an immunized camel. All isolated binders were expressed in bacteria in high yield (up to 10 mg/l) and possessed prolonged stabilities and high thermal stabilities. Epitope mapping revealed that each VHH interacted with different, non-overlapping epitopes on CEA, with affinities in the range of 0.9-55 nM. The isolated VHH specifically recognized CEA expressed on LS174T human adenocarcinoma cells as shown by flow cytometry. In addition, a recombinant fusion protein that contained the VHH with highest affinity for CEA

(cAb-CEA5), fused to *Enterobacter cloacae* P99  $\beta$ -lactamase ( $\beta$ L) was engineered. The immuno-conjugate could be readily purified from periplasmic fractions in high yields as a soluble protein without notable signs of aggregation. Both, the binding of the VHH and the enzymatic activity of the  $\beta$ L moiety are well preserved. The specific cytotoxic effect of the conjugate in combination with CCM prodrug on LS 174T human adenocarcinoma cells expressing CEA antigen has been demonstrated. Biodistribution of the chimeric protein in nude mice bearing sc LS 174T cells confirmed the specific targeting to the CEA expressing tumours, and a favourable tumor-to-organ ratio for antibody-dependent enzyme prodrug therapy. Outstanding *in vivo* therapeutic effects were recorded for this immunoconjugate in nude mice bearing sc LS 174T carcinoma tumour xenografts in combination with sub-lethal doses of the CCM prodrug.

Smaller size, higher solubility, higher intrinsic stability, more economic production, easier tailoring into pluripotent constructs, reduced immunogenicity and targeting novel epitopes are the main advantageous properties of the camel-derived single domain antibodies over antigen-binding fragments of conventional antibodies. Because of their excellent tumour targeting and the above properties, camel single domain antibodies are a promising format for cancer diagnosis/therapy to be used as monomer or as modular building unit for multivalent or multifunctional constructs. Interestingly, efforts are currently being made to increase the stability of scFv antibodies and to try to endow them with properties of camel single-domain antibody fragments<sup>6</sup>.

#### REFERENCES

- Hamers-Casterman, C., Atarhouch, T., Muyldermans, S., Robinson, G., Hamers, C., Bayjana Songa, E., Bendahman, N. and Hamers, R. (1993) *Nature* **363**, 446-448.
- Gharhoudi, M., Desmyter, A., Wyns, L., Hamers, R. and Muyldermans, S. (1997) *FEBS Lett.* **414**, 521-526.
- Lauwereys, M., Gharhoudi, M., Desmyter, A., Kine, J., Holzer, W., De Genst, E., Wyns, L. and Muyldermans, S. (1998) *EMBO J.* **17**, 3512-3520.
- Muruganandam, A., Tanha, J., Narang, S. and Stanimirovic, D (2002) *FASEB J.* **16**, 240-242.
- Cortez-Retamozo, V., Lauwereys, M., Hassanzadeh, G. G., Gobert, M., Conrath, K., Muyldermans, S., De Baetselier, P., and Revets, H. (2002) *Int. J. Cancer* **98**, 456-462.
- Visintin, M., Settanni, G., Maritan, A., Graziosi, S., Marks, JD. and Cattaneo, A. (2002) *J. Mol. Biol.* **317**, 73-83

S. MATSUMOTO, Y. KATAKURA, M. YAMASHITA, Y. AIBA,  
E. NOGUCHI, K. TERUYA, S. SHIRAHATA

## ESTABLISHMENT OF EFFICIENT CLONING METHOD FOR VARIABLE REGION GENES OF ANTIGEN SPECIFIC HUMAN MONOCLONAL ANTIBODY

*Department of Genetic Resources Technology, Kyushu University, Fukuoka,  
Japan*

**Abstract.** We have developed an *in vitro* immunization protocol of human peripheral blood mononuclear cells (PBMC) for generating human antigen-specific antibodies. By using this protocol, B cells producing antigen-specific antibody can be propagated within a week. In the present study, we tried to establish an efficient strategy to clone variable region genes of antigen-specific human monoclonal antibody by applying *in vitro* immunized PBMC to the phage display method. To evaluate the efficiency of our strategy, variable region genes prepared by PCR from PBMC immunized *in vitro* with mite-extract (ME) and non-immunized PBMC were applied to the phage display method. After concentrating the ME-specific phage antibody by several rounds of panning, the number of phage antibodies specific for ME and antigen specificity both increased by using *in vitro* immunized PBMC. These results demonstrate that efficiency in acquisition of variable region genes of antigen specific human monoclonal antibody can be improved by *in vitro* immunizing PBMC used as a source of antibody genes.

### 1. INTRODUCTION

Human monoclonal antibodies (mAbs) have a great potential for diagnosis and treatments of cancer, allergy and other diseases. However, we cannot immunize human with antigen by ethical problems. Monoclonal antibodies from mouse origin are relatively easy to produce, however, their therapeutic availability is restricted by their antigenicity. They cause human anti-mouse antibody (HAMA) response. At present, human monoclonal antibodies are mainly produced by humanizing mouse monoclonal antibodies with genetic engineering. But it is difficult to completely remove antigenicity derived from mouse. Therefore, we have developed an *in vitro* immunization (IVI) protocol of human peripheral blood lymphocyte (PBL) for generating human antigen specific antibodies. Until now, we have successfully generated human B cell clones producing CTB, KLH, or rice allergen specific antibody (1). However, this method has been restricted to the generation of low affinity IgM antibodies. In the present study, we tried to establish an efficient strategy to clone variable region genes of antigen specific human monoclonal antibody by applying *in vitro* immunized PBL to the phage display technique.

### 2. MATERIALS AND METHODS

497

*F. Gòdia and M. Fussenegger (Eds.), Animal Cell Technology meets Genomics, 497-499.  
© 2005 Springer. Printed in the Netherlands.*

### 2.1. Reagents

Recombinant human IL-2 was purchased from Genzyme corporation (Cambridge, MA, USA). Recombinant human IL-4 was purchased from Pepro Tech EC LDT. (London, England). Muramyl dipeptide (MDP) was purchased from Chemicon international Inc. (Temecula, CA, USA). L-Leucyl-L-Leucine methyl ester (LLME) was obtained from Boehringer GmbH (Mannheim, Germany).

### 2.2. *In vitro* immunization

Human peripheral blood lymphocytes (PBL) were separated by density-gradient centrifugation from a healthy donor. Lymphocytes from peripheral blood were treated with 0.25 mM LLME. The LLME-treated PBL were cultured for 8 days in ERDF medium containing 10% heat inactivated fetal bovine serum, MDP, IL-2, IL-4, 2-mercaptoethanol and Mite-Extract (ME). Antibody production and antigen specificity of supernatant of cultured PBL was measured by ELISA.

### 2.3. Construction of Phage Display Library

At first, mRNA was isolated from PBL and the VH (variable heavy) and VL (variable light) genes were prepared by RT-PCR. To obtain diverse variable region genes of antibody, specific primers for several families (2) antibody genes were prepared. Next, the heavy and light chain DNA fragments were joined with a linker DNA. The assembled ScFv (single-chain fragment variable) DNA was subsequently amplified with primers which attach *Sfi* I and *Not* I restriction site. The amplified product was digested with *Sfi* I and *Not* I for cloning into the pCANTAB5E phagemid vector. The ligated vector was introduced into competent *E.coli* TG1 cells. Phagemid-containing bacterial colonies were infected with M13KO7 helper phage to yield phage-displayed antibody ScFv fragments.

### 2.4. Detection of ME-specific phage clones by panning and ELISA

The phage-displayed antibody fragments were selected by panning against ME. Phage which display ME-specific antibody fragments bound to a ME-coated plastic vessel. Non-specific phage were thus removed due to their inability to bind to the vessel by washing. *E.coli* TG1 cells were infected with the phage which display ME-specific antibody. Cells were rescued with M13KO7 helper phage and panned against ME several more times to further enrich for ME-positive phage antibodies. Then the cells were plated on a solid medium. Colonies were picked and rescued individually. Phage from individual wells were then assayed by ELISA.

## 3. RESULTS AND DISCUSSION

### 3.1. Efficiency of applying *in vitro* immunized PBL to phage display method

15 positive clones were obtained from random picked 120 phage clones of *in vitro* immunized library, and 12 positive clones were obtained from random picked 120 phage clones of non-stimulated library. Immunized library slightly exceeded non-stimulated library in efficiency. Three markedly high reactive clones were obtained from *in vitro* immunized library, but such high reactive clones were not obtained from non-stimulated library (Figure 1).

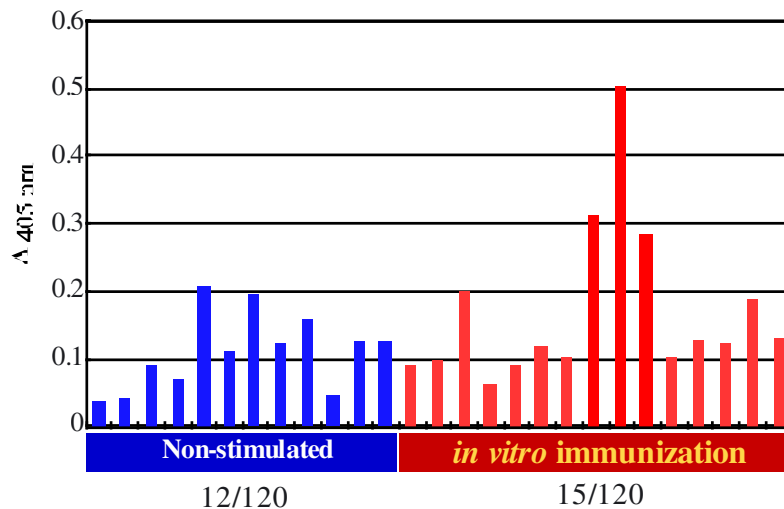


Figure 1. Reactivity of Phage Antibodies against ME

Results showed that the number of phage antibodies specific for Mite-Extract and antigen specificity both increased by using *in vitro* immunized PBL. These results demonstrate that efficiency in acquisition of variable region genes of antigen specific human monoclonal antibody can be improved by using *in vitro* immunized PBL as a source of antibody genes. Furthermore, it has been speculated that affinity maturation of lymphocyte can be occurred by *in vitro* immunization since especially high reactive clones were obtained from *in vitro* immunized library. We expect that the *in vitro* immunization and phage display hybrid protocol is a potentially powerful strategy to obtain variable region genes for antigen specific human antibody.

#### 4. REFERENCES

- Ichikawa, A., Katakura, Y., Teruya, K., Hashizume, S. and Shirahata, S. (1999) In vitro immunization of human peripheral blood lymphocytes: establishment of B cell lines secreting IgM specific for cholera toxin B subunit from lymphocytes stimulated with IL-2 and IL-4. *Cytotechnology* 31, 131
- Xiaowei Wang, B. David Stollar. Human immunoglobulin variable region gene analysis by single cell RT-PCR. *Journal of Immunological Methods* 244 (2000) 217-225

BORTH N., BÖHM E., GRILLARI J., LÖSCHER M., GROSS S.,  
VOGLAUER R., FERKO B., KUNERT R., KATINGER H.

## FROM GENE TO MONOCLONAL ANTIBODY: EFFICIENT SCREENING BY CELL SORTING

*Institute for Applied Microbiology, University of Natural Resources and  
Applied Life Sciences, Vienna, Austria (Muthgasse 18, 1190 Vienna, Austria)  
e-mail: nicole.borth@boku.ac.at*

### 1. INTRODUCTION

The screening for antigen-specific hybridoma cells with adequate production rates is still a very time, labour and money consuming procedure. Some alternatives such as phage display and single chain libraries have been described<sup>1</sup>. However, these also require intensive screening or affinity maturation and are often protected by proprietary rights. A reduction in the number of microtiter plates to be cultivated and tested by pre-selecting the fused cells that produce the right kind of antibody at high rates could therefore make the hybridoma technology more attractive, even for small research groups or for new genes at an early stage of research projects, when it is not yet clear whether the gene product is “worth” the effort.

In a research setting one is often faced with the problem of having identified a gene of interest, for instance by subtractive hybridisation or by selection of an interacting gene by a yeast-two-hybrid assay<sup>2-3</sup>. The establishment of a monoclonal antibody early on in the project is usually hampered by a lack of information about the protein, which prevents establishment of a purification protocol to obtain sufficient amounts for immunisation of mice. Nevertheless, exactly at these early stages it would be especially helpful for clarification of the function to be able to locate the protein in the cell, to quantify its concentration or to have an antibody for co-precipitation and Western Blots. To overcome these difficulties we have developed the strategy described in this paper.

### 2. METHODS AND RESULTS

#### *2.1. Isolation of genes and expression in yeast and insect cells*

SNEV (senescence evasion factor) is a nuclear protein presumably involved in mRNA splicing that was identified by a screening for genes that are differentially expressed in senescent versus early passage human endothelial cells<sup>2</sup>. Blom4 (Bring lots of money 4) was identified as a SNEV interacting protein by yeast-2-hybrid screening and is homologous to the subunit REXO70 of the rat exocyst complex<sup>3-4</sup>. Both genes are upregulated in young cells and are of interest for a better



understanding of the molecular mechanisms underlying replicative senescence in cultured cells. The genes were cloned into pBacPac8HA and pPICZA vectors after addition of a 6-His-tag to the 3'-end of the genes. After production in *Pichia pastoris* cells or Sf9 cells, respectively, the proteins were purified as described in 5.

### *2.2. Immunisation of Mice and Fusion*

Four mice each were immunised twice with 50µg of yeast derived purified antigen at three weeks intervals. Insect cell derived antigen was used for the third immunisation and the boost to avoid maturation of antibodies against traces of yeast or insect cell proteins. 3-5 days after the boost spleen cells were fused with Ag8.653 (ATCC CRL1580) mouse myeloma cells at a ratio of 3:1 according to the procedure described by StemCell Technologies, USA. 10-14 days after fusion the HAT selected cells were washed and sorted for IgG production.

### *2.3. Secretion Assay and Flow Cytometry*

The single cell secretion assay was described by Manz et al.<sup>6</sup> and modified to suit different proteins and cell lines by Borth et al.<sup>7</sup>. The principle is based on covering the cells stepwise with an affinity matrix consisting of biotinylated ConcanavalinA, Avidin, and a biotinylated goat-anti-mouse-IgG antibody. During incubation the monoclonal antibody secreted by each cell is bound to its surface and subsequently stained with an anti-mouse-IgG-FITC conjugate. Ag8.653 cells were treated the same way as negative control. Cells were analysed on a FACS Vantage (Becton Dickinson, USA) with two 5W Argon Lasers tuned to 488nm and multiline UV. Cells were sorted at 10 cells per well directly into two 96 well-microtiter plates using the Automatic Cell Deposition Unit. Fig. 1 gives an overview over the sort gates used for selection.

### *2.4. Testing and Repeated Sorts*

After this first enrichment step, clones were tested for IgG production and specificity. Positive clones were sorted again for high IgG-production at 2 cells/well (1 plates) to ensure monoclonality. In the case of blom4, this step was performed using a double staining protocol for IgG production and specificity (Fig. 1, bottom right). Cells were incubated with the antigen for 30 min at 4°C, washed in RPMI and then incubated with goat-anti-6His-FITC conjugate and goat-anti-mouse-IgG-PE conjugate. After testing and selection of specific clones the cells with the 5% highest production rates were finally sorted to obtain a stable and high producing subclone for production. Table 1 compares the number of plates sorted and of wells tested to those necessary when using limited dilution cloning.

## **3. DISCUSSION**

By adding a 6-His-tag on the genes several problems were solved: purification with a commercially available His-tag column was possible and the selection of specific mouse hybridoma cells using an antibody against 6-His. By cloning into two different cell types the antibody response of the mice was pushed

towards producing antibodies against the desired proteins and not against potentially more antigenic yeast or insect proteins. This strategy may not be applicable, however, if the desired protein is glycosylated. By sorting IgG producing cells a reduction in work load of a factor of ten is easily achieved. This includes not only testing, but also cell culture work. Using the antigen for staining during the first sort would further decrease the work load, however at this early stage it may be considered more important not to lose any of the antibody producing cells. During stabilisation of the specific hybridoma subclones the benefit of sorting is enhanced because several subclones have to be selected. Also, with sorting three subclonings are sufficient, while with limited dilution cloning 5-10 such subclonings are necessary to obtain a cell line with the desired properties.

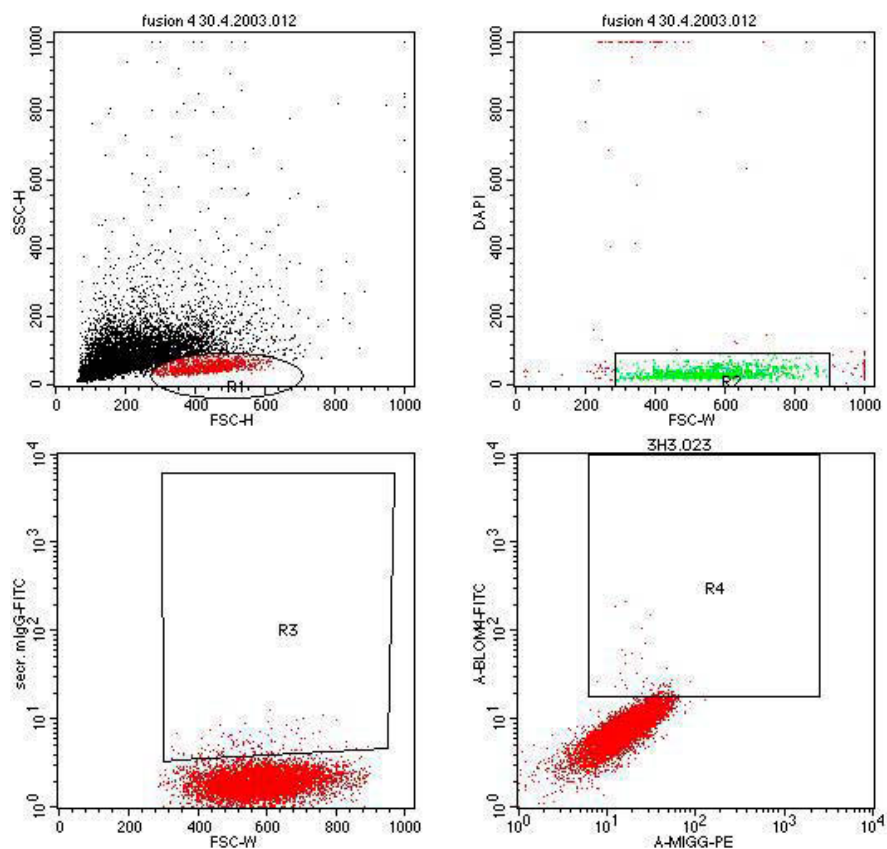


Figure 1. Sort gates and strategy: a gate is set on FSC/SSC to identify viable cells (top left).

This gate is refined by excluding cells that take up DAPI (top right). Finally on a plot of FSC-W (identifies single cells) against FL1, the cells with secreted IgG molecules caught on their surface are sorted (bottom left). Double staining for IgG-production and specificity: After application of the affinity matrix and secretion period, cells were incubated on ice with the antigen. After washing, cells were stained with an anti-mouse IgG-PE conjugate and an anti-6His-tag antibody conjugated to FITC (bottom right)

Table 1. Comparison of Cell Sorting to traditional Limiting Dilution Cloning (LDC): Values given for Cell Sorting are the averages calculated from 8 mice, values given for LDC are theoretical values calculated from the percentages given

	<b>Cell Sorting</b>	<b>LDC)</b>
% IgG positive cells (intracellular)	10	10
% IgG positive wells	80	10
% antigen specific of positive	5	5
Antigen specific antibodies isolated per mouse	2	2
wells tested (1 <sup>st</sup> Subcloning)	50	400
wells tested after 2 <sup>nd</sup> Subcloning (1 plate Sorting, 10 plates LDC per mAb) for 2 mAb	60	600
% high producers sorted in 3 <sup>rd</sup> sorting step	5	
Wells tested after 3 <sup>rd</sup> subcloning step for 2 subclones	40	400
<b>Results of Sorting</b>		
<i>IgG production after one sort (pg/cell/day)</i>	0,2-5	
<i>Stable high producers (&gt;20pg/cell/day) per mAb</i>	10	
<i>Final IgG production after three sorts (pg/cell/day)</i>	12-47	
<b>Total tested wells for 2 high producing mAb cell lines</b>	<b>150</b>	<b>1400 or more</b>
<b>Total plates cultivated for 2 high producing mAb cell lines</b>	<b>6</b>	<b>50 or more</b>

#### 4. REFERENCES

1. Knappik, A. et al. (2000) J Mol Biol, 296, 57-86
2. Grillari J. et al. (2000) Exp Gerontol, 35, 187-197
3. Grillari, J. et al. (2002) Submitted to FEBS Letters
4. Kee, Y. et al. (1997) Proc Natl Acad Sci U S A, 94, 14438-43
5. Yip, T.T. and Hutchens, T.W. (1994) Mol Biotechnol, 1, 151-64
6. Manz R. et al. (1995) PNAS 92, 1921-1925
7. Borth N. et al. (2000) Biotechn. Bioeng., 71, 266-273

A. J. CASTILLO, S. VÍCTORES, E. FAIFE, Y. RABASA,  
K. R. DE LA LUZ

## DEVELOPMENT OF AN INTEGRATED STRATEGY FOR RECOMBINANT CELL LINE SELECTION.

*Process Development Dept, Center of Molecular Immunology,  
PO Box 1600, Havana 11600, Cuba.*

**Abstract.** When developing cell culture processes based on recombinant mammalian cell lines, researchers faces very often problems related with early selection of that clone, which could better fit with the requirements needed for the future scale-up. Among desired characteristics for newly selected clones are high level and stable expression of desired protein and capability to reach high cell density in protein free-medium, in many cases under nutrient or oxygen limitations.

In this work an integrated methodology was developed for the final cell line/culture medium selection. For this aim kinetic parameters were determined in batch cultures and expression stability was studied during long term cultures. An integral multiparametric coefficient was calculated for each clone and five of twelve clones were pre-selected based on this value. The final selection was done based on resistance to apoptosis induction when these cell lines reached limiting conditions at the end of exponential growth phase.

### 1. INTRODUCTION

The loss of heterologous protein expression in recombinant mammalian cells is one of the major problems faced by industrial cell line developers and have been reported by several authors (Kim et al., 1999). By this reason the development of a procedure for obtention of stable and high producer cell lines is very important, especially for those processes based on long term continuous cultures.

The lack of high throughput clone selection procedure that could render with high efficiency clones with desired characteristics for further scale-up process (i.e. high specific production rates) have been pointed out (Grammatikos et al, 1997). Several authors have attempted to develop with relative success this kind of procedure (Massie et al, 2000; Al Rubeai et al, 2000).

In this work several clones were isolated in protein-free medium and an integrated methodology was developed for the final selection of the best combination of cell clone and culture medium attending stability of the expression during long term cell culture and specific rates determined by kinetic studies using spinner flasks.

Finally the resistance to apoptosis induction of the pre-selected clone/culture medium combination by nutrient limitation at the end of exponential growth phase was studied.

## 2. MATERIALS AND METHODS

Several clones of recombinant NSO myeloma expressing a humanized monoclonal antibody were adapted to grow in two different protein-free cell culture media: PFHM-II (Invitrogen) and Turbodoma HP (Dr. F. Messi Cell Culture Technologies).

Expression stability studies were carried out in 25 cm<sup>2</sup> T-flasks by duplicates. Cells were sub-cultured every 3 or 4 days during 45-50 days. Periodically cells were taken from each flask and seeded by triplicate in 24-well cell culture plates at 1 x 10<sup>5</sup> cells/mL per well. After 10 days IgG concentration in supernatant was tested by an anti-human IgG sandwich ELISA. Stability index (*K<sub>st</sub>*) was calculated as the surface under the curve in the IgG concentration versus culture time correlation.

Kinetic studies were carried out by triplicate in 250 mL spinner flasks (Integra). During these studies samples were taken daily or twice per day for cell counting by trypan blue exclusion method. After that, samples were centrifuged and stored at -70° C for IgG concentrations measurement.

The fraction of apoptotic population induced by nutrient limitation at the end of exponential growth phase was studied using Annexin V assay (Pharmingen).

## 3. RESULTS AND DISCUSSION

Specific growth and production rates, as well as maximum IgG concentration were determined for each clone and medium combination by kinetic characterization of batch cultures and the stability index from expression stability studies.

The integrated selection index (*K<sub>s</sub>*) was calculated using the following equation:

$$K_s = A K_{st,i} / K_{st,max} + B q_{abi} / q_{ab,max} + C [IgG]_i / [IgG]_{max} + D \mu_i / \mu_{max} \quad (1)$$

Where: *K<sub>st,i</sub>*, *q<sub>abi</sub>*, [*IgG*]<sub>*i*</sub> and  $\mu_i$  are the stability index, the specific antibody production rate, the antibody concentration at the end of the batch and the specific growth rate for a given clone respectively; *K<sub>st,max</sub>*, *q<sub>ab,max</sub>*, [*IgG*]<sub>*max*</sub> and  $\mu_{max}$  are the maximum values of stability index, specific antibody production rate, the antibody

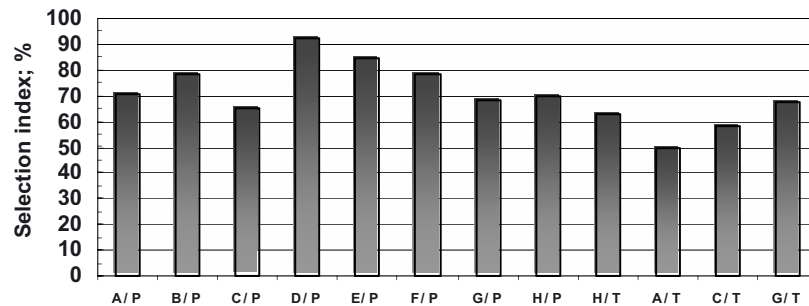


Figure 1. Selection index for different clone and culture medium combinations, where A to H: clone names; P: PFHM-II medium; T: Turbodoma HP medium.

concentration at the end of the batch and specific growth rate respectively among all studied clones. The weight coefficients  $A = 0.4$ ,  $B = 0.3$ ,  $C = 0.2$  and  $D = 0.1$  were defined in decreased order giving the highest value to the stability index and the lowest to the specific growth rate and in the way that their sum was the unity.

The values of  $K_s$  determined by equation 1 for tested clone/culture medium combinations are compared in the Figure 1. From these results the combinations with a  $K_s$  higher than 70 % were selected for further characterization attending their resistance to apoptosis induced by nutrient limitation at the end of exponential growth phase. After this assay (Figure 2) the clone B in PFHM medium showed the lowest fraction of apoptotic population, that renders it as the best candidate for further development. However if the process could be designed in order to avoid nutrient limitation (ex. perfusion instead batch or feed-batch) the best candidates could be the clones D or E cultured in PFHM-II medium, because they showed the highest values of integrated selection index.

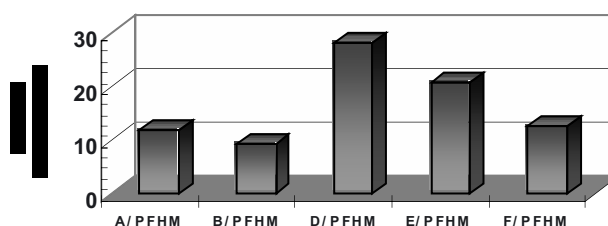


Figure 2. Percent of cell population in apoptosis induced at the end of exponential growth phase for pre-selected clones.

#### 4. CONCLUSIONS

We have developed an integrated strategy for cell line selection that considers the influence of the most important characteristics needed for a cell line during the process scale-up. In the present study the best candidate for further development is the clone B cultured in PFHM-II medium.

#### 5. REFERENCES

- Kim N. S., Kim S. J., Lee G. M., Heterogeneity within DHFR- mediated gene amplified population of CHO cells producing chimeric antibodies. *New Developments and New Application of Animal Cell Technology*, 1997, O. W. Merten et al. (eds), Proceedings of 15<sup>th</sup> ESACT Meeting, 81-83.
- Grammatikos S.I., Bergemann K., Werz W., Brax I., Bux R., Eberhardt P., Fieder J., Noé W., The real meaning of *high expression*, *Products from cells, cells as products*, 1999, A. Bernard et al. (eds), Proceedings of 16<sup>th</sup> ESACT Meeting, 11-15.
- B. Massie, D. Mosser, L. Bourget, A.W. Caron, Use of flow cytometry and micromanipulator for high efficiency cloning of cells co-expressing fluorescent proteins. In *Cell Culture Engineering VII*, 2000.
- M. Al-Rubeai, P. Holmes, High-throughput screening and selection of high producers by a rapid and objective immobilised surface display technique. In *Cell Culture Engineering VII*, 2000.

M. DEROUAZI<sup>1</sup>, P. GIRARD<sup>1</sup>, M. JORDAN<sup>1</sup>, C. DENOYA<sup>2</sup>  
AND F.M. WURM<sup>1</sup>

## GENE TRANSFER TO ANIMAL CELLS IN CULTURE BY MICROINJECTION: A NOVEL TOOL TO CREATE RECOMBINANT CELL LINES?

<sup>1</sup>*LBTC, Center of Biotechnology, EPFL, 1015 Lausanne Switzerland.*

<sup>2</sup>*Bioprocess Research and Development, Pfizer Inc, Groton USA*

**Abstract.** We are using microinjection of plasmid DNA into the cytoplasm and nucleus of Chinese hamster ovary (CHO) cells to better understand the mechanisms involved in DNA degradation and integration within the cell and to identify the requirements for the establishment of highly productive cell lines. Microinjection is an excellent tool for these studies since it allowed us to control the timing and the location of DNA transferred into single cells.

### 1. INTRODUCTION

The first barrier for the establishment of recombinant cell lines is gene transfer or more specifically, the delivery of plasmid DNA into the nucleus. The current gene transfer methods such as calcium phosphate coprecipitation (CaPi), lipofection, polymer-mediated delivery and electroporation do not allow control of the amount or subcellular location of the DNA delivered into each cell. The DNA fate during transit from membrane to the nucleus is yet not fully elucidated, but it has been shown that a dominant part of the DNA does not even reach the nucleus but is degraded<sup>3</sup>. Microinjection of naked DNA into specific cellular compartments allows both the copy number and the location of the plasmid DNA to be controlled.

We have investigated several parameters of microinjection including DNA concentration, timing of injection with regard to the cell cycle, and subcellular location of the injection in order to evaluate the feasibility of this technique for the establishment of highly productive stable cell lines.

### 2. RESULTS

#### *2.1. DNA concentration and location of injection affect protein expression level*

For the studies described below, pEGFP-N1 was dissolved in pure water because the use of buffered solutions resulted in lower GFP expression following microinjection (data not shown). The DNA concentration was found to be a critical parameter for successful microinjection. DNA concentrations from 0.5 to 1 mg/ml resulted in no

GFP expression while DNA concentrations in the range of 0.25 to 0.5 mg/ml resulted in GFP expression but no subsequent cell division. Reduction of the DNA concentration to 0.06 mg/ml resulted in both GFP expression and cell division following microinjection.

GFP expression was observed 2-3 hours after DNA injection. This result indicated that GFP began to accumulate 1-2 hours after microinjection since this protein must mature for at least one hour before it becomes fluorescent. In general, GFP expression was higher following microinjection into the nucleus as compared to microinjection into the cytoplasm (Fig. 1).

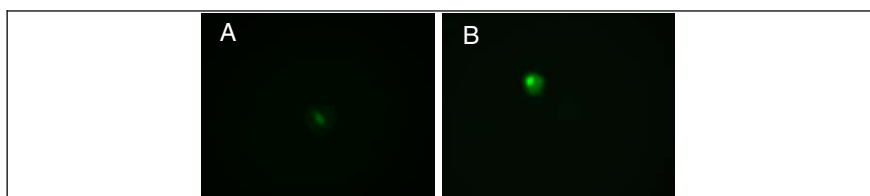


Figure 1. A: CHO cell expressing GFP 3 hours after microinjection into the cytoplasm. B: CHO cell expressing GFP 3 hours after microinjection into the nucleus.

## 2.2. Potential correlation between cell cycle stage at the time of microinjection and GFP expression

Results from CaPi transfections of synchronized CHO cell cultures demonstrated that the cell cycle plays an important role in transient transgene expression<sup>2</sup>, and Chida et al. (1998) showed a correlation between cell cycle and stable gene transfer. The frequency of stable transformation after injection is higher for cells in the G1/S boundary and in early S phase.

The effect of the cell cycle on GFP expression following microinjection was investigated by injecting cells at different time intervals after plating. CHO cells were seeded either 4 or 19 hours prior to microinjection. The position of the cells in the cell cycle at the time of microinjection was analyzed by flow cytometry. The culture plated one day prior to microinjection had 42% of the cells in the S-phase, while the culture plated 4 hours prior to gene transfer had only 28% (Table 1). Over 60% of the cells plated one day prior to microinjection were expressing GFP one day after injection into the cytoplasm. In contrast, only 32% of the cells were GFP-positive following microinjection of cells plated 4 hours prior to gene transfer.



Table 1: The cells were injected either 4 or 19 hours after plating. The cell cycle stage at the microinjection time was analyzed by flow cytometry. The transfection efficiency was assessed 3 and 24 hours after microinjection.

Injection time after plating	Location of injection	3h after injection	Day 1 after injection	G0/G1	S	G2/M
4 h	Cytoplasm	0	32%	35%	28%	37%
	Nucleus	30%	20%	35%	28%	37%
19 h	Cytoplasm	10%	64%	42%	42%	16%
	Nucleus	40%	20%	42%	42%	16%

2.3. Formation of GFP-expressing colonies after microinjection into the cytoplasm

Initially after injection into the cytoplasm, cells divided and expressed GFP at similar levels. Three to six days later, the formation of colonies with different morphologies was observed (Fig. 2), but GFP expression levels within individual cells of these colonies was heterogeneous.

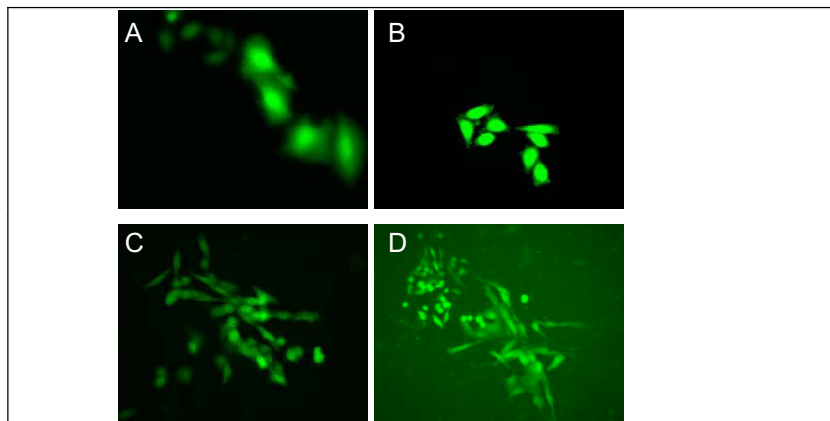


Figure 2. A and B: CHO cells expressing GFP two days after microinjection into the cytoplasm. C and D: Colonies of CHO cells expressing GFP 6 days after microinjection into the cytoplasm.

Nuclear injection of DNA resulted in very high GFP expression levels, as judged by visual examination, but these cells did not divide. The cause of this mitotic inhibition is not known.

### 3. CONCLUSION

Following microinjection of DNA into the cytoplasm, cells expressing GFP for up to six days were generated. We observed that the amount of DNA injected is critical. Since the injection volume is constant, DNA copy number can be modulated by changing the concentration of plasmid DNA. We identified conditions that allowed good expression of GFP while allowing the cells to continue to divide. The timing of injection may also have a strong impact on reporter protein expression level. Indications are that this is related to the cell cycle phase at the time of gene transfer. Microinjection is certainly a promising approach for the generation of stable cell lines since it allows the establishment of recombinant cells in a short period of time without major screening efforts. One key issue remaining is the question of the stability of the transgene expression in clones generated by microinjection.

### 4. REFERENCES

1. Chida K., Sueyoshi R. and Kuroki T. (1998) *Biochemical and Biophysical Research Communications* **249**: 849-852
2. Grosjean F., Batard P., Jordan M. and Wurm FM. (2002) *Cytotechnology* **38**: 57-62
3. Lechardeur D, Sohn K-J, Haardt M., Monck M., Graham RW., Beatty B., Squire J., O'Brodoovich H. and Lukac GL. (1999) *Gene Therapy* **6** : 482-497

### ACKNOWLEDGMENT

Special thanks to Frédéric Grosjean for flow cytometry analysis.

WYN FORREST-OWEN, LEKAN DARAMOLA,  
DIANE HATTON, RAY FIELD

## EVALUATION OF THE STABILITY OF NS0 CELL LINES EXPRESSING RECOMBINANT HUMAN IGG

*Cambridge Antibody Technology, The Science Park, Melbourn,  
Cambridgeshire SG8 6JJ, UK*

### INTRODUCTION

After antibody selection from phage display at CAT, lead scFvs are reformatted to human IgG and are produced using mammalian expression systems which are well suited to expression of proteins that require assembly and glycosylation. For large-scale production of IgG, such as that required for clinical trials and for market, stable recombinant myeloma cell lines (GS-NS0) are constructed. The stability of these recombinant NS0 cell lines in terms of growth and expression is critical for the success and yield of the IgG production process. However, not all recombinant cell lines show the desired stable expression profile. Here we present a comparative assessment of a stable and unstable cell line expressing the same recombinant IgG and discuss the causes of instability.

### METHODS

***Cell line construction and characterisation.*** NS0 host cells were transfected with CAT-derived human antibody genes using the GS-expression system (Bebbington *et al.*, 1992). Following the initial clonal transfection, two transfectants expressing the same recombinant IgG were selected for limiting dilution cloning. A high-producing clonal cell line from each parent transfectant expressing recombinant human IgG was identified and serum-free adapted. Growth and expression studies were carried out in shake flask cultures over 20-50 generations to evaluate the stability of these lines.

***Analysis of cell supernatants.*** The IgG present in cell supernatants was quantified by enzyme-linked immunosorbent assay (ELISA) and analysed by western blotting using specific antibodies to detect heavy and light chain polypeptides.

***Analysis of cells by flow cytometry.*** Intracellular antibody content of the cells was analysed using FITC-conjugated goat anti-human IgGs specific for heavy and light chains against a goat IgG-FITC isotype control (Bae and Lee, 1996). The fluorescence intensity was measured by flow cytometry.

## RESULTS

**Cell line expression stability.** Two clonal cell lines were isolated by limiting dilution cloning. One cell line was found to be stable in terms of growth and antibody expression over 58 generations whereas the other showed a rapid decrease in antibody production over 20 generations (Figure 1). The unstable cell line also showed an increase in maximum viable cell number over this period of 20 generations whereas doubling time remained constant.

**Western blot analysis of secreted proteins.** The decrease in the IgG expression in the unstable line correlates with decreased heavy chain expression whereas light chain expression remains constant (Figure 2).

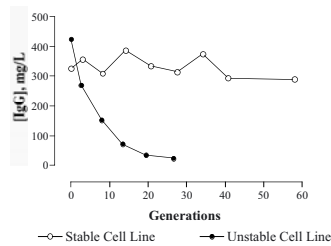


Figure 1. Final harvest titre of overgrow cultures from a stable and unstable cell line expressing human IgG

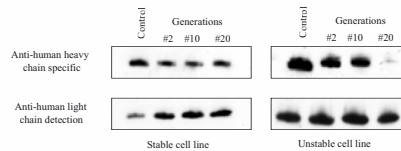


Figure 2. Western blot analysis of secreted protein from stable and unstable lines.

**Analytical cloning.** Cell stocks of the stable and unstable cell lines from early, middle and late generations were cloned by limiting dilution. Supernatants derived from the resulting single colonies were assessed by ELISA to detect assembled IgG. The analytical cloning data indicates an increasing proportion of non-IgG producing cells with time in the unstable cell line that explains the observed drop in IgG productivity. Moreover, as many of the non-IgG-producing clones express light chain alone this explains why levels of light chain protein are maintained by the parent cell line (Figure 3).

**Flow cytometric analysis of the stable and unstable cell lines.** The flow cytometric analysis of the stable and unstable cell lines confirms the findings of the analytical cloning showing loss of heavy chain production in the unstable cell line over time (figure 4).

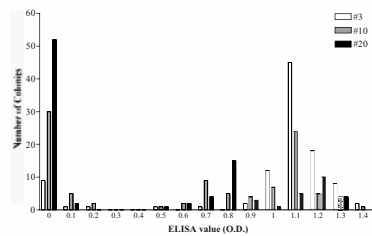


Figure 3. Dilution cloning of the unstable cell line at generations 2, 10 and 20

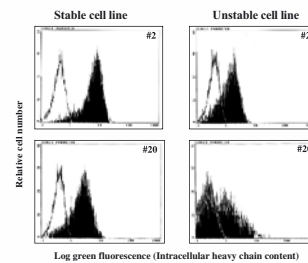


Figure 4. Flow cytometric determination of intracellular heavy chain (shaded peaks) of stable and unstable cell lines at generations 2 and 20.

**Analysis of clones derived from the unstable cell lines.** Non-producing, light chain only-producing and IgG-producing clones derived from the unstable cell line were identified by ELISA. The identities of these clones were confirmed by analysis of secreted protein using western blotting (Figure 5). Flow cytometric analysis confirmed that the clones have identical profiles of intracellular and secreted heavy and light chain production (Figure 6).

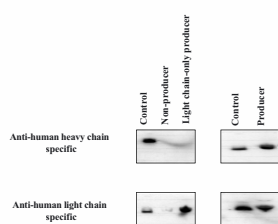


Figure 5. Western blot analysis of secreted protein of unstable line clones.

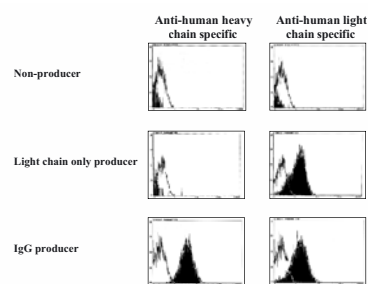


Figure 6. Flow cytometric determination of intracellular antibody contents of unstable line clones.

## CONCLUSIONS

The decrease in productivity of the unstable cell line results from an increase in the proportion of non-IgG-producing cells in the cell population. These non-IgG-producing cells include cells producing light chain only and non-producing cells that express neither heavy or light chain protein.

The non-IgG-producing cells were initially identified by analytical cloning but can also be detected in the parent cell line by flow cytometric analysis highlighting the potential of flow cytometry as an analytical tool.

Whilst there is a high probability that the unstable line was clonal, there is still a possibility that it may not have derived from a single cell. If this is the case then further rounds of cloning should derive a stable cell line and experiments are currently ongoing to assess this approach. Alternatively, the heterogeneity may have arisen spontaneously (*eg* during serum free adaptation and/or subculture) and further experiments to investigate this are ongoing by characterising and comparing the clones derived from the unstable cell line.

## REFERENCES

- Bae SW and Lee GM (1996) Influence of fluorescent antibody probe specificity on flow cytometric analysis of antibody-producing cells. *Journal of Immunological Methods* 189: 83-88.
- Bebbington CR, Renner G, Thomson S, King D, Abrams D and Yarranton GT (1992) High-level expression of a recombinant antibody from myeloma cells using a glutamine synthetase gene as an amplifiable selectable marker. *Bio/Technology* 10: 169-175
- Coller HA and Coller BS. Poisson statistical analysis of repetitive subcloning by the limiting dilution technique as a way of assessing hybridoma monoclonality. *Methods Enzymol* 1986; 121: 412-417.

C. GIESE<sup>2</sup>, C.D. DEMMLER<sup>2</sup>, G. GRADL<sup>1</sup> AND U. MARX<sup>2</sup>

## HIGH THROUGHPUT SCREENING AND SELECTION OF SINGLE CELLS IN SUSPENSION USING FLUORESCENCE PARAMETERS

<sup>1</sup> *Evotec Technologies GmbH,  
Schnackenburgallee 114, D-22525 Hamburg, Germany*

<sup>2</sup> *ProBioGen AG,  
Goethestrasse 54, D-13086 Berlin, Germany*

**Abstract:** Product specific cell based fluorescence-assays have been established and tested on two hybridoma cell lines using a microfluidic and dielectrophoretic cell handling device in combination with fluorescence-spectroscopic detection. Product specific secretion rates of suspended single cells can be quantified. Automation and high throughput screening of large numbers of cells will be realized.

### 1. INTRODUCTION

The production of Biopharmaceuticals may be optimised on many levels. In addition to the established fields of upstream and downstream process engineering, the cells, as the smallest production unit, are becoming the targets of optimisation efforts. Use of cells selected for sustainable high production can significantly reduce costs and improve process reproducibility and safety. Fully automated single cell screening procedures will potentially fill the currently existing gap between genetic cell engineering and conventional process development for industrial scale production of biopharmaceuticals. To find the best producer cells large numbers of samples must be screened. Cell specific production rates can be estimated using small and defined cell populations in multiparallel miniaturized culture volumes or by single cell screening. In order to calculate specific production rates, the exact number of cells must be determined. Single cell assays are the ultimate solution for cell selection since exact determination of both production and secretion rates via image analysis is possible on a per cell basis. Single cell selection processes require highly sensitive detection methods and assays and highly specialised cell handling technology. "Conventional" techniques such as FACS are inadequate.

### 2. TECHNOLOGICAL PLATFORM

#### 2.1. Cell Handling

Suspended single cells were handled by a combination of microfluidics and dielectric field forces using the Cytocon300<sup>TM</sup>-Technology. Microchannels and electrodes are integrated on a chip that can be placed on a microscopic unit (fig.1, left). Suspended cells are injected into the fluidic system, transported to the center part of the chip and fixed temporarily by dielectric field forces in an octopole field cage (fig. 1, right).

### 3. DETECTION AND SELECTION

#### *3.1. Fluorescence Based Secretion Assay*

Detection molecules, e.g. antibodies, antibody-fragments, protein A and protein G, which are labelled with fluorochromes (defined quantum yields) of high target-affinity (polyvalent binding sites) were used. Suspended cells are incubated with product specific detection molecules, washed and injected into the Cytocon<sup>TM</sup>300-system. Secreted proteins are caught specifically by detection molecules and form a pericellular localized corona of fluorescent precipitates. Intensity and thickness of the corona can be correlated to secretion capacity.

#### *3.2. Detection and Classification of Fluorescence Signals*

The Insight<sup>TM</sup>-Technology was used for spectroscopic detection of fluorescent molecules. Single cells are centered in the field cage and scanned by a confocal laser beam at equatorial plane. Events of emitted fluorescence-quanta are detected time resolved (fluorescence-spectra). Spectra are analyzed by autocorrelation-algorithms. Size and number of detected molecular aggregates can be derived and referred to the confocal volume of about 1fL. Whole equatorial sections will be monitored by beam-scanning and aggregates summarized (ligands, fig. 3). Images can be generated to visualize the distribution of molecular aggregates (fig. 2).

#### *3.3. Sorting of Cells, Cell Deposition and Outgrow*

Cells classified as high producers were selected by controlled microfluidics and dielectric gates after release out of the field cage. They are accelerated by sheath fluid and transported out of the microchip. Selected cells are deposited into miniaturized culture systems (96-well or 384-well plates). The outgrow frequency of selected single cell clones is 15 % compared to 22 % in reference culture prepared by limited dilution (1 cell / well).

#### *3.4. Selection Stability*

The stability of selected high and low producer clones (selected by FACS) was monitored over a period of 71 days, equivalent to 40-47 cell cycles. Selected high and low producers show constant ratios in production rates over culture time in

conventional culture (T-flask). Two clones of high producers selected by limited Dilution show constant ratios in production rates over 122 days of culture (equivalent to 183 resp. 232 cell cycles) but a consistent decline of productivity down to 47 % resp. 40%.

#### 4. REMARKS

Cytocon™300 and Insight™ are registered trademarks of Evotec OAI AG.

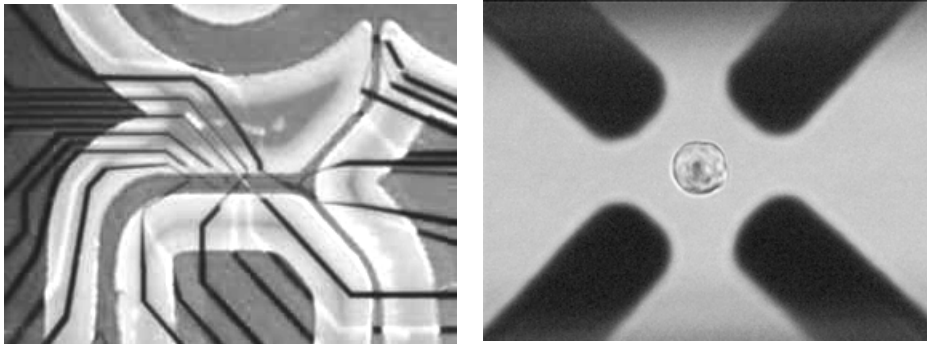


Figure 1. Microchannels and microelectrodes for cell handling (left)  
Single cell fixed in field cage (right)

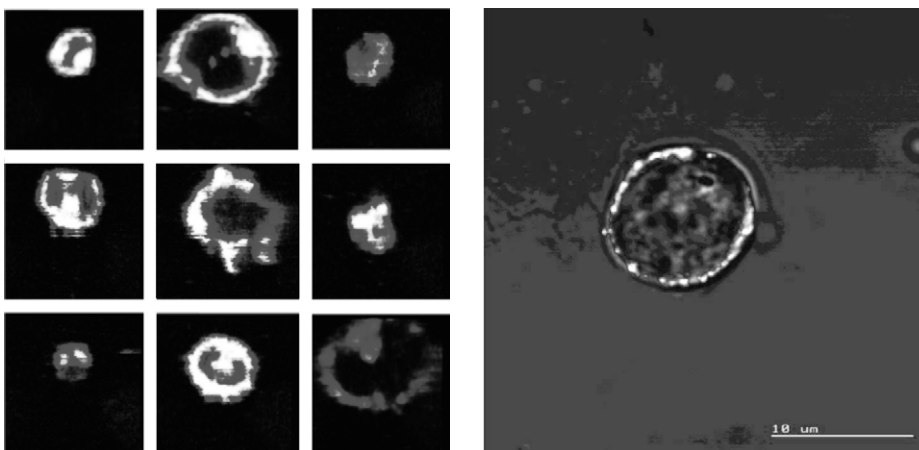


Figure 2. Cellular images showing fluorescent corona (Insight™-Scan, left)  
Overlay of confocal scanning and phasecontrast image  
(right, generated by P. Klein)



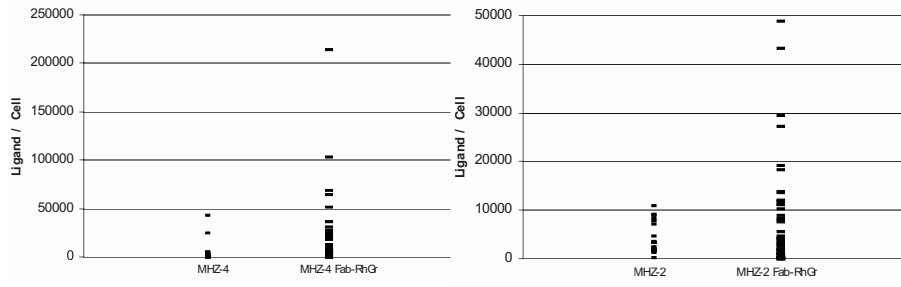


Figure 3. *Distribution of precipitated ligands per cell (50 cells shown; hybridoma cell lines) each left: unlabelled; each right: labelled*

R. KUNERT<sup>1</sup> S. WOLBANK<sup>1</sup>, M. CHANG<sup>2</sup>, S. PREIS<sup>2</sup>,  
W. STEINFELLNER<sup>1</sup>, N. BORTH<sup>1</sup> H. KATINGER<sup>1,2</sup>

## CONTROL OF KEY PARAMETERS IN THE DEVELOPMENT OF MAMMALIAN PRODUCTION CLONES

*1 Institute of Applied Microbiology, Muthgasse 18 A-1190 Vienna, Austria*  
*2 Polymun Scientific, Immunbiologische Forschung, Nussdorfer Laende 11,*  
*A-1190 Vienna, Austria, E-mail: R.Kunert@iam.boku.ac.at*

**Abstract.** The large scale production of recombinant proteins is mainly routed by the stability and production potential of the master cell bank. Biological safety of the product is accessed to the history of the cell line as well as to production conditions, down stream procedures and quality control. The quality of a recombinant cell line is assessed predominantly at the lab scale fermentation but at that time the physiologic and genomic status is already defined. For that reason it is inevitable to control parameters influencing the productivity and growth properties already during clone development. Clonal changes in transcriptional and translational behavior according to stress during selection and amplification have to be identified and comprised into the screening process. In different examples we have analyzed production titers and growth rates as well as genotypic variables concerning house keeping genes, selection markers and target genes providing information on the further development of recombinant clones.

### 1. INTRODUCTION

The generation of expression clones for the production of recombinant proteins for biopharmaceutical use has developed in the last twenty years concerning production systems and vector constructs. Expression in *E.coli* depends on the plasmid vector determining the strength of the promoter, the origin of replication (*ori*) controlling the plasmid copy number in the production system, but also the gene of interest affecting predominantly the translational machinery. A more complicated perspective is evident in mammalian cells. The development of a production clone is an interactive process, conducted by different variables that cannot be controlled per se but must be evaluated often at a very late stage of clone selection. Here we report data on the development of recombinant cell lines expressing different proteins that are applied intravenously at dosages from microgram to gram amounts and thus having diverse requirements regarding expression rate, product quality and purification.

### 2. MATERIALS AND METHODS

#### *2.1. Transfection of IgM (HB617) genes into CHO cells*

521

*F. Gòdia and M. Fussenegger (Eds.), Animal Cell Technology meets Genomics, 521-524.*

© 2005 Springer. Printed in the Netherlands.

Transfectants were generated by lipofection of CHO dhfr- cotransfecting two plasmids carrying the  $\mu$ -chain with selection marker and  $\kappa$ -chain with the joining chain as bicistronic expression cassettes under control of the CMV immediate early promoter. 24 hours after transfection, selection was started until clones arose in 96-well plates and primary transfectants were expanded to T-flasks for further analysis.

### 2.2. ELISA, Western-blot, FACS-analysis

Quantification of expressed proteins was accomplished by indirect double sandwich ELISA, and IgM content was quantified with polyclonal human IgM (Sigma).

The degree of polymerization of human monoclonal IgMs was analyzed in NuPAGE tris-Acetate 7% gels (NOVEX) using denaturing, non reducing conditions. Gels were blotted and polymeric IgMs were detected with alkaline phosphatase conjugated goat anti human  $\kappa$ -light chain.

Intracellular content of IgMs was analyzed by FACS. Cells were fixed, washed and stained with mouse anti-human  $\kappa$ -chain antibody conjugated with Quantum red and goat-anti-human  $\gamma$ -chain antibody conjugated with FITC simultaneously and analyzed in a FACS Vantage. Cells were excited with 250 mW laser power at 488 nm and fluorescence emission was measured with a 530/30 BP filter (F11) and a 660/20 BP filter (F13), respectively. Nonproducing host cells were used as negative control as their fluorescence was set between 0 and 10 on the logarithmic scale for both parameters. Compensation of spectral overlap from F11 to F13 was adjusted using cells stained only with goat-anti-human  $\gamma$ -chain FITC.

### 2.3. Real time PCR

Isolation of genomic DNA and total RNA was done with Wizard SV96 Genomic DNA purification System and Trizol reagent. RNA samples were digested with DNaseI and transcribed into cDNA with MMLV reverse transcriptase using oligo-dT<sub>(20)</sub> primer. Real time PCR (RT-PCR) was carried out using Rotor Gene 2000 thermocycler (Corbett Research, N.S.W. Australia) with Rotorgene software version 4.2. Each experiment was carried out with decimal dilutions of specific templates ( $10^7$  to  $10^2$  copies per  $\mu$ l). Purified PCR products amplified with the same primers and quantified with the Bioanalyzer were used as standards. All samples were measured in triplicate and standards were measured in duplicate. A non template control was run in every experiment to avoid detection of unspecific priming.

The absolute number of specific genes was calculated for each sample with three measurements giving a maximum standard deviation of 10%. These values were normalized by dividing them to the absolute gene copy number of beta-actin and expressed as a multiple of beta-actin resulting in relative gene copy numbers and relative transcription rates of heavy and light chain.

## 3. RESULTS AND DISCUSSION

### 3.1. Determination of generation of pentameric IgM in recombinant cell lines expressing IgMs of different specificity

Two different recombinant monoclonal antibodies of IgM subclass were expressed in CHO dhfr- cells and the pentameric IgMs were verified in Western-blot immunostaining. MAb 4E10 is a class switched isotype of an anti-HIV-1 antibody, while mAb HB617 was originally expressed as IgM and is directed against a glycosphingolipid. Both antibodies have the same constant regions in their genotype. We confirmed the presence of complete, covalently linked, polymeric antibodies in the culture supernatants using denaturing, non-reducing SDS-PAGE/Western-blot. The immunoblots revealed predominantly pentameric and monomeric form for the IgM isotype at an estimated ratio of about 1:2 for 4E10IgM and an exclusively pentameric form for HB617IgM (fig. 1).

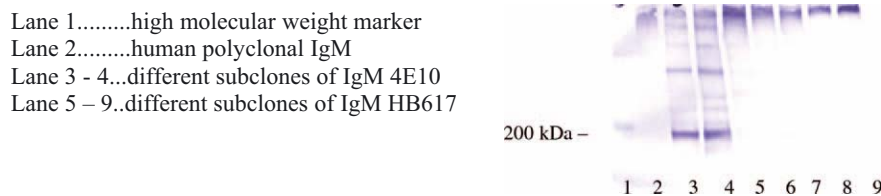


Figure 1. monomeric and oligomeric distribution of IgMs expressed in cell culture

Our data correspond with results published by others on the expression of polymeric IgM in lymphoid (Randall, King et al. 1990) and non-lymphoid cell-lines (Davis, Collins et al. 1989; Yoo, Coloma et al. 1999). We have compared different transfections with the HB617 plasmids under different conditions and even with and without serum in the cultivation medium and confirmed the pentameric structure of the expressed IgM. As shown in other recombinant hu IgMs the different potential to generate pentamers is determined in the variable region (Wolbank, Kunert et al. 2003). In other experiments we have expressed human IgA class switched antibodies and found also different distributions of oligomeric structures, that are specific for each antibody. In context with this, it may be plausible that antibodies that were also in their native form of IgM isotype form also pentameres when expressed in CHO cells.

### 3.2. Evaluation of early transfectants

Screening of early transfectants simplifies and minimizes the effort of laboratory intensive screening for recombinant production clones. A strong correlation between the gene copy number of the exogenous target gene and the expression titer of the POI (protein of interest) was often demonstrated in recombinant expression systems but only at very late stages of clone development. We have determined the gene copy numbers and transcriptional rates of different production clones expressing human monoclonal IgMs with RT-PCR and correlated the results to secretion rates and intracellular antibody content. Table 1 shows that specific productivity of three different subclones of HB617 compared to intracellular POI and homogeneity of the cell population. In this example clear preference for the B8 subclone is indicated.

Table 1. Comparison of specific production rate and intracellular antibody content of HB617 IgM clones

HB617 subclone	ELISA	FACS analysis relative geo mean		
	Qp [pg/cell/day]	% cells > blank	Fl1/FITC	Fl3/QuRed
B8	23,8	72	7,3	12,2
G9	0,6	5	3,9	2,6
D10	15,9	34	5,8	7,2

In parallel we have analyzed gene copy numbers and transcriptional activity of the three subclones B8, G9 and D10 as illustrated in figure 2. The results give an example of significant correlation of nucleic acids of the target gene with production rate of the clone. The gene copy number of the antibody's heavy and light chain were referred to a house keeping gene (beta-actin) that was set at 1 for gene copy number as well as transcriptional rate. In this example heavy chain and light chain of the recombinant antibody were expressed from two different plasmids after co-transfection and integration into the genome, both driven by the viral CMV promoter. This fact is reflected in the results of the RT-PCR finding similar amount of these two genes in gene copy number as well as transcription rate. The clone G9 that generates minor amounts of secreted and intracellular antibody also gives poor results to the amplification of target gene nucleic acids.

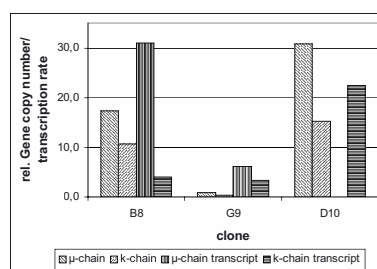


Figure 2. real-time amplification of genomic DNA and cDNA of exogenous genes in different subclones; D10  $\mu$ -chain transcripts were not analyzed

#### 4. LITERATURE

- Davis, A. C., C. Collins, et al. (1989). "Differential glycosylation of polymeric and monomeric IgM." *Molecular Immunology* 26(2): 147-52.
- Randall, T. D., L. B. King, et al. (1990). "The biological effects of IgM hexamer formation." *European Journal of Immunology* 20(9): 1971-9.
- Wolbank, S., R. Kunert, et al. (2003). "Characterization of Human Class-Switched Polymeric (Immunoglobulin M [IgM] and IgA) Anti-Human Immunodeficiency Virus Type 1 Antibodies 2F5 and 2G12." *Journal of Virology* 77(7): 4095-103.
- Yoo, E. M., M. J. Coloma, et al. (1999). "Structural requirements for polymeric immunoglobulin assembly and association with J chain." *The Journal of Biological Chemistry* 274(47): 33771-7.

CH. LATTENMAYER<sup>1</sup>, R. KUNERT<sup>2</sup>, H. KATINGER<sup>2,3</sup>

## ESTABLISHMENT OF SCREENING SYSTEMS FOR RECOMBINANT CELL LINES: EARLY PREDICTION OF THE SUITABILITY AS A PRODUCTION CLONE

<sup>1</sup>*ACBT (Austrian Center of Biopharmaceutical Technology), Austria*

<sup>2</sup>*IAM (Institute of Applied Microbiology), Vienna, Austria*

<sup>3</sup>*Polymun Scientific, Immunbiologische Forschung, Vienna, Austria*

**Abstract.** The present report describes at which state after transfection other parameters beside ELISA titers in the culture supernatant can be obtained in order to identify a clone suitable for production in pilot plant fermentation.

### 1. INTRODUCTION

At the IAM different recombinant cell lines expressing therapeutic proteins like human monoclonal antibodies, human hormones and human cytokines have been developed, which are produced in large quantities in pilot plant fermentation. Usually, early transfectants of recombinant cell lines are only screened by ELISA due to low sample volume and the need for fast results. Several other analytical methods allow further investigation of characteristics necessary for the identification of a production clone.

### 2. MATERIALS AND METHODS

#### *Transfection and Cultivation of Adherent CHO-Cells*

Dihydrofolate reductase deficient CHO-cells were cotransfected by lipofection with the plasmid encoding the amplification marker (dhfr) and the plasmid carrying the target gene. Cells were transfected in 96-well tissue culture plates. After screening by ELISA highest producers were subcultured into 24-well, then into 6-well plates before expansion into T25-tissue culture flasks.

#### *2.1. Determination of $q_p$ and Intracellular Titer*

Product titer in the supernatant was determined by ELISA while quantification of the intracellular titer of the protein was achieved by FACS analysis.

### 2.2. Measurement of Growth Kinetics by GCSS

Determination of growth rates with the GCSS (General Cell Screening System) is done by a high resolution turbidity measurement (700 nm) performed directly in the 96-well tissue culture plate (Steindl F., 1990). Therefore cells from T25-tissue culture flasks were seeded into these specially designed plates. Growth behavior of the cells was determined until the cells reached the stationary phase.

### 2.3. Determination of Nucleic Acids

Nucleic acids (mRNA, genomic DNA) were isolated from cells grown in 96-well and 6-well plates, as well as in T25-flasks. By real-time PCR the amount of target gene and amplification marker in relation to a housekeeping gene was determined.

## 3. RESULTS

### 3.1. Comparison of Growth Rates and $q_p$ of Different Clones

Figure 1. shows specific growth rates determined with GCSS, while Figure 2. demonstrates  $q_p$  of the same clones during 2 weeks of cultivation in T25-flasks.

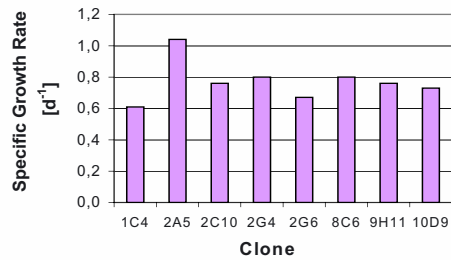


Figure 1. Growth rates of different clones

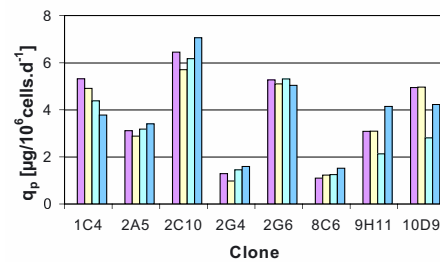


Figure 2.  $q_p$  of different clones

### 3.2. Product Secretion into the Cell Culture Supernatant

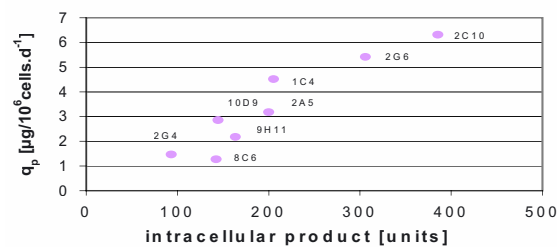


Figure 3. Product secretion

Figure 3. shows the relationship between  $q_p$  in the culture supernatant and the amount of intracellular product determined by FACS analysis.

### 3.3. Determination of Nucleic Acids

Figure 4. describes the development of genomic DNA levels of clone 2B1 in different cultivation vessels. Amplification pressure was raised from 0,048 to 0,096  $\mu\text{M}$  MTX before expansion into 6-well plates. In the 96-well plate no product titer was determined. Figure 5. demonstrates the correlation of mRNA (transcribed to cDNA) levels and product titers of different clones in T25-flasks.

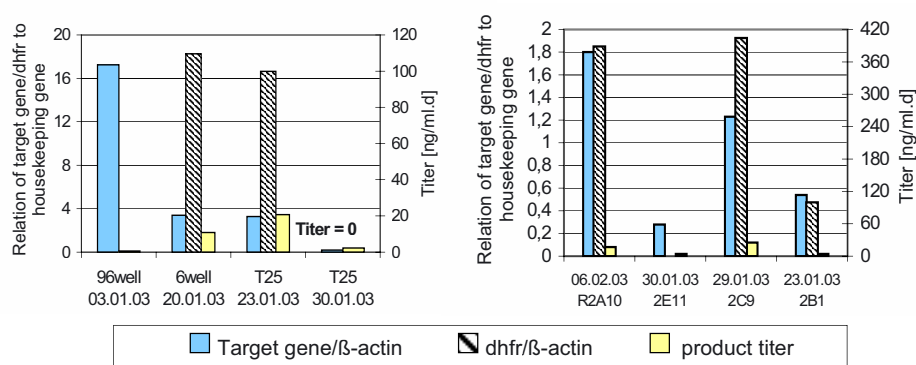


Figure 4. Genomic DNA levels versus titer

Figure 5. mRNA levels and product titers

## 4. CONCLUSION AND PROSPECTIVES

The project work so far demonstrated that gaining other parameters beside ELISA titers in early stages after transfection – in face of low available sample amount - is possible. Determination of nucleic acid levels as well as the rate of product secretion have proven to be additional criteria for a more reliable clone selection.

The relevance of all these parameters in order to predict the suitability of a clone to become a production clone has to be clarified retrospectively. The question whether a clone has to be fast growing and reaching high cell densities with a lower  $q_p$ , or the other way round in order to succeed in pilot plant fermentation remains unanswered for the moment. Experiments in fermenters after serumfree adaptation have just been started.

## 5. ACKNOWLEDGEMENTS

This research was kindly funded by the ACBT (Austrian Center of Biopharmaceutical Technology), a competence center supported by the Federal Ministry for Economy and Labour, federal states of Vienna and Tyrol.



E. TRUMMER<sup>1,3</sup>, D. MÜLLER<sup>1,2</sup>, W. STEINFELLNER<sup>1</sup>,  
R. KUNERT<sup>1</sup>, F. STEINDL<sup>1</sup>, F. HESSE<sup>3</sup>, H. KATINGER<sup>1,2</sup>

## CHARACTERISATION OF CHO SUBCLONES SHOWING PROFOUND CHANGES IN PERFORMANCE WHEN PROPAGATED IN DIFFERENT CULTIVATION SYSTEMS

*Institute of Applied Microbiology, Vienna, Austria<sup>1</sup>; Polymun Scientific,  
Vienna, Austria<sup>2</sup>; Austrian Center of Biopharmaceutical Technology,  
Vienna, Austria<sup>3</sup>*

### 1. INTRODUCTION

One of the major challenges in the establishment of recombinant mammalian cell lines for the manufacturing of biopharmaceutical products is the selection of a robust clone that shows both a high specific growth rate and a high specific productivity. This is often not easily achieved as cells tend to show a different behaviour when transferred from a T-flask or spinner culture to a bioreactor. This is supposed to be mostly due to the increase in shear stress that occurs in bioreactor systems. Since changes in cellular metabolism and physiology associated with the transfer of cells into bioreactors are not well understood we investigated this phenomenon using a system of five recombinant CHO subclones representing candidates for the establishment of a Master Cell Bank.

### 2. MATERIAL AND METHODS

Experiments were carried out with five serum-free adapted subclones of a recombinant CHO DHFR<sup>r</sup> line producing a monoclonal antibody. The bioreactor cultivation was performed in the multiple fermenter system Sixfors (Infors HT) in repeated batch mode. In the course of inoculum preparation cells were cultivated in T-flasks and spinner flasks (WV 0.125l and WV 0.5l). The General Cell Screening System (GCSS) was used as a tool for comparing growth characteristics of subclones derived from different cultivation systems in the course of inoculum preparation and bioreactor cultivation. It enables non-invasive determination of growth kinetics in 96 well plates [Steindl, 1990]. In addition, part of the inocula was used to perform batch cultivations in spinner flasks. The obtained results were compared with those found in the bioreactor. Cell concentrations were determined measuring the cell nuclei with a Coulter Counter after cell desintegration. Viability

was determined using a hemocytometer and the product concentration using an in-house developed ELISA.

### 3. RESULTS AND DISCUSSION

#### 3.1. Bioreactor cultivation

Shear stress present in bioreactors appeared to exert a major effect on three (7D3, 7E5/EF 29.11 and 17.12) of five subclones used in this study. Even if all of the subclones were cultivable in spinner cultures three of them could not be cultivated in the bioreactor due to enhanced formation of aggregates (Fig.1).

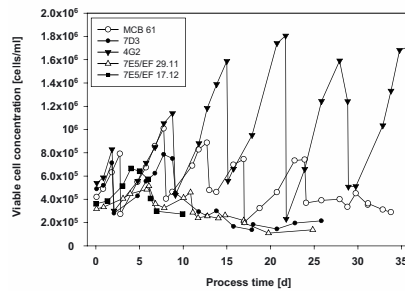


Fig 1: Progression of viable cell concentration in the course of repeated batches; one peak represents one batch

#### 3.2. Spinner versus Bioreactor

In comparing the results from spinner and bioreactor cultivation we were able to predict the specific productivity of the subclone during growth, whereas no predictions could be made regarding the specific growth rate (Fig.2).

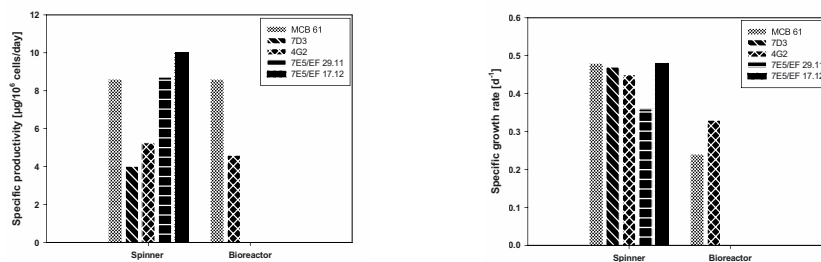


Fig.2: Specific productivities (A) and specific growth rates (B) obtained from batch cultivations in spinner and bioreactor

### 3.3. Aggregation phenomena

Regarding the robustness we found that cells with an increased potential to form aggregates already on the stage of spinner cultivation could not be cultivated in the bioreactor. Enhanced aggregate formation occurred rapidly. Therefore, aggregate formation in the spinner proved to be a good indicator for the robustness of a clone. Furthermore, we could observe adherence phenomena of cells cultivated in GCSS plates. This behaviour indicates that an active component was involved in the appearance of aggregation. Active adherence could not be observed for cells derived from T-flasks.

### 3.4. General Cell Screening System (GCSS)

The GCSS has proved to be a valuable tool to compare cells taken from different cultivation systems with respect to specific cell growth and specific productivity. In our study we found a clear change of these parameters after the transfer of cells from static to stirred systems (Fig.3 A/B).

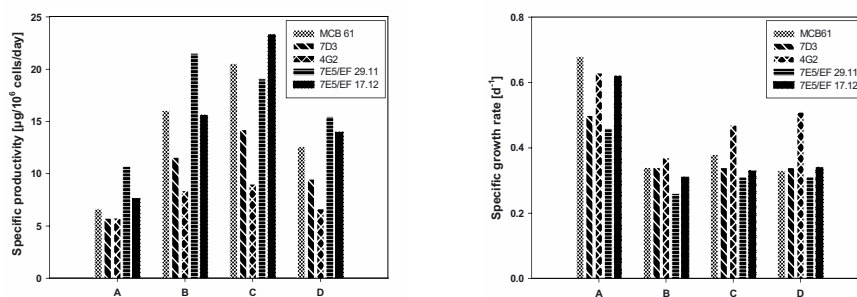


Figure 3: Specific productivities (A) and specific growth rates (B) determined in GCSS cultivation: cells were transferred from: A: T-175-flask B: Spinner 0,125l WV C: Spinner 0,5l WV D: Bioreactor

## 4. CONCLUSION

Three out of five investigated subclones were technologically irrelevant, as they were not cultivable in bioreactors. Our data revealed that changes in cell line performance occurred concomitant with changes in the cultivation systems. We could find a negative correlation between aggregation in spinner cultivation and growth in the bioreactor. In conclusion our data clearly indicate, that cultivation in stirred systems has to be performed to allow an estimation of cell line performance in bioreactors.

## 5. PERSPECTIVES

We have established a system of five subclones, which can serve as a model for the identification of parameters relevant for clone selection. Using this system we want to perform microarray analyses for a better understanding of gene expression profiles of cells undergoing physiological changes associated with shear stress. In addition, a proteomic approach is planned in order to identify proteins potentially implicated in the cellular response to stress factors. This combined analysis may provide essential information for cellular and metabolic screening efforts and could lead to a better strategy of clone selection and process optimization.

## 6. REFERENCES

Steindl F.: General Cell Screening System – A New Dimension in Screening & Cell Culture  
Int. Biotech. Laboratory News Edition 1990 Dez.

## 7. ACKNOWLEDGEMENTS

This work was funded by the AUSTRIAN CENTER OF BIOPHARMACEUTICAL TECHNOLOGY (ACBT), a competence center supported by the Austrian Federal Ministry of Economy and Labour, federal states of Vienna and Tyrol.

C. YALLOP, M. RAAMSMAN, M. ZUIJDERWIJK,  
Y. VAN NOORDENBURG, A. VOOYS, R. KEEHNEN,  
B. VAN MONTFORT, M. JANSEN, F. LAGERWERF, R. DIJKSTRA,  
M. BIRRENTA, M. DE VOCHT, S. RENGER, A. BOUT AND  
D.-J. OPSTELTEN

## HIGH LEVEL PRODUCTION OF RECOMBINANT IGG IN THE HUMAN CELL LINE PER.C6<sup>TM</sup>

*Crucell Holland bv, Leiden, The Netherlands*

### 1. INTRODUCTION

The number of recombinant proteins expected to gain approval as human therapeutics is expected to increase dramatically in the next few years. This increase is expected to create problems in manufacturing capacity, particularly for antibodies as they use a disproportionately high total production capacity due to the high doses required. This in turn has led to the optimisation of production platforms (largely CHO and hybridoma cell-lines SP2/0, NS0), to maximise product yields and efficiency. The human cell line PER.C6<sup>TM</sup> was recently shown to support antibody yields up to 500 mg L<sup>-1</sup> from batch cultures with a glycan pattern similar to that reported for human serum IgG (Jones et al 2003). It was therefore decided to develop a fed-batch process for this cell-line in order to establish it as a platform for recombinant antibody production.

### 2. MATERIALS AND METHODS

Two PER.C6 clones expressing different human recombinant antibodies were selected for this study. Both clones were generated using the protocol described previously (Jones et al 2003). Cells from a serum-free cell bank were thawed directly into 250 ml Erhlemeyer flasks (Corning), containing 25 ml serum free medium at a starting cell concentration of  $0.3 \times 10^6$  ml<sup>-1</sup>. Flasks were shaken at 100 rpm and maintained in logarithmic growth by passage every 1-3 days in a humidified incubator at 37°C and 5% CO<sub>2</sub>. Batch cultures were performed in ExCell VPRO (JRH Bioscience). Cell counts were performed using a CASY automatic cell counter (Schärfe Systems). Glucose, lactate, ammonia and phosphate concentrations were determined on cell-free culture supernatants using an Ektachem II analyser (Kodak). Amino acid concentrations were determined using the AccuTag HPLC

method (Waters) according to the manufacturers instructions. Antibody concentrations were determined by ELISA.

### 3. RESULTS

#### 3.1. Batch Cultures

Figure 1 shows a typical batch culture for each clone. Cell specific productivity and antibody production per day decreased on day 8 and 10 for clone 1 and 2 respectively, 1-2 days before maximum cell number was reached.

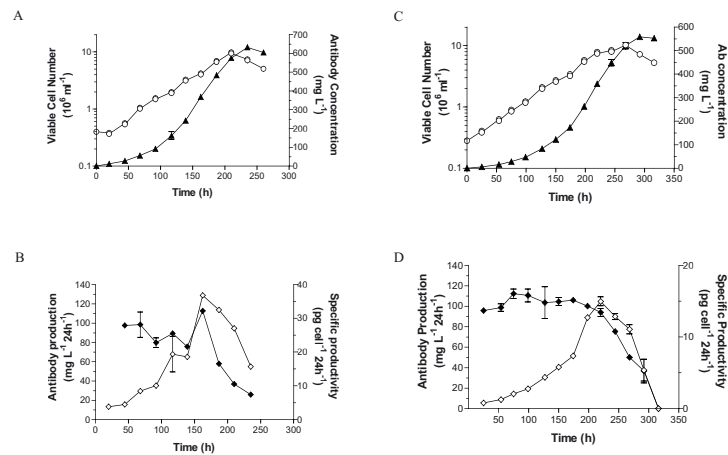


Figure 1. Viable cell number (open circles), antibody concentration (closed triangles), cell specific productivity (closed diamonds) and productivity per day (open diamonds) for PER.C6 clone 1 (A+B) and clone 2 (C+D).

#### 3.2. Metabolic Characterisation

The metabolite profile of both clones was similar (Figure 2 shows the profile for clone 1). The decrease in specific productivity for both clones correlated with depletion of phosphate, glutamine, leucine, isoleucine, serine, methionine, arginine and cystine. Ammonia, glutamate and alanine consumption occurred immediately following glutamine depletion suggesting a reversal of glutamine catabolism.

### 3.3. Design of Feed Strategy

A basic feed concentrate (glucose, glutamine, amino acids, salts and growth factors) was prepared and timing determined from the nutrient utilisation profile. The concentration of each nutrient in the feed was determined from the cell specific utilisation rate in order to supply each nutrient at the level required by the cells and limit overflow metabolism. These feed strategies resulted in an increase in antibody yield by greater than 50%, from 0.5-0.6g L<sup>-1</sup> to approx. 1.0g L<sup>-1</sup>. Figure 3 shows one typical experiment.

Feeds were added every two days. Additional components are currently being tested and the existing component concentrations further optimised.

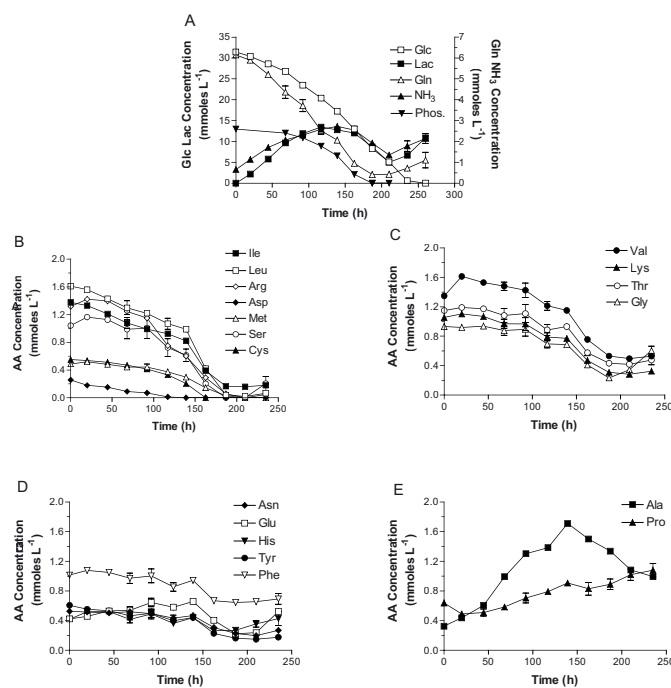


Figure 2. Metabolic profile of PER.C6 clone 1 grown in shake flask on VPRO.

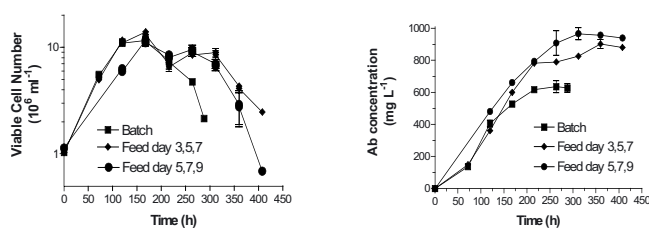


Figure 3. Viable cell numbers and antibody yields from batch cultures versus two feed strategies.

### 3.3. Product Quality

Analysis of purified antibody by IEF, SDS-PAGE and glycan analysis by HPAEC-PAD showed product quality to be essentially the same in the feed experiments as in the batch cultures (data not shown).

## 4. AFFILIATION

Crucell, Archimedesweg 4, 2333 CN Leiden, The Netherlands

## 5. REFERENCES

Jones D, Kroos N, Anema R, van Montfort B, Vooys A, van der Kraats S, van der Helm E, Smits S, Schouten J, Brouwer K, Lagerwerf F, van Berkel P, Opstelten D.-J, Logtenberg T and Bout A (2003). High level expression of recombinant IgG in the human cell line PER.C6. *Biotechnol. Prog.* 19: 163-169.



Z. DEEDS, A. ALBEE, B. DELONG, J. GIFFORD, S. ROSS,  
K. KAO, AND M. CAPLE

## CREATING A NEW MEDIUM TO HELP MEET THE VARIABLE NUTRITIONAL REQUIREMENTS OF CHINESE HAMSTER OVARY (CHO) CELL CLONES

*Sigma-Aldrich Biotechnology, 3050 Spruce Street, Saint Louis,  
MO 63103 USA*

**Abstract.** It is widely known that different recombinant protein expressing Chinese Hamster Ovary (CHO) cell clones can have variable nutritional requirements. Sigma-Aldrich has previously developed an Animal-Component Free Medium (CHO-AF, Product Code C5467) that for many CHO clones yields excellent growth and productivity. However, with some CHO clones it yields less than optimal performance. Therefore the need has arisen to create a second-generation medium that will complement CHO-AF.

The Dihydrofolate Reductase (DHFR) gene amplification system has become very popular for use in CHO clones. The DHFR system allows the gene of interest to be amplified with increasing concentration of methotrexate, leading to increased protein expression. The recombinant cell lines used in the optimization of this new medium were all DHFR clones expressing a variety of protein products, including a rIgG and rhM-CSF. Each cell line poses a unique challenge, as demonstrated by the differences in amino acid utilization rates.

Based on cell growth, r-protein production, and the amino acid consumption rates, CHO DHFR- Medium (Product Code C8862), was developed. The base formulation for CHO DHFR- was very different from that of CHO-AF, allowing for the development of a complementary animal-component free medium. Experiments have shown that CHO DHFR- promotes better growth and protein production than CHO-AF with many CHO clones, but there are still other cases where using CHO-AF is advantageous. The development of this new medium resulted in growth and recombinant protein production rates surpassing that of other commercially available media. Finally, the application of these two CHO animal-component free media in spinner flasks and 5-L bioreactors is discussed.

### 1. INTRODUCTION

Chinese Hamster Ovary (CHO) cells are one of the most frequently used cell lines for the expression of recombinant proteins that require post-translational modification to express full biological function. Since more and more biopharmaceutical companies are producing their potential therapeutic agents in CHO cells, there has been increased regulatory scrutiny of the medium in which the cells are grown. Animal component-free media have now come to the forefront for use with CHO cells. Sigma has previously developed a CHO Animal Component-free Medium (CHO-AF, Product Code C5467), to support the suspension culture of CHO cells and to achieve the desired recombinant protein expression. This CHO medium contains recombinant human insulin, plant hydrolysates, and proprietary iron chelators. All other components are also of non-animal origin, including amino

acids, vitamins, fatty acids and surfactants. CHO-AF has proven to be medium of choice for many recombinant protein producing cell lines, but not for all.

In order to obtain maximal growth and recombinant protein production with those clones for which CHO-AF is not optimal, Sigma has created CHO DHFR-Medium (Product Code C8862). Much like CHO-AF, CHO DHFR-Medium contains recombinant human insulin, plant hydrolysates, and proprietary iron chelators and is completely animal-component free. Many factors were considered while CHO DHFR-Medium was being developed, including amino acid analysis. This information allowed insight into the utilization rates of different cell lines.

The recombinant cell lines used in the development of this medium were all DHFR (Dihydrofolate reductase) clones. This cloning system allows one to greatly increase the gene of interest copy number within their specific clone, leading to increased recombinant protein expression. The cell lines that were studied produced either a recombinant antibody or a recombinant human growth factor.

Finally, CHO DHFR-Medium is compared to other commercially available media and is also tested in bioreactor experiments.

## 2. MATERIALS AND METHODS

Sigma-Aldrich Corporation (St. Louis, MO) supplied all chemicals, media and solutions unless otherwise stated.

Cell Lines. CHO 5/9 m alpha 3-18 (M-CSF) cells (ATCC #CRL-10154) were obtained from the American Type Culture Collection (ATCC). Cell line CHO-IgG is a proprietary clone expressing a recombinant antibody.

Cell Culture and Cell Growth Assays. Cells were grown in suspension in CHO-AF and were used to seed experiments done in 125mL or 250ml (100mL and 150mL liquid volume respectively) Techne Spinner flasks. The initial inoculum was 50,000 viable cells per milliliter. All conditions were run in duplicate. The cells were cultured in Forma incubators at 37°C and 5% CO<sub>2</sub>.

For bioreactor experiments, B. Braun Biotech International's Biostat® B 5 liter reactors were used. They were set-up with marine impellers and a 0.5 µm sparging stones. These were also seeded at 50,000 viable cells/mL.

Quantification of Recombinant Humanized IgG and Recombinant Human M-CSF. The IgG secreted into the medium by CHO IgG was measured by HPLC (Waters 2690 HPLC Millipore, MA) using a protein-G affinity column. Recombinant Human M-CSF was measured by a Quantikine® Human M-CSF Immunoassay supplied by R&D Systems (Catalog # DMC00).

## 3. DISCUSSION

Sigma's new product, CHO DHFR-Medium (C8862), was developed in response to data suggesting that our CHO-AF Medium (C5467) was not performing as expected with a significant amount of recombinant CHO cell clones. This is demonstrated in Figure 1, where CHO-AF yields sub-optimal growth and productivity with the

CHO-IgG cell line. CHO DHFR- is a vast improvement over this medium when considering the CHO-IgG clone. However, the variable requirements of different CHO clones are clearly shown by the results in Figure 2. Here the CHO-M-CSF cell line grew similarly in both media, but the rh-M-CSF production was much better in CHO-AF.

**Growth and recombinant IgG Production with CHO-IgG clone**

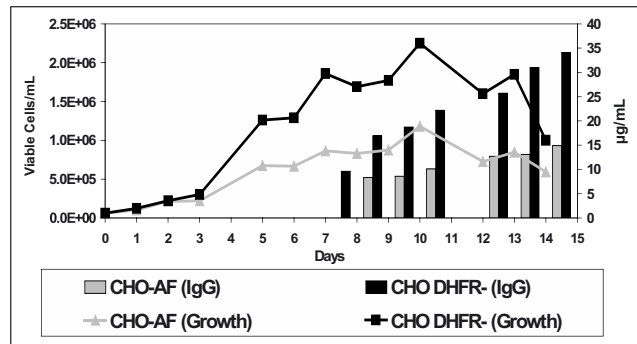


Figure 1. Comparison between CHO-AF and CHO DHFR- media for growth and recombinant IgG production.

**Growth and recombinant hM-CSF Production with CHO-M-CSF clone**

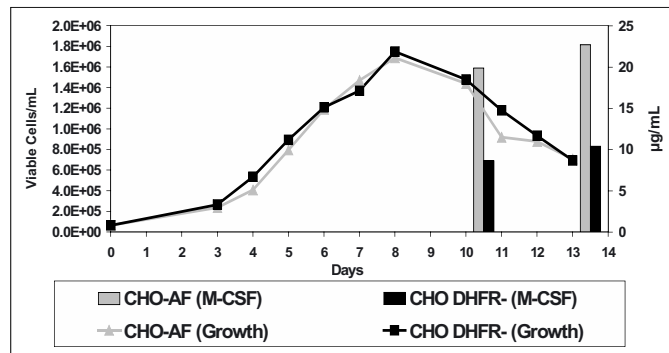


Figure 2. Comparison between CHO-AF and CHO DHFR- media for growth and recombinant M-CSF production

Furthermore, amino acid analysis gives even deeper insight into the variations amongst CHO clones. Aspartic acid (ASP) utilization is one example. Comparing the CHO-IgG and CHO-M-CSF cell lines in CHO DHFR- medium (data not shown), one sees that the aspartic acid level in both cultures has increased by day 7. This continues with the CHO-M-CSF cell line, to almost double the initial amount by day 12. However, the trend reverses with the CHO-IgG cell line, and by day 12 almost all of the available aspartic acid is utilized. Another interesting note is that

with the CHO-IgG cell line, differences can be seen in the amino acid utilization rates with the different media (data not shown). Again using aspartic acid as an example, we can see that in CHO-AF the increase in concentration is not seen on day 7, but much like C8862, most of the available aspartic acid is gone by day 12.

Figures 3 and 4 show how CHO DHFR- Medium compares to other commercially available media. With both cell lines, CHO DHFR- yields the highest growth and total recombinant protein production.

### Media Comparison - CHO-IgG

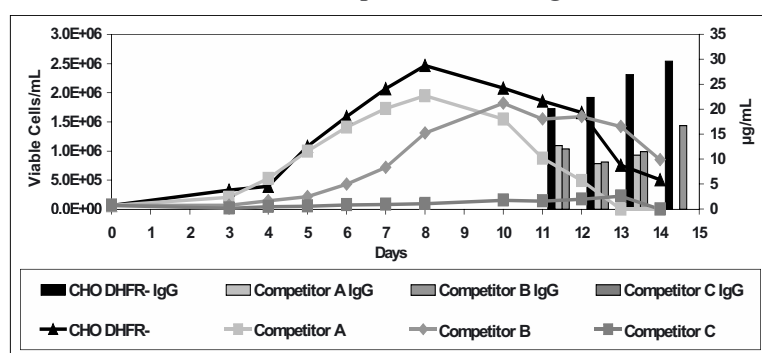


Figure 3. Performance Comparison with CHO-IgG clone

### Media Comparison - CHO-M-CSF

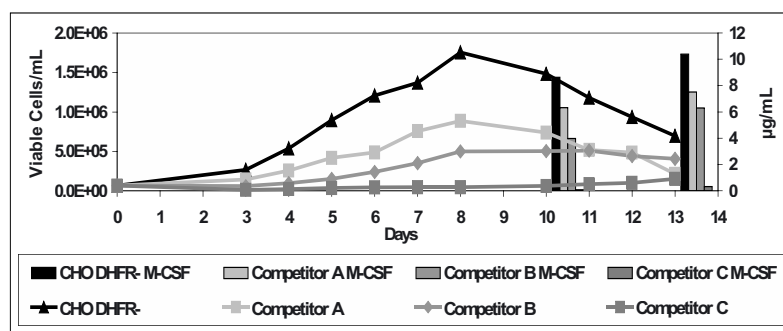


Figure 4. Performance Comparison with CHO-M-CSF clone.

Specific productivity (data not shown) further elucidates the need for multiple medium formulations. With the CHO-IgG cell line, CHO DHFR- had the highest specific productivity while CHO-AF was more in the range of the competitors. Conversely, with the CHO-M-CSF cell line CHO-AF yielded the highest specific productivity.

Scalability of CHO DHFR- was demonstrated in 5L B. Braun bioreactors, in both batch and fed-batch modes using the CHO-IgG cell line (data not shown).

B. DELONG, A. ALBEE, Z. DEEDS, J. GIFFORD, S. ROSS,  
K. KAO, and M. CAPLE

DEVELOPMENT OF AN EFFICIENT MEDIUM  
OPTIMIZATION KIT FOR FACTORIAL MATRIX  
DESIGN—A STATISTICAL APPROACH TO  
INCREASE CELL GROWTH AND PRODUCTIVITY OF  
RECOMBINANT CHO CELLS

*Sigma-Aldrich Biotechnology, PO Box 14508, Saint Louis, MO 63103 USA*

**Abstract.** Chinese Hamster Ovary (CHO) cells have been used for large-scale recombinant protein expression in the majority of pharmaceutical companies worldwide. The most challenging aspect of culturing recombinant CHO cell clones is providing for the diverse nutritional requirements that are unique to every transfected cell line. Therefore, using factorial matrix statistical assays to accelerate the optimization of cell culture medium has received great attention in many pharmaceutical companies. Based on the format of factorial matrix we have recently developed a component medium optimization kit. This kit which consists of one basal medium and 6 concentrated grouped media supplements (including Amino Acids, Vitamins, Iron chelator, Lipids, Hydrolysates and Metals) will provide an easy access to perform various factorial matrix assays. The statistical program predicts the most optimal levels of the components and additional matrix assays can be set up to confirm these results or narrow the search window for the components. Once the critical components have been optimized or identified they can be added directly to the medium to receive the most optimal growth and/or production. By using this medium optimization kit, we have demonstrated that this kit can be used successfully to achieve optimal growth and productivity in multiple CHO cell with unique nutritional requirements. Taken together, our data strongly suggests that a combination of grouped components and the use of a statistical approach can facilitate the timely development of the “best” medium for any given recombinant CHO clone.

## 1. INTRODUCTION

Chinese Hamster Ovary (CHO) cells have been of great interest to pharmaceutical companies because of the cell's ability to express human recombinant proteins on a large scale. However, developing cell culture medium is very challenging because there are several CHO cell clones, each having unique nutritional requirements. In order to assist pharmaceutical companies in improving their medium optimization process, Sigma-Aldrich has developed a medium component optimization kit that allows the customer to easily perform factorial matrix experiments. This kit consists of one basal medium and six concentrated grouped media supplements, which have been previously determined to have a significant effect on cell growth and recombinant protein production in CHO cells. We have tested this kit using two cell lines to demonstrate how the statistical program predicts the most optimal levels of each component for unique medium supplementation. Taken together, our results

indicate that this medium optimization kit is a powerful tool for timely medium development for any CHO clone.

## 2. MATERIALS AND METHODS

### 2.1. *Materials*

Two CHO cell lines were used for this development. CHO K1 cell (ATCC #CRL-61) is a non-producing CHO clone. CHO recombinant clone 1 is engineered to produce human recombinant IgG. Factorial matrix software used to generate data analysis was Design-Expert®, version 6.0.2 (Stat-Ease, Inc., Minneapolis, MN). All materials used in this work were obtained from Sigma-Aldrich Co. (St. Louis, MO) unless otherwise stated.

### 2.2. *Optimization Kit Design*

The Base Medium consists of low levels of Amino Acids, Metals, Iron, Vitamins, Lipids, and Hydrolysates so that each component can be titrated. It does not contain any amount of Insulin, Glucose or Glutamine.

Components included in the kit were determined from previous work developing a custom medium to have a significant effect on cell growth and production. Initial experiments titrated one component at several low and high levels while leaving the other components constant at their base levels in order to determine the appropriate levels of low and high titrations to suggest for customer use.

### 2.3. *Matrix Assay*

Once all component titration values had been determined, two full factorial matrix assays per cell line were set up testing three components at their two pre-determined levels (23 factorial matrix). Each assay consisted of a centerpoint which was 100% of the three components being titrated (the average amount between the low and high values) while the other components were kept constant at their base levels. Data used in Design-Expert® analysis consisted of cell days and average IgG production (ug/ml) at equal importance levels. The Base Medium is used only as a control.

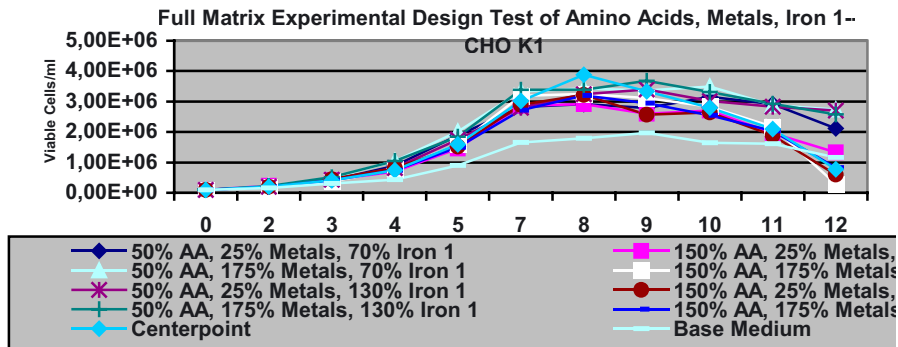
The media for each condition was formulated by adding back the appropriate amounts of each supplement being tested to the Base Medium. Iron 2, Insulin and Glucose were added back at a 100% level. All assays were run in duplicate in 125ml spinner flasks stored at 37°C, 5% CO<sub>2</sub>, and stirring at 80rpm and counted on a CASY®-1 cell counter (Scharfe Systems, Reutlingen, Germany) and by the trypan blue exclusion method. IgG concentrations were determined by HPLC using a Protein-G binding column. Data was then input into Design-Expert® for analysis.

### 3. RESULTS AND DISCUSSION

#### 3.1. CHO K1 Matrix Assays

In the first matrix assay Amino Acids (AA), Metals, and Iron 1 were tested at two levels each. As shown in Fig. 1, the Base Medium grew to  $1.5 \times 10^6$  cells/ml by day 7 while all conditions reached cell densities of about  $3 \times 10^6$  cells/ml. On day 12, the top conditions all have a low level of AA as the common factor.

Figure 1. Viable Cells/ml, average two spinners. Centerpoint equals 100% level of AA, Metals and Iron 1 with base levels of Vitamins, Lipids and Hydrolysates. Base Medium used as control.



The benefit of AA can also be seen in the cube graph (Fig. 2). Cube graphs demonstrate how interactions of the three components effect the cell growth results. With these graphs, use the highest number in each corner of a cube graph to determine the levels of each supplement that should be added back to the base medium. The cube graph for the first experiment only shows two results for growth— $2.58 \times 10^7$  and  $2.0 \times 10^7$ —which change on the X-axis only. There can be more results shown in a cube graph, but the fact that there are two numbers that differ on the X-axis alone shows that only AA effect the cell growth. The Metals and the Iron 1 show no effect because altering their low and high levels still result in the same cell growth number on the cube graph. These results are confirmed in the Normal Plot (Fig. 3), which shows the positive or negative effect of the supplements on cell growth. In a Normal Plot, components to the left of the line have a negative effect, components to the right of the line have a positive effect and components on the line are not significant. The Normal Plot for this experiment shows that only AA have a negative effect, but the Metals and the Iron 1 are on the line representing no effect on growth. Because Metals and Iron 1 do not appear to affect growth their levels were maintained at the centerpoint value of 100%.

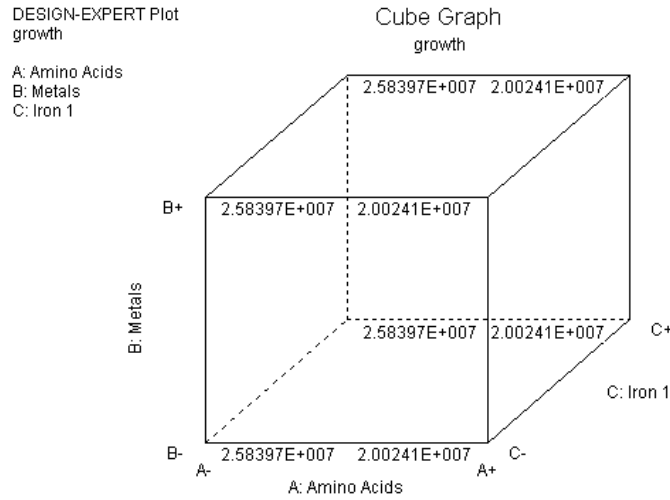


Figure 2. Design-Expert® graph depicts cell growth results in cube graph format. Amino Acids shown on X-axis, Metals on Y-axis, Iron 1 on Z-axis. Numbers represent cell days ( $e^7$ ).

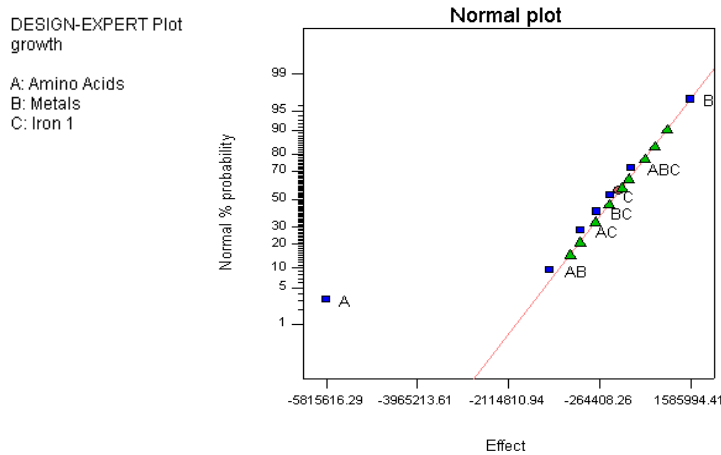


Figure 3. Design-Expert® Normal plot shows amount of effect supplements have on CHO K1 cells.

In the second matrix assay Vitamins, Lipids and Hydrolysates were tested at two levels each. The cube graph (data not shown) depicts that Vitamins have a relatively small effect, but they are more beneficial at the low level. The Normal Plot (data not shown) confirms this result by showing the Vitamin supplement having a slightly negative effect. The Normal Plot also shows Hydrolysates have a significantly positive effect and conditions combining negative Vitamins and



positive Hydrolysates can result in slightly positive interactions. Since the Normal Plot shows that Lipids do not have a significant effect, the level was maintained at the centerpoint value of 100%.

The predicted optimal level of the components tested for CHO K1 cells is: 50% Amino Acids, 100% Metals, 100% Iron, 150% Vitamins, 100% Lipids, and 150% Hydrolysates. Metals, and 100% Iron 1.

### *3.2. CHO Recombinant Clone 1 Matrix Assays*

In the third matrix assay Amino Acids (AA), Metals, and Iron 1 were tested at two levels each using CHO recombinant clone 1. The condition with the highest cell density has a high level of AA, a low level of Metals, and a low level of Iron 1 (data not shown). Again, the high cell density for this condition is confirmed in the cube graph and the Normal Plot (data not shown). The Normal Plot shows that Metals and Iron 1 are slightly negative, while AA have a positive effect. The average IgG production (data not shown) shows a difference in supplementation as well. The cube graph (data not shown) also shows that the biggest increase in IgG production comes from a high AA level. There are only two data results in the cube graph, representing that only AA have an effect on production. This trend is also seen in the Normal Plot (data not shown) by depicting that AA have a significantly positive effect while the other two supplements are insignificant.

In the final matrix assay Vitamins, Lipids and Hydrolysates were tested at two levels each. This matrix experiment shows some conditions have lower cell densities than the Base Medium. By day 12 the conditions which are lower all have a low level of Hydrolysates in common. The beneficial conditions, which have high levels of Hydrolysates, are portrayed in the cube graph (data not shown). On this graph, of the two highest data points, one has a low level of Lipids, while the other highest data point has a high level of Lipids. Because of this, it appears that the level of Lipids does not play a significant role. However, both of the two highest cell densities have a low level of Vitamins and a high level of Hydrolysates. These relationships are further demonstrated in the Normal Plot (data not shown), which shows Vitamins have a negative effect, Hydrolysates have a positive effect, and Lipids have no significance on growth. Even though some conditions were lower cell densities than the Base Medium, all conditions generated higher IgG production (data not shown). The cube graph representing production (data not shown) shows higher IgG production whenever there is a high level of Hydrolysates. An inverse relationship between Vitamins and Lipids is shown in the Normal Plot (data not shown) as having a negative effect, meaning Vitamins at a high level and Lipids at a low level will result in the highest productivity. It also shows that Hydrolysates have a positive effect.

The optimal medium obtained from this assay based on equal importance of cell growth and production is: 150% Amino Acids, 25% Metals, 70% Iron 1, 50 % Vitamins, 150% Lipids, and 150% Hydrolysates.

### 3.3. Test of Predicted New Formulation

From the two factorial matrix assays using CHO K1 cells, we obtained two predicted optimal growth formulations. Combining data from the two assays, a new medium was prepared: 50% Amino Acids, 100% Metals, 100% Iron, 50% Vitamins, 100% Lipids, and 150% Hydrolysates. The cell growth performance of this new medium was tested on CHO K1 cells (Fig. 4). The result clearly showed that CHO K1 cells grew to a 1.5-fold higher cell density in this new medium than that in the original Base Medium or in the two competitors' media tested.

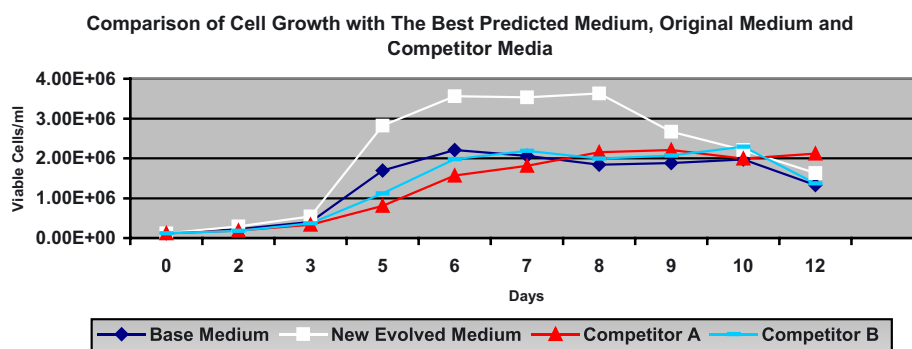


Figure 4. Test of cell growth with the best predicted medium using CHO K1 cells. New evolved medium is prepared according to the predicted best formulations obtained from two factorial matrix assays using CHO K1 cells. CHO K1 cells growing in this newly evolved medium give a 1.5-fold higher cell density as compared with the original medium (Base Medium) and two competitor's media.

### 3.4. Cell Line Comparisons

These results clearly demonstrate that using this medium optimization kit and Design-Expert® software on diverse CHO cell lines can generate a different optimized media formulation. In the cell lines tested there were some similarities observed such as both needed Vitamins at low levels and Hydrolysates at high levels, but there were also several differences seen between the two cell lines. The concentrations of Metals and Iron 1 had no significant effect on cell growth of CHO K1 cells, while with CHO recombinant clone 1 these supplements were found to be more beneficial at the low level. Furthermore, CHO K1 cells had higher growth when Amino Acids were at the lower level, but CHO recombinant clone 1 cells required Amino Acids at a high level for optimal growth. Also, CHO K1 cells

needed a lower level of Lipids for optimal growth, while the CHO recombinant clone 1 cells needed a higher level of Lipids.

#### 4. CONCLUSIONS

Factorial matrix design, a statistical approach, has greatly enhanced the process of cell culture medium development and optimization. Sigma-Aldrich's CHO Medium Component Optimization Kit is formatted to facilitate easy medium formula manipulation through factorial matrix assays. Using factorial matrix design and this CHO medium component optimization kit, an optimized medium formulation can be generated rapidly. By streamlining the process of medium optimization for any given recombinant CHO clone, Sigma-Aldrich's CHO Medium Component Optimization Kit can provide great benefits to the pharmaceutical industry.

#### 5. REFERENCES

- Bettger, William J. and Ham, G. (1982), Advances in nutritional research. *The Nutrient Requirements of Cultured Mammalian Cells, Chapter 9*, (H. Draper, ed.), Plenum Publishing Corporation, pp. 249-281.
- Moen, R., Nolan, T., and Provost, L., Quality Improvement through Planned Experimentation, Second Edition. McGraw Hill, Inc., New York (1999).

\*Design-Expert® is a registered trademark of Stat-Ease, Inc.

GIFFORD J., ALBEE A., DEEDS ZW., DELONG B., KAO K.,  
ROSS S. AND CAPLE MV.

## AN EFFICIENT APPROACH TO CELL CULTURE MEDIUM OPTIMIZATION -- A STATISTICAL METHOD TO MEDIUM MIXING

*Sigma-Aldrich Corporation, PO Box 14508, Saint Louis, MO 63178 USA*

**Abstract.** One of the most challenging aspects of culturing recombinant Chinese Hamster Ovary (CHO) cell clones is providing for the diverse nutritional requirements that are unique to every transfected cell line. In order to minimize the amount of time required for medium development, we have recently developed CHO Medium Optimization Kit 1 (Product Code CH0001). This kit consists of six diverse animal component-free CHO media (including two chemically defined media) to provide for a wide range of nutritional requirements. The format of this kit provides multiple media to screen, and functions as a platform for statistical medium optimization by using a three-point mixing design. After screening several different recombinant CHO clones against the six media, our data showed that we could increase cell growth and recombinant protein production over the original medium. Following a statistical approach provided by Design-Expert® computer software, we mixed the top three performing media and were able to further increase cell growth and productivity. The data can be further analyzed by Design-Expert® to yield a predicted best medium mixture to support maximum cell growth and productivity for a particular recombinant CHO clone. Our data strongly suggests that using CHO Medium Optimization Kit 1 with a combination of media screening and a statistical approach to media mixing, can facilitate the development of an optimized medium for any given recombinant CHO clone.

### 1. INTRODUCTION

Sigma's CHO Medium Optimization Kit 1 consists of six diverse animal component-free media designed to maximize cell growth and recombinant protein production in a wide variety of CHO clones. Two of these six media are chemically defined and all differ in amounts of amino acids, vitamins, salts, trace elements, recombinant human insulin and other organic compounds. The format of this kit allows the user to rapidly screen six CHO formulations for cell growth, recombinant protein production or any other criteria. If this initial screen yields satisfactory results, the researcher may decide that no further optimization is required. However, if the initial screening does not satisfy the specified criteria, a series of media mixing experiments can be performed.

There are two options for analyzing the data from the mixing experiments. The first option is to normalize the data for each criterion and visually analyze the criteria separately. The second method is a more in-depth approach, in which a Design-of-Experiment (DOE) software package can be used. The DOE software allows the researcher to look at multiple criteria together and assign importance

values to each criterion. Based on these user preferences, the software can predict one or several best-fit media designed specifically to meet the nutritional requirements of a particular cell line.

The convenient format of CHO Medium Optimization Kit 1 allows for a rapid screening of multiple diverse CHO formulations. In addition, the powerful mixture experiments coupled with the DOE software provide an invaluable tool for boosting cell growth and productivity. In either application, CHO Medium Optimization Kit 1 has the ability to significantly improve any medium development project

## 2. MATERIALS AND METHODS

*Cell Lines* CHO K1 cells (ATCC # CRL-61) were obtained from the American Type Culture Collection (ATCC). Cell line CHO IgG, expressing a proprietary recombinant antibody, was transferred from a customer to Sigma for custom medium development and optimization.

*Cell Culture and Cell Growth Assays* The media used in this study are CHO Protein-Free Animal Component-Free Media. Cells were grown in suspension in #C5467 and were used to seed experiments done in 125mL or 250ml (100mL and 150mL liquid volume respectively) Techne Spinner flasks. The initial inoculum was 50,000 viable cells per milliliter. The cells were cultured in Forma incubators at 37°C and 5% CO<sub>2</sub>. Spent medium samples were collected every day for the analysis of nutrients/metabolites and recombinant protein production. At the same time, the cells were counted using a Schärfe System Casy 1® Model TTC and viability was assessed using the Trypan Blue Exclusion Method.

*Quantification of Recombinant Humanized IgG* The IgG secreted into the medium was measured by HPLC (Waters 2690 HPLC Millipore, MA) using a protein-G affinity column.

## 3. RESULTS AND DISCUSSION

Sigma's CHO Medium Optimization Kit 1 (Product Code CH0001) contains six diverse animal component-free media designed to maximize cell growth and recombinant protein production in a wide variety of CHO cell clones. After the initial screening of all six media (data not shown), the user must decide whether additional optimization is desired. Based on criteria such as cell growth and recombinant protein production, the user can select the top three performing media from the initial experiment and complete a media mixing experiment (data not shown). Figure 1 illustrates the media mixes to be performed and the concept of the mixture triangle.

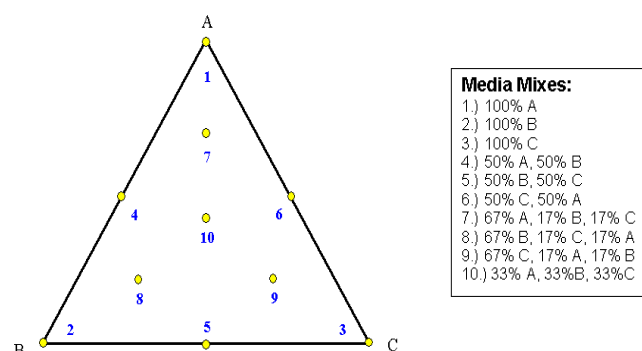


Figure 1. The three-point mixture diagram and corresponding media mixes. The three best performing media from the screening of all six media, are set to 100% at one of the three vertices of the mixtures triangle. Media mixing begins at 50% between two of the media along the sides of the triangle (numbers 4, 5 and 6). This is followed by a 67%, 17%, 17% mix of all three media within the interior of the triangle (numbers 7, 8 and 9). The final mix will be 33% of all three media as seen at the center point of the triangle (number 10).

The results from the mixing experiment can be analyzed by two methods. The first method, as represented in Figure 2, is accomplished by separately analyzing the data for each criterion. Using this method, the data can be normalized to one of the media and ranked or plotted directly on the mixture triangle to identify which mixes might reveal the best results. If the user desires a more in depth analysis, a Design-of-Experiment (DOE) software package such as Design-Expert (Stat-Ease, Inc.) can be used. Figure 3 shows the contour plots generated from our two criteria, cell growth and recombinant protein production. The result is a medium mixture near the center of the triangle that is predicted to produce the maximum cell growth and recombinant protein production for our particular clone. By altering the importance values assigned to each criterion, it is possible to generate an exact medium mix to maximize growth and productivity for any CHO clone (data not shown).

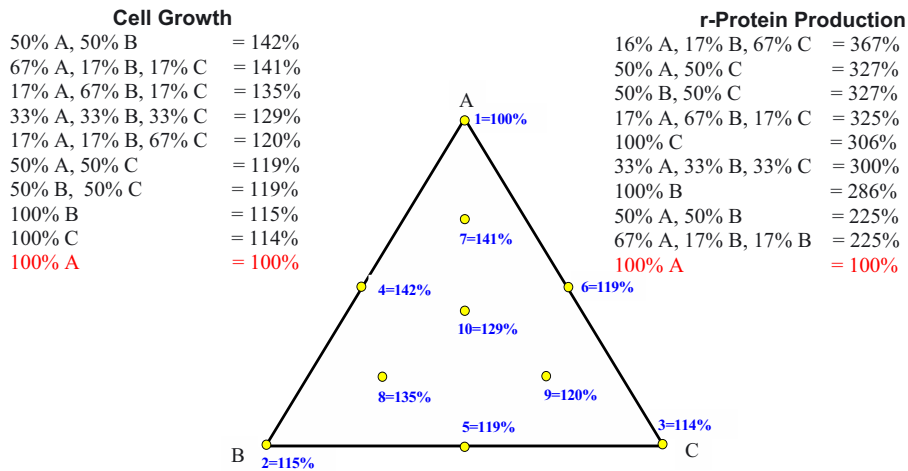


Figure 2. Data from the mixture experiment can be normalized and visualized in several methods. The data from the mixtures experiment in Figure 3 can be analyzed by normalizing the data to one of the media. In this example, the results from medium A represent 100%. Media can be ranked in terms of performance in the form of a list as seen on the left and right of the triangle. Another way of visualizing the data is to plot the values on the mixture triangle. The center diagram represents the normalized cell growth data. This method clearly indicates an increase in cell growth for the media mixes around numbers 4,7,8 and 10.

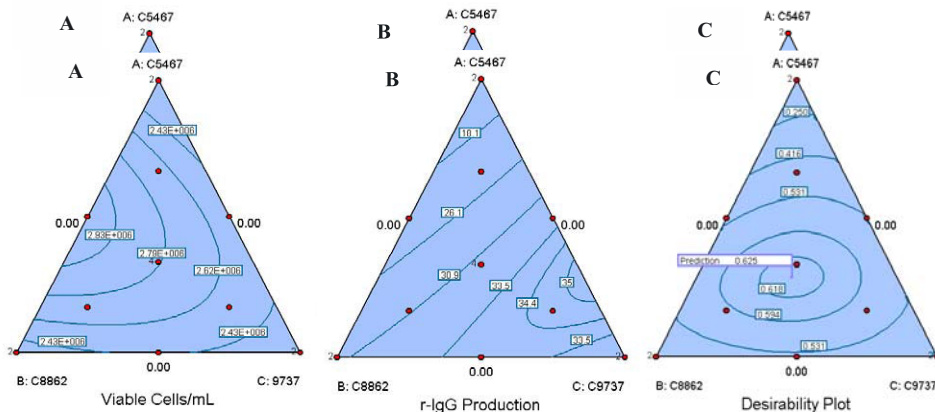


Figure 3. Data from the mixture assay can also be analyzed using Design-of-Experiment (DOE) software for a more precise analysis and optimization. A.) The contour plot for cell growth data indicates that the area with the best cell growth is located near a 50% mix between C8862 and C5467. B.) A similar contour plot for recombinant protein production. C.) During the optimization step, importance values can be assigned to each criterion, allowing each criterion to be weighted separately or together. The software then generates a desirability plot with values ranging from 0 to 1 (1 being the most desirable), indicating the exact point on the triangle where the most desirable mixes are located. The point predicted to yield maximum cell growth and r-IgG production corresponds to a mix of 29% C5467, 37% C8862 and 34% C9737.

Using either method for data analysis shows that the media mixes not only increased cell growth, but they also correlated with the highest levels of recombinant protein production. By using the media and techniques described in this kit, it is possible to develop an optimized medium for any CHO clone. The data presented has confirmed the value of using this approach to medium development.

#### 4. CONCLUSION

Sigma's CHO Medium Optimization Kit 1 consists of six diverse animal component-free media formulations designed for maximum cell growth and recombinant protein production in CHO cells. The convenient format provides multiple media formulations that can be screened for any recombinant CHO clone. The simple yet powerful media mixing experiments combined with DOE software allow researchers to rapidly elucidate an optimal medium mixture.

#### 5. REFERENCES

Moen, R., Nolan, T., and Provost, L., Quality Improvement through Planned Experimentation, Second Edition. McGraw Hill, Inc., New York (1999).

\*Design-Expert® is a registered trademark of Stat-Ease, Inc.



HERMANN, H. , BURIAN, R., WALDMANN, R.

## VIRUS INACTIVATION IN FOETAL CALF SERUM BY A COMBINED TREATMENT OF GAMMA- IRRADIATION AND UV-C IRRADIATION

*PAA Laboratories GmbH, Haidmannweg 9, 4061 Pasching, Austria*

Abstract Transmission of viruses by animal sera like Foetal Calf Serum (FCS) represents a considerable risk for humans and animals particularly when serum is used for production of pharmaceutical products such as vaccines. Procedures applicable for inactivating large numbers of different viruses both enveloped and non-enveloped, are therefore mandatory. The most used Gamma irradiation method accepted by FDA and EU guidelines efficiently abolish most of enveloped viral contaminants whereas “non-enveloped” viruses (e.g. Bovine Parvovirus) are not fully eliminated. For this purpose we have developed and validated UV-C irradiation in combination with Gamma irradiation as an efficient virus-inactivation method. Spiking experiments in FCS were performed and revealed constantly high clearance rates for various viruses such as bovine parvovirus, parainfluenza type III virus, bovine diarrhoe virus and different forms of mycoplasmas.

Experimental data showed that the combined UV-C and Gamma-treated sera maintained their growth promoting activities for various cell types. The validated process of UV-C treated FCS possesses a high inactivation capacity for the “non-enveloped” parvoviruses, a pathogen that cannot be destroyed easily by the Gamma irradiation alone. The UV inactivation procedure was performed with a novel computerised equipment. Only the combined irradiation of serum with Gamma and UV light offers under validated and controlled cGMP conditions the maximum possible raw material safety for biopharmaceutical production.

### 1. INTRODUCTION

Cell culture is routinely used in production of vaccines and production of recombinant proteins. The cell culture system commonly use medium supplemented with animal sera, the most common being foetal calf serum (FCS). Animal sera can contain viruses that cannot be removed with standard sterilization methods. Because FCS is a complex mixture of biologically sensitive components many of the treatments used to eliminate viruses negatively impact the growth-promoting properties. Under controlled conditions, serum products can be Gamma- irradiated to inactivate both animal and human viruses.

The process for 25 kGy irradiation–dosage itself is worldwide accepted from regulatory authorities for the inactivation of biological contaminants in medical reagents for the pharmaceutical industry. Most of the non-enveloped viruses are not fully eliminated by Gamma irradiation. While Gamma irradiation mainly breaks the virus proteins and the nucleic acids of lipid coated viruses, the UV-C irradiation method rather targets the viral nucleic acids, leading to an destruction of small, resistant viruses that are in lack of a viral lipid coat (“non-enveloped viruses”). The

combined application of Gamma- and UV-C-irradiation on FCS today offers the maximum safety of biopharmaceutical production. Both methods are robust and synergetic to each other.

## 2. METHODS

### **UV- irradiation treatment**

Foetal Calf Serum (FCS) spiked with different viruses and mycoplasmas is pumped through a UV-C irradiator (15 litre/h) with four UV lamps (40 Watt). During operation, the cylindrical irradiation chamber is set at a horizontal angle of 10° and rotated at 150 r.p.m. The serum is subjected to a fluence of 0.1 J/cm<sup>2</sup>.

### **Gamma Irradiation**

FCS spiked with viruses listed in table 1 was Gamma irradiated with a dosage of 35 kGy. The irradiation procedure was performed by Mediscan GmbH, Research Centre Seibersdorf, Austria using single box irradiation procedure.

### **Spiking procedure**

All procedures were performed in duplicate. For each spiking procedure 50 ml of the viruses listed in table 1 or 50 ml of mycoplasma were added to 950 ml FCS (in 1 liter standard plastic bottle). 2 x 2 ml of the spiked material were removed on each occasion as the load sample. Once the irradiation procedure was completed the irradiated FCS was collected and the volume was determined. Representative volumes of the output material together with load samples were stored at -5°C to further titration.

### **Titration of samples**

Generally, samples were tested undiluted in EMEM + penicillin/streptomycin or mycoplasma broth at various dilutions (10<sup>-3</sup>-10<sup>-7</sup>).

### **Plaque assay**

Dishes were seeded with Vero cells and allowed to grow to confluency. The cell sheet was inoculated with 0.5 ml of the sample and was allowed to absorb for 60-90 minutes. After removal of inoculum, dishes were overlaid with agarose containing neutral red and incubated until plaques were fully formed in the positive controls. Plaques were then counted.

### **Calculation of clearance rates**

Log reduction was calculated by subtracting the logarithm of the total p.f.u. recovered from the logarithm of the total p.f.u. added.

### **Growth promotion test with Acid Phosphatase Assay**

Cells are grown in 24-well plates at densities between 10<sup>4</sup> and 10<sup>5</sup> cells per well. The culture medium is removed and each well is washed with PBS. To each well 500 µl buffer containing 0.1 M Na-acetat, 0.1 % Triton-X-100 and 5 mM p-nitrophenyl phosphate are added. After incubation the reaction is stopped with addition of 500 µl NaOH, and colour development is assayed at 405 nm using a microplate reader.

### 3. RESULTS AND DISCUSSION

#### *Gamma irradiation at 35 kGy in single box container*

The international recommended dosage for products sterilized by Gamma irradiation is set at 25 kGy. New regulatory developments recommend to apply a minimum ionization of 30 kGy at all points to vials of FCS making it possible to obtain a minimum value of 25 kGy in the vial. Typically irradiation of fully loaded pellets need a higher maximum dosage (50 kGy achieve the requested minimum dosage). To obtain the new ionisation dosage of 30 kGy at all points we transfer the bottles filled with FCS in single boxes and set the Gamma irradiation at 35 kGy. The single boxes arrangement leads to extreme small energy distances between minimum and maximum dosage (35.7 kGy to 38.7 kGy). In contrast to fully loaded pellets where the maximum dosage influence the product quality the single box arrangement has only negligible impact on cell growth promoting properties of FCS (data not shown).

#### *UV-irradiation with a computer controlled machine*

The most used Gamma irradiation method accepted by FDA and EU guidelines efficiently abolish most of enveloped viral contaminants whereas "non-enveloped" viruses (e.g. Bovine Parvovirus) are not fully eliminated. Different to Gamma irradiation short wavelength ultraviolet light (UV-C) at 254 nm targets nucleic acids rather than proteins. The photons are emitted directly into the viral nucleic acids and induce photodimers, photohydrates which destroy the nucleic acid. Since viruses lack the repair enzymes, the genetic damage remains unrepaired. This is the reason why small, resistant viruses that are in lack of a viral lipid coat ("non-enveloped viruses") are very effectively destructed by UV-C irradiation. Furthermore proteins (e.g. growth factors and albumins in FCS) remain unaffected if irradiated with UV-C energy at 254 nm. For this purpose we developed a new UV-lab apparatus, the VIRALATOR™. The "VIRALATOR™", is a computer-controlled, UV-C irradiation machine specifically designed for the purpose of inactivating viruses, mycoplasma and other pathogens in biological fluids such as serum, plasma and protein solutions. It is used for the application at (bio)pharmaceutical upstream and downstream production processes, conforming with cGMP ("current Good Manufacturing Practices). The machine is validated for inactivation of contaminants in fluids with a maximum decay of 11 log steps (data not shown). The liquid product is fed through a slightly inclined rotating stainless-steel cylinder. The rotation presses the product against the inner wall of the cylinder forming a thin layer of fluid. This film is irradiated by two or four UV-lamps emitting the energy at 254 nm which are mounted along the axis of the cylinder. At the lower end the liquid reaches a collector cup and flows through the discharge valve in a container.

The following critical parameters are monitored: intensity of UV-lamps, cylinder rotations, fluid temperature before and after irradiation process and the through-put measured by a flow-meter.

**Combined UV-C and Gamma irradiation of Foetal Calf Serum (FCS)**

Viral inactivation by combined UV-C- and Gamma irradiation was investigated by spiking of FCS with several viruses and mycoplasmas (*table 1*). The table 1 shows the result after combined treatment. It could be demonstrated that the combination of these two synergistic inactivation processes will achieve clearance rates which are satisfactory under the aspects of biological safety. Also non-enveloped Parvoviruses show a significant log reduction of 6.7-9.8 steps (*table 1*).

*Cell growth-promoting activity of UV-C and Gamma irradiated FCS*

The influence of UV-C and Gamma irradiation on cell growth promoting properties of FCS was studied by comparing an UV-C / Gamma-treated serum with an untreated control. An acid phosphatase assay was used for this purpose.

In general, minor differences in cell growth could be observed by comparing UV-C / Gamma-treated serum and control over 14 days. This result shows that the combined UV-C / Gamma irradiation has only negligible impact on cell growth-promoting properties of FCS (*figure 1*).

## CONCLUSION

It can be assumed that the combined method is also applicable to other genera of viruses. Furthermore it is evident also bacteria, mycoplasmas and bacteriophages will be eliminated effectively by the combination treatment. In contrast to Gamma irradiation, UV-C irradiation is not an officially recognized virus inactivation process yet. The combination treatment of Gamma- and UV-C irradiation under validated and cGMP conditions can therefore be considered as an elementary improvement in product safety of biologic, bovine derived raw materials used in biopharmaceutical production.

Pathogen	Group	Genome	Envelope	Size (nm)	Clearance UV-Irradiation (Logs)	Clearance Gamma Irradiation (35 kGy) (Logs)	Clearance Combination UV-C/ $\gamma$ Irradiation (Logs)
BVDV	Pestiviridae	ssRNA	Yes	45-55	8	6.1	14.1
PI-3	Paramyxoviridae	ssRNA	Yes	100-200	7	7.5	14.5
Reo-3	Reo-viridae	dsRNA	No	70-80	4	6.7	10.7
IBR	Herpesviridae	dsDNA	Yes	100-200	6	7.1	13.1
BPV	Parvoviridae	ssDNA	No	18-25	8	1.8	9.8
PPV	Parvoviridae	ssDNA	No	18-25	5.5	1.2	6.7
Acholeplasma laidlawii	Mycoplasma				> 7	> 8	15
Mycoplasma agalactiae	Mycoplasma				> 7	> 8	15

Table 1: Clearance rates of viruses after combined UV-C irradiation and Gamma irradiation

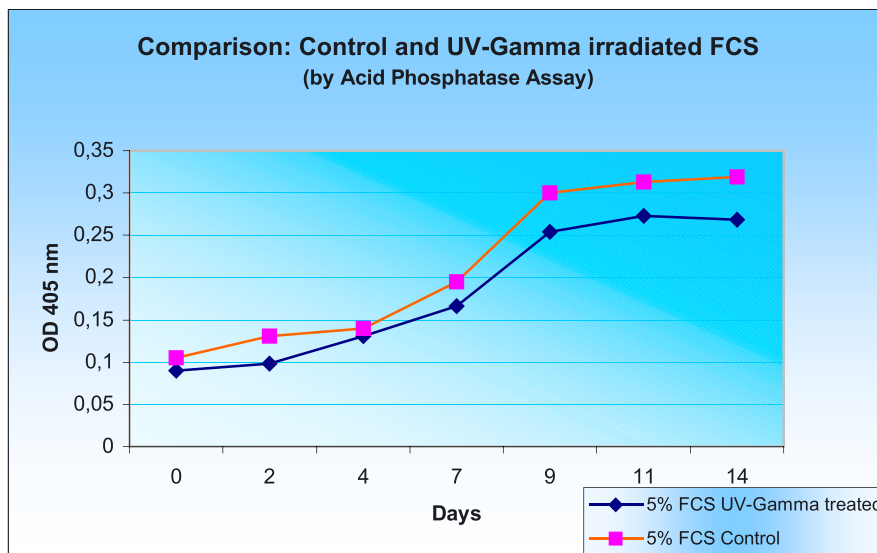


Fig. 1 : Comparison of control and UV-C / Gamma-irradiated 5 % foetal calf serum (FCS)

STACY HOLDREAD (1), CINDY HUNT (1), PERRY HAALAND (2),  
BRYCE CHANEY (2), WARREN PORTER (2),  
MOHAMMAD HEIDARAN (2), JON WANNLUND (1)

## ADVANCES IN MEDIA OPTIMIZATION: TWO AUTOMATED APPROACHES THAT INCREASE EXPRESSION WHILE REDUCING DEVELOPMENT TIME

*(1) BD Diagnostic Systems, Sparks, MD, USA (2) BD Technologies,  
Research Triangle Park, NC, USA*

### INTRODUCTION

There is no such thing as a universal medium. Through media optimization the ideal growth and production environment of a cell can be identified, resulting in optimal cell performance in a completely defined medium. If an even shorter development time is required, similar screening methods can be employed to evaluate a wide range of animal free peptones to select the best peptone or combination of peptones and the optimal concentration(s). Both partial and full optimization strategies provide a way to increase culture performance while decreasing or eliminating the amount of undefined or animal derived materials commonly used in cell culture media. These methods can be automated to further accelerate development time, increase assay reproducibility, and reduce laboratory costs.

### MATERIALS

Select Soytone, TC Yeastolate UF, TC Soy Plus UF, Bacto™ Proteose Peptone 3 (PP3), Difco Springer DS100 Soy Peptone UF (DS100), Wheat Peptone, Phytone™ Peptone, Phytone™ Peptone UF, BD Cell™ Chemically Defined Medium (BD Cell™ CD)

### METHODS

Individual components of a developmental CHO formulation were titrated to create a better-optimized medium. DS100, an ultra filtered soy peptone, was among the many components tested in 96 well plates where proliferation was determined using Alamar Blue™ and ELISA was used for PDGF production yields. Figure 1

demonstrates the increased performance achieved when one component is optimized. Figure 2 shows the performance of the optimized formulation in shaker flasks.

Cell performance can be enhanced when peptones are blended. Eight peptones were selected based upon prior studies demonstrating their performance in cell culture. Each peptone was titrated individually in BD Cell™ CD with 46/4 ATCC HB67 cells seeded at a density of  $2 \times 10^5$  cells/ml. Cell proliferation and antibody production were both evaluated to determine the optimal concentration for each peptone. These optimal concentrations were then blended in sets of two and three in BD Cell™ CD and set up in 96 well plates using Alamar Blue™ for cell proliferation determinations and ELISA for antibody production yields. Figures 3 and 4 represent a selection of the best and worst combinations and figure 5 shows the antibody production of the two-peptone blend media. These data demonstrate that high cell densities do not necessarily correlate with high antibody production. The peptone blending protocol can be automated to increase the number of combinations evaluated.

To demonstrate the need for a completely optimized medium an NS0 cell line was tested in 45 different proprietary chemically defined media in order to identify a potential candidate from which to begin the optimization. Once selected, several key components were titrated to determine optimal concentrations based upon Alamar Blue™ cell proliferation. Figure 6 shows the improved performance of the cell line when in the presence of the optimal concentration of the component.

## CONCLUSION

While many commercially available cell culture media exist, none are able to meet the specific requirements of every cell line. Optimization provides a way to increase cell proliferation and production by creating an ideal environment specific to the cell. One of the most important benefits of a complete optimization is increased cell performance with the elimination of undefined or animal derived components. Peptones used individually or in combination are suitable alternatives to complete optimization if time is critical. Performing these optimizations with automation can increase accuracy, increase the number of data points tested, and decrease the risk associated with human error (Figure 7).

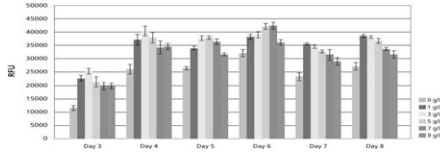


Figure 1. Developmental CHO Medium DS100 Titration

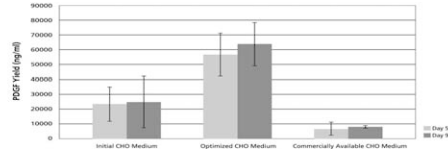


Figure 2. Developmental CHO Medium Optimization Study PDGF Production in Shaker Flasks

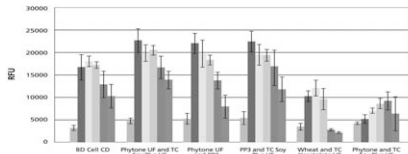


Figure 3. Two Peptone Blending Study in BD Cell CD 46/4 ATCC HB67

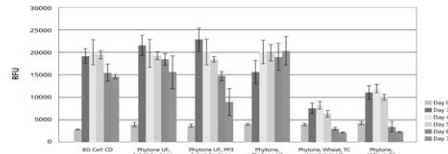


Figure 4. Three Peptone Blending Study in BD Cell CD 46/4 ATCC HB67

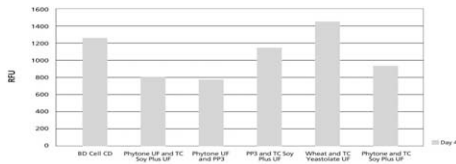


Figure 5. Two Peptone Blending Study in BD Cell CD Day Four Antibody Yield 46/4 ATCC HB67

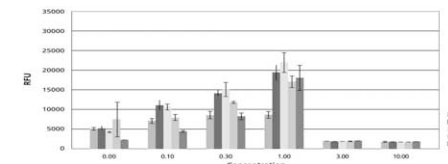


Figure 6. Calcium Chloride Titration NS0 Cells

Comparison of Automated Media Optimization and Conventional Media Optimization		
RD Automated Optimization	Number of Replicates	Conventional Optimization
N = 3	N = 10	
> 30 additions/minute (~45 minutes/plate)	Pipetting Speed	< 5 additions/minute (2-3 days/plate)
5	Number of Optimizations	84
50 fold less	Reagent Cost Savings	standard
1 day	Data Analysis Time	2 weeks
< 1 minute	Robotic Programming Time*	40 hours

Figure 7.

\*Based on Manual Programming of Liquid Handling Systems



## THE IMPORTANCE OF CHOLESTEROL FOR INSECT CELL GROWTH AND BACULOVIRUS PRODUCTION

*Department of Chemical Engineering, The University of Queensland,  
Brisbane, Australia*

### 1. INTRODUCTION

Cholesterol is believed to be an important component for insect cell culture in serum-free cultures to maintain good insect cell growth and to obtain good production of baculoviruses or recombinant proteins. This study aims to determine the effects of cholesterol on *Helicoverpa zea* cell growth in serum-free suspension culture and on the production of *Helicoverpa armigera* nucleopolyhedrovirus (HaSNPV). HaSNPV has the potential to be used as a biopesticide for the control of *Helicoverpa* pest species.

### 2. MATERIALS AND METHODS

The *H. zea* cell line (strain BCIRL-Hz-AM1) and HaSNPV (isolate UQ-AC53) were used in this study. VPM3 was an in-house made serum-free medium with a cholesterol level of 4.5 mg/L. Infections were carried out as shown in Fig. 1.

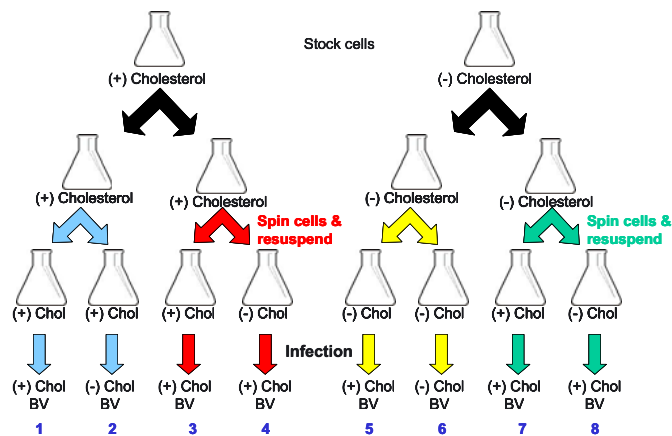


Figure 1: The approach taken to study the effect of cholesterol on baculovirus production.

## 3. RESULTS AND DISCUSSION

The growth of *H. zea* cells were not adversely affected by cholesterol-free medium (Table 1). Cell were maintained in cholesterol-free medium for more than 30 passages without any adverse effects on peak cell density (PCD), population doubling time (PDT) and growth rates.

Table 1. Effect of cholesterol on *Helicoverpa zea* cell growth.

Medium	PCD ( $\times 10^6$ cells/ml)	PDT (hours)	Growth rates ( $h^{-1}$ )	Dry weight (ng/cell)	TCP (ng/cell)
(+) cholesterol	$3.31 \pm 0.12$	$19.86 \pm 1.03$	$0.035 \pm 0.002$	$1.05 \pm 0.10$	$0.450 \pm 0.007$
(-) cholesterol	$3.15 \pm 0.10$	$23.16 \pm 1.58$	$0.030 \pm 0.002$	$1.02 \pm 0.15$	$0.510 \pm 0.009$

4 times higher cell specific yields were obtained in cholesterol medium. The quality and production of BV was affected by cholesterol. Real-time PCR results have confirmed that faster and higher BV production in cholesterol cultures.

Table 2. Infection.

Flask	Medium	Source of BV	PCD ( $\times 10^6$ cells/ml)	Cell specific yield (OB/cell)
1	(+) cholesterol	(+) cholesterol	0.92	265
2	(+) cholesterol	(-) cholesterol	1.91	60
5	(-) cholesterol	(+) cholesterol	1.88	63
6	(-) cholesterol	(-) cholesterol	2.53	22

Slightly higher OB production was obtained when cholesterol is present during infection (Table 3). This is different to the findings of Gilbert et al. (1996) which reported that cholesterol is essential for cell growth but not during infection.

Table 3. Infection.

Flask	Cells	Infection medium	PCD ( $\times 10^6$ cells/ml)	Cell specific yield (OB/cell)
3	(+) cholesterol	(+) cholesterol	0.59	231
4	(+) cholesterol	(-) cholesterol	1.05	161
7	(-) cholesterol	(+) cholesterol	0.55	168
8	(-) cholesterol	(-) cholesterol	1.02	130

More OB were observed in infected cells in cholesterol cultures (Fig. 4A) compared to cholesterol-free cultures (Fig. 4B). Cholesterol was reported as essential for normal morphogenesis of the ODV membranes (Bellonick et al., 1997). Normal ODV membrane morphogenesis (presence of membrane profiles and occluded virions) was observed in cholesterol-free infection cultures (Fig. 4D). However, nucleocapsid (arrows) numbers appeared to be lower in cholesterol-free infections (Fig. 4D) compared to cholesterol cultures (Fig. 4C), suggesting that this might lead to lower OB numbers.

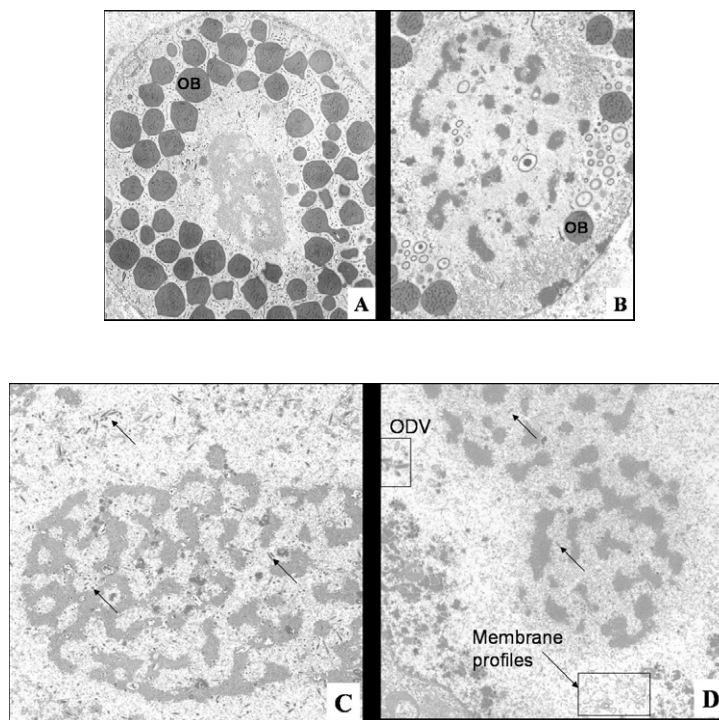


*Figure 2: Effect of cholesterol on virus morphogenesis. (A&C) Cholesterol infection cultures. (B&D) Cholesterol-free infection cultures.*

#### 4. CONCLUSIONS

Cholesterol is non-essential for *H. zea* cell growth in serum-free suspension culture. However, it is required for both the conditioning of the cells before infection and during infection to achieve high production yields of HaSNPV. Cholesterol is also important for the production of BV. The morphogenesis of ODV and OB occlusion

appeared normal in cholesterol-free infections but lower numbers of nucleocapsids were observed.

#### 5. REFERENCES

- Bellonick S, Akoury WE and Cheroutre M (1997) Importance of cholesterol for nuclear polyhedrosis virus (NPV) replication in cell cultures adapted to serum free medium. In: K Maramorosch and J Mitsuhashi (eds) *Invertebrate Cell Culture. Novel Directions and Biotechnology Applications* (pp. 141-147) Science Publishers, USA.
- Gilbert RS, Nagano Y, Yokota T, Fletcher T and Lydersen K (1996) Effect of lipids on insect cell growth and expression of recombinant proteins in serum-free medium. *Cytotechnology* 22: 211-216.

A. MARC, V. DEPARIS, C. DURRIEU, I. MARC, J.L. GOERGEN,  
I. CHEVALOT

## USE OF RAPESEED PROTEINS AND PEPTIDES AS SUPPLEMENTS IN INSECT CELL CULTURES

*Laboratoire des Sciences du Génie Chimique, CNRS-ENSAIA, BP 172,  
F-54505 Vandoeuvre-lès-Nancy, Cedex*

### 1. INTRODUCTION

Insect cell culture technology is widely used for the production of large quantities of biologically active recombinant proteins. However, the development of improved culture media able to support high-density suspension cultures of insect cells is required for large-scale productions. Currently, conventional media formulations for the culture of such cells are usually supplemented with fetal bovine serum (FBS). Because of the risks associated with the use of animal-derived materials, protein hydrolysates generated by acid or enzymatic hydrolysis from plant proteins became an interesting alternative to FBS. In particular, rapeseed proteins seem to be a valuable source for animal or insect cell cultures because of the high abundance of rapeseed cattle cake as raw material and its well-balanced amino acid composition.

The aims of this work were to test the ability of rapeseed proteins or hydrolysed derivatives to support the growth of Sf9 insect cells in low or serum-free media and to compare the kinetics of growth, substrate consumption and by-product formation during cultures performed with various medium combinations.

### 2. PREPARATION OF RAPESEED SUPPLEMENTS

The rapeseed concentrate and hydrolysate have been obtained from a basic extraction and an enzymatic hydrolysis of rapeseed cattle-cakes. The extraction procedure increases the proportion of proteins by a factor 2 (75%) compared to the level found in cattle cakes (33 %). Additional components such as fibres, lipids and ashes remain present at a low level. The concentrate contains mainly peptides with a molecular weight higher than 10 kDa. Alternatively, 74 % of the soluble peptides in the hydrolysate contain less than 10 amino acids, and a very low level of free amino acids is observed (table 1).

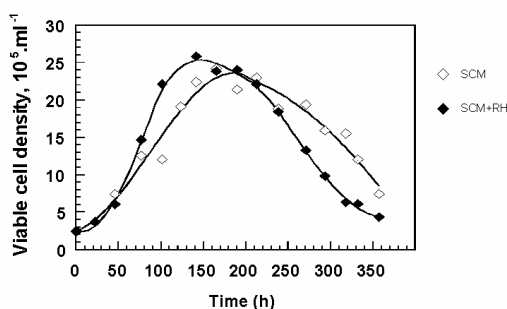
Table 1. Composition of the rapeseed protein concentrate and hydrolysate

	Degree of hydrolysis (%)	Free amino acids (% w/v)	Size < 1 kDa (% w/v)	Size 1-10 kDa (% w/v)	Size > 10kDa (% w/v)
Concentrate	N.A.	N.D.	9	17	74
Hydrolysate	32	1.2	74	23	3

(% w/v of soluble nitrogenous compounds)      N.A.: not applicable      N.D.: not determined

### 3. SF9 INSECT CELL CULTURES

#### 3.1. Serum-containing medium (SCM) with rapeseed hydrolysate (RH)

Figure 1. Growth kinetics of *Sf9* cells cultured in 250 ml erlenmeyer in SCM or SCM+RH

The addition of protein hydrolysate only slightly enhances the growth of *Sf9* cells in serum-containing medium, even if the maximal specific growth rate is higher (figure 1). The kinetics of carbohydrates, glutamine, lactate and ammonium ions are identical for both media. Sugars are consumed in the following order: glucose, then fructose and sucrose. Glutamine was never a limiting factor. Lactate and ammonium ions levels were not significant all over the culture.

#### 3.2. Serum-free medium (SFM) and rapeseed concentrate (RC) or hydrolysate (RH)

No cytotoxic effect of the rapeseed concentrate was observed (figure 2). The serum-free medium supplemented with the hydrolysate has a strong effect on both the maximal cell density (+ 60%) and the specific growth rate. With the three media, no differences in carbohydrate and lactate metabolisms have been detected. No limitation in glutamine occurred in all tested conditions since its consumption remained at a significant rate during the course of the culture.

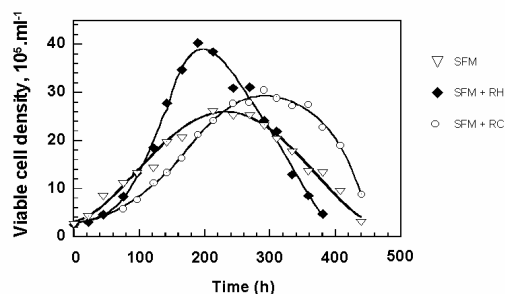


Figure 2. Viable cell density in SFM, SFM supplemented with RH or SFM with RC

### 3.3. Serum-free medium (SFM) and lactalbumin hydrolysate (LH)

The addition of lactalbumin hydrolysate does not affect strongly the growth of Sf9 cells in serum-free medium. However, without lactalbumin, the same maximal cell density is reached 100 h later and is maintained for a shorter period of time (table 2). The rapeseed concentrate was able to enhance the maximum cell density in a higher manner than lactalbumin, though a lower specific growth rate was obtained.

Table 2. Maximal viable cell density and specific growth rate of Sf9 grown in various media

Medium	SCM	SCM + RH	SFM	SFM + LH	SFM + RC	SFM + RH
$X_{\max}$ ( $10^6$ cells.ml <sup>-1</sup> )	2.3	2.6	2.5	2.5	3.0	4.0
$\mu_{\max}$ (h <sup>-1</sup> )	0.023	0.032	0.018	0.025	0.013	0.023

## 4. CONCLUSIONS AND PERSPECTIVES

From this work, it appears that the proteic concentrate from rapeseed does not present any cytotoxic effects on insect cells even in serum-free medium and that the rapeseed hydrolysate can enhance the growth of Sf9 cells more efficiently than the bovine lactalbumin hydrolysate. However, this effect is much lower with serum-containing medium. Interestingly, the supplementation of the media with rapeseed components does not induce any significant changes in cell metabolism. In future studies, rapeseed proteins and peptides will be tested with other cell lines. In particular, the metabolism of such peptides will be more deeply assessed and the effect of such plant components will be studied on recombinant proteins productivity and quality.

DIRK E. MARTENS, HENDRIKUS B.A. WEGKAMP,  
NICHOLAS H. SIMPSON, HANS H. HUTTINGA, TON KUNST  
AND ANDRÉ D. SIEMENSMA

NUTRITIONAL PERFORMANCE OF WHEAT-GLUTEN  
-DERIVED PROTEIN HYDROLYSATES IN  
HYBRIDOMA CELL CULTURES. A NUTRITIONAL  
FUNCTION STUDY.

<sup>1</sup> *Department of Agrotechnology and Food Science, Food and  
Bioengineering Group, Wageningen University, P.O. Box 8129,  
6700 EV Wageningen, The Netherlands*

<sup>2</sup> *Quest International Nederland B.V., P.O. Box 2, 1400 CA Bussum-  
Holland, The Netherlands*

## 1. INTRODUCTION

For the production of pharmaceutical proteins with animal cells often media are used containing components of mammalian origin. Since these components may contain infectious agents, industry aims at using media that are mammalian-source free. Wheat-gluten-derived protein hydrolysates are promising components for the development of such media. They are free of infectious agents and have been shown to be beneficial for animal cell cultures. The aim of this study was to elucidate the nutritional function behind the beneficial effect of wheat-gluten-derived protein hydrolysates and compare the performance of these hydrolysates to that of the meat-derived Primatone™ RL for a hybridoma cell-line.

## 2. MATERIAL AND METHODS

A murine hybridoma cell line was used producing a humanized monoclonal antibody. A serum-free medium was used supplemented amongst others with bovine serum albumin ( $1\text{g}\cdot\text{dm}^{-3}$ ) and Pluronic ( $0.8\text{g}\cdot\text{dm}^{-3}$ ).

Chemostats and perfusion cultures were performed in a  $3\text{ dm}^3$  bioreactor (Applikon Schiedam, the Netherlands) with a working volume of  $1\text{ dm}^3$ . The dissolved oxygen concentration was maintained at 50% DO. The pH was controlled at 7.2 and the temperature was maintained at  $37^\circ\text{C}$ . The dilution rate in the chemostats was controlled at  $0.64\text{ day}^{-1}$ . For the perfusion system cell retention was attained using an acoustic cell separator (Biosep  $10\text{ dm}^3$ , Applikon). A bleed rate of  $0.1\text{ day}^{-1}$  and a dilution rate of  $1\text{ day}^{-1}$  were applied.



The two control chemostats contained basic medium with the free amino acids of  $1.25 \text{ g.dm}^{-3}$  HyPep™ 4601. One chemostat contained  $1.25 \text{ g.dm}^{-3}$  HyPep™ 4601 and one contained the free amino acids of  $1.25 \text{ g.dm}^{-3}$  HyPep™ 4601 and  $1.15 \text{ g.dm}^{-3}$  HyPep™ 4605 Dev. The three perfusion cultures contained basic medium with respectively the free amino acids of  $2 \text{ g.dm}^{-3}$  HyPep™ 4602 Dev,  $2 \text{ g.dm}^{-3}$  HyPep™ 4602 Dev, and  $2.5 \text{ g.dm}^{-3}$  Primatone™ RL with  $0.29 \text{ g.dm}^{-3}$  glutamine. HyPep™ 4601, 4605 Dev and 4602 Dev all contain a large fraction of di- and tripeptides. HyPep™ 4605 Dev contains relatively more larger peptides. HyPep™ 4602 Dev contains 28% free amino acids, which is only slightly less than Primatone™ RL. HyPep™ and Primatone™ RL are protein hydrolysates from Quest International.

## 2. RESULTS

Figure 1 shows that upon addition of wheat-gluten-derived protein hydrolysates the cell density increases with 25%. Upon addition of Primatone™ RL, however, the viable-cell density more than doubled in the perfusion system. Viability and productivity (data not shown) remained constant upon addition of hydrolysate.

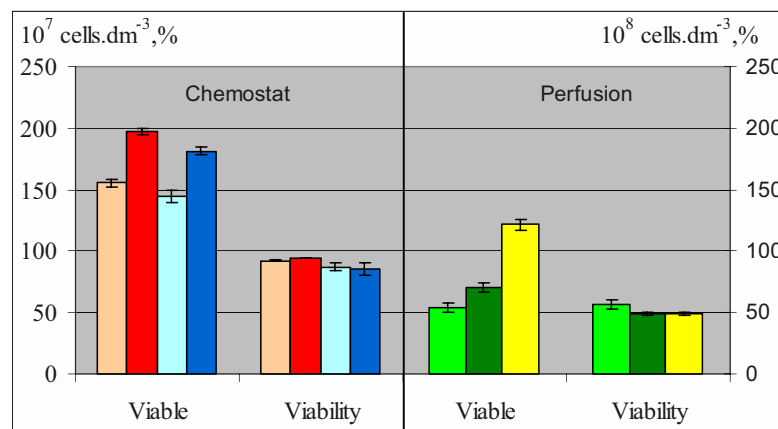


Figure 1. Steady-state viable cell concentration and viability in chemostats and perfusion culture for different culture conditions. ■ Control 4605, ■ HyPep 4605, ■ Control 4601, ■ HyPep 4601, ■ Control 4602, ■ HyPep 4602, ■ Primatone

In figure 2 it can be seen that upon addition of wheat-gluten-derived hydrolysates, the consumption rate of free amino-acid nitrogen decreases. In the chemostats it can be directly seen that this is compensated by the consumption of nitrogen in the form of peptides.

For the perfusion cultures the viability was low and a lot of peptides were released from dead cells. However, a decrease in peptide production can be seen at constant viability, indicating the consumption of peptides. Thus, the increase in cell density is probably caused by the availability of peptides as an additional source of nitrogen.

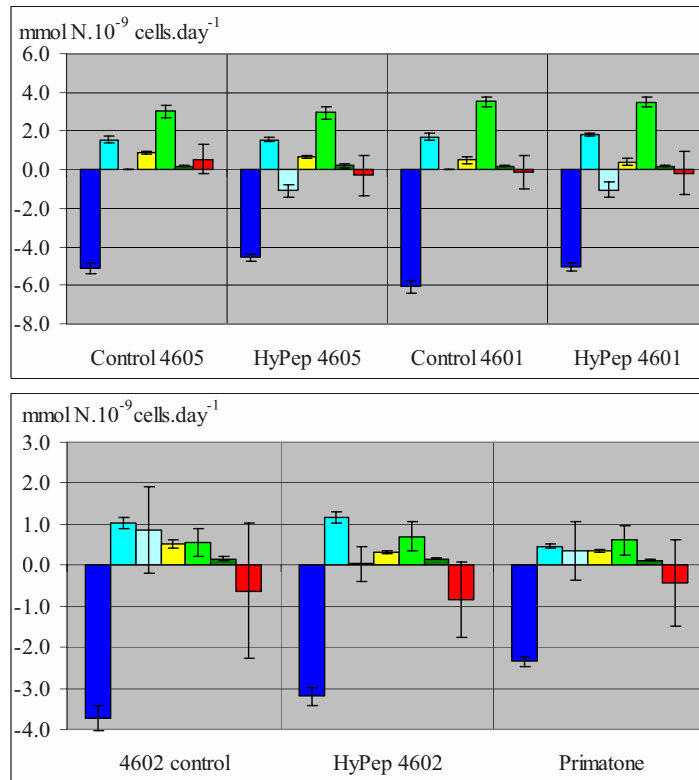


Figure 2. Nitrogen balances (■), for the chemostat (A) and perfusion cultures (B). Different nitrogen consumption rate contributions in the form of: ■ consumed free amino acids. ■ produced free amino acids. ■ peptide amino acids. ■ ammonia, ■ biomass, ■ product.

In the case of Primatone™ RL less nitrogen is wasted in the form of excreted free amino acids. This more efficient use of amino acids in addition to the consumption of peptides on the fact that slightly more free and peptide amino acids were present in the medium causes the extra increase in cell density seen for Primatone™ RL.

## CONCLUSIONS

Wheat-gluten-derived protein hydrolysates cause an increase in cell density due to the consumption of peptides that form an extra source of nitrogen and as such can replace Primatone™ RL.

Further research should study whether wheat-gluten-derived protein hydrolysates can also replace the function of Primatone™ RL that results in a reduction of nitrogen waste metabolism.

TALLEY D., CUTAK B., RATHBONE E., AL-KOLLA T.,  
ALLISON D., BLASBERG J., KAO K. AND CAPLE M.

## SYNTHECHOL™ SYNTHETIC CHOLESTEROL FOR CHOLESTEROL DEPENDENT CELL CULTURE -- DEVELOPMENT OF NON-ANIMAL DERIVED CHEMICALLY DEFINED NS0 MEDIUM

*Sigma-Aldrich Corporation, PO Box 14508, Saint Louis, MO 63178 USA*

**Abstract.** Traditional serum supplemented cell culture medium is fast becoming outdated as new technology permits the omission of most animal derived protein from the culture system. Cell lines derived from the NS0 myeloma cell line are rising in popularity for biopharmaceutical production, due to their high cell growth potential and their subsequent high production yields. However, because of their cholesterol auxotrophic nature, NS0 derived cell lines are particularly challenging for medium development. The first hurdle lies in the fact that there is no source of non-animal derived cholesterol. Second, cholesterol is not water-soluble and thus requires supplementation at the point of use. To address these issues, Sigma-Aldrich has produced SyntheChol™ (Sigma C1231); a synthetic, non-animal derived cholesterol. Initial results demonstrate that SyntheChol behaves similarly to animal-source cholesterol when dissolved in ethanol and supplemented in Hybridoma Medium, Animal Component Free (Sigma H4409). Furthermore, we have developed a sterile, liquid (500X), ready to add SyntheChol NS0 Supplement (Sigma S5442) with increased stability in cooler conditions. The results showed that SyntheChol NS0 Supplement is a stable and effective production-enhancing supplement as compared to both competitor supplements and natural cholesterol dissolved in ethanol. SyntheChol NS0 Supplement can be added to any medium prior to use. Finally, the development of the synthetic cholesterol, SyntheChol, has offered an opportunity of manufacturing an animal component-free, chemically defined NS0 medium.

### 1. INTRODUCTION

The NS0 cell line obtained from the European Collection of Cell Cultures (ECACC culture number 85110503) is described as a mouse myeloma cell line with lymphoblastic morphology. It is a subclone of the NS-1 cell line that is traditionally known to be cholesterol dependent for cell growth. This condition is particularly challenging for a serum free/protein free medium manufacturer. NS0 derived subclones are quickly gaining ground in the biopharmaceutical-manufacturing arena as a cell line of choice for several reasons. First, NS0 cells are very hardy, proliferative cells. Because they grow in suspension, they lend themselves easily to use in the larger and more complex stirred tank and perfusion bioreactor systems. Most importantly, NS0 recombinant clones are very productive.

Cholesterol is not water-soluble. The lipid-like characteristics of cholesterol make it appear hazy in liquid medium. This condition worsens over time and is

accelerated by storage in cooler conditions. Furthermore, until very recently there was no non-animal source of cholesterol on the market. Recently Sigma-Aldrich Corporation developed a non-animal, synthetic cholesterol, called SyntheChol™ (Sigma C1231). Using this newly created SyntheChol, we have further developed a sterile, ready to add (500X) liquid, SyntheChol™ NS0 Supplement (Sigma S5442) with increased stability in cooler conditions. In this study, the effects of SyntheChol and SyntheChol NS0 Supplement on cell growth and rIgG production in NS0 cells and NS0-derived recombinant clones are presented.

## 2. MATERIALS AND METHODS

Cell Lines and Cell Culture Media Stock NS0 and NS0 derived recombinant clone cell stocks were maintained in Hybridoma Medium, Animal Component Free (Sigma H4409), supplemented with 10mM L-Glutamine (Sigma G7513), and 5mg/L animal derived cholesterol (Sigma C3045 and/or C8667) or SyntheChol (Sigma C1231) which was dissolved in 200 proof ethanol.

Cell Culture and Cell Growth Assays Cell stocks were maintained at 37°C, 5% CO<sub>2</sub> and 95% Rh in an incubator. Stock cultures were between 50,000 and 1,000,000 cells/ml. For studies involving competitors' media and supplements, cell stocks were taken from serum containing basal medium and adapted to the respective test media. All cell stocks were harvested with at least 90% viability and were in log phase growth. All assays included a no cholesterol control and a cholesterol control. All reported results are the average of two replicate spinner flasks for each condition. Cell counts were done on a Scharfe Systems CASY-1 cell counter and a hemocytometer by Trypan Blue dye exclusion method.

Quantitation of Recombinant IgG Samples were centrifuged to remove cells and supernatants were submitted for analysis. An affinity chromatography method was employed utilizing a Dionex model #AD 20 UV VIS detector with a Protein G cartridge from Applied Biosystems catalog number 2-1002-00.

Mass Spectrometry Analytical comparison of animal-derived cholesterol (C8667) and SyntheChol (C1231), by reversed phase HPLC with UV and MS detection was performed using the following equipment and parameters: Waters 2690; Phenomenex C18 (2), 5 mm, 50 x 2 mm column; column temperature, 40 °C; isocratic mobile phase, 95% ACN 5% H<sub>2</sub>O; flow 0.100 mL/min; injection volume, 10 ul; run time 20 min; Micromass LCT; ionization by positive ion atmospheric pressure chemical ionization (APCI).

## 3. RESULTS AND DISCUSSION

As shown in Figure 1, SyntheChol, performs as well as both animal-derived cholesterol and fetal bovine serum in supporting NS0 cell growth. Furthermore, analytical data shows that the physio-chemical behavior of SyntheChol is in agreement with that of animal derived cholesterol (data not shown). The two products have similar chromatographic profiles. The UV chromatograms show that the samples are quite pure. The only major peak detected was that of cholesterol.

The two products yielded nearly identical mass spectra (background subtracted). The only major ion detected was  $m/z$  369.40. The monoisotopic molecular weight of cholesterol is 386.3549. Under the ionization conditions the C-O bond is extremely labile and the loss of the OH group results in a carbocation with the monoisotopic mass of 369.3521. This is in agreement with the observed peak in the mass spectra. The accurate mass measured for C8667 was 369.3555. The accurate mass measured for C1231 was 369.3548. These two masses are in agreement within

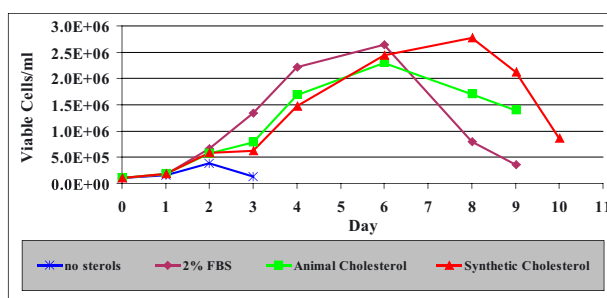


Figure 1. Comparison of animal derived cholesterol and synthetic cholesterol (SyntheChol, Sigma C1231) in supporting NS0 cell growth. Cell growth of NS0 cells were tested with Sigma hybridoma medium (H4409) supplemented with 2% FBS, 5 mg/L of animal-derived cholesterol and synthetic cholesterol. Both animal-derived and synthetic cholesterol were dissolved in Ethanol. The synthetic cholesterol exhibited growth characteristics comparable to the animal-derived cholesterol and FBS.

0.7 mDa.

In Figure 2, the SyntheChol NS0 Supplement (Sigma S5442) is then shown to perform as well as SyntheChol dissolved in ethanol and is offered as a sterile, ready to add supplement with increased stability in cooler conditions. This has been demonstrated in spinner flask culture and bioreactors.

The SyntheChol supplement is further shown to be as good as or better than a competitor's equivalent product with regard to growth of NS0 recombinant cells.

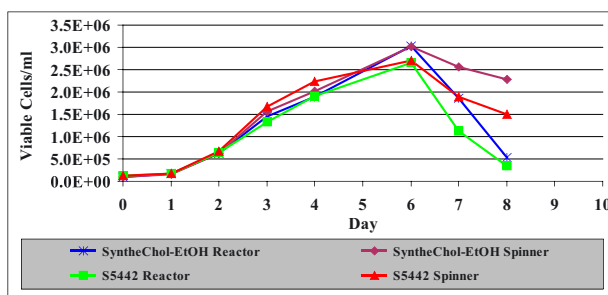
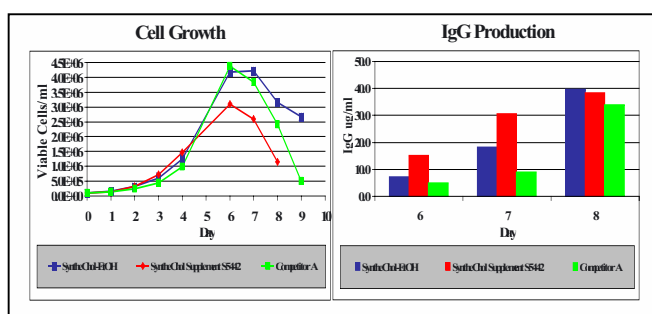


Figure 2. Comparison of NS0 cell growth in spinner flask and bioreactor with SyntheChol-EtOH and SyntheChol Supplement (Sigma S5442). NS0 cell growth was tested with Sigma hybridoma medium (H4409) supplemented with 5 mg/L of SyntheChol dissolved in ethanol or supplemented with SyntheChol Supplement (Sigma S5442). Both formats of SyntheChol support similar cell growth in spinner flask and 5 L bioreactor.

When used with an IgG producing NS0 derived recombinant clone the SyntheChol NS0 Supplement is as good as or better than the competitors' product with regard to IgG production (as shown in Figure 3). This data is further confirmed by the data obtained from a testing of the second recombinant NS0 clone (data not shown).



**Figure 3.** Cell growth and rIgG production of NS0 recombinant clone 1 were compared using the medium supplemented with SyntheChol-EtOH, Competitor A product and SyntheChol Supplement (Sigma S5442). NS0 cell growth was tested with Sigma hybridoma medium (H4409) supplemented with 5 mg/L of SyntheChol dissolved in ethanol or supplemented with SyntheChol Supplement (Sigma S5442). Although the cell growth is slightly lower in the medium with SyntheChol Supplement, the total IgG production and specific IgG productivity is higher or comparable to other tested samples in the NS0

#### 4. CONCLUSION

Sigma-Aldrich Corporation has produced the non-animal derived cholesterol called SyntheChol (Sigma C1231). This product promotes the growth of NS0 and NS0 derived cell lines in Hybridoma medium totally devoid of animal derived components (Sigma H4409). SyntheChol NS0 Supplement (Sigma S5442) enhances the solubility of the SyntheChol molecule for easier use. This supplement is supplied as a 500X concentrate, is sterile filtered, and ready for use. SyntheChol NS0 Supplement provides similar or better growth and rIgG production as compared with SyntheChol dissolved in ethanol and a leading competitor's product.

#### 5. REFERENCES

- Merten, O-W., Safety issues of animal products used in serum-free media, in *Animal Sera, Animal Sera Derivatives and Substitutes Used in the Manufacture of Pharmaceutical: Viral Safety and Regulatory Aspects*. Dev. Biol. Stand. Basel, Karger, 99, 167-180, 1999.
- Peppers, S., Allison, D., Johnson, T., Talley, D., Caple, M., Replacing the animal component in serum: evaluating raw materials of inclusion in optimized hybridoma media. *BioPharm.*, 14(5), 22-30, 2001.
- Gorfien, S., Paul, B., Walowitz, J., Keem, R., Biddle, W., Jayne, D., Growth of NS0 Cells in Protein-Free, Chemically Defined Medium. *Biotechnol. Prog.*, (16), 682-687, 2000.
- Wrotnowski, C., Cell culture media trends mirror bioindustry. *Gen. Eng. New*, 20(8), 8, 2000.

MANWARING, J., BARNETT, B., PENCE, B.,  
AND WHITFORD, W.

## NS0 DERIVATIVES: MAB PRODUCTION IN LARGE- SCALE SFM FORMATS

*Perbio Science/NV HyClone Europe, 9320 Erembodegem-Aalst, Belgium*

**Abstract** NS0 is a mouse myeloma cell popular in the construction of hybridoma and transfectoma for large-scale heterologous protein expression. For reasons of regulatory compliance, cost, batch consistency, downstream processing, and materials availability, commercial application of NS0 has moved toward one of many available serum free media (SFM) platforms. There exists today no full-complement SFM that will support the high performance culture of NS0 derivatives in large-scale culture. Nevertheless, solutions to many implementations have been developed, and high yield production in large-scale SFM applications is now possible.

### MATERIALS AND METHODS

Serum-free media: HyQ<sup>®</sup> ADCF-MAb<sup>™</sup>, a protein- and animal derived component- free (ADCF) medium; HyQ<sup>®</sup> SFX MAb<sup>™</sup>, a chemically defined (CD) protein-containing medium; and HyQ<sup>®</sup> SFM4MAb<sup>™</sup>, a rich, low-protein production medium with robust properties. Lipid supplements to support NS0 and other cultures include two cyclodextrin-based, CD and ADCF lipid dispersions. One, HyQ<sup>®</sup>LS-1000<sup>™</sup>, is a 1000x concentrate providing cholesterol and requiring dilution immediately prior to use. Another, HyQ<sup>®</sup>LS250<sup>™</sup> provides cholesterol and other lipids, and may be used in supplementation at any time prior to culture initiation and may be filtered after dilution. Cell lines employed to demonstrate performance include ECACC 85110503 null NS0, and a particularly troublesome proprietary pSV based NS0 transfectoma (rNS0) from this line. Culture modes include shake flask, 10L Celligen<sup>®</sup> and 3L Applikon<sup>®</sup> bioreactors. Employing our Metabolic Pathway Design<sup>™</sup> approach, HyClone is optimizing media and applications to the nutritional requirements and production kinetics of NS0 in specific culture modes. Also, attention is paid to supporting popular product purification approaches.

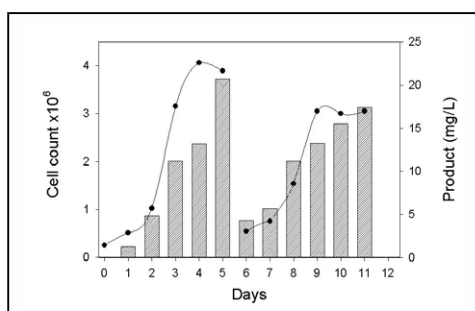
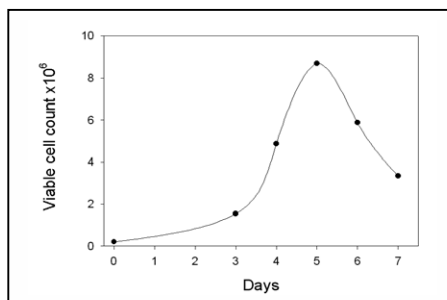
#### *NS0 Properties*

Robust growth, a sound regulatory pedigree, and success in a variety of fusion, transfection, selection and production approaches are properties that make NS0 a practical candidate for expression of product. Apoptosis is known to be an issue in the culture of murine myeloma, and their derivative hybridoma, especially under conditions of environmental or nutritional stress (1). Shear force sensitivity is of concern in suspension culture. Product secretion kinetics through the culture cycle of

many hybridoma, including NS0 are an issue. A variety of nutrient and culture environment perturbations have been shown to induce increased production rates (2). Cholesterol is required by all animal cells for a number of functions including the maintenance of membrane fluidity. As the need for expression in serum-free environments developed, it was discovered that NS1 and derivatives had become auxotrophs for cholesterol. Glutamine may be available to cells in culture through absorption from the ambient medium or production by glutamine synthetase from glutamate and asparagine. NS0 have been shown to be auxotrophs for glutamine. This phenotype is used as a popular selection system in transfectoma production (3).

### Growth Media

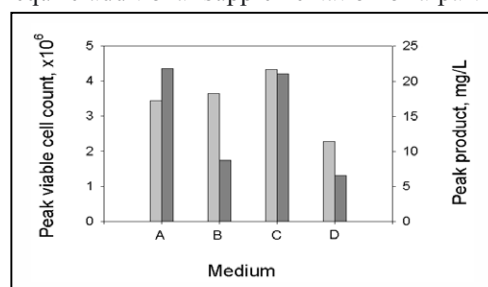
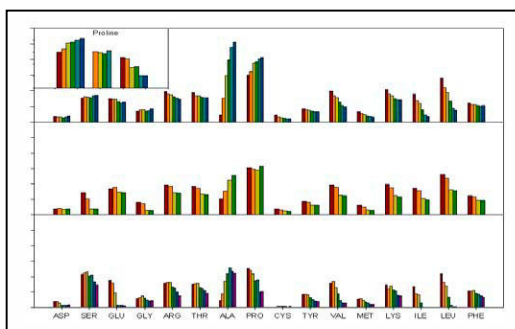
NS0 can be adapted to a number of commercially available serum-dependant culture media. Many researchers and commercial rprotein producers wish to avail themselves of the variety of SFM available. For example, suspension cultures of NS0, in HyQ<sup>®</sup> SFM4Mab<sup>™</sup> supplemented with HyQ<sup>®</sup>LS high cholesterol lipids, seeded at  $2 \times 10^5$  cells/ml supports culture densities to over  $8 \times 10^6$  cells/ml (Fig. 1). While much has been accomplished in this arena, NS0 derivatives still present unique challenges to large-scale SFM culture (4). Culture modes and scale appear to be of more than average import for SFM application. While there are some configurations of serum-free, and especially protein-free, culture that remain problematic, many of them have been successfully implemented. Many examples of high levels of cell density and total product accumulation in large-scale applications have been reported by private concerns that hold their formulas and procedures as trade secrets. We have



demonstrated the suitability of HyQ<sup>®</sup> SFM4Mab<sup>™</sup> and HyQ<sup>®</sup>LS Lipids to rNS0 in 10L perfusion bioreactor culture (Fig. 2). Sub-clones and derivatives of NS0, due to the diversity of their means of generation and maintenance, complicate the identification of “NS0” media requirements. Product expression, secretion, and net production in both hybridoma and transfectoma have been shown to be very dependant upon nutrient supplementation, alteration, timing and depletion as well as other culture environment perturbations. Various culture manipulations and nutritional regimens have been reported to increase net production in NS0. Many represent a common theme that cultures inhibited for



nominal cellular proliferation, can be stimulated to higher overall product accumulation on a per cell, culture volume, or time basis. However, most appear to be derivative/ medium/culture configuration dependant (5). Approaches to reducing the problem of apoptosis include avoiding particular nutritional and environmental stresses. Chemical additives that have been shown to reduce or inhibit apoptosis may be a consideration here, too. Iron transport is always an issue in the development of any SFM. Added transferrin will normally replace the transport potential provided by serum. In protein-free formulations, a variety of chelators and added iron have been shown to support most cultured cells, although many have a preference for particular complexes. Glutamine supplementation is an absolute requirement for these cells that cannot produce it on their own, but are obligate for an exogenous source. However, functional genes for glutamine catabolism from glutamate or other intermediates are available to NS0 from transfection or fusion to other cells. The most popular selection system for transfectoma production employs this system. Amino acid, vitamin, trace element and other ion concentration/ratio optima for various myeloma and derivatives, including NS0, have been reported for decades (6). General basal conditions, as well as high-density feeding and perfusion approaches for any particular application can be established from them. However, review of



these formulations, as well as direct experimentation, reveals significant sub-clone, derivative, basal formulation, and culture mode induced variation in these requirements. For example, it is not uncommon to see an NS0 producer reported to require additional supplementation of a particular amino acid in an application, and discover that your culture is either not utilising it, or actually producing it. For example, null NS0, rNS0, and rGS NS0 demonstrate divergent amino acid usage in HyQ® SFM4MAb™ (Fig.3). Lipids, due to their very limited solubility in aqueous media, are a special issue in culture media supplementation. The fact that NS0 require such a high concentration of a sterol (for example, 2– 6 mg/L of cholesterol) is a particular challenge to supplementation. There are many technologies available for this supplementation including the use of PC based vesicles, emulsions, microemulsions, carrier proteins, and carrier polymers such as one of the cyclodextrins (7). For example, HyQ® ADCF MAb™ (A), SFX MAb™ (B), SFM4MAb™ (C), and CCM-1™ plus the high cholesterol supplement HyQ® LS Lipids support rNS0 culture and production (fig. 4). Cholesterol loads efficiently into certain

cyclodextrins, and the resultant complex is filterable, stable, and innocuous, however, the nature of the association leads to instability in high dilution in some formulations. Products and systems are available for large-scale SFM applications of NS0 derivatives, yet adequate complete media (including sufficient cholesterol), and fed-batch system supporting supplements are not yet commercially available.

#### REFERENCES

1. Sauerwald TM, Betenbaugh MJ, (2002) Apoptosis in biotechnology: Its role in Mammalian Cell Culture and Methods of Inhibition. *Bioprocessing Journal*; Summer, 61-68.
2. Miller WM, et al, (2000) A kinetic analysis of hybridoma growth and metabolism in batch and continuous suspension culture: effect of nutrient concentration, dilution rate, and pH. Reprinted from *Biotechnol Bioeng*; (1988), Mar 20;67(6):853-71.
3. Keen MJ, Hale C, (1996) The use of serum-free medium for the production of functionally active humanized monoclonal antibody from NS0 mouse myeloma cells engineered using glutamine synthetase as a selectable marker. *Cytotechnology* 18:207-17.
4. Dempsey J, et al, (2003) Improved Fermentation Process for NS0 cell lines expressing human antibodies and glutamine synthetase. *Biotechnol. Prog*; 19, 175-8.
5. deZengotita VM, et al, (2000) Phosphate feeding improves high-cell-concentration NS0 myeloma culture performance for monoclonal antibody production. *Biotechnol Bioeng*; Sep. 5;69 (5):566-76.
6. Keen MJ, Hale C, (1996) The use of serum-free medium for the production of functionally active humanized monoclonal antibody from NS0 mouse myeloma cells engineered using glutamine synthetase as a selectable marker. *Cytotechnology* 18:207-17.
7. Keen MJ, Steward TW, (1995) Adaptation of cholesterol-requiring NS0 mouse myeloma cells to high density growth in a fully defined protein-free and cholesterol-free culture medium. *Cytotechnology* 17:203-211.

SATOSHI TERADA<sup>1</sup>, KANA YANAGIHARA<sup>1</sup>, KOZUE KAITO<sup>1</sup>,  
MASAO MIKI<sup>1</sup>, MASAHIRO SASAKI<sup>2</sup>, KAZUHISA  
TSUJIMOTO<sup>2</sup>, HIDEYUKI YAMADA<sup>2</sup>

## SILK PROTEIN SERICIN ACCELERATES PROLIFERATION OF VARIOUS MAMMALIAN CELLS

<sup>1</sup>*Department of Applied Chemistry and Biotechnology, Faculty of  
Engineering, Fukui University, 3-9-1 Bunkyo, Fukui 910-8507, Japan,*  
<sup>2</sup>*Technology Department, Seiren Co. Ltd. 1-10-1, KEYA, FUKUI 918-8560, JAPAN*

**Abstract.** Sericin protein derived from silkworm cocoon was added to the culture of various mammalian cell lines including human hepatoblastoma HepG2, human fibroblasts and so on. The proliferations of all cell lines tested were accelerated in the presence of sericin and its mitogenic activity was comparable to that of bovine serum albumin (BSA), one of the best supplements for the culture medium. Sericin derived from silkworm cocoons would be a preferable supplement for culture media because the risk of infection to human was not reported, while BSA is obtained from bovine serum and the risk of infection such as bovine spongiform encephalopathy cannot be avoided. Recombinant sericin peptides synthesized by *E. coli* (1) also stimulated the growth of hybridoma as well as sericin derived from silkworm did. These results indicate that sericin is a novel and suitable mitogenic supplement for mammalian cell culture.

### 1. INTRODUCTION

Although many serum-free media have been developed, most mammalian cells require bovine serum or its replacement in the culture medium. But the risk of infection such as bovine spongiform encephalopathy (BSE) could not be avoided. Therefore a novel factor for mammalian cell culture is strongly required and we propose silk protein sericin as such a factor.

Sericin, together with fibroin, is the major component of raw-silk. Sericin, a gummy coating on raw-silk filaments, is removed by a treatment called degumming in order to make silk lustrous and semitransparent. Degumming treatment is an alkaline scouring operation at a temperature of about 95°C. Recently, novel functions of sericin were reported. Sericin functions as an antioxidant to inhibit tyrosinase and lipid peroxidation (2). Feeding sericin to mice prevent them from colon carcinogenesis induced by 1,2-dimethylhydrazine (3). DMBA-TPA-induced skin tumorigenesis is also suppressed by sericin (4). Recombinant sericin peptide had protective effects against freezing stress in *E. coli*. (1).

We previously reported that sericin accelerates proliferation of various mammalian cell lines such as hybridoma (5). Here, it is reported that sericin induces proliferation of several human cells and that recombinant sericin peptides are also useful.

## 2. MATERIALS AND METHODS

Sericin was prepared from cocoons of *Bombyx mori*. One liter of 0.2 % sodium carbonate solution with 20 g of the cocoon was heated at 95°C for 2 hours and then filtrated with a glass microfiber filter in order to remove fibroin. The filtrate was dialyzed against deionized water and dried up by spray drying. The recombinant sericin peptides were synthesized in *E. coli* transfected with pQEserD and pQEserT, and prepared by the method of Tsujimoto (1). The peptide had a high proportion of hydrophilic amino acid residues (Ser, 45%; Gly, 16%; Thr, 11%; Asn, 11%).

Human hepatocarcinoma HepG2 was cultured in DME-medium supplemented with 10% FBS or in ASF104N medium (Ajinomoto, Japan). Human fibroblast was purchased and cultured in FGM. Hybridoma 2E3-O was cultured in ASF104 medium (Ajinomoto). Viable and non-viable cell densities were determined by the trypan blue exclusion method using a Neubauer improved hemocytometer (Erma, Tokyo, Japan).

## 3. RESULTS AND DISCUSSIONS

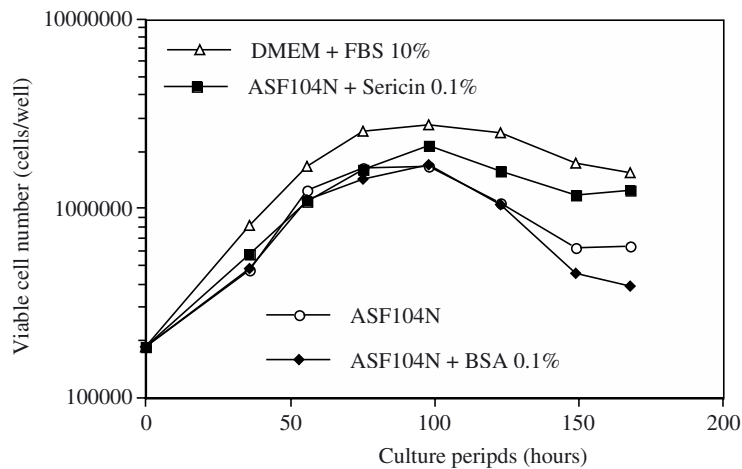


Fig.1 Effect of sericin on proliferation of human hepatocarcinoma HepG2

### 3.1. Effect of sericin on proliferation of human hepatocarcinoma HepG2

Human hepatocarcinoma HepG2 were cultured in DMEM supplemented with 10% FBS. 268,000 cells were seeded into each well and cultured for one day. Then medium was changed into ASF 104N serum-free medium supplemented with sericin or BSA. As shown in Fig. 1, sericin significantly improved the culture, while BSA failed to improve the culture.

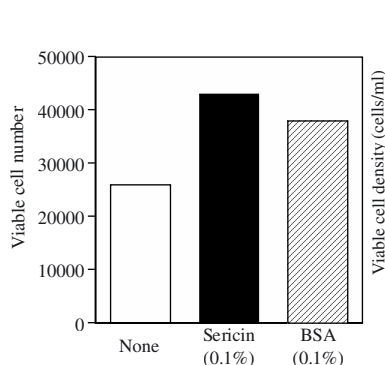


Fig.2 Growth of human fibroblast . 20,000 cells were seeded and cultured for 3 days.

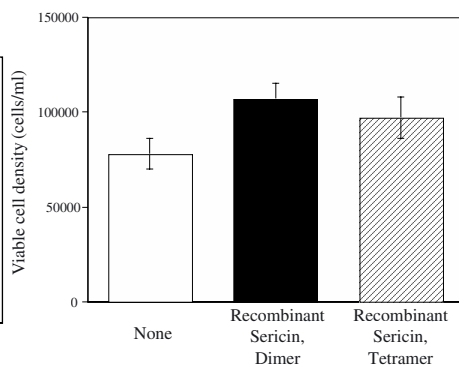


Fig.3 Effect of recombinant sericin peptides on proliferation of hybridoma

### 3.2. Effect of sericin on proliferation of human fibroblast.

Sericin was added into the culture of human fibroblast and the effect on the proliferation was assayed (Fig.2). In the presence of 0.1% sericin, fibroblast proliferate at higher rate than in the absence and than even in the presence of BSA.

### 3.3. Effect of recombinant sericin peptides

Recombinant sericin peptides were prepared. pQEserD and pQEserT encode dimer sericin and tetramer sericin peptides, respectively. 16,000 hybridoma cells were seeded in ASF104 medium with 0.03% sericin peptide and cultured for 3 days (Fig.3). Both dimer and tetramer sericin significantly accelerated the proliferation.

## 4. REFERENCES

- [1] Tsujimoto K et al. (2001) Cryoprotective effect of the serine-rich repetitive sequence in silk protein sericin. *J. Biochem.* 129: 979-986.
- [2] Kato N et al. (1998) Silk protein, sericin, inhibits lipid peroxidation and tyrosinase activity. *Biosci. Biotechnol. Biochem.* 62: 145-147.
- [3] Sasaki M et al. (2000) Silk protein, sericin, suppresses colon carcinogenesis induced by 1,2-dimethylhydrazine in mice. *Oncol. Rep.* 7: 1049-1052.
- [4] Zhaorigetu S et al. (2003) Silk protein, sericin, suppresses DMBA-TPA-induced mouse skin tumorigenesis by reducing oxidative stress, inflammatory response and endogenous tumor promoter TNF- $\alpha$ . *Oncology Reports.* 10: 537-543.
- [5] Terada S et al. (2002) Sericin, a protein derived from silkworms, accelerates the proliferation of several mammalian cell lines including a hybridoma. *Cytotechnology.* 40: 3-12.

T. BRUECKERHOFF<sup>1</sup>, J.-G. FRERICHS<sup>1</sup>, K. JOERIS<sup>2</sup>,  
K. KONSTANTINOV<sup>2</sup>, T. SCHEPER<sup>1</sup>

## IMAGE ANALYSIS BASED REALTIME-CONTROL OF GLUCOSE CONCENTRATION

*1) Institut für Technische Chemie, Universität Hannover, Callinstr. 3,  
30167 Hannover 2) Bayer Corporation, Dept. of Cell Culture and  
Bioprocess Engineering, 800 Dwight Way, Berkeley, CA 94701, USA*

**Abstract.** In-situ microscopy is the concept of monitoring micro organisms in the original production environment inside a fermentor. A new type of in-situ microscope suitable for both batch and long-term fermentation runs is presented. First results with the new type of in-situ microscope show that it is possible to integrate the in-situ microscopy system for process control purposes.

### 1. INTRODUCTION

To increase quality and yield of biotechnology processes, it is useful to obtain information about direct process parameters in real-time. Furthermore, online information about a cultivation is a requirement for a complete automation of the cultivation process. Up to now samples are taken off the bioreactor and cell number and viability are determined offline. It is not possible to control the process without interfering with it. In-situ microscopy is a new method based on image analysis that allows for counting of direct cell parameters online (Bittner et al., 1998, Suhr et al., 1995, Camisard et al., 2002). Images of cells are acquired directly in the bioreactor, the digital data is analysed automatically by image analysis algorithms and serves for controlling the bioprocess. A first in-situ microscopy application, according to industrial requirements, is described by (Joeris et al., 2002).

### 2. MATERIALS AND METHODS

#### *2.1. The in-situ microscopy system*

The in-situ microscope consists of the in-situ microscope hardware, the microcontroller, a compact PC with a frame grabber, an image analysis software and a control software for the microscope itself. In combination with the frame grabber and a progressive scan CCD-camera the in-situ microscope represents the image acquisition unit. The frame grabber digitizes the analog signal from the CCD-camera and the digital data can be evaluated by means of image analysis. To acquire in-situ

images the microscope fits into a bioreactor's standard 25 mm side port. The sampling zone is defined by two sapphire windows that work as slide and cover slip of a standard light microscope. In contrast to previous types of the in-situ microscope the new flow-through sampling zone consists of a fixed slide and a movable cover slip. The two steel tubes of the microscope are attached to stepper motors. To define the sampling zone volume a micro controller gives a signal to a stepper motor attached to the outer tube and the desired height of the sampling zone is adjusted. With a second stepper motor, attached to the interior tube, the objective is automatically focussed.

To monitor yeasts, achromatic objectives with a 20-fold magnification (overall magnification 400-fold) and numerical aperture of 0.4 are used. To monitor mammalian cell cultivations, achromatic objectives with a 4-fold magnification (overall magnification 80-fold) and a numerical aperture of 0.1 are used.

## *2.2. Online process control*

With the in-situ microscope it is possible to control the cultivation process based on direct cultivation parameters (e.g. cell concentration, cell size). For this purpose it is necessary to develop adequate algorithms for each cell type. In the following image analysis for mammalian cells is shown as an example. The image analysis algorithm is based on the algorithm described by (Frerichs, J.-G., 2000).

Image 1 in Figure 1 shows an image of CHO cells taken during a perfusion cultivation. The magnification is 80-fold. Two main features are visible in Image 1: cells and bubbles. In the first step of image analysis the background is separated from the bubbles and cells by automatic thresholding. Each region is labelled, bubbles and cells are separated. This step results in Image 2 that represents cells and Image 3 that represents bubbles. The bubble area is subtracted from the total field of view. This step is necessary to calculate the cell density. During the next step of image analysis (region growing) each area representing a single cell is evaluated. The outline of each cell is defined and cell size and cell volume are calculated. The results of image analysis allow to calculate the cell concentration.

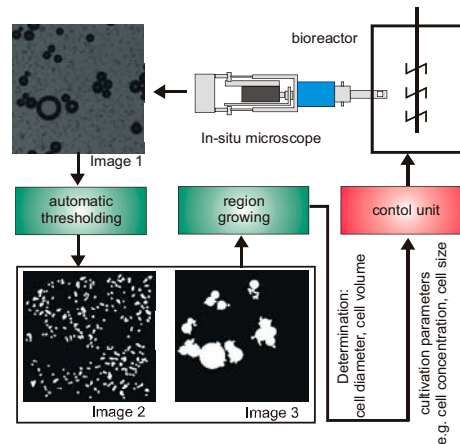


Figure 1. Image analysis embedded in the process control.

In a first attempt yeasts were used as a test organism because of the simple handling compared to mammalian cells. The image analysis for yeasts works similar but due to different cultivation conditions no bubbles occur.

### 3. RESULTS

For online process control of cultivation processes by in-situ microscopy it is necessary to monitor a wide range of cell concentration in the cultivation vessel without the possibility of dilution. To test the new flow-through sampling zone the yeast concentration in a 3 L bioreactor was permanently increased. The results show that there is a linear dependency between the cellular dry weight and single cells calculated with the image analysis software. Up to a cell concentration of about  $4 \cdot 10^8$  cells/mL it was possible to monitor the accumulation of yeasts in the bioreactor without recalibration.

Concerning mammalian cell cultivations, the in-situ microscope was tested in a perfusion system with 5 L working volume. The test organisms were CHO cells. The results of image analysis were compared to an automated cell counting system, Cedex (Innovatis, Bielefeld, Germany). Up to a cell concentration of about  $9 \cdot 10^6$  cells/mL it was possible to monitor the cultivation without recalibration.

The results allow for the embedding of the in-situ microscopy system in a cultivation regulating system. In a first step yeasts were used to test a process control based on in-situ microscopy. The aim of this yeast cultivation was to optimize the control of glucose concentration to minimize the production of ethanol and to maximize the growth rate. To run the complete cultivation at the optimal glucose concentration a regulating system based on the  $\text{CO}_2$  concentration in the exhaust air and the biomass calculated by the in-situ microscope was developed. The cultivation of the strain *S. cerevisiae* H620 was carried out in a 1,5 L bioreactor. A profile for the glucose concentration was run with a maximum of 0.08 g/L and a



minimum of 0.05 g/L. Images were taken and biomass was calculated every minute. During the cultivation no ethanol was produced, though the system is not very stable yet. However, these very early results of bioprocess control by direct cell parameters are very promising.

#### 4. REFERENCES

- Bittner, C., Wehnert, G., Scheper, T., 1998. In-situ microscopy for online determination of biomass. *Biotechnol. Bioeng* 60: 24-35.
- Camisard, V., Brienne, J.-P., Baussart, H., Hammann, J., Suhr, H., 2002. Inline Characterization of Cell Concentration and Cell Volume in Agitated Bioreactors Using In-Situ Microscopy: Application to Volume Variation Induced by Osmotic Stress. *Biotechnol. Bioeng.*, Vol. 78, No. 1.
- Frerichs, J.-G., 2000. Entwicklung eines In-situ Mikroskops zur bildgestützten On-line Überwachung von Bioprozessen., Ph. D. Thesis, University of Hannover.
- Joeris, K., Frerichs J.-G., Konstantinov, K., Scheper, T., 2002. In-situ microscopy: Online process monitoring of mammalian cell cultures. *Cytotechnology* 38: 129-134.
- Suhr, H., Wehnert, G., Schneider, K., Bittner, C., Scholz, T., Geißler, P., Jähne, B., Scheper, T., 1995. In-situ Microscopy for On-line Characterization of Cell Populations in Bioreactors, Including Cell Concentration Measurements by Depth from Focus. *Biotechnol. Bioeng.* 47, 106.

ARNE BURZLAFF, CORNELIA KASPER, THOMAS SCHEPER

## ONLINE ANALYSIS OF MICROCARRIER CULTIVATIONS

*Institut für Technische Chemie, Callinstr. 3, 30167 Hannover, Germany*

### 1. INTRODUCTION

In biotechnology, animal cell culture is widely used for the production of many biologicals such as vaccines, monoclonal antibodies, or other recombinant products. Microcarriers are being used in high-density cell cultures in several bioprocesses, which can be divided in three categories, a) high-yield production of cells or cell products, b) studies of cells in vitro, c) routine cell culture techniques. The advantage of this technique is that anchorage-dependent cells are growing on the surface of small spheres, so the disadvantages of a standard monolayer culture can be avoided by increasing the surface area with the use of microcarriers.

The cell densities achieved by this process can be 20 times higher per culture volume compared with a monolayer bottle, resulting in a higher yield.

Our aim was to develop an analytical system to monitor a microcarrier cultivation process. Therefore a model cell line (NIH-3T3) was grown on different microcarrier spheres. The most important criterion for the microcarriers was the size and size distribution, as flow cytometry is limited to smaller objects not exceeding 200  $\mu\text{m}$ .

### 2. MATERIAL AND METHODS

Several different microcarriers were used for the usability testing (Cytodex 1 and 3, 130-215  $\mu\text{m}$ , Amersham Pharmacia, Sweden; Glass Microcarriers, 90-150  $\mu\text{m}$  and Plastic Microcarriers 150-210  $\mu\text{m}$ , Cellon SA, Luxembourg; Polystyrene Beads 45.6  $\mu\text{m} \pm 6.5 \mu\text{m}$ , Polyscience, Germany).

The microcarriers were pretreated according to the manufacturers instructions. The inoculation density of the microcarriers was 2 g per liter culture medium with a cell density of  $2.5 \cdot 10^4$  cells per ml. Cultivations were carried out in 500 ml spinner flasks (Techne, England) in RPMI 1640 supplemented with 5 % newborn calf serum. During the first 3 h of cultivation an intermittent stirring was chosen with 2 min stirring at 30 rounds per minute followed by 30 min pause. Samples were drawn every 12 h for analysis of glucose, lactate concentration, phase contrast microscopy, in-situ microscopy and flow cytometry.

The large scale cultivation process was performed in a self-build 5 l steel tank reactor with an adjusted 25 mm port for the in situ microscope. The sampling zone of the microscope is located between an illuminated condenser and an objective with two sapphire windows working as slide and coverslip of a standard light microscope. The inoculation density of microcarriers and cells were identical with the small scale cultivations.

Flow cytometric analysis was done using the MacroSort module of the FACS Vantage SE (BD Biosciences) with a 200 and 400  $\mu\text{m}$  nozzle. All samples (5 ml) were washed once with PBS and fixed in 70 % ethanol for at least 1 h at  $-18\text{ }^{\circ}\text{C}$ . Prior to flow cytometric analysis, the microcarriers were rehydrated in 5 ml PBS and stained with Propidiumiodide (250  $\mu\text{l}$ ; 50  $\mu\text{g/ml}$  PBS).

### 3. RESULTS AND DISCUSSION

In-situ microscopy has proven to be a suitable tool for monitoring the plating efficiency and the cell density for every chosen microcarrier. The pictures obtained during fermentation had a similar quality with the phase contrast pictures (see Fig. 1).

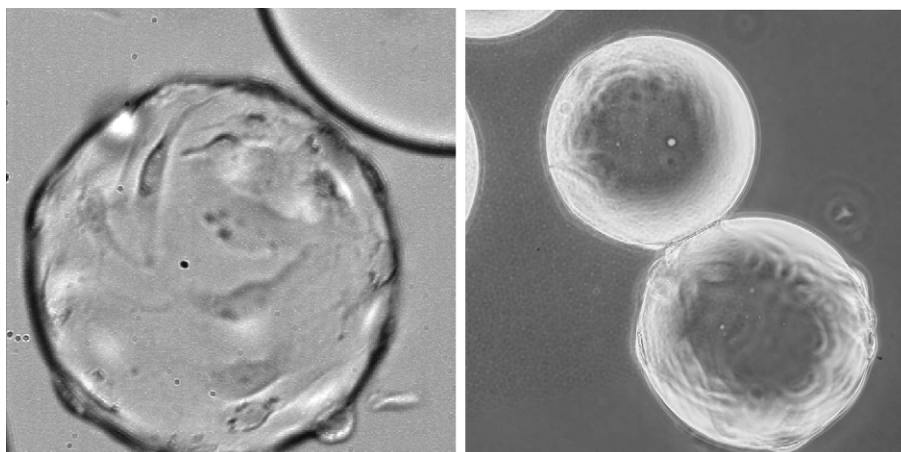


*Figure 1: Cytodex 3 microcarriers 65 h after inoculation with NIH-3T3 cells. Left picture showing an in-situ picture with 400 times magnification; right picture showing a phase contrast picture with 400 times magnification.*

One of the major limitations in flow cytometry analysis of microcarrier cultivations is the limited size range that can be detected. Usually the particles should be two to four times smaller than the nozzle size; all standard microcarriers were analysed using the 400  $\mu\text{m}$  nozzle, the model microcarriers with 45.6  $\mu\text{m}$  diameter were analysed using the 200  $\mu\text{m}$  nozzle. All chosen standard microcarriers caused tube or nozzle blocking. The 45.6  $\mu\text{m}$  polystyrene spheres have shown a good plating

efficiency and due to the small diameter were easily detectable by flow cytometry (see Figure 2).

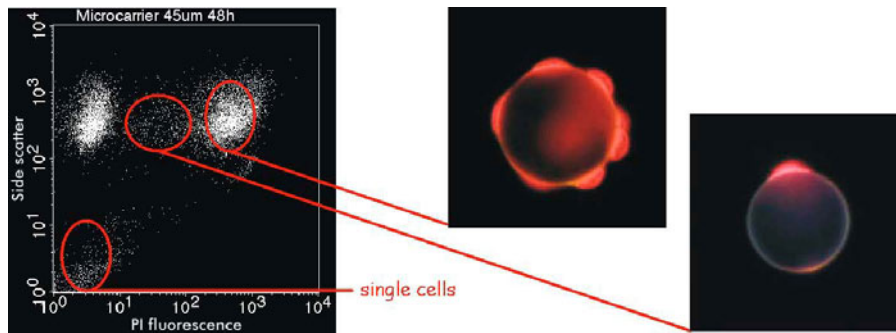


*Figure 2. Flow cytometric analysis of a sample, 48 h after inoculation with NIH-3T3 cells. Side scatter was plotted against fluorescence intensity, showing 4 populations corresponding to single cells, microcarriers with no cells and an increasing amount of cells attached to the surface.*

Flow cytometric analysis has shown a good correlation in judging the plating efficiency with the in-situ microscopy and microscopic analysis. By plotting sideways scattered light against fluorescence intensity four separate populations were distinguishable corresponding to single cells, microcarriers with no cells and an increasing amount of cells attached to the surface.

Both systems, in-situ microscopy and flow cytometry have proven to be a suitable method for gaining informations about cell density and plating efficiency fast and reliable.

CHETAN GOUDAR<sup>1,2</sup>, RICHARD BIENER<sup>3</sup>, JAMES MICHAELS<sup>1</sup>,  
JAMES PIRET<sup>2</sup> AND KONSTANTIN KONSTANTINOV<sup>1</sup>

## ERROR ANALYSIS DURING ESTIMATION OF METABOLIC FLUXES THROUGH METABOLITE BALANCING

<sup>1</sup>*Bayer HealthCare, Biological Products, 800 Dwight Way, Berkeley, CA  
94710 USA* <sup>2</sup>*Biotechnology Laboratory and Department of Chemical &  
Biological Engineering, University of British Columbia, Vancouver, BC  
Canada V6T 1Z3* <sup>3</sup>*Bayer AG Technology Services, Process Analysis,  
51368, Leverkusen, Germany*

**Abstract.** Accurate estimation of fluxes in a bioreaction network is critical as metabolic fluxes are a key determinant of cell physiology and function. The input data for metabolic flux estimation by the metabolite balancing technique includes the growth rate of cells and specific nutrient uptake and metabolite production rates. These rates are computed from experimental measurements of the primary cell, nutrient and metabolite concentrations. As a result, any error in experimental measurements of the primary variables propagates into the rate estimates, which in turn affect the accuracy of the resulting metabolic fluxes. In this study, we present analysis of the error associated with computing metabolic fluxes using a combination of experimental and theoretical approaches. Baby Hamster Kidney (BHK) and Chinese Hamster Ovary (CHO) cells were cultivated in perfusion culture at approximately  $20 \times 10^6$  cells/mL. Samples were periodically drawn from the bioreactors and analyzed for cell, nutrient and metabolite concentrations. The error associated with these primary variables was first determined by performing multiple measurements after which the Gaussian law of error propagation was used to estimate errors associated with specific rates and metabolic fluxes in an established metabolic network. This analysis helped establish relationships between the errors in metabolic fluxes and those in the primary variables allowing a priori prediction of the errors in metabolic fluxes.

### 1. INTRODUCTION

Mammalian cells are being increasingly used for the production of complex therapeutic proteins as they have the ability to correctly fold and glycosylate these proteins. To achieve optimal protein productivities in mammalian cell cultures, it is desirable to have a good understanding of the physiological state of the cells. Metabolic flux analysis (Stephanopoulos et al., 1998) offers a convenient framework for quantifying cellular metabolism by providing carbon flux estimates in a defined biochemical network. These fluxes are estimated either by performing a mass balance on the nutrients and metabolites (Metabolite balancing approach) or through the use of labeled carbon substrates followed by subsequent NMR or GC-MS analysis (Isotope labeling approach).

As metabolic fluxes provide valuable quantitative information on the physiological state of cells, it is important to adequately characterize the uncertainty

associated with their estimation. Metabolic flux estimation requires specific rate data which in turn are computed from primary variables such as cell, nutrient, metabolite and product concentrations. Hence errors in measurements of the primary variables will propagate into the flux estimates and it is important to quantify the nature and extent of the influence of primary variable errors on those in metabolic fluxes. Several approaches for characterizing errors in biochemical reaction networks have been proposed (Noorman et al., 1996; van der Heijden et al., 1994a; van der Heijden et al., 1994b; Wang and Stephanopoulos, 1983) and we apply some of these concepts to characterize the error properties of a biochemical reaction network for mammalian cells

## 2. THEORY

A general method for calculating error propagation is through computation of the total differential. For the function  $y=f(x_1, x_2, \dots, x_n)$  with  $n$  independent variables  $x_1, \dots, x_n$  the total differential is

$$d(y) = \frac{\partial f}{\partial(x_1)} dx_1 + \frac{\partial f}{\partial(x_2)} dx_2 + \dots + \frac{\partial f}{\partial(x_n)} dx_n = \sum_i \frac{\partial f}{\partial(x_i)} dx_i \quad (1)$$

The standard deviation can be calculated from

$$\Delta y^2 = \sum_i \left( \frac{\partial f}{\partial(x_i)} \right)^2 \Delta x_i^2 \quad (2)$$

If we introduce the relative error of  $x_i$  with respect to the expected value  $\bar{x}_i$

$$r_{x_i} = \frac{\Delta x_i}{\bar{x}_i} \quad (3)$$

the relative error can be derived from

$$(r_y \cdot \bar{y})^2 = \sum_i \left( \frac{\partial f}{\partial(x_i)} \right)^2 (r_{x_i} \cdot \bar{x}_i)^2 \quad (4)$$

## 3. RESULTS

The error associated with measurement of primary variables was determined by performing multiple measurements after the cell culture reached steady state. The errors associated with primary variable measurements are presented in Figure 1

while those for specific rate estimation are shown in Figure 2. The harvest cell density measurements were characterized by the highest relative error (~30%) and this is primarily because of the low cell density ( $\sim 0.1 \times 10^6$  cells/mL) in the harvest stream. Amino acid measurements were characterized by average relative errors on the order of 20% while relative errors in the other primary variables were less than 10%. These specific rates were subsequently used for metabolic flux estimation and the standard deviations associated with the calculated fluxes are shown in Figure 3.

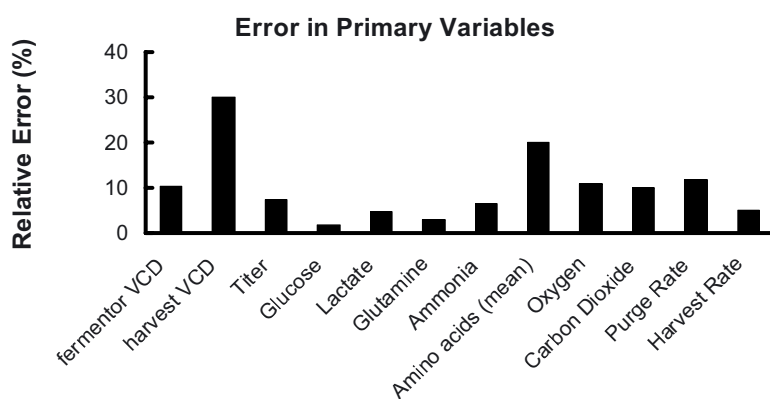


Figure 1. Relative errors in the primary variables used for specific rate estimation

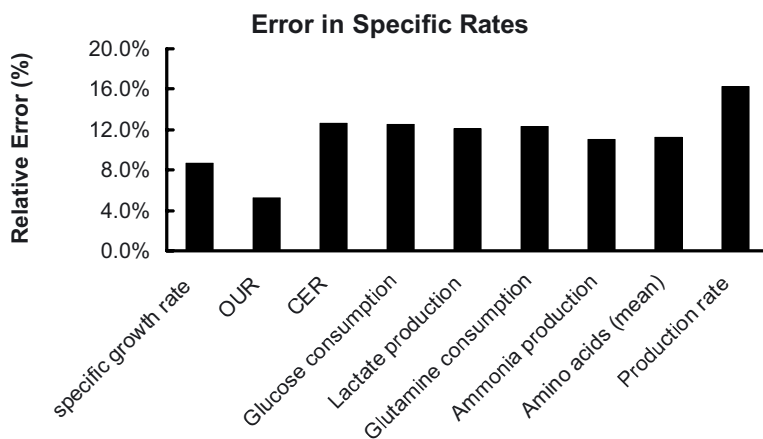


Figure 2. Relative errors in specific rates computed from the primary variables in Figure 1

	Reaction	metabolic flux (pM/cell/d)	standard deviation (pM/cell/d)		Reaction	metabolic flux (pM/cell/d)	standard deviation (pM/cell/d)
1	Glc → Glc6P	1.31110	0.16478	14	Glu → αKG + NH <sub>4</sub> <sup>+</sup>	0.46350	0.23649
2	Glc6P → 2 GAP	1.30830	0.13663	15	GAP + Glu → αKG + Ser	0.00090	0.02698
3	GAP → Pyr	2.51110	0.25527	16	GAP + Glu → αKG + Gly	0.10310	0.02676
4	Pyr → Lac	2.10300	0.23786	17	Lys → 2 AcCoA + 2 CO <sub>2</sub>	-0.05600	0.03691
5	Glc6P → Rib5P + CO <sub>2</sub>	0.00120	0.04162	18	Ile → AcCoA + SuCoA	0.12120	0.05661
6	Pyr → AcCoA + CO <sub>2</sub>	1.28990	0.36299	19	Leu → 3 AcCoA	0.09660	0.05665
7	Pyr + Glu → Ala + αKG	0.10860	0.00866	20	Glu → Pro	-0.01770	0.02349
8	AcCoA + OAA → αKG + CO <sub>2</sub>	1.56120	0.09744	21	Thr → SuCoA	0.11670	0.01208
9	αKG → SuCoA + CO <sub>2</sub>	2.01500	0.13480	22	Val → SuCoA + CO <sub>2</sub>	0.07470	0.03707
10	SuCoA → Fum	2.32760	0.12934	23	OAA + Gln → Asn + αKG	-0.18210	0.04925
11	Fum → OAA	2.32760	0.15589	24	OAA + Glu → Asp + αKG	-0.04260	0.04919
12	OAA → Pyr + CO <sub>2</sub>	0.99040	0.31180	25	3 ADP + NADH + 0.5 O <sub>2</sub> → 3 ATP + NAD <sup>+</sup>	8.96780	0.45038
13	Gln → Glu + NH <sub>4</sub> <sup>+</sup>	0.75640	0.07434	26	2 ADP + FADH <sub>2</sub> + 0.5 O <sub>2</sub> → 2 ATP + FAD	2.56400	0.23422

Figure 3. Errors in metabolic fluxes computed from the specific rates in Figure 2

#### 4. CONCLUSIONS

We have characterized the propagation of errors from the primary variables in a perfusion system into specific rates and subsequently into the estimated metabolic fluxes. Given the fundamental role that metabolic fluxes play in the description of cellular physiology, characterization of the uncertainty associated with the computed metabolic fluxes is critical. The approach presented in this study enables such a characterization and allows for robust characterization of cellular physiology from metabolic flux data.

#### 5. REFERENCES

- Noorman, H.J.; Romein, B.; Ch, K.; Luyben, A.M.; Heijnen, J.J. Classification, error detection, and reconciliation of process information in complex biochemical systems. *Biotechnol. Bioeng.* **1996**, *49*, 364-376.
- Stephanopoulos, G.; Aristidou, A.; Nielsen, J. *Metabolic Engineering. Principles and Methodologies*; Academic Press: San Diego, **1998**.
- van der Heijden, R.T.J.M.; Romein, B.; Heijnen, S.; Hellinga, C.; Luyben, K.C.A.M. Linear constraint relations in biochemical reaction systems: I. Classification of the calculability and the balanceability of conversion rates. *Biotechnol. Bioeng.* **1994a**, *43*, 3-10.
- van der Heijden, R.T.J.M.; Romein, B.; Heijnen, S.; Hellinga, C.; Luyben, K.C.A.M. Linear constraint relations in biochemical reaction systems: II. Diagnosis and estimation gross errors. *Biotechnol. Bioeng.* **1994b**, *43*, 11-20.
- Wang, N.S.; Stephanopoulos, G. Application of macroscopic balances to the identification of gross measurement errors. *Biotechnol. Bioeng.* **1983**, *25*, 2177-2208.



CHETAN GOUDAR<sup>1,2</sup>, RÜDIGER HEIDEMANN<sup>1</sup>, KLAUS  
JOERIS<sup>1</sup>, JAMES MICHAELS<sup>1</sup>, JAMES PIRET<sup>2</sup> AND  
KONSTANTIN KONSTANTINOV<sup>1</sup>

## GENERALIZED LOGISTIC EQUATION MODELING OF MAMMALIAN CELL BATCH CULTURES

<sup>1</sup>*Bayer HealthCare, 800 Dwight Way, Berkeley, CA 94710* <sup>2</sup>*Biotechnology  
Laboratory and Department of Chemical & Biological Engineering,  
University of British Columbia, Vancouver, BC Canada V6T 1Z3*

**Abstract.** We present a method for analyzing experimental data from mammalian cell batch bioreactors through functional approximation. Specifically, a 4-parameter generalized logistic equation (GLE) described time profiles of viable cell density while two reduced forms of the GLE with 3 parameters described nutrient uptake and metabolite/product formation. Experimental data were accurately described by the GLE and its reduced forms, suggesting the validity of this approach. These equations were analytically differentiable thereby allowing rapid estimation of specific rates, often variables of interest in a batch culture. From a computational standpoint, the approach presented in this study is significantly simpler in comparison to classical kinetic formulations involving Monod type kinetics. Overall, the simplicity of the approach presented coupled with its ability to accurately describe batch experimental data should make it an attractive option for modeling mammalian cells in batch culture.

### 1. INTRODUCTION

The conventional approach to model mammalian cells in batch cultures has been through the use of unstructured kinetic models that are variations on the classical Monod equation (Bree et al., 1988; Dhir et al., 2000). Simple Monod-type equations with one limiting substrate are easy to work with (Heidemann et al., 1998) while models involving multiple substrates are computationally difficult to implement as they involve nonlinear estimation of a large number of kinetic parameters from a system of nonlinear differential equations. A general approach that does not rely on the use of kinetic models and is applicable over the entire time course of the experiment is to fit polynomials to experimental data (Linz et al., 1997). However, as time profiles of cell, nutrient and product concentration exhibit exponential behavior, they are difficult to describe by polynomial functions (Stephanopoulos et al., 1998).

In the present study, we recognize the advantage of using a general functional representation of batch experimental data and present the application of a generalized logistic equation for modeling mammalian cells in batch cultures. A single equation was adequate to accurately describe time profiles of all experimentally measured variables and as this function was analytically differentiable, it allowed for rapid estimation of specific rates.

## 2. THEORY

### 2.1. Generalized Logistic Equation

It is desirable to have an analytically differentiable function that can describe experimental data accurately. Subsequent computation of the derivatives is trivial because they can be readily obtained from the differentiated form of the original function. Several functions were evaluated for this purpose and the following four parameter generalization of the logistic equation (Jolicoeur and Pontier, 1989) was found to provide the best description of experimental data

$$X = \frac{1}{C_1 \exp\left(\frac{t}{D_1}\right) + C_2 \exp\left(-\frac{t}{D_2}\right)} \quad (1)$$

where  $X$  is the independent variable and could be any of the state variables measured in the bioreactor including cell density, nutrient, metabolite or product concentration. The  $t$  is time and  $C_1$ ,  $D_1$ ,  $C_2$ ,  $D_2$  are model parameters, all non-negative.

## 3. RESULTS AND DISCUSSION

### 3.1. Description of Experimental Data

The time profiles of viable cell density for two experiments with CHO cells are shown in Figure 1. Experimental data were accurately described by the GLE. Specific growth rates were calculated from the time derivatives and these are also presented in Figure 1. Time profiles of glucose, lactate, glutamine and ammonia are shown in Figure 2 along with GLE equation fitted curves. The specific uptake rates for glucose and glutamine and specific production rates for lactate and ammonia were subsequently computed from the time derivatives.

### 3.2. Comparison with Existing Kinetic Approaches

The GLE and its reduced forms presented in this study allow for accurate functional representation of experimental data from mammalian cells in batch culture. As these functions can be readily differentiated and integrated, they allow for rapid estimation of specific rates and other related metabolic parameters that can be used to characterize the physiology of the system. While this approach is conceptually similar to polynomial approximation of experimental data, it is superior because the

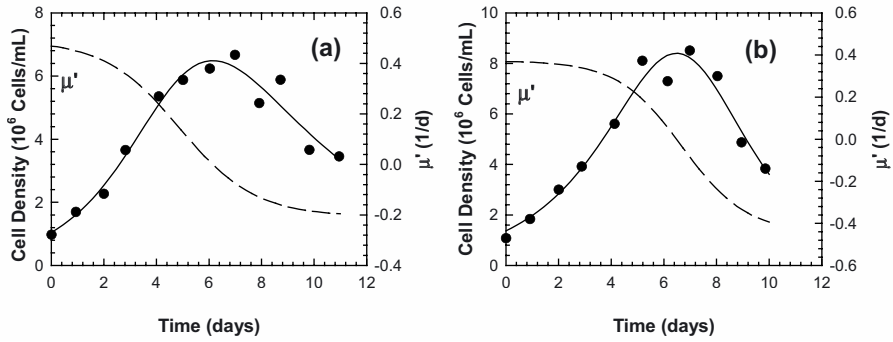


Figure 1. Viable cell density in two batch experiments with CHO cells. The points are experimental data while solid lines are fits to the GLE. The calculated specific growth rates are shown as dashed lines

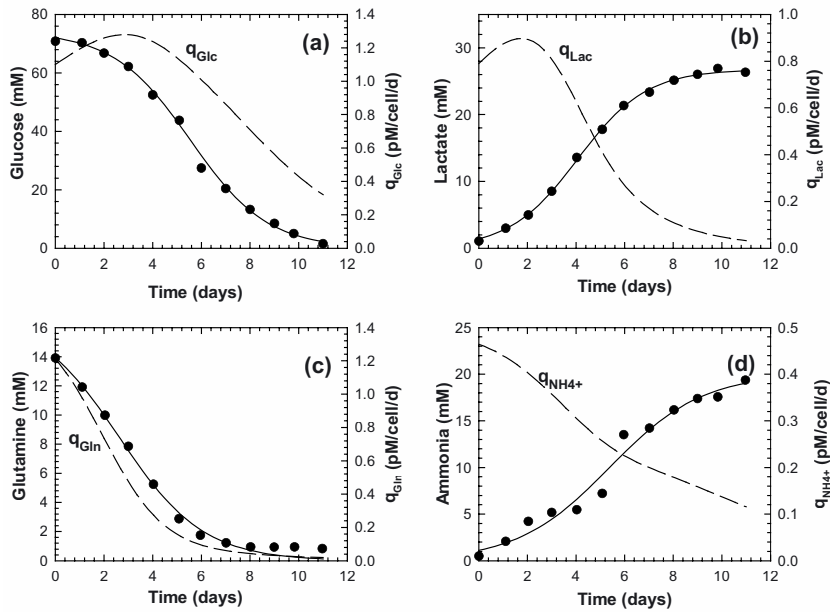


Figure 2. Time profiles of glucose, lactate, glutamine and ammonia in a batch culture with CHO cells. The points are experimental data while solid lines are fits to the GLE. The calculated specific uptake/production rates are shown as dashed lines

exponential nature of the time profiles of the state variables are difficult to describe by polynomial functions (Stephanopoulos et al., 1998). In the polynomial fitting approach different functional forms may be required for each of the state variables. Another advantage of the formulation presented in this study is that a single function can be used to describe all the major state variables (cell density, nutrient, metabolite and product concentrations) in a batch system.

#### 4. CONCLUSIONS

We have illustrated application of the functional approximation approach to analyze data from mammalian cells in batch culture through the use of a generalized logistic equation and its reduced forms. Time profiles of cell density, nutrients and metabolites were accurately described by the logistic equation and time derivatives of these variables were readily computed resulting in rapid and accurate estimation of specific rates. The general nature of this approach, coupled with the ability to rapidly obtain accurate estimates of specific rates should make it an attractive alternative for describing the dynamics of mammalian cell growth and protein production in batch culture. It can also serve as an important tool for designing optimal feeding strategies for mammalian cells in fed-batch culture

#### 5. REFERENCES

- Bree, M.A.; Dhurjati, P.; Geoghegan, R.F.; Robnett, B. Kinetic modeling of hybridoma cell growth and immunoglobulin production in a large-scale suspension culture. *Biotechnol. Bioeng.* **1988**, *32*, 1067-1072.
- Dhir, S.; Morrow, K.J.; Rhinehart, R.; Wiesner, T. Dynamic optimization of hybridoma growth in a fed-batch bioreactor. *Biotechnol. Bioeng.* **2000**, *67*, 197-205.
- Heidemann, R.; Lütkemeyer, D.; Büntemeyer, H.; Lehmann, J. Effects of dissolved oxygen levels and the role of extra- and intracellular amino acid concentrations upon the metabolism of mammalian cell lines during batch and continuous cultures. *Cytotechnology* **1998**, *26*, 185-197.
- Jolicoeur, P.; Pontier, J. Population growth and decline: A four-parameter generalization of the logistic curve. *J. Theor. Biol.* **1989**, *141*, 563-571.
- Linz, M.; Zeng, A.P.; Wagner, R.; Deckwer, W.D. Stoichiometry, kinetics and regulation of glucose and amino acid metabolism of a recombinant BHK cell line in batch and continuous culture. *Biotechnol. Prog.* **1997**, *13*, 453-463.
- Stephanopoulos, G.; Aristodou, A.; Nielsen, J. *Metabolic Engineering. Principles and Methodologies*; Academic Press: San Diego, 1998.

KLAUS JOERIS (2), JAN-GERD FRERICHS (1,3), THOMAS SCHEPER (1) AND KONSTANTIN KONSTANTINOV (2)

## IN-SITU MICROSCOPY BASED MONITORING OF MAMMALIAN CELL CULTURE PROCESSES

(1) *University of Hannover, Germany*

(2) *Bayer Corporation, Berkeley, CA, USA*

(3) *TEXYS GmbH, Germany*

### 1. THEORY

The in-situ microscope (ISM) is a utility developed to acquire images of mammalian cells, directly inside a bioreactor (in-situ) during a fermentation and is suited for either batch or long-term perfusion fermentation runs. The system fits into a 25mm standard port, features a retractable housing and can be serviced without interruption of the process. A sampling zone inside the bioreactor encloses a defined volume of culture and an image sequence is taken. The height of the sampling zone is set by the control program and can be adjusted during the cultivation to accommodate a wide range of change in cell density. Process relevant information like cell density is extracted from the images by digital image processing routines, currently under development for CHO and BHK cells. A detailed description of the system can be found in [1]. The following results show the averages of 20 images for each ISM measurement point. The Cedex results were also derived from series of 20 images.

### 2. RESULTS AND DISCUSSION

#### 2.1. BHK Perfusion Culture

BHK cells were cultivated in perfusion mode in a protein-free medium formulation. Experiments were conducted in a 15L bioreactor (Applikon, 12L working volume). The temperature was maintained at 35.5 °C and the agitation was kept constant at 70 rpm. Dissolved oxygen (DO) concentration was maintained at 50% air saturation by silicone cage aeration. Bioreactor pH was maintained at 6.8.

The cell accumulation phase and two days of the steady state are shown in figure 1. The focal setting of the microscope was changed on day two to facilitate the image processing. ISM 1 shows results obtained with an image processing routine developed in Optimas 6.1 (Media Cybernetics, Silver Springs, MD, USA). The routine used a local smoothing operation followed by segmentation based on a

threshold set for minimum variance of dark object gray values. Cells were detected as points with predefined diameter. ISM 2 shows the results of a slightly modified routine that gave better results at low cell densities.

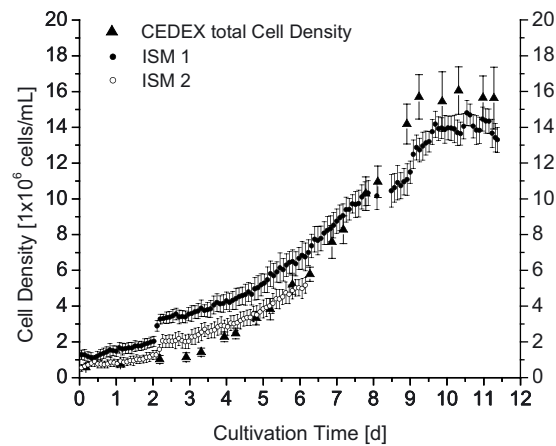


Figure 1. BHK Perfusion Culture.

## 2.2. CHO Batch and Fed-Batch Cultures

CHO cells were cultivated in batch (figure 2) or fed-batch mode (figure 3) in a protein-free medium formulation. Experiments were conducted in 15L bioreactors (10L working volume). The temperature was maintained at 36.5 °C and the agitation was kept constant at 40 rpm. Dissolved oxygen (DO) concentration was maintained at 50% air saturation by sparging a mixture of oxygen and nitrogen into the bioreactor. Bioreactor pH was maintained at 6.8 by the addition of either CO<sub>2</sub> or 0.3M NaOH.

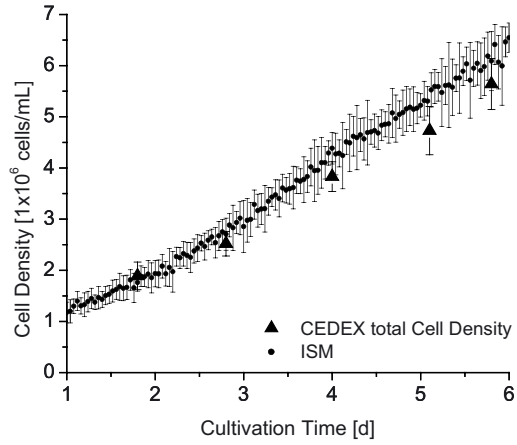


Figure 2. CHO Batch Culture.

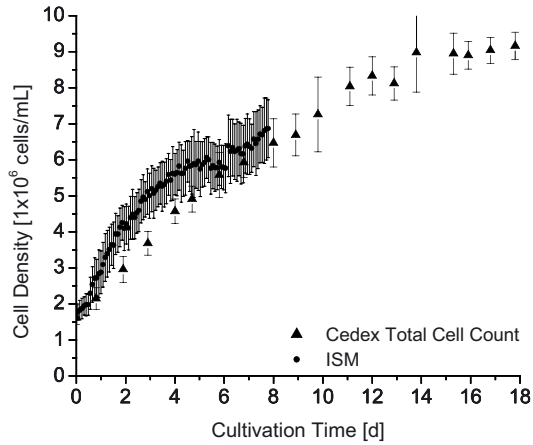


Figure 3. CHO Fed-Batch Culture.

The images were analyzed using the algorithm described in [2]. The algorithm was slightly modified for the fed-batch application. Only the first 8 days of this fed-batch are shown in figure 3, since the reprocessing of the images has not been completed yet.

### 3. SUMMARY

The in-situ microscope was successfully tested in CHO batch/fed-batch and BHK perfusion cultures. The results correlate well with the cell counts obtained by the Cedex system. It showed good stability and proved to be useful as an industrial application.

### 4. REFERENCES

- Joeris K, Frerichs JG, Scheper T, Konstantinov K, (2002), *Cytotechnology* 38:129-134  
Frerichs JG, (2000), Ph.D. Thesis, University of Hannover



MARTIN JORDAN

## A NOVEL DISPOSABLE MICROTUBE FOR RAPID ASSESSMENT OF BIOMASS IN CELL CULTURES

*Swiss Federal Institute of Technology Lausanne, Faculty of Basic Sciences,  
Institute of Biological and Chemical Process Sciences*

### 1. INTRODUCTION

Accurate and reproducible values of cell number form the basis of all experimental work with mammalian cells. I am presenting a prototype of a microtube system for the assessment of cell mass based on packed cell volume (PCV). Glass PCV tubes are currently being used, but they require large sample volumes (5-10 ml) and are dependent on swinging bucket rotors for centrifugation. The microtubes presented here were manufactured by Techno Plastic Products AG in Trasadingen, Switzerland and have been designed according to the following criteria:

- 1.) all cells settle into the calibrated capillary during centrifugation (up to 10'000g).
- 2.) the tubes are compatible with common fixed angle and swinging bucket rotors.
- 3.) up to 1 ml of sample fits into the tube.

### 2. RESULTS

The prototype of the PCV microtube is depicted in Fig. 1. Manufacturing of the final version is in progress and will have a distinct marking for direct reading of total cell volume in  $\mu\text{l}$ . Prototype tubes were rigorously tested using a centrifuge with a swinging bucket rotor for 1.5/2 ml tubes (Eppendorf 5417C, A-8-11 rotor). After a brief centrifugation, all cells were found within the defined capillary. The height of the cell pellet, visible to the naked eye, defines the volume that is occupied by the cells (Fig. 1). This volume is transformed into PCV (%) using the formula:

$$PCV (\%) = (\text{volume of cell pellet} / \text{volume of sample}) \times 100$$

After centrifugation the column of packed cells within the capillary still contains a given fraction of medium (filling the space between the cells). This fraction depends on the time and speed of centrifugation. Both parameters were studied separately and eventually defined to get reproducible results. Initially, 300  $\mu\text{l}$  of CHO-DG44 suspension cells (at a cell density of  $4.2 \times 10^6$  cells/ml and a viability of 98%) were pipetted into microtubes and centrifuged at different speeds (850 g = 3000 rpm, 9500 g = 10'000 rpm) (Fig. 2, left panel). The experiment was done in duplicate (series A and B), and each point represents the average of two PCV microtubes.

Even though the cells were pelleted within 30 seconds a 1 minute centrifugation period was chosen as the standard time. For this centrifugation period there was a strong effect on the PCV up to a speed of 2000 g (Fig. 2, left panel). Beyond 2000 g the volume of the pellet was further decreased, but to a lesser extent. Based on these results a speed of 2380 g (5000 rpm) was chosen as the standard for all further experiments.



**Figure 1.** Prototype PCV microtube. The depicted tube is manufactured from transparent polystyrene. The capillary has a volume of 5  $\mu$ l. A graduated scale for easily reading the PCV will be printed onto the tubes. Left: 2 samples in duplicate. Right: A sample with 3.6  $\mu$ l of packed cells corresponding to 1.6 million CHO cells.

Next, the effect of centrifugation time was studied for speeds of 5000 rpm and 10000 rpm (Fig. 2, right panel). Centrifugation for 30 seconds at 5000 rpm was not sufficient to achieve a compact pellet, but pellet size did not vary for centrifugation times between 1 and 10 minutes. At 10000 rpm the pellet became more compact with longer periods of centrifugation.

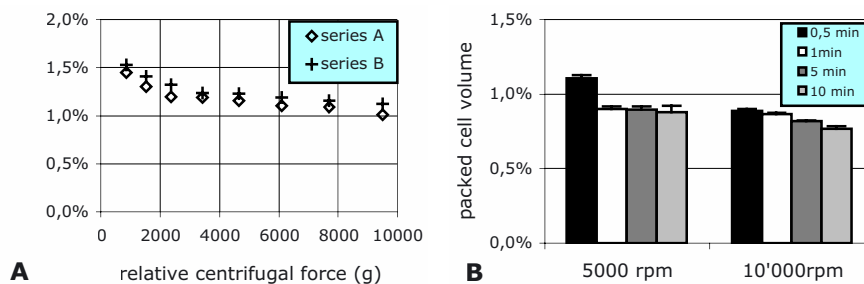


**Figure 2.** The packed cell volume of cells as a function of speed and centrifugation time. A) Effect of centrifugation speed. Per tube 300  $\mu$ l of CHO cells at  $4.2 \times 10^6$  cells per ml were added. B) Effect of centrifugation time. Per tube 400  $\mu$ l of CHO cells at  $3.2 \times 10^6$  cells per ml were added ( $n=4$ ).

The PCV can be calibrated as cell number per ml, making it a powerful method for quantitating cells. In order to demonstrate the reliability of the PCV method two different cell lines (NS0 and CHO) were used in a comparative study. Serial dilutions of the cells were carefully prepared and analysed by the trypan blue method, an automated counting method (Casy, Schärfe Systems), and PCV microtubes. All three methods correlated linearly with the dilutions (Fig. 3). Since the PCV was calibrated against the manual cell counts, the slope of these curves was identical. The Casy counts were close to the manual counts for the NS0 cells, a culture in which no aggregate formation occurred. For the CHO cells grown in serum-free medium we routinely saw small aggregates of about 10 cells at densities above 1 million cells per ml. This caused a systematic underestimation of the cell number when cells were counted with the Casy.

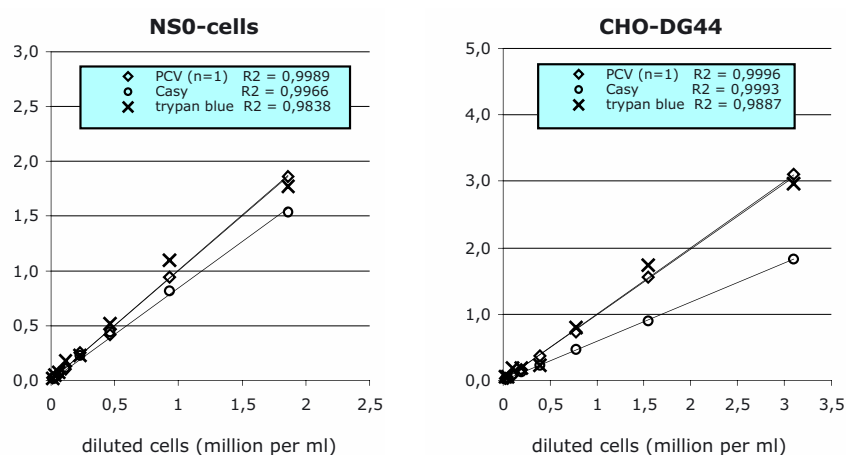


**Figure 3.** Quantitation of cell number by PCV in comparison with two established counting methods. NS0 cells and CHO cells were serially diluted and counted in parallel by PCV, Casy and trypan blue methods.

### 3. CONCLUSION

The disposable PCV microtubes represent a rapid and accurate approach for measuring the packed cell volume using only a small volume of sample. A centrifugation step of 1 minute at more than 2000g is sufficient to pellet the cells. The method covers a wide dynamic range starting at a detection minimum that is below 100'000 cells per ml. Since the capillary holds about 2 million cells and the loading volume is 1 ml or less, there is no upper detection limit. No dilution or further manipulation of the samples is needed in order to rapidly obtain a result that represents an absolute value. PCV can be calibrated against any desired value such

as cell number, protein content or metabolic activity. With these features the assay is one of the simplest and most rapid for obtaining precise information about a cell culture.

A. MARC, V. DEPARIS, A. JESTIN AND J.-L. GOERGEN

## INTRACELLULAR MONITORING OF BACULOVIRUS INFECTION OF SF9 INSECT CELLS AND R-PROTEIN PRODUCTION USING ANTI-ALPHA-1,3/4 FUCOSYLTRANSFERASE ANTIBODIES AND FLOW CYTOMETRY

*Laboratoire des Sciences du Génie Chimique, CNRS-ENSAIA, BP172,  
F- 54505 Vandoeuvre-lès-Nancy Cedex*

### 1. INTRODUCTION

Baculovirus/insect cells expression system is widely used for the production of active recombinant proteins. Several methods have been proposed to assess more accurately the progress of baculovirus infection and to have a better control of processes involving this expression system. However, these methods, on-line or off-line, such as the measurement of the oxygen uptake, the relative permittivity of the viable biomass, the cell density or viability by trypan blue might be subject to important errors or provide only an average value for the whole cell population <sup>1</sup>. Alternatively, flow cytometry has emerged in the past years as a potential tool to monitor baculovirus infection since this technique is able to give statistically valuable information about individual cells in a heterogeneous population <sup>2</sup>.

The aim of this study was to set up a flow cytometric method to monitor the infection of Sf9 insect cells by a recombinant baculovirus and to test more precisely by flow cytometry the extent of infection of insect cells by a baculovirus expressing the human  $\alpha$  1,3/4 fucosyltransferase (Fuc-TIII) in batch process.

### 2. DEVELOPMENT AND OPTIMIZATION OF THE IMMUNO FLUORESCENT LABELING PROTOCOL

In order to detect the fluorescent labelling by flow cytometry in combination with RALS properties, cells producing the recombinant Fuc-TIII were permeated and treated with rabbit anti Fuc-TIII and anti rabbit FITC sera (figure 1A). The specificity of the antibodies were verified by flow cytometry: the specificity of anti-Fuc TIII antibody (figure 1B, left) is shown by fluorescence histograms of non infected cells (1) labelled with the 1<sup>st</sup> and the 2<sup>nd</sup> Abs, (2) with the 2<sup>nd</sup> Ab only, (3) cells (48 hpi) or labelled with both Abs. The specificity of FITC-conjugated anti rabbit IgG was verified in a similar manner (figure 1B, right): fluorescence

histograms revealed infected cells (48 hpi) labelled with (1) no antibody, (2) the FITC-labelled antibody only, (3) or both antibodies.

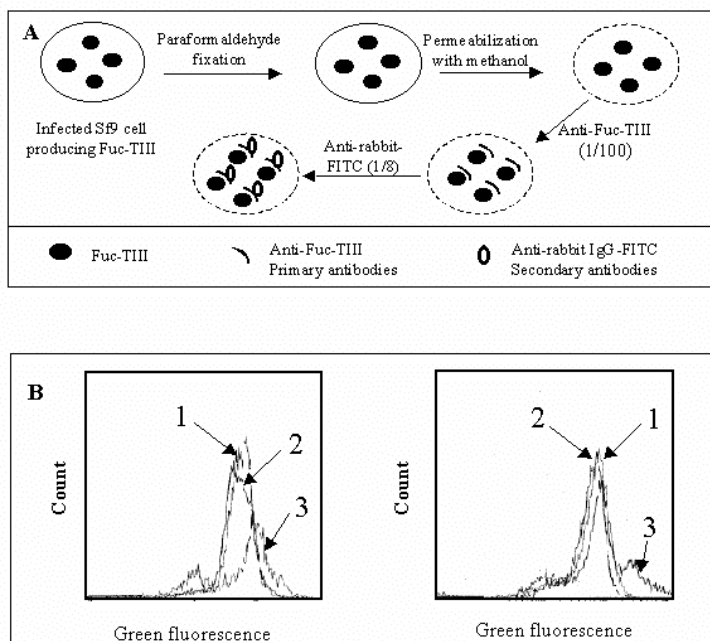


Figure 1: Staining procedure and antibody specificity as shown by flow cytometry

### 3. MONITORING OF BACULOVIRUS INFECTED SF9 CELLS GROWN IN SUSPENSION BATCH CULTURES

Suspension cultures of Sf9 cells were infected (figure 2) in the early exponential growth phase ( $5 \cdot 10^5$  cells. $\text{ml}^{-1}$ , left column) with a MOI of 0.1 pfu.cell $^{-1}$  (white symbols) or 10 pfu.cell $^{-1}$  (black symbols), or near the end of the growth phase ( $24 \cdot 10^5$  cells. $\text{ml}^{-1}$ , right column) with a MOI of 0.05 pfu.cell $^{-1}$  (white symbols) or 2 pfu.cell $^{-1}$  (black symbols). In these experiments, the vertical line represented the time of infection.

## 4. CONCLUSIONS

Using side-scattered light coupled to green fluorescence detection after immunolabeling of the recombinant protein, the method allowed monitoring of baculovirus infection of Sf9 batch cultures infected with different MOI and TOI. The technique was capable to precisely assess the extent of infection of the insect cells from 60 hours post infection. In asynchronously infected SF9 cell cultures, the two-step infection process (primary and secondary infection) was well characterised using this technique.

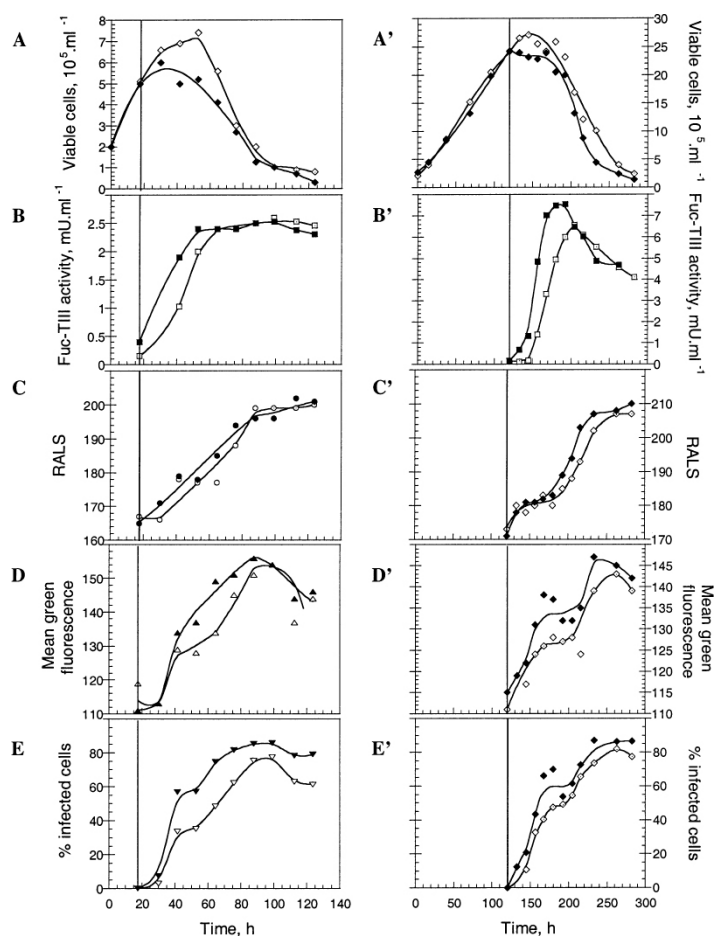


Figure 2: Baculovirus infection of Sf9 cells grown in batch culture

This technique is especially useful for the development of perfusion cultures, where infection with high MOI can be difficult because of the high cell densities and consequently the large quantities of virus required. In such processes, monitoring infection by flow cytometry as described in our study could help to choose a MOI in order to get an efficient infection of all cells in the culture.

## 5. REFERENCES

<sup>1</sup> Monica et al. 2000, *Biotechnol Prog.*, 16: 866-871.

<sup>2</sup> Deparis et al. 2003, *Biotechnol Prog.*, 19: 624-630.



H. MATSUOKA & T. TAKEDA

EFFECT OF GLUCOSE AND GLUTAMINE CONCENTRATION  
ON METABOLISM OF ANIMAL CELLS IN CHEMOSTAT  
CULTURE

*Teiko University of Science & Technology, Yamanashi, Japan*

1. INTRODUCTION

Glutamine is an essential amino acid that provides a major energy source in mammalian cells. It plays the role of both carbon and nitrogen sources. The concentration of glutamine strongly influences the cell metabolism that governs cell growth and monoclonal antibody productivity. Many experiments have been carried out in order to comprehend glutamine concentration on the cell metabolism, however the relationship remains somewhat unclear (Vriezen, N. and J. P. Dijken (1998), Matsuoka et al. (2001)). Recently, the technique for estimating intracellular metabolic fluxes from extracellular utilization and production rates has been developed. In this study a chemostat culture was carried out under a wide range of glutamine feed concentrations and intracellular metabolism was studied by using metabolic engineering technique.

2. MATERIALS AND METHODS

In this study chemostat culture under non-serum media was carried out in the wide range of glutamine feed concentration and change of the metabolism by using metabolic engineering technique was examined. A mouse-mouse hybridoma 4-8H was used. 4-8H was cultured in a 1 L fermentor with a 400 mL working volume at  $37 \pm 0.1$  °C. pH and DO were maintained at 7.2 and 40 % of air saturation by CO<sub>2</sub> and O<sub>2</sub> influx in the headspace, respectively. Agitation speed was 70 rpm. A fresh medium, which was composed on the basis of RPMI1640: DMEM: F12 = 2:1:1, adding 1 g/L insulin, 0.55 g/L, transferrin, 0.2 g/L ethanolamine, 0.67 g/L selenium and 1 % Penicillin-Streptomycin-Neomycin antibiotics mixture, was continuously supplied as dilution rate was 0.45 d<sup>-1</sup>. Concentrations of glucose, glutamine, glutamate, lactate, and ammonia were measured by YSI biochemical analyzer or enzymatically measuring kits. Other amino acids concentrations were determined by HPLC.

Intracellular fluxes were estimated by using the modified metabolic engineering method on the basis of Europa et al. (2000). When the stoichiometric matrix of mass balance,  $A$ , was constructed, the metabolic flux vector,  $x$ , is,

$$x = (A^T \Psi^{-1} A)^{-1} A^T \Psi^{-1} r$$

where  $r$  and  $\Psi$  is the specific rate vector and the correlation matrix, respectively. Amino acids composition was used reference data (Akimoto et al. (1997)).

## 3. RESULTS AND DISCUSSION

Experimental data was collected under five kinds of steady state conditions (*Table 1*); low glucose and low glutamine concentration (a-c), and high glucose and high glutamine concentration (d,e). In a-c, glutamine is a limiting factor because feed glutamine was completely consumed in the fermentor. In c-e, the limitation of glucose consumption is negligible.

*Table 1* Glucose and glutamine concentration of inlet and outlet to fermentor

		a	b	c	d	e
Glucose [mM]	in	7.3	7.4	7.2	26.5	25.8
	out	4.6	3.1	1.7	20.4	19.6
Glutamine [mM]	in	0.36	0.64	1.29	2.09	4.13
	out	0	0	0	0.54	1.61

*Figure 1* shows that glutamine consumption rate is strongly influenced on glutamine concentration. However glucose consumption rate is not so influenced in low glutamine concentration. *Figure 2* shows as follows,

1. Fluxes of amino acids except that of glutamine to glutamate are 10-times lower than those related to glycolysis (a-e).
2. 23-28 % of consumed glucose is utilized as a carbon source for proliferating cells (a-e).
3. The TCA cycle works well in very low glutamine concentration (a), as well as in both sufficient glucose and glutamine feeding (d,e).

*Figure 3* shows that the flux of pyruvate utilization to the TCA cycle is large in very low glutamine concentration (a), as well as in high glutamine concentration (d,e). *Figure 4* shows that the flux of catabolization of amino acids becomes larger, according to decrease of glutamine concentration (a-c). However the utilization rate of amino acids for biomass and IgG production does not influenced on glutamine concentration (a-e). The flux from glutamate to  $\alpha$ -ketoglutarate is less than half of the flux that glutamate enters the TCA cycle due to the action of transaminase in low glutamine concentration (a-c). However they are comparable in high glutamine concentration (d,e). It is suggested that the region of effective glutamine utilization to the TCA cycle exists in low glucose and low glutamine concentration range. In this region both catabolization rate of amino acids and glucose utilization rate to the TCA cycle are much larger.

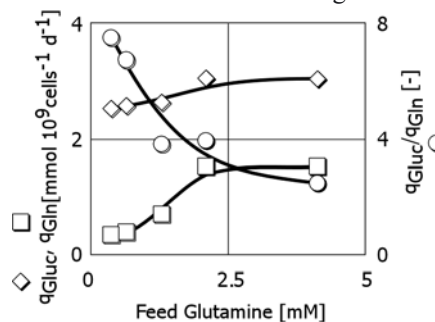


*Figure 1.* Specific glucose and glutamine consumption rates

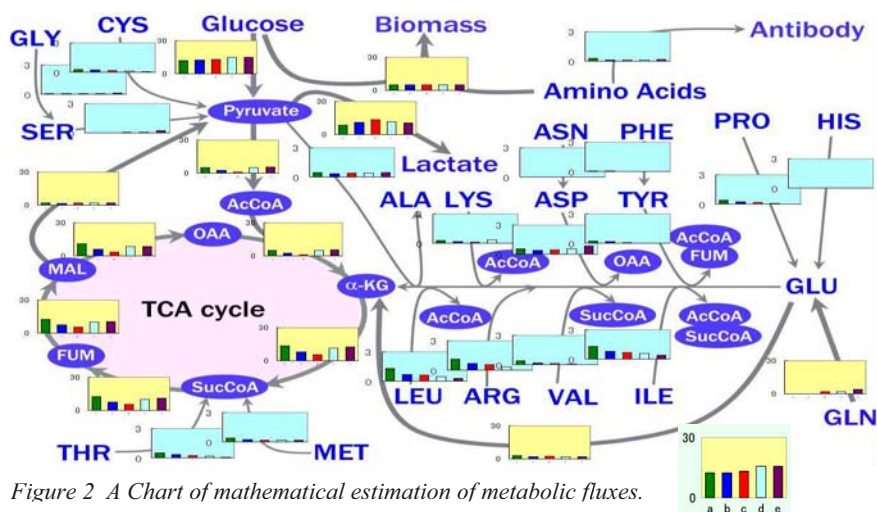


Figure 2 A Chart of mathematical estimation of metabolic fluxes.

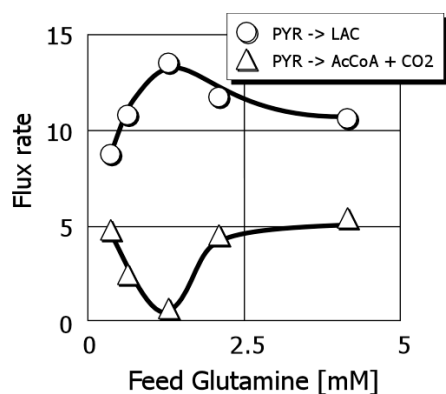


Figure 3. Two kinds of flux rates from pyruvate to lactate and acetyl-CoA.

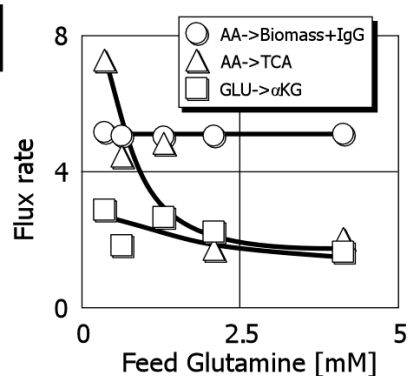


Figure 4. Three kinds of flux rates related to the utilization of amino acids.

#### 4. REFERENCES

- Matsuoka, H., Andoh, S., Matsuda, Y., Kaneko, H., Takeda, T. (2001). Influences of Glutamine Concentration on Cellular Metabolism in Continuous Culture of Hybridoma. In *Animal Cell Technology: From Target to Market*. pp 175-178. Kurokawa, H., Ogawa, T., Kamihira, M., Park, Y. S., Iijima, S. and Kobayashi, T. (1993) Kinetic Study of Hybridoma Metabolism and Antibody Production in Continuous Culture Using Serum-Free Medium. *J. Ferment. And Bioeng.* **76**; 128-133
- Vriezen, N., Bastiaan, R., Luyben, K. Ch. A. M., Dijken, J. P. (1997) Effects of Glutamine Supply on Growth and Metabolism of Mammalian Cells in Chemostat Culture. *Biotechnol. Bioeng.* **54**; 272-286
- Europa, A. F., Gambhir, A., Fu, P-C., Hu, W-S. (2000) Multiple Steady States with Distinct Cellular Metabolism in Continuous Culture of Mammalian Cells. *Biotechnol. Bioeng.* **67**; 25-34
- Akimoto, K., Okayasu, T., Ikeda, M., Sorimachi, K. (1997) The amino acid composition of mammalian and bacterial cells. *Amino Acids*, **13**, 379-391

*Department of Biosciences, Teikyo University of Science and Technology,  
Uenohara, Yamanashi 409-0193, Japan*

G. SCHMID AND D. ZACHER

## EVALUATION OF A NOVEL CAPACITANCE PROBE FOR ON-LINE MONITORING OF VIABLE CELL DENSITIES IN BATCH AND FED-BATCH ANIMAL CELL CULTURE PROCESSES

*F. Hoffmann-La Roche Ltd., Pharmaceuticals Division, Nonclinical  
Development, Biotechnology, CH-4070 Basel, Switzerland*

**Abstract.** A novel capacitance probe was evaluated and found to monitor well both exponential growth and importantly also death phases of batch and fed-batch CHO cell fermentations.

### 1. INTRODUCTION

The viable cell density is one of the most important parameters to monitor in any cell culture process. In development and production it can be useful e.g. for the timing of cell transfers in the inoculum train or from inoculum to production reactors and for the timing of feed additions in fed-batch processes. Culture turbidity, fluorescence, or capacitance properties have been used to estimate the biomass concentration on-line (1-4). The currently available and often employed optical density probes, however, have limitations when cell viabilities decrease as they measure culture turbidity rather than viable cell density (2).

Therefore we have recently begun to investigate a novel capacitance probe for the determination of viable cell counts in CHO cultures. Results are compared with data obtained from on-line turbidity measurements. Off-line analyses included packed-cell volume determinations, manual cell counting with a hemacytometer using the Trypan Blue exclusion method and cell number/cell-size distribution measurements with a CASY counter.

### 2. MATERIALS AND METHODS

CHO cell cultures were performed in serum-free medium based on a mixture of Dulbecco's, Ham F12 and Iscove's powdered media (5). The medium contains the 8kD ultrafiltered hydrolysate Primatone RL (Quest, NL) and insulin at 5mg/L. Bioreactor experiments were performed at 37°C in 25 l airlift bioreactors (Chemap, CH). pH was maintained at pH 7.2, while the dissolved oxygen (DO) level was kept at 30% air saturation. The gas flow rate was set at 1 l/min total flow rate with additional oxygen enrichment when necessary. The reactor was fitted with a novel capacitance probe (Biomass System<sup>®</sup>, Fogale, Nimes, F) and an optical density probe (Aquasant,

Bubendorf, CH). The capacitance data was recorded using Fogale's data acquisition software (X System) on a desktop PC. An on-line conductivity signal is also available. Off-line analyses included packed-cell volume determinations using graduated glass centrifuge tubes (Kimble, US), manual cell counting with a hemacytometer using the Trypan Blue exclusion method and cell number/cell-size distribution measurements with a CASY counter (Schärfe, D).

### 3. RESULTS AND DISCUSSION

Capacitance and conductivity signals were recorded for several batch and fed-batch CHO cell fermentations. Figure 1 presents the acquired data from one such run and points out the different phases of the cultivation, e.g. exponential and death phases

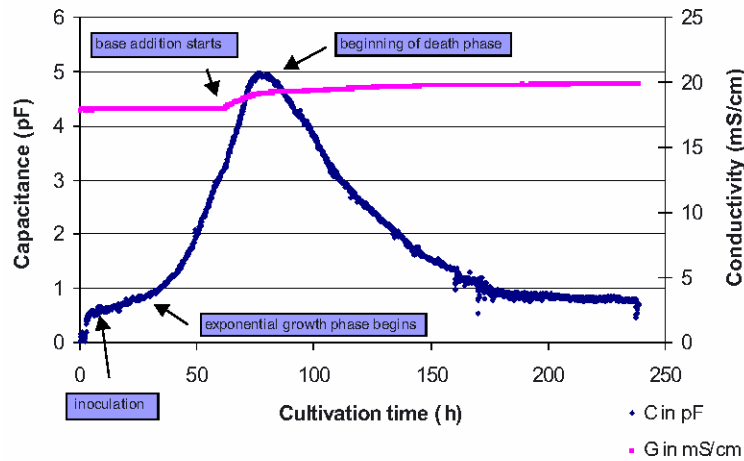
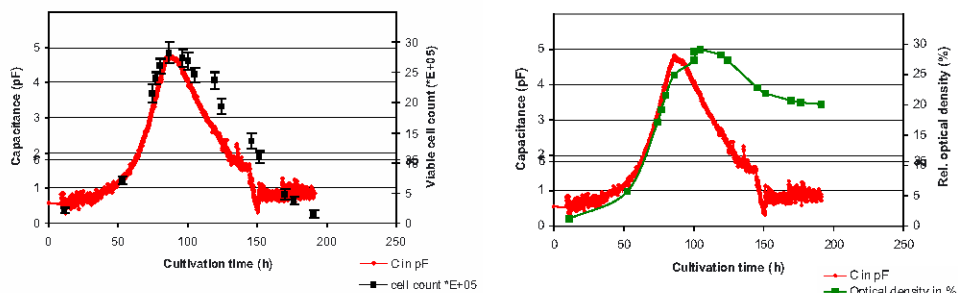


Figure 1. Capacitance and conductivity signals during CHO cell batch growth



Figures 2 and 3: Capacitance signal vs viable cell counts and rel. optical density

and the beginning of base addition. Figure 2 shows the excellent agreement of the capacitance signal with the viable cell counts determined by Trypan Blue staining or CASY counter (not shown) during the exponential growth phase. During the death phase, however, there is some discrepancy between the two data sets. A comparison of the on-line signals for capacitance and optical density (Figure 3) demonstrates that the culture turbidity fails to match the capacitance signal (and thus the viable biomass) completely during the death phase due to signal originating from dead cells/debris. However, the influence of physiological changes in cell state on the capacitance signal cannot be neglected and was indeed clearly identified, e.g. before and after feed additions during CHO fed-batch cultivations (Figure 4).

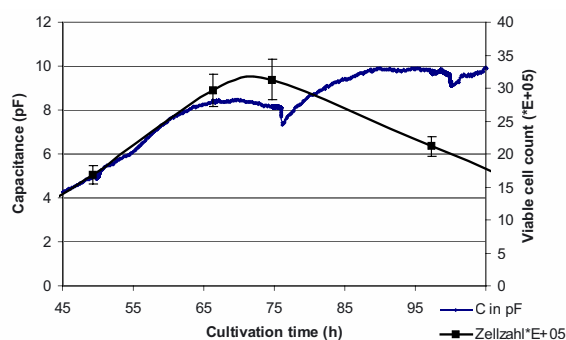


Figure 4: Fed-batch growth of CHO cells: Sensitivity of the capacitance signal to feed additions

#### 4. CONCLUSION

Exponential growth and importantly also death phases of CHO batch fermentations are described well by an on-line measured capacitance signal. Fed-batch cultivations demonstrate the sensitivity of the signal to physiological changes in cell state.

#### 5. ACKNOWLEDGEMENTS

We wish to acknowledge the productive interaction with Mr. Geoffrey Esteban (Fogale), Prof. Charles Ghommidh (University of Montpellier) and Mr. Jean-Pierre Christ (Infors) over the past months. During her internship in 2002/2003 D.Z. was supported by a F. Hoffmann-La Roche Ltd. stipend.

#### 6. REFERENCES

1. P. Wu, S.S. Ozturk, J.D. Blackie, J.C. Thrift, C. Figueroa, and D. Naveh, *Biotechnology and Bioengineering*, 45, 495-502 (1995).
2. R. Beri, J. Wayte, J. Swift, S. Abraham, and M. Brown, ACS Annual Meeting, Boston, September 1998.

3. K.B. Konstantinov, R. Pambayun, R. Matanguihan, T. Yoshida, C.M. Perusich, and W.-S. Hu, *Biotechnology and Bioengineering*, 40, 1337-1342 (1992).
4. I. Cerckel, A. Garcia, V. Degouys, D. Dubois, L. Fabry, and A.O.A. Miller, *Cytotechnology*, 13, 185-193 (1993).
5. E.-J. Schlaeger and B. Schumpp, *Journal of Immunological Methods*, 146, 111-120 (1992).



C. BASSENS\*, P. RIGAUX\*, V. HENDRICK\*, M. CHERLET\*,  
K. SATO\*, K. KOTARSKY\*\* AND J. WERENNE\*

## SODIUM BUTYRATE ENHANCEMENT OF PROTEIN EXPRESSION IN HELA CELLS: FOLLOW-UP OF A CHIMERIC REPORTER GENE BEHAVIOUR FOR PROCESS DEVELOPMENT

*\*Laboratory of Animal Cell Biotechnology, Department of Bioengineering,  
Faculty of Sciences, Université Libre de Bruxelles, Brussels, Belgium*

*\*\*Division of Molecular Neurobiology, Wallenberg Neuroscience Center,  
University of Lund, Lund, Sweden*

**Abstract :** We studied in chimeric EGFP-Photinus luciferase HeLa cells the expression of fluorescence and luminescence in different cell culture conditions (medium with or without Serum, static or dynamic conditions, in suspension or on microcarriers) as a model to follow the productivity of a recombinant protein . By studying the effect of Butyrate known as general but unpredictable stimulating agent for protein expression, we were able to establish the optimal conditions for efficacy ( concentration, time of addition, ...)

### INTRODUCTION

Chimeric EGFP-Photinus luciferase reporter gene has been proposed to improve clone selection and high-throughput screening, both for CHO and HeLa cells (1).

As the measure of the amount or the activity of recombinant protein produced in cell culture is a time and manpower consuming activity, a more straightforward essay of productivity would be useful to develop and optimize a process of production. Our aim in the present work was to evaluate the possibility of using the fluorescence or luminescence of such chimeric cells to follow the productivity under Butyrate treatment.

### MATERIAL AND METHODS

The HeLa cells construct described in the above mentioned paper (1) was used and EGFP and Luciferase expression were followed by fluorescence microscopy, or photometry, by cytofluorimetry or luminometry. In some experiments the CHO equivalent construction was also used. The gene being under the control of TRE, is an inducible system activated by ATP or phorbol esters. The cells were grown either in TC flasks or in Spinner flasks, either in suspension or on microcarriers, in medium with or without addition of Serum.

Butyrate being a general but unpredictable enhancer of protein expression, we have studied the fluorescent-luminescent properties of the cells to establish the optimal conditions for its use. We have also studied the effect of agitation on t-PA production in transfected CHO(2) in parallel to the expression of EGFP in the chimeric CHO.

## RESULTS

Under butyrate treatment, cell fluorescence and luminescence are enhanced.

Butyrate has a transitory effect which reached its maximum 16 hours after its addition. Its effect is function of its concentration as studied up to 5 mM where a toxic effect is already clearly visible.

ATP present an enhancing effect up to a saturation level at a concentration of 1mM. A synergic effect between ATP and Butyrate is observed.

Either in suspension or on microcarriers, it was shown that Butyrate enhanced greatly the protein productivity only during the early phase of culture.

The parallel study of the EGFP-luciferase CHO and t-PA-CHO (2) was of interest since we showed that the expression of t-PA by these cells readapted to Serum and grown on Cytodex 3 in spinner flasks, differed also significantly under different shear stresses. Those cells maintained their adhesion dependent growth up to an agitation in spinner at 200 rpm. Only at 300 rpm some detachment of the cells from the microcarriers can be observed together with subsequent mortality. It should be mentioned that this agitation at 300 rpm correspond to a critical shear stress of 1N/m<sup>2</sup>, as calculated by computational fluid dynamics, using "Fluent software" (3). Under this agitation however, as at 200 rpm, the t-PA productivity is higher than at 50 rpm.

## CONCLUSIONS

The fluorescent-luminescent system used was shown to be of interest to evaluate the influence of critical parameters affecting the action of butyrate which has general but unpredictable enhancing properties. In particular we screened easily in this way the optimal concentration and time of addition of butyrate to the culture in order to obtain a significant transitory increase of recombinant protein production. It must be mentioned that others, by using other kinds of fluorescent cells have reached similar conclusions independently (4). Our chimeric system offered however the possibility to follow two different recombinant proteins in parallel. The system may be also useful to predict the limit of acceptable shear stress for the production of a given recombinant protein.

As we were becoming aware that Lisa Hunt was following independently a similar track as us in Florian Wurm's laboratory, we expressed to her our wishes to collaborate with her along this line and she was reacting very positively with her usual enthusiasm. However she died soon after from a tragic mountain accident. We wished to reiterate at this occasion our remaining emotion in her memory.

## REFERENCES

- K. Kotarsky, C. Owman and B. Olde, A chimeric reporter gene allowing for clone selection and high - throughput screening of reporter cell lines expressing G-Protein-coupled receptors, *Anal. Biochem.* **288**, 209-215, 2001.
- V. Hendrick, P. Winnepeninckx, C. Abdelkafi, O. Vandeputte, M. Cherlet, T. Marique, G. Renemann, A. Loa, G. Kretzmer and J. Wérenne, Increased productivity of recombinant tissular plasminogen activator (t-PA) by butyrate and shift of temperature : a cell cycle phases analysis, *Cytotechnology*, **36**, 71-83, 2001.
- M. Cherlet, J. Castillo, V. Halloin and J. Wérenne, abstract JAACT-ESACT meeting, Kyoto, 1998.
- L. Hunt, P. Batard, M. Jordan and F. Wurm, Fluorescent Proteins in animal cells for process development : optimization of sodium butyrate treatment as an example, *Biotech.Bioengin.* **77**, 528-537, 2002

P. GIRARD<sup>1,2</sup>, M. DEROUAZI<sup>1</sup>, F. VAN TILBORGH<sup>1</sup>  
F.M. WURM<sup>1,2</sup>

## SCALABLE, SERUM-FREE, HIGH EFFICIENCY TRANSFECTION OF CHO CELLS USING AN ECONOMICAL DNA TRANSFER VEHICLE

<sup>1</sup>*LBTC, Center of Biotechnology, EPFL, 1015 Lausanne, Switzerland.*

<sup>2</sup>*ExcellGene SA, 11 rue de Malagny, 1196 Gland, Switzerland.*

**Abstract.** Reports on large-scale transient gene expression (TGE) in mammalian cells focus on two transfection technologies. Polyethyleneimine (PEI) and calcium phosphate (CaPi) mediated transfection have both been shown to work at scales beyond 10 liters. Unfortunately, both approaches yield higher recombinant protein (r-protein) levels in the presence of serum than in its absence. Since serum is a major cost factor and generally a hindrance to protein purification, our goal is to develop a productive large-scale TGE process in the absence of serum.

Large-scale TGE is a way of providing, within weeks, enough r-protein for many applications including development of downstream processing, activity testing, stability and formulation studies, and pre-clinical and animal studies. HEK 293 cells are the typical host for TGE, but r-proteins for medical applications are preferably produced in stable CHO cell lines. Thus, problems arise when comparing test results from transiently produced and stably produced material. To eliminate this problem we propose a TGE process in CHO cells.

CHO-DG44 cells were cultivated and transfected in a chemically defined media using PEI as transfection vehicle. The procedure, was scaled up to 20 liters, yielded expression levels in the same range as in HEK cells, *e.g.* around 8 mg/l for intracellular and for secreted proteins.

### INTRODUCTION

It is generally accepted that the fastest method for the production of r-proteins in mammalian cell, is transient gene expression (TGE)[1]. The classic calcium phosphate coprecipitation (CaPi) method and its modifications, polyethyleneimine (PEI) mediated transfection, as well as continuous flow electroporation, have been shown to be useful DNA-transfection methods. These three approaches have been shown to be economical, highly efficient and applicable at larger scales for cells in suspension, while commercially available liposomes are also efficient, but prohibitively expensive at larger scales. Human Embryonic Kidney cells (HEK 293) are usually used for TGE. In order to make TGE acceptable to the authorities as a means of producing proteins for early clinical studies and eventually for the manufacturing of orphan drugs and vaccines, we developed a method to transfect Chinese hamster ovary cells (CHO) under serum-free conditions.

## MATERIALS AND METHODS

Suspension CHO DG-44 cells were expanded in ProCHO5-CDM, (BioWhittaker) in shaken square flasks. A human IgG was expressed from plasmids containing the genes encoding for the light chain and for the heavy chain cloned into the pEAX8 backbone or into pMYC/EF1 containing a murine CMV promoter and an EF1 $\alpha$  enhancer. pEGFP-N1 (Clontech) was used as transfection efficiency marker as well as for optimization of transfections. PEI was used as transfection reagent. Prior to transfection, the growth medium was changed for the transfection medium. PEI and DNA were diluted individually into transfection solutions. The PEI solution was then added to the DNA, and after 10 minutes, the mixture was added to the cells. After 4 to 6 hours of incubation the culture was diluted with the growth medium. The transfection method was optimized in shaken 12-well plates (MicroSpin)[2], and then scaled up into bioreactors (BR).

In order to optimize the transfection conditions, different transfection solutions, 150 mM NaCl and 5% glucose, were tested together with different transfection media (RPMI, ProCHO5, DMEM/F12, fortified DMEM/F12, DMEM w/o Ca<sup>2+</sup>). Also, the amount of DNA (1-5  $\mu$ g/ml of transfection volume) and the ratio of PEI to DNA (1:2 to 5:1 w/w) were varied. Finally, the seeding cell density and different supplementation strategies were also optimized for transfections.

## RESULTS AND DISCUSSION

The best results were obtained using the following conditions: RPMI as transfection medium with cells seeded at  $2 \times 10^6$  cells/ml and a PEI:DNA ratio of 2:1, 2.5 mg/ml DNA in the ready to transfer DNA-vehicle cocktail. The transfection particles should be formed in the NaCl transfection solution. During the production phase glucose and glutamine had to be supplemented.

The presence of only a small concentration ( $\sim 0.2$  mM) of Ca<sup>2+</sup> in the medium seemed to be important for the outcome of the transfection, higher and lower concentration didn't work. Transfection in chemically defined medium tested was not possible, as the PEI DNA particles did not stick to the cells. Lower DNA concentrations, down to 1  $\mu$ g/ml, were possible with only a slight reduction of protein expression. The cells being transfected at high density, it was important to supplement the culture with glucose and glutamine during the production to avoid nutrient depletion and starving. This allowed a production phase of up to 10 days.

Table 1: PEI transfections at different scales. The lower expression at the 5 L scale is due to inefficient aeration/stripping in that reactor configuration.

Culture System	Product	Titer [mg/l]	Volume [l]	DNA	Comments
MicroSpin	GFP	~7	2 ml	2.5 µg/well	on day 5
MicroSpin	IgG (CMV)	5.5	2 ml	2.5 µg/well	at harvest
MicroSpin	IgG (EF1 $\alpha$ )	2.3	2 ml	2.5 µg/well	on day 3
BR 3 L	IgG (CMV)	5.5	1.2 L	2.5 mg	at harvest
BR 3 L	IgG (EF1 $\alpha$ )	7.8	1.2 L	2.5 mg	at harvest
BR 5 L	IgG (CMV)	2.3	4.5 L	5 mg	on day 3
BR 20 L	IgG (EF1 $\alpha$ )	6.1	13 L	18 mg	at harvest
BR 20 L	IgG (CMV)	2.0	13 L	18 mg	on day 3

The above protocol was then scaled up and applied to stirred bioreactors at various scales (see Table 1).

The relative simplicity of the transfection protocol using PEI and the absence of time critical steps allowed an easy scale up.

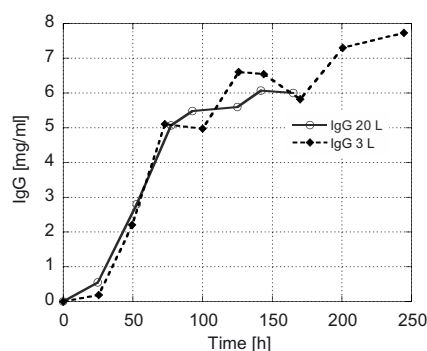


Figure 1: Production of an antibody in the 5 L and the 20 L bioreactor. CHO cells were transfected with 5 respectively 18 mg of plasmid DNA. 2% pEGFP-N1 were co-transfected as transfection efficiency marker.

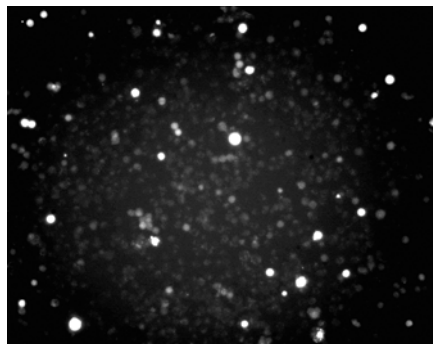


Figure 2: Cells transfected in the 20 L reactor with PEI showed GFP expression already 5h after transfection. The cells grew as single cells. 10% of the cells expressed GFP (visual estimate) with 2% of GFP encoding plasmid.

#### CONCLUSION

Serum-free, transient gene expression (TGE) in CHO cells using PEI is possible and readily scalable. The expression levels for intracellularly accumulated GFP as well as for secreted IgG are lower than those seen with HEK 293 cells [3]. Transient r-protein expression in CHO cells under serum-free conditions could be a step towards regulatory acceptance of the use of transiently produced clinical material. It is expected that differences in secondary modifications of proteins made transiently in CHO or by stable CHO cells would be minimal thus further enhancing the potential of TGE.

#### ACKNOWLEDGEMENTS

pMYC backbone was kindly provided by Seon-Young Kim, Laboratory of Cell Biology, Korea Research Institute of Bioscience and Biotechnology, 52 Eoundong, Yusong, Taejon 305-333, South Korea.

#### REFERENCES

1. Wurm, F. and A. Bernard, *Large-scale transient expression in mammalian cells for recombinant protein production*. *Curr Opin Biotechnol*, 1999. **10**(2): p. 156-9.
2. Girard, P., et al., *Small scale bioreactor system for process development and optimization*. *Biochem. Eng. J.*, 2001. **7**(2): p. 117-119.
3. Meissner, P., et al., *Transient gene expression: Recombinant protein production with suspension-adapted HEK293-EBNA cells*. *Biotechnol Bioeng*, 2001. **75**(2): p. 197-203.

J. M. JOHNSON, J. HARTSHORN, S. MCNORTON,  
J. A. PADILLA, T. MOHABBAT, S. LUO, AND  
K. ETCHBERGER.

## PROCESS OPTIMIZATION FOR AN NS0-DERIVED HYBRIDOMA CELL LINE IN A CHEMICALLY DEFINED, PROTEIN-FREE MEDIUM

*JRH Biosciences, Inc., 13804 W. 107th Street, Lenexa, Kansas 66215 USA;  
Corresponding author, e-mail Janice.johnson@jrhbio.com*

**Abstract.** A process optimization study was performed in stirred-tank bioreactors to determine parameter set points that maximize cell growth, viability, and monoclonal antibody (MAb) production. A statistical design of experiment (DoE) software package was used to determine parameter settings for dissolved oxygen (DO), pH, and temperature.

An immunoglobulin G (IgG) producing NS0-derived hybridoma cell line was adapted to growth in a chemically defined, protein-free and animal-component free medium. Growth and productivity were characterized at the 2L bioreactor scale. Results were analyzed based on variable responses including growth and productivity on a per-liter basis. Parameter ranges that yield optimal productivity were determined.

### 1. INTRODUCTION

To improve efficiency of external cellular conditions, it is necessary to optimize and control dynamic environmental changes for robust cell growth and antibody production. This can be done by using DoE software that utilizes algorithms in combination with advanced quantitative models.

DoE designed runs were performed in batch culture using NS0-derived hybridoma cells. Results show that the culture environment and process can be optimized to yield robust cell growth and high MAb production using statistically designed runs.

### 2. MATERIALS AND METHODS

#### *2.1. Cells and Medium*

SC-71 cells (NS0-derived hybridoma) stably expressing mouse IgG1 were purchased from the American Type Culture Collection, No. HB-277. Seed cultures were maintained in a 37°C, humidified incubator. The cells were cultured in 125 mL Erlenmeyer flasks (20 mL culture volumes) at 110 rpm in 5% CO<sub>2</sub>.



Stock cultures were maintained in EX-CELL NS0, by JRH Biosciences, Catalog No. 14650, supplemented with 40 mL/L L-glutamine (200 mM), and 2 mL/L Lipid Concentrate (500X), Chemically Defined, JRH Biosciences, Catalog No. 14100.

### 2.2. Bioreactors

Runs were conducted in 2L Applikon Biobundle™ bioreactors. Bioreactors were seeded at  $3 \times 10^5$  cells/mL in 1.5 L EX-CELL NS0 medium. DO, pH and temperature were monitored online and controlled using air, O<sub>2</sub>, N<sub>2</sub>, CO<sub>2</sub> and 7.5% NaHCO<sub>3</sub>. Samples (40 mL) were collected daily to monitor cell density and viability, and IgG production.

### 2.3. Analytical Methods

Cell density and viability were determined by Cedex (Innovatis) and by trypan blue exclusion with hemacytometer (data not shown). Once cell viability reached less than 60% as determined by hemacytometer, the runs were terminated. IgG production was quantified by HPLC analysis (Agilent Technologies). Lastly, runs were designed (Table 1) and analyzed with Fusion Pro™, a DoE software (S-Matrix Corporation).

## 3. RESULTS AND DISCUSSION

### 3.1. Growth

As shown in Figure 1, culture conditions with more than 30% DO levels were optimal for cell growth and viability when pH and temperature were maintained at 7.0 - 7.2 and 37°C, respectively. Lower temperatures (< 37°C) hindered cell growth in Runs 1 and 2.

### 3.2. Monoclonal Antibody Production

The conditions for Runs 3, 4, 5 and 6 yielded more than 200 mg/L IgG, whereas conditions for Runs 1 and 2 produced less than 100 mg/L IgG (Figure 2). The highest volumetric production level was reached with Run 3 (665 mg/L) for SC-71 cells in EX-CELL NS0 medium. A 7.4-fold increase in volumetric IgG production was achieved in Run 3 when compared to initial conditions in Run 1.

## 4. CONCLUSIONS

The parameters evaluated in this study have shown significant effects on cell growth, viability and production. Specifically, EX-CELL NS0 medium was shown to support favorable cell growth and superior MAb production at optimal DO, pH and temperature ranges. Temperature set at 37°C was a critical parameter of culture

and process conditions that generated more than 200 mg/L MAb. Specifically, higher MAb production was achieved with a combination of optimal levels of DO, pH and temperature (Run 3). At a lower temperature (35°C), cell growth was severely limited, regardless of DO percentage. Further optimization should continue to enhance production, making EX-CELL NS0 an ideal choice for a highly efficient and economic process.

4. TABLES AND FIGURES

Table 1. Run Design

Run No.	DO (%)	pH (Units)	Temperature (°C)
1	80	7.0	35
2	30	6.8	35
3	30	7.0	37
4	50	7.0	37
5	50	7.0	38
6	80	7.2	37

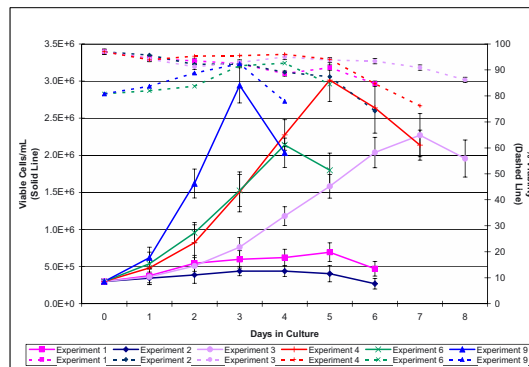


Figure 1. Growth and viability of SC-71 cells in EX-CELL NS0 medium. Runs 4 and 6 had higher peak cell densities than the Runs 1, 2, 3 and 5. Conditions for Runs 3 and 4 yielded extended culture longevities. Conditions for Runs 1 and 2 did not support cell growth.

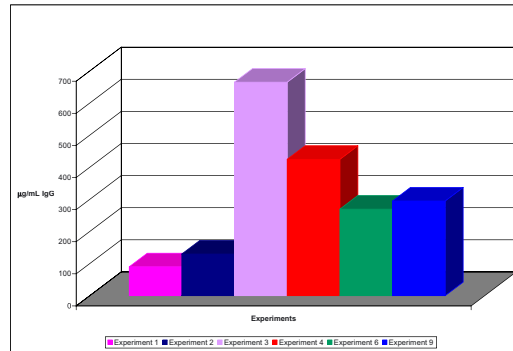


Figure 2. Cumulative IgG production in SC-71 cells. IgG production in Run 3 reached 665 mg/L and was significantly greater than production in other runs.

ALISON RIDLEY, JONATHAN DEMPSEY, CHRIS GEE,  
RICHARD TURNER, MATTHEW OSBORNE, STEVE RUDDOCK,  
CHRISTY RITCHIE AND RAY FIELD

IMPACT OF CHANGE IN FERMENTATION PROCESS  
PH AND DISSOLVED CARBON DIOXIDE  
CONCENTRATION ON SECRETED ANTIBODY  
STRUCTURE AND CELL PHYSIOLOGY OF A GS-NS0  
CELL LINE EXPRESSING A HUMAN ANTIBODY

*Cambridge Antibody Technology, Milstein Building, Granta Park,  
Cambridge, CB1 6GH, United Kingdom*

## 1. INTRODUCTION

Increased production of recombinant proteins from mammalian cells is a key focus of process development. Process pH is one factor well known to dramatically affect growth and productivity of some mammalian cells (1-3). Most mammalian cell culture systems use a bicarbonate based pH buffer system, in which pH setpoint is maintained by addition of carbon dioxide or bicarbonate. When pH set-point is lowered, more carbon dioxide is required to maintain pH, which may elevate the dissolved carbon dioxide ( $p\text{CO}_2$ ) to growth inhibitory levels (4). To counteract this, the bicarbonate concentration in the medium can also be reduced. Changes to pH and  $p\text{CO}_2$  have also been shown to affect protein glycosylation (5), which may affect protein function (6).

This study describes the impact of changing process pH and  $p\text{CO}_2$  on a GS-NS0 cell line expressing a human monoclonal antibody.

## 2. MATERIALS AND METHODS

Fermentation inocula were generated from characterised cell banks. Fermentations were performed in a scaled-down model of the manufacturing process. Initial  $p\text{CO}_2$  was varied by adjusting the process pH and by using media with low or standard sodium bicarbonate concentrations. Cell concentration was determined by trypan blue exclusion, from daily fermentation samples. Supernatants were analysed for antibody concentration by Protein A-HPLC. Antibody purified from the supernatants by Protein A was analysed by isoelectric focusing (IEF). The Cumulative Cell Hours (CCH) were calculated by summation of the areas between

adjacent viable cell concentrations over time. Cell doubling times were calculated from time of fermenter inoculation to time of maximum viable cell concentration. The specific antibody production rate ( $Q_p$ ) was calculated as the mean quantity of antibody produced per cell per day over the whole fermentation profile.

### 3. RESULTS AND DISCUSSION

Figures 1 and 2 show the influence of pH and initial  $pCO_2$  on CCH and  $Q_p$ . In both cases where pH is maintained but initial  $pCO_2$  is changed, the cells respond to the change in  $pCO_2$ . This data supports the hypothesis that the physiological effects are mainly due to initial  $pCO_2$  rather than pH.

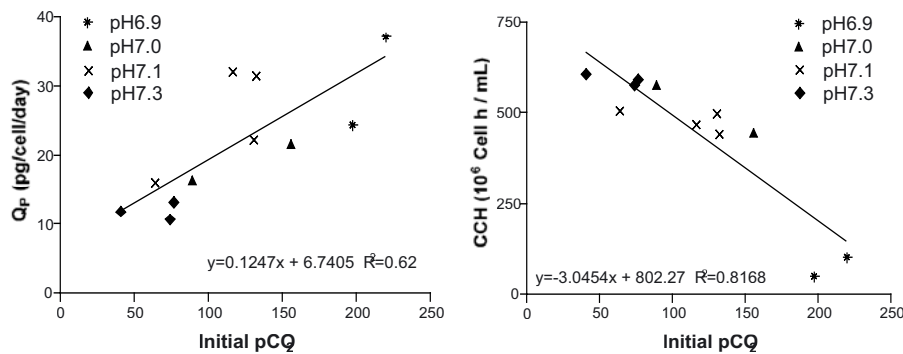


Figure 1: The influence of pH and initial  $pCO_2$  on  $Q_p$

Figure 2: The influence of pH and initial  $pCO_2$  on CCH

Figures 3 and 4 show the influence of the initial  $pCO_2$  on cell growth and antibody production, with standard error marked on each bar. Elevated initial  $pCO_2$  resulted in severe growth inhibition, which is shown through: reduced CCH, reduced maximum viable cell concentrations and longer doubling times.  $Q_p$  generally increased with elevated initial  $pCO_2$ . However, highest titres were achieved at an intermediate initial  $pCO_2$ . At elevated initial  $pCO_2$ , the process was less robust as shown by the large error bars.

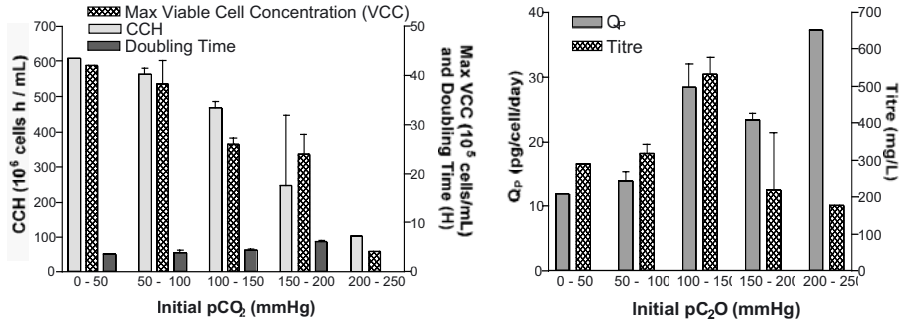


Figure 3: The influence of initial pCO<sub>2</sub> on Cell Growth (CCH and maximum VCC)  
 Figure 4: The influence of initial pCO<sub>2</sub> on antibody accumulation (Q<sub>p</sub> and titre)

Figure 5 shows an IEF gel for cells grown at mid and high initial pCO<sub>2</sub>. An additional basic band, as indicated, was evident in samples prepared from fermentations run at the highest extreme of initial pCO<sub>2</sub>. This additional basic band by IEF was not detected under any other conditions tested.

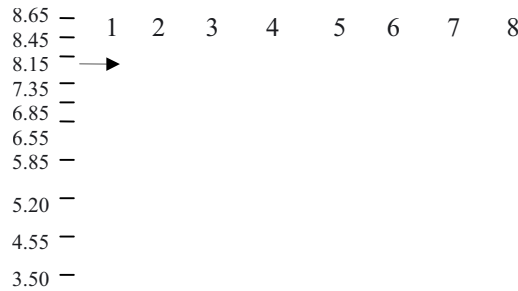


Figure 5: An IEF gel for cells grown at mid and high initial pCO<sub>2</sub>.

Lanes 1 and 7 show markers with the pI as indicated, Lanes 2 and 3 show antibody from fermentations with initial pCO<sub>2</sub> of 198-220mmHg. Lanes 4, 6 and 8 show antibody from fermentations with an initial pCO<sub>2</sub> of 100-150mmHg. Lane 5 shows an assay control.

4. CONCLUSIONS

- Changes to cell growth and productivity were not linked to pH alone, as shown by running fermentations at the same pH but with different initial pCO<sub>2</sub>.
- Increasing the initial pCO<sub>2</sub> of cultures caused growth inhibition. Initial pCO<sub>2</sub> above 150mmHg resulted in severe inhibition of cell growth and a lack of process robustness.
- Increasing initial pCO<sub>2</sub> resulted in increased Q<sub>p</sub>. However, the highest antibody titres were achieved when initial pCO<sub>2</sub> was sufficiently high to give high

$Q_p$  without resulting in severe growth suppression. In this series of experiments the highest titre was achieved at an initial  $pCO_2$  of approximately 130mmHg.

- An additional basic band occurred in IEF analysis of purified fermentation samples at the highest extreme of initial  $pCO_2$ . This represents a probable change in product structure and starts to define the upper limit of  $pCO_2$  tolerated in the manufacturing process.

## 5. REFERENCES

1. Wayte J. *et al.* The Genetic Engineer and Biotechnologist (1997) 17: 125-132.
2. McDowell C.L. *et al.* Spier RE, editor. In: The Encyclopaedia of Cell Technology (2000) 63-69. New York: Wiley-Liss.
3. Sauer PW *et al.* Biotech and Bioeng (2002) 67: 585-597.
4. deZengotita V.M. *et al.* Biotech and Bioeng (2002) 77: 369-380.
5. Borys M.C. *et al.* Biotechnology (1993) 11 (6): 720-724.
6. Jefferis R. Biopharm (2001) September: 19-27.

RODRÍGUEZ, E.N.; PÉREZ, M.; ORDAZ, Y.; CASANOVA, P.R.;  
MARTINEZ, L.; HERRERA, N.

## EXPERIMENTAL FACTORIAL DESIGN FOR THE STUDY OF SOME VARIABLES IN ROLLER BOTTLES CELL CULTURE.

*Center for Genetic Engineering And Biotechnology.  
Havana, Cuba.*

*E-mail: [elias.nelson@cigb.edu.cu](mailto:elias.nelson@cigb.edu.cu)*

*<http://www.cigb.edu.cu>*

**Abstract:** An experimental factorial design was developed to study influence of seed cell density, agitation rate and culture condition(open or closed system) in order to maximize the expression of recombinant protein transfected in CHO cell line.

A 2<sup>3</sup> experimental design included those independent variables was running and total protein expression and specific protein expression were measured as dependent variables. A low and high level was established for each variable assuming working experience and literature review. There were running 8 experiments keeping similar culture conditions except variables under study.

Multiple lineal regression model was fitted to the data and statistic parameters suggest a good correlation between independent and dependent variables

Results show that three independent variables have a statistic significance in the expression of target protein but not interaction between them.

These results are very useful in order to establish culture condition at large scale production of biopharmaceuticals and for validation purposes.

### INTRODUCTION

Roller bottle systems have been used for over 50 years in pharmaceutical and biochemical process.(Liu YL et al, 2003, Tsao EI et al, 1992)

Widespread use of the roller bottle is due to several reasons like simplicity and scalability of the technology, reduced developmental timelines, constant fluid-gas contact and capability to maintain sterile conditions.(Muzzio et al, 1999)

An experimental factorial design was developed to study influence of seed cell density, agitation rate and culture condition(open or closed system) in order to maximize the expression of recombinant protein transfected in CHO cell line.

### MATERIALS AND MÉTHODS.

The CHO cell line used is derived from wild type (ATCC CRL-9096) and transformed to express heterologous protein in our Institute (Center for Genetic Engineering and Biotechnology). The cells were cultivated in Dulbecco's Modified Eagle Medium (D-MEM) containing 5 % of fetal bovine serum (FBS) supplemented with 10 µg/mL gentamicine. Cells were kept at 37°C. Medium exchange was done



each 48-72 hours. Harvest medium was supplemented with insulin and collected each 48 hours.

An experimental factorial design was developed to study influence of seed cell density, agitation rate and culture condition (open or closed system) in order to maximize the expression of recombinant protein transfected in CHO cell line. A  $2^3$  experimental design included those independent variables was running and total protein expression and specific protein expression were measured as dependent variables. A low and high level was established for each variable assuming working experience and literature review. (Berson RE et al, 2002; Griffiths B, 2001; Elliot AY, 1990)

Variables	Unit	Low level (-1)	High level (+1)
Seed cell density ( $x_1$ )	Cell/cm <sup>2</sup>	20 000	60 000
Agitation rate ( $x_2$ )	rpm	0.2	1.0
Culture condition ( $x_3$ )		Closed system	Open system

Table 1 : Independent variables and levels of experimentation.

Open system is defined as bottle with vent filter in the cap that allow gas exchange with environment.

It was used expanded surface bottle 2.5X ( 2125 cm<sup>2</sup>).

There were running 8 independent experiments in parallel keeping similar culture conditions except variables under study.

Target protein was determined by specific ELISA assay developed in our Institute. Total proteins were measured by Bradford's method.

The statically analysis of the result was done with Statgraphics software.

## RESULTS AND DISCUSSION

There is not statistically significant relationship between variables respect total protein expression.

The results of the experiments respect target protein are summarized in the following table:

Experiment	X <sub>1</sub>	X <sub>2</sub>	X <sub>3</sub>	[target protein] (mg/mL)
1	-1	-1	-1	0.067
2	-1	-1	+1	0.055
3	-1	+1	-1	0.073
4	-1	+1	+1	0.063
5	+1	-1	-1	0.053
6	+1	-1	+1	0.046
7	+1	+1	-1	0.066
8	+1	+1	+1	0.052

Multiple linear regression model was fitted to the data. The general model included all variables and interactions:

$$Y = B_0 + B_1X_1 + B_2X_2 + B_3X_3 + B_{12}X_1X_2 + B_{13}X_1X_3 + B_{23}X_2X_3 + B_{123}X_1X_2X_3$$

Not significant variables or interactions were removed from the model. Adjusted model was:

$$Y = 0.059375 + 0.005125X_1 - 0.004125X_2 - 0.005375X_3$$

Results show that the three independent variables have statistical significance in the expression of target protein but not interaction between them.

P value in the ANOVA analysis is 0.0014 ( $p < 0.01$ ), therefore there is statistically significant relationship between variables at 99 % confidence level.

Others statistical results were:

- $R^2$  : 97.22 %
- Standard error of estimated: 0.002031
- Mean absolute error: 0.001187

Model suggest that best conditions for maximize target protein expression are higher level of seed cell density, lower level of agitation and the use of closed system.

There is an important difference between results at the best and worst scenario that should be taken in account for the productivity of the system. Further experiments should be addressed to clarify the influence of open system in the productivity of cell line and others variables should be studied.

These results are very useful in order to establish culture condition at large-scale production and for validation purposes.

## REFERENCES

- Liu YL, Wagner K, Robinson N, Sabatino D, Margaritis P, Xiao W, Herzog RW. Optimized production of high-titer recombinant adeno-associated virus in roller bottles. *Biotechniques* 2003 Jan;34(1):184-9
- Berson RE, Pieczynski WJ, Svihla CK, Hanley TR. Enhanced mixing and mass transfer in a recirculation loop results in high cell densities in a roller bottle reactor. *Biotechnol Prog* 2002 Jan-Feb;18(1):72-7
- Griffiths B. Scale-up of suspension and anchorage-dependent animal cells. *Mol Biotechnol* 2001 Mar;17(3):225-38
- Muzzio FJ, Unger DR, Liu M, Bramble J, Searles J, Fahnestock P. Computational and experimental investigation of flow and particle settling in a roller bottle bioreactor. *Biotechnol Bioeng* 1999 Apr 20;63(2):185-96
- Tsao EI, Bohn MA, Omstead DR, Munster MJ. Optimization of a roller bottle process for the production of recombinant erythropoietin. *Ann N Y Acad Sci* 1992 Oct 13;665:127-36
- Elliott AY. Nonperfused attachment systems for cell cultivation. *Bioprocess Technol* 1990;10:207-16

RODRÍGUEZ, E.N.; PÉREZ, M.; ORDAZ, Y.; CASANOVA, P.R.;  
MARTINEZ, L.; HERRERA, N.

## EVALUATION OF ROLLERCELL SYSTEM FOR HIGH SCALE PRODUCTION OF BIOPHARMACEUTICALS.

*Center for Genetic Engineering And Biotechnology.  
Havana, Cuba.*

*E-mail: [elias.nelson@cigb.edu.cu](mailto:elias.nelson@cigb.edu.cu)*

*<http://www.cigb.edu.cu>*

**Abstract:** RollerCell system is a self-contained, automated roller bottle processing system marketed by Cellon, S.A. RollerCell system consists of two main components, the RollerCell Bottle Packs and the RollerCell Processing Unit.

This system could replace traditional roller apparatus and performs all the tasks previously undertaken manually or by robotic processors.

Nowadays, roller bottles are still an election technology for culture of anchorage dependent mammalian cell for the production of recombinant proteins, especially those that should have complex posttranslational modifications. In that sense, it is important to have a technological option for the operation of roller bottles at large scale.

We have been using that system mainly for bottles processing in the production of a biopharmaceutical recombinant protein in parallel with traditional manual operation of roller bottles. We have collected interesting results comparing both systems respect labor cost, operation time, control contamination and requirements of skilled operators.

We have demonstrated the usefulness of RollerCell system for large scale production and its feasibility for these purposes.

### MATERIALS AND METHODS

Evaluation of two productive campaigns was done. First campaign was completely done with single bottles and the second with the RollerCell system equipped with roller bottle pack.(Cellon)

### RESULTS AND DISCUSSION

There are not differences between both systems in term of control contamination and target protein expression in evaluated campaigns.

It should be remark that our operators have a good training and enough incorporated skill in cell culture. May be that could mask any advantages in the application of the system to reduce directly contamination. Anyway, manual operation require as aseptic intervention as bottles composed the lot. In RollerCell system you require an aseptic intervention for each 20 bottles. The system reduce drastically the probability to introduce a contamination due to manipulation.

In RollerCell system monolayer is kept during all the cultivation time and has not observed damages to cell structure. In manual operation monolayer near bottle bottom almost always is lost due to impact of liquid. The damage is directly proportional to the operator skill. This problem is not reflecting it in protein expression results in our production and analytical conditions but it could be significant in larger production scale or with more accuracy analytical methods.

In manual system you need at least two operators. With RollerCell system just one operator can make all the activities, but is not recommended. We could have reduce personnel from 5 to 3 with the application of RollerCell system without lost of production capacity.

In our conditions an operator needs not less than 30 seconds to manipulate a flat bottle and not less than one minute to operate expanded surface bottles in order to drain all exhausted medium.

Lots of 40 expanded bottles required at least of 40 minutes to complete each operation of medium change.

With RollerCell system you can change media in not more than 10 minutes for the same number of bottles because the system is equipped with a peristaltic pump that feed 20 bottles at the same time.

Roller bottle system has been improved with drain sump in the roller bottle packs. This characteristic combined with the possibility of the system to tilt each rotor help to complete extraction of exhaust medium from bottles. It is difficult to drain individual expanded surface bottles because liquid is entrapped between bottle channels and operators have to make some draining movement for extract completely the liquid from the bottle.

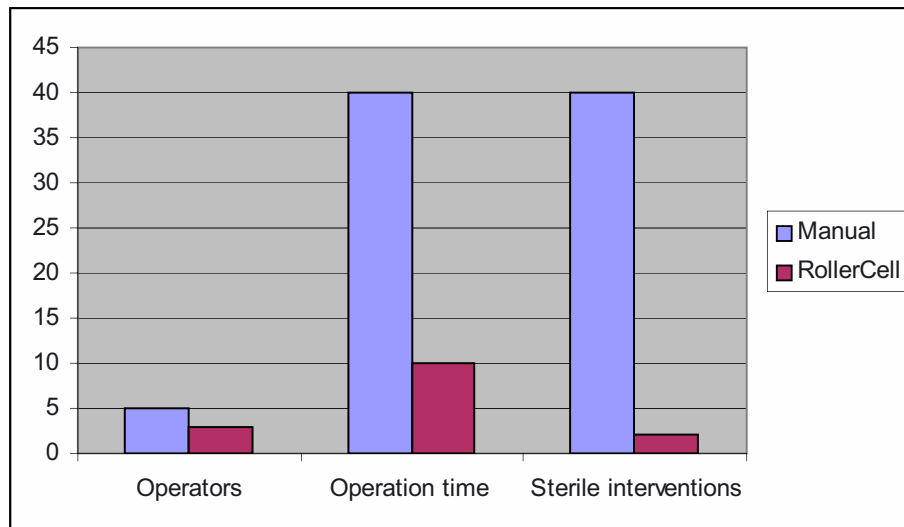


*Fig. 1 : Comparison of manual and automatic system operation.*

We have not yet exploited system facilities for trypsinisation.

We have detected two main difficulties in the operation of RollerCell system:

- Sometime pump does not pump liquid to all rollers tubing at the same time and that require further intervention (not aseptic) to adjust pump heads.
- Usually when you detect contamination in one bottle is sign of all bottles in the rotor are contaminated.

With the application of this automated system we have passed from milligram to grams scale production. RollerCell system may be used to process any commercially available flat walled or expanded surface roller bottles.

We have demonstrated the usefulness of RollerCell system for large-scale production and its feasibility for these purposes.

DE MATTEI, C., DE BERNARDI, N., GASPARI,  
F., CASTIGLIONI, S., ORLANDI, A., MURU, E., CAVENAGHI,  
L., NOLLI, M.L.

## STRATEGIES FOR THE PROCESS DEVELOPMENT OF MONOCLONAL ANTIBODIES FOR THERAPEUTIC USE

*Areta International via Roberto Lepetit 34, 21040 Gerenzano (VA) Italy*

**Abstract:** The launch on the market of an increasing number of antibody-based drugs had, as consequence, the parallel development of recipient cell lines, serum free media and bioreactors for production of big quantities of these molecules. Most of the destiny of a biopharmaceutical drug is played during the process development, a step that appears in all biotech projects but very often is not properly carried out with the hurry to go to production. This loss of accuracy at early stages of the development can cause problems in reliability of lots during manufacturing with potential risks of stopping/delaying the project in advanced phases of development. We describe here a strategy for the process development of monoclonal antibodies for clinical studies.

**Key words:** Mabs, Process Development, GMP, QC tests

### 1. INTRODUCTION

We are entering an era in which in addition to the traditional drugs of synthesis, semi synthesis or deriving from fermentation processes, new drugs including monoclonal antibodies, proteins, cells and DNA will be developed. The development of these new drugs, mostly produced by recombinant cell lines is bringing about a revolution in the production, analytical and regulatory field. Biological drugs producers have to organize production plants different from the traditional ones, able to guarantee the safety and quality control of the finished product. On the other end the ethic committees has to control on these new products and on the same time have a positive attitude to their development since they could be important novelties for the cure of diseases not curable today (1). In the case of monoclonal antibodies, one of the most successful biotech products, born as a tool for research and diagnosis, the development of recombinant cell lines able to produce chimerical and humanized antibodies at a high level of safety opened the way for the development of monoclonal antibodies as therapeutic agents (2). For a correct development of a therapeutic antibody the crucial step is the process development that has the objective to establish a robust cell culture process, a reproducible purification method and reliable analytical tests for manufacturing of controlled antibody lots for clinical trials (3).

## 2. METHODS

*Thawing of cells and Mycoplasma check.* One vial of NSO cells producing a chimeric antibody from a working cell bank (WCB) was thawed in RPMI + 10% FCS and put in quarantine until the results of the Mycoplasma test. (Mycoplasma detection kit, Roche Diagnostic).

*Kinetics of static culture.* The cells were cultivated in static culture (flask) in RPMI + 10% FCS and the viability related to cell density and antibody production monitored for one week together with the Glucose consumption and Lactate production.

*Adaptation to Serum Free Medium.* The recombinant cells were adapted to Serum Free Medium (SFM). Two types of SFM were tried and after evaluating the production related to viability, the CD Medium (Life Technologies) was selected.

*Bioreactors and mode of culture.* Two different types of bioreactors, one with a high surface volume ratio (Cell Line) and a more traditional one (Roller Bottles), were used for laboratory scale up of the chimeric antibody

*Development of a quantitative test to follow the production process.* An indirect quantitative ELISA, based on anti-human FC and an anti-human IgG peroxidase conjugated, was set up for monitoring the antibody during the cell culture process and purification steps. A standard curve with the purified antibody was used.

*Subclass determination of the Mab.* The class specificity of the Mab was determined by an ELISA set up in house using anti-human IgG and anti-human IgM immunoglobulins.

*Purification and analysis of chimeric Mab.* Cell culture supernatants were purified by Protein A and ion exchange chromatography (Mono Q Sepharose Fast Flow). At each step samples were checked by SDS-PAGE, WB, Elisa and for Endotoxin (LAL), Sterility.

*Development of Safety and Quality Control Tests.* To monitor the quality of antibody during production and analyze the purified bulk, Safety and QC tests were set up. The tests include assays for absence of contaminants (Sterility, LAL, Mycoplasma, BSA, Protein A, HCP), and for biochemical and biological characterization (SDS-PAGE and SEC, Western Blot, ELISA, IEF).

## 3. RESULTS AND DISCUSSION

The process development is a step of the project that determines the destiny of the biotech product. A correct process development may shorten the road of the product to the registration. It is therefore crucial at the stage of process development to acquire a deep knowledge of the discrepancies that could appear during the cell culture and purification process and solve them before going at large scale. At the same time at this stage, critical process parameters could be identified and test/measurements set up to keep them under control. The kinetics data of cells grown in medium with serum in static culture are very informative regarding the viability of the clone, the cell density to use in the scale up process and through the

glucose consumption and lactate accumulation give useful indications of the metabolic pathway and Mab production (Fig 1 and 2).

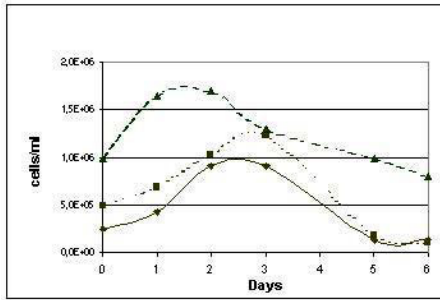


Figure 1 Viability Data  
 -◆-  $2.5 \cdot 10^5$ /ml, -■-  $5 \cdot 10^5$ /ml, -▲-  $1 \cdot 10^6$ /ml

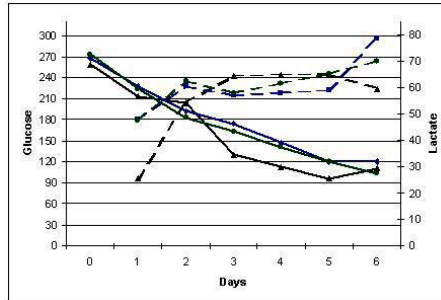


Figure 2 Glucose consumpt., Lactate prod  
 -◆-  $2.5 \cdot 10^5$ /ml, -■-  $5 \cdot 10^5$ /ml, -▲-  $1 \cdot 10^6$ /ml

The results of this experiment indicate that we can have the maximum cell density and viability at  $1 \cdot 10^6$ /ml concentration at 48 hours of culture. The Mab production, 25-30 mg/L, is the best compatible with the cell viability, glucose consumption and lactate accumulation. These data, together with those related to the difficulty in maintaining this level of Mab production in CD medium for more than 72 hours (data not shown) indicate that we can use the cells at  $1 \cdot 10^6$ /ml prepared in medium with serum (inoculums for the bioreactor) and the CD medium for the production phase with a short process (72 hours) that would avoid accumulation of dangerous catabolites. This strategy gave the best results using roller bottles as bioreactor.

The Mab purification from the cell culture supernatant included Protein A and anion exchange chromatography (Q Sepharose Fast Flow). Some trials both with protein G and with Protein A were performed at the beginning to see which resin would be the best for the chimeric antibody. Fig 3 shows that both resins elute the antibody with the same profile.



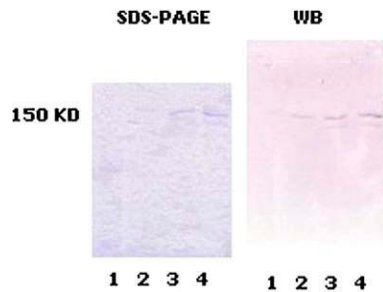


Figure 3 SDS-PAGE and Western Blot of:  
SN (1), Protein G (2), Protein A (3,4)

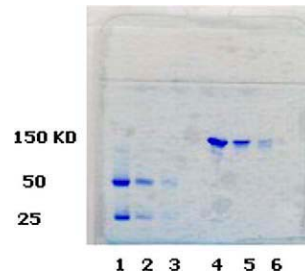


Figure 4. Quantitative SDS-PAGE of Purified  
Mab (1,2,3 reduced 4,5,6 not reduced)

Protein A was selected because of familiarity at regulatory level (4). Between the two purification steps the Mab was left 15 minutes at pH 3 for virus inactivation. After Mono Q Sepharose step the purified Mab was filtered on 18 nm filters for the second step of virus inactivation. The yield of antibody after the overall downstream process was 50%. The purified bulk was tested to specifications with safety and Quality Control tests demonstrating that it is appropriate to be used for clinical studies. The tests include those for Mab purity as the SDS-PAGE and Size Exclusion Liquid Chromatography (SEC). Fig 4 shows the SDS-PAGE in reducing and non reducing conditions of the Mab at different concentrations after the Mono Q Sepharose purification.

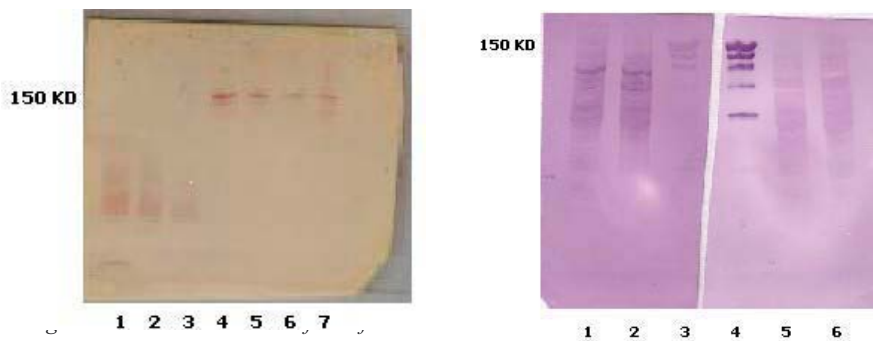


Figure 5 HCP WB test of Purified Mab  
Mab (1,2,3 protein A, other lanes Mab) (1,2,rec cells lysate, 3 , other lanes Mab)

Size Exclusion Chromatography indicates that > 95% of the antibody is constituted by the high molecular weight IgG1. Other tests were carried to demonstrate the absence of contaminants in the purified bulk like the Protein A, BSA and Host Cell Protein. Fig 5 shows that in the Mab preparation after Mono Q Sepharose there is no

Protein A. Since the limit of protein A in a Mab purified bulk should be <10 ng/mg and the sensitivity of the SDS-PAGE was 125-250 ng/sample, we have set up a quantitative sandwich Elisa that demonstrated that Protein A in the purified bulk was under the level required. Rabbit antisera specific for proteins of the parental myeloma cells and for those of the recombinant cell line were generated, and the Host Cell Protein assay was developed using them in Western Blot. Fig 6 demonstrates that in the myeloma lysate is present a low molecular weight band no longer present in the purified bulk antibody.

#### 4. CONCLUSION

The control of quality parameters at the level of process development of the chimeric antibody makes possible the production of controlled bulk that meets the specifications for in vivo use, enabling a more reliable scale up of the entire process.

#### 5. REFERENCES

- European Commission. Notice to applicants – Medicinal products for human use. 1998 Edition.
- Reichert. J.M. Monoclonal antibodies in the clinic. *Nature Biotechnology* 19 (2001) 819-822
- Dobhoff-Dier O., Bliem R. Quality control and assurance from the development to the production of biopharmaceuticals. *TIBTECH* 17 (1999) 266-270.
- Iyer H., Henderson F., Cunningham E., Hansen J., Bork C., Conley L., Webb J. Consideration during development of a protein A-based antibody purification systems. *BioPharm* 15 (2002) 14-20.

ANDREW S. TAIT<sup>1,2</sup>, MIKE HOARE<sup>2</sup>, JOHN BIRCH<sup>3</sup>, DOUGLAS  
J. GALBRAITH<sup>1</sup>, MICHAEL HINES<sup>1</sup>, CATHERINE J. BROWN<sup>1</sup>  
AND DAVID C. JAMES<sup>1</sup>

## OPTIMISATION OF PEI-MEDIATED TRANSIENT EXPRESSION IN CHINESE HAMSTER OVARY CELLS

<sup>1</sup>*School of Engineering, University of Queensland, St. Lucia, Queensland  
4072, Australia;* <sup>2</sup>*Department of Biochemical Engineering, University  
College London, London WC1 7JE, UK;* <sup>3</sup>*Lonza Biologics plc, 228 Bath  
Road, Slough, UK*

**Abstract.** The aim of this project is to develop transient gene delivery and expression strategies that can be employed in large-scale cultures of mammalian cells currently employed for therapeutic protein production (e.g. CHO, NSO). We have employed a model transfection system utilising the cationic polymer polyethylenimine (PEI) as a vehicle to deliver plasmid DNA encoding reporter gene constructs into suspension adapted Chinese Hamster Ovary cells. A key parameter in PEI-mediated transient gene expression is the PEI to DNA ratio. In our system expression was optimal at 10 moles PEI nitrogen to 1 mole DNA phosphate, which was conserved at different DNA to cell ratios. However, maximal reporter output was observed at a specific DNA:cell ratio. Addition of bovine serum albumin to growth medium was shown to increase both transgene expression (6 fold) and transfection efficiency (2 fold). Particle sizing data suggests that BSA acts to stabilise the PEI-DNA complexes at 300 nm. Therefore, these data imply that the specific properties of a PEI-DNA complex (particle size, charge etc), as well as the cellular "dose" of that complex may be important factors that regulate the uptake and intracellular fate of the recombinant DNA. In addition, small molecule inhibitors (SMI) were used to demonstrate that progression through the G2/M phase in the cell cycle is a pre-requisite for transgene expression. It was also observed that continued use of SMI throughout culture lead to an increase and an extension of transgene expression.

### 1. INTRODUCTION

The increase in the number of new recombinant therapeutic proteins under investigation and a desire to reduce development times of promising candidates has led to the investigation of strategies to more rapidly produce large quantities for pre-clinical and clinical trials. Transient gene expression has the potential to do this by removing the need to develop established cell lines to produce recombinant protein. Substituting transient gene expression in initial protein production could potential reduce the time required to produce sufficient quantities for pre-clinical trials by up to 6 months. However, this requires efficient transient gene expression at scale. We investigated the potential for scale-up of transient gene expression mediated by the polycation polyethylenimine. PEI condenses plasmid DNA to form a cationic complex that is taken into the cell by endocytosis. The mechanism by which DNA is transported to the nucleus for expression of the transgene is unclear at present.

## 2. MATERIALS AND METHODS

Plasmid DNA encoding firefly luciferase and enhanced green fluorescent protein were propagated in *E. coli* and purified using the standard procedure for Aurum™ maxipres (Biorad). CHO-S cells were maintained in CHO-S SFM II (Gibco) at 37 °C, 5 % CO<sub>2</sub>. Cells were transfected at  $2 \times 10^5 \text{ mL}^{-1}$  with the PEI-DNA complex. Experiments were performed in ultra-low binding 24-well plates (corning), with 1 mL per well, unless otherwise stated.

## 3. RESULTS AND DISCUSSION

### 3.1. Optimisation of PEI-mediated transient gene expression

Transient transfection was optimised with respect to PEI:DNA and DNA:Cell ratio using the firefly luciferase reporter gene. Maximum transgene expression was observed at a PEI nitrogen to DNA phosphate molar ratio of 10:1, which was conserved across all DNA concentrations investigated (Figure 1A). The optimal DNA concentration was found to be  $1 \mu\text{g mL}^{-1}$  (Figure 1A), equivalent to 1  $\mu\text{g}$  per  $2 \times 10^5$  cells (approximately 690,00 plasmids per cell). Expression levels at DNA concentrations greater than  $1 \mu\text{g mL}^{-1}$  did not plateau, as might be expected, but decreased. Further analysis of the data showed that there was a strong correlation between PEI concentration and cell specific growth rate, independent of the PEI:DNA ratio (data not shown). It was assumed that these cytotoxic effects lead to the reduction in transgene expression.

Addition of bovine serum albumin ( $6 \text{ mg mL}^{-1}$ ) to growth medium reduces PEI cytotoxicity (data not shown) and increased transgene expression and transfection efficiency nearly 6 fold and 2 fold respectively (Figure 1B). Particle sizing data obtained by photon correlation spectrometry indicates that BSA acts to reduce and

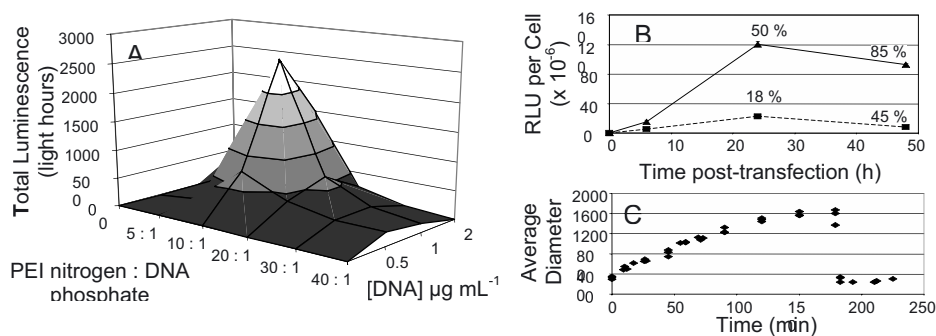


**Figure 1:** Optimisation of PEI-mediated transfection. **A:** PEI-DNA complexes were prepared under the conditions shown. Total luciferase was calculated from the integral of relative light units over 48 hrs. **B:** Luciferase expression in the presence (solid line) and absence (dashed line) of BSA. Transfection efficiencies are displayed as values on graph.  $n=3$ . **C:** DNA-PEI complexes were allowed to form for 3 hours, after which BSA was added ( $6 \text{ mg mL}^{-1}$ ).

stabilise the cationic size (Figure 1C), which has been suggested can increase transient transfection. It is unclear how BSA interacts with the PEI-DNA complexes, however, the addition of BSA before PEI in complex formation leads to a reduction in expression, suggesting that a loose association is better. These optimal conditions have been confirmed at shake flask scale.

### 3.2. Cell cycle analysis and manipulation

Cells blocked with nocodazole in G2/M phase exhibited expression at 8 hours post transfection, whereas cells blocked with hydroxyurea in G1/S phase exhibited expression from 12 hours post transfection (Figure 2A). This increase in reporter expression is associated with the cell population moving into G2/M phase (data not shown), suggesting cell division is required for transgene expression. CHO-S cells exposed to nocodazole throughout the culture showed elevated and prolonged transgene expression (Figure 2B). The presence of nocodazole increased transfection efficiency from approximately 85% to 98% 48 hrs post transfection (data not shown). Nocodazole holds cells in G2/M phase, during which nuclear membrane integrity is lost. We infer that the loss of nuclear membrane integrity during this phase facilitates passive nuclear localisation of rDNA and subsequent transgene expression. Comparable effects of nocodazole addition were achieved in shake flask cultures.

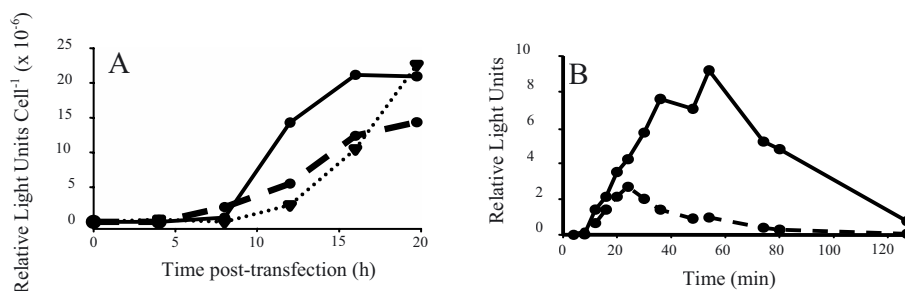


**Figure 2. Luciferase expression by synchronised cell populations.** *A:* CHO-S cells were synchronised by treatment with nocodazole (solid) or hydroxyurea (dots) 15h then transferred to fresh medium and transfected with a reporter plasmid encoding luciferase. *B:* As for A except nocodazole was maintained in culture medium post-transfection.

## 4. CONCLUSIONS

PEI-mediated transfection is increasingly being used as a means to transiently express recombinant proteins in mammalian cells. However, at present the mechanisms of DNA uptake and delivery to the nucleus are still poorly understood. We have demonstrated that manipulation of the transfection complex through the optimisation of PEI to DNA ratio and the addition of bovine serum albumin can increase expression levels dramatically. We have also shown that manipulation of the cell cycle with small molecule effectors can have the same effect. We are now using these strategies developed at small scale to maximise transient gene expression at scale.

YAO-MING HUANG, THU HUYNH, LE LY, WOLFGANG NOE,  
DAVID Y. H. CHANG

## DEVELOPMENT OF FED-BATCH PROCESS PRODUCING MONOCLONAL ANTIBODIES USING IN-HOUSE MEDIA

*IDEC Pharmaceuticals Co, Cell Culture Process Sciences, 11011 Torreyana  
Road, San Diego, CA 92121, USA*

**Abstract.** IDEC Pharmaceuticals has devoted efforts for maximizing monoclonal antibody (MAb) production to fulfill increasing clinical and market demand. Cell Culture Process Sciences is equipped with numerous 5L stirred-tank bioreactors that provide cultures a well-controlled environment suitable for parameter studies during early stages of process development. In-house medium development is an ongoing effort to ensure the full ownership of IDEC Mabs manufacturing process. Manipulation of amino acid contents in both basal and feed media can effectively promote cell growth and control toxic by-products. A harvest titer of 1-2 g/L MABs in a two-week fed-batch process is routinely achieved using IDEC-owned in-house medium. The resulting volumetric productivity is over 100 mg/L/day, comparable to a process using vendor's proprietary medium.

### 1. INTRODUCTION

Fed-batch culture is a frequently used method for the industrial manufacture of cell culture based recombinant therapeutic proteins. Process improvement often relies on a good basal medium as well as feeding strategies. This paper presents a few case studies of process improvement through manipulation of medium components using IDEC in-house media.

### 2. STRATEGY AND METHODS

#### *2.1. Cell culture*

The cell lines are DG44 derived CHO adapted to suspension in serum-free medium prior to the banking. They are maintained in chemically-defined media, including vendor's proprietary medium and IDEC's in-house medium.

For the bioreactor cultivation of CHO cells, an Applikon™ reactor with a working volume of 3L was used. The pH was adjusted using CO<sub>2</sub> gas and Na<sub>2</sub>CO<sub>3</sub>. Cell concentration and viability were estimated by trypan blue dye exclusion. The metabolites, including glucose, lactate, ammonium, and dCO<sub>2</sub> were measured using a Nova Bioprofile.

#### *2.2. In-house medium development*

IDEC's in-house medium is consisted of commonly used commercial media, enriched with trace elements, vitamins, and certain salts, to establish a balanced medium for generic IDEC cell lines. A fluorescent-based well plate assay was developed to facilitate identification of critical supplements and their optimal dosage. Medium development occurred concurrently with fed-batch process development to expedite the optimization process.

Amino acid analysis was performed using a reverse phase High Performance Liquid Chromatography (Agilent 1100) with the Zorbax Eclipse-AAA 75 mm columns.

### 3. RESULTS AND DISCUSSION

Table 1 summarizes that combinations of three amino acids (A1; A2; A3) in the basal medium have a significant impact on the specific growth rates and ammonium accumulations for the first three days of bioreactor cultivation. The best A1/A2/A3 ratio (0.5/1/1) sustained a high specific growth rate while reducing ammonium production.

Table 1. Basal medium composition affects growth rate and ammonium accumulation

A1/A2/A3 in basal medium (relative to 1X)	Specific Growth Rate ( $\text{day}^{-1}$ )	$\text{NH}_4^+$ Accumulation (mM)
0 / 0.1 / 9	$0.62 \pm 0.05$	$1.05 \pm 0.07$
0.5 / 0.5 / 5	$0.74 \pm 0.03$	$2.59 \pm 0.17$
0.5 / 1 / 1	$0.83 \pm 0.04$	$2.90 \pm 0.06$
1 / 1 / 1	$0.83 \pm 0.04$	$5.13 \pm 0.62$

Feed medium is generally based on the basal medium with minor adjustments made according to metabolite profiles. Figure 1 indicates that varying two amino acids (A3/A2) in the feed stream led to various levels of ammonium accumulation in 2-week fed-batch process. The resulting cumulative integrated cell growth (cICG) and titers were also greatly affected, as shown in Figure 1.

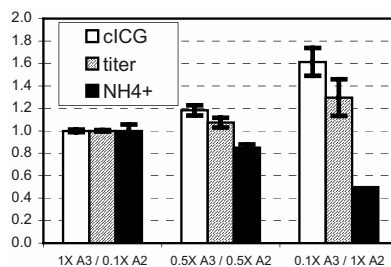


Figure 1. Impact of A3:A2 ratio in feed medium on fed-batch culture

To control toxic metabolite accumulation, some non-essential amino acids may be kept under rate-limiting conditions. It is observed that cumulative AA uptake rates are notably higher when feed amounts are doubled, even though there is no depletion of essential amino acids in the regular amount of feed (Figure 2). The antibody productivity did not improve with increasing amount of feeds or elevated AA uptake rates. Therefore, for a cost-efficient feeding strategy, it may be necessary to apply the concept of metabolism shift to boost titer performance.

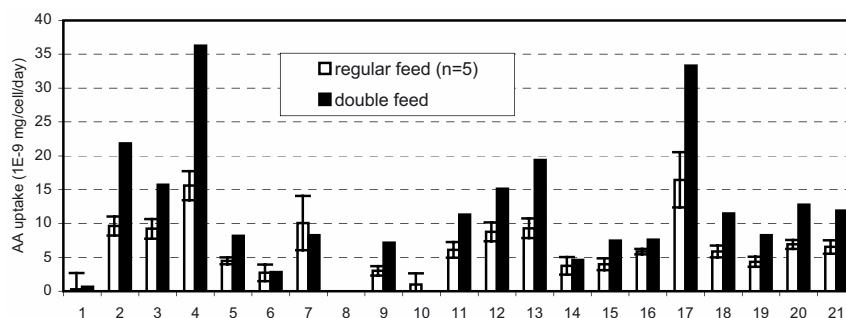


Figure 2. Cumulative amino acid uptake rates in response to double amount of feeds

Applying IDEC’s in-house medium from one cell line to other cell lines has proved successful with little adjustments needed (Figure 3). The fed-batch process using in-house medium delivered a volumetric productivity greater than 100 mg/L/day in fully amplified cell lines, comparable to optimized processes using vendor’s proprietary medium.

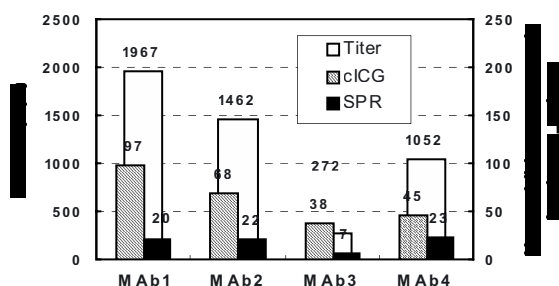


Figure 3. Applicability to 4 Mab Production

#### 4. CONCLUSIONS

Complete ownership of medium formulation can ensure full freedom of operation in process improvement as well as full control of vendor sourcing and medium quality. The insights gained during medium development also helped the optimization of cell-specific supplements and the elimination of unnecessary components in feeds.



KALLEL H. <sup>1</sup>, BELLILA A. <sup>1</sup>, FATHALLAH D. M. <sup>2</sup>

## PRODUCTION OF AN ANTI $\beta$ 2 INTEGRIN MONOCLONAL ANTIBODY BY A HYBRIDOMA CELL LINE GROWN IN A 2 LITER BIOREACTOR

<sup>1</sup> : *Viral Vaccines Research & Development Unit*

<sup>2</sup> : *Molecular Biotechnology Group, Laboratory of Immunology  
Institut Pasteur de Tunis. 13, Place Pasteur. BP 74. 1002 Tunis. Tunisia*

### INTRODUCTION

Anti  $\beta$ 2 integrin monoclonal antibodies hold a great potential for preventing inflammation-mediated tissue injuries in several pathological conditions. We have studied the production by a hybridoma cell line of monoclonal 107, an antibody that blocks the function of the human leukocyte adhesion molecule, CR3 or  $\beta$ 2 integrin CD11b/CD18. This antibody recognizes specifically the A-domain of the CD11b  $\alpha$  subunit. The overall aim of this work was to optimise the production of this antibody by a hybridoma cell line grown in a stirred tank bioreactor.

### MATERIALS & METHODS

*Cell line (Hybridoma)* : the 107 murine hybridoma was used throughout this study. This cell line produces an IgG2a monoclonal antibody.

*Culture medium* : RPMI-1640 was supplied by Invitrogen (Glasgow, UK). Foetal calf Serum (FCS) and bovine serum enriched with iron (NS) were obtained from Hyclone (Logan, USA).

*Culture conditions* : Cultures were carried out in 250 ml spinner flasks containing 200 ml of cultured cells, at 37°C in a 5% CO<sub>2</sub> incubator. The spinners were inoculated with 2x10<sup>5</sup> cells/ml. The experiments were carried out in duplicate. Samples were taken daily for cell count and for the measurement of glucose, lactate, ammonia, pH and antibody levels.

*Bioreactor cultures* : The cultures were performed in a 2 L bioreactor (Inceltech, France) equipped with a pitched blade impeller and a spin filter (pore size : 5 $\mu$ m) fixed on the axis. During cell culture proliferation step, the following conditions were applied : pH = 7.2, pO<sub>2</sub> maintained at 30 to 50%, temperature = 37°C and agitation rate = 20 to 35 rpm.

Perfusion was started after two days of culture. Perfusion rate was modulated according to cell density.

Samples were taken daily to determine cell density, cell viability, glucose, lactate, ammonia and antibody levels.

*Analytical methods* : The viable and total cell concentrations were determined using a hemacytometer and the trypan blue exclusion method.

Glucose and lactic acid concentrations were monitored by enzymatic assays, using glucose and lactate assay kits from Chronolab (Switzerland).

Ammonia level was quantified enzymatically by the UV-test Cat. N°. : 171-UV (Sigma, St. Louis, USA).

*ELISA test* : Immulon-2 ELISA plates were coated with recombinant protein, CD11b A-domain (2µg/well) at 37°C for 1 hour. Plates were washed once with PBS buffer, then blocked with 1% BSA at room temperature for 1 hour. After washing three times with 0.05% Tween 20, plates were incubated with MAb 107 (hybridoma culture supernatant diluted with PBS-1%BSA) at room temperature for 1 hour. After incubation, plates were washed three times, then incubated with a second MAb, goat anti mouse IgG conjugated with peroxydase (Sigma) at room temperature for 1 hour. Plates were then washed three times and incubated with the peroxydase substrate : o-phenylenediamine/H<sub>2</sub>O<sub>2</sub> (Sigma) for 30 minutes at room temperature. The results were quantitated using an ELISA plate reader at 492 nm.

## RESULTS

### *Effect of serum type and concentration on 107 hybridoma cell growth*

To optimize 107 hybridoma cell growth, we investigated the effect of serum type as well as serum concentration.

*Table 1 : 107 hybridoma cell growth and monoclonal antibody in different media. Cells were grown in spinner flasks.*

	<b>5% NS</b>	<b>10% NS</b>	<b>5% FCS</b>	<b>10% FCS</b>
Cell density/ml	0.73x10 <sup>6</sup>	1.2x10 <sup>6</sup>	0.6x10 <sup>6</sup>	10 <sup>6</sup>
Maximum specific growth rate (h <sup>-1</sup> )	0.026	0.038	0.027	0.031
MAb level (µg/ml)	29	32	28	31

As shown in Table 1, RPMI 1640 supplemented with 10% NS, resulted in the highest cell density and antibody level. Similar data were reported by Kallel et al. (2002) for another hybridoma cell line which produces an  $\beta$  2 integrin monoclonal antibody.

*Optimisation of cell growth and monoclonal antibody production in a 2-L bioreactor**Effect of inoculum viability**Table 2 : Effect of inoculum viability on 107 hybridoma cell growth in a 2-L bioreactor. The cells were grown in RPMI 1640 + 10% NS.*

	<b>Culture n°1</b>	<b>Culture n°2</b>	<b>Culture n°3</b>	<b>Culture n°4</b>
Inoculum viability (%)	66	71	75	77
Cell density/ml	0.24x10 <sup>6</sup>	0.245x10 <sup>6</sup>	1.5x10 <sup>6</sup>	1.8x10 <sup>6</sup>
Culture duration (day)	4	3	8	15

During cultures 1 and 2, we observed a cell density decrease one day after the inoculation of the bioreactor. However, for cultures 3 and 4, we noticed a cell growth. This behaviour is due to the viability of the inoculum used to start the different cultures.

To grow 107 hybridoma cells in a bioreactor, the viability of the inoculum should be higher than 75%.

*Table 3 : 107 hybridoma cell growth on RPMI 1640 +10% NS, in a 2-L bioreactor. The cultures were aerated continuously by air injection in the head space of the bioreactor and by sparging when necessary. Agitation rate was set at 30 rpm and pO<sub>2</sub> at 50%.*

	<b>Cell density/ml</b>	<b>Culture duration (day)</b>
Culture 1	0.598x10 <sup>6</sup>	4
Culture 2	0.720x10 <sup>6</sup>	3

Although both cultures were started with an inoculum viability higher than 75%, we observed a cell density decrease two days after the start of the culture. Monitoring of glucose level indicates that this nutrient is not limiting. Therefore, the decrease of cell density level observed is probably due to shear stress.

*Perfusion culture of 107 hybridoma cells*

To minimize shear stress effect on 107 hybridoma cell growth, agitation rate and pO<sub>2</sub> were reduced respectively to 20 rpm and 30%. The cultures were aerated continuously by air injection in the head space of the bioreactor but direct sparging was intermittent.

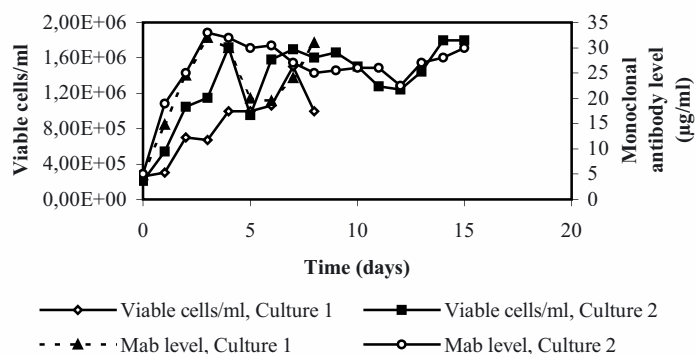


Figure 1 : Cell growth and antibody production in a 2-L bioreactor. The cells were grown in RPMI 1640 +10%NS in perfusion mode.

In these culture conditions and compared to the previous cultures, we reached a high cell density level ( $1.8 \times 10^6$  cells/ml). Cell viability was maintained around 80% during both cultures. The highest antibody concentration obtained was equal to 32  $\mu\text{g/ml}$ .

### CONCLUSION

We showed that in spinner flask, 107 hybridoma cell growth was optimal in the medium RPMI 1640 + 10%NS. In a 2-L bioreactor, we demonstrated that inoculum viability and shear forces affected cell growth. In the optimal conditions determined, we obtained a cell density level of  $1.8 \times 10^6$  cells/ml. Monoclonal antibody concentration and the specific productivity were equal respectively to 32  $\mu\text{g/ml}$  and 25  $\mu\text{g}/10^6$  cells/day.

### REFERENCES

- Héla Kallel, Hend Zaïri, Samia Rourou, Makram Essafi, M.Ridha Barbouche, Koussay Dellagi and Dahmani M. Fathallah (2002). Optimization of a hybridoma cell line growth and antibody production in a spinner flask using a Taguchi experimental design. *Cytotechnology*, 39, 9-14.

MIRIAM MONGE<sup>1</sup>, ANDREW SINCLAIR<sup>2</sup>

## ECONOMIC EVALUATION OF DISPOSABLES VS STAINLESS STEEL WITHIN A MODULAR PILOT PLANT FACILITY - A COMPARATIVE ANALYSIS

(1) *STEDIM, S.A. Aubagne, France*

(2) *Biopharm Services Ltd., Pharmadule-Modular pilot plant facility design,  
UK*

### INTRODUCTION

In a biopharmaceutical manufacturing environment where there are concerns about cost and capacity availability, companies need to take time to analyze their processes and look at the technology available allowing process optimization.

In this paper we present a Process comparison & Cost of Goods model comparing two technologies used in biomanufacturing:

- 1) Single-use disposable bag technology
- 2) Traditional stainless steel vessels.

The facility design of a Modular pilot plant facility using disposable technology has also been developed based on the above study in collaboration with **Pharmadule**. This will be presented in the Poster presentation .

### THE CONCEPT OF SINGLE-USE DISPOSABLE BAG TECHNOLOGY

Single-use bag systems manufactured in a range from 50ml to 3000L are intended to replace glass bottles or stainless steel vessels used for sterile fluid handling in biopharmaceutical manufacturing. The bag systems are provided pre-assembled, sterile and pyrogen-free, ready for process-use. The systems can be customized according to customer specifications.

### APPLICATIONS.

The bags can be used for a wide variety of bioprocess applications in USP and DSP, the most common being:

- Open bag systems for media and buffer formulation before sterile filtration
- Closed bag systems for storage of media, buffer, intermediate and bulk final product

- Manifold systems - a series of interconnected bags around a common central filling line allowing simultaneous distribution and sterilization of the fluid stream (in many cases the manifolds are fitted with a disposable sterilizing filter capsule on the filling line, 0.2 or 0.1 $\mu$ )

### QUALITY & VALIDATION

The bag systems are manufactured according to GMP and are tested according to US and European Pharmacopoeias, biocompatibility testing is carried out according to ISO 10993<sup>1</sup>. Chemical compatibility testing of bags and solutions is carried out according to ASTM<sup>ii</sup>. A model solvent approach has been developed by STEDIM for an extractables testing programme.

#### *INTRODUCTION TO THE PROCESS COMPARISON & COST OF GOODS MODEL*

The objectives of the simulation comparing the two technologies for sterile fluid handling in process are:

- Optimisation of capital requirements by maximizing asset utilization
- Measuring production rates
- Optimising production

### BASIS

The basis for the comparison is a commercially relevant monoclonal antibody process. Using information in the public domain we were able to put together a process operation that mimics many industrial operations. The manufacturing route adopted consists of a fermentation system run at 2000L scale. This scale of operation was selected on the basis that this is a common size employed for the supply of clinical quantities of material and for in market supply for the smaller indications. It also is a scale of operation that can be accommodated by commercially available disposable bag systems ranging from 50L to 2000L.

The modelling technique used is discrete event modelling as opposed to continuous modelling. Discrete event deals with time related events, mapping process sequences as opposed to continuous modelling that simulates time through equations.

The modeled process consists of the following operations covering the production of the monoclonal antibody from inoculation of the seed fermenter through to bulk purified sterile filtered product:

Seed fermenter, Production fermenter, Harvest centrifuge, UF concentration diafiltration, Protein A chromatography, UF concentration diafiltration, Ion exchange chromatography, UF concentration diafiltration, Gel permeation chromatography

The output from this manufacturing operation would supply a fill finish operation. Disposable bag technology is used wherever it is technically feasible within the process operation, namely Product hold, Media & Buffer hold. Vessel liners are used for all other operations where a quick changeover is required between batches and where the operation is not sterile, namely media & buffer prep.

#### ANALYTICAL APPROACH

- A resource constrained time based simulation was used as the basis for the analysis. This allowed a comparison of two parallel production lines of the same size. The main difference between the two production lines is that one uses disposable bags and the other uses stainless steel vessels. Both lines use the same production data.

#### COST OF GOODS ANALYSIS

At the end of a simulated operation the process simulation model automatically transfers key performance data to the COG spreadsheet such as:

- Capital requirements for:

CIP, Utility Systems, number and size of hold vessels used by the Vessel Sub Model,

□ Number of containers to support the large volume disposable bags required for the Disposable Sub Model

- Material Consumptions per Batch:

All critical utility consumptions, CIP chemical usage

- Number of disposable bags used by the Disposable sub model

Production rate

Outcomes:

<b>Capital Estimate</b>	
Stainless Steel Vessel Sub Model	€ 26,000,000
Disposable Bag Sub Model	€ 18,500,000
Overall Capital Saving	29%

*Table A Capital Requirements for the Two Sub Models*

There is a significant (29%) reduction in the capital requirement for the single use disposable bag production line compared to that required for the one based on stainless steel vessels (Table A). This is a result of a reduced requirement for CIP by the disposable bag sub model. For example the WFI generation capacity required for the disposable bag sub model is around 400L/hour however the stainless steel vessel sub model requires 1500L/hour of WFI capacity to achieve the same production rate. This effect is seen throughout the utility systems. Together with the reduced

vessel count and CIP requirement of the disposable bag sub model, this results in a capital saving of around € 7,5 million.

Does this reduction in capital result in a reduced cost of goods for the monoclonal antibody? In this analysis it does. Capital is factored in an amortized charge: this is based upon an 8 year plant life and 15% cost of capital and 5% residual value in the plant after the 8 years. In addition, for the disposable bag sub model there are higher consumable costs resulting from bag use. These are offset by utility savings and savings in quality costs. In this analysis it is estimated that the quality head count would be reduced by 5 for the disposable sub model, resulting from a reduced ongoing cost requirement for CIP & SIP annual validation and reduced paper work. The overall impact is a saving of 11% on the cost of goods resulting from a new plant installation based on disposable bags when compared to one based on stainless steel vessels.

#### OTHER ASPECTS COVERED IN THE POSTER PRESENTATION:

- Comparison of the environmental impact of the two technologies through the simulation
- Validation survey comparing Validation requirements for each technology
- Possible impact of the new disposable Aseptic Connector (ACD) on facility design
- Facility design Study carried out with Pharmadule, designing a modular pilot plant facility based on disposables around the given Process model. This facility demonstrates:
  - Once through material flow
  - No recycle
  - No wash up or Clean autoclave
  - Minimal CIP & Utilities

---

<sup>i</sup> ISO 10993-1, Biological Evaluation of Medical Devices

<sup>ii</sup> ASTM D1239-98, Standard test method for resistance of plastics films to extraction by chemicals.



JOHN CROWLEY<sup>1\*</sup>, CARINA SCHLUKEBIR<sup>1</sup>,  
MAIKEL DIJKSTAL<sup>1</sup>, SUZAN HOEKSMAS<sup>1</sup>, EDITH OLT HOF<sup>1</sup>,  
STEFANIE HUßMANN<sup>2</sup>, SYBILLE ESSER<sup>2</sup>, ANDREAS HERRMANN<sup>2</sup>,  
JOSE M. COCO MARTIN<sup>1</sup>, ROBERT HOF<sup>1</sup>.

## CGMP MANUFACTURING OF A FUSION PROTEIN IN MAMMALIAN CELLS USING A LARGE-SCALE ACOUSTIC PERFUSION SYSTEM.

<sup>1</sup> *DSM Biologics, Research & Development, P.O Box 424, 9700 AL  
Groningen, Netherlands.*

<sup>2</sup> *Cardion AG, Max-Planck straÙe 15a, D-40699 Erkrath, Germany.*

*\*John.Crowley@dsm.com*

### 1. INTRODUCTION

The constituents of a biotechnological broth are many and varied, but in general they can be grouped into classes either by size or function. A perfusion set-up involves the separation of various components of this broth so that cells are retained, harvest is captured and medium refreshment occurs. The increasing use of serum, protein and mammalian source free medium for the manufacture of biopharmaceuticals from mammalian cells has led to variable performance within a classical spin filter perfusion system. In this development, scale-up and GMP manufacturing program, the use of an acoustic cell retention system was investigated.

In this program, the influence of (a) temperature, (b) power input, (c) frequency selection and (d) medium flowrate on the 200L/day system was investigated using a CHO-K1 cell line producing a fusion protein in protein free medium. Each of these parameters was optimised which resulted in significantly higher, stable cell retention. A validation of the acoustic system was performed prior to cGMP manufacturing. The optimised set-up and system settings for the 200L/day system were successfully used during what is believed to be the world's first cGMP production run using the acoustic device at this scale.

### 2. MATERIALS & METHODS

One vial of a CHO-K1 MCB vial frozen in HyQ PF medium (Perbio, Netherlands) was used to inoculate a 100L working volume reactor. A 200L Biosep acoustic chamber with ASP991 controller (Applisens, Netherlands) was used as a cellular retention system.

## 3. RESULTS

Figures 1 to 4 were generated using a viable cell density of  $5 - 6 \times 10^6$  cells/ml.

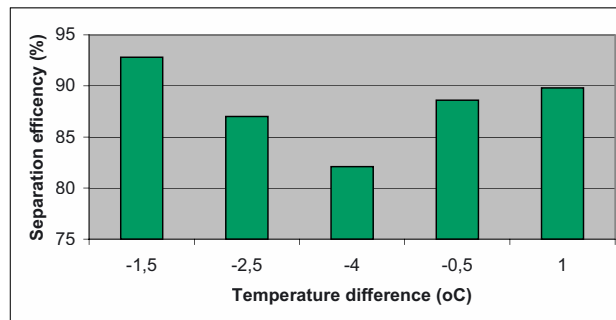


Figure 1: Separation efficiency (%) versus temperature difference ( $^{\circ}$ C) between cultivation temperature in fermenter and acoustic retention chamber for a 200L/day acoustic retention.

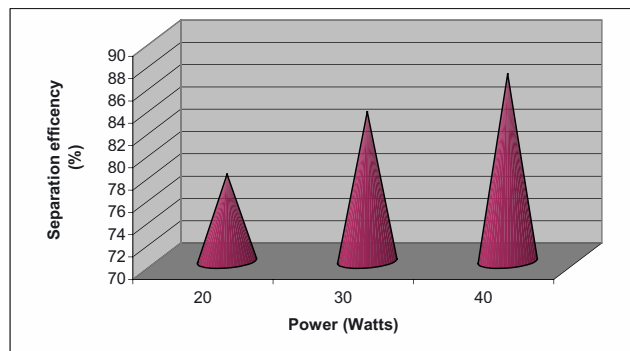


Figure 2: Separation efficiency (%) versus power usage (Watts).

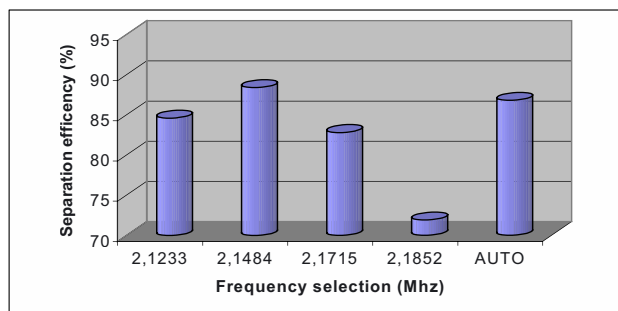


Figure 3: Separation efficiency (%) versus frequency selection (Mhz).

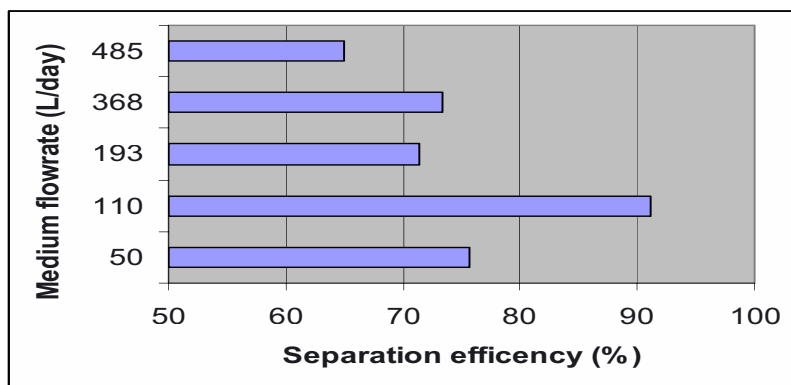


Figure 4: Medium flowrate (L/day) versus separation efficiency (%).

#### 4. SUMMARY & CONCLUSIONS

- ❖ Figure 1 demonstrates that separation efficiency is influenced by the temperature surrounding the acoustic chamber as a result of convective forces. A temperature difference of 1 – 1.5<sup>0</sup>C between the cultivation temperature in the reactor and temperature of the cooling chamber surrounding the acoustic chamber yielded the optimal performance.
- ❖ Figure 2 demonstrates the influence of power on separation efficiency. An increase in power improved separation efficiency up to a limit (other data not shown). A power setting of 40W yielded the best performance for this parameter.
- ❖ Figure 3 shows the influence of frequency selection on separation efficiency. 2.14MHz gave the best performance at this time point (during

steady state) however automatic frequency selection gave improved performance during logarithmic growth as the matrix was changing significantly (data not shown) hence affecting the acoustic field generated.

- ❖ Figure 4 shows the influence of medium flowrate on the separation efficiency. A flowrate of 110L/day gave the best performance at >90% cellular retention, however 485L/day still gave a separation efficiency of 63% demonstrating that this method appears to have significant potential for larger volume flowrates.

MCF DALM<sup>1,3</sup>, SMR CUIJTEN<sup>1</sup>, WMJ VAN GRUNSVEN<sup>1</sup>,  
A OUDSHOORN<sup>2</sup>, J TRAMPER<sup>3</sup> AND DE MARTENS<sup>3</sup>

## INFLUENCE OF CULTURE PARAMETERS ON VIABILITY IN PERFUSION PROCESS

<sup>1</sup> *Diosynth BV, PO Box 20, 5340 BH Oss, The Netherlands*

<sup>2</sup> *Applisens, De brauweg 13, 3125 AE Schiedam, The Netherlands*

<sup>3</sup> *Wageningen University, Department of Agrotechnology and Food sciences,  
Process engineering group, PO Box 8126, 6700 EV Wageningen,  
The Netherlands*

### INTRODUCTION

In many perfusion processes low viabilities are obtained during the production phase. A low viability may cause negative effects on product quality, which results from the release of proteases and neuraminidases from dead cells. Furthermore, intracellular proteins and cell debris interfere with down-stream processing and measurement and control of the process.

### OBJECTIVE

Determine if the viability in perfusion processes can be increased through changing the feed and bleed rate within the ranges used in production processes.

### MATERIALS AND METHODS

Hybridoma cells were cultured in a chemically-defined protein-free medium. Perfusion bioreactor runs were performed at a dilution rate of 0.5, 1.0 and 1.5 per day and at a bleed rate of 0.05, 0.10 and 0.20 per day. The BioSep (Applisens, NL) was used as cell retention device (figure 1). Viable and dead cell concentrations as well as the intra- and extracellular lactate dehydrogenase activities were measured daily.

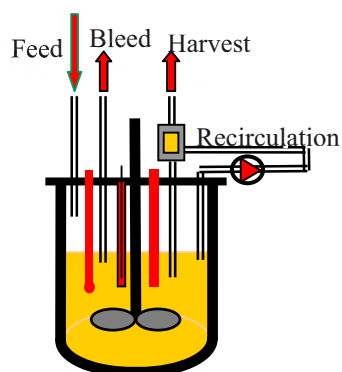


Figure 1. Experimental set-up perfusion bioreactor

## RESULTS AND DISCUSSION

Figure 2 shows that at a bleed rate of  $0.2 \text{ d}^{-1}$  the viability remained constant around 72% at all dilution rates. While in the bioreactor runs operated at a bleed rate of 0.05 and  $0.10 \text{ d}^{-1}$  the viability increased with dilution rate. However, lower viabilities were obtained.

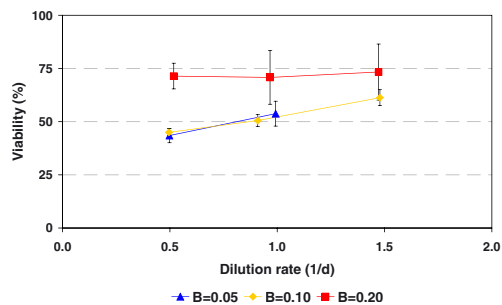


Figure 2. Viability in steady state at different feed ( $D$ ) and bleed ( $B$ ) rates

Figure 3 reveals that at a bleed rate of 0.1 and  $0.2 \text{ d}^{-1}$  the specific death rate was independent of the feed rate, with the distinction that the specific death rate at a bleed of  $0.2 \text{ d}^{-1}$  was significantly lower. At a bleed rate of  $0.05 \text{ d}^{-1}$  the death rate increased with dilution rate.

The viability is dependent on the death rate, bleed rate and lysis rate. This could explain the obtained differences in viabilities at the different feed and bleed rates.

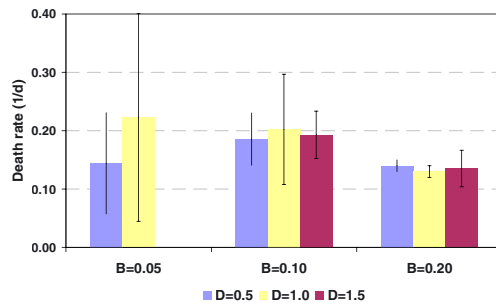


Figure 3. Death rate in steady state at different feed (D) and bleed (B) rates

### CONCLUSION

Even at low bleed rates a relatively high viability during the production phase can be attained. At a bleed rate of  $0.2 \text{ d}^{-1}$  a constant viability and death rate are obtained. This result is significantly different when compared to the other two bleed rates, where an increase in viability is observed at increasing dilution rates. Furthermore a higher death rate was observed at these two bleed rates. Further insight in the mechanism behind the observed relations should lead to an optimal choice of parameter settings.

### ACKNOWLEDGEMENTS

This work was supported by the ministry of economic affairs SENTER program contract nr BTS00093.

E.A. ELSAYED<sup>1</sup>, G.-W. PIEHL<sup>1</sup>, J. NOTHNAGEL<sup>1</sup>,  
R.A. MEDRONHO<sup>2</sup>, W.-D. DECKWER<sup>3</sup>, R. WAGNER<sup>1</sup>

## USE OF HYDROCYCLONE AS AN EFFICIENT TOOL FOR CELL RETENTION IN PERFUSION CULTURES

<sup>1</sup>*Cell Culture Technology, GBF, Braunschweig, Germany*

<sup>2</sup>*Chemical Engineering Dept., Federal University, Rio de Janeiro, Brazil*

<sup>3</sup>*Biochemical Engineering, Technical University, Braunschweig, Germany*

**Abstract.** A new specially designed hydrocyclone was successfully applied as cell separation system in 6-L and 30-L continuously perfused bioreactors. Cell concentration reached up to 10 million per mL and viability remained above 90 % for HeLa and CHO cells during operation.

### 1. INTRODUCTION

Several cell separating devices are used for retaining cells in the bioreactor during perfusion cultures. These devices are usually based on centrifugal force (centrifuges, hydrocyclones), filtration (spin-filters, tangential flow filters, dynamic filters), gravitational settling, ultrasonic and dielectrophoretic separation.

Although hydrocyclones use the same separation principle as centrifuges (sedimentation in a centrifugal field), they have no movable parts, the vortex motion is performed by the fluid itself, and stable eddies are generated by the high velocity of the tangential flow of the suspension. Moreover, they do not have high precision components which are expensive to manufacture and to operate. These properties suggest hydrocyclones for separating animal cells in continuously perfused bioreactor systems. However, few applications of hydrocyclones in animal cell processes have been reported so far. The reasons are, on the one hand, the low separation forces (density difference and organism size), and on the other hand, the high velocities required for reasonable separation efficacies combined with the unavoidable shear forces. In the present work we used a hydrocyclone, specially designed to avoid these disadvantages, for separating HeLa and CHO cells in continuously perfused bioreactors.



## 2. MATERIALS AND METHODS

### 2.1. Hydrocyclone

A new, specially designed double tangential inlet-hydrocyclone was used for cell retention. It is characterized by an overflow pipe diameter of 2 mm and an underflow orifice diameter of 2.5 mm.

### 2.2. Cell Lines and Culture Conditions

The recombinant Chinese hamster ovary cell line CHO-3D6 producing human anti-HIV antibody, kindly provided by Polymun Scientific (Vienna, Austria), was cultivated in protein-free SMIF6 medium (Invitrogen GIBCO-BRL Life Technologies, Paisley, UK). HeLa cells were cultivated in Hybridomed DIF-1000 medium (Biochrom, Berlin, Germany) supplemented with albumin, insulin and transferrin. 0.1 % Pluronic F68 was always added to the media. Both, CHO-3D6 and HeLa cells were cultivated in 1-L spinner flasks (Techne, Cambridge, UK) and then inoculated to a 6-L bubble-free aerated membrane bioreactor. The 30-L pilot membrane bioreactor (Bioindustrie Mantovane, Italy) was fully automated (Ubicon, GBF) and controlled by online glucose monitoring (Trace, Braunschweig, Germany). Cell culture process parameters were analysed by using standard methods.

### 2.3. Experimental Set-Up

The hydrocyclone was installed in the bioreactor system via an external recycling loop. Perfusion was performed by intermittent operation according to the glucose concentration using a pulsation-free pumphead (505L Watson-Marlow) equipped with a double tubing device (Marprene<sup>®</sup>, 9.6/2.4 mm).

## 3. RESULTS AND DISCUSSION

### 3.1. Cultivation of HeLa and CHO Cells in the 6-L Bioreactor

HeLa cells propagated in spinner flasks were transferred to the 6-L bioreactor resulting in an initial cell concentration of  $4.3 \times 10^5 \text{ mL}^{-1}$ . Within the first cultivation phase of 50 hours, the cell concentration increased to  $1.76 \times 10^6 \text{ mL}^{-1}$ , and glucose reached its minimal concentration of  $0.3 \text{ g L}^{-1}$ . Subsequently, hydrocyclone was started for perfusion to maintain glucose concentration above  $0.5 \text{ g L}^{-1}$ . The hydrocyclone was operated intermittently (3 min every 2-3 h) during the 12 days of perfusion. Viable cell concentration reached a maximum of  $1 \times 10^7 \text{ mL}^{-1}$  and cells grew with a growth rate of  $0.0124 \text{ h}^{-1}$  after 8 days resulting in a population

doubling time of  $2.3 \text{ d}^{-1}$ . Viability remained above 94 % for the whole cultivation process. In addition, the perfusion rate varied according to cell concentration reaching its maximum at the end of the cultivation with 1.83 reactor volumes a day.

CHO-3D6 cells cultivation in the 6-L bioreactor was started with a cell concentration of  $2.3 \times 10^5 \text{ mL}^{-1}$ . Cells grew with an adaptation phase of about 75 hours. Exponential growth started at a cell concentration of  $6.1 \times 10^5 \text{ mL}^{-1}$ . After 120 hours, when glucose reached its minimum concentration of  $0.8 \text{ g L}^{-1}$ , the hydrocyclone perfusion was started intermittently to maintain glucose above this level. After 235 hours of exponential growth with a rate of  $0.02 \text{ h}^{-1}$ , the cell concentration reached its maximum ( $3.9 \times 10^6 \text{ mL}^{-1}$ ). Viability was always above 90 %. The cell separation efficiency during the perfusion by the hydrocyclone was maintained above 85 %.

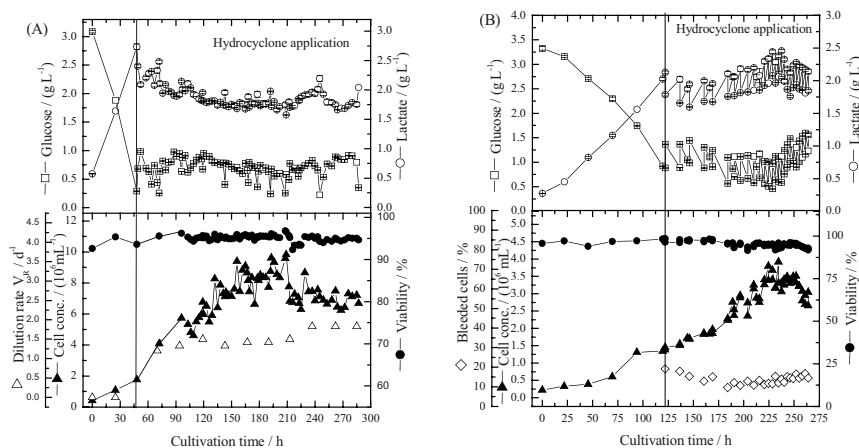


Figure 1. Cultivation of HeLa cells (A) and CHO-3D6 cells (B) in a continuously perfused 6-L bioreactor using a hydrocyclone.

### 3.2. Cultivation of HeLa Cells in a 30-L Continuously Perfused Bioreactor

Comparable performance of the hydrocyclone operation in a fully automated continuously perfused 30-L bioreactor has been obtained using the same hydrocyclone configuration as in the 6-L system (data not shown). Perfusion was started after 41 hours to maintain glucose above the minimum level. The cells grew exponentially with a growth rate of  $0.04 \text{ h}^{-1}$  up to a concentration of  $2.6 \times 10^6 \text{ mL}^{-1}$  after 90 hours. Viability remained above 93 % during the whole process.

#### 4. CONCLUSION

Hydrocyclones can be efficiently used as perfusion systems in continuous mammalian cell culture processes maintaining a viability above 90 %.

During the quasi steady state period of cultivation in 6-L bioreactors, the hydrocyclone was operated for 3 minutes within 2 hours at a flow rate of  $1 \text{ L min}^{-1}$  generating  $\Delta P \leq 1$  bar and a separation efficiency  $\geq 0.85$ . This corresponded to a residence time of less than 0.2 s within the hydrocyclone volume of  $2.1 \text{ cm}^3$ . Provided the residence time in the hydrocyclone is not significantly changed this hydrocyclone performance can be maintained with any other perfusion system.

#### 5. ACKNOWLEDGMENT

This work was supported in part by the German Academic Exchange Service (DAAD).

FIGUEREDO A, NAVARRETE J., VITÓN P., MARTÍNEZ E.,  
CASTRO A. AND E. CHICO

## EFFECT OF DIFFERENT VARIABLES ON THE LONG-TERM SPINFILTER CLOGGING DURING PILOT-SCALE ANIMAL CELL PERFUSION RUNS

*Center of Molecular Immunology (CIM), P.O. Box 16040, Havana City  
11600. Cuba. email alvio@ict.cim.sld.cu*

**Keywords:** animal cells, perfusion, spinline, filter clogging.

### 1. INTRODUCTION

The spinline SF is one of the most popular retention devices used on the animal cell perfusion culture. Although fouling remains as the major drawback of this device, studies addressing this phenomenon on a long term basis are rarely found in the literature.

In this work several variables that affect the long term behaviour of the SF were examined during pilot scale runs. Cell passage factor was examined as a possible candidate for an early indicator of spinline fouling. Effect of cell concentration and soluble DNA concentration on run longevity was study.

### 2. MATERIAL AND METHODS

Cell lines and culture media: A transfectoma cell line derived from NSO myeloma, producing a monoclonal antibody and a recombinant CHO cell line producing rhEPO were used. Cells were grown on protein free or serum supplemented media. Bioreactor and spinline: Pilot scale (30 L) stirred tank bioreactors were purchase from CHEMAP AG. Spinline were of stainless steel and 20 µm of mesh opening.

Analytics: Cell counts were done by exclusion method using trypan blue, DNA concentration was measured by dot-blot.

Experimental protocol: NSO and CHO perfusion runs were carried out using the same feeding policy. Temperature, pH and DO were controlled in 37 C; 6,5 – 7,0 and 20 – 100 % with respect to air saturation respectively.

Calculations: Cell passage factor was calculated as the division of total cell concentration inside the spinline by the total cell concentration in the bioreactor. Cumulative values were calculated by numerical integration.

3. RESULTS

3.1. Cell passage factor

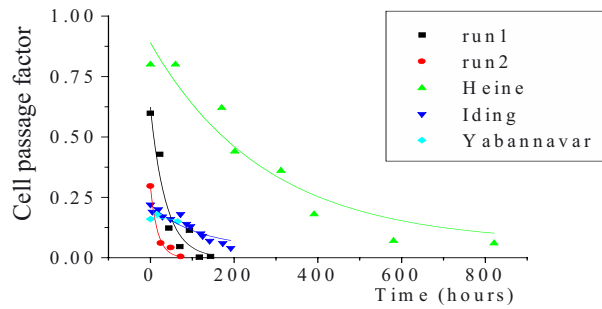


Figure 1. Profile of the cell passage ( $\alpha$ ) against time for perfusion runs. Two runs (run 1 and run 2) data are included together with 3 set of data found in the literature.

In figure 1, the profiles of cell passage factor of SF perfusion experiments including data extracted from the literature are shown. Table 1 shows the adjusted parameters of an exponential model describing the behaviour of  $\alpha$  in time.

Figure 2 shows right the average operational time and the average soluble cumulative DNA concentration of CHO (3 runs) and NSO (15 runs) perfusion runs. And left the total cumulative cell concentration (TCCC) inside/outside the SF vs. the operational time.

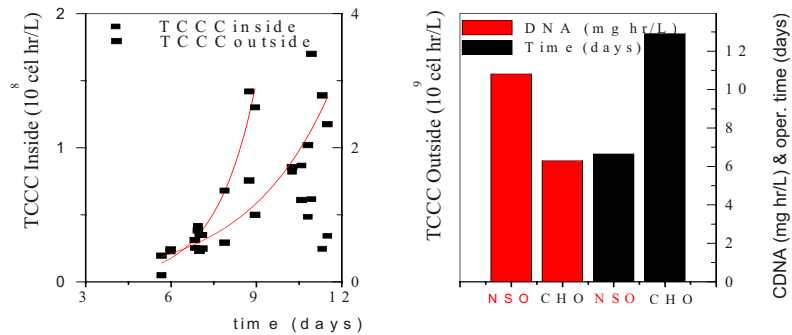


Figure 2. At right time (in days) elapsed before SF clogs and corresponding DNA cumulative (mg hr/L) concentration for NSO and CHO perfusion runs. Left: TCCC inside and outside the spinfilter at the time of clogging vs time of clogging.

Table 1. Adjusted parameters for exponentially falling function.

Reference	$\alpha_0$	$\beta(\text{hrs}^{-1})$	$r^2$	Number of data
Heine 1999	0,9232	0,081	0,94	7
Yabannavar 1994	0,2053	0,0091	0,95	5
Iding 2000	0,2377	0,008	0,92	12
Run 1	0,7731	0,0372	0,8176	7
Run 2	0,2935	0,0516	0,9394	4

#### 4. DISCUSSION

It can be seen from figure 1 and table 1 that the  $\alpha$  profile can be successfully adjusted to an exponentially falling function for several set of data. The sets of data corresponds to different conditions which provide clues about the possibility that such a behaviour is related to a general kinetic mechanism of obstruction for spinfilters rather than to an exception.

On the other hand, analysis of cumulative cell and DNA concentration in long term perfusion (figure 2 left) shows that CHO cells, which liberates less DNA, when compared with NSO cells, tend to clog less the SF. The role of this compound in the cell – sieve interaction is again observed (Esclade et al 1991).

The total cumulative cell concentration (TCCC) in the bioreactor exhibited a growing pattern as operational time increases as can be withdrawn from figure 2 right. This is consistent with the assumption that operational time is not a function of TCCC outside the SF. A similar trend is followed by the TCCC in the internal lumen of SF for runs which lasted less than 9 days where a similar conclusion to the previous can be taken. It is likely that runs that last less than 9 days were affected by overflowing of the SF which led to accelerated obstruction of it. A strikingly different behaviour for TCCC in the inside of the spinfiler is observed for runs which lasted more than 9 days. This observation leads to the conclusion that operational time is more sensitive to the amount of cell that are put in contact with the inner spinfiler surface than on the outer surface. (Trocha et al, 1997)

#### 5. REFERENCES

- Trocha M, von Rohr P. R. Sümeghy Z, 1997.. In Carrondo MJT (Ed) Animal cell technology. Kluwer. Dordrecht, p 405
- Esclade R. J. L, Carrel S, Péringer P. 1991. Biotechnol. Bioeng. 38: 159-168
- Iding K, Lüttermeyer D, Fraune E, Gerlach K, Lehmann J. 2000.. Cytotech. 34: 141-150
- Heine H, Biselli M, Wandrey C. 1999.. In: Bernard A, et al. (eds) Animal cell technology: Products from cells, Cells as products. Kluwer. Dordrecht. P 83
- Yabannavar, V. M., Singh, V., Connelly, N. V. 1994. Biotechnol. Bioeng. 43: 159-164.

Authors want to thank to the ESACT meeting organizing committee for the grant of a bursary to Figueredo A. to attend to the 18th ESACT meeting.

T. KEIJZER<sup>1</sup>, F. TRAMPLER<sup>2</sup>, A. OUDSHOORN<sup>1</sup>, H. V/D BERG<sup>1</sup>

## INTEGRATING ACOUSTIC PERFUSION IN MAMMALIAN CELL CULTURE: TEMPERATURE CONTROL

<sup>1</sup> *AppliSens, Schiedam, The Netherlands* <sup>2</sup> *Sonosep Technologies, Moedling, Austria*

### 1. INTRODUCTION

The BioSep cell retention system has a virtual (not physical) filter, which avoids clogging (Bierau, et al). The filter in the BioSep system is a field of standing waves, which are formed by exciting a ceramic transducer plate. Part of the energy that is applied to the transducer is transferred into heat. Therefore the BioSep systems should be cooled. The smaller systems (10L and 50L) are air cooled and the larger systems (200L and 1000L) are water cooled. The amount of heat that is produced is depending on the power that is applied to the system. However, the amount of power is not the only influence on the temperature in the system. Other parameters are the harvest flow rate, the temperature of the environment and the length of the recirculation loop. In this study several of these parameters were investigated to determine what settings are optimal for operating the different commercially available BioSep devices.

### 2. METHODS AND MATERIALS

All experiments were performed with a 7 L Applikon bioreactor with a 5L working volume. The bioreactor was heated to 37°C with a heating blanket controlled by an ADI 1030 controller. The BioSep 10 and 50L were placed on top of the bioreactor. Temperature was measured using thermocouples, placed as shown in figure 1. The thermocouple in the cuvette was placed in a metal tube. This was done to avoid any direct heating of the thermocouple by the field. The thermocouples in the recirculation loop were inserted into the liquid via a T-piece. The BioSep 200L was placed besides the bioreactor.

The BioSep 10L and 50L were cooled with compressed air (10-30L/min) of room temperature. The BioSep 200L had a circulating water jacket around the cuvette to assure that the temperature in the cuvette was homogeneous and similar to the bioreactor temperature. The circulating water temperature was set between 33 and 37°C.

For the BioSep 10L harvest line norprene food tubing size 14 was used, for the recirculation size 16 was used. With the BioSep 50L tubing size 16 was used for the harvest and size 15 for the recirculation. The BioSep 200L used size 35 for the harvest and the recirculation. For both the harvest and the recirculation line a variable speed pump was used. For each experiment the power was relative to the to harvest flow rate, at 0.6-1.2 W/L/day for the BioSep 10L and 0.2-0.4 W/L/day for the BioSep 50L and 200L. These power levels are used to maintain separation efficiencies above 95% in mammalian cell culture.

Most experiments were performed in demineralized water to determine temperature effects. Some experiments were done using a yeast suspension of 10 g/L in physiological salt solution (9 g/L NaCl in demi water), to determine the effect on the separation efficiency. Yeast was used as a model particle for mammalian cells. 10 g/L yeast is comparable to  $10 \cdot 10^6$  mammalian cells/ml, by volume. The separation efficiency was calculated by dividing the amount of cells in the harvest stream by the amount of cells in the suspension

$$Sep. eff. := \left(1 - \frac{C_h}{C_s}\right) * 100\% \quad (1)$$

with  $C_h$  = cell concentration in harvest and  $C_s$  = cell concentration is suspension. Cell concentrations were measured as described in Keijzer, et al.

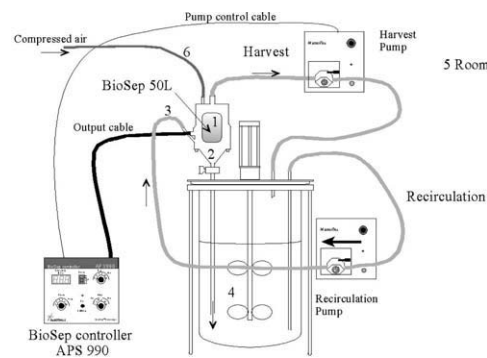


Figure 1: Experimental set-up of the temperature study with a 50L BioSep. Thermocouples were placed at position 1-6.

### 3. RESULTS

The temperature in and around the BioSep 10L was primarily influenced by two parameters, the flow rate of the recirculation and the power applied to the system.



Although the recirculation line was as short as possible (1.5m) the temperature decreased from 37°C to 25°C before it entered the BioSep, at 5L/day recirculation flow. When the recirculation flow was increased to 20L/day the temperature of the medium going into the BioSep increased to approximately 32°C. When the field was switched on the temperature in the BioSep increased 10 to 15°C. Air cooling was used to cool the temperature in the BioSep back to the bioreactor temperature. On average an air flow of 10L/min at 2W, 20L/min at 3W and 30L/min at 5 and 7W, was needed to reduce the temperature back to 37°C.

The temperature differences in the BioSep 50L were smaller. Again recirculation flow rate should have a minimal flow rate (50L/day in this case) to avoid that the recirculation temperature decreases below 33°C. Also the applied power did not effect the temperature in the cuvette as much as in the 10L, due to the lower power input per ml of medium. At 5W the temperature did not even increase above 37°C. At 7 W and 10W, air cooling of 20L/min and 30L/min, respectively, were sufficient to reduce the temperature below 37°C and closer to the recirculation temperature (figure 2).

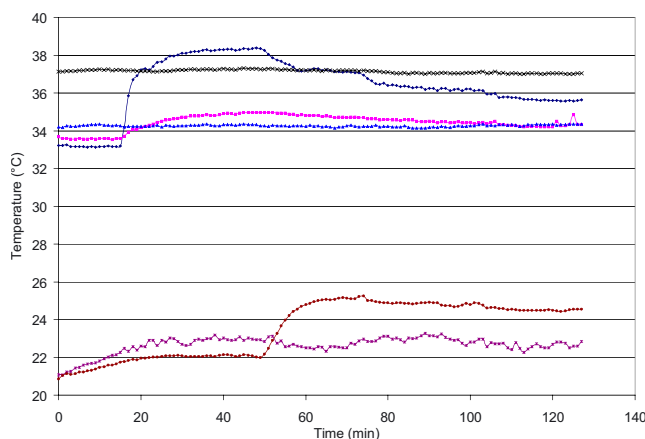


Figure 2. Temperature measurement at 20 L/day harvest, 60L/day recirculation, 7W switched on at  $t=16$  min, and air cooling of 10 ( $t=45$  min), 20 ( $t=73$  min) and 30L/min ( $t=101$  min).  $\diamond$ =cuvette(1),  $\blacksquare$ =funnel(2),  $\blacktriangle$ =recirculation(3),  $\times$ =bioreactor(4),  $*$ =room(5),  $\circ$ =air cooling(6)

Some tests were also performed with a yeast suspension to determine the effects of temperature and air cooling on the separation efficiency. With the BioSep 10L the separation efficiency did not change much with varying temperatures. Without any air cooling still separation efficiencies higher than 99% were measured. Since it did not change when the temperature became more homogeneous, it seemed that the separation efficiency was already at its upper limit. This was different for the 50L BioSep. Thermal streaming had a larger influence on the separation efficiency. With air cooling of 30L/min, the separation efficiency improved from 97.4% to 99.1%, at 10g/L yeast, 50L/day harvest and 150L/day recirculation.

For the BioSep 200L the recirculation did not decrease as much ( $\pm 35^\circ\text{C}$ ) as in the BioSep 10L, due to the higher relative flow speed. The temperature in the cuvette was approximately the same as the temperature of the water bath, before the field was switched on. When the field was switched on the temperature in the cuvette increased  $2\text{-}3^\circ\text{C}$ . Decreasing the water bath temperature by  $1^\circ\text{C}$  resulted in a decrease of the temperature in the cuvette of approximately  $0.7^\circ\text{C}$  at 20 W and  $0.4^\circ\text{C}$  at 40 - 60W. At any power setting the best separation efficiency was reached at a water bath temperature of  $36^\circ\text{C}$ . However at 40 and 60W a little more cooling was necessary to maintain a maximum temperature  $37^\circ\text{C}$  in the cuvette. The effect of the temperature on separation efficiency was minimal (99.0 and 98.8% SE at 36 and  $35^\circ\text{C}$  water bath).

#### 4. CONCLUSIONS AND RECOMMENDATIONS

The temperature differences in around the BioSep 10L can be relatively large. However this can be reduced by applying a minimal recirculation flow of 20L/day and applying air cooling when the field is switched on. Separation efficiency was not influenced by temperature in the 10L BioSep. This contrary to the BioSep50L, where separation efficiency improved when air cooling was applied. Therefore air cooling in the 50L is always recommended even when temperature does not increase above  $37^\circ\text{C}$ . The BioSep 200L had the best separation efficiency at  $36^\circ\text{C}$ . However at the higher power inputs the temperature increased above  $37^\circ\text{C}$  and more cooling is beneficial to the temperature of the medium and the effect on separation efficiency was minimal. All the experiments led to the following recommendations for cooling at different settings of harvest flow rate and power input. A temperature study in the 1000L BioSep will be done shortly.

*Table 1: Recommendations for air cooling of the 10L BioSep*

<i>Harvest (L/day)</i>	<i>Recirculation (L/day)</i>	<i>Power (W)</i>	<i>Air cooling (L/min)</i>
1-2	20	2	10
2-5	20	3	20
5-8	20	5	30
8-10	20	7	30

*Table 2: Recommendations for air cooling of the 50L BioSep*

<i>Harvest (L/day)</i>	<i>Recirculation (L/day)</i>	<i>Power (W)</i>	<i>Air cooling (L/min)</i>
5-20	50	5	10
20-40	100	7	20
40-50	100-150	10	30

*Table 3: Recommendations for the water bath setting of the 200L BioSep*

<i>Harvest (L/day)</i>	<i>Recirculation (L/day)</i>	<i>Power (W)</i>	<i>Water bath (°C)</i>
20-40	40-100	20	36
40-100	100-300	30	35.5
100-150	300-450	40	35
150-200	450-600	50-60	34

## REFERENCES:

- H. Bierau, A. Perani, M. Al-Rubeai, A.N. Emery. A comparison of intensive cell culture bioreactors operating with Hybridomas modified for inhibited apoptotic response. *Journal of biotechnology* 62, 195-207, 1998.
- T. Keijzer, F. Trampl, A. Oudshoorn, O. Doblhoff, H. Berg, Integrating acoustic perfusion in mammalian cell culture. Scale-up and performance characterisation. 2001 (poster)

## FLEXIBLE FED-BATCH PROCESS CONTROL OF ANIMAL CELLS

*Technische Universitaet Hamburg-Harburg, Bioprozess- und Bioverfahrenstechnik, Denickestraße 15, 21071 Hamburg, Germany, poertner@tuhh.de*

### INTRODUCTION

Fed-batch suspension culture of animal cells continues to be of industrial importance for the large scale production of pharmaceuticals. However, existing control concepts are still insufficient and metabolites produced during the cultivation may inhibit cell growth.

The combination of a model-based fed-batch process and the adaptive Open-Loop-Feedback-Optimal(OLFO)-controller /1, 2/ represents an effective tool, which couples an efficient cultivation concept and a high performance process control strategy. Characteristics are the transferability to different cell lines and cultivation systems, e.g. dialysis cultivation. Fed-batch cultivation using dialysis allows the improvement of maximum cell density and product yield via removal of low molecular weight metabolites. Major elements of this fed-batch control are a process model, a model parameter identification and an optimisation part (fig.1).

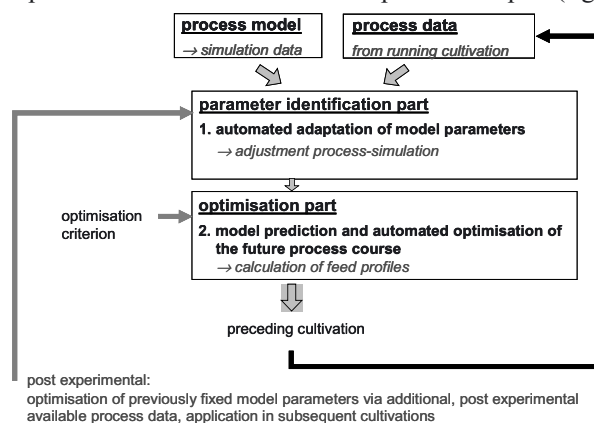


Fig. 1: Scheme of the adaptive, model-based process control strategy for fed-batch cultivation of animal cells

Using the process model, the course of important process variables from the end of the lag phase to the actual process time is calculated. Subsequently, an automated parameter identification takes place, based on the available process data. The optimisation part predicts the future course of process variables using the adapted model and calculates control functions (e.g. feed profiles) with respect to an optimisation criterion. The control cycle is repeated within a chosen time interval.

## MATERIALS & METHODS

The application to a NS0 cell cultivation for antibody production is presented.

Cell line: NS0 6A1 bcl-2, overexpressing bcl-2 for suppression of apoptosis, producing MAb for cancer therapy. The cell line was made available through Prof. Dr. M. Al-Rubeai, Animal Cell Technology Group, University of Birmingham, UK. No preliminary characterisation of the cell line, its uptake rates etc.

Model: Unstructured, unsegregated, 16 equations (10 coupled differential equations for the description of viable and total cell concentration and all major substrate and metabolite concentrations and 6 mostly Monod-type equations) and 14 variable model parameters. Shown in /2/ without dialysis.

Reactor: Membrane dialysis reactor (Bioengineering AG, CH): Culture chamber (2 L, working volume at inoculation 1 L) and dialysis chamber (8 L, working volume 4 L) separated by a cylindrical Cuprophane<sup>®</sup> dialysis membrane (cut-off: 10 kDa) and continuously perfused at a rate of 400 mL medium day<sup>-1</sup>.

Medium: Serum-free Pro CHO 4 CDM containing 23 mmol L<sup>-1</sup> glucose plus supplements.

Feed: 10fold concentrated DMEM/Ham's F12 (1:1) medium without salts containing 100 mM glucose.

Process: Control of glucose concentration at 16 mmol L<sup>-1</sup>. Run of the process control cycle (fig. 1) at every sampling starting at the end of the lag phase.

## RESULTS

Predicted and measured courses of important process variables of a dialysis fed-batch cultivation are shown in figure 2 over cultivation time. Each predicted value results from the model parameter optimisation and feed optimisation cycle (fig. 1) which was carried out at the time of the previous measurement.

The OLFO-controller realises process management and maintenance of the target glucose concentration in conjunction with the employed model. The use of dialysis cultivation for the removal of low molecular weight metabolites significantly enhances the performance of the process: Maximum cell density: 16·10<sup>6</sup> cells mL<sup>-1</sup> (3·10<sup>6</sup> without dialysis), product yield: 1030 mg MAb L<sup>-1</sup> (340). The application to a hybridoma cell cultivation without dialysis is presented in /2/. Time-space-yield considerations are described in /4/.

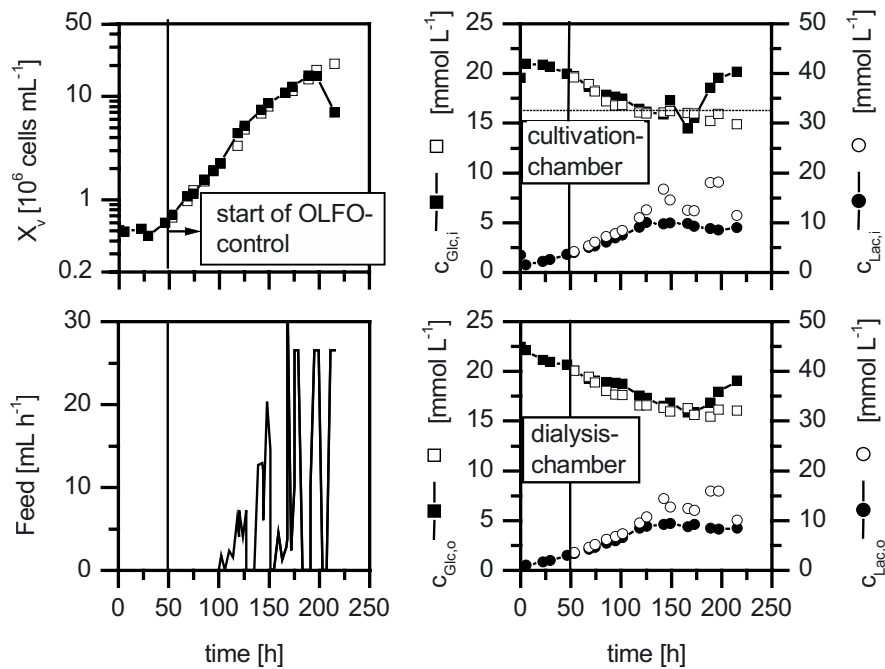


Fig. 2: Dialysis fed-batch cultivation of the NS0 cell line 6A1 bcl-2 by the OLFO-controller. Comparison of measured (filled symbols) and predicted (open symbols) process variables: a) viable cell concentration  $X_v$ , b) glucose concentration  $c_{Glc,i}$  and lactate concentration  $c_{Lac,i}$  in cultivation chamber c) glucose concentration  $c_{Glc,o}$  and lactate concentration  $c_{Lac,o}$  in dialysis chamber and d) calculated feed profile.

## REFERENCES

- /1/ Dreyfuss, S. E. (1962). Some types of optimal control of stochastic systems. *SIAM Journal of Control* 2: 120-134.
- /2/ Frahm, B., Lane, P., Atzert, H., Munack, A., Hoffmann, M., Hass, V. C., Pörtner, R. (2002). Automated, adaptive, model-based control by the Open-Loop-Feedback-Optimal (OLFO) controller for the effective fed-batch cultivation of hybridoma cells. *Biotechnology Progress* 18: 1095-1103.
- /3/ Frahm, B., Müller-Landré, B., Wiggers de Almeida, G., Singer, M., Rausch, M., Lane, P., Munack, A., Hass, V. C., Pörtner, R. (2003). Fed-batch cultivation of animal cells - a challenge for adaptive, model-based control. In: *Tagungsband zum 11. Heiligenstädter Kolloquium: Technische Systeme für Biotechnologie und Umwelt*: 503-509.
- /4/ Frahm, B., Müller-Landré, B., Wiggers de Almeida, G., Singer, M., Rausch, M., Lane, P., Munack, A., Hass, V. C., Pörtner, R. (2003). Fed-batch cultivation of animal cells - a challenge for adaptive, model-based control. In: *Tagungsband zum 11. Heiligenstädter Kolloquium: Technische Systeme für Biotechnologie und Umwelt*: 503-509.

OJITO MAGAZ, E., ARIAS M.A, CHICO VELIZ, E.

## DEVELOPMENT OF A FED-BATCH STRATEGY FOR THE PRODUCTION OF NS0-DERIVED HUMANISED MAB IN PROTEIN FREE MEDIUM.

*Center of Molecular Immunology. P.O. Box 16040, Havana City  
11600, Cuba.*

### INTRODUCTION

In order to meet the increasingly demand of therapeutic antibodies derived from mammalian cells to conduct clinical trials fed-batch culture has been established as alternative fermentation technology. A lot of feeding strategies has been implemented according to feeding medium composition (1, 2, 3). GS-NS0 cell line has been the most widely used host cell, which bear Glutamine -Sintetase expression vector, yet few information has rose from non GS-NS0 cell line fed batch-culture. Until now, out of 21 approved therapeutic products mammalian cell-derived only 2 are produced from NS0 cell line and in both cases using GS expression system and serum free media. Adaptations of NS0 cell line to commercially available protein free medium it is a hard work due to the cholesterol auxotrophy of this cell line. That's why few papers have been published about the role of cholesterol on specific Mab production rate in NS0 fed batch culture. Ojito et al 2001, demonstrated that the use of different cholesterol solutions in PFHM II medium improved the qMAb 1, 5 fold with respect to cholesterol free medium in batch culture. This fact allows for establish a fed-batch culture feeding only glucose and glutamine concentrated solutions in PFHM II medium with high amino acid content.

### MATERIALS AND METHOD.

Cell line and Culture Conditions. The cell line used was NS0-H7, which produce a humanised antibody against EGF receptor. The medium used throughout the experiments was PFHM II supplemented with Pluronic F68, glutamine and NaHCO<sub>3</sub>. Lipid supplements were Lipid Mixture 100X (S26), CD Lipid Concentrated (S49), Lipid # 37(S62), Lipid # 37 with fatty acids (S63), Lipid # 6 (S13)) and CD Lipid Concentrated with bovine cholesterol (S69). Cells were cultured in spinner flasks at 60 rpm and 36,5 °C. NaHCO<sub>3</sub> was use for pH control. The scheme of glucose and glutamine addition was based upon uptake metabolism. Feeding was initiated when viable cell concentration reached 1X 10<sup>6</sup>-cells/ mL in

order for maintains glucose and glutamine concentration above 5mM and 1mM respectively. Glucose and glutamine were added as concentrated solutions.

Analytical Measurements. Cell counts were carried out using hemocytometer and cells were quantified using trypan blue exclusion method. Glucose, Lactate and Ammonia were measured by Biolyzer DT60 II. Amino Acids were detected using a proprietary method from Water by Merck-Hitachi HPLC. IgG determination was performed through a specific ELISA.

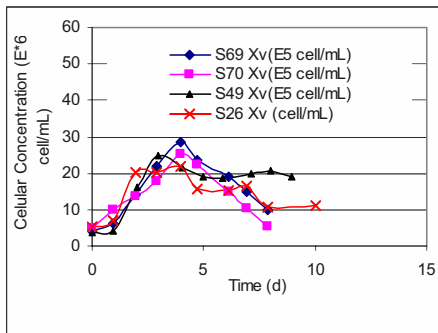


Fig.1 Fed-Batch culture w/o cholesterol

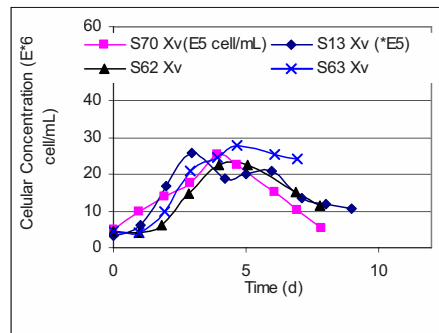


Fig.1 Fed-Batch culture with cholesterol

## RESULTS AND DISCUSSION.

### *Development of a fed-batch process.*

Two sets of experiments were carried out to evaluate the effect of fatty acid and cholesterol upon fed-batch performance. As shown in Figure 1 cell line NS0-H7 grew in medium PFHM II using different lipid supplementation. Control culture S70 reached  $2,53 \times 10^6$  cell/mL and viability index of  $118 \times 10^5$  cell/d/mL. When fed culture was performed using Lipid Mixture 100X cells reached a maximal viable cell density of 87 % with respect to that control culture. The same occurred with CD Lipid Concentrated where cells reached 98, 5 % with respect to control. In the case CD lipid concentrated plus bovine cholesterol the maximal Xv was 113% with regard to the control culture. **It could be concluded that lipid supplementation hadn't effect on maximal cell density and lipids don't constitute the**



**stoichiometric limitation.** Yet, lipid supplementation improved viability index in all cases evaluated in 123% respect to the control. Figure 2 shows that when cells were supplemented with non-animal derived cholesterol without fatty acid (S62, S63 and S13) the maximal cell density was over 100% with respect to the control culture. In these cases, the viability index was similar to that culture without fatty acid supplementation. In terms of metabolic load the maximal reached lactate concentration was over 30 mM, which has been reported to be inhibitory to NSO cell line in serum free medium.(4). In case of ammonia the average concentration obtained was over 5 mM confirming the impact of wasting products on overall cell growth. **If we look at that cellular dead pattern it can be observed that in this phase  $k_d > \mu$  which demonstrate that lactate concentration could be the responsible of that behaviours.**

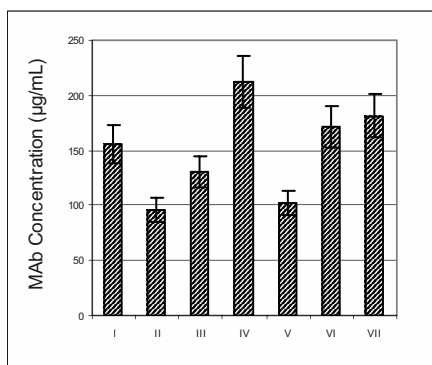


Fig.3. Maximum MAb Concentration

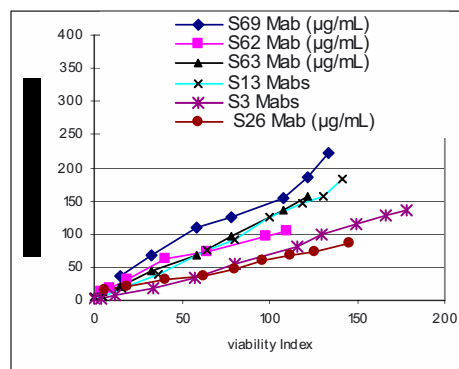


Fig.4. Effect of cholesterol on qMAb

#### Impact of cholesterol upon Mab productivity.

In terms of Mab concentration there was different outputs with regards to the type of lipid used (Figure 3). In case of S28 the maximal Mab concentration obtained was 92 mg/L which means 2 fold the value obtained in batch culture. For S49 the final value was 130 mg/L and when cholesterol was added to CD Lipid Concentrated (S69) the final Mab concentration was 220 mg/L, which represented 4,4 fold with respect to batch culture. This difference in the final Mab concentration between S49 and S69 was due to an increase in the specific Mab production rate. This increase was provoked by the addition of 5 mg/L of cholesterol varying from  $3 \times 10^{-7}$  up to  $5,2 \times 10^{-7}$   $\mu\text{g}/\text{cell h}$  demonstrating the value of medium optimisation instead of feeding strategy. For cholesterol supplemented cultures the final Mab average concentration was 165 mg/L. From these results two production patterns can be identified, one associated to culture supplemented with fatty acids without

cholesterol (S28, S49) and other associated with the cholesterol concentration in the basal medium. (Figure 4). These results allow for conclude that the use cholesterol increased the specific Mab rate in PFHM II medium.

#### CONCLUSIONS.

From the results presented here can be concluded that the fed batch culture feeding glucose and glutamine increase the final Mab concentration up to 150 mg/L in PFHM II medium. The lactate and ammonia concentration modified the dead phase getting fewer products due to lower values of viability index Cholesterol constituted an improvement of specific Mab production rate in NS0 cell line adapted to PFHM II medium. The use of glucose and glutamine as feeding solution no increase the qMab value over control culture. All these results demonstrated the feasibility of using recombinant non GS-NS0 cell line for production of proteins of high added value.

M. RENDALL, A. MAXWELL, D. TATHAM, P. KHAN, R.D.  
GAY, R.C. KALLMEIER, J.R.T. WAYTE & A.J. RACHER

## TRANSFECTION TO MANUFACTURING: REDUCING TIMELINES FOR HIGH YIELDING GS-CHO PROCESSES

*Lonza Biologics, Cell Culture Process Development, 228 Bath Road, Slough,  
Berkshire, SL1 4DX, UK*

### 1. INTRODUCTION

Chinese hamster ovary (CHO) cell lines are widely used by the bio-pharmaceutical industry for therapeutic protein manufacture. The rapid construction of high yielding recombinant CHO cell lines are a key economic consideration. Gene amplification is widely used to create high yielding CHO cell lines; however this can substantially increase the length of a cell line development programme. As a further consideration, adaptation to single cell suspension culture and to protein-free (or chemically-defined) media can be problematic, and impact project timelines; one solution is to use a host cell line pre-adapted to the desired culture conditions.

The work reported here describes the creation of high yielding GS-CHO cell lines for use in a chemically-defined fermentation process. This was achieved through improvements in the cell line construction process; focusing on the development of a pre-adapted host cell line, and the optimisation of the transfection and selection stages.

### 2. METHODS

A host CHO cell line pre-adapted to suspension culture and chemically-defined medium (CHOK1SV) was evaluated against the original host cell line (CHOK1). Host cells were transfected with genes coding for the antibody cB72.3 linked to the glutamine synthetase (GS) selectable marker. Transfectants were selected in serum containing glutamine-free medium. Successive productivity assays were performed by ELISA to select the highest yielding cell lines. High yielding cell lines were progressed to flask suspension cultures in a chemically-defined, animal component free medium and productivity assessed.

Growth and productivity kinetics were additionally evaluated in a platform chemically-defined GS-CHO fermentation process utilising a 10 L airlift bioreactor operated in fed-batch mode.

### 3. RESULTS

CHOK1SV and CHOK1 host cells were transfected with a GS-expression vector encoding the genes for the antibody cB72.3. Glutamine independent transfectants were selected and supernatants screened by ELISA for the presence of assembled antibody. A total of 341 transfectants were initially screened, all of which produced antibody. From these, 259 transfectants were selected for further assessments of productivity.

Following successive rounds of selection, thirty cell lines were selected for adaptation to suspension culture in protein-free medium and evaluated in shake-flask culture. Antibody concentrations up to 1150 mg/L were obtained and one of these high producing cell lines, LB01, was selected for further evaluation. These cell lines had not been subjected to gene amplification.

The development of a pre-adapted CHOK1SV host cell line resulted in a timeline reduction to within 6 months duration for the creation of high yielding GS-CHO cell lines adapted to chemically-defined medium (Figure 1).

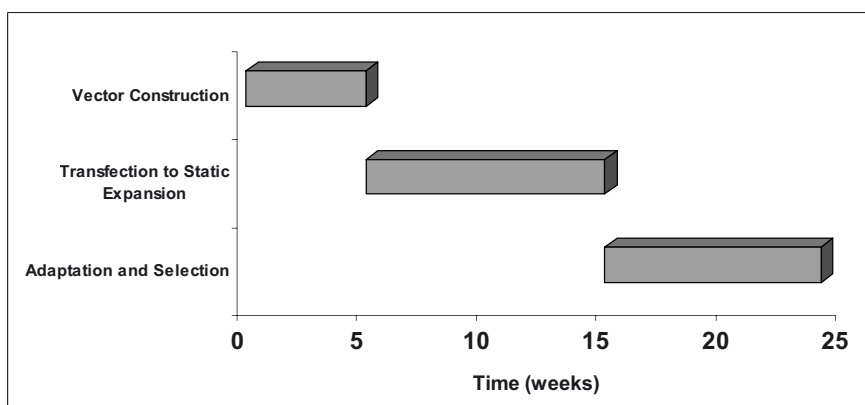


*Figure 1. Timeline showing steps performed to select high yielding GS-CHO cell lines adapted to chemically-defined medium. Use of pre-adapted CHOK1SV host has resulted in a substantial timeline reduction. High yielding GS-CHO cell lines can be created within six months.*

Two model cell lines: 22H11 (original CHOK1 host) and LB01 (created using the new CHOK1SV host), were grown in 10 L airlift bioreactors using successively improved versions of the GS-CHO fermentation process with chemically-defined medium and feeds. Medium and feed optimisation strategies enabled extension of culture duration, increased viable cell density and increased specific cellular productivity. In figures 2 and 3, cell growth and productivity data are shown comparing the performance of 22H11 and LB01 cell lines together with process improvements. Using the LB01 cell line with the improved process (V2.0), the antibody concentration at harvest was 2.8 g/L.

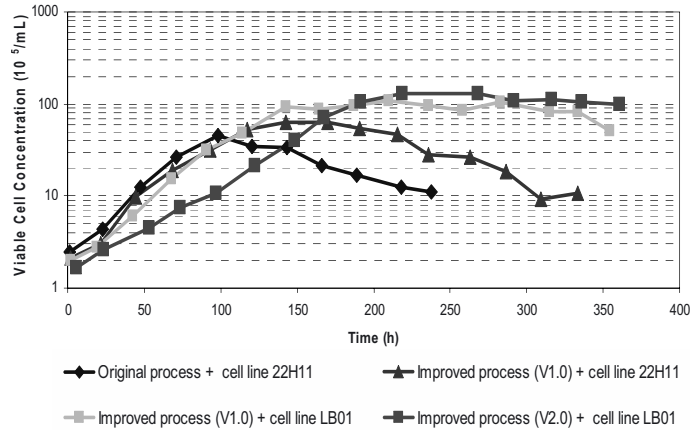


Figure 2. GS-CHO chemically-defined fed batch bioreactor culture process and cell line optimisation: Cell growth

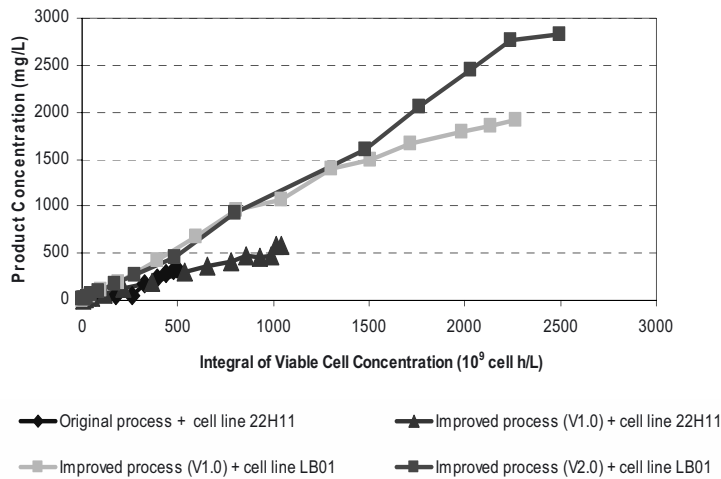


Figure 3. GS-CHO chemically-defined fed batch bioreactor culture: Productivity improvement by process and cell line optimization

#### 4. SUMMARY

CHOK1SV derived transfectants rapidly adapted to suspension culture in fully chemically-defined, animal component free medium. Productivity and timeline improvements were the result of changes made at all stages of the cell line

construction programme. Antibody concentrations of 2.8g/L were achieved in fed-batch bioreactor culture without gene amplification. Use of a host cell line pre-adapted to suspension culture and growth in chemically-defined medium, resulted in high yielding GS-CHO cell lines being developed within 6 months.

PAUL SAUER

## OPTIMIZATION OF A FED-BATCH PROCESS PRODUCING HUMANIZED ANTIBODIES

*Increasing Product Quantity While Maintaining Product Quality*

### INTRODUCTION

Previously we reported the development of a 1<sup>st</sup> generation fed-batch process (FBP-1) used to manufacture early-phase (I/II) clinical trial material for four humanized antibody product candidates (1). Antibody production at the 750 L bioreactor scale for the four products ranged from 0.37 to 0.60 g/L. Here we discuss a new 2<sup>nd</sup> generation fed-batch process (FBP-2) developed for the production of future clinical trial material.

FBP-2 was developed by optimizing the feed medium; specifically, the concentrations of all amino acids were, at a minimum, doubled, and the concentrations of select vitamins and trace elements – thought to promote oxidative metabolism – were significantly increased (2). Using FBP-2 at the 150 L pilot scale, final antibody concentration for three product candidates ranged from 1.1 to 1.4 g/L.

In a case study, extensive analytical characterization work was performed to establish comparability for one product candidate. Accelerated stability studies showed that FBP-2 culture duration impacted stability of the drug product. Overlaying vialled drug product with nitrogen gas resulted in a stability profile comparable to reference material produced using FBP-1. The mechanism of product degradation observed in FBP-2 is currently under investigation (3, 4).

### MATERIALS & METHODS

*Table 1. Bioreactor controller setpoints for 1<sup>st</sup> generation (FBP-1) and 2<sup>nd</sup> generation (FBP-2) fed-batch processes*

	<i>bioreactor scale</i>		
	<i>750 L</i>	<i>150 L</i>	<i>3 L</i>
DO (% air saturation)	30	30	30
temperature (°C)	37.0	37.0	37.0
agitation rate (rpm)	25–30	50–65	100–200
gas flow rate (slpm)	12	3.0	0.1–0.2

Table 2. Host cell line derivation for six cell lines producing humanized antibodies. Bioreactor data generated using WCB vials unless otherwise noted.

	cell line					
	B	C	G	H	J	K
host cell	Sp2/0	NS0	Sp2/0	Sp2/0	NS0	NS0

Table 3. Volume of basal medium, inoculum, and feed medium added to bioreactor.

	bioreactor scale		
	750 L	150 L	3 L
basal medium (L)	245	45	0.9
inoculum (L)	65	15	0.25
feed medium (L)	290	50	1.00
final working volume (L)	600	110	2.15

Table 4. Basal medium used in fed-batch bioreactor processes. BM-3 has been previously described (1). BM-4 is identical to BM-3 except that insulin has been removed. BM-4 is a completely defined, protein-free basal medium.

cell line	1 <sup>st</sup> generation (FBP-1) process				2 <sup>nd</sup> generation (FBP-2) process		
	B	C	G	H	C	J	K
basal medium	BM-4	BM-4	BM-3	BM-3	BM-4	BM-4	BM-4

Table 5. Fold increase in FBP-2 feed medium component concentration relative to FBP-1 feed medium component concentration. There are no new components in FBP-2 feed medium compared to FBP-1.

Feed medium component	FBP-2 feed medium component concentration (fold increase relative to FBP-1 feed medium)
amino acid #1	6.8
amino acid #2	6.8
amino acid #3	4.5
amino acid #4	4.5
amino acid #5	4.5
all other amino acids	2.3
vitamin #1	3.8
vitamin #2	3.8
vitamin #3	2.6
all other vitamins	1.3
trace element #1	6.9
trace element #2	6.9
trace element #3	2.9
trace element #4	2.6
all other trace elements	1.3
lipid #1	3.8
all other components	1.3



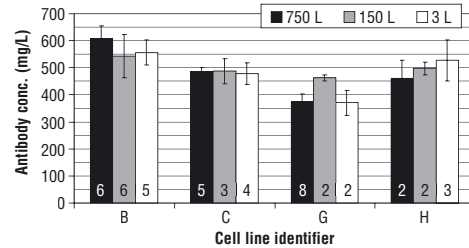


Figure 1. Bioreactor data for 1<sup>st</sup> generation fed-batch process at three different bioreactor scales (3 L, 150 L, and 750 L) using 4 different cell lines (B, C, G, and H). The number of replicates at each bioreactor scale is superimposed on the figure. Data show that the process is generic, scaleable, and reproducible. Coefficient of variation is <15% for all scales and all cell lines. Cell line identifiers are consistent with previously published data (1).

Table 6. Process data for 3 cell lines (C, J, and K) run at the 150 L bioreactor scale in the 2<sup>nd</sup> generation fed-batch process (FBP-2). Source of cells was either the WCB (Working Cell Bank) or the SB (Seed Bank). Cell line C produced 0.48 g/L in FBP-1 (see Figure 1) and 1.1 g/L in FBP-2 — the only difference between FBP-1 and FBP-2 is the amount of feed medium components added (as specified in Table 5).

cell line	150 L bioreactor runs	cell source	process duration (days)	final antibody conc. (g/L)
C	n = 1	WCB	12	1.13
J	n = 5	WCB	13	1.38 ± 0.07
	n = 6	WCB	10	1.03 ± 0.13
K	n = 1	SB	11	1.24

Table 7. Cell line C data generated at the 150 L bioreactor scale using two fed-batch processes: FBP-1 and FBP-2. Volumetric productivity increased 2.1 fold. Yield of cells on glucose increased 1.8 fold. Yield of antibody on glucose increased by 3.1 fold. Yield of lactate on glucose decreased by 50% indicating a shift toward aerobic or oxidative metabolism. Previous data (2) indicate that the shift toward oxidative metabolism involves some combination of vitamins #1–#3 and trace elements #1–#4 (see Table 5).

	FBP-1	FBP-2	fold change (FBP-2/FBP-1)
volumetric productivity (mg/L day)	46	95	2.1
cells produced / glucose consumed (10 <sup>9</sup> cells/g)	1.2	2.2	1.8
antibody produced / glucose consumed (g/g)	0.027	0.083	3.1
lactate produced / glucose consumed (g/g)	0.64	0.32	0.5

*Case Study: Effect of Increased Productivity on Product Quality*

A humanized antibody was evaluated in a Phase I clinical trial. Material for the Phase I trial was manufactured using cell line G, an Sp2/0-derived cell line, in the 1<sup>st</sup> generation fed-batch process (FBP-1). In order to increase process yield, cell line J, an NS0-derived cell line that produces the same humanized antibody as cell line G, was selected. In anticipation of a Phase III trial, we evaluated material produced by cell line J in FBP-2 to determine if it was comparable to reference (i.e., material produced by cell line G in FBP-1).

In Figures 2–4 below, “FBP-1” refers to reference material manufactured at the 750 L bioreactor scale, and “FBP-2” refers to material produced at the 150 L development scale. FBP-1 and FBP-2 material was clarified, purified using a series of filtration and chromatography steps, formulated, and vialled. Vialled material was used for all experiment conditions. As indicated in Figures 2–4, FBP-2 material was harvested (removed) from the bioreactor on various (specified) days post-inoculation (e.g., “FBP-2 (day 10)” refers to material that was harvested from the bioreactor 10 days after inoculation, and subsequently clarified, purified, formulated and vialled).

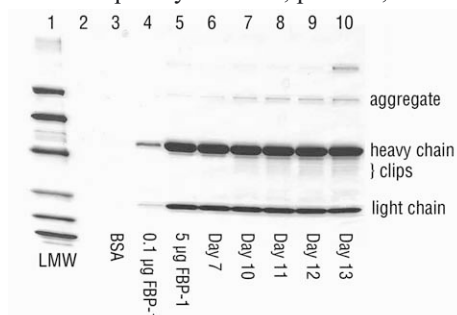


Figure 2. Effect of culture duration on product quality as measured by SDS-PAGE. Lanes 4 and 5 contain 0.1 µg and 5 µg of FBP-1 reference material. Lanes 6–10 contain FBP-2 material harvested from the 150 L bioreactor on days 7, 10, 11, 12, and 13. Progressive increase in clip and aggregate observed with increasing culture duration.

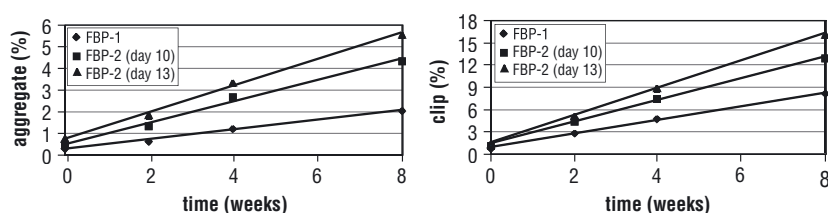


Figure 3. Effect of culture duration on drug product stability as determined by an accelerated stability study (50°C for 8 weeks). Degradants measured using SEC. FBP-1 denotes reference. FBP-2 material was harvested from a 150 L bioreactor on day 10 or day 13. The trend of increasing degradants (both percent clip and percent aggregate) is evident: FBP-2 (day 13) > FBP-2 (day 10) > FBP-1.

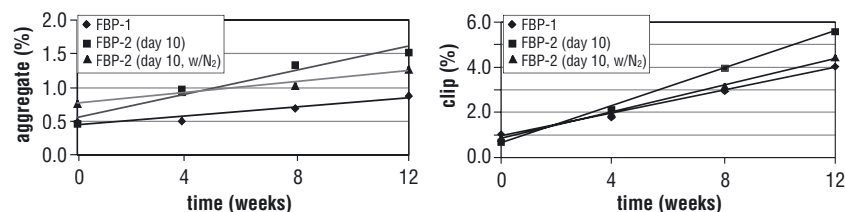


Figure 4. Effect of nitrogen overlay on drug product stability as indicated by accelerated stability study (37°C for 12 weeks). Degradants measured using SEC. FBP-1 denotes reference. FBP-2 is material harvested from a 150 L bioreactor on day 10 then overlaid with nitrogen (day 10, w/ N<sub>2</sub>), or not overlaid (day 10). With nitrogen overlay the rate of aggregate and clip formation of FBP-2 material is comparable to FBP-1 material.

## CONCLUSIONS

A 2<sup>nd</sup> generation fed-batch process (FBP-2) was developed by optimizing the feed medium. Specifically, the concentration of all FBP-2 feed medium components were increased relative to the concentration of FBP-1 feed medium components (see Table 5). As with FBP-1, FBP-2 remains a serum-free, protein-free process. Volumetric productivity of cell line C in FBP-2 was 2.1-fold greater than the volumetric productivity of cell line C in FBP-1 (1.1 g/L in 12 days vs. 0.37 g/L in 8 days). Two new NS0-derived cell lines (J and K) also achieved high volumetric productivity in FBP-2 (1.4 g/L in 13 days and 1.2 g/L in 11 days, respectively). The marked increase in oxidative metabolism in FBP-2 was most likely the result of an increase in the amount of a few select vitamins and trace elements added. Cells remained viable longer in FBP-2 compared to FBP-1, increasing process duration to 13 days. Increased culture duration had a negative impact on product quality for one antibody tested — increased amounts of clip and aggregate were observed in accelerated stability studies. Limiting FBP-2 culture time to 10 days and overlaying drug substance with nitrogen mitigated product stability problems while maintaining a significant product yield increase compared to FBP-1.

## REFERENCES

1. P. Sauer et al. A High-Yielding, Generic Fed-batch Cell Culture Process for Production of Recombinant Antibodies, *Biotech. and Bioeng.*, Vol. 67, No. 5, March 5, 2000, p. 585–597.
2. L. Qu. High Yield Fed-Batch Culture Under Oxidative Metabolism, *Cell Culture Engineering VIII*, Snowmass Village, CO, April 1–6, 2002.
3. K. Reid et al. Effects of Cell Culture Process Changes on Humanized Antibody Characteristics, WCBP, San Francisco, CA, January 8, 2003.
4. S. Gupta. Effect of Process Changes on the Stability of a Humanized Monoclonal Antibody, Waterside Conference, San Francisco, CA, May 4–7, 2003.

Paul Sauer, Protein Design Labs, Inc., Fremont, California, USA.

JENNIFER WALOWITZ, LIA TESCIONE, WILLIAM PAUL,  
DAVID JAYME AND STEPHEN GORFIEN

## OPTIMIZED FEEDING STRATEGY FOR NS0 CELLS

*Invitrogen Corporation, Grand Island, NY, USA*

### INTRODUCTION

NS0 is a non-immunoglobulin secreting, non-light chain synthesizing subclone of NS-1. We previously described development of cyclodextrin-based lipid supplements, which when added to a protein-free hybridoma culture medium made it possible to grow wild-type NS0 cells in a completely protein-free culture system lacking animal derived components (1). Peak cell density in this small-scale system exceeded previously reported results obtained in systems which contained animal derived components (2). However, productivity in batch culture systems may be limited by nutrient depletion and/or build-up of toxic metabolites. We have recently described development of a model fed-batch culture system in Chinese Hamster Ovary (CHO) cells for optimization of recombinant protein expression through nutrient supplementation (3). The goal of our present work was to improve productivity of a recombinant NS0 (rNS0) line in fed-batch bioreactors. Several approaches to provide rate-limiting nutrients to the cultures have been tested and indicate that feeding amino acids and lipids together improve productivity in these cells.

### MATERIALS AND METHODS

Variants of CD Hybridoma Medium (GIBCO 11279-023) were supplemented with 250X Cholesterol Lipid Concentrate (GIBCO 12531-018). CD Hybridoma Medium Partial Nutrient Supplement (PNS) was used in amino acid feeding strategies. It was prepared by mixing equal volumes of Acid Solubles (GIBCO 00-0336DG) and Base Solubles (GIBCO 00-0337DG) within 10 minutes of use and was fed at a 1:100 dilution to the cultures. A CD Hybridoma Medium 5 Amino Acid (5AA) Solution was similarly prepared. Glutamine was not present in either supplement. Cholesterol Lipid Concentrate (CLC), 1000X Aqueous Liquid (GIBCO 01-0025DG) was used in lipid feeding strategies at a 1:1000 dilution.

A proprietary rNS0 line expressing IgG was maintained in catalog and low glucose/low glutamine (low G/G) media. Cells were grown in shake flasks at 125 rpm at 37°C in a humidified atmosphere of 8% CO<sub>2</sub> in air.

Stirred tank CelliGen Plus<sup>®</sup> (New Brunswick Scientific Co., Inc., NJ) bioreactors with a 4 L working volume were seeded at  $3 \times 10^5$  viable cells/mL. Agitation (60 rpm), temperature (37°C), pH (7.30), and dissolved oxygen (25%) were controlled at the indicated setpoints. For low G/G conditions, glucose was monitored and controlled on-line at 1 g/L using a YSI analyser (YSI Inc., Yellow Springs, OH). The initial glutamine concentration was 2 mM. Beginning on day 2, bioreactors were fed the equivalent of 1 mM glutamine daily. PNS or 5AA Solution was fed on days 4 and 6. CLC was fed on days 3 and 5. Immunoglobulin content (4) and amino acids (3) were quantitated as previously described.

## RESULTS/DISCUSSION

We recently developed a nutrient supplementation strategy to optimize recombinant protein expression in CHO cells (3). A similar approach was used to improve antibody production in an rNS0 cell line. Initial experiments indicated that glucose and glutamine requirements were vastly different for the CHO and rNS0 systems. Since this rNS0 cell line lacks the glutamine synthetase (GS) enzyme, these cells require glutamine supplementation. rNS0 growth and IgG production were similar in catalog and low G/G media. Less overall ammonia was produced with the low G/G medium, so this condition was used in all further development work.

Since amino acid supplementation has been used to improve antibody production in mammalian cell lines (3, 5, 6), PNS was used in initial feeding experiments. A slight improvement in rNS0 production was seen at the end of the run. In order to reduce the amino acids in the feed, we looked at the amino acid consumption profile, which indicated that cystine, leucine, methionine, tyrosine, and valine were substantially reduced during the bioreactor run with low G/G conditions. A 5AA Solution was prepared with these amino acids. Similar results were seen with PNS and the 5AA Solution, which suggested that one or more other components might be limiting.

Since the rNS0 line is cholesterol dependent, cells were fed with CLC in addition to the amino acid supplements. Previous studies indicated that 250X Cholesterol Lipid Concentrate could not be used in feeding strategies because cyclodextrin levels became toxic to the cells. However, the 1000X CLC could be used because this supplement contributed less cyclodextrin to the cultures. The combined amino acid and lipid feed improved IgG production. Preliminary experiments suggested depletion of fatty acids, yet feeding fatty acids in addition to 5AA Solution did not improve productivity. In contrast, feeding with cholesterol and fatty acids in addition to 5AA Solution improved IgG levels.

Adapting rNS0 cells from catalog to low G/G medium, coupled with feeding 5AA Solution and CLC, resulted in a doubling of IgG levels (164  $\mu\text{g/mL}$ ) compared to the unfed catalog control (82  $\mu\text{g/mL}$ ). Yet, amino acid analysis revealed that glutamine levels were not detectable during most of the run, despite daily 1 mM feeds beginning on day 2. When the glutamine feed was increased to 2 mM, faster growth, but lower IgG levels were observed, as shown in Figure 1C. Amino acid analysis showed more rapid depletion of the other fed amino acids in the 2 mM

culture (Figures 1B and 1D). We hypothesize that the lower amino acid availability resulted in lower IgG production in the 2 mM bioreactor culture. IgG production was similar at both glutamine concentrations in shake flask cultures (Figure 1A), presumably as a result of less rapid depletion of amino acids (Figure 1B) and/or other nutrients. This suggests that optimization of feeding times and/or concentrations of other nutrients may further improve IgG production in bioreactors.

### SUMMARY

IgG production in an rNS0 culture was increased through development of amino acid and lipid feeding strategies in low G/G medium. This work has established the basis for further optimization studies with this cell line. While off-line HPLC analysis and a bolus feeding strategy were used in this work, on-line analysis can be used to continuously monitor depletion of amino acids and optimize feeding strategies (7). We are working to develop an on-line monitoring system to optimize nutrient concentrations and feeding rates.

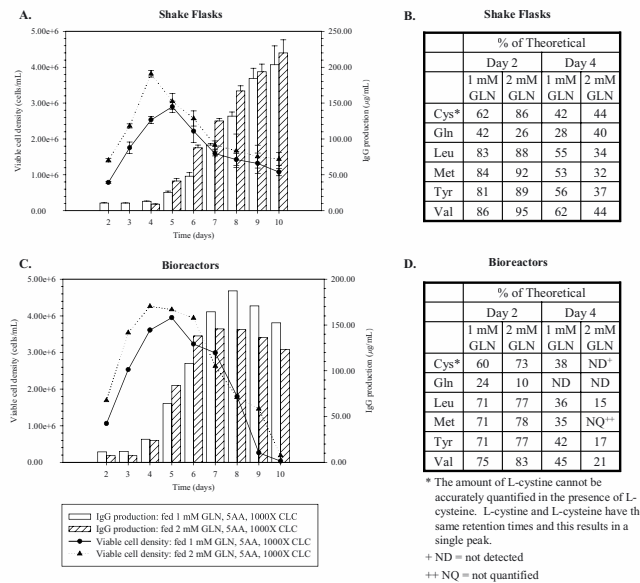


Figure 1. Effect of Glutamine Concentration on rNS0 Cell Growth, IgG Production, and Amino Acid Consumption Profile in Low Glucose/Low Glutamine Medium

## REFERENCES

1. Gorfien S, Paul B, Walowitz J, Keem R., Biddle W and Jayme D. (2000) *Biotechnol. Prog.* 16: 682
  2. Keen MJ and Steward TW. (1995) *Cytotechnology* 17:203
  3. Gorfien SF, Paul W, Judd D, Tescione L and Jayme DW. (2003) *BioPharm International* 16(4):36
  4. Walowitz J, Fike R and Jayme D. (2003) *Biotechnol. Prog.* 19:64
  5. Dempsey J, Ruddock S, Osborne M, Ridley A, Sturt S and Field R (2003) *Biotechnol. Prog.* 19: 175
  6. Martial-Gros A, Goergen JL, Engasser JM, and Marc A. (2001) *Cytotechnology* 37: 93
  7. Larson T.M, Gawlitzek M, Evans H, Albers U, Cacia J. (2002) *Biotechnol. Bioeng.* 77: 553
- CelliGen Plus<sup>®</sup> is a registered trademark of New Brunswick Scientific Co., Inc.

ALEXANDER TAPPE<sup>1</sup>, GERLINDE KRETZMER<sup>1</sup>, CORNELIA  
KASPER<sup>1</sup>, THOMAS SCHEPER<sup>1</sup>, EVGENIA G. VLAKH<sup>2</sup>,  
TATIANA B. TENNIKOVA<sup>2</sup>

## COMPARISON OF COMPLEMENTARY INTERACTIONS BETWEEN SYNTHETIC LIGANDS AND t-PA BY HPMDC

<sup>1</sup>*Institut für Technische Chemie, Hannover, Germany*

<sup>2</sup>*Institute of macromolecular compounds, St. Petersburg, Russia*

### 1. INTRODUCTION

Tissue plasminogen activator (t-PA) enables efficient dissolution of blood clots by converting plasminogen in its active form, plasmin, dissolving the major component of blood clots, fibrin. t-PA and plasminogen possess a high affinity binding site for fibrin, but also some synthetic polymers can provide the stimulating effects of plasminogen activation. High performance monolithic disk chromatography (HPMDC) is a very fast, efficient and suitable tool for the isolation of biological active compounds.

A step by step modelling of possible affinity pairs and different oligo/polymer forms of linear and branched lysine derivatives using HPMDC is shown. The results of the evaluation of these affinity interactions were compared to natural affinity counterparts to t-PA (monoclonal antibodies, plasminogen, fibrinogen). The results enable a practical choice of affinity systems to be used for the fast and efficient analytical and preparative methods for the down stream processing of recombinant production of t-PA.

### 2. IMMOBILISATION OF PROTEIN LIGANDS AND SOLID PHASE PEPTIDE SYNTHESIS

#### *2.1. solid phase peptide synthesis*

Solid phase peptide synthesis by Fmoc strategy was accomplished inside the cartridge (housing plus syringe). Deprotection of side chains was accomplished outside of the cartridge due to chemical irrisistance towards 90 % TFA.



### 2.2. Immobilisation of protein ligands

- wash disk with ethanol, ethanol-water (1:1) and water.
- immerse disk in 0.1 M sodium carbonate buffer (pH 9.3) for 2 hours.
- transfer disk to 1 ml 5.0 mg/ml protein solution in the same buffer.
- let reaction proceed for 16 hours at 34 °C without stirring.
- wash with initial sodium phosphate buffer.
- wash with PBS solution containing 0.02 % sodium azide for storage at 4 °C.

Taking into account the very high reactivity of epoxy groups of GMA-EDMA macroporous polymers, the immobilization was carried out as one step under static conditions. No spacers have been inserted as several publications have specified no dependence of separation efficiency of HPMDC for immobilization of peptides and proteins.

### 2.3. Analysis

Synthetic peptides were analyzed by RP-HPLC and size exclusion chromatography of acidic hydrolyzed samples. The amount of protein ligands coupled to the matrix was monitored by Lowry assay. Affinity characteristics were calculated from frontal analysis. Model solutions of t-PA from 0.01 to 0.5 mg/ml were used. ELISA was carried out to determine t-PA concentration of the samples. Purity was observed by SDS-PAGE with silver staining. Standard mixtures of proteins were passed through the sorbents. In all cases non-specific interaction did not exceed 2 % from applied protein sample.

Crude CHO cell supernatant was used to evaluate the purification efficiency of t-PA from a biological sample. The disk was loaded with sample in PBS buffer (pH 7.0, 10 mM, 150 mM NaCl). Specific bound t-PA was eluted with 0.01 M HCl after washing with 2 M NaCl. Flow rate was set to 2 ml/min. Total amount of t-PA was 3.5 µg.

## 3. RESULTS

The data in Table 1. shows that the amount of immobilized ligands is a function of molecular size of ligands. Highest capacity has been found for small ligands due to higher diffusion coefficient and less sterical hindrances inside the pores by blockage of functional groups after immobilization of molecules. While homo- and heteropeptides show no significant differences due to their small differences in size, capacity decreases for the rigid dendrimer  $K_{15}A$  molecules and proteins.

Adsorption capacity and values of  $K_{diss}$  show strong interaction between t-PA and mAbs as expected. A specific complex with t-PA and every second antibody is formed. Structure safety and biological function of proteins is preserved on the surface as even the plasminogen-t-PA complex shows high thermodynamic strength.

About 30 to 60 molecules of homopeptide forms of lysine bind to one t-PA molecule due to the size difference between t-PA-peptide complex and single peptide. A transition from linear to branched forms of lysine cause no significant changes in  $q_{ads}$ . Comparing dissociation constants it can be noticed that polymer

forms of lysine show less intensive coupling, while K<sub>12</sub> and dendrimeric ligands take intermediate position between polymer and short peptides. This can be caused by small differences in surface concentration of ligands, as it cannot be predicted whether a single-point or multi-point linkage of ligands with an adsorbent surface will occur. Affinity properties of GPRP are unaffected by introduced lysine residues or increasing its length.

Table 1. Affinity characteristics

<i>ligand</i>	$q_{\text{immobil.}}$ [ $\mu\text{mol } 10^2/\text{m}^2$ ]	$q_{\text{adsorb}}$ [ $\mu\text{mol } 10^2/\text{m}^2$ ]	$q_{\text{immobil.}}/q_{\text{adsorb}}$	$K_{\text{Dis}}$ [ $\mu\text{mol/L}$ ]
mAB	0.20	0.10	2.00	0.2
Plasminogen	0.45	0.05	9.00	0.9
Fibrinogen	0.05	1.30	0.04	14.0
K <sub>15</sub> A (dendrimer)	9.20	0.30	27.70	4.9
K <sub>12</sub>	13.10	0.30	43.00	4.5
K <sub>8</sub>	15.90	0.40	38.80	2.7
K <sub>4</sub>	16.60	0.30	58.80	1.0
K <sub>8</sub> GPRP	14.30	0.10	142.90	5.4
K <sub>4</sub> GPRP	14.30	0.10	158.90	4.9
GPRP	15.90	0.10	175.90	1.8

Table 2. shows the extraction of t-PA from crude CHO cell supernatant using GPRP- und polylysine ligands. The ligands with good affinity, GPRP and K<sub>15</sub>A, also provide the biggest adsorption capacity. GPRP shows even higher capacity than monoclonal antibodies. Purity was proved by SDS-PAGE.

Table 2. Yield of t-PA from biological samples

<i>synthetic ligand</i>	<i>t-PA</i> [ $\mu\text{g/ml}$ ]	<i>yield</i> [%]
mAB	2.6	74
K <sub>15</sub> A (dendrimer)	2.5	71
K <sub>12</sub>	1.3	37
K <sub>4</sub>	1.0	29
K <sub>8</sub> GPRP	1.4	40
K <sub>4</sub> GPRP	1.2	34
GPRP	3.0	86

C. ALTAMIRANO, A. ILLANES, R. CANESSA, S. BECERRA  
AND J. BERRIOS

## EFFECT OF NUTRIENT SUPPLEMENTATION ON THE BIOLOGICAL QUALITY OF tPA PRODUCED BY CHO CELLS ON SERUM-FREE MEDIUM

*Biochemical Engineering School. Universidad Católica de Valparaíso,  
Valparaíso, Chile*

### 1. INTRODUCTION

Optimization of media formulation is a key aspect for bioprocess development in animal cell cultivation because of its complexity and high cost. Elimination of fetal bovine serum (FBS) is nowadays enforced because of the well-reported drawbacks of its use. However, serum-free media implies a case to case design based on the particular supplements required for each strain. BIOPRO1 is a defined medium designed specifically for CHO cell cultivation by BioWhitaker Europe (Belgium). Recombinant tPA producing CHO TF 70R cells have been cultivated in BIOPRO1 but cell growth was somewhat lower than obtained in a FBS containing medium. The objective of this work is the improvement of BIOPRO1 for CHO TF 70R cultivation in terms of cell growth and tPA production and functionality.

### 2. MATERIALS AND METHODS

tPA producing cell line CHO TF 70R was kindly provided by Pharmacia & Upjohn (Sweden). BIOPRO1, kindly provided by BioWhitaker Europe, plus 20 mM of glucose and 6 mM of glutamine was supplemented with vitamins, lipids and aminoacids as indicated in Table 1 for each experiment ( $C_i$ ). A control experiment (CC) was also performed for each of the four series of experiments ( $S_i$  in Table 1). Cell concentration and viability, glucose, lactate, ammonia and aminoacids were determined as previously reported (Altamirano *et al*, 2000). tPA was determined by ELISA and tPA activity with a chromogen assay. A conjugated peroxidase antihuman-tPA IgG was used for Western Blott analysis.

## 3. RESULTS AND DISCUSSION

According to S1 experiments, a three-fold increase in biotin, cobalamine, benzoic acid and folic acid (C1) was enough to obtain the same result as in C2 (data not shown), where all vitamins were increased threefold with respect to the control. V-3BF supplement produced an increase in specific cell growth rate ( $\mu$ ), cell concentration and viability with respect to CC, as seen in Table 2. A slight increase in tPA production was observed as a consequence of a higher cell concentration, but specific activity remained unaltered. In S2 experiments, best results were obtained with C5 (Table 2) where the medium was supplemented with lipids (Chol+FA) and vitamin (V-3BF) mixtures. In S3 experiments, the concentration of such mixtures was increased and the best results were obtained with C7 (Table 2), which corresponds to a 50 % increase in lipid concentration. A substantial increase with respect to BIOPRO1 was obtained in terms of  $\mu$ , cell concentration, cell viability and tPA production. The addition of lipids had opposite effects with respect to tPA: the specific activity of tPA increased, but the specific productivity ( $q_{tPA}$ ) decreased.

Table 1. Medium culture composition on the different experiments

Culture	Supplements add to BIOPRO1 whit 20 mM glucose and 6 mM glutamine						
	V-3BF	V-MEM	Chol <sup>a</sup>	Chol+PA <sup>b</sup>	Chol+FA <sup>c</sup>	Ser+Pro	Asn
CC	---	---	---	---	---	---	---
C1(S1)	3X	---	---	---	---	---	---
C2(S1)	3X	3X	---	---	---	---	---
C3(S2)	3X	---	1 %v/v	---	---	---	---
C4(S2)	3X	---	---	1 %v/v	---	---	---
C5 (S2)	3X	---	---	---	1 %v/v	---	---
C6(S3)	6X	---	---	---	1 %v/v	---	---
C7(S3)	3X	---	---	---	1.5% v/v	---	---
C8(S3)	6X	---	---	---	1.5% v/v	---	---
C9(S4)	3X	---	---	---	1.5% v/v	2X	---
C10(S4)	3X	---	---	---	1.5% v/v	2X	2X

a: 0.22 mg/L Chol. b: 0.22 mg/L Chol and 0.01 mg/L PA. c: lipids concentrate (GibcoBRL, 11905). V-3BF: biotin, cobalamine, benzoic acid and folic acid mixture. V-MEM: vitamins mixture (Sigma, M6895). Cho: cholesterol. PA: palmitic acid. FA: fatty acids. 3X/6X: threefold/six fold increase with respect to BIOPRO1.

**Table 2.** Culture parameters of CHO cell cultures: effect of vitamins and lipids

Parameter	CC	C1	C5	C7
		% of control		
$\mu$ ( $\text{h}^{-1}$ )	0.016	114	150	165
$q_{Glc}$ ( $\text{nmol}/10^6\text{cell}\cdot\text{h}$ )	170	97	105	98
$q_{Lac}$ ( $\text{nmol}/10^6\text{cell}\cdot\text{h}$ )	365	98	95	90
$q_{Gln}$ ( $\text{nmol}/10^6\text{cell}\cdot\text{h}$ )	94	105	84	80
$q_{Amm}$ ( $\text{nmol}/10^6\text{cell}\cdot\text{h}$ )	150	91	67	61
$q_{tPA}$ ( $\text{ng}/10^6\text{cell}\cdot\text{h}$ )	19.8	97	88	84
$Xv$ ( $10^6\text{cell}/\text{mL}$ ) <sup>a</sup>	0.68	113	146	162
$\%Xv$ <sup>a</sup>	72	108	112	125
$tPA$ ( $\text{mg}/\text{L}$ ) <sup>a</sup>	0.71	106	128	148
$a_{tPA}$ ( $\text{U}/\text{mg}$ ) <sup>a</sup>	116	97	128	136

<sup>a</sup>: values obtained at 96 h of cultivation

A possible explanation is that cholesterol stiffens the plasmatic membrane, which increases its mechanical strength and therefore confers a higher viability (Jenkins *et al.*, 1994). This implies a lower protease release by cell lysis and increased product stability. However, this membrane stiffening may hinder the excretion of tPA, which would explain the decrease in  $q_{tPA}$ . Similar results have been obtained with interferon- $\gamma$ -producing CHO K1 cells (Castro *et al.* 1995). To design S4 experiments, the residual concentration of aminoacids was analyzed: Apart from glutamine, the lower residual aminoacid concentrations corresponded to Ser, Asn and Pro. Ser and Asn are not considered essential aminoacids; however, high consumption rates have been determined in other CHO cell lines (Castro *et al.*, 1995). Pro is required for most CHO cells, because the mother strain (CHO K1) is a Pro auxotroph (Keen *et al.*, 1995). In S4 experiments Ser and Pro (C9) and Ser, Pro and Asn (C10) were supplemented, to double their concentrations in BIOPRO1, to assess the specific effect of Asn. This effect is not apparent, since Asn could be limiting (it was consumed almost completely) while contributing to increase the level of ammonia. As seen in Table 3, best results were obtained in C10, where, longevity of the culture was increased in 25 h and cell concentration increased threefold with respect to CC, while  $q_{tPA}$ , reduced in C7, was restored to a value close to that in CC. Although there is no clear explanation for this behavior, stimulatory effect of specific aminoacids on protein production has been reported in the case of Arg in the production of thrombopoietin with CHO cells (Chung *et al.*, 2001). No effect on tPA identity was observed in any case, as revealed by Western Blott (data not shown).

**Table 3.** Culture parameters of CHO cell cultures in S4

Parameter	CC	C9	C10
		% of control	
$\mu$ ( $h^{-1}$ )	0.018	159	162
$q_{Glc}$ ( $nmol/10^6 cell-h$ )	181	95	94
$q_{Lac}$ ( $nmol/10^6 cell-h$ )	362	89	92
$q_{Gln}$ ( $nmol/10^6 cell-h$ )	87	83	80
$q_{Amm}$ ( $nmol/10^6 cell-h$ )	130	70	94
$q_{tPA}$ ( $ng/10^6 cell-h$ )	26.2	87	98
$X_V$ ( $10^6 cell/mL$ ) <sup>a</sup>	0.72	181	200
% $X_V$ <sup>a</sup>	66	130	139
$tPA$ ( $mg/L$ ) <sup>a</sup>	0.66	150	1.81
$a_{tPA}$ ( $U/mg$ ) <sup>a</sup>	102	104	96

a: values obtained at 121 h of cultivation

#### 4. CONCLUSIONS

A systematic approach for media supplementation with vitamins, lipids and specific aminoacids produced a substantial increase in t-PA production with no detrimental effect on its biological activity and identity. The effect of Asn on t-PA production was unexpected and needs to be further studied.

#### 5. REFERENCES

- Altamirano, C., Paredes, C, Cairó, J., and Gòdia, F. *Biotechnol. Progress.* **16** (2000): 69-75.  
 Chung, J., Kim, T., Sung, Y., Jun, S., and Lee, G. In: *Animal Cell Technology - ESACT* (2001), p107.  
 Castro, P., Hayter, P., Ison, A., and Bull, A. *Cytotechnol.* **19** (1995): 27-36.  
 Jenkins, N., Castro, P, Menon, S., Ison., and Bull, A. *Cytotechnol.* **15** (1994): 209-215.  
 Keen, M., and Rapson, N. *Cytotechnol.* **17** (1995): 153-163.

**Acknowledgements:** Work supported by Grant 1020793 from FONDECYT, Chile.

S. DUVAR (1), J. BERLIN (1), H. ZIEHR (1), H.S. CONRADT (2)

## MODULATION OF THE GLYCOSYLATION REPertoire OF A RECOMBINANT HUMAN EPO EXPRESSING MODEL CELL LINE UNDER DIFFERENT CULTURE CONDITIONS

(1) *GMP Facility, German Research Center for Biotechnology GBF ,  
Mascheroder Weg 1, D-38124 Braunschweig, Germany*

(2) *Protein Glycosylation, German Research Center for Biotechnology  
GBF , Mascheroder Weg 1, D-38124 Braunschweig, Germany*

Abstract. Differences in the glycosylation patterns of glycoprotein therapeutics might result in altered biological activity, e.g. clearance, immunogenicity, targeting to specific receptors. Therefore, the exact knowledge of the product quality is an aspect of primary importance for the further development of a production process.

We have chosen a model BHK-21 B cell line expressing human recombinant EPO for the evaluation of the effect of different culture conditions on the N- and O-glycosylation of the product in the culture supernatant.

The BHK-21 B cell line expresses an unusual N-glycan pattern which shows apart from di-, tri- and tetraantennary complex-type structures present, in a significant high NeuGc content, partial truncated glycans and about 20% of oligomannosidic structures with phosphate (Man<sub>5</sub>6GlcNAc<sub>2</sub>) when cultivated in T-flasks or spinner flasks.

After identifying the critical culture variables like pH, initial glutamine concentration, glucose starvation and cell density we tested different procedures to reduce the undesirable NeuGc content and increase the NeuAc content at the same time, and furthermore to significantly eliminate oligomannosidic glycan structures and optimise the total N-glycans towards the type of modification that are found in the international EPO standard preparation.

Analysis of the product quality (after immunopurification) was performed by applying carbohydrate mapping procedures including HPAEC-PAD and MALDI/TOF-MS (ESI-MS) techniques.

### 1. INTRODUCTION

Mammalian cells are the preferred production system for secreted pharmaceutical proteins. The glycosylation of these proteins is important for their biological activity. To determine the product quality, we analysed protein integrity and glycosylation pattern of human EPO as a biotechnologically relevant and sensitive pharmaceutical product under different physiological conditions. EPO is highly glycosylated and glycosylation, in particular terminal sialylation, is essential for *in vivo* activity. BHK cells have a heterogeneous glycosylation pattern that has been characterised in detail [2]. Under certain culture conditions the classical Gal $\beta$ 1-4GlcNAc-antenna of di-, tri- and tetraantennary oligosaccharides are changed to GalNAc $\beta$ 1-4GlcNAc modifies which are not acceptors for  $\forall$ 2-3 sialyltransferase

mediated sialylation. Therefore the product secreted by these cells is significantly undersialylated (results not shown).

## 2. RESULTS AND DISCUSSION

The purpose of this investigation was to identify critical process parameters which affect product consistency of EPO expressed by BHK cells.

Figure 1 shows the influence of different production systems on the glycosylation of recombinant EPO. The amount of oligomannosidic structures with phosphate ( $\text{Man}_5\text{-}_6\text{GlcNAc}_2$ ) was in spinner-flasks about four times higher than in batch or perfusion cultures in bioreactors. In batch culture the tetrasialylated structures increased almost three times compared to the spinner-flasks. The perfusion process could also improve the quality of EPO compared to the spinner-flask but the batch culture was the most efficient production system in terms of EPO quality.

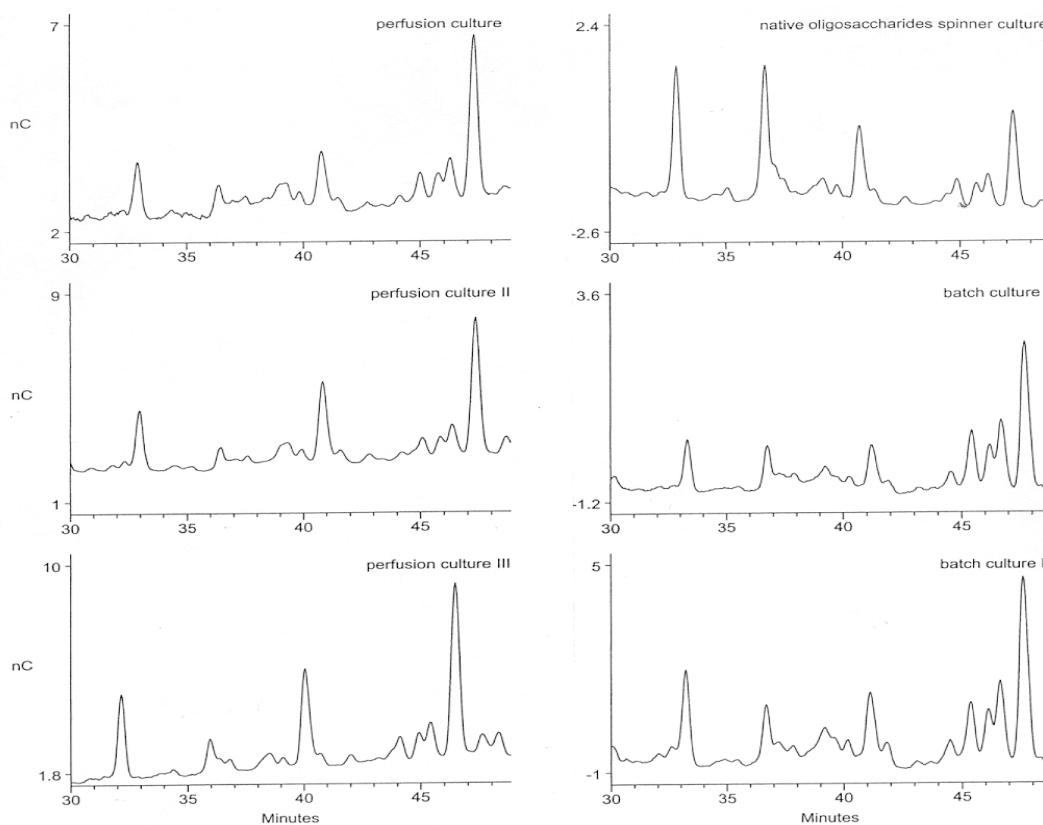


Fig. 1: HPAEC-PAD "mapping profile" of native oligosaccharides of rec-EPO from different cultivation systems.



The effect of  $\text{NH}_4\text{Cl}$  depends on the used culture medium (data not shown). In SMIF7 medium the amount of undesired NeuGc decreases in the presence of  $\text{NH}_4\text{Cl}$  less than in ProCHO5 medium. Also, the initial amount of NeuGc in SMIF7 medium is higher than in ProCHO5 medium. There is no detectable change in  $\text{Man}_6\text{-P}$  with or without  $\text{NH}_4\text{Cl}$ . In SMIF7 medium the cells react more sensitive towards  $\text{NH}_4\text{Cl}$ . The quantity of the total secreted EPO decreased in both cultures in presence of  $\text{NH}_4\text{Cl}$ . Our HPAEC-PAD data were confirmed with MALDI/TOF-MS (ESI-MS). The specific growth rate was significantly reduced whereas the specific glucose consumption decreased during the same culture.

We also analysed the effect of elevated glucose concentrations and different pH values (pH 7,2 and 6,8) on the glycosylation pattern of EPO. The effect of elevated glucose was a lower  $\text{Man}_6\text{-P}$  amount compared to the control culture with a low amount of glucose.

The addition of the V-ATPase inhibitor archazolide for three days caused a decrease in diantennary structures. The SDS-Page analysis showed light variations in the molecular weight. We also observed a decrease in glucose uptake with increasing concentrations of archazolide. Microscopical observations showed that the cell shape appeared more rounded than control cells without archazolide treatment (data not shown). These results could be explained with the inhibition of the transportation during the post-translational processing of the glycoprotein.

### 3. CONCLUSION

Our results show that it is important to characterise culture conditions that affect the post-translational modification of recombinant proteins in order to ensure consistency of secreted glycoproteins during a production process.

### 4. ACKNOWLEDGEMENTS

We gratefully acknowledge the collaborative contributions of the company GlycoThera GmbH (Dr. E. Grabenhorst and Mr. S. Kandzia).

### 5. REFERENCES

- Yang, M., Butler, M.  
Effects of Ammonia on CHO Cell Growth, Erythropoietin Production, and Glycosylation. *Biotechnology and Bioengineering*, Vol. 68, No. 4, May 20, 2000.
- Grabenhorst, E., Schlenke, P., Pohl, S., Nimtz, M., and Conradt, H.S.  
Genetic engineering of recombinant glycoproteins and the glycosylation pathway in mammalian host cells. *Glycoconjugate Journal* 16, 81 – 97, 1999.
- Schlenke, P., Grabenhorst, E., Nimtz, M., Conradt, H.S.  
Construction and characterisation of stably transfected BHK-21 cells with human-type sialylation characteristic. *Cytotechnology* 30; 17 – 25, 1999.

M. ETCHEVERRIGARAY, G. I. AMADEO, C. DIDIER, D. A.  
PEREIRA BACCI, F. A. CAVATORTA, R. KRATJE

## PHYSICOCHEMICAL ESTIMATION OF rhEPO POTENCY PRODUCED IN SUSPENSION CULTURE

*Laboratorio de Cultivos Celulares, Facultad de Bioquímica y Ciencias  
Biologicas, Universidad Nacional del Litoral, Santa Fe, Pcia. Santa Fe,  
Argentina*

### 1. INTRODUCTION

Most of recombinant products of animal cells are glycoproteins, and the consistency of glycosylation is extremely important during production. The oligosaccharide moieties play an important role, defining several biological properties like clearance rate, immunogenicity, and biological specific activity. The oligosaccharide residues on recombinant glycoproteins are highly variable depending on the host cell type, protein structure and cell culture conditions. Besides, the downstream processing protocol may influence the set of isolated glycoforms (Storring et al., 1998).

The aim of this work was to compare the molecule of recombinant human erythropoietin (rhEPO) produced in CHO cells grown in a perfused stirred tank bioreactor, and purified by two different methods, named A and B. We utilised physicochemical methods to analyse the purified isoforms in order to establish a correlation between these parameters and the biological activity of the hormone.

### 2. MATERIALS AND METHODS

#### *2.1. Cell Lines and Cultures*

A stable CHO.K1 cell clone transfected with the human EPO gene, obtained in our lab, was cultivated in a perfused 25 l stirred tank bioreactor (MBR AG, Switzerland). The media used consisted in a 1:1 mixture of DMEM and Ham's F-12 (Gibco BRL, USA) supplemented with 0.2% fetal calf serum (Bioser, Argentina).

#### *2.2. Purification Methods*

A three-step procedure was used for rhEPO purification (Amadeo *et al.*, 1996). Two alternative methods were employed for the second purification step (A and B).

### 2.3. Analysis of Samples

The total protein concentration was measured by Bradford. The rhEPO concentration was determined by RIA (Amadeo et al., 1999) and/or ELISA (Amadeo et al, 2002) in order to calculate the recovery and the purification factor of each purification step. The molecular weight and the purity of the final product were controlled by SDS-PAGE with silver staining. rhEPO was exposed to polyacrylamide gel isoelectric focusing in a pH 3-10 gradient and the bands were analysed by densitometry. The isoforms profile was obtained by capillary zone electrophoresis (CZE) (BioRad, USA). Taking into account the specific biological activity of the BRP standard and the relative abundance of its isoforms, it was possible to establish the activity of each form. Considering the CZE pattern of our samples, we estimated their potency and compared them with the *in vivo* activity measured in normocythaemic mice.

## 3. RESULTS AND DISCUSSION

The analysis of the three-step purification procedure for rhEPO by CZE established that 8 isoforms were obtained after the first step (Fig. 1).

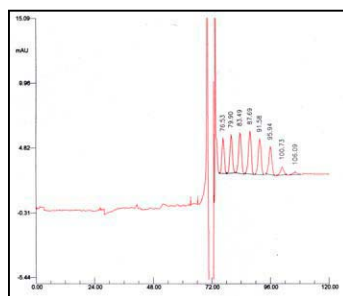


Fig. 1. Analysis of isoforms obtained after step 1 by CZE.

The second purification step was performed by two alternative methods, named A and B. Following method A, no variation in the number of isoforms was observed by CZE, but the relative proportion of each peak did vary. With method B, instead, two less glycosylated isoforms were eliminated (Fig. 2 and 3). SDS-PAGE analysis showed the difference in MW in each case (data not shown).

Glycoforms with isoelectric points (IP) ranging from 3.8 to 5.6 were isolated from cell culture supernatants by the three-step procedure with a total recovery of 54%. Method A allowed to separate a population of 8 isoforms (IP = 3.80 - 4.51), meanwhile method B rent a population of 6 isoforms (IP = 3.80 - 4.26). Two isoforms, less acidic, were eliminated by method B, and consequently, specific biological activity was increased from 90,000 IU/mg to 120,000 IU/mg.

The biological activity of different samples measured by the *in vivo* test was plotted against the potency estimated from the relative abundance of its isoforms by

CZE in the range from 40,000 IU/mg to 130,000 IU/mg (data not shown). The slope ( $\pm$  its confidential interval limits for  $\alpha = 5\%$ ) obtained by linear regression analysis was  $0.93 \pm 0.17$  ( $n = 18$ ), showing an adequate correlation between both parameters.

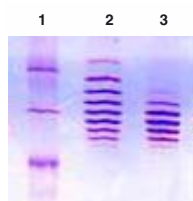


Fig. 2: Isoelectric focusing. Lane 1: IP markers. Lanes 2 and 3: purified isoforms by methods A and B, respectively.

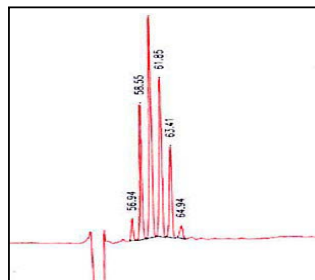


Fig. 3: Electropherogram of the purification product obtained with method B.

#### 4. CONCLUSIONS

The physicochemical analysis of rhEPO isoforms allowed us to establish the glycoform patterns obtained in every purification step and to evaluate the effect of modifications introduced in the process. It was possible to improve the overall process by means of accurate analysis of the quality of the molecule obtained in terms of desired isoforms. Finally, knowing the specific biological activity of each isoform, it was possible to predict the potency of each sample, considering its CZE pattern.

#### 5. REFERENCES

- Amadeo I, Kratje R, Etcheverrigaray M (1996) *Desarrollo del Downstream Processing de Eritropoyetina Humana Recombinante*. IV Jornadas de Comunicaciones Técnico-Científicas. Facultad de Bioquímica y Ciencias Biológicas, Universidad Nacional del Litoral. Santa Fe, Argentina.
- Amadeo I, Forno A, Bollati Fogolín M, Zuqueli R, Kratje R, Etcheverrigaray M (1999) *Controlling the quality of rhEPO during the production process*. In: *Advances in Modern Biotechnology* (J.V. Gaviñondo, M. Ayala, B. Acevedo, eds.), Elfos Scientiae, Havana, Cuba 5: 10.
- Amadeo I, Zenclussen ML, Oggero Eberhardt M, Kratje R, Etcheverrigaray M. (2002) *Cuantificación de rhEPO mediante un ELISA sandwich en diferentes estadios del proceso productivo*. XXIV Congreso Argentino de Química. Facultad de Bioquímica y Ciencias Biológicas, Universidad Nacional del Litoral. Santa Fe, Argentina.
- Storring PL; Tiplady RJ, Gaines Das RE; Stenning BE, Lamikanra A; Rafferty B; Lee J. (1998) *Epoetin alpha and beta differ in their erythropoietin isoform compositions and biological properties*. Br J Haematol, 100(1):79-89.

A.G. FORNO(1), M. ETCHEVERRIGARAY(1), M. NIMTZ(2),  
R.B. KRATJE(1)

POST-TRANSLATIONAL MODIFICATION OF  
RECOMBINANT HUMAN GM-CSF EXPRESSED BY  
STABLE-TRANSFECTED CHO CELLS UNDER  
DIFFERENT CULTURE CONDITIONS

(1) *Laboratorio de Cultivos Celulares, Facultad de Bioquímica y Ciencias  
biológicas, Universidad nacional del litoral, Santa Fe, pcia, Santa Fe,  
Argentina*

(2) *German Research Centre for Biotechnology (GBF), Braunschweig,  
Germany*

## 1. INTRODUCTION

Granulocyte-macrophage colony-stimulating factor (GM-CSF) is a pleiotropic cytokine that stimulates both the production of different hemopoietic cell lineages and the effector function of mature myeloid cells (Metcalf *et al.*, 1986). The sequence of mature human GM-CSF consists of 127 amino-acid residues, resulting in a predicted molecular mass of 14,465 Da. There are two *N*-linked glycosylation sites on Asn<sub>27</sub> and Asn<sub>37</sub>, and there are several *O*-linked glycosylation sites clustered on three serine residues near the *N*-terminus of the molecule (Kaushansky *et al.*, 1987).

The glycosylation of therapeutic proteins obtained in cell culture is essential for the clinical effectiveness of the extracted product. For this reason, it is necessary to fully characterise these recombinant glycoproteins with respect to their carbohydrate structures.

The aim of this work is focalised on the effect of adherent and suspension cell culture, with the purpose of clarifying whether the glycan structures change under different culture conditions. In this respect, the results presented here constitute the first characterisation of the oligosaccharides present in recombinant human GM-CSF (rhGM-CSF) for different growth cell conditions.

## 2. MATERIALS AND METHODS

### 2.1. Routine Cell Culture

A stable transfectant clone (GM-CSF 1P8B5) which expresses human GM-CSF (Bollati Fogolin *et al.*, 2000) was utilised in this work. This clone was derived from a CHO.K1 cell line transfected with a plasmid containing the gene for human GM-CSF. The suspension culture was performed in spinner flasks with Medium 1 supplemented with 0.2% FCS and stirred at 50 rpm. Daily, 50% of medium was removed and replaced by fresh medium while the cells were returned to the spinner flask. The adherent culture was performed in a Nunc Cell Factory™ also with Medium 1, which was changed twice a week.

### 2.2. Analysis of Samples

rhGM-CSF was purified from culture supernatant using immunoaffinity chromatography (CNBr-activated sepharose 4B coupled with monoclonal anti GM-CSF) as described by Forno *et al.* (2001). The samples were subjected to SDS-PAGE and analytical isoelectric focusing. Release of *N*-linked glycans from the samples was performed by PNGase F treatment. An aliquot of the sample was reduced and alkylated and Glu-C digestions were carried out. Mapping of proteolytic peptides was performed by MALDI/TOF-MS, and carbohydrate analysis was achieved using HPAEC-PAD and MALDI/TOF-MS.

## 3. RESULTS AND DISCUSSION

Multiple closely spaced bands in the apparent molecular mass range of 18-32 kDa, showing a similar pattern for both samples were observed on SDS-PAGE chromatography (figure not shown). In the isoelectric focusing experiment performed with a pH 2.5-6.5 gradient, at least 11 isoforms were observed, showing that the sample from adherent cultures contains less basic forms than the sample from suspension cultures (figure not shown). The HPAEC-PAD profiles showed no major differences in the *N*-glycan structures of both samples, with the presence of di, tri- and tetraantennary structures with and without *N*-acetylactosamine repeats as major components. The ratio of the peak areas corresponding to the liberated NeuAc and glycans indicates the overall degree of sialylation (Fig. 1).

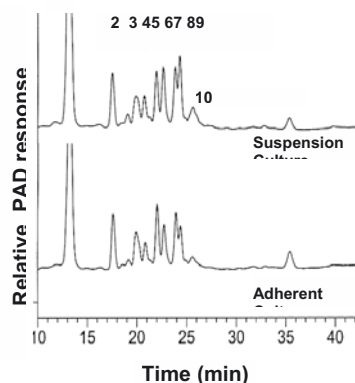


Figure 1. HPAEC-PAD mapping of neutral *N*-glycans of the suspension and adherent culture samples. The position of NeuAc (1), NeuGc (11), diantennary oligosaccharides structures (2), and triantennary oligosaccharides without (3 and 4), with one (6) and with two *N*-acetylactosamine repeats (8) are indicated. Other elution positions indicated are neutral tetraantennary oligosaccharides (5) and tetraantennary structures with one (7) and two *N*-acetylactosamine repeats (9).

The results of the *O*-glycosylation studies demonstrated GM-CSF forms containing either two or three *O*-glycan chains for both samples. A slightly higher content of *O*-glycan structures and an increased sialylation thereof was noticed for the product obtained from adherent culture. MALDI/TOF-MS of the desialylated GM-CSF forms (Fig. 2) showed that a higher proportion of the molecules from the suspension culture is lacking in the occupancy of one glycosylation site, indicating that site occupancy is the responsible for the differences observed in the isoform patterns.

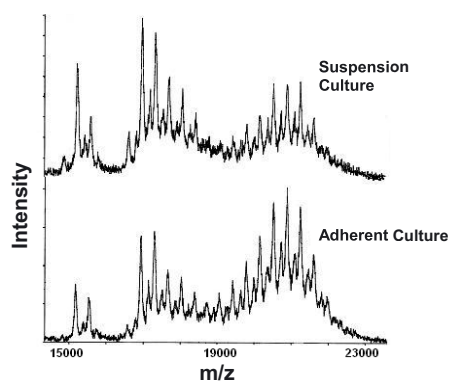


Figure 2. MALDI/TOF-MS spectrum of desialylated GM-CSF forms. The higher molecular mass zone (19,000 – 22,500 *m/z* region) corresponds to the *O*-glycosylated protein with both *N*-glycosylation sites occupied.

## REFERENCES

- Metcalf D., Begley G.G., Johnson G.R., Nicola N.A., Vada M.A., Lopez A.F., Williamson D.J., Wong G.G., Clark S.C., Wang E.A. *Blood* (1986) 67: 37-45
- Kaushansky K., O'Hara P.J., Hart C.E., Forstran J.W. and Hagen F.S. *Biochemistry* (1987) 26: 4861-4867.
- Bollati Fogolin M, Etcheverrigaray M, Kratje R. More Quality of Life by Means of Biotechnology, Hannover-Braunschweig, Germany (2000). Abstract Nr. 10.
- Forno A., Etcheverrigaray M., Kratje R. IX Jornadas de Jóvenes Investigadores de la Asociación de Universidades del Grupo Montevideo, Rosario, Argentina (2001). Abstract Nr. QU-12



S. NASCHBERGER<sup>1</sup>, K. RÜTTEN<sup>2</sup>, D. MÜLLER<sup>1</sup>  
AND H. KATINGER<sup>1</sup>

## SOFTMIX, A NEW SCALABLE MIXING SYSTEM FOR THE CULTIVATION OF SENSITIVE CELLS ON MICROCARRIER UNDER PROTEIN- FREE CONDITIONS

<sup>1</sup>*Institute of Applied Microbiology, University of Natural Resources and  
Applied Life Sciences, Muthgasse 18, A- 1190 Vienna, Austria*  
<sup>2</sup>*Rütten Engineering Ltd., Industriestrasse 9, CH- 8712 Stäfa, Switzerland*

### INTRODUCTION

The Softmix is an equipment providing soft mixing conditions in animal cell bioreactors. It is based on an agitation mechanism totally different from conventional impeller technology (Fig. 1). The essential part is a perforated plate with tapered holes dipped into the liquid oscillating vertically at a controlled frequency and amplitude (Fig. 1). The main difference in comparison to an impeller is a more homogenous energy distribution within the mixing zone due to the fluid flow across the holes (Tab. 1). The oscillation generates a low speed current ideal for the cultivation of shear sensitive cells over a wide range of mixing conditions. Additionally, the system is equipped with a sieve for carrier retention and perfusion .

### ENGINEERING CHARACTERISATION

For reactor characterisation  $k_L a$ - value, mixing time, maximum velocity of sinusoidal oscillation and stirrer tip speed were determined (Tab. 1-4). The system provides three aeration units (0.2  $\mu\text{m}$  microsparger, external circulation loop and headspace aeration). For  $k_L a$ - determination deionized water was aerated with air from zero (nitrogen saturated) to more than 90 % airsaturation (Fig.2; Tab. 2). The  $k_L a$  calculation was performed using the model in Fig. 2. The mixing time was determined by acid injection (2 M HCl) into the reactor and pH- measurement until no change in the signal was observed (Tab. 4).

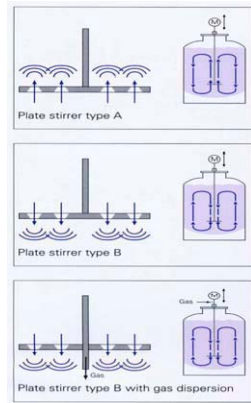
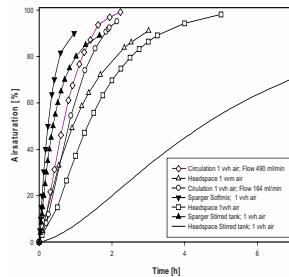


Figure 1. Mixing principle



Calculation model:  
 Exponential 2 Parameter  
 $\% \text{Airsat.} = a \times (1 - e^{-k_L a \times t})$   
 a... 100 % Airsaturation  
 $k_L a \dots k_L a\text{-value [h}^{-1}\text{]}$   
 t...time [h]  
 Program: Sigmaplot 8.0

Figure 2. Determination of  $k_L a$ -value

System	Parameter	Value [m/s]
Softmix reactor	Maximum velocity	0.28
Stirred tank reactor	Tip speed	0.31

Table 1. Comparison Softmix and stirred

Aeration system	Circulation Flow [ml/min]	Gasflow Air	$k_L a$ -Value [h <sup>-1</sup> ]
Circulation	164	1 vvh	1.061
Circulation	490	1 vvh	1.201
Headspace	0	1vvh	0.761
Headspace	0	1vvh	0.570
Sparger	0	1vvh	2.830
Sparger (STR)	0	1 vvh	1.728
Headspace (STR)	0	1 vvh	0.166

Table 2.  $k_L a$ - values Softmix- and stirred tank reactor

Aeration	$k_L a$ STR [h <sup>-1</sup> ]	$k_L a$ SM [h <sup>-1</sup> ]	F (= $k_L a$ SM / $k_L a$ STR)
Headspace	0.166	0.570	3.4
Sparger	1.728	2.830	1.6

Table 3. Comparison stirred tank reactor

Conditions	Mixing time [sec]
Softmix reactor	37
Stirred tank reactor	30
Comment	Time until no change in pH- value was observed

Table 4. Mixing time (STR..stirred)

The maximum velocity of sinusoidal oscillation (Softmix reactor) was calculated by  $v_{max}[\text{m/sec}] = A[\text{m}] \times \pi \times f[\text{sec}^{-1}]$  and the stirrer tip speed (stirred tank reactor; marine impeller) by  $v_{tip}[\text{m/sec}] = \text{rpm}[\text{sec}^{-1}] \times \pi \times \text{diameter}[\text{m}]$  (Tab. 1). All experiments were performed in the same vessel either equipped as Softmix or as stirred tank reactor.

Under these conditions the  $k_La$  value in the Softmix reactor was 3.4 (headspace) and 1.6 (sparger) higher than in the stirred tank reactor (Tab. 3). This enormous increase in oxygen transfer was achieved at comparable velocity maximum (sinusoidal oscillation) and stirrer tip speed (constant angular speed) (Tab. 1).

### SOFTMIX AS BIOREACTOR

For all experiments a protein- free medium formulation based on DMEM/HAM's F12 (1:1) was used. In order to find optimal conditions for Vero cells, we compared different microcarriers (Cytodex 1, Cytodex 3 and Cytopore 1) in spinner flasks (data not shown). All maximal cell concentrations found were in a range documented in literature. The macroporous carrier Cytopore 1 was best suited for this application (data not shown). However, in a stirred tank reactor it was not possible to cultivate Vero cells on microcarriers under these conditions (data not shown). In order to check the general applicability of the Softmix system for cultivation of cells on microcarriers a robust antibody producing CHO clone was cultivated first (Fig. 3). A cell concentration of  $1.4 \times 10^6$  cells/ml was reached. In the next step we cultivated Vero cells in the Softmix reactor in a perfusion mode and in contrary to the stirred tank reactor a cell concentration of  $1.0 \times 10^6$  cells/ml was reached (Fig. 4; F97). First efforts to improve the performance of the system by doubling of the carrier concentration to 2.4 g/l did not result in a further increase in cell concentration (Fig. 4; F103).

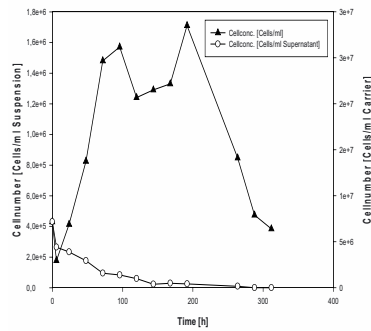


Figure 3. CHO cells on Cytopore (1.5 g/l) in the Softmix

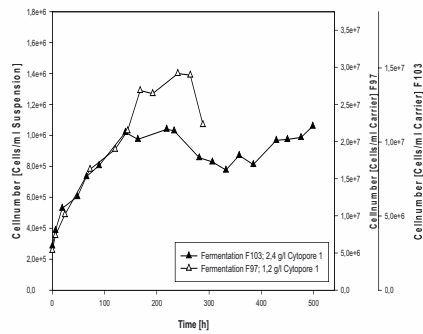


Figure 4. Vero cells on Cytopore 1 in the Softmix reactor

We found no indication for a substrate limitation (data not shown). Nevertheless, we think that a higher cell concentration is achievable with an optimized perfusion strategy.

The results obtained in this work demonstrated the applicability of the Softmix reactor as cultivation system for sensitive cells on microcarriers.

#### FUTURE ASPECTS

In order to optimize the Softmix system we will develop an adapted perfusion strategy. Furthermore a protocol for scale-up by carrier- to- carrier transfer will be established. Other carrier systems (Cytodex 1) will also be tested within this system. Based on the successful cultivation of sensitive cells on microcarriers and the excellent technical features, there are no restrictions for a scale- up of the Softmix system to industrial size.

#### LITERATURE

Microcarrier, Principles and Methods, Amersham Pharmacia Biotech, 2000

BOUZÓ L., OJITO E., ARIAS M.A., SUAREZ J., CHICO E.,  
ALVAREZ A., CHEA M., ALVAREZ I., DÍAZ C., VALIENTE O.

## ESTABLISHMENT OF FERMENTATION PROCESS FOR HREPO USING STIRRED TANK FERMENTERS IN PERFUSION MODE USING A COMMERCIAL PROTEIN- FREE CULTURE MEDIUM.

*Center of Molecular Immunology. P.O. Box 16040, Havana City  
11600, Cuba.*

### INTRODUCTION

The increasing needs for therapeutic proteins obtained from mammalian cell culture require the design of new production processes based in more powerful cell culture media. The commercial production of human recombinant Erythropoietin (hr EPO) has been done using different cell culture technologies as: rollers bottles, stirred tank fermentation, hollow fiber bioreactor. In recent studies Butler<sup>(1)</sup> has reported the production of this molecule in fluidized bed bioreactors. The trends in these production technologies are addressed to the removal of bovine serum from cell culture media and the introduction either serum free or protein free media which are specific for each cell line. The present work was addressed to obtain the scale up in stirred tank bioreactor (STR), using the HyQ PF-CHO MPS cell culture medium to produce hr EPO with quality characteristics similar to those obtained using other cell culture technologies. The growth and productivity of the CHO cell line transfected with the human EPO and cultured in different serum free or protein free cell culture media were studied. Moreover it was accomplished the study of expression stability during 60 days of continuous culture for the selected combination of clon- culture medium in order to guarantee the feasibility of the process.

### MATERIALS AND METHODS

**Cell line and Culture Conditions.** The cell line used was CHO-C31b, which produce a human recombinant EPO. The culture media used throughout the experiments were HyQ-SFX-CHO, HyQ-CCM5, HyQ-PF CHO MPS and PFHM II supplemented with Pluronic F68, glutamine and NaHCO<sub>3</sub>. Cells were cultured in 250 mL spinner flasks at 60 rpm and 36,5 °C. NaHCO<sub>3</sub> was use for pH control.

**Operation of a Perfusion 41L Fermenter.** Cells were cultured in a 41-L STR. Dissolved Oxygen Tension was controlled at 50%, pH varied between 6,8-7,0 and

temperature was controlled at 36,5°C. The stirred speed was 127 rpm. The dilution rate varied between 0,25 to 1,2 v. v. d. as the cellular metabolism change. Feeding was initiated when cell concentration reached about  $1,2 \times 10^6$  cell/ mL and glucose concentration was kept at 5mM.

**Analytical Measurements.** Cell counts were carried out using hemocytometer and cells were quantified using trypan blue exclusion method. Glucose, Lactate and Ammonia were measured by Biolyzer DT60 II. Amino Acids were detected using a proprietary method from Water by Merck-Hitachi HPLC. EPO and isoforms determinations were done through a specific ELISA and IEF techniques.

## RESULTS AND DISCUSSION.

### *Adaptation and selection of the medium.*

Among all media tested only in HyQ-CCM5 very low level of cell proliferation was observed with respect to the other media (Data not shown). The figures 1a and 1b show the cell growth and production profile of the cell line. In all cases the maximum cell density was over  $1,3 \times 10^6$  cell/ mL and the average specific growth rate was  $0.05 \text{ h}^{-1}$ . In terms of EPO titer, the best result was obtained in HyQ-PF CHO MPS medium, where the maximum EPO concentration reached  $37,8 \mu\text{g/ mL}$  which was 1,6 fold that obtained by the control culture in serum contained medium. For PFHM II medium the concentration was  $17 \mu\text{g/ mL}$  being 70 % lower than control culture. In the case of HyQ-SFX medium the value obtained was  $12,5 \mu\text{g/ mL}$  being lower than that obtained in PFHM II medium. From these results was selected HyQ-PF CHO MPS medium and a Working Cells Bank was made up for further experiments.

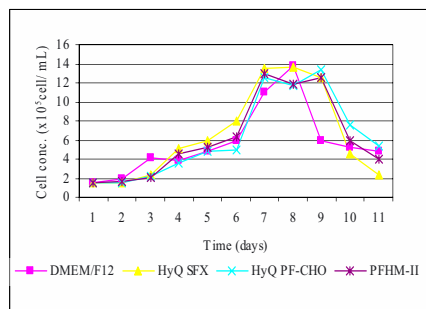


Figure 1.a Profile of growth of cellular line CHOC31B in different medium from culture.

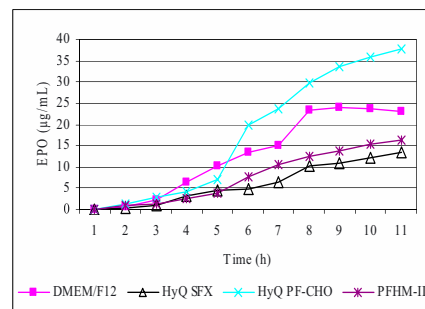


Figure 1.b Concentration of EPO in the time of cellular line CHOC31B.

### *Stability Study*

Once a medium was selected a stability study was carried out during 60 days in

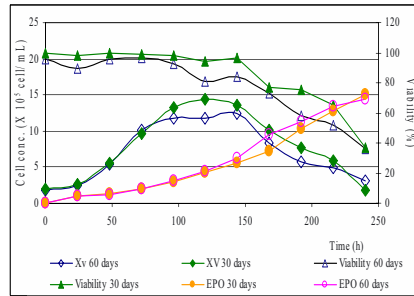


Figure 2. Cellular growth and concentration of EPO to two different times of culture.

order to demonstrate the feasibility of this cell line to be used in perfusion process.

The figure 2 shows that there isn't difference regarding to cell growth profile between cells at 30 and 60 days being the maximum cell density around  $1,4 \times 10^6$  cell/mL. The EPO production was also similar in both cases reaching over  $60 \mu\text{g}/\text{mL}$ .

This fact demonstrates the cells are stable in this medium and could be used in fermentation process up to 30 days.

*Fermentation Process at 41 L.*

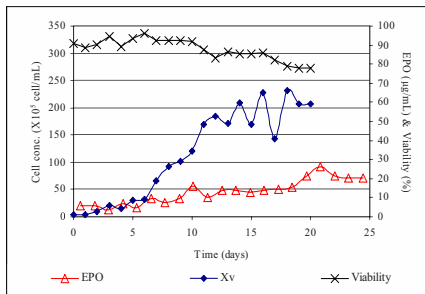


Figure 3. Fermentation in perfusion mode using a 41 L bioreactor for the EPO production.

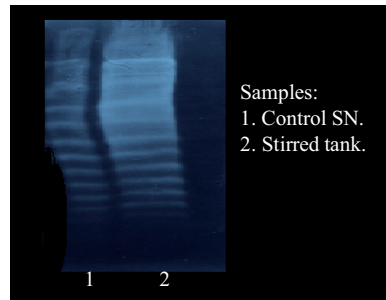


Figure 4. Pattern of isoforms of the molecule of EPO in different ways from culture.

The figure 3 shows the cell concentration increases over the time reaching a maximum cell concentration of  $23 \times 10^6$  cell / mL. During the exponential phase the EPO concentration reached  $12 \mu\text{g}/\text{mL}$  and in the plateau  $30 \mu\text{g}/\text{mL}$  being the specific production rate dependent upon the physiologic state of cells. Throughout the run the viability was kept over 80%. This process yielded 15 fermenter volumes and an output of 100 000 vials / run. The quality of the molecule is comparable with that obtained in hollow fiber and roller bottle as can be seen in the figure 4.

## CONCLUSIONS

- The HyQ PF-CHO MPS was the best medium for EPO production.
- The cell line CHO-C31b is stable HyQ PF-CHO MPS for more than 30 days.
- During the scaled up of the cells there was no loss of productivity.
- The quality of the molecule is comparable in different fermentation mode.

## REFERENCES

1. M-D. Wang, M. Yang, N. Huzel, M. Butler. 2001. Erythropoietin Production from CHO Cells Grown by Continuous Culture in a Fluidized-Bed Bioreactor. *Biotechnology and Bioengineering* 77: 194-203.
2. Heiko Meents, Barbara Enenkel, Rolf G. Werner, Martin Fussenegger. 2002. p27<sup>Kip1</sup>- Mediated Controlled Proliferation Technology Increases Constitutive sICAM Production in CHO-DUKX Adapted for Growth in Suspension and Serum- Free Media. *Biotechnology and Bioengineering* 79: 619- 627.
3. Geserick C, Bonarius HPJ, Kongerslev L, Hauser H, Müller PP. 2000. Enhanced productivity during controlled proliferation of BHK cells in continuously perfused bioreactors. *Biotechnology and Bioengineering* 69: 266- 274.



R. BRECHT<sup>1</sup>, H. BUSHNAQ-JOSTING<sup>1</sup>, S. ZIETZE<sup>1</sup>, R. NUCK<sup>2</sup>,  
C. KLOTH<sup>3</sup>, A. SCHWADTKE<sup>1</sup>, N. OBERMAYER<sup>1</sup>, U. MARX<sup>1\*</sup>  
S. KOCH<sup>1</sup>

## CONTINUOUS GMP PRODUCTION IN HOLLOW FIBRE BIOREACTORS – A VIABLE ALTERNATIVE FOR THE PRODUCTION OF LOW VOLUME BIOPHARMACEUTICALS

<sup>1</sup>ProBioGen AG Goethestrasse 54, 13086 Berlin, Germany, <sup>2</sup>Free University  
Berlin, Germany, <sup>3</sup>Medarex, Inc., Bloomsbury, NJ, USA, \*corresponding  
author. Phone +493092400611 Email: uwe.marx@probiogen.de

**Abstract.** Three different products; a murine monoclonal antibody from hybridoma cells, a human antibody and a recombinant protein from CHO cells, were produced in GMP compliant, pressure regulated hollow fibre bioreactor systems. The production runs were performed over a period of about 60 days. A high correlation between productivity in a 24h assay in T-flasks and the daily productivity of the cells per hollow fibre cartridge was observed.

In addition, production up to 90 days with high reproducibility is possible, as shown for the murine mAb. The different products were purified and subjected to extensive N-glycosylation analysis showing complex oligosaccharide structures. No correlation between the daily productivity and the percentage of sialylated structures was found, but a high reproducibility of the sialylation over different runs was observed with murine mAb.

### 1. INTRODUCTION

Recent trends in process science indicate a growing interest in continuous production processes. The requirement to show consistency for continuous processes is one of the major regulatory challenges that have to be met before production for market supply can begin. We have examined data from a number of hollow fibre bioreactor runs with different production cell lines and with the focus on scalability, reproducibility, durability and quality of the different products (glycosylation).

### 2. RESULTS AND DISCUSSION

#### 2.1. Comparison of production runs of different products

Three different pressure regulated bioreactor systems were used for the production runs: ASM 500, ASM 1000 and ASX (1,2 and 6 hollow fibre cartridges), BioVest Int., Minneapolis. Production runs were performed for a murine mAb from

hybridoma cells over a period of 58 days (ASM500), a human mAb from CHO cells (ASX, 60 days) and a recombinant protein from CHO cells (ASM 1000, 62 days).

Even though different cell types were used and the runs were not preceded by process development, we observed a high correlation between the productivity in a 24h assay and the productivity in the hollow fibre bioreactor, calculated for one cartridge (approximately 100 ml culture space), see figure 1. This correlation could be expressed as a factor which is very similar ( $\pm 20\%$ ) for the different products. This shows that the robustness of the production system is independent of the type of cell and product, and enables us to calculate the expected process amount at a very early stage of the pre-bioreactor cell culture. A major aim of further process development is to increase this factor by optimizing of process parameters.

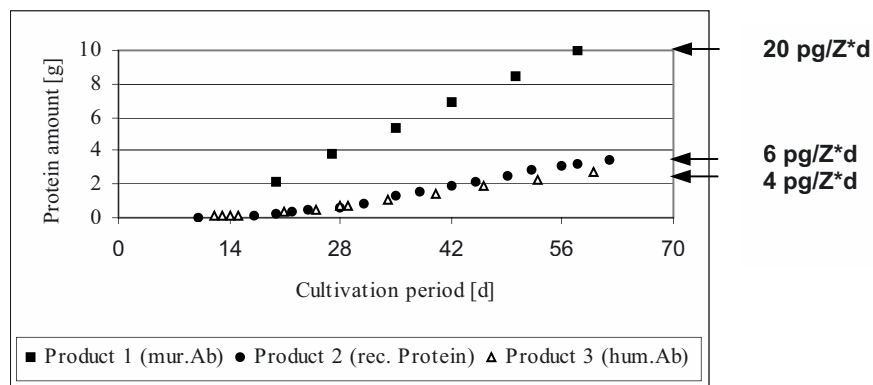


Figure 1. Cumulative protein amount in comparison with productivity in 24h assay

## 2.2. Comparison of different production runs for one product

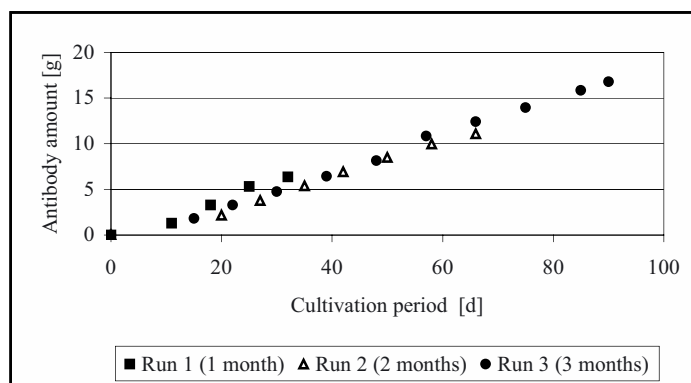


Figure 2. Consistency runs.

The murine monoclonal antibody was produced in an ASM 500 bioreactor three times over a period of about one, two and three months. As shown in figure 2, the daily productivity is highly reproducible and stable over longer cultivation periods of up to three months in the hollow fibre bioreactor.

### 2.3. Glycosylation analysis

The glycosylation pattern of the different products was analysed with a focus on rate and type of sialylation as an indicator for prolonged *in vivo* half-life [1]. The proteins were digested with trypsin and resulting peptides were deglycosylated by PNGase F digestion. The glycans were labelled with 2-aminobenzamide and separated by HPLC on a GlycosepC-column. Sialic acids were further characterized by sialidase treatment, DMB labelling and separation on a Bischoff Hypersil-ODS-column in comparison with the Sialic acid Reference Panel (Oxford GlycoSciences).

As shown in table 1, a totally different rate of sialylation for the three products was found and no correlation with the daily productivity in the hollow fibre bioreactor system could be observed. Typically N-glycolyl-neuraminic acid which was shown to be immunogenic [2], was found for the murine monoclonal antibody, whereas N-acetylneuraminic acid is the dominating sialic acid in the CHO-products.

High reproducibility in the sialylation rate was found for three different hollow fibre runs performed with and without FCS.

Table 1. Sialylation analysis

additives	<i>Hum. mAb</i>	<i>Rec. protein</i>	<i>Murine mAb</i>		
	Serum free	0.02% HSA	Serum free	Serum free	2% FCS
N-glycolyl-neuraminic acid	-	1,9	94,1	94,7	94,4
N-acetyl-neuraminic acid	100	99,1	5,9	5,3	5,6
Asialo-glycans	99,5	21,9	54,9	48,9	56,2
Monosialo-glycans	0,05	29,9	35,6	38,4	35,5
Disialo-glycans	0,45	40,6	9,3	12,8	8,3
Trisialo-glycans		6,5			
Tetrasialo-glycans		1,1			

### 3. REFERENCES

- [1] Kronman C, Chitlaru T, Elhanany E, Velan B, Shafferman A: Hierarchy of post-translational modifications involved in the circulatory longevity of glycoproteins. Demonstration of concerted contributions of glycan sialylation and subunit assembly to the pharmacokinetic behavior of bovine acetylcholinesterase. *J Biol Chem.* 2000 Sep 22;275(38)
- [2] Noguchi A, Mukuria CJ, Suzuki E, Naiki M: Immunogenicity of N-glycolylneuraminic acid-containing carbohydrate chains of recombinant human erythropoietin expressed in Chinese hamster ovary cells. *J Biochem (Tokyo).* 1995 Jan;117(1):59-62.

G. RODRIGUEZ, M.A. ARIAS, J. SUÁREZ, M. CHEA, L. BOUZÓ,  
R. CUERVO, I. ALVAREZ AND E. CHICO

## OPTIMIZING CULTIVATION STRATEGIES IN DIFFERENT SCALES OF HOLLOW FIBER BIOREACTORS

*Center of Molecular Immunology (CIM). P.O.Box 16040,  
Havana City 11600. Cuba.*

### 1. INTRODUCTION

In this study two empirically based optimization strategies are developed and tested during the cultivation of NSO and CHO cells in hollow fiber bioreactors. Both strategies address the changes in the nutrient feeding via Intracapillary Space (IC) medium flow as well as the improvement of the cellular environment in the Extracapillary Space (EC) by axial recirculation and controlling harvest/feed ratio in the EC space.

### 2. MATERIALS AND METHODS.

Cell lines: A recombinant myeloma cell line (NS0) that produces a humanized monoclonal antibody and a CHO cell line secreting rhEPO.

Bioreactors: Two different automated AcuSyst hollow fiber bioreactors models were used. The AcuSyst- Jr with cultivation area of 1,1 m<sup>2</sup> and an extracapillary volume of 65 mL was used for the cultivation of the NSO cell line. The AcuSyst X-Cell with a total area of 12.6 m<sup>2</sup> (six 2.1 m<sup>2</sup> cartridges) and a total extracapillary volume of about 750 mL was used for the growth of the CHO cell line.

Table 1: Optimization Rationale

	Basic Cultivation Procedure	Optimization criteria	
		CHO Cells	NS0 Cells
IC Space	Adjust IC feed flow to control Glucose concentration above 11 mM	Intensive IC-Feeding strategy without Glucose concentration control. (OVER-FEEDING)	Intensive IC-Feeding strategy without Glucose concentration control. (OVER-FEEDING)
EC Space	EC Cycling for mixing and balanced Harvest/EC-Feed ratio	An axial EC recirculation loop in addition to the EC Cycling to improve mixing in the cell growth compartment	Avoid excess of cell mass 'in suspension' by regular cell removal. Increase total protein concentration by reduce the Harvest/EC Feed ratio.

### 3. RESULTS AND DISCUSSION

#### 3.1 Cultivation of CHO cells in large scale ( $12.6 \text{ m}^2$ bioreactor). Results of the optimization

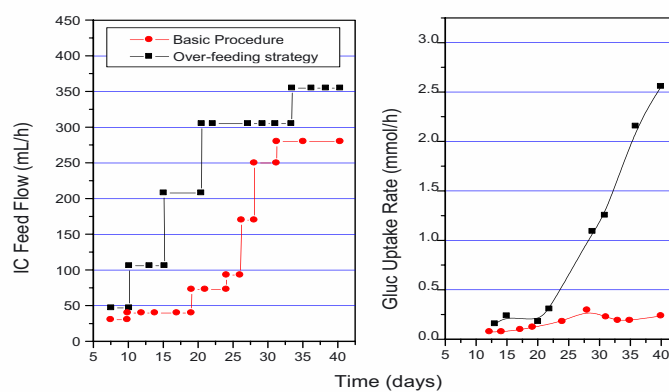


Figure1. Metabolic effect of the over-feeding on the cultivation of CHO cells. Medium flows are expressed per  $2.1 \text{ m}^2$  cartridge.

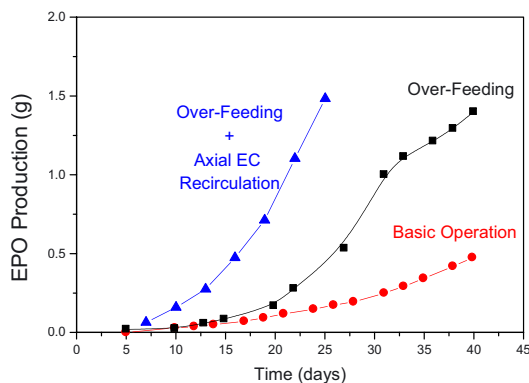


Figure 2. Cumulative rEPO production for the different cultivation strategies.

The rEPO production by the CHO cells increased also as a result of the IC overfeeding in comparison to the basic operation procedure, as can be observed in Fig.2. The optimization of the EC environment by the axial recirculation flow resulted in an additional increase of the protein production from the early phase of the fermentation, which indicates the productivity potential of the cell population when the limiting and/or inhibiting gradients are modified.

3.2 Cultivation of NS0 cells in pilot scale (1.1 m<sup>2</sup> bioreactor). Results of the optimization.

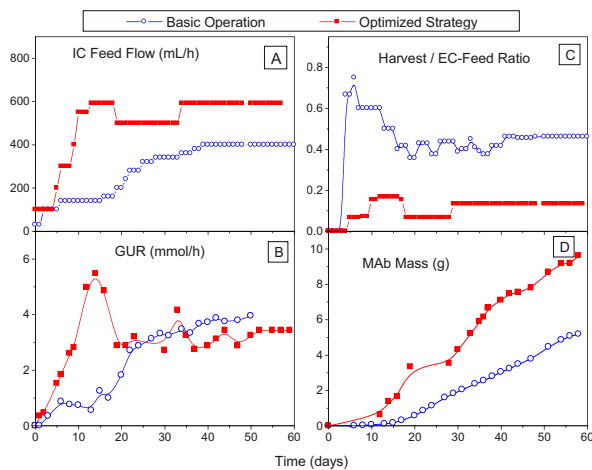


Figure 3. Experimental results of the cultivation of NS0 cells under basic and optimized operation.

The metabolic activity evaluated through the glucose uptake rate (GUR) is showed in the figure 3B. The use of the IC overfeeding strategy resulted in rapid increase in the fermenter GUR with a maximum reached when IC feed rate was adjusted to 600 mL/h (Fig 3B and 3C). However, the GUR profiles were very similar for both cultivation strategies from day 20 until the end of the cultivation time. A significant reduction in the Harvest/EC feed ratio was carried out during the fermentation done with the optimized strategy, as can be observed in the Fig. 3C. Table 2 shows the effect of the lower harvest flow on the accumulated EC parameters. As can be observed in Table 2, the new strategy resulted in a tenfold increase in the harvest concentration and a 6 fold reduce in the harvest volume with a positive impact on the downstream process.

*Table 2: EC accumulated parameters for both cultivation strategies.*

<b>EC process parameters</b>	<b>Basic Operation</b>	<b>Optimized strategy</b>
EC medium consumed	25 L	20L
Total harvest volume	11.54 L	1.99 L
Average MAb concentration in harvest	0.477 g/L	4.812 g/L

The combined optimization in the IC feeding as well as in the harvest/EC-feed ratio resulted in a significant improve in bioreactor productivity as can be observed in Fig. 3D, at the end of the cultivation time the NSO cells accumulated 10 g of recombinant antibody, for an almost twofold increase in productivity.

#### REFERENCES.

- Grammer, M.J et al. Effect of harvesting protocol on performance of a hollow fiber bioreactor. *Biotech. Bioeng.* **65**: 334-340, 1999

MICHAEL J. GRAMER

## INCREASING ANTIBODY PRODUCTION FROM HOLLOW FIBER SYSTEMS

*BioVest, Minneapolis, USA*

While hollow fiber bioreactor systems have been used for production of biologicals for almost 25 years, little data are available regarding optimization of these systems. This is due in large part to the lack of a good hollow fiber-specific screening tool. The purpose of this poster is to present recent findings using a novel tool developed specifically for this process: the micro hollow fiber bioreactor. The primary advantage of this tool is that no pumps are required, so that many conditions can be tested simultaneously. This tool has become an integral part of our development screening process, enabling quicker time to production of clinical material at reduced cost (*1*). Case studies are presented demonstrating the effect of medium and cell line on performance of hollow fiber bioreactors. Additional work demonstrates the value of cell side convection to enhance productivity in the short term and prolong productivity in the long term.

### 1. INTRODUCTION

Hollow fiber bioreactors consist of thousands of hollow fibers encased in a cylindrical shell. The fibers are semi-permeable with a molecular weight cut-off usually in the range of 10-30 kD. Cells are inoculated outside the fibers. Medium is circulated from a reservoir, through a gas-exchange cartridge, through the inside of the fibers, and is returned to the reservoir. The high rate of circulation is primarily to provide sufficient oxygen to the cells. The bulk of cell nutrition is provided by the non cell side medium, which is usually basal medium. A 160-ml bioreactor consumes about 10 L/day of non cell side medium. Cell side medium is fed at about 1 bioreactor volume per day to provide growth factors that do not cross the fiber; the product is harvested from the cell side at the same rate. The 10 L/day medium consumption from a 160-ml bioreactor produces the same as 10 L in a batch tank, but the cost is reduced since basal medium is the bulk of the feed. Downstream processing is simplified by placing an in-line filter on the harvest line, resulting in the collection of a concentrated, cell-free harvest ready for application to a purification column.

Scale up is linear, accomplished by increasing the bioreactor size, by connecting bioreactors in parallel, and by adding off-the-shelf instruments. The largest off-the-shelf instrument supports 20 160-ml bioreactors, equivalent to a 1500 L batch tank with kg production capacity. Hollow fiber instruments require only an outlet and a CO<sub>2</sub> source, which reduces overhead costs and allows for accelerated facility construction.

### 2. MICRO BIOREACTOR

751

*F. Gòdia and M. Fussenegger (Eds.), Animal Cell Technology meets Genomics, 751-753.*

© 2005 Springer. Printed in the Netherlands.



### *2.1. Description*

The micro bioreactor is a patented tool useful for screening media and cell lines for growth in a hollow fiber environment (2-5). The micro bioreactor is constructed similarly to a standard hollow fiber bioreactor. However, only 30 fibers are used. The fibers are encased in a 15-cm piece of silicone tubing which has an inside diameter of 0.635 cm. Cells are inoculated inside the fibers in total volume of 0.2-ml. Because of this small volume, the metabolic demand of the cells is relatively low, even at densities near 100 million viable cells per ml. The 4.6-ml space outside the fibers is large enough to serve as a medium reservoir, and the silicone tubing provides sufficient oxygen and carbon dioxide transfer to act as the gas-exchange cartridge. As a result, no pumps are required. The micro bioreactor is inoculated at 1-5 million viable cells per ml, placed in the incubator like a T-flask, and is harvested three days later. Micro bioreactor conditions which support better cell expansion at high viability result in better overall performance and production from a large scale hollow fiber system. Many conditions can be tested at once, enabling rapid optimization. The following case studies are presented in the poster.

*2.2. CASE STUDY 1: The micro bioreactor is more useful than a T-flask for predicting performance of a hollow fiber system.*

*2.3. CASE STUDY 2: Optimal growth in the micro bioreactor correlates with higher productivity in the hollow fiber system.*

*2.4. CASE STUDY 3: An NS0/GS cell line required increased serum on the cell side of the fiber.*

*2.5. CASE STUDY 4: CHO cells grow better in the micro bioreactor when adapted to PFM in suspension.*

*2.6. CASE STUDY 5: Selecting cells for optimal growth in a hollow fiber system.*

## 3. EFFECT OF CELL SIDE CONVECTION

Theoretical modeling suggests that enhanced convection is necessary for optimal HF performance. Accelerated cell side circulation provides some benefit, although severe channeling was seen as the bioreactor reached packed cell density. This channeling was not seen when ultrafiltration cycling was used; production was increased and prolonged (6-7). The value of cycling is visually demonstrated by the use of non-invasive NMR imaging. After reaching a packed cell density on day 14,

cycling was turned off. Overnight, there was a substantial reduction in viable cell density, correlating with reduced metabolic activity.

### 3. REFERENCES

1. Gramer, M.J., Hirschel, M.D. and Sly, J (2003) From discovery to the clinic: a robust strategy for rapid development of clinical manufacturing processes. *Bioprocess International*, 5, 62-66.
2. Gramer MJ and Britton TL (2002) Antibody production by a hybridoma at high cell density is limited by two independent mechanisms. *Biotechnol Bioeng* 79: 277-283.
3. Gramer MJ and Britton TL (2000) Selection and isolation of cells for optimal growth in hollow fiber bioreactors. *Hybridoma* 19: 407-412.
4. Gramer MJ and Poeschl DM (2000) Comparison of cell growth in T-flasks, in micro hollow fiber bioreactors, and in an industrial scale hollow fiber bioreactor system. *Cytotechnology* 34:111-119.
5. Gramer MJ and Poeschl DM (1998) Screening tool for hollow fiber bioreactor process development. *Biotechnol Prog* 14: 203-209.
6. Gramer MJ, Poeschl DM, Conroy MJ and Hammer BE (1999) Effect of harvesting protocol on performance of a hollow fiber bioreactor. *Biotechnol Bioeng* 65: 334-340.
7. Hirschel MD and Gruenberg ML (1988) An automated hollow fiber system for the large scale manufacture of mammalian cell secreted product. In: BK Lydersen (ed) *Large Scale Cell Culture Technology*. Macmillan. pp. 113-144.

CORY J. CARD, THOMAS SMITH, BRENT HUNSAKER,  
BILL BARNETT

PRODUCTION OF POLIOVIRUS, RUBELLA VIRUS,  
MEASLES VIRUS AND RECOMBINANT  
ADENOVIRUS IN PROTEIN-FREE MEDIA

*Perbio Science/Nv Hyclone Europe, Aalst, Belgium*

1. INTRODUCTION

The nutritional demands placed on cell culture media for long-term culture of mammalian cells and production of high virus titers are great. Traditionally, serum has been the principal source of vitamins and cofactors, essential nutrients, minerals and trace elements, attachment factors, transport and binding of essential nutrients, buffering capacity, protection from shear stresses, toxins, proteolysis, and free radicals, and regulation of growth. Hence, the development of an efficient serum-free or protein-free medium can become complex as an attempt is made to replace these functions; especially so when undefined and/or animal-derived components are to be avoided.

During viral infection, however, serum-free conditions have an advantage. Because of the inhibitive effect of serum on virus infectivity, serum content is often reduced or eliminated just prior to inoculating cultures. The level of nutrition available to cells during the infection, therefore, is reduced, and may limit the rate at which the host cell can produce virus. This is not the case in serum-free media, wherein the growth medium is identical to the medium during infection. This allows a high level of nutrients to be available to the cell during virus replication. Further action can be taken to increase the nutrient availability and virus/host cell interaction. These methods in large-scale cultures include concentration of the cell mass in stirred tank cultures by use of a spin-filter or hollow-fiber cartridge with suspension cultures and reducing agitation with microcarrier cultures to allow settling, and partial removal of the culture fluids. Once the cells are concentrated, the culture is inoculated with virus and maintained at a reduced agitation rate. At 4 to 6 hours post-inoculation the agitation rate is increased, and the working volume replenished using fresh serum-free medium. This process provides a high level of interaction between virus and host cell, while increasing the availability of nutrients at the time of demand.

## 2. MATERIALS AND METHODS

### 2.1 Cells

Stock cultures of HEK 293 cells (ATCC, CRL-1573), PER.C6\* (Crucell, Leiden, The Netherlands), and Vero (ATCC, CCL-81) were maintained at 37° C with 5% CO<sub>2</sub>/95% air in Dulbecco's Modified Eagle's Medium (DMEM) (HyClone, SH300022) supplemented with 10% fetal bovine serum (HyClone, SH30070). PER.C6 cultures were also supplemented with 10mM MgCl<sub>2</sub>.

### 2.2 Virus

Poliovirus Type I was obtained from Utah State University (Logan, UT) and was used in the vero cell studies. Ad5-GFP vector was obtained from Quantum Biotechnologies (Montreal, Quebec) and used in the HEK 293 studies. Ad5-LacZ vector was obtained from Crucell and used in the PER.C6 studies.

### 2.3 Cryopreservation

Cells maintained in serum-free medium during exponential phase growth with viabilities greater than 90% were cryopreserved using the following procedure.

Cells were centrifuged at 100 x g to produce a cell pellet. Supernatant was removed and stored for later use. Cell pellet was gently resuspended at a concentration of 10x10<sup>6</sup> cells/ml in the conditioned medium. An equal volume of fresh serum-free medium supplemented with 20% DMSO was slowly added (drop-wise) to adjust cell density to 5x10<sup>6</sup> cells/ml. The suspension was then transferred to plastic 1.8 ml cryovials (Nalge) at a volume of 1.0 ml. Cells were cooled at an approximate rate of -1.0° C/min to reach a final temperature of -70° C. Upon reaching the final temperature, vials were transferred to the vapor-phase of liquid nitrogen storage tanks. Care was taken to ensure cells do not remain at -70° C for longer than 24 h.

Cells were thawed by removal of vials from liquid nitrogen storage and placed immediately into a 37° C waterbath with gentle agitation, allowing vials to warm to 25° C. The vials were then disinfected using 70% isopropyl alcohol. Cell contents were transferred to a 15 ml centrifuge tube, and an equal volume of fresh, pre-warmed (25° C) serum-free medium was added drop-wise to the suspension. Tubes were allowed to stand for 5 min, then 3 ml of fresh, pre-warmed serum-free medium was added drop-wise to bring the total volume to 5 ml. Again, the tubes were allowed to stand for 5 min. Finally, an additional 5 ml of fresh, pre-warmed serum-free medium was added drop-wise to bring the volume to 10 ml, with an expected cell density of 5x10<sup>5</sup> cells. The cells were centrifuged at 100 x g for 10 min, pelleting the cells to remove the cryoprotectant. The supernatant was removed and the cells were gently resuspended in 10 ml of fresh, pre-warmed serum-free medium. A small sample of the suspension was counted to determine actual cell density. Viability assessment was not accurate for at least 24 h after thawing. Cell

suspensions were placed into a 25 cm<sup>2</sup> T-flask and incubated at 37° C, 5% CO<sub>2</sub>. Agitated, suspension cultures were initiated within 3.5 days, or when average viabilities were >90%, and normal population doubling times (24-36 h) were observed.

#### *2.4 HEK 293 and PER.C6 Virus Production Studies*

A 10 L working volume stirred-tank was seeded at 3x10<sup>5</sup> cells/ml and monitored for cell growth during a 72 h period. At 72 h post-seeding a cell count was obtained, and the cell suspension was concentrated using a hollow-fiber cartridge to remove 50% (5 L) of the working volume. The cell density was recorded following the concentration step to determine cell loss in the hollow-fiber. During the concentration step the agitation rate was decreased, and the bioreactor was inoculated with an appropriate virus titer. Virus and cells were left in the concentrated state for 4 h post-inoculation. Following the 4 h incubation, fresh medium was added to replenish the 10 L working volume, and the normal agitation rate was resumed. Samples were obtained every 24 h post inoculation for cell density/viability and viral titer determination.

#### *2.5 Vero Virus Production Studies*

The appropriate vessel was seeded with 1x10<sup>4</sup> cells/ml and monitored for cell growth until a 90% confluent monolayer was formed. Upon reaching 90% confluency 50% of the culture medium is removed, and the culture was inoculated with an appropriate virus titer. Virus and cells were left in the concentrated state for 4 h post-inoculation. Following the 4 h incubation, fresh medium was added to replenish the working volume. Samples were obtained at 72 h post-inoculation to determine virus titer.

### 3. RESULTS AND DISCUSSION

The ability of a serum-free medium to support cryopreservation and recovery of cells without the use of serum is a desirable, but demanding characteristic. Figure 1 documents the recovery of three cell lines following 6 months storage in the serum-free medium without the use of serum as an aid in cryopreservation. While all three cell lines displayed slow growth during the first passage after thawing, all resumed typical growth rates within three to four passages.

High yields of poliovirus were obtained using vero cells under protein-free conditions in static (T-flask), roller bottle, and suspension microcarrier cultures. Figure 2 depicts the yields of poliovirus obtained in each culture system under serum-free and serum-containing conditions. In each case, the serum-free condition outperformed the serum-containing condition with regard to virus yield. Both serum-containing and serum-free conditions yielded higher productivity in static and microcarrier cultures, compared to roller bottle cultures.

High yields of adenovirus vector were also obtained using serum-free culture of HEK 293 and PER.C6 cells, as shown in figures 3, and 4, respectively. Ad5 titers from HEK 293 cells reached approximately  $5.3 \times 10^{10}$  TCID<sub>50</sub>/ml, and  $3.3 \times 10^9$  TCID<sub>50</sub>/ml, respectively.

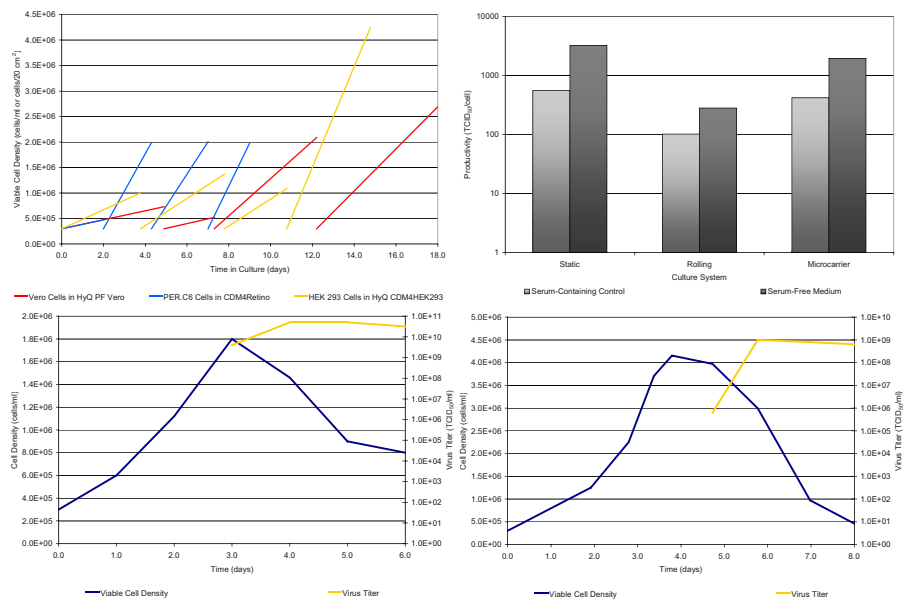


Figure 1. (Above Left) Vero, PER.C6, and HEK 293 cell growth obtained after thawing following a 6 month cryopreservation under serum-free conditions supplemented with 10% DMSO. Figure 2. (Above Right) Infectious titer of poliovirus produced under protein-free and serum-containing conditions using static, roller bottle, and suspension microcarrier cultures. Figure 3. (Lower Left) Viable cell density and Ad5 vector titer obtained in HEK 293 cells under animal-free conditions in a 10L NBS Celligen Plus stirred-tank culture. Figure 4. (Lower Right) Viable cell density and Ad5 vector titers obtained in PER.C6™ cells under chemically-defined, animal-free conditions in a 10L NBS Celligen Plus stirred-tank culture.

#### 4. SUMMARY

Although serum has traditionally been a necessity in cell culture, these studies have shown that the nutritional demands placed upon cells during vaccine or virus production can be met in serum-free conditions. In many circumstances, particularly with adherent-dependant cell lines, cell proliferation rates obtained in serum-containing conditions cannot be matched by serum-free conditions. However, this shortcoming is insignificant, as the productivity of cells in serum-free conditions during virus production appears to be much higher. This is most likely due to the availability of nutrients during infection, which is not attainable when reducing or eliminating serum from the culture medium.

## 5. REFERENCES

- Froud, S. J. (1999) The Development, Benefits and Disadvantages of Serum-Free Media. *Dev Biol Stand* 99: 157-166.
- Mather, J.P. (1998) Making Informed Choices: Medium, Serum, and Serum-Free Medium. *Methods Cell Biol* 37: 19-30.
- Merten, O.W. (1999) Safety Issues of Animal Products Used in Serum-Free Media. *Dev Biol Stand* 99: 167-180.
- Hierholzer, J.C., and Killington, R.A. (1996) in *Virology Methods Manual* (Mahy, B., Kangro, H. eds.), pp. 35-46, Academic Press, London, San Diego, New York, Boston, Sydney, Tokyo, Toronto.

CORY J. CARD, THOMAS SMITH, BRENT HUNSAKER,  
BILL BARNETT

SERUM-FREE PRODUCTION OF POLIOVIRUS: A  
COMPARATIVE STUDY USING MICROCARRIERS,  
ROLLER BOTTLES AND STATIONARY CELL  
CULTURE

*Perbio Science/Nv Hyclone Europe, Aalst, Belgium*

1. INTRODUCTION

Serum has been a necessity for many years, and continues to be important for the culture of attachment-dependant cell lines. The lack of serum in an adherent cell culture medium poses difficulties such as the attachment, spreading, and formation of a cell monolayer; proteolytic damage during monolayer dissociation; and limitations to the use of some culture systems. As the use of serum becomes more highly regulated the need increases for robust serum-free media allowing flexibility in use and meeting the nutritional requirements of the cells for high productivity. Many systems have been used in the production of viruses, including static cultures, roller bottles, and suspension microcarrier systems. A comparison of the surface area obtainable with each of these systems is listed in Table 1. Each system provides its own advantage(s). Large-scale static culture systems, such as the Nunc Cell Factories can allow adherent culture of cells without the expense of rolling apparatus and other handling equipment, while roller bottles offer ease and a classical approach in culture manipulations. Microcarriers offer an extremely high surface area to cubic space ratio, allowing high cell densities. However, each system has distinct disadvantages also, including difficulty in manipulating and monitoring cultures when using Cell Factories, a large space, time, and equipment requirement for roller bottle systems, and expensive stirred-tank equipment and increased difficulty in cell manipulation using the microcarrier approach. A direct evaluation comparing the productivity of each of these systems was performed using HyQ PF Vero, a novel protein-free medium for the culture of vero cells and virus production.



Table 1. Surface area comparison of various adherent-dependant culture systems

Culture Type	Surface Area per Unit	Equivalent Surface Areas	Surface area (cm <sup>2</sup> ) per Liter
Microcarrier -Cytodex 1	4,400 cm <sup>2</sup> /g	1L stirred vessel	4,400 – 22,000
Roller Bottles	850 cm <sup>2</sup> /bottle	5 – 26 bottles	4,250 – 8,500
Static - Cell Factory	632 cm <sup>2</sup> /layer	7 – 35 layers	3,160 – 4,200

## 2. MATERIALS AND METHODS

### 2.1. Cells

Vero cells (CCL-81) were obtained from the American Type Culture Collection (ATCC, Manassas, VA), and maintained in Dulbecco's modified Eagle's medium (DMEM) (HyClone, Logan, UT, SH30003) supplemented with 10% defined fetal bovine serum (FBS) (HyClone, SH30070). Cells were adapted to serum-free conditions by sub-culturing the cells from DMEM/10% FBS directly into HyQ PF Vero with no serum. Sterile, polystyrene 162 cm<sup>2</sup> T-flasks (Corning, Corning, NY, #3150), 850 cm<sup>2</sup> roller bottles (Corning, #431198), and Cytodex I (Amersham Pharmacia, #17-0448-01) microcarriers were used throughout these studies.

The content of serum supplemented to DMEM was reduced to 5% in the serum-containing stock cultures prior to performing the studies. Maintenance of the vero cells in serum-containing and serum-free media was accomplished by sub-culturing every three to five days. Cells were counted and viability assessed by use of an Improved Neubauer hemacytometer with trypan blue exclusion dye (Sigma, #T-8154).

### 2.2. Growth Evaluations

Vero cells were seeded at identical densities in each study to analyze growth in PF Vero as compared to serum-containing medium (DMEM/5%). These studies were performed in static, rolling, and suspension microcarrier cultures. Viable cell counts were performed at the time of sub-culturing.

### 2.3. Virus

Poliovirus type 2 was used in the virus production studies. The virus was passaged in vero cells for greater than four passages in either serum-containing or serum-free medium to establish viral stocks. Median tissue culture infectious dose (TCID<sub>50</sub>) assays were used to quantitate virus at each passage. These assays were performed in sterile, polystyrene, flat-bottomed, 96-well plates (Corning, #3585), using visually assessed cytopathic effect (CPE) as the endpoint.

#### 2.4. *Virus Production Assays*

Virus production assays were performed using serum-containing medium (DMEM/5% FBS) and HyQ PF Vero. Serum-containing medium was replaced at the time of infection with DMEM lacking serum (since substances are present in serum that suppress virus infection). Cells were inoculated at an approximate MOI of 0.1. After inoculation, cultures were incubated at 37° C, 95% air/5% CO<sub>2</sub> atmosphere for 72 h, then frozen and thawed three times to lyse cells and release virus particles. Lysate from each well was then collected and centrifuged to pellet and remove cellular debris. The supernatant containing virus was used to prepare 10 log<sub>10</sub> dilutions of each sample. Titrations for each clarified sample were performed in 96 well micro-titer plates using TCID<sub>50</sub> assays described previously.

### 3. RESULTS AND DISCUSSION

#### 3.1. *Growth Evaluations*

Vero cells were tested for their ability to attach, form a monolayer, and proliferate in serum-free conditions. The serum-free adapted vero cells were found to attach within 4 h of seeding in HyQ PF Vero medium. This was especially important when roller bottles or microcarriers were used. Due to the lack of protein in HyQ PF Vero, great care was taken to ensure all trypsin was either removed, or inhibited and later removed to prevent damage to the cells. If trypsin was not adequately removed, a sloughing of the monolayer after two days was observed. Figure 1 depicts growth of vero cells in serum-free and serum-containing media over a period of 17 passages in static culture. Small-scale static culture was readily maintained, and did not require as much from a serum-free medium with regard to attachment and other issues. Larger scale static culture is more difficult. Figure 2 shows 5 passages of vero cells in the two conditions cultured using roller bottles. Inadequacies of a serum-free medium can become apparent using this type of culture. However, with the serum-free medium used in these studies, the cells attached well and proliferated. Figure 3 shows two “passages” of vero cells cultured on Cytodex I microcarriers. This system places the highest demand on serum-free medium. In many cases, serum is supplemented to serum-free media in order to facilitate microcarrier culture. The serum-free medium in this case, however, promoted attachment of the vero cells to the microcarriers without additional supplementation or treatment.

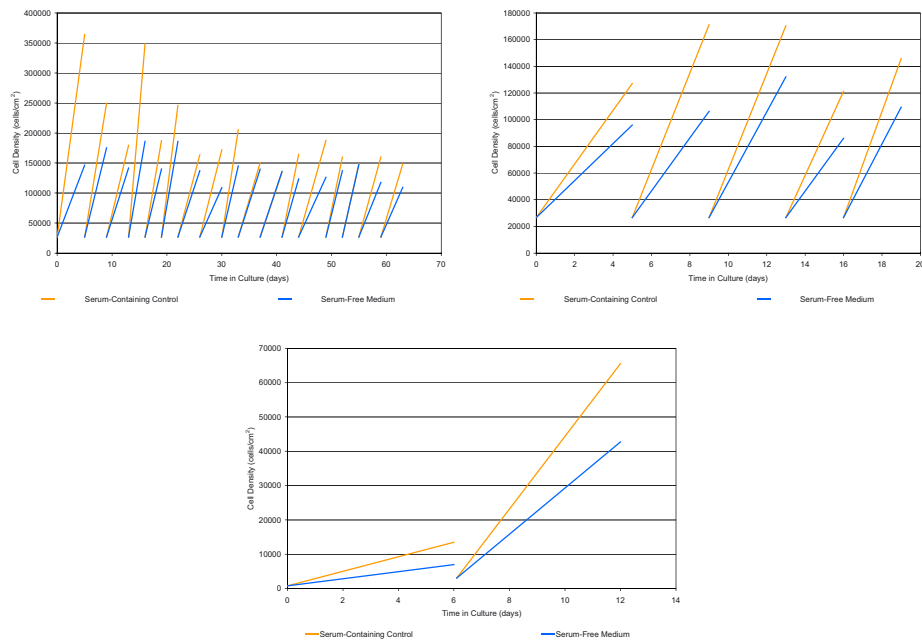


Figure 1. (Upper left) Long-term culture of vero cells in static culture under serum-free and serum-containing conditions. Figure 2. (Upper right) Growth of vero cells in roller bottle culture under serum-free and serum-containing conditions. Figure 3. (Left) Growth of vero cells in suspension microcarrier culture under serum-free and serum-containing conditions.

### 3.2. Virus Studies

Despite the fact the serum-free medium yielded lower overall cell growth, virus production was significantly enhanced with the serum-free medium when compared to DMEM. One possible explanation for the lower virus titers from the basal medium (DMEM) could be nutrient depletion during infection when serum is not present. Serum was removed (DMEM w/FBS was replaced with DMEM w/o FBS) immediately before inoculation to prevent serum interference with viral infection. Another possibility is that the proprietary composition of the serum-free media includes components that enhance virus production and/or virus stability. Yields of poliovirus in each system per unit volume are shown in Figure 4. This graph shows poliovirus production highest in static culture, and lowest in the microcarrier culture. However, due to the very low seeding density used in the microcarrier study, the productivity, or the amount of virus produced per cell, was observed to be very high in the microcarrier culture (Figure 5). This is a significant detail because of the

scalability of this system compared to the others. The roller bottle method was found to be lowest in virus productivity per cell compared to the other two systems.

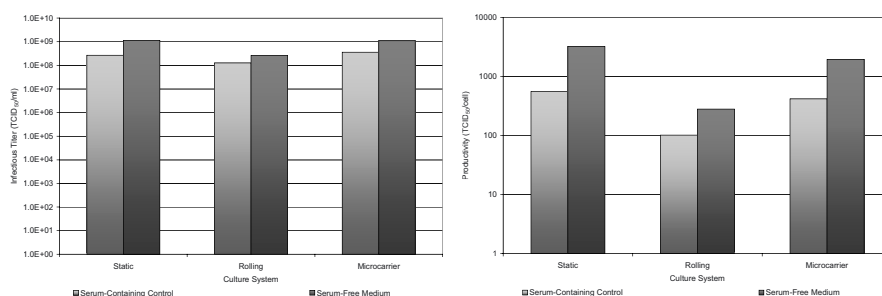


Figure 4. (Above Left) Production of poliovirus in vero cells in static, rolling, and suspension microcarrier culture under serum-free and serum-containing conditions. Figure 5. (Above Right) Productivity of vero cells with regard to infectious units produced per cell in static, rolling, and suspension microcarrier culture under serum-free and serum-containing conditions.

#### 4. SUMMARY

When eliminating serum from vero cell culture media, the immediate challenge is to obtain cell attachment and suitable division rates. It was discovered during the development of the medium that by supplying the appropriate nutritional components vero cells would firmly attach to a culture surface in a protein-free environment. This ability to promote attachment of vero cells facilitates culture of these cells in a variety of culture systems, including static, rolling, and suspension microcarrier culture. Though PF Vero did not produce cell-doubling rates equal to that of serum-containing medium, this protein-free medium produced higher yields of poliovirus than obtained with serum containing medium. A comparison of the three culture systems mentioned above revealed that, firstly, a serum-free medium can support a variety of culture and virus propagation methods, and secondly, that productivity of this cell line is dramatically changed depending upon the culture system used. Static cultures appeared to support the highest level of productivity, but scale-up with this type of system is cumbersome. Microcarrier cultures yielded high productivity, and are easily scaled-up.

#### 5. REFERENCES

- Froud, S. J. (1999) The Development, Benefits and Disadvantages of Serum-Free Media. *Dev Biol Stand* 99: 157-166.
- Mather, J.P. (1998) Making Informed Choices: Medium, Serum, and Serum-Free Medium. *Methods Cell Biol* 37: 19-30.
- Merten, O.W. (1999) Safety Issues of Animal Products Used in Serum-Free Media. *Dev Biol Stand* 99: 167-180.
- Hierholzer, J.C., and Killington, R.A. (1996) in *Virology Methods Manual* (Mahy, B., Kangro, H. eds.), pp. 35-46, Academic Press, London, San Diego, New York, Boston, Sydney, Tokyo, Toronto.

Y. GENZEL, R. ALT, U. REICHL

## GLUTAMINE-FREE MEDIA FOR VACCINE PRODUCTION PROCESSES

*Max Planck Institute for Dynamics of Complex Technical Systems,  
Magdeburg, Sandtorstr. 1, 39106 Magdeburg, Germany. e-mail:  
genzel@mpi-magdeburg.mpg.de*

### 1. INTRODUCTION

In animal cell culture technology high ammonia concentrations can limit cell growth and product formation, especially when focussing on achieving high cell densities for maximum yields. This high ammonia concentration normally results from glutamine metabolism and chemical decomposition [1]. To overcome such problems we have tested several options and developed a glutamine-free medium for cell lines used in industrial applications. Preliminary investigations were carried out in static cultures and roller bottles for BHK21, CHO and MDCK cells.

Detailed characterization of MDCK cell metabolism was done for an influenza vaccine production process [2] (equine influenza Newmarket 1/93 H3N8) in MDCK cells using this newly developed glutamine-free medium: The results for cell growth and virus replication in a large-scale controlled microcarrier culture (5 L bioreactor) are compared to those obtained for a gln-containing (2 mM) GMEM medium.

### 2. MATERIAL AND METHODS

Madin-Darby canine kidney (MDCK) cells were obtained from ECACC (No. 84121903) and grown in GMEM (Invitrogen) supplemented with glucose (final concentration 5.5 g/L), 10 % foetal calf serum (FCS) (Invitrogen), 2 g/L peptone (autoclaved 20% solution, International Diagnostics Group) and 4.0 mg/mL NaHCO<sub>3</sub> (Merck, p.a.) at 37°C. BHK21 (No. ACC61) and CHO-K1 (No. ACC110) cells were both obtained from DSMZ (Braunschweig, Germany). Composition of glutamine-free medium was according to a patent pending by R. Alt [3].

Cells were infected with equine influenza strain A/Equi 2 (H3N8) Newmarket 1/93 (NIBSC, Potters Bar, London, UK) in medium without serum containing low levels of porcine trypsin (12,5 mg/L; Invitrogen) to facilitate infection of cells at 37°C. Virus production was followed by titration of viral haemagglutinin (HA) [4]. Virus seed was stored at aliquots of 10 mL (2.1-2.4 log HA units/100 µL) at -70 °C, thawed and added at 2,5 mL/L, which corresponds to a moi of 0.025 based on plaque forming units of the virus seed. Cells (start cell concentration 2,1 x 10<sup>5</sup>

cells/mL, respectively  $3 \times 10^5$  cells/mL for gln-free medium) were grown in a 5 L bioreactor (B. Braun Biotech, Melsungen, Germany) on Cytodex 1 solid microcarriers (1.7 g/L) (Amersham Biosciences, Freiburg, Germany) in 4.5 L cell growth medium (CGM) (50 rpm, pH control (1 M NaOH) at pH 7.3, pulsed addition of pure oxygen at 40% pO<sub>2</sub>). For monitoring and process control a digital control system (PCS7, Siemens, Karlsruhe, Germany) was used. After 4 days cultivation the cells were grown confluent. The medium was removed and the remaining suspension was washed several times with PBS. To the remaining cell suspension, 3 L virus maintenance medium (VMM) containing 10 mL virus inoculum and 5 mL trypsin solution (10 g/L) were added.

### 3. RESULTS AND DISCUSSION

Preliminary experiments for the cultivation of MDCK cells at higher cell densities showed limitations with respect to availability of some medium components as well as due to inhibiting metabolites. One problem was the accumulation of ammonia, which could be overcome by a newly developed gln-free medium, which was tested for 3 different cell lines (MDCK, CHO-K1 and BHK21).

*Table 1. Metabolite concentrations of CHO, BHK21 and MDCK cells in gln-containing and gln-free media*

cell	basal medium	gln	p. nr <sup>a</sup>	gln <sup>b</sup>	NH <sub>3</sub> <sup>b</sup>	gluc <sup>b</sup>	lac <sup>b</sup>	HA <sup>c</sup>
CHO	GMEM	yes	19	-1.1	+1.9	-13.8	+25	0
CHO	GMEM	no	19	-0.06	+0.17	-10.5	+21	0
CHO	HAM's F12	no	19	-0.01	+0.03	-3	+5.3	n.d.
BHK21	GMEM	yes	18	-1.3	+1.2	-12.6	+23.3	0.96
BHK21	GMEM	no	19	-0.1	+0.18	-8.1	+16.6	0.96
MDCK	Optipro SFM	yes	38	-3.15	+1.82	-12	+21.1	n.d.
MDCK	Optipro SFM	no	36	-0	+0	-8.1	+19.8	n.d.
MDCK	GMEM	yes	20	-1.3	+0.9	-9.9	+14.4	1.93
MDCK	GMEM	no	20	-0	+0.03	-5.7	+12.6	2.25

<sup>a</sup>Highest passage number, <sup>b</sup>overall consumed (-) or released (+) gln, NH<sub>3</sub>, glucose & lactate (mM) in T25 & roller bottle (MDCK/GMEM); <sup>c</sup>virus titre in log HA units per 100 µL (4 days p.i.) in T75

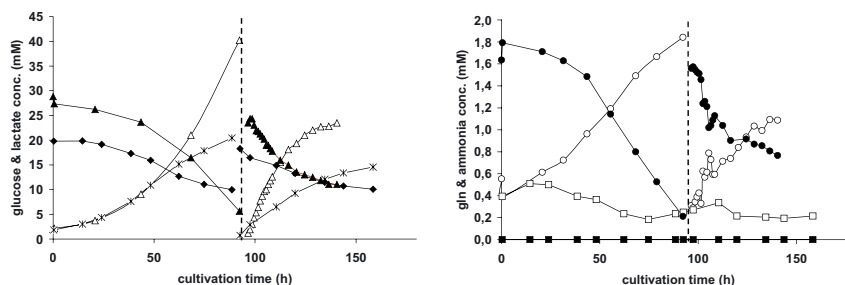


Figure 1. Metabolite concentrations ( $\blacktriangle$  gluc,  $\triangle$  lac;  $\bullet$  gln,  $\circ$   $\text{NH}_3$  in gln-cont. med.;  $\blacklozenge$  gluc,  $*$  lac,  $\blacksquare$  gln,  $\square$   $\text{NH}_3$  in gln-free med.) during growth of MDCK cells in a 5 L bioreactor & during influenza virus production (separated by dashed line) (Biochemistry analyzer YSI 7100 (YSI, Yellow Springs, USA) & Vitros DT60-II (Ortho Clinical Diagnostics, Neckargemünd, Germany).

For MDCK cell growth in a controlled 5 L microcarrier system there were several differences in metabolite levels between a gln-containing and our new medium. In the new medium ammonia production was reduced and there was significant lower glucose consumption and lactate production (fig. 1). While similar cell numbers were obtained, virus titre (fig. 2) was lower for the new medium.

Surprisingly, an uptake of glutamate was found during cell growth for both media. During virus replication the release of glutamate correlated with the increase of HA. This probably indicated the release of the intracellular pool of glutamate into the cell culture medium when virus was released by budding and cell breakage.

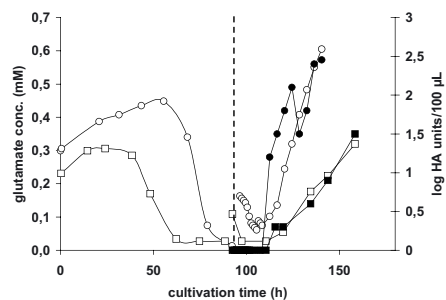


Figure 2. Glutamate concentration and influenza virus titre (HA) ( $\circ$  glu &  $\bullet$  HA in gln-cont. med.;  $\square$  glu &  $\blacksquare$  HA in gln-free med.) (Biochemistry analyzer YSI 7100 & titration of influenza virus by hemagglutination (HA) [4])

#### 4. CONCLUSIONS

The tested gln-free medium supported growth of different industrial cell lines to high passage numbers. The ammonia production was significantly reduced and the cells metabolized glucose at a lower rate but achieved similar growth rates. For the tested MDCK cells this new medium did not result in an increase in virus yield. However, for cultivation at higher cell densities and for ammonia-sensitive cells or virus strains this medium might be an alternative to achieve higher productivities [3]. Further investigations should be carried out for the use of this new gln-free medium composition in serum- and protein-free media. Currently we are comparing changes in cellular metabolism and characterizing metabolic fluxes in both media.

#### 5. REFERENCES

1. M. Schneider; I.W. Marison; U. von Stockar; J. Biotechnol., 1996, 46, 161-185.
2. Genzel Y.; Voges L.; Reichl U.; Proceedings from the 17th ESACT meeting: Animal cell technology: From target to market in June 2001, Tylösand, Sweden.; Eds. E. Lindner-Olsson; N. Chatzissavidou; E. Luellau; Kluwer Acad. Publ.. 2001, 344-346.
3. Alt R; Verfahren zur Kultivierung von Säugerzellen mit verminderter Hemmstoffproduktion; German patent pending, 2002, file nr: 102 26 455.4 (ruediger.alt@web.de)
4. Mahy BWJ, Kangro HO. Virology methods manual. Academic press, London 1996; 41-43.



B. HUNDT<sup>1</sup>, A. SCHÄNZLER<sup>2</sup>, U. REICHL<sup>3</sup>

## SERUM FREE CULTIVATION OF PRIMARY CHICKEN EMBRYO FIBROBLASTS IN MICROCARRIER SYSTEMS FOR VACCINE PRODUCTION

*1: Otto-von-Guericke-University Magdeburg, Chair of Bioprocess  
Engineering, Universitätsplatz 2, D-39106 Magdeburg, Germany*

*2: Impfstoffwerk Dessau-Tornau GmbH, PF 400214, D-06855 Rosslau, Germany*

*3: Max-Planck Institute for Dynamics of Complex Technical Systems,  
Sandtorstr. 1, D-39106 Magdeburg, Germany*

### 1. INTRODUCTION

Animal cells are a common substrate for production of viral vaccines. Optimization of virus yields is closely connected with profound knowledge of growth and metabolism of cells and virus-cell interactions. In our work we investigated a vaccine production process using primary chicken embryo fibroblasts (CEF). At present, the industrial process involves the cultivation of these cells in serum free medium (SFM) with roller bottles. Disadvantages are high input of consumables and time, a comparatively high contamination risk and only poor control of process parameters such as pH and pO<sub>2</sub>. So our aim was to establish a process for growing primary CEF in microcarrier systems using a serum free medium. Cultivations were performed in a stirred tank reactor and a novel wave bioreactor. Results regarding cell growth, metabolism and propagation of an orthopox virus strain in both systems are compared.

### 2. MATERIAL AND METHODS

Primary CEF were harvested from 11 day old chicken embryos obtained from specified pathogen free eggs (Charles River Laboratories, Germany). With a starting cell number of  $5 \cdot 10^5$  cells/mL cells were grown in a commercially available serum free medium (Invitrogen) supplemented with 1-2 % L-glutamine (200 mM, Invitrogen). Cells were cultivated in 5 L stirred tank reactor (4 L wv, B. Braun Biotech, Germany) and in 2 L wave bioreactor (1 L wv, Wave Biotech, CH). Online analytics: temperature, pH, and pO<sub>2</sub>. Offline the concentrations of glucose, lactate, glutamine, glutamate (YSI 7100, YSI, USA) and ammonium (Vitros DT60-II, Ortho Clinical Diagnostics, Germany) were measured. Additionally, amino acid

concentrations were determined (BioLC, Dionex, Idstein, Germany). Cells in stirred tank were cultivated on Cytodex 1 microcarrier (2 g/L, Amersham Biosciences, Germany) with 50 rpm, pH control (1 M NaOH) at pH 7.2, 37 °C, pulsed aeration with pure oxygen at 40 % pO<sub>2</sub>. Process parameters for wave bioreactor were the same except aeration rate (0,1 mL/min, sterile air with 5 % CO<sub>2</sub>), pH was not controlled, tilt rate was 8 min<sup>-1</sup> and tilt angle 5°. For virus propagation studies cell cultures were infected directly at the start of cultivation. Virus titer were measured after 5 days of cultivation using a TCID<sub>50</sub>-protocol developed and validated at Impfstoffwerk Dessau-Tornau.

### 3. RESULTS AND DISCUSSION

Preliminary experiments in spinner flasks (0,25 L wv) allowed to improve attachment of primary CEF on Cytodex 1 microcarrier in serum free medium (data not shown). Based on these results further investigations for cultivating CEF on microcarrier in stirred tank and wave bioreactor were carried out.

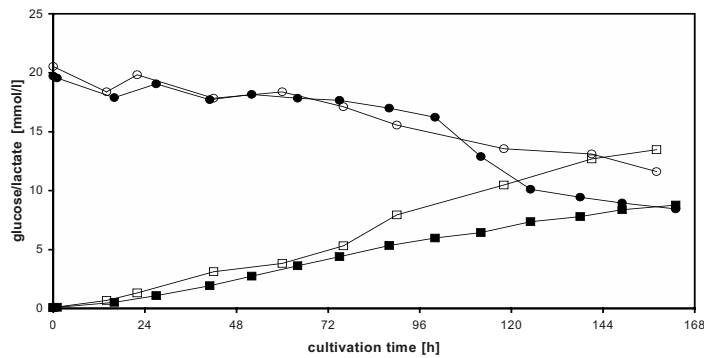


Figure 1. Comparison of glucose – lactate concentration profiles from stirred tank and wave bioreactor cultivation of primary CEF on Cytodex 1 in SFM (● glucose stirred tank ○ glucose wave bioreactor ■ lactate stirred tank □ lactate wave bioreactor)

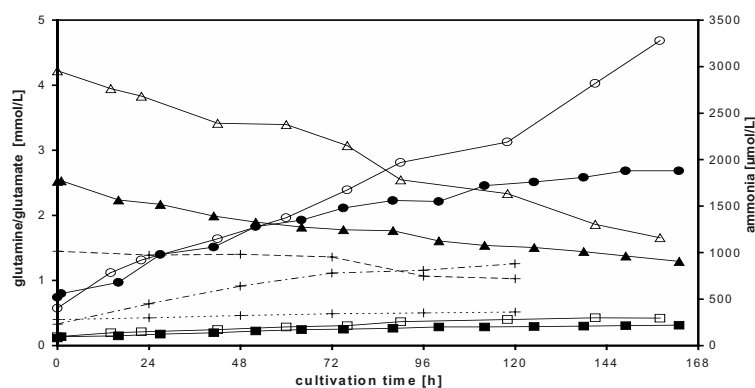


Figure 2. Comparison of glutamine/glutamate – ammonia concentration profiles from stirred tank and wave bioreactor cultivation of primary CEF on Cytodex 1 in SFM (▲ glutamine stirred tank △ glutamine wave bioreactor ■ glutamate stirred tank □ glutamate wave bioreactor ● ammonia stirred tank ○ ammonia wave bioreactor) (chemical glutamine decomposition is taken into account)

Analysis of glucose uptake shows that in the stirred tank cultivation less glucose is metabolized into lactate compared to a wave bioreactor (fig.1). Total molar yield  $Y_{lac/gluc}$  (related to possible stoichiometric yield) in the stirred tank is 38,5 % vs. 75 % in the wave bioreactor. In stirred tank ammonia release was significantly lower than in wave bioreactor, while glutamate concentration profile is the same for both vessels (fig. 2). Total molar yield  $Y_{amm/gln}$  for stirred tank is 1,25 compared to 1,16 for wave bioreactor. Metabolic data indicate a successful transfer of the process from roller bottles to microcarrier systems regarding cell growth.

A problem we faced in all serum free CEF cultivations was that cells detached microcarriers after a cultivation time of about 60-72 h and tended to form microspheroids (fig.3). Cell numbers for first 60 h of cultivation indicated that cells grew only with one doubling to a cell number of  $9 \cdot 10^5$  viable cells/mL. In serum supplemented medium these effects were not observed and primary CEF grew up to cell numbers of  $2-3 \cdot 10^6$  cells/mL [1]. Therefore we investigated growth of primary CEF under defined conditions in a perfusion chamber (3 mL vv, SFM, batch, standard conditions) for five days under a microscope. Analysis revealed a high motility and tendency for cluster formation of primary CEF's. This might be the explanation for the observed effect that cells detached from microcarriers and formed microspheroids. Signal-molecules that could be responsible for this are probably inhibited by components of fetal serum. Experiments with virus infection proved that both stirred tank and wave bioreactor supported virus propagation in the range known from roller bottle cultivations.

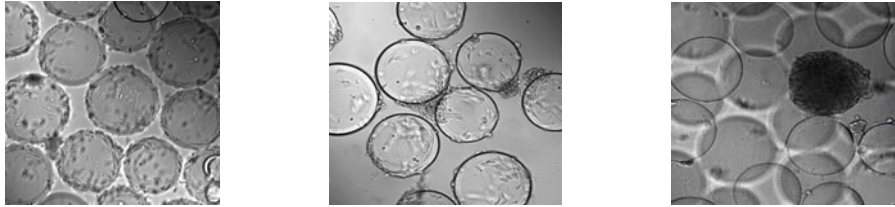


Figure 3. Primary CEF on Cytodex 1 in stirred tank after 24 h, 72 h and 144 h cultivation time (from left to right) (40x)

#### 4. CONCLUSIONS

We developed a process for the cultivation of primary CEF on microcarriers in SFM using a stirred tank reactor and a wave bioreactor. Cell growth was not satisfying so far, although virus titers were as high as in roller bottles. Further experiments should answer the question which factors influence the tendency for spheroid formation and if higher numbers of viable cells will result in higher virus yields. Focus of future work will be on additional analytics (MALDI-MS, flow cytometry), use of perfusion systems and medium design.

#### 5. REFERENCES

1. L. Zhang, Y. Zhang, C. Yan, J. Yu; Applied Biochemistry and Biotechnology, 1997, 62, 291-302

KALLEL H.<sup>1</sup>, ROUROU S.<sup>1</sup>, VAN DER ARK A.<sup>2</sup>, THALEN M.<sup>2</sup>,  
VAN DER VELDEN DE GROOT T.<sup>2</sup>

## DESIGN OF AN ANIMAL PROTEIN FREE MEDIUM TO SUSTAIN VERO CELLS GROWTH IN A STIRRED TANK BIOREACTOR

<sup>1</sup> *Viral Vaccines Research & Development Unit. Institut Pasteur de Tunis.  
13, Place Pasteur BP 74. 1002 Tunis. Tunisia.*

<sup>2</sup> *Laboratory of Process & Process Development. RIVM. PO Box 1,  
3720 BA Bilthoven, The Netherlands*

### INTRODUCTION

Animal cell culture was established as a manufacturing technology for the preparation of viral vaccines and therapeutics. This technology requires bovine sera for vigorous growth of cell lines. However, the use of bovine serum has several drawbacks such as bacterial endotoxins, immunogenic contaminants, lot to lot variability in terms of promoting cell growth and product formation, as well as a potential source of contamination with TSE. Thus current biotechnological approaches for the production of biologicals strongly recommend avoiding the use of serum.

The overall aim of this work was to develop an animal protein free medium suitable for optimal growth of Vero cells in agitated cultures.

### MATERIALS & METHODS

*Cell line* : Vero cells were used through out this study.

*Culture medium* : MEM, M199, Foetal Calf Serum and Insulin were supplied by Invitrogen (Glasgow, UK).

*Chemicals and peptones* :All chemicals were obtained from Sigma (St. Louis, USA). Peptones were supplied by Quest International (Naarden, The Netherlands).

*Microcarrier preparation* : Cytodex 1 and Cytodex 3 from Amersham Pharmacia Biotech (Uppsala, Sweden) were used throughout this study. They were prepared and sterilized according to manufacturer's instructions.

*Bioreactor cultures* : The cultures were performed in a 5 L bioreactor (Applikon, The Netherlands) equipped with a marine impeller and a spin filter (pore size : 18µm) fixed on the axis. During cell culture proliferation step, the following

conditions were applied : pH = 7.2, pO<sub>2</sub> maintained at 50%, temperature = 37°C and agitation rate = 25 to 40 rpm.

Recirculation was started after two days of culture. Recirculation rate was modulated according to cell density.

Samples were taken daily to determine cell density, cell viability, glucose, lactate, glutamine and glutamate levels.

*Cell counting* : 5 ml of Vero cell culture were washed three times with PBS then treated in 5ml of 0.1 M citric acid containing 0.1% crystal violet and 0.1% Triton X-100 and incubated at least for 1 hour at 37°C. The released nuclei were counted using an hemacytometer.

*Metabolite analysis* : Glucose, lactate, glutamine and glutamate concentrations were monitored by a YSI analyser.

## RESULTS

### *Selection of serum free media for Vero cells growth*

To design a serum free medium, we investigated the effect of different components (Table1) on Vero cells growth.

*Table 1 : Components tested to design a serum free medium for Vero cells growth.*

<b>Component</b>	<b>High level</b>	<b>Low level</b>
	5 g/l	1 g/l
<b><i>Hypep 5603</i></b>		
Hypep 4601	5 g/l	1 g/l
Hypep 7401	5 g/l	1 g/l
Hypep 4605	5 g/l	1 g/l
Hypep 1510	5 g/l	1 g/l
Transferrin	10 µg/ml	1 µg/l
Insulin	10 µg/ml	1 µg/ml
Selenium sodium	25 nM	0
Ethanolamine	100 µM	10 µM
Medium	M199	MEM

Using the method of experimental design, we selected two serum free media (SF-MEM and SF-M199) that sustain cell growth. As indicated in Table 2, SF-M199 medium seems to support Vero cell growth better than SF-MEM medium.

Table 2 : Vero cells growth in the selected SF-Media and in MEM supplemented with 7.5% FCS, in T-flasks. MEM<sup>+++</sup> and M199<sup>+++</sup> contain all components present in SF-MEM and SF-M199 media except the hyeps.

Medium	SF-MEM	SF-M199	MEM+7.5% FCS	MEM <sup>+++</sup>	M199 <sup>+++</sup>
<b>Cells/T25</b>	4.66x10 <sup>6</sup>	4.73x10 <sup>6</sup>	6.32x10 <sup>6</sup>	3.36x10 <sup>6</sup>	2.35x10 <sup>6</sup>

*Kinetics of Vero cells growth in the SF-M199 medium*

Table 3 : Vero cells growth in SF-M199 medium, in a 500 ml spinner flask on 2 g/l cytodex 1 and 2.5 g/l cytodex 3 and in a 5-L bioreactor on 2.5 g/l cytodex 1.

	Spinner flask cultures		Batch bioreactor culture
	2 g/l Cytodex1	2.5 g/l Cytodex 3	2.5 g/l Cytodex 1
Cell density/ml	1.33x10 <sup>6</sup>	1.17x10 <sup>6</sup>	1.87x10 <sup>6</sup>
Average specific growth rate (h <sup>-1</sup> )	0.0255	0.0235	0.0239

*Design of an animal protein free medium*

To eliminate animal proteins, we further optimised the composition of SF-M199 medium. Therefore, transferrin was substituted by an iron salt and a chelator (Yabe et al. 1987; Kovar and Franek, 1987). The medium obtained was called AFM-M199.

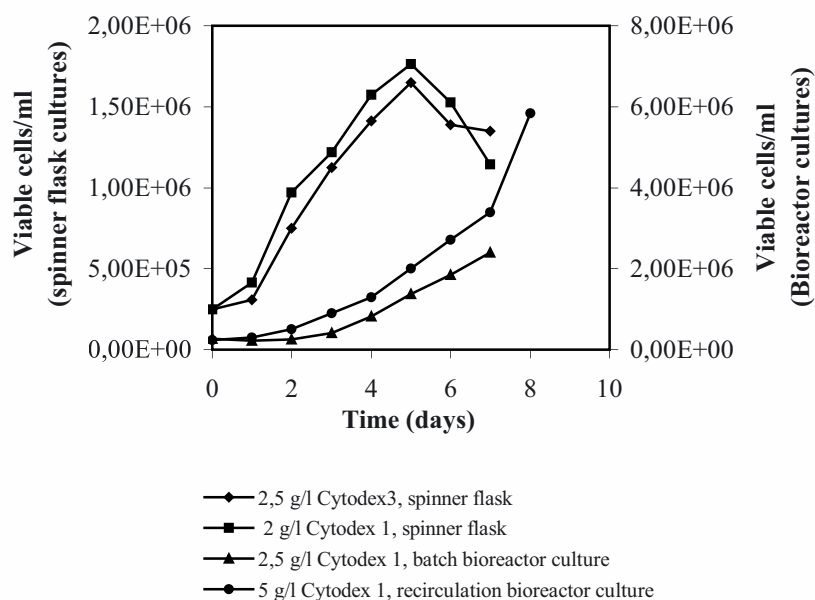


Figure 1 : Vero cells growth in AFM-M199 medium, in a 500 ml spinner flask on 2 g/l cytodex 1 and 2.5 g/l cytodex 3 and in a 5-L bioreactor on 2.5 g/l cytodex 1 run in batch and recirculation modes.

## CONCLUSION

We design an animal protein free medium AFM-M199 for the proliferation of Vero cells in a stirred tank bioreactor using cytodex 1 as a microcarrier.

## REFERENCES

- Kovar J, Franek F (1987). Iron compounds at high concentrations enable mouse hybridoma and myeloma cells to grow in a protein-free medium. In : Neijssel OM, van der Meer RR, Luyben KchAM (Eds.), Proc 4th European Congress on Biotechnology, Amsterdam, Elsevier Science Publishers, vol.3, pp 614-617.
- Yabe N, Kato M, Matsuya Y, Yamane I, Iizuka M, Takayuki H and Suzuki K (1987) Role of iron chelators in growth-promoting effect on mouse hybridoma cells in a chemically defined medium. In Vitro cell Develop Biol, 23, 815-820.



M. LECINA<sup>1</sup>, A. CASABLANCAS<sup>1</sup>, A. SOLEY<sup>1</sup>, C. VELA<sup>2</sup>, E. ESPUÑA<sup>3</sup>, J. DE GRÀCIA<sup>1</sup>, J.J. CAIRÓ<sup>1</sup>, F. GÒDIA<sup>1</sup>

## USE OF ON-LINE OUR MEASUREMENTS TO MONITOR AND IMPROVE INSECT CELL CULTURES FOR RECOMBINANT PROTEIN PRODUCTION

1. *Departament d'Enginyeria Química, ETSE, Campus Universitat Autònoma de Barcelona (UAB), 08193 Bellaterra, Barcelona, Spain.*
2. *INGENASA, Dept. de Investigació, C/Hnos. García Noblejas 41, 2º, 28037 Madrid.*
3. *LABORATORIOS HIPRA S.A., Dept. de Investigació y Desarrollo. Avda. La Selva 135, 17170 Amer.*

**Abstract.** On-line oxygen uptake rate measurements using a dynamic model are applied to Sf9 cultures infected with recombinant baculovirus. This measurement allows a sensitive monitoring of cell growth and post-infection process. Also, results are given on fed-batch and perfusion cultures where 8-10 · 10<sup>6</sup> cells/ml can be achieved by automatically adjusting the medium fed-rate on the basis of OUR on-line measurements.

### INTRODUCTION

Insect cells–baculovirus expression system- have been used successfully for the expression of several proteins. A way to improve protein production is to increase cell density at the infection time by using different culture strategies such as fed-batch or perfusion culture. The expression system used is strongly linked to the infection parameters (MOI, TOI and TPI), and to an appropriate nutrients in the medium in order to provide to the cells with all the substrates for feeding the synthesis of the protein of interest. To develop an automatic and optimized production method, a system variable that allow to correlate culture parameters as well as infection process parameters is needed. OUR is an easy measurable parameter that has been demonstrate to correlate well the physiological state of the cells. The results of its use in defining infection and culture strategies for Sf9 cells are described below.

### MATERIALS AND METHODS

*Cell line, medium and culture conditions.* The insect cell line used was *Spodoptera frugiperda* 9 (Sf9). The baculovirus strain was AcVP2.IBDV (kindly provided by LABORATORIOS HIPRA S.A. and INGENASA., respectively). The basal medium

used was IPL-41 insect cell medium (Sigma I0638) supplemented with 3.33g/l yeast extract (Sigma Y-1000) and lactalbumin hydrolysate (Sigma L90) and a 10% (v/v) of foetal bovine serum was added. Cultures were stirred at 100 rpm, grown at 27°C and pH=6.2. Density and viability were assessed by trypan blue exclusion method using an haemocytometer (Neubauer improved, Brand).

*Culture system.* Bioreactor Braun-MCD (2 L).

*Titer determination.* VP2 and Baculovirus titers were determined as previously reported (Martínez-Torrecuadrada et al., 2000).

*On-line measurement:* OUR was determined by the dynamic method (Kussow et al., 1995).

## RESULTS AND DISCUSSION

OUR monitoring in Sf9 bioreactor cultures: The OUR measurements obtained every two hours in insect cell cultures allowed a very accurate measurement of the viable cells curve, both in growth conditions and after infection (as show in figures 1 and 2 respectively). In addition this measure has less error than viable cell counting (20% error) and allows to determine the infection point where cell viability starts decreasing in good anticipation, this information being very relevant from the process point of view. It's interesting to note how in figure 2 remains relatively unchanged after infection, until it decreases sharply coinciding with maximum VP2 concentration.

Finally, it can be observed that since the TOI to the maximum of VP2 titer (figure 2) coincides to the theoretical TOI until the time when it was achieved the maximum cell concentration in a uninfected batch (figure 1). If the infection is performed, the substrate consumption is not expected to be higher than the control since metabolism is mostly restricted to the synthesis of VP2. Therefore it is anticipated that enough substrates are available to produce VP2.

Process strategies: As a previous step to increase VP2 production, fed-batch and perfusion strategies have been performed to obtain maximum cells densities. In both cases, the on-line OUR measurements is used to adjust the medium feeding rate to the reactor. In figures 3 and 4 it can be observed that  $8 \cdot 10^6$  and  $10 \cdot 10^6$  cells/ml were achieved, and that OUR curves made possible to detect infection point in the growth profiles due to nutrient limitations, being connected by the corresponding change in fed-rate. This sensitivity was not achieved by off-line cell counting.

## CONCLUSIONS

The use of on-line OUR determination, using a simple method, in Sf9 cell cultures infected with recombinant baculovirus is proven effective to follow cell growth, post infection periods, and to adjust the nutrient feeding to cell growth in fed-batch and perfusion system.

A detained study of the profile of OUR concludes the capacity to predict in real time the infection parameters (TOI and TPI), or the key moment of action to start a culture strategy to increase the cells density, evaluating the OUR derivates.

FIGURES

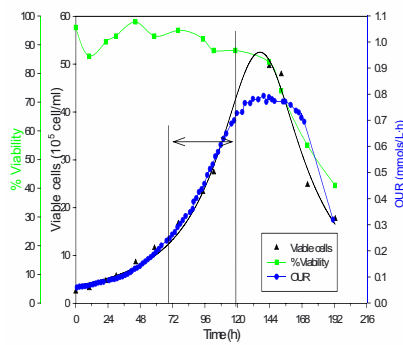


Figure 1: Profile in a batch culture.

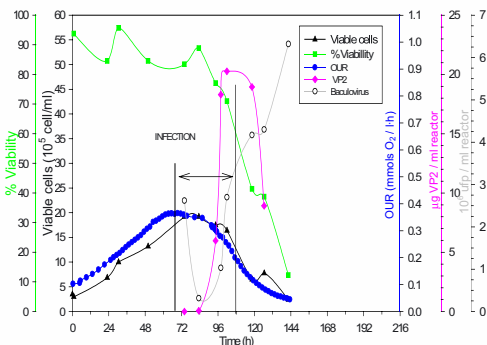


Figure 2: Profile in a infected batch culture.

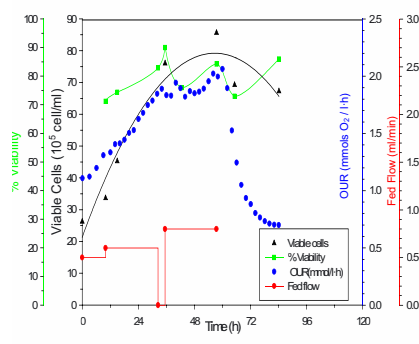


Figure 3: Profile in a fed-batch culture.

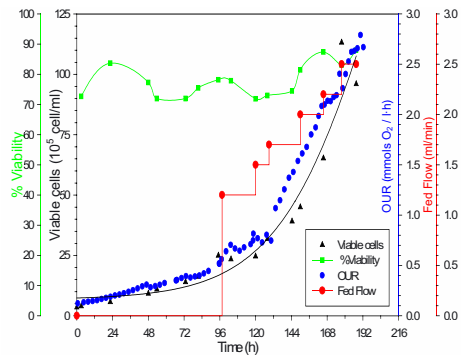


Figure 4: Profile in a perfusion culture.

REFERENCES

Kussow Ch. M., Zhou W., Gryte D. M. and Hu W. S.(1995). *Monitoring of mammalian cell growth and virus production process using on-line OUR measurement*. Enzyme and Microbial Technology. Path. 17: 779-778.

Martínez-Torrecuadrada, J.L, Lázaro B., Rodríguez J.F.and Casal J.I. (2000). *Antigenic proprieties and diagnostic potencial of baculovirus-expressed infectious Bursal disease virus proteins*. Clinical and diagnostic laboratory immunology. P:645-651.

N. MAZURKOVA, E. NECHAEVA, T. RYABICHEVA,  
N. VARAKSIN, T. SEN'KINA, T. SVIRIDENKO, T.  
KOLOKOLTSOVA, S. MARKUSHIN\*, YU. GENDON\*

## PRODUCTION OF LIVE INFLUENZA VACCINE IN MDCK CELL LINE

*Research Institute of Cell Cultures State Research Center of virology and  
Biotechnology "Vector", Koltsovo, Novosibirsk region, 630559, RUSSIA  
\* Research Institute of Viral Preparations, Moscow, RUSSIA*

**Key words:** influenza virus, vaccine, MDCK cells, cultivation

**Abstract.** Development of efficient vaccines against influenza, yet remaining a serious problem for many countries of the world, is a topical problem. Stable cell lines as a substrate are attracting the attention of influenza vaccine developers. It was demonstrated that unlike the influenza virus adapted to chick embryos, the influenza virus isolated from MDCK culture retains the antigenic properties of epidemiological strain.

Effects of various conditions of cultivation in cells (inoculation dose, compositions of growth and supporting media, and infectious dose of virus) on production efficiency of cold-adapted reassortant vaccine strains of type A and B influenza viruses were studied in experiments.

Selection of optimal biological additions to the nutrient medium, including additions involving plant hydrolysates, provided efficient reproduction of the virus (9.5–10.0 log EID<sub>50</sub>/ml) in MDCK cell line in the presence of 2 µg/ml trypsin. Stabilizers allowing the culture-grown live virus to be freeze-dried with preservation of the virus infectivity at a level of 8.5 log EID<sub>50</sub>/ml were studied. The parameters studied are key properties while developing the technology for manufacturing culture live vaccine against influenza using cold-adapted reassortant vaccine strains.

### 1. INTRODUCTION

The development of efficient vaccines against the influenza that has long remained a serious problem for most countries is a very urgent task. Stable cell lines used a substrate have begun to attract a great attention of the developers of influenza vaccines recently. It has been shown that influenza virus isolated on a MDCK cell culture preserves the antigenic properties of the epidemic strain unlike the strain adapted to chicken embryos. In addition, the production technology used to prepare cultural influenza vaccines allows the vaccine production to be increased during a short period, which is very important at an influenza pandemic and is very difficult to achieve when chicken embryos are used as a substrate. The development of a safe technology for production of a live influenza vaccine requires the removal of any products of animal origin (additives, enzymes and stabilizers) that should be replaced by substances of plant origin. The present work sought to develop a live cultural influenza vaccine using cold-adapted reassortant vaccine strains of influenza

virus types A and B cultivated on a MDCK cell line in a serum-free medium supplemented with plant additives and stabilizers of plant origin.

## 2. MATERIALS AND METHODS

**Influenza virus strains.** The cold-adapted reassortant vaccine strains A/47/Shandon/93/1 (H1N1) and A/47/Johannesburg/94/2 (H3N2) and B/60/Petersburg/95/20 were used in the work. **Cell lines.** The MDCK cell line was obtained from the Pasteur Institute (Paris, France). The cells were cultivated in serum-free MDSS2 medium. **Reproduction of viruses.** A three-day-old monolayer of MDCK cells was infected with viruses. The infected cells were incubated at 34°C, supplemented with MDSS2 containing 2 µg/ml trypsin and plant hydrolysates.

## 3. RESULTS AND DISCUSSION

The study of the reproduction of reassortants in a MDCK cell line was performed at an infection multiplicity from 0.005 to 0.0001 EID<sub>50</sub>/cell. The obtained results presented in Figure 1 demonstrate that the maximal virus titers ( $10^{9.5}$ – $10^{10.0}$

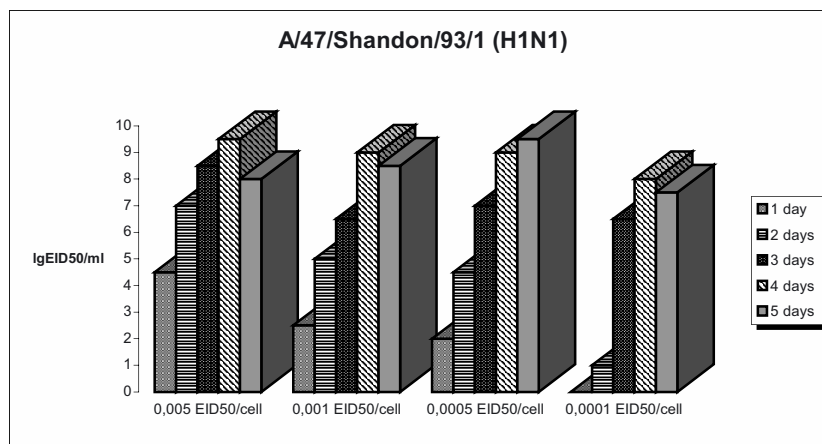


Figure 1. The dynamics of the accumulation of influenza viruses in a MDCK cell culture at different infection multiplicities

EID<sub>50</sub>/ml) are achieved at an infection multiplicity of 0.005 EID<sub>50</sub>/cell on day 4 for the cold-adapted strains of influenza virus type A and on day 5 for the cold-adapted strain of influenza virus type B. The infection multiplicity decreased to 0.0005 EID<sub>50</sub>/cell causes a 1-day shift in reaching the maximal titers. Further decrease in the infection multiplicity to 0.0001 EID<sub>50</sub>/cell does not promote an increase in infectious titers during 5 days of the experiment.

Plant protein hydrolysates at the concentration from 0.01% to 1.0% were introduced to the supporting nutrient medium as additives to enhance the specific activity of the influenza virus strains in the process of cultivation on a MDCK cell line. Stabilizers containing plant peptone solutions were used to maintain the specific activity of influenza virus in the processes of lyophilization and storage. As seen from Table 1, all the used hydrolysates are able to maintain the specific activity of influenza virus in the processes of lyophilization and storage at different conditions.

*Table 1. The study of the effects of plant protein hydrolysates on maintaining the specific activity of influenza virus A/H1N1 strain cultivated in a MDCK cell*

Level of hydrolysates (%)	Specific activity, log EID <sub>50</sub> /ml				Residual moisture, %
	Virus-containing liquid	Liquid semi-finished product	Dry semi-finished product	37°C , 7 days	
0	9.0	8.8	8.0	6.3	0.7
0.01	9.5	8.5	7.5	6.3	0.9
0.02	8.7	8.7	8.5	6.3	1.2
0.05	9.1	8.5	8.5	7.4	0.9
0.8	8.8	8.5	7.5	6.3	0.7
1	9.5	8.7	7.7	7.3	1.0

#### 4. CONCLUSION

The obtained data show that all the studied reassortant strains of influenza virus are able to reproduce at optimal infection multiplicities up to the titers of  $10^{9.5} - 10^{10.0}$  EID<sub>50</sub>/ml on a MDCK cell culture cultivated in a serum-free medium.

The introduction of plant hydrolysates into the medium allows to increase the reproduction of influenza virus in MDCK cells and to maintain the virus specific activity in the processes of lyophilization and storage at different conditions.

#### 5. ACKNOWLEDGMENTS

This Work was supported by the ISTC, Project 940B.

#### 6. REFERENCES

- Broun F. et.al., (1999) Inactivated Influenza Vaccines Prepared in Cell Cultures., *Dev.Biol. Stand.*, **98**; 13-21.  
 Merten O., Managuerra J., Hannoun C., et.al. (1999) Production of Influenza virus in serum- free mammalian cell cultures, *Dev.Biol. Stand.*, **98**; 23-37.

E. NECHAEVA, N. VARAKSIN, T. RYABICHEVA,  
T. GETMANOVA, N. MAZURKOVA, T. SENKINA,  
T. KOLOKOLTSOVA

## ELABORATION OF THE MICROENCAPSULATED FORMS OF THE VIRAL VACCINES

*State Research Center of Virology and Biotechnology Vector, Koltsovo,  
Novosibirsk region, 630559, Russia*

**Abstract.** Development of antiviral mucosal vaccines involving pH-dependent polymers and polymer complexes is a topical problem now. These polymers are capable of protecting the virus from acid gastric medium and releasing it in weakly alkaline intestinal medium. In addition, the majority of these polymers are capable of intensifying the immune response to the antigen introduced. SRC BV VECTOR with AOZT DELSI elaborated the method of microencapsulation of viral particles into a matrix of pH-dependant polymers under specific condition of their conformational transitions. Spherical or irregular-shaped particles with size of 1-30  $\mu\text{m}$  were produced. Examination of the immunogenic properties of the vaccine specimens has demonstrated the increase in the antibody titers of the animals immunized orally with the preparations containing polyacrylic acid copolymers with ethyl groups, sodium alginate-chitosan complexes and sodium alginate-spermidine complexes.

### 1. INTRODUCTION

Antigen delivery systems such as microencapsulation have emerged in recent years as an innovative approach to improving vaccine strategies (1,3). Development of antiviral mucosal vaccines using pH-dependent polymers and polymeric complexes is especially topical now because of their ability to protect the virus from the gastric medium and to release it in a weakly alkaline medium of intestines. The majority of polymers are also capable of boosting the immune response to an antigen introduced.

The goal of this work was to characterize the microencapsulated forms of measles and influenza viral vaccines involving pH-dependent polymers as a matrix.

### 2. MATERIALS AND METHODS

**The measles virus** vaccine strain Leningrad-16 and the **influenza virus** cold-adapted reassortant vaccine strain A/47/Shandon/93/1 were used. The following **polymers** were used as a matrix: copolymers of polyacrylic acid with 43% ethyl group substitution rate (molecular weight, 31 kDa), sodium alginate – spermidine ([N-3-aminopropyl]-1,4-aminobutylamine) complexes, carbopol, carbopol-polyvinylpyrrolidone complexes. The virus-containing liquid was supplemented with stabilizing solutions and polymers according to the technique developed. The

mixture was poured into ampoules and freeze-dried (2). **Electron microscopy:** preparations were dissolved in distilled water, mounted onto grids, stained with 2% aqueous solutions of phosphotungstic acid (PTA) with pH 2, 5, or 7, and analyzed with an electron microscope (“Hitachi-H 500”, Japan). The **specific activities** of microencapsulated measles vaccine were determined according to the cytopathic effect on Vero cells. The specific activity of influenza virus was determined by infecting 11-days-old developing chick embryos. The vaccine **immunogenicity** was determined by oral, subcutaneous and intranasal immunization of guinea pigs. The sera were studied using hemagglutination test on 28 day.

### 3. RESULTS AND DISCUSSION

Electron microscopy showed that the microparticle structure and density changed depending on the pH of medium. Microcapsules formed aggregates in an acidic medium, which dissociated into separate particles at pH 7.0 (Fig.). At increasing the pH, polyacrylic acid unfolded in the pH range of 4.5–8.0, and sodium alginate did at pH=3.5 (the 3D structure of spermine molecules remained constant) (2). Thus, the microcapsule morphology related to changes in the conformation of polymeric molecules. At a neutral pH, particles involving polyacrylic acid had a size of 0.5–10  $\mu\text{m}$ , and those formed of sodium alginate–spermidine had a size of 1–9  $\mu\text{m}$ .

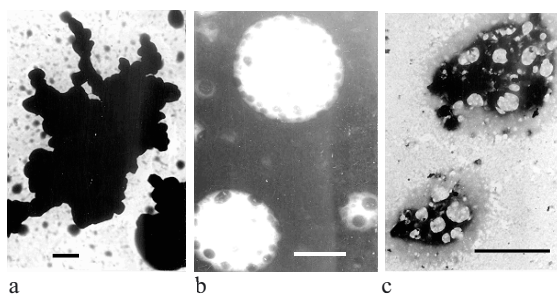


*Figure 1. Microcapsules containing 0,1% polyacrylic acid copolymers at pH=2 and 7 (a, b) or sodium alginate–spermidine complexes at pH=5 (c). Transmission electron microscopy. Bar=1  $\mu\text{m}$ .*

Upon freeze-drying, the level of virus-specific activity in the preparation remained sufficiently high (Tables 1, 2). Thus, the microencapsulated forms of viral vaccines studied contained active measles or influenza viruses.

Study of the vaccine immunogenicity has shown the increase in the antibody titers. The animals immunized three times orally with the preparations containing polyacrylic acid copolymers or sodium alginate-spermidine complexes displayed a 100% seroconversion, the mean geometric titers reached 56 – 84. After a single subcutaneous administration the best results were obtained for the sodium alginate-chitosan complexes; the mean geometric titers were amounted to 38.1. The triple



intranasal administration gave the titers up to 11 when using sodium alginate LVG - spermine and sodium alginate MVM - spermine as the microparticle matrix.

Table 1. Specific activity of the preparations of microencapsulated measles vaccine produced using copolymers of polyacrylic acid.

Concentration of polymer	Specific activity ( $\log TCID_{50}/0.5 \text{ ml}$ )	
	Liquid semi-finished vaccine	Microencapsulated vaccine
1.0%	4.70	3.36
0.5%	5.40	4.27
0.1%	5.36	4.31

Table 2. Specific activity of the preparation of microencapsulated influenza virus.

Polymers of matrix	Specific activity ( $\log EID_{50}/ \text{ ml}$ )	
	Liquid semi-finished vaccine	Microencapsulated vaccine
Polyacrylic acid copolymers	8.7	7.3
Carbopol	7.0	6.5
Carbopol-polyvinylpyrrolidon	6.5	6.0

#### 4. CONCLUSIONS

The microencapsulated measles and influenza virus vaccines involving pH-dependent polymers are capable of preserving the enclosed measles and influenza virus viable. Microparticles of pH-depending morphology have the size optimal for transport trough the intestine wall. The virus specific activity in the preparation studied is sufficiently high. Examination of the vaccine immunogenicity demonstrated the increase in the antibody titers of the animals immunized by oral, subcutaneous and intranasal administration.

#### 5. REFERENCES

- Eldridge J. H. et al. Biodegradable microspheres as a vaccine delivery system. //Mol. Immunol. (1991), Vol.28, No.3, pp. 287-294.  
 Nechaeva E.A. et al. Approach to microencapsulated form of the live measles vaccine. // Ann. N.Y. Acad. Sci. (2001), Vol.944, pp.186-187.  
 Offit P.A. et al. Enhancement of rotavirus immunogenicity by microencapsulation. //Virology (1994), Vol.203, No.1, pp. 134-143.

#### 6. ACKNOWLEDGEMENT

The work was supported by the ISTC grant No. 1035B.

K. SAUTTER (1,2), J. FIEDER (1), R. OTTO (1), B. ENENKEL (1)

## HTS-BASED DEVELOPMENT OF HIGH-PRODUCING CHO CELL LINES

(1)Boehringer Ingelheim Pharma GmbH & Co. KG, Biberach, Germany

(2) Bayerische Julius-Maximilians-Universität Würzburg, Germany

**Abstract.** A major problem when establishing high-producing cell lines is the variability of integration sites. Integration of plasmid DNA into the genome of host cells occurs at random. As a consequence, selection of high producers is very time-consuming, costly and critical. Therefore, strategies which simplify and fasten the selection process are advantageous. Here, we present a system, that identifies and selects those of the transfected cells, which show the highest GFP-expression correlating with the expression of a product gene. This high expression system comprises expression vectors and serum-free transfection, selection and cultivation of CHO-DG44 cells.

sICAM (secreted intracellular adhesion molecule) was chosen as an example for the expression of a monomeric therapeutic glycoprotein (480 amino acids) in CHO cells. For this, CHO-DG44 cells were transfected with the vector pBIDG-sICAM. It contains the open reading frames of sICAM and GFP in a bicistronic transcription unit, connected via an IRES (internal ribosome entry site) and driven by a CMV-enhancer and the strong CHO-promoter combination. The selection marker DHFR was expressed from a separate transcription unit. The additional expression of GFP enabled the use of a FACS-based selection strategy. Two to three weeks after the first selection in HT-free CHO-S-SFMII medium the top 5% GFP-expressing cells were selected. After a cultivation period of two weeks, again the top 5% GFP-expressing cells were isolated by FACS-sorting. This sequential sorting was carried out six times in total. A good correlation between sICAM-productivity and GFP-fluorescence could be shown. In shortest time, cell pools with a high specific productivity of up to 16 pg/cell and day were isolated only by FACS-based selection, without any MTX-amplification steps. By combining the GFP-based selection with one single MTX-amplification step it was possible to increase the productivity up to 30 pg/cell and day. These productivities were obtained by the amplification of a pool after the fourth sorting with 500 nM MTX as well as by the amplification of a pool after the sixth sorting with 2  $\mu$ M MTX. In contrast to a stepwise amplification, usually starting with a very low MTX-concentration (5 - 20 nM MTX), we had to use a higher MTX-concentration from the beginning to achieve an amplification effect. There was no significant increase in productivity resulting from the addition of 5 or 50 nM MTX to cells from the fourth sort or, respectively, from the addition of 500 nM MTX to cells from the sixth sort. Obviously, the level of DHFR in the starting pools was already that high that a

complete DHFR-inhibition could only be achieved with a high MTX-dose. Furthermore, the pre-sorted cell pools showed a better survival of the selection phase despite a high initial MTX-dose, meaning that a cell population with a high vitality was obtained in a shorter time period than with the conventional stepwise gene amplification strategy.

In another example, CHO-DG44 cells were co-transfected with the vector combination pBIDG-F19HC and pBIN-F19LC expressing the mAb F19 (a multimeric therapeutic glycoprotein). The humanized antibody F19 is directed against the surface molecule FAP, which is synthesized by reactive stroma fibroblasts. In the herein used vector configuration the both protein chains of the antibody were each expressed from their own vector, which in addition codes for either the DHFR or the neomycin selection marker in a separate transcription unit. Furthermore, the vector pBIDG-F19HC contains another selection marker, GFP, whose expression was linked to the expression of the heavy chain via an IRES-element. CHO-DG44 cells with a high expression of the mAb F19 could be isolated in a short period of time just by selecting the cells with a high GFP content by sequential FACS sorting. For this, the top 5% GFP-expressing cells were sorted out by FACS after an initial 2–3 week selection of the transfected cell pools in HT-free CHO-S-SFMII medium supplemented with 400 µg/mL G418. This sorting was carried out six times in total with a two week cultivation period between each sort. Surprisingly, a good correlation between F19-productivity and GFP-fluorescence could be shown, although both protein chains of the antibody were expressed from their own vector and although the GFP-based FACS sorting could only consider the expression of the heavy chain because of its transcriptional connection to GFP. The productivities were raised up to 10 pg/cell and day. In one single MTX-amplification step starting from a cell pool of the fifth sort, the productivities could be increased even further up to 37 pg/cell and day by adding 1000 nM MTX to the selection medium. At the same time, this strategy shortened the time needed for the selection of high producing cells to the half (i. e. about 120 days) compared to the conventional stepwise gene amplification strategy, which usually comprises 4 steps. This goes along with a significant reduction in developmental capacities and costs.

## Author Index

- Abbas, N. 125  
Abismil, C. 171  
Agathos, S.N. 175  
Aiba, Y. 147, 497  
Ailor, E. 59  
Aires-Barros, M.R. 325  
Alam, I.M. 187  
Albee, A. 537, 541, 549  
Alete, D.E. 71  
Al-Kolla, T. 577  
Allison, D. 229, 577  
Al-Rubeai, M. 439  
Alt, R. 767  
Altamirano, C. 719  
Alvarez, A. 739  
Alvarez, I. 739, 747  
Alves, P.M. 317,  
Amadeo, G.I. 727  
Antonsson, B. 359  
Aramaki, S. 249  
Arias, M.A. 697, 739, 747  
Arod, C.Y. 359  
Asensi, G.F. 489
- Baars, S. 377  
Backmann, N. 493  
Backstrom, M. 423  
Baldi, L. 365  
Ballabas, L. 397  
Barnett, B. 581, 755, 761  
Barthmaier, P. 393  
Barthold, M. 199, 241  
Bassens, C. 233, 625  
Battle, T. 359, 389  
Beccaria, A.J. 87  
Becerra, S. 719  
Beer, C. 83, 321  
Bellila, A. 663  
Bengala, A. 303  
Bengio, S. 447  
Bensellam, M. 233  
Berlin, J. 723  
Bernier, A. 295  
Berrios, J. 719
- Betenbaugh, M. 59  
Bezdetnaya, L. 261  
Biener, R. 431, 597  
Birch, J. 71, 655  
Birrento, M. 533  
Bisson, L. 87, 99  
Blasberg, J. 577  
Blocker, L. 465  
Blüml, G. 253  
Böhm, E. 501  
Bohnenkamp, H.R. 221  
Bollati Fogolin, M. 87  
Borth, N. 501, 521  
Bout, A. 533  
Bouzó, L. 739, 747  
Brandhorst, D. 277  
Brecht, R. 403, 743  
Brown, C.J. 655  
Brueckerhoff, T. 589  
Bruenker, P. 417  
Buhlmann, C. 51, 393  
Buholzer, P. 417  
Büntemeyer, H. 167  
Burg, M. 237, 285  
Burian, R. 555  
Burke, V. 281  
Burzlaff, A. 593  
Bushnaq-Josting, H. 743  
Butler, I.P. 137  
Buttkeriet, U. 277
- Cairns, M.T. 479  
Cairó, J.J. 103, 111, 779  
Calles, K. 155  
Canessa, R. 719  
Caple, M. 537, 541, 549, 577  
Card, C.J. 755, 761  
Carmo, M. 303  
Carpentier, E. 87  
Carrondo, M.J.T. 303, 317, 329  
Casablanca, A. 103, 779  
Casanova, P.R. 641, 645  
Castiglioni, S. 649  
Castilho, L.R. 489

- Castillo, A.J. 505  
 Castro, A. 683  
 Cavalcanti, J.M. 489  
 Cavatorta, F.A. 727  
 Cavenaghi, L. 649  
 Celeri, C. 309  
 Cham, B. 23  
 Chamow, S. 483  
 Chaney, B. 561  
 Chang, C. 483  
 Chang, D.Y.H. 459, 659  
 Chang, M. 521  
 Chea, M. 739, 747  
 Cherlet, M. 625  
 Cheung, K.Y. 187  
 Chevalot, I. 569  
 Chico E. 683, 739, 747  
 Chico Veliz, E. 697  
 Chung, J.Y. 475  
 Cleverley, S. 447  
 Coco Martin, J.M. 671  
 Conradt, H.S. 723  
 Cornudella, L. 111  
 Coroadinha, A.S. 303  
 Cortez-Retamozo, V. 493  
 Costa, M.J.L. 325  
 Cotten, M. 15  
 Crowley, J. 671  
 Cruz, P.E. 303  
 Cuervo, R. 747  
 Cuijten, S.M.R. 675  
 Cunha-Bakeev, C. 439  
 Cutak, B. 577  
 Czerny, K. 377
- Dalm, M.C.F. 675  
 Dang, C. 309  
 Daramola, L. 513  
 De Baetseelier, P. 493  
 De Bernardi, N. 649  
 De Graaf, A. 423  
 De Gràcia, J. 103, 779  
 De Jesus, M.J. 381  
 De la Luz, K.R. 505  
 De Leon Gatti, M. 23  
 De Mattei, C. 649  
 De Vocht, M. 533
- Deckwer, W.-D. 679  
 Deeds, Z. 537, 541, 549  
 Dejesus, M. 67  
 Del Aguila, E.M. 489  
 Delong, B. 537, 541, 549  
 Deluz, C. 471  
 Demmler, C.D. 517  
 Dempsey, J. 637  
 Denoya, C. 509  
 Deparis, V. 569, 613  
 Derouazi, M. 471, 509, 629  
 Derow, E. 365  
 Di Maiuta, N. 373  
 Díaz, C. 739  
 Didier, C. 727  
 Dierickx, P.J. 193  
 Dijkstal, M. 671  
 Dijkstra, R. 533  
 Dimopoulos, G. 3  
 Doblhoff-Dier, O. 253  
 Donahue, L.M. 229  
 Durocher, Y. 83, 87  
 Durrieu, C. 569  
 Duvar, S. 723  
 Dwek, R.A. 31
- Ebert, L. 377  
 Ehler, E. 213  
 Eigenmann, C. 381  
 El Abrid, H. 67  
 Elias, C.B. 87, 99  
 Elliott, L.O. 351  
 Elsayed, E.A. 679  
 Enenkel, B. 115, 791  
 Eriksson, K. 333  
 Eriksson, U. 133  
 Erny, A. 171  
 Espuña, E. 103, 779  
 Esser, S. 671  
 Essers, R. 423  
 Etchberger, K. 281, 633  
 Etcheverrigaray, M. 87, 727, 731
- Faife, E. 505  
 Fallon, E. 459  
 Fang, S.G. 151  
 Fargali, S. 199, 241

- Fathallah, D.M. 663  
 Feger, G. 359  
 Ferko, B. 501  
 Ferrara, C. 417  
 Ferreira, G.N.M. 325  
 Ferreira, T.B. 329  
 Fieder, J. 791  
 Field, R. 513, 637  
 Figueredo, A. 683  
 Figueroa, B. 59  
 Fischbach, T. 269  
 Flatman, S. 187  
 Forestell, S. 309  
 Forno, A.G. 731  
 Forrest-Owen, W. 513  
 Frahm, B. 693  
 Franěk, F. 107  
 Frerichs, J.-G. 589, 605  
 Fritchman, K. 369  
 Fujiki, I. 129  
 Fussenegger, M. 115, 213, 345
- Gadek, Z. 121  
 Galbraith, D.J. 655  
 Galbraith, D.N. 453  
 Garza, P. 459  
 Gaspari, F. 649  
 Gätgens, J. 423  
 Gaudry, J.-P. 359  
 Gay, R.D. 701  
 Gee, C. 637  
 Geisse, S. 373  
 Geldart, R. 465  
 Gelli, C. 385  
 Gendon, Yu. 783  
 Geny-Fiamma, C. 303  
 Genzel, Y. 767  
 Gerdes, C. 417  
 Gernold, N. 377  
 Getmanova, T. 787  
 Geyer, S. 309  
 Giese, C. 517  
 Gifford, J. 537, 541, 549  
 Girard, P. 365, 509, 629  
 Girod, P.-A. 411  
 Glassey, J. 439  
 Gleich, T. 381
- Goddard, C. 137  
 Gòdia, F. 103, 111, 779  
 Goedde, A. 377  
 Goergen, J.L. 261, 569, 613  
 Gonçalves, D. 303, 329  
 Gonçalves, J. 303  
 Gong, T. 309  
 Gorfien, S. 711  
 Goudar, C. 431, 597, 601  
 Gradl, G. 517  
 Gramer, M.J. 751  
 Greiffenberg, L. 397  
 Grillari, J. 289  
 Grosjean, F. 67, 159  
 Gross, S. 501  
 Guillemin, F. 261  
 Guttmann, J. 265
- Haaland, P. 561  
 Haas, R. 163  
 Hacker, D. 15, 67, 365  
 Häggström, L. 133, 143, 155  
 Hamann, D. 207  
 Hamasaki, T. 27, 249  
 Hann, L.E. 79  
 Hansson, G. 423  
 Hardwick, J.M. 59  
 Hardwicke, P. 439  
 Hartshorn, J. 281, 633  
 Hatton, D. 513  
 Hawrylik, S. 465  
 Heidaran, M. 561  
 Heide, M. 179  
 Heidemann, R. 125, 601  
 Heine, H. 359  
 Heineken, K. 483  
 Hendrick, V. 339, 625  
 Henke, M. 373  
 Henry, O. 295  
 Hensel, A. 183  
 Henze, S. 377  
 Hermann, H. 555  
 Herrera, N. 641, 645  
 Herrmann, A. 671  
 Herzer, S. 333  
 Hesse, F. 83, 95, 529  
 Hines, M. 655

- Hinterleitner, P. 253  
Hoare, M. 655  
Hoben, G. 207  
Hoeksma, S. 571  
Hof, R. 671  
Holdread, S. 561  
Hong, Y.J. 475  
Hu, W.-S. 23  
Huang, Y.-M. 459, 659  
Hundt, B. 771  
Hunsaker, B. 755, 761  
Hunt, C. 561  
Hunt, L. 67  
Hußmann, S. 671  
Huttinga, H.H. 573  
Huynh, T. 659  
Hwang, S.O. 475
- Iding, K. 167  
Illanes, A. 719  
Imada, T. 249  
Irani, N. 87  
Ishii, Y. 121
- Jacob, D. 295  
Jacquet, R. 365, 471  
Jaeger, M. 207, 265  
Jäger, V. 199, 241  
James, D.C. 71, 655  
Jansen, M. 533  
Jayme, D. 711  
Jean-Meret, J. 417  
Jestin, A. 613  
Joeris, K. 589, 601, 605  
Johnson, J.M. 281, 633  
Jordan, M. 159, 381, 509, 609  
Jourdain, C. 261  
Juanola, S. 111  
Jungfer, H. 289  
Jursik, C. 289
- Kabayama, S. 121, 249, 257  
Kagye, N. 339  
Kaito, K. 585  
Kallel, H. 663, 775  
Kallmeier, R.C. 701  
Kamba, Y. 339  
Kamen, A. 83, 87, 99, 295  
Kao, K. 537, 541, 549, 577  
Kashiwagi, T. 249, 257  
Kasper, C. 593, 715  
Katakura, Y. 121, 129, 147, 151,  
249, 257, 497  
Katinger, H. 153, 245, 289, 501,  
521, 525, 529, 735  
Keehnen, R. 533  
Keijzer, T. 687  
Keller, B. 345  
Kelm, J.M. 213  
Kessler, N. 171  
Khan, P. 701  
Kim, K.W. 75  
Kim, Y.H. 75  
Kimura, T. 273  
Kloth, C. 743  
Koch, S. 403, 743  
Koh, Y.W. 475  
Kolokoltsova, T. 783, 787  
Komatsu, T. 249  
Konstantinov, K. 125, 431, 589, 597,  
601, 605  
Korn, B. 377  
Kotarsky, K. 625  
Kratje, R. 87, 727, 731  
Kretzmer, G. 715  
Kreusel, D. 397  
Kunert, R. 253, 501, 521, 525, 529  
Kunst, T. 573  
Kuschel, M. 393
- Laffert, B. 385  
Lagerwerf, F. 533  
Landauer, K. 253  
Langlais, C. 377  
Lanthier, S. 99  
Lattenmayer, Ch. 525  
Lecina, M. 103, 779  
Lee, G.M. 75, 475  
Lee, M.S. 75  
Lehmann, J. 167, 285  
Lemmens, R. 333  
Leugers, S.L. 229  
Li, Y. 121, 249  
Lim, K.M. 23

- Lim, S.W. 475  
 Linde, V. 179  
 Lindskog, E. 155  
 Link, N. 345  
 Link, T. 423  
 Loa, A. 385  
 Locas, M.-C. 99  
 Loechel, S. 179  
 Losberger, C. 389  
 Löscher, M. 501  
 Lose, S. 199  
 Lowagie, S. 233  
 Lua, L.H.L. 565  
 Luedke, G. 51  
 Lundholt, B.K. 179  
 Luo, S. 633  
 Ly, L. 659  
  
 Majore, I. 199, 241  
 Malhó, R. 325  
 Mantalaris, A. 3  
 Manwaring, J. 581  
 Marc, A. 261, 569, 613  
 Marc, I. 569  
 Marcelino, I. 317  
 Marique, T. 339  
 Markushin, S. 783  
 Markvicheva, E. 261  
 Martens, D.E. 573, 675  
 Martin, J. 397  
 Martínez, E. 683  
 Martinez, L. 641, 645  
 Marx, U. 403, 517, 743  
 Matsumoto, S. 147, 497  
 Matsuoka, H. 617  
 Maxwell, A. 701  
 Mayer, H. 199  
 Mazurkova, N. 783, 787  
 McNorton, S. 281, 633  
 Medronho, R.A. 679  
 Meents, H. 115  
 Mehta, S. 351  
 Melville, M.W. 79  
 Mensah, P. 465  
 Merlin, J.L. 261  
 Mermod, N. 411  
 Merry, A.H. 31  
  
 Merten, O.-W. 303  
 Michaels, J. 431, 597, 601  
 Miki, M. 273, 585  
 Mikkelsen, I. 179  
 Möbest, D. 207, 265  
 Mohabbat, T. 633  
 Molinas, M.B. 83  
 Mols, J. 175  
 Monge, M. 667  
 Montague, G. 439  
 Morenweiser, R. 333  
 Morisawa, S. 121, 249, 257  
 Moritz, T. 277  
 Moser, S. 417  
 Müller, D. 253, 529, 735  
 Muru, E. 649  
 Mussa, N.A. 187  
 Muyldermans S. 493  
  
 Naschberger, S. 735  
 Navarrete, J. 683  
 Nechaeva, E. 783, 787  
 Nelving, A. 95  
 Neumann, T. 393  
 Niebruegge, S. 285  
 Niede, S.J. 179  
 Nielsen, L.K. 163  
 Nimtz, M. 731  
 Nissom, P.M. 23  
 Noe, W. 459, 659  
 Noguchi, E. 497  
 Noll, T. 221, 269, 423  
 Nolli, M.L. 649  
 Noone, C.B. 479  
 Nossed, Å. 155  
 Nothnagel, J. 679  
 Nowrouzian, M.R. 277  
 Nuck, R. 403, 743  
  
 Obermayer, N. 743  
 Ogawa, A. 273  
 Ojito Magaz, E. 697  
 Ojito, E. 739  
 Okediadi, C. 465  
 Olsen, M. 309  
 Olthof, E. 671  
 Ong, P.F. 23



- Opalka, B. 277  
 Opstelten, D.-J. 533  
 Ordaz, Y. 641, 645  
 Orlandi, A. 649  
 Osborne, M. 637  
 Otsubo, K. 121, 249  
 Otto, R. 791  
 Otubo, K. 257  
 Oudshoorn, A. 675, 687  
  
 Padilla, J. 281, 633  
 Paschoalin, V.M.F. 489  
 Passamani, P. 103  
 Paul, C. 403  
 Paul, W. 711  
 Peeters-Joris, C. 175  
 Peixoto, C. 317  
 Pence, B. 581  
 Pereira Bacci, D.A. 727  
 Pérez, M. 641, 645  
 Perriard, J.-C. 213  
 Perrier, M. 99  
 Pfragner, R. 245  
 Philip, R.J. 23  
 Pias, S. 465  
 Picasso, S. 365, 471  
 Pick, H.M. 471  
 Piehl, G.-W. 679  
 Piret, J. 431, 597, 601  
 Pluschkell, S. 465  
 Porter, W. 561  
 Pörtner, R. 693  
 Præstegaard, M. 179  
 Prats, E. 111  
 Prchal, M. 289  
 Preckel, T. 51  
 Preis, S. 521  
 Pronold, B.J. 229  
 Puchacz, E. 483  
 Puentener, U. 417  
  
 Quel, G. 237  
  
 Raamsman, M. 533  
 Rabasa, Y. 505  
 Racher, A.J. 71, 701  
 Rahmati, S. 459  
  
 Rathbone, E. 577  
 Raymond, I. 483  
 Reff, M. 59  
 Reichl, U. 767, 771  
 Reid, S. 163, 565  
 Rendall, M. 701  
 Renger, S. 533  
 Rennebeck, G. 229  
 Revets, H. 493  
 Rey, L. 359  
 Ridley, A. 637  
 Rigaux, P. 625  
 Rink, A. 23  
 Rist, L. 183  
 Ritchie, C. 637  
 Roche, G. 171  
 Rodríguez, E.N. 641, 645  
 Rodriguez, G. 747  
 Rohde, M. 241  
 Ross, S. 537, 541, 549  
 Rourou, S. 775  
 Rudd, P.M. 31  
 Ruddock, S. 637  
 Ruediger, M. 237  
 Rütten, K. 735  
 Ryabicheva, T. 783, 787  
 Ryll, T. 483  
  
 Sandig, V. 403  
 Sanny, A. 23  
 Santambie, P. 447  
 Sasaki, M. 585  
 Sato, K. 625  
 Sauer, P. 705  
 Sautter, K. 791  
 Schänzler, A. 771  
 Schatten, R. 377  
 Scheper, T. 589, 593, 605, 715  
 Scheuermann, T. 377  
 Schick, M. 377  
 Schlukebir, C. 671  
 Schmid, G. 621  
 Schneider, M. 265  
 Schneider, Y.-J. 175  
 Schroeder, M. 285  
 Schultz, E. 377  
 Schulz, C. 87

- Schulz, R. 199  
Schütt, P. 277  
Schwadtke, A. 743  
Seeber, S. 277  
Sen'kina, T. 783, 787  
Senter, P. 493  
Sheehan, A.J. 137  
Shirahata, S. 121, 129, 147, 151,  
249, 257, 497  
Sidler, F. 183  
Siemensma, A.D. 573  
Sifi, I. 309  
Silva, J.T. 489  
Simon, S. 339  
Simpson, N.H. 573  
Simula, A.P. 137  
Sinacore, M. 79  
Sinclair, A. 667  
Smales, C.M. 71  
Smith, T. 479, 755, 761  
Soley, A. 103, 779  
Sousa, M. 317  
Sousa, P.M. 489  
Spaeni, M. 417  
Spens, E. 143  
Spielmann, M. 345  
Stadler, G. 245  
Stahl, F. 199  
Stark, G.B. 207, 265  
Steindl, F. 529  
Steinellner, W. 521, 529  
Stephan, J.P. 351  
Suarez, J. 739, 747  
Subashi, A. 465  
Sumnall, T. 369  
Suter, T. 417  
Svensson, I. 155  
Sviridenko, T. 783  
Swartzwelder, F.J. 229  
  
Tait, A.S. 655  
Takaki, M. 257  
Takeda, T. 617  
Talabardon, M. 459  
Talley, D. 577  
Tamura, T. 147  
Tan, K.S. 23  
  
Tappe, A. 715  
Tario, J.D. 229  
Tatham, D. 701  
Teixeira, M. 303  
Ten Buren, B. 373  
Tennikova, T.B. 715  
Terada, S. 273, 585  
Teruya, K. 121, 129, 147, 151, 249,  
257, 497  
Tescione, I. 711  
Tewes, M. 277  
Thalen, M. 775  
Thiel, G. 403  
Thinsky, A-L. 339  
Thrift, J. 125  
Tilsaghani, C. 369  
Toallati, M. 233  
Toemoe, S. 397  
Tramper, J. 675  
Trampler, F. 687  
Tromba, P. 365  
Trummer, E. 529  
Tsai, S.P. 351  
Tsujiimoto, K. 585  
Tsunematu, T. 129  
Turner, R. 637  
  
Umana, P. 417  
Unterluggauer, F. 253  
  
Valer, M. 51, 393  
Valiente, O. 739  
Van de Berg, H. 687  
Van de Goor, J. 351  
Van den Ark, A. 775  
Van den Heuvel, J. 87  
Van der Velden de Groot, T. 775  
Van der Wielen, C. 193  
Van Grunsven, W.M.J. 675  
Van Montfort, B. 533  
Van Noordenburg, Y. 533  
Van Tilborgh, F. 629  
Van Zant, G. 229  
Varaksin, N. 783, 787  
Varley, J. 3  
Vasi, J. 333  
Vela, C. 103, 779

- Verhoeve, F. 175  
Verissimo, C. 317  
Vernet, A. 171  
Víctores, S. 505  
Vitón, P. 683  
Vives, J. 111  
Viviani, A. 183  
Vlakh, E.G. 715  
Voglauer, R. 245, 289, 501  
Vooyo, A. 533
- Wade, B.J. 137  
Wagner, R. 83, 87, 95, 679  
Waldmann, R. 555  
Walowitz, J. 711  
Wannlund, J. 561  
Wayte, J.R.T. 701  
Weber, C.C. 345  
Weber, W. 345  
Wegkamp, H.B.A. 573  
Werenne, J. 233, 339, 625  
Wermelinger, T. 183, 403  
Werner, A. 285  
Wernery, U. 493  
Whitford, W. 581  
Wieser, M. 245  
Winkler, I. 397  
Winkler, K. 403  
Wirth, M. 83, 87, 321  
Wlaschin, K. 23  
Wolbank, S. 521  
Wollner, S. 207  
Wong, A. 351
- Wong, C.F. 23  
Wong, K. 23  
Wu, M.-H. 3  
Wurm, F.M. 15, 67, 159, 365, 381,  
471, 509, 629  
Wurm, Y. 397
- Xu, Q.H. 151
- Yallop, C. 533  
Yamada, H. 585  
Yamaguchi, A. 273  
Yamasaki, G. 125  
Yamashita, M. 147, 151, 497  
Yanagihara, K. 585  
Yandell, C.A. 137  
Yap, M. 23  
Yoshizaki, K. 129  
Yuk, I. 309
- Zacher, D. 621  
Zahn-Zabal, M.M. 411  
Zeng, W. 483  
Zerlin, M. 397  
Zhang, C. 431  
Zheng, L. 351  
Zhu, M. 465  
Ziehr, H. 723  
Zietze, S. 403, 743  
Zörner, K. 423  
Zubov, V. 261  
Zuijderwijk, M. 533  
Zweigerdt, R. 237, 285

## Subject Index

- 107 hybridoma cell growth 664, 666
- 107 hybridoma cells 665
- 293T cell line 325, 326, 327
- 30-L continuously perfused bioreactors 679
- 5L stirred-tank bioreactors 659
- 6-L continuously perfused bioreactors 679
- accumulation of osmoprotectants 3
- ACF-v1 process 466, 467, 469, 470
- acid phosphatase assay 556
- acoustic perfusion 687
- active recombinant proteins 613
- activity testing 629
- adeno-associated virus (AAV) 333, 334, 335
- adenoviral vector production kinetics 299
- adenoviral vectors (AdV) 281, 295
- adenovirus 281, 282
- adenovirus infection kinetics 329
- adenovirus production 295
- adoptive immunotherapy 289
- agitation mechanism 735
- akt1 inhibitors 179, 181
- Alamar Blue ® metabolism 209, 211
- alemtuzumab antibodies 417
- allogenic cytotoxicity assay 290
- alternative cultivation systems 381
- Alzheimer disease 51
- amino acid concentrations 95
- amino acid feeding strategies 711
- amino acid supplementation 210, 211, 712
- amino acids 535, 541, 542, 545, 546, 569, 617, 618, 705
- ammonia 533
- ammonia concentrations 767
- analytical cloning 514
- animal cell bioreactors 735
- animal cell culture 439, 593, 775
- animal cell cultures use in pharmaceutical industry 439
- animal cell membranes 9
- animal cells 683, 693, 771
- animal cells metabolism 617
- animal component-free media 537
- animal host cell lines 87
- animal protein free medium 775, 777
- animal protein-free cultivation 175
- annexin V apoptosis measurements 53
- annexin V binding 125
- anoxic hypothermic preservation (AHP) 168
- anti  $\beta$ 2 integrin monoclonal antibodies 663
- anti-alpha-1,3/4 fucosyltransferase antibodies 613
- anti-apoptotic genes 273
- antiapoptotic genes expression 111
- antibodies 487, 488, 493, 502, 518
- antibody production 76, 148, 534, 751
- antibody production processes 3
- antibody production rate 3
- antibody productivity in hybridoma 3
- antibody productivity in transfectoma 3
- antibody stability 3
- antibody-antigen recognition 36
- antibody-dependent cellular cytotoxicity (ADCC ) 417-421
- antibody-fragments 518
- antigen presenting cells (APCs) 34
- antigenic peptide loading 32
- antigens 148
- antigen-specific hybridoma 501
- anti-HIV-antibody production 253
- apoptosis 51, 59, 60, 118, 125, 129, 581
- apoptosis detection 112
- apoptosis induction 52, 505
- apoptotic cell death 121
- arginine 534
- arylsulfatase B (ASB) 43, 47
- ASBEST 45, 46, 47
- ATF tech 313
- ATP 87, 89, 121, 122

- autologous cytotoxicity assay 291  
Aven 61, 63
- baby hamster kidney (BHK) cells  
597, 605
- bacterial endotoxins 775  
*Baculovirus* 453-456  
baculovirus expression system 779  
baculovirus expression vector system  
(BEVS) 92, 93, 378, 379  
*Baculovirus* production 565  
Baculovirus/insect cells expression  
system 613  
baculoviruses 163  
base medium 542  
batch animal cell culture 621, 622  
batch culture 125, 534  
batch fermentation 589, 605  
batch production 298  
Batch-fed suspension culture 309  
Bayer CHO cell lines 128  
BHK-21 B cell line 723  
BHK-21 cells 489, 767  
bioartificial liver support 167  
bioinformatic tools 377  
biologicals production 751  
biomechanical properties analysis  
265  
Biopesticide 565  
biopharmaceutical products  
manufacturing 529  
biopharmaceutical industry 701  
biopharmaceutical manufacturing  
447, 667  
biopharmaceuticals 641, 645  
biopharmaceuticals cloning 489  
biopharmaceuticals expression 489  
biopharmaceuticals production 517  
bioreactor cultivation 530  
bioreactor design 265, 267  
bioreactors 312, 313, 325, 381, 411,  
432, 459, 461-463, 529, 530, 537,  
589, 590, 597, 605, 634, 665, 747  
bioreactors experiments 538  
biosensor immuno assay (BIA) 345,  
347, 349  
BioSep system 687-690
- biotherapeutics production 453  
blastocysts 237  
bone marrow 229  
bone tissue engineering 199  
bone tissue implants 199, 241, 243  
Bovine Aortic Endothelial cells  
(BAE) 317, 318  
bovine FSH glycoprotein 479  
bovine serum 775  
bovine serum removal 739  
bovine spongiform encephalopathies  
453  
bovine viral risks 453  
Bradford's method 642  
breast cancer 423  
breast cancer cells 183, 184  
breast cancer immunotherapy 221  
BSA 585-587  
BSE 585  
butyric acid 26  
BV production 566, 567
- calcium accumulation 7  
calcium phosphate 159  
calcium phosphate (CaPi) 629  
calnexin (CNX) 475-478  
calreticulin (CRT) 475-478  
camel single-domain antibodies 493  
cancer 51  
cancer cell encapsulation 261  
cancer immunotherapy 493  
cancer treatment 417  
capillary gel electrophoresis CGE  
393  
CaPO<sub>4</sub>-mediated transfection 373,  
374  
Caprine Jugular (CJE) 317, 318  
carbohydrate mapping procedures  
723  
carbohydrate metabolism 570  
carbon 617  
carbon source 209, 211  
carbonic anhydrase (CA) 171  
cardiomyocyte-derived microtissues  
213  
cardiomyocytes 285  
caspase activation 125

- caspase activity 51
- cDNA cloning 489
- cDNA microarray 23, 27
- cDNA 359, 360, 480, 522
- cell adhesion 9
- cell analysis 222, 513
- cell banks 637
- cell culture 52, 59, 116, 304, 317, 340, 538, 555, 578
- cell culture data-based modelling 439
- cell culture management software 397
- cell culture media 562, 578, 755
- cell culture medium optimization 549
- cell culture platform technology 459
- cell culture production 659
- cell cycle distribution 3
- cell death 51, 163
- cell density 222, 423, 432, 634
- cell density effect 297
- cell growth 3, 76, 111, 143, 329, 633, 775
- cell growth assays 538, 578
- cell growth increase 541
- cell growth rate 3
- cell growth suppression 249
- cell isolation 222
- cell line construction 513
- cell line engineering 417
- cell line expression stability 514
- cell line physiology 295
- cell lines 4, 43, 71, 104, 112, 295, 303, 310, 311, 321, 370, 381, 385, 397, 403, 405, 408, 419, 483, 484, 485, 486, 521, 537, 538, 550, 578, 581, 694, 743, 784
- cell lines screening 752
- cell population analysis 411
- cell preparation 230
- cell retention tool 679
- cell separation system 679
- cell shape 9
- cell side convection 752
- cell size 9
- cell specific production rates 517
- cell specific productivity 534
- cell supernatants analysis 513
- cell therapy 59, 233
- cell transfer 529
- cell viability 4
- cell volume change 3
- cell-based assays 385
- cell-cell fusion (CCF) 483, 484, 485, 486, 488
- cell-cell fusion (CCF) clones 486, 487
- CELLine flasks 369, 370
- cells selection 340
- cellular metabolic rate 3
- cellular metabolism 434, 435, 436
- cellular senescence 129
- CELO adenovirus Gam1 gene 15, 16
- cGMP 454, 557
- cGMP manufacturing 671
- chemically-defined protein-free medium 675
- chemostat culture 617
- chemostats 573
- chimeric EGFP-Photinus luciferase 625
- Chinese hamster ovary cells (CHO) 15-17, 23, 79, 115, 351, 403, 483, 533, 561
- Chinese hamster ovary cells (CHO) , genomic exploration 23
- CHO cDNA library 24
- CHO cDNA microarray 24
- CHO cell clones 537, 541, 542, 549, 550, 553
- CHO cell cultures 441, 444, 621, 623
- CHO cell lines 125, 546, 553, 641, 701, 711, 716, 747, 791
- CHO cells 62, 67, 69, 137, 138, 159, 175, 180, 188, 411, 412, 413, 419, 423, 425, 429, 431-436, 454, 465, 470, 471, 472, 475, 479, 489, 509, 510, 521, 523, 525, 541, 590, 597, 602, 605, 606, 611, 625, 626, 629, 632, 655, 659, 679, 683, 685, 719, 731, 739, 743, 744, 747, 748, 767, 767
- CHO expression system 479

- CHO sequences 25, 26
- CHO subclones 529
- CHO-AF 537, 538, 540
- CHO-DG44 cells 115, 116, 118
- CHO-DG44 cells 791
- CHO-IgG 539, 540
- CHOK1 701, 702, 721, 727
- CHOK1 cells 489
- CHOK1SV 701, 702
- cholesterol 565, 567, 577, 697, 699
- cholesterol dependent cell culture 577
- CHO-M-CSf 539, 540
- chromatographic resins 333
- chromatography 467
- chromatography sorbents 447, 450
- classical cell culture technology 381
- clearance rates calculation 556
- clinical trails 333
- clinical-scale expansion 230
- cloning 44
- cloning method 497
- closed bag systems 667
- co-expressed recombinant protein 471
- collagen expression 208, 211
- colorectal carcinoma (CRC) patients 291
- commercial protein-free medium 739
- complex therapeutic proteins 597
- conditioned medium (CM) 133-135
- conditioned medium factors 143, 144
- congenital disorders of glycosylation (CDG) 31
- continuous flow electroporation 629
- cord blood (CB) 270
- cord blood hematopoietic stem and progenitor cells (HSPC) 269
- cost of goods analysis 669
- co-transfected cell lines 487
- cross validation 440, 441
- cryopreservation 167, 386
- cryopreservation procedure 385
- cryopreserved cells 385
- CryoStock 397-400
- cultivation 783
- culture conditions 104, 112, 723
- culture dishes 411, 412
- culture maintenance 4
- culture media 95
- culture media composition 330
- culture osmolarity 10
- culture parameters influence 675
- cultured fathead minnow (FHM) 193
- cumulative cell hours (CCH) 637
- cystine 534
- Cytocon300™ technology 518
- Cytodex 737, 738, 772
- Cytodex 3 microcarriers 339
- cytokine analysis 222
- cytokines 222-226, 269, 270
- cytomegalovirus (CMV) 84
- cytoskeletal organization 9
- cytotoxic unconjugated mabs as drugs 417
- data augmentation techniques 440
- data-based modelling of cell cultures 439
- dendritic cells (DC) 221, 223, 224, 245
- design-of-experiment (DOE) software 549, 551
- device master files (DMF) 232
- diabetes 273
- dihydrofolate reductase (DHFR) 351, 537
- dihydrofolate reductase (DHFR) systems 71
- disposables vs stainless steel 667
- DMSO 385
- DNA 83, 84, 118, 122, 122, 123, 160, 161, 257, 296, 348, 352, 361, 472, 498, 509, 522, 630, 649, 655, 656, 657, 791
- DNA concentrations 509, 510, 683, 684
- DNA gel electrophoresis 125
- DNA laddering 51, 53
- DNA methylation 15
- DNA microarray 4, 199, 202
- DNA microarray techniques 7
- DNA preparation 52
- DNA replication 60

- DNA transfections 112  
DNA-transfection methods 629  
DOE software package 633  
double stable cell line 476  
downstream processing 629  
drug identification 385  
Dulbecco's Modified Eagle Medium (DMEM) 95, 96, 233, 764
- E. coli* cells 490  
*E. coli* system 378  
E1B-19K protein 60, 61, 62, 63  
early transfectants 523  
economical DNA transfer vehicle 629  
EGF 242  
electrodes 518  
electrolysed-reduced water (ERW) 121, 249, 257, 258  
electron microscopy 321  
embryonic stem cells (ES) 237, 285, 286  
EMCV 115  
empirically based optimization strategies 747  
endoplasmic reticulum (ER) 31, 34  
ER strains 317  
endothelial cells culture 339, 341  
enhanced green fluorescent protein (EGFP) 15, 159, 160, 161  
enhanced green fluorescent protein (EGFP) fluorescence 457  
enhanced yellow fluorescent protein (EYFP) 15  
enveloped viral particles 321, 323  
enzyme-linked immunosorbent assay (ELISA) 112, 148, 152, 187, 351, 498, 506, 513, 514, 522, 525, 527, 530, 561, 562, 642, 650, 664, 698, 702, 716, 719, 740  
enzyme-linked immunospot (ELISPOT) 148  
epigenetic effectors 15  
EPR 303  
EPR spectroscopy 305, 307  
Epstein Barr virus positive cell lines 111  
erythropoietin (EPO) 84, 88, 89  
eukaryotic systems 453  
European Collection of Cell Cultures (ECACC) 577  
experimental factorial design 641  
expression strategies 655  
external shear stress 59  
extracapillary Space (EC) 747  
extracellular histone cells 155  
extracellular matrix formation 207  
extracellular metalloproteases 175  
extracellular protein factors 134
- FACS 51, 518, 522, 525, 527  
FACS analysis 45, 47  
factorial matrix design 541, 547  
fed batch reactor culture 253-255  
fed-batch animal cell culture 621, 622  
fed-batch bioreactors 711  
fed-batch culture 659, 779  
fed-batch process-1 (FBP-1) 698, 705-709  
fed-batch process-2 (FBP-2) 698, 705-709  
fed-batch production 298, 314  
fed-batch strategy 697  
feed strategy 535  
feeding strategies 659  
fermentation inocula 637  
fermentation process 739  
fetal bovine serum (FBS) 569  
fibroin 585  
filter clogging 683  
final antibody concentration 3  
flexible fed-batch process control 693  
flow cytometry 116, 230, 231, 513, 515, 593, 594, 595, 613  
fluidized bed culture 253, 254  
fluidized bed reactors 739  
fluorescence based secretion assay 518  
fluorescence microscopy 116  
fluorescence parameters 517  
fluorescence signals 518  
Fmoc strategy 715



- foetal calf serum (FCS) 555, 558  
 formulation studies 629  
 freezing 386  
 fructose 210, 211  
 full open reading frame (ORF) clones 377, 378, 379  
 fusion protein 671
- Gam1 16, 19  
 gamma-irradiation method 555, 556, 557, 558  
 gene amplification 701  
 gene expression 7, 411  
 gene expression analysis 4  
 gene expression experiments 10  
 gene therapy 59, 329  
 general cell screening systems (GCSS) 526, 529, 531  
 generalized logistic equation (GLE) 601, 602, 604  
 genes 377, 378  
 gibbon ape leukaemia virus (GALV) 303, 304, 305, 306, 307  
 global information management 397  
 gluconeogenesis 423  
 glucose 210, 533, 535, 542, 593, 617  
 glucose consumption 6  
 glucose uptake rate (GUR) 750  
 glucose-limited perfusion process 423  
 glutamate 618  
 glutamate consumption 6  
 glutamine 534, 535, 542, 617, 618  
 glutamine synthetase (GS) 71, 701  
 glutamine-free media 767  
 glycan epitopes 32, 37  
 glycans 37-40  
 glycoengineering 418, 421  
 glycoforms 31  
 glycolysation 43  
 GlycoMAb 418, 421  
 glycoprotein therapeutics 723  
 glycoproteins 31, 35, 727  
 glycosylation 34, 46, 423, 429, 456, 463, 479  
 glycosylation analysis 745  
 GM-CSF concentration 223
- GMP 649  
 GMP production 743  
 Grace cells 103, 104  
 graft versus host disease (GVHD) 229  
 granulocyte-macrophage colony-stimulating factor (GM-CSF) 731-733  
 green fluorescence protein (EGFP) 84  
 green fluorescent protein (GFP) 43, 48, 112, 179, 791, 792  
 green fluorescent protein (GFP) expression 509-512  
 growth factors 242, 535  
 growth kinetics 526  
 GS-NS0 cell line 637  
 GS-NS0 expression system 3, 4
- Haine River waste-water samples 193  
 harvest 360  
 Heartwater 317  
 heavy chain (HC) 33, 34, 188  
 heavy-chain antibodies (HCAs) 493  
 HEK 293 cells 83, 84, 85, 281, 296, 365, 629, 632, 756-758  
 HEK.EBNA cells 373, 374  
 HEK293EBNA cells 359, 360, 361, 363, 365, 366, 389, 391  
 HeLa cells 625, 679  
*Helicoverpa armigera*  
 nucleopolyhedrovirus (HaSNPV) 565, 567  
*Helicoverpa* pest species 565  
 hemacytometer 4  
 hematological malignancies 417  
 hematopoietic stem cells (HSC) 229  
 hepatocytes 167, 168  
 HEPES 386  
 heterohybridoma 404  
 hGH 88  
 HHPAEC-PAD 723, 725, 732  
 high glucose perfusion culture 425  
 high level heterologous gene expression 403

- high performance monolithic disk chromatography (HPMDC) 715, 716
- High-Five™ cells 91, 92, 93, 99
- histone H4 155
- HIV-1 325, 327
- hollow fiber 741
- hollow fiber bioreactors 369, 739, 743, 744, 747, 752
- hollow fiber systems 751
- host cell lines 309
- host cell proteins (HCP) 448
- hours post infection (HPI) 329
- human anti-mouse antibody (HAMA) response 497
- human cell line PER.C6™ 533
- human factor IX (FIX) 489, 490, 491
- human G-CSF 490
- human hepatoblastoma HepG2 585, 586
- human IgG 630
- human immunoglobulin loci 403, 405
- human lymphocytes 148
- human medullary thyroid carcinoma (MTC) cell 245, 247
- human monoclonal antibodies 147, 637
- human mouse heterohybridoma 403, 404,
- human peripheral blood lymphocytes (PBL) 147-149, 151, 153, 498, 499
- humanized antibodies 705
- humanized monoclonal antibody 573
- hybridization 24
- hybridoma 585
- hybridoma cell cultures 573
- hybridoma cell lines 111, 517, 663
- hybridoma cells 403, 675
- hybridoma cultures 107, 108, 109
- hydrocyclone use 679
- hydrogen peroxide 129
- hydrosylates 541, 542, 544, 546
- hyperglycemia 273, 275
- hyper-osmotic culture 3
- hyper-osmotic pressure 3, 75, 76
- hyper-osmotic stress 75
- hyperoxic hyperthermic preservation (HHP) 168, 169
- hypo-osmotic culture 3
- hypo-osmotic pressure 3
- Hypo-Thermosol (HTS) 386
- HyQ PF-CH) MPS 739
- ICB-BEVS 91
- IDEC cell culture platform 460
- IDEC cell culture process flow diagram (PFD) 459
- IDEC in-house media 659, 660
- idiotype-dendritic cell vaccine 277
- idiotypic determinant (Id) 277, 278
- IgG 533
- IgG mRNA transcription rate 3
- IL-10 151, 152, 153
- IL-4 concentration 223
- IMAC 447, 450
- immunobiological analysis 223
- immunocytochemistry 481
- immunogenic contaminants 775
- immunogenicity 788
- immunoglobulins 36
- immunostaining 321
- impeller technology 735
- in vitro* immunization 498, 499
- in vitro* immunization method (IVI) 147, 148, 149, 151, 152
- in vitro* protocol 497
- infection 299, 389
- infection parameters 779, 781
- infectious agents 573
- influenza vaccine production process 767
- influenza virus 171, 783, 787
- influenza virus strains 784
- inoculum viability 665
- insect cell cultures 443, 569, 779
- insect cell growth 565
- insect cell/baculovirus expression system 441
- insect cells 91, 103, 453
- Insight™ technology 518
- in-situ microscopy (ISM) 589, 591, 593, 594, 595, 605, 608

- insulin 137, 275, 542  
 insulinoma cell line 273, 274  
 interferon 340, 341  
 internal ribosome entry site (IRES)  
   111, 115, 116  
 Intracapillary Space (IC) 747  
 intracellular fluxes 617  
 intracellular nucleotide pools 95  
 ion balance 6  
 ion concentration measurements 6  
 ion exchange 447  
 ion-exchange chromatography 333,  
   337  
 IPL-41 103, 104  
 iron 542, 545, 546  
 iron chelator 541  
 isoelectric focusing (IEF) 637, 639,  
   740  
 isoleucine 534  
  
 job module 399  
  
 K<sup>+</sup> concentration 7  
 Kaposi sarcoma tissues 111  
 killer-T-cells (KTCs) 289, 290, 291  
  
 lab-on-a-chip technology 51  
 lactate 91, 92, 533  
 lactate concentration 593  
 lactate metabolism 570  
 lactate production 6  
 large scale cell culture strategies 233  
 large-scale acoustic perfusion system  
   671  
 large-scale protein production 365  
 large-scale recombinant protein  
 expression 541  
 large-scale SFM formats 581  
 large-scale static culture systems 761  
 large-scale transient gene expression  
   (TGE) 629, 632  
 LC 188  
 leader-sequence 45  
 lentiviral transduction 217  
 leptin Fc 403-405  
 leucine 534  
 lipids 541, 542, 544, 546  
  
 long time storage of pre-inoculated  
 multi-well plates 385  
 Long<sup>TM</sup> R<sup>3</sup>IGF-I 137, 138, 139, 140  
 long-term fermentation 589, 605  
 long-term spinfilter clogging 683  
 low glucose perfusion culture 426  
 low volume bioreactors 743  
  
 MAb 459, 460, 461, 497, 649, 652,  
   653, 697, 699, 700, 743  
 Mab production 459, 581, 633, 635,  
   651, 659  
 Madin-Darby canine kidney (MDCK)  
   cells 171, 767, 768, 770, 783, 784,  
   785  
 major histocompatibility class I  
   (MHCI) peptide antigens 31, 33  
 MALDI/TOF 723, 725, 732, 733  
 MALDI-TOF-MS 72, 76, 77, 406,  
   407  
 mammalian antibiotic sensor  
   technology (MAST) 345, 346,  
   347, 349  
 mammalian cell batch cultures 601,  
   602  
 mammalian cell culture 59, 60, 213,  
   321, 414, 585, 687  
 mammalian cell culture processes  
   605  
 mammalian cell lines 87, 471  
 mammalian cells 15, 43, 67, 71, 359,  
   365, 423, 431, 590, 591, 597, 609,  
   637, 645, 671, 755,  
 mammalian expression systems 373  
 mammalian production clones 521  
 manifold systems 668  
 mannose-6-phosphate receptor 43  
 MAP assays 321  
 MAPK phosphorylation 137, 139  
 mass spectrometry 578  
 Master Cell Bank 529  
 matrix assay 542, 543, 545  
 matrix metalloproteases (MMP)  
   175, 176  
 matrix-attachment region (MAR)  
   elements 411, 412, 413, 414  
 maturation cells 223

- MDBK cells 339  
measles virus 787  
measles virus production  
media optimization 561  
media screening 752  
medium 4, 43, 104, 112, 340, 659, 694, 740  
medium ion concentration 4  
medium mixing method 549  
medium optimization kit 541, 549, 550, 553  
medium supplementation 541  
membrane stability 262  
membrane thickness 262  
mentionine 534  
mesenchymal stem cells (MSC) 233, 234, 235, 241  
metabolic characterisation 534  
metabolic flux analysis (MFA) 431, 432  
metabolic fluxes 597  
metabolism 4, 207  
metals 541, 542, 543, 545, 546  
micro bioreactor 752  
micro hollow fiber bioreactor 751  
microcapsules 261-263  
microcarrier cell culture 318, 319  
microcarrier cultivations 593  
microcarriers 340, 341, 594, 626, 761  
microchannels 518  
microencapsulated forms of viral vaccines 787  
microfluidic technology 393, 395  
microinjection 509, 510, 511  
microscopic live imaging 159  
microtiter assay 208  
microtube system 609  
mini membrane bioreactor 269  
minic small tumors 261  
mistletoe extracts 183  
mistletoe lectins 184  
mistletoe polysaccharides (MS) 184  
mitochondria 115, 116, 118  
mitosis 159  
mixed lymphocyte reaction 224  
MLV-A 322  
mobilized peripheral blood 229  
modified anoxic hypothermic preservation (MAHP) 168, 169  
modular pilot plant facility 667  
molecular therapy 325  
monoclonal antibodies 497, 501, 502, 506, 593, 649, 659  
monoclonal antibody process 668  
monoclonal antibody production 369, 634  
monoclonal antibody productivity 111  
mouse leukaemia virus (MLV) 303  
mouse myeloma cells 419  
MRC-5 385  
mRNA 71, 79, 351, 352, 354  
MTC cell lines 246  
MTX 791, 792  
MUC-1 glycoprotein 423  
mucopolysaccharidosis VI (MPS VI) 43, 47  
multicellular spheroids 261  
multi-drug-resistant human-pathogenic bacteria 345  
multiple myeloma (MM) 277  
multiple apoptosis parameters 51  
multiplicity of infection (MOI) 163, 164, 165, 329, 330  
murine monoclonal antibody 743  
murine myeloma 581  
myocardial microtissues 216  
natural peptides 107, 108, 109  
neonatal mouse cardiomyocytes (NMC) 214, 215  
neonatal rat cardiomyocytes (NRC) 214, 215, 217  
neo-tissues 265  
neural red uptake (NRU) 193  
NH<sub>4</sub><sup>+</sup> production 6  
NIF production 466  
nitrogen 617  
N-linked glycosylation 31  
non-ACF process 467  
non-animal defined NS0 medium 577  
non-Hodgkin's lymphoma 417

- normoxic hypothermic preservation (NHP) 168
- novel capacitance probe 621
- NRW 121
- NS0 403, 483, 581, 582, 583
- NS0 cell cultivation 694
- NS0 cell lines 611, 697
- NS0 cells 143, 145, 650, 711, 747, 750,
- NS0 derivatives 581, 582, 584
- NS0 derived cell lines 577, 578
- NS0 myeloma 683
- NS0-derived hybridoma 633
- nucleic acid capture assay (NACA) 351, 352, 353, 354
- nucleic acid quantitation 321
- nucleic acids 527
- Nunc Cell Factories™ 309, 312, 313, 761
- nutrient depletion 59
- nutrient supplementation 719
- nutrient supplementation strategy 712
- nutritional function study 573
  
- ODV membranes 567
- oligosaccharide moieties 727
- O-linked glycosylation 31
- oncolytic adenoviral vectors 309
- on-line OUR measurements 779
- ONYX-4XX vectors 309, 315
- open bag systems 667
- open-loop-feedback-optimal (OLFO) controller 693
- optimal peak cell density (OPCD) 163, 164, 165
- optimization kit design 542
- orthopaedic reconstructive surgery 199
- osmotic pressure 3
- osteogenic cells 199
- OUR monitoring 780
- oxidative stress 257
  
- packed cell volume (PCV) 609-611
- PAGE analysis 44, 45
- pancreatic  $\beta$  HIT-T15 cell 121, 122
  
- Parkinson disease 51
- partial least squares regression (PLS) 95, 97
- PCR 497
- PDGF production yields 561
- peak cell density (PCD) 566
- peanut lectin (PNA) 171, 172
- PEI 655, 656, 657
- PEI-mediated transient expression 655, 656
- peptides 569
- peptones 562
- perfusion 683
- perfusion culture 110, 125, 573, 679, 779,
- perfusion process low viabilities 675
- perfusion production 298, 314
- peripheral blood mononuclear cells (PBMCs) 289, 290, 292, 497
- pH dependent polymers 787
- phage display library 498
- phagocytosis 224
- pharmaceutical industry 439
- pharmaceutical production 693
- pharmaceutical proteins 573
- phase contrast microscopy 593
- phosphate 533, 534
- Phosphatidylserine 52
- phosphatidylserine exposure 51
- pilot scale airlift fed-batch culture 254
- pilot-scale animal cell perfusion runs 683
- plant hydrolysates 537
- plaque assay 556
- plasmid constructs 112, 116
- platinum nanocolloids (PtNCs) 249, 250, 251
- poliovirus production 755, 761
- polyethyleneimine (PEI) 629-632
- polyethyleneimine (PEI) mediated transfection 373, 375, 629
- polymers 787
- population doubling time (PDT) 566
- pre-clinical trials 333
- premature senescence 129

- primary chicken embryo fibroblasts (CEF) 771-774
- principal component analysis (PCA) 95, 98
- process development 649
- process optimization 667
- production quality analysis 723
- production system 369
- program cell death (PCD) 59
- proprietary iron chelators 537
- protein analysis 447
- protein expression monitoring 448
- protein ligands immobilisation 716
- protein production 411
- protein purification optimization 450
- protein quantitation 393, 395
- protein sizing 393
- ProteinChip® technology 447
- protein-free conditions 735
- protein-free culture medium 711
- protein-free medium 143, 755, 761, 765
- proteins 377, 378
- P<sub>SV40</sub> promoter 346, 347
- purification 361, 447, 450, 451, 467
- PYC2 87-88, 99
  
- QC tests 649
- Qiagen 4
- quasi real-time metabolic flux analysis (QRT-MFA) 431, 432, 436
  
- rabbit mesenchymal stromal cells 241, 242
- radial basis function (RBF) neural networks 440, 443, 444
- rapeseed hydrolysate (RH) 570, 571
- rapeseed proteins 569
- rCHO cells 75, 76, 77, 78
- reactive oxygen species (ROS) 121, 249, 250, 251, 257, 258
- real time PCR 522, 526
- real-time PCR results 566
- recombinant adenoviral (AV) vectors 329, 330
- recombinant adenovirus production 755
  
- recombinant antibodies 403, 408, 483
- recombinant cell line selection 505
- recombinant cell lines 509, 525
- recombinant clones 521
- recombinant glycoprotein expression 479
- recombinant human EPO (rhEPO) 723-725, 727-729
- recombinant human GM-CSF (rhGM-CSF) 731, 732, 739
- recombinant human insulin 537
- recombinant humanized IgG 550
- recombinant IgG 513, 578
- recombinant mammalian cell lines 529
- recombinant mammalian cells 505
- recombinant NS0 cell lines 513
- recombinant protein levels 629
- recombinant protein production 779
- recombinant proteins 373, 377, 389, 393, 441, 472, 521, 569, 626, 637, 641
- recombinant retroviruses 303
- recombinant therapeutic proteins 655
- redistribution™ 179, 181
- Refine Technology ATF™ 309
- replicative senescence 129
- retentate chromatography SELDI mass spectrometry 447, 448, 449, 451
- retention devices 683
- retroviral vector stability 303
- retroviral vectors 322, 323
- reverse phase 447
- rickettsia *Ehrlichia ruminantium* (ER) 317, 318, 319
- rickettsiae *Cowdria ruminantium* 339, 341
- rickettsiae stocks 340
- rituximab antibodies 417
- RNA 522
- RNA transcription rate 3
- RNAi 19
- rNS0 line 711
- roller bottle systems 641

- roller bottles 340, 341, 369, 370, 739, 741, 761
- RollerCell bottle packs 645
- RollerCell procesing unit 645
- RollerCell system 645, 646, 647
- root mean squared error (RMSE) 440, 441, 443
- r-protein 365, 367
- rubella virus production 755
- ruminant endothelial cells 317, 318
- RW 121, 122, 123
  
- salts 535
- Scaffold attachment regions (SARs) 411, 412
- scanning 24
- screening systems 525
- SDS-PAGE 393, 394, 652, 653, 716, 717, 725, 728
- SEAP 346, 347
- secreted intracellular adhesion molecule (sICAM) 791
- seed train 360
- senescence evasion factor (SNEV) 501
- sequencing 25
- sericin 585-587
- serine 534
- serum concentration 329
- Serum Free 293 II Medium (SFM) 95, 96
- serum free media 776
- serum-containing medium (SCM) 570, 571
- serum-free cultivation 175, 771
- serum-free cultures 133
- serum-free expansion medium preparation 230
- serum-free media 115, 143, 569, 570, 571, 581, 585, 621, 755, 756, 763, 771
- serum-free PER.C6™ cells 281
- serum-free production of poliovirus 761
- serum-free suspension culture 373
- serum-reduced media 200
- Sf9 cells 155, 157
- Sf9 cultures 389, 779, 780
- Sf9 insect cells 569, 570, 571, 613, 614, 615
- shuttle 43
- sialylation 745
- silk protein sericin 585
- single-cell secretion assay 502
- single-use bag systems technology 667
- size exclusion liquid chromatography (SEC) 652
- slot and western blot analysis 476
- sodium butyrate 625
- Softmix 735, 737, 738
- solid breast tumors 417
- solid phase peptide synthesis 715
- specific formation rate 144
- specific growth rate 144
- spiking procedure 556
- spinfilter 683
- spinner 530
- spinner flasks 340, 341, 529, 537, 625, 626
- stability studies 629
- Statgraphics software 642
- stationary cell culture 761
- Stemline™ hematopoietic stem cell expansion media 229, 230, 232
- stirred tank bioreactor 663
- stirred tank fermenters 739
- stirred-tank bioreactors 633, 775
- storage system 398
- stirred tank bioreactor (STR) 736, 737, 739
- stromal cell lines 269, 271
- subcloning 377
- surface enhanced laser desorption ionization (SELDI ) 447
- synthetic cholesterol 577
- synthetic ligands 715
- synthetic peptides 107, 108, 109
  
- T. ni* proliferation 133
- TC flasks 340, 625
- TC-100 cells 103, 104
- TCA 87
- T-cell receptors (TCRs) 34, 35

- T-cell recognition 34  
telomerase activity 246  
telomere length 246  
temperature control 687  
T-flasks 529  
therapeutic antibodies 697  
therapeutic antibody glycoforms 417  
therapeutic proteins 731  
therapeutic strategies 245  
therapeutics preparation 775  
tissue culture (TC) 234, 235  
tissue engineering 207, 208, 265  
tissue plasminogen activator (t-PA)  
715, 719  
tissue-engineered biohybrid tissues  
265  
titration of samples 556  
TOF-MS 448  
total cumulative cell concentration  
(TCCC) 685  
toxin accumulation 59  
TPO biological activity 477  
TPO productivity 475  
trans-epithelial electrical resistance  
(TEER) 171, 172  
transfection 44, 360, 362, 373  
transfection of CHO cells 471  
transfection technologies 629  
transfectoma cell line 683  
transient gene delivery strategies 655  
transient transfection 159  
translation rate 3  
transplanted islets death 273  
trastuzumab 417  
*Trichoplusia ni* cells 133  
trypan blue dye-exclusion method 4  
tumor cell lines 289, 309, 311  
tumor cells cultivation 263  
tumor necrosis factor- $\alpha$ (TNF- $\alpha$ ) 147,  
148, 149  
two-dimensional polyacrylamide gel  
electrophoresis (2-D PAGE) 75,  
78  
UK-279, 276 production 465, 466  
umbilical cord blood (CB) 229  
unconjugated antibodies 417  
universal medium 561  
University of Wisconsin Solution  
(UW) 386  
unstable cell lines 514, 515  
UV-C irradiation 555, 556, 557, 558  
vaccination 329  
vaccine production 783  
vaccine production processes 767  
vaccines 593  
vascular endothelial growth factor  
(VEGF) 213, 214, 217  
vector envelopes 306-308  
vector stability 299  
vero cells 762, 775, 776, 788  
versatile disposable culture system  
381  
veterinary vaccine 317  
VHH 493-495  
viability 633, 634  
viability cell count 5  
viral infection 59, 755  
viral particles 333, 334, 335  
viral vaccines preparation 775  
viral vectors 333  
virus contamination 321  
virus production 304  
virus production assays 763  
virus purification 304  
virus removal strategies 321  
virus stability assay 304  
viscotoxin 184  
vitamins 541, 542, 544, 705  
VLPs 325, 326, 455  
volume regulation mechanism 9  
water 9  
western analysis 44, 45  
western blot analysis 514, 522, 523,  
719, 721  
western blots 501, 654  
wheat-gluten-derived protein  
hydrolysates 573  
working cell bank (WCB) 650, 740  
yeast pyruvate carboxylase 87  
yeast two-hybrid system 378  
yeast-2-hybrid screening 501  
z-VAD-fmks 125, 128